



Celebrating 40 Years

36th ANNUAL MIDWINTER MEETING

ABSTRACT BOOK

February 16-20, 2013
Baltimore Marriott Waterfront Hotel
Baltimore, Maryland, USA

ARO OFFICERS FOR 2012-2013

PRESIDENT: **John C. Middlebrooks, PhD (2012-2013)**
University of California at Irvine
Department of Otolaryngology
Irvine, CA 92697-5310

PRESIDENT ELECT: **Jay T. Rubinstein, MD, PhD (2012-2013)**
University of Washington
Virginia Merrill Bloedel Hearing Research Center
Box 357923
Seattle, WA 98195

PAST PRESIDENT: **Debara L. Tucci, MD (2012-2013)**
Duke University Medical Center
Division of Otolaryngology-HNS
Box 3805
Durham, NC 27710

**SECRETARY/
TREASURER:** **John P. Carey, MD (2011-2014)**
Johns Hopkins School of Medicine
Department of Otolaryngology-HNS
601 North Caroline Street, Room 6255
Baltimore, MD 21287-0910

EDITOR: **Linda J. Hood , PhD (2012-2015)**
Vanderbilt University
Department of Hearing and Speech Sciences
1215 21st Ave S, MCE S Tower, Room 8310
Nashville, TN 37232-8242

HISTORIAN: **David J. Lim, MD**
House Ear Institute
2100 W. Third Street, Fifth Floor
Los Angeles, CA 90057

**COUNCIL MEMBERS
AT LARGE:** **Barbara Canlon, PhD (2012-2015)**
Karolinska Institute
Department of Physiology & Pharmacology
Von Eulers Vag 8
Stockholm 171 77
SWEDEN

Ruth Y. Litovsky, PhD (2011-2014)
University of Wisconsin
Waisman Center 521
1500 Highland Avenue
Madison, WI 53705

Dan H. Sanes, PhD (2010-2013)
New York University
Center for Neural Science
4 Washington Place
New York, NY 10003

**ARO Executive
Director:** **Haley Brust**
Talley Management Group
19 Mantua Road
Mt. Royal, NJ 08061
(856) 423-7222 ext: 103
(856) 423-0041
hbrust@talley.com
headquarters@aro.org

ABSTRACTS OF THE 36TH ANNUAL MIDWINTER MEETING OF THE



PRESIDENT'S MESSAGE 2013

Welcome back to Baltimore for the ARO MidWinter Meeting. The Baltimore Waterfront Marriott has been a comfortable venue for us in the past, and we're looking forward to another great meeting in 2013. This is a special year for the ARO -- the 40th anniversary of the association. Trivia fans will note that this is only the 36th MidWinter Meeting, but the meetings began some years after the ARO was founded. We'll have a few reminiscences from the podium after the Awards meeting on Monday, and we all can share our own tall tales in the reception afterwards.

The meeting begins Saturday morning with the Presidential Symposium on "Ears and Brains at the Cocktail Party". Those of you with jet-lag may or may not be disappointed that we're not serving drinks at that early hour. Instead, the distinguished speakers will address the challenges of recognizing speech and other important sounds in complex auditory scenes. The topics include normal and electrical hearing, psychophysical and physiological results from humans and animals, and multisensory integration. Saturday, following the afternoon sessions, we will have a chance to practice our cocktail-party hearing in the welcome reception, once again sponsored by Springer. Also, be sure to attend the ARO Business Meeting at 6 pm Sunday to keep in touch with the workings of this fine organization.

Larry Lustig and his Program Committee have put together an excellent program, which includes a few format changes. In response to many comments from past meeting attendees, symposia and workshops will be limited in duration to two hours, which will permit a larger number of such sessions. Also, there are two symposia organized by young investigators, which will feature the innovative work of post-docs and early-career faculty. Those of us who are challenged to be in multiple places at once will have it even worse this year -- at most times there will be three simultaneous podium sessions to choose from in addition to posters. We suffer from a mixed blessing of too much good science!

Be sure to attend the Presidential Lecture and Awards ceremony, which will honor the Award of Merit Winner, Karen P. Steel. Dr. Steel will tell us about "What's the Use of Genetics?". After her lecture, we will adjourn to the Honors Reception, which is upgraded this year to also honor the 40th anniversary of the ARO.

Ruth Litovsky has been spearheading efforts with the Students and Post-docs in ARO (spARO) to offer enhanced mentorship opportunities for students, post-docs, and early-stage faculty. There will be two sessions everyday, Saturday through Tuesday, at noon and 1 pm. Topics include "Building mentoring relationships", "Publish or perish and grant applications", and "Work-life balance", among others. Check the program for details on the specific topics and location of these events. Also, be sure to check the program for the spARO Town Hall meeting and social at Heavy Seas Alehouse.

We are grateful to the exhibitors for their contributions to the financial support of this meeting. They include Intelligent Hearing Systems, Interacoustics, NIDCD National Temporal Bone Registry, Plural Publishing, Springer, and Tucker-Davis Technologies. Be sure to check out their wares in the poster room. We thank the National Institute on Deafness and Other Communication Disorders for their generous funding support. Support for travel awards came from NIH, Advanced Bionics, American Academy of Audiology Foundation, American Academy of Otolaryngology - Head and Neck Surgery Foundation, Cochlear Americas, Cochlear Limited, Elsevier, Hearing Health Foundation, Knowles Hearing Center, Otonomy, and Pfizer. Finally, we thank Springer for sponsoring the Welcome Reception and MED-EL Corporation for sponsoring the Travel Awards Luncheon.

We thank the Talley Management Group for continuing to keep the ARO and the Mid-Winter Meeting running smoothly. After 11 years of outstanding service to the ARO in various capacities, Lisa Astorga has moved on, to be replaced by the capable services of Executive Director Haley Brust, Meeting Manager Kathy Baumer, and Meetings Coordinator Danielle Barsuglia.

Think about getting more involved in the ARO organization. There are many opportunities to serve on committees. The new committee members will be appointed shortly after the MidWinter Meeting by the new president, who will be Jay Rubinstein. If you are interested in serving on a committee, please indicate your interest on the post-meeting questionnaire. Also, consider speaking with or dropping an email to Jay or the chair of the committee of your choice.

Finally, don't miss a chance to let down your hair at the Hair Ball Tuesday evening with the popular band, Rollex. Here's a chance to see a side of your colleagues that you might have missed at the poster sessions.

I thank you for the opportunity to serve the ARO as President this past year, and I wish you all a very stimulating and enjoyable conference.

John C. Middlebrooks
ARO President, 2012-2013

CONFERENCE OBJECTIVES

At the conclusion of the MidWinter Meeting, participants should be better able to:

- Explain current concepts of the function of normal and diseased states of the ear and other head and neck structures
- Recognize current controversies in research questions in auditory neuroscience and otolaryngology
- Describe key research questions and promising areas of research in otolaryngology and auditory neuroscience

REGISTRATION

The 2013 MidWinter Meeting Registration Desk is located on the Third Floor Level and will be open and staffed during the following hours:

Friday, February 15	12:00 pm - 6:30 pm
Saturday, February 16	6:30 am – 6:00 pm
Sunday, February 17	6:30 am - 6:00 pm
Monday, February 18	7:00 am - 6:00 pm
Tuesday, February 19	7:00 am - 6:00 pm
Wednesday, February 20	7:00 am - 12:00 pm

ADMISSION

Conference name badges are required for admission to all activities related to the 36th Annual MidWinter Meeting, including the Exhibit Hall and social events.

PROGRAM AND ABSTRACT BOOKS

A limited supply of the abstract and program books will be available for purchase at the ARO MidWinter Meeting Registration Desk. Electronic copies of the books are also available online at www.aro.org.

MOBILE DEVICES

As a courtesy to the speakers and your fellow attendees, please switch your mobile device(s) to silent while attending the sessions.

RECORDING POLICY

ARO does not permit audio or photographic recording of any research data presented at the meeting.

ASSISTED LISTENING DEVICES

A limited amount of assisted listening devices are available at the ARO MidWinter Meeting Registration Desk, courtesy of Phonak.

A SPECIAL NOTE FOR THE DISABLED

ARO wishes to take steps that are required to ensure that no individual with a disability is excluded, denied services, segregated or otherwise treated differently than other individuals because of the absence of auxiliary aids and services. If you need any auxiliary aids or services identified in the Americans with Disabilities Act, or any assistance in registering for this course please contact ARO Meetings Department at meetings@aro.org; via telephone at 856-423-0041, option 2; or write to ARO Meetings Department, 19 Mantua Road, Mt. Royal, NJ 08061.

2013 ARO MIDWINTER MEETING

General Chair

John C. Middlebrooks, PhD (2012 - 2013)

Program Organizing Committee

Lawrence R. Lustig, MD, *Chair* (3/11-2/14)

Jianxin Bao, Ph.D (3/12-2/15)

Julie Arenberg Bierer, PhD (3/11-2/14)

Steve D.M. Brown, PhD (3/10-2/13)

Yale E. Cohen, Ph.D. (3/11-2/14)

Richard Hallworth, PhD (3/12-2/15)

Stefan Heller, PhD (3/10-2/13)

Keiko Hirose, MD (3/10-2/13)

Gay R. Holstein, PhD (3/11-2/14)

Lisa L. Hunter, PhD (3/11-2/14)

Ruth Y. Litovsky, PhD (3/11-2/14)

Douglas Oliver, PhD (3/10-2/13)

Alec N. Salt, PhD (3/10-2/13)

Su-Hua Sha, MD (3/12-2/15)

Council Liaison: Lawrence R. Lustig, MD

spARO Representative: Thomas Welch

Program Publications

Linda J. Hood, PhD (2012-2015)

Animal Research Committee

Rickie R. Davis, PhD, *Chair* (3/10-2/13)

Esperanza Bas Infante, PhD (3/12-2/15)

Robert Keith Duncan, PhD (3/11-2/14)

Sherri Marie Jones, PhD (3/11-2/14)

Amanda Lauer, PhD (3/12-2/15)

Edward Lobarinas, PhD (3/11-2/14)

Karen S. Pawlowski, PhD (3/11-2/14)

Suhrud M. Rajguru, PhD (3/10-2/13)

Claus-Peter Richter, MD, PhD (3/12-2/15)

Saima Riazuddin, PhD (3/10-2/13)

Soroush G. Sadeghi (3/11-2/14)

Council Liaison: Dan H. Sanes, PhD

spARO Representative: Ann Hickox

Award of Merit Committee

M. Charles Liberman, PhD, *Chair* (3/10-2/13)

Karen B. Avraham, PhD (3/11-2/14)

Jeffrey T. Corwin, PhD (3/11-2/14)

Charley Della Santina, MD PhD (3/12-2/15)

Judy R. Dubno, PhD (3/10-2/13)

Peter G. Gillespie, PhD (3/10-2/13)

Brian C. J. Moore, PhD (3/12-2/15)

Dan H. Sanes, PhD (3/11-2/14)

Robert V. Shannon, PhD (3/10-2/13)

Eric D. Young, PhD (3/12-2/15)

Council Liaison: David J. Lim, MD

Diversity & Minority Affairs Committee

Howard W. Francis, MD, *Chair* (3/10-2/13)

Gail S. Donaldson, PhD (3/12-2/15)

Avril Genene Holt, PhD (3/11-2/14)

Frank Lin, M.D. PhD (3/11-2/14)

Raju Metherate, PhD (3/10-2/13)

Neeliyath A. Ramakrishnan, PhD (3/10-2/13)

Khaleel Razak, PhD (3/12-2/15)

Xiaorui Shi, MD, PhD (3/10-2/13)

Dwayne D. Simmons, PhD (3/11-2/14)

Peter S. Steyger, PhD (3/11-2/14)

Council Liaison: Dan H. Sanes, PhD

spARO Representative: Yoojin Chung, PhD

External Relations Committee

Carey D. Balaban, PhD, *Chair* (2012-2014)

Anne Luebke, PhD, *Chair* (2009-2014)

Paul D. Allen, PhD (3/10-2/13)

Corne Kros, PhD (3/12-2/15)

Hainan Lang, MD, PhD (3/12-2/15)

Charles J. Limb, MD (3/10-2/13)

Anna Lysakowski, PhD (3/10-2/13)

George Pollak, PhD (3/12-2/15)

Pamela Roehm, MD, PhD (3/12-2/15)

Mario A. Svirsky, PhD (3/10-2/13)

Council Liaison: Ruth Y. Litovsky, PhD

spARO Representative: Adrian KC Lee

Finance & Investment Committee

Dennis R. Trune, PhD, MBA, *Chair* (2010-2014)

Steven Wan Cheung, MD (3/10-2/14)

Sharon G. Kujawa, PhD (3/12-2/15)

Jean Luc Puel, PhD (3/10-2/13)

Robert Raphael, PhD (3/12-2/15)

Ex-officio: John P. Carey, MD

International Committee

Robert K. Shepherd, PhD, (Australia) *Chair* (2012-2014)

Karen Banai, PhD, (Israel) (3/12-2/15)

Deniz Baskent, PhD, (Netherlands) (3/10-2/13)

Byung Yoon Choi, MD, (Korea) (3/12-2/15)

James Fallon, PhD, (Australia) (3/10-2/13)

M'hamed Grati, Eng., Ph.D., (USA) (3/11-2/14)

Benedikt Grothe, PhD, (Germany) (3/12-2/15)

Bo Hong, Ph.D., (China) (3/12-2/15)

W. Wiktor Jedrzejczak, (Poland) (3/10-2/13)

Goran Laurell, MD, (Sweden) (3/10-2/13)

Takayuki Nakagawa, MD, PhD, (Japan) (3/11-2/14)

Azel Zine, PhD, (France) (3/10-2/13)

Council Liaison: Robert K. Shepherd, PhD

spARO Representative: Simon Jones, PhD

JARO Editorial Board

Paul B. Manis, PhD, *Editor-in-Chief* (2011-2016)
Robert P. Carlyon, PhD (2010-2013)
Laurel H. Carney, PhD (2010-2013)
Christian Chabbert, PhD (2012-2015)
Nigel P. Cooper, PhD (2010-2013)
Donna Fekete, PhD (2012-2015)
Andrew Griffith, MD, PhD (2011-2014)
Joseph W. Hall, PhD (2012-2013)
Manuel Malmierca (2012-2015)
Jennifer Melcher (2012-2013)
Cynthia F. Moss (2009-2013)
Shawn Newlands, MD, PhD (2012-2015)
Dominik Oliver, PhD (2012-2015)
Sunil Puria, PhD (2010-2013)
Anthony J. Ricci, PhD (2010-2013)
Christoph Schreiner, MD, PhD (2012-2015)
Susan E. Shore, PhD (2012-2015)
Laurence O. Trussell, PhD (2009-2013)

Long Range Planning Committee

Karina S. Cramer, PhD, *Chair* (2012-2014)
Steven H. Green, PhD (3/11-2/14)
Troy Hackett, PhD (3/12-2/15)
Andrej Kral, MD, PhD (3/10-2/13)
Lina A. Reiss, PhD (3/10-2/13)
Edwin W. Rubel, PhD (3/11-2/14)
George Spirou, PhD (3/12-2/15)
Konstantina M. Stankovic, MD, PhD (3/11-2/14)
Doris Wu, PhD (3/12-2/15)
NIDCD Rep: Amy Donahue, PhD
Council Liaison: Karina S. Cramer, PhD
President-Elect: Jay T. Rubinstein, MD, PhD
International Committee Chair: Robert K. Shepherd, PhD
spARO Representative: Wei Zhao

Membership Committee

Colleen Garbe Le Prell, PhD, *Chair* (2012-2014)
Eric Bielefeld, PhD (3/12-2/15)
Glenis R. Long, PhD (3/12-2/15)
Tianying Ren, MD (3/12-2/15)
Chris J. Sumner (3/12-2/15)
spARO Representative: Jazz Bailey, PhD

Nominating Committee

Debara L. Tucci, MD, *Chair* (3/12-2/13)
Judy R. Dubno, PhD (3/12-2/13)
Anil K. Lalwani, MD (3/12-2/13)
Peter G. Gillespie, PhD (3/12-2/13)
Jennifer Stone, PhD (3/12-2/13)

Publications Committee

Anil K. Lalwani, MD, *Chair* (2011-2013)
Thomas B. Friedman, PhD (3/11-2/14)
Paul A. Fuchs, PhD (3/10-2/13)
Philip X. Joris, MD, PhD (3/10-2/13)
Charles J. Limb, MD (3/11-2/14)
Erick Xi Lin, PhD (3/12-2/15)
Xue Z. Liu, MD, PhD (3/12-2/15)
Paul B. Manis, PhD (3/10-2/13)
John S. Oghalai, MD (3/12-2/15)
Elizabeth S. Olson, PhD (3/10-2/13)
Alan R. Palmer, PhD (3/10-2/13)
Susan E. Shore, PhD (3/11-2/14)
Daniel Tollin, PhD (3/12-2/15)
Ex-officio, JARO Editor: Paul B. Manis, PhD
Ex-officio, Springer Representative: Ann Avouris
Secretary/Treasurer: John P. Carey, MD
Council Liaison: Linda J. Hood, PhD
spARO Representative: Jeffery Lichtenhan

Travel Awards

Marlan R. Hansen, MD, *Chair* (2008-2014)
Jin Woong Bok, PhD (3/12-2/15)
Angelika Doetzlhofer, PhD (3/12-2/15)
Dianne Durham, PhD (3/11-2/14)
Robert Froemke, PhD (3/12-2/15)
Samuel Gubbels, MD (3/12-2/15)
Ronna P. Hertzano, MD, PhD (3/10-2/13)
Michael Hildebrand, PhD (3/12-2/15)
Avril Genene Holt, PhD (3/11-2/14)
Yunxia Wang Lundberg, PhD (3/11-2/14)
Yehoash Raphael, PhD (3/11-2/14)
Alexander A. Spector, PhD (3/10-2/13)
Li Xu, MD, PhD (3/12-2/15)
Ex-officio, NIDCD Dir: James F. Battey, MD, PhD
Council Liaison: Linda J. Hood, PhD (3/12-2/13)
spARO Representative: Judith S. Kempfle, MD

Executive Offices

Association for Research in Otolaryngology

19 Mantua Road
Mt. Royal, New Jersey 08061
Phone: (856) 423-0041
Fax: (856) 423-3420
E-Mail: headquarters@aro.org
Meetings E-Mail: meetings@aro.org



**Karen P. Steel, PhD
2013 Award of Merit Recipient**

Award Lecture: What's the Use of Genetics?

Karen P. Steel
2013 Recipient of the ARO Award of Merit

The Association for Research in Otolaryngology has chosen to honor Karen P. Steel with the 2013 Award of Merit. For everyone at ARO, this is such a clear choice. Karen's work has crossed all boundaries and sub-disciplines at ARO. Her warm and wonderful personality, genuine smile and willingness to give advice at any time, has made Karen one of the most well-recognized scientists in our field and at ARO. Karen has been at the forefront of mouse genetics in hearing from the early days of the field, and continues to lead the field with her discoveries. For all these reasons, the society and its members have chosen to honor and thank Karen Steel for her invaluable contributions.

Karen began her scientific education at the University of Leeds, UK, where she studied genetics and zoology, and graduated in 1974. She then decided to focus on mouse genetics for her Ph.D. studies and obtained her Ph.D. in Genetics from the Department of Human Genetics and Biometry, University College London, in 1978.

To link her structural and developmental findings with function, for her first post-doctoral training, Karen moved to the new MRC Institute of Hearing Research in Nottingham to learn auditory electrophysiology, and she established the mouse genetics facilities and deafness research program there. An early interest was the structure and function of the tectorial membrane, an extracellular matrix lying over sensory hair cells in the cochlea. She used novel approaches to investigate its electrical and chemical properties, and discovered that it maintained its own electrochemical environment. She pursued a second postdoctoral position at the Institut für Zoologie in München, Germany, after which time she returned to the UK in 1983 to take on a research position at the MRC Institute of Hearing Research in Nottingham. She was made an honorary Professor of Genetics in 1995. In 2003, Karen moved a bit south to the Sanger Institute. While continuing her research in deafness, a major effort there was setting up the Mouse Genetics Project, a large-scale program that created over 700 new mouse mutants using the EUCOMM/KOMP targeted embryonic stem cell resource. Using an electrophysiological approach, Karen's group discovered 12 new genes underlying deafness among the first 500 lines studied, confirming the value of this approach in gene discovery. Karen is now a Professor of Sensory Function at the Wolfson Centre for Age-Related Diseases at King's College London.

Since her early postdoctoral work, Karen has focused on identifying genes underlying deafness and understanding the molecular and physiological basis for the dysfunction. She has published phenotypic descriptions of over 80 different mouse mutants representing 36 loci, and together with collaborators, her group has identified 37 mutations in 21 different genes by positional cloning. For several of these, Karen has collaborated with human geneticists to identify mutations in the same genes in humans with deafness. Despite the common assumption that hearing loss is due to sensory hair cell degeneration, her analysis of this large panel of mutants showed that degeneration is an epiphenomenon, not a primary cause of deafness. Furthermore, there is a very wide range of primary defects in the ear that can cause deafness.

Karen has made so many seminal discoveries in the field of hereditary deafness; only a few will be listed here. Karen was the first to demonstrate that lack of melanocytes in the stria vascularis of mice with white spotting pigmentation defects caused abnormal stria function leading to deafness. In 1995, in collaboration with Steve Brown, Karen identified the first gene involved in deafness, *Myo7a*, mutated in the shaker1 mouse mutant as well as in people with Usher syndrome type 1B. Since these early reports, her group has analyzed the pathology of these mice in detail using ultrastructural and electrophysiological approaches, and discovered that myosin VIIa appears to anchor the cell membrane to the actin core of stereocilia on top of hair cells, and that without functional myosin VIIa protein, the membrane-bound transduction channel complex is loosely coupled to the core and readily slips, closing the channel. Karen's team also found the first indications of retinal anomalies in both *Myo7a* and *Cdh23* mouse mutants, giving clues to the causes of long-term retinal degeneration in humans with similar mutations. Over the years, Karen has worked on the following mouse mutants: deafness, jerker, quivering, viable dominant spotting, shaker1, splotch, Light, whirler, Snell's waltzer, bronx waltzer, Varitint-waddler, Tailchaser, waltzer, slalom, Headturner, Headbanger, wheels, Beethoven, submarine, light coat and circling, Doarad, flouncer, Hush Puppy, Belly Spot and Deafness, dearisch, diminuendo, and more. Most of these names are synonymous with "Karen Steel."

In 1997, Karen coordinated (which began as a conversation with Rudi Balling over a beer) a successful bid to the European Commission (EC) for funds to add a screen for deafness and balance defects to two large-scale ENU mutagenesis programs that were just beginning in Munich and Harwell, with other partners in Tel Aviv and Paris. She made a tremendous impact in another EC consortium, EuroHear. This was indeed an exciting time for ENU and these mice continue to contribute an enormous amount of information about auditory and vestibular mechanisms. Karen's group devised the screen and characterized the new mutants, and went on to map and identify new mutations. They identified 24 mutations in 13 different genes, 9 of which were not previously known to be involved in deafness, including the first microRNA involved in a Mendelian disorder.

Karen's primary interest over the years has been the genetics of deafness, using mouse mutants to gain access to the molecules involved in normal development and function. More broadly, she has remained interested in understanding the process of disease from the molecular defect to the function of the whole organism, and she has studied a range of other defects in addition to deafness, such as balance disorders, retinal dysfunction and pigmentation anomalies. Karen adopted a phenotype-driven approach, starting with mouse mutants with a hearing defect, defining the phenotype and identifying the mutant gene by positional cloning.

Today, Karen's current research is moving towards understanding the reasons for the decline in hearing with age, as this is a major problem in the human population. She is looking at whole exome resequencing data from people with age-related hearing loss (ARHL), as well as investigating mouse mutants with progressive hearing loss, to look for common mechanisms.

During her career, Karen Steel has taken an active public role and has served on many national and international bodies, including the *Hearing Research* editorial board, *Mammalian Genome* editorial board, Scientific Advisory Board of the Mouse Genome Database at the Jackson Laboratory, Organizing Committee of the Molecular Biology of Hearing and Deafness Conference, International Mouse Genome Nomenclature Committee, ARO Council, and was President of the International Mammalian Genome Society. She has also been an expert witness to the House of Lords Select Committee on Ageing, scientific advisor to the charities Deafness Research UK and SENSE, deputy Chairman of the MRC Neurosciences Board, and a member of the Wellcome Trust Neurosciences and Mental Health Funding Committee.

Karen has been recognized for her tremendous achievements. She was awarded the Kresge-Mirmelstein Prize for Excellence in Hearing Research in New Orleans in 1998, was elected as a Fellow of the Academy of Medical Sciences in London in 2004 and a Fellow of the Royal Society in 2009. In 2012, Karen was awarded the €1 million Brain Prize from the Grete Lundbeck European Brain Research Foundation with Professor Christine Petit from the College de France "for their unique, world-leading contributions to our understanding of the genetic regulation of the development and functioning of the ear, and for elucidating the causes of many of the hundreds of inherited forms of deafness."

Karen's contribution to the field has resulted in 128 manuscripts and 80 invited commentaries, reviews, books, book chapters and databases. A landmark paper was published in 1980 in *Nature*, describing "The nature of inherited deafness in deafness mice" (the gene was subsequently found in 2002). For many years, she was editor of the *Hereditary Deafness Newsletter*, which kept everyone in the field updated on the latest findings in the field, long before the internet. There is no question that everyone in the field looks first to what Karen is doing, what she has recently published, and what she will talk about in her next lecture. Unpublished data is the norm and she has always shared a wealth of information with anyone who asks. Her incredibly generous nature to collaborate or more often than not, provide reagents (most notably, mice), is unparalleled.

Most of all, Karen has been a mentor to countless students and post-doctoral fellows. She has been an inspiration to all, and especially women, scientists throughout Europe and the US, and a model for dedication and perseverance. Karen is truly an outstanding recipient of the 2013 ARO Award of Merit.

Karen B. Avraham

Past Presidents

1973-74 David L. Hilding, MD
1974-75 Jack Vernon, PhD
1975-76 Robert A. Butler, PhD
1976-77 David J. Lim, MD
1977-78 Vicente Honrubia, MD
1978-80 F. Owen Black, MD
1980-81 Barbara Bohne, PhD
1981-82 Robert H. Mathog, MD
1982-83 Josef M. Miller, PhD
1983-84 Maxwell Abramson, MD
1984-85 William C. Stebbins, PhD
1985-86 Robert J. Ruben, MD
1986-87 Donald W. Nielsen, PhD
1987-88 George A. Gates, MD
1988-89 William A. Yost, PhD
1989-90 Joseph B. Nadol, Jr., MD
1990-91 Ilsa R. Schwartz, PhD
1991-92 Jeffrey P. Harris, MD, PhD
1992-93 Peter Dallos, PhD
1993-94 Robert A. Dobie, MD
1994-95 Allen F. Ryan, PhD
1995-96 Bruce J. Gantz, MD
1996-97 M. Charles Liberman, PhD
1997-98 Leonard P. Rybak, MD, PhD
1998-99 Edwin W. Rubel, PhD
1999-00 Richard A. Chole, MD, PhD
2000-01 Judy R. Dubno, PhD
2001-02 Richard T. Miyamoto, MD
2002-03 Donata Oertel, PhD
2003-04 Edwin M. Monsell, MD, PhD
2004-05 William E. Brownell, PhD
2005-06 Lloyd B. Minor, MD
2006-07 Robert V. Shannon, PhD
2007-08 P. Ashley Wackym, MD
2008-09 Paul A. Fuchs, PhD
2009-10 Steven Rauch, MD
2011-12 Karen B. Avraham, PhD
2012-13 Debara L. Tucci, MD

Award of Merit Recipients

1978 Harold Schuknecht, MD
1979 Merle Lawrence, PhD
1980 Juergen Tonndorf, MD
1981 Catherine Smith, PhD
1982 Hallowell Davis, MD
1983 Ernest Glen Wever, PhD
1984 Teruzo Konishi, MD
1985 Joseph Hawkins, PhD
1986 Raphel Lorente de Nó, MD
1987 Jerzy E. Rose, MD
1988 Josef Zwislocki, PhD
1989 Áke Flóck, PhD
1990 Robert Kimura, PhD
1991 William D. Neff, PhD
1992 Jan Wersäll, PhD
1993 David Lim, MD
1994 Peter Dallos, PhD
1995 Kirsten Osen, MD
1996 Ruediger Thalmann, MD & Isolde Thalmann, PhD
1997 Jay Goldberg, PhD
1998 Robert Galambos, MD, PhD
1999 Murray B. Sachs, PhD
2000 David M. Green, PhD
2001 William S. Rhode, PhD
2002 A. James Hudspeth, MD, PhD
2003 David T. Kemp, PhD
2004 Donata Oertel, PhD
2005 Edwin W. Rubel, PhD
2006 Robert Fettiplace, PhD
2007 Eric D. Young, PhD
2008 Brian C. J. Moore, PhD
2009 M. Charles Liberman, PhD
2010 Ian Russell, PhD
2011 Robert V. Shannon, PhD
2012 David P. Corey, PhD
2013 Karen P. Steel, PhD

2013 TRAVEL AWARD RECIPIENTS

Yaneri Aguilar-Ayala, MSc
Heike Althen, PhD
Eric Applebaum, BS
Charles Askew, BA
Gregory Ball, PhD
Alexander Billig, MSc
Kris Boyen, MSc
Katarina Brunette, PhD
Jin Chen, PhD
Soyoun Cho, PhD
Cat Connelly, BS
Mathieu Forgues, BA
Brian Gartrell, MD
Sabine Grimm, PhD
Abderrahmane Hedjoudje, MD
Emma Holmes, PhD
Vanessa Irsik, BA
Salima Jiwani, MSc
Olympia Kremmyda, MD, PhD
Jianyi Lee, PhD
Robert Mackinnon, BA
Moline McKay, BS
Nina Mistry, MBChB, BSc
Scott Montgomery, BS
Karina Needham, PhD
Se-Kyung Oh, MS
Melissa Papesh, AuD
Braulio Peguero, BA
Carol Pham, PhD
Sripriya Ramamoorthy, PhD
Dong-Dong Ren, PhD, MD
Elodie Richard, PhD
Dorea Ruggles, PhD
Seiji Shibata, MD
Erika Skoe, PhD
Jae-Jin Song, MD, PhD
Daniel Stolzberg, PhD
Sundeep Teki, MSc
Alexander Thompson, BSc
Emily Tignor, MD
Corstiaen Versteegh, MSc
Tian Wang, MD, PhD
Melissa Watts, MD
Michael Wiebel, MD
Tanika Williamson, BS
Qian Zhang, MD, PhD

Michelle Allen-Sharples, BS, MD, PhD
Carly Anderson, BSc
Justin Aronoff, PhD
Erin Bailey, BS
Matthew Barton, MD
Vikrant Borse, MSc
Emilie Brun, PhD
Joseph Burns, PhD
Ananthakrishna Chintanpalli, PhD
Cynthia Chow, BS
Joseph Crew, PhD
Marie Gadziola, BSc
Carolina Glogowski, BS
Heiner Hartwich, PhD
Lara Li Hesse, MD
Chengcheng Huang, BS
Ayaka Iwata, MS
Julia Korchagina, MSc
Eric Larson, PhD
James Lupo, MD
Karen Martin, MSc
Diana Mendus, PhD
Doreen Moeckel, PhD
Gowri Nayak, PhD
Lisa Nolan, PhD
Cristen Olds, BS
Alexandra Parbery-Clark, BSc
Richard Penninger, PhD
Lana Pollock, BS
Caitlyn Reed, BS
Nicole Renaud, PhD
Astin Marie Ross, PhD.
Tim Schoof, Mrs
Shaked Shivatzki, BSc
Michael Slama, PhD
Kevin Stebbings, BSc
Karima Susi, PhD
Andrew Thomas, BA
Jennifer Thorton, PhD
Joshua Tokita, MD
Kyle Walsh, PhD
Ningyuan Wang, PhD
Angela Wenzel, MD
Conor Wild, PhD
Yazhi Xing, MD
Ken Zhao, BS

ISSN-0742-3152

The *Abstracts of the Association for Research in Otolaryngology* is published annually and consists of abstracts presented at the Annual MidWinter Research Meeting. A limited number of copies of this book and previous books of abstracts (1978-2011) are available. Please address your order or inquiry to Association for Research in Otolaryngology Headquarters by calling (856) 423-0041 or emailing headquarters@aro.org.

This book was prepared from abstracts that were entered electronically by the authors. Authors submitted abstracts over the World Wide Web using Mira Digital Publishing's PaperCutter™ Online Abstract Management System. Any mistakes in spelling and grammar in the abstracts are the responsibility of the authors. The Program Committee performed the difficult task of reviewing and organizing the abstracts into sessions. The Program Committee Chair, Dr. Lawrence R. Lustig and the President, Dr. John C. Middlebrooks, constructed the final program. Mira electronically scheduled the abstracts and prepared Adobe Acrobat pdf files of the Program and Abstract Books. These abstracts and previous years' abstracts are available at www.aro.org.

Citation of these abstracts in publications should be as follows: **Authors, year, title, Assoc. Res. Otolaryngol. Abs.: page number.**

For Example:

Joni Doherty, 2013, Identification of Target Proteins Involved in Cochlear Otosclerosis, Assoc. Res. Otolaryngol. Abs.: **1125.**

Table of Contents

Abstract Number

Presidential Symposium

A: Ears and Brains at the Cocktail Party 1-6

Symposium

B: Biologically Inspired Mechanisms of Parsing the Acoustic Scene..... 7-13

Podium

C: Genetics 14-28

D: Auditory Protheses and Drug Delivery 29-43

NIDCD Workshops

EA: Training/Career Development Workshop 44

Early Stage/New Investigator Workshop 44

Poster

E1 Inner Ear: Damage and Protection - Noise Trauma 45-60

E2 Auditory Pathways: Brainstem - Aging 61-64

E3 Auditory Pathways: Brainstem - Cellular Physiology 65-77

E4 Auditory Pathways: Cortex and Thalamus - Neural Mechanisms and Coding 78-104

E5 Development IV 105-119

E6 Inner Ear: Anatomy and Physiology I 120-134

E7 Inner Ear: Damage and Protection - Animal Models of Inner Ear Damage 135-142

E8 Inner Ear: Hair Cells - Molecules and Mass Spec 143-152

E9 Inner Ear: Hair Cells - Outer Hair Cells and Prestin 153-158

E10 Inner Ear: Membranes and Fluids 159-163

E11 Otoacoustic Emissions I 164-171

E12 Physiological Psychophysics 172-183

E13 Regeneration III 184-193

E14 Psychophysics IV 194-210

E15 Speech Perception: Acoustic 211-219

E16 Tinnitus: Animal Behavior Models 220-226

E17 Tinnitus: Clinical 227-237

E18 Vestibular Basic Research I 238-255

Workshop

F: Assessing Tinnitus in Animals: Progress and Pitfalls 256-260

Symposium

G: Optogenetics: Studying Hearing Under a New Light 261-268

Podium

H: Development I 269-276

Symposium

I: News about Tinnitus 277-281

J: Optical Approaches for Studying Auditory Processing 282-287

Podium

K: Development II 288-296

Symposium

L: Insulin-like Growth Factor Signaling in Development and Protection... 297-302

Podium

M: Inner Ear Damage and Prevention I 303-309

N: Aging 310-317

O: Inner Ear Damage and Prevention II 318-323

Poster

P1	Inner Ear: Genetic Disorders	324-337
P2	Auditory Pathways: Brainstem - Auditory Nerve.....	338-342
P3	Auditory Pathways: Brainstem - Development	343-351
P4	Auditory Pathways: Brainstem - Sound Localization	352-364
P5	Auditory Pathways: Cortex and Thalamus - Neural Correlates of Perception.....	365-383
P6	Auditory Pathways: Cortex and Thalamus - Plasticity and Learning	384-386
P7	Auditory Prosthesis: Auditory and Central Measures	387-402
P8	Auditory Prosthesis: Implantable Hearing Aids, Middle Ear Stim, and Conductive HL	403-408
P9	Clinical Audiology	409-422
P10	Clinical Otolaryngology.....	423-436
P11	External or Middle Ear Physiology.....	437-446
P12	Middle Ear Pathology and Treatment.....	447-457
P13	Inner Ear: Hair Cells - Synaptic	458-464
P14	Inner Ear: Hair Cells - Transduction	465-473
P15	Psychophysics III.....	474-494
P16	Psychophysics and Speech.....	495-503
P17	Sound Localization: Dynamics, Spectral Cues, and Heads	504-522
P18	Speech Perception: Attention	523-527
P19	Tinnitus: Central Nervous System.....	528-535
P20	Vestibular Basic Research II	536-552

Symposium

Q:	Prestin at 13 - Progress, Problems, and Prospects.....	553-558
R:	Translating Science into Rehabilitation for People with Hearing Loss	559-565

Podium

S:	Regeneration I.....	566-573
----	---------------------	---------

Symposium

T:	Intercellular Signaling During Sensory System Development	574-579
----	---	---------

Workshop

U:	Hyperacusis: What's the Impact?	580-584
----	---------------------------------------	---------

Podium

V:	Regeneration II and External Middle Ear	585-591
----	---	---------

Get Your Research Funded

W:	592
----	-------	-----

Symposium

X:	Noise-induced Hearing Loss: Scientific Advances	593-598
----	---	---------

Podium

Y:	Psychophysics I.....	599-604
Z:	Hair Cells - Transduction I.....	605-610
AA:	Psychophysics II.....	611-614
BB:	Hair Cells - Transduction II	615-620

Poster

CC1	Aging	621-638
CC2	Auditory Pathways: Brainstem - Physiology	639-645
CC3	Auditory Pathways: Brainstem - Cellular Anatomy and Circuitry.....	646-650
CC4	Auditory Pathways: Cortex and Thalamus - Cochlear Implants and Hearing Dysfunction.....	651-661
CC5	Auditory Pathways: Midbrain - Auditory Physiology	662-675
CC6	Auditory Pathways: Midbrain - Cellular Anatomy and Circuitry	676-682
CC7	Auditory Prosthesis: Electric and Acoustic Hearing Preservation	683-692
CC8	Auditory Prosthesis: Optical Stimulation.....	693-698
CC9	Cochlear Drug Delivery	699-709
CC10	Genetics	710-735

CC11	Inner Ear: Anatomy and Physiology II	736-744
CC12	Inner Ear: Damage and Protection - Inflammatory Response and Prevention	745-761
CC13	Inner Ear: Mechanics and Modeling I	762-782
CC14	Regeneration III	783-792
CC15	Speech: Perception - Auditory Prostheses	793-800
CC16	Clinical Vestibular	801-820
CC17	Inner Ear: Anatomy and Physiology III	821-840
Symposium		
DD:	Supporting Cells: Lessons from Studies of Glia	841-845
Podium		
EE:	Localization Mechanisms and Mapping	846-853
Symposium		
FF:	The Non-Lemniscal Auditory Thalamus	854-859
GG:	Cognitive Factors Influencing Speech Understanding	860-864
HH:	Manganese Enhanced MRI (MEMRI): Advantages for Functional Imaging	865-872
Young Investigator Symposium		
II:	Short and Long-term Neural Plasticity in the Auditory Brainstem	873-880
Podium		
JJ:	Hair Cells - Anatomy & Physiology I	881-885
Young Investigator Symposium		
KK:	The Neurophysiology of Human Auditory Processing	886-894
Podium		
LL:	Hair Cells - Anatomy and Physiology II	895-899
Poster		
MM1	Auditory Nerve	900-918
MM2	Auditory Pathway: Brainstem - Evoked Potentials	919-934
MM3	Auditory Pathways: Brainstem - Tinnitus	935-938
MM4	Auditory Pathways: Cortex and Thalamus – Multisensory	939-959
MM5	Auditory Pathways: Cortex and Thalamus - Speech, Language, and Vocalizations	960-965
MM6	Auditory Pathways: Midbrain - Sound Localization	966-972
MM7	Auditory Prosthesis: Bilateral	973-980
MM8	Auditory Prosthesis: Current Steering and Shaping	981-986
MM9	Auditory Prosthesis: Music and Cognitive Effects	987-991
MM10	Auditory Prosthesis: Optimizing Methods	992-1002
MM11	Development III	1003-1017
MM12	Inner Ear: Damage and Protection - Auditory Nerve	1018-1027
MM13	Inner Ear: Damage and Protection - Drug Ototoxicity	1028-1047
MM14	Inner Ear: Mechanics and Modeling II	1048-1063
MM15	Otoacoustic Emissions II	1064-1074
MM16	Psychophysics IV	1075-1084
MM17	Sound Localization: Binaural Mechanisms	1085-1097
MM18	Tinnitus: Midbrain	1098-1105
Podium		
NN:	Auditory Nerve	1106-1115
OO:	Genetic Hearing Loss	1116-1125

1 Choosing from the Conversation Smorgasbord of a Cocktail Party

Barbara Shinn-Cunningham¹

¹*Boston University*

At a rollicking party, conversations ebb and flow all around. Although the noise level may make it difficult to hear some exchanges, there are often multiple discussions that could be understood. This is very convenient if you find yourself in dull conversation about, say, motor homes, while the group behind you is sharing some racy gossip about one of your colleagues. In such situations, you can satisfy social expectations by monitoring what is happening in front of you, even though you are really processing the chatter from behind. This real-life example illustrates the various factors that can affect the ability to communicate in social settings. Early psychoacoustic work focused on understanding how a competing masker sound interferes with the early sensory representation of information about an important message, and how much of that message must be represented cleanly for it to be understood. While such details determine whether or not you understand a message when there is only one source demanding your attention, such as in a phone conversation, that is not how you operate when you navigate a busy street or argue some controversial issue with impassioned colleagues at a faculty meeting. How your brain focuses on different conversations depending on your interests governs what knowledge you take away from a cocktail party as surely as the does the fidelity of the sensory representation.

2 A View of the Precedence Effect Through the Owl's Ears

Terry Takahashi¹, Brian Nelson¹, Caitlin Baxter²

¹*University of Oregon*, ²*University of Maryland*

In nature, sounds of interest are followed by reflections from nearby surfaces. Yet, for short delays, the sound arriving directly from the source dominates perception. This phenomenon, "localization dominance" (LD), is part of the precedence effect. To better understand the neural mechanisms of the precedence effect, we conducted neurophysiological and psychoacoustical experiments in the barn owl (*Tyto alba*), with a direct sound (ds) that overlaps with a simulated echo.

We found that LD requires deep amplitude modulations (AMs) when the onset and offset delays are removed. Without these AMs, the owl localized the leading and lagging sounds with equal frequency, in spite of the fact that the lagging carrier was a delayed copy of the lead. To explain these observations, we developed the "envelope model". When there are two sound sources with overlapping amplitude spectra, the frequency-specific binaural cues are biased toward values corresponding to the momentarily-louder source. Neurons in the owl's auditory space map discharge if, as the binaural cues begin to approximate those of its spatial receptive field, the amplitude is rising. The envelope model computes the relative incidences of this conjunction to predict the number of spikes evoked by the lead and lag sources. The model suggests that LD occurs because a peak in the

lead obscures the rising edge of the corresponding peak in the lag.

Reflected sounds and independent, competing sounds are on a continuum of similarity to the ds. When the lead and lag sounds have different envelopes (but identical, but delayed carriers) there are no corresponding peaks. In such case, the strengths of the lead and lag sounds' neural representations, which can be computed by the envelope model, are determined by the arbitrary shapes of the envelopes. Results show that the owl localizes the sound predicted to have the stronger representation.

Our results suggest that 1.) The temporal relationship between the lead/lag pair is determined not from the carrier, but from the ongoing envelope disparities. 2.) LD is due to the superposition of the waveforms in the ears and the selectivity of neurons for upward AMs, suggesting echoes need not be actively suppressed. 3.) Lead/lag pairs and a pair of independent sounds are represented on the space map according to the same principles.

3 Neural Bases of Concurrent Sound Segregation in Primate Auditory Cortex

Yonatan Fishman¹, Christophe Micheyl², Mitchell Steinschneider¹

¹*Albert Einstein College of Medicine*, ²*University of Minnesota*

The ability to perceptually separate concurrent sounds (e.g., voices) is critical for successful hearing in complex acoustic environments (e.g., a cocktail party or noisy cafeteria). Neural mechanisms underlying concurrent-sound segregation are poorly understood and are thought to involve central auditory processes. Here, we present results of electrophysiological studies in primary auditory cortex (A1) of awake monkeys that aim to shed light on these neural mechanisms. We examine neural correlates of two perceptual phenomena reflecting key principles of concurrent sound segregation: (1) "pop-out" of mistuned components in harmonic complex sounds, exemplifying segregation based on inharmonicity, and (2) segregation of concurrent harmonic complex sounds (e.g., vowels) based on a difference in their fundamental frequency (F0).

In relation to (1), we find that responses to harmonic complex tones (HCTs) containing a mistuned component are enhanced in neural populations that are tuned to the frequency of the mistuned component, relative to responses evoked by 'in-tune' HCTs. This response enhancement parallels the increased perceptual salience of mistuned harmonics reported in human psychoacoustic studies. Mistuned sounds also evoke temporal discharges which are phase-locked to lower frequency "beats" in the stimuli. Thus, a local increase in firing rate or a difference in temporal response pattern in A1 may contribute to concurrent sound segregation based on inharmonicity.

In relation to (2), using a stimulus design employed in auditory-nerve studies (Larsen et al., 2008), we found that neural responses in A1 convey sufficient spectral ('rate-place') and temporal ('phase-locking') information reflecting the harmonic structure and F0s of two simultaneous and spectrally overlapping HCTs to enable their perceptual segregation. Lower harmonics (1-6) of the

HCTs were better resolved in neural 'rate-place' representations than higher harmonics (7-12), consistent with psychoacoustic findings in humans. Furthermore, introducing an onset asynchrony between the HCTs enhanced the neural representation of their harmonics, consistent with the improved ability to perceptually segregate asynchronous sounds. F0s below 350 Hz were also represented in temporal discharges phase-locked to the periodicities of the HCTs. Findings suggest that A1 contains sufficient spectral and temporal information for extracting the pitch of HCTs via harmonic templates and periodicity detectors, and for segregating concurrent HCTs based on a difference in F0. Improved understanding of central mechanisms contributing to concurrent sound segregation may facilitate the development of more effective approaches toward alleviating deficits in speech and music perception in hearing-impaired listeners.

4 Cortical Encoding of Auditory Objects at the Cocktail Party

Jonathan Z. Simon¹

¹*University of Maryland*

A visual scene is perceived in terms of its constituent visual objects. Similar ideas have been proposed for the analogous case of auditory scene analysis, though their hypothesized neural underpinnings have not yet been established. Here, we investigate how auditory objects are individually represented in auditory cortex, using magnetoencephalography (MEG) to record the neural responses of human listeners. Subjects selectively listen to one of two competing streams, in a variety of auditory scenes. The auditory streams may overlap spatially, spectrally, or both.

First we demonstrate that attentional gain does not act globally on the entire auditory scene, but rather acts differentially on the separate auditory streams. This stream-based attentional gain is then used as a tool to individually analyze the different neural representations of the competing auditory streams.

In the acoustically richest example, subjects selectively listen to one of two competing speakers mixed in a single channel. Individual neural representations of the speech of each speaker are observed in auditory cortex, with each being selectively phase locked to the rhythm of the corresponding speech stream, and from which can be exclusively reconstructed the temporal envelope of that speech stream. The neural representation of the attended speech, originating in posterior auditory cortex, dominates the responses. Critically, when the intensities of the attended and background speakers are separately varied over a wide intensity range, the neural representation of the attended speech adapts only to the intensity of that speaker, but not to the intensity of the background speaker. This demonstrates object-level intensity gain control in addition to the object-level attentional gain.

Overall, these results indicate that concurrent auditory objects, even if spectrally overlapping and not resolvable at the auditory periphery, are indeed neurally encoded individually as separate objects, in auditory cortex.

5 Cochlear Implants in Real-Life Auditory Scenes: Limitations and Opportunities

Jan Wouters¹

¹*ExpORL, Dept. Neurosciences, University of Leuven, Belgium*

Cochlear implants are up to now the most successful man-made interfaces to the neural system. The auditory nerve is stimulated electrically which leads to a partial restoration of hearing and auditory perception for persons with severe hearing impairment. Speech understanding of cochlear implant (CI) recipients in quiet environments can be very good, but considerably worse in more real-life and adverse listening situations.

Although modern CIs use up to 22 stimulation channels, the information transfer is still very limited for the perception of fine spectro-temporal details to allow the perception of music and speech communication in common real-life auditory scenes. The limitations have become clear after years of research. Major limitations are related to reduced spectral resolution and the lack of matching of the coding of temporal and spectral aspects of pitch.

However, temporal aspects of the input sound, such as the speech envelope and periodicity can very well be transmitted in CIs. Examples will be given of enhanced representation of these features in the signal coding leading to improved directional hearing and speech perception in challenging listening scenes.

Furthermore, some signal processing approaches introduce speech enhancements in noisy conditions at the cost of significant signal distortions. These distortions are evaluated as detrimental for sound quality in normal hearing and hearing impaired, but are hardly noticeable by most cochlear implant recipients. This opportunity for further improvements in auditory perception in CI will be discussed.

6 Dynamic Faces Speed Up Vocal Processing in the Auditory Cortex

Asif Ghazanfar¹

¹*Princeton University*

The dynamics and deformations of the face during speech lead to a variety of visual motion cues related to the auditory components of speech; they are integral to face-to-face communication. In noisy, real world environments, visual cues provide considerable intelligibility benefits to the perception of auditory speech and faster reaction times. We are currently investigating the neural correlates of this behavioral advantage by investigating what role the auditory cortex of macaque monkeys plays in the audiovisual integration of their "coo" vocalizations. Monkeys detected visual, auditory or audiovisual coo vocalizations produced by monkey avatars in a background of noise (~60 dB) as fast and as accurately as possible. The loudness of the auditory vocalization (i.e. signal to noise ratio or SNR) relative to the noise background was varied. Decreasing SNR of the auditory-only vocalizations led to an increase in reaction times

(RTs). Audiovisual RTs were faster than RTs to both auditory- and visual-only conditions. Under these behavioral conditions, we recorded spiking activity and local field potential (LFPs) in the lateral belt auditory cortex. We found that, at least in part, the activity in auditory cortex co-varied with behavior. First, a decrease in SNR of the auditory-only vocalization increased latency and decreased the magnitude of spiking responses. Second, surprisingly, we found that spiking responses were faster for audiovisual compared to auditory vocalizations—a parallel with decreasing reaction times. Spiking responses were however absent to visual-only vocalizations — suggesting sub-threshold effects of visual input. Thus, we analyzed the LFP responses to identify the network dynamics that could mediate this speed-up. We found that the inter-trial phase coherence in the 10 – 30 Hz band of the LFP was suppressed for audiovisual compared to auditory vocalizations. Suppression was maximal for the largest SNR and decreased with the decrease in SNR. This suggests that visual input into auditory cortex changes the state of network dynamics in this frequency band. We also found that the onset of visual mouth motion led to an increase in the inter-trial phase coherence in the 10 – 30 Hz band immediately after visual onset. These results suggest that during the detection of visual vocalizations, visual cues speed up and alter the dynamics of the circuits in auditory cortex that process vocalizations.

7 A Temporal Integration Mechanism Enhances Frequency Selectivity Between Brainstem Inputs and Inferior Colliculus Neurons

Chen Chen^{1,2}, Heather Read¹, Monty Escabi¹

¹University of Connecticut, ²SUNY Downstate Medical Centre

Mammals can accurately resolve frequency components in sounds, a task that is essential for sound recognition. Despite its importance, there is little direct evidence for how frequency selectivity is preserved or newly created across auditory structures. Here we demonstrate a dramatic enhancement in frequency selectivity between putative input (PIN) and target inferior colliculus neurons (ICN) that is created through temporal integration of the converging inputs. PIN receptive fields are broadly tuned and exhibit temporally delayed and spectrally interleaved excitation and inhibition not present in IC. A radical sharpening of tuning is accomplished by temporal integration of the converging inputs. A neuron model accurately replicates the finding and demonstrates that this integration degrades timing precision but enhances spectral selectivity through interference of spectrally in- and out-phase IC inputs. This contrasts current models that require local inhibition to enhance selectivity and supports a fast computational strategy to enhance frequency selectivity in IC.

8 Making a Case for Integration Time-Constants: Do Sparse Representations Scale Hierarchically?

Monty Escabi¹, Chen Chen², Heather Read¹

¹University of Connecticut, ²SUNY Downstate Medical Center

Neural codes that are minimally redundant and sparse have been proposed as efficient strategies for representing natural sounds. Prevailing theories hold that neural responses to sound shift hierarchically from highly redundant dense codes in the auditory periphery to a selective sparse codes in cortex. On the other hand, computational models that use sparse coding principles can account for receptive field features in auditory nerve (Lewicki 2002), midbrain (Carlson et al. 2012), and cortex (Klein et al 2003). These seemingly conflicting views can be reconciled if one considers the neural integration times for phase-locked activity, which increase systematically from the auditory nerve to auditory cortex. Here we demonstrate that most inferior colliculus (ICC) neurons in the cat respond with a single precise action potential within their spectrotemporal response field (STRF), which defines their integration time. Population activity was likewise sparse with few neurons active for a typical integration time and neuron-to-neuron correlations where minimal (5% of pairs) and strictly confined to 1/3 octave. Responses from primary auditory cortex (A1) are similarly sparse if each structure is analyzed at their respective integration time scales (10 msec ICC; 50 msec A1). This indicates that sparse representations scale hierarchically with neural integration times and that measures of sparseness should be referenced on the time-scales relevant to the sound feature represented at each stage of the auditory pathway.

9 Associative Learning Enhances Population Coding in the Avian Auditory Cortex by Inverting Inter-Neuronal Correlation Patterns

James Jeanne^{1,2}, Tatyana Sharpee³, Timothy Gentner¹

¹UC San Diego, ²Harvard Medical School, ³Salk Institute

Cortical encoding of acoustic signals involves the coordinated activity of millions of neurons. Although learning can alter encoding in individual cortical neurons, it is unknown how this plasticity extends to neural populations. Correlated inter-neuronal activity, a property not observable in single neuron responses, can greatly impact population encoding and is thus a potential target for learning driven plasticity. To test this possibility, we measured the simultaneous activity of multiple auditory cortical neurons in songbirds trained to recognize natural segments of song. We show that learning inverts the canonical positive relationship between correlated signal (tuning function similarity) and correlated noise between pairs of neurons. This inversion enhances the ability of neural populations to discriminate between those song segments that are relevant for behavior. These results reveal the inter-neuronal correlation relationship as a novel target for learning-dependent plasticity.

10 Sensitivity and Invariance to Temporal Transformations of Vocalizations in the Primary Auditory Cortex

Isaac Carruthers¹, Ryan Natan¹, Maria Geffen¹

¹*University of Pennsylvania*

One of the central tasks of the mammalian auditory system is to represent information about acoustic communicative signals, such as vocalizations. However, the neuronal mechanisms underlying vocalization encoding, and sensitivity to its temporal transformations, in the central auditory system are poorly understood. To learn how the auditory cortex encodes information about con-specific vocalizations, we presented a library of natural and transformed ultra-sonic vocalizations (USVs) to awake rats, while recording neural activity in A1 using chronically implanted multi-electrode probes. The vocalizations were presented in their original form, reversed temporally, dilated or compressed. For responses of each neuron to each stimulus group, we fitted a simple, yet novel predictive model: a generalized linear-non-linear model (GLNM) that takes the frequency modulation and single-tone amplitude as the only two input parameters. Many neurons reliably and selectively responded to original USVs. Our GLNM accurately predicted their responses to previously unheard USVs. Neurons with high model prediction accuracy were typically tuned to tone pips in the ultra-sonic vocalization frequency range. However, accurate model performance is also reported for neurons that were tuned to lower frequencies. We next tested the changes in neuronal responses to temporally transformed and reversed versions of the original vocalizations. The model prediction accuracy was lower for temporally transformed, rather than original or reversed vocalizations, whether the model was fitted on the original or the transformed vocalizations, whereas the mean firing rate was not affected by the transformations of the stimulus. Our results demonstrate that A1 processes original USVs differentially than transformed USVs, indicating specialization for temporal statistics of the original vocalizations.

11 Auditory Coding of Individual Vocalizations in Scenes

Sarah Woolley¹

¹*Columbia University*

Background

Processing communication vocalizations is a crucial, natural function of the auditory system. Central auditory circuits generate representations of vocalizations that lead to perception and guide behavior. An important part of understanding how auditory processing leads to perception of communication vocalizations in complex scenes is explaining mechanisms whereby neural representations of vocalizations are extracted from neural representations of scenes.

Methods

We trained songbirds to discriminate among individual vocalizations and tested their abilities to recognize those vocalizations in auditory scenes at varying signal to noise ratios. We then recorded the responses of single auditory

midbrain, primary forebrain and higher forebrain neurons to the same vocalizations at varying intensities and in scenes at varying signal to noise ratios. Using analysis of recorded spike trains, pharmacological and stimulus manipulations, and simulations, we generated and tested a simple neural circuit model that explains the transformation in neural representations of vocalizations and scenes along the ascending auditory pathway.

Results

We found that the neural representation of vocalizations transformed from a dense and redundant code in the midbrain and primary forebrain into a sparse and distributed code in the higher forebrain. Sparse coding neurons were better than dense coding neurons at extracting individual vocalizations from auditory scenes, and generated neural representations of target vocalizations in scenes at signal to noise ratios that matched behavioral detection. A simple neural circuit of fast excitation and delayed inhibition transforms dense input into sparse output, and facilitates the neural extraction of an individual vocalization from a complex auditory scene.

Conclusions

Our findings suggest that the neural representation of vocalizations transforms significantly between the primary and higher auditory forebrain, from a dense and non-selective code to a sparse, highly selective and distributed code. The higher forebrain sparse code is sensitive to acoustic context, relies on inhibition, and serves as a mechanism for the neural extraction of one vocalization from a complex scene.

12 Mechanisms of Attention in Auditory Scene Analysis

Mounya Elhilali¹

¹*Johns Hopkins University*

The mechanisms by which a complex auditory scene is parsed into coherent objects depend on poorly-understood interactions between task-driven and stimulus-driven attentional processes. It is widely believed that detecting a target amidst ambient noises or competing sounds is not only mediated by top-down processes that direct listeners' attention to the signal of interest; but is also modulated by the listening environment, statistics of the auditory scene and prior information that listeners have or gather about the scene. Here, we explore the role of exogenous (stimulus-driven) processes in forming priors about our listening environments; and their interaction with endogenous (listener-directed) attentional processes. Our findings indicate that listeners operate in an optimal way by integrating all information from both task instructions and stimulus and scene cues in an effective manner. We propose a computational framework that integrates the role of both endogenous and exogenous processes in foreground/background organization and auditory object formation.

13 Natural Sound Statistics and Auditory Scene Analysis

Josh McDermott¹, Eero Simoncelli²

¹Massachusetts Institute of Technology, ²Howard Hughes Medical Institute, New York University

Auditory scene analysis involves estimating individual sound sources from the signal that enters the ear, which often contains mixtures of multiple concurrent sources. The segregation of sounds from a mixture is a classic ill-posed problem in perception, and can be solved only with the aid of prior assumptions about the sound sources that occur in the world. In this talk we will present a theoretical framework by which these assumptions about sound sources can be related to natural sound statistics. We view sound segregation as the task of distinguishing actual sound sources from the many possible incorrect alternatives – sound signals that are physically consistent with the mixture received by the ears but which did not occur in the world. Our approach stems from the observation that incorrect estimates of individual sources must tend to be partial mixtures of the true sources. Sound properties that have different values for individual sources compared to mixtures should thus aid segregation, as they could serve to distinguish correct and incorrect source estimates. By comparing the properties of individual sound sources with those of their mixtures, we can assess the theoretical utility of different potential segregation cues. We will discuss the results of such statistical analyses of various corpora of natural sounds, their implications for theories of segregation, and how these implications might be tested experimentally.

14 A Mutation in *PNPT1*, Encoding the Mitochondrial RNA-Import Protein PNPase, Causes Hereditary Hearing Loss

Simon von Ameln¹, Geng Wang², Redouane Boulouiz³, Mark A. Rutherford⁴, Geoffrey M. Smith⁵, Yun Li⁶, Hans-Martin Pogoda⁷, Gudrun Nürnberg⁸, Barbara Stiller¹, Alexander E. Volk¹, Guntram Borck¹, Jason S. Hong⁵, Richard J. Goodyear⁹, Omar Abidi³, Peter Nürnberg⁸, Kay Hofmann¹⁰, Guy P. Richardson⁹, Matthias Hammerschmidt⁷, Tobias Moser⁴, Bernd Wollnik⁶, Carla M. Koehler², Michael A. Teitell⁵, Abdelhamid Barakat³, Christian Kubisch¹

¹Institute of Human Genetics, Ulm, Germany, ²Department of Chemistry and Biochemistry, University of California at Los Angeles, Los Angeles, USA, ³Institut Pasteur du Maroc, Casablanca, Morocco, ⁴University Medical Center Göttingen, Göttingen, Germany, ⁵David Geffen School of Medicine at UCLA, Los Angeles, USA, ⁶Institute of Human Genetics, Cologne, Germany, ⁷Institute for Developmental Biology, Cologne, Germany, ⁸Cologne Center for Genomics, Cologne, Germany, ⁹University of Sussex, Brighton, UK, ¹⁰Institute for Genetics, Cologne, Germany

Background

A subset of nuclear encoded RNAs has to be imported into mitochondria to ensure proper replication and transcription of the mitochondrial genome and hence mitochondrial function. Polynucleotide phosphorylase (PNPase, encoded by *PNPT1*) is one of the few components known to be

involved in this poorly characterized process in mammals. In our present study we investigated a consanguineous Moroccan family with autosomal recessive non-syndromic hearing impairment (*DFNB70*) and identified a homozygous missense mutation in *PNPT1* as the underlying cause of disease.

Methods

Family members were evaluated by detailed medical history interviews, a physical examination, and underwent an otological examination and pure-tone audiometry. To identify the chromosomal locus underlying the sensory disorder, we performed genome-wide homozygosity mapping. Coding exons and adjacent splice sites of all positional candidate genes within the linked interval were analysed by PCR amplification of genomic DNA followed by direct Sanger sequencing. RT-PCR was applied to investigate *PNPT1* expression in various murine tissues including the cochlea. In zebrafish the expression of the *PNPT1* ortholog was analyzed by in situ hybridization. To investigate the cellular localization of PNPase within the cochlea, we performed immunohistochemistry on cochlear cross-sections and in organ of Corti whole-mount preparations. The ability of the PNPase mutant to assemble into functional trimers was analyzed by blue-native gel electrophoresis and mitochondrial RNA import assays were conducted in yeast and mammalian cells.

Results

By positional cloning we identified a homozygous *PNPT1* missense mutation (c.1424A>G predicting the protein substitution p.Glu475Gly) of a highly conserved PNPase-residue within the second RNase PH-domain in a family with autosomal recessive non-syndromic hearing impairment. The immunohistological staining pattern demonstrated a broad PNPase distribution in the inner ear including the sensory hair cells and spiral ganglion neurons. In vitro analyses in bacteria, yeast, and mammalian cells showed that the identified mutation results in a hypofunctional protein leading to disturbed PNPase trimerization and reduced mitochondrial RNA import.

Conclusion

In summary, we elucidated a hereditary disturbance of the mitochondrial RNA import by the identification of a hypofunctional mutation in *PNPT1* in congenital severe hearing impairment, demonstrating the rather unexpected and specific importance of PNPase for auditory function.

15 Gene Expression Profiling of Young and Adult Mouse Cochlea by RNA-Seq in Strains with Normal and Age-Related Hearing Loss

Anne B. S. Giersch^{1,2}, Jun Shen², Nahid G. Robertson¹, Cynthia C. Morton^{1,2}

¹Brigham and Women's Hospital, ²Harvard Medical School

Background

Age-related hearing loss is the most common sensory deficit that reduces the quality of life in the aged population. Its social impact will become more

pronounced as life expectancy increases. Despite the discovery of many deafness genes, pathophysiology of progressive hearing impairment due to aging remains elusive. We hypothesize that gene expression profiling of the cochlea from mouse models with various degrees of age-related hearing loss will reveal the molecular mechanism and inform potential target selection for prevention and treatment.

Methods

We performed gene expression profiling of mouse cochlea by next-generation sequencing (RNA-Seq). A multi-factorial design was used. Cochleas from mouse strains with good hearing past one year of age (CBA/CaJ and B6.CAST-Cdh23^{Ahi+}) or with documented age-related hearing loss (Coch^{G88E/G88E} and Coch^{-/-} in a CBA background and C57BL/6J) were dissected at discrete ages ranging from one week through late adulthood. PolyA selected mRNAs were extracted and the derived cDNA samples were fragmented, indexed, pooled, and sequenced by Illumina HiSeq. Biological replicates were used for all conditions. Expression levels of all transcripts were analyzed and differential gene expression analyses were performed.

Results

We created gene expression profiles of mammalian cochlea at various ages by RNA-Seq. With total reads of at least 30 million, more than 16,000 genes were detectable, and expression levels were highly reproducible. We detect significant systematic differences in gene expression profiles between C57BL/6J and CBA/CaJ strain backgrounds, regardless of age. Comparing mouse models with or without age-related hearing loss of the same genetic background, we find that few genes show statistically significant differential expression at young ages before the onset of hearing impairment, but the number of genes dramatically increases to hundreds at later stages. In addition, hundreds of genes show significant temporal changes on both genetic backgrounds. This postnatal to adult cochlea specific gene expression dataset will eventually be added to the publicly accessible Shared Harvard Inner Ear Database (SHIELD: <https://shield.hms.harvard.edu>).

Conclusion

We have surveyed gene expression in mammalian cochlea by RNA-Seq and identified genes that show age-related differential expression. Systematic differences exist between different genetic backgrounds. Temporal gene expression profiles in the cochlea may suggest candidate targets for prevention and treatment of age-related hearing loss. By providing online access to the fully annotated dataset, we expect it to become a useful resource for the research community.

16 Deep Sequencing Identifies Novel MicroRNAs in the Mouse Inner Ear

Anya Rudnicki¹, Lilach M. Friedman¹, Ofer Isakov², Inbal Weiss¹, Tal Elkan-Miller¹, Noam Shomron², Karen B. Avraham¹

¹Dept. of Human Molecular Genetics, Sackler Faculty Medicine, Tel Aviv Univ., Tel Aviv, Israel, ²Dept. of Cell & Developmental Biology, Sackler Faculty Medicine, Tel Aviv Univ., Tel Aviv, Israel

Background

MicroRNAs (miRNAs) are small non-coding RNAs that regulate gene expression post-transcriptionally. By binding to sequences in the 3' untranslated region (UTR) of mRNAs, a miRNA can inhibit target mRNAs by translational suppression and mRNA destabilization. miRNAs clearly play an important role in the inner ear, since mutations in miRNAs lead to deafness in humans and mice. Conditional knock-out mouse mutants have shown that miRNAs are vital for development of the sensory neurons, sensory epithelia and inner ear morphogenesis.

Methods

To further characterize miRNAs in the mammalian inner ear, we used Illumina deep sequencing to identify novel miRNAs in mouse inner ear sensory epithelia and differentially-expressed miRNAs in cochlea and vestibule. Short RNA molecules were sequenced from cochlear and vestibular sensory epithelia of newborn C57Bl/6 mice by high-throughput DNA sequencing. The reads were aligned to the mature *Mus musculus* miRNA database, allowing one mismatch to occur between a read and the reference, due to isomiRs. The reads that were not mapped to known miRNAs were used to predict novel pre-miRNAs or pri-miRNAs, according to the known characteristic read pattern for each type of novel RNA, using the DARIO algorithm. We selected miRNAs with the following criteria: seed regions conserved between mouse and human, highly expressed in the sensory epithelia, and located in introns of genes expressed in the inner ear due to possible co-expression.

Results

A total of 7,732,589 and 8,452,794 small RNAs were found in the cochlear and vestibular samples, respectively. These included miRNAs, snoRNAs, transfer RNAs and ribosomal RNAs. For miRNAs, 440 and 458 were identified in the cochlea and vestibule sensory epithelium, respectively. In addition, we identified three novel mouse miRNAs. qRT-PCR and in situ hybridization validated expression of these miRNAs in the inner ear. Predictions of gene-targets to these miRNAs were verified by luciferase assays. The interaction between the miRNAs and a number of their targets is being studied.

Conclusion

We have generated and analyzed a comprehensive dataset of small RNA sequences from the mouse inner ear. The analysis revealed novel miRNAs with potential regulatory effects on development. Based on the function

of the targets, these miRNA-target pairs may be involved in cell signaling, apoptosis, membrane structure, and conductance of voltage-gated channels, with implications for hearing and mechanisms leading to deafness.

Supported by the Israel Science Foundation and NIH-NIDCD R01-DC005641.

17 Genome Wide Association Analysis and Expression Studies Involved in Hearing Function and Age-Related Hearing Loss

Giorgia Girotto¹, Dragana Vuckovic¹, Annalisa Buniello², Morag Lewis², Beatriz Lorente², Karen Steel², Paolo Gasparini¹

¹Medical Genetics - Department of Medical Sciences - IRCCS-Burlo Garofolo/University of Trieste, ²Wellcome Trust Sanger Institute, Wellcome Trust Genome Campus, Hinxton, Cambridge CB10 1SA, UK

Background

Only few genes have been involved in normal hearing function and age-related hearing loss (ARHL). To reach the goal of increasing our knowledge on the genetic bases of both hearing function and ARHL an integrated strategy has been designed based on: A) Genome Wide Association Studies (GWAS) on different hearing traits (low, medium and high Pure Tone Average, the separated thresholds and the Principal components), B) expression studies in mice using immunohistochemistry and confocal microscopy of genes identified by the GWAS and C) genotype-phenotype relationships

Methods

Three meta-analyses using 3681 samples coming from isolated populations located in Europe (Italy, Croatia and Ukraine), Caucasus (Armenia, Azerbaijan, Georgia) and Central Asia (Uzbekistan, Kazakhstan, Tajikistan and Kirghizstan) were carried out. Two GWAS for hearing quantitative traits (one sex separated), and one for ARHL (qualitative traits) have been performed. In order to confirm our findings, expression studies in wild-type mice (at 4 and 5 days postnatal) using immunohistochemistry and confocal microscopy were then carried out on genes identified by the GWAS. Genotype-phenotype relationships have been performed using mean values for each frequency and comparing the 3 different genotypes of a given SNP

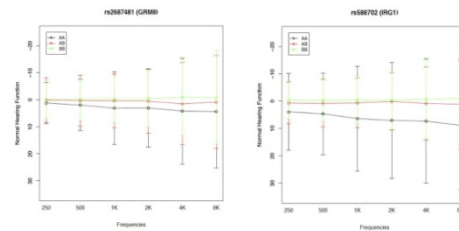
Results

By meta-analysis of data in these populations, some significant and suggestive loci ($p < 10^{-6}, 10^{-7}$) have been found and some of them map to known hereditary hearing loss loci whose genes still need to be identified (Girotto et al. JMG 2011). A list of 22 strong candidate genes has been defined to be included in the expression studies. 5 of them (Arsg, Slc16a6, Dclk1, Gabrg3, Csm1) show strikingly specific expression in the cochlea (e.g. at the top of sensory hair cells and in the marginal cells of the stria vascularis) while the other 10 (Ptprd, Grm8, GlyBP, Evi5, Irg1, Rimp2, Ank2, Mbd1, Rbfox1, Cdh13) are located in multiple cell types in the cochlea. As regards the possible

genotype-phenotype correlation, an example is reported in Figure 1 where Irg1 and Grm8, being both expressed in many cell types in the cochlea, show similar pattern at all the frequencies in the three genotypes. Moreover, some interesting findings have been obtained comparing phenotype/genotype data with the localization of the expression

Conclusion

Preliminary results prove the useful combination of GWAS, expression studies and genotype/phenotype data to provide new insights into the molecular basis of hearing function and ARHL suggesting new targets for treatment and prevention



18 Exome Sequencing Reveals Mutations in ATP6V1B2 as a Cause of Dominant Deafness-Onychodystrophy (DDOD) Syndrome

Yongyi Yuan^{1,2}, Qing Chang², Feng Xin¹, Jianjun Wang², Xukun Yan¹, Weiwei Guo¹, Binfei Zhou², Jianguo Zhang^{3,4}, Jing Wu⁵, Qingyan Zhu³, Changxin Gao⁵, Jun Wang^{3,6}, Xi Lin², Pu Dai¹

¹Chinese PLA General Hospital, ²Emory University School of medicine, ³BGI-CShenzhen, ⁴T-Life Research Center, Fudan University, ⁵BGI-Tianjin, ⁶Department of Biology, University of Copenhagen

Background

Dominant deafness and onychodystrophy syndrome (DDOD syndrome) is characterized by congenital sensorineural hearing loss, dystrophic or absent of nails. Cornical and hypoplastic teeth were also present in some cases. The DDOD syndrome as an autosomal dominant condition was first recognized in 1961 and subsequently identified in five other unrelated families. The genetic etiology of DDOD is not yet determined.

Methods

We collected two Chinese DDOD pedigrees. The probands showed identical phenotypes: congenital hearing impairment, absent of all the toe nails, little finger and thumb nails, absent of the distal little finger bones as well as onychodystrophy like malacia and pitting of the middle three finger nails. The whole-exome sequencing was performed in two probands and their parents using the genomic DNA extracted from peripheral blood. The on-target mean depth of exome sequencing was >130 fold,

resulting in >99% of the targeted base pairs being sufficiently covered. Single-nucleotide variations and indels of patients and their parents were filtered by dbSNP132, the 1000 Genomes Project, HapMap8 databases and BGI YH database. Candidate genes of inner ear from the Morton Human Fetal cDNA library were also used in the filtering. Immunohistochemistry and specific gene knockdown by using morpholino antisense oligos were carried out to investigate the pathogenic mechanism of DDOD-related gene mutations.

Results

Mutations in four genes, ATP6V1B2, ACTG1, PABPC1 and CDC27 were identified in the two affected probands by our analysis strategy. Since the quality scores of PABPC1 and CDC27 SNPs were low, we concentrated on confirmatory sequencing of the variations in the ATP6V1B2, ACTG1 by Sanger sequencing. A common heterozygous de novo mutation 1516 C>T (R506X) in the ATP6V1B2 was verified. While the ACTG1 variant turned out to be a false positive. Conservation analysis of amino acids in nine ATP6V1B2 orthologs indicated the arginine in 506 is highly conserved in evolution. In addition, the 1516 C>T mutation in ATP6V1B2 was not detected in 1053 ethnically matched normal controls. Immunohistochemistry labeling of the ATP6V1B2 in the cochlea identified its expression in the hair cells, spiral ganglia, spiral limbus, interdental cells, spiral prominence and fibrocytes. Mice injected with ATP6V1B2 morpholino antisense oligos into the scala media of cochlea showed significant hearing loss in the injected side, while contralateral control showed normal hearing.

Conclusion

Exome sequencing data identified a mutation in the ATP6V1B2 as the cause of DDOD. Preliminary functional study supported that ATP6V1B2 plays a vital role in normal hearing.

19 Beyond Hearing Sensitivity : Added Value from Primary ABR Phenotypic Screening

Neil Ingham^{1,2}, Selina Pearson², Karen P. Steel^{1,2}

¹Kings College London, ²Wellcome Trust Sanger Institute

Background

The Sanger Institute's Mouse Genetics Project (MGP) generates targeted knockout mice and characterizes the effect of the mutant allele using a wide range of phenotyping tests designed to cover a number of common disease areas. Hearing is assessed in mice aged 14 weeks.

Methods

Mice are anaesthetized using Ketamine / Xylazine and their auditory brainstem responses (ABRs) recorded to click and a range of tone-pip stimuli. Thresholds are estimated and used to build audiometric profiles for mutant and control mice. In addition, click-evoked ABR waveforms are analysed in more detail. Individual responses recorded at 20dB and 50dB sensation level and a mean response

waveform for each mutant group are superimposed on a reference range waveform calculated from large numbers of control wildtype mice of the same genetic background. These plots are used to assess altered waveform shapes in mutant mouse lines. Input-Output Functions are calculated for wave 1 and wave 3 amplitude and latency and plotted over a reference range for each parameter to quantify abnormal waveforms parameters.

Results

We have identified a number of mutant lines which demonstrated abnormal click-evoked ABR waveforms despite having normal threshold sensitivities. A variety of mutant lines were identified having affected wave 1 or wave 3 amplitude or latency. For example, Ppp5c homozygote mutants exhibited increased wave 1 amplitudes, Usp42 homozygote mutants had reduced wave 1 and wave 3 amplitudes, Atp5a1 heterozygote mutants showed reduced wave 3 amplitudes and Sesn3 homozygote mutants showed prolonged wave 3 latencies. Reduced wave amplitude could have a number of underlying causes. Reduced neuronal numbers could give reduced evoked potential generator activity and maybe indicate neurodegeneration phenotypes. Desynchronized neuronal activity could also result in reduced wave amplitude and may indicate abnormal synaptic activity along the auditory brainstem pathway. Altered wave latencies are also seen and may indicate deficits in neuronal conduction or synaptic efficiency.

Conclusion

Estimation of hearing sensitivity using ABRs can identify abnormal auditory phenotypes involving raised thresholds. However, detailed assessment of ABR waveforms can identify a wider range of potential auditory system phenotypes.

20 Collateral Damage: Spontaneous Mutations from a Targeted Knockout Programme

Morag Lewis^{1,2}, Francesca Carlisle², Selina Pearson², Jing Chen^{1,2}, Johanna Pass^{1,2}, Zahra Hance², Thomas Keane², Jacqueline White², Neil Ingham^{1,2}, Karen Steel^{1,2}

¹King's College London, ²Wellcome Trust Sanger Institute

Background

The Sanger Institute's Mouse Genetics Project (MGP) aims to generate knockout mice and characterise the effect of the null allele using a broad spectrum of phenotyping tests, one of which is the Auditory Brainstem Response. During standard phenotyping, several lines were found to display a variety of hearing defects which did not segregate with the knockout allele, and were probably due to spontaneous mutations.

Methods

DNA from four of these lines was sent for comparative genome hybridisation and whole exome sequencing, along with DNA from the embryonic stem cell lines used to make the knockout alleles. The mutations from two of the lines have also been mapped using a backcross. Further

characterisation has been carried out by ABR, endocochlear potential (EP) measurements, middle ear dissection, inner ear clearing, immunohistochemistry and scanning electron microscopy of the organ of Corti.

Results

The sequencing results show a background of mutations present in ES cells, many common to both cell lines. Mapping has proven effective in identifying the mutation responsible for the rapid progressive hearing loss seen in one of the four lines, which has been identified as a new allele of *S1pr2*, a gene known to be important for hearing. These mice have normal gross morphology of middle and inner ears, and while hair cell degeneration was observed from 5 weeks old in affected mice, some intact hair cells are still visible at 9 weeks old in mice with no ABR responses at all. Their EP measurements, however, are decreased from an early age, and there are subtle defects in the stria vascularis of affected mice. We are currently mapping a second line, and have identified a critical region and several candidates for the low frequency hearing loss phenotype common to this and several other MGP mouse lines.

Conclusion

The intriguing phenotypes of these spontaneous mutations are an unexpected benefit of the Mouse Genetics Project and its extensive phenotyping screen. The first mutation identified is a novel allele of a known hearing gene that offers a useful model of progressive hearing loss. Identifying the gene responsible for the unusual phenotype of low frequency hearing loss will further extend our understanding of the ear and the genes responsible for its maintenance and function.

[21] Thrombospondin Genes Are Required for Normal Cochlear Development and Maintenance

Diana Mendus¹, Felix Wangsawihardja¹, Vidya Sundaresan¹, Mirna Mustapha¹

¹Stanford University

Background

Recent studies reveal important roles for cell-adhesion molecules such as thrombospondins (TSPs) in promoting synapse formation during brain development and in repairing synaptic connection after stroke.

Methods

For our efforts to identify genes involved in cochlear synapse formation and functional maturation, we hypothesize that cell adhesion proteins that are also upregulated during cochlear synaptogenesis and/or adulthood are important for these processes. In this study, we examine whether TSPs are involved in synapse formation and maintenance in the cochlea using recombinant mouse models of these genes.

Results

Our preliminary data using microarray and qPCR analysis on TSP genes 1-4 from whole cochlea revealed significant

increase in TSP2-4 expression during a critical window of postnatal cochlear development with TSP1 expression picking up later in adulthood. Our auditory brain stem response (ABR) test on TSP1 and TSP2 mutants reveal elevated threshold in TSP2 mutants but not in TSP1 mutants at an early age. These data suggest a role for TSP2 in synapse functional maturation that is important for the onset of hearing. However, one-year old TSP1 mutant mice show an increase in ABR threshold at higher frequencies and decreased amplitude of response compared to wild type controls, suggesting a role for TSP1 in synapse maintenance. Our physiology data is in agreement with the roles predicated for these genes based on our expression studies. Counting of afferent and efferent synapse numbers in TSP2 and TSP1/2 mutants versus wild type mice does not show significant differences between these groups. Our next step would be to examine whether the synapses in the TSP mutant mice are functional using electrophysiology. To test the role for these genes in the recovery of the cochlea from noise injury, we exposed TSP2 and TSP1/2 mutant mice to a noise insult and measured ABR threshold after a recovery period. Data from these experiments showed that these mice were unable to recover from the noise injury compared to wild type controls indicating a deficit in repair mechanisms in these mice.

Conclusion

Our results, taken together, indicate that TSPs 1 and 2 are both involved in different aspects of cochlear functional maturation, repair and maintenance and these genes are now candidates for screening in human patients with congenital and age-related hearing impairment.

[22] An Inducible RtTA Mouse Line for Gene Manipulation and Fate Mapping in Supporting Cells and Glia Within the Auditory and Balance Sense Organs of the Inner Ear

Bradley Walters¹, Jian Zuo¹

¹St. Jude Children's Research Hospital

Background

Sox10 is an SRY-related HMG-box (Sox) transcription factor that has been shown to be expressed in several cell types within the central and peripheral nervous systems. The reverse tetracycline transactivator (rtTA) protein is a variant of the *E. coli* tet-repressor protein that induces the expression of genes containing a tet-operator (tetO) sequence only when in the presence of tetracycline or its derivative doxycycline. Knock-in of the rtTA sequence to the endogenous Sox10 locus thereby allows for the specific expression of the rtTA protein in Sox10 expressing cells and temporal and quantitative control over TetO promoted gene expression by dosing regimen of doxycycline.

Methods

In this study, Sox10rtTA mice (MGI ID 3513104) were bred with mice containing a TetO-lacZ transgene, and X-gal staining and beta-galactosidase immunostaining were used to map Sox10 promoter activity in the sensory organs

of the inner ear at various embryonic and postnatal ages. Sox10rtTA mice were also bred with mice that had a TetO-Cre transgene and a CAG-promoted, floxed-stop TdTomato reporter so that the fate of Sox10 positive cell types could be determined.

Results

Both models reveal widespread Sox10 reporter expression in the cochlea and balance organs at several ages and at varying levels across cell types depending upon age or upon the concentration of doxycycline administered. For both hearing and balance organs, the majority of reporter expression was in supporting cells (SCs) and glia, and, in the cochlea, in the greater epithelial ridge (GER). With late embryonic induction, lower doses of doxycycline resulted in decreased reporter expression in SCs, but not in GER cells, suggesting a dose-responsiveness for the TetO transgene, but perhaps also lower Sox10 promoter activity in SCs than GER cells. Fate mapping and reporter expression at embryonic and neonatal ages suggests that prosensory precursor cells that give rise to both HCs and SCs express Sox10, but that Sox10 expression is downregulated in HCs while being maintained in supporting cells well into adulthood.

Conclusion

These findings suggest that Sox10 may be an important factor in prosensory cell fate decisions and in the maintenance of SC fate in the hearing and balance organs. Furthermore, the Sox10rtTA mouse line represents a powerful model for fate mapping and/or genetic manipulation of Sox10 expressing SCs and glia in the mouse inner ear.

This work was supported in part by the NIH, ONR, HHF, NOHR, and ALSAC.

23 The LINC Complex Is Essential for Hearing in Humans and Mice

Danielle R. Lenz¹, Henning F. Horn², Zippora Brownstein¹, Shaked Shivatzki¹, Amiel A. Dror¹, Orit Dagan-Rosenfeld¹, Kyle J. Roux³, Serguei Kozlov⁴, Kuan-Teh Jeang⁵, Moshe Frydman^{1,6}, Brian Burke², Colin L. Stewart², Karen B. Avraham¹

¹Dept. of Human Molecular Genetics, Sackler Faculty Medicine, Tel Aviv Univ., Tel Aviv, Israel, ²Institute of Medical Biology, A*STAR, Singapore, ³Sanford Children's Health Research Center, Sioux Falls, SD, USA, ⁴National Cancer Institute, Frederick, MD, USA, ⁵Laboratory of Molecular Microbiology, NIAID-NIH, Bethesda, Maryland, USA, ⁶Sheba Medical Center, Tel Hashomer, Israel

Background

Young adults in two Israeli families of Iraqi Jewish ancestry presented with a high-frequency hearing impairment. The pattern of hearing loss in the families suggested autosomal recessive inheritance and the new deafness locus was named DFNB76. To obtain further insight into the role of Syne4 in epithelial cells, we created mice harboring a targeted disruption of the *Syne4* gene by homologous recombination in embryonic stem cells. Hearing loss of

mutant mice was detected already at P15 and progressed to all frequencies by P60. The *Syne4*^{-/-} mice became a mouse model for DFNB76 once a *SYNE4* mutation was found in the two families. Syne4 is a member of the KASH domain family. The nuclear envelope (NE), as the interface between the nucleus and cytoplasm, displays several major structural features, the most prominent of which are the inner and outer nuclear membranes (INM and ONM). Localization of KASH proteins to the ONM is dependent upon Sun domain proteins of the INM.

Methods

Linkage and homozygosity mapping, massively parallel and Sanger sequencing identified the human mutation. Mouse inner ears of *Syne4* and *Sun1* knock-outs were analyzed by scanning electron microscopy, auditory brainstem response (ABR), and behavioral testing. Immunolocalization of Syne4, Sun1, prestin and sodium potassium ATPase defined morphology and protein expression.

Results

SYNE4 was identified as the gene responsible for progressive high frequency hearing loss in the two families. Full-length Syne4 localized to the NE, whereas the mutant protein was found throughout the cytoplasm. In both *Syne4* and *Sun1* mutants, the OHCs began to degenerate in a basal to apical gradient, while the IHCs remained intact. Loss of Syne4 and Sun1 results in abnormal positioning of the nucleus in OHCs.

Conclusion

Hearing loss is caused by defects in either of two proteins that localize to the nuclear membranes of hair cells: Syne4, which localizes to the ONM and Sun1, which localizes to the INM. Mutations in *SYNE4* lead to deafness in humans and the *Syne4* mouse mutant serves as an ideal model to study this form of human deafness. The findings in the mice suggest that abnormal nuclear positioning leads to OHC death either due to interference with their sound-induced motility or to a compromised ability of abnormal OHCs to withstand the mechanical rigors of motility.

Supported by NIH/NIDCD grant R01-DC011835 and Singapore Biomedical Research Council and Singapore Agency for Science, Technology and Research (A*STAR).

24 Pathological Features in LmnaDhe/+ Mutant Mouse Provide a Novel Model of Human Otitis Media and Laminopathies

QING ZHENG¹, Yan Zhang^{1,2}, Heping Yu¹, Min Xu³, Fengchan Han¹, Cong Tian⁴, Suejin Kim¹, Elisha Fredman¹, Jin Zhang¹, Cindy Benedict-Alderfer¹

¹Case Western Reserve University, ²Second Hospital, Xi'an Jiaotong University School of Medicine, ³Xi'an Jiaotong University School of Medicine, ⁴University of Maine

Background

Genetic predisposition is recognized as an important pathogenesis factor of otitis media (OM) and associated diseases

Methods

The following assays were used:

Tympanometry analysis, ABR thresholds and DPOAE. histological and immunofluorescent staining. Scanning electronic microscopy, RT-PCR for gene expression. serum phosphate and calcium assays. Peritoneal macrophage migration in vivo and quantification assay

Results

We found that heterozygous mice with the Lmna allele, disheveled hair and ears (LmnaDhe/+), exhibit early-onset, profound hearing defects and other pathologic features of human laminopathy, which result from LMNA mutation. We assessed the effects of LmnaDhe/+ mutation on the development of OM and pathologic abnormalities characteristic of laminopathy. We found malformation and abnormal positioning of the Eustachian tube accompanied by OM in all of the LmnaDhe/+ mutant mice (100% penetrance) as early as postnatal day 12. Scanning electronic microscopy demonstrated ultrastructural damage to the cilia in middle ears that exhibited otitis media. Hearing assessment revealed significant hearing loss paralleling that in human OM. Expression of NF- κ B, TNF- α and TGF- β , which correlated with inflammation and/or bony development, was upregulated in the ears or in the peritoneal macrophages of LmnaDhe/+ mutants. Rugous, disintegrative and enlarged nuclear morphology of peritoneal macrophages and hyperphosphatemia were found in LmnaDhe/+ mutant mice, and together these features resemble the pathology of human laminopathies possibly revealing some profound pathology, beyond OM, associated with the mutation.

Conclusion

The LmnaDhe/+ mutant mouse provides a novel model of human otitis media and laminopathy.

25 TRPM7 Is Required for Neurotransmission by Zebrafish Hair Cells

Sean Low¹, Serhiy Pylawka¹, Jim Hudspeth¹

¹The Rockefeller University and Howard Hughes Medical Institute

Background

In an attempt to identify vertebrate genes required for hearing and balance, we undertook an examination of zebrafish mutants with defects in other forms of mechanosensation. One touch-unresponsive mutation, touchdown, arises in the gene encoding the transient-receptor-potential channel TRPM7. Because touchdown mutants also fail to initiate escape behaviors in response to water movements that are ordinarily detected by the lateral-line system, we attempted to identify the role of TRPM7 in hair cells of the lateral line.

Methods

We performed whole-mount in situ hybridization to pinpoint the cells in which TRPM7 is expressed. Electrophysiological recordings were then made from neuromast hair cells and lateral-line afferent neurons in touchdown mutants, wild-type siblings, and mutants in which the expression of wild-type TRPM7 had been selectively restored in hair cells. Finally, we examined the afferent synapses of hair cells by electron microscopy, immunohistochemistry, and pH-sensitive probes.

Results

Expression analysis demonstrated trpm7 transcripts in neuromast hair cells. Electrophysiological recordings from hair cells and their afferent neurons in touchdown mutants revealed normal microphonic responses but no tonic, hair cell-driven neural activity. Consistent with a requirement for the channel in hair cells, cell-specific expression of TRPM7 restored tonic activity in the afferent neurons of mutants. These findings, coupled with a role of mammalian TRPM7 in neurotransmission by cultured neurons, prompted a structural investigation of hair-cell synapses in the mutants. We found that touchdown larvae possess the structural elements of hair-cell synapses but lack acidified synaptic vesicles.

Conclusion

Our results demonstrate that TRPM7 is required for neurotransmission by zebrafish hair cells and suggest that the channel is necessary for proper pH regulation of synaptic vesicles, a process required for neurotransmitter filling.

[26] Role of the ATP-Gated P2X2 Ion Channel in Progressive Nonsyndromic Hearing Loss DFNA41 and in Noise-Related and Age-Related Hearing Loss

Denise Yan¹, Taro Fujikawa², M'hamed Grati¹, Hongbo Zhou³, Bechara Kachar², Gary D. Housley⁴, Peter R Thorne^{5,6}, Allen F. Ryan⁷, Mary-Claire King⁸, Xue-Zhong Liu¹

¹University of Miami Miller School of Medicine, Dept of Otolaryngology, ²National Institute on Deafness and other Communication Disorders National Institutes, Laboratory of, ³University of Kentucky Medical Center, Dept of Otolaryngology, ⁴University of New South Wales, Sydney, Dept of Physiology and Translational Neuroscience Facility, S, ⁵School of Medical Sciences, University of Auckland, New Zealand, Dept of Physiology, ⁶Section of Audiology, School of Population Health, University of Auckland, ⁷University of California, Otolaryngology Research Division, Dept of Surgery and Dept of Neuroscience, ⁸University of Washington, Dept of Medicine, Division of Medical Genetics

Background

Extracellular ATP is a purinergic signaling molecule that influences developing and mature cochlea via both ionotropic P2X and metabotropic P2Y receptors in sensory, neural, and secretory cochlear tissues. A role of ATP signaling in regulating hearing sensitivity to noise is supported by evidence that noise and metabolic stress trigger ATP release into the endolymph. Sustained noise exposure also causes up-regulation of P2X2 receptor mRNA and protein expression in the organ of Corti, that is highly expressed in developing inner ear neuroepithelium. There is evidence in both mice and humans that there is a heritable component to noise-induced hearing loss, with no known genes directly associated with noise- and age-related human hearing loss. We identified *P2RX2* p.V60L variation that co-segregates with inherited dominant and progressive hearing loss DFNA41, and determined how it affects the function of the P2X2 channel.

Methods

We used patch-clamping measurement of HEK293 cells expressing GFP-*P2RX2* to evaluate its physiology. We used confocal microscopy of MDCKII cells expressing GFP-*P2RX2* to quantify its ATP-induced permeability to FM1-43 dye. We performed ballistic transfections and confocal microscopy to examine the targeting properties of GFP-P2X2 in inner ear hair cells and support cells. We examined Auditory Brainstem Recordings and inner ear histology of aging mice and of mice exposed to noise from P2X2 (-/-) knockout colony.

Results

We show that both wild-type and p.V60L mutant P2X2 receptors are preferentially targeted to the apical plasma membranes of hair cells and supporting cells, excluding mislocalization of the heteromeric channel as a cause of deafness in heterozygous individuals. We also show that P2X2 p.V60L receptors have aberrant electrophysiological characteristics, and that co-expression of mutant and wild-

type subunits results in severe reduction (~60%) of permeability of the heteromeric channel to FM1-43 dye, suggesting a dominant-negative effect of the mutant protein on channel function. Moreover, stimulation by ATP evokes an inward current response in cells expressing wild-type *P2RX2*, but not in cells expressing *P2RX2* p.V60L. Finally, we find that loss of function of P2X2 receptors in mouse contributes to noise-related and age-related hearing loss.

Conclusion

Critical functions of P2X2 receptors are abolished by the *P2RX2* p.V60L mutation. These results indicate that *P2RX2* p.V60L is responsible for DFNA41 and that loss of function of P2X2 receptors contributes to both noise-related and age-related hearing loss.

[27] Defining the Pendred Syndrome-DFNB4 Disease Spectrum by High Throughput Sequencing of 101 Candidate Genes Expressed in the Lateral Wall of the Murine Membranous Labyrinthine in Patients with Enlarged Vestibular Aqueducts

Fatemeh Alasti¹, Michael Hildebrand¹, Tao Yang¹, Philine Wangemann², Elliot Shearer¹, Matthew Ritchie³, Gordon Myth³, Richard J.H. Smith¹

¹MORL laboratories, Department of Otolaryngology, University of Iowa, Iowa, USA, ²Department of Anatomy and Physiology, Kansas State University, Manhattan, USA, ³The Walter and Eliza Hall Institute of Medical Research, Melbourne, Australia

Background

Pendred syndrome (PS) and non-syndromic enlarged vestibular aqueduct (EVA) are recessive disorders characterized by sensorineural hearing loss and inner ear malformations that range from Mondini dysplasia to isolated EVA. Mutations in *SLC26A4*, encoding the anion exchanger pendrin, are the major cause of the PS-EVA-DFNB4 disease spectrum. However, in a small percentage of patients carrying only a single mutation in *SLC26A4*, additional mutations have been identified in cis- and trans- regulatory elements of *SLC26A4* (its promoter and the transcriptional regulator *FOX11*), as well as in the potassium channel *KCNJ10*.

Methods

To identify additional genes that may interact with pendrin, we have used a microarray-based strategy to quantitate gene expression in the lateral cochlear wall in mice with a targeted deletion of *Slc26a4* (*Slc26a4*^{-/-} mutants). To select candidate genes for further study, network analysis was used to define gene-gene correlations based on expression data, filtering for all possible interacting partners of *SLC26A4*, *FOX11* and *KCNJ10*. We also included genes implicated in murine deafness for which no human counterpart has been identified (Heatmap database).

Results

Targeted genomic enrichment has been used to capture all coding sequence of genes on our candidate list. The genes included on the optimized platform, which we call EVASeq, are composed of potassium channels, sodium channels, solute carriers, carbonic anhydrases, and some genes related to ATP catalysis. In addition, we have included 3 known EVA genes, 4 known deafness genes and some genes with other functions. To comprehensively define the EVA phenotype, all patients with EVA and one or no mutations in *SLC26A4* are being screened for variants in both EVASeq genes and OtoSCOPE genes. Data analysis is performed using a locally installed Galaxy framework running a custom pipeline for variation annotation.

Conclusion

The results of this study will provide novel insight into the PS-EVA-DFNB4 disease spectrum.

Targeted gene categories included on EVASeq	#
Potassium Channel genes	18
Sodium Channel genes	4
Solute Carrier genes	20
Carbonic Anhydrase genes	9
Other Trans-membrane genes	7
ATP Catalyzes	4
Known EVA genes	3
Known deafness genes	4
Others	33

28 Mutation of *SLC45A3* in Familial and Sporadic Menière's Disease

Colleen A. Campbell¹, Benjamin J. Boese², Charley C. Della Santina³, Cheng Li⁴, Nicole C. Meyer¹, Lauren T. TeGrootenhuys¹, Jennifer Webster⁵, Dietrich A. Stephan⁶, Hossein Najmabadi⁷, Ahmad Danashi⁷, Israt Jahan¹, Bernd Fritzscht¹, Karin Fredrickson², Andrew P. May⁸, Bruce J. Gantz¹, John P. Carey³, Lloyd B. Minor³, Marlan R. Hansen¹, Tim T. Harkins^{9,10}, Richard J.H. Smith¹
¹University of Iowa, ²454 Life Sciences, ³The Johns Hopkins University, ⁴Harvard School of Public Health, ⁵Translational Genomics Research Institute, ⁶The Institute For Individualized Health, ⁷Genetics Research Center, University of Social Welfare and Rehabilitation Sciences, Tehran, Iran, ⁸Fluidigm Corporation, ⁹Roche Applied Science, ¹⁰Life Technologies

Background

Menière's disease (MD) is a complex idiopathic disorder of the inner ear characterized by the symptom triad of vertigo, sensorineural hearing loss and tinnitus. Its incidence varies around the world and is estimated at 1-2 per 1,000 Caucasian individuals. Most cases of MD are sporadic although 5-14% of individuals report a family history in which MD segregates as a dominant but incompletely penetrant disease. To date, a genetic contribution to sporadic and/or familial MD has not been identified reflecting the challenges that complex diseases present to causative gene discovery.

Methods

We completed linkage analysis in a large family segregating MD and confirmed genetic findings in 570 patients with sporadic MD. Expression of the gene and its encoded protein in the membranous labyrinth were defined by in situ hybridization and immunohistochemistry.

Results

The genome-wide linkage scan defined a candidate interval on 1q32 that segregated with the MD phenotype. Targeted exon capture and pyrosequencing of coding sequence within the interval identified a 36-bp deletion in *SLC45A3*. We found the identical deletion in five of 570 patients with sporadic MD. In situ hybridization and immunohistochemistry confirmed that *SLC45A3* and its encoded protein, Prostein, are expressed in the cochlea and endolymphatic sac.

Conclusion

Through the use of two complementary human genetics approaches – 1) segregation analysis with targeted-sequence capture and massively parallel sequencing; and, 2) candidate gene sequencing in a large MD cohort as a test of the common-disease-rare-variant hypothesis – we have identified *SLC45A3* as the first gene causally related to MD. A deletion in *SLC45A3* is found in 1% of persons with MD across five populations. The encoded protein, Prostein is expressed in the cochlea and endolymphatic sac where it is hypothesized to play a role in osmotic regulation. (This research was supported in part by a grant from the American Otological Society (RJHS).)

29 The Static Force Dependence of Sound - Transmission Efficiency in Round Window Stimulation

Hannes Maier¹, Rolf Salcher¹, Burkard Schwab¹, Thomas Lenarz¹

¹Medizinische Hochschule Hannover

Background

The Direct Acoustic Cochlea Stimulator (DACS, Phonak Acoustic Implants) is intended to stimulate the cochlea directly by a piston. An alternative approach to the round window (RW) is successfully done with other devices, having the advantage of being independent of the presence of any middle ear structure. Here we investigate the impact of static force applied to the RW on actuator output and performance.

Methods

The obtainable maximum equivalent sound pressure output of round window stimulation was determined experimentally in fresh human temporal bones (TBs) in analogy to the ASTM standard (F2504.24930-1).

First the stapes footplate (SFP) displacement in response to sound applied to the external ear canal was determined. ASTM compliant TBs were implanted with the actuator axis perpendicular to the RW membrane. The stimulation was performed by means of a prosthesis with a spherical tip (\varnothing 0.5mm) attached to the actuator as interface to the RW membrane.

SFP vibration in response to actuator stimulation was measured in a series of positions relative to the RW membrane. Starting at a position without contact to the RW, the position of the actuator was moved in increments of 50 μ m into the RW membrane and the resulting axial static force load was determined. From the SFP response to sound and actuator stimulation the achieved equivalent sound pressure level at the tympanic membrane was calculated for each step.

Results

10 TBs were found within the acceptance range of the ASTM standard and contributed data to further analysis. At moderate axial static force (3.90 ± 0.70 mN; MV, SD) an average sound equivalent sound pressure level of ~ 103 - 120 eq. dB SPL (@ $1V_{rms}$) was found for frequencies ≤ 4 kHz. At higher frequencies (6 - 10 kHz) the achieved output dropped to ~ 90 dB SPL. This static force loading was below the actuator safe operating limit (< 50 mN) and at least a factor 10 below the rupture limit of the RW.

The magnitude of the transfer function from the RW to the SFP increased monotonically with the applied forces (0 to >40 mN), allowing even higher output by increasing the axial load.

Conclusion

Sound transmission efficiency to the RW crucially depends on the static contact force applied to the RW. Our results demonstrate the possibility of round window stimulation with the DACS actuator at moderate static forces with

sufficient output to treat moderate and pronounced sensor neural hearing loss components.

30 Estimating Round Window Vibroplasty Efficiency: A Comparative Temporal Bone Study of Forward and Reverse Ossicular Chain Stimulation

J. Eric Lupo¹, Kanthaiha Koka², Herman A. Jenkins¹, Daniel J. Tollin^{1,2}

¹University of Colorado School of Medicine Department of Otolaryngology, ²University of Colorado School of Medicine Department of Physiology and Biophysics

Background

Mechanical stimulation of the round window membrane (round window vibroplasty, RWV) with an active middle ear implant (AMEI) has demonstrated functional benefit in clinical reports in patients with mixed and conductive hearing losses. Current published standards for objective measurement of AMEI performance are based on stapes velocity in human cadaver temporal bones for AMEIs coupled to the ossicular chain (ossicular chain vibroplasty, OCV). Here, stapes velocity is a reasonable measure of the input to the cochlea via the AMEI because the system is driven in the forward direction. However, these standards may not be applicable when estimating the efficiency of RWV as the stapes or umbo velocities may change in complex ways though stimulation of the cochlea by the round window. Previous work from our lab in an animal model revealed stapes velocity measures underestimate the RWV efficiency for frequencies above 4 kHz compared to cochlear microphonic measurements. In the current study, we sought to expand upon this hypothesis.

Methods

In the current set of temporal bone experiments (N=5), we measured stapes and umbo velocities, H_{sv} and H_{uv} , respectively, via laser Doppler vibrometry in response to acoustic and AMEI generated tone pip stimuli (0.25 to 8 kHz) delivered by OCV and RWV for varying intensity levels. H_{sv} and H_{uv} in RWV and OCV were normalized with the representative acoustic H_{sv} and H_{uv} to estimate the AMEI efficiency in each condition, which was analyzed in 3 frequency ranges (low 0.25-1 kHz, med 1-3 kHz and high 3-8 kHz).

Results

In comparing the efficiency estimated from H_{sv} and H_{uv} in RWV, measurements revealed that the H_{uv} underestimated AMEI efficiency by 10, 6 and 15 dB (low, medium and high frequency ranges, respectively). In OCV, H_{uv} underestimated AMEI efficiency by 5 dB, 13 dB and 21 dB (low, medium and high frequency ranges, respectively).

Conclusion

The vibromechanical energy delivered by RWV measured at the stapes or umbo is subjected to losses from the cochlea and the ossicular chain. Transmission losses are proposed to occur secondary to third window effects within the cochlea in addition to ossicular chain inefficiencies.

With the addition of intracochlear pressure measures, better estimation of efficiency of RWV may be obtained in future studies.

31 Use of Temporal Envelope Cues Recovered from Temporal Fine Structure for Cochlear Implant Users When Original Speech Envelopes Are Severely Degraded

Jong Ho Won¹, Hyun Joon Shim², Christian Lorenzi³, Jay Rubinstein⁴

¹*Dept. of Audiology & Speech Pathology, Univ of Tennessee Health Science Center, Knoxville, TN 37996,*

²*Department of Otolaryngology, Eulji General Hospital, Eulji University, Seoul, 139-231, Korea,* ³*Equipe Audition, CNRS, Universite Paris Descartes, Ecole normale superieure, Paris, 75005, France,* ⁴*V.M. Bloedel Hearing Research Center, University of Washington, Seattle, WA 98195, USA*

Background

Won et al. [J. Acoust. Soc. Am. 132, 1113-1119 (2012)] reported that cochlear implant (CI) sound processor generates recovered amplitude modulation (AM) cues from broad-band speech frequency modulation (FM) and CI users can use these cues for speech recognition in quiet. For commercially available implant processing today, such FM-to-AM conversion is the only mechanism of transmitting FM (i.e., acoustic temporal fine structure, TFS) information for CIs. Therefore it is important to further study the role of FM-to-AM conversion for CI users in various acoustic environments. The present study aimed to determine whether the FM-to-AM conversion mechanism is important for CI users when original speech AM cues are severely degraded.

Methods

Original speech AM cues were degraded by either manipulation of the acoustic signals or of the sound processor. The manipulation of the acoustic signals included the presentation of background noise, simulation of reverberation, and amplitude compression. The manipulation of the sound processor included the change of input dynamic range and the number of channels. For each of these conditions, multiple levels of envelope degradation were tested. Speech perception was measured for CI users and compared for stimuli having both AM and FM information (intact condition) or FM information alone (FM condition). Consonant identification or word recognition were used as speech perception measures.

Results

As original speech envelopes were degraded more, speech perception performance was reduced for both intact and FM conditions, but performance was always better than chance. Performance for intact and FM conditions became similar for stimuli having severe envelope degradation, suggesting that speech perception for CI users in such a challenging acoustic environment could be determined by the use of recovered envelope cues. This is further supported by significant correlations

between speech perception for intact and FM stimuli as well as electrode output measurements.

Conclusion

The present study demonstrates that the envelope cues recovered from speech TFS convey important phonetic information for CI users when they are communicating in an acoustic environment which degrades the original speech envelope cues.

[This work was supported by NIH T32-DC000033 and an educational fellowship from Advanced Bionics Corporation.]

32 Efficient Coding for Auditory Protheses

Zachary Smith¹

¹*Cochlear Ltd.*

Background

Conventional cochlear implant (CI) sound coding strategies (e.g. CIS, ACE) convey information from multiple spectral bands by sampling the temporal envelope of each channel with fixed-rate pulses. We investigated an experimental sound coding strategy, called Fundamental Asynchronous Stimulus Timing (FAST), which employs a sparse, yet temporally precise, representation of temporal envelope. We hypothesized that the FAST strategy would provide better temporal sensitivity to ITD and F0 cues while using significantly less stimulation power than conventional strategies.

Methods

Several types of listening experiments were conducted comparing the ACE and FAST strategies in bilateral and unilateral CI subjects. These include 1) speech understanding in quiet and in noise, 2) ITD sensitivity of speech stimuli, 3) ITD-based spatial release from masking, and 4) F0 sensitivity. Additionally, battery life during take-home usage was examined to compare power consumption across strategies.

Results

Initial results indicate that speech understanding is equivalent across strategies, while FAST provides significantly better ITD sensitivity and ITD-based spatial release from masking. Additionally, subjects reported 2-3 times more battery life with FAST over ACE.

Conclusion

Results suggest that a temporally sparse coding strategy, such as FAST, provides a sufficient representation of speech sounds while allowing for more precise and efficient coding of temporal envelope. This development could lead to better hearing outcomes with CIs and future device miniaturization.

33 Benefits of Intermodal Training for Sound Localization Following Bilateral Cochlear Implantation

Amal Isaiah^{1,2}, Tara Vongpaisal^{2,3}, Andrew King², Douglas Hartley^{2,4}

¹University of Maryland, ²University of Oxford, ³Grant Macewan University, ⁴University of Nottingham

Background

Arguably, cochlear implants (CIs) are the most successful neural prosthesis developed. Although most individuals are fitted with a CI in one ear only, bilateral CIs are increasingly being offered to children with the aim of improving sound localization and speech perception in noise. However, adults with long-term hearing loss are rarely offered bilateral CIs. We developed an animal model of bilateral CI (Hartley et al., 2010) to examine the potential detrimental effects of long-term hearing loss on sound localization following bilateral CI and possible strategies to remediate them.

Methods

Ferrets were fitted with bilateral (n=4) or unilateral (n=4) CIs after either early (n=4) or late (n=4) induction of hearing loss by ototoxic antibiotic injections. They were subsequently assessed for their sound localization accuracy within a free-field environment, using a positive conditioning paradigm. Animals that performed poorly were reassessed after a modified intermodal training paradigm that consisted of localization trials in which visual cues (light flashes) were randomly interleaved with sound-alone stimuli. In acute physiological recordings that followed behavioral assessments, we examined interaural timing difference (ITD) and interaural level difference (ILD) sensitivity of primary auditory cortical (A1) neurons in response to single biphasic current pulses presented binaurally to the intracochlear electrode arrays under direct, computer control.

Results

Compared with normal-hearing ferrets, animals with late-onset hearing loss and bilateral CI performed poorly on the sound localization task. However, these animals performed significantly better than bilaterally implanted ferrets with early-onset hearing loss or animals with unilateral CI. The latter performed no better than chance, regardless of the duration of deafness. Strikingly, intermodal training led to significantly improved sound localization accuracy in bilaterally implanted ferrets with early-onset hearing loss. In these animals, cortical sensitivity to ITDs and ILDs in A1 was much greater than in ferrets that did not receive intermodal training.

Conclusion

Our results show that despite the absence of auditory input during development, intermodal training led to improved sound localization accuracy in animals with bilateral CIs. Our recording data reveal a possible neural substrate for this by showing improved binaural sensitivity of A1 neurons in these animals. These findings support investigation of a similar paradigm for auditory

rehabilitation in human CI users, specifically where current implantation criteria exclude bilateral implantation in individuals with pre-lingual onset of hearing loss.

Supported by the Wellcome and Rhodes Trusts.

34 Early Deafened, Late-Implanted Cochlear-Implant Users Enjoy Listening to Music

Christina Fuller^{1,2}, Lisa Mallinckrodt¹, Bert Maat¹, Deniz Baskent^{1,2}, Rolien Free^{1,2}

¹University Medical Center Groningen, Department of Otorhinolaryngology / Head & Neck Surgery, NL,

²University of Groningen, Graduate School of Medical Sciences (Behavioural & Cognitive Neurosciences)

Background

The early-deafened, late implanted (EDLI) CI users are an only recently implanted, and therefore understudied, group of CI users. The outcomes of implantation are mostly unknown for this group. Therefore, this study evaluated the outcome of implantation in EDLI CI users for the second most important acoustical stimulus next to speech, the self-perceived perception and enjoyment of music. Additionally, the correlations of these measures were explored with the self-reported quality of life, the self-reported everyday hearing ability and a behaviorally measured speech perception test.

Methods

The inclusion criteria for participation were: severe hearing loss at least since preschool (5-7 years of age), implanted > 16 years and > one year of CI-experience. Thirty-seven qualifying EDLI CI users, all patients of our clinic, were sent four questionnaires to quantify: 1) Dutch Musical Background Questionnaire (enjoyment and perception of music); 2) Nijmegen Cochlear Implant Questionnaire (health-related quality of life); 3) Cochlear Implant Functioning Index (auditory related functioning); 4) Speech, Spatial and Qualities of Hearing scale (hearing ability). As a complementary behavioral measure, a speech perception in quiet test (phoneme recognition in meaningful words reported in percent correct) was completed.

Results

Twenty-two EDLI CI users were included. A majority (60%; 12 out of 22) reported music to sound pleasant through their CI. The subjective quality of the sound of music was scored positively. No correlations were observed between the self-reported perception and enjoyment of music, the quality of life, everyday hearing ability and the behavioral scores of speech perception. The self-reported health-related quality of life of the NCIQ and the auditory related functioning of the CIFI were positively correlated with the behavioral measures of speech perception

Conclusion

The overall results indicate that, differently than for post-lingually deafened CI users, the group of EDLI CI users subjectively enjoy the perception of music and rate the quality of music positively. No correlations between the subjective perception of music and the health-related

quality of life, everyday hearing ability and speech perception were shown. An explanation for the absence of correlations could be that this group of CI users rates their perception of music to a different anchor point than the post-lingually deafened adults, which may be attributed to the lack of exposure to music with acoustical hearing. The findings of our study may give additional support for implantation of this special group.

35 Musical Interval Perception with Normal Hearing and Cochlear Implants

Xin Luo¹, Megan Masterson¹, Ching-Chih Wu¹

¹Purdue University

Background

Little is known about cochlear implant (CI) users' ability to perceive pitch intervals (i.e., the size of pitch changes between notes) important for melody recognition. This study systemically investigated musical interval perception of CI users via clinical processors using both subjective and objective tests that are suitable for patients even with little musical experience.

Methods

Subjects were adult CI users (n=6) and normal-hearing (NH) listeners (n=6). Interval size estimation was tested for musical intervals from 1 to 24 semitones using a scale from 1 to 100. Pitch interval discrimination threshold was measured for standard intervals from 0 to 9 semitones using a 2AFC task and an adaptive procedure. Both rising and falling intervals were tested in a high (around 349.2Hz) or a low (around 174.6Hz) pitch range. In the melodic interval adjustment test, subjects adjusted a scaling factor that started from a random value and was applied to all the intervals of a familiar melody to produce the most correct melody. Subjects were also asked to rate the degree that each adjusted melody was in tune.

Results

CI users had poorer performance than NH listeners. Estimated interval sizes were generally a linear increasing function of physical interval sizes in semitones for NH listeners, but a stepwise increasing function for CI users. Estimated sizes increased more rapidly for falling intervals than for rising intervals in the low pitch range, but for rising intervals than for falling intervals in the high pitch range. The pitch interval discrimination thresholds increased as the standard interval increased from 0 to 1 semitone and from 7 to 9 semitones, but were relatively constant for standard intervals from 1 to 7 semitones. There were no consistent patterns in interval discrimination thresholds between falling and rising intervals in the low and high pitch ranges. In the melodic interval adjustment test, NH listeners were sensitive to subtle interval changes and found the melodies with an interval scaling factor of ~1 the most correct. CI users often preferred expanded intervals with scaling factors >1. However, the found scaling factors varied across trials, melodies, and subjects, and seldom produced a completely in-tune melody.

Conclusion

The results revealed significant effects of pitch range and direction on musical interval perception. Subjective estimated interval sizes cannot be explained by objective interval discrimination thresholds. Subjects with better interval discrimination seemed to have better judgments of musical intervals in familiar melodies.

36 Vocal Singing in Prelingually-Deafened Children with Cochlear Implants and Hearing Aids

Li Xu¹, Qiaoyun Liu², Mengchao Zhang², Heather Nutter¹

¹Ohio University, ²East China Normal University

Background

Vocal singing plays an important role in people's social and communicative aspects of daily life. Profoundly deaf children who use cochlear implants or hearing aids frequently have difficulty perceiving and producing discrete pitch patterns. The purpose of the present study is to investigate vocal singing abilities in children with cochlear implants and hearing aids.

Methods

Three groups of participants, aged between 2 and 7 years old, were recruited: (1) nine cochlear implant users, (2) twelve hearing aid users, and (3) ten normal-hearing, age-match children. Each child was asked to sing a familiar song. The fundamental frequency (F0) and duration of each note of the recorded songs was extracted. The sung songs were then compared against the original score based on the following five different metrics: (1) contour direction, (2) compression ratio, (3) mean note deviation, (4) mean interval deviation, and (5) note duration ratio deviation. The first four metrics were pitch-based measures and the fifth one was a rhythm-based measure.

Results

Results showed that children who use cochlear implants and hearing aids performed similarly with each other in pitch- and rhythm-based measures, but the performance was significantly poorer than that of the normal-hearing children.

Conclusion

Either cochlear implant or hearing aid has failed to provide satisfactory rehabilitation to prelingually-deafened children in vocal singing due to inadequate pitch information that is transmitted to the auditory system through the devices.

Work supported in part by a grant from the NIH/NIDCD and research contract from the Advanced Bionics.

37 Is High Intensity Electrical Stimulation Excitotoxic in Hearing Cochleae? Evidence from the Mouse Model

Jonathan Kopelovich¹, Chuka Ifeanyi¹, Barbara Robinson¹, Hakan Soken², Shawn Goodman³, Marlan Hansen¹

¹University of Iowa Department of Otolaryngology Head and Neck Surgery, ²Eskisehir Military Hospital, Department of Otolaryngology, ³University of Iowa Department of Communication Sciences and Disorders

Background

Excitotoxicity after high intensity electrical stimulation is one proposed mechanism for hearing loss seen after cochlear implantation in patients with residual hearing. Consistent with this hypothesis, data from cochleotypic cultures exposed to high intensity electrical current reveal damage at the level of the primary afferent synapse with relative sparing of hair cells.

Methods

33 three month old C57Bl6J mice underwent round window implantation with a platinum wire electrode. 20 of these were exposed to acute electrical stimulation (ES: 100Hz monopolar charge balanced biphasic pulses) at high intensity (eABR saturation). Hearing was tested using ABR and DPOAE pre-implantation and at 1 week. After euthanasia (1 week), cochleae were prepared for either histopathology (5 ES, 4 sham) or immunohistochemistry (15 ES, 9 sham). Contralateral ears were also examined.

Results

Post-implantation ABR thresholds were significantly elevated in sham and electrically stimulated cochleae compared with pre-implantation and contralateral thresholds with a trend towards higher thresholds in electrically stimulated cochleae. DPOAEs were undetectable in cochleae with the highest thresholds. Histology revealed hair cell loss in 2/5 stimulated and 0/4 unstimulated mice. Interestingly, if hair cell loss was evident in the basal turn – it was also evident in the mid cochlea. Currently we are quantifying hair cells, afferent synaptic structures, and neural innervation based on immunolabeling.

Conclusion

C57Bl6J mice suffer a large decrement in hearing (42+/-4dB) after round window implantation – likely due, in part, to the proportionate effect of middle ear effusion relative to size. Loss of hair cells is apparent only in stimulated mice. These data provide support for an “electrotoxic effect” but suggest that only mice lacking significant middle ear effusion (intact DPOAEs) after implantation should be used in future analyses. Work is ongoing to pinpoint the cochlear structures most affected.

38 Effects of Age on the Preservation of Residual Hearing with Cochlear Implants

Andrew Wise^{1,2}, Sam Irving¹, Robert Shepherd^{1,2}, James Fallon^{1,2}

¹Bionics Institute, ²University of Melbourne

Background

Cochlear implant (CI) recipients with residual hearing in their implanted ear receive both electric and acoustic stimulation. As a result, optimal hearing preservation is a major factor in achieving the best possible auditory experience for these patients. However, a small but significant number of CI patients lose their residual hearing following implantation, although the mechanisms of this loss are not clear.

Methods

To determine the effects of age on the preservation of residual hearing, this study evaluated hearing preservation, using auditory brainstem response recordings, in both neonatal (n=8) and adult onset (n=3) partially deaf cats. All animals received approximately 6 months intra-cochlear electrical stimulation from a clinical CI and speech processor, after stabilisation of their systemic aminoglycoside induced partial hearing loss.

Results

All animals had measurable residual hearing in the low- to mid-frequency range (below 8 kHz, apical to the intra-cochlear electrode array) throughout the experiment. There was no significant loss of hearing in the neonatally deafened animals during the chronic stimulation period (paired T-test, p= 0.13). In contrast, the adult onset group exhibited a significant hearing loss of approximately 8 dB (paired T-test, p= 0.03). Interestingly, there was no difference in the severity of the loss between the low- (1 & 2 kHz) and mid-frequency (4 & 8 kHz) regions (t-Test, p = 0.5).

Conclusion

These results indicate that CI use per se, does not result in a significant loss of residual hearing (i.e. no change in threshold for the neonatally deafened group). However, age may be a factor in the preservation of residual hearing with CI use, as a small loss was observed in the adult onset group. These results need to be confirmed with a larger sample size, and confounding factors (such as the total duration of deafness) also need to be further examined.

39 The Effects of Neurotrophins and Chronic Electrical Stimulation Delivered to the Deafened Guinea Pig Cochlea

Andrew Wise^{1,2}, Remy Pujol^{1,3}, Tom Landry^{1,2}, James Fallon^{1,2}, Robert Shepherd^{1,2}

¹Bionics Institute, ²University of Melbourne, ³University of Montpellier

Background

Spiral ganglion neurons (SGNs) in the deafened cochlea undergo continual degeneration ultimately resulting in cell death. The exogenous application of neurotrophins (NTs)

can prevent SGN loss, with the survival effects enhanced by chronic intracochlear electrical stimulation (ES) from a cochlear implant. Furthermore, NT treatment can enhance resprouting of the SGN peripheral processes. However, little is known about the changes to the SGNs that occur following ES and NT treatment. Here we examine the ultrastructural changes to SGNs and their peripheral processes following delivery of brain derived neurotrophic factor (BDNF) and chronic ES.

Methods

Adult guinea pigs (n=14) were deafened using a single application of an aminoglycoside and loop-diuretic. Two weeks later each animal was unilaterally implanted with a scala tympani electrode array containing a cannula for NT delivery. A commercial cochlear implant was used to deliver chronic intracochlear ES over a four week treatment period. Cochleae were collected and prepared for examination on a transmission electron microscope.

Results

Chronic NT treatment was effective in reducing the loss of SGNs and their peripheral processes following deafness. SGN soma in deafened controls exhibited enlarged cytoplasmic vacuoles while the myelin sheath typically remained intact. The peripheral processes were significantly larger in NT treated cochleae, with or without ES, compared to deafened cochleae not treated with NTs ($p < 0.0005$). Finally, resprouting processes were observed within the osseous spiral lamina, the spiral limbus and the scala tympani.

Conclusion

This study has shown that exogenous NT delivery was effective in reducing the retraction of peripheral processes and SGN degeneration that normally occurs following deafness. Degeneration of the SGN soma precedes loss of the myelin sheath. Resprouting of peripheral processes was promoted by NT treatment. Processes were observed within the scala tympani, raising the potential of a direct connection between the SGNs and the electrode array that may improve the nerve-electrode interface.

40 Safety of Intratympanic Gel Polymer Injection for Treatment of Cytomegalovirus-Induced Hearing Loss

Nicholas Jabre¹, Emily Greinwald², Jonette Ward³, Daniel Choo³

¹University of Cincinnati College of Medicine, ²University of Wisconsin, ³Cincinnati Children's Hospital Medical Center

Background

Cytomegalovirus (CMV) is the leading infectious cause of congenital hearing loss, affecting 0.6 per 1000 newborns each year. Intratympanic injection of cidofovir (CDV) can rescue hearing in CMV-infected guinea pigs, but therapeutic benefit is limited by drug loss through the Eustachian tube. Sustained delivery of CDV to the intracochlear space can be accomplished by direct application of drug-infused gel polymer to the round window membrane. However, the safety of this technique

is poorly described. The objective of this study is to determine whether intratympanic delivery of CDV using a gel polymer is a safe treatment for CMV-induced hearing loss.

Methods

Non-infected guinea pigs were injected intratympanically with one of four gel polymer combinations (Gel A, Gel B, Gel A + CDV, Gel B + CDV). Auditory brainstem response measurements were obtained prior to injection and at 21, 28, or 35 days post-injection. Hearing loss was classified as mild (<20 dB), moderate (20-40 dB), or profound (>40 dB) based on decibels lost in post-treatment hearing thresholds. The middle ear and cochlea were then evaluated microscopically for signs of inflammation (edema, cell infiltrate, bleeding). Inflammation was classified as mild (1/3), moderate (2/3), or severe (3/3) based on the number of inflammatory factors present.

Results

Moderate-to-profound high frequency hearing loss and moderate-to-severe ear inflammation were measured in all treated guinea pigs regardless of gel polymer combination used. Hearing loss and inflammation were maximal at day 21 and improved by day 35. However, measurements never returned to pre-treatment baseline.

Conclusion

Intratympanic injection of CDV-infused gel polymer holds great potential as treatment for CMV-induced hearing loss, but has not yet reached an acceptable level of safety. Further research is warranted to develop a safe method of drug delivery that may one day provide treatment for affected infants.

41 Protein Transduction Utilizing Arginine-Rich Cell-Penetrating Peptides Into the Cochlea

Ryosei Minoda¹, Toru Miwa¹, Takao Yamada¹

¹Kumamoto University

Background

Various approaches, including viral vectors, electroporation, microinjection, and liposome encapsulation, have been used to introduce target molecules into the cells to manipulate them. In 1988, Green and Frankel independently discovered that HIV TAT proteins were able to cross cell membranes. Short peptide sequences, such as these, have been referred to as cell-penetrating peptides (CPPs). CPPs are a class of short cationic peptides that are able to traverse the cell membranes in many types of mammalian cells. Many macromolecules have been attached to these peptides and subsequently internalized. The cargo molecules delivered into cells maintain their biological activities. Among CPPs, arginine-rich CPPs have been the most widely studied. We assessed protein transducing abilities of nine-arginine-rich CPP into embryonic inner ears and adult inner ears.

Methods

Ptotein transduciton into the developing inner ear: CD-1 pregnant mouse dams with E11.5 embryos were anesthetized. The uterus was exposed using a low midline laparotomy. EGFP conjugated to nine-arginine peptide (EGFP-9R), or EGFP alone was injected into the otocysts.

Ptotein transduciton into the adult inner ear: Gelatin foam with soaked in EGFP-9R or EGFP alone in was placed at the round window of adult CD-1 mouse cochleae.

Protein transducing abilities was assessed periodically.

Results

In the embryos that underwent EGFP-9R inoculation, EGFP-9R expression was detected in the lining cells in the otocysts and in their vicinity in a diffuse manner. Expression of EGFP-9R was maintained for 12–18 hours after otocystic inoculation. Embryos that underwent EGFP-9R inoculation developed to term normally, and P30 mice that underwent EGFP-9R inoculation showed normal auditory function.

In adult EGFP-9R mice, EGFP-9R expression was detectable in the cochlea upto 36 hours post-treatment.

Conclusion

Ptotein transduciton may provide a useful strategy for delivering a target molecules into embryonic inner ear and/or adult mice inner ear. Ptotein transduciton via the round window membrane may be a potentially useful method for delivering therapeutically relevant molecules into the inner ear.

42 Steroid Treatment Partially Suppresses the Altered Inner Ear Gene Expression in Murine Autoimmune Disease

Dennis Trune¹, Fran Hausman¹, Beth Kempton¹, Dongseok Choi¹

¹Oregon Health & Science University

Background

It has been decades since the first identification of inner ear disorders in systemic autoimmune diseases and their control by glucocorticoids. However, little is known of the mechanisms by which systemic inflammatory diseases cause hearing loss or the molecular impact of steroids on these dysfunctional processes. Although hearing recovery is generally attributed to the immune suppressive functions of glucocorticoids, they also are known to affect inner ear mineralocorticoid-receptor driven processes of ion and water homeostasis. Clarification of these steroid controlled mechanisms in the ear is critical for effective therapeutic control of many forms of hearing loss. Therefore, studies were conducted to assess the inner ear molecular processes at risk in murine lupus and the impact of glucocorticoid treatment.

Methods

Systemic disease and hearing loss develop in autoimmune MRL/MpJ-*Fas*^{pr}/J mice at 3 months of age. Therefore, inner ear gene analyses were conducted on 3.5 week old and 5.5 month old mice, as well as 5.5 month old mice treated systemically with the glucocorticoid prednisolone

for 2 weeks. Inner ears were harvested, RNA extracted, and 6 ear samples for each treatment group processed on the Affymetrix 430 2.0 Gene Chip. Genes for the treated and untreated older mice were statistically analyzed for up or down expression against the young mice.

Results

Approximately 7,500 genes were significantly up or down regulated by systemic disease (FDR $p < 0.05$). If a cutoff of 1.5 fold or more overexpression or 0.67 or less underexpression was applied to these significantly affected genes, there still were 1,303 (up) and 1,029 (down) inner ear genes affected. Steroid treatment reduced this number by approximately 20%. Inflammation related genes and ion homeostasis related genes were examined further since these two mechanisms presumably play a significant role in cochlear function during autoimmune disease. Steroid treatment reduced the number of overexpressed inflammatory genes by 30% and decreased the number of underexpressed ion homeostasis genes by 50%.

Conclusion

Thousands of inner ear genes are affected by systemic autoimmune disease and oral steroids play a role by reversing some of these induced molecular processes. Furthermore, the efficacy of steroids in controlling hearing loss probably involves more inner ear mechanisms than simple immune suppression.

(Supported by NIH-NIDCD R01 DC005593 and ARRA Supplement DC005593-S1)

43 Magnetic Nanoparticles to Deliver Drugs to the Ear

Azeem Sarwar¹, Didier Depireux¹, Reza Basiri¹, Roger Lee¹, Irving Weinberg², Ben Shapiro¹

¹U of Maryland, ²Weinberg Medical Physics

Background

In the inner ear, noise trauma can induce injury and inflammation. The damage should be ideally treated by the timely local delivery of drugs to the affected relevant structures in a limited region of the cochlea. To this end, nanoparticles are a natural candidate because of their biocompatibility, the ability to load them with a variety of drugs, and the promise that they can deliver their payloads without causing additional injury or trauma to the inner ear.

Methods

We are using superparamagnetic nanoparticles with a maghemite core, made biocompatible with a chitosan matrix loaded with fluorescent proteins for visualization. We have characterized the distribution of these particles in the cochlear space as a function of their diameter, duration of exposure to an external magnetic field and other delivery parameters while the particles are being actively steered by a configuration of magnets, either pulling from the contralateral side of the skull or pushing from the ipsilateral side.

Results

We are able to deliver nanoparticles with a remarkably uniform density throughout a target area of the cochlea, thus leading to the hope we can deliver drugs in a targeted, uniform manner at a pre-determined therapeutic level. We have also tested in a rat model the effectiveness of magnetically pushed nanoparticles functionalized with prednisolone in preventing the emergence of hearing loss post-trauma.

Finally, we have also observed the possibility of using the nanoparticles to deliver drugs from the ear canal into the middle ear, with a view to cure or reduce otitis media without the need to administer drugs systemically or to compromise the integrity of the eardrum.

Conclusion

The use of biocompatible magnetic nanoparticles, functionalized with appropriate molecular agents, will lead to the ability to deliver specific drugs at pre-determined concentrations in specific parts of the ear.

44 NIDCD Workshops: Training/Career Development Workshop and Early Stage/New Investigator Workshop

Roger Miller¹, Janet Cyr¹, Shiguang Yang¹, Kausik Ray¹
¹NIDCD

Background

NIDCD will offer two concurrent workshops targeted to two specific audiences with limited experience submitting grant applications to NIH.

Methods

Workshop #1: Applying for NIDCD Training and Career Development Grants.

Workshop #2: Early Stage Investigators (ESI) and New Investigators (NI).

Results

Workshop #1: Applying for NIDCD Training and Career Development Grants.

This workshop will include an overview of research training and career development opportunities appropriate for graduate students, postdoctoral fellows and new clinician investigators. The discussion will include the submission and review of individual NRSA fellowship awards (F30, F31 & F32), as well as the mentored career development awards (K08, K23 & K99/R00). Drs. Janet Cyr and Shiguang Yang will lead the presentation.

Workshop #2: Early Stage Investigators (ESI) and New Investigators (NI).

If you have plans to submit an R01 application for the first time, or have been unsuccessful with past R01 applications, then this workshop is for you. We will begin with a quick overview on how grant applications are processed including: assignment to NIDCD; preparation for review at different study sections; and when to contact staff during this process. Our goal is to provide information

that facilitates a successful grant submission as a new (NI) or early stage investigator (ESI), use of the NIH Research Grant (R01), Exploratory/ Developmental Research Grant (R21), SBIR/STTR applications from a small business, and the NIDCD Small Grant Award (R03). Other issues will be addressed during the question/answer session. Drs. Roger Miller and Kausik Ray will lead the presentation.

Conclusion

These two sessions are intended for graduate students, postdoctoral fellows, new clinician investigators, and Early Stage Investigators (ESI) and New Investigators (NI).

Available funding mechanisms appropriate for new investigators will be discussed.

45 Protective Mechanism of the Outer Hair Cells from Traumatic Noise by Prior Whole-Body Heat Stress

Michio Murakoshi¹, Yoko Kitsunai¹, Naohiro Yoshida¹, Koji Iida¹, Shun Kumano¹, Toshimitsu Kobayashi¹, Hiroshi Wada¹

¹Tohoku University

Background

The outer hair cell (OHC) motility results in cochlear amplification, leading to high sensitivity and sharp frequency selectivity of mammalian hearing. Unfortunately, however, OHCs are vulnerable to acoustic overstimulation. The OHCs have been reported to be protected from such traumatic exposure by prior sublethal conditioning, such as nontraumatic sound exposure, heat stress, etc. However, the mechanisms underlying conditioning-related cochlear protection remain unknown. In the present study, therefore, the effects of whole-body heat stress on the structure and function of OHCs were analyzed.

Methods

CBA/JNCRj strain male mice, aged 10–12 weeks (25–30 g), were used. The animals were anesthetized and placed in an aluminum boat floating in a hot water bath (46.5°C) to raise their rectal temperature up to 41.5°C. It was maintained at that temperature for 15 min. To evaluate the effects of heat stress on the structure of OHCs, Young's modulus of OHCs, the amount of filamentous actin (F-actin) in OHCs and the expression level of heat shock protein 27 (HSP27) in the cochlea were measured before and after heat stress by atomic force microscopy (AFM), confocal laser scanning microscopy (CLSM) and Western blotting, respectively. To evaluate the effects of heat stress on the function of OHCs, distortion product otoacoustic emissions (DPOAEs) and the expression level of prestin in OHCs were evaluated before and after heat stress by an ER-10C acoustic system and CLSM, respectively.

Results

Heat stress caused an increase in Young's modulus of OHCs at 3–6 h after its application (Fig. 1) along with an increase in the amount of F-actin (Fig. 2). Heat stress was

also found to increase HSP27 in the cochlea and to enhance the DPOAE amplitude. On the other hand, the expression level of prestin was not changed by heat stress. These results suggest that heat stress induces HSP27 expression and thus increases F-actin in OHCs, increasing their stiffness, resulting in protection of the ear against noise induced hearing loss.

Conclusion

Conditioning with heat stress structurally modifies OHCs so that they become stiffer due to an increase in the amount of F-actin. As a consequence, OHCs possibly experience less strain when they are exposed to loud noise, resulting in protection of mammalian hearing from traumatic noise exposure. In contrast with F-actin, heat stress did not affect the amount of prestin.

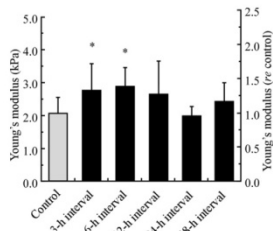


Fig. 1. The mean and standard deviation of Young's moduli of the apical-turn OHCs in the control group ($n = 10$) and the anesthesia + heat groups with 3-h ($n = 13$), 6-h ($n = 5$), 12-h ($n = 8$), 24-h ($n = 7$) and 48-h ($n = 12$) intervals. Statistical analysis indicated significant differences between the control group and the anesthesia + heat groups with 3-h and 6-h intervals, as shown by asterisks ($P < 0.05$ by Student's t -test).

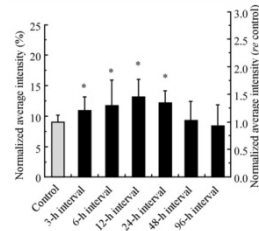


Fig. 2. The mean and standard deviation of the normalized average intensities of F-actin labeling in the control group ($n = 13$) and the anesthesia + heat groups with 3-h ($n = 10$), 6-h ($n = 8$), 12-h ($n = 6$), 24-h ($n = 10$), 48-h ($n = 10$) and 96-h ($n = 8$) intervals. Statistical analysis indicated significant differences between the control group and the anesthesia + heat groups with intervals of 3 h, 6 h, 12 h and 24 h, as shown by asterisks ($P < 0.05$ by Student's t -test).

46 Dose-Dependent D-Methionine Administration Significantly Reduces Permanent Impulse Noise-Induced Hearing Loss (NIHL) in Chinchillas

Kathleen Campbell¹, Robert Meech¹, Daniel Fox¹, Tim Hargrove¹, Steven Verhulst¹

¹Southern Illinois University School of Medicine

Background

In previous animal studies, D-methionine (D-met) demonstrated otoprotection from drug-induced (cisplatin and aminoglycosides) and NIHL secondary to steady state noise exposures. In small scale Phase 1 and 2 clinical trials, D-met also protected from radiation-induced oral mucositis and cisplatin-induced hearing loss. D-met markedly reduced NIHL in animals when administered prior to and during steady state noise exposures or when first started 1 to 7 hours after these noise exposures. The purpose of this study is to determine the lowest D-met dose that is maximally effective in preventing impulse noise-induced hearing loss with noise exposures analogous to repeated M16 rifle fire. Currently we are preparing for clinical trials with the Department of Defense to prevent hearing loss for impulse noise exposures. If D-met prevents or reduces impulse noise-induced hearing loss, it could attenuate one of the most common causes of NIHL in soldiers.

Methods

Cohorts comprised five groups of 3 year old male Chinchillas laniger with ten animals per group. Groups

received intraperitoneal injections of D-met at 0 (saline control), 25, 50, 100, or 200 mg/kg/dose every 12 hours beginning 2.5 days before and ending 2.5 days after noise exposure. Animals were exposed to simulated M-16 weapon fire at 155 dB peak SPL (150 repetitions at 2/s). ABR thresholds were tested at baseline and on post-noise exposure day 21. Left and right ear thresholds were determined using tone-bursts centered at 2, 4, 6, 8, 14, and 20 kHz frequencies. Cochleae were harvested after the 21 day ABR and percentage of remaining outer hair cells measured.

Results

Significant reduction in ABR threshold shift at $p \leq 0.05$ occurred at 8 and 20 kHz for 100 and 200 mg/kg/dose groups and at $p \leq 0.01$ for 14 kHz in the 100 mg/kg/dose group. Hair cell analyses are in progress.

Conclusion

D-met can significantly reduce ABR threshold shift resulting from simulated M-16 weapon fire over a range of auditory frequencies and D-met dosing levels with 100mg/kg appearing to be optimal.

NIHL reduces troop redeployment and survivability /lethality on the battlefield. Current US military costs exceed 2 billion dollars annually D-met may be able to reduce NIHL in our military populations.

Acknowledgements: Funding: DoD Army Research and Materiel Command, #11342008.: We thank Simon Martin, Danielle Hummel for data collection.

47 Auditory Phenotypes of 129S6 and CBA Mice After High-Intensity Noise Exposures

Ayaka Iwata^{1,2}, Carol Robbins^{1,2}, Bruce Tempel^{1,2}

¹University of Washington, Department of Otolaryngology-HNS, ²V.M. Bloedel Hearing Research Center

Background

Noise-induced hearing loss (NIHL) is a major health problem, and its effects are debilitating and irreversible. Using genetically homogenous mice as our animal model reduces inter-animal variability, and enables us to systematically assess inter-strain differences in vulnerabilities to NIHL. These phenotypic differences can be utilized to isolate the underlying genes involved. The inbred mouse strain 129S6/SvEvTac (S6) has been reported to be a remarkably noise resistant (NR) strain when exposed to noise levels that cause significant permanent threshold shifts (PTS) in the good hearing CBA/CaJ (CB) strain. Hirose and Liberman, 2003, assessed the noise exposure damage present when CB were exposed up to 116 dB SPL, which we use for comparison. Here we aimed to characterize the true extent of the NR phenotype in S6 by examining the effects of severe high-intensity exposure levels that cause dramatic PTS.

Methods

30 day old male unrestrained and unanesthetized S6 or CB mice were exposed to an octave-band noise (8-16 kHz) at high intensities (109 dB SPL, 115 dB SPL, or 118dB SPL) for two hours. A pre-conditioning stimulus was given immediately prior in order to avoid audiogenic seizure and death. Noise-induced PTS were assessed using distortion product otoacoustic emissions (DPOAEs) and auditory brainstem responses (ABRs). Mice were tested one or two days prior to noise exposure for baseline, then again one and two weeks after the exposure. Inner ears were harvested after the final tests. Cochleas were then fixed and the organ of Corti was isolated from its bony confinement by fine whole-mount dissections. The tissue was then stained for immunohistochemical studies.

Results

After exposure to 118 dB SPL, the most intense acoustic trauma delivered in this study, both S6 and CB mice experienced 60-80 dB threshold shifts. Halving the power to 115 dB SPL resulted in a similar severe PTS in CB, but caused S6 mice to split into two different sensitivities. Half of the S6 pool endured a dramatic PTS, but the other half experienced partial acoustic protection. Hearing loss from 109 dB SPL exposure was less traumatic. The pattern of hair cell loss seen at the histological level is consistent with the degree of injury seen.

Conclusion

Our findings characterize the striking noise resistance phenotype of S6 mice by delivering noise exposures more intense than those used to date to study this strain.

Support: DoD DM102092; HHMI 80-0380

48 Mitochondrial Peroxiredoxin 3 Regulates Hair Cell Survival in the Cochlea

Hong-Wei Zheng¹, Fu-Quan Chen¹, Jochen Schacht², Su-Hua Sha¹

¹Department of Pathology, Medical University of South Carolina, ²Kresge Hearing Research Institute, University of Michigan

Background

Mitochondrial peroxiredoxin 3 (Prx3) regulates intracellular redox balance and stress-induced apoptosis. Cochlear damage induced by traumatic noise, aminoglycosides and aging has been suggested to be linked to reactive oxygen species, disturbing cellular homeostasis. We therefore investigated the role of Prx3 in acquired hearing loss.

Methods

Auditory brainstem responses as measure of auditory function - Anti-Prx3 staining of surface preparations to determine expression of Prx3 in outer hair cells - Delivery of Prx3 siRNA to the round window via intra-tympanic application - Prx3 protein and mRNA levels from organ culture explants measured by Western blot and quantitative RT-PCR - hROS formation by fluorescence staining.

Results

In vivo, Prx3 increased transiently in mouse cochlear hair cells after traumatic noise, kanamycin treatment, or with progressing age before any cell loss occurred; when Prx3 declined, hair cell loss began. Maintenance of high Prx3 levels with the radical scavenger 2,3-dihydroxybenzoate prevented kanamycin-induced hair cell death. Conversely, reducing Prx3 levels with Prx3 siRNA increased the severity of noise-induced trauma. In explants of the murine organ of Corti, reactive oxygen species and levels of Prx3 mRNA and protein increased concomitantly at early times of gentamicin challenge. When Prx3 levels declined after prolonged treatment, hair cells began to die. The radical scavenger p-phenylenediamine maintained Prx3 levels and attenuated gentamicin-induced hair cell death. Gentamicin treatment also elevated levels of the transcription factor c-Myc, which targets the Prx3 gene, while a c-Myc inhibitor abolished the effect of gentamicin on both Prx3 mRNA and protein.

Conclusion

Our results suggest that Prx3 is up-regulated via c-Myc in response to oxidative stress and that maintenance of Prx3 levels in hair cells is a critical factor in their susceptibility to inner ear insults.

The research project described was supported by R01 grants DC009222 (to SHS) and DC-03685 (to JS) from the National Institute on Deafness and Other Communication Disorders, National Institutes of Health.

49 Prestin Regulation in Residual Outer Hair Cells After Noise-Induced Hearing Loss

Anping Xia¹, Rosalie Wang¹, William Clifton², Patrick Raphael¹, Simon Gao¹, Fred Pereira², Andrew Groves³, John Oghalai¹

¹Dept. of Otolaryngology - Head and Neck Surgery, Stanford University, ²Bobby R. Alford Dept. of Otolaryngology - Head and Neck Surgery, Baylor College of Medicine, ³Dept. of Neuroscience, Baylor College of Medicine

Background

The outer hair cell (OHC) motor protein prestin is necessary for electromotility. Previously, we found that OHC prestin expression was higher in Tecta transgenic mice with hearing loss. In the present study, we sought to determine the effects of noise-induced hearing loss on prestin expression.

Methods

We exposed cohorts of 5-6 week-old CBA mice to white noise (4-20 kHz at 100 dB SPL) for 4 hours.

Results

We assessed the cochlear epithelium by immunolabeling for prestin and myosin VIIa, and observed the expected pattern of OHC loss at the basal end of the cochlea. We then quantified prestin and found a significant increase in the fluorescence intensity from residual OHCs within the

basal region of noise-damaged cochleae. We used whole cochleae preparations to measure prestin protein and found that the prestin/myosin VIIa ratio was elevated 1.7 fold at 7 days after noise exposure. We also measured mRNA expression changes in noise-damaged mice at 0.5, 3, 7 and 28 days after noise exposure. Noise exposure caused a significant increase in the prestin/myosin VIIa ratio. This effect was first detected at day 7 and persisted through day 28. ABR and DPOAE thresholds were elevated 30-40 dB immediately after noise. While most of the threshold shift recovered within 3 days, there was additional gradual recovery over the next month. At the 12 kHz cochlear location, where no OHCs were lost, the threshold and sharpness of masked tuning curves demonstrated full recovery by day 7. At the 32 kHz location, where partial OHC loss occurred, a near-complete recovery of tuning curve threshold and sharpness was found by day 7.

Conclusion

Taken together, we conclude that OHC prestin mRNA begins to become up-regulated >3 days after noise exposure and that prestin protein and cochlear amplifier function improve in an associated fashion with it. Prestin regulation may serve to partially compensate for OHC loss.

50 Renexin as a Rescue Regimen for Noise Induced Hearing Loss

Shi-Nae Park¹, Sang A Back², Hong Lim Kim³, Dong Kee Kim², Kyoung-Ho Park², Sang Won Yeo²

¹The Catholic University of Korea, ²Department of Otolaryngology-Head & Neck Surgery, ³Laboratory of Electron Microscopy, Integrative Research Support Center, The Catholic University of K

Background

Renexin (SK Chemicals Co Ltd, Korea) is a new combination drug of ginkgo biloba extract and cilostazol, which is known to have neuroprotective effect, anti-apoptotic effect and blood flow improvement effect. To evaluate the effect of Renexin on rescuing noise-induced hearing loss, we compared hearing and cochlear morphologies among different concentrations of Renexin-administered mice groups and control groups after noise exposure.

Methods

Mice were exposed to white noise at 110-dB sound-pressure level for 60 minutes at the age of 1 month. Different concentrations of Renexin (90mg/kg and 180mg/kg) were administered per oral for seven consecutive days after noise exposure. Auditory brainstem responses and distortion product otoacoustic emissions (DPOAE), cochlear pathology including efferent nerve endings were evaluated and compared among Renexin groups and control groups (noise and normal controls). Western blotting was performed to observe α -synuclein expression in the cochlea.

Results

Compared with mice of noise control, 90mg/kg and 180mg/kg Renexin groups showed less severe hearing loss from low to high frequencies at 7 days after noise exposure and their effects of rescuing hearing loss were dose-dependent manner. Various cochlear morphologic studies showed the far less severe outer hair cell damages in 180mg/kg Renexin-group compared to noise control group. Even 90mg/kg Renexin group showed the rescuing effect on outer hair cells after noise exposure. Efferent nerves under outer hair cells were more prominent in Renexin-groups compared to noise control group. Immunohistochemistry and western blot assay of α -synuclein also demonstrated a stronger expression of this synaptic vesicular protein in Renexin groups in dose dependent manner.

Conclusion

Renexin seemed to rescue hearing loss and cochlear damage after noise exposure in mice. Further studies to investigate the mechanism of Renexin on rescuing noise induced hearing loss will be necessary.

51 The Auditory System Functions in a Circadian Manner

Inna Meltser¹, Gabriella Schmitz Lundkvist¹, Vasiliki Basinou¹, Barbara Canlon¹

¹Karolinska Institutet

Background

Circadian rhythmicity is essential for many bodily functions. A master clock is found in the hypothalamus, the suprachiasmatic nucleus (SCN), and is known to synchronize and coordinate rhythms to regulate various physiological functions including metabolism, inflammatory responses, oxidative reactions, feeding, sleep-wake patterns and the hypothalamic pituitary adrenal axis. Since the sensitivity of the auditory system can be modulated by the hypothalamic pituitary adrenal (HPA) axis and glucocorticoid receptors our working hypothesis is that the auditory system may function in a circadian manner.

Methods

Circadian oscillations of the PER2 protein were performed using tissues obtained from knock-in PERIOD2::LUCIFERASE (PER2::LUC) transgenic mice with a C57/B6 background. Ethical permission was granted by Stockholm's Norra Djurförsöksetiska Nämnd. Cochlear explants were placed under photomultiplier tube detector assemblies mounted inside a light tight incubator at 36.5°C. Acoustic trauma was free field broadband noise at 6 - 12 kHz at intensity of 100 dB SPL for 1 h. Auditory sensitivity was assessed with auditory brainstem response (ABR) thresholds for the frequency of 6, 12, 16 and 24 kHz. The equipment for the ASR apparatus consisted of two startle chambers (SR-LAB; San Diego Instruments, San Diego, CA).

Results

Functional auditory responses were found to vary with the time of day. The amplitude of the acoustic startle response

was higher and latencies shorter during day compared to night. Moreover, a greater loss of auditory function was found when noise trauma was delivered at night. The isolated peripheral auditory organ, the cochlea, was shown to have a self-sustained circadian rhythmicity of the expression of the clock gene protein product PERIOD2 that changed during development. Glucocorticoids were shown to synchronize the rhythm of the mouse cochlea-clock and to kick-start oscillations in the central auditory structures, cochlear nucleus and inferior colliculus. The expression of the interleukin-6 and the neurotrophic factor BDNF in the cochlea was differentially altered after noise trauma applied during day versus night, which may be associated with the subsequent hearing loss.

Conclusion

The fact that the auditory system shows circadian rhythmicity is an important finding with clinical importance since noise-induced hearing disorders are an important public health issue and are exponentially increasing in the human population.

52 Auditory Responses in Bats Show Strong Resistance to Noise Impairment Compared to Gerbils

James Simmons¹, Andrea Simmons¹, Jonathan Barchi¹, Hiroshi Riquimaroux², Keizo Fukushima², Kota Kobayashi²
¹Brown University, ²Doshisha University

Background

Echolocating big brown bats are active at night and use their hearing as the dominant sense for orienting, for finding food, and for navigating through complex surroundings such as dense vegetation. Their near-total, moment-to-moment reliance on hearing in the 10-100 kHz range makes them potentially vulnerable to hearing impairment from intense sound exposures and from aging. Their own sonar broadcasts are ~120-130 dB SPL, but there are known mechanisms that reduce self-stimulation to about 75-75 dB SPL per sound. However, they also fly frequently in their roosts or in swarms, where they experience prolonged, virtually continuous exposure to ~100 dB SPL levels from other bats without evident impairment of echolocation. Further, bats have a very long lifespan of 20 years or more and yet they retain their sonar-guided abilities in the wild and in laboratory psychophysical tests.

Methods

To explore the implications of the bat's acoustic lifestyle on protection of hearing, we compared big brown bats and gerbils for the impact of noise exposure on the magnitude of neural responses (cochlear microphonics, local field potentials, evoked potentials) to short, wideband frequency modulated (FM) stimuli.

Results

In experiments with broadband noise exposure equated for hearing range (20-100 kHz for bats, 3-30 kHz for gerbils), auditory responses to all FM sounds in gerbils decline in amplitude by up to 20 dB 1 minute after exposure and

remain low for at least one hour. Recovery is complete after 10-12 hours. In bats, auditory responses to downsweeping FM sounds decline by 3-5 dB at 1 minute following exposure but have fully recovered by 30 minutes. Responses to upsweeping sounds are not affected.

Conclusion

The bat's critical reliance on hearing for echolocation may have led to enhancement of its auditory protective mechanisms over the entire lifespan.

53 Lack of Brain-Derived Neurotrophic Factor in the Cochlea But Not in the Brain Hampers Inner Hair Cell Synapse Physiology, But Protects Against Noise Induced Afferent Fiber Loss

Marlies Knipper¹, Annalisa Zuccotti¹, Stephanie Kuhn², Stuart L. Johnson², Christoph Franz¹, Wibke Singer¹, Dietmar Hecker³, Hyon-Soon Geisler¹, Iris Köpschall¹, Karin Rohbock¹, Katja Gutsche⁴, Julia Dlugaiczek³, Bernhard Schick³, Walter Marcotti², Lukas Ruettiger¹, Thomas Schimmang⁴

¹University of Tuebingen, Tuebingen Hearing Research Center, ²Department of Biomedical Science, University of Sheffield, ³Department of Otolaryngology, Saarland University Hospital, ⁴Instituto de Biología y Genética Molecular, Universidad de Valladolid

Background

The precision of sound information transmitted to the brain depends on the transfer characteristics of the inner hair cell (IHC) ribbon synapse and its multiple contacting auditory fibers. We found that brain derived neurotrophic factor (BDNF), so far assumed to maintain spiral ganglia neuron survival, differentially influences IHC characteristics in the intact and injured cochlea.

Methods

We generated conditional knockout mice in combination with exocytosis measurements, calcium currents, auditory brainstem responses, ABR wave analysis, high resolution confocal microscopy.

Results

Using conditional knockout mice (BDNFPax2 KO) we found that resting membrane potentials, membrane capacitance and resting linear leak conductance of adult BDNFPax2 KO IHCs showed a normal maturation. Likewise, in BDNFPax2 KO membrane capacitance (ΔC_m) as a function of inward calcium current (ICa) follows the linear relationship typical for normal adult IHCs. In contrast the maximal ΔC_m , but not the maximal size of the calcium current, was significantly reduced in high frequency but not low frequency cochlear turns correlated with a loss of IHC ribbons in these turns and a reduced activity of the auditory nerve (ABR wave I). Remarkably, a noise-induced loss of IHC ribbons, followed by reduced activity of the auditory nerve and reduced centrally generated wave II and III observed in control mice, was prevented in equally noise-exposed BDNFPax2 KO mice. This did not occur

when BDNF was deleted in a mice model that lead to deletion of BDNF in central brain neurons.

Conclusion

Data describe a differential beneficial and harmful role of BDNF in the intact, respectively injured cochlea with dramatic impact on central sound processing that are discussed in a more widespread context of brain disorders. Supported by a grant from the Marie Curie Research Training Network CavNET MRTN-CT-2006-035367, Deutsche Forschungsgemeinschaft, grant DFG-Kni316-8-1

54 Investigating Long-Term Recreational Noise-Induced Hearing Loss in an Adult Population

Robert Mackinnon¹, Heather Fortnum¹, Dave Moore^{2,3}, Marcel Vlaming¹, Christian Fullgrabe²
¹NIHR Nottingham Hearing Biomedical Research Unit, Nottingham, UK, ²MRC Institute of Hearing Research, Nottingham, UK, ³Cincinnati Children's Hospital Medical Center, Cincinnati, OH

Background

There is a great deal of concern about the risk of noise-induced hearing disturbances caused by listening to loud music. While there is clear evidence to support short term hearing disruption in some circumstances (Zhao et al. 2010), there is little, and mixed, evidence to support longer-term or permanent damage (Meyer-Bisch 1996, Tambs et al. 2004). A large scale study specifically investigating long-term recreational music exposure and any relationship between loud music exposure and hearing loss, tinnitus or hyperacusis is reported.

Methods

Participants were invited to complete two tasks using their home computer: First, an online English language speech-in-noise test. This was a modified digit triplet test presented at this conference last year (Vlaming et al. 2012). This test was optimised to detect high-frequency hearing loss, such as that caused by noise exposure; Second, a newly developed online long-term retrospective self-report questionnaire. The questionnaire contained questions on participants' hearing, otological history, and most importantly asked for a life-history of their exposure to loud music. We anticipated recall of such a life history would be difficult. The use of a questionnaire tool called a "calendar instrument" has been shown to be useful in some interviewer-administered retrospective surveys (eg. Belli et al. 2007). As no studies were identified where a calendar instrument was used in an online, self-report context, we also compared a questionnaire using the instrument to a "standard" questionnaire in a set of two experiments (n=212). In the main study, commencing in October 2012, self-reported music exposure is compared to both hearing test result and self-rated hearing questions, whilst controlling for other relevant factors.

Results

In the comparison of the questionnaire types, participants rated the questionnaires as being equivalent for difficulty,

ease of use, and accuracy of recall ($p < 0.001$). They rated the calendar instrument as being more than moderately helpful. No difference in data reliability was detected, but significantly more exposure was reported using the calendar ($p < 0.05$), a finding taken to indicate better recall of exposures in other calendar instrument studies. Further analysis is continuing in 2012.

Conclusion

In addition to the above data, we will present results of the main screening experiment that will show the relationship between loud music exposure and hearing disturbances.

55 One Critical Subcellular Damage That Switches Noise-Induced Temporary to Permanent Threshold Shift

Ruqiang Liang¹, Han Zhou¹, Guangjie Zhu¹, Debin Lei¹, Leqing Wu², Jianxin Bao¹
¹Washington University, ²Baylor College of Medicine

Background

Noise is the most common occupational and environmental hazard. Noise-induced hearing loss (NIHL) is the second most common form of sensorineural hearing deficit, after presbycusis. Low levels of noise exposure cause temporary threshold shift (TTS) only but not permanent threshold shift (PTS). Although promising approaches have been identified for reducing both TTS and PTS, currently there are no effective medications to prevent NIHL. Development of an efficacious treatment has been hampered by unknown cellular and molecular pathways involved in NIHL.

Methods

CBA/CaJ mice at 2 months old were exposed for 2 hours to 8-16 kHz octave band noise at 90 or 93 dB sound pressure level (SPL). There were also a no-noise control group and a group treated with zonisamide (120 mg/kg) just before the 93 dB noise exposure. TTS and PTS were measured one day and two weeks after noise exposure, respectively. Whole-mount fluorescent immunostaining of presynaptic ribbons by C-terminal binding protein 2 (CtBP2) and postsynaptic glutamate receptor 2/3 (GluR2/3) patches were analyzed by confocal microscopy and quantified by the imaging analysis software Volocity and our own custom program.

Results

Compared to the noise exposure at 90 dB causing only TTS, PTS was observed after exposure to 93 dB noise. The number of IHC ribbons and GluR2/3 patches was only slightly decreased after 90 dB noise exposure (0.78 and 0.59, respectively, averaged across 5, 10, 20, 28.3, and 40 kHz regions); while a significant synaptic loss was observed after 93 dB noise exposure (3.44 and 3.31, respectively, on average). Prophylactic administration of zonisamide reversed this synaptic loss after 93 dB noise exposure back to the loss similar to the 90 dB noise. Most importantly, no PTS was observed in the zonisamide-treated 93 dB noise group with reduced synaptic loss. Zonisamide saved about two ribbon synapses between

IHC and SGNs on average across five frequencies examined.

Conclusion

Differences in cellular damage between TTS only and PTS have been observed, however, it was unknown what kind of cellular damage was critical for this difference. We have discovered that one critical difference between TTS only and PTS is a significant loss of synapses between inner hair cells (IHCs) and spiral ganglion neurons (SGNs) in cochleae with PTS, and this cellular damage can be prevented by a T-type calcium channel blocker (i.e., zonisamide).

56 Mmp7 Knock-Out Potentiates Noise-Induced Functional Loss of the Cochlea

Qunfeng Cai¹, Bo Hua Hu¹

¹State University of New York at Buffalo

Background

Metalloproteinases (MMPs), a family of zinc-dependent endopeptidases, play an important role in degrading the extracellular matrix. We recently reported the involvement of this gene family in noise-induced cochlear pathogenesis. The study showed that Mmp7 was not constitutively expressed in the rat cochlear sensory epithelium, but was significantly upregulated after noise exposure. To investigate the role of Mmp7 in noise-induced cochlear pathogenesis, we examined the cochlear responses to acoustic trauma in Mmp7 knock-out mice and compared the response differences between the knock-out and the wild-type control mice.

Methods

B6.129-Mmp7tm1Lmm/J mice were used as experimental subjects and C57BL/6J mice were used as control subjects. Both the experimental and the control mice were exposed to a broadband noise at 120 dB SPL for 2 hours. Auditory brainstem responses were measured before and at various times after the noise exposure. After the final hearing test, the animals were sacrificed. The cochleae, kidney, liver and inferior colliculus were collected for transcriptional analysis of Mmp7 expression. The cochlear tissues collected were also used for pathological assessments.

Results

The expression of Mmp7 was not detected in any examined tissues (the cochlea, kidney, liver, and inferior colliculus) in the knock-out mice, but was detected in the kidney and liver in the wild-type mice, indicating that the knock-out mice lack Mmp7 expression. Under physiological conditions, the knock-out mice exhibited a similar threshold level of auditory brainstem responses as compared with the control animals, suggesting that Mmp7 knock-out does not affect normal hearing sensitivity. After the noise exposure, Mmp7 expression became detectable in the wild-type subjects, but remained undetectable in the knock-out mice, indicating that the Mmp7 knock-out mice lack the Mmp7 response to the acoustic overstimulation. As compared with the control mice, the knock-out showed

a slightly greater hearing loss at 2 hours after the noise exposure (61 ± 19 dB for the wild-type mice vs. 67 ± 13 dB for the knock-out mice), but the difference was not statistically significant. Noticeably, the difference increased at 3 weeks after the noise exposure (37 ± 21 dB for the wild-type mice vs. 50 ± 12 dB for the knock-out mice, $p < 0.01$), suggesting that the lack of the Mmp7 response in the knock-out mice potentiates noise-induced hearing loss.

Conclusion

This study suggests that Mmp7 participates in the recovery process of noise-induced cochlear injury.

57 Isolation of the Sensory Cell-Enriched, OHC-Enriched and IHC-Enriched Samples from Mouse Cochleae with the High Integrity of RNAs for Transcriptional Analyses

Qunfeng Cai¹, Bo Wang¹, Bo Hua Hu¹

¹State University of New York at Buffalo

Background

Analyses of molecular mechanisms of sensory cell degeneration rely on the collection of high quality of sensory cell samples from the cochlea. Traditional methods for collection of whole cochlear tissues or the sensory epithelium tissue are relatively easy, but the collected tissues contain a large quantity of non-sensory cells. The methods that are suitable for the collection of sensory cell-specific samples, such as in vitro hair cell isolation, a fluorescence activated cell sorting, and laser capture microdissection, are time consuming and unable to maintain the integrity of RNAs. The current investigation was designed to develop a microdissection technique for collection of high quality sensory cell-enriched samples from mouse cochleae for transcriptional analyses.

Methods

A microdissection technique was developed to isolate three types of cochlear samples from mouse cochleae: the sensory cell-enriched, OHC-enriched, and IHC-enriched samples. We also developed a method of image analysis for normalization of starting materials for transcriptional analyses. Using a pre-amplification technique, we examined the expression pattern of 12 reference genes (18SrRNA, Actb, Hprt, Hsp90ab1, Nono, Ppia, Rpl13a, Tbp, B2m, Ldhal6b, Gusb, and Tfrc) in the sensory cell-enriched samples, and identified the stable reference genes after exposure to a broadband of noise at 120 dB SPL for 1 hour.

Results

The reported method provided several advantages over the currently-available techniques. First, the cell types in each sample could be clearly defined. The sensory cell-enriched sample contained the hair cells and three types of supporting cells, Deiters cells, pillar cells and inner sulcus cells. The OHC-enriched sample contained OHCs, Deiters cells and pillar cells. The IHC-enriched sample contained IHCs, pillar cells and inner sulcus cells. Second, the integrity of RNAs extracted from the samples is well preserved. Third, the tissue could be collected from a

defined cochlear site, suitable for the analysis of a site-specific change in gene expression. Using this technique for sample collection, we found expression of all 12 examined reference genes in the sensory cell-enriched samples. Among these genes, eight (18SrRNA, Actb, Hprt, Hsp90ab1, Nono, Ppia, Rpl13a and Tbp) were relatively stable after exposure to the intense noise. Finally, we have successfully applied this method to sample collection from rat cochleae.

Conclusion

The reported microdissection technique is able to provide sensory cell-enriched samples with the well-preserved RNA integrity.

(Supported by NIH R01 DC010154)

58 Apoptosis and Molecular Mechanism Involved in Cochlear Implant Trauma

Adrien Eshraghi¹, Chhavi Gupta¹, Thomas Van De Water¹, Jorge Bohorquez¹, Carolyn Garnham², Esperanza Bas¹, Dustin Lang¹

¹Department of Otolaryngology, University of Miami,

²MED-EL GmbH Innsbruck, Austria

Background

We described previously, the pattern of hearing loss post cochlear implantation (CI) and electrode insertion trauma (EIT) in animal models. This loss of hearing post CI has both an acute component (direct trauma) and an early post operative component (cellular and molecular damage) that develops over the period of at least a week following the initial trauma event. We demonstrated that insertion of a cochlear implant electrode array, not only causes direct tissue trauma and cell losses via necrosis, but also generates molecular events that will contribute further to a loss of residual hearing; e.g. oxidative stresses and release of pro-inflammatory cytokines that can lead to the initiation of programmed cell death; activation of the caspase pathway which can result in apoptosis; generation of pro-apoptotic signal cascades via, for example, mitogen-activated protein kinases/c-Jun-N-terminal kinases (MAPK/JNK); these may initiate programmed cell death within the damaged tissues of the cochlea. To gain a better understanding of the molecular mechanisms involved, we have investigated this process in a Guinea pig model of CI and tested the otoprotective effect of an inhibitor of JNK pathway.

Methods

Animals were exposed to EIT with and without treatment of JNK pathway inhibitor : AM-111 at round window. Immunostaining for HNE, activated Caspase-3, CellROX® and phospho-c-Jun were performed at 6hrs, 12hrs and 24hrs post-EIT. Neurofilament, Synapsin and FITC-Phalloidin staining for hair cells counts are performed at 90 days post-EIT. Guinea pig hearing thresholds were measured by ABR responses before and after cochlear implantation in four groups: EIT; pre-treated with hyaluronate gel ½ hr before EIT (EIT+Gel); pre-treated with hyaluronate gel/AM-111 ½ hr before EIT (EIT+AM-111), unoperated contralateral ears as controls.

Results

We observed an increase in ABR thresholds, post-EIT in the cochleae of EIT only and EIT+Gel treated animals. There was no significant increase in hearing thresholds in either EIT+AM-111 treated or unoperated control ears were observed. We observed protection of organ of Corti sensory elements (i.e. hair cells (HCs), supporting cells (SCs), nerve fibers and synapses) provided by AM-111 at 3 months post-EIT.

Conclusion

Molecular mechanisms involved in program cell death (PCD) of hair cells are different than the one involved in PCD of support cells. Local delivery of AM-111 prevented EIT-induced hearing, HCs losses and neural elements at 3 months.

59 Do Supernumerary Sensory Cells in the Cochleae of Rbl2 Null Mice Provide Protection from Noise-Induced Trauma?

Katyarina E. Brunette¹, JoAnn McGee^{1,2}, Sonia Rocha-Sanchez³, Sarah Stimmler¹, Edward J. Walsh^{1,2}

¹Boys Town National Research Hospital, ²Creighton University School of Medicine, ³Creighton University School of Dentistry

Background

The Rbl2 null mouse is unique among mutant animal models characterized by the presence of supernumerary cochlear hair cells in that sensitivity to sound is normal in spite of the presence of an extra row of inner hair cells and extra rows of outer hair cells in the apical half of the cochlea (Rocha-Sanchez et al., 2011). The availability of a mouse model exhibiting extra sensory cells and normal thresholds creates an opportunity to determine if extra sensory cells offer protection from hearing loss resulting from exposure to environmental noise that causes permanent hearing loss in control mice. The purpose of this study was to address this question directly.

Methods

A key element of the experimental design was to select potentially traumatizing noise bands that targeted cochlear regions populated with supernumerary sensory cells (the apical half of the cochlear spiral) and otherwise normal cochlear regions in the basal half of the end organ. Separate groups of Rbl2 null and wild-type (WT) mice were exposed to octave-wide bands of noise centered on 5.7 kHz or 11.3 kHz that were delivered for one hour at 120 and 110 dB SPL, respectively. Auditory brainstem responses (ABRs) to brief tone-bursts were used to estimate the magnitude of hearing loss produced by noise exposure, and to track recovery from hearing loss on a daily basis for the first four post-exposure days and at approximately 7, 14, 30 and 60 days thereafter.

Results

Immediately following exposure to traumatizing noise, ABR thresholds were elevated as much as 60 dB relative to pre-exposure, baseline values in both Rbl2 null and WT mice.

Recovery of function progressed at approximately the same rate and was nearly complete for both Rbl2-deficient and control mice following exposure to the noise band centered on 11.3 kHz. However, Rbl2 null mice exposed to the noise band centered on 5.7 kHz recovered more completely than WT mice over the course of the first two weeks following exposure, but thresholds to tone-bursts increased in Rbl2^{-/-} mice studied 30 and 60 days following noise exposure and threshold-frequency curve profiles observed at the two month post noise exposure time point were similar to those observed in WT cohorts.

Conclusion

Findings reported here suggest that mice exhibiting supernumerary sensory cells are less vulnerable to consequences of noise trauma than WT cohorts in the short term, but not under long term conditions.

60 Methylene Blue Prevents Noise Induced Hearing Loss

Teresa Wilson¹, Irina Omelchenko¹, Sarah Foster¹, Alfred Nuttall¹

¹Oregon Hearing Research Center

Background

The present study was performed to determine whether methylene blue, a powerful synthetic redox compound, can provide protection against noise induced hearing loss. Originally synthesized as a textile dye, methylene blue is currently being examined as a treatment for many human ailments including acute lung injury and Alzheimer's disease. In low doses, methylene blue, which is highly cell permeable and readily crosses the blood-brain barrier, acts as an electron shuttle in mitochondria transferring electrons to oxygen thereby greatly reducing superoxide production. Additionally, methylene blue has been shown to directly inhibit the activity of both inducible and constitutive forms of nitric oxide synthetase (NOS).

Methods

Male CBA/CaJ (8 weeks old) mice (n=5/group) were injected with methylene blue (0.5 mg/kg IP) or water at 24 and 1 hr prior to exposure to the moderately damaging noise levels of 110 dB SPL, 4-45 kHz for 3 hrs. At 1 day, 1 week and 2 weeks, Auditory Brain Stem Response (ABR) was measured. The ABR to a 1-ms rise-time tone burst at 4, 8, 12, 16, 24, and 32 kHz was recorded and thresholds obtained for each ear. The effect of methylene blue on NOS and NADPH oxidase activities were measured using DAF-FM and CellROX Deep Red Reagent, respectively.

Results

The results revealed that prior treatment with methylene blue provided significant protection against noise induced hearing loss across all measured frequencies.

Conclusion

Here, we provide evidence that pre-treatment with low dose methylene blue can prevent hearing loss due to loud sound exposure. The mechanism behind this protection is likely the strong antioxidant properties of methylene blue

that prevent loud sound induced free radicals from damaging the tissues of the inner ear. Supported by NIDCD DC 00105.

61 Auditory-Based Cognitive Training Improves the Subcortical Differentiation of Stop Consonants in Older Adults

Travis White-Schwoch¹, Samira Anderson^{1,2}, Nina Kraus¹
¹Northwestern University, ²University of Maryland

Background

Speech sounds are differentiated by acoustic cues which the auditory brainstem represents with tremendous fidelity. However, aging degrades the neural precision of subcortical speech encoding due to converging sensory and cognitive factors. Auditory training may prevent or reverse age-related declines in sensory processing. In animals, short-term perceptual training can reverse the effects of aging indexed by single neuron activity in auditory cortex.

Methods

We investigated the use of perceptual training to improve subcortical speech sound differentiation in older adults. We collected auditory brainstem responses to the stop consonants [ba] and [ga], which differ in their consonant-vowel (CV) transition formant trajectories, and so elicit brainstem responses which are out of phase in the transition period. After a first test, a group of older adults (ages 55-69) completed eight weeks of training which directed attention to speech transition cues by adaptively expanding and compressing CV transitions. After training we again collected brainstem responses.

Results

With training, subcortical consonant differentiation improved, indexed by an increase in the phase difference between responses in a time and frequency band corresponding to the CV transition. These changes in physiology were accompanied by improvements in speech perception, notably, hearing in noise. An active control group showed no changes.

Conclusion

In older adults, perceptual training can induce plasticity at fundamental stages of auditory processing. Specifically, training can improve the fidelity with which the brainstem transcribes rapidly-changing speech cues, which are especially vulnerable to the effects of aging. This plasticity can instill real-world communication benefits for listening in everyday situations. Supported by NIH (RO1 DC01510) and the Knowles Hearing Center.

62 Training Reverses Central Processing Effects of Sensorineural Hearing Loss in Older Adults

Samira Anderson^{1,2}, Travis White-Schwoch¹, Nina Kraus¹
¹Northwestern University, ²University of Maryland

Background

Aging is accompanied by a loss of sensory function, and hearing impairment can be especially devastating due to reduced communication ability. Older adults report that speech, especially in noisy backgrounds, can be uncomfortably loud yet still unclear. Improving audibility through amplification provides only a partial remedy; impaired speech processing may limit the benefits of increased auditory input. Hearing loss may result in enhanced encoding of the slowly varying envelope (contributing to perceived loudness), dominating the response to the extent that the details of the rapidly varying fine structure (contributing to perceived clarity) are less salient. We hypothesized that older adults with hearing loss can be trained to reweigh envelope cues relative to the temporal fine structure.

Methods

We recruited older adults (ages 55 to 79) who were randomly assigned to an experimental or an active control group, both of which completed 8 weeks of computer-based auditory/cognitive training. All participants were tested pre- and post-training with electrophysiological, perceptual, and cognitive measures. We compared the effects of training in subgroups of participants with normal hearing and hearing impairment.

Results

After training, the experimental group with hearing loss had improved subcortical speech-in-noise processing. In particular, the relative representation of the envelope to the temporal fine structure was restored to that of individuals with normal hearing. No changes were noted in the active control group. Importantly, improvements in speech encoding were related to improvements in speech perception.

Conclusion

Central processing deficits associated with hearing loss can be restored through training. The speech-evoked brainstem response can be used as an index of these changes. This work is supported by the NIH (RO1 DC01510) and the Knowles Hearing Center.

63 Medial Olivocochlear Efferents: Changes in *Shaker-2* Mice with Congenital Deafness

Kirupa Suthakar^{1,2}, Catherine Connelly^{1,2}, David Ryugo^{1,2}
¹Garvan Institute of Medical Research, ²University of New South Wales

Background

One of the main consequences of hearing loss is the impaired ability to understand speech in noisy environments. Medial olivocochlear (MOC) efferents are believed to be involved in this process due to their cholinergic damping effects on outer hair cell (OHC)

function. Because deafness represents an extreme form of hearing loss, we examined changes in MOC neurons of hearing and deaf *shaker-2* mice using immunohistochemistry for the enzyme Choline Acetyltransferase (ChAT). Differences in MOC cell features observed between these two groups of animals will guide future studies on milder forms of hearing loss.

Methods

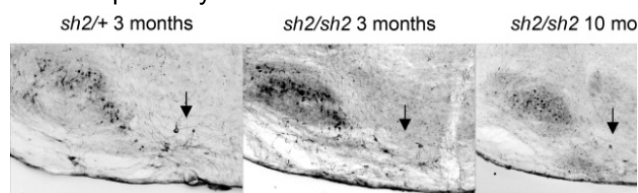
ChAT staining was performed in hearing and deaf *shaker-2* mice at various ages, and changes in immunopositive cell size and number were quantified. Additionally, some animals received injections of fluorogold into the round window of the cochlea to retrogradely label MOC neurons. Double labeling was used to determine what proportion of immunopositive cells of the superior olive were in fact MOC efferents.

Results

By 3 months of age, the OHCs of deaf *shaker-2* mice have completely degenerated in the basal region of the cochlea (Gong et al., 2006). At this age, our data reveal that the MOC cells of deaf *shaker-2* mice are significantly smaller (~20%) than those of age-matched hearing heterozygotes. By 10 months of age there is noticeable MOC cell loss and a ~50% reduction in cell size compared to normal hearing mice. These preliminary results indicate that MOC cell size and number progressively decreases with duration of deafness.

Conclusion

MOC efferents are implicated in the modulation of afferent input by regulating OHC activity, suggesting a critical role in extracting sound signals from noise. Abnormalities in MOC cell characteristics that accompany deafness indicate that central auditory dysfunction is linked to peripheral damage. Furthermore, the pathology of MOC efferents is progressive, suggesting a use-dependent deterioration. It remains unclear, however, if this change is due to a loss of afferent input to MOC cells or the loss of their peripheral targets. Future studies will examine changes in MOC cells in non-congenital forms of hearing loss beginning at different ages in order to determine which factors most contribute to the degradation of this reflexive pathway.



64 Synaptic Transmission at Endbulb of Held Synapses During Age-Related Hearing Loss in CBA/Caj Mice

Ruili Xie¹, Paul Manis¹
¹University of North Carolina at Chapel Hill

Background

Age-related hearing loss (AHL) is a slow process in which peripheral hearing sensitivity diminishes with age. The

changes in the central auditory system, particularly in the cochlear nucleus, however, are less clear. Here, we investigated synaptic transmission at the endbulb of Held synapse between the auditory nerve and cochlear nucleus neurons during ARHL.

Methods

CBA/CaJ mice bred in-house were reared under standard vivarium conditions in microisolater cages until 31-38 days old, 85-105 days old, and 15-19 months old. Auditory brainstem evoked responses (ABR) to clicks were measured in each animal prior to preparation of brain slices. Voltage-clamp recordings were then made from bushy cells in parasagittal slices of the cochlear nucleus to measure the excitatory postsynaptic currents (EPSC) evoked by auditory nerve stump stimulation.

Results

The ABR showed ~10 dB SPL increase in hearing threshold in 15-19 month old mice relative to the two younger groups. However, the amplitude of the 1st ABR waveform increased more slowly with increasing intensity in both older groups, suggesting that hearing loss was present even in the 85-105 day old animals in spite of normal thresholds. When stimulating the auditory nerve in slices, we found that the EPSC amplitude in bushy cells was reduced while the paired-pulse ratio was increased in the oldest group. Furthermore, there was a significant increase in asynchronous release at the end of 400 Hz trains in the oldest group.

Conclusion

CBA mice exhibit decreased ABR amplitudes by 100 days of age, in spite of near-normal thresholds. Furthermore, at the first central site of synaptic transmission, AHL is associated with both weaker synaptic transmission (decreased release probability) and a compromised ability to sustain temporally precise transmitter release.

65 Unilateral Cochlear Implant Stimulation Maintains the Molecular Balance of the Plasticity Marker GAP-43 in Auditory Brainstem Circuits

Nicole Rosskothén-Kuhl¹, Robert-Benjamin Illing¹
¹Neurobiological Research Laboratory, University-ENT-Clinic, Freiburg, Germany

Background

In early life, millions of synapses develop in the mammalian brain. At this stage, high levels of phosphoprotein GAP-43 were detected in neuronal somata, axons and immature synapses. With maturation of the nervous system, synthesis of this protein decreased in most neurons, including those of the central auditory system. However, some regions maintain levels of GAP-43 mRNA, among them the lateral superior olive (LSO) and the central inferior colliculus (CIC). An additional region is the hippocampus, known for its involvement in learning. It is still unknown what happens molecularly in the brain if one ear or both fail in adulthood? Can a cochlear implant (CI) help to replace the missing input on the molecular

level? This study investigated the correlation between GAP-43 mRNA expression and symmetry of bilateral sensory inputs within the auditory system of rats.

Methods

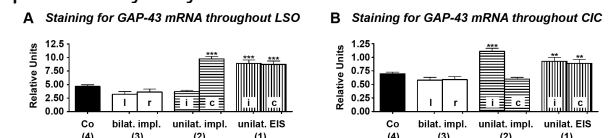
For quantification, GAP-43 mRNA levels were determined in LSO and CIC. To create different auditory input conditions, we worked with four experimental groups of young adult, wild-type Wistar rats. (1) Rats with a unilateral CI, stimulated for up to 7 days, rats with unilateral (2) or bilateral (3) CI(s) for up to 10 weeks without stimulation, and (4) normal hearing controls.

Results

We found that GAP-43 mRNA levels shifted as a function of activity balance and activity patterns. The control group (4) and the unstimulated rats with bilateral CIs (3) had almost identical GAP-43 mRNA levels on both sides of the brain in LSO and CIC. By contrast, mRNA levels were significantly unbalanced for the unstimulated group with only one CI (2). In contralateral LSO, GAP-43 mRNA expression increased as compared to control level. Ipsilateral CIC reached significance against control level after long-term implantation of 3 or 10 weeks. By monaural CI stimulation (1), GAP-43 mRNA levels were left-right symmetrical for LSO and CIC. Still, levels were higher than in control rats in LSO for all stimulation times and in CIC by 7 days of EIS.

Conclusion

Overall, our data suggest that GAP-43 is more than a marker for neurite outgrowth and early stages of synaptogenesis. When activity input is different between left and right ear of adult rats, this imbalance is displayed by levels of GAP-43 mRNA expression. Remarkably, the balance can be completely sustained if the hearing impaired ear became activated by simple stimulation patterns by way of a CI.



Simplified results of GAP-43 mRNA quantification.

Summarized staining results of GAP-43 mRNA in LSO (A) and CIC (B) indicate that GAP-43 mRNA levels were unbalanced between left and right side of the brainstem if auditory activity was reduced on one side only. By inserting and directly activating a cochlear implant on the deafened side, mRNA levels increased significantly against control levels but maintained left-right balance. Significant differences against control staining level are displayed by asterisks: (***) = $p < 0.001$, (**) = $p < 0.01$. l: left; r: right; i: ipsilateral; c: contralateral; Co: control group; unilat.: unilateral; bilat.: bilateral; impl.: implantation; EIS: electrical intra-cochlear stimulation.

66 Presynaptic Ion Channels Regulate Quantal Size in the Calyx of Held

Hai Huang¹, Laurence Trussell¹
¹Oregon Health & Science University

Background

Synaptic vesicles accumulate transmitter using energy from the proton electrochemical potential ($\Delta\mu_{H^+}$), composed of an electrical potential ($\Delta\psi$) and a chemical gradient (ΔpH). Previous studies suggested that glutamate uptake into synaptic vesicles by the vesicular glutamate transporter (VGLUT) is dependent mostly on $\Delta\psi$ rather than ΔpH . Recently, a study showed that rat brain synaptic

vesicles express a $K^+(Na^+)/H^+$ monovalent cation exchanger activity that converts ΔpH into $\Delta \psi$ and promotes synaptic vesicle filling with glutamate (Goh et al, 2011). Manipulating presynaptic K^+ at the calyx of Held, a giant glutamatergic terminal in the auditory brainstem, influenced quantal size, indicating that synaptic vesicle K^+/H^+ exchange regulates glutamate release and synaptic transmission. Although the intracellular K^+ concentration is relatively stable, the Na^+ concentration may fluctuate widely during spike activity, raising the question of whether Na^+ may have a regulatory influence on VGLUT activity.

Methods

Whole-cell electrophysiology and Na^+ -imaging recordings were made from the calyx of Held in brainstem slices of P8-14 rats.

Results

Our experiments showed that intracellular Na^+ strongly affects glutamate uptake: increasing Na^+ in the presynaptic recording pipette potentiated mEPSC amplitude (quantal size) while decreasing Na^+ in the pipette reduced mEPSC. We found that hyperpolarization-activated cyclic nucleotide-gated (HCN) ion channels control the resting Na^+ concentration and that blocking HCN channels with Cs^+ reduced the amplitude of mEPSCs. Moreover, modulating HCN channels with forskolin or 8-Br-cAMP increased mEPSC size.

Conclusion

Plasma membrane ion channels control intracellular Na^+ and therefore regulate glutamate uptake and synaptic transmission. Because high-frequency spike activity leads to Na^+ accumulation in terminals, we expect activity dependent facilitation of glutamate uptake will speed vesicle replenishment and sustain synaptic transmission.

67 Synaptic and Membrane Properties of Neurons in the Ventral Nucleus of the Lateral Lemniscus (VNLL) of Mice

Veronika Auer¹, Franziska Caspari¹, Gülçin Vardar¹, Ursula Koch¹

¹FU Berlin, Institute of Biology, Neurophysiology

Background

Neurons in the lateral lemniscus receive numerous inputs from lower auditory brainstem nuclei and send prominent inhibitory projections to the inferior colliculus. Based on the anatomical inputs and physiological properties, neurons in the lateral lemniscus can be subdivided in at least two distinct nuclei, the dorsal (DNLL) and the ventral nucleus of the lateral lemniscus (VNLL). Whereas properties of DNLL neurons have been well described, less is known about neurons in the VNLL. Neurons in the VNLL receive excitatory inputs from the contralateral ventral cochlear nucleus (VCN) and inhibitory inputs from the ipsilateral medial nucleus of the trapezoid body (MNTB). However, little is known about the physiological properties of these neurons. Therefore, we started to characterize the membrane and synaptic properties of neurons in the VNLL of mice.

Methods

Biophysical membrane properties and synaptic inputs were characterized by whole-cell patch-clamp recordings of VNLL neurons in acute brain slices from P10/11 and P17/18 C57Bl6J mice. Excitatory and inhibitory synaptic currents were evoked by stimulating the incoming fibers of the lateral lemniscus with a glass electrode placed $\sim 50 \mu m$ ventral to the recorded neuron. Underlying synaptic receptors were determined by pharmacological blockade of the respective receptors. VNLL neurons were identified by their dorsal/ventral position within the lemniscal fiber tract. Only neurons in the most ventral part in the fiber tract were analyzed.

Results

VNLL neurons predominantly displayed an onset-type firing pattern in response to depolarizing current step injections (1s). During hyperpolarizing current injections these neurons exhibited a prominent depolarizing voltage sag. This indicates that both low threshold K^+ -channels and HCN-channels are expressed in the VNLL.

Stimulating the incoming fibres evoked both excitatory and inhibitory synaptic responses. In P17/18 mice excitatory synaptic currents were mediated by AMPA and NMDA receptor. Both AMPA and NMDA receptor currents had large amplitudes. Inhibitory synaptic responses had fast time constants (around 2 ms) and were largely mediated by glycine at postnatal day 17/18.

Conclusion

Our results show that synaptic and membrane properties of VNLL neurons, that are located in the lemniscal fiber tract, are fairly uniform. These neurons receive large excitatory and inhibitory inputs and display membrane properties that ensure precise integration of excitatory and inhibitory inputs.

68 Competing Mechanisms of Short-Term Synaptic Plasticity in the Chick Cochlear Nucleus

Stefan Oline¹, R. Michael Burger¹

¹Lehigh University

Background

In the auditory system, stimuli of different frequencies are processed in parallel frequency-tuned circuits, beginning in the cochlea. Activity of avian auditory nerve fibers reflect this frequency-specific topographic pattern, known as tonotopy, and impart frequency tuning onto their postsynaptic target neurons in Nucleus Magnocellularis (NM). While all NM neurons perform the basic function of encoding the timing properties of acoustic stimuli, physiological specializations exist along the tonotopy that reflect the characteristic frequency (CF) of their auditory nerve fiber inputs. One known feature of synaptic physiology that has not been investigated across the tonotopic axis of NM is short-term synaptic plasticity.

While the utility of comparing synaptic plasticity across different neurons in different brain regions is limited, NM offers a rather homogenous population of neurons with a

distinct topographical distribution of synaptic specialization that is ideal for the investigation of short-term synaptic plasticity. We have previously demonstrated that synapses with a high CF are more resistant to short-term synaptic depression, which is due in part to a larger readily releasable pool (RRP) and a faster rate of recovery than their low CF counterparts. In this study, we examined the contribution of current amplitude and postsynaptic mechanisms to the observed difference in depression.

Methods

We used in vitro whole-cell patch clamp with chickens aged E19-P1. Brainstem slices were collected, and slice order determined tonotopic position of NM neurons. A stimulating electrode was placed in a position proximal to the cell until a unitary evoked excitatory postsynaptic current (EPSC) was observed. Cyclothiazide (40 μ M) was added to aCSF to evaluate receptor desensitization.

Results

Superimposed on the tonotopic distribution of synaptic depression, we show that larger inputs show more depression, regardless of characteristic frequency. Experiments with cyclothiazide showed that larger EPSCs also caused larger AMPA receptor desensitization. However, this postsynaptic effect was small relative to presynaptic components of short-term synaptic depression, and was not sufficient to explain the tonotopic distribution of depression.

Conclusion

Across the tonotopy of NM, high CF synapses are more resistant to depression than their low CF counterparts. We show that larger EPSCs exhibit greater depression, even within frequency regions. In addition, the magnitude and distribution of postsynaptic receptor desensitization did not reflect the difference in short-term synaptic depression across the tonotopy. Therefore, the presynaptic mechanisms of RRP size and vesicle recovery are the most likely mechanisms that underlie synaptic specialization in NM.

69 How Does Jaundice Cause Deafness in a Model Mouse?

Emanuele Schiavon¹, Helen Parker¹, Ian D. Forsythe¹
¹*Dept. Cell Physiol. & Pharm., University of Leicester, LE1 9HN. UK.*

Background

Acute bilirubin encephalopathy (ABE) and Chronic bilirubin encephalopathy (or kernicterus) are serious neurological events with an incidence of 1/100,000 and 1/150,000 in newborns in the United Kingdom. Both conditions are associated with hyperbilirubinaemia -Jaundice- (Maisels, *Early Human Development*, vol. 85 pp 727-732, 2009) where increased plasma levels of free bilirubin cross the blood-brain-barrier and cause neuronal damage in the CNS (Haustein et al, *J. Physiol.*, Vol. 588.23 pp 4683-4693, 2010). The link with vulnerability of the auditory system is well documented, but the mechanism(s) of bilirubin neurotoxicity remain unclear. To investigate

damage in the brainstem auditory pathway we focused on a giant synapse that has a pivotal role in the circuitry involved in sound localization. This synapse, between the anterior ventral cochlear nucleus (aVCN) and the neurons of the medial nucleus of the trapezoid body (MNTB), is known as calyx of Held (Kopp-Scheinflug et al, *Hearing Res.*, vol. 279 pp22-31, 2011)

Methods

Hyperbilirubinaemia was induced in CBA mice by a single intraperitoneal injection of free bilirubin (0.5 mg/g and Sulfadimethoxine 0.3mg/g) and the auditory function was monitored by recording in vivo auditory brainstem responses (ABR) 4h-24h and 5 days afterwards. We used an in vitro slice preparation to study transmission at the calyx of Held combined with multi-photon imaging and immunohistochemistry for the presynaptic marker VGLUT2 (vesicular glutamate transporter 2). Additionally the acute effect of bilirubin was investigated on slices from untreated animals, using patch clamp recording.

Results

We showed a deficit of ABRs at 4h which had recovered by 24h and 5 days after injection. Using multi-photon imaging and immunohistochemistry for VGLUT2 we found disruption of the synapses at the calyx of Held at both 4h and 24h after injection. Patch clamp recordings showed a decrease in the threshold for the firing of action potentials in the MNTB, after acute perfusion of the slices with free bilirubin. In control experiments, bilirubin caused no change in the amplitude of evoked EPSCs mediated by AMPA or NMDA receptors.

Conclusion

We conclude that this mouse model for hyperbilirubinaemia exhibits an acute damage to the auditory system, involving a disruption of the synapses at the level of calyx of Held and provides a good model for further understanding mechanisms of injury caused by jaundice.

This research was funded by Action On Hearing Loss UK.

70 Intrinsic Firing Heterogeneity in the Cochlear Nucleus Improves Population Coding of Temporal Fluctuations During Noisy Current Stimulation

Jheeyae Ahn¹, Lauren Kreeger¹, Katrina MacLeod¹
¹*University of Maryland*

Background

There is widespread evidence for intrinsic property diversity in many brain areas, but the role of such diversity in neural coding is not well understood. While neurons in the timing pathway of the avian auditory brain stem are fairly stereotyped in their firing properties, those in the intensity pathway show a broader range of biophysical diversity. Previous research investigated how the intrinsic properties of the cochlear nucleus angularis (NA) influenced the response to noisy current injections during recordings from slices in vitro that simulated the arrival of

many nerve inputs. All physiological subtypes of NA neurons showed reliable, stimulus-locked firing to fluctuating noisy currents, but the degree of spike train reliability and precision correlated with cell type (Kreeger et al., 2012, *J Neurophysiol.*) In this study, we investigated how well the stimulus was encoded by individual NA neurons, how the diversity of intrinsic properties affected encoding and whether this diversity led to better population coding of the stimulus.

Methods

Patch-clamp recordings were made from chick (E17-18) brain stem slices while delivering filtered Gaussian white noise current stimuli. We used reverse correlation methods to reconstruct an estimate of the stimulus using the spike-triggered averages (STA) and assessed by cross-correlation with the original stimulus (low-pass, 300 Hz).

Results

To compare reconstructions across neurons with different properties, identical noise stimuli were presented during separate recordings from 60 NA neurons. Reconstruction estimates showed high degree of correlation with the original stimulus (0.50 ± 0.08). STAs generated by two, uncorrelated noise stimuli were very similar within a given neuron, but differed across neurons for the same stimulus, suggesting that each neuron had a unique sensitivity to the current fluctuations. Comparing spike trains across neurons to identical stimuli, differences were observed in number and timing of spikes, but there were also many correlated, precise spike events. Combining information from spike trains drawn from the population improved stimulus reconstruction estimates (0.67 ± 0.02 , 40 cells).

Conclusion

Temporal fluctuations in current inputs were efficiently coded by individual NA neurons and combining information across the population improved coding due to biophysical diversity. Highly reliable firing has also been observed in NA in vivo during repeated broadband noise stimuli (Steinberg and Pena, 2011 *J. Neurosci.* v31:3234), suggesting temporal envelope fluctuations may be encoded via the intensity pathway. Whether intrinsic property diversity contributes to envelope coding in vivo remains to be seen.

[71] Development of Kcna1 Dominant-Negative Lentivectors in the Central Auditory System

Jennifer Thornton^{1,2}, Jessica Weatherstone^{1,3}, Jin Li^{1,2}, Bruce Tempel^{2,3}

¹The Virginia Merrill Bloedel Hearing Research Center, University of Washington, Seattle, WA, ²Dept. of Otolaryngology, University of Washington School of Medicine, Seattle, WA, ³Dept. of Pharmacology, University of Washington School of Medicine, Seattle, WA

Background

Throughout the nervous system, potassium channels are required for efficient signaling and action potential timing. In the central auditory system, the voltage-activated,

delayed rectifier Kv1.1 subunit, encoded by the *Kcna1* gene, is important to sustain the firing rate and timing of action potentials via its regulation of a low-voltage activated current (IKL) (Brew et al 2003; Gittelmann and Tempel 2006; Kopp-Scheinflug et al 2003). To study how altered Kv1.1 channels affect functioning in the central auditory system it is necessary to establish an animal model that has mutated channels in the auditory system only. As Kv1.1 is expressed throughout the central nervous system, a necessary means to achieve this specificity in the auditory system is via localized stereotaxic injections of lentiviral vectors. The main goal of this study is to generate and establish lentivectors with a dominant negative *Kcna1* mutation as a means of studying desynchronized activity in the central auditory system.

Methods

Recombinant lentiviruses were developed to provide a range of interference with endogenous Kv1 subunits. GFP-expressing lentivectors were produced by introducing AU1-tagged Kv1.1 cDNAs encoding wildtype and mutant to the lentivector. For in vivo expression, lentiviruses were injected into the anteroventral cochlear nucleus (AVCN) of adult mice, which projects monosynaptically to the medial nucleus of the trapezoid body (MNTB). AVCN location was confirmed stereotaxically and also by detection of multi-unit activity. GFP intensity and the density of transfected neurons in both the AVCN and MNTB were determined using immunocytochemistry.

Results

We have produced repeatable Kv1.1 dominant negative lentiviral injections in the AVCN of adult mice, and this resulted in transfection of both AVCN neurons and MNTB pre-synaptic calyces. Additionally, we established a timeline of integration of the mutant Kv1.1 subunit into the genome of AVCN bushy cells. Using antibodies to the AU1-tag, we determined the time required for mutant Kv1.1 subunits to integrate into the MNTB calyces of Held.

Conclusion

These results suggest that it is possible to use a *Kcna1* dominant negative lentivector as a means to disrupt Kv1.1 channel activity in the central auditory system. After optimizing the lentivector injections, we can record single unit activity from MNTB principal cells to determine what effect disrupted Kv1.1 activity will have on the physiological responses of these cells. Support: NIDCD R01-DC02739 (BLT) and 5T32DC00018-30 (JLT).

[72] Imaging Synaptic Zinc Release in the Dorsal Cochlear Nucleus with Newly Developed Zinc Sensors and Chelators

Charles T Anderson¹, Robert Radford², Zhen Huang², Wei Lin², Stephen Lippard², Thanos Tzounopoulos¹

¹University of Pittsburgh, ²MIT

Background

Vesicular zinc exists at many glutamatergic synapses in the brain. This transition metal is loaded into presynaptic glutamatergic vesicles and is co-released with glutamate

during synaptic transmission. The molecular layer of the dorsal cochlear nucleus (DCN) contains high levels of vesicular zinc. Our group has recently reported that synaptically-released zinc initiates endocannabinoid synthesis that subsequently modulates synaptic strength. However, the amount of synaptic Zn²⁺ that reaches the postsynaptic membrane during synaptic stimulation remains unknown, mainly due to lack of appropriate zinc sensors and chelators.

Methods

Here, we have used new generation of fluorescent zinc sensors and chelators to examine how much, and under what conditions zinc is released in the DCN.

Results

We have found ZnT3-mediated zinc release following electrical stimulation with zinc-sensitive fluorescent probes.

Conclusion

We provide evidence for ZnT3-mediated zinc release in the DCN.

73 Glutamate-Activated Currents in Unipolar Brush Cells

Carolina Glogowski¹, Laurence Trussell¹

¹Oregon Health & Science University

Background

Unipolar brush cells (UBCs) of the dorsal cochlear nucleus (DCN) and vestibular cerebellum receive glutamatergic mossy fiber input on a complex brush-like dendrite. Studies of cerebellar UBCs identified different subtypes of UBC based on immunohistochemical markers and physiological profiles. We have examined auditory UBCs, and compared them to cerebellar UBCs with respect to the physiology of the mossy input and glutamate sensitivity.

Methods

Patch-clamp recordings were made on coronal slices from DCN or parasagittal slices from vestibular cerebellum in P16-23 mice. A monopolar or bipolar glass electrode was used for extracellular stimulation. Glutamate was pressure ejected from a pipette positioned near the dendritic brush. Mouse lines included mGluR2-GFP and wildtype C57/Bl6. GABA_A and glycine receptors were blocked to prevent inhibitory transmission.

Results

EPSCs evoked by extracellular stimulation evoked NBQX-sensitive EPSCs with a profile similar to that reported by Rossi et al. 1995: a small, fast inward current followed by a very slow delayed inward current. Occasionally, a train of stimuli would result in a delayed outward current consistent with a glutamate-activated K⁺ current. However synaptic responses were painfully rare. To explore glutamate sensitivity of UBCs, we therefore applied brief puffs of 1 mM glutamate. A variety of response profiles were elicited in different cells, suggestive of different cell types. Overall the results indicated the presence of at least 3 glutamate receptor subtypes in UBCs. 1) AMPA receptors (defined by

sensitivity to NBQX), which generated a small, rapid inward current followed by an outward current and lastly a slow inward current. In some cases the AMPA current was negligible, but in all cases the current was markedly increased by cyclothiazide, a blocker of AMPAR desensitization. 2) A slow outward current blocked by mGluR2 antagonist, consistent with a GIRK channel. 3) A slow inward current blocked by antagonists to mGluR1 receptors.

Conclusion

UBCs express an array of glutamate receptors which generate complex response profiles. The high expression of metabotropic glutamate receptors coupled to K⁺ channels and other cation channels could grant these cells with a unique role in processing multisensory signals in the structures where they are present.

74 Dependence on Otoferlin (And Background Strain) of Magnitude and Convergence of Auditory Nerve Inputs on Cochlear Nuclear Bushy Cells

Samantha Wright¹, Xiao-Jie Cao¹, Donata Oertel¹

¹University of Wisconsin

Background

Even before the onset of hearing, patterned spontaneous activity that starts in the cochlea ascends through auditory pathway (Tritsch et al. 2007; Tritsch and Bergles 2010). Otoferlin acts as a calcium sensor at synapses of inner hair cells, mediating synaptic transmission. In otoferlin *-/-* mice, inner hair cells release little neurotransmitter throughout the life of the animal (Roux et al. 2006; Longo-Guess et al. 2007). Bushy cells in the anteroventral cochlear nucleus receive most excitatory input through large terminals, the end bulbs of Held. End bulbs in otoferlin mutants are smaller and more wispy (Wright et al., 2012). We compare the number of inputs and the magnitude of evoked excitatory postsynaptic currents (EPSCs) in bushy cells of otoferlin *-/-* mice with *+/-* and *+/+* hearing control mice to learn how activity early in development affects end bulbs of Held.

Methods

Stimulation of bundles of auditory nerve fibers evoked EPSCs in bushy cells in slices that grew in steps of widely varying sizes with shock strength, reflecting the recruitment of converging fibers (Cao et al., 2007; Cao and Oertel, 2010).

Results

The average number of steps was not different in deaf otoferlin *-/-* mice (4.2 ± 1.5 steps, n=36) and hearing *+/-* and *+/+* controls (3.4 ± 1.9 steps, n=36) (p = 0.06) (P15-P22) suggesting that the number of inputs is not strongly affected by spontaneous and acoustically driven activity. Evoked EPSCs were enormous in all three genotypes, with maximal currents exceeding 60 nA in some cells. Unitary EPSCs in hearing *+/-* and *+/+* mice were significantly smaller (5.2 ± 6.2 nA, n=36) than in deaf otoferlin *-/-* mice (7.6 ± 8.8 nA, n=36, p = 0.01). Because measurements of

such large synaptic currents are sensitive to series resistance compensation in patch clamp recordings, the measurements of amplitude must be viewed as approximate.

The unexpectedly large EPSCs in the +/+ C57BL/6J and C3HeB/FeJ background (maximal EPSCs 19.9 ± 12.2 nA, $n=18$), prompted a comparison of maximal EPSCs in various wild type strains recorded in our lab. We find large differences in the magnitude of maximal EPSCs between strains. In ICR mice maximal EPSCs were 2.7 ± 1.4 nA ($n=23$); in C57Bl/6 and 129S hybrids, maximal EPSCs were 1.0 ± 0.1 ($n=3$); in another hybrid strain, AKR, C57Bl6, LG, and BALBc, maximal EPSCs were 3.6 ± 1.4 nA ($n = 6$).

Conclusion

Activity and background strain matters.

75 Munc13 Proteins Differentially Regulate Short-Term Plasticity at the Calyx of Held Synapse in the Mammalian Auditory Brainstem

Samuel Young¹, Zuxin Chen^{1,2}, Benjamin Cooper³, Frederique Varoqueaux³

¹Max Planck Florida Institute, ²Huazhong University of Science and Technology, ³Max Planck Institute for Experimental Medicine

Background

Numerous molecular interactions at the active zone of synapses regulate the reliability of synapses to encode information over a wide range of frequencies in response to action potentials. In the CNS, the Munc13 gene family encodes critical molecules in the regulation of synaptic transmission and plasticity and consists of three genes, Munc13-1, Munc13-2 and Munc13-3, that express four Munc13 isoforms. Currently, it is unknown why despite the presence of Munc13-2 or Munc13-3, they are functionally dispensable at some synapses or why their loss in other synapses leads to increases in frequency-dependent facilitation. We addressed these questions at the calyx of Held synapse, a giant synapse in the auditory brainstem, that places a premium on speed and reliability of information transfer for auditory signal processing and allows for biophysical dissection of the different regulatory steps in CNS synaptic transmission.

Methods

Acute brainstem slices containing the MNTB were prepared from Munc13-2 KO, Munc13-3 KO, or Munc13-2-3 DKO or wild-type mice. Electrophysiology experiments to study AP-evoked EPSC's were performed by afferent fiber stimulation in conjunction with patch clamp recording of the MNTB. To quantitatively understand the dynamics of the readily releasable pool of vesicles we performed paired recordings of the calyx/MNTB synapse. Quantitative immunohistochemistry experiments measuring Munc13 isoform levels at the calyx were done using the Munc13 XFP knockin animals. Experiments used mice before the

onset of hearing (p9-11) or when the calyx is more functionally mature (p18-p21).

Results

We report that the calyx of Held synapse expresses 3 isoforms of Munc13 (Munc13-1, ubMunc13-2, and Munc13-3). Using detailed electrophysiological analyses of the Munc13 KO mice lines, we report that loss of both Munc13-2 and Munc13-3 leads to an increase in the rate of calcium-dependent recovery and a reduction in the readily releasable pool, but with no change in the fast releasing vesicle pool size but a selective loss of the slow releasing vesicle pool size. Using Munc13XFP knock-in mice, quantitative immunohistochemistry revealed that Munc13-1 is the dominant isoform. We also find that only the Munc13-1 isoform is highly colocalized with bassoon at the active zone.

Conclusion

Based on our data, we conclude that Munc13-2 and Munc13-3 isoforms compete with Munc13-1 to differentially regulate calcium-dependent recovery and the slow pool to fast pool conversion in central synapses.

76 Physiology of Golgi Cell-granule Cell Synapses in the Cochlear Nucleus

Daniel Yaeger¹, Laurence Trussell¹

¹Oregon Health & Science University

Background

The cochlear nucleus contains diverse granule cell domains conveying multimodal signals from mossy fibers to the molecular layer of the dorsal cochlear nucleus (DCN). Little is known about inhibitory cells that modify these multimodal signals at the level of the granule cell. A previous study (Balakrishnan and Trussell 2008) showed prominent GABAergic and glycinergic inputs to granule cells in rat, but did not identify the sources of these inputs. We have used mouse lines in which GFP is expressed in inhibitory neurons and tdTomato is expressed in granule cells to facilitate identification of these cell types in different regions of the cochlear nucleus. Moreover, we explored modulation of inhibition by metabotropic receptors.

Methods

Single or paired patch-clamp recordings were made on slices from P16-23 mice. A monopolar or bipolar glass electrode was used for extracellular stimulation. Mouse lines included mGluR2-GFP, GlyT2-GFP, and GABA_Aα6-tdTomato. AMPA and NMDA receptors were blocked to prevent glutamatergic transmission.

Results

Extracellular stimuli reliably elicited IPSCs in granule cells from DCN and granule cell lamina. As in rat, IPSCs were mediated by GABA and glycine receptors, suggesting that presynaptic fibers released both transmitters. Paired recordings made from either GFP-expressing, non-unipolar brush cell neurons in mGluR2-GFP or GlyT2-GFP positive neurons synaptically coupled to granule cells revealed that at least one source of inhibition to auditory granule cells is

local interneurons. For convenience, we collectively term these interneurons Golgi cells, although it is possible they represent a diverse class. Paired recordings always showed smaller IPSCs than with extracellular stimulation, implying that 3-4 Golgi cells converge on single granule cells.

A previous study demonstrated muscarinic and metabotropic glutamate receptor 2-mediated hyperpolarization of mouse Golgi cells (Irie et al., 2006). We confirm this report but also observed potent inhibition of evoked IPSCs in granule cells by carbachol or by LY354740. The effect of carbachol was mimicked by oxotremorine M, indicating the presence of muscarinic receptors. In paired recordings in which the presence of a presynaptic spike could be verified, synaptic inhibition persisted, indicating that inhibition is not generated by prevention of presynaptic spikes. Nevertheless, modulation of short-term plasticity of IPSCs by carbachol suggested that carbachol acted at a presynaptic site.

Conclusion

Golgi cells may control the efficacy of multimodal inputs to the DCN. Modulation of inhibition by metabotropic receptor systems may provide a means for state-dependent gating of these signals.

77 Noise-Induced Changes of Neuronal Spontaneous Firing Rates in Mice Cochlear Nucleus and Inferior Colliculus Brain Slices

Moritz Gröschel^{1,2}, Jana Ryll², Romy Götze², Arne Ernst¹, Dietmar Basta^{1,2}

¹Unfallklinik Berlin, Germany, ²Humboldt-University Berlin, Germany

Background

A noise trauma leads beside damage in the periphery to profound changes in the central auditory system. Recent work demonstrated that noise exposure has a strong and rapid impact on central neuroanatomy and neurophysiology. Despite an increase in apoptotic cell death and a subsequent reduction in cell densities, a single noise trauma is often followed by an elevation of spontaneous neural activity in auditory brain structures as demonstrated by electrophysiological recordings or activity-dependent imaging techniques. As most of these studies were performed in vivo, it remains unclear to what extent particular brain areas are responsible for the observed hyperactivity. Acute in vitro preparations provide the opportunity to investigate intrinsic properties of brain structures disconnected from ascending or descending neuronal input. It was the aim of the present study to investigate spontaneous firing activity at different time points after noise exposure in brain slices of the lower auditory pathway, namely the cochlear nucleus (CN) and inferior colliculus (IC).

Methods

Normal hearing mice (NMRI strain) were exposed to a broadband noise (5-20 kHz, 115 dB) for 3 hours under anaesthesia and have been investigated immediately

(acute group) or 7 or 14 days after trauma. Hearing thresholds were determined by auditory brainstem response audiometry. To investigate changes in spontaneous neural activity in vitro, electrophysiological single-unit recordings were carried out in the dorsal and ventral cochlear nucleus (DCN and VCN) and IC brain slices. Unexposed mice served as normal hearing controls.

Results

The ABR results demonstrate that hearing loss in the animals was highest immediately after noise exposure and recovered significantly within one week. However, a significant permanent threshold shift was present even at day 14 after noise exposure. Spontaneous neuronal activity was significantly increased in the acute group on the level of the DCN and VCN, no significant changes occurred in the IC. One week after noise trauma, firing rates did not differ from control animals in any investigated structure. However, after 14 days, spontaneous activity was significantly elevated in the DCN as well as in the IC.

Conclusion

The data underline our previous findings that a noise trauma is acutely affecting central cellular properties and induces short-term plasticity, particularly in brainstem structures. Further, long-term physiological changes seem to appear slowly and might thus differ from the early effects, whereby the DCN and the IC (but maybe not VCN) are supposed to serve as key structures during this development.

78 Filter Widths Throughout the Auditory System

Toby Wells¹, Chris Sumner¹

¹MRC Institute of Hearing Research

Background

Frequency selectivity is a fundamental and extensively studied property of the auditory system, yet it is not clear whether it is established at the periphery or if central mechanisms make a contribution. This is, in part, because two distinct approaches are taken, psychophysics and physiology, the results of which are difficult to compare. Psychophysical estimates are made using masking paradigms, whilst many physiological measurements in the past were made using pure-tone responses. Also, psychophysics measures detection thresholds, which are not necessarily comparable to the mean spike rates used in physiology.

Methods

To try and reconcile the differences between these two fundamentally different approaches, we measured auditory filter widths of single neurons, as well as multi-unit activity, in two brain regions; the inferior colliculus (IC) and primary auditory cortex (A1). This was performed in the anesthetized guinea-pig. Unlike most similar physiological experiments we used notched-noise masking of a pure-tone signal, which is more typically seen in psychophysics. Signal detection theory methods were used to convert spike firing rates into neurometric functions, similar to

psychometric functions. Threshold signal to noise ratio values were calculated and $roex(p, r)$ functions used to estimate filter size. In addition $roex(p, p_u, r)$ functions were fit to pure-tone response areas, allowing a direct comparison to the masking approach.

Results

In the IC notched-noise results were relatively homogeneous and corresponded well with previous experiments in the literature, which used more traditional pure-tone methods and in more peripheral auditory brain regions. Simultaneously masked bandwidth estimates were significantly broader than forward masked ones, which concurs with results in psychophysics. However, pure-tone derived estimates were significantly broader than notched-noise ones calculated within the same unit (by a factor of ~2). In A1 pure-tone calculated bandwidths were equally as broad, but more surprisingly, notched-noise bandwidths were narrower than seen in the IC and behaviour.

Conclusion

Frequency selectivity seems to be consistent from the periphery to the IC, but sharper in A1. This may be due to a number of reasons; the assumptions we make that allow us to interpret the activity of cells and convert firing rates into signal detection performance may not hold for the more complex A1 cells, or perhaps cortex uses a sub-optimal method for pooling cell activity when performing a detection task. The cause is still being investigated.

79 Electrophysiological Recordings from the Parabelt Areas in Macaques

Yoshinao Kajikawa¹, Deborah Ross¹, Charles Schroeder^{1,2}, Troy Hackett³

¹Nathan Kline Institute, ²Columbia University, ³Vanderbilt University

Background

According to anatomical connection patterns, primate auditory cortex has 3 hierarchical regions - core, belt and parabelt. Every region contains several areas. In macaques, the core and most of the belt regions stretch posterior-to-anterior on the superior temporal plane. Tonotopic gradients across areas run parallel in core and belt areas. Parabelt is elongated on the superior temporal gyrus (STG) and divided into caudal (CPB) and rostral (RPB) areas. Based on connection patterns and functional features, CPB and RPB are speculated to be parts of caudal "where" and rostral "what" pathways, respectively. Functional segregation between areas was suggested for the macaque belt by electrophysiological studies. However, the functions and physiological properties of macaque STG remain unknown, as does the relationship between CPB and RPB. We mapped auditory responses in PB of an awake macaque monkey, using a chronic chamber technique to make electrode penetrations perpendicular to STG.

Methods

Linear array multielectrodes were used to record field potential and multiunit activity (MUA) simultaneously across the laminar depth of STG cortices. We used a battery of sounds including pure tones (0.3 to 32 kHz), 1/3 oct. band-pass noises (BPN), broad band noises (BBN), click trains, sinusoidal amplitude modulation (SAM) tones, FM sweeps, and conspecific vocal sounds, and were delivered binaurally. We defined a best frequency (BF) at each penetration site using responses to tones and BPN.

Results

Many sites in STG appeared "tuned" to tones and BPN. Topographic patterns of BF were similar between tones and BPN, with a common low BF zone that could be a border between CPB and RPB. In the putative CPB, most sites responded to tones and formed a tonotopic gradient roughly in parallel to those in A1/CL. About 50 % of RPB sites did not respond to tones, and RPB had no clear tonotopic gradient. Latencies of responses to BBN were longer in RPB than CPB.

Conclusion

Our implant technique allowed direct access to Macaque STG. We mapped acoustic response properties in parabelt areas. While PB areas may prefer complex or vocal sounds to simple sounds, they also responded surprisingly well to tones and BPN with spectral tuning. RPB had smaller fraction of tone-responsive sites, suggested more selectivity to sounds in RPB than CPB. Shorter response latencies in CPB suggested a possibility of CPB-to-RPB projections.

80 Impact of Low Dose GABA on Temporal Responses: Comparison Between MGB and IC

Rui Cai¹, Donald M. Caspary¹

¹Southern Illinois University School of Medicine

Background

Previous studies demonstrated that neurons at higher levels of the auditory system respond to sinusoidal amplitude modulated (SAM) stimuli with large and complex variations in spike rate. Our preliminary medial geniculate body (MGB) findings and a number of earlier studies in the inferior colliculus (IC) found that GABA played a role in controlling response rate and shaping SAM response properties. The presence of high affinity GABAA receptors in MGB and the present iontophoretic studies suggest MGB neurons display a heightened sensitivity to GABA application. The present study quantifies the potency of GABA under parallel experimental conditions comparing the GABA 50% inhibitory dose (ID50) for MGB and IC neurons.

Methods

A commercially available, carboxystar-6, was used for recording and drug delivery (GABA, 10mM). Rate modulation transform functions (rMTFs) were generated from responses of isolated single units and occasional small clusters within MGB and IC in response to randomly

presented SAM (2-512 Hz, 450ms duration, 100% modulation depth, BBN or BF carrier). Retaining currents were set at -15nA and drug delivery dosage (eject current amplitude) ranged from 0nA up to 100nA with 5 or 10nA steps.

Results

In MGB and IC, rMTFs can be categorized into low pass, high pass, bandpass, band-reject response types. GABA dose-dependent effects were obtained from 34 MGB and 10 IC units, focused on bandpass and band-reject response types. Spike counts at -15nA retaining current was considered as the control condition for each unit. The percentage change in spike count was obtained at different ejection doses. A linear fit curve was applied to the percentage value against ejection current for each unit and ID50 values were calculated. The median ID50 in MGB was 11.72, and the mean was 14.01 ± 3.00 (Mean \pm SE). IC neurons were significantly less sensitive GABA application than MGB neurons ($p < 0.001$, independent t-test), with a median ID50 value of 51.28 and mean of 49.56 ± 6.75 .

Conclusion

These results find that MGB neurons are three times as sensitive to GABA application as IC neurons. This difference is likely due to the presence of high affinity GABA_A receptors in MGB. It has been suggested that, due to the presence of these high affinity GABA_ARs, ambient GABA levels may uniquely gate and shape the ascending information from MGB to auditory cortex. These data also suggest a specific role for these receptors in temporal processing in the MGB.

81 Cortical Spectrotemporal Processing with Age-Related Hearing Loss

Michael Trujillo¹, Khaleel Razak¹

¹Univ. California, Riverside

Background

Presbycusis (age-related hearing loss) is the most prevalent hearing impairment in humans. It affects ~40% of people older than 65 years. One major symptom of presbycusis is impaired speech recognition. Hearing aid amplification is only a partial solution, indicating central auditory system plasticity. The central changes have been insufficiently characterized. Here we studied cortical processing of frequency modulated (FM) sweeps to evaluate spectrotemporal representation plasticity in a mouse model of presbycusis (C57bl/6 strain).

Methods

Single unit electrophysiology in mice anesthetized with ketamine/xylazine was used to record FM selectivity. We compared cortical (both A1 and AAF) FM sweep rate selectivity across three age groups: Young ('Y', 1-2 mo), Middle-age ('M', 6-8 mo) and Old ('O', 14-20 mo). Sweep rates between 0.06-22 kHz/msec (linear sweeps) were tested. Neurons were classified as fast-pass, slow-pass, band-pass or all-pass based on response selectivity.

Results

Three main results were observed with age: 1) There were less fast-pass and band-pass neurons and more slow-pass neurons. 2) Selectivity of fast-pass and band-pass neurons was shifted towards slower sweep rates. Overall selectivity of band-pass neurons was reduced 3) Response variability to stimulus repetitions in terms of magnitude, first-spike latency and inters-spike intervals was increased.

Conclusion

Thus, processing of spectrotemporal cues becomes slow and noisy with presbycusis.

82 Consonance-Dependent Modulation of Phase Synchrony in the Auditory Cortex of Rats

Tomoyo Isoguchi¹, Takahiro Noda¹, Ryohei Kanzaki¹, Hirokazu Takahashi^{1,2}

¹The University of Tokyo, ²PREST, JST

Background

Many sounds in the environment have a rich sound spectrum, which is related to the qualia of the sound such as consonance or dissonance of chords. However, the information processing of the consonance of the chord in the auditory cortex is not fully understood. In this study, we targeted a phase locking value (PLV) of local field potential (LFP) and investigated whether PLV represents consonance of the chord consisting of two pure tones.

Methods

A microelectrode array with a grid of 96 recording sites recorded LFPs in the fourth layer of the auditory cortex of anesthetized naive rats in response to continuous pure tones and chords. In the pure tone condition, we randomly presented 9 pure tones (12, 13.5, 14.4, 15, 16, 18, 19.2, 20, and 24 kHz, 60 dB SPL) for 30 seconds continuously, each of which was interleaved with a silent block of 30 seconds. In the chord condition, we made 8 chords by combining 12-kHz pure tone and one of other 8 pure tones, and presented them in the same way as the pure tone condition. The recorded LFPs were bandpass filtered in 5 bands (theta, 4 - 8 Hz; alpha, 8 - 14 Hz; beta, 14 - 30 Hz; low gamma, 30 - 40 Hz; high gamma, 60 - 80 Hz) and PLVs were calculated in each band. First, a median of PLV among all pairs of recording sites within the auditory cortex in each silent and stimulus block was calculated. Second, a difference of median of PLV in the stimulus block with respect to that in the adjacent silent block was calculated as Δ PLV. Finally, a difference of Δ PLV of a chord with respect to Δ PLV of the higher-frequency composition tone of the chord was evaluated in consonant (low composition, 12 kHz; high composition, 15, 16, 18 or 20 kHz) and dissonant chords (low composition, 12 kHz; high composition, 13.5, 14.4 or 19.2 kHz) (Fig.1).

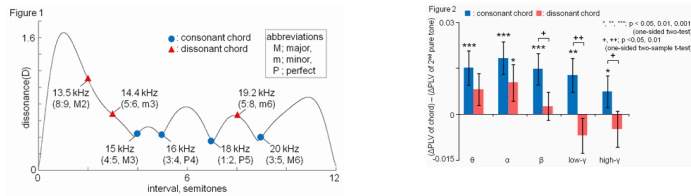
Results

Δ PLVs of consonant chord were significantly larger than Δ PLVs of pure tone in all bands, while Δ PLVs of dissonant chord were not significantly larger except alpha band (Fig. 2). Especially in beta, low gamma and high gamma band,

Δ PLV increase in a chord was larger in consonance than dissonance.

Conclusion

These results suggest that the phase synchrony within the auditory cortex is modulated according to the complex sound spectrum, such as consonance of the chords.



83 Measurement of Auditory Cortical Network Responses to Potassium Channel Openers

Calvin Wu¹, Nicole Calderon¹, Kamakshi Gopal¹, Guenter Gross¹, Ernest Moore¹

¹University of North Texas

Background

Potassium (K⁺) channels are primary regulators of neuronal excitability, with significant roles in neuropathic pain, epilepsy, cardiac arrhythmia, hearing loss, and tinnitus. In recent years, a novel class of drugs – K⁺ channel openers – has been shown to exert anticonvulsive and neuroprotective effects by activating K⁺ currents that induce hyperpolarization. Retigabine, a first-in-class channel opener of a voltage-gated K⁺ channel subclass (K_v7), is the prime candidate currently undergoing clinical trials for the treatment of epilepsy.

Methods

We present quantitative measurements of the modulatory effect of K⁺ channel openers on the activity pattern of spontaneously-active neuronal networks, and discuss the potential therapeutic value of K⁺ channel openers on pathological auditory cortical activity such as tinnitus. Networks derived from dissociated auditory cortices of mouse embryos were grown on microelectrode arrays (MEAs) to assay the drug-induced changes in network spike production, burst patterns, and action potential waveforms.

Results

We assessed the effects of retigabine, flupirtine (structural analog of retigabine), isopimaric acid, and NS1619 (activator of large-conductance calcium-sensitive potassium channels). The EC₅₀ values were 8.0, 4.0, 7.8 and 5.8 μ M, respectively. Despite comparable potency – flupirtine (EC₅₀: 4.0 μ M) > NS1619 (5.8) > isopimaric acid (7.8) > retigabine (8.0) – and full efficacy, each K⁺ channel opener exhibited differential burst properties under low concentration (2.0 μ M), and distinct K⁺ waveform component alteration of action potentials under high concentration (20 μ M).

Conclusion

This study, using the *in vitro* auditory cortical network model coupled with the MEA platform for rapid drug screening and identification of mechanisms, may serve as the basis for developing and re-purposing K⁺ channel openers as potential drugs for the treatment of tinnitus.

84 Multiscale Functional Imaging of Auditory Cortical Areas in Awake Mice

John Issa¹, Ben Haeffele¹, Eric Young¹, David Yue¹

¹Johns Hopkins University

Background

Classic electrode studies support robust spatial organization of sensory cortices, comprised of distinct areas with remarkable functional specialization and segregation. In the mouse auditory cortex, auditory subregions with distinctive receptive field properties have been observed: AI, AAF, UF, DP, and All. For example, in AI and AAF, preferred frequencies appear organized spatially along a rostrocaudal gradient; neurons in UF prefer high frequencies (>40 kHz); and All contains neurons with multi-peaked tuning (J Comp Physiol A., 181(6):559-71).

However, these studies may underestimate the actual heterogeneity of neuronal responses because the methodologies used may be biased towards strongly responding neurons. More recent two-photon Ca²⁺ imaging studies, where a large number of individual neurons can be imaged simultaneously, have revealed diverse receptive fields among nearby neurons (Nat Neurosci., 13(3):353-68) and even between nearby spines on the same neuron (J Neurosci., 32(5):1589-601). These results suggest a high diversity of response properties in auditory cortex, contrasting with the well-organized and distinctive auditory field maps expected from prior studies. To reconcile these contrasting perspectives, we here combined functional transcranial fluorescence imaging registered with two photon Ca²⁺ imaging of individual neurons in the auditory cortices of awake mice.

Methods

The left auditory cortical areas of adult mice were initially characterized by functional transcranial fluorescence imaging. The large imaging field (~5 mm) permitted simultaneous imaging of all auditory fields. Next, we undertook two-photon Ca²⁺ imaging of layer 2/3 neurons, as registered to transcranial images via blood vessel landmarks.

Results

Transcranial imaging rapidly identified multiple, well-demarcated auditory cortical areas, including AI, AAF, UF, and All. Response properties and spatial organization exhibited remarkable agreement with the consensus view of earlier electrode studies, such as strong rostrocaudal gradients of preferred frequency in AI and AAF. Under two-photon Ca²⁺ imaging, the average response, taken by summing firing across individual neurons, accorded well with the global profile of corresponding cortical regions.

Beyond this clear overall congruence, single-neuron activity exhibited significant divergence in precise responses among neighboring neurons, leaving room for higher-order representations of acoustic stimuli. Compared to anesthetized mice, single-neuron activities in awake animals were often enhanced, favoring well-resolved characterization of response profiles.

Conclusion

The combination of transcranial functional imaging and two-photon Ca²⁺ imaging promises to reveal how global receptive-field organization intersects the neural activity of individual neurons across multiple spatial scales.

85 Morphological Analysis of Auditory Thalamus in BXSB/MpJ Mice

Jane Mattley¹, Dr Lucy A. Anderson¹, Dr Jennifer F. Linden^{1,2}

¹*UCL Ear Institute*, ²*Dept. Neuroscience, Physiology & Pharmacology, University College London*

Background

In the BXSB/MpJ inbred mouse strain, approximately half the animals spontaneously develop nests of displaced neurons in cortical layer I, called ectopias. Neocortical ectopias have also been reported to occur in humans with developmental disorders such as dyslexia. Interestingly, although the ectopias occur outside the auditory cortex, both human studies and studies of rats with induced cortical malformations have observed an association with anatomical abnormalities within the auditory thalamus. Previously, we have shown that ectopic male BXSB/MpJ mice have an auditory thalamic processing deficit, despite apparently normal hearing sensitivity. The aim of this current study was to determine whether these animals also have anatomical abnormalities in the auditory thalamus.

Methods

Auditory brainstem responses and extracellular thalamic recordings were collected from urethane-anaesthetised male BXSB/MpJ mice during monaural presentations of free-field auditory stimuli. All experiments were necessarily performed blind to the ectopic status of the animal. Following in vivo physiological recordings, brain tissue was processed for histology. Alternate coronal brain sections were stained for cytochrome oxidase to differentiate thalamic subdivisions, and Nissl substance to reveal cortical ectopia and thalamic cell density. Volumes of cortical ectopias and auditory thalamic subdivisions were calculated using area estimates obtained by drawing borders on images of stained sections. Cell packing densities were estimated with a pixel-based density index, calculated from the mean of median pixel intensities across different image squares for the same subdivision and animal.

Results

Most ectopic animals had a single ectopia (volume 0.001-0.036 mm³), located in the motor cortex. Ectopia volume was found to correlate with auditory thalamic processing deficits; animals with larger ectopia in motor cortex had

larger deficits ($p < 0.05$). However, anatomical analysis showed no significant differences in thalamic volume or cell density between ectopic and non-ectopic mice, for either the whole auditory thalamus or any individual subdivision.

Conclusion

Cortical ectopias in BXSB/MpJ mice were not associated with any significant changes in auditory thalamic morphology; however, ectopia volume correlated with physiological deficits in auditory thalamic processing. These results suggest that the deficits might arise outside the auditory thalamus, and perhaps that motor cortex ectopias and auditory thalamic processing deficits have a common underlying developmental cause.

Acknowledgements

Supported by the Wellcome Trust, Deafness Research UK, and a UCL Impact Award.

86 An Emergent Spectro-Temporal Representation for Natural Sounds Based on Sustained Firing of Central Auditory Neurons

Michael Carlin¹, Mounya Elhilali¹

¹*Johns Hopkins University*

Background

Natural sounds evolve over many concurrent timescales, from tens to hundreds of milliseconds, yet the mechanisms by which the auditory system calibrates internal neural dynamics to the information-bearing components of these signals remains unclear. Recent data suggests the presence of a neural code based on sustained firing rates, whereby central auditory neurons exhibit strong, persistent responses to their preferred stimuli. In this work, we examine how this code may underlie aspects of how the auditory system learns to represent sound.

Methods

We explore how a coding strategy that maximizes sustained firing rates of model neurons influences the shapes of spectro-temporal receptive fields (STRFs) in the central auditory system.

Results

We demonstrate the emergence of richly structured STRFs that capture the structure of natural sounds over a wide range of timescales, and show how the emergent ensembles resemble those commonly reported in physiological studies. We also show how the emergent ensembles capture the full range of spectro-temporal modulations observed in natural sounds, forming a discriminative representation that captures the full range of modulation statistics that characterize natural sound ensembles.

Conclusion

The results suggest that a coding strategy based on sustained firing rates may underlie part of the neural code for representing sounds in the central auditory system.

87 Cell Type-Specific Cholinergic Regulation of Action Potentials in Layer 6 Neurons of Auditory Cortex

Takuya Mieda¹, Hideki Kawai¹

¹Soka University

Background

Layer 6 of primary auditory cortex (A1) contains neurons that control cortical gain of auditory information by providing feedback to primary thalamic neurons in the ventral division of medial geniculate nucleus (MGv) and by modulating thalamorecipient neurons in the middle layer of A1. Since cholinergic inputs to A1 regulate receptive field of MGv neurons, neuromodulatory mechanisms of cortical neurons, particularly of layer 6 neurons, may be critical for gating of auditory information. Many previous studies have revealed cholinergic regulation of neuronal excitability in the neocortex. However, little has been studied about the regulation of layer 6 neurons. As a step toward understanding cellular mechanisms of sensory gating, we investigate intrinsic membrane properties and cholinergic regulation of neuronal excitability in layer 6 neurons.

Methods

In auditory thalamocortical slices, we have recorded membrane potentials of layer 6 neurons using whole-cell patch clamp recording techniques. Cholinergic ligands were tonically applied to examine their effects on intrinsic membrane properties and action potentials elicited by current injections. Cell type and morphology of recorded neurons were analyzed by examining the expression of glutamic acid decarboxylase 67 kDa (GAD67) - an inhibitory neuronal marker - using immunofluorescent staining method and by histochemical analysis of biocytin-filled neurons.

Results

Based on spike firing properties and immunofluorescent staining, we divided neurons into three groups: regular spiking (RS), inhibitory RS (iRS), and fast spiking (FS) neurons. Tonic application of acetylcholine (ACh; <100 μ M, ~5 min) increased resting membrane potentials, input resistance, and spike frequency while decreasing spike onset time in all layer 6 neurons recorded. In RS neurons, ACh decreased spike threshold for the first spike as well as repolarizing afterhyperpolarization (fAHP) with little changes in spike width and peak amplitude. In iRS neurons, ACh greatly increased spike threshold, spike width, and fAHP while decreasing peak amplitude. Meanwhile, in FS neurons, ACh had little effects on spike threshold, peak amplitude, and spike half-width, but decreased fAHP.

Conclusion

ACh increased the excitability of all layer 6 neurons we recorded by increasing resting membrane potentials and input resistance. Analysis of action potentials revealed the difference in cellular mechanisms of cholinergic regulation in RS, iRS, and FS neurons.

88 Neurochemical, Physiological and Anatomical Studies of the Auditory Thalamotectal Projections of the Mouse

Alexandria Lesicko¹, Daniel Llano¹

¹University of Illinois at Urbana-Champaign

Background

Descending projections are found at virtually every level of the central auditory system. Though many of these projections have garnered attention in recent years, the auditory thalamotectal pathway remains poorly characterized. The purpose of the current study was to provide an initial characterization of this pathway, using neurochemical and physiological approaches. We examined immunoreactivity for two calcium-binding proteins, calbindin and calretinin, in auditory thalamotectal cells since these proteins are found in the medial and dorsal divisions of the medial geniculate body. As thalamotectal cells arise from the dorsal and medial divisions of the medial geniculate body, we hypothesize that they will be immunoreactive for either calbindin or calretinin, like their neighboring cells in these regions. We also studied the electrophysiological properties of identified thalamotectal cells.

Methods

A fluorescent retrograde tracer, either red polystyrene Fluospheres (for physiological studies) or Fluorogold (for immunostaining studies), was injected into the inferior colliculus of mice to label thalamotectal cells. Fluorogold-injected animals were perfused, had brains removed and tissue sections that contained labeled thalamotectal cells were immunostained for either calbindin or calretinin. Living brain slices were obtained from Fluosphere-injected animals, and whole-cell patch clamp was used to study the physiological properties of these cells. Recorded cells were filled with biocytin for morphological characterization.

Results

We found that the vast majority of retrogradely-labeled cells (>90%) were negative for either calbindin or calretinin. Positive controls with retrogradely labeled thalamocortical cells showed strong immunostaining for both calbindin and calretinin. Physiologically, thalamotectal cells showed little bursting behavior and did not show typical bitufted thalamic morphology.

Conclusion

Mouse auditory thalamotectal neurons do not exhibit strong positivity for calbindin or calretinin, do not show bursting and do not have typical thalamocortical cell morphology. Based on these results, it is possible that these cells form a distinct class of thalamic neurons that differ from neighboring auditory thalamic cells.

89 Temporal Modulation Context Affects the Cortical Representation of Amplitude Modulated Signals in Awake Monkeys

Ralph Beitel¹, Brian Malone¹, Maike Vollmer², Marc Heiser³, Christoph Schreiner¹

¹UCSF, ²Comprehensive Hearing Center Wuerzburg, Germany, ³UCLA

Background

Sinusoidal amplitude modulated (SAM) signals are often used in psychophysical studies of temporal processing in the auditory system. Proposals about encoding of SAM sounds in the brain include filterbank models tuned to modulation frequencies as well as models that favor information processing across modulation frequencies. In this physiological study we presented pairs of modulated stimuli (SAM1/SAM2) to awake monkeys and investigated the effects that SAM1 had on cortical responses to SAM2.

Methods

Two squirrel monkeys were trained to sit facing a speaker with head restrained during recording sessions. Multiunit responses were recorded in core auditory cortex with a linear 16-channel silicon probe. The carriers for modulated signals were pure tones near channel best frequency (BF) or 2-octave bandwidth noise centered on channel BF. SAM2 modulation frequencies were typically presented from 4 to 512 Hz in pseudorandom order. The effects of stimulus context were investigated by comparing the shapes of modulation transfer functions (MTFs) when each SAM2 stimulus (1-s) was preceded immediately by a SAM1 stimulus (1-s) at a constant frequency (4, 10, 32, or 96 Hz) or by an unmodulated stimulus. Responses to SAM2 signals presented alone were also studied. Modulation depth was 100% for all SAM stimuli.

Results

The spike rates to SAM2 presented alone or preceded by an unmodulated stimulus were similar and were usually higher than spike rates to SAM2 stimuli preceded by SAM1 stimuli. In comparing the effect of different SAM1 modulation frequencies on SAM2 spike rates, higher SAM1 modulation frequencies generally resulted in a significant reduction in SAM2 spike rates when compared to lower SAM1 frequencies. This reduction in spike rates occurred over a broad range of SAM2 modulation frequencies (± 2 oct) and tended to be larger for SAM2 modulation frequencies nearer to the modulation frequency of the preceding SAM1 segment. Compared to rate MTFs, the effects of stimulus context on MTFs defined by temporal metrics (vector strength and trial-to-trial response similarity) were small.

Conclusion

Temporal context significantly affects cortical responses to SAM signals in a manner consistent with the idea of adaptation within a broadly tuned modulation frequency channel. In contrast, a preceding unmodulated stimulus had no consistent effect on the responses to modulated stimuli, suggesting that preceding modulation was

necessary as well as effective for the observed spike rate effects.

Supported by grants Silvio O. Conte MH077970, NIDCD RO1-DC-02260, the Coleman Memorial Fund, and Hearing Research Inc.

90 Noradrenergic Gating of Long-Term Cortical Synaptic Plasticity

Ana Raquel Martins^{1,2}, Robert Froemke^{1,3}

¹Skirball Institute of Biomolecular Medicine, New York University School of medicine, ²BEB PhD programme, CNC, University of Coimbra, ³Center for Neural Sciences, NYU

Background

Neuronal networks of the cerebral cortex are plastic, maintaining the capacity to reorganize throughout life. While neuromodulator release is required for cortical plasticity, it is uncertain how subcortical neuromodulatory systems, such as the noradrenergic locus coeruleus, interact with and refine cortical circuits.

Methods

Here we determine the dynamics of auditory cortical receptive field plasticity at the synaptic and spiking levels using in vivo whole-cell recording. Adult rats were anesthetized, stimulation electrodes were implanted in the locus coeruleus, and a craniotomy performed over the primary auditory cortex. After mapping the tonotopic field of the primary auditory cortex, intracellular recordings were made (usually in layer V) from cortical neurons, and pure tones of varying frequencies and intensities were presented to the animal to characterize tonal receptive fields.

Results

Pairing sensory stimulation (pure tones) with locus coeruleus activation (to release noradrenalin) dramatically changed the tuning properties of cortical neurons. For most recordings, pairing induced large increases of tone-evoked synaptic and spiking responses, degrading neuronal tuning across all frequencies. Changes in tuning curve shape continued to evolve over tens of minutes to emphasize and disambiguate the paired stimulus from other unpaired stimuli. Multiple cell recordings from the same animal for hours after a single episode of locus coeruleus pairing suggested that these changes in AI tuning stabilized after three to six hours and could persist for 11+ hours.

Furthermore, some AI neurons were initially unresponsive to auditory stimuli. During and after locus coeruleus pairing, however, tone-evoked responses could suddenly emerge, persisting for the duration of post-pairing recordings (30+ min). This suggests the involvement of the locus coeruleus arousal system in the integration of 'silent neurons' into a specific auditory memory trace or cortical representation of certain, potentially behaviorally important sensory stimuli.

Moreover, our data suggests that the locus coeruleus itself seems to undergo local activity changes that at least partially underlie the cortical changes observed.

Conclusion

We hypothesize that such changes to cortical tuning curves have important implications for the detection and/or discrimination of different sensory inputs, and that the subcortical sensitization of locus coeruleus plays a major role in the cortical changes observed.

91 The Effect of Sound Source Location on Multi-Peak Frequency Tuning in the Primary Auditory Cortex of Marmoset Monkeys

Yi Zhou¹, Xiaoqin Wang²

¹Dept. Speech and Hearing Science, Arizona State University, ²Dept. Biomedical Engineering, Johns Hopkins University

Background

When the listening environment contains multiple sound sources emitting sounds from various spatial locations, sound source identification becomes difficult to achieve. On the other hand, the auditory system routinely streams together isolated sound elements into a coherent perceptual image using multiple grouping cues, such as harmonicity and common onset. For example, pure tones that are harmonically related can be fused into a single auditory event regardless of their spatial locations. To understand the underlying neural mechanisms, this study investigated whether auditory cortex neurons treat sounds originating from the same source or different sources in different ways.

Methods

Single-unit data was collected from the primary auditory cortex (A1) of awake marmoset monkeys. The experiments were conducted in free field with multiple loudspeakers positioned in the frontal hemifield. To analyze the efficacy of spectral integration in A1, our analyses focused on neurons showing multi-peak frequency tuning profiles in response to a pair of pure-tone stimuli delivered from the same loudspeaker.

Results

The two-tone paradigm revealed substantial inhibitory activity in frequency tuning of neurons. We observed that many multi-peak neurons showed either excitatory or inhibitory sensitivity at distant frequencies with particular harmonic ratios to their best frequency (BF), e.g., 1/2BF or 2BF. Interestingly, presenting the two tones from two different spatial locations did not change the multiple-peak tuning profiles of a majority of neurons. In some neurons, inhibitory interactions were observed when a pure tone with a distant frequency (e.g., 2BF) was presented from the location showing no excitatory responses to BF.

Conclusion

These observations provide an interesting example of location invariance in cortical spectral processing. The data show that A1 neurons can integrate harmonically related

excitatory or inhibitory inputs across a broad spatial domain.

92 Structured Sparse Encoding for Automated Segmentation of Calcium Imaging Data

Benjamin Haeffele¹, Rene Vidal¹, John Issa¹, David Yue¹, Eric Young¹

¹Johns Hopkins University

Background

Advances in fluorescent microscopy and improvements in synthetic and genetically encoded calcium indicators have enabled recordings of calcium dynamics from large numbers of neurons. However, as the number of recorded neurons increases, segmenting the neuron boundaries from the raw fluorescent data becomes increasingly challenging and presents a significant bottleneck in the data analysis. Several methods have been suggested to automate the image segmentation process but their application has been limited by decreased performance in the presence of image noise, overly restrictive model assumptions, or excessive computation time.

Methods

To address these issues, we have developed an image segmentation algorithm which uses structured sparse encoding to learn a basis of dictionary elements and then decomposes the fluorescence data into segmented regions and estimated spike trains simultaneously. To demonstrate the utility of our method we use it to segment two photon calcium image data taken from the auditory cortex of awake mice. The cortex was virally transfected with the genetically encoded calcium indicator GCaMP5, and images were acquired at multiple levels of optical resolution. Robust activity was observed in response to both natural mouse calls and pure tone stimuli.

Results

Our method requires minimal user input or parameter tuning, makes no assumptions about region morphology, is robust to noise, and is easily modified to accommodate a wide variety of calcium dynamics. When applied to data taken at multiple levels of optical resolution, our method is able to identify neural boundaries and estimate spike trains from both cell bodies and dendritic processes.

Conclusion

Structured sparse encoding provides a robust, efficient, and highly flexible method to decompose neural calcium image data into both segmented cell boundaries and estimated spike trains.

93 Intracortical Inputs to Neurons in Layer 4 of Primary Auditory Cortex

Megan Kratz¹, Paul Manis¹

¹University of North Carolina at Chapel Hill

Background

One task of the auditory system is to identify auditory objects in the environment. Auditory objects often contain component frequencies from across the hearing range.

This presents unique challenges for the neural circuitry that processes sound, as it requires extensive lateral connectivity between different parts of the tonotopic map. One of the earliest sites in the auditory pathway where convergence from across the entire cochlear partition can take place (aside from octopus cells of the cochlear nucleus) is the primary auditory cortex (A1). Here, we investigate the sources of intracortical input from across the tonotopic axis onto Layer (L) 4 neurons in mouse primary auditory cortex.

Methods

We use thalamocortical slices of P35-43 CBA/CAJ mouse A1 that cut across the tonotopic map. We then record excitatory post-synaptic currents from L4 neurons while stimulating potential presynaptic partners throughout A1 using laser scanning photostimulation and glutamate uncaging. Uncaging sites were designed on a dense, overlapping hexagonal grid so that any presynaptic neuron will likely be activated by stimulation at multiple adjacent sites. This approach allows us to use the spatial correlation of stimulation-evoked events to more confidently determine the presence and location of presynaptic cells.

Results

While input maps to individual L4 neurons are heterogeneous, they share some common features. Discrete, discontinuous inputs from other L4 neurons ~ 300 μm caudal (towards the low-frequency end of the tonotopic map) to the cell are evident in about 40% of cells, as are similar inputs from L4 neurons ~ 300 μm rostral. Inputs were also seen from L6 neurons both ~ 300 μm rostral and caudal, although few cells receive inputs from all of these locations. L4 neurons also receive "columnar" inputs. Nearly all cells receive L4 input from the immediate vicinity of the cell, while approximately 30%, 22% and 50% of cells receive same-column input from L2/3, L5, and L6, respectively.

Conclusion

These results suggest that information from different tonotopic locations is combined with thalamocortical inputs in L4 neurons. The non-contiguous but regular organization of the input zones is consistent with a modular processing circuit. The (putative) cross-tonotopic connections shown here may be tuned to help amplify or fill-in harmonic structure, aiding our ability to detect, identify, and attend to auditory objects.

Supported by NIDCD R01DC009809 to PBM.

94 Cortical Auditory Evoked Potentials to Frequency Changes with Varied Size, Velocity and Direction

Marc Lammers^{1,2}, Marjolijn van der Waals¹, Gijsbert van Zanten^{1,2}, Wilko Grolman^{1,2}, **Huib Versnel**^{1,2}
¹University Medical Center Utrecht, ²Rudolf Magnus Institute of Neuroscience

Background

Cortical auditory evoked potentials (CAEPs) in response to brief changes in sounds (e.g., vowel transitions, or changes in level or frequency) may be suitable for assessing suprathreshold neural processes related to speech perception. These CAEPs evoked by sound changes are also referred to as acoustic change complexes (ACCs) and are composed of a typical P₁-N₁-P₂ waveform morphology (N₁ latency ≈ 100 ms after stimulus change). In this study we explored ACCs to small frequency modulation (FM) sweeps following 1000-Hz pure tones. Size, velocity and direction of the FM sweep were systematically varied.

Methods

Ten young adult human subjects with normal hearing participated. Stimuli were tones of 3300 ms with three components: a) a reference tone of 1000 Hz with a duration of 3000 ms, b) an FM sweep with a frequency change Δf , c) a tone with a frequency of 1000- Δf or 1000+ Δf Hz and a duration of 300 ms. The silent interval between stimuli was 200 ms. Sound level was 75 dB SPL. Three frequency changes were used: 0.029, 0.086 and 0.257 octave; four FM velocities were used: 3.2, 9.5, 28.6 and 85.7 octave/s; both up and down sweep directions were presented. The ACCs were recorded with Ag/AgCl electrodes at Cz referenced to the contralateral mastoid. For each stimulus condition, ACC waveforms were averaged over 100 presentations.

Results

As previously shown in literature, the ACC amplitude increased with increasing frequency change. The amplitude doubled when the change was increased with a factor 9. Further, the amplitude increased with about 25% when velocity was increased with a factor 27. Finally, the ACC amplitudes tended to be larger for downward frequency changes.

Conclusion

The primary factor determining the ACC amplitude is the size of the frequency change. A secondary factor is velocity of the change. For clinical purposes, for instance when assessing thresholds of responses to frequency changes, an appropriate stimulus to evoke ACCs would be a fast FM sweep following a long pure tone.

95 Oxytocin-Based Neuromodulation of Mammalian Social Behavior

Bianca Jones¹, Robert Froemke²

¹New York University School of Medicine, ²New York University

Background

Social interactions are essential for normative development and lifelong physical and mental health. The neuromodulator oxytocin is believed to be important for some forms of social behavior, specifically parent-child bonding and maternal behavior. Here we investigate a fundamental form of rodent social behavior that depends on both social cues and modification of neural substrates: pup retrieval.

Methods

To initiate pup retrieval behavior, mouse pups produce ultrasonic vocalizations (USVs) when separated from the nest. Dams and other experienced caregivers use these acoustic signals to locate and retrieve isolated pups. Importantly, virgin female mice can also learn a variety of maternal behaviors, including pup retrieval, and we hypothesize that oxytocin plays a major role in this form of learned social behavior (Pedersen et al., Science 1982). However, it is unclear how oxytocin impacts the activity of the cortex, leading to the robust increase in maternal behavior.

Results

We confirmed that virgins can also learn to retrieve pups. Furthermore, learning is accelerated after either systemic or cortical application of oxytocin. Virgins were first tested for initial retrieval abilities. Virgins were then co-housed with a dam and her pups for up to three days, with some animals receiving oxytocin and other animals receiving saline. After 12 hours of co-housing, 16/31 (~50%) animals injected with oxytocin learned to retrieve pups, but only 6/24 (25%) control saline-injected virgins retrieved pups. Similarly, 7/9 animals receiving oxytocin infusion into left auditory cortex via cannula retrieved pups within 12 hours, but 0/4 cannulated virgins receiving saline infusion retrieved pups. Finally, infusing the GABA-A receptor agonist muscimol into left auditory cortex, to inactivate local circuitry, reduced or fully prevented pup retrieval in 6/9 experienced animals. Infusion into right auditory cortex did not seem to significantly affect retrieval.

Conclusion

This demonstrates that left auditory cortex is required for USVs to engage pup retrieval. Furthermore, these data suggest that oxytocin-based neuromodulation, paired with acoustic stimuli, can modify auditory cortex to enable or improve learned social behavior.

96 Functional Organization of Spectrotemporal Processing in Human Temporal Lobe

Patrick Hullett¹, Niman Mesgarani², Christoph Schreiner³, Edward Chang²

¹UCSF & UCB Joint Graduate Group In Bioengineering, UCSF, ²Department of Neurological Surgery, UCSF., ³Coleman Memorial Laboratory, Department of Otolaryngology-HNS, UCSF

Background

Functional organization within the nervous system often reveals key insights into the information being represented and the processing taking place. In the human auditory system, tonotopic organization is a prominent organizing principle up through the primary auditory cortex, but less is known about the functional organization of higher auditory areas. It is of considerable interest to determine what organizing principles, if any, are present in higher-order auditory areas in humans. Here we use ECoG recordings in conjunction with advanced techniques for computing spectrotemporal receptive fields to investigate what forms of functional organization are present in areas beyond primary auditory cortex.

Methods

To characterize functional organization in higher-order auditory areas, we recorded auditory responses to natural speech in the temporal lobe of awake humans using electrocorticography (ECoG). Although restricted to rare clinical settings, ECoG provides high spatiotemporal resolution of neural activity, which is ideal for investigating questions of functional organization in the auditory system. Using the high gamma component of ECoG recordings in three patients who passively listened to speech, we computed spectrotemporal receptive fields (STRF's) using maximally informative dimension (MID) analysis and looked for functional organization based on the spatial distribution of STRF's across the temporal lobe.

Results

Parameters derived from each STRF, including best spectral modulation, best temporal modulation, best frequency, bandwidth, and temporal integration were mapped onto cortex to characterize the functional organization of spectrotemporal processing. One prominent outcome of this analysis shows functional organization based on spectral and temporal modulation tuning. First, there is a spectral-temporal trade-off in which regions tuned to high spectral modulations prefer low temporal modulations while regions tuned to high temporal modulations prefer low spectral modulations. Second, there are smooth transitions from high spectral modulation tuned regions to high temporal modulation tuned regions thus forming an organized distribution of modulation tuning across temporal lobe auditory cortex.

Conclusion

These results indicate that modulation tuning is a dominant organizing feature within temporal lobe auditory cortex. Although other forms of functional organization are

present, organization based on modulation tuning is most descriptive of temporal lobe activity in response to complex signals like speech. At the level of the temporal lobe, these maps imply the extraction of spectrotemporal modulation content is a critical step in the process of speech perception.

97 Functional Topography of Thalamocortical and Intracortical Inputs to Layers 4 and 6b

Charles Lee¹, Kazuo Imaizumi¹

¹Louisiana State Univ. School of Veterinary Medicine

Background

In the auditory forebrain, thalamocortical axons transfer information from the thalamus to layers 4 and 6b of sensory cortical areas. Yet, receptive field properties in layer 6 are generally more complex than those in layer 4. Thus, it remains an open question whether such differences reflect distinct inheritance patterns from the thalamus or if instead they are derived from local cortical circuits.

Methods

To distinguish between these possibilities, we utilized in vitro slice preparations containing the intact thalamocortical pathways in the auditory and somatosensory systems. Responses from neurons in layers 4 and 6b that resided in the same column were recorded using whole-cell patch clamp. Laser-scanning photostimulation via uncaging of glutamate in the thalamus and cortex was then used to map the functional topography of both thalamocortical and intracortical inputs.

Results

We found that the thalamocortical inputs to layers 4 and 6b originated from the same thalamic domain, but the intracortical projections to the same neurons differed dramatically, with those to layer 6b originating from different laminar regions than those to layer 4.

Conclusion

Our results suggest that the intracortical projections to layer 6b likely contribute more to their complex receptive fields, while the thalamocortical inputs to layer 6b instead may be concomitantly attenuated. As such, the functional circuitry of the thalamocortical network is comprised of concurrent and convergent networks that lead to computationally divergent outcomes emerging from the intracortical network.

98 Subcollicular Sources of Projections to the Auditory Thalamus in the Rat

Albert S. Berrebi¹, F.-Javier Bernardo², Yongming Jin³, Marcelo Gomez-Alvarez², M-Auxiliadora Aparicio², Emmanuel Marquez², David Sloan¹, Enrique Saldana^{2,4}

¹West Virginia University, ²University of Salamanca, ³Cleveland Clinic, ⁴Institute of Biomedical Research of Salamanca (IBSAL)

Background

It is generally assumed that the main source of ascending projections to the auditory thalamus is the inferior colliculus (IC). However, several isolated reports suggest that the medial geniculate body (MGB) receives direct projections from different auditory subcollicular nuclei (e.g. Henkel, *Brain Res* 259:21–30, 1983 [cat]; Angelucci et al., *J Comp Neurol* 400:417–439, 1998 [ferret]; Malmierca et al., *J Neurosci* 22:10891–10897, 2002 [rat]; Berrebi et al., *ARO Abstr* 35:250, 2012 [rat]). This is particularly relevant because evidence presented at this meeting indicates that, contrary to the long-held tenet, the medial division of the MGB (MGBm) is not a major target of the IC (Saldaña, Symposium on “The non-lemniscal auditory thalamus”).

Methods

To systematically investigate the sources of ascending projections to the auditory thalamus, we made iontophoretic injections of the sensitive retrograde tracer FluoroGold into the auditory thalamus and analyzed the distribution of the neuronal cell bodies labeled in all subcollicular auditory nuclei.

Results

We obtained cases with injection sites centered in different regions of the auditory thalamus, including the ventral, dorsal and medial divisions of the MGB, the posterior intralaminar nucleus, the marginal zone and the posterior limitans nucleus.

In the classical auditory nuclei, abundant retrogradely labeled neurons were found in the contralateral dorsal cochlear nucleus and lateral superior olive; in the ipsilateral medial superior olive (MSO), superior paraolivary nucleus (SPON), and ventral nucleus of the lateral lemniscus; and in the dorsal nucleus of the lateral lemniscus and the nucleus sagulum of both sides. We also found numerous labeled neurons ipsilaterally in the ventrolateral tegmental area, located medial to the ventromedial portion of the VNLL, as well as in an ill-defined territory wedged between the medial nucleus of the trapezoid body and the SPON. In the cases with the most retrograde labeling, the percentage of labeled neurons in some nuclei, such as the ipsilateral MSO and SPON, approached 50%.

Conclusion

Because FluoroGold injection sites tend to be large and usually include more than one subdivision of the auditory thalamus, we are currently performing a quantitative, multivariate analysis to infer the relative contribution of each one of the subcollicular nuclei to the innervation of each region of the auditory thalamus.

These findings improve our understanding of the organization of the auditory pathway, shed light on the complex parcellation of the auditory thalamus, and provide novel morphological frameworks for future functional studies.

[99] Modulation of Auditory Steady-State Response (ASSR) as a Function of Frequency Ratio Characterizing Three-Note Chords

Asuka Otsuka¹, Masato Yumoto², Shinya Kuriki³, Seiji Nakagawa¹

¹The National Institute of Advanced Industrial Science and Technology (AIST), ²Graduate School of Medicine, The University of Tokyo, ³Research Center for Advanced Technologies, Tokyo Denki University

Background

Chords composed of tones characterized by simple frequency ratios are perceived consonant whereas chords of complex ratios are perceived dissonant. In theory, perception of dissonance is attributed to sensation of beats/roughness. The neuronal processing of beats/roughness is reflected in the auditory cortical steady-state response (ASSR), an oscillatory evoked response phase-locked to the temporal envelope periodically amplitude-modulated at rates of difference frequencies (ΔF). Intracranial recording revealed that the ASSR was correlated to energy of ΔF and exhibited larger activities for dissonant than consonant chords. However, effect of frequency ratio on the ASSR was yet unclear because the physical parameters of Δf contained in each chord differed in terms of modulation rate, number of frequency components and spectral energy. The present study therefore aimed at exploring more simply the modulation of neuromagnetic ASSR as a function of frequency ratio.

Methods

Six kinds of stimulus chords composed of three sinusoids were prepared. The frequency ratio was varied systematically from 4:5:6, 6:7:8, through to 14:15:16, corresponding to chords containing 5th, 7th, to 15th overtone series. The carrier frequencies of each chord were defined for the envelope to be amplitude-modulated at ΔF of 40 Hz. The spectral energy of all frequency components was equalized at 70 dB SPL by real-ear measurement and inverse filtering method. A sinusoidally amplitude-modulated (SAM) chirp tone was presented as a control to capture the neuronal frequency characteristics of the ASSR.

Results

Clearly elicited 40-Hz component was identified as the ASSR. Equivalent current dipole (ECD) of the ASSR was estimated using a single dipole model per hemisphere. The strength of the ECD moment for 5th and 7th chords characterized by simple frequency ratio was significantly smaller than that for 11th, 13th and 15th chords of complex frequency ratio despite that the acoustic parameters, i.e., the frequency as well as the spectral energy of ΔF to

which the ASSR was synchronized was physically equal and further that the neuronal frequency characteristics was compensated by responses to the SAM chirp tone.

Conclusion

The results of the present study suggest that information that exists in natural world such as simple frequency ratio is processed in energy-saving manner whereas artificial information induces larger activations. Attentional gating of thalamocortical function as well as resonance effect with the spontaneous rhythmic activities might be candidates for the underlying mechanism.

[100] MANTA – an Open-Source, High Density Electrophysiology Recording Suite for MATLAB

Bernhard Englitz^{1,2}, Stephen David³, Shihab Shamma^{1,2}

¹Ecole Normale Supérieure, ²University of Maryland, ³OHSU

Background

The distributed nature of nervous systems necessitates to record from a large number of sites in order to break the neural code, whether single cell, local field potential (LFP), μ ECOG, electroencephalographic (EEG), magnetoencephalographic (MEG) or in vitro micro-electrode array (MEA) recordings are considered. High channel-count recordings also optimize the yield of a preparation and minimize the time-investment for the scientist. Currently, data acquisition (DAQ) systems with high channel counts (>100) can be purchased from a limited number of companies at considerable prices/headstages. These systems are typically closed-source and thus prohibit custom extensions or improvements by end users.

Methods

We have developed an open-source MATLAB-based DAQ system MANTA (MATlab N-Times Analog) which combines high channel counts (up to 1500 channels/PC), usage of analog or digital headstages, low per channel cost (<\$90/channel), feature-rich display & filtering, a user-friendly interface, and a modular design permitting easy the addition of new features. MANTA is licensed under the GPL and free of charge.

Results

The system has been tested by daily use in multiple setups for >1 year, recording reliably from 128 channels. It offers a growing list of features, including integrated spike sorting, PSTH and CSD display and fully customizable electrode array geometry (including 3D arrays), some of which are not available in commercial systems. MANTA runs on a typical PC and communicates via TCP/IP and can thus be easily integrated with existing stimulus generation/control systems in a lab at a fraction of the cost of commercial systems.

Conclusion

With modern neuroscience developing rapidly, MANTA provides a flexible platform that can be rapidly adapted to

the needs of new analyses and questions. Being open-source, the development of MANTA can outpace commercial solutions in functionality, while maintaining a low price-point.

101 Cytoarchitecture and Parvalbumin Immunoreactivity of the Auditory Cortex in the Chinchilla

Natalia Jara¹, Romina Falcon¹, Constantino Dragicevic¹, Jose Luis Valdes¹, Paul H. Delano^{1,2}

¹*Fisiologia y Biofisica, ICBM, Universidad de Chile,*

²*Servicio Otorrinolaringologia, Universidad de Chile*

Background

Although chinchillas (*Chinchilla laniger*) have been widely used as a model to study middle ear and cochlear anatomy, there are relatively few studies focused on auditory cortex morphology. The bifurcation of the middle temporal artery has been proposed as a vascular landmark to identify primary auditory cortex in chinchillas. In addition neuronal responses to brief tones with a latency <15 ms, have been postulated to be generated in the primary auditory cortex of chinchillas. Here, we measured auditory cortex evoked potentials and correlate these findings with cytoarchitecture (Nissl) and parvalbumin immunoreactivity of the auditory cortex.

Methods

Ten adult chinchillas were anesthetized and placed in a stereotaxic frame inside a sound attenuated room. Macroscopic vascular landmarks were measured from bregma. An electrophysiological characterization of the auditory cortex was performed using tones at different frequencies (1-8 kHz) and intensity levels (20-80 dB SPL). An electrolytic cortical lesion was made by a current pulse (1 mA for 15 s) throughout the recording electrode and the cytoarchitecture (Nissl) and immunohistochemistry with Parvalbumin were evaluated.

Results

The bifurcation of the middle temporal artery was found in 8 animals, located in average at: 2.6 ± 0.9 mm (X axis), 10.0 ± 1.9 mm (Y axis), and 3.9 ± 1.3 mm (Z axis) as measured from bregma. The response latency of this brain position was shorter than 15 ms only in three animals. The average cortical thickness of sites with latencies < 15 ms was 2070 ± 119 μ m, while that of sites with latencies between 15-20 ms was 2230 ± 279 μ m ($p > 0.05$). Both auditory cortices were thicker than parietal sensory cortex (1395 ± 187 μ m; $p < 0.001$). These thickness differences were mainly due to thicker layers V and VI in both auditory fields ($p < 0.01$). The density of parvalbumin (+) neurons was similar in parietal and auditory cortex exhibiting higher counts in layers IV and V.

Conclusion

The primary auditory cortex of the chinchilla was located in the bifurcation of the middle temporal artery in 30% of the experiments. A noticeable feature of the chinchilla auditory cortex was its thickness around 2 mm, which depends mainly on thick layers V and VI. Parvalbumin (+)

immunoreactivity was found mostly in layers IV and V. To guarantee the exact location of the primary auditory cortex in chinchillas, electrophysiological confirmation is needed in every experiment.

Supported by FONDECYT 1120256 and Fundaci3n Guillermo-Puelma.

102 Middle Latency Auditory Evoked Potentials in Response to Feature-Conjunction Deviants Suggest Processing Downstream to Simple Deviant Processing

Heike Althen^{1,2}, Sabine Grimm^{1,2}, Carles Escera^{1,2}

¹*Institute for Brain, Cognition and Behavior (IR3C),*

University of Barcelona, ²*Cognitive Neuroscience*

Research Group, University of Barcelona

Background

The violation of a regular sound pattern by irregular or novel stimuli is reflected by the mismatch negativity (MMN), a component of the human auditory evoked potential (AEP), with a latency of 100-250 ms and main sources in the auditory cortices. Evidence for auditory novelty detection however has also been reported in the middle-latency range (MLR) of the human AEP at latencies from 20 to 40 ms after change onset, in particular for simple feature deviants. According to a hierarchical view of auditory novelty detection, more complex types of regularities should be encoded at higher levels of the auditory pathway than simple regularities. In fact, MMN can be triggered by a so-called feature conjunction deviant, which combines features of different standard stimuli, e.g. the frequency of one standard and the location of another standard. In this study, we aimed at examining if the detection of conjunction deviants becomes already evident in the MLR of the human AEP.

Methods

A conjunction paradigm was applied (standard 1 [45%] = 800 Hz, presented from the left side; standard 2 [45%] = 1200 Hz, presented from the right side; deviant 1 [5%] = 800 Hz, presented from the right side; deviant 2 [5%] = 1200 Hz, presented from the left side), while subjects were concentrating on a subtitled movie. In a second session a frequency oddball paradigm was presented, in order to compare the deviance-related modulations of the AEP in response to a simple and a more complex regularity violation. The electroencephalogram was recorded from 64 electrodes. Different frequency filters for the analysis of the MLR and the long-latency range AEP were applied. The data of 17 subjects was statistically tested for differences in amplitudes and latencies of the MLR components and MMN elicited by standard and deviant stimuli.

Results

A significant MMN was obtained at fronto-central electrodes for both experimental paradigms. MMN in the oddball condition was significantly bigger than MMN in the conjunction condition. In the middle-latency range, the components Na, Pa and Nb showed no deviant-related modulations in response to the conjunction deviant. In the

oddball condition, however, the amplitude of the Nb component was enhanced in response to the deviant, compared to the standard.

Conclusion

This outcome suggests that the detection processes of an auditory feature conjunction deviant start at auditory cortical areas lying downstream to the areas processing a simple auditory deviant.

103 Early Deviance Detection Within an Intensity Pattern Regularity: An

Electrophysiological Study in Humans

Sumie Leung¹, Sabine Grimm¹, Miriam Cornella¹, Carles Escera¹

¹University of Barcelona

Background

Recent oddball studies showed that auditory change detection responses exist in the first 50 ms after sound onset, in the middle latency response (MLR) range. These deviance-related MLR responses occur much earlier than the Mismatch negativity (MMN), an electrophysiological correlate of the brain's pre-attentive auditory change detection system, observed as an auditory evoked potential at 100-250ms. However, when complex paradigms were employed, these early deviance effects were not as consistent, suggesting that different levels of information were encoded in two separate time ranges, hence supporting the notion of a functional hierarchy of auditory deviance detection. In the present study, we further tested this notion by examining if such early responses could be elicited by changes within an intensity pattern.

Methods

In order to obtain optimal MLR, we used an "up-chirp" stimulus that was designed to compensate for the cochlear traveling wave delay. It starts with a low frequency (50Hz) and ends with a high frequency (8000Hz), with a duration of 16.7ms. Electroencephalography (EEG) data were obtained from sixteen healthy participants. Participants were presented with a sequence of chirps that followed a rising intensity pattern (55, 65, 75, 85dB). This pattern was violated 15% of the time, with a pattern in which the third and the fourth tones had the same intensity (55, 65, 75, 75dB). We compared the responses elicited by the third (standard) and the fourth (deviant) chirps within the rare pattern, in both MLR and MMN latency ranges.

Results

In the MLR range, the deviant led to an enhanced Pa response (corrected $p = 0.030$) at around 42 ms when compared to the standard. No significant differences were observed between deviant and standard responses for other MLR components (Na, Nb). In the MMN range, we observed a double-peaked negativity on the difference waveform (deviant minus standard) at 78-108ms and at 175-205ms respectively.

Conclusion

Our results suggest that the human brain is capable of detecting an auditory pattern change as early as 42ms. Although there is a possibility that the observed effect could be due to repetition enhancement, it is unlikely to be the case, especially since repeated stimuli have been shown to reduce neuronal responses, as demonstrated by stimulus-specific adaptation in animals and sensory gating in humans. The present study has shown, for the first time, that deviance detection within an intensity pattern regularity could be reflected electrophysiologically in human MLR.

104 Neuromechanistic Temporal Models of Pitch Perception Using Slope Detectors

Chengcheng Huang¹, John Rinzel¹

¹New York University

Background

Despite the importance of pitch in auditory scene analysis, the neural mechanisms for pitch detection remain unclear. The existence of pitch-selective neurons in nonprimary auditory cortex suggests a separate pathway for pitch processing and a possible pitch map in cortex (Bendor & Wang 2005). Most existing pitch models are one of two types: pattern matching (spectral) or autocorrelation (temporal). While these models can predict pitch in many cases, development of neuronal implementations is immature. We have developed two mechanistic temporal models using two different slope detector units, extracting pitch information explicitly as a place code and temporal spike trains respectively.

Methods

We developed a firing rate (mean field) model and a biophysical cellular (HH-like) model each with phasic behavior, i.e. each has an onset-only response followed by low steady state during the stimulus regardless of stimulus amplitude (Figure1). These models can serve as slope detectors, since stimulus needs to rise fast enough to initiate a response. The population model has a graded response and resonant frequency, while the cellular model can produce precise phase-locking. Using a tonotopic array of such (uncoupled) units with a broad footprint for afferent input, the models can respond at the period corresponding to the perceived pitch as reported in human psychoacoustic studies.

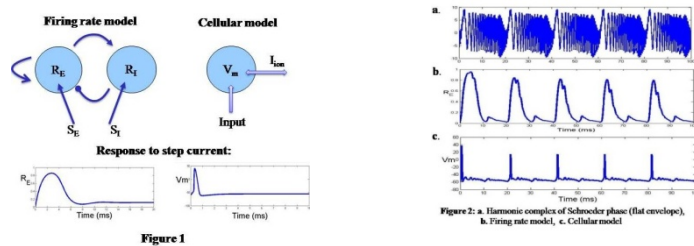
Results

Our models can encode the fundamental frequency of missing fundamental harmonic complexes while being unresponsive to individual components when presented alone. The response amplitude decreases as the lowest order of harmonics increases, consistent with the decrease in salience of human pitch perception. For shifted harmonics, our models also reproduced the perceived pitch which is not the fundamental frequency. Moreover, our model is not sensitive to phases of the harmonics. With alternating phase and Schroeder phase our results are consistent with psychoacoustic studies (Figure2). Our population models represent the extracted pitch in two

ways. The resonant units have preferred pitch, thus representing pitch with a place code. The phase-locking units encode pitch as temporal periodic firing, in which case another stage is needed to transform into rate code.

Conclusion

Using an array of slope-detector units that receive input from broad frequency channels, our models can extract pitch not only for missing fundamental complexes, but also encode correctly in special cases when pitch does not correspond to periodicity or envelope. Different from the pattern matching and autocorrelation models, our models do not require a bank of coincidence detectors and delay lines.



105 Combinatorial Regulation of Hair Cell Induction by Co-Transfection of ATOH1 and Transcription Factors

Ryoukichi Ikeda^{1,2}, Kwang Pak^{1,2}, Chavez Eduardo^{1,2}, Allen Ryan^{1,2}

¹University of California San Diego, ²VA Medical Center

Background

Overexpression of the basic helix-loop-helix transcription factor (TF) Atoh1 has been shown to induce the transformation of supporting cells in the organ of Corti into hair cells (HCs). Evaluating potential regulatory region of the *pou4f3* gene, a likely target of Atoh1 in HCs, we identified a cluster of binding sites for Atoh1 and a number of other TFs, a feature that was highly conserved across a widely separated mammalian species. We previously tested three of these (TCF3, GATA3 and SP1) and found that two (TCF3 and GATA3) enhanced the ability of Atoh1 to activate the gene and induce Myo7A expression in nonsensory cells.

Methods

To test the hypothesis that the remaining TFs act in combination to regulate the *pou4f3* gene, we transfected by electroporation neonatal mouse (postnatal day 1.5) organ of Corti with plasmids encoding these TFs for which highly-conserved binding sites have been identified in the *pou4f3* gene and which are expressed in the developing organ of Corti: CUX1, E2F1, ETS2, ETV4, FOXM1, HES1, HES5, GABPA, GATA1, GATA2, MAX, MAZ, MEIS, NERF, NFE2, NMYC, PATZ1 and USF2. We used a transgenic mouse in which 5' DNA from the *pou4f3* ATG drives expression of GFP to assess the regulation of this gene, and labeled the cultures with anti-myosin 7A to identify transition to a HC-like phenotype.

Results

We identified several additional TFs that had enforced the effect of Atoh1 while others inhibited or did not influence Atoh1.

Conclusion

These results suggest that Atoh1 acts in concert with a subset of other TFs that find that find to adjacent DNA element to control the expression of the *pou4f3* gene, and more generally to induce a HC phenotype. These TFs could be used to enhance HC regeneration.

106 Tonotopy Organization of the Vertebrate Cochlea May Require a Gradient of Shh Signaling

Eun Jin Son¹, Ji-Hyun Ma¹, HongKyung Kim¹, Doris K.

Wu², Jinwoong Bok¹

¹Yonsei University College of Medicine, Seoul, Korea,

²National Institute on Deafness and other Communication Disorders, Rockville, MD, USA

Background

Precise perception of sounds is crucial for verbal communication as well as daily activities of human life. Frequency discrimination first occurs at the peripheral auditory organ, the cochlea, which is tonotopically organized such that hair cells are tuned to high frequency sounds at the base of the cochlea and to low frequencies at the apex. However, the underlying mechanisms for tonotopy remain obscure. It has been shown that graded levels of Sonic hedgehog (Shh) signaling provide unique positional information in various tissues including neural tube and limbs. Since the developing cochlea receives graded Shh signaling along the cochlear duct, higher at the apex and lower at the base, it has been suggested that the gradient of Shh signaling may confer unique positional identities along the cochlear duct, contributing to the establishment of tonotopy.

Methods

To test this hypothesis, we upregulated Shh signaling in the developing mouse cochlea using the *cre/lox* approach as well as implanting Shh-soaked beads to the developing chicken cochlea.

Results

When Shh signaling was ectopically activated in the cochlear duct of *Pax2^{Cre/+}; Smo^{M2/+}* mutants, genes that are preferentially expressed in the apical cochlear regions such as *Fst*, *Msx1*, and *EphrinB2*, were upregulated throughout the cochlear duct, whereas expression of *A2m*, which is normally restricted to the base, was downregulated. These results suggest that Shh may specify regional identity of the developing cochlea. Hair cell phenotypes cannot be evaluated in these mutants due to early lethality. In contrast, implanting beads soaked with Shh proteins into the chicken otocyst *in ovo* generated hair cells at the base of the basilar papilla with stereocilia morphologies that resembled those located more apically in controls.

Conclusion

Our results suggest that high Shh signaling promotes apical cochlear identity and a gradient of Shh signaling may facilitate the establishment of the tonotopic organization of the auditory organ in vertebrates.

107 PTEN Plays Multiple Roles by Regulating Both PI3K/Akt and MEK/Erk Signaling Pathway During the Mammalian Inner Ear Development

Junko Murata¹, Mayumi Sakuraba¹, Tohru Kimura², Akira Suzuki³, Tak Mak⁴, Hideyuki Okano⁵, Toru Nakano², Katsuhisa Ikeda¹

¹Juntendo University School of Medicine, ²Osaka University Graduate School, ³Medical Institute of Bioregulation, Kyushu University, ⁴Campbell Family Institute for Breast Cancer Research, ⁵Keio University School of Medicine

Background

The PI3K/Akt signaling pathway has been shown to integrate multiple developmental signals to promote cell growth, proliferation and survival, and these effects of PI3K/Akt signaling are counteracted by the tumor suppressor PTEN (phosphatase tensin homologue) through its phosphatase activity. In this study, we investigate the regulatory role of PTEN in mammalian inner ear morphogenesis, using mice in which *PTEN* gene is specifically eliminated from developing inner ear.

Methods

To disrupt PTEN function within the inner ear, we crossed *PTEN^{fllox}/PTEN^{fllox}* mice (Suzuki A, Mak TW et al., 2003) with doubly heterozygous mice for the *Foxg1-Cre* allele (Hebert JM, McConnell SK, 2000) and the *PTEN-fllox* allele. Offspring with the genotype *Foxg1^{Cre/+}; PTEN^{fllox}/PTEN^{fllox}* (*PTEN*-cko) survived through E18.5, and the immunoreactivity of PTEN had disappeared and the activation of Akt was indeed increased in *PTEN* conditional knock-out (cko) inner ear.

Results

PTEN cko inner ear was hypertrophic, and especially, the diameter of cochlear duct had extraordinarily increased. The increased number of PHH-positive, proliferating cells implicated that the cell proliferation was prolonged in *PTEN* cko inner ear. In *PTEN* cko littermates, the extra OHCs are found in patches that alternated with regions containing the normal three rows. The additional IHCs appear in places, however, less frequently compared to the case of OHCs.

As Myosin VI- immunopositive OHCs were found only in the apical-middle turn of *PTEN* cko cochlea and not in that of wild type cochlea, the differentiation of HCs seemed to be accelerated in *PTEN* cko mutants. The extent and relative positioning of Sox2 and p27Kp1 expression were unchanged in *PTEN* cko mutants at E13.5, which imply that the prosensory formation is almost normal in *PTEN* cko cochlea.

The expression of activated Akt was increased by deletion of *PTEN*, especially in the neurons and the out side of the

prosensory region. Recent reports have showed that PTEN also negatively regulates MEK/Erk pathway. Indeed, activated Erk was expressed in the supporting cell progenitors at E15.5 and E17.5 in *PTEN* cko mutants, which was not observed in WT controls.

Conclusion

The multiple roles PTEN were clarified by analyzing the inner ear of *PTEN* cko mouse. PTEN regulate the MEK/Erk signaling pathway, in addition to the PI3K/Akt signaling pathway. PTEN controls the premature differentiation of HCs and the prolonged continuous cell proliferation to complete the adequate mammalian inner ear morphogenesis.

108 Characterization of Hippo Signaling During Development and Regeneration of Inner Ear Sensory Hair Cells

Matthew Barton¹, Yuan-Chieh Ku¹, Michael Lovett¹, Mark Warchol¹

¹Washington University School of Medicine

Background

The loss of sensory hair cells (HCs) is a leading cause of deafness in humans. Although the mammalian inner ear is unable to replace lost/damaged HCs, birds and other non-mammalian vertebrates can regenerate HCs after injury. The Hippo signaling pathway constitutes an evolutionarily conserved kinase cascade involved in regulation of organ size, cell proliferation, and tissue regeneration. Despite these well-documented roles in growth control, Hippo signaling remains unexplored in the ear. The purpose of this study is to begin characterization of the Hippo pathway in the context of inner ear biology, with focus on development and regeneration of sensory HCs.

Methods

Immunocytochemical techniques were used to characterize the expression patterns of several core Hippo signaling components (e.g. SAV1, NF2/Merlin, MST1/2, LATS1/2, YAP1, and TAZ) within the developing mouse inner ear. Illumina sequencing was used to identify expression of Hippo pathway genes in organotypic cultures of normal and Streptomycin-damaged chick utricles and cochleae.

Results

Temporal changes in the distribution of several Hippo signaling components, including SAV1, NF2/Merlin, and YAP1 indicate that the Hippo pathway may be involved in the regulation of terminal mitosis and/or onset of HC differentiation during mouse organ of Corti development. In mature avian sensory epithelia, RNA sequencing revealed robust expression of numerous canonical Hippo signaling components, including SAV1, STK3/4, LATS1/2, NF2, YAP1, TAZ/WWTR1, DIAPH1/3, DLG2, and MOB2, as well as the upstream Hippo signaling regulators alpha-catenin, FAT1-4, and DCHS1/2. Several TEAD family transcription factors (1, 3, and 4), which are required for YAP1-mediated induction of proliferation, demonstrated significant expression levels as well. Finally, sequencing

data revealed alterations in YAP1 target gene expression (e.g. MYC, DIAPH1, TP53BP2, TP63, TP73, E2F1, and Cyclin E) throughout the time course of avian HC regeneration *in vitro*.

Conclusion

Despite its roles in cell proliferation and tissue regeneration in other organ systems, Hippo signaling has not been studied in the inner ear. The data presented here describe the localized expression of key Hippo signaling molecules within sensory epithelia of avian and murine inner ears, and provide evidence to support putative roles for Hippo signaling during sensory epithelial development and HC regeneration.

109 Age-Related Changes in the Expression of Vesicular Glutamate Transporter 3 in the Rat Cochlea

Zhe Peng¹, Guopeng Wang¹, Shusheng Gong¹

¹Beijing Tongren Hospital, Capital Medical University, Beijing, China

Background

Vesicular glutamate transporters 3 (VGLUT3) plays an important role in hearing maintaining, and knockout mice in which are totally deaf and auditory brainstem responses (ABRs) indicates an early defect. Yet the exact mechanism in the cochlea is not well established. Although the presence of VGLUT3 in fetal and postnatal auditory hair cells are confirmed, the age associated changes of VGLUT3 expression in aging animals remains unclear and the research doesn't involve spiral ganglion cells (SGCs). Elucidation of developmental and aging dynamics of VGLUT3 expression in the auditory epithelium and SGCs is conducive to functionally understanding auditory glutamatergic transmission.

Methods

We characterized the expression profile of VGLUT3 in the rat cochlea and SGCs during postnatal development and aging by using immunohistochemistry and quantitative real-time polymerase chain reaction (qRT-PCR).

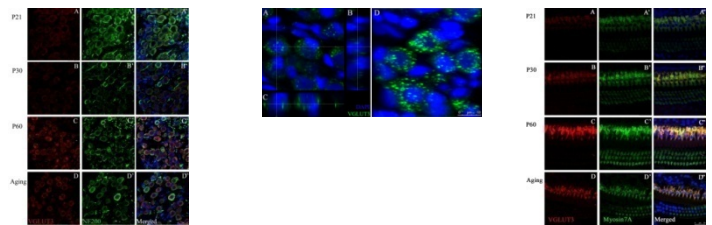
Results

We found that the expression of VGLUT3 in the cochlea varied from different age groups. VGLUT3 expressed in the inner hair cells (IHCs) and SGCs in the cochlea as early as the post-natal days, and present a dynamic variation during the development. We noted that postnatal 14 days (P14) was a key time point when the expression of VGLUT3 in IHCs sharply increased and VGLUT3 expression peaked in the adult. VGLUT3-immunopositive puncta was found in the cytoplasm of SGCs from P7 but not in IHCs. And VGLUT3 was also detected in the cochlea of aging rat. In IHCs, no apparent difference of VGLUT3 expression was found between the aging and adult rat. Although in SGCs, the amount of SGCs decreased in comparison with that of adult, the fluorescence of VGLUT3 in SGCs present little change with the method of immunohistochemistry. Slc17a8 gene expression trend evaluated by qRT-PCR is similar with that

of the VGLUT3 protein expression. And no statistic difference was found in the mRNA expression level between the groups of adult and aging rats.

Conclusion

VGLUT3 expression of the cochlea exists age-related changes. At the hearing onset stage (P14), its expression in IHCs is obviously intense and reach peak at the adult. VGLUT3-immunopositive puncta was found in the cytoplasm of SGCs from P7 but not in IHCs. Except for the decreasing with the SGCs loss, there are no obvious VGLUT3 expression changes in the aging rat cochlea. Since it is present in early developmental stages and its expression increases with maturing and still maintains to the aging, VGLUT3 is likely to have developmental and physiological roles in rat cochlear.



110 Characterization of Myosin7a in the Cochlear and Vestibular Ganglia of the Developing Chick

Amanda Hall¹, Jennifer Rowsell¹

¹Washington College

Background

The cochlear vestibular ganglion (CVG) comprises a cluster of undifferentiated neurons that delaminate beginning around embryonic day 2 (E2). The CVG will then divide into two separate populations; the cochlear and vestibular ganglion by (E6.5). Various transcription factors have been shown to play a role in the differentiation of both cochlear and vestibular neurons in mice (Kim et al., 2001; Lawoko-Kerali et al., 2004; Lu et al., 2011). Previous work from our lab has demonstrated a possible role for NeuroD and Gata3 in influencing neuroblast cell fate decision in chicks (Jones and Warchol, 2009).

Methods

We utilized immunohistochemistry to characterize the expression of Myosin7a in the developing chicken inner ear neurons from E3 to E11.

Results

We are investigating whether Myosin7a, an actin-dependent molecular motor protein, may play a role in the decision of a neuronal precursor to become a cochlear or vestibular neuron. The onset of Myosin7a expression was detected at E4 in a subset of neuronal precursors. Expression becomes restricted to vestibular neurons at E5 and persists as late as E7.

Conclusion

Our results indicate that Myosin7a may be playing a role in the development of vestibular neurons.

111 Septin7 Expression and Function in the Inner Ear of Embryonic Mouse

Hiroko Torii¹, Atsuhiko Yoshida¹, Norio Yamamoto¹, Takayuki Nakagawa¹, Juichi Ito¹

¹*Dep. Otolaryngology, Head and Neck Surgery, Graduate School of Medicine, Kyoto University*

Background

Septin proteins are GTP-binding proteins that are evolutionally conserved through eukaryotes except plants. Septin complex can interact with membrane, myosin, and microtubules. Their functions include formation of the cortical rigidity, control of the vesicular transportation, and compartmentalization within plasma membrane. These functions contribute to the formation of the cellular polarity that is important characteristics of epithelial cells. Our previous reports showed that Septin7, a core protein of multimeric Septin complex, was expressed in the embryonic cochlea (Yoshida et al. *Hear Res* 2012).

Methods

To identify the roles of Septin7 in the development of inner ears, we crossed Septin7 floxed mice with Foxg1Cre mice because conventional Septin7 knockout mice were embryonic lethal. Then we investigated the inner ear morphology of the mice using paint filling and the expression patterns of several markers related to early inner ear development.

Results

Macroscopic morphology by paintfilling on E17.5 inner ears showed remarkable underdeveloped inner ear with only cystic structure. Normal otocyst was formed in E10.5 but later development of the inner ear goes on abnormally.

Conclusion

This result shows that Septin7 plays significant role in early developmental stage of inner ear.

112 Exploring MicroRNA Expression Patterns in Zebrafish and Chicken Inner Ear

Kaidi D. Zhang¹, Donna M. Fekete¹

¹*Purdue University*

Background

MicroRNAs (miRNA) are small single-stranded RNAs that mediate post-transcriptional repression of gene expression by binding with target mRNA 3'UTRs. Mice with conditional knockouts of Dicer1 in embryonic inner ear have severe neurosensory defects and hair cell degeneration in three studies, revealing the importance of miRNAs in hair cell maturation and maintenance. Using published data from miRNA expression screens in mice, as well as miRNA target gene prediction algorithms, we created a list of miRNAs to interrogate for cross-species conservation of expression in the inner ear. Our aim was to use these model organisms to understand the roles of individual miRNAs in the developing inner ear.

Methods

Digoxigenin-labeled locked-nucleic acid probes for miR-19b, 93, 99, 124, 130b, 141, 199, 200a, 200b and 200c were purchased from Exiqon. We performed whole-mount in situ hybridization of zebrafish embryos at 1, 2, 3 and 5 days post fertilization (dpf). A similar method was applied to whole mounts of the chicken basilar papilla (BP) on embryonic day 17 to localize miR-96.

Results

We found that miR-200a and miR-141 were weakly expressed in inner ear hair cells and highly expressed in lateral line neuromasts and olfactory epithelia. At 2dpf and 5dpf, miR-124 gave strong signal in the eye. Broad expression in the head was observed for miR-93. We were unable to detect expression of miR-19b, 99, 130b or 199 in zebrafish at the tested ages. In the chicken BP, miR-96 was expressed in hair cells with a pronounced longitudinal gradient (high apex, low base).

Conclusion

We confirmed the evolutionary conservation of inner ear expression for the miR-200a family in zebrafish, adding miR-141 to the list of genes associated with mechanosensory organs. However, it is proving challenging to identify additional miRNA families associated with the inner ear in zebrafish. In chicken embryos, the miR-96 expression gradient (apex higher than base) matched that reported for the mouse cochlea after 2 weeks of age (Weston et al., 2011). In mice, this pattern for the miR-183 family emerged from an inverse gradient at postnatal day 0 (base higher than apex). A developmental timecourse of expression for the BP is underway to ask if this spatiotemporal expression pattern is also conserved. Expression analysis of miR-9 in the BP is also ongoing.

113 Temporal-Spatial Expression of MicroRNAs in Mouse Inner Ear Sensory Epithelium

Marsha Pierce¹, Colby Bradfield¹, Minh Nguyen¹, Sharalyn Steenson¹, Garrett Soukup¹

¹*Creighton University*

Background

MicroRNAs (miRNAs) post-transcriptionally regulate gene expression and are required in the development of the inner ear. Previous studies demonstrate that ~100 miRNAs are expressed in mouse inner ear. Certain of these miRNAs exhibit hair cell specific expression including the miR-183 family (miR-183, miR-96, and miR-182) that is known to impact hair cell differentiation and maintenance. However, little is known about the remainder of inner ear miRNAs. To gain greater perspective on cell-specific expression and function of inner ear miRNAs, we have completed an expression survey of 76 miRNAs.

Methods

In situ hybridization using a digoxigenin (DIG)-labeled, locked nucleic acid (LNA) probe complementary to each miRNA was performed on embryonic or neonatal mouse

inner ear. miRNA expression was visualized using anti-DIG antibody conjugated to alkaline phosphatase and BM purple as a chromogenic substrate. Tissues were whole-mounted or sectioned for microscopic imaging.

Results

Many miRNAs are detected in the mouse inner ear by microarray analysis and quantitative PCR. Our survey of miRNA expression patterns using *in situ* hybridization on neonatal mouse inner ear showed that many such miRNAs were ubiquitous with high or low detection, or undetected. Relatively fewer miRNAs or miRNA families showed cell-specific expression patterns that included sensory neurons or epithelia. Of particular interest are those miRNAs that exhibited sensory epithelium and hair cell-specific expression in embryonic and neonate mouse inner ear. These included miR-9, miR-200 family (miR-141, miR-200a, miR-200b, miR-200c, miR-429), and miR-204 family (miR-204, miR-211) in addition to miR-183 family.

Conclusion

Results suggest that relatively few yet highly conserved miRNA families contribute exclusively to the development of sensory epithelia and hair cells in the mouse inner ear, whereas many other miRNAs might serve relatively general albeit important functions.

114 Keratan Sulfate Mediates Zebrafish Otolith Formation

Kevin Thiessen¹, Kenneth Kramer¹

¹Creighton University

Background

More than 50 human proteins have been identified in which mutations are associated with congenital hearing loss. While many of these proteins have glycans attached to them, little is known about the role these sugars have in mechanosensory function. The glycosaminoglycan keratan sulfate (KS) is consistently found in the extracellular matrixes that directly overlie sensory hair cells and are critical to mechanosensory function. We sought to define the expression of KS during early zebrafish otolith development, identify which enzymes were responsible for KS synthesis, and characterize otolith development in KS-deficient zebrafish embryos.

Methods

Zebrafish embryos were collected for KS-immunohistochemistry at developmental stages when otic structures were first visible, including the otic placode (16 hours post fertilization, hpf), otocyst (18 hpf), and otolith (19.5 hpf). Early stages of otolith development were also examined at 21, 24, and 27 hpf. *In situ* hybridization with probes for putative KS-synthesizing enzymes was done using embryos collected at the same stages. Morpholinos were injected at 1-cell stage, and otoliths were examined at 27 hpf.

Results

KS is expressed at the earliest stages of zebrafish otolith development. While KS is actively synthesized by the cells

surrounding the otocyst beginning at 16 hpf, KS is not found in the otolith until 24 hpf, approximately 6 hours after the earliest otolith-localized protein, Oc90. KS forms a layered biomatrix that complements the expression of the otolith matrix protein OMP1. We identified *b3gnt7b*, *chst2b*, and *chst1* as putative KS-synthesizing enzymes there were expressed in the otic placode concomitant with early KS expression. Morpholino knockdown of either *b3gnt7b*, *chst2b*, or *chst1* resulted in embryos with deformed or absent otoliths.

Conclusion

During early zebrafish otolith development, KS synthesis and secretion are temporally distinct. We identified genes responsible for three of the four steps of KS synthesis during zebrafish otolith development; and using morpholino knockdown of each gene, we have demonstrated that KS is required for zebrafish otolith formation.

115 The Role of the Notch Signaling Pathway in Supporting Cell Development

Dean Campbell¹, Angelika Doetzlhofer¹

¹Johns Hopkins University, SOM, Department of Neuroscience and Center for Sensory Biology

Background

The sensory epithelium of the cochlea is responsible for the perception of sound. This specialized epithelium consists of sensory hair cells and glial-like supporting cells. Auditory supporting cells provide structural and functional support to hair cells and are critical for cochlea homeostasis and function. Despite the fact that these cells are functionally important to hearing and a possible unit of regeneration within the inner ear, little is understood about the molecular mechanisms involved in their differentiation. A good candidate pathway for being involved in supporting cell differentiation is the evolutionarily conserved Notch signaling pathway, which is highly activated in the sensory progenitors fated to differentiate into supporting cells. It is well established that activation of the Notch signaling pathway in these sensory progenitors results in the up-regulation of Atoh1 antagonists preventing these progenitor from adopting a hair cell fate. We hypothesize that the Notch pathway, in addition to repressing the hair cell fate in bi-potential progenitor cells, promotes supporting cell differentiation by up-regulating genes important for this process.

Methods

We used DAPT, a gamma secretase inhibitor, to disrupt the Notch signaling pathway in cultured developing cochlea (E15.5) for 18 hours. We analyzed the resulting changes in gene expression with Affymetrix exon arrays and we used RT-qPCR for microarray data validation. Using RT-qPCR we analyzed supporting cell specific gene expression in the Cre inducible dominant negative mastermind like 1 (DN-MAML1) transgenic mice. The expression of DN-MAML1 disrupts Notch signaling by preventing the formation of the activated Notch transcriptional complex.

Results

Acute DAPT inhibition of the Notch signaling pathway uncovered more than 200 cochlear epithelial genes that are positively regulated by the Notch signaling pathway. Based on function and supporting cell specific expression we selected 24 genes for further validation in the DN-MAML1 transgenic mouse line. Our results indicate that a vast majority of the selected genes showed a decrease in expression in this Notch mutant.

Conclusion

In summary, our data shows that a significant subset of supporting cell specific genes are regulated by the Notch signaling pathway, suggesting that this pathway positively regulates supporting cell differentiation.

116 The Role of the Lin28b/Let-7 Axis in Cochlea Differentiation

Erin Golden¹, Angelika Doetzlhofer¹

¹Johns Hopkins University

Background

The development of the mammalian auditory sensory epithelium is a carefully orchestrated process that results in the generation of several highly specialized cell types from a single progenitor cell pool. These mechanosensory hair cells and supporting cells are critical for hearing, but the molecular mechanisms regulating their differentiation are largely unknown. Using a high throughput screen we identified that the heterochronic gene Lin28b is selectively expressed in auditory sensory progenitors. This RNA-binding protein maintains cells in a pluripotent state by two distinct mechanisms; it enhances translation of growth-related genes and represses the expression of the let-7 family of microRNAs. We hypothesized that the Lin28b/let-7 miRNA axis is playing an important role in the transition of cochlear progenitor cells to a differentiated state.

Methods

We used both in situ hybridization and quantitative PCR to characterize the temporal and spatial expression pattern of Lin28b and the let-7 miRNAs during cochlea differentiation. In order to address the role of Lin28b in cochlea differentiation, we used both lentiviral-infected organotypic cochlea cultures and a doxycycline-inducible transgenic mouse line to overexpress Lin28b prior to hair cell differentiation.

Results

During cochlea development, Lin28b is expressed in the undifferentiated cochlea sensory progenitor cells, but drastically decreases as sensory progenitors differentiate. Conversely, let-7 miRNA expression increases with progressive sensory epithelium differentiation. Overexpression of Lin28b within the undifferentiated cochlea led to a significant slowing in the timing of hair cell differentiation. While hair cells do eventually form in the Lin28b overexpressing cochlea, Lin28b overexpressing hair cells lag in their maturation and stereocilia formation.

Conclusion

We found that the Lin28b/Let-7 axis plays an important role in the timing of hair cell differentiation and maturation. Here we shall discuss the gene targets and molecular mechanisms underlying Lin28b's role in cochlea differentiation.

117 Normal Morphogenesis of Auditory Hair Cells Requires Both Non-Muscle Myosin IIA and IIB

Jie Fang¹, Xuefei Ma², Lin Gan³, Robert S. Adelstein², Jian Zuo¹

¹Dept. of Developmental Neurobiology, St. Jude Children's Research Hospital, ²Genetics and Developmental Biology Center, National Heart, Lung, and Blood Institute,

³University of Rochester School of Medicine and Dentistry

Background

In humans, the heavy chains of the non-muscle myosin II (NMII) family are encoded by three genes, MYH9 (NMIIA), MYH10 (NMIIB) and MYH14 (NMIIC). Mutations in either MYH9 or MYH14 cause hearing defects. The mechanisms of these defects are unclear. NMII has been shown to play significant roles in junction formation and cell shape changes. Recent studies have suggested that NMII is involved in cochlear duct extension and patterning during the organ of Corti development. However, it is still not clear what roles NMIIA and NMIIB have during hair cell development and maturation.

Methods

To investigate the roles of NMIIA and NMIIB in hair cells, we used the Cre-loxp system to specifically delete (cKO) NMIIA and NMIIB in hair cells since both NMIIA and NMIIB germline knockout mice are embryonically lethal. We bred NMIIA floxed and NMIIB floxed mice with the hair cell specific Cre mouse line Gfi1-Cre to generate NMIIA cKO, NMIIB cKO and NMIIA and NMIIB double cKO mice. Auditory brainstem responses (ABR) were monitored in each mouse model. Whole mount immunohistochemistry was performed for hair cell morphologic analysis.

Results

Neither NMIIA cKO nor NMIIB cKO mice showed any ABR hearing defects or detectable morphological defects in the organ of Corti. NMIIA and NMIIB double cKO mice show significant hearing defects and abnormal hair bundle shapes. These abnormal hair bundles do not have the normal V-shape, instead they show an asymmetric V-shape or S shape.

Conclusion

Normal morphogenesis of auditory hair cells requires both non-muscle myosin IIA and IIB.

This work was supported in part by grants from the National Institutes of Health (DC006471, DC008800, and CA21765 the Office of Naval Research (N000140911014, N000141210191, and N000141210775), NOHR, and the American Lebanese Syrian Associated Charities (ALSAC)

of St. Jude Children's Research Hospital. J. Zuo is a recipient of The Hartwell Individual Biomedical Research Award.

118 **Plastin-1 Controls Vestibular Stereocilia Length**

Jocelyn Krey¹, Francisco Rivero², Peter Gillespie¹
¹Oregon Health & Science University, ²The Hull York Medical School

Background

The mechanosensory hair bundle consists of organized rows of actin-filled stereocilia of increasing heights. During development, stereocilia form through the assembly of actin filaments into tight parallel bundles by actin-bundling proteins. Stereocilia then increase in diameter and length through the addition of new actin filaments and the elongation of existing filaments within the actin paracrystal. Although plastin-1 (PLS1) is a member of one of the three classes of actin-bundling proteins known to be enriched in hair bundles, little is known about its function in stereocilia assembly.

Methods

We used mass spectrometry to identify and quantify proteins of hair bundles purified from P21-P25 mouse utricles. Protein abundance and localization was carried out with quantitative immunoblotting and confocal immunocytochemistry. Morphometric analysis of stereocilia was conducted with confocal images of phalloidin-labeled utricles.

Results

We tested the importance of PLS1 in stereocilia development by examining the vestibular hair bundles from *Pls1*-null mice. *Pls1*-null mice do not display behavioral evidence of overt auditory or vestibular dysfunction and auditory and vestibular hair cells appear to develop normally. To test whether loss of PLS1 is compensated by upregulation of another actin-bundling protein, we used mass spectrometry to quantify proteins in purified mouse hair bundles from wildtype and *Pls1*-null mice. In wildtype mice, PLS1 is the second-most abundant protein in the bundle and the most abundant actin-bundling protein of those we detected (PLS1, FSCN2 and ESPN). PLS1 was absent from the bundle in *Pls1*-null mice but no other actin-binding proteins increased in expression or were mislocalized. Using mass spectrometry and immunoblotting, however, we detected a significant ~30% decrease in the total amount of actin within the bundles of *Pls1*-null mice. Morphometric analyses of vestibular bundles indicated that stereocilia of adult (P21) *Pls1*-null mice were significantly shorter in length (~20%) than those of wildtype mice, with no change in kinocilia length or the staircase architecture of the bundle. Stereocilia at early postnatal stages (P4-P6) were also shorter than those of wildtype mice, although the difference was smaller (~10%).

Conclusion

Our results suggest that PLS1 is not essential for the initial assembly of stereocilia, but that it does play an important

role in regulating the elongation of stereocilia. The difference in stereocilia between *Pls1*-null and wildtype mice was greater later in development, suggesting that PLS1 is used for stereocilia lengthening between P4 and P21.

119 **Absence of Plastin1 Results in a Reduction of the Width of Inner Hair Cell Stereocilia and a Moderate Hearing Loss**

Ruth Taylor¹, Stuart Johnson², Eva-Maria Grimm-Gunter³, Walter Marcotti², Francisco Rivero³, Andrew Forge¹, Nicolas Daudet¹

¹University College London, ²University of Sheffield, ³University of Hull

Background

The stereocilia of hair cells contain a central core of F-actin filaments, organized into tightly packed parallel bundles. Proteins that bind to F-actin and promote such assembly are known as actin-bundling proteins, some of which such as espin, harmonin and eps8 are critical for stereocilia formation. However the function in the inner ear of the most abundant actin-bundling protein expressed in stereocilia, plastin1 (*pls1*, also known as fimbrin), has not been examined. In the intestinal brush border of mice in which the gene encoding plastin1 has been disrupted (*plastin1* KO mice) there are changes in microvillar dimensions, missing microvillar rootlets and reduction in the thickness and organisation of the terminal web underlying the microvilli at the apical end of the cell (Grimm-Gunter et al. 2009). This suggests the possibility that stereocilia and auditory function may be affected in *plastin1* KO mice.

Methods

The organs of Corti of *plastin1* KO mice and their wildtype and heterozygous littermates (P8 to >6months) were examined by immunohistochemistry, and scanning and transmission electron microscopy. Auditory function of adult mice (P30+) was tested by auditory brainstem responses to click and tone pip (8-40kHz) stimuli. Biophysical properties of hair bundle mechanotransduction were examined in organs of Corti from P6 animals.

Results

Hair cells developed normally in the vestibular and auditory epithelia of *plastin1* KO mice. However, auditory brainstem responses revealed that *plastin1* KO mice have a moderate hearing loss across most frequencies compared to their wildtype and heterozygous littermates. Ultrastructural studies of adult mice cochleae showed a significant reduction in the width of inner hair cell stereocilia but no effect on height, or general organization of the bundle. Outer hair cells showed no such defect. Cuticular plate depth and stereociliary rootlets of both hair cell types were also unaffected. In outer hair cells at P6, the extent of adaptation of mechanotransduction current was increased and fast time constant of adaptation reduced compared to wildtype littermates.

Conclusion

Plastin1 is important for correct formation and maintenance of inner hair cell stereocilia and defects due to its absence may account for the threshold shifts seen in plastin1 KO mice.

Ref: Grimm-Gunter et al.(2009)*Mol Biol Cell* 20, 2549-2562.

120 Organ of Corti Vibration Measured in the Intact Living Mouse Cochlea

Wenxuan He¹, Hongzheng Zhang^{1,2}, Tianying Ren¹

¹Oregon Health & Science University, ²Southern Medical University

Background

The current knowledge of the cochlear mechanical process comes mainly from the direct measurement of the basilar membrane vibration. To understand how sounds excite mechanotransduction channels of sensory hair cells, it is critical to measure the vibration near the channels.

Methods

The sub-nanometer vibration of the organ of Corti was measured in sensitive mouse cochleae using a newly developed scanning heterodyne low-coherence interferometer (SHLI). The object beam of the SHLI was focused on the reticular lamina of the organ of Corti through the intact round window membrane, basilar membrane and cellular structures of the organ of Corti. The vibration magnitude and phase were measured as a function of frequency at different sound levels. The reticular lamina location was determined by measuring the tissue reflectivity as a function of the transverse location.

Results

At low sound levels, the vibration magnitude increased with frequency and reached the maximum at the best frequency. As the sound level increased, the response peak shifted toward low frequencies and the peak magnitude saturated. In sensitive cochleae, the organ of Corti vibration showed high sensitivity, sharp tuning and strong nonlinearity. Upon the death, the vibration magnitude decreased dramatically across different frequencies and showed broad tuning and the linear growth. Compared to the basilar membrane vibration, the organ of Corti vibration showed higher sensitivity and stronger nonlinearity with no significant difference in the peak frequency and phase.

Conclusion

The current data demonstrate the active mechanical response of the organ of Corti in mice. These results provide essential information for studying the molecular mechanisms of cochlear amplification using genetically modified mice.

121 Auditory Responses to Stimulation at Soft Tissue Sites Before and After Fixation of Mobile Components of the Middle Ear

Ronen Perez¹, Cahtia Adelman², Haim Sohmer³

¹Dept of Otolaryngology, Shaare Zedek Medical Ctr affiliated to the Hebrew University Medical School, ²Speech and Hearing Center, Hadassah University Hospital, ³Dept of Medical Neurobiology, Hebrew University-Hadassah Medical School

Background

A new mode of auditory stimulation, namely, Soft Tissue Conduction (STC), which complements air conduction (AC) and bone conduction (BC) has been recently described. Since STC stimulation uses the same bone vibrator as in BC, it is possible that STC is simply a form of BC. The present study was conducted in order to investigate this possibility.

Methods

Six sand-rats initially underwent ablation of the left cochlea and opening of the right bulla. This was followed by measurement of auditory nerve and brainstem responses (ABR) thresholds to AC, BC and STC stimuli. AC stimuli were given through an insert earphone, BC through a bone vibrator to the skull and STC by applying the same bone vibrator to the sub-mental area. After baseline threshold measurements, the middle ear ossicles including the stapes footplate and the round window were totally fixated by immobilizing them with super glue (cyanoacrylate), thus eliminating the classical BC mechanisms. After the glue had dried, the AC, BC and STC ABR thresholds were determined again in the presence of the immobilization and compared to baseline measurements.

Results

Initial mean ABR thresholds before and after immobilization of the round window and ossicles in response to AC stimulation were 53.3 ± 6.8 and 91.7 ± 11.3 dB pe SPL respectively. In response to BC stimulation the thresholds were 81.7 ± 6.8 before and 80.8 ± 7.4 dB (instrument settings) after. With STC stimulation at the sub-mental area ABR thresholds were 99.2 ± 2.0 before and 98.3 ± 4.1 dB (instrument settings) after the immobilization. Thus, mean air conduction responses were significantly elevated by 38.4 dB (two tailed paired t-test, $p < 0.00001$) (conductive hearing loss), but mean BC and STC thresholds were virtually unchanged following the immobilization (in each, mean thresholds improved non-significantly by less than 0.9 dB; BC $p = 0.61$, STC $p = 0.36$).

Conclusion

Even though the two windows were no longer mobile and bulk fluid flow is therefore no longer possible, and a pressure difference across the basilar membrane would not be induced, STC and BC thresholds were not altered. These and additional results from previous experiments provide evidence that STC may not be variant of BC, and that STC activation at low sound intensities may not be based on a passive traveling wave which requires two mobile windows.

122 Effect of Exposure to Intense Tones on Otoacoustic Emissions and Neural Thresholds

Jonathan Siegel^{1,2}, Karolina Charaziak^{1,2}

¹Northwestern University, ²Hugh Knowles Center, Roxelyn and Richard Pepper Dept. of Comm. Sci. and Disord

Background

When the ear is stimulated with a pure tone the cochlea emits an “echo” at the frequency of the tone, so called stimulus-frequency otoacoustic emissions (SFOAEs). It has been hypothesized that SFOAEs at low probe levels originate within the peak of the traveling wave on the basilar membrane. This implies that SFOAE should carry place specific information about cochlear function and should be especially sensitive to small changes in the gain of the cochlear amplifier as compared to other type of emissions, specifically distortion product (DP) OAEs. Here we tested this prediction by recording SFOAEs and DPOAEs in chinchillas’ ears before and after exposure to an intense tone that resulted in clear shift compound action potential (CAP) thresholds.

Methods

All measures were obtained in anesthetized male chinchillas. The SFOAEs were measured for low level probes (30 dB SPL) varied from 0.3 to 12 kHz in fine steps with the suppression method. The suppressor was fixed near the probe frequency at moderate level. Additionally, SFOAE were measured with a second, high-frequency suppressor present (fs/fp ratio 1.2 – 2.5) to eliminate confounding effects of possible contributions from generators basal to the place of the probe frequency. DPOAEs were measured across a wide (f2=0.5-20 kHz frequency range (35/50 dB SPL, f2/f1=1.2). Animals were exposed to an intense tone (3 kHz, 100 dB SPL) to produce ~40 dB CAP thresholds shifts near 4 kHz and OAE tests were repeated.

Results

Even though in most cases SFOAE levels dropped following the exposure at frequencies where changes in CAP thresholds were evident, the SFOAE level shifts were always smaller and poorly correlated with amount of the shift observed for CAP. Measuring SFOAEs using the second high-frequency suppressor usually did not improve the match between SFOAE and CAP levels shifts. DPOAEs usually demonstrated a larger drop in level than SFOAEs that often better mapped the CAP threshold shift. However a variety of cases were noted ranging from DPOAE under- as well as over-estimating CAP threshold shifts.

Conclusion

SFOAE do not appear to be a more sensitive and accurate tool for evaluating changes in cochlear amplification as compared to DPOAEs measured with low stimulus levels.

Supported by NIH Grant DC-00419 (M. Ruggero) and Northwestern University.

123 Transient Evoked Otoacoustic Emissions in Ears Exposed to an Intense Tone

Jonathan Siegel^{1,2}, Karolina Charaziak^{1,2}

¹Northwestern University, ²Hugh Knowles Center, Roxelyn and Richard Pepper Dept. of Comm. Sci. and Disord

Background

It is commonly believed that otoacoustic emissions (OAEs) evoked with low level transient stimuli (TEOAEs) arise over a region of the basilar membrane mapped to the frequency content of the stimulus. This implies that TEOAE evoked with a narrow-band stimulus (tone-pip) should a) not contain energy outside of the band of the stimuli, b) be sensitive to changes in cochlear function only at frequencies within the stimulus band. We evaluate these predictions by measuring TEOAEs in chinchillas before and after exposure to an intense tone causing localized elevation in neural thresholds (CAP).

Methods

All measures were obtained in anesthetized male chinchillas. TEOAE were measured with the compression method using tone-pips (1 ms) centered at 1, 4 and 12 kHz. The stimulus level was fixed at 50 dB peSPL except few cases where additional recordings with lower levels were collected. Localized damage to the cochlea was induced with exposure to 3 kHz tone at high level to produce ~40 dB CAP threshold shifts at 4-6 kHz. Emissions were recorded before and after the exposure.

Results

For 1 kHz stimuli, TEOAEs showed small changes post-exposure, with the largest changes at the shortest delays. For 4 kHz stimuli, the spectra of TEOAEs pre-exposure usually had a frequency content similar to stimulus; but, an additional band centered around 0.5 kHz was usually present even for TEOAEs evoked with lower-level tone-pips. This low-frequency band was particularly sensitive to acoustic trauma. The TEOAE centered around 4 kHz showed less consistent changes, typically a drop in amplitude with or without a change in fine structure. The 12 kHz emissions showed reduced amplitude only if CAP thresholds were elevated at the highest frequencies.

Conclusion

Given large threshold shifts near 4 kHz, the lack of consistent changes in the spectra of TEOAE evoked by 4 kHz tone pips near the center frequency of the stimulus suggests that the emissions originate partly in locations remote to 4 kHz place. But the 0.5 kHz band seems to represent an intermodulation distortion generated near the 4 kHz place since its amplitude was clearly reduced post-exposure. Changes to TEOAE fine structure as well as observed enhancements in amplitudes, particularly for 1 kHz stimuli, suggest that TEOAEs generally represent contributions from sources distributed over a wider region of the basilar membrane than hypothesized.

Supported by NIH Grant DC-00419 (M. Ruggero) and Northwestern University.

124 Endocochlear Potential Powered Electronics

Andrew Lysaght^{1,2}, Patrick Mercier³, Saurav Bandyopadhyay³, Anantha Chandrakasan³, Konstantina Stankovic^{2,4}

¹Harvard - MIT, ²Massachusetts Eye and Ear Infirmary, ³Massachusetts Institute of Technology, ⁴Harvard Medical School

Background

The endocochlear potential (EP) is a + 70-100 mV electrochemical gradient generated between the intermediate and marginal cells of the stria vascularis and found within endolymph of the scala media. The EP provides approximately half of the electrochemical force driving auditory transduction currents and is critical to the cochlea's impressive sensitivity and dynamic range. Despite its role in powering active processes of the inner ear, the EP has never before been used as a power source for electronic devices.

Methods

Surgical exposure of a guinea pig cochlea was performed. The bulla was opened to provide access to the round window (RW) while maintaining the integrity of the tympanic ring and middle ear ossicles. Pulled glass micro-electrodes were advanced through the RW to access the fluid spaces of the inner ear. The negative electrode was inserted into the perilymph-filled scala tympani and the positive electrode through the RW and BM into the endolymph-filled scala media. Electrodes were connected to a novel designed, anatomically-sized, ultra-low quiescent-power energy harvester integrated with a wireless transmitter (endo-electronics chip). The impact of experimental procedures on the physiological function of the ear was assessed via tone-pip audiogram and measurement of the compound-action potential (CAP).

Results

The endo-electronics chip was successfully operated for periods of up to 5 hours while utilizing a guinea pig EP as the power source. During this time the EP remained stable, with no decline indicative of long-term damage from over-taxing the energy supply. CAP testing performed before and immediately after electrode insertion demonstrated that electrodes could be placed without causing hearing impairment. Comparison of CAP results before and after prolonged current draw similarly confirmed that power extraction is possible without sacrificing hearing performance.

Conclusion

We have demonstrated that it is possible to utilize the mammalian EP as the source of energy for electronic devices, in this case a radio-transmitter capable of broadcasting sensory information to external devices. This has been accomplished without significantly compromising the ear's ability to transduce sound. With improvements in

electrode design, this biologic battery may provide novel opportunities to sustainably power sensors or drug-delivery actuators in the vicinity of the ear, eye and brain of mammals; enabling transformative opportunities for new diagnostics and therapies in hearing research and related fields.

125 Endolymphatic Microphonics to Low-Frequency Tones and Noise, and Their Suppression by Higher-Frequency Sounds: A Study Relevant to Wind Turbine Noise

Alec N. Salt¹, Jeffery Lichtenhan¹

¹Washington University School of Medicine, St. Louis, MO

Background

Large cochlear microphonics (CM) recorded from scala media have been reported with infrasonic fluid-injected stimuli (Salt and DeMott, JASA 106:847; 1999). In the current study we investigate endolymphatic CM responses with a variety of low-frequency acoustically-delivered stimuli.

Methods

DC-coupled CM recordings were made from endolymph of the first and third turns of guinea pig cochleae in response to tonal and low-pass filtered frozen noise stimuli.

Results

In response to tonal stimuli, the maximum CM amplitude – the peak of the growth curve as stimulus level was varied – increased markedly as frequency was lowered. Specifically, the maximum CM amplitude averaged 4.0 mV at 500 Hz (n=9), 10.8 mV at 50 Hz (n=11), and 17.2 mV at 5 Hz (n=11). The large CM to 5 Hz stimulation was suppressed by the simultaneous presentation of a 500 Hz stimulus. A similar suppression of low-frequency responses was observed when microphonic was evoked with low-pass filtered noise and the filter cutoff frequency was increased. CM, measured as a spectral average across the 12-125 Hz range with the low pass noise cutoff frequency at 125 Hz, averaged -70.1 dB re 1V (n=5). As the filter cutoff frequency was increased in half-octave steps, CM responses across the 12-125 Hz range decreased progressively, reaching -78.7 dB re 1V (n=5) with the cutoff filter at 1.4 kHz.

Maximum endolymphatic CM amplitude from the first cochlear turn in response to tones and low-pass filtered noise was lower in amplitude than in the third turn. Additionally, noise-evoked measures showed smaller changes as the filter cutoff frequency was varied.

Simultaneously recorded output from a microphone in the ear canal was virtually unchanged as the noise-stimulus filter was varied, demonstrating that the changes to endolymphatic CM did not result from variations in signal power.

Conclusion

These data show that in the absence of higher-frequency sounds, endolymphatic responses to infrasonic stimuli can

be substantially larger than to stimuli in the audible range. These large responses are relevant to situations where people are exposed to very low-frequency sounds when ambient noise levels are low. This occurs within people's homes located near wind turbines. Although the house structure attenuates the higher frequency sounds, it does not attenuate the infrasound generated by the wind turbine to the same degree. If the ear responds strongly under conditions such as this, it may account for sleep disturbances and other symptoms that some living near wind turbines report.

126 Logic of Sound Level Encoding in the Auditory Nerve

Jérôme Bourien¹, Youg Tang¹, Mark Lenoir¹, Sabine Ladrech¹, Charène Batrel¹, Régis Nouvian¹, Jean-Luc Puel¹, Jing Wang¹
¹*inserm*

Background

The mammalian cochlea encodes sound level over a large dynamic range, through the progressive recruitment of three auditory nerve fibers pools, the high-, medium- and low- spontaneous rate (SR) fibers, with different threshold and dynamic range.

Methods

Using a combination of pharmacological, anatomical and computational approaches, we investigate the weight of each auditory fibers pool on the sound-evoked compound action potential (CAP), as a proxy of sound level dynamic range.

Results

Our results demonstrate that CAP thresholds and amplitude are independent of the low-SR fibers but rely on the high- and medium-SR fibers. This argues against a continuum activation of all the auditory nerve fibers to encode the full sound-level dynamic range. In addition, we suggest that intrinsic properties of high-SR fibers suffice to explain CAP dynamic range.

Conclusion

Our results show that substantial auditory nerve fibers loss can co-exist with normal hearing and call for relevant clinical tests to detect hidden auditory nerve fibers degeneration.

127 Spiral Ganglion Myelination Across Mammalian Species

Rudolf Glueckert^{1,2}, Helge Rask-Andersen³, Wei Liu³, Anneliese Schrott-Fischer¹
¹*Medical University Innsbruck, ²University Clinics Innsbruck, ³Uppsala University Hospital*

Background

Only human lacks a myelin sheet around the soma. The meaning for this difference remains unclear and may be related to facilitate synchronous activity or preprocess the auditory signals.

Methods

We performed a comparative and quantitative analyses of the spiral ganglion in various species including humans, monkey, pig, sheep, guinea pig and mice. Further we analyzed the structure of monopolar spiral ganglion neurons (SGNs) in human in cases of noise induced hearing loss and Wolfram disease in human and compare this with SGN degeneration in animal models.

Results

Results show that human type I neurons have cell bodies that are unmyelinated to 90-97%. The type II cells making up approximately 3-5% are completely unmyelinated in mammalian species including peripheral and central axons. The unmyelinated nature in human is true for at all frequency levels.

Findings highlight the marked morphological differences in the structure of the spiral ganglion between human and other mammalian species.

Conclusion

The presence of intimate contacts between spiral ganglion neurons in man around their perikarya supports the hypothesis of transcellular communication.

The lack of a rigid myelin layer may also elucidate the healing mechanism when peripheral axons are lost retrograde to hair cell death and explain the robust survival of monopolar SGNs.

128 Human Spiral Ganglion is Unmyelinated – Why Is So?

Helge Rask-Andersen¹, Wei Liu¹, Rudolf Glueckert², Anneliese Schrott-Fischer²
¹*Uppsala University Hospital, ²Medical University Innsbruck*

Background

Thorough morphologic analysis of the human spiral ganglion obtained after direct fixation of surgical specimens in normal hearing individuals show that they are unmyelinated contrary to animals studied so far. The reason for this difference remains obscure but may be essential both for understanding the normal physiology and pathology especially after sensory deafferentiation.

Methods

In here we analyzed systematically the structure of the human spiral ganglion at various frequency levels in optimally fixed specimens from normal hearing individuals undergoing petroclival meningioma surgery. Verification of the normal hearing is demonstrated by audiometry. The inner ear as well as the auditory pathways were unaffected by disease.

Results

Results show that human type I neurons have cell bodies that are unmyelinated to 90-97%. Central and peripheral axons are myelinated in 100%. The type II cells making up approximately 5% are also completely unmyelinated including peripheral and central axons. The unmyelinated nature is verified at all frequency levels. In addition the

unmyelinated type I cells often form cellular clusters with intimate contacts between somata. At these places separating satellite glial cells is often incomplete forming direct contacts between individual cell body surface membranes. This may allow for electric cross excitation and facilitate trans-cellular communication between cells at the level of the ganglion.

Conclusion

Findings highlight the marked morphological differences in the structure of the spiral ganglion in different species. The exceptional conditions of the human spiral ganglion raises questions about the possibility of generating specific complex and dynamic auditory responses essential for human speech communication. The conditions may also play an important role for the unique preservation properties of the human spiral ganglion cells following sensory hair cell loss.

129 Cooperative Release of Synaptic Vesicles at a Hair Cell Ribbon Synapse

Geng-Lin Li¹, Henrique von Gersdorff²

¹Department of Biology, University of Massachusetts Amherst, ²The Vollum Institute, Oregon Health & Science University

Background

According to the classic quantal theory of synaptic transmission in the NMJ, each release site (or active zone) has a low release probability and can release only one synaptic vesicle in response to one presynaptic action potential. In addition, the releases of synaptic vesicles are independent from each other. However, synchronized release of a few synaptic vesicles from the same release site, i.e., multivesicular release, has been demonstrated at hippocampal synapses, retinal bipolar cell ribbon synapses and hair cell ribbon synapses. At bipolar cell ribbon synapses the release of synaptic vesicles has been shown to be coordinated and binomial, but not cooperative. At hair cell synapses, however, the spontaneous multivesicular release events have been suggested to be cooperative. In the present study, we investigated whether synaptic vesicle releases from frog auditory hair cells are cooperative during physiologically relevant stimulations.

Methods

Paired patch-clamp recordings were made on hair cells and their connected afferent fibers in bullfrog amphibian papilla. Hair cells were stimulated with sinusoidal voltage-clamp commands (400 Hz, with 5, 10 and 20 mV peak-to-peak amplitudes, centered at -55 mV), which mimic hair cell voltage responses *in vivo* to pure sound tones. Excitatory Postsynaptic Currents (EPSCs) were recorded from afferent fibers, and individual synaptic events were detected with a sliding template technique. Based on our previous study on single vesicle (or quanta) events, the quantal contents were calculated for the evoked EPSC events.

Results

By varying the strength of stimulation, we found that although the failure rate of EPSCs can be as high as ~40%, the majority of the EPSC events still contains 2~3 vesicles. A simple binomial model cannot account for this finding. However, the data can be fit well with a simple cooperative release model where the release of one synaptic vesicle increases the probability of nearby vesicles being released, thus producing a nearly synchronous multivesicular event.

Conclusion

The release of synaptic vesicles from auditory hair cells under physiological stimulations is cooperative and cannot be described by a simple binomial distribution.

130 Hair Cell and Neural Potentials Recorded at the Round Window in Gerbils

Mathieu Forgues¹, Heather Koehn¹, Askia Dunnon¹, Craig Buchman¹, Oliver Adunka¹, Douglas Fitzpatrick¹

¹University of North Carolina

Background

Electrocochleography measured at the round window contains both hair cell and neural responses. Responses from the hair cells are the cochlear microphonic (CM) and summing potential (SP). Responses from the auditory nerve are the compound action potential (CAP) and auditory nerve neurophonic (ANN). The CAP and SP are relatively isolated and can be readily identified in the waveform. The CM and ANN are both present in the ongoing part of the response; the CM follows the fine structure of all frequencies and the ANN is the evoked response correlate of phase locking in the auditory nerve. Because these signals are mixed, it is a challenge to separate them.

Methods

ECoG potentials were measured from the round window of Mongolian gerbils to tones of different frequencies and intensities. Forward masking was also used in an attempt to attenuate the neural response. Gerbils were either normal hearing or had a pattern of high frequency noise induced hearing loss (NIHL) similar to many cochlear implant recipients.

Results

In normal hearing gerbils, distortions in the ECoG waveform, likely attributable to phase locking associated with the ANN, were present to low frequencies at low and moderate intensities. At high intensities, distortions were present at all frequencies, suggesting saturation of stereociliary movement. Forward masking with a masker 30 dB louder than the probe reduced the signal and distortions across the frequency range including high frequencies, suggesting that a preference for closed channels in stereocilia persists for a time after the stimulus. In gerbils with NIHL, the ongoing part of the ECoG saturated at relatively low intensities indicating a loss of spread of excitation.

Conclusion

These results show that distortions in the ECoG attributable to phase locking in nerve fibers are restricted to low frequencies at low and moderate intensities, and that forward masking is present in hair cells at high intensities.

131 Firing Patterns of Afferent Calyces Differ with Epithelial Zone in the Immature Rat Sacculle

Jocelyn Songer^{1,2}, Ruth Anne Eatock^{1,2}

¹Harvard Medical School, ²Massachusetts Eye and Ear Infirmary

Background

The mammalian vestibular epithelium has unique calyceal synapses between type I hair cells and the postsynaptic afferent terminal. Two classes of vestibular afferents form calyceal endings: calyx-only fibers innervate the central striolar zone of the epithelium, and dimorphic fibers form both calyceal and bouton endings on hair cells and innervate either the striola or the extrastriola. Striolar afferents have irregular spike timing whereas extrastriolar afferents have regular spike timing. From work on isolated vestibular ganglion cell bodies, irregular spiking is thought to correlate with the transient responses to current steps, and regular spiking with sustained responses. Here we investigate these proposed relationships with whole-cell recordings from striolar and extrastriolar calyces in the epithelium, where spiking initiates.

Methods

Whole-cell current clamp recordings were made from calyces in a semi-intact preparation of the immature (postnatal days 2-9) rat saccular epithelium and attached nerve. Nomarski optics and fluorescent dye fills were used to identify the morphology of the afferents.

Results

Striolar calyces responded to depolarizing current steps with a single spike at the stimulus onset, consistent with recordings from vestibular ganglion. At 25-29°C, 19 of 24 calyces were silent, and the remaining five had low and irregular spontaneous activity: 6 ± 2 spikes/s, $CV = 1.14 \pm 0.25$, Fano factor = 0.24 ± 0.06 , $n = 5$. In contrast, most extrastriolar calyces gave sustained responses to depolarizing current steps (12/16). They were also more likely to fire spontaneously (9/16) and the firing was higher-rate and more regular: 15 ± 2 spikes/s, $n = 9$, $p < 0.014$; $CV = 0.22 \pm 0.08$, $p < 9e-4$; Fano factor = 0.013 ± 0.008 , $p < 1.8e-4$.

Firing rates are expected to be higher at body temperature. Indeed, in 7 complex calyces recorded at 35-37°C, four fired spontaneously, with higher firing rates than recorded at room temperature (thermal Q10 of 3).

The spontaneously active striolar calyces were from P7 or P8 animals, while many of the silent calyces were from P2-

P4 animals, raising the possibility that spike activity increases with maturation.

Conclusion

Striolar calyces had transient responses and irregular spontaneous activity. Extrastriolar calyces had sustained responses and regular spontaneous activity. These results suggest that in vivo differences in spike regularity between the striolar and extrastriolar zones are preserved in our preparation, and are consistent with evidence correlating specific ion channels with firing patterns and spike timing.

132 Discharge Regularity and Information Transmission in the Mammalian Crista

Jay M Goldberg¹

¹University of Chicago

Background

Two themes are common in vestibular organs. 1) Regular and irregular afferents exist side-by-side. 2) The two kinds of afferents differ in their response dynamics. Can a rationale be provided for these two themes? In particular, can we explain why there is a close association between response dynamics and discharge regularity despite the fact that there is both experimental and theoretical evidence that these two discharge properties are not causally related? One possibility is that the association is needed for the efficient encoding of sensory information.

Methods

Efficient encoding can be measured by the mutual information between stimulus and response. For this reason, we calculated upper-bound estimates of mutual information (MIUB) at several frequencies (f). MIUB is proportional to the square of the ratio between $G(f)$, the conventional rotational gain (in spikes per s/deg per s) and CV, the coefficient of variation of the background discharge. Gains and CVs were obtained from Ramachandran and Lisberger (2008) over a frequency range from 0.5-10 Hz.

Results

Reflecting a flat gain and a low CV, the MIUB of regular units is uniformly high throughout the frequency spectrum. High-gain irregular (dimorphic) units are characterized by a high CV and a frequency-dependent gain increase; the result is an MIUB with an upward slope that crosses the regular curve near 1 Hz. Low-gain irregular (calyx) units are especially phasic; given their low gain, high CV and phasic response dynamics; their MIUB curve rises steeply, but only crosses the regular curve at frequencies approaching 20 Hz.

Conclusion

Regular and high-gain irregular units provide more efficient coding at low and high frequencies, respectively. Low-gain irregular units may be specialized to handle rapid head saccades with peak head velocities approaching 500 deg/s. The superior performance of irregular units at high frequencies depends on a 10-fold frequency-dependent gain increase, which can be achieved only by the high

sensitivity to depolarizing inputs of the hair cells synapsing on such units. This same characteristic is needed to produce an irregular discharge. A need for high synaptic sensitivity may explain the association between an irregular discharge and phasic response dynamics.

133 The Anatomy of the Lamprey Ear: Morphological Evidence for Horizontal Canal Equivalent in the Labyrinth of Lamprey, *Petromyzon Marinus*

Caitlyn Reed¹, Bernd Fritsch², Adel Maklad³
¹University of Mississippi Medical center, ²University of Iowa, ³University of Mississippi Medical Center

Background

Jawed vertebrates' (Gnathostome') inner ears have three semicircular canals arranged orthogonally in the three Cartesian planes: one horizontal (lateral canal) and two vertical canals each with its own ampulla containing a canal crista uniformly polarized toward (horizontal crista) or away (vertical cristae) from the utricle. Canals with cristae function as a detector for angular acceleration movements in their respective planes. In jawless craniates, cyclostomes (hagfish and lamprey), the horizontal canal is missing. The hagfish inner ear has one doughnut shaped torus (equivalent to the two vertical canals) vertical canal, and the lamprey has reportedly only two vertical canals. These observations on the anatomy of the cyclostomes' inner ear have been unchallenged for over a century, and the question of how these jawless vertebrates perceive angular acceleration in the horizontal (yaw) plane remains open.

Methods

In the present study we sought an answer to this question by reevaluating the anatomy of the inner ear in the sea lamprey, *Petromyzon marinus*, using stereoscopic dissection and scanning electron microscopy.

Results

In contrast to all gnathostomes, the lamprey has two horizontal canals in each labyrinth. In contrast to jawed vertebrates, the horizontal canals in lampreys are located on the medial surface in the labyrinth rather than on the lateral surface. These radical differences suggest that the horizontal canal's evolved twice and independently as a lateral canal associated with only one crista in gnathostomes and as two symmetric medial demi-canals, each associated with the horizontal leg of the tripartite canal ampulla.

Conclusion

Given that the sensory epithelia of the canal cristae in hagfish, lampreys and gnathostomes differ in structure and distribution and that lampreys and hagfish apparently are a monophyletic taxon, it is most parsimonious to assume that each canal system with associated cristae evolved independently from proto-chordate precursors ears that likely had no canals or cristae but served only as gravistatic (statocyst) sensors as in most aquatic non-vertebrates.

134 Differences in the Diameter of Facial Nerve and Facial Canal in the Pathophysiology of Bell's Palsy – a Three-Dimensional Temporal Bone Study

Melissa Vianna^{1,2}, Meredith Adams¹, Patricia Schachern¹, Paulo Lazarini², Michael Paparella³, Sebahattin Cureoglu¹
¹University of Minnesota, ²Santa Casa of Sao Paulo, ³Paparella Ear Head and Neck Institute

Background

Bell's palsy is hypothesized to result from virally mediated neural edema. Ischemia occurs as the nerve swells in its bony canal, blocking neural blood supply. Since viral infection is relatively common and Bell's palsy relatively uncommon, it is reasonable to hypothesize that there are anatomic differences in the diameter of the facial nerve canal that predispose some patients to develop paralysis. Measurements of the facial nerve and canal as it follows its tortuous course through the temporal bone are difficult without a 3D view. In this study, 3D reconstruction was used to compare anatomic differences in temporal bones of patients with and without a history of Bell's palsy.

Methods

Of 78 patients that presented with facial paralysis from the human temporal bone (HTB) collections of the University of Minnesota and MEEI, 6 patients met diagnostic criteria for Bell's Palsy (BP): 5 unilateral and 1 sequential bilateral case. Three-dimensional models were generated from HTB histopathologic slides with reconstruction software (Amira®), and the diameters of the facial canal (FC) and facial nerve (FN) were measured at the midpoint of the labyrinthine, tympanic, and mastoid segments. Measurements were compared between HTB with BP to the contralateral, unaffected side of each case (CLS) and to 10 age-matched normal controls using non-parametric tests.

Results

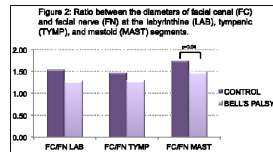
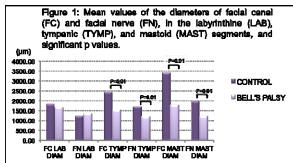
The mean diameter of the FC and FN was significantly smaller in the tympanic and mastoid segments ($p=0.01$) in the BP group than in the control group. There was no difference between groups in regards to the diameter of the labyrinthine segments (fig.1). The FC to FN diameter ratio (FC/FN) was smaller in each of the three segments in the BP group compared to controls, but the difference was statistically significant only in the mastoid segment (fig.2). There were no significant differences between the diameters of the FC or FN between the BP and contralateral sides.

When comparing the BP and control groups, the narrowest part of the FC was the labyrinthine segment in the control group and the tympanic segment in the BP.

Conclusion

This study suggests an anatomical difference in the diameter of the FC in the tympanic and mastoid segments but not in the labyrinthine segment in patients with Bell's palsy. These findings suggest that there may be a site of

anatomical predisposition in the FC that may have treatment implications.



135 Developing a Mouse Model for Cochlear Implantation

Nina Mistry¹, Shakeel R Saeed¹, Andrew Forge¹, Ruth R. Taylor¹

¹Centre for Auditory Research, UCL Ear Institute

Background

Animal models are the only means of assessing the effects of cochlear implantation (CI) at a cellular and molecular level. Mice are an excellent model for auditory research and this is in part due to the range of naturally occurring and genetically-modified strains which mimic human deafness. To date, there are very few studies of CI in mice. Our aim was to create a mouse model of CI and subsequently assess the effects of CI on cochlear ultrastructure and function.

Methods

Surgical techniques were developed and refined using cadaveric dissection prior to live surgery. C57Bl6 mice (early-onset hearing loss model) were the initial CI group. Access to the round window was gained and implantation using a specialised electrode array (n=6) and dummy implant (n=12) performed. The contralateral cochlea acted as a control. Auditory brainstem response (ABR) audiometry prior to and at time-points following CI was undertaken. Cochleae were fixed and decalcified before being prepared for histological examination.

Results

All mice recovered well following surgery. Postoperative ABR testing revealed a mean elevation in thresholds of 10dB when compared to preoperative levels. This was a permanent threshold shift in the majority of cases. Correct placement of the electrode array was confirmed using cone beam CT and light microscopy. Initial analysis revealed encapsulation of the implant in tissue with features suggesting the presence of fibrosis. Immunolabelling using a leucocyte marker, CD45, revealed greater numbers of positively labelled cells within the basal turn of implanted cochleae compared to controls. This was particularly seen within the region of the spiral ligament and basilar membrane, suggesting enhanced recruitment of these cells.

Conclusion

Our results show that mouse CI via the round window is achievable and holds many translational benefits. Patient studies have suggested that fibrous encapsulation reduces implant efficacy, prompting the necessity for replacement in some. Further investigation into the presence of inflammation and fibrosis using this mouse model will

therefore help identify measures to potentially reduce these effects. The model will allow for future research using eluting electrode arrays as a means for drug delivery to cochleae, ultimately to enhance patient outcomes.

136 Preservation of Residual Low Frequency Hearing in a Guinea-Pig Model of Non-Electrically Active Cochlear Implantation

Lisa S. Nolan¹, Kristien Verhoeven², Shakeel Saeed^{1,3}, Andrew Forge¹, Ruth R. Taylor¹

¹UCL Ear Institute, U.K., ²Cochlear Technology Centre, Belgium., ³The Royal National Throat, Nose and Ear Hospital, London, U.K.

Background

Electro-acoustic stimulation (EAS) with Cochlear™ Hybrid implants is a same-ear bimodal concept that has extended the traditional implantation candidacy criteria to patients that have retained some functional hearing in the low frequencies. Hearing loss in such candidates is targeted with electrical stimulation of the basal cochlear turns, encoding the high frequencies, in concert with acoustic stimulation of the low frequency apical turns. However, the perceptual benefits gained through EAS are hampered by clinical evidence that some patients eventually lose a considerable amount of residual hearing in the implanted ear. The aetiology of this loss of low-frequency sounds is currently unknown; an inflammatory-fibrotic 'foreign body' response triggered post-implantation (PI) is one mechanism thought to be involved. To identify the molecular mechanism(s) underlying this loss of low-frequency hearing, we have established an animal model of residual hearing in the guinea-pig and developed a soft surgical approach for cochlear implantation via the round window.

Methods

Guinea-pigs were treated with gentamicin (125mg/kg) for 10 consecutive days, a procedure in our laboratory that has consistently shown to produce hair cell loss restricted to the basal turns. Auditory brainstem responses (ABRs) to click and tone pip stimuli (4-40 kHz) were recorded to confirm residual low frequency hearing. Guinea-pigs were implanted with a 14-electrode array. Additional ABR recordings were taken pre-implant and monitored until sacrifice: 2 days, 1 week and 1 month PI. Auditory bullae were fixed and tissue prepared for histological processing.

Results

Little elevation in ABR thresholds was evident in implanted ears 2 days PI compared to contralateral control ears. At 1 week PI threshold shifts of 10-20dB were identified in implanted ears compared to control, that exhibited minimal further deterioration in hearing up to one month PI. At 2 days PI, a soft tissue covering the electrode array was observed, which at 1 week PI had expanded to encapsulate the electrode array. One month PI, tissue consistent with the appearance of neo-osteogenesis was observed along the implant pathway externally from the round window. Immunofluorescence analysis with an anti-CD45 antibody showed enhanced immunoreactivity in the

scala tympani of implanted ears compared to controls; CD45 positive cells consistent with the morphology of macrophages were identified from 2 days PI.

Conclusion

Threshold shifts following cochlear implantation manifest within 1 week PI in a guinea-pig model of residual hearing, which is consistent with the timing of fibrosis observed in the scala tympani over the electrode array.

137 Novel *In Vitro* Model for Cochlear Electrode Induced Mechanical Trauma Studies

Esperanza Bas¹, Chhavi Gupta¹, John Dinh¹, Ly Vu¹, Christine Dinh¹, **Thomas Van De Water**¹

¹University of Miami Ear Institute, Miami, FL

Background

Mechanical trauma from cochlear implant electrode insertion can lead to inflammation and oxidative stress reactions within the cochlea that result in the apoptosis of the auditory hair cells (HC) and initiation of intracochlear fibrosis. To gain insight into the molecular mechanisms that can cause this trauma initiated loss of auditory HC and cochlear fibrosis and the otoprotective effects of dexamethasone (DXM) observed in our previous *in vivo* studies, an EIT *in vitro* model was created and characterized.

Methods

Cochleae from 3 days rat pups were divided into: 1) Control untreated; 2) EIT; 3) EIT+ DXM (50 μ M). In groups 2 and 3, a 0.3 mm diameter monofilament fishing line was introduced through a small cochleostomy performed next to the round window membrane, in order to achieve a high angle of insertion, i.e. between 110-150°. Organ of Corti explants were dissected and then either untreated or treated with DXM. HC counts, gene expression for pro-inflammatory cytokines (i.e. TNF α and IL-1 β), pro-inflammatory inducible enzymes (i.e. iNOS and COX-2) and growth factors (i.e. TGF β 1, TGF β 3 and CTGF), oxidative stress (i.e. CellROX), and analyses of apoptosis pathways (i.e. Caspase-3, AIF and Endo G) were carried out on all explants.

Results

Expression levels of both TNF α and IL-1 β inflammatory process related genes increased significantly in response to EIT and these increases were prevented by DXM treatment. EIT in this *in vitro* model also caused a significant increase in oxidative stress and loss of HCs that was prevented by treatment with DXM. EIT-induced HC losses were caused by conversion of procaspase-3 to its active form. The strongest effects of these EIT-initiated changes were observed mainly in the basal and middle turns of the EIT explants.

Conclusion

This new EIT-model of insertion trauma provides a useful tool for understanding the mechanisms involved in both

inflammation-induced HC losses and the initiation of fibrosis that can occur following cochlear implantation.

138 Cochlear Electrode Implantation Trauma Causes Over-Expression of TGF- β 1 and Activation of the Wnt/ β -Catenin Pathway in an *In Vitro* Model

Esperanza Bas¹, Yamil Selman^{1,2}, Bradley Goldstein¹, Chhavi Gupta¹, Adrien Eshraghi¹, Thomas R. Van De Water¹

¹University of Miami-Ear Institute, ²University of Virginia

Background

The insertion of a CI electrode array can be associated with an inflammatory response that is known to induce loss of auditory hair cells and growth of fibrotic tissue around the electrode array. This fibrotic process can have a negative impact on the function of a patient's implant. Wnt/ β -catenin/Tcf signaling induces the expression of Axin2, which in turn participates in a negative feedback loop to limit the intensity of a Wnt-initiated signal. From previous work we know that trauma to the cochlea induces the expression of TGF- β 1 and we hypothesize that this growth factor can co-operate with the Wnt pathway to elicit fibrosis.

Methods

Cochleae from 3 days rat pups were divided into: 1) Control untreated; 2) TGF- β 1; 3) TGF- β 3; 4) EIT; 5) EIT+ TGF- β 1 (10 ng/ml); and 6) EIT+ TGF- β 3 (10 ng/ml).

qRT-PCR for Axin2, Wnt4, Wnt5b and CTGF was performed in organ of Corti (oC) explants and lateral wall tissues (LW) after 96 hours of incubation.

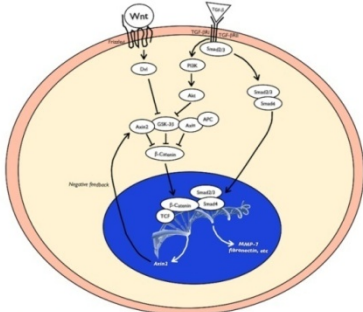
Results

Upon EIT, CTGF was up-regulated in oC and LW tissues, compared to control explants. Addition of TGF- β 1 and TGF- β 3 to the LW tissues resulted in the upregulation of CTGF. In the EIT-TGF- β 3 oC explants the CTGF levels were as low as the control group. Axin2 mRNA levels were remarkably increased in oC explants either treated with TGF- β 1 or TGF- β 3. Wnt4 was downregulated in the LW tissues by the addition of TGF- β 1 and TGF- β 3, but no differences were observed between control and EIT groups. While Wnt4 levels were not altered in the oC explants, a decrease in Wnt5b mRNA levels was observed upon EIT, and in groups 2 and 3 compared to 1. Interestingly Wnt5b was upregulated in the EIT group treated with TGF- β 3.

Conclusion

Induction of EIT in the cochlea triggers a fibrogenic response as part of the wound healing process, in which TGF β s are key role players. oC cells and LW cells play different roles. While there is an increase on the Wnt/ β -catenin activation pathway upon EIT in oC, exacerbated by TGF- β 1 treatments, a downregulation of the Wnt5b was observed. This is consistent with previous reports that indicate antagonism between the canonical and noncanonical Wnt pathways. Our results suggest that the

Wnt pathways do not participate in the fibrotic response initiated by the lateral wall tissues.



139 Age Related Changes in the Inner Ear of the Mouse Model of Metabolic Syndrome

Kazuma Sugahara¹, Junko Tsuda¹, Eiju Kanagawa¹, Yoshinobu Hirose¹, Takefumi Mikuriya¹, Makoto Hashimoto¹, Hiroaki Shimogori¹, Hiroshi Yamashita¹
¹Yamaguchi University

Background

The metabolic syndrome is characterized by obesity concomitant with other metabolic abnormalities such as hypertriglyceridemia, hyperlipidemia, elevated blood pressure and diabetes. It is known that the prevalence of hearing loss is high in the patients with diabetes. However, the causes of hearing loss have not been clear. In the present study, we evaluated the hearing function in animal model of diabetes with obesity.

Methods

TSOD male mice used in study were derived from the Tsumura Research Institute. Age- and sex- matched non-diabetic TSNO mice served as controls. Blood samples were collected from TSOD and TSNO mice at 3, 5, 8 months of age. Blood glucose concentrations of TSOD mice were significantly higher than those of controls. In addition, Body weights of TSOD mice were greater than those of controls.

Results

We evaluated the ABR thresholds of animals in 3, 5, 8, 12 month of age. There was no different in ABR thresholds between TSOD mice and controls in 3 or 5 month of age. However, the elevation of ABR thresholds were observed in 8 month aged TSOD mice. The thresholds of 8 months aged TSOD mice were significantly larger than those in controls. The histological examination showed the thickened vessel wall of cochlear modiolus, and the arterial stenosis in the stria vascularis. In addition, the gene expression profiles were analyzed using the Affymetrix GeneChip®. The microarray analysis indicated the expression of growth factors such as IGF-1 in the model mouse related with control mouse.

Conclusion

The understanding of changes in the inner ear of the model animals might be of importance in future prophylactic approaches to prevent hearing loss in the patient with metabolic syndrome.

140 A Novel Animal Model for Studying Blast Injuries of the Inner Ear Using Laser-Induced Shock Waves

Takaomi Kurioka¹, Takeshi Matsunobu¹, Katsuki Niwa¹, Atsushi Tamura¹, Akihiro Kurita², Satoko Kawauchi³, Yasushi Satoh⁴, Shunichi Sato³, Akihiro Shiotani¹

¹Department of Otolaryngology, National Defense Medical College, Japan, ²Department of Otolaryngology, Saitama Red Cross Hospital, Japan, ³Department of Biomedical Information Science, National Defense Medical College, Japan, ⁴Department of Anesthesiology, National Defense Medical College, Japan

Background

Recently, the number of blast injuries of the inner ear has increased in frequency in the general population. Inner ear injury may result in the temporary or permanent sensorineural hearing loss, but their mechanisms underlying this phenomenon are not fully understood. The majority of animal models for these injuries use explosive or complex experimental settings, limiting the laboratory study of blast injury. Recent studies have revealed that brain and pulmonary injuries caused by laser-induced shock waves (LISW) would be useful models to study blast injury.

Methods

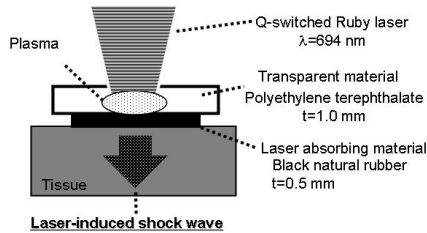
The aim of this study was to establish a small-animal model for inner ear injuries associated with blast injury, using LISW with high controllability, and easy experimental settings. A LISW was generated by the irradiation of an elastic laser target with 694nm nanosecond laser pulses of a ruby laser. Anesthesia was initially induced in Sprague-Dawley rats (5w). After transmastoidal cochlear laser-irradiation at 6.6 J/cm², 7.3 J/cm², 8.3 J/cm² in rats, we investigated the auditory brainstem response (ABR) and distortion product otoacoustic emission (DPOAE) after the laser irradiation, and outer hair cells (OHCs) loss was examined using surface preparation technique. Immunohistochemical analyses for 8-hydroxy-2-deoxyguanosine (8-OHdG) were performed to examine the amount of oxidative DNA damage that occurred in cochlea.

Results

ABR and DPOAE measurements revealed that this animal model has the auditory dysfunction associated with inner ear damages. With regard to the peak pressure of laser-induced shock wave, there was a better improvement for the 6.6 J/cm² group as compared to the 8.3 J/cm² group. Furthermore a significant lower survival rate of OHCs was observed of the 8.3 J/cm² group as compared to that of 6.6 J/cm² group and strong immunoreactivities against 8-OHdG were observed in the inner ear tissues of the laser-irradiation rats. These data suggested that 6.6J/cm² group seems to be a temporary hearing loss (TTS) models and 8.3J/cm² group to be a permanent hearing loss (PTS) models.

Conclusion

Animals exposed to transmastoidal cochlear laser irradiation showed functional and morphological changes of the inner ear similar to other studies in blast injury. Although the underlying mechanism of blast injury seems to be complicated, this novel rat model of blast injury using LISW is suitable for detailed studies of blast inner ear injury in the laboratory.



141 Hearing Impairments and Cochlear Changes in Type1 Diabetes Model Mice and Diet-Induced Obesity Mice

Takeshi Fujita¹, Daisuke Yamashita², Sayaka Katsunuma², Shingo Hasegawa², Hitoshi Tanimoto², Ken-ichi Nibu²

¹Mitsui Memorial Hospital, ²Kobe University Graduate School of Medicine

Background

Recent several population-based studies suggested the association between diabetes and hearing impairment. However, the impact of diabetes on hearing impairment has not been as well recognized in comparison with the known complications affecting the renal, visual, and peripheral nervous systems. In addition, the association between obesity and hearing loss also has been reported.

Methods

1. Type1 diabetes model

Streptozotocin induced male C57BL/6J diabetic mice were used. Hearing function was evaluated 1, 3 and 5 months after induction of diabetes (n = 10 per time point) using auditory evoked brainstem responses (ABR). Mice (n = 8) were exposed to loud noise (105 dB) 5 months after induction of diabetes. ABR were measured before and after noise exposure. Cochlear blood flows were measured by laser-Doppler flowmeter. Spiral ganglion cells (SGCs) were counted. Vessel endothelial cells were observed by CD31 immunostaining.

2. Diet-induced obesity model

C57B/6J and CBA/N male mice were used. Obesity was induced with a high fat diet (HFD32, CLEA Japan). Hearing function was evaluated 1, 3 and 5 months (B6, n = 10 per time point) and 1 year (B6, n=10 and CBA, n=9) after induction of high fat diet.

Results

1. Type1 diabetes model

Chronologic changes in the ABR threshold shift were not significantly different between the diabetic group and

controls. However, vessel walls in the modiolus of the cochleae were significantly thicker in the diabetic group than the control group. Additionally, recovery from noise-induced injury was significantly impaired in diabetic mice. Reduced cochlea blood flows and SGC loss were observed in diabetic mice cochleae after noise exposure.

2. Diet-induced obesity model

At 5 month after induction of obesity, compared to the baseline, ABR threshold shifts were significantly increased in Control at 32kHz compared with Obesity model in B6 mice. Moreover, 1year after induction, ABR thresholds were significantly increased in Control at all frequencies. However in CBA mice, ABR thresholds were significantly increased in Obesity model compared with Control at all frequencies at 1 year after induction.

Conclusion

Our data suggests that diabetic cochleae are more susceptible than controls to loud noise exposure, and decreased cochlear blood flow due to sclerosis of the vessels and consequent loss of SGCs is a possible mechanism of hearing impairment in diabetic patients.

142 Attempts to Rescue Outer Hair Cell Loss Induced by Dysfunctional Prestin in 499 Prestin Knockin Mice

Emily Love¹, Roxanne Edge¹, Jing Zheng¹, Jonathan Siegel¹, Mary Ann Cheatham¹

¹Northwestern University

Background

Prestin is the motor protein responsible for outer hair cell (OHC) somatic electromotility. Removal of prestin results in a change in cochlear mechanics, as well as a loss of amplification. In order to study this process, a knockin (KI) mouse model was created to preserve physical/anatomical OHC properties, which are altered in prestin knockout (KO) mice. The resulting 499 prestin KI (Dallos et al., 2008) was created by replacing 2 of prestin's 744 amino acids: V499G/Y501H. These mice have vastly reduced electromotility and sensitivity, but maintain normal OHC length and stiffness. Although 499 OHCs appear WT-like, hair-cell death is accelerated relative to that documented in mice lacking prestin protein.

Methods

Because the loss of OHCs complicates the interpretation of experimental results, we implemented three interventions. First, 499 KI's were backcrossed to BAK KO mice (C57BL6), which lack the mitochondrial pro-apoptotic gene *Bak*, in the hope of reducing apoptotic cell death. Second, because oxidative stress is a major cause of OHC death, another group of 499 KI mice was fed the antioxidant diet, Protandim (Liu et al., 2009). This approach in chemoprevention is thought to decrease the effects of oxidative stress by increasing the expression levels of superoxide dismutase, as well as catalase activities. Finally, 499 KI mice were backcrossed onto the FVB murine strain in order to avoid the relatively early onset age related hearing loss associated with the original

129/B6 499 KIs. Hair-cell loss was documented by constructing cytochrome oxidase at 42 days of age.

Results

A significant reduction in OHC death (Student's t-test) was observed in FVB/499KI mice, and in mice receiving the Protandim diet, intimating an increased preservation of OHCs. 499 KI mice that were also homozygous for the *Bak* gene failed to show any improvement in OHC death.

Conclusion

Since the benefit obtained for FVB/499 KI mice was more dramatic than that achieved with Protandim, these results provide guidance for future interventions designed to ameliorate progressive OHC loss. (Work supported by NIDCD Grants DC00089 and DC010633, and the Knowles Hearing Center).

143 In-Depth Proteomic Analysis of Mouse Cochlear Sensory Epithelium by Mass Spectrometry

Lancia Darville¹, Bernd Sokolowski¹

¹University of South Florida, Morsani College of Medicine, Tampa, FL 33647

Background

Identification (ID) of the complete proteome in sensory organs such as the cochlea is challenging due to small amounts of tissue and because membrane proteins, such as ion channels, are difficult to isolate and identify. Several proteomic techniques have been developed, including 2D-DIGE, antibody microarray and mass spectrometry. However, mass spectrometry in conjunction with separation methods can provide a more comprehensive proteome because of its ability to enrich protein samples, detect low molecular weight and hydrophobic proteins, and identify low abundant proteins by reducing its dynamic range.

Methods

We used several separation techniques to maximize protein ID, applied Filter Assisted Sample Preparation (FASP) for detergent removal, and varied protein digestions prior to using nano liquid chromatography tandem mass spectrometry (MS), to obtain an in-depth proteome analysis of 30-day-old mouse cochlear sensory epithelium. In the first approach, we fractionated extracted proteins using gel-eluted liquid fraction entrapment electrophoresis (GELFrEE). In the second, proteins were digested and separated by strong cation exchange (SCX) or weak anion exchange (WAX) chromatography. We also compared single tryptic digestions with double tryptic or tryptic and LysC digestions.

Results

Double digestion with SCX fractionation identified 3390 proteins with a 1% false discovery rate (MaxQuant), of which 497 were in the plasmalemma and 19 of these were ion channel α -subunits. GELFrEE yielded 2173 proteins, of which 511 were absent when using SCX. Gene ontology annotation showed that 59% and 51% are binding proteins

and 32% and 40% are catalytic proteins when comparing SCX and GELFrEE, respectively. GELFrEE identified 10 ion channel α -subunits with one unique channel not observed by SCX. The distribution of biological processes, cellular components, and protein classes were comparable between different separation methods. Combining the results from the different techniques resulted in 4187 total protein IDs, including 21 ion channel α -subunits. Additional protein data filtering using Scaffold produced similar ion channel IDs at 95% confidence, but with 19% higher numbers of identified channels.

Conclusion

The results show that the application of multiple approaches is needed to provide an exhaustive proteome analysis of the cochlear sensory epithelium that includes many membrane proteins.

Supported by NIDCD grant R01 DC004295 to BS.

144 Large-Scale Proteomic Analysis of Cholesterol-Rich Membrane Microdomains in Cochlea

Paul Thomas¹, Liqian Liu¹, R. Keith Duncan¹

¹University of Michigan

Background

Compartmentalization of membrane proteins into microdomains is a key feature of cell signaling. These microdomains include buoyant, detergent-resistant membrane (DRM) specializations that are high in cholesterol and often enriched with cholesterol-binding proteins like caveolin and flotillin. Importantly, disruption of these domains with cholesterol-chelating cyclodextrins has proven extremely ototoxic (Ward et al., *Pediatr Res*, 2010). Using ultraperformance liquid chromatography-tandem mass spectrometry, we probed the protein composition of DRM fractions from the chick cochlea to gain insight into the structure and function of these domains.

Methods

Cochlear homogenates were pooled from 12 chicken basilar papillae (2 - 4 weeks old) and lysed in buffer containing 0.25 - 2% Triton X-100. Membrane proteins were separated by sucrose-gradient fractionation. Equal volume fractions were collected and probed for cholesterol content, protein concentration, and common markers of raft (caveolin) and non-raft (transferrin receptor) membrane domains. Twenty μ g of protein from the DRM fractions were separated by SDS-PAGE, divided into ten equally sized gel segments, trypsin digested, and analyzed by nano-LC-MS/MS with an LTQ Orbitrap Velos Pro (MSBioworks).

Results

Homogenization in 0.5% Triton maximized protein concentration and enriched cholesterol in the DRM while optimally separating caveolin and transferrin receptor. From three independent samples, we identified 930 DRM proteins, with a false discovery rate of \sim 0.5%. The majority of these proteins were predicted by topology and ontology to be associated with cell membrane though only

~25% with the plasma membrane specifically. Identified proteins included caveolin, flotillin, prohibitin, erlin, and the GPI-anchored protein Thy-1, each common to lipid microdomains. Top terms in a process ontology analysis were metabolic processes (cluster frequency 35.4%), localization (24.4%), transport (21.3%), and cell communication (14.7%). Eight of the ten most abundant proteins in the DRM were associated with ion transport and energy metabolism.

Conclusion

Our results show that scaffolding proteins common to lipid rafts are enriched in the cochlea and that hundreds of other proteins segregate with these scaffolds. Cholesterol-rich microdomains have been widely associated with compartmentalized cell signaling, cell proliferation, excitability, exocytosis, and oxidative signaling. Our results revealed that proteins involved in energy metabolism and oxidative stress are abundant in cholesterol-enriched DRMs, offering a link between cholesterol disruption and hearing dysfunction which may explain cyclodextrin-induced ototoxicity.

Supported by P30-DC005188 and Action on Hearing Loss

145 Generation of Atoh1-RtTA Transgenic Mice to Transiently Alter Gene Expression in Hair Cells

Jennifer Dearman¹, Brandon Cox¹, Jian Zuo¹

¹St. Jude Children's Research Hospital

Background

The Cre/loxP system has been commonly used for cell type specific control of gene expression, resulting in many significant advances for the hearing field. However Cre-mediated excision of the floxed region is permanent and in many cases, transient control of gene expression is desired. This can be achieved using the tetracycline-inducible system, where the reverse tetracycline transactivator (rtTA) protein binds to the promoter and activates transcription of a second transgene which contains a tetracycline response element (TRE). The rtTA protein can only bind to TRE and activate transcription in the presence of doxycycline, making it transient as the binding does not occur when doxycycline is removed. Cell-type specific expression can be achieved using cell-type specific promoters/enhancers to express the rtTA protein. Here, we used the well characterized Atoh1 enhancer to drive expression of rtTA. Atoh1 is a basic helix-loop-helix transcription factor that is required for the differentiation of hair cells in the inner ear and of granule cells in the cerebellum. In the inner ear, Atoh1 is expressed during late embryonic development and is down-regulated by postnatal day 6-7 (P6-7).

Methods

We used a construct that contains the Atoh1 enhancer followed by rtTA-IRES-hPLAP-SV40 Intron-poly A. The addition of the internal ribosome entry site (IRES)-human placental alkaline phosphatase (hPLAP) gene in the

construct allows visualization of rtTA transgene expression (Chow et al., Dev. Dyn. 2006).

Results

We have obtained 12 transgenic founder mice and thus far 6 founders have given germline transmission. We are characterizing these transgenic mice using hPLAP staining in the inner ear and cerebellum and will further characterize their rtTA activity using TetO-lacZ reporter mice and doxycycline injection at early postnatal ages.

Conclusion

In addition to providing transient control of gene expression, these Atoh1-rtTA mice can be used in combination with other existing supporting cell-specific Cre or CreER mice for genetic manipulation of two genes in the inner ear in vivo. There is a second poster from our lab discussing a supporting cell specific rtTA allele (Sox10-rtTA; see Bradley Walters et al.).

146 Actin-Binding Protein 12 Is a Component of the Hair Cell's Cuticular Plate

Lana Pollock¹, Divya Indrakanti¹, Brian McDermott¹

¹Case Western Reserve University

Background

The filamentous actin-based mesh of the hair cell cuticular plate is hypothesized to anchor the stereocilia in place at the apical surface of the cell. However, the precise role of the cuticular plate in hair bundle morphology and hearing remains unknown. Additionally, little is known about the molecular mechanisms that shape actin to build the unique structure of the cuticular plate.

Methods

By analysis of the zebrafish hair cell transcriptome, we identified several hair cell-expressed candidate molecules that could potentially be involved in hair bundle or cuticular plate morphogenesis based on their known actin-shaping activities in other tissues. We analyzed the localization patterns of these candidate molecules by immunolabeling in mouse hair cells as well as by expression of GFP-fusion proteins in zebrafish hair cells. We are also currently working to generate zebrafish mutants of each of these candidate genes using zinc-finger nucleases or transcription activator-like effector nucleases. Analyses of these mutants will help us to elucidate the role of these molecules in hair cell structure and hearing.

Results

We found that one candidate, Actin-Binding Protein 12 (ABP12), localizes throughout the cuticular plate in mouse vestibular hair cells. Ongoing analysis of GFP-ABP12 fusion protein expression in transgenic zebrafish hair cells also indicates a possible cuticular plate localization pattern.

Conclusion

We hypothesize that ABP12 is a key regulator of cuticular plate morphology and function. Future analyses of the effects of genetic perturbation of *abp12* on hair bundle

morphogenesis, function, and hearing will allow further elucidation of the molecular mechanisms shaping the cuticular plate and may also allow us to advance our understanding of the role of the cuticular plate in hearing.

147 Differential Distribution Pattern of the Non-Classical Spectrin Beta-V in the Inner Ear Sensory Hair Cells During Evolution

Samantha Papal^{1,2}, Christine Petit^{1,2}, Aziz El-Amraoui^{1,2}

¹*Institut Pasteur*, ²*Unité de Génétique et Physiologie de l'Audition, INSERM UMRS587; UPMC Paris 06*

Background

Within the mammalian auditory organ, outer hair cells (OHCs) amplify sounds by electromotility – the voltage-dependent contraction and elongation of the lateral plasma membrane (LPM). Electromotility is driven by the OHC transmembrane protein prestin. The actin- and spectrin-based cortical lattice that underlies the LPM is also important in this process; however, the precise composition of the cortical lattice, and the way in which it interacts with prestin (defective in a human deafness), have been unknown. In the mouse inner ear, we found that spectrin beta-V (which exists as an alpha-II/beta-V heterodimer) that is almost twice the length of conventional beta spectrins, forms the spectrin-based cytoskeleton that provides OHCs with the flexibility required for sound amplification.

Methods

Immunofluorescence microscopy analyses, Confocal laser scanning microscopy

Results

We detected spectrin beta-V in the vestibular epithelia where it displays a punctuated cytoplasmic distribution pattern. Interestingly, unlike in OHCs, no co-localisation was observed with alpha-II spectrin throughout the cytoplasm of vestibular hair cells. A co-localisation was, however, observed with Golgi-labeled structures, which suggests this spectrin involvement in protein/membrane trafficking. Because spectrin beta-V distribution pattern varies among inner ear sensory cell types, we analysed further its distribution pattern in *Xenopus* inner ear. We show that the protein is present also in the hair cells, essentially in the apical region of the cells, at the level of the cuticular plate. Faint labeling was also observed at the cell-cell junctions. This spectrin beta-V labeling in frog correlates with the distribution of the *Drosophila* beta-Heavy spectrin observed in the apical region of epithelial cells.

Conclusion

Altogether, our findings support changes during evolution in the distribution pattern of the non-classical spectrin beta-V within the inner ear sensory hair cells.

148 Immunocytochemical Localization of Oncomodulin (Ocm) in the Human Inner Ear

Ivan Lopez¹, Dwayne Simmons², Larry Hoffman¹, Gail Ishiyama³, Akira Ishiyama¹

¹*Dep Head and Neck Surgery David Geffen School of Medicine UCLA*, ²*Dep Integrative Biology & Physiology, UCLA*, ³*Dep Neurology, UCLA*

Background

In the present study, we determined the distribution of oncomodulin (Ocm), a member of the parvalbumin family, relative to other EF-hand CaBPs by immunocytochemistry in the human inner ear using auditory and vestibular endorgans (macula utricule and cristae ampullaris) microdissected from human temporal bones obtained at autopsy and macula utricule obtained from ablative surgery. We also determined Ocm immunolocalization in the mouse cochlea and vestibule for comparative purposes (Simmons et al., *J Comp Neurol*, 518:3785-3802, 2010).

Methods

All human subjects (n=4, aged 82-85 years old) had documented normal auditory and vestibular function. The macula utricule acquired from patients undergoing surgery for acoustic neuroma (n=3, ages, 42, 44, 56) year old) was also used. Formalin fixed frozen sections obtained from the cochlea; macula utricule and crista were incubated with affinity purified rabbit polyclonal antibodies against recombinant full-length rat Ocm. Immunoreactivity was visualized using secondary antibodies labeled with Alexa 488 or horse-radish-peroxidase and DAB.

Results

In the human and mouse cochlea Ocm was exclusively located in outer hair cells (OHCs). The expression of Ocm was uniformly the base to apex. In contrast to the cochlea, Ocm expression was substantially reduced in human vestibular tissues at older adult ages (normal autopsy). In the human macula utricule from younger individuals (surgical specimens) Ocm immunoreactivity was located to hair cells in the central portion of the sensory epithelia resembling the striola.

Conclusion

The high degree of conservation of Ocm expression in the human and mouse suggest that Ocm may play an important role in calcium homeostasis. In addition it can be used as a marker for specific cells types in the vestibular sensory epithelia.

149 Slo Is Targeted to the Basolateral Membrane Using a Dihydrophobic Amino Acid Motif

Jun-Ping Bai¹, Joseph Santos-Sacchi², Dhasakumar Navaratnam¹

¹*Yale University Dept. of Neurology*, ²*Yale University Dept. of Surgery*

Background

Large conductance K channels (BK) are important for determining the receptor potential of inner hair cells that allow a graded response to sustained sound induced

depolarization and is essential for accurate sound encoding. These channels consist of an alpha subunit (Slo) and a variable number of auxiliary subunits. Slo is localized to the lateral wall of inner hair cells where they lie adjacent to ryanodine receptors, which are thought to be the site of Ca release and subsequent activation of these channels in a hair cells operating voltage range (-80 to -60mV). Similarly, these channels are thought to mediate efferent synaptic output in mid to high frequency outer hair cells. BK channels are localized at the basolateral surface of OHCs where its activation is thought to occur by Calcium induced Calcium release from the ER. The distribution of the ER in these OHCs mirrors that of efferent synaptic release sites.

Proteins are targeted to the basolateral surface of polarized epithelial cells using a number of intrinsic sequence motifs. In this study, we explore the role of a number of these motifs in targeting Slo to the basolateral surface of the cell.

Methods

We used MDCK cells as a model system and established that Slo is targeted to the basolateral surface of these cells. We identified four dihydrophobic motifs (DXXLL or D/EXXXLL) and one potential tyrosine motif (ΦXXY) that could target Slo to the basolateral surface of the cell. We then mutated these residues individually and transfected MDCK cells with Slo containing these mutations. The expression of these mutants on the basolateral surface of was quantified using confocal microscopy.

Results

We determined that LI976 was critical for adequate targeting of Slo to the basolateral surface of MDCK cells. Substitution of these residues with either alanine or glutamine residues resulted in the loss of basolateral targeting with the protein retained within the Golgi. Finally, we establish that Slo uses a trafficking pathway that includes clathrin/AP1B since LLC-PK1 cells that lack the AP1B subunit show deficient Slo targeting to the basolateral surface of the cell.

Conclusion

Slo uses a dihydrophobic targeting sequence (LI976) and the clathrin/AP1B pathway to traffic to the basolateral surface of the cell.

150 cGMP Pathways in Mammalian Cochlear Hair Cells Underlying the Regulation of Intracellular $[Ca^{2+}]$ by CGMP-Gated CNGA3

Michael Wiebel¹, Lucio Pereira¹, Marian Drescher¹, Robert Silver², Dakshnamurthy Selvakumar¹, Neeliyath Ramakrishnan¹, Dennis Drescher¹

¹Wayne State University, ²Syracuse University

Background

The expression of olfactory/cone photoreceptor form(s) of cGMP-gated CNGA3 transcript in vestibular hair cells and CNGA3 protein in mammalian cochlear hair cells (Selvakumar et al., Biochem. J. Cell 443: 463-476, 2012) predicts a need to regulate cGMP pathways in hair cells.

In vestibular hair cells, regulation occurs in part via cone photoreceptor cGMP-phosphodiesterase 6c, PDE6c, but not PDE5.

Methods

Primers for the specific transmembrane isozymes of guanylyl cyclase and phosphodiesterase, and GCAP1 and GCAP2, that are utilized in vision and olfaction were applied in RT-PCR to rat organ of Corti and isolated cochlear hair cells. These primers crossed introns and all products were sequenced. Calcium fluorescence imaging was utilized to determine calcium responses in individually isolated cochlear hair cells to inhibitors of the cGMP-pathway isozymes.

Results

We show that transcript for cone photoreceptor PDE6c is expressed in singly-isolated inner and outer hair cells from the cochlea of the adult rat. Transcript for the cone photoreceptor guanylyl cyclase isozyme, GC-E, has been identified in cochlear inner hair cells. Transcript for photoreceptor isozyme GC-F, GCAP1 and GCAP2 have been found in an isolated organ of Corti (OC) cochlear subfraction. GCAP1 and GCAP2 regulate activation of GC-E and GC-F, and GCAP2 is recognized as being a protein binding partner of the hair cell ribbon synapse protein, ribeye. Transcript for the olfactory/photoreceptor form of CNGA3 has been identified in cochlear outer hair cells, and as functionally predicted for this cGMP-gated ion channel, inhibitors of PDE6c caused an overall elevation of intracellular Ca^{2+} in singly-isolated outer hair cells over minute time intervals, as opposed to a decrease in intracellular Ca^{2+} that would be the consequence if voltage-gated calcium channel inhibition via PKG-phosphorylation were the primary determinant of intracellular Ca^{2+} . Given the expression of cGMP-pathway proteins in the OC that are found in photoreceptors, we considered and confirmed transcript expression of photoreceptor rhodopsin and cone medium-wave sensitive opsin in rat organ of Corti, pointing to a mammalian correlate of the rhodopsin cascade identified in Johnston's organ of *Drosophila*.

Conclusion

cGMP pathways in mammalian cochlear hair cells modulate hair cell intracellular Ca^{2+} and include components that are clearly identifiable as photoreceptor isozymes in retinal cGMP-cascades. These results support the suggestion that across evolution "different sensory modalities utilize common signaling cascades" (Senthilan et al., Cell 150: 1042-1054, 2012).

151 USH1 Proteins Form an Adhesion Belt Around the Basolateral Region of the Photoreceptor Outer Segment, Including the Calyceal Processes That Are Absent from Mice

Aziz El-Amraoui¹, Iman Sahly², Eric Dufour², Cataldo Schietroma², Vincent Michel¹, José-Alain SAHEL³, Christine Petit²

¹Institut Pasteur, Génétique et Physiologie de l'Audition, Inserm UMRS587, UPMC, Paris, France, ²Institut Pasteur, Institut de la vision, Inserm UMRS587, UPMC, Paris, France, ³Inserm UMRS968, Institut de la Vision, Département de Génétique, Paris, France

Background

The Usher syndrome is the first cause of inherited deaf-blindness in humans. USH1 Animal models wherein Usher syndrome type I (USH1) proteins — myosin VIIa (USH1B), harmonin (USH1C), cadherin-23 (USH1D), protocadherin-15 (USH1F) and sans (USH1G) — were targeted at different maturation stages of the auditory hair cells have proven efficient to unravel the role of USH1 proteins in proper organization of the hair bundle, the sound receptive structure, and functioning of the mechano-electrical machinery. By contrast, the mechanisms underlying USH1 retinal dystrophy remain unknown because mutant mice lacking any of the USH1 proteins do not display retinal degeneration. This discrepancy between the mouse and human retinal phenotypes has made it particularly difficult to elucidate the roles of USH1 proteins in the human retina. We addressed this issue here.

Methods

Immunohistochemistry, Confocal microscopy, Coimmunoprecipitation experiments, immunogold and scanning electron microscopy.

Results

We found evidence for the existence of major differences between rodents and primates in the structural and molecular architecture of photoreceptors at the interface of the inner and outer segments, and for a differential distribution of USH1 proteins associated with this particular region. In macaque photoreceptors, all USH1 proteins — myosin VIIa, harmonin, cadherin-23, protocadherin-15, sans — colocalized at membrane interfaces i) between the inner and outer segments in rods and ii) between the microvillus-like calyceal processes and the outer segment basolateral region in rods and cones. This pattern, conserved in humans and frogs, was mediated by the formation of an USH1 protein network, which was associated with the calyceal processes from the early embryonic stages of outer segment growth onwards. By contrast, mouse photoreceptors lacked calyceal processes and had no USH1 proteins at the inner-outer segment interface. Rodent photoreceptors also lack the long, rigid, F-actin roots of the calyceal processes, penetrating into the inner segment of the photoreceptor, and which confer a relationship between the inner and outer segments that is very different from that in photoreceptors lacking these structures.

Conclusion

Together, our findings accounts for why mice are poor models for retinal defects caused by USH1. They led us suggest that USH1 proteins form an adhesion belt around the basolateral region of the photoreceptor outer segment in humans, and that defects in this structure probably cause the retinal degeneration in USH1 patients.

Grants: EEC FP7, HEALTH-F2-2010-242013 (TREATRUSH), ANR-07-MRARE-009-01, ANR-10-LABX-65, and the Fondation Voir et Entendre.

152 The Striated Organelle and Their Spectrin Connection in Inner Ear Hair Cells

Robstein Chidavaenzi¹, Anna Lysakowski¹

¹University of Illinois at Chicago

Background

Spectrins are a prominent family of cytoskeletal proteins initially described in red blood cells, where they were assigned the function of maintenance of the erythrocyte membrane's biconcave form. Non-erythrocytic forms of these proteins have since been identified, and their functional roles have grown just as steadily as the number of binding partners. In our work we are only beginning to appreciate the integral role that they play in inner ear hair cells in general, and the striated organelle in particular.

Methods

We used confocal and electron microscopy methods (Lysakowski et al., 2011), combined with co-immunoprecipitation (CoIP) and mass spectrometry analyses. For the CoIP experiments, each tissue type (vestibular, cochlear, and brain), was run in two parallel tubes - one for the bait antibody (mouse anti- α -II spectrin) and one for the control mouse IgG. The tissue extracts and sepharose G conjugated to antibody or IgG were incubated overnight at 40C. After the reaction, the flow-through and CoIP elution products were analyzed using western blots and mass spectrometry for determining interacting protein identities. The mass spectrometry was done for us by our Core proteomics facility. Protein identifications were accepted if they could be established at greater than 95.0% probability and contained at least 2 identified peptides.

Results

We have evidence that the striated organelle is composed of α II and β II spectrin, whereas the other isoforms, viz. α I, β I, β III, β IV, and β V spectrin, are not involved. α II and β II spectrin also localize to the cuticular plate and, hence, can be found in all hair cell types. On the other hand, the other non-striated organelle spectrins, although still present in hair cells, exhibit different or more restricted distribution patterns. Legendre et al. (2008, J. Cell Science 121: 3347-3356) recently showed that besides α II and β II spectrin, mammalian outer hair cells have β -V spectrin in their lateral walls, but they found no evidence of β I, β III or β IV spectrins using immunofluorescence. By contrast, in our immunofluorescence experiments we have observed β I

spectrin in outer hair cells but not in inner hair cells, and we are currently working out the distribution of β III spectrin which preliminary evidence suggests is also present in cochlear hair cells.

Conclusion

We present further evidence of the distribution patterns of the spectrins and highlight how interacting partners differ, which might point to the different roles that spectrins play in inner ear hair cells.

153 Membrane Recycling of Outer Hair Cells

Csaba Harasztosi¹, Emese Harasztosi¹, Anthony W.

Gummer¹

¹University Tubingen, Germany

Background

Efferent innervation of outer hair cells (OHCs) is probably important for modulating the mechanical impedance of the organ of Corti, and afferent innervation for feedback to the brainstem. Synaptic communication at the subnuclear pole of OHCs is thought to require tightly regulated exocytic and endocytic activities, membrane recycling. Rapid endocytic activity of OHCs in the guinea-pig cochlea has been already studied using the fluorescent membrane marker FM1-43 (Griesinger et al., 2004; Kaneko et al., 2006; Meyer et al., 2001). It was demonstrated that vesicles were intensively endocytosed at the apical pole of OHCs and transcytosed to different locations, namely into the basolateral membrane and through a central strand towards the nucleus. Since the significance of the endocytic activity in the subnuclear region of OHCs is still not clear, in this study we investigated rapid endocytic activity located at the synaptic pole of OHCs.

Methods

In response to application of FM1-43, confocal laser scanning microscopy was used to visualize membrane recycling of OHCs isolated from the functionally mature guinea-pig cochlea. Perfusion system was used that maintained constant laminar flow around the entire OHC. This system guarantees that upon application, the dye arrives at the same time and concentration to both the apical and basal poles of the OHC.

Results

After dye application, the fluorescence intensity immediately started to increase in both the infracuticular and subnuclear regions ($t < 1$ s). Signal intensity changes were recorded in the apical and basal poles relative to the signal at the membrane. Measured 5 s after onset of FM1-43 application, the normalized signal intensity at depths of 1, 2, 4 and 6 μ m deep beneath the membrane were 0.28 ± 0.02 , 0.15 ± 0.03 , 0.08 ± 0.03 and 0.06 ± 0.04 in the basal pole (N=5) and 0.39 ± 0.17 , 0.16 ± 0.03 , 0.09 ± 0.04 and 0.04 ± 0.03 in the subcuticular area (N=5), respectively. These data show no significant difference in fluorescence signal intensity changes between the opposite poles of the OHC - the subnuclear and the subcuticular areas.

Conclusion

Therefore, it is concluded that stained vesicles appearing in the subnuclear pole in that time interval cannot have derived from apical endocytic activity, but were locally endocytosed. Consequently, endocytic activities in both basal and apical poles of the OHC probably contribute equally to balance the exocytosis-evoked membrane surface increase - the membrane recycling.

154 Prestin Is Targeted to the Basolateral Membrane Using a Tyrosine Motif

Yifan Zhang¹, Jun-Ping Bai², Joseph Santos-Sacchi³, Dhasakumar Navaratnam²

¹Choate Rosemary Hall School, ²Yale University Dept. of Neurology, ³Yale University Dept. of Surgery

Background

The presence of the motor protein prestin in the basolateral wall of outer hair cells (OHCs) is critical for proper OHC function and cochlear amplification.

Proteins are targeted to the basolateral surface of polarized epithelial cells using a number of intrinsic sequence motifs. In this study, we explored the role of a number of these motifs in targeting prestin to the basolateral surface of the cell.

Methods

We used MDCK cells as a model system and established that prestin is targeted to the basolateral surface of these cells. We identified five potential tyrosine motifs (Φ XXY) that could target prestin to the basolateral surface of the cell. We then mutated these residues individually and transfected MDCK cells with prestin containing these mutations. The expression of these mutants on the basolateral surface of was quantified using confocal microscopy.

Results

We determined that Y520 was critical for adequate targeting of prestin to the basolateral surface of MDCK cells. We also established that substitution of Y520 with Phe and Ser resulted in a wild type phenotype and markedly disorganized targeting respectively. These data confirm that the signature important for basolateral targeting is dependent on the phenol ring and not on the OH side chain of the Tyr residue. Additionally, we confirm the lack of importance of an adjacent negatively charged group of residues in targeting prestin to the basolateral surface. Finally, we establish that prestin uses a pathway using clathrin/AP1B since LLC-PK1 cells that lack the AP1B subunit show deficient prestin targeting to the basolateral surface of the cell.

Conclusion

Prestin uses a tyrosine targeting sequence (520Y) and the clathrin/AP1B pathway to traffic to the basolateral surface of the cell.

155 Can Oncomodulin Directly Regulate Prestin's Function?

Chongwen Duan¹, Kazuaki Homma¹, MaryAnn Cheatham¹, Peter Dallos¹, Jing Zheng¹

¹Northwestern University

Background

Prestin is a unique voltage-dependent motor protein responsible for the somatic electromotility of outer hair cells (OHCs) (Zheng et al., 2000), a process that is essential for providing the high sensitivity and frequency selectivity of mammalian hearing. Oncomodulin, also called β -parvalbumin, is a calcium-binding protein, selectively and abundantly expressed in OHCs (Sakaguchi et al., 1998). Oncomodulin's mRNA developmental pattern is similar to prestin's, starting with expression around P3, and peaking around P10 (Yang et al., 2004, Belyantseva et al., 2000). Furthermore, both prestin and oncomodulin mRNAs are down-regulated by the same microRNA (Lewis et al., 2009). It is also known that an exceptionally high level of oncomodulin protein is found in the soma of OHCs, which is surrounded by the prestin-embedded basolateral membrane (Hackney et al., 2005). In prestin-KO mice, augmented expression of oncomodulin is observed at both mRNA and protein levels (Miller et al., 2010). Similar expression patterns and regulation arrangements between prestin and oncomodulin indicate possible functional connections between these two important OHC-specific proteins.

Methods

In order to explore the association between prestin and oncomodulin, we investigated whether oncomodulin can directly bind to prestin. We created various prestin mutants by PCR. These mutant prestins include point mutations and deletions at various positions. Several biochemical methods including co-immunoprecipitation, SDS-PAGE/Western blot, and protein purification, were used to identify prestin's amino acids that are important for oncomodulin binding.

Results

Experimental evidence suggests that prestin's C-terminal domain has a significantly higher binding capability than control proteins.

Conclusion

Since prestin is expressed in the OHCs, whose mechanical property is significantly modulated by intracellular calcium (Dallos et al., 1997), it is reasonable to postulate that oncomodulin-prestin interaction at least partially underlies the calcium-dependent change in the mechanical properties of OHCs (Work supported by NIH Grants DC011813, DC010633, DC00089, and the Knowles Hearing Center).

156 Functional Consequences of Direct Calmodulin Binding to Prestin and Other SLC26 Transporter C-Terminal Domains:

Inhibition of Transport by Calcium/Calmodulin

Jacob Keller¹, Kazuaki Homma¹, Jing Zheng¹, Peter Dallos¹, Mary Ann Cheatham¹

¹Northwestern University

Background

Several studies have shown that calcium influences the function of various members of the SLC26 protein family (Lamprecht et al., 2009; Loriol et al., 2008), including prestin (Frolenkov et al., 2000), the central force-delivering protein in the mammalian cochlear amplifier (Zheng et al., 2000). The mechanistic connection between calcium and SLC26 proteins, however, has heretofore not been elucidated. We have previously presented bioinformatic and biochemical evidence that calmodulin binds directly to intrinsically-disordered regions (IDRs) in the intracellular carboxy-terminal domains of several, if not all, SLC26 members in a calcium-dependant manner (Jacob and Dallos, 2009).

Methods

We performed ratiometric measurements of intracellular pH changes in cultured cells expressing various SLC26 proteins, the kinetics of which reflect the magnitudes of anion transporter activities of the expressed transporter proteins. The effects of the calcium ionophore, calcimycin, and the calmodulin inhibitor, trifluoperazine (Vandonselaar et al., 1994), were examined in order to demonstrate functional ramifications of calmodulin binding to SLC26 proteins.

Results

Calmodulin binding to IDRs within intracellular domains of SLC26 proteins is expected to be induced by increased intracellular calcium upon calcimycin treatment. Our experiments indicate that this binding significantly reduces the kinetics of pH change, and that the inhibition of calmodulin by trifluoperazine significantly alleviates this calcimycin-induced inhibitory effect.

Conclusion

Our results strongly indicate that the functional consequence of calmodulin binding to the IDRs in the intracellular carboxy-terminal domains of SLC26 transporters is inhibitory. We also discuss some ideas about potential ramifications for prestin electromotility and cochlear amplification.

This work is supported by NIH grants DC00089 (to MAC), DC010633 (to JZ), and by the Knowles Hearing Center.

157 Effects of the Elevation of Intracellular Calcium on the Outer Hair Cell Plasma Membrane Motors

Ghanshyam Sinha¹, Gregory Frolenkov¹

¹Department of Physiology, University of Kentucky

Background

It has been proposed that calcium signaling in outer hair cells (OHCs) may regulate cochlear function. An increase of intracellular calcium is known to affect the stiffness of

the cortical cytoskeleton in OHCs. It has been also proposed but never directly demonstrated that the increase of intracellular calcium may regulate the operation of the prestin-based plasma membrane motors. Calcium concentration within an OHC may be elevated either through the calcium influx from outside of the cell or through calcium release from the *subsurface cisternae*, an endoplasmic reticulum-like structure of the OHCs. The OHC cortical cytoskeleton and the membrane motors elements are located at the lateral wall of the OHC in close proximity to the *subsurface cisternae*.

Methods

We used photo-activatable (caged) calcium chelators to release free calcium within the OHC and fast calcium imaging to monitor the propagation of calcium signal along the cell. Whole cell patch clamp recordings were used to simultaneously measure the OHC non-linear capacitance.

Results

In acutely isolated organ of Corti explants loaded with *o*-nitrophenyl EGTA (NP-EGTA) UV laser illumination with duration less than 20 ms produced rapid rise in intracellular calcium concentration measured by calcium indicator fluo-4. After an initial calcium spike we observed a diffusive propagation of calcium longitudinally along the OHC with an estimated speed of $\sim 1 \mu\text{m/s}$. The calcium-induced calcium release, if present, was difficult to resolve. Puff application of 5 μM ryanodine to OHCs resulted in only moderate calcium responses. Thapsigargin (50 μM), an inhibitor of the endo/sarco-plasmic reticulum ATPase, does not apparently affect the propagation of uncaged calcium along the OHC. In the presence of cesium in the patch pipette, the whole-cell currents were not affected by the release of calcium into the cytosol. However, the non-linear capacitance decreased by $\sim 10\%$ after about one minute after surge of intracellular calcium.

Conclusion

1) Our data suggests a minimal contribution of calcium-induced calcium release in propagation of calcium signals along OHC. 2) However, a decrease of non-linear capacitance after calcium uncaging indicates potential modulatory effect of intracellular calcium on prestin-based plasma membrane motors.

158 The Relationship of Prepulse Effect and Prestin Density in an Inducible Prestin Cell Line

Feng Zhai^{1,2}, Lei Song¹, Junping Bai¹, Chunfu Dai², Joseph Santos-Sacchi¹

¹Yale University, ²Fudan University

Background

Mechanical activity of the outer hair cell (OHC) underlies the enhanced sensitivity and frequency resolving power of the mammalian cochlea. Prestin, a member of the SLC26 anion transporter family, has been identified as the molecular motor for electromotility. The voltage dependence of prestin's nonlinear capacitance (NLC) depends on long term holding potential. We call this a

prepulse effect. The relationship of prepulse effect and prestin density in an inducible prestin cell line remains to be elucidated.

Methods

HEK293 cells were cultured in DMEM containing 50 U/ml each of penicillin and streptomycin, 10% fetal bovine serum at 37°C in a CO2 incubator (5%). All whole cell recordings were made on single cells growing on a coverslip at 2h, 4h, 6h, 10h and 24h after tetracycline induction. The NLC traces show the change of membrane capacitance C_m in response to voltage across the membrane V_m , which was fit with a Boltzmann equation.

Results

We assayed four different parameters of NLC, Q_{sp} , z , V_h and ΔV_h , to delineate prestin function. Q_{sp} , charge movement per unit of membrane surface, increases with time in a sigmoidal manner. In contrast to Q_{sp} , which takes days to reach its asymptotic level, the z value reaches a maximum level of 0.8e 6h after induction. V_h values reach its asymptotic value 6h after induction, shifting in the depolarizing direction with time. ΔV_h , the difference between V_h with long term holding potentials (1 min) of -100mV and +50mv holding potentials, an index of the prepulse effect upon V_h , increases steadily from 2h and reaches its peaks 10h after induction.

Conclusion

The prepulse effect upon V_h increases with prestin density, and may correspond to early molecular maturation events.

159 Morphological and Functional Changes in a New Animal Model for Meniere's Disease

Naoya Egami¹, Akinobu Kakigi¹, Taizo Takeda², Tatsuya Yamasoba¹

¹University of Tokyo, ²Nishinomiya Municipal Center Hospital

Background

Meniere's disease (MD) is histologically characterized by endolymphatic hydrops (EH) in the inner ear. There is considerable evidence that water homeostasis in the inner ear is regulated partly via the vasopressin-aquaporin2 (VP-AQP2) system. EH is considered to be the result of incoordination of inner ear water homeostasis, which involves excessive production of endolymph and/or reduced absorption of endolymph. Until recently, however, the detailed mechanisms underlying the over-accumulation of endolymph were unclear. We aimed to examine both morphological and functional changes of the inner ear system in our novel combined animal MD model, involving the combination of surgical obliteration of the endolymphatic sac and duct and the administration of desmopressin (vasopressin type 2 receptor agonist; V2 agonist).

Methods

In experiment No. 1, guinea pigs used in morphological studies underwent surgical obliteration of the

endolymphatic sac and duct in one ear and were maintained for a week or 4 weeks, and divided into with or without desmopressin administration. We quantitatively assessed EH in the cochlea, vestibules and semicircular canal. In experiment No.2, we performed vestibular examination. We recorded spontaneous nystagmus and observed the presence or absence of balance disorder in normal control group, desmopressin administration group and surgical treated groups with or without desmopressin administration.

Results

In experiment No. 1, both the increase ratio (IR) of the scala media area and the proportion of the endolymphatic space in the saccule were significantly higher in the Combined group than in the Surgical groups. There were no significant differences in the degree of hydrops in the utricle or semicircular canal among ear groups. In experiment No. 2, all animals of the Combined groups showed spontaneous nystagmus and balance disorder; meanwhile, the Surgical groups were found to be asymptomatic.

Conclusion

Our experimental animals not only presented severe EH in the cochleae and saccules, but also showed episodes of balance abnormalities along with nystagmus. EH may be exacerbated due to endolymphatic sac dysfunction combined with the effect of desmopressin and acute V2 effect, which may accompany vestibular abnormalities that are similar to the vertigo attack in patients with MD.

160 Do Autoimmunity to IgG1 and Their Immune Complex Reaction Cause Meniere's Disease?

Sung Huhh Kim¹, Jin Young Kim², Won-Sang Lee¹, Jae Young Choi¹

¹Yonsei University College of Medicine, ²Yonsei University

Background

This study was performed to identify autoimmune reaction as a main pathologic mechanism of Meniere's disease. Authors tried to identify main target antigens in Meniere's disease which causes inner ear damage and endolymphatic hydrops of Meniere's disease.

Methods

First, proteins which only exist in the endolymphatic sac (ES) luminal fluid of Meniere's disease were identified by proteomic analysis (LC-MS/MS, n=3). Based on the result, authors conjectured pathophysiology of Meniere's disease and performed protoarray with the sera of Meniere's disease patient (n=10) and compared the result with those of normal controls (n=10). With the data of protoarray, we identified target antigens reacted with autoantibodies of patients' sera. Then, we examined if the target antigens also exist in the human endolymphatic sac tissues and ES luminal fluid of patients using proteomic analysis (LC-MS/MS).

Results

Proteins only exist in the luminal fluid of Meniere's disease but not in the control were 9 proteins; eight of them were immunoglobulin and one was interferon regulatory factor. This infers that immunologic or autoimmune reaction could be the pathologic mechanism of Meniere's disease. In the protoarray, 18 antigens showed increased reaction more than two folds when compared with normal controls. Among the antigens, only one protein, IgG1, exist in the human ES sample and ES luminal fluid and it showed increased reaction with the sera of Meniere's disease more than 200 folds.

Conclusion

This result means that autoimmune reaction to IgG1 and immune complex formation can be the pathologic mechanism of Meniere's disease like other rheumatologic diseases such as rheumatoid arthritis and SLE. For validating the results, immunoprecipitation with the ES luminal fluid and IgG1 protein and mass analysis of immune reaction with Meniere's disease patients' sera should be performed.

161 An Electromotility Mechanism Driven by the Tectorial Membrane

Roozbeh Ghaffari¹, Scott Page^{1,2}, Shirin Farrahi^{1,2}, Dennis Freeman^{1,2}

¹MIT Research Laboratory of Electronics, ²MIT Department of Electrical Engineering & Computer Science

Background

The mammalian cochlea is a remarkable sensor capable of detecting and analyzing sounds that generate subatomic vibrations. This extraordinary sensing property is widely believed to depend on electromotility of outer hair cells. Here we describe an additional electromotility mechanism driven by the tectorial membrane (TM), whereby transduction currents acting on TM fixed charge groups generate local TM deformations that could contribute to hair bundle motion.

Methods

We developed a microaperture chamber to test TM electrical properties by positioning isolated mouse TMs as an electrochemical barrier between two fluid-filled compartments. This setup allowed both measurement of TM interfacial voltages and application of electrical stimuli.

To determine TM fixed charge density, we measured DC interfacial potentials between the TM and the surrounding baths as a function of bath ionic concentration. The resulting voltages were fit by a model based on the Donnan relation.

To measure TM electromotility, AC electric fields were applied to the TM in its middle and marginal zones, which normally overlie the hair bundles. Electrically-evoked displacements in the bulk of the TM were visualized and quantified using a stroboscopic computer vision system and Doppler optical coherence microscopy.

Results

The net charge of the TM was large (-7.1 mmol/L at physiological pH), representing 1 fixed charge molecule for every 25 cations in endolymph. The high density of fixed charge contributes significantly to TM compressive stiffness and also suggests that electrical stimuli could generate an electromechanical response.

Electrically-evoked TM motions were nanometer-scaled (~ 5 -200 nm), increased linearly with electric field amplitude (0.05-20 kV/m) and decreased with frequency (1-1000 Hz). This frequency dependence can be understood in terms of the interplay between electrophoresis and electro-osmosis.

Conclusion

Results reported here show that the TM contains a high density of fixed charge that contributes to its compressive stiffness and can generate electrically-evoked displacements. These displacements may have important implications for cochlear mechanisms. Although the electric fields applied in this study were large, they are in the range that can be generated near hair cell transduction channels. The low pass nature of the TM's frequency dependence suggests that this mechanism may be particularly relevant at low frequencies and in the cochlear apex. TM electromotility thus could be important in the deflection of cochlear hair bundles *in vivo*.

162 Hearing Impairment at Low and High Frequencies After Loss of Mammal-Specific Tectorial Membrane Component Carcinoembryonic Antigen Cell Adhesion Molecule 16 (CEACAM16)

Lukas Rüttiger¹, Andreas Bress¹, Robert Kammerer², Kishiko Sunami³, Marlies Knipper¹, Wolfgang Zimmermann⁴

¹University of Tübingen, ²Institute of Immunology Greifswald, ³Osaka City University Medical School, ⁴University Hospital of Munich

Background

The mammal-specific, secreted CEACAM16 is a member of the carcinoembryonic antigen gene family. CEACAM16 is exceptionally well conserved among species. CEACAM16 is selectively expressed in the inner ear. We studied the hearing function and the cochlear expression of CEACAM16 to elucidate its importance for auditory function in young and aged Ceacam16^{-/-} mice.

Methods

Ceacam16^{-/-} mice were analysed for age related and trauma induced hearing deficits by ABR and DPOAE measurements and exposure to noise. In cochlear sections of Ceacam16^{-/-} mice the tectorial membrane was inspected and gene expression was studied by *in situ* hybridisation and immunohistochemistry. Protein expression was furthermore studied by Western blot analyses.

Results

CEACAM16 is specifically expressed in the inner ear. The hearing phenotype of Ceacam16^{-/-} mice was similar to the observed hearing-impairment in members of human Family 1070 with non-syndromic autosomal dominant hearing loss (DFNA4) who carry a missense mutation in CEACAM16.

Conclusion

CEACAM16 can probably form higher order structures with other tectorial membrane proteins and influences the physical properties of the tectorial membrane. Evolution of CEACAM16 might have been an important step for the specialization of the mammalian cochlea, allowing hearing over an extended frequency range.

163 Remodeling and Biosynthesis of Glycosaminoglycans Revealed Using a BODIPY-Xyloside Conjugate in the Vestibular System

Holly Holman¹, Vy Tran¹, Lynn Nguyen¹, Sailaja Arungundram¹, Balagurunathan Kuberan¹, Richard Rabbitt^{1,2}

¹University of Utah, ²Marine Biological Laboratory

Background

Examination of proteoglycan biosynthesis and remodeling in the semicircular canals and utricle using a novel BODIPY-xyloside conjugate. Xylosides are known to enter the Golgi apparatus and prime the production of glycosaminoglycans (GAGs). When conjugated with a fluorescent reporter and introduced into the inner ear endolymph, we found newly expressed fluorescent GAGs *in vivo*. We provide a new powerful tool to study inner-ear glycobiology and associated disorders.

Methods

Adult oyster toadfish (*Opsanus tau*) of either sex weighing 500 gm with rostral-caudal length greater than 25 cm were obtained from the Marine Biological Laboratory (Woods Hole, MA), and all experiments were carried out in accordance to the approved protocols at the Marine Biological Laboratory and the University of Utah. The BODIPY conjugated xyloside used in this study (BX, VY-IIB 57A) was synthesized following a previously described technique (Kuberan et al., *ChemBioChem*. 2008). Two microliters of a 2 μ M BX in DMSO is diluted in endolymph and administered via glass micropipette into the dorsal extreme of the anterior endolymphatic canal. Single unit afferent recordings and fluorescence imaging were done *in vivo*. After ~ 4 hours, the inner ear was harvested and fixed for either confocal or 2-photon imaging (Olympus FV1000/MPE), or biochemical analysis. Western blotting was performed using mouse anti-heparin sulfate proteoglycan (AbD Serotec), and mouse anti-chondroitin sulfate proteoglycan (Invitrogen).

Results

Within minutes BX post injection, fluorescence was detectable in the crista of the anterior and horizontal canals. BX was not fluorescent in the lumen of the canal

or ampulla, showing incorporation into the cells was a precursor to fluorescence. The time course and spatial distribution of fluorescence development suggests ongoing GAG production occurring at different rates among different vestibular structures. Hair cells expressed strong and persistent fluorescence, with the brightest fluorescence localizing at the apical end of the cell. Multi photon imaging showed strong phalloidin labeling of stereocilia and a BX primed fluorescent kinocilium glycolyx. The epithelial lining of the endolymphatic space and supporting cells also expressed fluorescent GAGs. BX revealed GAG ultrastructural features of the cupula including long fluorescent projections from the crista to the ampullary apex.

Conclusion

A novel xyloside conjugate administered into the endolymph, demonstrates priming of fluorescent GAGs in the inner ear. Additionally, we report strong expression in the vestibular organs of chondroitin sulfate and heparin sulfate proteoglycans. This study reveals GAG ultrastructure, time course of GAG production, remodeling and repair in the ear.

164 Experimental OAE Growth Rates and General Properties of a Dynamical System

Renata Sisto¹, Arturo Moleti², Filippo Sanjust¹, Teresa Botti², Federica Longo²

¹INAIL Research, ²University of Rome 'Tor Vergata'

Background

The dynamical properties of the active feedback mechanism localized in outer hair cells can be recognized in the otoacoustic emissions (OAE) I/O curves. OAEs seem therefore to be able to reflect the fundamental characteristic of the cochlear amplifier.

Methods

High-resolution SFOAE and DPOAE spectra have been measured at different stimulus levels in young healthy subjects using a chirp technique. TEOAE were measured with the double evoked paradigm. A time-frequency filtering method was applied to separate OAE components from different generation mechanisms according to their different phase-gradient delay. In the TEOAE and SFOAE cases, time-frequency analysis permitted separation of the main reflection component from a shorter latency component, and from multiple-reflection components. In the DPOAE case, the overlap component and the main reflection component have been separated.

Results

SFOAEs are thought to be generated by a place-fixed mechanism due to linear reflection from cochlear roughness. The SFOAE complex response is consistent with that measured in the time domain for TEOAEs. If the peak BM response is compressive as $p^{1/3}$, a saturated response

$p^{1/3}$ is expected in the case of peak reflection both in the TEOAE and in the SFOAE. This prediction is well confirmed by the present work. A reduced compression

level is shown by the TEOAEs and SFOAEs shorter latency components, which seem therefore attributable to reflections from more basal cochlear regions.

A linear growth rate has been found over a wide stimulus level range for the DP overlap component. This finding is coherent with a cubic distortion source in which the BM displacement follow a compressive behavior as $p^{1/3}$. As the overlap component is the source for the reflection component, when the first one grows linearly, the reflection one is expected to grow as $p^{1/3}$. This prediction is also confirmed by the experimental results.

Conclusion

The characteristics of the growth rate of the time-frequency separated OAEs components seem to reflect the dynamics of the cochlear active gain.

A compressive BM response growing as $p^{1/3}$, as predicted for a dynamical system operating at the Hopf bifurcation, is consistent with the experimental data.

165 What You See Is Not What You Get:

DPOAEs Versus Intracochlear DPs

Barden B. Stagner¹, Glen K. Martin^{1,2}, Brenda L.

Lonsbury-Martin^{1,2}

¹Research Service, VA Loma Linda Healthcare System, Loma Linda, CA, ²Dept. of Otolaryngology--Head & Neck Surgery, Loma Linda University Medical Center, Loma Linda, CA

Background

The characteristics of distortion product otoacoustic emissions (DPOAEs), ie, distortion products (DPs) measured in the ear canal have been thoroughly described. In contrast, there is relatively little known concerning the behavior of intracochlear DPs (iDPs) propagated toward the DP frequency place (f_{dp}) on the basilar membrane (BM). Detailed comparisons of iDPs to DPOAEs could provide valuable insights on the extent to which DPOAEs can be assumed to mirror DPs within the cochlea.

Methods

Whitehead et al (1995) described a technique whereby the behavior of iDPs could be inferred by interacting a probe tone with the DP of interest to produce a secondary DPOAE. The behavior of the 'secondary' DPOAE was then used to deduce the characteristics of the iDP. In the present study, this technique was used in rabbits to directly compare DPOAE f_2/f_1 -ratio functions, level/phase maps, and interference response areas (IRAs) to their iDP counterparts. $2f_1-f_2$ and $2f_2-f_1$ DPOAEs were collected with f_1 and f_2 primary-tone levels from 75-35 dB SPL. During the collection of these DPOAEs, a 50-dB SPL f_3 was placed at a DP/ f_3 ratio of 1.25 to evoke a secondary DPOAE at $2f_3-(2f_1-f_2)$ or $2f_3-(2f_2-f_1)$. In some experiments, a fixed 4th interference tone (IT) was presented, or was alternatively swept in frequency and level to produce an IRA describing the effects of the IT on DPOAEs and iDPs.

Results

It was found that low primary-level DPOAE f_2/f_1 -ratio functions peaked around $f_2/f_1=1.25$, while the corresponding iDP ratio functions peaked at $f_2/f_1\approx 1.0$. Also, notches observed in DPOAE f_2/f_1 ratio functions were not present in their iDP counterparts. Additionally, ITs above f_2 at narrow f_2/f_1 settings often enhanced the DPOAE, while the iDP remained unaffected. And, level/phase maps showed rapid phase variation with f_{dp} for the narrow ratio $2f_1-f_2$ and all $2f_2-f_1$ DPOAEs, while the corresponding iDPs evidenced relatively constant phase.

Conclusion

DPOAEs often provide poor representations of iDPs, because distributed DPOAE components directed toward the ear canal are often in cancellation, while iDP components directed toward f_{dp} add in phase.

166 Mechanical Two-Tone-Distortions in the Movement of the Tympanal Membrane of Insects

Doreen Moeckel¹, Manfred Kössl¹, Manuela Nowotny¹

¹Goethe-Universität Frankfurt

Background

During stimulation with two pure-tones, tympanal organs of insects emit pronounced distortion-product otoacoustic emissions (DPOAEs) that are indicative of non-linear ear mechanics. There is evidence that the scolopidia, the auditory mechanoreceptors in tympanal organs, are involved in their frequency-specific generation [Möckel et al.: J Comp Physiol A193, 2007]. Our current study aims to measure the mechanical correlates of DPOAEs within the movement of the tympanal membrane of the locust *Schistocerca gregaria*.

Methods

We analysed the movement of the tympanal membrane during stimulation with two pure-tones f_1 and f_2 . Both stimuli f_1 and f_2 had been optimized to evoke large emissions using a closed system to record sensitive DPOAEs in insects. The same frequencies were then used for the open system measurements required by the laser Doppler vibrometry. The laser measurement points were arranged around the potential generation site of the emissions, that is, the attachment point of the scolopidial mechanoreceptors at the tympanal membrane. Stimulation levels of f_1 and f_2 started at 30 dB SPL and reached up to 70 dB SPL.

Results

During stimulation with two pure tones f_1 and f_2 , the amplitude response of the tympanal membrane showed additional peaks at the emission frequency $2f_1-f_2$. The $2f_1-f_2$ mechanical displacement level was 43 dB below the f_2 amplitude which is comparable to the OAE recording situation when using a closed acoustical measurement system. The $2f_1-f_2$ tympanum displacements amounted up to about 0.25 nm for single measurement points located close to the attachment area of the scolopidia. The threshold to evoke a $2f_1-f_2$ mechanical response in the

tympanum movement during these open-system measurements lay at about 50 dB SPL stimulation level.

Conclusion

We demonstrate the existence of mechanical two-tone-distortions in the movement of the tympanal membrane at the $2f_1-f_2$ frequency. The largest displacement amplitudes and therefore potential place of their generation lies close to the attachment point of the dendrites of the receptor cells.

Funding. This project was supported by a grant from the Deutsche Forschungsgemeinschaft (No. 841/1-1), and by a "Nachwuchswissenschaftler/innen im Fokus" grant from the Goethe Universität, Frankfurt, Germany.

167 Time-Frequency Analysis of Transiently Evoked Otoacoustic Emissions Measured with Different Acquisition Protocols

Wiktor Jedrzejczak¹, Krzysztof Kochanek¹, Henryk Skarzynski¹, Andrew Bell², Piotr Skarzynski¹

¹Institute of Physiology and Pathology of Hearing,

²Research School of Biology, College of Medicine

Background

Transiently evoked otoacoustic emissions (TEOAEs) are commonly recorded as average responses to a repetitive click stimulus. If the click train has constant polarity, a linear average results; if it contains a sequence of clicks of differing polarity and amplitude, a nonlinear average can be calculated. The purpose of this study was to record both protocols from the same set of ears and characterize the differences between them.

Methods

Time-frequency (TF) analysis of the recorded signals was done by decomposing them into their basic waveforms. For this, a method of high-resolution adaptive approximation was used, a technique based on the matching pursuit (MP) algorithm.

Results

It was shown that the main difference between TEOAEs recorded with the linear and nonlinear methods is found in the 0-5 ms post-stimulus time window. It was assumed that the signal derived from the linear protocol was contaminated by stimulus artifact. After removal of this artifact, the time-frequency properties of TEOAEs recorded under both the linear and nonlinear protocols were similar. However reproducibility and signal to noise ratio were higher for the linear TEOAEs. Additionally, it was shown that TEOAEs recorded under the linear protocol appear to be less dependent on the presence of synchronized spontaneous otoacoustic emissions (SSOAEs).

Conclusion

TF analysis has shown that the main difference between CEOAEs recorded with the linear and nonlinear methods is found in the 2.5-5 ms post-stimulus time window, and it affects frequencies below 2.2 kHz. The difference is mainly due to stimulus artifact in the linear protocol. This artifact can be removed, either by the MP method or by a

combination of windowing and linear filtering, a process that still leaves the high-frequency, early OAE response intact. TF analysis verifies the reliability of the proposed method.

168 The Effect of Probe Frequency on the Time-Course of Recovery from the Medial Olivocochlear Reflex

Kyle P. Walsh¹, Jordan A. Beim¹, Magdalena Wojtczak¹

¹University of Minnesota

Background

Different methods for estimating the effect of the medial olivocochlear reflex (MOCR) on stimulus-frequency otoacoustic emissions (SFOAE) in humans appear to yield different estimates of the time-course of recovery from the effect. The effect of the MOCR elicited by broadband noise, calculated by extracting changes in the relationship between the ear-canal pressure produced by two brief simultaneous probe tones relative to the sum of the pressures produced by the tones presented in separation decayed over ~600-700 ms after the offset of the elicitor [K. P. Walsh, E. G. Pasanen, and D. McFadden (2010). Overshoot measured physiologically and psychophysically in the same human ears. *Hear. Res.* 268, 22-37]. In comparison, the MOCR effect elicited by a notched-noise, estimated from changes in the ear-canal pressure using a continuous fixed-level probe was substantially shorter, on average ~160 ms [B. C. Backus and J.J. Guinan, Jr. (2006). Time-course of the human medial olivocochlear reflex. *J. Acoust. Soc. Am.* 119, 2889-2904]. Aside from using different methods for estimating effects of efferent activation, the two studies also used different probe frequencies (4 versus 1 kHz). Thus the question remains as to whether the differences in recovery times are due to differences in methodology or due to a frequency dependence of the recovery from the MOCR.

Methods

The time-course of recovery was estimated using continuous fixed-level (40-dB SPL) probes with frequencies of 1, 2, 4 and 6 kHz. For each probe, a 60-dB SPL ipsilateral broadband noise with a 2-octave notch around the probe frequency was used to elicit the MOCR. The ear-canal pressure was measured in the presence and absence of the elicitor to extract changes in SFOAE at the probe frequency due to the elicitor. A heterodyne technique was used to calculate complex-valued ear-canal pressure at the probe frequency.

Results

Changes in SFOAE following the offset of the elicitor, expressed in terms of the proportion of the magnitude of SFOAE measured using a suppression paradigm for each probe frequency, were fitted with an exponential to estimate the time of recovery. The time constants from the best exponential fits to the normalized changes in SFOAE magnitude increased with increasing probe frequency.

Conclusion

The data suggest that the time of recovery from the effect of the MOCR estimated using SFOAEs increases with increasing probe frequency.

[Supported by NIH grant R01DC010374.]

169 Probing Otoacoustic Emissions in the Budgerigar (*Melopsittacus Undulatus*)

Christopher Bergevin¹, Wei Dong², Laurel Carney³

¹York University, ²Columbia University, ³University of Rochester

Background

Given the complex nature of their vocalizations, birds have become an increasingly attractive model for studying neurophysiological mechanisms underlying the processing of complex sounds. However, much is still unknown about the function of the peripheral auditory system in birds, and there are significant physiological differences between birds and mammals (e.g., hair cell distribution, lower prestin density, structure of the tectorial membrane). The present study explores this issue by characterizing several types of otoacoustic emissions (OAE) in the budgerigar (*Melopsittacus undulatus*).

Methods

Birds were lightly anesthetized using either isoflurane (gas) or ketamine and xylazine (injectable, sub-cutaneous) and were expected to fully recover following the recording session (typically 1-2 h long). Feathers about the external auditory meatus were gently trimmed and the OAE probe was then sealed to the head using vaseline.

Results

While no spontaneous emissions were observed, physiologically-sensitive evoked emissions were readily measurable. Though not thoroughly explored, emissions magnitudes exhibited a degree of sensitivity upon both the depth and type of anesthesia used, consistent with previous reports.

Conclusion

OAEs were confined to the most sensitive regions of the audiogram. Tuning estimates derived from stimulus-frequency OAEs suggest auditory filter bandwidths similar to those of chicken (*Gallus gallus domesticus*). Relative to mammals, distortion-product OAEs exhibited both similarities (e.g., shallow 2f1-f2 DPOAE phase-gradients for larger fixed f2/f1 ratios) and differences (e.g., reduced magnitude fine structure).

Work supported by NIH DC001641.

170 Comparison of MOC Efferent Effects on SFOAEs, DPOAEs and Compound Action Potentials

Maria A. Berezina-Greene^{1,2}, John J. Guinan Jr. ^{2,3}

¹Harvard-MIT HST, *Speech and Hearing Bioscience and Technology Program*, ²Eaton Peabody Laboratories, *Mass Eye & Ear Infirmary, Boston MA USA*, ³Department of

Background

Otoacoustic emissions (OAEs) have been used as a non-invasive way to assess the effects of medial olivocochlear (MOC) efferents in humans and laboratory animals. However, the MOC effect that is relevant for hearing is the inhibition of auditory-nerve (AN) fiber responses. Nonetheless, there has been little work on the relationship between MOC effects on OAEs and neural responses.

Methods

We measured stimulus-frequency OAEs (SFOAEs), distortion-product OAEs (DPOAEs) and AN compound action potentials (CAPs) evoked by tone pips in deeply anesthetized albino guinea pigs. MOC efferent neurons were activated by electrical shocks at the floor of 4th ventricle. DPOAE tones had a frequency ratio of 1.2 with the higher-frequency tone 10 dB SPL above the lower-frequency tone. SFOAEs were separated from the probe sound by taking the difference of the ear-canal sound at the SFOAE frequency with and without a suppressor tone 50 Hz above the probe frequency and 20 dB SPL above the probe level. SFOAE, DPOAE and N1 level functions were measured with and without MOC stimulation. To keep the MOC effects frequency specific, probe tones above 50 dB SPL were not used. The MOC effects for SFOAEs, DPOAEs and CAPs were quantified by the MOC-induced shift to higher levels of the amplitude-level functions. Comparisons of MOC effects on CAP and emissions were done at 5-10 dB above the CAP threshold level. For the vast majority of collected data, this corresponded to 25-35 dB SPL.

Results

Our preliminary results suggest that in animals with good hearing the MOC inhibition of SFOAEs and CAPs are comparable for tones near 7-8 kHz. For tones below 7-8 kHz, the MOC inhibition tended to be larger on CAPs than on SFOAEs. In several animals there were tone frequencies for which the SFOAE amplitude-level and/or phase-level functions were non-monotonic with MOC stimulation and monotonic without MOC stimulation. Preliminary results suggest that the MOC effects on DPOAEs are smaller than MOC effect on SFOAEs and CAPs.

Conclusion

In the mid-frequency region, MOC effects on SFOAEs and on gross neural responses are similar. More work is needed to characterize the relationship outside of this frequency region, and between MOC effect on DPOAEs and CAPs in all frequency regions. Supported by RO1DC00235, P30DC005209. Maria Berezina-Greene is also supported by NSF GRFP.

171 Determination of Primary- And Secondary-Source Components Using Short-Pulse Distortion Product Otoacoustic Emissions

Dennis Zelle¹, Anthony Gummer¹, Ernst Dalhoff¹
¹Tübingen Hearing Research Centre

Background

According to a widely-used model, distortion product otoacoustic emissions (DPOAEs) evolve from interference of a so-called primary- and secondary-source component within the cochlea. The presence of two components can be visualized during the onset of the f₂ primary if signal blocks recorded with suitable primary-phase variations are averaged in the time domain (Whitehead et al., 1996). Recently, we showed that sampling the resulting time signal at an appropriate time instant leads to reliable extraction of the primary-source component (Vetevnik et al., 2009). However, the secondary-source component is not always reliably quantified, especially if both contributions are approximately in phase. Here, we present a new method using short-pulse DPOAEs that enables the quantification of both sources independent of their respective phase.

Methods

DPOAEs were acquired from four subjects with distinctive fine structure. The f₂ tone was pulsed for 8ms, whereas the f₁ tone was presented continuously. The ratio f₂/f₁ was kept constant at 1.2, with f₂ increasing from 1.7kHz to 2kHz in steps of 20Hz. Primary-tone levels were between 25 and 65 dB SPL. For the investigated frequency range, the primary-source component attains its steady state approximately 8–10ms after onset of the f₂ tone, while the secondary-source component is delayed by another 8–10ms. Presenting the f₂ primary with a short pulse of 8ms leads to suppression of the primary-source component during the rise of the secondary-source component. Cancellation of the primary tones and other DPOAE waveforms, except for the cubic component of interest at 2f₁–f₂, was achieved using ensemble averaging with suitable phase shifts between adjacent signal blocks (Whitehead et al., 1996).

Results

DPOAE amplitude and phase responses show considerable differences depending on the relative interference phase, particularly at time instants shortly after the decay of the primary-source component. DPOAE signals with destructive interference show a distinctive notch separating the contributions of the two components and rapid phase jumps close to 180°. A phase variation of 90° indicates the quadrature condition, whereas an invariant phase implies constructive interference. In the latter case, using the short-pulse technique, the size of the secondary source can be detected 16–20ms post-onset.

Conclusion

Short-pulse DPOAEs present a promising approach to separate and quantify the two source components with a single-frequency measurement, thus avoiding the

otherwise necessary acquisition of DPOAEs over a broader frequency range.

172 Insights from a Structural Theory of Pitch: Existence Region, Sound Level Dependence and Discriminability

Jonathan Laudanski^{1,2}, Yi Zheng², Romain Brette²
¹Neurelec, ²Equipe Audition, Ecole Normale Supérieure, Paris

Background

Pitch is a fundamental auditory percept which is perceived by many species and for humans constitutes the basis of melody production. Clearly, what distinguishes sounds with a pitch from other sounds is the temporal regularity of the signal. In other words, sounds with similar period are perceived with similar pitch. However, solely defining pitch as the perceptual correlate of periodicity raises a few discrepancies. Periodic sounds elicit pitch only within a certain domain of existence. There are small but significant level-dependencies of pitch for low frequency pure tones. Finally, although independent of the exact harmonic content (e.g. missing fundamental); the resolvability strongly determines the salience and discriminability of pitch. Here, we propose that pitch is the perceptual correlate of the similarity structure in the vibration pattern of the basilar membrane.

Methods

We use both analytical method and data analysis to study the implications behind the detection of the similarity structure. Analytical derivations are used to obtain an implicit equation linking the phase difference at two basilar membrane locations, the sound level and the estimated pitch. We analyze previously published guinea-pig auditory nerve fibers (ANF) responses to low frequency tones (Palmer and Shackelton 2009) and fit von Mises distribution to the period histogram to obtain an analytical description of the phase probability distribution.

Results

We describe the similarity structure along the basilar membrane by identifying positions whose vibrations are equal but with possible time delay. From this mathematical definition, we derive two types of structure: across channel and within channel similarity. We show that across-channel similarity is only possible for resolved harmonics while within channel similarity is possible for both resolved and unresolved harmonics. In our framework, the maximal delay allowed set the lower limit of perceived pitch and we demonstrate the implications of resolvability on this lower limit. In the case of a pure tone, the pitch shift with level is computed using phase distribution from ANF and compared to results from the psychophysics. Finally, we estimate tone discriminability as a function of F0 using vector strength.

Conclusion

Our work provides new insights into possible mechanisms used for pitch perception.

173 Effect of Efferent Activation on Cochlear Gain and Compression Estimates

Vit Drga¹, Christopher Plack², Ifat Yasin¹
¹University College London, ²University of Manchester

Background

Behavioural and physiological evidence suggests that the amount of gain applied to the basilar membrane may change during the course of acoustic stimulation due to efferent activation of the cochlea (Liberman, 1996). This study used the Fixed Duration Masking Curve (FDMC) method (Yasin et al, 2012) to estimate human cochlear gain and compression, both with and without a precursor sound. In the FDMC method, masker level at threshold for a 10-dB SL, 4-kHz signal is obtained in the presence of an on-frequency (4 kHz) and off-frequency (1.8 kHz) forward masker, as a function of signal duration, with total masker- and signal duration set to 25 ms, and masker-silent interval set to 0 ms. A short-duration masker ensures that accurate estimates of basilar membrane gain and compression can be obtained in the absence of efferent activation. Presentation of a precursor prior to the masker-silent stimulus can be used to infer the time- and level-dependence of the efferent effect.

Previous psychophysical studies examining the decay characteristics of the efferent effect have varied either precursor level or post-precursor delay, but not both together. The present study varies both variables to investigate each separately and also their interaction. The use of the FDMC technique ensures that the effect of the precursor on gain can be measured independently of any masking effects by the precursor. This has been a confound in previous behavioural studies.

Methods

FDMCs were obtained from five listeners with and without a precursor noise (500-ms, 1-kHz wide noise band centered at 4 kHz). The precursor was presented at levels of 20, 40, 60 and 80 dB SPL, with silent intervals between precursor and masker (P-M interval) of 0, 50, 100 and 200 ms. A 2-way ANOVA showed a significant effect for precursor level [$F(3,12) = 14.09$, $p < 0.001$], P-M interval [$F(3,12) = 5.28$, $p = 0.015$] and interaction between precursor level and P-M interval [$F(9,36) = 2.94$, $p = 0.01$].

Results

Estimated gain decreased as precursor level increased, and for a given precursor level, gain increased as the P-M interval increased, consistent with a decay of the efferent effect.

Conclusion

It appears that effect of P-M interval on recovery of gain increases with precursor level.

174 The Effect of Preceding Tones on Frequency Discrimination

Samuel R. Mathias^{1,2}, Christophe Micheyl³, Andrew J. Oxenham³

¹Max Planck Institute for Human Cognitive and Brain Sciences, ²Center for Computational Neuroscience and

Neural Technology, Boston University, ³Department of Psychology, University of Minnesota

Background

Demany and colleagues have suggested that the auditory system contains automatic frequency-shift detectors (FSDs) that bind successive sounds together. These hypothetical units appear to be tuned to optimally detect frequency shifts of around 1.5 semitones. The present work details six experiments that may provide more evidence for the existence of FSDs.

Methods

All the experiments used the same basic procedure. Each trial contained a sequence of three pure tones, referred to as (from earliest to latest) the 'precursor', the 'standard', and the 'test' tones. Listeners discriminated frequency shifts between the standard and the test tones (Δ_2); the directions of these shifts were randomly upward or downward, and their magnitudes were fixed to the same point on each listener's psychometric function. Listeners were told to always ignore the frequency shifts between the precursor and the standard tones (Δ_1), whose values ranged from 0 to 9 semitones, and whose direction on each trial was independent of the direction of Δ_2 . Sensitivity (d') and bias (c) were measured as a function of Δ_1 .

Results

In almost all conditions and experiments, there was a consistent nonmonotonic relationship between d' and Δ_1 . Sensitivity declined as a function of increasing Δ_1 up to approximately 1.5 semitones, and further increases in Δ_1 increased sensitivity. The 'dip' in d' when Δ_1 equaled 1.5 semitones was observed even though the precursor and the standard tones were separated by a 500-ms interval, meaning that the results are unlikely to be caused by masking. The dip was observed when listeners judged the direction of frequency shifts and when they simply detected frequency shifts. Neither altering the timbre nor the perceived spatial location of the precursor tones so that they sounded perceptually dissimilar to the remaining tones removed the dip. The dip was not influenced by whether the frequency of the standard tone was roved or fixed over trials, nor by whether the value of Δ_1 was random or blocked for 100 sequential trials. The relationship between c and Δ_1 was less consistent across listeners and across experiments.

Conclusion

FSDs provide a convenient explanation for the present results if one assumes that (a) listeners discriminate small frequency shifts using FSDs, and (b) FSDs were activated—and consequently fatigued by—the irrelevant frequency shift on each trial. Thus, maximal fatigue would have occurred on trials in which Δ_1 equaled 1.5 semitones. [Work supported by NIH R01 DC05216]

175 Neural Correlates of Auditory Streaming in the Human Brainstem

Shinpei Yamagishi¹, Takanori Ashihara¹, Sho Otsuka², Shigeto Furukawa³, Makio Kashino^{1,3}

¹Tokyo Institute of Technology, ²The University of Tokyo,

³NTT Communication Science Laboratories

Background

Neural correlates of auditory streaming have been reported both in subcortical and cortical sites. However, convincing evidence for neural correlates of streaming in the human brainstem is still limited. Here, we examined the correlation between the auditory brainstem frequency-following response (FFR) and behavioral reports of perceived streaming for a prolonged exposure to a repeated acoustic pattern that may evoke perceptual bistability between a single coherent stream and two segregated streams.

Methods

The stimulus was a repeated triplet-tone sequence (ABA-ABA-...; A: 315-Hz tone, B: 400-Hz tone, -: silence). The duration of each tone was 50 ms, which included rising and falling cosine ramps of 10 ms. The duration of silence was 60 ms. The frequency difference between A and B tones was four semitones. Fifteen normal-hearing adults aged 19 - 34 participated in the experiment. The experiment consisted of 48 sessions. In each session, participants were presented with 200 repetitions of ABA-triplets. While listening, they pressed a button corresponding to one-stream or two-stream percepts whenever they experienced perceptual switching. At the same time, the FFR was recorded using a vertical one-channel electrode montage. The electrode placements were Cz (active), ipsilateral earlobe (reference), and forehead (ground). The recorded FFR was segmented at every onset of ABA- triplets and classified according to behavioral reports (one-stream or two-stream), then averaged within each perceptual category. The results were evaluated in terms of the amplitude of the average FFR at the stimulus frequencies. The phase locking value (PLV) was also examined. To derive the PLV of a given tone, first, the difference between fourier-transformed stimuli and corresponding FFR was computed for each tone presentation and expressed as an unit vector on the complex plane. Then, the PLV was determined as the length of the vector average across presentations.

Results

The averaged FFR amplitude and PLV to the second A tone (A2) in the triplet were significantly smaller for one-stream than two-stream percepts. For other tones, no significant change was observed between one-stream and two-stream percepts. Moreover, when participants perceived one stream, the averaged FFR amplitude and PLV to A2 were significantly smaller than those to A1. When participants perceived two streams, these differences were not significant.

Conclusion

The results demonstrated significant changes in the FFR according to perceived streaming for the physically constant stimulation, indicating neural correlates of auditory streaming in the human brainstem.

176 Effect of Phase Curvature on Forward and Backward Masking: Evidence Against Efferent Activation

John Deeks¹, Sheila Flanagan¹, Robert Carlyon¹
¹Medical Research Council

Background

Carlyon and Datta (1997) measured forward masking of a 1-kHz signal by Schroeder-phase harmonic complexes. The positive Schroeder-phase masker caused the auditory filter centred on 1-kHz to have a highly modulated output and produced less masking than a negative Schroeder-phase masker, which produced an output with a flatter envelope. This was attributed to fast-acting compression in the auditory system attenuating the peaks of the more modulated auditory filter output. Wojtack and Oxenham (2009) obtained similar results for a 1-kHz signal frequency (f_s) with masker components between 400-1600 Hz, but no phase effect when the masker components were all below f_s . They attributed this to the portion of the basilar membrane tuned to 1-kHz responding linearly to the off-frequency masker. However, for $f_s=6$ -kHz, a masker phase effect was observed for masker components below f_s . They suggested that this off-frequency masker may cause the efferent system to attenuate the response to the 6-kHz probe.

Methods

Experiment 1 replicated Wojtack and Oxenham main findings. For $f_s=1$ -kHz the forward masker contained consecutive equal-amplitude harmonics of 100 Hz: 400–1600 Hz (on-frequency) or 100–600 Hz (off-frequency). The phase of the n th harmonic equalled $C\pi n(n-1)/N$ where $C=-1$ or 1 . For $f_s=6$ -kHz the on- and off-frequency maskers spanned 4800-7200 Hz and 1600-4000 Hz, respectively. C was -1 or 0 . Experiment 2 measured backward masking for $f_s=6$ -kHz with the off-frequency masker.

Results

For Experiment 1, on-frequency maskers showed phase effects at both f_s , while off-frequency maskers showed a phase effect only with $f_s=6$ kHz. For Experiment 2 a substantial phase effect was observed for most listeners, and, across all six listeners tested, the size of this effect correlated highly significantly with that in the analogous forward masking condition ($r=0.97, p<0.001$). A control forward-masking experiment with a long masker-signal gap showed no masking, ruling out the possibility that, in experiment 2, the backward masker in one interval affected detection of the signal in the previous interval.

Conclusion

The results of both experiments are consistent with fast-acting compression in the auditory system reducing the 'effective level' of stimuli that produce 'peaky' auditory filter

outputs. The 1-kHz data are consistent with compression rising entirely in outer-hair-cells, while the phase effect observed for $f_s=6$ -kHz and off-frequency maskers suggest an additional effect (possibly compression in inner-hair-cells, auditory nerve fibres or brainstem). Experiment 2 showed that phase effects with off-frequency maskers are not caused by efferent activation, which cannot act retrospectively.

177 The Effect of Cochlear Nonlinearities on Binaural Masking Level Differences

Nicolas Le Goff¹, Armin Kohlrausch^{2,3}
¹Technical University of Denmark, ²Philips Research Europe, ³Eindhoven University of Technology

Background

The binaural masking level difference (BMLD) has been shown to be constant (10–15dB) for masker spectrum levels from 70dB/Hz down to 30–40dB/Hz and to gradually decrease with lower levels (McFadden, 1968; Hall and Harvey, 1984). The decrease at low levels was larger in an asymmetric condition where the masker was attenuated in only one ear. McFadden predicted the data by assuming that an external and an internal noise would interaurally decorrelate the internal representations of the stimuli. In the present study, the role of nonlinear cochlear processing and asymmetric masker level on the BMLD was investigated using an equalization–cancellation (EC) based binaural model framework.

Methods

The BMLD was measured for 500-Hz target tones presented in 3-kHz-wide maskers. BMLDs were obtained as a function of masker level in one symmetric and two asymmetric masker conditions: (i) NoS π : thresholds were measured for masker spectrum levels between 50 and -10dB/Hz, with the same level at both ears; (ii) No'S π '50: same as first condition but the masker was attenuated in one ear only and fixed at 50dB/Hz in the non-attenuated ear; (iii) No'SII'20: same as second condition but with a masker level of 20dB/Hz in the non-attenuated ear. An EC based binaural model with a frontend including nonlinear peripheral processing (Jepsen et al., 2011) was used to predict these results.

Results

The BMLD obtained in the No'S π '50 condition was smaller than that obtained in the NoS π condition at all masker levels between 50 and -10dB/Hz. The difference in BMLD between the two conditions gradually increased with decreasing masker level from 50 to 20dB/Hz and remained constant between 20 and -10dB/Hz. The proposed model could account for these data. A model analysis suggested that the increase in BMLD difference between the No'S π '50 and NoS π conditions results from a decrease in interaural correlation at the output of the periphery, and is a consequence of the cochlear nonlinearity at levels between 20 and 50dB/Hz. For levels below 20dB/Hz, cochlear processing becomes linear and the model predicts that the difference in BMLD between the

symmetric and the two asymmetric conditions is constant, in line with the experimental data.

Conclusion

A model was proposed to account for the effect of level asymmetry on BMLD. The modeling results suggest that cochlear nonlinearities affect the analysis of binaural cues at higher processing stages such that signals carrying interaural level differences can become interaurally decorrelated.

178 The Audiogram Fails to Reveal Deficits from Significant Inner Hair Cell Loss in Chinchillas Treated with Carboplatin

Edward Lobarinas¹, Richard Savli², Karlee Maerten¹, Dalian Ding²

¹University of Florida, ²University at Buffalo

Background

The audiogram is the most widely used clinical measure of hearing. It has been useful in detecting and describing acquired hearing loss as a consequence of ageing, a history of noise exposure, otologic disease and/or exposure to ototoxic drugs that preferentially damage the outer hair cells of the inner ear. These hearing losses lead to increased thresholds and poorer tuning. In contrast, despite their extensive innervation of afferent auditory nerve fibers (>90%), little is known about how loss of inner hair cells impacts auditory perception and it is not clear if the audiogram is useful in detecting sensory deficits associated with selective inner hair cell loss. Previous physiological studies in chinchillas with carboplatin induced selective inner hair cell loss suggest reduced compound action potentials at the level of the cochlea but near normal potentials at the inferior colliculus and auditory cortex. The purpose of the present study was to determine if the audiogram could reveal deficits associated with carboplatin induced inner hair cell loss in the chinchilla.

Methods

To determine if selective inner hair cell loss impacts the audiogram, chinchillas were first trained to respond to tonebursts across a broad frequency range (250-11,300 Hz) using an established avoidance paradigm. Subjects were then treated with a single 75 mg/kg dose of carboplatin, a dose known to induce 30-90% inner hair cell loss and reevaluated. Finally subjects were sacrificed and the extent and pattern of inner hair cell loss was correlated with post-carboplatin audiometric data.

Results

Chinchillas treated with carboplatin showed selective inner hair cell loss of 30-90%; results consistent with previous reports. Relatively large lesions (>80%) were needed before a significant threshold shift could be observed. However, this effect was only evident at the higher frequencies with lower frequencies showing no changes and was present in about half the animals.

Conclusion

These data suggest that audiometric threshold assessment does not reveal the presence of inner hair cell lesions even when these extend over a large region of the cochlea. We suggest that conventional audiometry is likely insensitive to inner hair cell loss in humans as well. Only small populations of inner hair cells appear to be necessary for detecting tone stimuli in a quiet background.

179 Auditory Filter Bandwidths in the Common Marmoset (*Callithrix jacchus*)

Michael Osmanski¹, Xiaoqin Wang¹

¹Johns Hopkins University School of Medicine

Background

The common marmoset has emerged as a promising non-human primate model in auditory neuroscience. However, a full appreciation of the physiological response to sound will require a basic understanding of auditory perception and behavioral sensitivity in this species, including measures of auditory frequency selectivity.

Methods

We measured frequency selectivity in marmosets by estimating auditory filter bandwidths using a psychophysical task in which tone thresholds were measured as a function of notched noise masker bandwidth. The resultant threshold data was used to estimate the auditory filter equivalent rectangular bandwidths (ERBs) using procedures originally developed for human subjects. We tested five different frequencies spanning much of the hearing range of this species (250 Hz, 500 Hz, 1000 Hz, 7000 Hz, and 16000 Hz).

Results

Marmosets have ERBs that are generally comparable to those measured in other mammalian species, although ERBs in marmosets tend to be wider than those measured in humans. This was true for all frequencies tested except 7000 Hz, where marmoset filter bandwidths are narrower than those measured in humans. Wider bandwidths likely means that, at most of the frequencies tested here, marmosets have poorer spectral resolution compared to humans. Narrower filter bandwidths at 7000 Hz probably reflects the fact that this is approximately the frequency of best hearing in this species and also the frequency around which most of the spectral energy in marmoset vocalizations is concentrated.

Conclusion

Differences in the size of human and marmoset filter bandwidths may reflect a series of tradeoffs between basilar membrane length (which is half that measured in humans), hearing range (which extends about 10 kHz higher than in humans), and the need to process species-specific communication signals centered in a particular range of frequencies. [Research supported by NIH grants DC003180, DC005808]

180 Hcn1 Null Mutant Mice Show Delays in Processing Sounds on Time Scales from 1 Ms to Over 2 Seconds in Tasks That Provide Animal Models for Speech Encoding, Temporal Summation, and Forward Masking

James Ison¹, Paul Allen², Donata Oertel³
¹U. Rochester, ²U. Rochester, ³U. Wisconsin

Background

In vitro studies of auditory brainstem neurons demonstrate that their precise timing depends on a low input resistance that gives them a short time constant (Oertel, 1983), and that this feature depends in part on a hyperpolarization-activated, mixed cation conductance (gh) in channels that contain Hcn1 subunits (Cao & Oertel, 2011; Kopp-Scheinpflug et al. 2011).

Methods

Here we examine the functional significance of this conductance in behavioral comparisons of Hcn1 +/+ mice (n = 63) and Hcn1 -/- mice (n = 60) using standard startle reflex (ASR) modification measures to determine: (1) their threshold for gap detection; (2) temporal summation of near-response-threshold tone pips; and (3) the rate of recovery from (a) suprathreshold gaps and (b) from suprathreshold noise bursts in a refractory paradigm. We measured also their ABR thresholds and suprathreshold amplitudes.

Results

Gap detection thresholds were delayed by 1 ms in -/- mice, but they had higher and more persistent response suppression from suprathreshold gaps than +/+ mice: the between group difference began at a 30 ms interval after the gap and lasted for over 100 ms. The peak of 2-pulse temporal summation was delayed in -/- mice from 2 to 3 ms, with +/+ mice responding more at short delays but less at longer delays of 3 to 4 ms. The refractory (suppressive) effect of one startle stimulus on the response to the second stimulus was more persistent in -/- mice, with the groups being different at 1 and 2 second recovery times, but not at 4 seconds. ABR thresholds in young adults (median age ~ 60 PND) were equal up to 24 kHz, but -/- mice showed a hearing loss of ~20 dB at 32 and 48 kHz. P1 for clicks had near identical latencies (means of 1.46 and 1.43 ms), but the -/- mice had smaller P1 amplitudes (and also a smaller baseline ASR). The -/- mice also had a significantly smaller peak amplitude about 1 ms after P1 but higher levels of asynchronous activity beyond 4 ms.

Conclusion

These in vivo behavioral and electrophysiological findings extend the in vitro data in showing that the Hcn1 gene contributes to temporal processing for complex auditory stimuli, but in addition, that it must contribute also to very high frequency hearing.

181 Physiologically-Based Envelope Cues for Diotic and Dichotic Tone-In-Noise Detection

Junwen Mao¹, Laurel H. Carney¹
¹University of Rochester

Background

The goal of studying masked detection is to understand what cues listeners use to detect signals in noise. Envelope cues derived from the stimulus predict detection performance successfully for both diotic and dichotic conditions. Here, it was hypothesized that predictions of detection performance based on envelope cues derived from physiological models would be similar to predictions using stimulus-based envelope cues.

Methods

500-Hz tones of 300-ms duration were detected in 300-ms narrowband and wideband reproducible Gaussian noises. Model predictions of the variance in detection performance across a set of reproducible noise waveforms were computed for both diotic and dichotic conditions.

The stimulus-based envelope cue for the diotic condition was computed from a modified envelope-slope (ES; Richards, 1992, JASA 91:3424; Davidson, *et al.*, 2006 JASA 119:2258) model. A bandpass filter extracted the 40 to 140 Hz envelope frequency range, which contained the most information about tone presence. For the dichotic condition, the slope of the interaural envelope difference (SIED) model, which examined the difference between the envelopes at the two ears, was used to predict listeners' detection performance.

For the physiologically-based envelope models, the stimulus was passed through a human version of the auditory-nerve (AN) model (Zilany *et al.*, 2009, JASA 126:2390; Ibrahim and Bruce, 2010, *The Neurophysiological Bases of Auditory Perception*, pp. 429) to obtain the synaptic response. Model AN responses were used as inputs to a same-frequency inhibition and excitation model for the cochlear nucleus (Nelson and Carney, 2004, JASA 116:2173). A bandpass modulation filter simulated an amplitude-modulation tuned inferior colliculus (IC) cell. Envelope-slope information was calculated as the derivative of the modulation filter response. The model decision variable was the integral of envelope slope over time.

Results

For the diotic condition, predictions based on the model IC response were similar to those of the modified ES model. For the dichotic condition, predictions based on binaural physiological envelope cues were similar to those of the SIED model. Moreover, for the dichotic wideband waveforms, predictions from both the stimulus-based and physiological envelope models were better than those of other dichotic models.

Conclusion

Physiological models for processing envelope cues predicted a similar amount of the variance in both diotic and dichotic detection performance as the stimulus-based

envelope cues. Thus, known physiological mechanisms are feasible for extracting and using monaural and binaural envelope cues for detection.

[Support: NIH DC010813]

182 Discrimination of Partial USVs by CBA/CaJ Mice

David Holfoth¹, Erikson Neilans¹, Michael Dygert¹, Micheal Dent¹

¹University at Buffalo, SUNY

Background

Mice are a commonly used model in hearing research, yet little is known about how they perceive their own ultrasonic vocalizations (USVs). Recent studies illustrate that mice are poor at discriminating between some of these vocalizations (Neilans et al. ARO 2013 abstract). For example, discrimination accuracy in mice is low for calls that are reversed in time, which is surprising when compared to similar studies in humans and other animals. This leads to the question of how much information the mice need from their calls in order to identify them and which portions of the USVs are most important for recognition. To answer these questions, the present study looks at how well mice can discriminate targets containing small portions of a call from a repeating background containing the whole call. Based on human and bird studies, we hypothesized that discrimination performance would be higher as more of the call was deleted, and that there would be an asymmetry in discrimination abilities depending on whether the beginning or the end of the call was omitted.

Methods

CBA/CaJ mice were trained and tested in a discrimination task using operant conditioning procedures. The mice were required to discriminate target stimuli from a background call to receive water/chocolate milk reinforcement. The target stimuli were incomplete versions of the repeating background stimulus, containing either one-third (initial third, middle third, and last third) or two-thirds (initial two-thirds, last two-thirds, and middle third removed) of the whole call. The first twenty responses for each target stimulus were recorded and analyzed.

Results

The discrimination results show that performance was very low for all targets. Discrimination accuracy did not improve with decreasing durations (two-thirds versus one-third), and results were similar across every partial-USV target. The mice could not discriminate small portions of the calls from the whole call.

Conclusion

The current results suggest that different portions of the call do not contain any more information than other portions of the call, contrasting with past results from humans and birds. This indicates that mice maybe perceiving their vocalizations differently from humans and birds. However, these calls are in the ultrasonic range and

are shorter in duration than any human or bird vocalizations and thus may be difficult to compare.

183 Enhancement and Suppression Estimated from Growth of Masking Functions

Erica L. Hegland¹, Elizabeth A. Strickland¹

¹Purdue University

Background

Threshold for a signal in a simultaneous masker may decrease when the signal is delayed from masker onset or when a precursor is added. When the masker has energy at the signal frequency, the results have been modeled as a decrease in cochlear gain, which could be consistent with the medial olivocochlear reflex (MOCR). When the masker lacks energy at the signal frequency, the results are consistent with a decrease in suppression, but this has not been directly demonstrated. One way to estimate suppression is to compare thresholds for a signal in simultaneous and forward masking using a masker that is approximately an octave below the signal frequency. Because the masker response at the signal place should be linear, the difference in thresholds between the two conditions yields the amount of suppression of the signal in dB. In the present experiment, enhancement and suppression were measured from the same data.

Methods

Ten subjects with normal hearing were tested. The signal was 4 kHz and 6 ms in duration. Maskers were narrowband noise centered at 2.4 kHz (off-frequency) and 4 kHz (on-frequency). Growth of masking functions were measured with masker level fixed and signal level varied. In the baseline condition, the masker duration was 20 ms. The signal immediately followed the masker or was presented in the center of the masker. For the comparison condition, the duration of the simultaneous masker was lengthened by 40 ms prior to signal onset, or a separate, fixed-level precursor was presented immediately before the masker.

Results

Enhancement was calculated for a fixed masker level as the difference in signal threshold for the short simultaneous masker and the long simultaneous masker or the precursor + masker. To calculate suppression, the masker level necessary to mask a fixed signal level was estimated from the data. Suppression was calculated as the masker level in the forward masking condition minus threshold in the simultaneous masking conditions. Suppression was greatest for the short masker and decreased in the long masker or the precursor + masker conditions. The amount of enhancement depended on the amount of decrease in suppression and the slope of the input/output function in the region of the signal level.

Conclusion

Results suggest that for these conditions, enhancement is consistent with a decrease in suppression coupled with the effects of compression.

184 Survival and Integration of Mouse Inner Ear Progenitor/stem Cells in the Cochleas of Hearing-Impaired Guinea Pigs

Luiz Barboza Jr¹, Karina Lezirovitz¹, Daniela Zanatta¹, Bryan Strauss¹, Regina Mingroni-Netto¹, Jeanne Oiticica¹, Luciana Haddad¹, Ricardo Bento¹

¹*Universidade De São Paulo*

Background

In mammals, damage to the sensory receptor cells (hair cells) of the inner ear results in permanent sensorineural hearing loss. Here, we investigate whether postnatal mouse inner ear progenitor/stem cells (mIESCs) can survive and integrate after transplantation into the basal turns of neomycin-injured guinea pig cochleas. We also studied the potential effects of the cell transplantation on auditory function.

Methods

Eight adult guinea pigs were deafened by intratympanic neomycin delivery. After 7 days, the animals were randomly divided in two groups. The study group (n=4) received a transplantation of 1 X 10⁵ LacZ-positive mIESCs in culture media to the scala tympani. The control group (n=4) received culture media only. Fourteen days after the transplantation, functional analyses were performed by auditory brainstem response (ABR) measurement, and the animals were sacrificed. The presence and distribution of mIESCs were evaluated by immunohistochemistry of longitudinal sections of the cochlea from the study group. Non-parametric tests were used for statistical analysis of the data.

Results

Intratympanic neomycin delivery damaged hair cells and increased auditory thresholds prior to cell transplantation. There were no significant differences between auditory brainstem thresholds before and after transplantation in individual guinea pigs. Some mIESCs were observed in all scalae of the basal turns of the injured cochleas, and a proportion of those cells expressed the hair cell marker myosin VIIa. Some transplanted mIESCs integrated in the cochlear basilar membrane. There was no evidence of inflammatory infiltration in any of the guinea pigs' cochleas.

Conclusion

Although mIESC implantation resulted in no obvious effect on auditory thresholds, our experiments demonstrated the survival, migration, integration and expression of a hair cell marker in transplanted cells.

185 Treatment for Connexin30 Deletion Associated Hearing Loss Utilizing Otocyst Trans Uterine Gene Transfer in Mice

Toru Miwa¹, Ryosei Minoda¹, Takao Yamada¹

¹*Department of Otolaryngology-Head and Neck Surgery, Kumamoto University, Japan*

Background

Mutation in gap junction beta-6 (GJB6), the gene that codes for Connexin30 (Cx30), causes hereditary deafness in humans and mice. In our previous study, we show that electroporation-mediated transfection of Cx30-targeted shRNA (shRNA-Cx30) into the normal mouse otocyst induced the knockdown of endogenous Cx30 in the cochlea, lack of endocochlear potential (EP) and severe hearing impairment. Now then, we investigated whether trans-uterine gene transfer therapy could cure hearing loss in Cx30 knockout mice.

Methods

At embryonic day 11.5 (E11.5), EGFP-fused Cx30 plasmid vector was microinjected through the uterus into the otic vesicle of Cx30 knockout mice and electroporated. Electroporated embryos were delivered at E18.5. Some fetuses were removed to prepare frozen sections, and some fetuses were raised by surrogate mothers until functional and morphological assessments on postnatal day 30 (P30). An auditory brainstem response (ABR), endocochlear potential (EP), immunohistology were used for the assessments. As a control, EGFP plasmid was used.

Results

Immunohistological analyses revealed that Cx30-positive cells were detected in the medial walls, the prosensory lesions, the lateral walls and the spiral ganglions at E18.5; they were detected in the spiral limbus, organs of Corti, stria vascularis, spiral ligaments and spiral ganglions in the treated ears at P30. There was no Cx30 expression in the non-treated right ears. The treated side ears exhibited significant amelioration of the auditory threshold compared with the non-treated right ears. (n=4, p<0.02). The treated ears showed normal EPs (n=2).

Conclusion

Cx30-deficient homozygous mice exhibit severely impaired hearing and lack endocochlear potentials. Trans-uterine transfer of normal Cx30 genes into the otocysts of Cx30 - deficient homozygous mice reversed the downregulation of Cx30 in the cochleae, and thereby restored their auditory functioning. Trans-uterine gene transfer into the otocyst is a novel treatment for genetic hearing loss.

186 Combined Expression of MicroRNAs and Transcription Factors for Promoting Hair Cell Differentiation

Prashanth Sripal¹, Jason Pecka¹, Timothy Hallman¹, Kirk Beisel¹, Garrett Soukup¹

¹Creighton University

Background

Damage to mechanosensory hair cells (HCs) of the inner ear causes permanent hearing loss in millions of people each year. Although some vertebrate species can regenerate HCs, human auditory HCs lack regenerative capacity. An emerging paradigm in regenerative strategies is to utilize a combination of crucial factors to achieve cell reprogramming. The transcription factor (TF) Atoh1 is indisputably required for HC development and represents the standard for regenerative strategies. However, microRNAs (miRNAs) post-transcriptionally regulate gene expression and are also required for HC differentiation and maintenance. These include miRNA-183 family members miR-183, miR-96, and miR-182. Additionally, other TFs including Pou4f3 and Gfi1 are necessary for hair cell differentiation and survival. Our objective is to apply a combination of these crucial factors to hair cell generation.

Methods

To determine whether a combination of miRNAs and TFs can generate HCs more effectively than Atoh1 alone, we have developed a novel vector for expression of miRNAs and multiple TFs from a single transcript. The transcript produces miR-183 family members from an intron, and individual TFs (Atoh1, Pou4f3, and Gfi1) and red fluorescent protein (RFP) from a single open reading frame by ribosomal cleavage of intervening viral peptide elements. This parent construct was used to generate a series that contain different combinations of factors, and certain constructs were converted to adenovirus vectors (AdVs) for gene delivery. miRNA and protein expression was examined in mouse otic precursor cells (IMO-2B1) by quantitative PCR (qPCR) and fluorescence microscopy. AdVs were used to infect mouse induced pluripotent stem cells (iPSCs), and development of HC-like morphology was assessed by fluorescence microscopy.

Results

Elevated expression of miR-183 family members in IMO-2B1 cells was observed by two different qPCR methods for mature miRNA detection. RFP expression in IMO-2B1 cells observed by fluorescence microscopy is indicative of factor expression given that RFP is produced from the final open reading frame of each construct. However, vectors encoding more factors yielded less RFP expression than those with fewer factors. Preliminary assessment of AdV effects on iPSCs using f-actin staining showed that the combination of miR-183 family and Atoh1 produced morphologically HC-like cells. In comparison, Atoh1 alone marginally affected iPSC cytomorphology.

Conclusion

Preliminary results suggest that combining HC-specific miRNAs and TFs provides a more effective means for cell

reprogramming and HC differentiation that might be useful in therapeutic strategies for HC repair and regeneration.

187 Development of Acoustic Sensor for Wide-Range Frequency Selectivity Using Non-Uniform Thick Ladder-Like BAM

Takayuki Kobayashi¹, Takayuki Nakagawa², Juichi Ito², Satoyuki Kawano¹

¹Graduate School of Engineering Science, Osaka University, ²Graduate School of Medicine, Kyoto University

Background

The basilar membrane in a cochlea has an important role to realize the frequency selectivity. In previous study [1], the authors developed a bionic auditory membrane (BAM) which mimics cochlear functions and proposed to use it as a sound processor. Although the basic applicability of the BAM was confirmed, the frequency range in which the BAM could work was narrower than the human audible range. One of the reasons is the uniform thickness of the BAM, though the thickness of the basilar membrane is varied by location. Therefore, we have newly developed a non-uniform thick ladder-like BAM. While the previous BAM has a trapezoidal membrane structure, the device is designed as an array of beams.

Methods

The non-uniform thick BAM was fabricated by the grayscale lithography based on MEMS (microelectromechanical systems) processes. The vibration characteristics of the BAM in air was measured as a preliminary experiment and evaluated the efficiency of the thickness change. The vibrations of beams were measured by laser Doppler vibrometer. Since the cochlea is filled with lymph fluids, the vibration characteristics of the BAM immersed in liquids were also measured. Here, the BAM was fixed in a liquid filled channel and the acoustic waves were applied by a piezoelectric actuator.

Results

The BAM consists of 64 micro beams and the thicknesses are successfully changed from 3.02 μm to 139 μm . The length and the width of beams are also changed from 750 μm to 1500 μm and from 50 μm to 600 μm , respectively. The frequency range is quantitatively evaluated using the ratio $f_{\text{max}}/f_{\text{min}}$ between the maximum first mode resonant frequency f_{max} and the minimum one f_{min} . The range in the non-uniform thick BAM is 10.9 times wider than that in the uniform one, indicating the successful control of the frequency range by the thickness change. The result in liquid shows that the resonant frequency is decreased by the fluid-structure interaction compared with that in air. From this effect, the ratio in liquid is 3.13 times larger than that in air.

Conclusion

Although the resonant frequency of the BAM is still higher than the human audibility, these experimental results prove the feasibility of the new BAM as an acoustic sensor which can work over the full range of the human audible frequency.

[1] T. Inaoka *et al.*, Proc. Natl. Acad. Sci. USA, Vol. 108, No. 45 (2011), pp. 18390-18395

188 Development of a Selective Hair Cell-Spiral Ganglion Neuron Double Ablation Model to Study Cochlear Implantation in Combination with Stem Cells

Leila Abbas¹, Marcelo N. Rivolta¹

¹Centre for Stem Cell Biology and Department of Biomedical Sciences, University of Sheffield, UK

Background

Animal models that resemble lesions observed in clinical conditions are of great value to explore future therapies. We are interested in developing the potential applications of stem cells for the treatment of hearing loss, particularly in combination with cochlear implants. We have previously employed the gerbil auditory neuropathy model developed by Lang *et al.* (JARO 6; 63-74, 2005) to study the ability of hESC-derived otic neuroprogenitors (hONPs) to repopulate the damaged spiral ganglion and to restore auditory function. After topical application of ouabain to the round window, permanent auditory neuron degeneration is induced, leading to a rise of ABR thresholds in response to click and tone stimuli. After an infusion of hONPs into the modiolus, we have evidence that the transplanted cells can graft and differentiate into bipolar, β III-tubulin positive neurons which contact the hair cells and project to the brainstem. Moreover, we have obtained a significant improvement in the mean auditory thresholds. This model shows preservation of the DPOAE responses, demonstrating that the hair cells remain intact.

Methods

We are currently exploring a 'double ablation' model, in which aminoglycoside antibiotics are used to abrogate hair cells alongside the ouabain-induced neuropathy. We have explored several paradigms of aminoglycoside application, with variable degrees of success.

Results

On one hand, application of gentamicin or kanamycin directly to the round window, or systemic kanamycin followed by the diuretic bumetanide does not induce hair cell loss. Alternatively, the combined application of kanamycin and furosemide is very effective in killing the hair cells, substantially raising ABR thresholds. In this condition however, the spiral ganglion neurons are preserved even months after aminoglycoside application, resembling the variable preservation of neurons after hair cell damage observed in humans.

Conclusion

The ability to damage selectively hair cells or neurons adds flexibility to a model system for studying stem cell transplantation. Moreover, the combined application of aminoglycosides and ouabain should prove ideal to study the effects of a fully-implantable, cochlear stimulator to substitute for hair cell function combined with the stem cell-replacement of spiral ganglion neurons, thus facilitating the

application of cochlear implants to a broader range of patients.

189 Partial Regeneration Following Cisplatin Ototoxicity in Zebrafish Lateral Line

Alisa Genualdi¹, Mark Warchol¹

¹Washington University School of Medicine

Background

Cisplatin is a chemotherapeutic agent that is used to treat a variety of solid tumors. Ototoxicity is a frequent side effect, often resulting in permanent sensorineural hearing loss. Nonmammalian vertebrates are capable of regenerating hair cells after aminoglycoside injury, but the avian ear cannot regenerate after cisplatin ototoxicity (EL Slattery, ME Warchol, J Neurosci, 2010). The current study analyzed hair cell death and regeneration in the zebrafish lateral line after cisplatin administration.

Methods

Zebrafish larvae (5 days post-fertilization) were treated for 4 hours in 1000 μ M cisplatin and then allowed to recover for 1-10 days. Other fish were exposed to cisplatin, followed by treatment for 24-72 hours with the γ -secretase inhibitor DAPT (50 μ M). After fixation, specimens were immunolabeled for HCS-1, in order to identify hair cells. Hair cells were quantified from 10 individual neuromasts along the posterior lateral line of each fish.

Results

We first examined hair cell numbers within three specified neuromasts evenly distributed along the length of the posterior lateral line. We found that neuromasts of unexposed (control) fish contained 9.3 ± 3.4 HC/neuromast. However, at 1 day after cisplatin exposure, hair cell numbers had decreased, to 1.7 ± 0.5 HC/neuromast. Quantification of hair cells numbers at 10 days after cisplatin revealed that neuromasts now contained 5.5 ± 3.0 HC's ($p < 0.0001$). Treatment with DAPT for 72 hours after cisplatin exposure resulted in only a very slight increase in hair cell numbers, compared to controls.

Conclusion

Consistent with previous studies (e.g. H Ou *et al.*, Hearing Res, 2007), our data indicate that treatment for 4 hours in 1000 μ M cisplatin results in the death of most hair cells within neuromasts of the posterior lateral line. Additionally, our data show that the zebrafish lateral line can regenerate hair cells after cisplatin ototoxicity. Previous studies of regeneration after aminoglycoside ototoxicity (e.g., JA Harris *et al.*, JARO, 2003; EY Ma *et al.*, J Neurosci, 2007) indicate that hair cell recovery is complete within three days of injury. However, our data show that regeneration after cisplatin ototoxicity is still incomplete after 10 days recovery. In addition, inhibition of Notch signaling (via treatment with DAPT) does not result in a substantial increase in hair cell numbers. Since hair cell regeneration is mediated by epithelial supporting cells, our observations suggest that cisplatin may have toxic effects on both hair cells and supporting cells.

190 Hearing Improvement by Gene Therapy in a Mouse Model Created by a Conditional Knockout of *Gjb2* Gene

Takashi Iizuka¹, Hideki Mochizuki², Tomoko Nihira³, Ayako Inoshita¹, Yoshinobu Kidokoro¹, Takeshi Nara⁴, Kazusaku Kamiya¹, Osamu Minowa⁵, Tetsuo Noda⁶, Katsuhisa Ikeda¹

¹Department of Otorhinolaryngology, Juntendo University Faculty of Medicine, Tokyo, ²Department of neurology, Osaka University Graduate School of Medicine, Osaka, ³Department of Neurology, School of Allied Health Sciences, Kitasato University, Sagami-hara, ⁴Department of Molecular and Cellular Parasitology, Juntendo University Faculty of Medicine, Tokyo, ⁵Mouse Functional Genomics Research Group, Riken, Yokohama, ⁶Department of Molecular Biology, Cancer Institute, Tokyo

Background

Hereditary deafness affects about 1 in 2,000 children and mutations in the *GJB2* gene, coding the gap junction, are the major causes in various ethnic groups, which require normal gene transfer in the early developmental stage to prevent deafness. Mice present an ideal model for inner ear gene therapy because their genome is being rapidly sequenced and their generation time is short. In order to establish the fundamental therapy of congenital deafness, we generated targeted disruption of mouse *Gjb2* gene using Cre recombinase controlled by P0. Using this animal model, we examined the potential of gene therapy in the inner ear, using the homozygous mutant mice and the heterozygous mutant mice.

Methods

Adeno-associated virus vectors (AAV) carrying *Gjb2* gene were injected into the scala tympani through the round window of the cochlea of the homozygous mutant adult and neonatal mice.

Results

In the adult mice, the expression of Cx26 was observed in the fibrocytes of the spiral ligament and spiral limbus, but was not seen in the supporting cells and failed to improve the hearing ability. However, in the neonatal mice, the expression of Cx26 was seen in the supporting cells and the hearing ability was improved. In the histological analysis, the organs of Corti of the homozygous mutant mice injected AAV carrying *Gjb2* gene were higher than the non-injected homozygous mutant mice.

Conclusion

The present paper will present the data regarding introduction of the virus vector into the *Gjb2* knockout mouse at the neonatal stage.

191 Cochlear Gene Transfer Mediated by Adeno-Associated Virus: Comparison of Two Surgical Approaches

Wade Chien^{1,2}, Devin McDougald¹, Lisa Cunningham¹
¹NIDCD/NIH, ²Johns Hopkins

Background

Hearing loss is one of the most common disabilities affecting the US population. Gene therapy offers the possibility of delivering corrective genes to the cochlea, potentially improving hearing. Currently, the most commonly used surgical methods for viral gene therapy delivery to the cochlea are the round window and the cochleostomy approaches. However, the patterns of viral infection and the effects on hearing have not been directly compared between these two approaches. In this study, we compare the patterns of cochlear infection and effects on hearing between these two surgical approaches using adeno-associated virus serotype 8 (AAV8) as the gene delivery vehicle.

Methods

CBA/J mice were used in this study. AAV8-GFP was delivered to the cochlea by either the round window or the cochleostomy approach. Auditory brainstem-evoked response (ABR) was used to examine hearing thresholds before and after surgery. Animals were examined at 1, 2, 3, and 4 weeks after surgery for the patterns of cochlear infection and hearing loss.

Results

Cochlear gene transfer was successful through both surgical approaches. In both approaches, the inner and outer hair cells, supporting cells, and the stria vascularis were infected with AAV8-GFP. The cochleostomy approach caused a greater amount of hearing loss than the round-window approach.

Conclusion

The round window approach and the cochleostomy approach are both successful at AAV-mediated gene transfer to the cochlea. The round window approach resulted in less hearing loss compared to the cochleostomy approach.

192 Essential Role for CBP in Tlx3-Mediated Neuronal Differentiation from Mouse Embryonic Stem Cells

Atsushi Shimomura¹, Eri Hashino¹

¹Indiana University School of Medicine

Background

The histone acetyltransferase CBP is a known transcriptional co-activator and has been shown to bind homeobox proteins, including Tlx3. The association of CBP with the homeobox proteins appears to be critical for evoking transcriptional activation of their target genes. Using Tlx3-expressing mouse embryonic stem cells (ESCs), we have shown that: (1) Tlx3 regulates Ngn1 expression only after neural induction; (2) Tlx3 binds CBP only after neural induction. We hypothesized that, upon

neural induction, CBP may be recruited to and bind Tlx3 occupying the Ngn1 locus, which causes conformational changes in chromatin through acetylation of histone H3/H4 and subsequent transactivation of Ngn1.

Methods

To test which region in Tlx3 is required for CBP binding, we generated several Tlx3 mutants, including Tlx3 Δ C lacking the C-terminus domain, and Tlx3 Δ HD lacking the homeodomain. We also generated ESC lines stably expressing wild-type Tlx3 and Tlx3 Δ HD, which were grown in neural induction medium for 4 or 7 days. To evaluate the functional outcome of impaired Tlx3-CBP binding, we measured changes in intracellular Ca²⁺ levels.

Results

Immunoprecipitation of HEK293 cells co-expressing CBP and one of these Tlx3 mutants revealed that the homeodomain in Tlx3 is required for its binding to CBP. qRT-PCR and Western blot analyses of samples collected from ESC-derived neurons revealed that Tlx3-CBP binding is essential for proper expression of Ngn1, but not Tau. In addition, a significantly smaller glutamate-induced Ca²⁺ influx was detected in Tlx3 Δ HD-expressing ESC-derived neurons when compared to wild-type Tlx3-expressing neurons.

Conclusion

These results strongly suggest that epigenetic regulation of Tlx3-mediated transcription can modulate efficiency of synaptic transmission in ESC-derived neurons.

193 Human Embryonic Stem Cell Incorporation Into the Mouse Cochlea in Vitro

Wade Chien^{1,2}, Matthew Kelley¹
¹NIDCD/NIH, ²Johns Hopkins

Background

Hearing loss is one of the most common disabilities affecting the US population. It is often caused by a loss of hair cells and/or spiral ganglion cells in the cochlea. Stem cell therapy offers the possibility of replacing these damaged and missing cells with functional ones and can potentially improve hearing function. One of the major hurdles of cochlear stem cell therapy is the lack of incorporation of transplanted cells into the neurosensory epithelium. In this study, we examine the patterns of human embryonic stem cell (hESC) incorporation into the mouse cochlea in vitro.

Methods

Mouse cochlear explants were dissected from E13, E15, E17, and P0 animals. WA07 hESCs were dissociated into single cells and co-cultured with mouse cochlear explants for 6 days. The patterns of hESC incorporation into the mouse cochlear explants were examined.

Results

Human embryonic stem cells were successfully incorporated into the mouse cochlear explants from E13 and E15 age groups. However, no hESC incorporation

was seen when co-cultured with mouse cochlear explants from E17 and P0 age groups. Several hESCs differentiated into neuron-like cells in all cochlear explants examined. Many of these neuron-like cells sent processes to make contact with mouse hair cells. No hair cell-like cells were seen to have differentiated from hESCs in all co-cultures examined.

Conclusion

E13 and E15 mouse cochleae were more susceptible to hESC incorporation into the neurosensory epithelium compared to older age groups. In addition, many hESCs readily differentiated into neuron-like cells and made contact with the mouse hair cells.

194 Auditory Scene Analysis in Birds: Spectrotemporal Cues Facilitate Streaming

Mary M. Flaherty¹, Erikson G. Neilans¹, Amanda K. Martin¹, Micheal L. Dent¹

¹State University of New York at Buffalo

Background

An animal's ability to accurately separate sounds from multiple sources in the environment is crucial for its survival. Understanding how different auditory cues in conspecific and heterospecific sounds are perceived by animals and what information facilitates acoustic segregation versus fusion will improve our knowledge of auditory scene analysis. The current study utilizes birdsong to measure streaming in budgerigars (*Melopsittacus undulatus*) and zebra finches (*Taeniopygia guttata*). A set of experiments was conducted to 1) determine the role of intensive, spatial, temporal, and spectral cues on streaming; and 2) to establish what specific cue properties are the most important for auditory scene analysis.

Methods

This study uses operant conditioning procedures to determine how conspecific and heterospecific cues affect streaming. Both species were trained to differentially peck keys in response to either a synthetic zebra finch song consisting of five syllables (whole song) or to the same song with one syllable omitted (broken song). Probe trials were presented to the birds on a small portion of all trials where the missing syllable was manipulated. In the first experiment, the original missing syllable was included but (1) varied in spatial location, (2) varied in intensity, (3) occurred earlier or later in time, or (4) varied in its spectral properties from the original whole song. In the second experiment, different stimuli were inserted into the missing syllable location, including a (1) zebra finch call, (2) budgerigar call, (3) budgerigar warble element, and (4) zebra finch syllable not found in the original training song. In both experiments, if the birds respond as hearing a whole song, it implies that the altered content is perceptually fused with the rest of the syllables to form one auditory stream.

Results

Results from Experiment 1 suggest that spatial and spectral cues have the most influence on streaming, while intensive and temporal cues are less informative. In Experiment 2, the probe stimuli that were more likely to be grouped with the surrounding broken song were probes that were the most temporally and spectrally similar to the original syllable and to the surrounding zebra finch song.

Conclusion

These results support the idea that spatial, spectral, and temporal cues are all somewhat important for the streaming of birdsong by zebra finches and budgerigars. These findings are consistent with previous results from humans and other animals.

195 Aesthetic Perception of Fractal Structure in Melodic Stimuli

Summer K Rankin¹, Charles J Limb¹

¹Johns Hopkins School of Medicine

Background

$1/f$, or fractal, structure is prevalent in nature, biology, and art: landscapes (coastlines, mountains), physiology (heart rate), and visual artwork (Pollock's paintings). Studies have demonstrated that subjects have an aesthetic preference for fractal images when compared to images created with non-fractal structure or random noise. Fractal analysis characterizes long-term correlation and self-similarity by taking sequential aspects of a time series into account.

Methods

A behavioral study was conducted to assess subjects' aesthetic perceptions of melodies with varying degrees of structure. Melodies were created using three types of noise: $1/f^0$ (white) contained no long term correlation or fractal structure; $1/f^1$ (pink) contained fractal structure and long-term correlation; $1/f^2$ (brown) contained highly correlated values. Fourteen adult subjects (musician and non-musician) with normal hearing were instructed to listen to each melody and answer the following questions: 1) Please classify the sequence using a likert scale from 1=ugly to 11=beautiful, 2) Rate the complexity of the sequence (1=least complex to 11=most complex), 3) How musical is the sequence? (1=very un-musical to 11=very musical), and 4) Which type of noise created this melody? Subjects were shown a picture of white, pink, and brown noise.

Results

Results showed that subjects were able to differentiate between white, pink, and brown melodies ($p < .01$) when asked to rate the complexity of the melody and when asked which type of noise was used to create the melody ($p < .01$). White melodies were rated as the most complex, pink melodies were the second most complex, and brown melodies were rated as the least complex. Subjects rated white and pink melodies significantly higher than brown on the measures of beauty and musicality ($p < .01$), showing

that subjects preferred white and pink to brown, but did not prefer the pink over white or vice versa.

Conclusion

Music must be predictable enough for people to attend to, but also contain enough violations of expectancy to keep the stimulus novel. The melodies that exhibited white or pink structure, received higher aesthetic ratings than the brown melodies. Possibly because the white and pink melodies were more unpredictable, and therefore more interesting than the brown melodies which were highly repetitive. Researchers have suggested that neural systems have evolved to encode these $1/f$ signals more efficiently than non-fractal signals; this could explain a conscious, aesthetic preference for $1/f$ stimuli.

196 Delayed Recovery of Auditory Stream Segregation: Cognitive and Acoustic Disruptions Are Additive

Graham Raynor¹, Julia Jones Huyck¹, Ingrid Johnsrude¹, Miriam Heavenrich¹

¹Queen's University

Background

People routinely segregate a mixture of sounds into distinct percepts. Previous research indicates that this useful perceptual organization can be disrupted by abrupt changes in auditory scene (Bregman, 1978) or by shifts in attention (Cusack et al., 2004). Here we examined the extent to which switches in attention between tasks and/or abrupt changes in auditory scene (1) cause a segregated percept to "re-set" to an integrated one and (2) influence the amount of time required to recover the segregated percept.

Methods

During each 12s trial, participants were cued to detect targets either in a two-tone (ABA-) auditory sequence for which segregation builds up over time, or in an unrelated distractor task in the opposite ear (Figure 1). Targets in the ABA task were 50ms delays of the B tone 'skips' (Thompson et al, ref) that occurred with 50% likelihood at 3s, 6s, or 9s after trial onset. Target detection sensitivity (d') on the ABA task is much higher when the percept is integrated compared to segregated. The distractor task required listeners to discriminate between two noise types with different amplitude envelopes. Across trials (Figure 2), either the attended task changed (the participant started to attend to the other task in the opposite ear), the auditory scene changed (the stimuli switched ears and the participant 'followed' the stimuli to the contralateral ear), both the task and auditory scene changed simultaneously (the participant kept listening to the same ear, but started doing the other task), or neither changed.

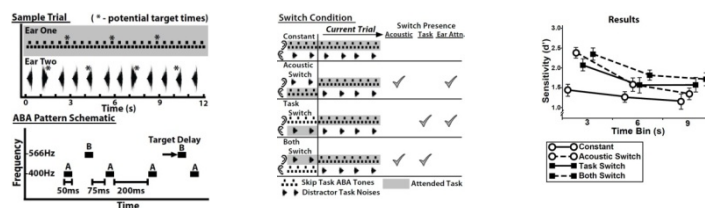
Results

Performance (Figure 3) was analyzed with a 4 (Switch Type) by 3 (Time) MANOVA. Sensitivity early in the trial (3s) indicated that changes in task, auditory scene, or both caused the perceptual organization to "re-set" (high d'). When only the task or auditory scene changed,

participants generally showed a return to segregation (low d') by the middle of the trial (6s). However, when both task and auditory scene changed, participants did not show segregation by the end of the trial (9s).

Conclusion

The delayed recovery of segregation following changes in the auditory scene and attended task (even if the attended ear stayed constant) demonstrates an additive effect of cognitive and acoustic disruptions on the buildup of segregation, suggesting that these two disruptions act via different mechanisms.



197 Recovering Sound Sources from Embedded Repetition and Directed Attention: Effect of Spectral Information on Sound Segregation

Keiko Masutomi¹, Nicolas Barascud², Tobias Overath², Makio Kashino^{1,3}, Josh H. McDermott⁴, Maria Chait²
¹Tokyo Institute of Technology, ²UCL Ear Institute, ³NTT Communication Science Laboratories, ⁴Massachusetts Institute of Technology

Background

McDermott et al. demonstrated that listeners can identify novel 'target' sounds from mixtures if they are presented multiple times across different distractors, even in conditions where single mixtures were impossible to segregate [McDermott, et al. (2011) PNAS. 108(3):1188-93]. Their results indicate that the auditory system can recover sound sources from mixtures by detecting repeating spectro-temporal structure embedded in the acoustic input. In the present series of experiments we aim to investigate whether this repetition-based sound segregation requires selective attention to sounds or whether it can occur partially outside the focus of attention. We adapted the original paradigm of McDermott et al. to a dual task design in which subjects are required to perform a difficult 'decoy' task concurrent with presentation of the sequence of sound mixtures.

Methods

Trials consist of ten sound mixtures, each composed of a repeating target and a distractor that changes from mixture to mixture. At the end of a trial, participants judge whether a subsequently presented probe appeared in the sound mixtures (a test of their ability to segregate the sounds in the mixture). Concurrently, subjects are presented with 'decoy' visual (Exp1, 2) or auditory (Exp3) stimuli. We manipulate the attentional load of the decoy task by instructing subjects to perform (in different blocks) 'low load' and 'high load' tasks on these signals. They are instructed (and explicitly motivated) to focus their attention

on the 'decoy' task, and guess if unsure about the sound-mixture task.

In Experiment 1 we use a rapid sequence of serially presented visual stimuli (digits). In the 'low load' condition listeners are required to report whether an underline appeared with one of digits. In the 'high load' condition, they are required to memorize the digit order – a task that requires significant attentional and echoic memory resources. In Experiment 2, we use a multiple object tracking visual task, which is attentionally demanding but does not rely on echoic memory. In Experiment 3, we employ a decoy auditory task in which listeners are required to memorize a sequence of rapidly presented sounds.

Results

This study is ongoing. The result of experiment 1 demonstrate that a concurrent, high load, visual task results in similar performance levels to those measured during a low load task.

Conclusion

Our results suggest that listeners can segregate novel sounds from mixtures when attention is directed elsewhere, providing support for repetition-based segregation as automatic, bottom up process.

198 Perceptual Asymmetry Induced by the Auditory Continuity Illusion

Dorea Ruggles¹, Andrew Oxenham¹
¹University of Minnesota

Background

Listening for messages within mixtures of maskers is both challenging and relevant to daily communication. One aspect of this listening challenge is that masked, or obscured, portions of messages are often perceptually "filled in" to create a continuous stream of information. This auditory continuity illusion has been studied primarily with the stimuli presented in isolation, and it is unknown whether the continuity illusion occurs in more complex situations when attention is not directed towards the interrupted stimulus.

Methods

Young normal-hearing participants listened for target tones in "clouds" of masking tones and noises with pseudo-random spectro-temporal locations. The basic experimental task was to listen for a long (300ms) tone in a cloud of short (100 ms) tones, and its counterpart condition was to listen for a short tone in a cloud of long tones. These two conditions have previously illustrated perceptual asymmetry in auditory object searches and were compared to listeners' ability to detect illusory long tones, created by interspersing a 100-ms noise between two short (100-ms) tones within a cloud of other short tones and noise. Individual thresholds for perceiving the continuity illusion in the absence of other stimuli (pulsation thresholds) were also measured.

Results

Detection of physical long and short tones confirmed previously reported perceptual asymmetry based on tone length. Illusory long tones were more readily detected than the short tones, but produced statistically significantly poorer performance than the physical long tones. Individual pulsation thresholds for the illusion alone were not found to be related to ability to detect the illusion within a cloud of masking tones and noise.

Conclusion

The results suggest that the continuity illusion can occur to some extent in the presence of a complex acoustic background, and in the absence of focused auditory attention towards the target tone. Previous reports have attributed perceptual asymmetry of long and short tones to the relatively greater number of duration-specific midbrain and cortical neurons tuned to long tones. If so, our results suggest that the illusory long tones may also activate some proportion of the neurons tuned to long-duration stimuli, suggesting a relatively early, and possibly pre-attentive locus for the continuity illusion. [Supported by NIH grant R01 DC 07657.]

199 Spectral Motion Contrast: Another Factor in Speech Context Effects?

Ningyuan Wang¹, Andrew Oxenham¹

¹Department of Psychology, University of Minnesota

Background

Spectral contrast effects, such as the auditory negative afterimage, may help normalize the incoming sound and produce perceptual constancy in the face of the variable acoustics produced by different rooms, talkers, and backgrounds. Such contrast effects may be particularly important for speech perception; indeed, a number of speech context effects have been explained in terms of static, or long-term, spectral contrasts. The present study examines another candidate for speech context effects, based on dynamic, rather than static, spectral contrasts. In particular, we attempt to dissociate effects of the long-term spectrum from those due to spectral motion or glides.

Methods

In the first experiment, we measured the effect of a preceding 500-ms spectral glide on the perceptual boundary between upward and downward spectral motion of a brief (50-ms) target glide. In the second experiment, the perceptual boundaries between [ba-da] and [da-ga] were measured for various precursors that included static and/or dynamic spectral components.

Results

Results from the first experiment confirmed earlier reports of a contrastive perceptual motion aftereffect, whereby a downward precursor glide resulted in a shift in the perceptual boundary between perceived upward and downward motion towards upward motion. The effect appeared to be spectrally local, with the strongest aftereffects occurring when the precursor and target were

presented within the same spectral region. Preliminary results from the second experiment suggest that the perceptual boundaries for phonemes can in some cases also be influenced by both the average spectral location and the spectral motion of the preceding sound.

Conclusion

Both static and dynamic spectral cues seem to play a role in inducing speech context effects. Thus, spectral motion contrast may be another factor that influences speech perception in natural contexts. [The first author is supported by a studentship from Advanced Bionics.]

200 Acoustic Amplitude-Modulation Detection and Speech Identification in Fluctuating Noise for Cochlear Implant Users

Dan Gnansia¹, Diane Lazard², Agnès Léger³, Claude Fugain⁴, Denis Lancelin³, Bernard Meyer⁴, Christian Lorenzi³

¹Neurelec, ²Institut des Neurosciences de Montpellier U1051, ³Equipe Audition (UMR LPP 8158 CNRS, Univ. Paris Descartes), Ecole normale supérieure, Paris, France, ⁴AP-HP, Service ORL, Hôpital Beaujon, Clichy, France

Background

This psychophysical study aimed to assess whether the limited capacity of cochlear implant users to identify speech in various listening conditions (in quiet, in the presence of a steady-state or fluctuating noise) is determined by a reduced capacity to perceive slow temporal modulations.

Methods

This was achieved by measuring (i) phoneme identification in quiet and in the presence of a steady-state or fluctuating (8 Hz) masking noise and (ii) amplitude-modulation detection thresholds at 8 Hz for a group of 17 cochlear implant users. All patients were tested in free field at 70 dB SPL with their own clinical sound processor.

Results

Consistently with previous studies, modulation detection thresholds at 8 Hz were highly variable across patients, ranging from -1 to -22 dB (re: 100% modulation). Phoneme identification scores measured in quiet were correlated with modulation detection thresholds at 8 Hz. Phoneme identification scores measured with a steady-state noise masker were generally correlated with modulation detection thresholds at 8 Hz at positive signal-to-noise ratios (0 and +6 dB). Phoneme identification scores measured with a fluctuating noise masker at a negative signal-to-noise ratio (-3 dB) were not correlated with modulation detection thresholds at 8 Hz.

Conclusion

These results suggest that auditory sensitivity to slow temporal modulations is an important predictor of cochlear implantation success in real-life listening situations. However, sensitivity to slow modulations does not seem to explain the limited capacity of most cochlear implant

patients to benefit from fluctuations in background noise maskers.

[201] A Direct Test of the Temporal-Coherence Model of Auditory Streaming

Coral Hanson¹, Christophe Michey², Laurent Demany³, Shihab Shamma⁴, Andrew J. Oxenham²

¹Augustana College, ²University of Minnesota, ³CNRS, ⁴Universite Bordeaux, ⁵Ecole Normale Supérieure

Background

According to a recently proposed model of auditory scene analysis, sequences of temporally coherent sounds are grouped perceptually into a single auditory “stream”. Results consistent with this hypothesis were obtained in an earlier study, which involved an integration-promoting task. The current study sought to test the influence of synchrony on streaming using subjective measures and a segregation-promoting task.

Methods

In experiment 1, listeners indicated whether they heard sequences of alternating or synchronous tones at two frequencies (A and B) as one stream or two streams. A-B frequency separations of 1, 3, 6, 9, and 15 semitones were tested. In experiment 2, listeners detected occasional changes in the level of tones at one frequency (e.g., B) while the level of tones at the other frequency was randomly varied, thus forcing listeners to attend selectively to the target tones. In Experiment 3 the frequency of the distractor tone alternated by a small amount (1 semitone) between bursts within each trial to test whether this would facilitate segregation of the target tones.

Results

Consistent with previous findings, the results of experiment 1 showed a marked increase in the probability of reporting segregation as frequency separation increased from 1 and 9 semitones. For synchronous tones, the results were more variable: some listeners showed large effects of frequency separation while others did not; however, on average, the probability of reporting segregation for large frequency separations (6 semitones or more) was lower, and flatter, for synchronous tones than for alternating tones. Consistent with the results of experiment 1, the results of experiment 2 showed more consistent and robust increases in sensitivity (d') with frequency separation for alternating than for synchronous tones. The results of experiment 3 showed no beneficial effect of frequency changes in the distractor tones on the segregation of the target tones.

Conclusion

Overall, the results provide partial support for models in which auditory streaming depends not just on frequency separation (e.g., channeling models) but also on the relative timing of events - with synchrony promoting stream integration, even for relatively large frequency separations. However, they also underscore the existence of large interindividual differences in the influence of relative tone timing on both “subjective” and “objective” (i.e.,

performance-based) measures of perceptual organization. [Work supported by grant R01 DC 07657.]

[202] The Effect of Visual Cues on Auditory Segregation

I-Fan Lin¹, Maria Chait², Makio Kashino¹

¹NTT Communication Science Labs, ²The Ear Institute, University College London

Background

Previous work has indicated that, visual stimuli presented in synchrony with a targeted auditory stream can affect auditory segregation under certain conditions (van Ee et al., 2009). The present series of experiments are designed to elucidate the properties of this visual effect on auditory segregation and its possible mechanisms. Specifically, we aim to ascertain whether the visual effect exists in both one-stream and two-stream conditions and whether it is affected by the temporal properties of the auditory sequence.

Methods

In Experiment 1 (one-stream), acoustic sequences consisted of pure tones at 3 different frequencies, separated by 2 semitones, that were presented in random order. Subjects (N=6) were instructed to identify a 'target pattern' which consisted of 3 tones in a particular order. The tones were presented isochronously (REG condition) at 2 or 4 Hz, or in a random temporal pattern (RAND condition) with a mean rate of 2 or 4 Hz. Visual stimuli were a black fan shape (1/3 of a circle) with a radius of approximate 2 degrees. To reduce after-image effects, the stimuli cycled between 3 orientations (0-120 degrees, 120-240 degrees, 240-360 degrees). Visual stimulation varied according to 3 conditions: (1) no visual stimulation, (2) synchronous with the auditory signals, and (3) presented independently of the auditory signals at a rate of 3 Hz.

In Experiment 2 (two-stream), the auditory stimuli contained two sequences separated by 5 semitones, and participants were cued to attend to one of them. The temporal regularity pattern of the attended and ignored sequences was manipulated independently, resulting in 4 conditions: RAND-RAND, RAND-REG, REG-REG, and REG-RAND. Only rate of 2 Hz was used in this experiment (experiments using faster rates are ongoing). Visual stimuli were absent or presented in synchrony with the attended auditory sequence, with the ignored sequence, or at a fixed rate of 3 Hz (independently of the auditory stimulation).

Results

In Exp 1, the visual stimulation had no effect on auditory pattern recognition. In contrast, in the RAND-REG and REG-RAND conditions in Exp 2, participants' performance was improved when visual stimuli were synchronized with the attended auditory stream. Moreover, in the REG-RAND condition, visual stimuli that were synchronized with the distractor auditory stream resulted in degraded performance.

Conclusion

Our results suggest a role for audio-visual coherence in auditory segregation. Relevant control conditions are in progress.

203 Bayesian Modeling of Human Performance in an Auditory-Categorization Task

Adam Gifford¹, Yale Cohen¹, Alan Stocker¹

¹University of Pennsylvania

Background

Categorization is a natural and adaptive process that is seen in all animals. That is, despite a great deal of variability within and across stimuli, animals typically ignore some sources of variation while treating others equivalently. The categorization process is complicated by the fact that (1) animals have to generalize over a large stimulus space to tolerate multiple category exemplars, and (2) a stimulus' category membership can be "ambiguous" since it can belong to multiple categories with overlapping boundaries. The mechanisms by which animals resolve these complications are not fully understood. Using auditory stimuli, we tested how asymmetric prior probabilities for a stimulus' category membership affected a listener's decisions on the categorization of a stimulus. Next, we tested whether the listener's performance matched the behavior of different Bayesian ideal categorization models.

Methods

Stimuli were pure-tones chosen from a continuous range of frequencies (500-5550 Hz), with the lower (log) 2/3 of this range assigned to one category ("A") and the upper (log) 2/3 assigned to a second category ("B"). Thus, each category had a frequency range that was unique to each category and a range that overlapped with both categories. Category priors across their respective frequency ranges were box-shaped such that all tones within a category were equally likely. Category prior probabilities were manipulated by varying the number of trials that presented a tone originating from either category A or B. Subjects performed 3 blocks of a 2-alternative forced choice experiment, with each block of trials having a different prior probability for category A [$p(A) = 0.25, 0.5, \text{ or } 0.75$]. After hearing a tone, subjects reported the category membership of the stimulus with a gamepad. Subjects received feedback regarding their decision.

Results

Our results demonstrated that increasing the category prior $p(A)$ led to an increased bias toward selecting category A. While this result was consistent with a Bayesian model, a more detailed analysis suggested that subjects were not able to learn the exact shape of the prior distributions. As a result, a Bayesian model with the assumption of Gaussian priors for categories A and B was also compared to subject performance.

Conclusion

These findings offer insight into how the auditory system may represent prior information and solve probabilistic inference tasks.

204 Temporal Integration for Detection of a Tonal Signal in a Comodulated Masker: Effects Related to Signal-To-Noise Ratio

Emily Buss¹, Joseph Hall¹, John Grose¹

¹UNC Chapel Hill

Background

Temporal integration for the detection of a tonal signal is often greater in a spectrally wide comodulated masker than in either a narrow or a wide random-noise masker. The present experiments assessed the contribution of higher maximum signal-to-noise ratios (SNRs) for longer signals, due to variations in the masker level over time. Whereas a brief signal might coincide with a dip or a peak in the masker envelope, increasing the signal duration would tend to increase the maximum SNR. This factor was expected to confer particular benefit in comodulated maskers due to the ability to 'listen in the dips.'

Methods

Temporal integration was assessed in normal-hearing adults in both the narrowband and the band-widening CMR paradigms. In some conditions, the signal was temporally centered in a masker envelope dip, and in others the signal was presented randomly with respect to the masker envelope.

Results

On average, temporal integration in a comodulated masker was substantially smaller when the brief signal coincided with a masker envelope dip than when it was presented at a random point in the masker envelope. For the slowest modulation rate tested (13 Hz), integration in the condition where the brief signal coincided with a masker envelope dip was less than that observed in steady noise, a result that is consistent with the integration of 'multiple looks' at the signal during epochs of improved SNR. In contrast to results for the comodulated masker, integration was insensitive to signal timing for the narrowband and random maskers.

Conclusion

The results obtained here are consistent with the conclusion that the relatively large temporal integration sometimes obtained for signals in a comodulated masker is due to greater maximum SNR for longer signals. When this factor is controlled for, integration may be comparable to or less than that observed in a steady masker.

This work was supported by a grant from NIH NIDCD R01-DC007391.

205 “Glimpsing” a Target Harmonic Complex in a Temporally Interrupted Masker

Yi Shen¹

¹University of California, Irvine

Background

When two sounds (a target and a masker) are presented simultaneously, listeners are typically more successful in identify features in the target sound if the masker sound contains temporal gaps. This benefit could be a consequence of the improved target-to-masker ratio (TMR) during the temporal gaps, or it might be interpreted that the temporal gaps in the masker provide a cue that promotes the perceptual segregation of the two sounds.

Methods

In the current study, sensitivity to changes in spectral profile was measured for a harmonic complex target sound. The target was always presented with a simultaneous harmonic masker that was temporally interrupted. Performance thresholds were collected as functions of differences in fundamental frequency (from 0 to 10 semitones) and target-to-masker ratio (from -20 to 10 dB). Besides thresholds, relative decision weights were estimated independently for the masker, the portions of the target that temporally overlapped the masker (target-overlap), and the portions of the target that were in the masker gaps (target-gap).

Results

Profile analysis thresholds improved with increasing fundamental-frequency difference, TMR, and gap duration. At low TMR's, the target-gap stimulus dominated the responses whereas the target-overlap contributed little to the responses, indicating that listeners conducted the task by glimpsing the target in the masker gaps. At high target-to-masker ratios, the target-overlap and target-gap contributed equally to the responses.

Conclusion

When it is advantageous to do so (e.g., at low TMR's), listeners perform profile analysis of the target using glimpses of the target during the temporal gaps of the concurrent masker. When the gap duration is short and the fundamental-frequency difference between the target and masker is small, the masker cannot be totally ignored. The efficiency of glimpsing the target improved as the fundamental-frequency difference increases.

206 Efficient Parameter-Based Estimates of Auditory Filters

Yi Shen¹, Virginia Richards¹

¹University of California, Irvine

Background

Performance-based methods currently used to estimate auditory filter parameters are time-consuming, making routine estimates difficult. An adaptive “parameter-based” Bayesian adaptive procedure for the rapid estimation of auditory filter parameters was proposed and tested.

Methods

The power spectrum model of masking was assumed with an efficiency parameter K and a two-parameter roex (r , p) filter, yielding a 3-D space of model parameters. A logistic psychometric function linked the model to behavioral responses. The task was the detection of a tone added to a notched noise, yielding a 2-D stimulus space composed of potential normalized notch bandwidths and signal strengths in dB SPL. Following Kontsevich and Tyler [1999; Vis. Res. 39, 2729-2737], a one-step-ahead search algorithm with an entropy-based criterion was adopted in which the next stimulus to be tested was the one that decreased the total expected entropy in the parameter estimation.

Results

The procedure was successful for most young normal-hearing listeners in that parameter estimates obtained from the proposed procedure and 100-150 trials were as reliable as those obtained using 2000 trials with a performance-based procedure. For a few listeners, the procedure failed to converge to reasonable parameter estimates, and for them, the performance-based measures were also variable. By introducing a “lapse” term into the psychometric function, the parameter-based procedure converged rapidly (100-150 trials) and reliably even for these few listeners.

Conclusion

The current data provided a proof-of-concept that estimates of auditory filters for young, normal hearing listeners could be achieved in as few as 150 trials. This parameter-based procedure can be extended to include other populations and other well-modeled psychophysical function.

207 Effects of Prior Frequency Separation and Prior Perception on Auditory Stream Segregation: Same or Different Effects?

David Weintraub¹, Joel Snyder¹

¹University of Nevada, Las Vegas

Background

Previous studies have shown that the perceptual segregation of low- (A) and high- (B) frequency tones in a repeating ABA pattern depended on two aspects of the previous context. First, sequences were more likely to be organized into separate streams when preceded by a context sequence that had a small frequency separation (Δf) between A and B tones, despite the fact that small frequency separations during the context tends to result in perception of one integrated stream during the context. Second, studies also showed that sequences with the same Δf as the preceding context sequence were more likely to again be organized into separate streams when preceded by a context that was also heard as segregated. Despite differences in the direction of these effects (i.e., contrastive vs. facilitative for effects of prior Δf and prior perception, respectively), it could be that the effect of prior Δf actually reflected a contrastive effect of prior perception when the Δf between context and test changed, and was

not due to the size of the Δf per se. To test this hypothesis, the effect of prior perception was measured separately for conditions in which the context and test sequence had matching or mismatching Δf .

Methods

Stimuli consisted of a repeating ABA pattern arranged into a 6.72-sec context sequence and a subsequent 6.72-sec test sequence. The Δf between A and B tones in the context sequence was 3, 5, or 7 semitones. The Δf in the test sequence was always 5 semitones. Participants continuously reported whether they heard the A and B tones grouped into the same or separate streams.

Results

Context sequences were more likely to be organized into separate streams when the Δf was large. Test sequences were more likely to be organized into separate streams when the preceding context Δf was small or was also organized into separate streams. Importantly, the effect of prior perception was facilitative regardless of whether the Δf between context and test matched or mismatched.

Conclusion

These results do not support the theory that the apparent effect of prior Δf reflected a contrastive effect of prior perception when the Δf between context and test changed. Therefore, we conclude that the effects of prior perception and prior Δf reflect distinct contextual influences of immediate prior listening. [Supported by NSF BCS1026023]

208 The Role of Object Perception in Change Deafness: Behavioral and Event-Related Brain Potential Findings

Vanessa Irsik¹, Melissa Gregg¹, Joel Snyder¹

¹University of Nevada, Las Vegas

Background

Change deafness is the failure to notice obvious changes occurring in an auditory scene. We sought to determine if change deafness is a fundamental sensory process, rather than a reflection of verbal memory limitations that would be predicted to only occur for recognizable sound objects. We also examined whether successful encoding of objects within a scene is related to successful detection of changes.

Methods

Event-related potentials (ERPs) were recorded while listeners completed a change-detection task and an object-encoding task with scenes composed of recognizable or unrecognizable sounds. For the change-detection task, listeners heard a scene composed of four concurrent sound objects, followed by 350 ms of silence, followed by another four-object scene that was either the same or different (three of the same objects plus one new object). Listeners then indicated whether the two scenes were the "same" or "different". Finally, for the object-encoding task, listeners heard a probe sound and indicated whether it was present or absent in one or both of the preceding scenes.

Results

More change deafness occurred for the unrecognizable sounds, compared to recognizable sounds. ERPs from Scene 1 revealed an enhanced positivity from 315-660 ms at right temporal electrodes for detected changes, but only for recognizable sounds. ERPs from Scene 2 revealed an enhanced P3 during detected changes for both recognizable and unrecognizable sounds. Performance on the object-encoding task revealed that change deafness was reduced, but not eliminated, when recognizable objects were accurately encoded. Neural responses recorded during the change-detection task with recognizable sounds revealed an enhanced P2 in both Scene 1 and Scene 2 when objects were not accurately encoded.

Conclusion

The data are consistent with the conclusion that change deafness is at least partly an auditory sensory phenomenon and not solely a product of verbal memory. Enhanced neural activity for recognizable sounds in Scene 1 might reflect more accurate mapping of objects onto pre-existing representations in memory during Scene 1 or better segregation of objects based on their acoustics. The enhanced P3 for detected changes in Scene 2 may indicate that conscious change detection has occurred. A parsimonious interpretation of the finding of a smaller P2 during successful object encoding is that better performance on the object-encoding task is supported by more efficient object representations, which also leads to better change detection performance. [Supported by Army Research Office grant W911NF-I2-I-0256]

209 Comodulation Masking Release (CMR) in Treefrogs and a Frog-Inspired Auditory Filterbank to Investigate Its Neural Correlates

Norman Lee¹, Christophe Micheyl¹, Alejandro Vézlez^{1,2}, Mark Bee¹

¹University of Minnesota, ²Purdue University

Background

Noisy social settings can impair the auditory system's ability to detect, recognize and localize sound sources. Female Cope's gray treefrogs (*Hyla chrysoscelis*) encounter this situation when attempting to find potential mates that call in loud, mixed-species choruses. Natural sources of noise may exhibit temporal envelope fluctuations that are correlated across the frequency spectrum, and this comodulation may be exploited by the auditory system for improved signal processing. Comodulation masking release (CMR) may depend on across-channel or within-channel frequency processing, or both. The anuran auditory periphery provides a unique opportunity to assess independently these contributions because anurans possess two distinct sensory organs in their inner ears, the amphibian papilla (AP) and the basilar papilla (BP), each responsible for processing mostly non-overlapping frequency ranges.

Methods

In this study we developed a frog-inspired auditory filterbank to investigate the correlation structure of natural frog choruses. This filterbank is more biologically pertinent than models with equal bandwidth and evenly spaced filter bands, or models based on the human auditory periphery. In a meta-analysis, a rounded exponential function (roexp) was applied to fit VIIIth nerve frequency tuning curves from several anuran species. The roexp function successfully described the filter shapes of AP and BP units, and was used to construct a filterbank.

Results

The output of this filterbank showed envelope fluctuations from different frequency bands of the chorus structure to be highly correlated. In behavioral experiments, we tested for CMR in *H. chrysoscelis*. Signal recognition thresholds were estimated for calls in quiet, or in the presence of “chorus-shaped noise” comprised of two narrowband noises centered on the two spectral peaks (1.3 and 2.6 kHz) present in the male advertisement call. The two narrowband noises were either 1) unmodulated (flat), 2) independently modulated (deviant), or 3) comodulated with identical modulators. At higher masker levels (73 dB SPL), subjects experienced an approximate 3 dB and 6 dB release from masking in comodulated noise compared to deviant or flat noise, respectively. This masking release was absent at a lower masker level of 53 dB SPL.

Conclusion

Our results confirm CMR-like processes that may contribute to improved call recognition in *H. chrysoscelis*, and we provide a first description of an anuran auditory filterbank as an analytical tool for predicting and explaining empirical results underlying mechanisms of auditory processing.

[This work supported by NIDCD R01 5R01DC009582.]

[210] Spatial Release from Masking Improves Temporal Pattern Recognition in Cope’s Gray Treefrog

Jessica L. Ward¹, Mark A. Bee¹

¹University of Minnesota

Background

For social species, such as humans, birds and frogs, that gather in large and noisy social groups, auditory mechanisms that improve acoustic signal recognition in noise are particularly important for successful communication. One way receivers in such environments might isolate target signals from competing sounds is by exploiting spatial separation between sources. We tested the hypothesis that spatial release from masking improves temporal sound pattern recognition in Cope’s gray treefrogs (*Hyla chrysoscelis*). Like many other frogs, male gray treefrogs form loud breeding “choruses” where they produce calls with species-specific temporal structures that females use to recognize potential mates. To choose a mate of the correct species, females must correctly recognize the temporal pattern conveyed by the pulse rate

(≈ 50 Hz) of calls amid competing calls and high levels of background noise. This ability is necessary to avoid mating with a closely-related species with spectrally similar, pulsatile calls having a slower pulse rate (≈ 20 Hz). If spatial release from masking improves temporal pattern recognition, we predicted females would be more likely to choose calls with faster pulse rates in the presence of artificial chorus noise originating from spatially separated sources compared with co-localized conditions.

Methods

To measure behavioral decisions of subjects, we used a phonotaxis assay requiring females to approach one of two alternating synthetic calls differing only in pulse rate. Subjects were presented with all pairwise combinations of alternatives having pulse rates of 20, 30, 40, and 50 Hz. These tests were replicated in quiet and in the presence of artificial chorus noise presented from separated or co-localized conditions.

Results

In quiet conditions, females showed strong and consistent selectivity favoring call alternatives with faster versus slower pulse rates. Hence, faster pulse rates constituted the “correct” behavioral response measured in quiet conditions. While error rates were higher in noise, subjects were significantly more likely to choose correct pulse rates when signals and noise were separated by 180° compared with the co-localized condition.

Conclusion

Spatial separation between sources improved the ability of subjects to make correct behavioral decisions based on analyses of temporal sound patterns. These results support the hypothesis that spatial release from masking improves temporal sound pattern recognition in the context of a cocktail-party-like communication problem in frogs. [This work was supported by 5R01DC009582.]

[211] Phonemic Restoration: Studying the Effect of Voice Alternation

Jeanne Clarke^{1,2}, Monita Chatterjee³, Etienne Gaudrain^{1,2}, Deniz Baskent^{1,2}

¹University Medical Center Groningen, NL, Department of Otorhinolaryngology / Head & Neck Surgery, ²University of Groningen, Graduate School of Medical Sciences (Behavioural & Cognitive Neurosciences), ³Boys Town National Research Hospital

Background

This study focuses on the importance of voice continuity for phonemic restoration (PR). The restoration effect can be observed by the increase in intelligibility when silent interruptions in a sentence are filled with noise, and is a measure of the auditory system’s top-down compensation for speech degradation. Poor PR performance was previously observed with cochlear-implant (CI) users, where the fundamental frequency (F_0) is not well delivered and thus pitch cues are missing. Based on this, we hypothesized that the continuity of pitch and vocal-tract-length (VTL) is important for PR, as these cues can be

used to group speech segments in interrupted speech. Disrupting this continuity should therefore decrease both overall intelligibility of interrupted speech and restoration effect.

Methods

Sentences originally spoken by a male talker were processed in STRAIGHT into four voice conditions: (1) unmodified vocal characteristics, (2) only F_0 shifted up toward that of a typical woman value, (3) only VTL shortened to that of a typical woman size, and (4) both F_0 and VTL modified simultaneously. The continuity of these vocal characteristics was then disrupted by alternating the synthesised voices across segments of meaningful interrupted sentences. Intelligibility of processed sentences was assessed with normal hearing, Dutch native speakers.

Results

Our preliminary results showed that disrupting the continuity of vocal-characteristics reduces overall intelligibility when VTL was manipulated (alone or together with F_0), but not when only F_0 was manipulated. However, phonemic restoration was present and unaffected in all voice conditions.

Conclusion

Although phonemic restoration is generally linked to the continuity illusion, the effect of restoration was preserved even when the continuity of vocal characteristics was disrupted to the degree that the listeners attributed different segments of speech to different talkers. In contrast, overall intelligibility was affected by the manipulation, in agreement with literature on speaker-normalization on the one hand and fusion of segments of interrupted speech on the other hand. However, the listeners perhaps took advantage of speech redundancy for restoration and compensated for distorted voice characteristics by taking advantage of other cues (such as linguistic and contextual cues). Further, as speech redundancy is very low in CI simulations and actual CIs, these results may suggest that the reduced PR effect observed in CI users or normally hearing listeners attending to CI simulations is unlikely to be only due to the poor pitch representation provided by the implant or the simulation.

212 Contribution of Spectral and Temporal Cues to Phonetic Discrimination in Infants

Laurianne Cabrera^{1,2}, Josiane Bertoncini¹, Christian Lorenzi²

¹Universite Paris Descartes-CNRS, ²Ecole Normale Supérieure

Background

A previous study (Cabrera, Bertoncini & Lorenzi, 2011) investigated the perception of spectral and temporal cues in normal-hearing (NH) 6-month-old infants by using noise-vocoded speech stimuli and a headturning preference procedure. Noise-vocoders degraded selectively frequency-modulation (FM, the rapid variations with a rate close to the center frequency of the auditory filter) and

amplitude-modulation (AM, the relatively slow variations in amplitude over time) cues. Vocoders also degraded the spectral resolution of speech signals by extracting AM within 4 broad frequency bands. After one or two minutes of familiarization, infants discriminated voicing (/aba/ versus /apa/) in each vocoded condition, but their reaction differed according to the type of degradation (see figure 1). These results suggested that the relatively fast FM and AM cues are not essential for infants to discriminate voicing in silence. The present research extended this initial study by assessing the ability of infants to discriminate two phonetic contrasts [voicing and place of articulation (/aba/ versus /ada/)] using an infant-controlled familiarization time. Tone-excited vocoders were used in order to limit potential distortions of AM cues introduced by the vocoder processing (Kates, 2011).

Methods

Four tone-excited vocoders were designed to reduce (i) FM cues, (ii) AM cues to their slowest variations (<16 Hz), (iii) and the spectral resolution of speech signals (from 32 to 8 bands). Discrimination abilities were assessed for 160 French 6-months who reached a familiarization criterion and completed a test phase including presentation of novel and familiar stimuli.

Results

Six-month-olds discriminated voicing and place in each vocoded condition. However, differences appeared in the time required to reach the familiarization criterion: infants required more time to be fully familiarized when fast AM cues were severely reduced (see figure 2).

Conclusion

NH 6-month-olds did not require fast FM and AM speech cues to distinguish voicing and place of articulation. This corroborates the idea that fine spectro-temporal details do not play a major role in phonetic discrimination in quiet for both infants and adults. Nevertheless, longer exposure to vocoded stimuli was required when fast AM cues were attenuated, suggesting that periodic, F_0 -related, envelope cues are perceived and used by infants.

Figure 1. Mean looking times measured for familiar (Fam) and novel (Nov) stimuli sequences and for each noise-vocoder condition during the test phase (data adapted from Cabrera, Bertoncini & Lorenzi, 2011; error bars show standard errors). Mean looking times obtained after one minute of familiarization for the "32-band AM+FM speech" and "4-band AM speech" conditions are shown in the leftmost part of the panel. Main effects of the sequences were obtained with a significant preference for novel sequences in the "32-band AM+FM speech" condition (t(21)=2.51, p=0.03) and a significant preference for familiar sequences in the "4-band AM speech" condition (t(21)=2.43, p=0.02). Mean looking times obtained after two minutes of familiarization for the "32-band AM speech" and "2-band AM+16Hz speech" conditions are shown in the rightmost part of the panel. Main effects of the sequences were obtained with a significant preference for novel sequences in the "32-band AM speech" condition (t(19)=2.99, p=0.014) and a significant preference for familiar sequences in the "2-band AM+16Hz speech" condition (t(19)=2.55, p=0.023).

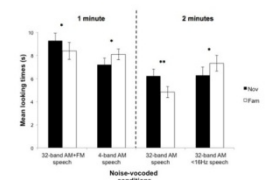
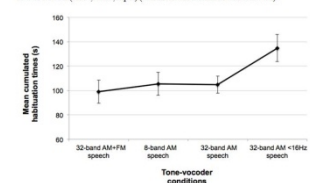


Figure 2. Mean habituation times in each (tone-excited) vocoder condition across stimuli (/aba/, /ada/, /apa/) (error bars show the standard errors).



213 Effect of Temporal Characteristics of Priming on Speech Recognition

Richard Freyman¹, Charlotte Morse-Fortier¹, Amanda Griffin¹

¹University of Massachusetts

Background

When a listener hears speech that has been degraded, a striking change in perception takes place once s/he knows the content of the message. For example, a listener first hearing speech processed through a noise vocoder with a small number of channels will hear the signal as a noisy distorted sound. This sound may or may not be interpreted as speech, and is likely to have limited intelligibility. However, after listeners are informed of the content of the message and the presentation of the vocoded sample is repeated, listeners are often impressed about how easy it is to understand the distorted speech. Quantification of the effect is difficult, because once the content is known, the listener could simply remember it and repeat it whether or not it the degraded message was correctly perceived. In this study, a forced-choice discrimination task was used to alleviate this difficulty. Listeners reported whether a printed sentence (the prime) and an acoustically presented sentence were the same or different. The specific goal of this study was to determine the importance of the relative timing of the prime and the acoustic presentation.

Methods

Normal-hearing subjects listened to nonsense sentences that had been processed with a four-channel noise vocoder. They also read the sentences printed on a computer screen. On half the trials one of three key words in the nonsense sentence was replaced with a non-rhyming foil word. The subjects' task was to determine whether the sentence they heard was the same as the sentence they read. The printed (prime) sentence was delivered at a time that ranged from two seconds before to two seconds after the acoustic presentation.

Results

As expected from previous results from a similar task using masked speech, the delivery of the written prime before the acoustic sentence produced significantly better discrimination performance than the reverse. Additional analysis focused on the comparison between the effects of simultaneous delivery of the prime versus prior delivery of the prime, and investigated the effects of fine differences in timing of the prime within a few hundred milliseconds of the acoustic presentation.

Conclusion

The effect of priming in improving speech recognition was reaffirmed. If data analysis indicates that the precise timing of the delivery of the prime is of importance, it could have implications for how priming should be delivered as part of an auditory training program. [Work supported by NIH DC01625.]

214 The Relative Roles of Temporal Neural Cues in Predicting Speech Intelligibility

Michael Wirtzfeld¹, Ian Bruce¹

¹McMaster University

Background

Speech intelligibility predictors based on the contributions of envelope (ENV) and time fine structure (TFS) neural cues have many potential applications in hearing and communications research. However, establishing robust correlates between subjective speech perception and these neural cues has not been straightforward. The spectro-temporal modulation index (STMI) metric¹ has been able to predict the effects of presentation level on intelligibility in normal-hearing and hearing-impaired listeners² and the effects of different hearing aid compression schemes³. Despite these results, the STMI metric cannot explain speech intelligibility for "auditory chimaeras"⁴ where speech information is primarily in the TFS⁵, motivating the inclusion of TFS neural cues in the predictive models.

Methods

A speech corpus of 1,750 sentences divided into five chimaera types, subjectively evaluated by 5 normal hearing listeners, was used⁵. Using sentence pairs consisting of an unprocessed NU-6 sentence and one of five respective chimaeric forms, model auditory nerve responses⁷ were simulated. The resulting spectro-temporal characterizations, termed auditory nerve "neurograms," were subsequently processed by the STMI metric as well as the neural similarity (NSIM) metric⁶. The latter metric can capture TFS cues along with ENV related information, unlike the STMI⁵.

To investigate the ability of these metrics to predict percent-correct phoneme scores for the NU-6 chimaeras, 3 linear regression models were considered. Model 1 uses ENV and TFS with one interaction term, while Model 2 uses STMI with TFS and one interaction term. Model 3, using only the STMI metric, provides a basis of comparison.

Results

Table 1 summarizes the predictive performance of the 3 models. Relative to the STMI only, which considers only ENV cues, both Model 1 and Model 2 provide better predictive performance with the inclusion of the NSIM TFS term. It is interesting to note the combination of STMI with NSIM TFS explained more variation than the NSIM TFS and its native ENV pairing.

Conclusion

In this experimental framework, speech intelligibility predictions based solely on ENV neural cues are inadequate. Including complementary TFS cues provides better predictive performance.

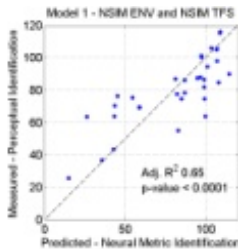
¹ Elhilali et al., Speech Comm 2003; ² Zilany & Bruce, IEEE EMBS Conf on Neural Eng 2007; ³ Leung & Bruce, IHCON 2008; ⁴ Smith et al., Nature 2002; ⁵ Ibrahim &

NSERC Discovery Grant 261736

Prediction of RAU Transformed % Correct CVC NU-6 Words

Model 1		Model 2	
ENV	258.2 (0.0002)	STMI	231.6 (< 0.0001)
TFS	-2.5 (0.986)	TFS	483.1 (< 0.0001)
ENV x TFS	397.8 (0.443)	STMI x TFS	-347.2 (0.09)
Adj. R ²	0.65	Adj. R ²	0.83
p-value	< 0.0001	p-value	< 0.0001

Regression coefficients for NSIM ENV, NSIM TFS and STMI terms and their interaction are shown along with their p-values in parenthesis. Overall goodness of fit as indicated by the Adj. R² value is also shown.



215 Consonant Identification Using Temporal-Fine Structure and Recovered Envelope Cues

Jayaganesh Swaminathan¹, Charlotte Reed¹, Louis Braidia¹, Lorraine Delhorne¹, Joseph Desloge¹
¹Massachusetts Institute of Technology

Background

The present study examined the contribution of recovered envelopes (RENVs) to the utilization of temporal-fine structure (TFS) speech cues for normal-hearing (NH) listeners. The Hilbert Transform has been used to separate speech into envelope and fine-structure components; however, this processing may not completely isolate these two components. Specifically, it has been shown that when a broadband signal is filtered through a narrow filter (such as a cochlear filter of a NH listener), the TFS component yields an envelope at the output of the filter that is similar to the envelope of the band (Ghitza, 2001). Thus, speech-reception performance with TFS signals may depend on the use of RENVs in addition to rapidly-varying fine-structure cues.

Methods

Consonant-identification experiments were conducted using speech stimuli (16 consonants in /a/-C-/a/ syllables) processed to present TFS or RENV cues. For TFS conditions: speech was filtered into *N* adjacent frequency bands over a range of 80-8020 Hz; the TFS component was extracted within each band; and the *N* resulting TFS signals were recombined to create the TFS stimulus. For RENV conditions: the TFS stimulus was filtered into *M* adjacent bands; the envelope components were extracted to yield the RENVs for each band; and the resulting

RENVs were used to modulate tone carriers equal to the center frequency of each of the *M* bands.

Experiment 1 examined the effects of exposure and presentation order using 16-band TFS and 40-band RENV speech. Experiment 2 examined the effect of varying the number of RENV bands from 4 to 40 with constant, 16-band TFS processing. Experiment 3 examined the effect of varying the number of TFS bands from 1 to 40 with constant, 40-band RENV processing.

Results

Preliminary results for Experiment 1 indicate that, with sufficient exposure, performance on TFS and RENV speech was comparable at roughly 55%-correct and that prior exposure to TFS speech aided in the identification of RENV speech. For Experiments 2 and 3, the dependence of performance on the number of TFS and RENV bands will be described.

Conclusion

This study investigates whether performance observed in previous studies of TFS speech may have been affected by the ability of NH listeners to recover envelopes from the TFS stimuli. The poor performance previously reported for hearing-impaired listeners with TFS speech may be related to an inability to recover envelopes due to broadened auditory filters.

216 The Relationship Between Background Noise Envelope Power and Speech Intelligibility in Adverse Conditions

Søren Jørgensen¹, Rémi Decorsière¹, Ewen MacDonald¹, Torsten Dau¹

¹Centre for Applied Hearing Research, Technical University of Denmark

Background

Classical models of speech perception, such as in the speech intelligibility index (SII), assume that the long-term speech-to-noise ratio and the spectral characteristics of the background noise determine intelligibility. In addition, the integrity of speech envelope fluctuations has been known to play a role in conditions with reverberation. However, recent studies have demonstrated that the inherent envelope fluctuations of the background noise also play a crucial role for the speech intelligibility in adverse conditions (Jørgensen and Dau, JASA 2011; Stone et al., JASA 2011, 2012). This is reflected in the speech-based envelope power spectrum model (sEPSM) proposed by Jørgensen and Dau (JASA, 2011), which uses the signal-to-noise envelope power ratio (SNR_{env}) as the main predictor of speech intelligibility. Here, a multi-resolution sEPSM (mr-sEPSM) is presented and evaluated in conditions with stationary and fluctuating interferers as well as in conditions where the background noise envelope power is varied systematically using a modulation processing tool (Decorsière et al., submitted). The central hypothesis is that the speech intelligibility is a monotonic function of SNR_{env}.

Methods

Model predictions were compared to literature and own data for speech mixed with three stationary and five fluctuating interferers. In addition, predictions were compared to new data obtained for speech mixed with a modified stationary speech-shaped noise (SSN) where the noise envelope power was attenuated or amplified in the modulation-frequency range between 4 and 20 Hz, while keeping the overall energy of the signal the same.

Results

Lower speech reception thresholds (SRT), i.e. better speech intelligibility, were obtained with the fluctuating noises in comparison to the stationary SSN, demonstrating speech masking release (MR). When the SSN envelope power was attenuated by 20 dB, the SRT decreased by 2 dB relative to the unprocessed SSN, suggesting a release from modulation masking. When the SSN envelope power was amplified by 20 dB, the noise took on a fluctuating character and led to an MR of 10 dB. The mr-sEPSM accounted well for the data in all conditions.

Conclusion

The envelope power of the noise alone plays a crucial role for speech intelligibility in adverse conditions. The mr-sEPSM-predictions were in good agreement with the data obtained in the various experimental conditions with stationary and non-stationary interferers, supporting the hypothesis that the SNR_{env} is a powerful objective metric for speech intelligibility prediction.

217 Abnormal Speech Processing for Hearing-Impaired Listeners in Frequency Regions Where Absolute Thresholds Are Normal

Agnes C. Leger^{1,2}, Brian C.J. Moore³, Christian Lorenzi^{1,2}
¹*Institut d'Etude de la Cognition, Ecole Normale Supérieure, Paris, France*, ²*Laboratoire Psychologie de la Perception, Université Paris Descartes, UMR CNRS 8158, Paris, France*, ³*Department of Experimental Psychology, University of Cambridge, Cambridge, UK*

Background

Speech intelligibility is reduced for listeners with sensorineural hearing loss, especially in noise. The extent to which this reduction is due to reduced audibility or supra-threshold deficits is still debated. The specific influence of supra-threshold deficits on speech intelligibility was investigated.

Methods

The intelligibility of nonsense speech signals in quiet and in various noise maskers was measured for normal-hearing (NH) and hearing-impaired (HI) listeners with hearing loss in high-frequency regions. Participants in both groups had a wide range of ages. The effect of audibility was limited by filtering the signals into low (≤ 1.5 kHz), mid (1-3 kHz) and low+mid (≤ 3 kHz) frequency regions, where pure-tone sensitivity was normal or near-normal for the HI listeners. The influence of impaired frequency selectivity on speech intelligibility was investigated for NH listeners by

simulating broadening of the auditory filters using a spectral-smearing algorithm. Temporal fine structure sensitivity was estimated for NH and HI listeners by measuring sensitivity to interaural phase differences. Otoacoustic emissions and brainstem electrical responses were measured.

Results

HI listeners showed mild to severe intelligibility deficits for speech in quiet and in noise. Similar deficits were obtained for steady and fluctuating noises. Simulated reduced frequency selectivity also led to deficits in intelligibility for speech in quiet and in noise, but these were not large enough to explain the deficits found for the HI listeners. The results suggest that speech deficits for the HI listeners may result from suprathreshold auditory deficits caused by outer hair cell damage and by factors associated with aging. The influence of temporal fine structure sensitivity remains unclear.

Conclusion

Speech intelligibility can be strongly influenced by supra-threshold auditory deficits. Audiometric thresholds within the "normal" range (better than 20 dB HL) do not imply normal auditory function.

218 A Blind Binaural Speech Intelligibility Prediction Model

Stefano Cosentino¹, John Culling², Tiago Falk³, Torsten Marquardt¹, David McAlpine¹
¹*University College London*, ²*University of Cardiff*, ³*University of Quebec (INRS-EMT)*

Background

The ability to hear out speech in noisy environments is considerably enhanced using both ears compared with purely monaural listening. Brain mechanisms underlying enhanced speech recognition in noise have been studied intensively and a number of binaural models have been proposed in order to predict speech intelligibility. Despite several of these models being able to achieve high correlations with subjective ratings, however, their practical usage is limited, as they all require a priori knowledge of the room acoustics, such as the room impulse response (RIR). Here, we develop and evaluate a blind measure to predict speech intelligibility based on an auditory-inspired model.

Methods

The proposed binaural model implements an equalization-cancellation stage together with a modulation frequency estimation stage. The binaural advantage was obtained as a combination of the Better Ear and Binaural Unmasking advantages. Our model "BiSIM", was first tested in anechoic using a single speech interferer paradigm. In a second set of experiments, the model was tested in conditions involving up to three simultaneous interferers in anechoic environments.

Results

Predictions from the model were compared with those obtained with an established "non-blind" model proposed by Lavandier and Culling (2010, *J. Acoust. Soc. Am.* 127, 387-399), as well as with data from studies investigating subjective SRTs (Speech Receptive Thresholds). Our experimental data indicate that the proposed blind model provides reliable predictions in anechoic rooms and single interferer, with correlations as high as 0.99. In multiple masker conditions, the models can still reliably predict subjective SRTs, although smaller correlations were found.

Conclusion

The proposed binaural blind model was successfully tested in anechoic environments, and in conditions involving multiple interferers. The data also suggest the importance of modulation energies in predicting binaural speech intelligibility. Further investigations will be directed towards solving some of the model limitations.

219 Effects of Glottal Phase on Negative Level Effects ("rollover") in Speech Perception

Van Summiers¹, Eric Thompson², Nandini Iyer², Douglas Brungart¹

¹Walter Reed National Military Medical Center, ²Wright-Patterson Air Force Base

Background

Speech recognition performance worsens above moderate presentation levels (~72 dB SPL). This "rollover" in performance is most evident in noisy conditions and is seen for both normal hearing and hearing impaired listeners. In a number of psychophysical tasks, level differences appear to influence auditory processing more for very "peaky" waveforms (such as a glottal wave) than for less modulated signals. The current research examined whether varying the shape of the glottal source exciting the speech envelope might influence the amount of rollover in speech scores at high levels.

Methods

Experienced normally hearing listeners were tested on sentences from the Modified Rhyme Test (MRT) at a +12 dB signal-to-noise ratio. Sentences were set to a levels of 48, 56, 64, 72, 80 or 88 dB SPL and then high-pass filtered with a 2.5 kHz cutoff frequency. Original MRT stimuli were presented along with stimuli that were resynthesized by applying a 64-channel vocoder to an excitation signal consisting either of noise or one of three types of harmonic complexes with different phase relationships generating different amounts of waveform peakiness (random phase, Schroeder-phase, or cosine phase).

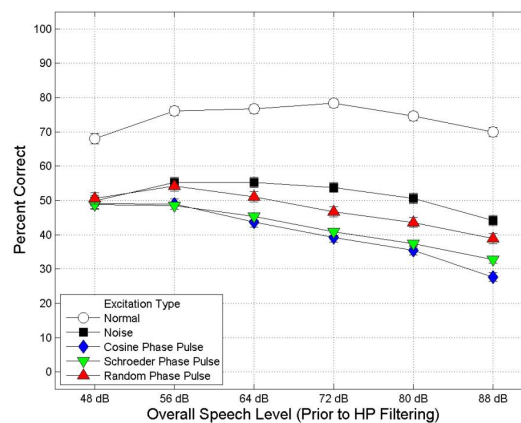
Results

Unprocessed MRT sentences produced higher scores than any of the resynthesized stimuli. Consistent with previous findings, unprocessed sentences showed rollover with a decrease in scores of ~10% as levels increased from 72 to 88 dB SPL. The processed sentences all showed similar performance at the lowest (48 dB SPL) level but varying

amounts of rollover as levels increased. The stimuli synthesized using the peakiest (cosine-phase) source function showed the most rollover, decreasing by more than 20% between 56 and 88 dB SPL.

Conclusion

The greater rollover seen for the peaky cosine-phase stimuli may be related to recent results on auditory localization (Brungart and Simpson, *Proc Int Conf Aud Disp*, 2008) which showed that vertical localization accuracy decreases for peaky click-train stimuli as levels increases from 50 to 80 dB SPL. Stimuli with less peaky waveforms did not show this level dependence. The current results may indicate that the peaky glottal waveform underlying natural speech contributes to rollover at high presentation levels. Development of speech synthesis techniques using less peaky glottal sources may lead to more intelligible speech stimuli when high presentation levels are required, as is often necessary to address audibility issues in hearing-impaired listeners.



220 Pilot Experiments for a Behavioral Model to Detect Tinnitus in Guinea Pigs

Amarins Heeringa^{1,2}, Martijn Agterberg³, Hans Segenhout¹, Nima Ilbegi⁴, Pim van Dijk^{1,2}

¹University Medical Center Groningen (UMCG), dept. of Otorhinolaryngology, Groningen, ²University of Groningen, Graduate School of Behavioral and Cognitive Neurosciences, ³Radboud University Medical Centre, Donders Institute for Brain, Cognition and Behaviour, Nijmegen, ⁴University of Groningen, Groningen, The Netherlands

Background

To confirm the presence of tinnitus in animals, behavioral models aim at assessing the inability to detect silence. We explored whether guinea pigs can be trained to detect silence. Initially, we replicated earlier experiments, that showed how guinea pigs can be conditioned to an external sound stimulus. Subsequently, we tested whether guinea pigs could be trained to detect a silent gap in noise.

Methods

Seven male guinea pigs were trained in a shuttle box with two compartments to shuttle at the presence of a conditioned stimulus (CS). When subjects failed, an air puff (the unconditioned stimulus, US) was applied as a

motivator. A training consisted of 10 daily sessions, with each session containing 20 trials. Hearing thresholds were determined using auditory brainstem responses.

Results

Guinea pigs could be conditioned to a broadband noise (BBN) burst. After 10 training sessions, most animals (5/7) showed >85% correct avoidance responses (CAR) to the CS. Additionally, animals were able to generalize between sound levels ranging from 58 dB to 88 dB, where a higher sound level providing better performance. Subsequent training of these same animals to a silent gap in noise was unsuccessful.

Conclusion

We were able to replicate and confirm the findings of Agterberg et al.: Guinea pigs could be rapidly conditioned to a BBN. In contrast, gap detection performance was much poorer, possibly due to the previous trainings to BBN. Therefore, currently ongoing experiments are aimed at conditioning naïve guinea pigs to a silent gap.

221 Tinnitus or Hearing Loss: What Is Gap Detection Actually Measuring?

Ryan Longenecker^{1,2}, Alex Galazyuk¹

¹Northeast Ohio Medical University, ²Kent State University, Biomedical Sciences

Background

Gap-induced prepulse inhibition of the acoustic startle reflex (GPIAS) has become a popular technique for tinnitus assessment in laboratory animals. This method has been praised for its relative behavioral simplicity but challenged on its fundamental principles. The skepticism is derived from the concern that sound exposed animals might be detecting hearing loss, rather than tinnitus, caused by unilateral exposure. This question should be definitively answered before this method will be accepted as a reliable test for tinnitus. The goal of this study was to address this question. Assuming that the tinnitus percept is centrally generated, we wanted to test whether it can be detected using the unexposed (intact) ear following unilateral sound exposure.

Methods

To induce tinnitus, CBA/CaJ mice were sound exposed unilaterally to a narrowband noise (116 dB) centered at 12.5 kHz for 1 hour under general anesthesia (Ketamine/Xylazine). Auditory brainstem responses were recorded before and after sound exposure to insure its effectiveness. Before and at different time points after sound exposure, GPIAS performance was monitored in every mouse for behavioral evidence of tinnitus.

Results

Prior to sound exposure all mice demonstrated good gap detection at all frequencies tested (8, 10, 12.5, 16, 20 kHz), with two ears intact or with either left or right ear obstructed. After sound exposure about half of exposed mice displayed consistent deficits in gap detection at or bordering the frequencies at or bordering the exposure

frequency (12.5 kHz) suggesting the presence of tinnitus. Following tinnitus confirmation with two ears unobstructed, the sound exposed ear was blocked with a silicone ear plug (Kwik-Sil WPI) and the test was repeated. In this testing condition the vast majority of animals exhibited analogous gap detection deficits as in the initial test with two ears unobstructed.

Conclusion

Following unilateral sound exposure, GPIAS reveals gap detection deficits using the unexposed ear. This strongly suggests that these deficits are not linked to hearing loss but represent behavioral evidence of tinnitus.

222 Loss of Gap-Induced Suppression of Acoustic Startle in Hamsters Following Intense Sound Exposure

Guoyou Chen¹, Calvin Lee¹, Nauman Manzoor¹, James Kaltenbach¹

¹Cleveland Clinic

Background

Suppression of acoustic startle by gaps in noise has been found to be reduced following exposure to intense sound or treatment with salicylate. This is often interpreted as evidence of tinnitus, the argument being that tinnitus fills in the gap when the pitch of the tinnitus is similar to that of the background noise. Here, we investigated the use of this method to test for the induction of tinnitus in Syrian golden hamsters.

Methods

We tested: 1) the relationship between startle response amplitude and startle stimulus level (57-120 dB SPL) with no background noise, 2) the effects of adding 70-85 dB SPL background noise on the startle amplitude, and 3) the effects of 50 ms gaps in the background noise on startle using various combinations of background noise and startle stimulus levels to determine what conditions are optimal for maximizing both the degree of gap-induced startle suppression and the weakening of this suppression effect following intense sound exposure. The tests were conducted in control (n=9) and intense tone exposed (10 kHz, 115 dB SPL, 4 hrs) hamsters (n=9).

Results

We found that hamsters display vigorous startle responses that grow in amplitude with increases in startle stimulus level. Exposed animals showed no change in startle thresholds relative to those in controls but showed an enhancement of startle at high startle stimulus levels. Addition of background noise preceding the startle stimulus had little effect on startle in control animals but had a strong suppressive effect on startle in sound exposed animals. When gaps were embedded in background noise preceding the startle stimulus, startle was further suppressed at all background noise levels and at all startle stimulus levels in control animals. In contrast, there was a marked reduction of gap-induced suppression of startle in exposed animals. Thus, weakening of gap induced suppression of startle paradoxically occurred

simultaneous with a strengthening of suppression of startle by background noise. The weakening of gap induced suppression of startle was not accompanied by changes in the suppression of startle by brief pulses that preceded the startle stimulus.

Conclusion

The loss of gap suppression after sound exposure without a corresponding change in prepulse inhibition is consistent with the interpretation that the exposure caused induction of tinnitus in hamsters. The results are also suggestive of different inhibitory mechanisms that control startle magnitude which are differentially affected by acoustic overstimulation. (Supported by NIH grant R01 DC009097).

223 Two Major Improvements for Using the Gap Detection Method to Assess Tinnitus-Like Behavior in Mice

Jianxin Bao¹, Yong Zhang¹, Debin Lei¹, Zoe Lu¹, Yixin Chen¹, Olivia Mao¹

¹Washington University

Background

Tinnitus is a major, growing health problem that affects the quality of life of millions of people. While formally defined as the perception of sound in the absence of a physical sound stimulus, people with tinnitus also report concentration difficulties, irritability, sleep disruption, anxiety and depression. There currently is no reliable treatment for tinnitus mainly due to a lack of understanding of its molecular mechanisms. With extensive molecular tools such as transgenic methods, mouse models for tinnitus would greatly facilitate this area of research. Although several animal behavior models including the gap detection method have been developed to study tinnitus in various types of animals, these methods have been difficult to apply in mouse studies. One major weakness of the gap detection method for mice is the use of average amplitude ratios between gap prepulse inhibition reflex and startle reflex as a measurement for tinnitus-like behavior. There are two reasons behind this weakness. First, the amplitude reduction of the startle reflex has been consistently observed after tinnitus induction. In addition, the neural pathway is different between the startle reflex and gap pre-pulse inhibition reflex. Second, we have found that most of behavior data is not normally distributed.

Methods

To solve these two issues, we first adopted the Kernel density method to select data for each trial, which solved the issue of abnormal data distribution. Next, we use the amplitude ratios between gap prepulse inhibition reflex and prepulse inhibition reflex as a measurement for tinnitus-like behavior.

Results

With these two major improvements, we can detect tinnitus-like behavior at specific frequencies in most of mice only one hour after sodium salicylate injection (350 mg/kg). This modified method is currently being tested in a noise-induced tinnitus mouse model.

Conclusion

One main goal of our studies is to study molecular mechanisms underlying tinnitus pathology in mice. With our two major improvements, the gap detection method can be an effective way to determine tinnitus-like behavior in mice, which paves way for us to study molecular signaling pathways involved in tinnitus.

224 Simulated Small Arms Fire Exposure in Rats Results in Reduced Gap Inhibition of the Acoustic Startle Reflex Suggesting Induction of Tinnitus

Dave Dolan¹, Susan Shore¹, Josef Miller¹, Karin Halsey¹, Diane Prieskorn¹, Ariane Kanicki¹, Peter Ghisleni¹, Rick Altschuler¹

¹KHRI

Background

Hearing loss resulting from exposure to ammunition discharge is a common finding in our military population. Both hearing loss and tinnitus are the leading causes for disability discharge from military service. Prevention or reduction of hearing loss and tinnitus would be of great social and economic benefit. Here we present preliminary findings of an animal model using simulated small arms fire (SAR) to induce hearing loss and tinnitus.

Methods

Sprague Dawley rats were unilaterally exposed to 50 biphasic impulses via a compression driver over a 2.5 minute period. The impulse level was either 152 or 160 dB SPL. Control rats received sham noise exposure. ABR measurements evaluated the effect of the exposure. The acoustic startle response (ASR), pre-pulse (PPI) and gap inhibition (GI) were used to evaluate the development of tinnitus.

Results

Sham treated animals showed stable ABR thresholds and consistent ASR, PPI and GI throughout the experiment. In general, animals exposed to the 160 dB stimulus showed significant unilateral ABR threshold shifts and reduced startle amplitudes sometimes resulting in "floor" effects and inconclusive PPI and GI ASR results. Animals exposed to the 152 dB stimulus showed reduced elevations in ABR thresholds compared to the 160 dB exposure. Startle amplitudes were either unaffected by the 152 dB exposure or increased in amplitude. PPI remained intact post exposure. In over half of the animals receiving the 152 dB stimulus GI decreased, suggesting the presence of tinnitus. In some animals, the presence of the gap in noise caused enhancement of the startle response, suggestive of the presence of hyperacusis.

Conclusion

More than half of the rats exposed to SAR exhibited reduced GI of the ASR but intact PPI, indicative of the induction of tinnitus by this exposure condition. Supported by DOD grant W81XWH-10-PRMRP-IIRA and NIDCD P30 grant DC005188

225 Effect of Low-Level Laser Therapy on Salicylate-Induced Tinnitus in Rat

Young-Min Park¹, Woo Sung Na¹, Min Young Lee¹, Jae Wook Lee¹, Il Yong Park¹, Myung-Whan Suh², Chung-Ku Rhee¹, **Jae Yun Jung**¹

¹Dankook University, ²Seoul National University Hospital

Background

Tinnitus is a perception of sounds without external source. Mainly because of the subjective nature of the disorder and our lack of knowledge of its pathophysiology, treatment of tinnitus has been unsuccessful. Low-level laser therapy (LLLT) has been introduced as an alternative treatment for tinnitus. Although many studies have been conducted for assessing a meaningful relief of tinnitus intensity, there has been no study to quantify the effect of LLLT on the treatment of tinnitus in animal model. Therefore, the aim of this study was to measure the effect of LLLT on salicylate-induced tinnitus in the rat model using GPIAS (gap prepulse inhibition of acoustic startle).

Methods

10 Sprague Dawley rats (8 weeks; 240~280g) were divided into 2 groups, one for the laser group (n=5) and another for the control group (n=5). Rats of both group were treated with 400mg/kg/day of sodium salicylate for 8 consecutive days. Tinnitus was monitored using GPIAS 2 hours after first salicylate treatment, and every 24 hours during 9 days of treatment. Rats in laser group was irradiated with wavelength of 830 nm diode laser at 165mW/cm² for 30 min to each ear daily for 8 days.

Results

GPIAS value of both two groups was significantly decreased after sodium salicylate administration, which means tinnitus was well induced in both groups. The day after treatment start, LLLT had a tendency to increase GPIAS value of study group and a statistically significant difference was noted at 120 hours after drug administration. No significant changes in NBPIAS were observed before and after salicylate injection over the entire testing period.

Conclusion

Our result shows that LLLT may provide a feasible therapeutic approach to control tinnitus. Further experimental studies are needed to find better method to facilitate LLLT efficacy and possible mechanism.

226 Single Dose Alcohol Has Protective Effect on Behavioral Deficits Post Blast-Exposure

Diana Peterson¹, Gregory Mlynarczyk¹

¹Iowa State University

Background

Alcohol has been shown to have both neuroprotective and deleterious effects after traumatic brain injury. Alcohol acts on numerous receptors within the brain (including GABAergic receptors). Non-chronic alcohol consumption works by keeping GABAergic receptors open longer, and

thus increasing neural inhibition. During blast-exposure, we have observed micro-tears centered on GABAergic neurons. We hypothesize that single-use alcohol may increase the efficacy of intact or slightly damaged GABAergic neurons and thus help re-stabilize circuitry that has sustained damage to GABAergic neurons.

Methods

To test this hypothesis, animals were orally gavaged ethanol either immediately prior or 2 days post blast exposure. They were monitored for motor ability with RotoRod and Versimax. They were also monitored for tinnitus with acoustic startle tests. To allow statistical comparisons of behaviors pre/post blast-exposure in each animal, all tests were performed both prior and post blast-exposure.

Results

Thirty minutes after alcohol administration all animals had a significant motor impairment. Analysis of behavioral measures pre/post blast-exposure indicated that the alcohol groups performed better in motor tests and had decreased incidences of tinnitus after blast-exposure.

Conclusion

We conclude that single-dose alcohol has protective effects on behavioral measures of injury after blast-induced traumatic brain injury.

227 Prevalence of Tinnitus and Its Relationship with Anxiety and Depression

Abby McCormack^{1,2}, Heather Fortnum¹, Mark Edmonson-Jones¹, Robert Pierzycki¹, Oliver Zobay², Dave Moore²

¹NIHR Nottingham Hearing Biomedical Research Unit,

²MRC Institute of Hearing Research

Background

In the 1980s, about 10% of UK adults reported experiencing prolonged, spontaneous tinnitus lasting for more than five minutes. However, the current prevalence is unknown and large-scale studies of tinnitus are lacking. Furthermore, although many people learn to live with tinnitus, for some people it can be severely distressing. Clinical studies indicate a strong association between tinnitus and mental health, with increased risk for depression and anxiety among tinnitus patients. However little is known about how the severity of tinnitus is related to these disorders. The aim was to update the prevalence of tinnitus and further examine the association between the severity of tinnitus and anxiety and depression.

Methods

A cross-sectional design study of 502,713 people (54.4% female; 45.6% male) from across Britain aged between 40-69 years who participated in UKBiobank between 2006-2010. UKBiobank is a resource set up to support research intended to improve the prevention, diagnosis and treatment of illness. Two questions on tinnitus asked whether participants had experienced ringing or buzzing for more than five minutes at a time, and if so how much it worries, annoys or upsets them. Participants were also

asked whether they had visited a GP/psychiatrist for nerves, anxiety, tension or depression, and specific questions on depression, including whether they had ever been depressed for at least a week, their longest period of depression, and number of depressive episodes. Associations between these factors and tinnitus characteristics were investigated using multiple regression techniques.

Results

17.7% of participants experienced tinnitus at least some of the time and, of these, 20.2% (3.6% of the total) had moderate or severe tinnitus, suggesting the prevalence of tinnitus in this age group could be much higher than previously thought. Of the whole sample, 34.1% indicated having seen a doctor (11.6% had seen a psychiatrist) for nerves, anxiety, tension or depression. 53.2% of the sample indicated being depressed for at least a week. The mean longest period of depression was 15.9 weeks and the mean number of depressive episodes was 6.3.

Conclusion

Data on prevalence and severity of tinnitus within the UK Biobank participants, and its relationship with anxiety and depression, suggest a stronger than expected association between these conditions in the UK's middle-aged population. These data will contribute to appropriate resourcing, prevention, identification and management strategies for people with tinnitus in the medium term.

228 Prefrontal Cortex Activity Is Related to the Tinnitus Percept – Group Differences and Correlations Revealed by Functional Magnetic Resonance Imaging

Anna Seydell-Greenwald¹, Amber Leaver¹, Theodore Turesky¹, Susan Morgan², H. Jeffrey Kim³, Josef Rauschecker¹

¹Georgetown University Medical Center, ²Georgetown University Hospital, ³Georgetown University Hospital - HNS

Background

Tinnitus, a phantom “ringing in the ears” affecting 10-15% of the population, is commonly attributed to changes in the central auditory system following damage to the peripheral auditory system. There is also increasing evidence for a role of non-auditory (especially limbic and prefrontal) brain areas in tinnitus, e.g. from group comparisons based on anatomical magnetic resonance imaging and resting-state magnetoencephalography (MEG). Compared to MEG, functional magnetic resonance imaging (fMRI) has superior spatial resolution; however, the vicinity of the sinuses leads to signal loss in ventral prefrontal cortex. The present study used a modified data acquisition scheme that ameliorates this problem and employed multiple conditions with auditory stimulation to further elucidate the role of ventromedial prefrontal cortex (vmPFC) in tinnitus.

Methods

Functional MRI was performed on 20 tinnitus patients and 20 control participants without tinnitus, who were matched for age, sex, and hearing loss. Each patient, and his or her matched control, listened to band-passed noise bursts at center frequencies spanning the human hearing range, one of which was matched to the patient's tinnitus frequency. In a control condition, no sound was played. To avoid compromising the conditions by scanner noise, fMRI data were acquired intermittently rather than continuously, and images were acquired in tilted slices to avoid cutting through the sinuses and improve the fMRI signal in ventral prefrontal cortex. Questionnaires assessed tinnitus-related measures such as tinnitus loudness, tinnitus distress, noise sensitivity, depression, and anxiety.

Results

When comparing patients and controls regarding the fMRI signal change between the condition with stimulation at the tinnitus frequency and the condition without stimulation, significant group differences were found in right vmPFC and right superior temporal gyrus (STG), including the putative location of primary auditory cortex. Post-hoc analyses constrained to these regions revealed a strong correlation between tinnitus loudness and vmPFC activation in tinnitus patients, especially during stimulation at the tinnitus frequency ($r = 0.74$). In contrast, correlations with tinnitus distress, noise sensitivity, depression, and anxiety were negligible.

Conclusion

These fMRI findings add to the evidence that vmPFC plays a role in tinnitus perception. The absence of correlations between vmPFC activation and measures of depression, anxiety, and tinnitus distress indicate that this role is not in the emotional evaluation of the tinnitus percept. Instead, the strong correlations between vmPFC activation and tinnitus loudness agree with our hypothesis that vmPFC activation can modulate the tinnitus percept (Rauschecker et al., 2010).

229 Tinnitus-Related Dissociation Between Cortical and Subcortical Neural Activity in Humans with Mild to Moderate Sensorineural Hearing Loss

Emile de Kleine¹, Kris Boyen¹, Pim van Dijk¹, Dave R.M. Langers¹

¹University Medical Center Groningen

Background

Tinnitus is a phantom sound percept that is strongly associated with peripheral hearing loss. However, only a fraction of all hearing-impaired subjects develops tinnitus. This may be based on differences in the function of the brain between those subjects that develop tinnitus and those that do not.

Methods

Cortical and sub-cortical sound-evoked brain responses in 34 hearing-impaired chronic tinnitus patients and 19 hearing level-matched controls were studied using 3-T

functional magnetic resonance imaging (fMRI). Auditory stimuli were presented to either the left or the right ear at levels of 30-90 dB SPL. We extracted neural activation as a function of sound intensity in eight auditory regions (left and right auditory cortices, medial geniculate bodies, inferior colliculi and cochlear nuclei), the cerebellum and a cinguloparietal region.

Results

The activation correlated positively with the stimulus intensity, and negatively with the hearing threshold. We found no differences between both groups in terms of the magnitude and lateralization of the sound-evoked responses, except for the left medial geniculate body and right cochlear nucleus where activation levels were elevated in the tinnitus subjects. We observed significantly reduced functional connectivity between the inferior colliculi and the auditory cortices in tinnitus patients compared to controls, both for ipsilateral and contralateral connections.

Conclusion

Our results suggest abnormal thalamic gating in the development of tinnitus.

230 Functional Connectivity Between Auditory, Default-Mode, and Cognitive-Control Networks in Tinnitus and Hearing Loss

Jennifer Melcher^{1,2}, Inge Knudson^{1,2}

¹Mass. Eye and Ear Infirmary, ²Harvard Medical School

Background

It is hypothesized that aberrantly correlated activity among brain areas may be important to sustaining the tinnitus condition, defined as the perception of phantom sound and the emotions surrounding the percept. The present study tested this hypothesis by comparing functional connectivity between human subjects with tinnitus and without. Functional connectivity indicates the degree to which activity in one brain area is temporally correlated with that in another.

Methods

Functional magnetic resonance imaging (fMRI) was performed on subjects in three groups: (1) high-frequency hearing loss and tinnitus (HFL-tinnitus), (2) clinically normal hearing sensitivity and tinnitus (cNH-tinnitus) and, (3) no tinnitus and threshold-matched to group 2 (cNH-control). A structural MRI of each subject was also obtained and segmented into regions of interest (ROI) comprising cortical gray matter. The ROIs were used to seed connectivity analyses of the fMRI data. Specifically, a correlation coefficient was calculated between the fMRI signal time-course within an ROI and the signal time-course of each voxel in the brain, resulting in a spatial map of correlations with the ROI seed. White matter and cerebrospinal fluid signals were regressed out. Maps of correlation for each subject were smoothed and entered into a second-level analysis for inter-group comparison.

Results

In the absence of any explicit sound stimulus, primary auditory cortex (PAC) of the cNH-control group showed: (1) positive correlations with both adjacent and contralateral auditory cortical areas (including contralateral PAC), (2) positive correlations with supplementary motor cortex (SMA) and pre-SMA, nodes of a previously-defined cognitive control network, (3) negative correlations with posterior cingulate/precuneus (PCC), right and left parietal lobes and, medial prefrontal cortex. The regions showing negative correlations are major nodes in the default mode network, which is active when external demands (e.g. listening) are not being placed on a subject. While cNH-tinnitus and HFL tinnitus subjects showed correlations between PAC and the same brain areas as cNH-controls, the magnitude of the correlations with non-auditory areas (but not auditory ones) was reduced. The reductions were significant in SMA/pre-SMA and PCC. They were greatest for the HFL tinnitus group.

Conclusion

The results demonstrate a conduit by which exogenous auditory information can interact with endogenous signals of the cognitive-control and default-mode networks and further suggest that this conduit may not operate normally in those with tinnitus, and especially those with hearing loss and tinnitus.

231 The Relation Between Perception and Brain Activity in Gaze-Modulated Tinnitus

Kris Boyen¹, Margriet J. van Gendt¹, Emile de Kleine¹, Dave R.M. Langers¹, Pim van Dijk¹

¹University Medical Center Groningen

Background

Tinnitus is a phantom sound percept that can be severely disabling. Its pathophysiology is poorly understood, partly due to the inability to objectively measure neural correlates of tinnitus. Gaze-modulated tinnitus (GMT) is a rare form of tinnitus that may arise after vestibular schwannoma removal. Subjects typically describe tinnitus in the deaf ear on the side of the surgery that can be modulated by peripheral eye gaze. This phenomenon offers a unique opportunity to study the relation between tinnitus and brain activity.

Methods

We included 18 patients with GMT and 9 controls. Pure-tone audiometry was performed in all subjects. Subjects with tinnitus also performed tinnitus matching tasks for six gaze directions. Cortical and sub-cortical brain responses were studied using 3-T functional magnetic resonance imaging (fMRI). The scanning paradigm included the same six gaze directions and one bilateral sound condition.

Results

In normal-hearing control subjects, peripheral gaze resulted in inhibition of the auditory cortex, but no detectable response in the medial geniculate body and inferior colliculus. In patients with GMT, peripheral gaze (1) reduced the cortical inhibition, (2) inhibited the medial

geniculate body, and (3) activated the inferior colliculus. Furthermore, increased tinnitus loudness was represented by increased activity in the cochlear nucleus and inferior colliculus and reduced inhibition in the auditory cortex.

Conclusion

The increase of cochlear nucleus and inferior colliculus activity with peripheral gaze is consistent with models of plastic reorganization in the brainstem following vestibular schwannoma removal. The decrease of activity in the medial geniculate body and the reduced inhibition of the auditory cortex support a model that attributes tinnitus to a dysrhythmia of the thalamocortical loop, leading to hypometabolic theta activity in the medial geniculate body. Our data offer the first support of this loop hypothesis of tinnitus, independent of the initial experiments that led to its formulation.

232 Auditory Evoked Magnetic Fields in Individuals with Tinnitus

Magdalena Sereda¹, Peyman Adjamian², Alan R. Palmer², Mark Edmondson-Jones¹, Deborah A. Hall¹

¹NIHR Nottingham Hearing Biomedical Research Unit,

²MRC Institute of Hearing Research

Background

Recent theories postulate that some forms of tinnitus are likely to be perceptual consequence of altered neural activity in the central auditory system triggered by damage to the auditory periphery. Despite reduced input from the cochlea and auditory nerve after noise exposure or ototoxic drugs, many animal studies have observed changes in sound-evoked firing rate, as well as amplitude of the evoked responses in inferior colliculus and auditory cortex. However, human electrophysiological evidence is rather equivocal. While some studies reported increased N1/N1m amplitude and shorter latencies in tinnitus patients compared to controls, others reported reduced N1/N1m amplitudes and prolonged latencies, and some found no differences.

Methods

The present study used magnetoencephalography (MEG) to seek evidence for altered evoked responses in people with tinnitus compared to controls. We have measured evoked magnetic fields in response to 300-ms tone bursts were presented at 40 dB SL in 22 people with tinnitus as well as in 13 participants with normal hearing and no tinnitus and 7 participants with matched hearing loss but without tinnitus. We applied channel-space analysis to compare the amplitudes and latencies of N1m responses to four different tone categories: a control tone, edge frequency, dominant tinnitus pitch and a tone within the area of hearing loss. All participants were screened to exclude hyperacusis.

Results

In agreement with the previous literature we found decreasing N1m amplitudes and only minimal shift in N1m latencies with increasing frequencies. Amplitudes of the evoked responses differed depending on the tone

category, but there was no difference in this pattern across tinnitus and control groups. Overall, N1m amplitudes to the dominant tinnitus pitch were significantly smaller than for the control and audiometric edge frequencies and were similar to the tone within the hearing-loss region.

Conclusion

Dominant tinnitus pitch is typically within the area of hearing loss. We thus conclude that differences in the evoked responses pattern in participants with tinnitus were related more to the hearing loss than to the presence of tinnitus. This indicates lack of a generalised tinnitus-specific hyperexcitability in response to sound stimuli.

233 "Distressed Aging" - The Differences in Brain Activity Between Early- And Late-Onset Tinnitus

Jae-Jin Song¹, Dirk De Ridder¹, Winfried Schlee², Paul Van de Heyning³, Sven Vanneste¹

¹Brai@-n, TRI & Department of Neurosurgery, University Hospital Antwerp, Belgium., ²Department of Clinical and Biological Psychology, University of Ulm, Germany.,

³Brai@-n, TRI & ENT, University Hospital Antwerp, Belgium.

Background

Recent findings regarding different characteristics according to the age of tinnitus onset prompted us to conduct a study on the differences in tinnitus-related neural correlates between late-onset tinnitus (LOT; mean onset age, 60.4 years) and early-onset tinnitus (EOT; mean onset age, 29.7 years) groups.

Methods

We collected quantitative electroencephalography findings of 29 participants with LOT and 29 with EOT, as well as those from 59 controls. Then, LOTs were subdivided into 14 high distress (HD)/15 low distress (LD), while EOTs into 14 HD/15 LD. We then compared the results using resting state electroencephalography source-localized activity and connectivity analyses.

Results

Compared to the EOT and older control groups, the LOT group demonstrated increased localized activity and functional connectivity in components of previously described tinnitus distress networks, as well as the default mode and intrinsic alertness networks, such as the prefrontal cortices, dorsal anterior cingulate cortex, and insulae. On subgroup comparisons, the ACC was activated more in HD-LOT participants than in LD-LOT participants, while the orbitofrontal cortex was activated more in HD-EOT than in LD-EOT.

Conclusion

The current findings of intrinsic differences in tinnitus-related neural activity between the LOT and EOT groups may be applicable for planning individualized treatment modalities according to age of onset. Moreover, differences with regard to the age of tinnitus onset may be

a milestone for future studies on onset-related differences in other similar pathologies, such as pain or depression.

234 Establishing the Tinnitus/Epilepsy Connection

Christine Ouellette¹, Avril Genene Holt², Anthony Cacace¹

¹Wayne State University, ²Wayne State University School of Medicine

Background

Throughout history, parallels have been drawn between tinnitus and epilepsy. Tinnitus is described as the perception of ringing or buzzing in the absence of external stimulation while epilepsy is often characterized by seizures that are recurrent and unprovoked. Similarities between the two conditions include suggested mechanisms related to underlying electrophysiology (neuronal hyperactivity, bursting discharges, neural synchrony across brain areas), alterations in intrinsic neurochemistry (reduced intra-cortical inhibition), and changes in gamma aminobutyric (GABA) and glutamate receptors after kindling and noise induced hearing loss (Valentine et al., 2004). There are also treatment modalities common to both, including: pharmacological, electrical (vagus nerve stimulation, VNS), magnetic (repetitive transcranial magnetic stimulation, rTMS), and deep brain stimulation (e.g., Engineer et al., 2011; Connor et al., 2012; Fisher, 2012). Understanding the link between tinnitus and epilepsy may provide new treatment strategies for these conditions.

Methods

We have developed and collected results from an online survey made available to members of the American Tinnitus Association (ATA). The survey remained accessible for five weeks and more than 250 members with tinnitus (between the ages of 18 and 80) responded.

Results

The incidence of epilepsy has been reported to be 3% of the population in the United States. The prevalence of active epilepsy in our society has been reported to be as high as 1%. In the current study we found that five percent of the respondents that report tinnitus were also diagnosed with epilepsy.

Conclusion

These results suggest that epilepsy may occur with greater frequency in the tinnitus population than in the general population. Further investigation into a possible tinnitus/epilepsy link should include surveys regarding tinnitus/epilepsy perception administered to epilepsy sufferers. These survey results begin to lay a foundation for studies examining common mechanisms between tinnitus and epilepsy.

235 Defining Uncertainties in Tinnitus

Treatments

Deborah Hall¹, Najibah Mohamad¹, Lester Firkins², David Stockdale³

¹NIHR Nottingham Hearing Biomedical Research Unit,

²James Lind Alliance, ³British Tinnitus Association

Background

A James Lind Alliance (JLA) Tinnitus Priority Setting Partnership has identified and prioritise unanswered research questions about tinnitus assessment, diagnosis and treatment. This process gives a voice to members of the public and clinicians and is driven by them.

Methods

Our methods included the following four steps: (1) established a working partnership between representatives for patients and clinicians; (2) designed and disseminated a questionnaire to identify and collect tinnitus uncertainties; (3) reduced the 2483 submitted questions down to a list of 170 edited questions by pooling duplicates and removing questions that had already been answered by systematic review; and (4) prioritised these remaining questions to create a 'top 10'.

Results

The highest ranked question (A) (Table 1) concerned management strategies and combined three separate questions asking about lifestyle changes, promoting habituation and learning to live with tinnitus. This is of the most concern to people with tinnitus. Systematic reviews have criticised the poor quality of trials [1-2] and an international standard has been proposed [3]. For hearing healthcare professionals, the second question (B) asked whether cognitive behaviour therapy (CBT)/psychological therapy, delivered by audiology professionals, is effective for people with tinnitus. Systematic reviews support a moderate benefit to patients from CBT [4], but studies tend to involve trained psychologists delivering the therapy which is not the usual model of care in the UK. C addressed the effectiveness of management strategies for patients with tinnitus and insomnia. Whilst sound therapy is commonly used by tinnitus patients at night, it is unknown whether it improves sleep because this is rarely an outcome measure [5]. We will present evidence to support all 10 research uncertainties and propose research strategies to take this work forward.

Conclusion

The top 10 questions are now registered on the NHS Evidence UK Database of Uncertainties about the Effects of Treatments (DUETs). It is managed by the National Institute for Health and Clinical Excellence (NICE). Outcomes are being widely disseminated to major stakeholders including tinnitus researchers and funders of biomedical research.

References:

[1] Hoare et al. *Laryngoscope* 2011;121:1555-1564.

- [2] Savage & Waddell. BMJ Clinical Evidence. Web publication date: 3 Feb 2012 (based on July 2011 search).
 [3] Landgrebe et al. Journal of Psychosomatic Research 2012;73:112–121.
 [4] Hesser et al. Clinical Psychology Review 2011;31:545–553.
 [5] Hobson et al. Cochrane Database of Systematic Reviews 2010, Issue 12. Art. No.: CD006371. DOI:

The top 10 tinnitus research uncertainties.

A	What management strategies are more effective than a usual model of audiological care in improving outcomes for people with tinnitus?
B	Is Cognitive Behaviour Therapy (CBT), delivered by audiology professionals, effective for people with tinnitus? Here comparisons might be with usual audiological care or CBT delivered by a psychologist.
C	What management strategies are more effective for improving tinnitus-related insomnia than a usual model of care?
D	Do any of the various available complementary therapies provide improved outcome for people with tinnitus compared with a usual model of care?
E	What type of digital hearing aid or amplification strategy provides the most effective tinnitus relief?
F	What is the optimal set of guidelines for assessing children with tinnitus?
G	How can tinnitus be effectively managed in people who are Deaf or who have a profound hearing loss?
H	Are there different types of tinnitus and can they be explained by different mechanisms in the ear or brain?
I	What is the link between tinnitus and hyperacusis (over-sensitivity to sounds)?
J	Which medications have proven to be effective in tinnitus management compared with placebo?

236 Epidemiology and Risk Factors of “Significant” Tinnitus: A UK Retrospective Study Using National Health Service (NHS) Records

Deborah Hall¹, Carlos Martinez², Christopher Wallenhorst², Don McFerran³

¹NIHR Nottingham Hearing Biomedical Research Unit,

²Pharmaepi, ³Colchester Hospital University NHS Foundation Trust

Background

Tinnitus remains one of the commonest chronic hearing-related conditions in the Western world. Long-term incidence studies are particularly valuable for identifying factors associated with developing the condition. This knowledge can inform the allocation of public health resources or target prevention campaigns. Only two

studies (Beaver Dam, Wisconsin, USA and Blue Mountains Hearing Study, Sydney, Australia) have so far assessed the long-term incidence of tinnitus in the general population. Their approach to risk factor modelling had some limitations. The aims of this study were to estimate the incidence rate of ‘significant’ tinnitus that burdens the NHS in the UK and to identify risks factors for developing the condition based on factors defined *a priori*.

Methods

Data was extracted from the Clinical Practice Research Datalink and Hospital Episode Statistics between 1 January 2001 and 31 December 2011. ‘Significant’ tinnitus was operationally defined as patient access to primary care and onward secondary referral, with a recording of tinnitus (n = 23,672). A gender- and age-matched control cohort included patients without a recording of tinnitus (n = 53,958). The choice of risk factors was defined according to a broad literature search (19 categories) and a breakdown according to period of exposure to various medications.

Results

The 10-year cumulative incidence of ‘significant’ tinnitus was 55.4 per 10,000 (95% CI:54.6–56.2). In other words, approximately one in 180 patients in the total population is likely to experience significant tinnitus within a 10-year period. Incidence rate steadily increased during the study period. Risk analysis used a conditional logistic regression model which controlled for confounding bias and accounted for age and hearing loss. Relative risk estimates are presented as adjusted odds ratios and 95% CI. Many otologic conditions increased risk, as did head injury, rheumatological disease, anxiety and depression. Tinnitus incidence appeared to be unaffected by heart disease, use of lipid controlling drugs and alcohol consumption. Histories of diabetes mellitus, smoking, treated hypertension and pregnancy emerged as potential protective factors.

Conclusion

Tinnitus is a symptom that may be part of a specific otological condition but can also be associated with non otological disease processes. Unfortunately there is no objective measurement for tinnitus and consequently diagnostic uncertainty exists, meaning that the NHS data should be interpreted with some degree of caution. Nevertheless these epidemiological data support the growing case for developing an effective referral and management pathway for people with tinnitus.

237 Changes of Tinnitus in Sudden Sensorineural Hearing Loss: The Relationship Between Tinnitus Pitch and the Audiogram

Tae Su Kim¹, Byoung Soo Shim¹, Jong Woo Chung¹, Joong Ho Ahn¹, Chang-Hee Kim², Hong Ju Park¹
¹Asan medical center, ²Konkuk university hospital

Background

Different mechanisms of tinnitus, such as lateral inhibition and homeostatic plasticity, have been proposed. The aim of this study was to explore the changes of tinnitus in patients with SSNHL at initial and 1 month follow-up examinations by analyzing the relationship between tinnitus pitch and audiogram shape.

Methods

Thirty-six patients with SSNHL and new onset tone-like tinnitus were enrolled. The tinnitus pitch was compared to the frequency of maximum hearing loss (HL) and the audiogram edge at initial and 1 month follow-up examinations.

Results

At initial examination, the tinnitus pitch was in the same range with the edge frequency. The tinnitus pitch showed a significant correlation with both the edge frequency and the frequency of maximum HL. The edge frequency ($r=0.461$, $p=0.005$) had more significant correlation than the frequency of maximum HL ($r=0.333$, $p=0.047$). At 1 month follow-up, the tinnitus pitch increased significantly compared to the initial stage and was similar to the frequency of maximum HL. The tinnitus pitch showed a significant correlation with the frequency of maximum HL ($r=0.519$, $p=0.001$), but not with the edge frequency ($r=0.155$, $p=0.366$).

Conclusion

Significant relationship of tinnitus pitch with the edge frequency at initial examination suggests that reduced lateral inhibition and cortical reorganization play a role in generating tinnitus at acute stage of hearing loss. Significant relationship of tinnitus pitch with the frequency of maximum HL at initial and follow-up examinations suggests that tinnitus is generated and persists by homeostatic mechanism.

238 A New in Vitro Model to Investigate the Biological Mechanisms Involved in the Alteration and Restoration of the Vestibular Neuronal Network

Emilie Brun¹, Sophie Gaboyard², Eric Wersinger², Christian Chabbert¹
¹INSERM U1051, ²Sensorion-Pharmaceuticals

Background

Background: It is commonly assumed that a large proportion of vestibular disorders results from transient synaptic decoupling between vestibular hair cells and their cognate nerve afferents. However the poor spatial resolution of current imaging techniques available in

human prevents the direct observation of the biological changes that occur following the synaptic insult. Using an animal model of vestibular excitotoxic insult, we previously demonstrated that selective impairment of the first sensory-neural synapse triggers the expression of altered vestibular behavior that replicates the symptomology encountered in human vestibular disorders. We also reported a high propensity of the vestibular synapses to spontaneously repair (Brugéaud et al. 2007). Such synaptic plasticity has been further confirmed in an organotypic culture model (Travo et al. 2012). More recently, we deciphered the time course of the vestibular lesion and functional restoration in an animal model of vestibular excitotoxic insult and demonstrated the correlation between the synapse impairment and the altered vestibular behavior (Gaboyard et al. poster # 247 ARO 2011). Present study was designed to develop an experimental model to access the intimate mechanisms of the vestibular lesion and restoration through several technical approaches such as imaging, histology, molecular biology and electrophysiology.

Methods

Method: this in vitro model consists in a three-dimensional mouse organotypic culture derived from previously detailed protocol (Gaboyard et al., 2005). Briefly, vestibular sensory epithelia and Scarpa's ganglion were removed with particular attention paid to preserve synaptic connections between hair cells and primary neurons. Organotypic slices were produced and maintained in culture up to 15 days and the synaptic integrity studied using a multidisciplinary approach: immunocytochemistry, 3D reconstruction and quantification by morphometric analysis and, transmission electron microscopy. Finally, the function of the synaptic transmission has been evaluated in parallel using the patch-clamp technique.

Results

Results: Observations of our in vitro model at different time point allowed us to show: (1) a clear integrity of most hair cells and vestibular neurons as attested by preservation of intact mitochondria and subcellular organelles; (2) a synaptic plasticity process with uncoupling and spontaneous repair occurring with a time course comparable to our previously described in vivo model (Gaboyard et al. 2011); 3) newly formed synapses in the process of maturation: incomplete calyces present synaptic ribbons with many vesicles facing synaptic post-densities.

Conclusion

Conclusion: This model provides a new tool to further investigate the intimate mechanisms of protection and/or repair by imaging, electrophysiology and molecular technics.

239 Experimental Mechanical Response of the Utricle to Dynamic Inertial Stimulus

Wally Grant¹, Myles Dunlap¹

¹VA Tech

Background

Few experimental studies have made direct measurement of otolith organ mechanical properties and none using dynamic stimuli. All previous analysis and experimental efforts regarding utricle mechanical motion have always concluded it is an overdamped system. Here, the utricle of the turtle was oscillated over a frequency range using an inertial stimulus, causing a measurable shear displacement of the combined gelatinous and column filament layers, the shear layer (SL). This experimental work revealed that the utricle is an underdamped system.

Methods

The utricle and its surrounding membranous sac were removed from the skull and maintained under compatible aqueous solution throughout. The membranous sac was opened to expose the dorsal surface of the otoconial layer (OL) of the utricular macula. The utricle periphery was then fixed to a glass slide with strands of dental floss. The glass slide was mounted onto a piezoelectric actuated platform that was located in a fixed stage light microscope. The piezoelectric actuator oscillated the neuroepithelium layer (NEL) of the utricle in its plane of normal acceleration stimulus. A controlled sinusoidal-sweep that increased from 0 to 500 Hz over 5 seconds was applied. This natural inertial stimulus produced a measurable shear displacement in the SL. The displacements of a reference point for the NEL and OL were filmed at 2000 frames/sec with a high-speed video camera during the oscillations. Image registration was performed on the video to track OL and NEL reference point displacements to better than 15 nm. The displacement waveforms were converted into frequency response data, and then used in a frequency domain system identification technique to determine the system mechanical properties of: (1) natural frequency, and (2) damping coefficient of the shear layer.

Results

Properties were measured for 21 utricles with a mean and 95% confidence interval in parenthesis: natural frequency $\omega_n = 373$ (350, 396) Hz, damping ratio $\zeta = 0.50$ (0.47, 0.53), and shear modulus $G = 9.52$ (8.32, 10.71) Pa. Within the acceleration ranges tested the utricle behaved as a linear system, nonlinearities were not observed in amplitude or frequency.

Conclusion

The results indicate that the utricle performs as a linear underdamped second-order system for inertial stimuli. In comparison to an overdamped system ($\zeta > 1$), a $\zeta = 0.50$ provides improved transient-response to head accelerations, increasing bandwidth.

(Supported by: NIH NIDCD R01 DC 005063)

240 Noise-Induced Vestibular Deficits in

Rats

Courtney Jernigan¹, Adams Briscoe¹, Xuehui Tang¹, Adel Maklad², Jerome Allison¹, William Mustain¹, Wu Zhou^{1,3}, Hong Zhu¹

¹Dept Otolaryngology, University of Mississippi Medical Center, ²Dept Anatomy, University of Mississippi Medical Center, ³Dept Neurology, University of Mississippi Medical Center

Background

The vestibular system responds naturally to head acceleration. Because vestibular end organs are connected to the auditory end organs by continuous fluid pathway within the membranous labyrinth, the vestibular system also responds to sound. It is well known that extensive noise exposure leads to sensorineural hearing loss. It has been suggested that noise exposure also leads to vestibular deficits in humans, but little is known about the underlying mechanisms. In the present study, we established a unilateral noise-induced hearing loss rat model to study the influence of noise exposure on the vestibular system.

Methods

Sprague-Dawley rats were anesthetized with isoflurane. Continuous broadband white noise at an intensity of 116 dB pSPL was delivered to the left ear via an insert ear phone. A hard plastic infant tip adapter was placed at the end of sound-conducting tubing and placed into a speculum that was sealed in the ear canal. The contralateral ear canals were sealed from air-conducted sound exposure. The rats received noise exposure 3 hours per day for 5 consecutive days. Hearing level was monitored by measuring ABR threshold (0.1 ms clicks).

Results

After 5 days of exposure, ABR thresholds of the ipsilateral ears increased from 28 ± 2.7 dB HL to 70.8 ± 7.8 dB HL and were at 64.5 ± 3.0 dB HL 7 days post-noise exposure. A 20-30dB temporary threshold shift was observed on the contralateral side, which may result from bone-conducted noise exposure from the left side. The vestibular functions of noise exposed rats were assessed by swimming tests. The morphology of vestibular hair cells was examined by scanning electron microscopy.

Conclusion

Conclusion: Our preliminary results indicated that vestibular deficits were induced by the unilateral noise exposure. Ongoing studies are to characterize the effects of air-conducted and bone-conducted noise exposure on the vestibular system and examine the underlying neural mechanisms.(supported by NIH R01 DC012060-01)

241 Cellular Correlates of Coding Deficits Associated with Partial Lesions of the Vestibular Epithelia

Larry Hoffman¹, Kristel Choy¹, David Sultemeier¹, Ivan Lopez¹

¹*Geffen School of Medicine at UCLA*

Background

Clinical investigations of Meniere's disease treatments have demonstrated that partial physiologic dysfunction may be induced by transtympanic gentamicin therapy. However, the cellular correlates of such functional compromise have yet to be elucidated through comparable animals studies. The goals of the present study were to induce partial lesions of the vestibular epithelia through intraperilympatic gentamicin administration and document the resulting physiologic deficits in the discharge of individual afferent neurons. Furthermore, we investigated the associated alterations among cellular constituents of the epithelia.

Methods

Adult male chinchillas underwent a surgical procedure under isoflurane anesthesia to administer 2.5 μ l of gentamicin solution through an implanted stainless steel cannula providing direct perilymphatic access at the superior semicircular canal. The concentration of this solution was adjusted so that the final administered quantity was 0.5 or 0.75 μ g. After 4 weeks animals were reanesthetized (sodium pentobarbital) for recording spontaneous and evoked discharge from individual afferent neurons projecting in the superior vestibular nerve. At the conclusion of the recording session, vestibular epithelia were harvested for immunohistochemical analyses.

Results

Administration of 0.75 μ g gentamicin resulted in partial lesions represented by calyx retraction in the cristae central zones and utricular striola. The morphology of intermediate- and peripheral-zone calyces, as well as extrastriolar calyces, appeared intact. To date, afferents recorded from these specimens that projected to the horizontal crista exhibited greater CVs for a given spontaneous discharge rate compared to untreated specimens. Coupled with what appear to be low sensitivities and coherence measures in response to stimulus frequencies \geq 1.6Hz, these data suggest lower signal:noise ratios among responding afferents. The phase measures of some afferents' responses suggested they represented remnant dimorphic afferents projecting from the crista central zone. No evidence of induced lesions were observed subsequent to 0.5 μ g gentamicin administration, where the cristae and utriculi exhibited normal distributions of anti-calretinin and anti-KCNQ4 immunoreactive calyces. Afferent discharge characteristics in these specimens could not be distinguished from untreated specimens. Further analyses to reveal hair cell densities and additional cellular markers are ongoing.

Conclusion

These results demonstrate that partial lesions of the vestibular epithelia may be induced by quantities of gentamicin as low as 0.75 μ g, though the dosage window for producing lesions compatible for detailed study is surprisingly narrow. Calyces projecting to the crista central zones are most severely affected, yet recorded responses indicate that central zone hair cells are functional.

242 Effect of Low Level Laser on Vestibular System After Ototoxic Damage

Myung-Whan Suh¹, Jae-Hwan Hyeon², Jae-Yun Jung³, Bong Jik Kim¹, Chung-Ku Rhee⁴

¹*Seoul National University Hospital*, ²*Dankook University Hospital*, ³*Dankook University College of Medicine*, ⁴*Dankook University, Medical Laser Research Center*

Background

Already applied in numerous areas, laser-induced phototherapy is widely applied as a noninvasive treatment promoting cell recovery and repair processes. It is especially notable that low-level laser therapy (LLLT) has been approved by the U.S. Food and Drug Administration for the treatment of several diseases, including carpal tunnel syndrome and alopecia. In the present study, the ability to recover vestibular function after gentamicin exposure was assessed using an 830 nm diode laser

Methods

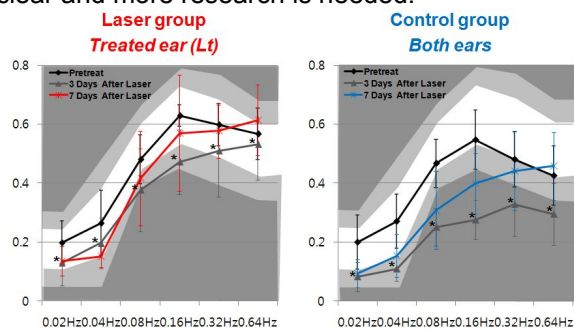
Gentamycin (110mg/kg/day) was injected intravenously for three days in 17 rats. Eight rats were irradiated (830 nm diode laser, transtympanic) in the left ear at an energy output of 200mW for 30 min for 7 days in a row (L group) and 9 rats served as a control (C group). Gain and asymmetry of Sinusoidal Harmonic Acceleration (SHA, 0.02-0.64Hz) were measured before the gentamicin exposure and also after the 1st, 3rd and 7th irradiations. After the 7th treatment, hair cells were observed using a confocal laser scanning microscope. The lateral canal ampullae were sectioned in the axis vertical to the crista ampullaris and 1 representative section were obtained per 50 μ m (6 samples/ampulla). The sections were stained with phalloidin and DAPI, and the number of hair cells was counted for quantitative comparison.

Results

After 7 days of LLLT, the gain of the left ear (LLLT ear) was significantly higher than that of the right ear (non-treated ear) in the L group. Also, the asymmetry was deviated to the right side (15-33%), reflecting that the vestibular function of the left ear has recovered while that of the right ear has not. On the contrary, the gain of the C group did not recover in both ears after 7 days. The asymmetry was symmetrical ($<\pm 10\%$), implying that bilateral vestibular weakness did not recover in neither of the ears after gentamin exposure. The number of hair cells was 145.5 \pm 25 in the left ear (LLLT ear), and 139 \pm 25 in the right ear (non-treated ear) of the L group. Although the number of hair cells was larger in the left ear when compared with that of the right ear, it did not reach a statistical significance.

Conclusion

Low level laser treatment may promote the recovery of vestibular functions after systemic gentamicin injection. But whether this effect is via improved hair cell survival is not clear and more research is needed.



*p<0.05, Comparison between laser group treated ear (Lt) and control group both ears

243 Novel Cytoplasmic Extensions Link Basal Portions of Type II Hair Cells with Other Elements in Adult Mammalian Vestibular Epithelia

Tot Bui Nguyen¹, Glen MacDonald¹, Jennifer Stone¹
¹University of Washington

Background

Mammals have two types of vestibular hair cells – type I and II - that differ with respect to their morphology, physiology, and innervation. A recent study of adult mice (Golub et al., 2012, J. Neuroscience, in press) showed that all hair cells that are spontaneously regenerated in utricles are type II-like and have branched extensions of their cytoplasm that reach several cell lengths. In this study, we examined undamaged utricles from adult mice and gerbils for evidence for this cell type in normal epithelia.

Methods

Vestibular end organs from 2-45 week-old mice or adult gerbils were dissected, fixed, and immunolabeled as whole-mounts with antibodies to the hair cell antigens, myosin VIIa, myosin VI, and calretinin and/or with antibodies to neural proteins (neurofilament, β II tubulin) and pre- and post-synaptic proteins (Ctbp2, PSD95, SV2, and ChAT). End organs were analyzed using confocal microscopy. Three-dimensional reconstructions of hair cells were generated using Fiji image segmentation.

Results

Image analysis revealed that many type II hair cells in adult mice and gerbils have one or more cytoplasmic processes that project basolaterally from the each cell. Hair cell processes have a variety of shapes and sizes, ranging from oval “blobs” to long branched processes that extend several cell lengths. In mice, hair cell processes have a high density of Ctbp2-positive pre-synaptic ribbon components. They are also closely associated with post-synaptic specializations and ChAT immunolabeling, suggesting they receive inputs from efferent fibers. Three-dimensional reconstructions suggest that nearby type II

hair cells seem to contact one another by their processes, and they confirm that type II hair cell processes contact calyces of type I hair cells. In mice, hair cell processes are first seen during the second postnatal week.

Conclusion

Many type II hair cells in mature rodents have a dramatic feature that has not been described before: one or more cytoplasmic processes that extend underneath type I hair cells, synapse on other cell types (most likely afferent nerves or hair cells), and receive synaptic input from other cells (most likely efferent nerves). Prior studies may have failed to notice this specific morphology of type II hair cells because they analyzed thin sections, young animals, or focused on type I hair cells. These observations suggest that direct communication amongst type II hair cells and cellular elements other than afferent fibers could modulate neural signaling in the vestibular system.

244 Persistent and Quantal Synaptic Currents in Vestibular Calyx Terminal

Stephen Highstein¹, Mary Anne Mann¹, Richard Rabbitt^{2,3}
¹Marine Biological Laboratory, ²Marine Biological Laboratory, ³University of Utah

Background

The unique morphological structure of the vestibular calyx has generated speculation concerning communication between Type I hair cells and the calyx inner leaflet membrane. Quantal and non-quantal transmission has been suggested. To examine this we recorded from calyces in the isolated lagenar macula of the turtle, *Trachemys scripta elegans*.

Methods

The lagenar epithelium was dissected, otoconia enzymatically removed and the tissue placed upon the fixed stage of an upright microscope for DIC and fluorescence imaging. Recording was performed employing the whole cell patch clamp technique. Patch electrodes were loaded with a fluorescent dye for viewing following recording. A fluid jet was employed to deflect hair bundles. The composition of the fluid in the jet was varied between a sodium-dominated perilymph like solution to a potassium-dominated endolymph like solution.

Results

All recordings were confirmed to have been taken from calyceal terminals by visualizing the terminal and its axon leaving the tissue employing wide field fluorescence imaging. Two types of excitatory post-synaptic currents (EPSC) were observed in voltage clamped vestibular calyx terminals held at -60mV. Miniature (mEPSCs) whose frequency could be increased by deflecting the hair bundle and an amplitude graded inward post-synaptic current that persisted for as long as the bundle was held deflected (pEPSC). pEPSCs developed and decayed with a time constant of ~ 200msec. Both types of EPSCs occurred simultaneously in a subset of cells. pEPSC varied from 0 to 200pA depending upon the cell and the intensity of bundle deflection. The frequency of mEPSCs adapted

during prolonged bundle deflection while pEPSCs did not. Varying the solution in the fluid jet (cf. methods) did not affect the character of the responses. CNQX reversibly blocked the mEPSCs without affecting the pEPSC, while TTX reversibly blocked the pEPSC without affecting the mEPSCs.

Conclusion

Results imply that mEPSCs convey timing and high frequency information while pEPSCs convey low frequency and tonic signals (e.g., gravity), presumably at a much lower energetic cost to the hair cell. The fact that the pEPSC did not adapt to maintained bundle deflections suggests it reflects the tonic component of the transduction current.

Supported by NIH 1R01DC008142 (SMH) and DC006685 (RDR)

245 Sodium Channel Distribution in Vestibular Afferents

Anna Lysakowski¹, Steven D. Price¹

¹Univ. of Illinois at Chicago

Background

The sodium channel isoform Na_v1.6 is the canonical sodium channel at the node of Ranvier and the axon initial segment. We have been investigating Na channel distribution with various Pan-Na_v and Na_v isoform-specific antibodies in vestibular afferents to determine whether Na_v1.6 or some other isoform is the main isoform present at the AIS region of vestibular afferents.

Methods

Methods used were similar to those used in our recent publication (Lysakowski et al., 2011), with the exception that most tissue was vibratome-sectioned rather than frozen-sectioned and lower concentrations (0.05%) of Triton X-100 were used.

Results

Our results indicate that Na_v1.6 is present at the heminode of dimorphic vestibular afferents, but not at pure calyx afferent heminodes. We determined the afferent class and location of the heminode by co-labeling with calretinin (a calyx afferent marker) and nodal marker antibodies, such as ezrin, βIV-spectrin, neurofascin-186 and ankyrinG, and paranodal and juxtapanodal marker antibodies, such as Caspr1, ankyrinB, K_v1.1 and K_v1.2, and myelin basic protein. Our search for the Na_v isoform at calyx heminodes led us to investigate various other isoforms, including Na_v1.1-1.3, 1.5, 1.7 and 1.8, in addition to various Pan-Na_v antibodies. Each antibody labels subsets of heminodes, although we have not yet quantified the proportions of individual isoforms expressed within each afferent class. Pan-Na_v and Na_v1.2 label the entire lower outer surface of the calyx in dimorphic afferents, down to the heminode. Calyx afferents are labeled with Na_v1.3 and Na_v1.8 antibodies in a similar pattern. The majority of calyx afferent heminodes are located above and the

majority of dimorphic afferent heminodes below the basement membrane.

Conclusion

We conclude that while Na_v1.6 has a role as the major player at the vestibular dimorphic afferent heminodes, other isoforms have supporting roles.

Supported by NIH R01-02058.

246 A Constitutive Null Mutation for Calretinin Has No Effect on Excitability of Vestibular Ganglion Neurons

Gang Q. Li¹, Ruth Anne Eatock¹

¹Massachusetts Eye & Ear Infirmary

Background

Work with transgenic animals has shown that calretinin, a fast calcium binding protein, can modulate the electrical activity of certain CNS neurons. Calyx-only vestibular ganglion neurons (VGNs), which innervate type I cells in central zones of the sensory epithelia, express high levels of calretinin. The calretinin-positive, calyx-only afferents have irregular firing, in contrast to the regular firing of calretinin-negative afferents to peripheral zones. We used calretinin-null mice (obtained from S. Schurmans) to investigate whether calretinin plays a role in the firing properties of calretinin-positive calyx-only VGNs.

Methods

VGNs were isolated from mice (60-90 days old) lacking functional calretinin (CR ^{-/-}), heterozygotes (CR ^{+/-}), and their wild-type littermates (CR ^{+/+}), and cultured overnight. Whole-cell currents and voltages were recorded with the perforated patch clamp method.

Results

Two groups of VGNs were identified based on their responses to depolarizing current steps between 50 and 500 pA: “transient” spikers made one-two spikes at step onset and “sustained” spikers made more than two spikes. As reported for VGNs from young rats (P0-P14), transient spikers are larger and have more negative resting potentials and larger current thresholds for spiking. Previous work associated the transient firing pattern with irregular afferents, which include the calyx-only, calretinin-expressing afferents, and the sustained firing pattern with regular afferents, which are calretinin-negative (Kalluri et al., J Neurophysiol. 104:2034, 2010). We hypothesized that effects of the calretinin null mutation would manifest most strongly in transient spikers. Neither transient nor sustained spikers, however, showed significant differences with genotype in spike parameters (height, width, current and voltage thresholds, afterhyperpolarizations) or firing patterns.

We also attempted to calibrate the endogenous Ca²⁺ buffering of VGNs, using spike properties and firing patterns as assays. After recording in perforated-patch mode to determine firing properties in endogenous buffering, we ruptured the membrane and replaced endogenous buffering with the fast synthetic Ca²⁺ buffer,

BAPTA. For all 4 BAPTA concentrations used (0.002, 0.1, 1, and 10 mM), membrane rupture was followed by a small depolarization and small effects on spike properties and firing pattern. Because these effects did not vary with BAPTA concentration, we expect that they reflect some other difference between the endogenous intracellular solution and the pipette solution.

Conclusion

VGN spike properties were resistant to constitutive changes in calretinin expression and acute changes in Ca²⁺ buffering.

247 Distribution of 5-HT_{1F} Receptors in Monkey Vestibular Ganglia

Habiba Vongtau¹, Carey Balaban¹

¹University of Pittsburgh

Background

Migraine and balance disorders are often comorbid with psychiatric disorders. Clinical data suggest that serotonergic mechanisms play an important role in vestibular contributions to migraine and balance disorders. Both 5-HT_{1B} and 5-HT_{1D} receptors are expressed extensively in inner ear ganglion cells of monkeys and rats. This study describes the distribution of another target of triptans, the 5-HT_{1F} receptor, in vestibular ganglion cells of monkeys.

Methods

Decalcified, paraffin embedded temporal bone sections (8 – 10 microns) from 5 adult macaques monkeys were stained immunohistochemically for 5-HT_{1F} receptors with a diaminobenzidine chromagen. Polyclonal, primary antibodies (Imgenex 78120/78121, 1:1000-5000) recognized human 5-HT_{1F} N- or C-terminus. A series of 12 bit digital images were taken with a 20X objective and neuronal somatic area and intensity of immunoreactive vestibular ganglia were quantified using Meta-Morph software. Data were normalized by subtracting background values and analyzed statistically employing SYSTAT 11 (SYSTATSoftware, Inc.).

Results

Virtually all vestibular ganglion cells were immunopositive for 5-HT_{1F} receptors, with staining confined to distinct cell regions. Staining of inferior and superior vestibular ganglia was more intense in small cells, punctate in some medium cells and polarized regionally in some large cells. Analyses of average somatic neuronal immunoreactive intensity identified a population of mainly medium sized cells with high standard deviation of intensity corresponding to punctately stained cells. Centrally directed ganglion cell processes were immunoreactive as well as ganglion cell dendrites, cochlear inner hair cells, vestibular hair cells and blood vessels in vestibular maculae and cristae.

Conclusion

Although the 5-HT_{1F}, 5-HT_{1B} and 5-HT_{1D} subtypes are expressed in almost all vestibular ganglia, they show

slightly different cellular distribution patterns. Interestingly, 5-HT_{1F} receptors are expressed in analogous regions in trigeminal, dorsal root and vestibular systems. We therefore propose that 5-HT_{1F} receptors may act in concert with other subtypes in vestibular ganglia, in mediating serotonergic involvement in the comorbidity of migraine and balance disorders. In addition, 5-HT_{1F} receptor expression in cochlear inner hair cell afferents suggests that this receptor could be exploited as a pharmacological target in treatment of audiovestibular symptoms of migraine.

248 Are There Differences in Infectability, Reactivation, or Production of Herpes Simplex Type I Virus in Superior Versus Inferior Vestibular Ganglion Neurons?

Shruti Nayak¹, Vladimir Camarena², Pamela Roehm¹

¹New York University School of Medicine, ²Hussman Institute for Human Genomics of Miami University

Background

Vestibular neuritis is extremely common condition causing spinning vertigo, which results in at least 15% of all complaints of dizziness to primary care physicians. In these patients, involvement of the inferior vestibular ganglion is rare (36% or less), and exclusive involvement is even less common (5%). Many authors have found evidence that vestibular neuritis results from herpes simplex type I (HSV1) infection or reactivation in the vestibular ganglion. In this study we used an *in vitro* cell culture system of herpes infection and reactivation to determine whether there are intrinsic differences in HSV1 infection, reactivation, or virion production in inferior versus superior vestibular ganglion neurons (VGNs).

Methods

Primary cultures of rat superior and inferior vestibular ganglion neurons were cultivated separately. Neurons were lytically and latently infected with HSV1 modified with a US11-green fluorescent protein (GFP) chimera. Percent lytic infection and baseline reactivation rates were assessed by fluorescent microscopy for GFP fluorescence. Trichostatin A (TSA) was applied to cultures and reactivation of HSV1 was assessed by fluorescent microscopy. Production of HSV1 virions was assessed by viral titer on Vero cells. The number of cells latently infected for both types of neurons was determined by fluorescent *in situ* hybridization for LAT transcripts.

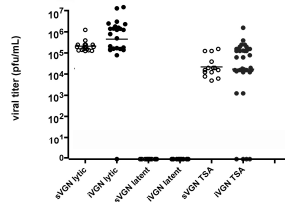
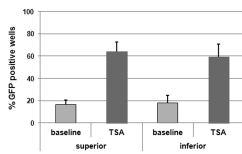
Results

Lytic infection rates were equivalent between the two ganglia, with 100% lytic infection rate at an multiplicity of infection of 3. Lytic infections yielded similar amounts of plaque forming units (pfu; 3.25 x 10⁵ v. 6.6 x 10⁵ pfu/mL). Numbers of LAT positive neurons by FISH were not significantly different for superior and inferior ganglia. Latently infected superior and inferior ganglion cultures showed no differences in rates of baseline (16.8% v. 17.9%, *p*>0.05) and TSA-induced (64.3 v. 59.7%, *p*>0.05) HSV1 reactivation as measured by GFP fluorescence. Production of HSV1 virions was also not different between

reactivated, latently infected superior v. inferior VGNs (3.5×10^4 v 2.6×10^4 pfu/mL).

Conclusion

Differences in the prevalence of superior and inferior vestibular neuritis are unlikely to result from intrinsic differences in HSV1 infection or virion production between the neurons contained in these ganglia. Other factors, such as the length and width of the bony canal containing the ganglia and nerves and accessibility of the ganglia by cerebrospinal fluid, may account for the discrepancy in involvement of the two ganglia.



249 Functional Analysis of TRPV1 and TRPA1 Channels in Rat Vestibular Ganglia

Takefumi Kamakura^{1,2}, Yusuke Ishida², Yukiko Nakamura², Takahiro Yamada², Tadashi Kitahara¹, Yasumitsu Takimoto^{1,2}, Arata Horii¹, Atsuhiko Uno¹, Takao Imai¹, Suzuyo Okazaki¹, Hidenori Inohara¹, Shoichi Shimada²

¹Dept. of Otorhinolaryngology-Head and Neck Surgery, Osaka University Graduate School of Medicine, ²Dept. of Neuroscience and Cell Biology, Osaka University Graduate School of Medicine

Background

Transient receptor potential vanilloid (TRPV)-1 and transient receptor potential ankyrin (TRPA)-1 are both cation channels co-expressed in sensory neurons such as dorsal root ganglia (DRG) and trigeminal ganglia (TG). TRPV1 is activated by noxious heat (>43°C), protons, capsaicin, and anandamide to name a few, while TRPA1 is activated by noxious cold stimuli (<17°C), alkaline pH (>8.5), cinnamaldehyde, mustard oil, allyl isothiocyanate and icilin to name a few. TRPV1 has been reported to be expressed in vestibular ganglia (VG) and suggested to be associated with vestibular function and/or dysfunction. On the other hand, in DRG and TG neurons, TRPV1 is co-expressed with TRPA1, but expression of TRPA1 in VG neurons has not been reported yet. Moreover, it is unclear whether TRPV1 and TRPA1 are functional as ion channels.

We studied the histological and functional expression of TRPV1 and TRPA1 in rat VG neurons.

Methods

We examined the TRPV1 and TRPA1 mRNA expression and localization by RT-PCR and in situ hybridization experiments and their functional analysis by Ca²⁺-imaging experiments.

Results

RT-PCR specifically amplified TRPV1 and TRPA1 transcripts from rat VG. In situ hybridization experiments showed TRPV1 expression in majority of VG neurons and also TRPA1 expression. In Ca²⁺-imaging experiments, capsaicin, a TRPV1 agonist, induced significant increases in intracellular calcium ion concentration ([Ca²⁺]_i) in rat primary cultured VG neurons, which were almost completely blocked by capsazepine, a TRPV1 selective antagonist. Cinnamaldehyde, a TRPA1 agonist, also caused [Ca²⁺]_i increase, which were completely inhibited by HC030031, a TRPA1 specific antagonist. Moreover, in some VG neurons, [Ca²⁺]_i increase was evoked by both capsaicin and cinnamaldehyde in the same neurons. We examined a total of 114 VG neurons and 21.9% (25/114) responded to capsaicin, 28.1% (32/114) to cinnamaldehyde, and 12.3% (14/114) both to capsaicin and cinnamaldehyde.

Conclusion

In summary, our data showed histological and functional expression of TRPV1 and TRPA1 in VG neurons. Ca²⁺-imaging experiment suggested that these two channels can be co-expressed in the same neuron. It is suggested that TRPV1 and TRPA1 in VG neurons might participate in vestibular function and/or dysfunction such as vertigo.

250 Opioid Receptor Mediated Inhibition of the Calcium Currents in Vestibular Ganglion Neurons of the Rat

Enrique Soto¹, Emmanuel Sesena¹, Rosario Vega¹

¹Universidad Autonoma de Puebla, Mexico.

Background

Opioid receptors have been shown to be expressed in vestibular endorgans, but studies of their mechanism of action at cellular level are scarce. With the aim to determinate the opioid receptors function we evaluated the modulation of the voltage-gated calcium current (I_{Ca}) by the μ opioid receptor activation (MOR) in afferent neurons isolated from the vestibular ganglia of the rat.

Methods

Young (P7-10) and prepubertal (P28-30) rats were studied using the perforated whole cell voltage clamp technique.

Results

The use of MOR agonists [D-Ala², N-Me-Phe⁴, Gly⁵-ol]-enkephalin (DAMGO), Met-enkephalin or endomorphine-1 inhibited the I_{Ca} in vestibular neurons at both ages studied. The DAMGO inhibition was dose-dependent with an IC₅₀ of 33 nM. The action of DAMGO was prevented by the co-application of MOR antagonist H-D-Cys-Tyr-D-Trp-Arg-Thr-Pen-Thr-NH₂ (CTAP) or in neurons pre-incubated with pertussis toxin (18-24 h, 500 ng/ml). Co-application of 8-Br-cAMP with DAMGO, reverted the inhibition induced by DAMGO and recovered 92 % of the control current, indicating that cAMP is the second messenger involved in the inhibition of I_{Ca} by MOR. The application of the protein kinase A inhibitor H-89 mimicked the DAMGO effect, and the co-application of H-89 and DAMGO did not add their

effects. In contrast, the co-application of porbol-myristate was unable to recover the DAMGO inhibition. DAMGO inhibited the LVA and HVA currents. The use of nickel, nifedipine and ω -ctx-GVIA showed that DAMGO inhibited both the low and the high voltage activated Ca^{2+} currents. In current clamp experiments the MOR activation increased the duration and decreased the amplitude of the action potential and decreased the repetitive discharge in response to depolarizing current pulse injection.

Conclusion

We concluded that in isolated vestibular afferent ganglion neurons the μ opioid receptor inhibits the T-, L- and N-calcium current, through the activation of a $G_{i/o}$ protein that leads to a decrease of the cAMP levels and the subsequent decrease of the PKA activity. The negative modulation of the Ca^{2+} current would modify the postsynaptic signal integration in the synapse between the hair cell and the vestibular afferent neuron and also at the central level decreasing the neurotransmitter release in the synapse between the vestibular afferent neurons and vestibular nucleus neurons.

251 Modification of the Hodgkin-Huxley Equations According to Experimental Data from Vestibular Afferent Neurons

Tamara Alexandrova^{1,2}, Vladimir Alexandrov^{1,2}, Rosario Vega¹, Maribel Reyes¹, Alicia Angeles¹, Galina Sidorenko², Nelly Shulenina², Enrique Soto¹

¹Universidad Autónoma de Puebla, ²Moscow State University

Background

Development of the vestibulo-sensorial conflict in microgravity leads to increased delays of the gaze fixation reaction (3 fold time increase in comparison with terrestrial conditions). The use of a micro accelerometer and a micro gyroscope, established on a helmet of a cosmonaut, are thought to help reduce such delay development. The use of a processing unit of the information from technical devices will provide the adequate correcting signals.

Methods

In this work the afferent neuron discharge is modeled on the basis of a Hodgkin-Huxley (HH) modified differential equations system.

The functional parameters and numerical data used in the model have been obtained from experimental measurements in the vestibular afferent neurons of the rat.

Results

The novelties of the simplified system that we are proposing are the following:

1. In the description of the potassium current (I_k) we have introduced a parameter of inactivation h_k of the I_k and in this connection we use one more equations of Kolmogorov for the description on the average dynamics of this parameter.

2. It has been mathematically justified the reduction of an order of the mathematical model in the presence of a small

parameter δm at a derivative of the subsystem describing on the average dynamics of activation parameter m of I_k .

3. The integral $n + h = c = \text{const}$, where n is the activation parameter of the I_k and h is the inactivation parameter of the sodium current (I_{Na}), were used as a simplification of the HH equations in various models (Rubin, 2000). In our work it is modified according to experimental data as $n + h = c(v)$ where v is the voltage.

Conclusion

Thus, modified model is presented in the form of Cauchy equations of the third order with small parameter in the right part of last equation describing on the average dynamics of the new parameter h_k .

The mathematical analysis of the model leads to conclude that this can be used as a part of a complete model of information processing in the vestibular end organs, that can be numerically solved using a microprocessor and used for the design of an automatic correction of the gaze stabilization in extreme conditions such as microgravity.

Supported by RF Ministry of education and science 2012, No 11.519.11.2045 and by SRE-Mexico-Russia project.

252 Afferent Responses to Efferent Stimulation in the Murine Vestibular System

Glenn Schneider¹, Meir Plotnik², Joseph C. Holt¹

¹University of Rochester, ²Rehabilitation Hospital Sheba Medical Center

Background

The vestibular organs of nearly every vertebrate receive a prominent efferent innervation whose activation modulates the ongoing discharge of vestibular afferents. Responses of mammalian vestibular afferents to efferent stimulation are effectively excitatory and have been extensively characterized in squirrel monkey and chinchilla. However, there is little data regarding the underlying cellular and synaptic mechanisms. The use of transgenic mouse models in tandem with pharmacological manipulation provide a powerful opportunity to parse out the various receptors and downstream effectors involved in mammalian efferent responses. The purpose of this study was to begin characterizing the response of mouse vestibular afferents to stimulation of efferent neurons.

Methods

C57Bl6 mice were anesthetized with urethane/xylazine, fitted with a tracheal cannula, and connected to a ventilator. A posterior craniotomy and cerebellar aspiration were performed to expose the right vestibular nerve and floor of the fourth ventricle. Glass microelectrodes were used to record the discharge of vestibular afferents in CNVIII, visually identified just as it exits the otic capsule. The discharge regularity (CV^*) of each afferent was computed from interspike intervals taken from background activity. To electrically stimulate vestibular efferents, shock trains (1-5s, 200-333/s) were delivered to an electrode array consisting of four wires spaced 400 μ m apart. The array was lowered into the floor of the fourth ventricle along the midline. The facial nerve was transected

bilaterally and/or tubocurarine was administered IP to block muscle contractions.

Results

We have recorded from a total of 26 units. Similar to that reported in squirrel monkey and chinchilla, mouse vestibular afferents were excited following midline efferent stimulation. This excitation consisted of a modest, fast perstimulus excitation (10-30 spikes/s) and slower excitation persisting for 50-60 seconds after the stimulus. Efferent responses were routinely observed in regularly to moderately regularly-discharging afferents ($CV^* < 0.15$) whereas most of the responses in irregularly-discharging afferents ($CV^* > 0.15$) were unexpectedly small or absent. These observations may be related to the stimulus location, as midline placement of the array would be predicted to stimulate predominantly contralateral efferent fibers, presumed from studies in other species to innervate mostly regular afferents.

Conclusion

Like previous mammalian studies, mouse vestibular afferents are excited by the midline activation of efferent neurons. The resulting excitation consists of fast and slow components differing in both their activation kinetics and duration. These results will be compared to those obtained with the additional stimulation of ipsilateral efferent neurons.

[253] Loss of Alpha-Calcitonin Gene-Related Peptide (CGRP) Reduces Vestibuloocular Reflex (VOR) Gain

Anne E. Luebke¹, Joseph C. Holt¹, Paivi M. Jordan¹, Harrod Ling², Jillian S. Caldwell², Kathleen E. Cullen²
¹University of Rochester Medical Center, ²McGill University

Background

All hair cell systems contain an efferent innervation originating in the brainstem and projecting to the hair cells and/or afferent processes innervating the sensory epithelium. However, the functional role of the brain's efferent projection back to the vestibular component of the inner ear remains a mystery. Previous studies have characterized the neuroanatomy of this efferent vestibular system (EVS) projection, yet have not revealed its role in modulating vestibular system function. Calcitonin-gene related peptide (CGRP) is a neuroactive peptide known to act at the synapses between vestibular and cochlear efferent fibers and their targets. In the cochlea, we and others have found that lateral olivocochlear fibers contain CGRP and have determined that the loss of CGRP in knock-out mice reduces sound-evoked activity of the cochlear nerve by ~20%. Because CGRP is also an EVS neuropeptide, we have begun to investigate whether and how the loss of CGRP influences vestibular system function in CGRP null (-/-) mice.

Methods

We determined that in CGRP null (-/-) mice, CGRP staining was absent in all vestibular canals and extraocular muscles using immunohistochemistry to

detect CGRP. In contrast, AChE staining in the canal and extraocular muscles was comparable in normal and CGRP null (-/-) mice. To test vestibular function, mice were secured with the horizontal semicircular canals level with the horizontal plane and eye movements were recorded using an infrared camera system (Stahl et al. 2000). Turntable velocity was measured and data acquisition was controlled online. To elicit the VOR, mice were rotated in the yaw axis at frequencies of 0.2-4 Hz, at a peak velocity of 15°/s.

Results

We have found that the loss of CGRP drastically reduced the VOR gain by ~50%. However, one alternative explanation for the deficit observed in CGRP null (-/-) mice is that it reflects a non-vestibularly related effect of the CGRP removal at the level of the extraocular motor neurons and/or their innervations of the extraocular muscles. We have tested this possibility indirectly using immunohistochemistry, and directly by confirming that the relationship between vestibular quick phase amplitude and its peak velocity is comparable in normal and CGRP null (-/-) animals.

Conclusion

The efferent vestibular system (EVS) neurotransmitter CGRP plays a key role in the development of the VOR gain. Information from these studies may also contribute to future drug therapies aimed at enhancing vestibular function. (Supported by funds from NIH-NIDCD, CIHR, and McGill University Dawson Chair)

[254] Sensitivity of Semicircular Canal Afferents to Temperature Gradients and Pulsed Infrared Radiation

Suhrod Rajguru^{1,2}, Holly Holman³, Micah Frerck³, Stephen Highstein⁴, Richard Rabbitt^{3,4}

¹Department of Biomedical Engineering, University of Miami, ²Department of Otolaryngology, University of Miami, ³Department of Bioengineering, University of Utah, ⁴Marine Biological Laboratory

Background

In the present study we aimed to determine the effect of changes in temperature induced at the vestibular neuroepithelium on the resting discharge rate and sensitivity of semicircular canal afferents. The temperature gradients were introduced by perfusion of temperature controlled artificial perilymph and with pulsed infrared radiation. In addition we have also examined the role of inhibitory and excitatory convergent synaptic inputs from the hair cells to the exquisite temperature sensitivity of the vestibular labyrinth.

Methods

The experiments were conducted in the oyster toadfish, *Opsanus tau* and responses of single afferent fibers were recorded. The temperature changes were generated by perfusion of the entire labyrinth with temperature-controlled artificial perilymph solution. The temperatures were controlled between 5° to 38°. In addition, the responses of

the afferents were recorded in response to pulsed laser radiation (Capella laser, Lockheed Martin Aculight, $\lambda = 1860\text{nm}$). The fish core temperature was maintained at ambient using a sea-water bath. The changes in spontaneous discharge rate, their regularity, adaptation to step hair bundle displacements and responses to sinusoidal head rotations of single-units were recorded. The roles of GABAergic and Glutamatergic hair cell inputs to the temperature-controlled responses were examined. Following fixation, epithelia containing injected afferents were processed for two-color fluorescence for biocytin and GABA, and whole mounts were imaged by two-photon microscopy.

Results

A variety of afferent responses to thermal perfusion and infrared irradiation were observed. Some of the recorded afferents showed an increase in the resting discharge rate with increased temperature while the others reduced their discharge rate. The responses to pulsed infrared radiation varied in the same afferents with increased and reduced temperatures. The arborization patterns of the vestibular afferents receiving GABAergic and Glutamatergic hair cell inputs were studied.

Conclusion

The results indicate that the convergent hair cell inputs may play a role in the temperature sensitivity of the vestibular labyrinth.

This work was supported by NIH NIDCD R01DC011481, R01DC006685 and R01DC01060.

255 Vestibulo-Ocular Reflex Eye Movement Responses to Infra-Red Laser Stimulation of the Mammalian Labyrinth

Peter J. Boutros¹, JoongHo Ahn², Gene Y. Fridman², Chenkai Dai², David Lasker², Charles C. Della Santina^{1,2}

¹Johns Hopkins University, Department of Biomedical Engineering, ²Johns Hopkins University, Department of Otolaryngology – Head & Neck Surgery

Background

The aim of this study was to determine whether IR stimulation can evoke vestibulo-ocular reflex (VOR) responses in mammals. Rajguru *et al.* recently reported that pulsed infrared (IR) laser stimulation of hair cells can modulate afferent fiber activity in neurons innervating the crista ampullaris of the toadfish vestibular labyrinth. Extending this approach to mammals, Ahn *et al.* demonstrated similar afferent responses to IR stimulation of the crista of chinchillas (*C. lanigera*). Since these single-unit electrophysiologic responses included a mix of large excitatory, inhibitory, and mixed responses from canal afferents apparently independent of caloric-induced endolymph convection, whether prosthetic IR stimulation can evoke significant VOR eye movement responses has been unclear.

Methods

Using the same approach to fiber placement when measuring single-unit electrophysiologic responses of superior and horizontal canal afferents during IR stimulation, the left bullae of adult, wild-type 450-650 g chinchillas were opened under isoflurane general and local field block anesthesia. A hole was drilled in the superior canal thin segment at its junction with the ampulla. A 400 μm optical fiber was positioned in the superior canal and oriented inferomedially (toward the superior and horizontal canal cristae). Isoflurane was titrated down until VOR responses to whole-body rotation about the horizontal canal axis in darkness were recovered. IR stimulation was then delivered by a Capella Infrared Neural Stimulator (Lockheed-Martin Aculight, Bothell, WA, USA) at 1870 nm wavelength, with repetition rates of 200-400 pulses/s, and pulse widths of 200–350 μs .

Results

In two out of four chinchillas, eye movements were observed during IR stimulation of the labyrinth, with peak slow phase velocity exceeding 15°/s and direction consistent with left horizontal semicircular canal inhibition.

Conclusion

Stimulation of the mammalian vestibular labyrinth using infrared laser stimulation produced VOR responses consistent with modulation of activity in the horizontal canal. Whether this is due to cupular deflection (e.g., via convection) or a more direct action on hair cells and/or afferents is not yet known, but can be determined by characterizing the dependence of responses on head orientation and on the status of hair cells after ototoxic injury. Further study of IR as an alternative means of prosthetically stimulating the mammalian vestibular labyrinth is warranted.

Supported by a research contract from Lockheed-Martin-Aculight

256 Introduction to the Workshop - "Assessing Tinnitus in Animal Models: Progress and Pitfalls"

M. Charles Liberman¹

¹Massachusetts Eye and Ear Infirmary

Understanding tinnitus mechanisms requires work in animal models; however, the measurement of a phantom percept in an animal presents obvious challenges. Several techniques for tinnitus assessment have been developed, including conditioned avoidance to foot shock, and gap-prepulse inhibition of the acoustic startle reflex. This Workshop aims to improve understanding of the strengths and weaknesses of the different approaches, and to promote the refinement of their application.

1) Two 20-minute talks will introduce the topic. The first will summarize the psychophysics of tinnitus in human subjects. The second will review the behavioral strategies devised to assess the presence of tinnitus in animals, as

well as the evidence for which parts of the brain each test engages, and the existing data on cross-test validation.

2) Next, two 15-minute talks will describe specific applications of the tests: a) one conditioned avoidance test and one startle-reflex test. Each speaker, who is also the test's developer, will describe test design, rationale, training requirements and reproducibility of results.

3) Lastly, a moderated 60-minute panel discussion will include the speakers, a representative of the Tinnitus Research Consortium (<http://www.ncbi.nlm.nih.gov/pubmed/22245715>) and other tinnitus researchers. Audience members can bring 1-2 relevant slides to frame their question and/or facilitate discussion, with a time limit of 3 minutes per participant.

257 Behavioral Strategies for Tinnitus Assessment in Animals

Brad May¹

¹*Johns Hopkins University*

Animal models provide a critical context for controlled laboratory studies of the physiological mechanisms of tinnitus. A longstanding challenge for this research is verification of phantom sound perception in non-human subjects that cannot verbally report the subjective properties of experimentally induced tinnitus. This presentation will introduce the types of behavioral strategies that have been used for tinnitus assessment in animals. We will begin by summarizing the basic experimental methods for inducing tinnitus. Then, we will demonstrate how the altered perception of silence can serve as an objective behavioral marker of tinnitus status. We will describe how the context of behavioral testing can be arranged to quantify additional subjective characteristics of tinnitus, such as its pitch and magnitude. The validity of these animal models will be assessed by comparing outcomes that have been obtained with different behavioral approaches from animals that have been treated with comparable induction methods. As tinnitus investigators seek high-throughput behavioral methods for screening animals, reflex-based methods have supplanted conditioning paradigms that may demand a substantial time investment in each subject. A concern raised by these new approaches is whether a change in reflexive behavior adequately reflects abnormal auditory processing in the parts of the brain that relate most directly to tinnitus perception.

258 Psychophysics of Tinnitus in Human Subjects

James Henry¹

¹*National Center for Rehabilitative Auditory Research*

Background

Over 30 years ago formal efforts were undertaken by the CIBA Foundation in London to promote international cooperation in tinnitus research. A central concept in the CIBA Symposium was that standardization of tinnitus measures would advance international understanding and facilitate work on tinnitus. As a result of these efforts a

clinical assessment battery was recommended to include pitch match, loudness match, maskability, and residual inhibition. Many tinnitus researchers and clinicians routinely obtain these measures. However, normative data do not exist to facilitate interpretation of the measures.

Methods

We have conducted studies since 1995 to develop computer-automated, self-guided tinnitus assessment procedures that can be used in a standardized fashion. The automated system has undergone numerous iterations and was eventually redesigned to enable clinical implementation. The Tinnitus Evaluation System (TES) now comprises a laptop computer (with custom programming) and a small patient-control box (TES Podiometer, or "Pod") that is hard-wired to a set of insert earphones.

Results

Measures obtained with the TES included (1) hearing threshold; (2) loudness match; (3) pitch match; (4) bandwidth match; (5) minimum masking level; and (6) residual inhibition. Repeated testing with research participants has documented response reliability for all of these tests. In general, all of these measures are reliable upon repeated testing except for pitch matching.

Conclusion

Normative data are important to identify relationships between measures of tinnitus perception and other factors that could help to: (1) elucidate underlying mechanisms of tinnitus; (2) facilitate a more definitive assessment of the association between these measures and measures of tinnitus impact; and (3) predict specific types of therapy that might be most beneficial to an individual patient.

259 A Startle-Reflex Based Test for Tinnitus

Jeremy Turner^{1,2}

¹*SIU School of Medicine, ²Illinois College*

The startle reflex, first explored systematically in the late 1930s by Landis and Hunt, has developed into a valuable tool for behavioral neuroscience research with many applications. The reflex and its habituation are routinely used to assess sensorimotor adverse effects in preclinical toxicology testing and drug development. The reflex can also be elevated through fear conditioning (known as fear-potentiated startle) and this technique has been used for several decades in the search for the neural basis of fear and anxiety, as well as in the development of anxiolytics. Another valuable feature of the startle reflex is how preceding sensory cues presented before the startle stimulus (optimally 50-150 ms), have the ability to reduce, or inhibit the reflex. This feature, generally referred to as prepulse inhibition (PPI) of the startle reflex, has been used to conduct audiometric/psychophysical testing in animal models (most notably by the laboratories of Ison, Willott, and their colleagues). PPI has also been used to document sensory processing deficits in human and animal models of schizophrenia and related disorders. A recent adaptation of the startle reflex test has been

proposed for the measurement of tinnitus. In this test, the startle reflex is inhibited when a silent gap embedded in a background noise is used as the inhibitory preceding cue. The hypothesis is that if an animal has ringing in the ears the silent gap cue would serve as a less salient stimulus, and thus a less effective inhibitor of the subsequent startle reflex. This presentation will review the use of the gap technique for measuring tinnitus and will discuss what has been learned about its applications. We will also discuss some of the challenges in using this technique and some of the questions that still remain.

Grant support provided by the Tinnitus Research Consortium.

[260] A Conditioned-Avoidance Based Test for Tinnitus

Shaowen Bao¹, Sungchil Yang¹, Benjamin Weiner¹, Li Zhang¹

¹*University of California, Berkeley*

Tinnitus is conscious perception of phantom sounds. We developed a behavioral test for tinnitus in a rodent model, in which this conscious perception drives a volitional active avoidance response (as compared to an autonomous, reflexive response). Our rationale is based on the assumption that while reflexes could be elicited subconsciously, volitional responses require decision-making that is based on conscious sensory perception. The behavioral procedure is divided into a training phase and a testing phase. In the training phase, animals learn to avoid foot shocks by crossing a barrier that separates the two compartments of a shuttle box when any sound is played. After training, animals are subjected to noise-induced hearing loss (NIHL) and begin the testing phase. A post-NIHL increase in barrier-crossing behavior in the absence of a sound is taken to indicate the presence of a tinnitus percept. This tinnitus measure is reproducible. Furthermore, it is correlated with the reduction of cortical GAD65 expression, supporting a role of the auditory cortex in the presumptively conscious tinnitus perception.

[261] Optogenetics: Molecules and Hardware for Control of Neurons

Edward Boyden¹

¹*MIT*

We have developed tools for the optical control of specific cell types embedded within the nervous system. These tools are now being used scientifically to reveal new targets for treating neural disorders, and also may clinically support prototype treatments for diseases ranging from blindness to post-traumatic stress disorder. A key aspect of our prosthetics is our development of a suite of fully-genetically-encoded reagents (e.g., ChR2, Halo, Arch, Mac, ArchT, Jaws, Chronos, and others) that, when expressed in specific neuron types in the nervous system, enable their activities to be powerfully and precisely activated and silenced in response to pulses of light. These tools are in widespread use for analyzing the causal role of defined cell types in normal and pathological brain functions. In this talk I will briefly give an overview of the

field, and then I will discuss a number of new tools for neural activation and silencing that we are developing, including new molecules with augmented amplitudes, novel color and light-sensitivity capabilities, and unique new capabilities. I will also describe new devices for high-channel-count light delivery into the awake behaving nervous system. Finally, I will talk about how these tools can be used to enable systematic analysis of neural circuit functions in the fields of emotion, sensation, and movement, and in neurological and psychiatric disorders, as well as our pre-clinical work on translation of such tools to support novel ultraprecise neuromodulation therapies for brain disorders.

[262] Luminopsin and Clomeleon: Novel Optogenetic Tools for Controlling and Monitoring Neuronal Activity

Ken Berglund¹

¹*Duke University Medical Center*

Over the past several years optical tools for observing and controlling neuronal activity have vastly expanded, from genetically encoded optical reporters to various light-driven actuators. However, there are unmet needs which require developing novel tools. We have developed two such tools, namely luminopsin and Clomeleon. I will provide proofs of principles for the two techniques and summarize their applications in neuroscience research.

First, it would be advantageous to manipulate neuronal activity acutely and invasively as well as chronically and non-invasively, using the same genetic construct. Luminopsin allows activation of genetically defined populations of neurons by means of localized physical light and a systemically applied chemical using the same construct. Luminopsin was created by fusing a light-sensing channelrhodopsin with a light-emitting protein, *Gaussia luciferase*. The channelrhodopsin in this chimeric molecule can be activated by physical light (standard optogenetic approach) as well as by light generated by the luciferase acting on its substrate coelenterazine, CTZ (chemical genetic approach). We transiently transfected cultured neurons with luminopsin constructs and demonstrated the feasibility of using CTZ-activated bioluminescence to modulate ongoing neuronal activity. Specifically, application of CTZ depolarized the membrane potential of luminopsin-expressing neurons, which enhanced neuronal excitability and caused neurons to fire more action potentials in response to synaptic input. Thus, luminopsin expands the current approaches of manipulating neural activity in the brain by allowing channelrhodopsins to be activated by a diffusible molecule as well.

Second, while there are several approaches to image synaptic excitation and action potential firing in neurons, synaptic inhibition has remained largely invisible, partly due to a lack of appropriate indicators. Clomeleon is an optogenetic tool that was intended to shed a light literally to synaptic inhibition mediated by chloride (Cl). Clomeleon is a fusion protein of Cl-sensitive yellow and Cl-insensitive cyan fluorescent proteins. Through fluorescence resonance energy transfer (FRET), it enables ratiometric

measurements of intracellular Cl concentration, which reflects and dictates synaptic transmission mediated by Cl. We developed and characterized transgenic mouse lines that express Clomeleon in different parts of the brain. Specifically, we have utilized these mice to demonstrate developmental Cl change in immature neurons and both phasic and tonic forms of synaptic inhibition in more mature neurons in the hippocampus and the cerebellum, respectively. In conclusion, Clomeleon provides an array of unique applications to address Cl regulations in neurons and possibly in other cell types in the least invasive manner.

263 High-Speed Optogenetic Mapping of Brain Circuitry

George Augustine^{1,2}

¹KIST, ²Duke-NUS Medical School, Singapore

Although the basic anatomy and cellular components of the brain have been known for more than a century, we still do not understand how the brain works. This is in large part due to technical limitations in our ability to identify the function of brain circuits. New optogenetic technologies promise to greatly increase our understanding of brain circuit function.

By scanning small spots of laser light, synaptic circuits can be mapped in brain slices from transgenic mice expressing channelrhodopsin-2 (ChR2). These light spots photostimulate presynaptic neurons expressing ChR2, while postsynaptic responses can be monitored in neurons that do not express ChR2. Correlating the location of the light spot with the amplitude of the postsynaptic response elicited at that location yields maps of the spatial organization of the synaptic circuits. This approach yields maps within minutes, which is 10,000 times faster than can be achieved with conventional paired electrophysiological methods.

We have applied this high-speed technique to map local circuits in many brain regions. In cerebral cortex, we observed that maps of excitatory inputs to pyramidal cells were qualitatively different from those measured for interneurons within the same layers of the cortex (PNAS 104: 8143). In cerebellum, we could use this approach to quantify the convergence of molecular layer interneurons on to Purkinje cells and found that at least 7 interneurons form functional synapses with a single Purkinje cell. The number of converging interneurons is reduced by treatment with gap junction blockers, indicating that electrical synapses between interneurons contribute substantially to the spatial convergence. Remarkably, gap junction blockers affect convergence in sagittal cerebellar slices but not in coronal slices, indicating sagittal polarization of electrical coupling between interneurons. By measuring limb movement, this approach also can be used in vivo to define motor maps non-invasively (J. Neurosci. Meth. 179: 258).

In summary, ChR2-mediated high-speed mapping promises to revolutionize our understanding of brain circuitry.

264 Gating Thalamocortical Synaptic Plasticity and Auditory Cortical Map Plasticity After the Early Critical Period

Stanislav Zakharenko¹

¹St. Jude Children's Research Hospital

Gating thalamocortical synaptic plasticity and auditory cortical map plasticity after the early critical period

Jay A. Blundon, Sungkun Chun, Ildar T. Bayazitov, Rachel Chassan, and Stanislav S. Zakharenko

Department of Developmental Neurobiology, St. Jude Children's Research Hospital, Memphis, TN 38105, USA

The learning of behaviorally important sensory information is accompanied by an expansion of cortical representation areas in the sensory cortices. The substrate of this cortical plasticity is unknown. In the auditory cortex of neonates, cortical plasticity is induced by passive exposure to tones, but in adults, it requires active learning or pairing tones with the activation of cholinergic inputs. Like cortical plasticity, long-term potentiation (LTP) and long-term depression (LTD) at thalamocortical excitatory synapses can be induced in neonates but not in adults. Using single-cell electrophysiology, two-photon glutamate uncaging, and optogenetics in thalamocortical slices containing the auditory thalamus and auditory cortex, we determined that postsynaptically expressed LTP and LTD at thalamocortical synapses in the auditory cortex can be unmasked in mature mice by cortical disinhibition and activation of cholinergic projections emanating from the nucleus basalis. Cholinergic projections activate M₁ cholinergic receptors (M₁Rs) at thalamic presynaptic terminals and sustain glutamate release from thalamic projections to the auditory cortex via negative regulation of adenosine signaling. Experiments in slices and in vivo showed that deletion of A₁ adenosine receptors bypasses the M₁R-dependent requirement for LTP and LTD and permits cortical plasticity in the auditory cortex in adult mice, which is induced by passive tone exposure. These data suggest that synaptic plasticity at thalamocortical synapses underlies experience-dependent cortical plasticity in sensory cortices.

265 A Comparison of Electrical and Optical Activation of Midbrain and Cortical Pathways in Mice Expressing Channelrhodopsin-2 in the Cochlear Nucleus

Keith Darrow¹, Michael Slama^{1,2}, Judith Kempfle^{1,2}, Edward Boyden³, Daniel Polley^{1,2}, M. Christian Brown^{1,2}, **Daniel Lee^{1,2}**

¹Massachusetts Eye and Ear Infirmary, ²Harvard Medical School, ³MIT

Background:

The majority of auditory brainstem implant (ABI) users have reduced performance compared to cochlear implant

users. One possible explanation for this discrepancy is that existing ABI electrode designs are based on electrical stimulation and may have significant current spread and poor selectivity. This reduces the number of effective acoustic channels and increases side effects, such as dizziness or facial twitching from activation of non-auditory centers. Optogenetic activation of neurons (using channelrhodopsin-2, ChR2) has been used successfully in a number of systems as a way to improve selectivity of stimulation compared to electrical current. We hypothesize that cochlear nucleus (CN) neurons transfected with AAV-ChR2 can mediate responses along the ascending auditory pathways.

Methods:

The CN of CBA/J mice were virally-transfected with AAV2/ChR2. Pressure injection of viral vector was made into the dorsal cochlear nucleus, followed by an incubation period of two to four weeks. Subjects were then reanesthetized, and blue light (480nm) was delivered via flexible optical fiber to the surface of the CN. Auditory brainstem responses (ABR) were measured and multi-channel recordings of neural activity were made in inferior colliculus (IC) and auditory cortex (Actx) during acoustic, electrical, and light stimulation. The presence of ChR2-expression in CN neurons was confirmed with post-experiment histology.

Results:

Light-mediated responses were recorded from the IC during pulsed blue light exposure, correlating with ChR2 expression within the CN. Responses increased with elevated radiant levels and diminished when the optical fiber was directed away from the CN. Responses evoked with stimulation using a large-diameter (400 μ m) fiber showed a broad pattern of excitation in IC similar to electric stimulation. The extent of excitation and threshold of responses did not appear to depend on stimulation rate. An increase in neural activation of auditory cortical neurons was also observed during optical stimulation. No significant increase in neural activity was measured in cases where ChR2 expression was outside the auditory brainstem and in control cases. Finally, there was no measurable auditory artifact while using the blue light laser.

Conclusions:

Neurons expressing AAV-ChR2 in the CN can mediate light activation of auditory pathways in the midbrain and cortex in vivo. This approach has the potential to offer more selective stimulation of limited regions of the CN by delivering precise light stimulation via light-emitting diode-based optodes.

Supported by the Bertarelli Foundation, MED-EL, and NIH.

266 Infrared Neural Stimulation (INS), an Alternative to Neural Interfaces

Claus-Peter Richter^{1,2}

¹Northwestern University, ²Biomedical Engineering

Background: Infrared neural stimulation describes a method, by which an infrared laser is used to stimulate neurons, their axons, or their dendrites. Pulses of mid-infrared laser radiation are delivered to native, non-modified neural tissue to depolarize the neurons. The main advantage of INS is the possibility of stimulating neuron populations with a high spatial resolution when compared with electrical stimulation. Implantation of a miniaturized light source into the cat cochlea demonstrated that stimulation evoked a behavioral response of the animal and showed that stimulation over weeks of time was possible. At the wavelengths used for INS, the energy is primarily absorbed by water in the tissue and is converted into heat. Recently, it has been demonstrated that local heating of the neural tissue by the laser pulse induces a capacitive and depolarizing current at the cell membrane. To translate the technique into a clinical application it is important to know the energy required to stimulate the neural structure. With this study we provide measurements of the radiant energy, radiant power, and radiant exposure at the target structure that is required to stimulate the auditory neurons.

Methods: Flat polished fibers were inserted into scala tympani that the spiral ganglion was in front of the optical fiber. Angle polished fibers were inserted along scala tympani and the beveled surface of the fiber allowed directing the radiation beam perpendicular to the spiral ganglion by rotating the fiber.

Results: The radiant exposure for stimulation at the modiolus for flat and angle polished fibers was on average 6.78 ± 2.15 mJ/cm². With the angle polished fibers, changing the orientation of the optical beam by $\sim 90^\circ$ from an orientation that resulted in a maximum INS-evoked response, decreased the response amplitude by about 50%. An orientation of the beam that was opposite to the orientation with the maxima, resulted in a minimum.

Conclusions: Optical stimulation is possible with flat polished and side firing optical fibers. When compared with electrical stimulation, an optical implant would require similar amounts of energy to simulate the neurons.

This work was supported with federal funds from the National Institute on Deafness and Other Communication Disorders, National Institutes of Health, Department of Health and Human Services, under Contract No. HHSN260-2006-00006-C / NIH No. N01-DC-6-0006, DC011855-01A1, DC011481-01A1 and by Lockheed Martin Aculight.

267 Optogenetic Control of Mouse Outer Hair Cells

***Alfred Nuttall**¹, Teresa Wilson¹, Tao Wu¹, Hrebesh Subhash², Irina Omelchenko¹, Yuan Zhang¹, Sripriya

Ramamoorthy¹, Michael Bateschell¹, Lingyan Wang¹, John Brigande¹, Zhi-Gen Jiang¹

¹Oregon Hearing Research Center, ²Department of Biomedical Engineering, Oregon Health & Science University

Background: Normal hearing in mammals depends upon both sound detection by inner hair cells (IHCs) and sound amplification by outer hair cells (OHCs). The somatic motility of OHCs driven by membrane potential changes is a major component of the cochlear amplification process. A variety of methods have been utilized to study OHC motility. However, all these techniques have considerable limitations such as being invasive and having a lack of cellular precision and temporal-spatial resolution. To overcome these limitations, we used an optogenetic approach based on channelrhodopsin-2 (ChR2), a direct light-gated non-selective cation channel (NSCC) derived from the blue-green algae *Chlamydomonas reinhardtii*.

Methods: Patch-clamp and whole cell recordings were performed on the auditory cell line, HEI-OC1, and on isolated mouse OHCs expressing ChR2-tdTomato. For in vivo analysis, ChR2(H134R)-tdTomato was conditionally expressed in OHCs under control of a prestin-CreER^{T2} transgene. Auditory Brain Stem responses and histological analysis were conducted on these mice.

Results: We showed that 100 ms light pulses ($\lambda = 473$ nm, 1 mW/mm²) elicited a typical ChR2 current in ChR2(+) HEI-OC1 cells: an inward current rapidly rising to a peak (-15.9 ± 2.1 pA/pF at -60 mV), and then relaxing to a sustained current with reduced amplitude in solutions blocking all K channels. The I/V plot showed a reverse potential (V_r) near 0 mV. With regular Na⁺ rich extracellular and K⁺ rich intracellular solutions, similar ChR2 currents were elicited with the V_r at ~0 mV. I-clamp mode showed that the light pulse transiently depolarized ChR2(+) HEI-OC1 cells by ~11.7 mV. In comparison, in ChR2(-) HEI-OC1, the light elicited no response in membrane current or potential. In isolated mouse ChR2(+) OHCs, similar ChR2 currents were elicited with ~-4.0 pA/pF at -60 mV in solutions blocking K conductances, with I-V plots showing a V_r at ~0 mV. In isolated ChR2(-) OHCs, the light elicited no current or potential change. Analysis of adult (8 weeks) mice with OHC-specific ChR2-tdTomato expression revealed that nearly 100% of OHCs expressed the transgene and possessed normal ABR and DPOAE levels.

Conclusions: This is the first demonstration that ChR2 was successfully expressed in mouse OHCs and HEI-OC1 cells and functionally exhibited a light-activated NSCC and depolarization. The data suggests a novel approach to modulate OHC membrane potential, the driving force of transduction current and the regulator of somatic motility and represents a step towards a potential non-invasive clinical intervention of cochlear amplification. Supported by NIDCD DC 00105, 00141 and 004716.

268 Optogenetic Stimulation of the Auditory Nerve

Tobias Moser^{1,2}, Victor H. Hernandez^{1,3}, Gerhard Hoch¹, Kirsten Reuter^{1,3}, Zhizi Jing^{3,4}, Matthias Bartels⁵, Gerhard

Vogt⁶, Carolyn W. Garnham⁶, George J. Augustine^{7,8}, Sebastian Kügler⁹, Tim Salditt⁵, Nicola Strenzke⁴
¹InnerEarLab, Department of Otolaryngology, University of Goettingen School of Medicine, ²Center for Molecular Physiology of the Brain, Bernstein Center for Computational Neuroscience, ³Bernstein Focus for Neurotechnology, Goettingen, Germany, ⁴Auditory Systems Physiology Group, Dept. of Otolaryngology, University of Göttingen Medical Center, ⁵Department of Physics, University of Goettingen, Germany, ⁶MED-EL Company, Innsbruck, Austria & MED-EL Germany, Starnberg, Germany, ⁷Program in Neuroscience and Behavioral Disorders, Duke-NUS Graduate Medical School, Singapore, ⁸Center for Functional Connectomics, Korea Institute of Science and Technology, Republic of Korea, ⁹Viral Vectors Laboratory, Dept. of Neurology, University of Goettingen Medical School

When hearing fails, electrical stimulation of spiral ganglion neurons (SGNs) by cochlear implants (CIs) enables speech comprehension despite poor frequency and intensity resolution. Optical SGN stimulation may improve CI coding by enabling more independent information channels to the CNS. We employed the light-gated ion channel, channelrhodopsin-2 (ChR2), to render SGNs sensitive to light. Stimulation of ChR2-expressing SGNs by blue light activated the auditory pathway in hearing mice and in deaf mice. ChR2-mediated auditory brainstem responses (oABR) had a threshold of 2 μ J/mm² and a dynamic range of more than 20 dB. In summary, optogenetic stimulation of SGNs is feasible.

269 The Role of Actomyosin Contractility in PCP Regulation in the Organ of Corti

Jianyi Lee¹, Robert Adelstein², Robert Ross³, Xiaowei Lu¹
¹Department of Cell Biology, University of Virginia Healthsystem, Charlottesville, VA 22908, USA, ²National Heart, Lung, and Blood Institute, National Institutes of Health, Bethesda, MD 20892, USA, ³Department of Medicine, UCSD School of Medicine, La Jolla, CA 92161, USA

Background

Planar cell polarity (PCP) in the organ of Corti (OC) is manifested by the uniform orientation of stereociliary bundles towards the lateral edge of the cochlear duct. Proper orientation of stereociliary bundles is essential for normal hearing function as they are directionally sensitive to vibrations along the basilar membrane. In addition to the core cassette of non-canonical Wnt/PCP pathway genes, Protein tyrosine kinase 7 (*Ptk7*) was identified as a novel regulator of PCP in vertebrates. In *Ptk7* mutant mice, outer hair cells (OHCs) display stereociliary bundle misorientation along with extra rows of OHCs in the apex, similar to core PCP mutants.

Methods

We hypothesize that *Ptk7* and the core Wnt/PCP pathway converge on myosin II to mediate PCP in the organ of Corti. Myosin II-based contractile tension between supporting cells and hair cells orient hair cell PCP. To test this hypothesis, we are taking a multipronged approach

combining mouse genetics, organotypic cochlear explant culture, small molecule inhibitors and live cell imaging to elucidate the role of the actomyosin cytoskeleton in hair cell PCP.

Results

We show that *Ptk7* and the core Wnt/PCP pathway differentially regulate a contractile myosin II network in supporting cells. Moreover, *Ptk7* and the Wnt/PCP pathway act in concert to promote junctional planar asymmetry of vinculin, a tension-sensitive actin-binding molecule. To gain mechanistic insight into this process, we are currently analyzing the dynamics of myosin II during PCP signaling in the organ of Corti by live imaging of cochlear explants expressing a GFP-Myosin IIB fusion, and assessing the effect of perturbing the actomyosin cytoskeleton on contractile behaviors of myosin IIB. We also generated conditional vinculin knockout mutants and observed PCP defects in the vinculin mutant inner ear. These results suggest a model whereby PCP signaling mediates polarized contractile forces along the medial borders of hair cells to orient their stereociliary bundles. Details of our analysis will be presented at the meeting.

Conclusion

Our results support the hypothesis that *Ptk7* and the non-canonical Wnt/PCP pathway act in concert to mediate myosin II-based anisotropic tension at contacts between hair cells and supporting cells. We showed previously that hair cell PCP is controlled by Rac-PAK signaling. We propose that polarized contractile tension between OC epithelial cells regulates the spatial pattern of Rac-PAK activity to orient hair cell PCP.

270 Patterning of the Organ of Corti Is a Multi-Step Process That Involves Dual Modes of Notch Signaling

Martin Basch¹, Takahiro Ohyama², Warren Pear³, Pamela Stanely⁴, Susan Cole⁵, Thomas Gridley⁶, Bridgett McNulty¹, Neil Segil², Andrew Groves¹

¹Baylor College of Medicine, ²House Research Institute, ³University of Pennsylvania, ⁴Albert Einstein College of Medicine, ⁵Ohio State University, ⁶University of Maine

Background

Notch-mediated lateral inhibition is a well-characterized patterning mechanism in the organ of Corti; however, it is insufficient to explain the intricate array of hair cells and supporting cells in the mammalian cochlea. Here we propose a dual mode of Notch action that is dose-dependent and acts differentially on progenitors that generate inner and outer hair cells.

Methods

We compared several mutants of the Notch pathway in the inner ear, analyzing the appearance of supernumerary hair cells and whether or not they were accompanied by transdifferentiation of associated supporting cells. We are also pharmacologically manipulating levels of Notch signaling in organotypic cochlear cultures to evaluate a dose dependency effect.

Results

In inner ear conditional mutants where some components of the Notch signaling pathway have been deleted, we do not observe supernumerary outer hair cells nor transdifferentiation of supporting cells to a hair cell fate. By contrast, we do observe supernumerary inner hair cells and their associated supporting cells.

Conclusion

Our results so far support a model in which low levels of Notch signaling might be sufficient to pattern inner hair cells, border cells and inner phalangeal cells whereas higher levels of Notch may be required to correctly regulate the proportions of outer hair cells and pillar and Deiters' cells.

271 Vangl2 Directs Supporting Cell Morphogenesis and Is Not Essential for the Postnatal Refinement of Hair Cell Planar Polarity

Catherine Copley¹, Michael Deans¹

¹Johns Hopkins University School of Medicine

Background

Auditory hair cells have a distinctive planar polarity evident in the polarization and orientation of the stereocilia bundle. Mutations in the core planar cell polarity (PCP) gene *vangl2* result in hair cells that form polarized bundles but are misoriented and have bundle polarities that are not coordinated with neighboring cells. In addition there is a gradient of phenotypic severity ranging from the least affected basal to the most affected apical turn of the cochlea. This gradient is similar to the progression of hair cell maturation suggesting that active refinement could correct planar polarity phenotypes in the basal cochlea of *vangl2* knockout (KO) mice.

Methods

Since the *vangl2* deletion results in perinatal lethality, *vangl2* conditional knockouts (CKO) were generated to test this hypothesis. When crossed with *pax2-Cre*, *vangl2* is deleted from the inner ear yielding planar polarity phenotypes similar to *vangl2* KOs at late embryonic stages. Early postnatal development was assayed using anatomical techniques and auditory function in adults was assayed by ABR and DPOAE.

Results

Pax2-Cre; *vangl2* CKO mice are viable and do not have the lethal neural tube defect that occurs in the *vangl2* KO. Quantification of planar polarity through postnatal development demonstrates a continuation of the maturational refinement processes initiated during late embryogenesis, and auditory hair cell orientation is largely corrected within 10 days of birth although some misoriented cells persist in the extreme apical turn of the cochlea. In contrast a similar refinement of vestibular hair cell planar polarity in the striola region of the utricular maculae does not occur during this period. In addition the *pax2-Cre*; *vangl2* CKO has profound changes in the shape

and distribution of the apical surfaces of Outer Pillar Cells and Deiters' Cells. These changes in supporting cell morphology are persistent, and are not corrected during the period of planar polarity refinement. ABR analyses of adults show a 10-20 decibel shift in auditory threshold across all tested frequencies and DPOAE measurements indicate that this mild hearing deficit is of cochlear origin.

Conclusion

Together these data support the hypothesis that a *vangl2*-independent refinement mechanism actively reorients auditory hair cells during the first 10 days of postnatal development. *Vangl2* is required during supporting cell development however it is unclear if this reflects a 'conventional' planar polarity activity. Nonetheless since the altered supporting cell morphology is not refined these changes in supporting cell shape likely underlie the hearing deficits measured in *vangl2* CKOs.

272 GSK3 Is an Essential Regulator of Cell Fate Decisions in the Mouse Cochlea

Takayuki Okano^{1,2}, Matthew Kelley¹

¹NIDCD/NIH, ²Kyoto University

Background

The development of the cochlear sensory epithelium requires the orchestration of multiple developmental events including cell cycle-exit, precise cell fate specification, and organized alignment of hair cells and supporting cells. Many of the signaling pathways required to coordinate these processes remain unknown. In the central nervous system the cytoplasmic molecule Glycogen Synthase Kinase 3 (GSK3) acts as an integrating molecule for multiple proliferation and differentiation signals. In particular, GSK3 is regulated by receptor tyrosine kinase, canonical Wnt, and Sonic hedgehog signaling pathways. While canonical Wnt signaling has been implicated in auditory versus vestibular fate specification, prosensory formation and hair cell differentiation, functional role(s) for GSK3 in the developing cochlea have not been examined.

Methods

To begin to identify the functional role(s) for GSK3 signaling in cochlear development, we established explant cultures from E13.5 mouse embryos. GSK3 was inhibited using one of two different pharmacological inhibitors (BIO-acetoxime and CHIR99021).

Results

Inhibition of GSK3 leads to several unique phenotypes including a disruption in hair cell arrangement, an increase in the number of inner hair cells (confirmed based on expression of *Fgf8*), and a widened gap between the row of inner hair cells and the first row of outer hair cells. This phenotype was markedly different from the phenotype observed in explants treated with the canonical Wnt agonist, suggesting that the effects of GSK antagonism are not a result of activation of canonical Wnt signaling. Inhibition of GSK3 also leads to a decrease in expression

of *Bmp4* in cochlear explants, suggesting that BMP may be a target of GSK3.

Conclusion

Our data suggest that non-Wnt-related GSK3 signaling plays an important role in cochlear development that may include regulation of inner and outer hair cell fates.

273 The Role of *Atoh1* in the Cochlear Development

Tiantian Cai¹, Michelle Seymour¹, Frederick Pereira¹, Huda Zoghbi¹, Andrew Groves¹

¹Baylor College of Medicine

Background

Atoh1, the mouse homolog of *Drosophila* proneural gene *atonal*, is a basic helix-loop-helix (bHLH) transcription factor that is the earliest known gene expressed in differentiating hair cells. There is a severe phenotype in the cochlea of *Atoh1*-null mice: massive cell death in the presumptive sensory epithelia begins at embryonic day 15.5 (E15.5) and results in the complete absence of hair cells and supporting cells, suggesting the necessity of *Atoh1* in the development of the organ of Corti.

Methods

To dissect *Atoh1*'s function during hair cell development, we established a conditional knockout (CKO) system that allows us to delete *Atoh1* from hair cells at different stages. By exposing pregnant or neonatal mice to tamoxifen to activate Cre-mediated recombination in hair cells, *Atoh1* was removed from hair cells at stages between E15.5 and postnatal day 0 (P0).

Results

We analyzed *Atoh1* protein expression in mice in which both copies of the *Atoh1* gene have been replaced by an *Atoh1-GFP* fusion sequence. Based on our results of GFP immunohistochemistry and quantitative PCR in these mice, *Atoh1* expression initiates in the prosensory domain of the cochlea as early as E13.5. As the cochlea develops, *Atoh1* expression is up-regulated and maintained in hair cells until postnatal stages, when it starts to be down-regulated and disappears from hair cells before the onset of hearing. We analyzed the number of hair cells and supporting cells in the cochleas of the *Atoh1*-CKO animals and found there is a critical time window (about two days after *Atoh1* expression) in which *Atoh1* is required to maintain the survival of the cells in the organ of Corti. We also examined the hair bundles in the CKO hair cells and found the hair bundle formation also requires *Atoh1* expression in a time-dependent manner. In addition, auditory brainstem response (ABR) was measured in the CKO animals in which *Atoh1* was removed at E17.5. Although we observed comparably normal hair cell formation in the basal region of the cochlea in these mice at neonatal stages, we could not detect ABR responses at any frequency in these mice at the age of 6 weeks, indicating an essential role of *Atoh1* in maintaining the proper function of hair cells after their differentiation.

Conclusion

Our study suggests *Atoh1* might have multiple functions in the survival, differentiation and maturation of hair cells during cochlear development.

274 Using Novel Mouse Mutants to Elucidate BHLH Transcription Factor Regulatory Interactions in Ear Neurosensory Development

Ning Pan¹, Israt Jahan¹, Jennifer Kersigo¹, Karen Elliott¹, Bernd Fritsch¹

¹University of Iowa

Background

Cross-regulation between transcription factors plays crucial roles in cell differentiation and development. In developing ears, studies have shown extensive intra- and intercellular interactions among the three proneural basic helix-loop-helix (bHLH) transcription factors, Neurog1, Neurod1 and Atoh1. Together with interactions with a group of diffusible factors and other transcription factors, they form a regulatory network that determines neurosensory cell identity.

Methods

We generated several novel mouse mutants and characterized their inner ear neurosensory development and gene expression using immunohistochemistry and *in situ* hybridization.

Results

Using *Neurod1* conditional knockout mutant mice, we show that the absence of *Neurod1* results in upregulation of *Atoh1* expression and hair cell formation within the sensory ganglion, suggesting that *Neurod1* negatively regulates *Atoh1* to suppress hair cell fate in neurosensory precursor cells to develop as neurons. Moreover, the deletion of *Neurod1* also results in premature and increased expression of *Atoh1* and formation of ectopic inner hair cells in the outer hair cell region in the apex of the organ of Corti. Interestingly, the phenotype of ectopic inner hair cell formation can be partially suppressed by deleting one copy of *Atoh1* gene, suggesting that the expression level of *Atoh1* may control type-specific hair cell differentiation. To further investigate the cross-interactions between *Atoh1* and *Neurod1*, we combined the deletion of *Neurod1* with the *Atoh1* 'self-terminating' conditional knockout, in which the Cre expression is driven by an *Atoh1* enhancer element and activated when Atoh1 protein binds. In addition to the Atoh1 self-regulatory binding site, the enhancer element also contains a putative Neurod1 binding site. The resultant mutant mice showed increased hair cell loss throughout the cochlea compared with the *Atoh1* 'self-terminating' mutant. This suggests that *Atoh1* expression may be more rapidly reduced due to increased Cre expression, which is possibly the combined effect of both the direct elimination of *Neurod1* inhibition on Cre expression and the indirect increased *Atoh1* self-promoting activity.

Conclusion

Our results suggest that the cross-interactions between *Neurod1* and *Atoh1* may provide molecular basis of neurosensory cell fate determination and type-specific hair cell differentiation. We will quantitatively measure and compare the expression level of relevant genes in these different mutant ears. Our data will help to further define the bHLH transcription factor regulatory network and the role of *Atoh1* expression level and duration in hair cell differentiation and maintenance, which will provide crucial information for reconstituting the organ of Corti.

275 Function and Regulation of Hey1 and Hey2 in Cochlea Development

Ana Benito Gonzalez¹, Angelika Doetzshlofer¹

¹Johns Hopkins University

Background

The mouse auditory sensory epithelium consists of mechano-sensory hair cells (HCs), critical for our ability to detect sound, and supporting cells (SCs). Both cell types derive from a common pro-sensory progenitor. At E14.0, shortly after terminal mitosis HC and SC differentiation initiates in a basal to apical gradient. Very little is known about the molecular mechanisms controlling the timing of HC and SC differentiation. Hey1 and Hey2, two highly redundant bHLH transcriptional repressors are highly expressed in cochlear pro-sensory progenitors and are rapidly down-regulated as differentiation occurs.

1. Based on their known function as Atoh1 antagonists and their high expression in pro-sensory progenitors, we hypothesize that Hey1 and Hey2 function in maintaining an undifferentiated progenitor state.
2. Hey1 and Hey2 have been commonly described as Notch effector genes. However, our recent findings suggest a more complex regulation mechanisms for Hey2 during cochlear development. A good candidate pathway to regulate Hey2 in pro-sensory progenitors is the Sonic hedgehog (Shh) pathway, which has been shown to play an inhibitory role in HC differentiation.

Methods

1. Pax2-Cre Hey1 fx/fx Hey2 null mice were used to genetically delete both Hey1 and Hey2 in the developing cochlea.
2. We cultured E13.5 Atoh1/GFP transgenic cochlea explants in the presence of Shh and cyclopamine and vehicle control and used qPCR to analyze changes in gene expression. In addition effects on HC differentiation were analyzed over a three day period monitoring HC specific Atoh1/GFP expression.

Results

1. Consistent with abnormal timing of differentiation, Hey1 Hey2 double knockout mice have complex hair cell patterning defects. We observe in the Hey1 Hey2 double mutant sensory epithelium ectopic IHCs from base to apex and ectopic OHCs in the base and mid cochlear regions. However, we observe in the apex of the Hey1 Hey2 mutant cochlear only two rows of OHCs.

2. Our results indicate that Shh positively regulates Hey2 expression at the pro-sensory stage. Moreover, cochlea explants treated with Shh show a delay in HC differentiation, while in those treated with the Shh antagonist, Cyclopamine, HC differentiation occurs earlier.

Conclusion

1. Our results show a patterning defect that suggests an early onset of HC in absence of Hey1 and Hey2 in the double knockout mutant mice possibly leading the altered phenotype.

2. Based on our findings we hypothesize that Shh pathway negatively controls HC differentiation through a Hey2 dependent mechanism.

276 Maintenance of Cell Fate in the Organ of Corti: Molecular Biology of Atoh1 Regulation by Hes/Hey Genes

Yassan Abdolazimi^{1,2}, Neil Segil^{1,2}

¹House Research Institute, ²University of Southern California

Background

A regular mosaic of hair cells and supporting cells characterizes the sensory regions of the inner ear. Genetic experiments indicate that this mosaic arises partly through Notch-mediated lateral inhibition leading to regulation of Atoh1 gene expression. During embryonic development, Atoh1 up-regulation is required for hair cell differentiation of selected sensory progenitors, and coincident inhibition in the surrounding progenitors, which subsequently differentiate as supporting cells. A requirement for Notch signaling continues to be required during perinatal maturation of the organ of Corti to maintain the fate of supporting cells. The molecular basis of Atoh1 gene regulation during these processes remains to be studied.

We have investigated the role of the Hes/Hey family of transcriptional repressors in the suppression of Atoh1 expression, and thus the maintenance of supporting cell fate. Hes/Hey expression in most perinatal supporting cells depends on the continued activation of the Notch signaling pathway. Blocking Notch signaling leads to Atoh1 activation and supporting cell transdifferentiation. Our working hypothesis is that Atoh1 is actively suppressed in supporting cells by Hes/Hey factors. In response to the loss of Notch activity in supporting cells, Atoh1 up-regulation is mediated by a process of disinhibition caused by the loss of Hes/Hey activity. Experiments supporting this hypothesis will be described.

Methods

Chromatin immunoprecipitation (ChIP), organ culture, FACS purification of hair cells and supporting cells, in vitro transfection, site-directed mutagenesis, and molecular reporter assays were used to investigate the role of Hes/Hey genes in regulation of Atoh1 expression.

Results

Hes/Hey gene expression is rapidly downregulated when Notch signaling is blocked, and Atoh1 is rapidly up-

regulated. ChIP assays provide evidence of direct binding of Hes/Hey proteins to the Atoh1 gene in a model cell line. Transfection assays indicate that Hes/Hey are sufficient to bring about Atoh1 transcriptional down-regulation, and that this likely occurs through direct binding to Atoh1 gene regulatory regions, and the changes in epigenetic regulation that accompany this binding.

Conclusion

Hes/Hey genes contribute to the regulation of Atoh1 through a mechanism that involves direct binding of these transcription factors to Atoh1 gene regulatory elements. Regulation of Atoh1, Hes/Hey genes and the importance of these observations to both the maintenance of the differentiated state, and regeneration, will be discussed.

277 Tinnitus Specific Trait in Animals

Marlies Knipper¹

¹University of Tuebingen, Tuebingen Hearing Research Center

Tinnitus is a non-curable stress-related brain disorder, that is mostly noise-induced and whose origin is unknown. We have addressed the molecular and physiological basis of this disease using a combined approach that included behaviorally tested tinnitus (Rüttiger et al., Knipper, *Hear Res* 2003), hearing measurements (including DPOAEs, ABRs and ABR wave analysis) and markers that trace network activity (Arc/Arg3.1). Data analysed the first time equally hearing impaired animals that were behaviorally distinguished in hearing impaired animals with and without tinnitus. We compared animals between the periphery of the cochlea and the auditory cortex, including the hippocampus and amygdala. We also included an analysis of altered responsiveness after stress priming. We unraveled a tinnitus specific trait that may explain some of the existing controversies about the molecular basis of tinnitus.

Acknowledgements. This work was supported by the Marie Curie Research Training Network CavNET MRTN-CT-2006-035367, the Deutsche Forschungsgemeinschaft DFG-Kni-316-4-1 and Hahn Stiftung (Index AG).

278 Short-Term Traumatic and Long-Term Non-Traumatic Noise Exposure Both Increase Spontaneous Firing Rate and Synchrony in Cat Auditory Cortex

Jos Eggermont¹

¹University of Calgary

Following traumatic noise exposure, resulting in a permanent hearing loss, the primary auditory cortex characteristic frequency (FF)-place map becomes reorganized. Instead of representing the frequency region of the hearing loss, now those neurons are tuned to the edge frequency of the audiogram, resulting in an over representation thereof. For this reorganized cortical region, spontaneous firing rates (SFR) are approximately doubled and spontaneous neural firings are occurring in a more synchronized way. Following frequency-restricted long-term moderate level (<70 dB SPL) stimulation with noise or other multi-frequency sounds, no changes in ABR

thresholds are found and DPOEAs remain normal. Yet, in auditory cortex the region with CFs in the frequency range of the sound exposure becomes much less responsive, it's SFR decrease as well as the slope of the driven-rate-level functions. In contrast, on both the low- and high-frequency side, the cortical gain is increased leading to increased SFR, increased neural synchrony and increased slope of the driven-rate-level functions. These changes require up to two weeks to establish and more than 3 months for recovery in quiet. Important differences are that the increased SFR following noise trauma is not accompanied by increased cortical gain, whereas this is the case following the long-term moderate level exposure. Following traumatic noise exposure, tinnitus is a frequent finding, and from the results induced by long-term moderate level noise one would expect the same, i.e., tinnitus but in the absence of hearing loss or peripheral auditory damage, but likely accompanied by hyperacusis.

[279] Psychoacoustic and Electrophysiological Imaging of Tinnitus

Larry E. Roberts¹

¹*McMaster University*

BACKGROUND: Neural mechanisms that detect changes in the auditory environment rely on processes that predict sensory state. This principle suggests that in tinnitus there is a disparity between what the brain predicts it is hearing (this prediction coded by aberrant neural activity occurring in frequency regions affected by hearing loss) and the acoustic information delivered to the brain by the damaged cochlea. This disparity may activate auditory attention, facilitating through subcortical neuromodulatory systems forms of neural plasticity that entrench aberrant neural changes underlying the tinnitus sound. This talk will summarize behavioral and functional brain imaging evidence for persisting auditory attention in tinnitus and present a qualitative model describing how attention may operate in normal hearing and in tinnitus.

METHODS: We measured hearing function, tinnitus spectra, and residual inhibition (RI) functions in 28 individuals with tinnitus, and hearing function in 31 age-matched controls without tinnitus. Audiometric thresholds to 16 kHz were comparable in the two groups. We then probed neural activity with 40-Hz amplitude modulated tones using either a 500 Hz carrier frequency in the range of normal hearing or a 5000 Hz carrier in the tinnitus spectrum and the region of audiometric threshold shift. Each subject adjusted the loudness of the probe stimulus to match a 1000 Hz sound (in the range of normal hearing) presented at 65 dB SL. This procedure may control for changes in central gain related to hearing loss and reveal consistent electrophysiological findings presently lacking in the tinnitus literature. Two responses were extracted from 128 channel EEG, the 40-Hz steady state response (ASSR) localizing to A1 and the N1 transient response localizing to A2, both responses known to be attention sensitive. The responses were also measured after a masking sound (band limited noise, center frequency 5000 Hz) presented for 30 seconds that yielded RI in tinnitus.

RESULTS: N1 amplitude was larger at both probe frequencies and ASSR amplitude at 500 Hz in the tinnitus group compared to controls. At 5000 Hz ASSR amplitude was smaller in tinnitus than controls. The group difference in N1 was not affected by masking, but the group difference in ASSR amplitude was abolished by masking.

CONCLUSIONS: These results can be interpreted assuming that (1) frequency-nonspecific auditory attention is activated by a failure of auditory prediction in tinnitus, and (2) neuroplastic changes occurring in the tinnitus frequency region bind neurons into synchronous activity underlying the tinnitus percept.

[280] Neuroimaging of Tinnitus-Related Changes in the Human Central Auditory System

Pim van Dijk¹, Kris Boyen¹, Margriet van Gendt¹, Dave Langers¹, Emile de Kleine¹

¹*University Medical Center Groningen*

Tinnitus is associated with peripheral hearing loss in the majority of cases. However, only a minority of people with a peripheral hearing loss experiences tinnitus. Evidently, peripheral hearing loss is not a sufficient condition to develop tinnitus, and brain-related factors have been hypothesized to play a role in the development of tinnitus. We applied functional MRI to investigate brain mechanisms involved in tinnitus.

One specific hypothesis that we tested is that tinnitus is related or even caused by reorganization of the tonotopy in the auditory cortex. However, an fMRI study in subjects with tinnitus and (near) normal hearing did not show reorganization. A second hypothesis, that assumes that tinnitus is related to reduced inhibition, predicts that sound-evoked responses may be enhanced in tinnitus. This hypothesis was tested by a comparison of subjects with and without tinnitus, respectively, and matched moderate hearing loss. There was no clear evidence of enhanced responses in the tinnitus subject group, which did not support the hypothesis. An additional analysis investigated the correlation between activity in auditory structures in the brainstem, thalamus and cortex. As was to be expected, the brainstem and cortex each have a strong functional connection with the thalamus. However, the functional connectivity between the brainstem and cortex was reduced in tinnitus subjects. This reduced connectivity may be an indicator of abnormal gating of auditory information in the thalamus. A third experiment was performed in subjects with gaze-modulated tinnitus. These subjects all underwent acoustic schwannoma surgery. They were selected for the ability to modulate the loudness of their tinnitus by peripheral gaze. An increase of the tinnitus loudness was associated with an increase of activity in the brainstem and a reduction of inhibition in the cortex. Furthermore, lateral gaze was associated with inhibition of activity in the thalamus. This unexpected inhibition again suggests abnormal thalamus function in tinnitus.

Together, these data show that tinnitus does not require reorganization of the cortical tonotopic map. Rather, functional correlates of tinnitus suggest a pivotal role of the thalamus in tinnitus. These correlates could either be a consequence of tinnitus, or may reflect a pre-existing vulnerability to develop tinnitus. Also, they could arise as a consequence of inherent mechanisms in the central auditory system or could be induced by interactions with non-auditory structures. Future research must help to understand these causal relations, which may help to develop new therapies for tinnitus.

281 Stress and Tinnitus: Population and Experimental Data

Sylvie Hébert^{1,2}, Dan Hasson³

¹Université de Montréal, ²International laboratory for research on BRAin, Music, and Sound (BRAMS),

³Karolinska Institutet, Stockholm, Sweden

Title :Stress and tinnitus: Population and experimental data

Sylvie Hébert
Dan Hasson

Hearing problems are a public health issue with prevalence figures far more common than previously estimated. There are well-established risk factors of hearing problems such as age, sex and noise exposure history. Our population studies systematically demonstrate an association between symptoms of long-term stress and increased prevalence of hearing loss and tinnitus. In particular, emotional exhaustion has been found a stronger predictor of both tinnitus presence and severity than traditional risk factors, e.g. noise at work, sex and hearing loss. Our experimental studies involving cortisol analyses, a stress-related hormone, also support an association between tinnitus and long-term stress. In particular, in tinnitus there is an increased sensitivity of the hypothalamus-pituitary-adrenal (HPA) axis to negative feedback. Such HPA axis disturbance has been described in other clinical populations such as patients with chronic fatigue syndrome and burnout. Altogether these findings have implications on treatment options for individuals suffering from severe tinnitus and suggest that measures of stress need to be taken into account in order to proactively intervene and prevent hearing problems. In this session, we will summarize our recent population and experimental findings about the associations between stress and hearing problems, and more specifically tinnitus.

282 Light on Network Dynamics in Primary Auditory Cortex

Israel Nelken¹

¹Hebrew University, Jerusalem, Israel

The last few years have seen the introduction of a number of exciting new techniques to auditory neuroscience, including calcium imaging of large populations of neurons and optogenetic techniques for the identification of neurons and manipulation of their responses. In this talk, I

will highlight one application of these techniques - the study of the correlation structure of large neuronal ensembles, and its modification by experience. Auditory cortex is malleable by experience, but previous studies of experience-dependent changes in auditory cortex emphasized modifications at the single-neuron level or modifications of the tonotopic map. Here, I will describe a study of the influence of a dramatic yet natural experience in the life of female mice - giving birth and becoming a mother - on neuronal ensembles in primary auditory cortex. Groups of neurons in layers 2/3 of mothers and age-matched controls were monitored using in-vivo two photon calcium imaging, verified and complemented by electrophysiological recordings from single neurons. Stimuli consisted of a set of artificial sounds and natural pup vocalizations. While response profiles of single neurons showed subtle changes in mothers relative to non-mother controls, population dynamics underwent large changes as measured by a large increase in pairwise and higher-order noise correlations: pairwise noise correlations essentially double in size in mothers relative to non-mother controls, independently of the tested stimulus. We used decoding techniques to estimate the influence of the increased noise correlations on stimulus coding. Surprisingly, decoding performance remained essentially the same in the two groups and was not affected by removing noise correlations from the responses. Thus, the correlated activity of the cortical network appears to be essentially orthogonal to its information-carrying capabilities.

283 Two-Photon Imaging of Neuronal Activity in the Mouse Auditory Cortex Reveals Spontaneous Categorization of Sounds

Brice Bathellier¹, Lyubov Ushakova¹, Simon Rumpel¹

¹Research Institute of Molecular Pathology (IMP)

In categorical perception a set of smoothly changing stimuli is perceived in a discontinuous manner. The neuronal correlates of this phenomenon are poorly understood. Here, we used in vivo two-photon calcium imaging to analyze sound-evoked activity patterns in local neuronal ensembles of the mouse auditory cortex. For that we used a large library of ~70 different sound stimuli containing pure-tone pips and various complex sounds. We found that activity patterns are highly constrained into few discrete response modes, which is surprising given how many patterns could theoretically be generated by the combination of already a few neurons. Such a low number of observed response modes suggest that local activity patterns form a discrete representation of sounds. Using on-line synthesis of sounds to tailor stimuli that allow precise probing of a given neuronal population, we observe highly non-linear dynamics indicating an antagonistic 'winner-takes-all'-like competition between response patterns. The high constrain on patterns that can be evoked implies that the information encoded locally is very low. However, we observed that different combinations of sounds were associated in a response mode in different local populations so that combining the

information of multiple local populations forms a representation that allows discrimination of more than 80% of sound pairs on a single trial basis. To test if discrete representations of sounds in the auditory cortex reflect auditory percepts in the mouse we trained mice in a go/no-go task to discriminate a positively reinforced sound and a negatively reinforced sound. We here used a novel assay where the spontaneous responses of mice to non-reinforced off-target sounds reported the perceived similarity of many off-target sounds to the reinforced target sounds. We observed non-linear categorization behavior in response to linear morphings of two target sounds. Interestingly, we observed a good match of the prediction based on global activity patterns recorded in the imaging experiments and behaviorally measured perception, including its non-linearities. In summary, our results suggest that local non-linear dynamics shape the cortical representation of sounds into a basis set of spontaneous categories that are available for behavioral decisions.

284 Micro-Organization and Plasticity of the Primary Auditory Cortex

Patrick Kanold¹

¹*University of Maryland*

The auditory cortex is a laminated structure organized into radial columns that adaptively processes sensory information from the external environment. The precise nature of the transformation of sensory information at the level of cortical networks is unknown. We use in vivo two-photon calcium imaging techniques to measure response properties and functional organization of primary auditory cortex neurons in mouse. We find that frequency selectivity in supragranular layers is heterogeneous on small spatial scales. In contrast to the supragranular layers, heterogeneity of frequency selectivity is lower in thalamorecipient layers indicating a rapid laminar transformation of the spatial representation of frequency selectivity. These findings reveal a transformation of sensory representations that occurs across a single cortical layer within the auditory cortex, which could generate sequentially more complex analysis of the acoustic scene incorporating a broad range of spectro-temporal sound features.

The local spatial heterogeneity of frequency selectivity in supragranular layers is likely created by sampling of diverse inputs to supragranular neurons by intra- and inter-laminar connections. The large frequency range of inputs available to each neuron might provide a substrate for a large degree of plasticity in individual neurons. We tested the capacity of auditory cortex neurons to rapidly change tuning properties by using micro-stimulation of top-down projections to auditory cortex and pairing such stimulation with a particular sound. We find that the frequency tuning of individual neurons can rapidly be changed leading to an increase in the representation of the paired sound. Collectively, these results provide insight into how sensory information is represented and adaptively transformed in auditory cortex.

285 In Vivo Two-Photon Calcium Imaging of Dendritic Spines in Auditory Cortex

Xiaowei Chen^{1,2}, Arthur Konnerth¹

¹*Institute of Neuroscience, Technical University Munich,*

²*Brain Research Center, Third Military Medical University*

The dendritic spines are key structures for receiving excitatory inputs and for synaptic plasticity. Understanding the individual functional properties and spatial arrangement of afferent synaptic inputs on dendrites is essential to dissect how the information is processed by neurons in the mammalian brain. However, the small size and high density have precluded the functional study of dendritic spines in vivo with standard methods. We have recently established a new variant of high-resolution two-photon imaging (LOW-power Temporal OverSampling, LOTOS) to detect calcium transients in single spines of mouse cortical neurons in vivo. Using this technique together with whole-cell patch-clamp recordings, we have studied two questions: 1) how is the spatial arrangement of sound-evoked inputs on dendrites in auditory cortex; 2) how individual synapses support cortical up-states in vivo. For the first question, we find that calcium signals require the activation of NMDA (N-methyl-D-aspartate) receptors. Active spines are widely distributed on basal and apical dendrites and pure-tone stimulation at different frequencies reveals both narrowly and widely tuned spines. Interestingly, spines tuned for different frequencies were highly interspersed on the same dendrites: even neighboring spines were mostly tuned to different frequencies. These results demonstrate that NMDA-receptor-dependent single-spine synaptic inputs to the same dendrite are highly heterogeneous (Chen et al., *Nature*, 2011). For the second question, we demonstrate that NMDA receptor-dependent subthreshold synaptic spine calcium signals are present during up-states, but nearly absent during down-states. We estimate that more than 500 excitatory synapses are active during an up-state. Importantly, similar patterns of spine calcium signaling are observed during spontaneous and sensory-evoked activity, indicating that cortical up-states and sensory stimulation-evoked cortical responses may be driven by highly overlapping sets of up-stream cortical neurons. These results identify the dendritic pattern of glutamatergic synaptic inputs on the level of single spines during cortical up-states. Altogether, with the high-resolution two-photon imaging technique, we open a way for in vivo functional study of the sensory information processing and the cortical network dynamics at single synapse level.

286 Single Neuron and Local Network Plasticity – Insights from Motherhood

Adi Mizrahi¹

¹*Hebrew University*

Understanding sound processing in the auditory cortex can benefit from recent imaging methods like two-photon laser scanning microscopy. One advantage of imaging is that it allows measurements at high spatial resolution and from multiple cells simultaneously. I will describe our recent experiments using in vivo two photon imaging to study how

pure tones and natural sounds are represented in layer 2/3 neurons in the primary auditory cortex (A1) of virgin vs. primiparus mother mice. To obtain a mechanistic understanding of network plasticity we targeted excitatory and inhibitory neurons selectively. We used either wild type NMRI mice or a cross between a knock-in parvalbumin positive driver mouse with a tdTomato reporter mouse. For calcium imaging we injected Fluo-4AM into L2/3 and imaged the cortex with a Prairie two-photon microscope. Electrophysiology was limited to juxtosomal recording either using blind patch or using visual guidance. Using calcium imaging we found that local populations display low signal correlations but high and variable noise correlations. Using electrophysiology we show that PV neurons provide a unique form of inhibition onto excitatory neurons. Moreover, PV neurons change their inhibitory pattern onto excitatory cells following the transition to motherhood and when multisensory inputs are processed. Our data show that plasticity in mothers is tunneled via modulation of feedforward inhibition.

[287] Corticostriatal Projections Mediate Auditory Decisions

Anthony Zador¹, Petr Znamenskiy¹
¹*Cold Spring Harbor Laboratory*

How does the brain use auditory signals to guide behavior? Representations of the acoustic world are constructed in the auditory cortex (ACx), but how these representations are used to effect behavioral choices is largely unknown. Auditory information is relayed from the ACx to a number of cortical and subcortical targets by distinct, largely non-overlapping populations of pyramidal neurons. We hypothesized that the ACx drives subjects' choices through its projection to the striatum. To test this hypothesis, we measured the contribution of striatal projection neurons to behavioral decisions by specifically manipulating their activity in rats performing auditory discrimination. We find that the projection of the ACx to the striatum drives auditory decisions in rats.

We first developed a novel auditory task—inspired by classic experiments by Newsome and colleagues in which a random dot stimulus was used to study the representation of visual motion in cortical area MT of macaque monkeys—designed to exploit the tonotopic organization of the ACx. We trained rats to discriminate low- and high-frequency “cloud-of-tones” stimuli (overlapping 30msec pure tones distributed over three octaves) in a two-alternative choice task. Subjects were required to report whether low or high tones were overrepresented; performance varied smoothly with stimulus frequency.

To test the ability of corticostriatal neurons to influence auditory discrimination in this task, we specifically targeted the expression of Channelrhodopsin-2 (ChR2) or Archaeorhodopsin-3 (Arch). We then implanted optical fibers into the ACx and limited light intensity to limit the perturbation to a restricted frequency band.

Activation of corticostriatal neurons by ChR2 biased the subjects to select the choice port associated with the neurons' frequency tuning. Furthermore, inactivation of corticostriatal neurons by Arch made subjects less likely to select the choice port associated with the preferred frequency of the inactivated neurons.

These results show not only that the ACx is causally involved in this task, but also that information propagates beyond the ACx via the corticostriatal projection. As striatal projections are widespread in cortex, our results may point to a general mechanism through which sensory cortex influences decisions.

[288] The Chromatin Remodeling Protein CHD7, Mutated in Charge Syndrome, Is Required for Proper Hair Cell Development and Cochlear Innervation

Elizabeth Hurd¹, Lisa Beyer¹, Yehoash Raphael¹, Donna Martin¹

¹*The University of Michigan*

Background

CHD7 is a chromatin remodeling protein that is necessary for proper formation of the mammalian inner ear. Humans with CHARGE Syndrome and *CHD7* heterozygous mutations exhibit mixed sensorineural/conductive hearing loss and inner ear dysplasia, including abnormalities of the semicircular canals and Mondini malformations. Prior studies in the mouse have demonstrated that reduced *Chd7* dosage in the ear disrupts expression of genes which are critical for morphogenesis and neurogenesis; however, the effects of *Chd7* deficiency on cochlear development have not been explored. In mice, complete loss of *Chd7* function results in intrauterine death by E11, several days prior to development of the sensory epithelium and its innervation. To overcome this early lethality and to uncover molecular mechanisms of CHD7 function, we have studied *Chd7* null phenotypes using inner ear specific *Cre* and *Chd7-flox* alleles.

Methods

We performed a detailed analysis of inner ears from mice with *FoxG1-Cre*-mediated *Chd7* conditional deletion, using whole-mount immunofluorescence, paint-filling, and scanning electron microscopy (SEM).

Results

FoxG1-Cre;Chd7 conditional knock-out (CKO) ears have underdeveloped, hypoplastic cochleae, with abnormal rotation of the mid-cochlear region and twisting of the apex that is detectable by E14.5. Myosin-VIIa staining of early postnatal CKO ears shows abnormal rows of outer hair cells along the length of the organ of Corti; at the tip of the apex, hair cells are completely disorganized and do not form typical orderly rows. SEM shows normal stereociliary bundle orientation and supernumerary hair cells throughout the length of the cochlea in CKO mice. Supernumerary hair cell stereocilia appear either cochlear-like or vestibular-like. Innervation of cochlear hair cells in

the *Chd7* CKO mice is also disrupted, with Neurofilament-positive neurites that extend to the lateral edge of the sensory epithelium. These neurites form loops that project beyond the hair cells, turn and extend backwards toward their site of origin in the cochlear ganglion.

Conclusion

Chd7 is necessary for elongation of the cochlear epithelium, hair cell differentiation and organization, and extension of neurites in the organ of Corti. Phenotypes in *Chd7*-CKO mice are similar to those observed with disrupted retinoic acid and Notch pathways. We conclude that CHD7-mediated chromatin remodeling regulates early patterning and regulation of hair cell number and differentiation, perhaps via altered retinoic acid and Notch signaling. Further experiments treating *Chd7* mutant ears with agents that alter retinoic acid or Notch signaling will explore this possibility.

289 An Analysis of a Sprouty Gene Dosage Series Reveals Compensatory Regulation of the Size of the Otic Placode

Jian Zhang¹, Amanda Mahoney Rogers¹, Katherine Shim¹
¹Medical College of Wisconsin

Background

In the mouse, at 8 – 9 somite stages (s), the otic placode becomes morphologically distinct as a pseudostratified region of ectoderm on either side of the hindbrain. These otic placodes are a committed embryonic progenitor pool that contributes to the mature population of mechanosensory hair cells, supporting cells and innervating neurons of the inner ear. We are studying the role of the *Sprouty* (*Spry*) gene family (of which there are four murine members, *Spry1* – 4) in otic placode induction. *Spry* genes encode antagonists of signaling downstream of receptor tyrosine kinases, including FGF receptors. In *Spry1*^{-/-}; *Spry2*^{-/-} double mutants, the otic placode is enlarged due to an aberrant, increased response of tissue to FGF induction.

Methods

Mutant combinations of *Spry1* and *Spry2* are generated by crossing β -actin *cre*/ β -actin *cre*; *Spry1*^{-/+}; *Spry2*^{-/+} males to *Spry1*^{fllox/fllox}; *Spry2*^{fllox/fllox} females. Embryos are analyzed by in situ hybridization, immunofluorescence, and histology. The size of the otic placode is measured by ImageJ on images of serial sagittal sections through the otic placode. Cell proliferation is quantified as the total number of cells stained for phospho-Histone-H3 per volume of otic placode.

Results

By analysis of a *Sprouty* gene dosage series, we find that similar to *Spry1*^{-/-}; *Spry2*^{-/-} double mutants, the otic placode is also enlarged in *Spry1*^{-/+}; *Spry2*^{-/-} and *Spry1*^{-/-}; *Spry2*^{-/+} mutant embryos at 9 – 11 s, a stage at which cells have committed to an otic fate. Interestingly, unlike *Spry1*^{-/-}; *Spry2*^{-/-} double mutants, enlargement of the otic placode is not maintained in *Spry1*^{+/+}; *Spry2*^{-/-} and *Spry1*^{-/+}; *Spry2*^{-/+} mutant embryos by 17 - 20 s, and the size of the otic

placode is restored to normal. Preliminary data suggest that a reduction in cell proliferation may help to reduce the size of an enlarged otic placode. Experiments exploring other mechanisms that explain the size correction of the otic placode are ongoing and will be presented.

Conclusion

These data suggest that organ-intrinsic mechanisms, such as modulation of cell proliferation, exist to correct aberrant enlargements of the otic placode, even after these cells have committed to an otic fate.

290 Retinoic Acid Signaling Regulates Tonotopic Patterning in the Developing Chick Cochlea

Benjamin Thiede¹, Zoe Mann², Yuan-Chieh Ku³, Michael Lovett³, Matthew Kelley², Jeffrey Corwin¹

¹University of Virginia, ²National Institute of Health,

³Washington University School of Medicine

Background

Frequency tuning depends on the basilar membrane's resonance properties and the responses of hair cells (HCs). In the chick cochlea, there is a longitudinal gradient of HC phenotypes. Proximal-end HCs contain 250 or more stereocilia that reach a maximum length of 1.5 μ m, while distal-end HCs contain 50 or fewer stereocilia that reach a maximum length of 5.5 μ m. At locations between those ends, the number and length of stereocilia grade from HC to HC. We sought to discover what signals pattern the development of this gradient of HC phenotypes.

Methods

Using transcriptome sequencing we sought to identify components of signaling pathways that are differentially expressed along the tonotopic axis of the E6.5 chick cochlea. We used qPCR to check these results and to evaluate expression at other ages.

To test whether treatments would affect phenotypes that are linked to HC position, we cultured cochleae from E6.5 embryos for 6 days in a control medium or media supplemented either with all-trans retinoic acid (RA) or citral, a RA synthesis inhibitor. We used Scanning EM to assess stereocilia length and number, qPCR to assess expression of the B1 subunit of the BK channel, and immunostaining to assess Calbindin expression (phenotypes that all differ along the longitudinal axis).

Results

In our analysis of the sequence data we discovered opposing longitudinal gradients of mRNA expression for an enzyme involved in the synthesis of RA and an enzyme involved in RA degradation. RALDH3, a RA synthesis enzyme, is expressed in a proximal-to-distal descending gradient, while CYP26C1, a RA metabolizing enzyme, is expressed in a distal-to-proximal gradient. However, a reverse (distal-to-proximal) gradient of RALDH3 is expressed at E10 and persists in the P14 cochlea. Through immunostaining, we confirmed that RALDH3 protein is expressed in the sensory epithelium.

When we cultured E6.5 cochleae in control medium for 6 days they developed the expected longitudinal gradient of HC phenotypes. In contrast, cochleae we cultured with RA developed HCs with distal-like phenotypes throughout the sensory epithelium. Cochleae cultured with the RA synthesis inhibitor, citral, developed HCs with more proximal-like phenotypes.

Conclusion

RA is a candidate morphogen that may influence the longitudinal patterning of HC phenotypes in the developing chicken cochlea. The evidence for a RA gradient we observed suggests that it may have an important role in the development of tonotopy.

291 A Gradient of Bmp7 Regulates Tonotopic Development in the Chick Basilar Papilla

Zoe Mann¹, Benjamin Thiede², Weise Chang¹, Michael Lovett³, Helen May-Simera¹, Jeff Corwin², Matthew Kelley¹
¹NIH, NIDCD, ²University of Virginia, School of Medicine, ³Washington University, School of Medicine

Background

The auditory system of vertebrates that perceive sound in air is organized based on the separation of sounds into their component frequencies. Tonotopy, is present in the sensory epithelia of the mammalian cochlea and avian/reptilian basilar papilla (BP), as well as in higher auditory structures including the brain stem and cortex. Manifestations of tonotopy along the longitudinal axis of the cochlea/BP vary between classes with changes in basement membrane characteristics predominating in mammals, while gradients in hair cell phenotype are foremost in birds and reptiles. Despite the significance of tonotopic organization for auditory function, the molecular and cellular factors underlying development of tonotopic organization remain unknown.

Methods

To identify signaling molecules that regulate positional identity along the chick BP, we determined the developmental timing for acquisition of positional identity (E6.5) using known markers for tonotopy and then Affymetrix expression arrays to compare gene expression between proximal and distal halves of the BP. Amongst those genes differentially expressed, Bmp7, in particular, displayed a significant expression gradient from distal to proximal. Graded expression was confirmed using both in situ hybridization and quantitative real-time qPCR and was found to persist even in the post-hatch BP (P12).

To determine the effects of disruption of the Bmp7 gradient, in vitro explant cultures were established at E6.5 and incubated for 6 days in either control media, or media supplemented with either Bmp7 or the Bmp antagonist, Noggin. Changes in positional identity along the tonotopic axis were assessed using known gradients in hair cell morphology including hair cell density, stereocilia length and number and the expression levels and cellular

localization of Calbindin. Potential downstream targets of Bmp7 were identified by western blot and qPCR.

Results

Contrast to control explants, which developed a normal tonotopic gradient, explants maintained in media with a uniform concentration of Bmp7 showed changes in tonotopic phenotypes consistent with a conversion of the entire BP to a distal identity. Similarly, treatment with Noggin converted the entire BP to a proximal phenotype. Furthermore, analysis of downstream targets suggests that Bmp7 acts through interactions with the FGF and MAPK signalling pathways.

Conclusion

Bmp7 is expressed in a gradient along the tonotopic axis of the chick BP and disruption of that gradient induces phenotypic changes consistent with alterations in positional identity. These results suggest that Bmp7 signaling plays a major role in specification of hair cell positional identity, and tonotopic organization, along the BP.

292 ephrin-B2 Is Required for Proper Development of an Inner Ear Transport Epithelium

Steven Raft¹, Mark Henkemeyer², Doris Wu¹
¹NIH/NIDCD, ²UT Southwestern Medical Center

Background

Identification of shaker/waltzer behavior and a collapsed labyrinth in mice lacking *EphB2*, as well as in CD1 mice heterozygous for deletion of the *ephrin-B2* (*Efnb2*) C-terminus, suggested a role for B-class Eph-ephrin signaling in endolymph homeostasis. This was confirmed by the finding of decreased utricular [K⁺] in circling *Efnb2* C-terminal deletion heterozygotes. However, the effects of these perturbations on the developing ear's transport epithelia remained undefined.

Methods

We have generated mice that lack *Efnb2* in developing ear tissues (*Efnb2* CKO) and are viable until shortly after birth.

Results

At an early stage, *Efnb2* CKO embryos display delayed outgrowth of the endolymphatic epithelium from the otocyst; this is preceded by a decreased rate of cell proliferation and heightened apoptosis. Delayed appearance of the structure is accompanied by disrupted patterning of endolymphatic duct and endolymphatic sac epithelia, as determined by mis-expression of genes in the Gbx, Dix, and Wnt families, and tissue-level mis-localization of protein and mRNA elements in an ionocyte differentiation pathway and the Notch signaling pathway. In the CKO, mRNA and protein components of the ionocyte differentiation and Notch signaling pathways are altered with respect to cellular-level abundance, but sub-cellular localization of ion transport proteins and transcription factors is maintained. Components of the

dysregulated ionocyte differentiation pathway include: the anion exchanger Pendrin (*Slc26a4*), mutations of which account for an estimated 5-8% of hereditary pre-lingual deafness in humans; the B1 subunit of an ATP-dependent proton pump (*Atp6v1b1*), mutations of which cause Renal Tubular Acidosis with Hearing Loss in humans; and Foxi1, a transcription factor and only known activator of *Slc26a4* and *Atp6v1b1* transcription in the ear. The utricle and saccule of *Efnb2* CKO fetuses display giant otoconia and abnormal aggregations of pre-otoconial matter, which we interpret as morphological markers of endolymph abnormality. We also investigated the relevance of these fetal CKO phenotypes to balance disturbance in adult mice. Tissue-level mis-localization of the ionocyte differentiation pathway was deemed a quantitative trait, as its metrics are significantly increased in *Efnb2* C-terminus deletion heterozygous fetuses of the CD1 circling strain compared with *Efnb2* C-del heterozygous fetuses of a non-circling strain.

Conclusion

These analyses, together with characterizations of *Efnb2* protein and mRNA expression, indicate that *Efnb2* is required for proper growth, differentiation, and activity of the endolymphatic epithelium over a wide period of embryonic development.

293 Secreted Semaphorins Control SGN Peripheral Axon Motility and Hair Cell Innervation

Thomas Coate¹, Matthew Kelley¹
¹NIH/NIDCD

Background

During cochlear development, peripheral axons from spiral ganglion neurons (SGNs) navigate through different cell types before synapsing with inner or outer hair cells (IHCs or OHCs). Projections from type I SGNs (95% of the total population) form synapses with IHCs, whereas projections from type II SGNs (the remaining 5%) extend past IHCs and pillar cells before innervating OHCs. In addition, after extending into the OHC layer, type II processes turn abruptly toward the cochlear base. The guidance mechanisms that mediate these projection patterns are poorly understood. In these studies, we have found that class 3 secreted Semaphorins (Sema3s), which bind Neuropilin/Plexin (Nrp/Plxn) co-receptor complexes, may play roles in type I and type II SGN navigation.

Methods

To determine expression patterns for these factors, we used both *in situ* hybridization and immunostaining. To investigate the function of Sema3-Nrp/Plxn interactions in the cochlea, a combination of *in vitro* culture assays and mutant mouse models were examined. In addition, specific changes in embryonic SGN growth cone behaviors in response modulating Sema3-Nrp/Plxn interactions were visualized using a live imaging mouse model in which sparse numbers of SGNs express a red fluorophore (*NgnCreERT2; R26R-tdTomato*) while all hair cells express a green fluorophore (*Atoh1-nGFP*).

Results

Developing SGNs express Nrp1, Nrp2 and PlxnA3 whereas specific cell types within the cochlear epithelium express several Sema3s. *Sema3a* is expressed by cells of the lesser epithelial ridge and appears in an apex-to-base concentration gradient. *Sema3f* is expressed by lateral support cells within the organ of Corti. The loss of Semaphorin-Nrp signaling in Nrp mutant mouse models or by Nrp function-blocking antibodies *in vitro* leads to increased numbers of SGN peripheral processes in the OHC region and abundant type II SGNs that do not turn toward the base. Using our imaging model, we determined that adding exogenous Sema3A or Sema3F leads to the collapse of different subsets of SGN growth cones suggesting distinct roles for these guidance cues during cochlear development.

Conclusion

Overall, these data suggest that secreted Semaphorin-mediated activation of Nrp/Plxn complexes may act to restrict type I SGN processes to the IHC region. These data also reveal a signaling system that drives the apex-to-base migration of type II spiraling fibers.

294 Generation of 'Three-Eared' Frogs Reveals Molecular and Activity-Based Guidance of Central Projections

Karen Elliott¹, Bernd Fritschsch¹
¹University of Iowa

Background

As new sensory organs arose in evolution, such as the ear, connections between the sensory system and CNS were formed. How these inner ear neurons find their central target in the hindbrain to transmit sound and movement information is not yet known. Development of the inner ear hair cells and neurons depends upon transcription factors such as Pax2/5/8 and several basic helix-loop-helix (bHLH) atonal family members. In the well-studied visual system, retinal ganglion cells (RGCs) similarly depend upon Pax2 and a bHLH atonal family member for their development. Given the molecular similarities of inner ear and eye development and the ability of inner ear afferents and RGCs to form a space-map in the CNS, it seems likely that the ear and eye use similar mechanisms for axon guidance. Projections of RGCs to the superior colliculus/tectum are guided by molecular cues (Eph/Ephrin) as well as activity-based mechanisms (formation of ocular dominance columns) in order to produce a topographical map of the environment. In this study, we generated 'three-eared' frogs in order to determine the amount of overlap or segregation of axonal projections when two ears are forced to innervate the same area of the hindbrain.

Methods

We transplanted an additional ear rostral to the native ear, either maintaining its orientation or rotating by 90 degrees. This allowed us to have the same or differential activity between the two ears, respectively. Swimming behavior

was observed and axonal projections were labeled by implanting lipophilic dyes into the native and transplanted ears.

Results

Embryos in which the transplanted ear was in line with the native ear swam normally, whereas embryos in which the transplanted ear was rotated by 90 degrees swam aberrantly. Afferent axons from the two ears projected to overlapping areas when the transplanted ear was in line with the native ear. In contrast, when the transplanted ear was rotated by 90 degrees, afferent axons from the two ears were segregated from each other, forming 'vestibular dominance columns' reminiscent of the ocular dominance columns formed from varying activity between the two eyes.

Conclusion

These results suggest that afferents of transplanted ears rotated 90 degrees interfere with vestibular processing as indicated by the aberrant swimming. In addition, the partial overlap and segregation of afferent innervation in the two 'three-eared' frog models implies that both molecular and activity-based mechanisms affect central projections.

295 Identification of Multiple Marshalin Isoforms and Their Expression During Cochlear Development

Jing Zheng¹, Chongwen Duan¹, Peter Dallos¹, MaryAnn Cheatham¹

¹Northwestern University

Background

The organ of Corti is composed of a group of highly polarized hair cells and their surrounding supporting cells, the latter having an unusual cytoskeletal structure. Microtubules (MT) and their networks play crucial roles during the development of the organ of Corti, which derives from simple epithelial cells. Marshalin has been identified as a MT minus-end-binding protein. MTs are present in loose dynamic networks in HCs (Slepecky et al., 1995), and tightly packed stable bundles in SCs (Angelborg and Engstrom, 1972). Although it is not known what factors contribute to form these distinctive patterns, we propose that Marshalin may be involved.

Methods

RNA was isolated using an Absolutely RNA@RT-PCR Miniprep Kit (Stratagene). RNA quality was measured by a 2100 Bioanalyzer (Agilent). Reverse transcription was performed by thermostable reversed transcriptase (Roche) at 55°C for one hour followed by PCR reactions using various primer sets. After cloning Marshalin cDNA into a mammalian expressing vector pEGFP-N2, plasmids encoding various marshalin isoforms were transiently transfected into opossum kidney (OK) cells. Marshalin-induced cytoskeletal changes were investigated using immunofluorescence.

Results

We discovered eight marshalin isoforms ranging from 863 to 1280 amino acids and carrying various protein-protein interacting domains including coiled-coil (CC), calponin homology, proline-rich (PR), and MT-binding domains referred to as CKK. We examined structural changes in the cytoskeleton induced by expressing two of these marshalin isoforms in OK cells. Marshalin containing CC and PR domains induce thick structures with marshalin surrounding MT-containing bundles. Marshalin isoforms lacking these CC and PR domains also induce MT-based bundles but in a more slender form. These data suggest that marshalin is an important scaffolding protein, capable of modifying cytoskeletal networks through its interaction with various protein partners. To further investigate the function of different isoforms in vivo, we examined marshalin mRNA expression during organ of Corti development. Marshalin mRNA associated with each of the eight isoforms is detected at different developmental stages ranging from E17 to adult.

Conclusion

These data suggest that marshalin isoforms are abundantly expressed in the mammalian cochlea and that they play various roles in regulating cytoskeletal structures. The expression of one or more specific domains allows marshalin to interact with different protein partners to shape and maintain the architecture of the organ of Corti. (Work supported by NIH Grants DC011813, DC010633, DC00089, and the Knowles Hearing Center).

296 MafB Is Necessary for Hearing Function and Auditory Synapse Development

Wei-Ming Yu¹, Jessica Appler¹, Allison Nishitani¹, Ye-Hyun Kim^{1,2}, Jeffrey Holt^{1,2}, Lisa Goodrich¹

¹Harvard Medical School, ²Children's Hospital Boston

Background

Auditory information is transmitted from the inner ear to the brain by spiral ganglion neurons (SGNs). To faithfully transmit sound information from hair cells to the brain, developing SGNs form a specialized synapse on hair cells, the ribbon synapse. The ribbon synapse is specialized for encoding acoustic signals with high temporal precision over a long period of time. Studying the molecular mechanism underlying how ribbon synapses develop may help us understand how sound information is transmitted and may lead to the development of new therapies for patients with hearing loss. We have identified the transcription factor MafB as a potential master regulator of auditory synapse development based on its specific expression in SGNs, functions in other developing systems, and ability to control the expression of known synaptic molecules.

Methods

To investigate the function of MafB in auditory synapse development, we generated a floxed allele of MafB and specifically removed MafB protein from SGNs. To complement MafB conditional knock-outs (*MafB^{CKO}*), we created a strain of mice (*MafB^{OE}*) that prematurely and

excessively express MafB upon Cre-mediated recombination.

Results

MafB^{CKO} mice are viable and exhibit no obvious behavioral abnormalities. Analysis of auditory function in *MafB^{CKO}* mice by auditory brainstem responses shows that the mutants can still detect sound even at low intensities, consistent with the normal preservation of hair cell function seen upon measuring DPOAEs. However, the neural response was significantly decreased and delayed relative to controls, suggesting that MafB is required for proper SGN activity. Immunostaining for the presynaptic ribbon marker RIBEYE/CtBP2 and postsynaptic AMPA receptor subunit GluR2 revealed that the number of ribbon synapses is reduced in *MafB^{CKO}* animals. In contrast to *MafB^{CKO}*, *MafB^{OE}* show increased ribbon synapses with altered cellular distribution. *MafB^{CKO}* mice show normal SGN firing properties and have an intact olivocochlear efferent system, indicating that the reduction of ribbon synapses is not a consequence of impaired activity of SGNs or the efferent system.

Conclusion

These results suggest that MafB is required for normal formation of synapses between hair cells and SGNs. More detailed analyses of the MafB mutant mouse models together with genome wide studies to identify MafB downstream genes will be performed to help us understand how MafB contributes to the development of auditory synapses.

297 An Overview of IGF Signaling

Derek LeRoith¹, Derek LeRoith¹

¹*Mt Sinai Sch of med*

The insulin/insulin-like growth (IGF) system comprises insulin, IGF-1 and IGF-2 as the ligands, six IGF binding proteins (IGFBPs) and three receptors; two receptors are functional as tyrosine kinases, the IR and the IGF-1R.

Most of the functional activity of the IGF ligands occurs via the IGF-1R, a transmembrane tyrosine kinase receptor. Activation of the IGF-1R leads to activation of the PI3Kinase and MAPKase pathways that are important for growth and development, cell survival and certain differentiate functions in adult tissues.

The IGF system is ubiquitous affecting almost every function of the body. Numerous gene-deletion mouse models of the IGFs, the IGFBPs and the IGF-1R have been created to established the whole body and tissue-specific effects of the IGF system, including the nervous system.

In this presentation, we will address the major signaling processes involved in cellular function and the effects of deletion or overexpression of the IGF system in tissue function focusing where applicable on the nervous system.

298 Regulation of Olfactory Stem Cell Self-Renewal and Differentiation

Russell Fletcher¹, Melanie Prasol¹, Jose Estrada¹, Yoon Gi Choi¹, John Ngai¹

¹*University of California, Berkeley*

Tissue regeneration is a complex process that requires the coordination of stem cell proliferation and differentiation to maintain or repair the structure. The olfactory epithelium is a sensory neuroepithelium whose constituent cell types – including the olfactory sensory neurons – are continuously replaced during the lifetime of the animal. Following severe injury that results in the loss of mature cell types, the olfactory epithelium is reconstituted by the proliferation and differentiation of adult tissue stem cells. The regenerative capacity and limited number of cell types make the olfactory epithelium an excellent model for investigating stem cell regulation in vivo. Previous studies have identified the horizontal basal cell (HBC) as the multipotent neural stem cell of the olfactory epithelium; the molecules and pathways regulating this adult tissue stem cell are unknown, however. Using whole genome expression profiling of FACS-purified HBCs, we characterized the mRNA and miRNA transcriptomes of HBCs under conditions of quiescence and proliferation/differentiation. Through these studies we identified groups of genes associated with different phases of the HBC life cycle. In addition, we found that p63, a member of the p53 tumor suppressor gene family, is highly enriched in quiescent HBCs. p63 is a key regulator of stem cell self-renewal and differentiation in all stratified epithelia investigated to date. Through conditional inactivation of the p63 gene in HBCs we found that p63 is required cell-autonomously for olfactory stem cell renewal and functions to repress HBC differentiation. These results demonstrate a critical role of p63 in olfactory stem cell renewal and differentiation, where p63 serves as a “molecular switch” that controls these two alternate cell fates. Our studies provide the first molecular insights into the genetic network regulating stem cell dynamics in the olfactory epithelium and reveal an unexpected parallel between stem cell regulation in this sensory neuroepithelium and other epithelial tissues. Current work is focusing on identifying the downstream targets and interaction partners of p63 in the regulation of olfactory stem cell dynamics.

299 IGF Signaling Regulates Cellular Differentiation in the Organ of Corti

Matthew Kelley¹, Takayuki Okano¹, Norio Yamamoto¹, Weise Chang¹

¹*NIH/NIDCD*

Insulin-like growth factor signaling is known to regulate multiple aspects of embryonic development including proliferation, growth, and differentiation. Mutations in members of the Igf signaling pathway lead to deafness in both humans and mice, demonstrating a role for this pathway in auditory function. While deletion of *Igf1* results in post-natal loss of spiral ganglion neurons, any other effects of Igf signaling within the developing sensory epithelium were not known.

In situ hybridization for members of the Igf signaling pathway during embryonic cochlear development indicated complex patterns of expression for Igf1 and 2, Igf1r, and six Igf binding proteins. Igf1 and 2 are strongly expressed in Kölliker's organ while Igf1r is expressed within the developing cochlear sensory epithelium.

Deletion of Igf1r results in shortened cochleae and defects in formation of the lateral and posterior semi-circular canals. Within the organ of Corti, Igf1r mutants exhibit decreased numbers of hair cells and a delay in hair cell differentiation. Analysis of the expression of developmental marker genes, including Sox2, p27kip1, and Atoh1 suggests that prosensory development is largely unaffected in Igf1r mutants, but that the transition from prosensory cell to hair cell is significantly delayed. Further analysis of Igf signaling in cochlear explants indicates independent effects on both cochlear elongation and hair cell differentiation, and suggests that the effects of Igf in the cochlea are regulated through PI3 kinase/AKT signaling.

Igf binding proteins can act as either enhancers or antagonists of Igf signaling. Igfbp3 expression is restricted to the prosensory domain prior to E14, but becomes down regulated in cells that develop as hair cells. Disruption of Notch signaling results in a loss of Igfbp3 as well as early differentiation of hair cells. These results imply that Igfbp3 could play a role in the timing of hair cell differentiation, possibly through antagonism of Igf signaling within the ear.

Overall, these results demonstrate an important role for Igf signaling in regulation of the transition between uncommitted prosensory cell and differentiating hair cell. Defects arising from disruption of this pathway could underlie the hearing loss observed in both humans and mice with perturbations of Igf signaling.

300 Insulin-Like Growth Factor 1 Deficiency and Hearing Loss

Isabel Varela-Nieto¹, Silvia Murillo-Cuesta¹, Lourdes Rodriguez de la Rosa¹, Rafael Cediél Algovia²
¹CSIC-UAM CIBERER IdiPAZ, ²UCM

Insulin like growth factor 1 (IGF-1) plays a central role in embryonic development and adult tissue homeostasis. Accordingly, it is an essential factor for the regulation of cochlear development through controlling apoptosis and late neuronal differentiation. In the cochlea, IGF-1 actions are mediated by a network of protein kinases (RAF, AKT and p38 MAPK) that modulate the expression and activity of transcription factors (AP1, MEF2, FoxG1 and FoxM1) leading to the regulation of cell cycle and metabolism.

IGF-1 deficiency causes hearing loss in mice and men, whereas low serum levels of IGF-1 are associated with human syndromes showing hearing loss and with premature presbycusis. Animal models are fundamental to understand the genetic, epigenetic, and environmental factors that contribute to human hearing loss. Mouse IGF-1 plasmatic levels decrease with ageing, concomitantly hearing loss and retinal degeneration occur, in a normal ageing process that is accelerated in the heterozygous *Igf1*^{+/+} mouse. Furthermore, low IGF-1 levels predispose to increased damage after noise-exposure. In the *Igf1* null

mouse, hearing-loss is caused by early neuronal loss and age-related stria vascularis alterations. In summary, our data suggest that serum IGF-1 levels could be a novel diagnostic tool for hearing loss and support the hypothesis that IGF-1-based treatments have potential for the protection or repair of hearing loss.

301 Clinical Efficacy of Topical IGF1 Treatment for Sudden Deafness

Takayuki Nakagawa¹

¹Kyoto University

Background

Several works from different laboratories have indicated that the insulin-like growth factor (IGF) signaling plays important roles in embryonic development and adult homeostasis of the cochlea. These findings encouraged us to investigate the efficacy of IGF1 in the treatment of sudden sensorineural hearing loss (SSHL). For this purpose, we have developed the drug delivery system using gelatin hydrogels for sustained, topical delivery of IGF1 into the cochlear fluid. Here we report clinical efficacy of topical IGF1 application via gelatin hydrogels for SSHL patients refractory to systemic steroid application.

Methods

A prospective, single-armed trial was designed using a historical control of hyperbaric oxygen therapy. Patients with SSHL that showed no recovery to systemic glucocorticoid administration were recruited. We applied gelatin hydrogels impregnated with recombinant human IGF1 in the round window niche. The primary outcome measure was the proportion of patients showing hearing improvement 12 weeks after the test treatment. The secondary outcome measures were the proportion of patients showing improvement at 24 weeks and the incidence of adverse events. We also performed retrospective chart review of these patients to figure out alterations in thresholds of pure tone audiometry (PTA).

Results

In total, 25 patients received the test treatment at a median of 23 days after the onset of SSHL. At 12 weeks after the test treatment, 48% (P = 0.086) of patients showed hearing improvement, and the proportion increased to 56% (P = 0.015) at 24 weeks. No serious adverse events were observed. These findings indicate that topical IGF1 application using gelatin hydrogels is well tolerated and may be efficacious for hearing recovery in patients with SSHL refractory to systemic steroids. In analyses of audiometric alterations, significant improvements of PTA thresholds were identified. Interestingly, the time course of hearing recovery is very slow. The major recovery of hearing appeared 4 weeks after application, and a few patients demonstrated further recovery of hearing until 24 weeks after treatment. These findings suggest that not only protection of hair cells but also other regenerative processes may be involved in mechanisms for hearing recovery.

Conclusions

A clinical trial of topical IGF1 application in SSHL patients indicates the potential of IGF1 as a therapeutic agent for

SSHL, and the need of further basic experiments to explore mechanisms for hearing recovery by IGF1.

302 Mechanisms of Cochlear Hair Cell Protection by IGF-1

Norio Yamamoto¹, Yushi Hayashi¹, Takayuki Nakagawa¹, Juichi Ito¹

¹*Dep. Otolaryngology, Head and Neck Surgery, Graduate School of Medicine, Kyoto University*

We have investigated the role of insulin like growth factor-1 (IGF-1) in cochlear hair cell protection. IGF-1 protects mammalian cochlear hair cells from noise exposure or from ischemic stress. The clinical trial for the treatment of idiopathic sudden sensorineural hearing loss cases that was refractory to the systemic steroid treatment showed improved hearing threshold in 56% of patients who were treated with IGF-1.

To establish more effective protocols of IGF-1 therapy for sensorineural hearing loss we tried to elucidate the mechanisms of cochlear hair cell protection by IGF-1 using cochlear explant culture of neonatal mice. We used neomycin as a method of hair cell impairment that was protected by IGF-1 in the explant culture system.

This system enables us to add various inhibitors at the most effective timing and concentration to clarify the downstream signal pathways of IGF-1 exerting the cochlear hair cell protection. We examined inhibitors of PI3K, Akt, MEK, and PKC that constitute the components of major downstream signal pathway of IGF-1. All tested inhibitors attenuated the effect of IGF-1 although the Akt inhibitor only attenuated the protection of inner hair cells, indicating that IGF-1 treatment could activate several kinds of downstream signal pathways. The specific action of Akt was confirmed by immunohistochemistry of phospho-Akt that was detected around inner hair cells. To clarify the effector of IGF-1 in the protection of hair cells, we performed comprehensive gene expression profiling using microarray. We identified two specific effector genes of IGF-1 signal, Gap-43 and Netrin1, in our experimental system.

To elucidate the cellular mechanisms involved in IGF-1 action, we examined the apoptosis and cell proliferation status after IGF-1 treatment. Decrease of apoptotic hair cell numbers and proliferation of Hensen's cells and Claudius' cells were observed when explant culture impaired by neomycin was treated with IGF-1. Contribution of the supporting cell proliferation to the maintenance of outer hair cells was confirmed by treatment with two different proliferation inhibitors, aphidicholin and mimosine.

In conclusion, these results indicated that IGF-1 activated several downstream cascades and, as a result, it promoted the proliferation of supporting cells and inhibited the apoptosis of cochlear hair cells in neonatal mice.

303 Identification of Novel Downstream Effectors of IGF-1 Signal Pathways Using a Comprehensive Gene Expression Analysis

Yushi Hayashi¹, Norio Yamamoto¹, Takayuki Nakagawa¹, Juichi Ito¹

¹*Kyoto University*

Background

We have revealed that insulin-like growth factor1 (IGF-1) protects cochlear hair cells of neonatal mice against aminoglycoside via both the phosphatidylinositol 3-kinase (PI3K)/Akt pathway and the mitogen-activated protein kinase kinase /extracellular signal-regulated kinase (MEK/ERK) pathway. However the effector genes of PI3K/Akt and MEK/ERK which work directly on cochlear hair cell protection have not been unveiled so far. To identify the effectors of IGF-1, we screened whole sets of expressed genes in the cochlear explant cultures using microarray and confirmed the results using quantitative RT-PCR (qRT-PCR).

Methods

1. Total RNA was extracted from the cochlear explant cultures of neonatal mice that were treated with only neomycin or both neomycin and IGF-1 for various durations. cDNAs were prepared from the total RNA and the expression levels of whole genes were compared between the control and IGF-1-treated groups using microarray provided by Affymetrix. We picked up the genes whose expression levels increased twofold in the experimental groups compared with those in the control groups. The differences in the expression levels were confirmed by qRT-PCR.

2. To confirm the identified genes were really at the downstream of the IGF-1 pathways, the changes of their expression levels after treatment with AKT or MEK inhibitor were tested using qRT-PCR.

Results

The expression levels of Gap43 and Ntn1 were up-regulated in the IGF-1-treated cochlear explant cultures compared with the control samples. The expression levels of Gap43 and Ntn1 were significantly reduced by the addition of Akt inhibitor or MEK inhibitor.

Conclusion

As effectors of IGF-1 signaling in the context of hair cell protection from aminoglycoside, we identified two kinds of genes, Gap43 and Ntn1 whose expression level increase was canceled by the addition of the PI3K or MEK inhibitor. These findings indicated that Gap43 and Ntn1 are the downstream effectors of IGF-1 in the cochlear sensory epithelium that are under the regulation of both the PI3K/Akt and MEK/ERK pathways.

304 Lmo4 Signaling in Cisplatin Mediated Ototoxicity

Samson Jamesdaniel¹, Sneha Hinduja¹

¹*The State University of New York, Buffalo, NY*

Background

The transcriptional regulator Lmo4 was recently identified as the major nitrated cochlear protein in cisplatin ototoxicity. Nitrated Lmo4 was localized in a number of critical cell types including outer hair cells, spiral ganglion neurons, and strial cells. Moreover, cisplatin treatment significantly decreased Lmo4 levels in the cochlea. The functional significance of a decrease in Lmo4 levels was indicated by an increased expression of activated caspase 3 in the inner and outer hair cells, upon silencing cochlear Lmo4 with siRNAs. These findings demonstrated the crucial role of Lmo4 in mediating cisplatin ototoxicity. However, the molecular signaling associated with cisplatin-induced modulation of cochlear Lmo4 is poorly understood.

Methods

Wistar rats were treated with a single dose of 16 mg/kg cisplatin and cochlear expression of mRNAs and proteins associated with Lmo4 signaling were evaluated, 3 days post treatment. A custom gene array was designed to investigate at least ten known binding partners and downstream targets of Lmo4, while proteins of interest were assessed by immunoblots. Co-treatment with 100 mg/kg/day Trolox was used to inhibit cochlear nitrosative stress and prevent cisplatin-induced ototoxicity.

Results

RT-PCR analysis of cochlear mRNA levels, indicated that cisplatin treatment modulated the expression levels of several binding partners and targets of Lmo4. Particularly, the cochlear expression of *Esr1* was significantly up-regulated by cisplatin treatment, while the expression of *Jak1* and *Stat3* was down-regulated. Co-treatment with antioxidant Trolox, which is also an inhibitor of peroxynitrite, attenuated their cisplatin-induced modulation in the cochlea. Further evaluation of the cochlear protein levels of *Stat3*, a downstream target of Lmo4 that is implicated in drug mediated apoptosis, supported the observed changes in the mRNA levels. Cisplatin treatment significantly decreased *Stat3* protein expression ($p < 0.001$), while co-treatment with Trolox attenuated the cisplatin-induced decrease in *Stat3* expression, in the cochlea ($p < 0.01$). Trolox co-treatment has previously been reported to prevent cisplatin-induced hearing loss. Therefore, these results illuminate a potential role of the key downstream players, *Jak1* and *Stat3*, in cochlear Lmo4 signaling and implicate their importance in mediating the ototoxic effects of cisplatin.

Conclusion

Based on these findings we hypothesize that cisplatin-induced nitration of Lmo4 decreases the cochlear expression of Lmo4 and facilitates the modulation of its binding partners *Esr1* and *Jak1*, which in turn represses

Stat3 and augments cochlear apoptosis. (Funded by NIH/NIDCD: R03DC010225, SJ)

305 Oral Capsaicin Prevents Cisplatin Ototoxicity

Leonard Rybak¹, Debashree Mukherjee¹, Kelly Sheehan¹, Vickram Ramkumar¹

¹*Southern Illinois University School of Medicine*

Background

Ototoxicity and nephrotoxicity are dose-limiting side effects of cisplatin, a widely used anticancer drug. Data from our laboratory suggest that cisplatin ototoxicity is linked, in part, to activation of transient receptor potential vanilloid 1 (TRPV1) receptor in the cochlea. Direct activation of TRPV1 by capsaicin (a TRPV1 agonist) produced transient hearing loss (~25 dB shifts) for 24h, which recovered by 72 h. This temporary threshold shift was not associated with damage or loss of outer hair cells. We found increases in stress response genes like TRPV1, NOX3 NADPH oxidase and pro-inflammatory moieties like iNOS, COX2 and TNF- α , but no increases in pro-apoptotic molecules like p53 or bax. Furthermore, capsaicin administration by the trans-tympanic route (50 μ l of 0.1 μ M) 24h prior to cisplatin (11 mg/kg, i.p) attenuated cisplatin induced hearing loss. We therefore hypothesized that oral administration of capsaicin would also help ameliorate cisplatin induced hearing loss.

Methods

Male Wistar rats were used for this study. Baseline ABRs were recorded, capsaicin or PBS was administered by oral gavage (2% in water, 1ml) 24h prior to cisplatin administration (11 mg/kg, i.p). Post treatment ABRs were recorded 72 h after cisplatin administration. Cochleae were collected for morphological analysis by scanning electron microscopy (SEM), gene expression by real time RT-PCR and immunohistochemistry of the mid-modiolar sections of the rat cochleae.

Results

Cisplatin treatment produced ~25 dB shift in hearing threshold. This cisplatin induced hearing loss was attenuated to (<10 dB) by both trans-tympanic as well as oral capsaicin pre-treatment. Preservation of hearing was associated with no significant damage or loss of OHCs in rats pretreated with trans-tympanic capsaicin prior to cisplatin administration as seen morphologically in SEM images, when compared to rats treated with vehicle plus cisplatin.

Conclusion

Oral capsaicin (levels equivalent to those when consuming spicy food) can attenuate cisplatin induced hearing loss. To our knowledge this is the first report showing the efficacy of oral capsaicin works as a pre-conditioning stimulus that ameliorates cisplatin ototoxicity. (Supported by NIH grants R01DC02396 to LPR, funds from SIU School of Medicine).

306 Effect of Somatostatin and Octreotide on Spiral Ganglion Neurites and Gentamicin-Induced Auditory Hair Cell Loss

Soledad Levano¹, Yves Brand¹, Michael Sung¹, Eric Wei¹, Vesna Radojevic¹, Cristian Setz¹, Daniel Bodmer¹

¹Universitätsspital Basel

Background

Somatostatin (SST), a peptide with hormone/neurotransmitter properties is known to affect targets in the CNS. It has been shown that SST receptors are expressed in the developing spiral ganglion and organ of Corti (OC) as well in the adult mammalian inner ear. SST has previously been shown to protect against gentamicin-induced auditory hair cell loss in vitro. We hypothesize that SST plays a role in spiral ganglion (SG) neurite outgrowth and that octreotide, a clinically used somatostatin analog, can protect hair cells from gentamicin-induced damage. Therefore the effect of SST and octreotide on SG neurite length and number was analyzed. In addition, we assessed the effect of octreotide on gentamicin-induced hair cell loss in vitro.

Methods

OC and SG explants were extracted from 5-day old wistar rats. SG explants were treated with different concentrations of SST or octreotide. Protection of auditory hair cells from gentamicin-induced toxicity was tested using two concentrations of octreotide. OC explants were preincubated with or without octreotide following by addition of gentamicine.

Results

Octreotide and SST increased SG neuronal survival. We observed more neurites per spiral ganglion explants treated in the SST and octreotide samples compared to control. The effect was dose dependent and statistical significant (ANOVA, $p < .05$). The length of neurites was slightly decreased at the lowest SST concentration (1uM) and at all octreotide concentrations (1uM-20uM) used compared to controls (ANOVA, $p < .05$). There was significantly less hair cell loss in OC treated with gentamicin in presence of octreotide compared to samples treated with gentamicin alone (ANOVA, $p < .01$).

Conclusion

Decreased hair cell loss in octreotide-treated samples that had been exposed to gentamicin provides evidence for a protective effect of octreotide in aminoglycoside-induced hair cell death in vitro. The effect of SST and octreotide on both length and number of SG neurites in vitro points to a possible involvement of SST in cochlear development.

307 Role of STAT1-P53 Axis in Mediating Gentamicin-Induced Cellular Stress and Hair Cell Death

Michael Brenner¹, Debashree Mukherjea¹, Puspanjali Bhatta¹, Vickram Ramkumar¹, Leonard Rybak¹

¹Southern Illinois University School of Medicine

Background

The aminoglycoside antibiotics, including the prototype gentamicin, are a well known cause of irreversible hearing loss. Reactive oxygen species (ROS) formation within the cochlea is a critical event for ototoxicity and hair cell death. In cisplatin-treated rat cochleae, ROS lead to activation of signal transducer and activator of transcription 1 (STAT1) and p53-mediated killing. We therefore hypothesized that ROS activation of the STAT1 – p53 axis may also mediate hair cell death after gentamicin therapy. We further predicted that pretreatment with the putative otoprotectant transplatin could decrease cellular stress and prevent cell death.

Methods

All assays were conducted using UB/OC-1 cells, a conditionally immortalized cell line derived from the organ of Corti. Gentamicin was administered at 0, 100 μ M, 500 μ M, or 1mM doses, and transplatin was administered at 0, 5, and 10 μ M doses. Gene expression was determined by real-time RT-PCR. MTT Tetrazolium dye reduction proliferation assays were used for assessment of cell viability. ROS formation was evaluated with H2DCFDA dye fluorescence assay using confocal microscopy. For immunocytochemistry (ICC), UB/OC-1 cells were treated with gentamicin for 24 hours and probed for TNF-alpha, NADPH oxidase isoform-3 (NOX3), transient receptor potential vanilloid 1 (TRPV1), and p-STAT by immunofluorescence.

Results

Gentamicin treatment increased STAT1 and p53 expression on real time RT-PCR. MTT proliferation assay demonstrated a 15% decrease in cell viability with gentamicin versus untreated control cells at 48 hours. Gentamicin-induced ROS formation was confirmed by live imaging by fluorescence confocal microscopy, and NOX3 prevalence was also seen to be increased. Gentamicin also resulted in increased prevalence of phosphorylated STAT1 (pSTAT1) at Ser727 residue and pSTAT1-responsive genes on ICC. Translocation of pSTAT1 to cell nuclei was confirmed with merged images with nuclear stain (DAPI). The TRPV1 channel, thought to play a role in gentamicin uptake, was also upregulated by gentamicin. On MTT assay, pretreatment with transplatin prior to gentamicin conferred complete protection from cell death at 48hrs, with an absorbance profile equal to controls. Transplatin pretreatment also normalized prevalence of NOX3, pSTAT1, TRPV1, and TNF-alpha to baseline levels on ICC.

Conclusion

These data suggest that the STAT1-p53 axis mediates gentamicin-induced hair cell death, with transplatin

conferring otoprotection. Transplatin prevents reactive oxygen species formation and attenuates cellular stress, providing a potential mechanism for decreased STAT1-p53 activation.

308 The JNK Signaling Complex in Hair Cell Damage

Allen F. Ryan^{1,2}, Kwang Pak^{1,2}, Jeffrey N. Savas³
¹UCSD-SOM, ²VAMC, ³The Scripps Research Institute,
Chemical Physiology

Background

Hair cell (HC) damage involves multiple molecular substrates. Among these, signaling via the c-Jun N-terminal kinase (JNK) pathway is thought to play a central role in noise, aminoglycoside and age-related HC loss.

Methods

We evaluated signaling molecules upstream of JNK using proteomics and specific inhibitors, in a gentamicin (GM)-induced in vitro model of HC loss. We also used proteomics in an in vivo model of noise-induced hearing loss, by comparing cochlear proteins from mice exposed to brief noise at an intensity that induces only temporary threshold shift (TTS), versus exposure to an intensity that induces permanent threshold shift (PTS). To assess the role of different JNK isoforms we evaluated, in vitro, GM-induced HC damage in mice deficient in JNK1 or JNK2.

Results

Inhibitor data indicated that GM activates small GTPases including kRas, Rac and cdc42. Inhibitors also implicated mixed lineage kinases and JNK itself. Comparison of proteins from cochleas with TTS versus those with PTS identified rapid, noise-induced reductions in several small GTPases of the Ras and Rho families in PTS cochleas compared to their levels in TTS cochleas. This is consistent with high levels of activation leading to degradation. A cdc42/Rho activating protein, a protein downstream from RhoA, and other JNK-interacting proteins were also reduced. Preliminary in vitro data from mice deficient in JNK1 or JNK2 indicate that JNK1 plays a protective role while JNK2 mediates HC damage. This illustrates the complex nature of signaling related to HC death, in which survival and damage pathways compete to determine the fate of the cell.

Conclusion

Our results support the idea that JNK signaling, including activation of upstream Ras and Rho family GTPases, is involved in HC damage due to both drugs and noise. In addition, we identified new molecular candidates for roles in regulating this pathway within the HC, providing additional targets for potential pharmacological manipulation, and potentially identified a protective JNK isoform.

309 Chemotherapy for the Future: Novel Aminoglycosides Dissecting Antibacterial Activity and Ototoxicity

Jochen Schacht¹, Tanja Matt², Dmitri Shcherbakov², Ng Chyan Leong³, Kathrin Lang³, Su-Hua Sha¹, Déborah Perez-Fernandez⁴, Rashid Akbergenov², Martin Meyer², Stefan Duscha², Pietro Freihofer², Srinivas R. Dubbaka⁴, Jing Xie¹, Andrea Vasella⁴, V. Ramakrishnan³, Erik C. Böttger²

¹University of Michigan, ²University of Zurich, ³MRC Molecular Biology, Cambridge, ⁴ETH Zürich

Background

Ototoxicity is thought to be inherent to aminoglycosides, compromising the clinical use of these important antibacterials. While we have shown clinically successful pharmacological mitigation of aminoglycoside-induced hearing loss (New Engl. J. Med. 354:1856-1857, 2006), chemotherapy of the future would benefit from aminoglycosides effective against multi-drug resistant bacteria but with no or little ototoxic potential.

Methods

Chemical synthesis; in-vitro translation assays; crystallography; site directed mutagenesis; antibacterial activity; reactive oxygen species; ototoxicity in murine organ culture and in guinea pig in vivo.

Results

Our mechanistic concept postulates a key role for the mitochondrial ribosome (mitoribosome) in aminoglycoside ototoxicity (PNAS 105:20888-20893, 2008). We have previously reported on the finding (PNAS 109:10984-10989, 2012) that apramycin, a structurally unique aminoglycoside in veterinary oral use for treatment of intestinal infections, shows low activity towards eukaryotic ribosomes, including hybrid ribosomes carrying the aminoglycoside-susceptibility A1555G allele. In murine cochlear explants, apramycin caused only little hair cell damage. In guinea pig in vivo, and in contrast to gentamicin, ototoxicity developed more gradually and only at higher concentrations. In accordance with its lesser toxicity, apramycin did not elicit free-radicals (ROS) at low concentrations. However, for both gentamicin and apramycin, the ROS marker nitrotyrosine appeared at antibiotic levels that caused loss of hair cells. This correlation with ototoxicity – rather than with drug concentration – supports the notion that generation of ROS is an integral part of the mechanisms that lead to cell death. Based on this proof-of-concept that antibacterial activity can be dissected from aminoglycoside ototoxicity, we have now developed aminoglycoside compounds with low ototoxic potential.

Conclusion

Together with three-dimensional structures of apramycin-ribosome complexes at 3.5 Å resolution, our results provide a conceptual framework to develop less toxic aminoglycosides by hypothesis-driven chemical synthesis. For the present, apramycin's high efficacy against drug-resistant strains combined with low ototoxic potential

makes it a drug of immediate clinical interest. New lead compounds promise a safety margin (antibacterial efficacy vs. ototoxicity) more than an order of magnitude better than gentamicin.

Support: Grants from the University of Zurich and the European Community (PAR, FP-7 HEALTH-2009-241476) to ECB and grant DC-003685 from the National Institutes on Deafness and Other Communication Disorders, NIH, to JS. VR was supported by the Medical Research Council (UK) and the Wellcome Trust.

310 Cisplatin-Induced Influences on Age-Related Changes in Auditory Physiology in the Fischer 344/NHsd Rat

Eric Bielefeld¹

¹The Ohio State University

Background

Cisplatin (CDDP) was approved for use by the FDA in 1978. A large proportion of the oncology patients who underwent successful CDDP treatment did so early in their life spans. Therefore, there is a population of patients with CDDP-induced hearing loss, or who received CDDP without detectable threshold shift, who are now reaching their sixth, seventh, and eighth decades of life, the times when age-related hearing is expected to set on. This population prompted the current study in which Fischer 344/NHsd rats, a model of age-related hearing loss in the cochlea, were exposed to cisplatin at age 7 months. The quiet-aged Fischer 344/NHsd rat develops hearing loss in the high frequencies between the ages of 9 and 12 months of age, and the hearing loss spreads to mid and low frequencies as the animals age from 12 to 24 months.

Methods

Eight animals received a single dose of 7 mg/kg CDDP in saline delivered intraperitoneally (i.p.) in a 30-minute infusion, while six animals received i.p. saline only as controls. All animals were aged 7 months at the time of the CDDP exposure. Auditory physiology in the form of auditory brainstem response (ABR) thresholds and supra-threshold amplitude input-output functions, along with DPOAE input-output functions, were evaluated monthly to assess the development and magnitude of age-related hearing loss in the CDDP-exposed and saline control rats. Monthly testing was performed for 11 months after the exposures until the animals were 18 months of age.

Results

The ABR threshold results revealed an acute threshold shift at the highest frequencies tested (30-40 kHz) within one month after CDDP exposure, and then earlier onset and greater severity of age-related hearing loss in the mid-to high-frequency range (15-30 kHz) by age 15 months. ABR input-output functions also showed acute effects of CDDP, followed by gradual amplitude reductions over time in the CDDP-exposed ears.

Conclusion

The results suggest that CDDP ototoxicity early in adulthood alters the trajectory of age-related hearing loss in the Fischer 344/NHsd rat. The age-related hearing loss of the Fischer 344/NHsd rat is associated with outer hair cell pathology, but the accelerated age-related hearing loss observed in the current study cannot yet be linked to a specific underlying pathology. Anatomical studies of the cochleae from the subjects are ongoing.

311 Age-Related Changes in Inner Hair Cell – Auditory Nerve Connections and Ntf3 Expression in the Cochlea of UMHet4 Mice

Richard Altschuler¹, David Dolan¹, Ariane Kanicki¹, Cathy Martin¹, Nan Deng¹, Karin Halsey¹, Richard Miller¹

¹University of Michigan

Background

We found a significant decline in the number of inner hair cell – auditory nerve (IHC-AN) connections across turns by 22-24 months of age in normal female UMHet4 mice. There was no further decrease at 27-29 months of age. On the other hand, auditory brain stem response (ABR) threshold shifts and hair cell loss were largely confined to apical / low frequency regions at 22-24 months and both measures showed considerable further decrement at 27-29 months. This suggested differences in underlying mechanisms. Recent studies show a role for NT3/Ntf3 in inner hair cell – auditory nerve synapse development, maintenance, regulation and regeneration (Wang and Green, 2012, Wan et al, 2012). We therefore looked for changes in Ntf3 gene expression at 22-24 months as well as changes in Gdnf and Bdnf, which can serve as survival factors for spiral ganglion neurons.

Methods

UMHet4 mice are a genetically heterogeneous four-way cross between female MOLF/EiJ x 129S1/SvImJ F1 mice and male C3H/HeJ x FVB/NJ F1 mice, all are negative for the Ah11 allele that generates hearing loss appearing in young adults. Mice were tested at 5-7 months, 22-24 months and 27-29 months for ABR, assessed for hair cell loss along the cochlear spiral and for IHC-AN connections based on CTBP2 immunostaining. Gene expression of Ntf3, Bdnf and Gdnf in the cochlea was compared between 5-7 month and 22-24 month old animals using qRT-PCR.

Results

There was a significant decrease of well over 50% in Ntf3 (NT3) gene expression in the cochlea of 22-24 month old UMHet4 mice compared to 5-7 month mice. Bdnf showed a smaller decrease in gene expression with considerable variability such that it was not significant. There was no decrease in Gdnf gene expression.

Conclusion

Given the findings by Wan et al (2012) and Wang & Green (2012) that NT3 regulates and maintains IHC-AN connections, the large age-related decrease in Ntf3 gene expression we find in the mouse cochlea by 22-24 months of age could result in a decreased ability to maintain the

full number of connections found in young animals. This could, in turn, explain our finding a 20-34% percent age-related decrease in IHC-AN connections.

Studies were supported by NIH grant AG025164 and NIDCD P30 grant DC005188

312 Hearing Loss and Changes in Brain Volume in Older Adults

Frank Lin¹, Luigi Ferrucci², Yang An², Joshua Goh², E. Jeffrey Metter², Christos Davatzikos³, Michael Kraut¹, Susan Resnick²

¹Johns Hopkins, ²National Institute on Aging, ³University of Pennsylvania

Background

Cross-sectional neuroimaging studies have demonstrated that audiometric hearing loss is associated with reduced volumes in the auditory cortex while epidemiologic studies have demonstrated that hearing loss is independently associated with accelerated cognitive decline and incident dementia. Whether hearing loss is associated with brain regions outside auditory cortex and with trajectories of brain volume decline is unknown.

Methods

We prospectively followed 126 individuals (ages 56-86) without prevalent dementia in the neuroimaging substudy of the Baltimore Longitudinal Study of Aging for a mean of 6.4 years with annual magnetic resonance brain scans. Audiometry was performed before the baseline scan, and hearing loss was defined as a speech-frequency pure tone average > 25 dB. Mixed-effects regression models were used to compare regional brain volume trajectories of individuals with hearing loss versus normal hearing.

Results

Accelerated volume declines over the follow-up period in whole brain, regional temporal lobe volumes (parahippocampus, superior, middle, and inferior temporal gyri), and cingulate gyrus were observed in individuals with hearing loss compared to those with normal hearing ($p < .05$). These results were robust to adjustment for multiple confounders and were consistent with voxel-based analyses.

Conclusion

Hearing loss is independently associated with accelerated whole brain and superior temporal gyrus atrophy among older adults. Whether hearing loss is an early marker or possibly a modifiable risk factor for structural brain aging deserves further study.

313 Cortical Evoked Potential Measures as Biomarkers of Binaural Temporal Processing in Older Adults

Ann Eddins¹, Bryce Romershausen¹, David Eddins¹

¹University of South Florida

Background

Temporal envelope and fine structure cues in binaural tasks such as the masking level difference (MLD) provide measurable advantages for detecting signals in

background noise. Compared to younger listeners, however, older adults often show reduced performance on such binaural tasks, thought to be due in part to diminished temporal processing with age and peripheral hearing loss. It is not clear to what extent diminished perceptual performance reflects age-related changes in central auditory encoding of envelope cues, fine structure cues or both. The purpose of this study was to evaluate the utility of cortical evoked potential measures as biomarkers of binaural temporal envelope and fine structure cues in an MLD paradigm in older adults.

Methods

Psychophysical and cortical evoked potential thresholds were measured for diotic (S_o) and dichotic (S_π) tonal signals presented in continuous diotic (No) maskers in ten older adults with essentially flat, mild to moderate (35-55 dB HL) sensorineural hearing loss. The MLD was computed as the threshold difference in dichotic (NoS_π) versus diotic (NoS_o) conditions. The contribution of stimulus envelope cues was examined using narrowband noise (50 Hz) with varying degrees of envelope fluctuation (Gaussian vs. Low-noise noise), and the contribution of fine structure cues was evaluated using low and high center frequencies (500 vs. 4000 Hz).

Results

Cortical evoked potential thresholds were within 10-15 dB of behavioral thresholds and highly correlated with behavioral thresholds. Both behavioral and evoked-potential MLDs were largest in the 500 Hz Gaussian noise condition where envelope and fine structure cues were available. MLDs were reduced in 500 Hz low-noise noise where envelope cues were minimized while fine structure cues were present. MLDs also were reduced in the 4000 Hz Gaussian noise condition where envelope cues were available but fine structure cues were not. Compared to young adults with normal hearing, MLDs in older adults were significantly smaller at 500 Hz in both Gaussian and low-noise noise, primarily due to reduced masking release in dichotic conditions, but were minimally different for 4000 Hz conditions. Notably, N1 and P2 latencies were longer in Gaussian noise dichotic conditions for older compared to younger adults.

Conclusion

The results indicate that cortical evoked potential measures may have utility as biomarkers of binaural temporal processing in older adults and other clinical populations.

314 Genes on Chromosome 17 Contribute to Age-Related Hearing Loss in 129S6/SvEvTac

Braulio Peguero¹, Linda Robinson¹, Bruce L Tempel^{1,2}

¹Otolaryngology-HNS & VMBHRC, University of Washington, ²Dept. of Pharmacology, University of Washington

Background

Presbycusis is one of the main causes of acquired deafness. Mice with age-related hearing loss (AHL) are

used as models of presbycusis because of their homology to the human auditory system. From the eight AHL loci described to date, three have led to the identification of genes that contribute to AHL. The 129S6/SvEvTac (S6) mouse is commonly used for gene targeting and noise resistance studies; however, S6 also has early-onset AHL. A similar AHL phenotype was mapped to Chromosome (Chr) 17 and Chr 10 in the genetically related 101H strain. Our objectives are: to use S6 to improve our understanding of AHL mechanisms, to identify the physical location of the AHL gene(s) for S6, and to determine whether 101H and S6 share similar genes that contribute to AHL.

Methods

Hearing experiments were conducted in S6 and 101H mice. We used auditory brainstem responses (ABRs) to measure hearing thresholds at six frequencies between 8kHz and 40kHz. Single-nucleotide polymorphisms (SNPs) were used in combination with Taqman assay for genotyping. By selectively backcrossing S6 to a good hearing strain, CBA/CaJ (CB), we are creating six novel recombinant-inbred (congenic) CB mouse strains with fragments of Chr 17 from S6. We hypothesize that genes within Chr 17 contribute to AHL in the S6 strain.

Results

By 4 weeks of age, S6 mice have an average hearing loss of 22dB (SPL) between 24-40kHz compared to CB. A congenic strain with the proximal 30Mb of Chr 17 from S6, CB-S6-(prox-D17Mit29), has similar hearing loss of 23dB between 24-40kHz. The proximal 30Mb region of Chr 17 contains upwards of 500 known genes of which 9 have been implicated with hearing. New congenic lines were generated to localize the causal gene with higher resolution. Congenic mouse CB-S6-(rs1348286-rs13482938) and CB-S6-(rs13482886-rs13482938) maintain a high frequency hearing loss in the 24-40kHz region while CB-S6-(prox-rs13482886) has hearing threshold indistinguishable from CB.

Conclusion

These data locate the causal genes between 21Mb and 28Mb on Chr 17. A complementation test is being conducted between the above congenic lines to determine if 101H share a common allele with S6 that produces the AHL phenotype. These studies will help identify genes causing AHL thereby elucidating homologous genes in humans that may contribute to presbycusis.

Supported by NIH DC06305, DoD DM102092, NIH T32 GM007108-36

315 The Aging Auditory System of the Common Marmoset (*Callithrix jacchus*)

Michelle Valero¹, Rama Ratnam¹

¹University of Texas at San Antonio

Background

The purpose of this study was to determine the effects of aging on auditory function in common marmosets (*Callithrix jacchus*). This species has increased in popularity as a model for auditory research, but little is known about the effects of aging on auditory function in the marmoset.

Methods

Hearing sensitivity and neural function were assessed in 15 young (1-4 yrs), 10 older-adult (5-8 yrs), and 10 aged (8-12 yrs) males using auditory brainstem responses (ABRs). Cochlear function was assessed in the same subjects using distortion-product otoacoustic emissions (DPOAEs). Significance of group differences was determined using effect size (Cohen's *d*) and bootstrap resampling.

ABR tone-burst stimuli were presented in 3-kHz steps from 3-9 and 15-24kHz at 74 dB SPL to assess the peak latency of waves I, II, and V. Tone-burst levels were reduced to determine threshold. Threshold was defined as the tone-burst level which elicited two repeatable waveforms (Pearson's $r > 0$, $p < 0.001$) with peaks that were distinguishable from the noise floor.

For DPOAEs, f_2 ranged from 3-24kHz in 1/5-octave steps ($f_2/f_1 = 1.21$), and L_1 was increased from 50-74 dB SPL in 6-dB steps.

Results

Consistent with the behavioral audiograms measured by other groups, ABR thresholds were lowest in each group at 6 kHz. ABR thresholds of older-adult males were significantly elevated at 3, 9, 15, and 18 kHz when compared to the young males. Thresholds of aged males were significantly elevated at all stimulus frequencies when compared to the young, and were significantly greater than older adults at 24kHz.

The ABR wave V latency, but not wave I and II latencies, was significantly prolonged in older-adults at 6, 18, and 21 kHz. In aged marmosets, wave I, II, and V latencies were delayed compared to the young males in a non-frequency specific manner.

DPOAE levels were reduced significantly in aged males, but not older-adult marmosets, at a wide range of frequencies and primary-tone levels.

Conclusion

These data suggest that the decline in hearing sensitivity observed in male marmosets does not progress from high- to low frequencies, that cochlear function may be preserved until late in life, and that central auditory dysfunction may precede peripheral deficits in this species.

316 Ventriloquism Effect in Young and Elderly Normal-Hearing Listeners

Marnix Stawicki^{1,2}, Piotr Majdak³, Deniz Baskent^{1,2}

¹University Medical Center Groningen, Department of Otorhinolaryngology / Head & Neck Surgery, NL,

²Research School of Behavioural and Cognitive Neurosciences, University of Groningen, the Netherlands,

³Austrian Academy of Sciences, Acoustics Research Institute, Vienna, Austria

Background

The success in fitting hearing aids depends, among others, on the ability to combine the auditory and visual information for speech perception. The audiovisual integration can be observed in the ventriloquist effect, where an observer localizes sound at a visually dominated spatial position. In this study, the suitability of the ventriloquist effect as a measure for the audiovisual integration was investigated. Assuming that elderly subjects have a greater ability for audiovisual integration, the effect of the age was also taken into account.

Methods

Minimum audible angles (MAAs) in the horizontal plane were measured in an acoustic lateralization task with a visual distracter. The acoustic stimulus was a 500-Hz pure tone presented via headphones at a lateral angle at the right or left side by filtering the stimulus with generic head-related transfer functions. Each lateral side was tested in an adaptive 3-up-1-down run, starting at the angle of 10°, and decreasing after three succeeding correct responses. Two runs, corresponding to the two sides, were randomly interleaved. The MAA was the difference between the lateral angles obtained from the two runs averaged over the last four reversals. The visual stimulus consisted of a yellow circle on a black screen presented in the center. The conditions were: no visual stimulus (No-V, listener-specific baseline), temporarily-synchronized audiovisual presentation (Sync) and asynchronous audiovisual presentation (Async). Sync and Async conditions corresponded to a measure of the audio-visual integration and distraction, respectively. All conditions were tested three times in a normalized Latin-square design. In order to eliminate hearing-loss as confounder, all subjects were normal hearing as assessed by pure-tone audiometry.

Results

For younger subjects (N=16), the MAAs in Sync were significantly ($P<0.02$) larger than in No-V. Preliminary results for elderly subjects (N=3) were not significantly different to that for younger subjects.

Conclusion

Stable MAAs, showing a significant ventriloquism effect, confirm the use of our procedure to investigate audiovisual interactions via headphones. Both elderly and young subjects showed similar baseline MAAs, demonstrating the suitability of our procedure for comparing different age groups. Similar MAAs were found in the integration and distraction conditions. The final results will be discussed in

the light of the contribution of visual information in younger and elderly listeners.

317 The Elderly Can Benefit from Top-Down Repair: Aging and Phonemic Restoration

Deniz Baskent^{1,2}, Jefta Saija^{1,2}, Elkan Akyurek^{2,3}

¹Department of Otorhinolaryngology, University Medical Center Groningen, The Netherlands, ²Research School of Behavioral and Cognitive Neurosciences, University of Groningen, The Netherlands, ³Department of Experimental Psychology, University of Groningen, The Netherlands

¹Department of Otorhinolaryngology, University Medical Center Groningen, The Netherlands, ²Research School of Behavioral and Cognitive Neurosciences, University of Groningen, The Netherlands, ³Department of Experimental Psychology, University of Groningen, The Netherlands

Background

This study investigated the effect of age on the top-down repair of degraded speech using phonemic restoration of interrupted sentences.

Methods

Perception of meaningful sentences interrupted with silent intervals was measured with and without a filler noise in the gaps, with young (<26 years, average 22 years) and elderly (>62 years, average 66 years) normal-hearing listeners. The phonemic restoration effect, observed by an increase in intelligibility after the addition of the filler noise, provided a measure of top-down repair of interrupted speech. Further, the speaking rate of sentences was altered (by slowing down and speeding up by a factor of two) to observe the effects of cognitive processing speed on restoration.

Results

Consistent with literature, older adults performed worse than younger adults in general. However, despite the lower intelligibility scores with interrupted speech with silent gaps, once the filler noise was added, intelligibility reliably increased by large amounts. Hence, the elderly showed a remarkably robust restoration effect. Slowing down speech helped the elderly adults gain more benefit than young adults with respect to phonemic restoration. This can be explained in terms of age-related cognitive slowing, as slowed speech gives elderly more time to extract cues from the speech and process them. Speeding up speech had a detrimental effect on speech intelligibility regardless of noise for both participant groups. This negative effect was larger for elderly than young adults, which can again be explained by cognitive slowing accompanying aging. With speeded speech there was a negative phonemic restoration effect, where inserting noise reduced the intelligibility of interrupted speech.

Conclusion

Even though elderly adults perform worse than young adults in understanding interrupted speech, they are still able to use top-down processes to extract cues and restore meaningful sentences when noise is added to the interruptions. It is conceivable that elderly rely on their life-long experience with language, as well as their rich vocabulary accumulated over a long time, to use these resources to effectively restore interrupted speech. When speech is slowed down such that the elderly are given more time to process the sentences, extract its cues and

derive its content the restoration effect is strongly visible. When speech is speeded up, there is a detrimental effect of noise, producing very poor performance, as well as an reversed restoration effect. These results indicate that top-down repair could also be affected by age-related cognitive slowing.

318 Endogenous Differences in Mitochondrial Metabolism Bias Sensory Cell Responses to Ototoxic Challenge

Heather Jensen Smith¹, Richard Hallworth¹, Michael Nichols¹

¹Creighton University

Background

Aminoglycosides (AG), including gentamicin (GM), are the most frequently used antibiotics in the world despite the risk of irreversible cochlear damage and hearing loss (HL) associated with their use. High-frequency outer hair cells (OHCs) reliably generate and succumb to a barrage of AG-triggered pro-apoptotic signals, while inner hair cells (IHCs) display truncated pro-apoptotic signaling and greater survival rates. Although there are numerous causes of HL and deafness, reactive oxygen species (ROS) are now well-known instigators of multiple HL pathologies including: AG-induced ototoxicity, noise-induced and age-related HL. Given that ROS are normal byproducts of ATP synthesis that can rise to lethal levels when mitochondrial metabolism is perturbed, intrinsic differences in I/OHC mitochondrial metabolism may explain why high-frequency OHCs are profoundly sensitive to mitochondrial-mediated damage during various cochlear pathologies.

Methods

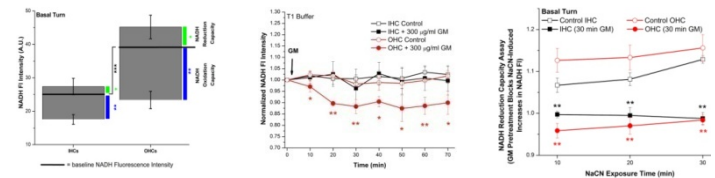
Mitochondrial metabolism was compared in apical, low-frequency (20% of cochlear length) and basal, high-frequency (80% of cochlear length) IHCs and OHCs obtained from acutely-cultured, intact cochlear (organ of Corti) explants harvested from mice (postnatal day 5 ± 1d). Real-time changes in the reduced (NADH, fluorescent) and oxidized (NAD⁺, non-fluorescent) states of the metabolic intermediate, nicotinamide adenine dinucleotide, were used to measure both endogenous and GM-induced differences in IHC and OHC mitochondrial metabolism. NADH reduction and oxidation capacities were compared using sodium cyanide and FCCP, respectively.

Results

Despite similar quantities of functional mitochondria, endogenous NADH fluorescence was greatest in high-frequency OHCs. The dynamic range of NADH metabolism was also greatest in high-frequency OHCs (Left Fig.). Akin to adult cochlear preparations, GM rapidly decreased NADH fluorescence in high-frequency OHCs (Center Fig.). This decrease was shown to be due to a substantial decline in NADH reduction capacity rather than an increase in NADH oxidation (Right Fig.).

Conclusion

Basal turn, high-frequency OHCs are metabolically responsive a number of changes in their microenvironment including GM and elevated glucose concentrations. High-frequency IHCs and low-frequency IHCs and OHCs are substantially less sensitive to their microenvironment. The observed GM-induced decrease in mitochondrial metabolism in basal turn, high-frequency OHCs is consistent with the well-known enhanced susceptibility of high-frequency OHCs to undergo apoptosis after AG exposures. This metabolic predisposition may bias basal turn OHC responses to a variety of cochlear insults, particularly those involving energy metabolism and ROS production.



319 RNA-Seq Sequencing Reveals the Involvement of the Complement Pathway in Noise-Induced Cochlear Damage

Minal Patel¹, Qunfeng Cai¹, Bohua Hu¹

¹State University of New York at Buffalo

Background

Exposure to intense noise causes sensory cell damage in the cochlea. Previous investigations have revealed multiple signal transduction pathways involved in cochlear degeneration, suggesting that noise-induced damage is a multifactorial process. To further explore novel signaling pathways, we examined the global transcriptome of noise-traumatized cochlear sensory epithelia using the next generation RNA-seq sequencing technique.

Methods

Young rats were exposure to a broadband noise at 120dB (SPL) for 2 h, and were sacrificed at 1 day post-noise exposure. The cochlear sensory epithelia were collected for total RNA isolation. The control animals received the same treatment except for the noise exposure. The samples from the two groups were used for cDNA library preparations and subsequently used for sequencing on the Illumina HiSeq 2000. Verification of the RNA-sequencing results was achieved using qRT-PCR and immunohistology.

Results

Our sequencing results revealed an average of 176 ± 21million reads for the normal control samples. Using a cut-off value of RPKM ≥ 0.1, we identified 12041 gene transcripts in the normal cochlear sensory epithelium. Comparing the RNA-seq data with the q-RT-PCR data of selected genes examined in our previous investigation, we revealed a high correlation between the two data sets. In the cochlear samples collected 1 day after exposure to the broadband noise at 120dB (SPL) for 2 h, we found 164 ± 47 million reads, similar to the value seen in the normal

cochleae. Using the cut-off value of RPKM ≥ 0.1 , we identified 11874 gene transcripts. Among these gene transcripts, 71 were upregulated and 7 were downregulated. Using bioinformatic DAVID analysis, we found that these expression-altered genes are linked to multiple signaling pathways. Among these pathways, the complement pathway, an immune response-related pathway that participates in clearing dying cells from tissues, has not been implicated in cochlear pathogenesis. Further qRT-PCR and immunolabeling assessments confirmed that the two genes (C1s and Cfi) identified by RNA-seq for the complement pathway were indeed involved in the pathogenesis of the organ of Corti. Importantly, the change in Cfi was associated with sensory cell death.

Conclusion

Identification of C1s and Cfi in the cochlear sensory epithelium following acoustic trauma highlights the presence of a cochlear inflammatory response, which may be modulated towards reducing the extent of sensory cell damage.

(Supported by NIH R01 DC010154-01A2 to BH Hu).

320 A Novel Treatment Reduces Hearing Loss, and Cochlear and Brain Injury After Noise and Blast

Jianzhong Lu¹, Wei Li¹, Xiaoping Du¹, Weihua Cheng¹, Donald Ewert¹, Robert Floyd², Richard Kopke^{1,2}

¹Hough Ear Institute, ²Oklahoma Medical Research Foundation

Background

High level steady state noise and blast can lead to cochlear injury and hearing loss and stress and/or injury to brainstem and cortical and other auditory centers. Military personnel exposed to blast can experience, hearing loss, tinnitus, and other associated co-morbidities related to memory and orientation impairment for example. Because noise-induced hearing loss and tinnitus continue to be ongoing prevalent problems despite traditional hearing conservation programs, research is being pursued to achieve a pharmacological treatment for these injuries. Here we report that a novel pharmacological therapy reduces cochlear and brain stress/injury and permanent hearing loss induced by high level steady state noise as well as blast.

Methods

Male Long-Evans pigmented rats had baseline ABR and DPOAE testing followed by exposure to either 115 dB SPL narrow band noise for 1 hour or 3 or 4, 14 p.s.i. blasts. One hour after the noise/blast exposure rats were treated with an intraperitoneal injection of a nitron (HPN-07) plus the glutathione prodrug n-acetylcysteine (NAC), or, with solution vehicle only. Serial ABR and DPOAE measurements were made up to 21 days post exposure. At different time points animals were euthanized and cochlear and brain tissues were harvested and processed for histological and immunohistochemical analysis.

Results

Treatment substantially reduced permanent hearing loss induced by narrow band noise or blast. Inner and outer hair cell losses were also substantially reduced after noise or blast trauma with treatment. Treatment also reduced injury biomarker expression in the brainstem, hippocampus, and auditory cortex after blast exposure. After noise exposure, treatment reduced c-fos expression in the cochlear nucleus.

Conclusion

These data suggest it may be possible to develop a pharmacological approach that not only reduces blast-and noise-induced cochlear damage and hearing loss but reduces brain injury associated with a blast and the stress response in the cochlear nucleus associated with high level noise exposure. This could have implications for noise or blast induced tinnitus. It may also have implications for the treatment of mild traumatic brain injury associated with blast in military personnel. Further research is needed to establish the extent of brain injury recovery and tinnitus reduction that might be possible with this treatment approach. A single pharmacological treatment that addressed both cochlear injury as well as brain injury associated with high level noise or blast could be useful in treating several co-morbid conditions experienced by military personnel.

321 Subcutaneous Etanercept Attenuates Noise-Induced Hearing Loss

Debashree Mukherjee¹, Kelly Sheehan¹, Leonard Rybak¹, Vickram Ramkumar¹

¹Southern Illinois University School of Medicine

Background

Noise induced hearing loss (NIHL) is the most common cause of hearing loss in adults. Our laboratories as well as others have shown that noise exposure induces reactive oxygen species (ROS) generation in the cochlea which initiates an inflammatory response. We have shown that noise exposure increases the expression of pro-inflammatory mediators such as tumor necrosis factor- α (TNF- α), inducible nitric oxide synthase (iNOS) and cyclooxygenase-2 (COX2), and increased CD14 positive cells in the rat cochlea. Therefore, we hypothesized that inhibition of the inflammation could be a potential therapeutic strategy for treating NIHL. In this study, we tested the effectiveness of the TNF- α receptor inhibitor (Etanercept - ETA) against NIHL.

Methods

To determine the utility of ETA to protect hearing, baseline ABR testing was recorded. Rats were then administered vehicle (saline) or ETA by the transtympanic (TT) (250 μ g in 50 μ l saline) or subcutaneous (SC) (2.5 mg/kg) routes, followed by noise exposures at 3 and 7 days following ETA treatments. To determine the efficacy of ETA against noise trauma, rats were treated with saline (via the IT or SC routes) or ETA at 24 or 48h following noise exposure. Noise was administered at 122 dB OBN (centered at 16 kHz) for 1 h. Post-treatment ABRs were recorded 21 days

after noise exposure. Cochleae were harvested for morphological analysis by scanning electron microscopy (SEM), immunohistochemistry and gene expression studies.

Results

Rats treated with ETA (SC route) 2h following noise showed almost complete protection from NIHL (<5dB ABR shift) and significant protection up to 24h. ETA administration (TT route) provided significant protection at 16 and 32 kHz (<25dB ABR shift). Administration of ETA 7d prior to noise exposures provided significant protection from hearing loss. This Otoprotection afforded by ETA was associated with preservation of outer hair cells, decreased gene expression of stress-response genes, such as NOX3 NADPH oxidase and TRPV1 and pro-inflammatory mediators such as TNF- α , iNOS and COX2.

Conclusion

ETA significantly reduced noise induced hearing loss when administered within 2h-24h after noise exposure. It was also shown to mediate otoprotection when administered up to 7days prior to noise exposure. These findings support the clinical use of etanercept (FDA approved) to prevent and treat NIHL. (Supported by HHF).

322 Expression of Inflammatory Cytokines and Ion Homeostasis Genes in the Cochlea Is Up-Regulated by Lipopolysaccharide-Induced Sepsis

Lourdes Quintanilla-Dieck¹, Frances Hausman¹, Barbara Larrain¹, Dennis Trune¹, Peter Steyger¹
¹Oregon Health & Science University

Background

The mechanism by which sepsis-induced inflammation enhances aminoglycoside trafficking into the cochlea remains poorly understood. This study sought to determine if sepsis and/or aminoglycosides induced changes in gene and protein expression of inflammatory-mediated cytokines and ion homeostasis proteins in the cochlea.

Methods

Three groups of mice received one of the following treatments: systemic lipopolysaccharides (LPS) for 6 hours for sepsis induction, systemic gentamicin for 3 hours, or both LPS and then gentamicin treatment. A fourth group served as controls. After sacrifice, cochleae were collected and underwent either RNA extraction for PCR, or protein extraction for enzyme-linked immunosorbent assay (ELISA). A total of 32 cytokine and ion homeostasis genes/proteins were analyzed.

Results

Cochlear gene expression analysis revealed that gentamicin alone did not induce significant inflammation or other changes in the cochlea within 3 hours. However, significant inflammatory and ion homeostasis gene up-regulation was seen with bacteria-derived LPS treatment. The most up-regulated cytokine genes with LPS were interleukin (IL)-6, macrophage inflammatory protein (MIP)-

2 α , and neutrophil activating protein (CXCL)-1. In the cochlear protein quantification experiments, the cytokines found in greatest quantity were IL-6, MIP-2 α , and CXCL1. A similar distribution was observed when measuring the cytokines in the serum. The ion homeostasis genes that LPS up-regulated in a biologically significant manner (fold change ≥ 1.5) were gap junction- α 1, claudin-4, and claudin-14. Gentamicin treatment did not modulate these LPS-induced changes.

Conclusion

Sepsis induces a systemic pro-inflammatory state that can enhance aminoglycoside uptake by cochlear tissues. After LPS administration in mice, which induces systemic inflammation, there is statistically significant up-regulation of cytokine gene and protein expression, and of specific ion homeostasis genes, in the cochlea regardless of aminoglycoside exposure. Interestingly, the most significant cytokines found in the gene expression analysis were also those seen in the protein quantification experiments. Given that cytokines increase permeability across blood-endothelial barriers, this phenomenon could enhance aminoglycoside trafficking into cochlear tissues. LPS-induced up-regulation of ion homeostasis gene expression may provide additional clues to the mechanisms by which enhanced aminoglycoside trafficking into the cochlea during systemic infection occurs. Thus, systemic infection may synergistically enhance the cochlear uptake of aminoglycosides and subsequent ototoxicity.

Supported by NIH-NIDCD grants R01 DC004555 (PS), R01 DC005593 (DT), and Department of Otolaryngology at OHSU

323 Inner Ear Changes in Niemann-Pick Disease Type C (NPC), and in NPC Therapy, in the Mouse

Anna M. Taylor¹, Joyce J. Reppa¹, Charles G. Wright^{1,2}, Elena Koulich¹, Karen S. Pawlowski^{1,2}
¹UT Southwestern Medical Center, ²UT Dallas

Background

Niemann-Pick disease type C (NPC) is a rare autosomal recessive lipid storage disorder that affects lysosomal transport of cholesterol and results in progressive neural and visceral organ dysfunction and eventual death. The central auditory system has been shown to be affected in NPC. Peripheral auditory system effects are reflected in reduced distortion product otoacoustic emissions (DPOAEs). We studied morphological changes in the NPC mouse inner ear.

The FDA approved 2-hydroxypropyl-beta-cyclodextrin (Cyclo) for treatment in NPC patients in 2009, under compassionate use status. At that time, Cyclo had been shown to effectively alleviate symptoms and increase life expectancy in mice. Initial results in humans are promising. However, Cyclo treatment in cats causes rapid and irreversible hearing loss. A better understanding of the development of hearing loss in the peripheral auditory system in NPC, with or without the administration of Cyclo,

could lead to treatment advancements. Therefore we also studied the ototoxicity of Cyclo in mice.

Methods

Adult mice were given either a high single or low repeated doses of Cyclo(1,000-8,000 mg/kg body weight, subcutaneously). ABRs were recorded at 4, 16, and 32 kHz before and after treatment. Inner ear tissue from normal, Cyclo- treated and BALB/c-npc1NIH mice was processed and sectioned for light and electron microscopic viewing. The opposite ears were micro-dissected for organ of Corti analysis.

Results

Changes were seen in NPC mice at the stria vascularis, nerve endings in the organ of Corti and in the spiral ganglion. Cyclo administration caused significant ABR threshold shifts at 4 kHz and 16 kHz 3 weeks following a high single dose. Less robust changes were seen in the mice given lower repeat doses. These results were also reflected in the organ of Corti pathology.

Conclusion

Neural changes seen in the present study are consistent with damage in the central nervous system that is known to occur in NPC. Surprisingly, while the hair cells require cholesterol for normal functioning, they appear to be relatively unaffected. The DPOAE changes are more likely due to stria damage. The changes seen after Cyclo treatment appear to be related to the loss of membrane cholesterol in the outer hair cells. New treatments are being tested and will be discussed. (Funding: Ara Parseghian Medical Research Foundation (JJR) & Pharmacology Training Grant at UT Southwestern, NIH T32 GM007062 (Mangelsdorf))

324 Molecular Mechanisms of the PRPS1

Deafness

Denise Yan¹, Alexandra A. DeSmidt², Julia Dallman², Zhengyi Chen³, Zhongmin Lu², Xue Zhong Liu¹

¹University of Miami, Department of Otolaryngology,

²Department of Biology, University of Miami, ³Department of Otolaryngology and Laryngology, Massachusetts Eye and Ear Infirmary, Harvard Medical School

Background

PRPP (phosphoribosylpyrophosphate) synthetases (PRPSs) are a family of enzymes that catalyze the synthesis of PRPP, a substrate in and an allosteric regulator of nucleotide synthesis. *PRPS1* loss-of-function missense mutations cause X-linked nonsyndromic sensorineural deafness type 2 (DFNX1) (Liu et al. 2010) or syndromic deafness including Arts syndrome and X-linked Charcot-Marie-Tooth disease-5 (CMTX5). However, the molecular mechanisms of the enzymatic aberration in DFNX1, as well as the biological effects of *PRPS1* mutations, are not understood.

Methods

To investigate the pathogenic mechanism of the *PRPS1* deafness associated mutations, we have used the

antisense morpholino (MO) technology to knock down *Prps1* gene function in zebrafish.

Results

By RT-PCR, we found that injection with M3, an acceptor site-targeting MO in *Prps1b* into zebrafish embryos, results in production of aberrantly spliced message mRNA. Our development study shows that there is a delayed hatching in M3 morphants and they have abnormalities in both anterior and posterior otoliths. Measurements of larval zebrafish inner ear and of saccular otolith growth indicates that the total inner ear and saccular otolith area of larval zebrafish injected with M3 are smaller compared with those measured in controls. Furthermore measurements of microphonic potentials revealed that the microphonic responses from the morphant's ears were considerably reduced compared to those measured in controls, indicating that these morphants had impaired mechano-electrical transduction.

Conclusion

Overall, our findings emphasize the need for tight regulation of PRS-I activity and imbalances in nucleotide metabolism affect nearly the whole cellular function. As the metabolic enzyme critical for nucleotide biosynthesis, PRS-I is a promising target for drug in prevention and treatment of hearing loss.

325 Noise Exacerbates Hypoxia-Associated Changes in the Alport Mouse Cochlea

Scott Montgomery¹, Jennifer Brinkmeier², Brendan Smyth¹, Michael Anne Gratton¹

¹Saint Louis University, ²University of Michigan

Background

Mice modeling the recessive form of Alport Syndrome have thickened stria capillary basement membranes (SCBMs). The cochlea of Alport mice is inherently hypoxic with significant differences post-noise exposure in ABR thresholds, EP magnitude and Na,K-ATPase activity compared to wild-type (WT) littermates. Our previous studies show Alport mice exhibit increased heparan sulfate proteoglycan in SCBMs and upregulation of hypoxia-regulated genes/proteins (i.e. facilitated glucose transporter-1, vascular endothelial growth factor) in the cochlea. These data suggest that reduced transcapillary movement of oxygen, metabolic nutrients and waste due to altered SCBM filtration properties creates a hypoxic microenvironment in scala media. We hypothesize that the combination of thickened SCBMs and metabolic stress drives the Alport cochlea into a glycolytic state to meet ATP demand for cellular metabolism and auditory transduction.

This project aimed to quantify energy states and oxidative stress in the cochlear lateral wall (LW). Levels of LW intracellular ATP and total glutathione, including oxidized to reduced GSSG/GSH ratio, were measured. To further characterize the biochemical dysregulation occurring in this hypoxic microenvironment, these assays were conducted after exposure to metabolic stress.

Methods

Lateral wall tissue was microdissected from 7-9 week Alport mice and their WT littermates. A subset of each genotype was subjected to noise (10 kHz OBN, 120 dB SPL, 10h). The LW was homogenized and pelleted by centrifugation. The supernatant was assayed for ATP and glutathione levels by flash/ glow luminometry. Data was referenced to protein concentration.

Results

Inherent metabolic differences were observed post-noise between WT and Alport mice. From quiet to post-noise, the WT LW has a robust, aerobic increase in intracellular ATP, de novo total glutathione (GSH+GSSG) synthesis and maintenance of GSSG/GSH ratio. In contrast, the post-noise Alport LW intracellular ATP level remains unchanged, with only a modest increase in total glutathione and a substantial increase in GSSG/GSH ratio.

Conclusion

The current study confirms and extends our previous work demonstrating that the Alport LW is essentially hypoxic, with an inability to efficiently regulate intracellular ATP and maintain GSSG/GSH ratio post-noise exposure. This implies that oxidative stress/free radical formation from mitochondrial dysfunction underlies the decreased physiological measures (ABR, EP, Na,K-ATPase) in the Alport cochlea. These results prompt further investigation of mitochondrial respiration through studying energy charge balance (e.g. ADP/ATP ratio), ROS formation, as well as glycolytic respiration (e.g. pyruvate/ lactate ratio)

326 Reactive Oxygen Species Generation and Detection in the Stria Vascularis of Alport Mice

Eric Applebaum¹, Osama Tarabichi¹, Michael Anne Gratton¹

¹Saint Louis University

Background

Alport syndrome is a hereditary defect in type IV collagen genes. Mice modeling the recessive form of Alport syndrome demonstrate progressive thickening of stria capillary basement membranes (SCBM), a mild high frequency hearing loss and sensitivity to noise. Our previous studies show that the cochlea is hypoxic and exhibits upregulation of hypoxia-regulated genes/proteins (i.e. HIF-1a, GLUT-1, VEGF). Noise-exposed Alport mice are unable to modify intracellular ATP levels, resulting in increased oxidized to reduced glutathione (GSSG/GSH) ratio, indicating disrupted mitochondrial respiration. Mitochondrial dysfunction, with loss of redox homeostasis and formation of excessive free radicals, may play an important role in the pathogenesis of the hearing loss associated with Alport syndrome. A method for detecting/quantifying ROS formation in the stria could be utilized to examine whether thickened stria capillary basement membranes result in mitochondrial dysfunction under conditions of metabolic stress.

This project sought to:

--develop a protocol using the fluorescent marker MitoSox (Invitrogen), an indicator of mitochondrial ROS generation in vitro, to measure oxidative stress in vivo.

--determine the level of reactive oxygen species generation in Alport stria vascularis with and without metabolic stress.

Methods

Cochlea lateral wall (LW) tissue was microdissected from 7-9 week old Alport mice and their WT littermates. A subset of each genotype was subjected to noise (10 kHz OBN, 120 dB SPL, 10h). The experimental LW was incubated (0.625M MitoSox, 10min) prior to mounting flat, stria upward, using DAPI gold. The contralateral LW served as a control, mounted directly in DAPI Gold. Slides were kept at 4°C until visualization. The total time for dissection, incubation and mounting was ≤ 35 minutes. The LW was visualized with confocal microscopy. Two-channel z-stacks, ROS and nuclear stain, were analyzed with Volocity software to quantify non-nuclear ROS.

Results

--Protocol developed to quantify ROS using confocal microscopy to detect MitoSox in unfixed, isolated cochlear tissue.

--Staining patterns of MitoSox correlate to expected areas of ROS formation in the stria vascularis based on predicted areas of greatest mitochondrial density.

--WT and Alport mice in quiet demonstrate similar ROS levels.

--Following noise exposure, ROS levels differ between the WT and Alport mice.

Conclusion

--ROS formation in the stria vascularis can be reliably imaged and quantified.

--Mice exhibiting thickened SCBMs and cochlear hypoxia demonstrate mitochondrial dysfunction under conditions of metabolic stress.

--Mitochondrial dysfunction contributes to the pathogenesis of the hearing loss associated with Alport syndrome.

327 IGF-1 Deficit Predisposes to Noise-Induced Hearing Loss in Mice

Silvia Murillo-Cuesta^{1,2}, Adelaida Celaya², Lourdes Rodríguez-de la Rosa^{1,2}, Rafael Cediel³, Julio Contreras³, Carlos Avendaño⁴, Isabel Varela-Nieto^{1,2}

¹CIBERER, ²IIBM CSIC-UAM, ³Veterinary Faculty UCM, ⁴Medicine Faculty UAM

Background

Human IGF-1 deficiency (ORPHA73272, OMIM608747) is a rare disease associated with poor growth rates, mental retardation and syndromic hearing loss. Equally, Igf1^{-/-} mice are dwarfs with poor survival rates and congenital profound deafness. IGF-1 is a neuroprotective agent, and accordingly, the physiological age-related decrease in circulating IGF-1 levels have been related to cognitive and brain alterations. Igf1^{-/-} mice present undetectable serum levels of IGF-1 throughout its life, whereas Igf1^{+/-} and Igf1^{+/+} littermates show an age-dependent decrease in

IGF-1 serum levels, especially from 6 months of age on2, 3, which correlates with the increase in ABR thresholds. However, there is little information on the effect of low levels of IGF-1 on the susceptibility to noise induced hearing loss (NIHL) and the potential protective actions of IGF-1 against this condition.

Methods

We have studied the susceptibility of Igf1+/- and Igf1+/+ mice to NIHL at different ages, with functional (auditory brainstem responses, ABR), morphological (cochlear histology and stereological hair-cell quantification) and molecular (RT-qPCR, Western Blotting) studies.

Results

Noise-exposure experiments with 1 and 3 months-old mice did not reveal differences between genotypes, both genotypes were equally sensible to NIHL. However, 6 month-old Igf1+/- presented a greater susceptibility to noise damage, with higher threshold shifts and a poorer recovery compared to noise-exposed Igf1+/+ mice. Igf1+/- mice showed severe morphological changes, including the massive loss of hair cells, as well as alterations in the main IGF-1 signalling pathways. These changes correlated with low IGF-1 serum levels in the heterozygous mice, compared to wild type.

Conclusion

These results support the idea that low levels of IGF-1 predisposes to higher susceptibility to NIHL, Therefore, IGF-1-based therapies could contribute to prevent or ameliorate age related and noise-induced hearing loss.

Acknowledgements: This research was funded by grants from the Spanish Ministry of Science and Innovation SAF2011-24391 and Intra-CIBERER programs to IV-N. SMC and LRR hold contracts from CIBERER.

References: 1Cediell et al. *Eur J Neurosci.* 2006 Jan;23(2):587-90; 2Riquelme et al. *Front Neuroanat.* 2010 Jul 13;4:27 ; 3Rodriguez-de la Rosa et al. *Neurobiol Dis.* 2012 May;46(2):476-85.

See also communication num. 33

328 Preliminary Results of Treating Deafness in Connexin Knockout Mice Using Retinoids

Yeunjung Kim¹, Qing Chang¹, Xi Lin¹

¹Emory University School of Medicine

Background

Connexin mutations represent the most common cause of nonsyndromic hereditary deafness, with 10-50% of all patients in different ethnic populations bearing mutations specifically in the GJB2 gene, which encodes the connexin (Cx) 26. Previous studies have shown the promise of treating nonsyndromic hereditary deafness caused by Cx mutations by increasing expressions of the affected Cx or even the remaining Cx levels (e.g. Cx26 in the absence of Cx30). Retinoids, the family of vitamin A derivatives, have been utilized to increase expression of the Cx levels (e.g. Cxs26, 30 and 43) in dermatological and oncological

studies, some of which involve syndromic deafness conditions caused by the Cx mutations such as keratitis-ichthyosis-deafness (KID) syndrome and palmoplantar keratoderma with deafness. Moreover, retinoids have been used to treat various types of hearing loss in both clinical and experimental applications, with promising results in vivo and in vitro. Yet the impact of retinoids on Cx expression in the inner ear is largely unknown.

Methods

In this study we examined the impact of retinoid derivatives in the mouse inner ear by surgically implanting gel foams soaked in the retinoids (e.g. retinyl palmitate and retinyl acetate) at the round window on postnatal day 1 (P1). At P10, the cochlea was harvested and examined for morphological changes and the expression of Cx26 and Cx30.

Results

Application of retinyl acetate greatly reduced the Cx30 expression, at concentrations 30 μ M and greater, to the level below that detectable by immunoblotting. For the expression of Cx26, there was a concentration dependent decrease assayed by immunoblotting. Furthermore, application of retinyl palmitate dramatically affected the development of the sensory epithelium, causing the tunnel of Corti to stay in a closed state. The mechanism underlying such a profound morphological change may also point to the modulation of the gene expression of cochlear Cxs, as seen in the conditional Cx26 null mouse models we previously reported. Further studies will be conducted to investigate the gene expressions in response to applications of retinoids, the impact on hearing, and to determine the mechanism underlying the closure of the tunnel of Corti.

Conclusion

Our findings point to a delicate relationship between different Cxs and retinoids in the inner ear development, and may be an important step in fully understanding the underlying mechanisms of retinoids in treating hearing loss.

329 Connexin26 Mutations That Cause Hereditary Deafness Lead to Macromolecular Complex Degradation of Cochlear Gap Junction Plaques

Kazusaku Kamiya¹, Keiko Karasawa¹, Osamu Minowa², Katsuhisa Ikeda¹

¹Juntendo University, ²RIKEN, BioResource Center

Background

Hereditary deafness affects about 1 in 2000 children and GJB2 gene mutation is most frequent cause for this disease in the world. GJB2 encodes connexin26 (Cx26), a component in cochlear gap junction.

Methods

In this study, we analyzed macromolecular change of gap junction plaques with two different types of Cx26 mutation as major classification of clinical case, one is a model of

dominant negative type, Cx26^{R75W+} and the other is conditional gene deficient mouse, Cx26^{ff}P0Cre as a model for insufficiency of gap junction protein.

Results

Gap junction composed mainly of Cx26 and Cx30 in wild type mice formed large planar gap junction plaques (GJP) along the cell junction site with the adjacent cells in normal inner sulcus cells and border cells. In contrast, Cx26^{R75W+} and Cx26^{ff}P0Cre showed fragmented small round GJPs around the cell junction site and marked decrease of total gap junction area. In Cx26^{ff}P0Cre, some of the cells with Cx26 expression due to their cellular mosaicism showed normal large GJP with Cx26 and Cx30 only at the cell junction site between two Cx26 positive cells. These indicate that bilateral Cx26 expressions from both adjacent cells are essential for the formation of the cochlear linear GJP, and it is not compensated by other cochlear Connexins such as Connexin30.

Conclusion

In this study, we demonstrated a new molecular pathology in most common hereditary deafness with different types of Connexin26 mutations, and this machinery can be a new target for drug design of hereditary deafness.

330 Morphological Changes of Cochlear Gap Junction Plaques in Brn4 Deficient Mouse, a Mouse Model of DFN3 Non-Syndromic Deafness

Yoshinobu Kidokoro¹, Kazusaku Kamiya¹, Keiko Karasawa¹, Osamu Minowa², Katsuhisa Ikeda¹

¹Juntendo University Faculty of Medicine, ²BioResource Center, RIKEN

Background

Brn4, which encodes a POU transcription factor, is the gene responsible for DFN3, an X chromosomelinked nonsyndromic hearing loss. Brn4 deficient (KO) mice show low endocochlear potential (EP), hearing loss and severe ultrastructural alterations in spiral ligament fibrocytes [Minowa O et al., Science, 1999].

In humans, mutations in the connexin26 (Cx26) and connexin 30 (Cx30) genes, which encode gap junction proteins and are expressed in cochlear fibrocytes and nonsensory epithelial cells (cochlear supporting cells) to maintain proper EP, are well known to be responsible for hereditary sensorineural deafness. The molecular pathologies of Brn4 deficiency causing low EP are still unclear.

Methods

It has been hypothesized that gap junction in the cochlea provide an intercellular passage by which K⁺ are transported to maintain high levels of the endocochlear potential essential for sensory hair cell excitation. In this study, we analyzed the formation of gap junction plaques in cochlear supporting cells of Brn4 KO mice in different stages by confocal microscopy and three dimensional graphic construction.

Results

Gap junction composed of mainly of Cx26 and Cx30 in wild type mice showed horizontal linear gap junction plaques along the cell-cell junction site with the adjacent cells and these formed pentagonal or hexagonal outlines of normal inner sulcus cells and border cells. However, the gap-junction plaques in Brn4 KO mice did not show normal linear structure, but the round small spots were observed around the cell-cell junction site. The size of gap junction units of Brn4 KO mice was significantly shorter than control mice.

Conclusion

Our results demonstrated that Brn4 gene mutation affects on the accumulation and localization of gap junction proteins at the cell border among cochlear supporting cells. It may suggest that Brn4 significantly associates with cochlear gap junction properties to maintain proper EP in cochlea as well as the mutations of Cx26 or Cx30.

331 Evaluation of Auditory Function in Slc44a2 Mutants on an ARHL-Resistant Genetic Background

Thankam Nair^{1,2}, Pavan Kommareddi^{1,2}, Irina Laczkovich^{1,2}, Bala Naveen Kakaraparthi^{1,2}, Danielle Miller^{1,2}, Ariane Kanicki^{1,2}, Lisa Kabara^{1,2}, Thom Saunders², David Kohrman^{1,2}, David Dolan^{1,2}, Thomas Carey^{1,2}

¹KHRI, ²University of Michigan

Background

SLC44A2 (CTL2, choline transporter-like protein 2), is a target of antibody-induced hearing loss and carries the HNA3a, 3b antigen of transfusion related acute lung injury (TRALI). We developed a knockout mouse to investigate the function of Slc44a2 protein in hearing. Exons 3-10 that span the first extracellular loop were targeted for deletion. Determining the effect of the deletion on hearing has been complicated by the line's 129/C57BL/6J genetic background, which is susceptible to age-related hearing loss (ARHL) in part due to the *Cdh23*^{753A} allele at the *Ahl* locus. We therefore bred the line to FVB, which carries the ARHL-resistant *Cdh23*^{753G} allele at *Ahl*, and evaluated hearing in this genetic context.

Methods

We backcrossed B6.129-*Slc44a2*^{del-ex3-10/Tec} to FVB mice, which carry the ARHL-resistant *Cdh23*^{753G} allele at *Ahl*, then genotyped subsequent intercross progeny for the *Cdh23*⁷⁵³ variant and for the *Slc44a2* deletion using PCR-based assays. Intercross progeny were tested at 1.5 months and 4.5 months of age for ABR at 12, 24 and 48 kHz.

Results

Eighteen intercross mice were genotyped and evaluated for auditory function. Three mice were *Slc44a2*^{del-ex3-10/del-ex3-10}*Cdh23*^{753G/G}, two were *Slc44a2*^{del-ex3-10/del-ex3-10}*Cdh23*^{753G/A}, two were *Slc44a2*^{+/+}*Cdh23*^{753G/G}, and two were *Slc44a2*^{+/+}*Cdh23*^{753A/G}. Eight mice were *Slc44a2*^{del-ex3-10/+}*Cdh23*^{753G/G} and one was *Slc44a2*^{del-ex3-}

^{10/+} *Cdh23*^{753G/A}. Progressive hearing loss at 48kHz occurred in three mice with homozygous *Slc44a2* exon 3-10 deletion and wild type *Cdh23*^{753G/G} (75, 73, 60dB) and two with homozygous *Slc44a2* exon 3-10 deletion heterozygous for *Cdh23*^{753G/A} had hearing loss (35, 105dB). Of four mice homozygous for wt *Slc44a2*, two with *Cdh23*^{753G/G} and one with *Cdh23*^{753G/A} had no hearing loss, but one with *Cdh23*^{753G/A} had a high frequency hearing loss (48 kHz, 60dB SPL). Of nine mice heterozygous for *Slc44a2*^{del-ex3-10/+}, six had high frequency hearing loss (45-80dB SPL) five with *Cdh23*^{753G/G}, and one with *Cdh23*^{753G/A} three others (2 *Cdh23*^{753G/G}, 1 *Cdh23*^{753G/A}) had normal hearing.

Conclusion

Significant high frequency hearing loss occurred by 4.5 months in nearly all mice carrying the *Slc44a2* exon 3-10 deletion, even in those carrying an ARHL-resistant allele of *Ahl*. This result is consistent with a role for the *Slc44a2* gene in normal auditory function.

332 Hearing Threshold Differences Among C57BL/6J (Wild-Type), FVB/NJ (Wild-Type), and *Cdh23*^{ahl} Corrected FVB.B6.129 Mice

Bala Naveen Kakaraparthi^{*1}, Irina Laczkovich^{*1}, Thankam Nair², Pavan Kommareddi², Danielle Miller², Lisa Kabara², Ariane Kanicki², David Dolan², David Kohrman², Thomas Carey²

¹KHRI, University of Michigan * These authors contributed equally to this work, ²KHRI, University of Michigan

Background

C57BL/6J mice and embryonic stem cells from 129S/129X1 strain, used to develop knockout strains, share a *cadherin23* G->A mutation at codon 753 designated *Ahl1* or *Cdh23*^{ahl}. This creates problems for hearing research due to early-onset presbycusis detectable at high frequencies (HF) from 1.5 months of age. We developed a *SLC44A2* (CTL2, choline transporter-like protein 2), which is a target of antibody-induced hearing loss, knockout mouse using B6.129 strain to examine CTL2 function. The knockout mouse exhibited HF hearing loss, but because the background strain was a confounder, we backcrossed to FVB/NJ (*Cdh23*^{+/+}). We compared hearing in wild type (wt) C57BL/6J, FVB/NJ, and FVB.B6.129.

Methods

We backcrossed B6.129 homozygous for *Cdh23*^{ahl/ahl} to FVB/NJ, wt for *cadherin23*, and tested offspring for the *Cdh23*^{ahl/ahl} mutation. After a second backcross to FVB/NJ, the mice were interbred and tested for the *Ahl1* polymorphism (CCGGTGAG vs. CCAGTGAG) by PCR and Msp1 digestion, which yields a 600bp band from the mutant (CCAG) and two bands of 200 and 400bp from the wt allele (CCGG). We compared the wt (*Cdh23*^{+/+}) FVB.B6.129 mice without the *Ahl* mutation to wt C57BL/6J (*Cdh23*^{ahl/ahl}) mice and FVB/NJ (*Cdh23*^{+/+}) controls by testing their auditory brainstem response (ABR) at 12, 24, and 48 kHz at 1.5 months, 3 months, and 4.5 months of age.

Results

Sixteen C57BL/6J mice were tested, and some were euthanized at intervals to examine ears for inner ear morphology. At 1.5 months old, the average hearing threshold at 48 kHz was ~59.5dB (thresholds > 50 dB translate to hearing loss). Progressive HF hearing loss occurred at 3 months (~87.5dB) and 4.5 months of age (109dB). Three FVB/NJ controls had averages of 30dB at 1.5 months and ~36dB at 3 months at 48 kHz. The two *Cdh23*^{ahl} corrected mice (*Cdh23*^{+/+}) also exhibited normal hearing, with averages of 25dB at 1.5 months and 20dB at 4.5 months at 48 kHz.

Conclusion

C57BL/6J mice exhibit progressive HF hearing loss from 1.5 months onward. FVB/NJ backcrossing and *Cdh23*^{ahl} correction resulted in normal hearing thresholds that remained constant up to 4.5 months of age. The results demonstrate that correction of the *Ahl1* mutation in the C57BL/6J and 129 strains is necessary for knockout experiments of genes involved in hearing acuity.

333 Examining the Role of Gtf2ird1 Deletion in Auditory Physiology and Behavior in a Murine Model of Williams-Beuren Syndrome

Eleni P. Asimacopoulos^{1,2}, Ann E. Hickox^{1,3}, Lucy Osborne⁴, Konstantina M. Stankovic^{1,2}

¹Eaton-Peabody Laboratory, Massachusetts Eye and Ear Infirmary, ²Department of Otolaryngology and Laryngology, Harvard Medical School, ³Program in Speech and Hearing Bioscience and Technology, Harvard-MIT, ⁴Collaborative Program in Neuroscience, University of Toronto

Background

Williams-Beuren Syndrome (WBS) is a genetic disorder typified by a constellation of features, including craniofacial and neuro-developmental abnormalities, which have been investigated substantially. However, less is known about the etiologies of auditory abnormalities associated with WBS such as hyperacusis, tinnitus, and high-frequency hearing loss. Here we examine auditory physiological and behavioral characteristics of mice with deletion of *Gtf2ird1*, one of the 26 genes located within the WBS region of chromosome 7, that display neuro-developmental features characteristic of WBS.

Methods

Mice that were homozygous knock-out (KO) for the *Gtf2ird1* gene were compared with heterozygous (HET) and wild-type (WT) littermates on measures of auditory function. Auditory brainstem response (ABR) and distortion product otoacoustic emissions (DPOAEs) were measured to assess cochlear and retro-cochlear function in young (~8wks) mice, as well as in older (~17wks) mice that were noise-exposed (8-16 kHz, 100 dB SPL, 2 hrs) at 6wks. The same groups of mice underwent acoustic startle response (ASR) and prepulse inhibition (PPI) of startle tests to assess supra-threshold auditory behavior.

Results

In the young cohort, KO and HET mice showed slight elevation of ABR and DPOAE thresholds compared to WT littermates, especially for high (> 22 kHz) frequencies. ABR waveform morphology was comparable across genotypes with the exception of a larger amplitude wave 2 in KO and HET mice compared to WT for supra-threshold, mid-frequency (8-22 kHz) stimuli. Behavioral responses to 16 kHz prepulses and to broadband startle stimuli were similar across genotypes. In the older, noise-exposed cohort, ABRs of KO and HET mice diverged, with KO mice showing lower thresholds and greater preservation of ABR wave amplitudes.

Conclusion

This study is one of the first to examine auditory function and behavior in a mouse model of WBS. Young mice with homozygous or heterozygous deletion of *Gtf2ird1* show subtle auditory threshold elevation, similar to some individuals with WBS. Reflex-based tests of auditory function reveal no significant behavioral differences and no obvious indication of hyperacusis-like behavior. Interestingly, in an older cohort of mice with history of acoustic overexposure, KO mice showed greater preservation of thresholds and supra-threshold neural response to sound compared to HET littermates. Taken together with the known expression of *Gtf2ird1* in the adult murine cochlea, further investigation is warranted to understand the role of this gene in the normal and injured ear.

334 A Mouse Model of Progressive Bone Remodeling and Mixed Hearing Loss

Sharon G Kujawa¹, Penelope W.C. Jeffers², Arthur G Kristiansen², Michael J McKenna¹

¹Harvard Medical School, Massachusetts Eye and Ear Infirmary, ²Massachusetts Eye and Ear Infirmary

Background

Otosclerosis is a disease of the otic capsule that is among the most common causes of acquired hearing loss. We have previously demonstrated that the osteoprotegerin (OPG) knockout mouse exhibits active bone remodeling within the otic capsule and progressive, apparently mixed (conductive and sensorineural) hearing loss (Zehnder et al 2006), characteristics seen in otosclerosis. Both the bone remodeling and the threshold elevations are responsive to treatment with bisphosphonates (Adachi et al 2008). OPG mutants used in these studies, however, existed in C57BL/6J (B6), a strain with rapidly progressive, age-related hearing loss (AHL). We have now bred the mutation into the normal hearing, normally aging CBA/CaJ strain, allowing for better assessment of the nature of the hearing loss attributable to OPG deficiency and the long-term efficacy of drug treatment. Here, we describe the age-progressive auditory pathophysiology and histopathology of the OPG mutant in the new background.

Methods

Experiments were conducted on an age-graded series (4 to 64 wk) of OPG-deficient (-/-, +/-) mice and wildtype (+/+)

littermates in the 10th generation of transfer to CBA/CaJ. Animals underwent auditory function testing using DPOAEs and ABRs (5.6 – 44.06 kHz). Paraffin-embedded middle ear and cochlear tissues (H&E stained) were examined by light microscopy to characterize the histopathology.

Results

OPG -/- (but no +/- or +/+) mice demonstrate abnormal remodeling of bone within the otic capsule. Foci show osteoclastic bone resorption and formation of new bone, and are progressive in number, size and location as animals age. Marrow spaces in bone are dramatically enlarged. Functional assays reveal progressive hearing loss in -/- compared to age-matched +/- and +/+ mice. Mild/moderate high frequency loss by ABR at 4 weeks progresses to severe loss across frequency by 32 weeks. DPOAE losses exceed those by ABR before limitation by a lower response ceiling. This asymmetry suggests conductive involvement affecting both forward and backward transmission through the middle ear, producing compound loss in the DPOAEs. Heterozygotes are wildtype-like in structure and function at all ages.

Conclusion

The OPG -/- mouse in CBA/CaJ shows progressive otic capsule bone remodeling and hearing loss without the complication of B6-related AHL. Studies aimed at clarifying the relative hearing loss consequences of the middle ear vs. cochlear sites of lesion are underway, to support our efforts to characterize long-term effects of drugs with potential efficacy in the treatment of otosclerosis. Research supported by NIDCD: RO1 DC03401

335 Restoration of Hearing in VGLUT3 Knock Out Mice Using Virally-Mediated Gene Therapy (P1-3 Injection)

Kevin Burke¹, Omar Akil¹, Rebecca Seal², Chuansong Wang³, Aurash Alami¹, Matthew During³, Robert Edwards⁴, Lawrence Lustig¹

¹Department of Otolaryngology- HNS, University of California San Francisco, San Francisco, ²Department of Neurology, University of Pittsburgh, Pittsburgh, PA, ³Comprehensive Cancer Center, The Ohio State University, Columbus, OH, ⁴Department of Neurology University of California San Francisco, San Francisco

Background

Mice lacking the vesicular glutamate transporter 3 (VGLUT3 KO) are born deaf due to the absence of glutamate release from the inner hair cells. In a prior study, we demonstrated correction of this genetic defect through virally-mediated gene therapy, using an in vivo microinjection of adeno-associated virus with a VGLUT3 insert (AAV-VGLUT3) into the endolymph of P10-12 VGLUT3 KO mice.

Methods

In the present study, in vivo microinjection of AAV-VGLUT3 via direct injection through the round window membrane was performed on P1-3 VGLUT3 KO mice.

Results

ABR testing demonstrated restoration of hearing in all VGLUT3 KO mice, to thresholds equivalent to those seen in wild-type mice. Long-term follow up showed that in the P1-3 rescued mice, 100% of animals had preservation of normal ABR thresholds through 9 months. In contrast, in mice rescued at P10-12, only 11% of animals demonstrated hearing preservation at this same time point. Immunofluorescence with anti-VGLUT3 antibody demonstrated robust VGLUT3 expression (100% of IHC transfected) within the inner hairs cells of the rescued VGLUT3 KO mice. In contrast, in mice rescued at P10-12, only 40% of IHC were transfected using the same amount of virus. Lastly we noticed an improved startle-response to hand clap of the P1-3 injected as compared to the P10-12 rescued mice. However, reduced spiral ganglion cell counts that are seen in the KO mouse were not reversed in the P1-3 rescued mice.

Conclusion

The results of this study again demonstrate functional recovery of hearing in a genetic model of human deafness due to loss of VGLUT3 function, using virally mediated gene therapy. Furthermore, earlier injection of the virus showed higher efficacy in hearing recovery, normalization of hearing to wild type ABR levels, greater longevity of the hearing response and better startle to hand clap than the mice rescued at P10-12. However, there was still no difference in the spiral ganglion cell counts between KO and rescued mice, suggesting that pre-natal spontaneous inner hair cell release of glutamate helps maintain normal spiral ganglion cell numbers through birth.

336 Otopathology in Congenital Toxoplasmosis

Felipe Santos¹, Mehti Salviz², Jose Montoya³, Joseph Nadol¹

¹Harvard Medical School, ²Mass Eye and Ear, ³Stanford Medical School

Background

Toxoplasmosis is a parasitic infection caused by *Toxoplasma gondii*. If fetal infection occurs early in gestation severe inflammation and necrosis can cause brain lesions, chorioretinitis and hearing loss. Hearing loss in congenital toxoplasmosis may be preventable with early diagnosis and treatment.

Methods

The temporal bones of nine subjects with congenital toxoplasmosis were removed at autopsy and studied under light microscopy. Cytocochleograms were constructed for hair cells, the stria vascularis and cochlear neuronal cells.

Results

Three of nine subjects (33%) were found to have parasites in the temporal bone. The organism was identified in the internal auditory canal, the spiral ligament, stria vascularis and saccular macula. The cystic form of the parasite was

not associated with the inflammatory response seen in the active tachyzoite form.

Conclusion

We infer that the hearing loss of toxoplasmosis is likely the result of a postnatal inflammatory response to the tachyzoite form of *T gondii*. Our findings have implications for the early identification and management of Toxoplasmosis.

337 Role of Smac/DIABLO in TNF α -Induced Auditory Hair Cell Loss in Vitro

Seo Moon¹, Christine Dinh¹, Esperanza Bas¹, Chhavi Gupta¹, Xue Zhong Liu¹, Thomas Van De Water¹

¹University of Miami, Department of Otolaryngology

Background

Second mitochondria-derived activator of caspases/Direct inhibitor of apoptosis protein (IAP)-binding protein with low PI (Smac/DIABLO) is a mitochondrial protein involved in apoptosis. Following an apoptotic stimulus, Smac is released into the cytoplasm, binds to the IAPs and releases basal inhibition of caspases to initiate apoptosis. Recently, a Smac mutation has been identified as a genetic cause of progressive non-syndromic hearing loss, DFNA64. Up to now, few studies have investigated the molecular mechanisms behind Smac activation in auditory hair cells (HC). Although Smac is known to be involved in the intrinsic pathway, studies have linked Smac expression to the extrinsic pathway through tumor necrosis factor alpha (TNF α) activity (a pro-inflammatory cytokine expressed in the cochlea in response to a variety of insults) and c-Jun N-terminal kinase (JNK).

Methods

Organ of corti (OC) explants were dissected from 3-day old rats and cultured in the following conditions: (1) No treatment (2) TNF α (1 μ g/ml); (3) TNF α + JNK-inhibitor (SP-600125, 10 μ M); (4) JNK-inhibitor alone; (5) Smac-N7 peptide (50 μ M); (6) Smac-N7 + Caspase-3 inhibitor (5 μ M); and (7) Caspase-3 inhibitor alone for either 24, 48 or 96 hrs in vitro. For HC viability, OC were fixed, and stained with FITC-phalloidin after 96 hrs in vitro and HCs with intact cuticular plates and stereociliary bundles were counted in the basal turns. Real-time PCR was utilized to obtain Smac gene expression levels after 24 and 48 hrs in vitro. ANOVA with Tukey HSD post hoc was performed with p-value < 0.05.

Results

OC explants exposed to either TNF α or Smac-N7 displayed significantly less viable HCs in the basal turn when compared to explants in: control media; TNF α + JNK-Inhibitor; JNK-Inhibitor alone; Smac-N7 + Caspase-3 inhibitor; and Caspase-3 inhibitor alone. TNF α ototoxicity initiated time-dependent increases in Smac gene expression compared to control explant expression levels.

Conclusion

TNF α -initiated loss of auditory HCs in vitro likely involves both JNK activation and Smac expression. HC loss in OC

explants treated with Smac-N7 peptide was abrogated by caspase-3 inhibitor. These results suggest a close relationship between TNF α , activated JNK, Smac, and caspase-3 activation. However, further in vitro studies involving Smac protein expression, JNK and selective caspase activation, and TUNEL assay are necessary to further delineate the role of Smac in programmed cell death in auditory HCs.

338 Brain Changes That Accompany Hearing Loss

Catherine Connelly^{1,2}, Amanda Lauer³, Tan Pongstaporn¹, Alexandar A. Boreki¹, David K. Ryugo^{1,2}
¹Garvan Institute of Medical Research, ²University of New South Wales, ³Johns Hopkins University

Background

Synaptic features of the central nervous system change as a consequence of alterations in sensory input. Studies of partially deaf cats show atrophic changes in brainstem synaptic morphology and postsynaptic ultrastructure (Ryugo et al., 1998), and congenitally deaf white cats exhibit even more severe brainstem pathologies, such as synaptic hypertrophy (Ryugo et al., 1997) and a redistribution of excitatory and inhibitory synaptic terminals (Tirko et al., 2009). This study aims to confirm and expand our understanding of hearing loss as it applies to the central auditory system in mouse models of hearing loss.

Methods

Three mouse strains (aged 1-7 months) representing distinct hearing phenotypes were used: CBA/CaH, which maintains normal hearing thresholds throughout adulthood; DBA/2, which begins to exhibit high frequency hearing loss starting at ~3-4 weeks of age; and shaker-2, where homozygote mutants are congenitally deaf. Hearing thresholds were verified with auditory brainstem responses (ABRs) prior to tissue collection. Cochlear nuclei from mice of various ages and degrees of hearing loss were analyzed with light and electron microscopy. Synaptic features were labeled using glutamate transport immunohistochemistry and/or injections of neurobiotin in the auditory nerve. Spherical bushy cell (SBC) size, endbulb of Held morphology, and the distribution of axosomatic primary excitatory and/or secondary inhibitory endings were quantified.

Results

Our results show that the size of the postsynaptic SBC soma, endbulb arborization, and number of inhibitory endings onto SBCs are directly correlated to hearing sensitivity. The CBA/CaH mouse does not experience a significant elevation in hearing thresholds from 1-7 months of age, and its SBC area, endbulb arborization, and ratio of primary excitation to secondary inhibition onto SBCs remain relatively unchanged. In contrast, as hearing thresholds increase in the DBA/2 mouse, a slight decrease in all three parameters is observed. However, total auditory loss as seen in the congenitally deaf shaker-2 mouse gives rise to more drastic decreases in SBC area, endbulb arborization, and inhibition onto SBCs.

Conclusion

Preliminary data show that congenital and acquired hearing loss result in abnormal brain morphology, which can be correlated to the degree and duration of hearing loss. Based on the present results, it seems important to determine which abnormalities can be remedied by treatment methods such as sound amplification. Future studies will test the hypothesis that an amplified sound environment slows the progression of brain pathologies in comparison to that of long-term, unattended hearing loss.

339 Synapse Size, AMPA and NMDA Receptor Numbers, and Their Distribution Are Regulated in an Input-Specific Manner in the Cochlear Nucleus

Maria Rubio¹, Yugo Fukazawa², Naomi Kamasawa³, Ryuichi Shigemoto⁴
¹University of Pittsburgh, ²Nagoya University, ³Max Plank Institute at Jupiter, ⁴National Institutes for Physiological Sciences

Background

Synapse size (i.e. size of the postsynaptic density, PSD) varies between synaptic contacts and often correlates with fundamental properties of synaptic transmission (Rollenhagen and Lübke, 2006; Xu-Friedman and Regehr, 2004). PSD size has been shown to be proportional to the number of ionotropic glutamate receptors (iGluRs), namely AMPA-type and NMDA-type (AMPA and NMDA receptors, respectively), whose content and spatial arrangement in the synapse primarily determine synaptic quantal size in many glutamatergic synapses in the CNS (Ganeshina et al., 2004; Takumi et al., 1999). However, these anatomical, molecular and functional parameters and their correlation to electrophysiological properties of synaptic transmission in glutamatergic synapses in the binaural and monaural auditory pathways remain unknown. This information will be important for understanding normal auditory processing and for the hearing impaired.

AMPA and NMDA receptors mediate excitatory transmission at auditory nerve (AN) and parallel fiber (PF) synapses in the cochlear nucleus (Raman et al., 1994; Manis and Molitor, 1996). Previously, the expression of AMPA and NMDA receptors at AN and PF synapses was analyzed with preembedding immunolabeling or postembedding immunogold labeling methods (Petralia et al., 1996; Rubio and Wenthold, 1997; Rubio, 2006; Wang et al., 1998). However, neither of these techniques allows efficient detection of synaptic iGluRs. Thus, due to the technical difficulty in revealing synaptic molecules at high detection efficiency, a relationship between iGluR content and the PSD size cannot be established.

Methods

In this study we used freeze-fracture immunogold labeling (FRIL) to determine how morphological and molecular differences could relate to synaptic transmission at AN and PF synapses. FRIL allows a highly sensitive and quantitative detection of molecules of interest in the synapse (nearly 1-to-1 detection sensitivity of functional

AMPA receptors) and provides a two dimensional (2D) landscape of the plasma membrane and receptor arrangement (Masugi-Tokita et al., 2007; Tarusawa et al., 2009).

Results

We observed substantial differences in the size of the PSD and AMPAR and NMDAR content between the AN and PF synapses on their postsynaptic targets.

Conclusion

Our results suggest that synapse size, AMPAR and NMDAR numbers and their 2D-distribution are regulated in an input-specific manner in the cochlear nucleus. These morphological and molecular properties may play important roles in shaping transmission at individual connections and normal auditory processing.

340 A New Vertebrate-Specific Presynaptic Protein as Molecular Component of the Endbulb of Held

Friederike Wetzel¹, Thomas Dresbach¹

¹University of Goettingen

Background

The endbulb of Held's exceptional size has made it an important model system for the study of synaptic transmission. Furthermore, the structure of the endbulb of Held has been extensively studied to gain more insight into the process of synaptic differentiation. However, little is known about the molecular composition of endbulbs of Held. We have recently identified Mover, a vertebrate-specific 266 kDa protein, as a component of the calyx of Held. Here, we have begun to study the molecular composition of endbulbs of Held with a particular focus on vertebrate-specific presynaptic proteins, assuming that this relatively small family of proteins may confer specific features to specialized presynaptic nerve terminals. To initiate this study, we characterized the localization of Mover within the auditory pathway.

Methods

To initiate this study, we characterized the localization of Mover within the auditory pathway by using immunohistochemistry.

Results

We find abundant Mover immunoreactivity in auditory nuclei of the brainstem, e.g. the cochlear nucleus, lateral superior olive, medial nucleus of the trapezoid body, inferior colliculus. In the anteroventral cochlear nucleus (AVCN) the immunoreactivity for Mover exhibits a punctate pattern surrounding the somas of bushy cells. The pattern of Mover is similar compared to other synaptic markers, i.e. Synapsin or Synaptophysin, but not to a glia cell marker, i.e. glial fibrillary acidic protein (GFAP). To further examine the cellular localization of Mover in presynaptic terminals in the AVCN we performed immunofluorescence staining with anti-VGLUT1, anti-VGAT and anti-Mover antibodies. At synaptic terminals ending on bushy cells we find co-localization of Mover with both VGLUT1 and VGAT.

Conclusion

Hence, we conclude that Mover is a molecular component of presynaptic endings in the anteroventral cochlear nucleus, including the endbulbs of Held.

341 Pulsed Infrared-Evoked Intracellular Calcium Transients in Cultured Neonatal Spiral Ganglion Neurons

Vicente Lumbreras¹, Michael Finale¹, Esperanza Bas², Chhavi Gupta², Suhrud Rajguru^{1,2}

¹Department of Biomedical Engineering, University of Miami, Miami, FL, ²Department of Otolaryngology, University of Miami, Miami, FL

Background

Recent work has illustrated the feasibility of in vivo neural activation with pulsed infrared light. In the present study we analyze the response of cultured neonatal spiral ganglion cells to infrared radiation (IR), $\lambda = 1860$ nm, in vitro. In agreement with the previous studies, we show that pulsed IR evokes intracellular Ca²⁺ transients in the target cells.

Methods

Experiments were performed on rat spiral ganglion neurons. Neonatal animals (P2 and P3) were decapitated, and both inner ears were removed from the base of the cranium. The spiral ganglion was isolated, the cells were dissociated and plated in culture dishes coated with poly-D-lysine. After 4 days, the cells were loaded and incubated for 45 minutes with calcium-sensitive dye Fluo-4 AM dissolved in DMSO and mixed with Pluronic F-127. In a limited set of experiments, the entire organ of corti was isolated from adult rats and used to study Ca²⁺ responses. IR stimulation was achieved with a 400 μ m optical fiber connected to a Capella laser (Lockheed Martin Aculight) operating at 1860 nm. IR was focused on the target cells under the guidance of a pilot light. Image sequences measuring fluorescence intensity differences were collected using a confocal microscope connected to a camera. The analysis of the image sequences was done with

ImageJ (NIH) and Matlab (MathWorks) software.

Results

The spiral ganglion neurons responded with an increase in fluorescence synchronized in time with the pulsed IR stimulation applied. At low frequency laser pulses, a pulse-by-pulse response was observed with distinct peaks of fluorescence corresponding to intracellular calcium transients were observed. A wide range of pharmacological array was tested to identify the intracellular Ca²⁺ release site.

Conclusion

Pulsed IR consistently evoked calcium related responses in neurons. The results suggest that Pulsed IR can effectively stimulate neurons without any modifications and can find applications in neuroprostheses including in the auditory and vestibular systems.

This work was supported by NIH NIDCD R01DC011481-02A2 (Rajguru, SM).

342 Stochastic Properties of Neurotransmitter Release Expand the Dynamic Range of Endbulb Synapses

Hua Yang¹, Matthew Xu-Friedman¹

¹University at Buffalo, SUNY

Background

The probabilistic nature of neurotransmitter release has been evident since the first recordings of synaptic potentials, but its functional effects are unknown. When the average size of synaptic potentials is near threshold, the stochastic properties of release potentially introduce noise and unreliability into postsynaptic spiking. This is important in the auditory system, where sound stimuli are encoded in the precise timing of spikes, so the loss or mistiming of spikes could reduce auditory acuity. We examined this by studying synapses formed by auditory nerve fibers onto bushy cells in the mouse anteroventral cochlear nucleus. These synapses show significant depression, and have particularly large quanta (~100 pA) so fluctuations in the number of released vesicles could impact spiking.

Methods

All experiments were carried out using standard patch clamp methods in brain slices from CBA/CaJ mice aged P15-21 at near-physiological temperature.

Results

We measured the variability of EPSCs in voltage-clamp experiments. We then studied the impact of this variability using dynamic clamp, by comparing responses to synaptic conductances that took on the average value against those that fluctuated from trial to trial. Variability in the probability of postsynaptic spiking was almost entirely accounted for by variability in synaptic conductance, as spike threshold is highly stable. For conductances that were on average above threshold, stochastic variability reduced the probability of spiking, but for conductances that were on average below threshold, it increased spiking.

Conclusion

Our results indicated that a decreased gain allowed postsynaptic spike probability to encode more information about average EPSC amplitude, which increased the dynamic range of the synapse. Furthermore, stimuli that caused significant synaptic depression could still influence spiking because of the stochastic properties of neurotransmitter release. However, stochastic aspects of release introduced variability in the timing of postsynaptic spikes, indicating a trade-off in rate vs. time codes.

343 Heteromeric Purinergic P2X2/3 Channels Enhance Action Potential Firing of Developing Auditory Brainstem Neurons

Sasa Jovanovic¹, Claudio Coddou², Beatrice Dietz¹, Jana Nerlich¹, Tamara Radulovic¹, Stanko S. Stojilkovic², Rudolf Rübsamen¹, Ivan Milenkovic¹

¹Faculty of Biosciences, Pharmacy and Psychology, University of Leipzig, Germany, ²NICHD, NIH, Bethesda, USA

Background

In developing auditory system, purinergic signalling attunes activity in the cochlea and in the brainstem. Endogenous release of ATP contributes to action potential generation in the inner hair cells and enhances glutamate-driven firing of the cochlear nucleus (CN) bushy cells (BCs). Modulatory effects of ATP diminish with maturity, both in the periphery and in the central auditory neurons. In the brainstem, only specific cell types undergo purinergic modulation, including cochlear nucleus bushy cells, principal neurons in the medial nucleus of the trapezoid body and some neurons in the lateral superior olive. Here, activation of P2X receptor channels (P2XRs) can evoke suprathreshold membrane depolarization and action potentials by a mechanism engaging cytosolic calcium signals and subsequent activation of the protein kinase C. While the P2Rs associated with cochlear development have been largely characterized, evidence about the possible P2XR types related to maturation of central auditory neurons is still sparse.

Methods

We used *in vivo/in vitro*-electrophysiology and fluorometric calcium measurements to determine the exact receptor type mediating the ATP effects in the CN BCs. Experiments were performed on Mongolian gerbils, P13-16 for *in vivo*-, and P7-12 for slice recordings. To delineate receptor properties, we compared characteristics of native P2XR responses measured *in vivo* and in slices with the data obtained from HEK293 cells expressing recombinant rat P2X2R, P2X3R, or P2X2/3R.

Results

In vivo extracellular recordings in combination with iontophoretic application of AF-353, a selective antagonist of P2X2/3R and P2X3R, revealed that respective receptor subunits mediate the enhancement of spontaneous and sound evoked activity induced by the endogenous ATP release on BCs. Pharmacological characterization of responses recorded from BCs in slice preparation is consistent with P2XRs resembling mixed P2X2 and P2X3 characteristics. The desensitization profile of the currents following application of ATP γ S and α - β -meATP corresponds to heteromeric P2X2/3Rs. Finally, analogous response properties were recorded in HEK293 cells expressing heteromeric P2X2/3R, but not homomeric P2X2R nor P2X3R.

Conclusion

We provide evidence that purinergic modulation of action potential firing in developing auditory brainstem is

conveyed by the heteromeric P2X2/3R. Given the role of P2X2/3R in the neuronal re-organization in developing cochlea (pruning of promiscuous hair cell-SGN connections), and the transient enhancement of spiking activity of auditory brainstem neurons shown here, it is reasonable to assume that P2X2/3R might play a more general role in development of the auditory system.

344 PSD-95 Expression During Giant Synapse Formation in the Chicken Cochlear Nucleus

Luisa Fensky¹, Stefanie Kurth¹, Jule Buchholz¹, Hermann Wagner¹, **Thomas Kuenzel¹**
¹RWTH Aachen University

Background

In the cochlear nucleus, auditory nerve axons form giant synaptic terminals (Endbulbs of Held) on a specific subset of neurons only. It is yet unknown how this target-specific increase in terminal size is regulated on a molecular level during development. The "postsynaptic-density protein of 95kD" (PSD-95) is a central organizer of the postsynapse, involved in adjusting excitatory synaptic strength and size. It is also implicated in the development of the presynapse by transsynaptic interaction with neuroligins/neurexins. We thus hypothesized that PSD-95 expression should be present in the cochlear nucleus and the dynamics of expression should be temporally related to the increase in synaptic terminal size.

Methods

We tested this with fluorescent double immunolabeling of PSD-95 and a presynaptic marker protein (synaptic vesicle protein 2) in embryonic chicken brain cryosections from embryonic days E10 to E17. This was supported by anterograde tracing of auditory nerve axons at E15 and E16. Staining was visualized with a confocal laser-scanning microscope and analyzed with custom software.

Results

We found that PSD-95 was expressed at synaptic sites in all auditory brainstem nuclei of the embryonic chicken. In the mid- to high-frequency parts of nucleus magnocellularis, a maximum in the extent of PSD-95 immunosignals was evident before and at the time of maximal increase of presynaptic signal area. This was not seen in the low-frequency region of nucleus magnocellularis. Anterograde tracing corroborated that dynamics of synaptic immunosignals correlate with rapid structural changes of presynaptic terminals in the rostral regions at E15/E16.

Conclusion

The results support the hypothesis that PSD-95 may be involved in molecular regulation of giant synaptic development. The chicken system will allow functional studies of this protein and its binding partners in the future.

345 A Co-Culture of Chicken Cochlear Ganglion and Auditory Brainstem Neurons to Investigate Regulation of Endbulb Synapse Formation in Vitro

David Goyer¹, Stefanie Kurth¹, Kai-Oliver Seibel¹, Hermann Wagner¹, Thomas Kuenzel¹
¹RWTH Aachen University

Background

In birds, the axons of cochlear ganglion neurons project into two subdivisions of the cochlear nucleus in the auditory brainstem, the nucleus magnocellularis and the nucleus angularis. Only in nucleus magnocellularis specialized axosomatic synapses, the Endbulbs of Held, are formed. These terminals are strongly enlarged, sometimes engulfing nearly three quarters of the postsynaptic cell. The molecular basis for the determination of this giant synapse during development is still largely unknown. To address this, we established a co-culture system of cochlear ganglion (CG) and auditory brainstem neurons of the embryonic chicken.

Methods

One cell culture well was divided by an upright glass coverslip with a thickness of 130µm, creating 2 separate compartments. In one compartment auditory brainstem neurons of embryonic day 7 were seeded out. Three days later, CG neurons of embryonic day 10 were explanted into the second compartment. The coverslip was lifted after the cells had settled to allow neurite growth between compartments. Neurons were characterized via immunocytochemical staining against neurofilament and synaptic vesicle protein 2 (SV-2) at various days in vitro. SV-2 puncta size for both neuron types was measured and the CG's neurite outgrowth onto auditory brainstem neurons was characterized.

Results

Staining against neurofilament revealed a distinct bipolar morphology of the CG neurons and a strong axon growth, reminiscent of the in vivo situation. If there were brainstem neurons present, the CG neurons showed a profound axon outgrowth into the brainstem neurons' compartment, indicating that brainstem neurons may emit growth cues that attract CG neurons. We also could demonstrate the existence of SV-2 in the CG neurons' axon terminals, showing that these neurons already express and transport the machinery for synapse formation as early as E10. SV-2 puncta of CG neurons appeared to be larger than those of auditory brainstem neurons and even larger when axons of CG neurons are in vicinity of auditory brainstem neurons.

Conclusion

We were able to construct a co-culture system with viable CG and auditory brainstem neurons. Our results indicate that in vitro innervation of brainstem neurons by CG neurons is possible. The differential SV-2 puncta size shows that this co-culture system is a promising tool for further investigation of molecular aspects of Endbulb-formation and developmental control of synaptic terminal size.

346 Structural and Functional Remodeling at the Developing Mouse Calyx of Held-MNTB Synapse During Unilateral Hearing

Giovanbattista Grande¹, Jaina Negandhi¹, Robert V Harrison¹, Lu-yang Wang¹
¹Hospital for Sick Children

Background

Ability to locate sound is immediately impaired following a unilateral earplug but improves toward normal over several days to weeks. This suggests the reweighting of auditory cues toward the intact ear in subjects experiencing unilateral hearing deficits lead to some form of synaptic plasticity in sound localization circuits to maintain function. To examine this, we investigated the structural and functional properties at the calyx of Held-MNTB synapse in mice developing with unilateral hearing.

Methods

Experiments were performed in brainstem slices from P16-19 mice that underwent unilateral surgery to remove left middle ear ossicles at P5. Advantages to this approach are that the structural and functional properties of this synapse are well-characterized at P16-19 and because calyx terminals, which originate from globular bushy cells of the cochlear nucleus, only innervate principal cells of the contralateral MNTB, it allows for an ideal 'in-mouse' comparison. That being, we can quantify synaptic properties of cells located in the sound-deprived (SD) right MNTB with those located in the left MNTB (CTL) which are exposed to more auditory input.

Results

ABRs confirmed unilateral hearing deficits and could be detected at ~10 dB following click stimulation in normal hearing wild types (WT) and the right ear of surgical animals. Left ear ABRs had higher thresholds (65 dB) and late wave (III-V) latencies were significantly longer versus the intact right ear. Synaptic strength in CTL MNTB was enhanced based on a higher paired-pulse ratio (108%), lower probability of release (0.11) and reduced EPSC depression (25.5% of initial) in MNTB neurons following high-frequency stimulation compared to SD (respectively 95%, 0.14, 18.9%) and WT (95%, 0.17, 18.6%) synapses. Remarkably, the relationship between synaptic input and spiking properties (failure rate at 300-400 Hz) amongst the populations of MNTB neurons (WT vs SD vs CTL) were unchanged. Although failure rates were similar, SD synapses were more excitable. Calyx morphology was more complex in both the CTL and SD MNTBs compared to WTs based on the degree of branching and fenestration expected at this age. This was surprising given the classic view that the transformation from spoon to fenestrated structure is strongly driven by sound-evoked activity.

Conclusion

We characterize the structural and functional remodeling that occurs at the calyx of Held-MNTB synapse in mice developing with unilateral hearing loss as a means to maintain sound localization circuit function.

347 A Tetanus Toxin Mouse Model to Study Activity Dependent Processes in Auditory Circuitries

Heiner Hartwich¹, Hans Gerd Nothwang¹

¹Department of Neurogenetics, University of Oldenburg, Oldenburg, Germany

Background

Neuronal activity is essential for the formation and maintenance of neuronal circuits. Previous work using cochlear ablation or gene knockouts suggested an important role of both spontaneous and acoustically driven activity for proper development and function of the central auditory system. However, these studies often suffered from ambiguity in the interpretation, as primary and secondary effects might be confounded. Furthermore, they represent irreversible processes which do not allow to challenge the plasticity of the auditory system by switching neuronal activity on and off. We therefore wished to implement a system to block neurotransmission in auditory circuits in an inducible and reversible manner.

Methods

A triple transgenic mouse model was generated to silence synaptic transmission. A Cre recombinase drives a tetanus toxin light chain (TxLC) - eGFP fusion protein in a doxycycline dependent manner. Here, we used the *Egr2::Cre* driver line to express TxLC-eGFP from early embryonic stages (E9.5) in rhombomeres 3 and 5 derived cells. These should result in silencing of large parts of the developing auditory brainstem such as the neurons of the AVCN, DCN, and SOC.

Results

Immunohistochemistry demonstrated expression of TxLC-eGFP in the absence of doxycyclin in the triple transgenic mouse line. Anatomical analyses of Nissl-stained sections revealed a severe reduction (41%) of the MNTB volume in adult (P25) mice. This volume reduction correlated well with a 47% decrease in cell number. These values are close to those reported for an auditory brainstem specific *Cav1.3* conditional knockout mouse, indicating an important role of excitation-transcription coupling in the developing auditory brainstem. At birth, a moderate volume reduction of 27% was already present. Currently, a similar analyses is conducted for the LSO.

Conclusion

Our data suggest that TxLC is expressed in the auditory brainstem and results in synaptic silencing. In addition, the anatomical results reveal that spontaneous activity is required for formation of auditory circuits. Further studies will investigate the precise mechanisms resulting in cell loss and the critical time windows for neuronal activity in auditory circuits. Finally, the approach presented here can be combined with different Cre-driver lines to block neurotransmission in any neuronal subpopulation.

348 Developmental Expression of *ErbB4* Is Required for Normal Cochlear Nucleus Organization

Kathleen Yee¹

¹University of Mississippi

Background

As the first synaptic site to receive input from the inner ear, the cochlear nucleus (CN) is a critical locus in the brain for auditory processing. Extensive literature exists on the anatomy and physiology of the CN during functional hearing, including hearing onset and decline, yet relatively less is known about the CN during its development. The laboratory is interested in elucidating molecules that contribute to the mature organization of the CN. Since the tyrosine kinase receptor *ErbB4* has been shown to be a molecule critical for developmental events, including migration and differentiation, the role of *ErbB4* in CN development and maturation was investigated.

Methods

Methods employed include in situ hybridization with digoxigenin-labeled riboprobes, general histological staining (cresyl violet, and hematoxylin and eosin) and immunohistochemistry. Analyses were performed in age-matched wild type and *ErbB4* homozygous null mice.

Results

In situ hybridization shows that perinatal *ErbB4* expression is spatiotemporally dynamic. At E16.5, expression is detected in the dorsal and ventral regions of the CN anlage. At postnatal day 0, *ErbB4* mRNA is expressed in the molecular/granule cell layer and by cells within the deep dorsal and ventral regions of the CN. Examination of the mature CN in wild type and *ErbB4* homozygous null mice permits assessment of the developmental impact of this gene. General histological staining shows perturbed dorsal CN organization including variable thickness of the molecular layer and altered organization of the granule cell layer. Immunohistochemical localization of vesicular glutamate transporter 1 (vGlut1; Millipore) shows vGlut1-expressing auditory nerve fiber terminals in the CN (Zhou et al., 2007) and reveals an expansion of the central core of the ventral CN in *ErbB4* null mice compared to wild-type controls.

Conclusion

These data show that developmental expression of the receptor tyrosine kinase *ErbB4* contributes to the normal anatomical organization of the CN. The change in cellular arrangement within the molecular and granule cell layers in *ErbB4* (-/-) dorsal CN suggests that *ErbB4* may be involved in CN neuronal migration or survival. The difference in pattern of vGlut1 immunohistochemical localization in the ventral CN between *ErbB4* null and wild type mice suggests that *ErbB4* may be important for the positioning of glutamatergic neurons and their afferents. Together, these anatomical changes further indicate that circuitry underlying sound localization may be critically dependent on *ErbB4* expression.

349 Afferent Regulation of Elongation Factor 2 in Auditory Brainstem Neurons: Cell Survival and Dendritic Reorganization

Yuan Wang¹, Ethan McBride¹, Edwin Rubel¹

¹Virginia Merrill Bloedel Hearing Research Center, University of Washington

Background

Afferent inputs regulate neuronal cell survival and dendritic morphology in the auditory brainstem. Using the chick nucleus magnocellularis (NM) and nucleus laminaris (NL) as models, we study the involvement of elongation factor 2 (eEF2), a translational factor that regulates protein synthesis, in afferent deprivation-induced cell death in NM and dendritic retraction in NL. Previously, we have found that afferent deprivation induced by cochlea removal leads to rapid reductions in the level of phosphorylated eEF2 (p-eEF2) in NM neurons. The current study continues to explore the role of eEF2 activity by asking what causes observed reductions in p-eEF2 and whether these changes are associated with cell survival in NM. In addition, we examine the involvement of eEF2 in afferent regulation at a subcellular level in NL, where unilateral cochlea removal leads to selected retraction of deprived dendritic arbors but not other arbors of the same neurons with normal innervation from the other intact cochlea.

Methods

The chick hatchlings (P4-10) received unilateral cochlea removal and survived for up to 48 hours. Fixed sections collected from these and unoperated animals were immunostained for eEF2, p-eEF2, eEF2 kinase (EF2K, a major mechanism that phosphorylates eEF2), and phosphorylated EF2K (p-EF2K) using specific antibodies. Cell apoptosis in NM was evaluated by a dramatically decreased intensity of Nissl stain in the cytoplasm. Staining patterns in NM and NL were imaged. Average optic intensities of the staining were quantified and compared between different manipulation and survival groups.

Results

At 6 hours post-surgery, we found notable increases in the level of EF2K and p-EF2K immunoreactivities in the deprived NM, in parallel with dramatic decreases in phosphorylated, but not total, eEF2. In addition, we found a strong correlation of the p-eEF2 level with the intensity of Nissl staining at 12 hours in NM. In NL, we found significant decreases in the p-eEF2 level in deprived NL domain as compared to the intact domain of the same NL neurons, as early as 3 hours following unilateral cochlea removal.

Conclusion

Afferent inputs rapidly regulate the level of phosphorylated eEF2 in auditory neurons in NM and NL. Such regulation can be either global and associated with cell survival, or confined to specific subcellular components that undergo structural changes later. One possible mechanism underlying this regulation maybe activity-dependent eEF2 kinase signaling.

350 Co-Release of GABA/glycine and Glutamate in Immature Auditory Brainstem from Distinct Vesicle Populations with Different Release Probabilities

Javier Alamilla¹, Deda Gillespie¹

¹McMaster University

Background

Principal neurons of the lateral superior olive (LSO) compute interaural level differences by integrating ipsilaterally derived excitatory signals arising in the cochlear nucleus with contralaterally derived inhibitory (glycinergic) signals arising in the medial nucleus of the trapezoid body (MNTB). During the first postnatal week, glycinergic terminals in the MNTB-LSO pathway release GABA and glutamate. While GABA and glycine are known to be co-packaged, whether glutamate is co-released from the same or a different subset of vesicles has been an open question.

Methods

In acute rat brainstem slices postnatal day 4-8 (P4-8), we made whole cell voltage clamp recordings in the LSO, using reversal potentials and pharmacology to isolate different neurotransmitter responses.

Results

We examined paired-pulse ratios (PPRs) for GABA/glycine- and glutamate-mediated transmission, finding significant differences in PPR for glycine (0.66 ± 0.03 and 0.58 ± 0.03) and AMPA (0.79 ± 0.02 and 0.77 ± 0.03 ; $p < 0.001$, MW-test) at 20 and 50 Hz. We next replaced calcium in the perfusate with strontium to desynchronize vesicle release and analyzed miniature synaptic events after electrical stimulation in the MNTB. In the presence of Sr⁺⁺, picrotoxin, and CNQX, two populations of synaptic events could be discerned based on rise time (0.62 ± 0.03 vs 6.59 ± 1.3 ms at P4-5, $n=12$; 0.61 ± 0.04 vs 4.96 ± 0.25 ms at P7-8, $n=12$; $p < 0.001$, Wilcoxon t) and decay time (2.17 ± 0.1 vs 21.77 ± 1.9 ms at p4-5, and 2.30 ± 0.3 vs 26.1 ± 3.3 ms at P7-8; $p < 0.001$). Miniature events with fast kinetics disappeared in strychnine ($10 \mu\text{M}$; $n=13$), whereas events with slow kinetics disappeared in D-APV ($50 \mu\text{M}$; $n=11$). Coefficients of variation for kinetics parameters also differed significantly for gly-R and NMDA-R events. In the presence of TTX ($1 \mu\text{M}$), as with Sr⁺⁺, a majority of miniature events (>98%) were fit by a single exponential. Despite fewer miniature events in TTX, we saw no differences in kinetics between evoked and spontaneous miniature synaptic events.

Conclusion

Our data are consistent with a model in which GABA/glycine and glutamate are packaged in distinct subsets of synaptic vesicles, allowing for their control by different release machinery and resulting in differing release probabilities at individual MNTB terminals.

351 Synaptic Function in the Auditory Nervous System in the Preterm Baboon Brain

Sei Eun Kim¹, Cynthia Blanco¹, Jun Hee Kim¹

¹University of Texas Health Science Center, San Antonio

Background

Prematurity is one of the leading causes of perinatal mortality and long-term disability. Extremely premature children often suffer from developmental delays; in particular, intellectual, cognitive, academic, and language difficulties. Poor reading-speaking abilities are associated with an auditory processing disorder. Fetal auditory development is essential for early brain maturation and healthy neuronal circuitry. However, the cellular mechanisms that lead to impaired auditory processing in the developing brain are still poorly understood. We have studied developmental changes in synaptic formation and functions in the auditory nervous system in baboon brain born prematurely.

Methods

We recorded electric signals from a single synapse in preterm and full term baboon brainstem slices (125 day; 67 % gestation and 185 day gestational age controls, respectively) using whole-cell patch clamp recordings, and examined local synaptic formation in auditory brainstem using immunofluorescence microscopy.

Results

We identified multiple nuclei, the lateral and medial superior olivary nuclei (LSO, MSO) and the medial nucleus of trapezoid body (MNTB), which were prominent nuclei within the superior olivary complex under light microscope in preterm baboon brainstem slices. In preterm baboon brain, the MNTB principal neurons formed synapses with the calyx of Held terminals expressing a high density of vesicular glutamate transporters, and displayed spontaneous excitatory postsynaptic currents, which are mediated by the 2-amino-3-(3-hydroxy-5-methyl-isoxazol-4-yl) propanoic acid (AMPA) receptors. In whole-cell patch clamp recordings, the MNTB neurons showed the burst of action potentials (~100 Hz) in response to current injections.

Conclusion

At 67% gestation, preterm baboon showed prominent neuronal circuitry and synaptic formation in the auditory brainstem, thus the functional maturation of synapses during late gestation period is critical for the development of auditory processing.

352 A Biophysical Cable Model for MSO Neurons as Generators of the Neurophonic

Joshua Goldwyn¹, Myles McLaughlin², Eric Verschooten³, Philip Joris³, John Rinzel¹

¹New York University, ²UC Irvine, ³K.U. Leuven

Background

The medial superior olive (MSO) is an early stage of binaural processing and sound localization in mammals. In vivo recordings of single cell activity in the MSO are rare due to the presence of strong sound-evoked local field

potentials (LFPs) in the brain stem. These LFPs, known as the auditory neurophonic, are believed to reflect post-synaptic current flow in MSO neurons and are a more accessible signal of *in vivo* neural activity. To date, however, the exact generators of the LFPs remain unclear, and there has been no quantitative theory that links the neurophonic to activity of individual MSO neurons.

Methods

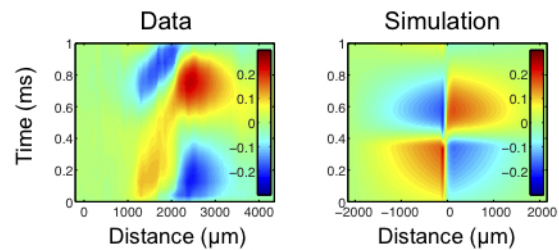
We use biophysically-based cable models of MSO bipolar neurons to predict how single cell neural dynamics can generate the experimentally observed population-level neurophonic (McLaughlin et al 2010). Passive cable theory (Rall 1977, e.g.) provides initial insights which are complemented by simulations of a model that includes voltage-gated currents (Mathews et al 2010). Motivated by anatomical and neurophysiological observations we make two simplifying, yet plausible, assumptions: 1) MSO neurons are identical bipolar cells arrayed with spatial symmetry; 2) afferent inputs to a subpopulation of MSO cells are in synchrony with each other. With these assumptions, we formulate a one-dimensional model of the population-summed neurophonic and relate simulation results to *in vivo* data.

Results

We find that post-synaptic dendritic current flow in the MSO neuron models can generate extracellular potentials that qualitatively resemble LFPs evoked by monaural tones (see figure). Our simulations make some non-intuitive predictions for responses to binaural beat stimuli. For instance, the spatial spread of LFPs depends on the degree of coincidence of bilateral inputs with coincident inputs generating fields that are most localized near the model MSO neurons. In ongoing work, we use these predictions to help interpret experimental data.

Conclusion

Our modeling provides a biophysically-based foundation to assess how cellular and synaptic properties generate the neurophonic. We have shown that, for monaural stimuli, the bipolar morphology of MSO neurons can create dipole-like LFPs with a half cycle phase shift between sink and source. This confirms and extends earlier conceptualizations of the neurophonic (Galambos et al 1959, McLaughlin et al 2010). These findings contrast with a study of the neurophonic in barn owls which suggested that pre-synaptic currents are the dominant generators of brain stem LFPs in that system (Kuokkanen et al 2010).



In vivo recordings and simulation results for responses to monolateral 1kHz tone. Color map is extracellular potential after 10Hz high pass filtering.

353 In Vivo Whole-Cell Recordings from Principal Neurons of the Medial Superior Olive

Tom P. Franken¹, Michael T. Roberts², Liting Wei¹, Nace L. Golding², Philip X. Joris¹

¹Lab. of Auditory Neurophysiology, KU Leuven, Leuven (Belgium), ²Sect. of Neurobiology & Ctr. for Learning and Memory, University of Texas at Austin

Background

In vivo intracellular data from medial superior olive (MSO) neurons have not been reported. Such data are essential to understand how sensitivity to interaural time differences (ITD) is generated in these cells. Its absence has led to controversies, for example regarding the origin of internal delays and the nature of the coincidence process.

Methods

We performed *in vivo* whole-cell current clamp recordings in the superior olivary complex (SOC) of young gerbils under general anesthesia. Patch clamp electrodes were filled with an internal solution containing biocytin. Neurons were characterized with threshold tuning curves, monaural and binaural sinusoidal tones, binaural beats and broadband noise. We separated postsynaptic potentials (PSPs) and spikes in the voltage signal using criteria of amplitude and repolarization speed. At the end of the experiment the animal was perfused and the brainstem sectioned, so that biocytin-filled cells could be retrieved using routine histological methods.

Results

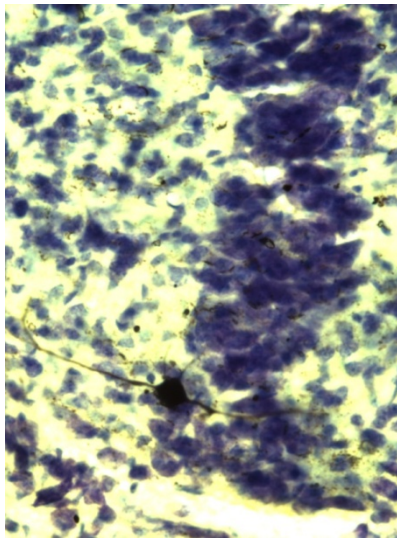
We obtained *in vivo* intracellular voltage responses for a variety of SOC neurons. Sensitivity to ITD as well as histology (cf. Figure) confirmed several of them to be MSO principal neurons. Analysis of the spontaneous activity showed remarkably high and continuous subthreshold activity. Driven activity, both to monaural and binaural stimulation, consisted of discrete excitatory events rather than a stimulus-like analogue waveform. Inhibitory PSPs were not obviously apparent as discrete events, either in the spontaneous signal or in the acoustically driven signal. The rise time and duration of subthreshold excitatory PSPs were close to the values previously reported for MSO neurons in brainstem slices. By comparing the response to ipsilateral and contralateral sounds, we found that rise times of subthreshold events triggered from opposing ears were not consistently different. The precision of phase

locking (the vector strength of spikes) was higher than that of subthreshold events. The relation between characteristic frequency and histological location shows that the high-frequency representation is surprisingly limited.

Conclusion

In conclusion, we made the first *in vivo* whole-cell recordings from MSO neurons. While our results do not preclude a role for inhibition, they suggest that ITD sensitivity is determined primarily by the relative timing of discrete, similarly shaped EPSPs.

Supported by a Ph. D. fellowship of the Research Foundation - Flanders (FWO) to TPF, grants from NIH (1R21DC011403), FWO (G.0961.11) and BOF (OT-09-50).



354 Activity Dependent Duration of Inhibition in an Echo Processing Circuit

Julian Ammer^{1,2}, Felix Felmy¹

¹Ludwig-Maximilians University, Munich, ²Graduate School of Systemic Neurosciences, LMU, Munich

Background

To localize primary sound sources in reverberant environments, the auditory system has to suppress the directional information of echoes. An elementary step of this process seems to be implemented in the circuitry of the dorsal nucleus of the lateral lemniscus (DNLL). The DNLL generates an exceptionally long lasting GABAergic inhibition that suppresses responses to trailing sounds for tens of milliseconds in the contralateral DNLL termed persistent inhibition (PI). It has been suggested that this PI underlies the suppression of directional information during echoes. However, *in vitro* single GABAergic IPSC decay with a time constant of ~ 4 ms, being too fast to explain the PI. Data from juvenile gerbils suggest that the appropriate inhibitory time course might be adjusted in an activity dependent manner. In this study we describe the cellular basis of the PI and its dependence on activity.

Methods

The cellular basis of PI was analyzed using *in vitro* patch clamp recordings in acute brain slices from P30-35

Mongolian Gerbils at near physiological temperatures. To do so recordings of pharmacologically isolated, fiber stimulated GABAergic responses as well as current and conductance injections into postsynaptic DNLL neurons were carried out.

Results

The GABAergic IPSC decay time course slowed with increasing stimulation frequencies, strength and pulses number indicating an activity dependent process. Pharmacological dissection of the underlying synaptic mechanisms showed that transmitter spill over and asynchronous release mediate the increase of GABAergic decay time constants. The factors that influence the conversion of this inhibitory conductance into effective IPSPs were analyzed. GABAergic IPSPs are strongly hyperpolarizing, as the chloride reversal potential is ~ -90 mV. The membrane properties between the resting potential and the reversal potential indicate that synaptic GABA conductances are integrated passively. A steady state approximation based on these findings shows that larger synaptic conductances cause slower IPSPs. The injection of synaptic conductances shows that these membrane properties transform the activity dependent slowing of IPSCs into a long lasting hyperpolarization. Finally, this hyperpolarization is indeed sufficient to suppress action potentials for tens of milliseconds.

Conclusion

Taken together, our data indicate that activity-dependent, hyperpolarizing inhibition can mimic the persistent inhibition *in vivo* underlying the suppression of space information during echo perception.

355 Systematic Variation of Conduction Velocity Achieves Isochronic Inputs

Armin Seidl^{1,2}, Edwin Rubel^{1,2}, Andres Barria^{1,3}

¹University of Washington, ²Virginia Merrill Bloedel Hearing Research Center, ³Department of Physiology and Biophysics

Background

Proper function of brain circuitry relies on the exact timing of signal propagation. In the avian brainstem, the circuit responsible for sound segregation consists of internal axonal delay lines innervating an array of coincidence detector neurons that encode interaural time differences (ITDs). Information from the ears gets transferred to nucleus magnocellularis (NM) neurons on each side of the brainstem and individual NM axons project to the dorsal dendritic region of the ipsilateral nucleus laminaris (NL) and to the ventral region of the contralateral NL, resulting in NL neurons receiving segregated input from both ears. These pathways are thought to represent a circuit similar to the Jeffress Model of sound localization. This model assumes equivalent delays from the two ears when a stimulus originates from straight ahead, leading to ITDs of less than 10 μ s. To accomplish this, action potential (AP) speed and travel distance have to be timed precisely - in the microsecond range - to ensure coincident arrival of information at individual detector neurons in NL.

We previously reported that internode distance and axon diameter of NM neurons vary systematically within individual axons to compensate for axonal length differences, suggesting that conduction velocities of specific axon segments are precisely regulated; shorter axon segments should propagate APs slower than longer axon segments.

Methods

In the current study, conduction velocities in different NM axon segments were measured. To this end, we recorded from single NM neurons in whole-cell current-clamp mode and determined the difference in the travel time of antidromic APs, elicited at two different locations along the axon. The axons were visualized with biocytin, and with the axon segment length between the stimulation sites conduction times were determined.

Results

Our results show that longer contralateral axons projecting across the midline conduct APs faster than the shorter axons in the ipsilateral loop. Conduction velocities calculated for physiological temperatures and axon length measurements show that conduction times of the ipsilateral and the contralateral NM axon branch are almost equal, leading to coincident arrival of inputs at NL when ITD is 0.

Conclusion

These combined anatomical and functional properties lead to the arrival of appropriately timed binaural inputs to coincidence detector neurons. Conduction velocity is systematically regulated within two different branches of the same axon and the parameters responsible for conduction velocity of NM axons must be regulated precisely during development to achieve coincidence detection.

356 A Model MSO Neuron Approaches the Measured Frequency Range of Fine-Structure ITD Sensitivity

Andrew Brughera¹

¹Boston University

Background

Sound from an acoustic source located to the side arrives first at the near ear, producing an interaural time difference (ITD). Sensitivity to ITD is derived in the left and right medial superior olive (MSO) of the auditory brainstem. MSO neurons receive bilateral excitation via the anteroventral cochlear nuclei (AVCN), and inhibition via the medial and lateral nuclei of the trapezoid body (MNTB and LNTB, contralaterally and ipsilaterally driven, respectively). For pure-tone acoustic inputs, in-vivo measurements in cat MSO have focused on frequencies from 150 to 1000 Hz, and recently in gerbil MSO from 800 to 2000 Hz. Fine-structure ITD sensitivity to 2 kHz is reported in both species, and effectively modeled above 800 Hz using bilateral excitation (EE) and frequency-dependent cochlear delays. This study models neural mechanisms underlying ITD sensitivity within an MSO

neuron incorporating realistic action potential propagation and an accurate number of synaptic inputs.

Methods

Existing ion-channel dynamics equations from gerbil MSO neurons were incorporated into a Hodgkin-Huxley model MSO neuron comprising two dendrites (contralateral and ipsilateral), soma, and axon. Four excitatory synapses were applied to each dendrite, zero to eight inhibitory synapses to the soma. Synaptic strength and speed were adjusted. Each synapse was driven by a point process with discharge patterns reflecting an AVCN bushy cell, or TB neuron, stimulated at characteristic frequency at 60 dB SPL. Active channel mechanisms were emphasized by minimizing passive leakage currents at resting potential, which was slightly lower in the axon than in the dendrites and soma.

Results

Large action potentials were limited to the model axon with minimal back-propagation to the soma. At 150 Hz, the model MSO neuron with bilateral excitation and inhibition (EII) produced a broadly tuned rate-ITD function ranging from 0 to 120 spikes/s and monaural responses around 50 spikes/s, matching measurements in cat MSO. At 1600 Hz, using faster synapses the EII model MSO neuron matched rate-ITD functions from gerbil MSO (ranging from 10 to 100 spikes/s), but monaural responses were weaker than in gerbil. From 300 to 1250 Hz, bilateral excitation and contralateral inhibition captured ITD responses in cat and gerbil MSO.

Conclusion

The model MSO neuron matched rate-ITD functions for pure-tones approaching the frequency range of fine-structure ITD sensitivity. Ion-channel mechanisms restricted back-propagation of action potentials, and supported ITD sensitivity for an accurately small number of synaptic inputs.

357 Tonotopic Gradient of Intrinsic and Synaptic Properties in the Rat Principal LSO Neurons

Jimena Ballester¹, Roberta Donato¹, Simon Foster¹, David McAlpine¹

¹UCL-Ear Institute

Background

The lateral superior olive (LSO) and medial superior olive (MSO) are the first nuclei in the ascending auditory pathway that encode binaural information. The classical view of the function of the LSO is that it encodes interaural level differences by weighting excitatory and inhibitory inputs originating from the ipsilateral and contralateral cochlear nucleus respectively. Nevertheless, it has been shown that LSO neurons are heterogeneous both in their intrinsic properties (Barnes-Davies et al., 2004; Remme et al., 2012) as well as in their synaptic inputs (Tsuchitani 1977). Moreover, some of these characteristics vary along the tonotopic axis. In addition, it has been shown that LSO neurons are capable of encoding interaural time

differences in the envelope of high frequency sounds (Joris and Yin 1995). Therefore, it has become clear in recent LSO neuronal models the importance of including this heterogeneity to fully understand the encoding properties of the LSO. The aim of the present work is to study the intrinsic electrical properties of principal LSO neurones and the characteristics of their synaptic inputs along the tonotopic axis.

Methods

Patch clamp whole cell recordings were made in LSO cells from P14 rat brainstem slices. Resonant properties of pLSO neurones were evaluated applying a current ZAP stimulus. Synaptic activity was evoked by use of a concentric bipolar stimulator placed at the fibre bundle that projects from the ipsilateral AVCN to the LSO.

Results

We demonstrate a gradient of resonances in the rat LSO where most of the pLSO cells from the lateral limb exhibit a peak resonance around 300 Hz while all the medial ones exhibit low-pass profiles. To further investigate the pLSO cells intrinsic ability to process high frequency inputs, action potentials were evoked either by injecting current pulses or by synaptic stimulation at rates ranging from 50 to 700 Hz.

Conclusion

Our data indicate a gradient in resonance filter properties along the presumed tonotopic gradient of the LSO of the rat that could underpin a transition in neural coding from one favouring extraction of temporal information conveyed in the stimulus envelope to one favouring the extraction of stimulus energy (level).

358 The Influence of Waveform Envelope Shape on the Rate-ITD Functions of Neurons in the Inferior Colliculus

David Greenberg¹, Mathias Dietz^{1,2}, Torsten Marquardt¹, David McAlpine¹

¹Ear Institute, University College London, London, UK, ²Medizinische Physik, Universität Oldenburg, Oldenburg, Germany

Background

It is possible to design envelope waveforms with each segment - pause, attack, sustain, and decay – assigned an independent duration. Klein-Hennig et al. (2011, J. Acoust. Soc. Am. 129 p. 3856-3872) conducted psychoacoustic experiments utilising these envelope waveforms to determine the threshold interaural time differences (ITDs) for different waveform envelope shapes and revealed that a short duration attack segment preceded by at least 4ms of pause is optimal for discrimination performance, whilst sustain and decay segment durations were of only minor influence.

Methods

Using tungsten microelectrodes, we recorded rate-vs.-ITD functions of single neurons in the inferior colliculus (IC) of anaesthetised guinea pigs. For each neuron, carrier

frequencies corresponded to the neuron's characteristic frequency (CF). Responses for 3 envelope shapes were analysed: (1) short attack-long decay (1.5ms-15ms), (2) long attack-short decay (15ms-1.5ms), and (3) a short attack-short decay (1.5ms-1.5ms) pseudo square-wave envelope. The current study assesses how each envelope waveform segment influences the rate-ITD function of IC neurons for each envelope shape.

Results

Rate-ITD -functions for the short-long stimuli (1) were better modulated than those to the long-short (2), indicating improved ITD discriminability in the presence of a waveform envelope with a short attack segment duration. Each neuron For most neurons, the shape of the rate-ITD functions, and therefore ITD sensitivity, for the various envelopes differed considerably a wide range of neural ITD sensitivity to different is unique in the shape of its rate-ITD-functions for each envelope shapes was observed. NThe neural ITD discrimination threshold is herewas defined as the smallest significant difference in response rate to any reference ITD . The responses of the first 28 neurons to be measured revealed 21/28 to have a significant ($d'^{\geq 2}$) ITD discrimination threshold for the short-long stimulus compared to 8/28 for the long-short stimulus. Average thresholds for the neurons in the top quartile of this subset were 167 μ s for the short-long and 1000 μ s for the long-short stimulus.

Conclusion

The data indicate the importance of fast-attack envelopes in providing for high-resolution ITD sensitivity in high-CF neurons. The physiological data show strong correspondence with human performance in envelope-ITD discrimination tasks.

359 GABA_B Receptor Mediated Adaptation in Medial Superior Olive Neurons

Annette Stange¹, Andrea Lingner¹, Michael H Myoga¹, Felix Felmy¹, Ida Siveke¹, Michael Pecka¹, Benedikt Grothe¹

¹Ludwig-Maximilians-University Munich

Background

It is well established that human listeners adapt in their judgement of the lateral position of low-frequency sound sources depending on the nature, timing and location of preceding sound stimulation. Recently it has been shown that interaural level difference processing in the lateral superior olive (LSO), which is important for localizing high-frequency sounds, is subject to binaural adaptations mediated by GABA_B receptors (Magnusson et al. 2008). The location of low-frequency sounds is first encoded in the medial superior olive (MSO) that precisely detects interaural differences in the arrival time of a sound at the two ears (ITDs). GABA_B receptors are expressed in the MSO, but in contrast to LSO neurons it is unclear whether MSO neurons also adapt their binaural sensitivity.

Methods

Here, we performed human psychophysical experiments and *in vivo* extracellular recordings of single MSO neurons in adult Mongolian gerbils to investigate adaptation in ITD-based sound localization using the same stimulus paradigm in both approaches. Moreover, we applied pharmacological manipulations *in vivo* and *in vitro* to determine the synaptic mechanism underlying neuronal adaptation.

Results

Our human psychophysical and *in vivo* electrophysiological studies show that adapter tone pips change human perception of the location of test tones and spike rates of gerbil MSO neurons, respectively. Specifically, we find that the spike rates during the test tones were negatively correlated with the spiking activity of individual MSO neurons to the adapter, suggesting an activity-dependent adaptation. Importantly, a similar reduction in spiking activity as found during the tone-evoked adaptation could be elicited by iontophoretically applying GABA without presenting adapter sounds. Moreover, the overall spike rate decreased strongly during application of the GABA_B receptor agonist baclofen, and conversely, antagonizing GABA_B receptors with CGP 55845 increased spiking activity. In line with this, *in vitro* patch-clamp studies revealed that GABA_B receptors modulate both excitatory and inhibitory inputs to the MSO in a dose-dependent manner.

Conclusion

Taken together, our results suggest that MSO neurons adapt their spike rate according to their preceding spiking activity through a GABA_B receptor mediated feedback loop. This feedback loop might serve as a dynamic adjustment during changing environments.

360 NMDA-Dependent Enhancement of Rate Coding in the Auditory Brainstem

Ida Siveke¹, Julian Ammer¹, Felix Felmy¹, Benedikt Grothe¹

¹Ludwig-Maximilians-Universität München

Background

Low frequency neurons in the dorsal nucleus of the lateral Lemniscus (DNLL) are sensitive to interaural time differences. They directly inherit this sensitivity from neurons of the superior olivary complex. Coincidence detector neurons in the superior olivary complex translate the binaural temporal code into a rate code. A major role of DNLL neurons at the second stage of this binaural pathway is suggested to be enhancing the rate code generated at the site of coincidence detection (Pecka et al. 2010). This enhancement is due to a reduction in the variability of neuronal responses in the DNLL compared to the superior olivary complex. However the cellular mechanisms of this enhancement are unclear. Interestingly, recent *in vitro* data from our lab showed that the synaptic NMDA currents amplify the postsynaptic activity in adult DNLL neurons (Porres et al. 2011, Ammer et al. 2012).

Methods

In this study we now linked the *in vitro* results to the *in vivo* measured enhancement investigating the role of NMDA currents on the neuronal activity of DNLL neurons in adult Mongolian gerbils using a combined *in vivo* and *in vitro* approach. While pharmacological blocking the NMDA current we measured the contribution of NMDA receptor mediated activation on the binaural responses in terms of rate, time, and variability *in vivo*.

Results

In vivo the neuronal activity in adult gerbils is significantly reduced after blocking the NMDA current. Besides the onset of the response to pure tones is strongly reduced by applying NMDA antagonists. This reduction of the ongoing component resulted also in shorter responses to tone stimulation. Furthermore the fano factor, a measure of response variability, significantly increases after blocking the NMDA current, which implies a higher variability in the neuronal response after blocking. The NMDA receptor induced enhancing of the rate code directly enhanced the neuronal coding of interaural time differences. This NMDA dependency is in line with *in vitro* findings that show a reduction in the number of spikes in response to fibre stimulation in a frequency dependent manner.

Conclusion

Taken together a NMDA sensitive component amplifies neuronal activity in the DNLL. This supports a transition from a predominantly temporal to rate-code information at this second stage of the binaural pathway.

The study is funded by the Deutsche Forschungsgemeinschaft (SFB 870)

361 Axonal Organization of Inhibitory Inputs to Binaural Brainstem Circuit

Kathryn Tabor¹, Rachel Wong², Edwin Rubel²

¹NIH/NICHD, ²University of Washington

Background

A fundamental question in neuroscience is how connections between neurons underlie information processing. In the chicken auditory brainstem, excitatory and inhibitory inputs to the nucleus laminaris (NL) are thought to be organized in a way that optimizes the computation of interaural time differences (ITDs), a binaural cue for encoding the location of a sound source. Neurons in NL are bipolar, with dorsal and ventral dendritic lamina receiving excitatory input from separate ears. Excitatory axons innervate narrow bands across NL to construct a precise tonotopic map. Orthogonal to its tonotopic map, NL is arranged by preferred ITD such that neighboring neurons have adjacent receptive fields along the horizontal plane. Computational and physiological studies demonstrated that the sensitivity of NL neurons to ITDs is modulated by an inhibitory feedback circuit via the superior olivary nucleus (SON). To better understand the structural arrangement of inhibitory inputs that provide this modulation, we determined the pattern of axonal

arborizations of individual SON axonal arborizations innervating NL.

Methods

We performed in vitro intracellular dye filling to label individual SON neurons and their terminal axonal arborizations in NL in embryonic day 18-21 chickens. Immunolabeling for GABAergic synapse components was performed on this tissue to ascertain the spatial distribution of synaptic contacts of single SON axons. Images were acquired using fluorescence microscopy and analyzed using FIJI and Matlab software. Measurements of arborizations (i.e. length, area, shape and location) and synaptic patterning (i.e. density and location) were compared between tonotopic regions and the two dendritic laminae of NL.

Results

The arborization patterns of SON axons were largely variable. While some axons targeted a specific dendritic lamina of NL (similar to excitatory inputs), others innervated both laminae relatively equally. In addition, some SON axons innervated a specific frequency region of NL while others extended across almost the entire tonotopic axis. SON axons in the later group did not innervate all frequency regions uniformly, but instead showed a high density of branches and synapses in a confined region and a significantly lower density of branches and synapse in surrounding frequency regions.

Conclusion

In contrast to the highly stereotyped and precisely targeted excitatory inputs to NL, the spatial patterns of inhibitory inputs from SON to NL are diverse. Further analyses will quantify the patterns of axon arborizations. This information will provide a more thorough understanding of how inhibitory input enhances frequency mapping and spatial segregation in ITD pathways of the brainstem.

362 Frequency Region Differences in Outward Currents of the Nucleus Laminaris in Chicken

William Hamlet^{1,2}, Yong Lu^{1,2}

¹Northeast Ohio Medical University, ²Kent State University

Background

In order to determine the location of a sound in horizontal space, specialized neurons in the auditory system compare arrival times of inputs (interaural time differences; ITD) from both ears. In chick, neurons in the nucleus laminaris (NL) compute ITD along a tonotopic axis. In vitro data suggests middle and high characteristic frequency (CF) neurons encode ITD more accurately than low CF neurons. It has been proposed that the presence of strong Kv currents partially explains this observation. The purpose of this work was to further study Kv currents in NL neurons across the tonotopic axis in order to better understand their role in ITD coding.

Methods

Brainstem slices (275-300 μ m) were prepared from chick embryos (E18). An Axopatch 200B amplifier was used to perform whole-cell voltage-clamp experiments. Recordings were made at room temperature, in the presence of TTX (1 μ M), and at a holding potential of -60 mV. Leak subtraction was implemented using a linear regression of current measured between -100 and -85 mV.

Results

Total Kv-currents in high CF neurons (at 0 mV, 12.0 ± 2.4 nA) were larger than in low CF neurons (at 0 mV, 7.1 ± 1.17 nA; $p = 0.03$). After accounting for size differences between cells, data confirmed that high CF neurons (at 0 mV, 0.34 ± 0.06 nA/pF) possess more total-Kv current density than low CF neurons (at 0 mV, 0.15 ± 0.05 nA/pF; $p < 0.01$). Furthermore, the V1/2 of total Kv current was substantially more hyperpolarized in middle (-16.9 ± 3.7 mV) and high CF (-15.4 ± 3.5 mV) than low CF neurons (1.2 ± 4.3 mV; $p < 0.001$). High CF neurons also possessed more Kv current at rest. Despite variations of voltage-gated sodium and Kv channels along the tonotopic axis, the two currents did not co-vary along the frequency axis. Finally, a small inactivating component of Kv current was present in middle and high but rarely in low CF neurons.

Conclusion

The results of this study indicate that high CF neurons in the NL possess stronger and more active Kv current than low CF neurons. Interestingly, there were few significant differences between middle CF neurons and low or high CF neurons. More work is needed to examine Kv currents in adult chicken and address how Kv currents improve ITD coding across different frequency regions.

363 Group II mGluRs Induce LTD of GABAergic Transmission in Avian Auditory Brainstem Neurons

Zhengquan Tang¹, Yong Lu¹

¹Northeast Ohio Medical University

Background

Since its discovery, chemical long-term depression (LTD), a persistent reduction in synaptic efficiency induced by agonists for transmitter receptors such as metabotropic glutamate receptors (mGluRs), has been extensively studied at excitatory glutamatergic synapses. However, group II mGluR (mGluR II)-induced LTD at inhibitory synapses has not been reported. We previously found that mGluR II agonist DCG-IV suppressed GABAergic IPSCs of chicken cochlear nucleus magnocellularis (NM) neurons, and recovery after washout of the agonist (~20 min) was incomplete. We hypothesized that mGluR II induced LTD of GABAergic transmission in NM neurons.

Methods

Brainstem slices (300 μ m in thickness) were prepared from chick embryos (E17-20). Whole-cell voltage-clamp experiments were performed with an AxoPatch 200B amplifier, at a holding potential of -70 mV, at 34-36 °C.

IPSCs were recorded (once every 30 s, for > 1 h) in the presence of antagonist for AMPA receptors.

Results

DCG-IV (4 μ M) induced a strong initial inhibition followed by LTD of IPSCs, which was blocked by mGluR II antagonist LY341495. DCG-IV application without synaptic stimulation of the GABAergic afferents failed to induce LTD, indicating that presynaptic spike activity was required to form the LTD, and more importantly, DCG-IV was washed out rapidly. Analyses of the failure rate and coefficient variance (CV) of IPSCs revealed presynaptic actions of mGluR II. NMDAR antagonist APV did not change the LTD, indicating that the LTD is NMDAR independent. Blocking adenylyl cyclase and PKA by pre-incubating slices for 1 h in ACSF containing SQ22536 and KT5720, respectively, eliminated the LTD. Surprisingly, blocking mGluR II increased the frequency without affecting the amplitude of mIPSCs, suggesting that ambient glutamate activated mGluR II. A low frequency stimulation (LFS, 1 Hz, for 15 min) protocol that activated both the glutamatergic and GABAergic pathways to NM induced LTD, which was blocked by LY341495, confirming chemical LTD induced by mGluR II activated by synaptically released glutamate and excluding electrical LTD induced by LFS of the GABAergic afferents.

Conclusion

Our finding of mGluR II-induced LTD of GABAergic synapses represents a novel form of long-term plasticity in the central auditory system, and provides evidence supporting the model we previously proposed in which tonic activity of mGluRs regulates the GABAergic transmission in NM, enhancing temporal information processing of sounds. Supported by NIH NIDCD Grant DC008984 to YL.

364 Action Potential Initiation in MSO Principal Neurons Examined with Light-Regulated Voltage-Gated Ion Channel Blockers

Kwang Woo Ko¹, Richard H Kramer², Nace Golding¹
¹Section of Neurobiology and Center for Learning and Memory, Univ. of Texas at Austin, ²Dept. of Molecular and Cell Biology, Univ. of California at Berkeley

Background

The principal neurons of medial superior olive (MSO) compute microsecond temporal differences in arrival time of sounds to the two ears. The axon initial segment (AIS) is thought to be the site of action potential initiation in MSO neurons, but despite its crucial position, the technical difficulty in isolating the effects of voltage-gated ion channels in the AIS from those of the soma and dendrites has precluded a clear understanding of how AIS properties influence the coding of auditory information.

Methods

We examined action potential initiation in gerbil brainstem slices containing the MSO at 35°C. To investigate the specific functional roles played by the AIS, we combined

whole-cell patch recordings and confocal imaging with recently developed photoswitches (e.g. QAQ) which provide a wavelength-dependent block of voltage-gated Na, K, and some Ca channels at specific subcellular locations. Both QAQ (200 μ M) and Alexa 568 (50 μ M) were applied through the pipette via diffusion and allowed to equilibrate in MSO neurons for >10 min., and neuron morphology was visualized. Simulated EPSCs were delivered through the recording electrode both during field illumination at 380 nm and after ion channels were focally blocked by scanning a 488 nm laser over regions of interest. These effects were immediately and fully reversible upon return to 380 nm illumination.

Results

Using intracellular QAQ, we compared the effects of ion channel blockade at either the AIS, soma, or entire cell. In slices from P13~14 gerbils, 488 nm illumination of the axon up to 50 μ m from the soma induced either a complete failure in action potential initiation or an increase in voltage threshold (-47 to -39 mV, $p=0.0002$, $n=6$). By contrast, somatic block provided a far smaller increase in threshold (-47 to -45 mV, $p=0.015$; $n=6$). Similar results were obtained in MSO neurons from gerbils >P18. These results are consistent with the primary effects of QAQ on the voltage-gated Na channels underlying the action potential.

Conclusion

We find that action potential threshold is established primarily by Na channels in the AIS, with surprisingly little contribution from somatodendritic Na channels. Thus spike initiation in the AIS appears electrically isolated from the influence of Na channels in the soma and dendrites.

365 Stimulus Specific Adaptation in the Auditory Thalamus of Awake Rats

Ben Richardson¹, Kenneth Hancock^{2,3}, Donald Caspary¹
¹Southern Illinois University School of Medicine, Springfield, IL, ²Eaton-Peabody Laboratories, Massachusetts Eye and Ear Infirmary, Boston, MA, ³Department of Otolaryngology and Laryngology, Harvard Medical School, Boston, MA

Background

Novelty detection by single neurons in the mammalian auditory system has been suggested to be a real-time filtering or gating mechanism of acoustic information. Selective adaptation of a neuron's response to repetitive/high-probability stimuli, but not rare/low-probability stimuli in a given domain is known as stimulus specific adaptation (SSA). Quantification of SSA using specific indices and stimulus protocols has allowed for the quantification of a single neurons' ability to respond selectively to novel stimuli. As defined by these metrics, SSA occurs in the inferior colliculus, medial geniculate body (MGB) and auditory cortex of anesthetized rodents. However, only auditory cortex has been examined and found to display SSA in awake animals.

Methods

Individually-advanceable tetrode microdrives were implanted to record single unit responses in the auditory thalamus (MGB) of awake Fischer Brown Norway rats. To determine the presence of SSA in MGB of awake rats, two stimulus paradigms were used to evoke SSA: the oddball paradigm and isointensity random and non-random frequency function pairs.

Results

Single units in the MGB of awake Fischer Brown Norway rats display SSA in response to two different paradigms. SSA was stronger in the non-lemniscal regions of the MGB and was most dramatic at lower intensities where 27 of 57 (47%) young adult single units displayed SSA. However, when SSA level, intensity and time course were compared to SSA responses of aged MGB single units, there were no significant age-related differences.

Conclusion

These data provide a description of SSA in the MGB of awake rats using two different stimulus SSA-inducing paradigms. Findings indicate that SSA is not dependent on arousal level nor the anesthetized state, but is a common response in the MGB of awake rats. SSA did not appear to be overtly altered in the aged auditory thalamus of awake rats. Determining the relevance of SSA to acoustic scene coding in a whole animal, what region in the auditory neuraxis and what neurotransmitters, receptors and membrane conductances are responsible for the generation of SSA remain as primary goals in the study of SSA.

366 Stimulus-Specific Adaptation in Real and Model Neurons

Israel Nelken¹, Flora Antunes¹, Itai Hershenhoren¹, Leila Khouri¹, Tohar Yarden¹, Amit Yaron¹

¹Hebrew University

Background

Stimulus-specific adaptation (SSA) is the reduction in the responses to a repeated stimulus that is not, or only partially, generalized to other stimuli. SSA is extremely sensitive, showing frequency hyperacuity, and being induced by frozen tokens of white noise 'tone clouds'. However, the mechanisms underlying SSA are still unclear. Along the non-lemniscal pathway, SSA is found as early as the inferior colliculus (IC), but along the lemniscal pathway, SSA first appears in primary auditory cortex (A1). Two different mechanisms may therefore underlie the generation of SSA in the lemniscal and the non-lemniscal pathway.

Methods

We studied two possible models for the generation of SSA. The first model is feed-forward, based on adaptation of excitation in narrow frequency channels that impinge on a single output neuron. The second is a recurrent network model, based on the tendency of networks with depressing synapses to generate 'population spikes'. Population spikes are more likely to occur for rare than for common

stimuli, giving rise to SSA. We generated predictions for responses to oddball and control sequences from both models. We compared the responses predicted by these models to responses recorded extracellularly from the IC, and intracellularly and extracellularly from auditory cortex of halothane-anesthetized rats.

Results

The feed-forward model predicts responses to a deviant tone to be smaller than responses to the same tone occurring with equal probability among many others ("deviant among many standards"). In IC, the feed-forward model fits nicely the data: neurons showing strong SSA are widely-tuned, as expected from the integration of many narrowly tuned inputs; and the responses to deviants in oddball sequences are indeed smaller than the responses to deviants among many standards. In contrast, in cortex, the predictions of the feed-forward model fail to a large extent: responses to deviants are larger than predicted, and are essentially equivalent to the responses to deviants among many standards, both for membrane potential responses and for spiking responses. The network model, on the other hand, reproduces the cortical results.

Conclusion

SSA in IC and in cortex seem to be due to different mechanisms. While in IC, widely-tuned neurons show SSA that is compatible with feed-forward adaptation of excitation in narrow frequency channels, A1 neurons do not conform to this model, but seem to be reasonably well described by a model that relies on network dynamics for the generation of SSA.

367 A Functional Near-Infrared Spectroscopy Study (fNIRS) of the McGurk Effect in Normal-Hearing Adults

Carly Anderson^{1,2}, Rebecca Dewey^{1,2}, Douglas Hartley^{2,3}

¹NIHR Nottingham Hearing Biomedical Research Unit,

²Division of Otorhinolaryngology, University of Nottingham,

³MRC Institute of Hearing Research

Background

Human speech perception is multimodal in nature, involving cross-modal binding of auditory and visual input. The McGurk effect can be elicited when incongruent audio-visual information, such as visual "ga" and audio "ba", are integrated and result in a novel fused percept that differs from both the audio and visual percept, such as "da". Functional MRI studies have correlated greater cortical responses in the auditory cortex with perception of the McGurk effect. In this study we used fNIRS to measure hemodynamic responses in the auditory cortex of normal-hearing adults to a stimulus designed to elicit the McGurk effect (McGurk stimuli) and stimuli that does not elicit the McGurk effect (non-McGurk stimuli).

Methods

Behavioural tests were performed in order to establish the efficacy of the McGurk stimuli. Adult normal-hearing participants (n=18, female n=12) were presented with the McGurk stimuli (audio "ba" with visual "ga") and were

asked to report the syllable that they perceived in an open-choice response task. In a separate session, we assessed fNIRS responses to McGurk and non-McGurk stimuli. Non-McGurk stimuli included audio alone “ba”, visual alone “ga”, and audio “ga” with visual “ba”.

During the fNIRS experiment, hemodynamic responses were measured using 3x3 arrays of optodes (Hitachi-ETG4000 system) placed bilaterally over the temporal lobes. All stimuli were presented five times in a pseudorandom order and interleaved with a baseline condition.

Results

The behavioural response task revealed that in 78% of subjects the McGurk stimuli elicited a novel fused percept that neither matched the audio nor the visual input. Fewer subjects reported a percept that matched the auditory component of the McGurk stimulus (17%) or the visual component (5%). Thus far we have completed fNIRS measurements in ten participants. Ongoing analysis will compare hemodynamic responses in the auditory cortex to the McGurk and non-McGurk stimuli.

Conclusion

The 78% rate of susceptibility to the McGurk effect is consistent with previously reported rates. Therefore our findings suggest that the present McGurk stimulus is an effective stimulus for eliciting the McGurk Effect in normal-hearing adults. Our future research aims to acquire fNIRS data in a cohort of cochlear implanted adult subjects. Accordingly, we aim to compare hemodynamic responses to McGurk stimuli in the auditory cortex of normal-hearing and cochlear implanted adult populations.

This work is supported by the University of Nottingham and the NIHR.

368 Plastic Changes of the Auditory Core Fields After Behavioral Conditioning to a Natural Sound

Ryouta Numata¹, Hisayuki Ojima², Tomohiro Ishida¹, Masato Taira², Junsei Horikawa¹

¹Graduate school of Computer Science and Engineering, Toyohashi University of Technology, ²Graduate school of Medical and Dental Sciences, Tokyo Medical and Dental University

Background

Reversing in time is sometimes used to elucidate whether neuron's responsiveness to a given complex sound is specific or not. In electrophysiological recordings made from auditory cortex (AC) of untrained animals, some neurons show dissociated (different) and others show associated (similar) responses when pairs of natural sound and its time-reversed version (REV) are used as stimuli. However, it is not known whether the same response properties are still preserved in conditioned cortex. There may be the possibility that the conditioned stimulus would change the neuronal network and that the changed network might facilitate or suppress activation evoked by its REV. We compared the activation properties evoked by

such a stimulus pair between naive and fully conditioned AC.

Methods

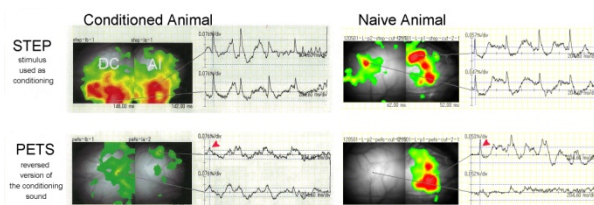
Guinea pigs (Hartley, 300 to 500g) were operant-conditioned to a digitized footstep sound (FSS) with food as reinforcer, resulting in 2 weeks in the induction of distinctive response behaviors in more than 95% trials. These included quick head swaying and/or circling locomotion initiated soon after the onset of conditioning sound. AC including core fields (CORE) of both untrained naive and trained groups was subject to voltage-sensitive dye optical imaging under ketamine anesthesia.

Results

Animals conditioned to the FSS did not respond behaviorally to its REV (rFSS) in most trials. Naive animals did not respond behaviorally to either stimuli at all. Optically-measured neuronal activity was evoked across the CORE to either stimulus type whether animals had been trained or untrained, but its extent and strength were varied between the stimulus types and also between the training experience. A remarkable contrast in response pattern to FSS and rFSS was found in the conditioned cortex, with a strong activation to FSS and a weak activation to rFSS. On the contrary, in the naive animals, the strong activation was evoked by the FSS, like in conditioned animals, but the activation evoked by rFSS was relatively strong, being generally greater than that evoked in the conditioned cortex.

Conclusion

Although neuronal mechanisms underlying this asymmetry in the response contrast to the different stimuli between the conditioned and non-conditioned cortex are currently unknown. One plausible explanation would be that a potential change in neuronal network is induced by the sound used for conditioning (FSS) and that this plastic change might not permit the sound with the opposite temporal structure to activate the cortex or subcortical stations. Supported by KAKENHI to H.O. (no.22500368).



369 Task-Dependent Activations of Human Auditory Cortex During Pitch and Spatial Tasks

Teemu Rinne^{1,2}, Noora Ovaska¹, Suvi Talja¹

¹Institute of Behavioural Sciences, University of Helsinki, Finland, ²Advanced Magnetic Imaging Centre, Aalto University School of Science, Finland

Background

It is generally accepted that spatial and nonspatial auditory information is processed in separate streams in human

auditory cortex. However, our previous studies have shown that activations during spatial discrimination and spatial memory tasks are highly similar to those observed during pitch discrimination and pitch memory tasks (Rinne et al, 2009, 2012). In the present study, we systematically compared fMRI activations during discrimination and memory tasks performed on sounds varying in both pitch and location. In different conditions, subjects performed the tasks on sounds in which both features varied or only the task-relevant feature varied and the task-irrelevant feature was absent (not salient). To observe pure task effects, subjects were also instructed to perform the discrimination tasks on sounds in which both features were absent. In addition, the different stimulus conditions were presented during a visual task. We expected that this paradigm would reveal task-dependent and stimulus-dependent activations associated with spatial and nonspatial processing.

Methods

In different blocks, subjects (N = 22) performed pitch/spatial discrimination, pitch/spatial memory or visual tasks. Auditory stimuli were noise bursts (duration 200 ms, mean rate 0.9 s) consisting of two 90-ms parts separated by a 20-ms gap. Sounds varied in pitch (200–1400 Hz; IRN), location (-120–120°; HRTF), and pitch/location salience.

Results

Initial fMRI data analysis showed that the auditory tasks (discrimination or memory) modulated activations in supratemporal areas extending from the anterior insula to IPL. As in our previous studies, direct comparisons of the two types of auditory tasks revealed stronger activations in temporal and insular areas during discrimination than memory tasks, while areas in the IPL were more activated during memory than discrimination tasks. Further, pitch tasks were associated with stronger activations than location tasks in the lateral STG/STS, while location tasks enhanced activations in areas of the IPL. During visual tasks, pitch-varying sounds enhanced activations in the lateral STG and HG, while location-varying sounds enhanced activations in more medial areas in the PT.

Conclusion

Activation differences between discrimination and memory tasks were strong and widespread, whereas differences between pitch and location tasks and between visual task blocks with pitch-varying or location-varying sounds were less pronounced. These results demonstrate that activations to spatial and nonspatial sounds strongly depend on the behavioral task and that these activations cannot be explained only by stimulus-dependent processing of physical features of sounds.

370 Beyond the Auditory Scene: Non-Auditory Predator Cues Modulate Auditory Responses of Single Neurons in the Mouse Amygdala

Jasmine Grimsley¹, Emily Hazlett¹, Sharad Shanbhag¹, Jeffrey Wenstrup¹

¹Northeast Ohio Medical University (NEOMED)

Background

Female mice emit a low frequency harmonic (LFH) call in two different contexts, during mating and in response to physical threat or pain. Male mice respond differently to the LFH call in the presence of predator odor or female urine; it is aversive in the presence of cat fur but not in the presence of female urine. The basolateral amygdala (BLA) has auditory inputs from both auditory thalamus and cortex and has been shown to code the valence of social vocalizations. We tested whether there were neural correlates of the behavioral valence change in the responses of BLA units.

Methods

Local field potentials (LFPs) and spiking activity were recorded simultaneously from the BLA of 10 awake, freely moving male mice in response to the LFH call and broadband noise (BBN). Signals were transmitted wirelessly from custom multi-electrode implants using a 16-channel wireless headstage (TBSI Technologies). Responses to sounds were recorded from animals in 4 contexts: clean chamber, neutral condition (cotton wool stimulus), cat fur, and female mouse urine. Responsiveness, for LFPs and spikes, was assessed using t-tests comparing background activity to the post stimulus activity. A rate modulation index (RMI) was computed during each context to quantify the spike discharge of responsive neurons.

Results

LFPs showed significant auditory-evoked elements for both BBN and the LFH. Responses were typically significantly modulated by both cat fur and female urine and often by the cotton wool bud. Thirty of 64 single neurons responded to the sounds; both excitatory and inhibitory responses were common. The RMI of responses to BBN and LFH changed with acoustic context. The mean absolute RMI value did not change in the presence of cat fur, suggesting that the sounds were equally detectable in each context. However, for individual neurons, the spike discharge patterns changed. The RMI in response to the LFH call increased in the presence of cat fur (Wilcoxon rank, $p=0.004$); 14 of 30 neurons switched from inhibition or no response to excitation, while 3 of 30 neurons increased their excitation. The RMI of BBN responses decreased in the presence of cat fur (Wilcoxon rank, $p=0.025$), representing a generalized shift to suppression (15 of 30 neurons) or to greater suppression (5 of 30 neurons).

Conclusion

Auditory responses in the mouse BLA, to both BBN and the LFH call, are differently modulated by non-auditory

contextual cues. Supported by NIDCD grant R01 DC 00937.

371 Retention of Auditory Memory During Breaks in Perceptual Training

David F Little¹, Beverly A Wright¹

¹*Northwestern University, Evanston, IL, USA*

Background

What circumstances are required for auditory perceptual learning to occur? One circumstance, indicated by recent findings, is that learning across days requires a sufficient amount of training per day. This suggests information is accumulating over the course of practice and must reach some learning threshold to enable across-day improvement. Interestingly, the memory of this accumulated information appears to decay, because a break in the midst of otherwise sufficient practice can disrupt learning. Here we asked whether this memory begins to decay immediately after practice ceases, as for declarative memory, or instead is retained for some time before decaying. We did so by comparing the ability of two mathematical models, with either immediate or delayed decay, to predict previously reported human learning data.

Methods

Four training groups practiced frequency discrimination (standard: two 15ms 1kHz tones separated by 100ms) for 6-8 days. Each day, groups practiced 360 trials (short-training), 900 trials (long-training), 720 trials with a 30-minute break after 360 trials (30' break), or 720 trials with a 6-minute break after every 120 trials (5x6' breaks). A control group only participated in pre- and posttests.

We tested immediate- and delayed-decay models, each with 64,000 parameter settings, by Monte Carlo simulation. For each model and parameter setting, we determined how well the amount of decay corresponded with the amount each group learned.

Results

Only the long-training ($p < 0.001$) and 5x6' breaks ($p = 0.020$) groups showed evidence of learning; the other groups did not (short-training, $p = 0.296$ and 30' break, $p = 0.423$; ANCOVA vs. controls with pretest and day as covariates).

With their best fitting parameters, both models predicted which groups learned and which did not. However, the average performance across all parameters was better for the delayed- than the immediate-decay model (Bayes Factor 7.23). The estimated delay of decay was ~5 minutes.

Conclusion

Auditory perceptual learning appears to require sufficient training per day for learning to occur across days. Our model evaluations suggest that information accumulated during the course of this training is retained in memory for ~5 minutes in the absence of practice. This memory appears to be distinct from declarative memory where

decay seems to begin immediately, and from echoic or working memory, which last for less time. The limitations of this memory store place constraints on perceptual training schemes.

Support: NIH/NIDCD-DC04453, NSF/DGE-0948017.

372 Attentional Mechanisms for Recognizing Acoustic Scene

Kailash Patil¹, Mounya Elhilali¹

¹*Johns Hopkins University*

Background

Humans exhibit a remarkable ability at processing complex acoustic information from their surroundings and identifying the nature of the environment where they are. This ability is further heightened when guided to detect particular target sounds, even in presence of distracting sounds or ambient noises.

Methods

In the present study, we explore the neural underpinnings of auditory scene recognition in a biomimetic computational model. We exploit the detailed multi-resolution spectro-temporal analysis performed by the mammalian auditory cortex to perform an intricate mapping of sound events present in different acoustic scenes. This framework is further extended by exploring the role of task-driven attention in modulating sensory processing of acoustic information; and ultimately enhancing the ability to detect target sounds of interest.

Results

We demonstrate the ability of the system to outperform previous systems at the task of acoustic scene recognition. We further show the adaptability of the system to recognize particular targets in a noisy environment.

Conclusion

We discuss the relevance of our results in tasks of auditory scene identification and target sound recognition; as well as the role of cortical processes and top-down attentional modulation in sound processing and perception of complex acoustic scenes.

373 Cortical Representations of Music in Human Listeners

Elizabeth Camenga¹, Katya Dombrowski², Benjamin Walsh³, Francisco Cervantes Constantino³, Krishna Puvvada³, Marisel Villafañe-Delgado³, Jonathan Z. Simon³

¹*University of Wisconsin La Crosse*, ²*Princeton University*,

³*University of Maryland*

Background

Cortical neural representations of music in humans are investigated using analysis techniques already demonstrated for analogous cortical representations of speech (Ding and Simon, PNAS 109(29), 11854-11859).

Methods

Using magnetoencephalography (MEG), we present and analyze neural responses to spectrally and rhythmically diverse samples of music. The neural responses are characterized by a temporal response function (TRF) generated via reverse-correlation with the stimuli.

Results

Correlations between actual and predicted responses to musical stimuli are comparable to those obtained using speech stimuli, but unlike the speech case, there is substantial diversity in TRF temporal profiles. The TRFs fall into at least two categories based on the polarity of the earliest peak. Critically, pairwise correlations of TRFs between subjects for each stimulus are generally higher than pairwise correlations of TRFs between stimuli, indicating that the encoding mechanism is robust across subjects.

Conclusion

This suggests that the underlying mechanism for encoding music in the brain is feature-dependent, and may specifically depend on the rhythmicity of the music.

374 A Neuromechanistic Model of Auditory Streaming

John Rinzel¹, Ernest Montbrio²

¹New York University, ²Universitat Pompeu Fabra.

Barcelona

Background

Interleaved tone sequences (AB_AB_... and ABA_ABA_...) are commonly used to study auditory streaming. For ranges of A-tone and B-tone frequency differences (DF) and presentation rate (PR) stimuli are ambiguous, leading to different percepts, integration or segregation with bistability and alternations between integration and segregation during long presentations. Neurophysiological results for A1 support a two-dimensional feature mapping (tonotopy and periodotopy) and reveal neuronal dynamics consistent with integration-segregation switching. While phenomenological models for perceptual bistability exist, the development of neuronally-based models is immature.

Methods

We have developed idealized firing-rate models with a 3-population recurrent network architecture for the 'percept formation' stage (see Figure). Inputs to the network embody the tonotopic and periodotopic representation in A1, e.g. population A responds most to the A-tone while population AB is most responsive to frequencies midway between A-tone and B-tone frequencies. If A and B are alternately activated by the interleaved sequence with little activity in AB (say for large DF) we say that segregation is being perceived. Integration occurs when AB is dominant (or equi-active with A and B), say for small DF. Activation is partially retained in the silent gaps between tones by recurrent excitation with slow, NMDA-like, facilitatory synapses. Competition for percept dominance occurs by lateral inhibition and slow negative feedback from firing-

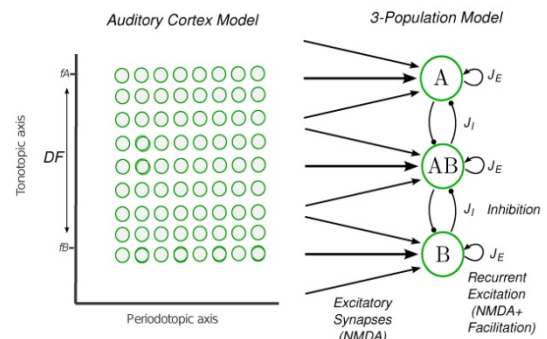
rate adaptation underlies integration-segregation alternations.

Results

First, we show that by implementing tonotopy and periodotopy in an A1 model we can account for: 1) experimentally observed A1 neuronal responses to interleaved A and B tones and 2) differential suppression phenomenon i.e., frequency selectivity of A1 neurons improves with repetition of AB sequences (Fishman et al, 2001). For a range of input and coupling parameter values, the model shows coexistence between the integration and segregation states – bistability, consistent with stimulus ambiguity. When adaptation is strong enough, the model produces regular transitions between these two coexisting states. The percent of time that integration or segregation is dominant depends on the input values.

Conclusion

Our model provides a neuronally-based rationale for specifying inputs to a percept formation network, enabling us to model the effects of changing DF and PR. While bistability has been modeled for the visual case (say, binocular rivalry) inputs are typically constant in time. The dynamical aspects of the interleaved auditory stimuli (with silent gaps between tones) present new challenges for modeling bistable perception that we have overcome by utilizing synaptic dynamics (NMDA-like slow decay and facilitation) to avoid re-setting activity variables between tones.



375 Receptive Field Changes in Primary and Secondary Auditory Cortex as Correlates of Streaming in Behaving Ferrets

Yanbo Xu¹, Pingbo Yin¹, Shihab Shamma^{1,2}

¹Neural Systems Lab., The Institute for Systems Research, University of Maryland, ²Department of ECE, University of Maryland

Background

Alternating two-tone sequences are usually perceived as two streams when the tones are far apart, while synchronous two-tone sequences evoke a unified single stream percept regardless of their separation. Consequently, it was hypothesized that the receptive fields (RFs) in auditory cortex would be different when listening

to these two types of sequences, with the latter inducing broadly tuned receptive fields compared to the former.

Methods

Ferrets were trained to listen attentively to the two-tone sequences until they transitioned to a random sequence of tones, at which point they were to approach a spout for a water reward. Responses were recorded in the primary auditory cortex (A1), and also in an adjacent secondary auditory field on the posterior ectosylvian gyrus (PEG) during behavior and in the passive listening. For the tone sequences, one tone (B-stream) was usually fixed at a neuron's BF, while the other tone (A-stream) varied between 0.25 to 2 octaves away from the first tone in different trials. The final random sequence allowed us to measure the neuron's RFs at the end of the two-tone sequences.

Results

In A1, both two-tone sequences evoked phase-locked responses that rapidly adapted after the onset of the trial, reaching a steady state level after 3-4 tones. When the animal was attentively listening, however, the responses to the two types of sequences diverged considerably. The alternating tone responses became more suppressed relative to the passive listening. By contrast, responses to the synchronous sequence were enhanced. This difference in responses was also evident in the RFs of the neurons at the end of each sequence. Since the alternating and synchronous trials were randomly presented, the results suggest that these RFs differences built up rapidly within each trial that typically lasted between 1-3 seconds. Preliminary responses from the PEG reveal a somewhat different picture, with weaker phase-locking and far noisier RFs, making similar response measurements to the A1 very difficult.

Conclusion

In summary, we believe that response changes such as those in A1 are mediated by rapid plasticity in the connectivity among the responding neurons. Specifically, we hypothesize that during behavior, stimulating neurons incoherently induces mutually suppressive connectivity, while the opposite is true for coherent stimulation. These patterns of RFs change are consistent with the idea that stimulus coherence is the key in inducing the streaming percepts and the organization of complex auditory scenes.

376 Task-Dependent Spatial Responses in Auditory Cortex of Common Marmosets

Evan Remington¹, Xiaoqin Wang¹

¹Johns Hopkins University School of Medicine

Background

Auditory cortex is essential for behaviors involving sound localization in mammals. Although spatial processing in auditory cortex has been extensively studied in passive subjects, there are few studies of spatial processing under behaving conditions. In this study, we investigated how representation of space by auditory cortex neurons is

modulated as specific regions of space become behaviorally relevant.

Methods

We recorded single-unit responses in auditory cortex of marmosets (*Callithrix jacchus*), an arboreal New World monkey, while they performed a spatial discrimination task with either a contralateral or ipsilateral stimulus bias. We asked whether any observed changes in response properties would depend on either the spatial parameters of the task, or the spatial tuning properties of the neurons themselves.

Results

We found a population of neurons for which firing rates to target locations recorded during task engagement were increased when compared to those recorded during passive listening. There was also a smaller increase in firing rates to target locations in hit trials compared to miss trials. A subset of neurons showing increased firing rates to targets also had increased firing rates to background (non-target) locations. Neurons which showed increased firing in response to one target location tended to have increased firing rates to other target locations as well, and neurons with increased firing rates in the one behavior condition (e.g. contralateral stimulus bias) tended to also have increased firing rates in the opposite condition. Furthermore, neurons with increased firing rates included those preferring both contralateral and ipsilateral locations in the passive condition.

Conclusion

Taken together, these results showed that responses of a subset of neurons in auditory cortex are modulated by spatial tasks.

377 Laminar Recordings of Task-Related Receptive Field Plasticity with Multisite Depth Electrodes in the Primary Auditory Cortex (A1) of the Behaving Ferret

Diego Elgueda¹, Michael Locastro¹, Bernhard Englitz^{1,2}, Mounya Elhilali³, Shihab Shamma^{1,2}, Jonathan Fritz¹

¹Neural Systems Lab, Institute for Systems Research, University of Maryland, College Park, MD, USA, ²Auditory Behavior & Computational Neuroscience Lab, École Normale Supérieure, Paris, France, ³Department of Electrical and Computer Engineering, Johns Hopkins University, Baltimore, MD, USA

Background

Previous studies have shown task-related receptive field plasticity (RFP) in A1 neurons (Fritz et al., 2003) during performance of simple spectral discrimination tasks. Two open questions were: (1) whether adaptive RFP changes also occurred during performance of temporal discrimination tasks, (2) whether such RFPs were equiprobable for A1 neurons in all cortical layers, or located preferentially in certain layers or cell types.

Methods

We trained ten ferrets to perform two auditory discrimination tasks in which they learned to discriminate between broad-band rippled noise stimuli and narrow-band tones (spectral task), and/or between low and high-rate click trains (temporal task). The basic behavioral paradigm for both tasks was conditioned avoidance (Fritz et al., 2003). We recorded from behaving head-fixed ferrets, using simultaneous multichannel recordings, and demonstrated plasticity at a single-unit and population level for temporal tasks. To explore the question of RFP laminar specificity, we recorded from A1 in three trained ferrets during behavior using near-perpendicular penetrations with multisite depth electrodes that allowed for simultaneous recording from all cortical layers, and comparison of RFP in each layer. We reconstructed the laminar location by using CSD (current source density) analysis on the LFP from all sites. We compared the STRFs (spectrotemporal receptive fields) recorded during a pre-behavior quiescent state and then during active discrimination behavior in all neurons.

Results

Many neurons showed STRF plasticity along the time axis during performance of temporal tasks. To help clarify whether these changes were specific for temporal tasks, or whether they might also occur in spectral tasks, we recorded from A1 neurons under both task conditions. We found STRFs throughout the depth of the electrode recording sites, and ~65% of all STRFs showed task-related plasticity for either spectral and/or temporal tasks. Our preliminary data suggests greater STRF plasticity occurs in supragranular layers. Some plastic cells showed RFP for only one task condition. About 60% of plastic neurons showed RFP for *both* tasks, however the effects were often different. We also observed task-related changes in neuronal responses to task stimuli that were not captured by the STRF which were found in all layers.

Conclusion

A1 neurons demonstrate remarkable, task-related RFP for both spectral and temporal tasks. Our results give first insights into the laminar location of this type of attention-driven RFP, and also indicate that the STRF adapts to task conditions along both the time and frequency axis.

378 Comparison of Neuronal Responses in Ferret Frontal Cortex During Positive and Negative Versions of an Auditory Long-Term Pitch Memory Task

Pingbo Yin¹, Kayla Kahn¹, Shihab Shamma¹, Jonathan Fritz¹

¹ISR, University of Maryland College Park

Background

An earlier study on ferret frontal cortex (FC) revealed persistent neuronal responses to auditory target stimuli over a time course of minutes to hours (Fritz et al., 2010) following performance of auditory discrimination tasks. In order to explore the role of the FC in auditory long-term

memory, we developed a new auditory task that requires information retrieval from long-term pitch memory.

Methods

Six ferrets were trained to classify single tonebursts into three frequency ranges (Low, Middle, High). Three animals were trained on a positive reinforcement (PR) task version, in which they learned to lick a waterspout for reward (Go-response) when the toneburst fell in the middle frequency range, and to stop licking the waterspout after tonebursts in either the low or high frequency range (NoGo response). In the PR task, licking during Nogo stimuli lead to a timeout. Three additional ferrets were trained on a conditioned avoidance (CA) version of the task, in which they received mild shock if they licked to tones in the middle range (Nogo stimuli), but could lick freely through the tones in both low and high range (Go stimuli). Each trial simply consisted of the presentation of a single toneburst, and the animal's response. Each daily session consisted of 100-200 trials. After animals were trained, they were implanted with headposts to secure head position during task performance. We recorded chronically from the FC of behaving, headfixed ferrets, using an independently-moveable multiple electrode system.

Results

All ferrets learned the basic discrimination, with either training paradigm (PR or CA), in an average of one month. Moreover, although toneburst stimuli in the initial training set had wide frequency spacing, animals generalized and readily transferred to a denser stimulus set with new frequencies, after learning the original task. Preliminary neurophysiological results from the PR task indicate the presence of two neuronal classes in FC that were strongly activated during task performance and selectively preferred tonal frequencies that corresponded to either Go stimuli or Nogo toneburst stimuli (Yin et al 2012). We will compare neuronal response from FC during the CA version of the task to those obtained in FC of animals trained on the PR version of the task.

Conclusion

These preliminary results provide insights into how the FC encodes, represents, classifies and retrieves the associative meaning of sensory stimuli during performance of an auditory long-term memory pitch task under different valence conditions.

379 Human Cortical Auditory Evoked Offset and Onset Response Sensitivity to Signals in Noise

Lucas Baltzell^{1,2}, Curtis Billings^{1,2}, Frederick Gallun^{1,2}

¹National Center for Rehabilitative Auditory Research (NCRAR), Portland VA Medical Center, ²Department of Otolaryngology/Head & Neck Surgery, Oregon Health & Science University

Background

Cortical auditory evoked potentials (CAEPs) can be elicited by both the onset and the offset of an auditory stimulus.

However, in both the clinical and research literature, offset responses have been both underreported and understudied in comparison to onset responses. Furthermore, while single unit animal studies have demonstrated important differences in the specific characteristics of the neural populations responsible for the onset and offset response, far-field studies (EEG and MEG) have tended to suggest that onset and offset responses are not physiologically independent.

The gap in resolution between single unit and far-field recordings is significant enough that, despite certain observable differences in the characteristics of the neural populations that respond to onsets and offsets, the usefulness of offset CAEPs in the neurophysiologic characterization of auditory processing and processing disorders remains to be convincingly demonstrated. The goal of studying offset responses in addition to onset responses then, is to determine how and when offset responses differ from onset responses such that additional information about the encoding of the stimulus may be obtained.

We report that offset responses are sensitive to changes in absolute signal level while SNR (signal-to-noise ratio) is held constant.

Methods

Billings et al. (2007): Responses were recorded from 13 young normal-hearing subjects, who were presented a 1-kHz tone (757 ms) at 7 signal levels (range: 30 to 90 dB SPL).

Billings et al. (2009): Responses were recorded from 15 young normal-hearing subjects, who were presented a 1-kHz tone (757 ms) at 2 signal levels (60 and 75 dB SPL).

Results

We find that, while peak latency and amplitude of onset responses are not sensitive to changes in absolute signal level if signal-to-noise ratio is held constant, offset latencies and amplitudes are, while also being sensitive to changes in SNR.

Conclusion

Cortical Auditory Evoked Offset responses are not simply less salient versions of onset responses, but can be measurably different even in far field recordings. In the present findings, offset responses indicate that the cortex is sensitive to absolute signal level cues in the encoding of signals in noise, a sensitivity not apparent in onset responses.

[Research was supported by VA/RR&D (C6971M) and NIH/NIDCD (R03-DC010914)]

380 Bold Response in the Auditory Cortex of Non-Human Primates Matches Pitch Percept Across Different Repetition Rates

Simon Baumann¹, Sukhbinder Kumar¹, Li Sun¹, Alexander Thiele¹, Timothy D Griffiths¹

¹Newcastle University

Background

Pitch is a fundamental percept with a complex relationship to basic acoustic stimulus properties such as frequency composition and temporal regularity of sounds. Thus a neuronal correlate of pitch is best identified by looking for neural responses that match the varying pitch percept to changing stimulus attributes.

Methods

Here we measured the BOLD response across the lower and upper limit of the pitch percept to regular interval noise (RIN) in the auditory brain upstream from the inferior colliculus (IC) of two rhesus macaques. The data were recorded in a Bruker 4.7 T vertical scanner during fixation of a visual stimulus. In three different experiments we presented RIN stimuli at repetition rates from 8 Hz to 2048 Hz and we used fixed-amplitude random-phase broadband noise as control.

Results

In both animals, widespread areas in the auditory cortex, particularly in lateral and anterior core and belt, showed a progressive increase in the BOLD response to increasing repetition rates beginning at the lower limit of pitch in humans of about 30 Hz. This effect was most pronounced bilaterally in a region between the core areas A1 and R and the adjacent belt areas. The response increase levelled off in a plateau between 256-512 Hz. Responses in the IC and the medial geniculate body (MGB), while showing stronger response to repetitive sounds than noise, did not show a modulation of the response across the lower pitch level. At 1024 Hz and above, coinciding with the upper limit of pitch to RIN in humans, all areas in the auditory cortex, MGB and IC showed a progressive decay in the BOLD response.

Conclusion

Macaques show a response profile in the auditory cortex that matches the pitch percept across the lower and upper human pitch limit. Behavioural tests in macaques suggest a similar lower pitch limit than humans [1]. The effect is consistently strongest in an area that has previously been highlighted as a "pitch center" in marmosets [2], supporting its role a candidate for a neural correlate of pitch. These findings are in line with results from single unit recordings in macaques [3]. Responses in the IC and the MGB across the lower pitch limit do not match perception, suggesting that the pitch percept arises at the level of the cortex.

[1] Joly O et al. ARO (2013).

[2] Bendor D, Wang X. Nature 436, 1161-1165 (2005).

[3] Kikuchi Y et al. ARO (2013).

381 A Modeled Auditory Evoked Potential Predicts Attentional Modulation of Averaged and Single Trial EEG Signals

Inyong Choi¹, Barbara G. Shinn-Cunningham¹
¹Boston University

Background

Human listeners easily can focus attention on a target sound within a complex auditory scene, though the underlying mechanisms of auditory attention are still largely unknown. Attention is known to modulate the cortical representation of the auditory scene, an effect that alters auditory evoked potentials (AEPs). These AEPs consist of different components with different latencies originating from different brain locations. Observing how attention modulates different AEP components can help us understand which neuronal centers have roles in selective attention.

Methods

Three competing isochronous tone sequences were presented (left, center, and right). Each stream had a different rhythm. AEPs were measured while listeners selectively directed attention to either the left or right competing stream.

The AEPs from different attentional conditions were compared. A model based on a superposition of Gaussian mixture functions convolved with a train of pulses with a pulse at each stimulus onset was used to generate predicted AEPs. By finding the model parameters that achieve the best match with measured AEPs, we derive a quantitative measure of attentional modulation.

Further, we analyzed single trial EEG results to predict which stream was attended on that trial, based on template-matching pattern classification. Different AEP components were incorporated into the templates, in order to compare which components were most useful in determining which stream a listener attended.

Results

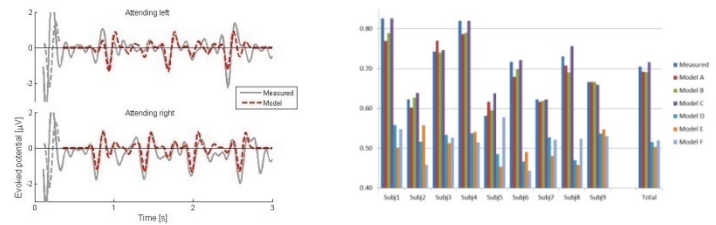
Measured AEPs showed strong attentional modulation. The best fitting models attenuate AEP components from the ignored streams by 20dB, while evoking strong P1, N1, and P2 components at onset events in the attended stream. The highest correlation between the measured AEPs and modeled was 0.80, averaged over mid-frontal 22 channels.

P1 and P2 components were important for predicting the averaged AEP shapes, but had no influence on single-trial classification of which direction a listener was attending. In contrast, the model containing only the N1 component ("Model C") achieved the best classification accuracy: 72%, for a 3-second-long single trial.

Conclusion

Attention strongly modulates the cortical representation of a complex auditory scene. This modulation causes the AEPs in response to an ignored stream to be attenuated by 20dB, on average. The N1 component is the strongest marker for predicting the direction of a listener's attention from a single trial. The proposed modeling framework can

be a useful tool for investigating mechanisms underlying auditory attention, and can provide a feature basis for a brain-computer interface paradigm using EEG and auditory stimuli.



382 Late Auditory Evoked Potentials in Responses to Informational Masking Stimuli

Matthew Richardson^{1,2}, Peter Bremen^{2,3}, Carol Q. Pham^{1,2}, John C. Middlebrooks^{2,3}, Fang-Gang Zeng^{1,2}, Myles Mc Laughlin^{1,2}

¹Hearing and Speech Laboratory, University of California Irvine, ²Center for Hearing Research, ³Dept. of Otolaryngology, University of California Irvine

Background

The auditory system creates a neuronal representation of the acoustic world based on cues present at the listener's ears. Parsing individual sources becomes challenging when multiple sources are active. The current study aims to understand the neuronal mechanisms underlying this process known as auditory scene analysis (ASA).

Here, we measured late auditory evoked potentials (LAEPs) in response to complex signal-in-masker stimuli designed to elicit informational masking (IM). Published psychophysical data show large inter-subject variability in response to these IM stimuli. Our aim is to develop a LAEP-based paradigm that could test whether this large variability is detectable in neuronal responses.

Methods

Stimuli consisted of a five-component tone complex, 50 ms in duration, repeated four times at a rate of 10 Hz (total duration 350 ms). The signal was one component fixed at 4000 Hz, and the four masker components either varied in frequency across bursts or were fixed in frequency. Signal and masker were gated synchronously. All energetic masker (EM) frequencies were drawn from a $\pm 1/3$ -octave band centered at signal frequency, whereas IM frequencies occupied a broad range outside of the signal band.

We obtained mismatch-negativities (MMNs) using an optimized oddball paradigm: One standard (masker alone), randomly interleaved with five deviants (signal + masker). Deviant signal levels were 30, 50, 60, 70, and 90 dB SPL. Masker components were fixed at 60 dB SPL. Subsequently, subjects performed a psychophysical 2-AFC detection task with an adaptive tracking procedure.

Results

In IM conditions, MMN components of all three subjects decreased systematically with decreasing signal level. In contrast, for EM only the highest signal level elicited significant MMNs. Accordingly, MMN thresholds were

lower for IM (30-50 dB SPL) but not for EM (70-90 dB SPL). In accordance with previously reported psychophysical data, neural thresholds displayed large inter-subject variability for IM. In one subject we tested psychophysical thresholds and found a strong positive correlation with neuronal thresholds ($R^2 = 0.99$ $N = 4$ $p < 0.001$).

Conclusion

We demonstrated that 1) it is possible to record meaningful LAEPs for these relatively long and complex stimuli 2) MMNs systematically vary with subjective task difficulty and 3) where available, neuronal thresholds correlate well with behavior. Although more data are needed to solidify these findings, our experiments potentially provide an important insight into the relationship between behavior and cortical activity during ASA.

383 Neural Correlates of Musical Discourse: An fMRI Study of Interactive Jazz Improvisation

Gabriel Donnay¹, Summer Rankin², Mónica López-González², Patpong Jiradejvong², Charles Limb²
¹University of Pennsylvania, ²Johns Hopkins University School of Medicine

Background

Interactive generative musical performance provides a suitable model for communication because, like natural linguistic discourse, it involves an exchange of ideas that is unpredictable, collaborative and emergent.

Methods

We utilized functional magnetic resonance imaging to investigate a form of jazz improvisation called trading fours, during which two musicians participate in a call and answer exchange akin to a 'musical conversation'. Eleven professional jazz piano players participated in this study. Two experimental paradigms were used during scanning, one of low complexity and one of high complexity. In the low complexity task, the subject and experimenter either traded a one octave, ascending and descending D Dorian scale (control task) or traded four measure improvisations (experimental task). Improvisation was heavily restricted to continuous, monophonic quarter notes in the key of D Dorian. In the high complexity task, the subject and experimenter either traded four measures of a memorized jazz composition (control task), or traded four measure improvisations (experimental task). All tasks were performed with accompaniment from a prerecorded rhythm section.

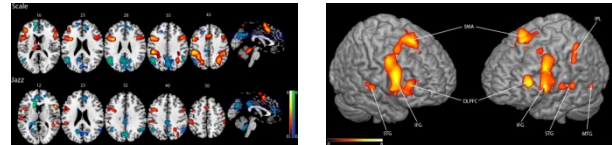
Results

SPM8 was used to analyze all functional neuroimaging data. Imaging data contrast analyses of improvised trading conditions vs. memorized trading conditions revealed activation of perisylvian language areas linked to processing of syntactic elements in music, including inferior frontal gyrus and posterior superior temporal gyrus. Furthermore, this form of improvised musical communication was associated with significant

deactivation of angular gyrus and supramarginal gyrus, brain structures directly involved with semantic processing for language.

Conclusion

Perisylvian language areas that subservise syntactic function are active during improvised musical communication. These findings support the idea that the exchange of ideas in music does not involve traditional semantic processing. Furthermore, these findings suggest that neural regions for syntactic processing may be domain-general for communication rather than domain-specific for language.



Activations	Left Hemisphere						Right Hemisphere											
	BA	Scale	Jazz	Control	Scale	Jazz	Control	Scale	Jazz	Control	Scale	Jazz						
Perisylvian Language Areas																		
IFG/IFC	44	5.43	-46	36	12	5.29	52	22	14	3.84	-54	18	29	5.46	50	18	14	
IFG/PCp	44	4.6	-52	10	16	4.3	52	19	19	4.26	-56	14	26	4.23	58	12	4	
STG	22	2.91	-46	-42	9	3.91	56	-40	2	4.01	-62	-24	8	4.55	54	10	-4	
Sensorimotor																		
SMA	6	6.21	-2	10	48	5.78	6	18	46	5.35	-2	12	58	4.62	10	14	62	
Temporal																		
ITG	20						9.3	58	-54	8					4.52	60	-52	8
MTG	37	3.39	-52	-56	-13	7.6	58	-48	-4						4.52	60	-52	8
Fusiform Gyrus	37									4.59	-28	-58	-14	2.82	24	-49	-14	
Parietal																		
IPL	2,40	11.08	-48	-32	39	6.17	36	-54	50	4.55	-56	-30	48	3.43	56	-28	52	
IPC	7	5.99	-22	-46	48	5.86	26	-58	50					3.33	18	-48	64	
SMC	2,40	7.47	-46	-32	39	3.91	36	-38	40	3	-52	-20	42	4.01	60	-24	48	
Occipital																		
Mid OC	18													4.59	38	38	12	
Mid OC	18,19	4.21	-30	-86	16	5.58	32	-62	38					3.4	34	-72	38	
Sup OC	19	2.87	-22	-66	39	4.56	30	-64	38					3.11	32	-64	42	
Prefrontal Cortex																		
ULPFC	46	6.56	-50	12	42	3.08	46	18	20	3.58	-42	40	24					
MFG	9,9	5.63	-42	46	18	3.26	34	40	4,05	-42	40	36	3,29	28	8	52		
DFC	9	3.63	-28	8	39	4.78	26	4	24									
Precentral Gyrus	6,44	6.08	-52	12	32	3.78	58	10	36	4.08	-52	2	48	4.05	50	2	40	
Deactivations																		
Region	BA	Scale	Jazz	Control	Scale	Jazz	Control	Scale	Jazz	Control	Scale	Jazz						
Sensorimotor																		
Temporal																		
MTG	10								-3.91	-46	2	-26	-3.72	48	2	-22		
Parietal																		
IPL	46	-3.95	-46	-54	36	-5.58	56	-56	38	-4.71	-44	-54	44	-3.77	48	-52	46	
SMC	40	-7.75	-12	54	16	-3.01	8	60	16					-3.16	6	46	40	
Prefrontal Cortex																		
MFG	6	-4.89	-20	40	22					-3.16	-26	52	8					
IFG	8,10	-3.66	-14	52	30	-4.6	16	42	26	-3	-22	56	16	-4.82	22	52	8	
Precentral Gyrus	6,44					-3.52	24	-16	64									
Other																		
Angular Gyrus	39	-5.12	-44	-60	34	-8.08	56	-54	36	-5.14	-44	-56	44	-4.92	62	-52	32	
Preuneus	31	-4.09	-4	-66	30	-3.85	4	-68	34	-4.42	-4	-68	30	-3.35	24	-44	4	

384 Juvenile Auditory Learning Is Associated with Diminished Cortical Synaptic Inhibition

Emma Sarro¹, Vibhakar Kotak¹, Dan Sanes¹
¹New York University

Background

Auditory associative training that occurs during development leads to improved performance in adulthood (Sarro and Sanes, 2011), indicating that developing animals display a unique benefit from sensory experience. To test whether functional adjustments in primary auditory cortex accompany such learning, we assessed inhibitory synaptic function, which has been implicated in cortical plasticity (Froemke et al., 2007).

Methods

Juvenile gerbils were trained on an amplitude modulation detection task from postnatal day (P) 23 to 40. Subsequently, we generated thalamocortical brain slice

preparations on the final day each animal received training, and assessed inhibitory synaptic function. Spontaneous inhibitory synaptic currents (sIPSCs) were recorded in layer 2/3 pyramidal neurons of thalamorecipient auditory cortex following blockade of ionotropic glutamate receptors and sodium spikes.

Results

Auditory associative learning was accompanied by an immediate reduction in both the amplitude and frequency of sIPSCs, and this decrease persisted for several days. However, following longer training durations, sIPSC amplitude and frequency approached or exceeded control levels. Finally, those juveniles that did not display significant learning, also showed control-like inhibitory currents.

Conclusion

Thus, a limited period of diminished inhibition may facilitate associative learning in developing animals.

385 The Effects of Reward Expectation on Neural Responses in Primary Auditory Cortex (A1) During the Learning and Performance of a Tone Detection Task

Nikolas Francis¹, Bernhard Englitz¹, Catherine Burke¹, Jonathan Fritz¹, Shihab Shamma¹

¹University of Maryland

Background

The neural network underlying reward and reward expectation has not traditionally included primary sensory cortices. However, recent studies in behaving animals have shown that neurons in A1 can encode target expectation and that neurons in V1 (primary visual cortex) can encode reward timing. To explore the effects of reward expectation on A1 coding of target sounds, we studied amplitude-modulation (AM) coding of target tones in A1 during task conditions involving expectation of a water reward.

Methods

Two ferrets were trained on a conditioned avoidance (CA) tone detection task. In each trial, a series of rippled noise stimuli was followed by a 4 Hz AM tone. During each testing session, a different AM carrier (ie. target) frequency was used. Animals were trained to lick from a waterspout for 1.5 seconds after AM tone offset, but to refrain from licking during a variable duration (1-4 second) target AM tone to avoid a mild tail-shock. Blocks of trials in a given session had fixed duration tones allowing the animal to accurately anticipate reward timing. While a ferret was learning the task, we recorded single-units in A1 using a moveable 64-channel multi-electrode array in a behaving, head-fixed ferret to study the plasticity of A1 responses to the task sounds over the time course of learning (~1 month).

Results

During task performance in the trained animal, the spike-rate steadily increased over the duration of the target AM

tone. The synchrony of spiking to the 4 Hz AM was decreased during the task. Consistent with previous findings (Fritz et al, 2003; Atiani et al., 2009), we also saw an overall suppression of spike-rate during the CA task, and persistent task-dependent frequency-specific changes in the shape and gain of spectro-temporal response fields (STRFs).

Conclusion

Our results suggest that reward anticipation in combination with inhibited reward-seeking behavior in the CA task leads to a build-up of A1 responses to target sounds as the reward time approaches. The decreased AM spike synchrony during the task reflects, in part, a combination of the decreased AM-feature salience for successful task performance, the suppressed overall spike-rate during the task, and an increase in the jitter of spike timing across trials during behavior. We will further discuss task-dependent effects on STRF tuning, and the effects of learning the task on A1 responses to the task sounds during learning.

386 Dynamics of Plasticity in Human Auditory Cortex During Course of Perceptual Learning

Serin Atiani^{1,2}, Robert J. Zatorre^{1,2}, Marc Schönwiesner^{1,3}

¹Montreal Neurological Institute, ²McGill University,

³Université de Montréal

Background

Establishing the link between behavior and its underlying neural mechanism is one of the central goals of neuroscience. Probing the representation of behaviorally significant sensory experiences is critical to understanding the functional dynamics of our sensory systems. The significance of the auditory system coupled with humans' unique ability to learn and adapt makes the human auditory system well suited to studying these questions. In this study we manipulate the behavioral significance of stimuli through training participants on an acoustic task and observe the changes in their representation that take place over the course of learning. Our experiment is designed to take advantage of auditory neurons' selectivity to spectro-temporal features of sound (Klien et al 2000, Theunissen et al 2000, Depireux 2001, Schönwiesner & Zatorre 2009). We use dynamic ripples, complex broadband stimuli with a drifting sinusoidal spectral envelope (Kowalski et al 1996), to measure modulation transfer functions (MTF) for voxels in auditory cortex, while participants are actively listening to a series of these ripples as they perform the task

Methods

Twelve participants were presented with a series of dynamic ripple stimuli and were trained to identify a target ripple with a unique spectro-temporal combination from a set of 16 different ripples with 4 spectral and 4 temporal modulation rates. Training took place during 5 consecutive days. Functional brain images were acquired with a 3T MRI scanner on the first, second and fifth day during task performance. We used the ripples heard during the task to

map spectro-temporal (MTF) of voxels in auditory cortex (method described in: Schönwiesner & Zatorre 2009)

Results

Participants' performance improved through the course of training to reach optimal performance by the fifth day. We observe task related changes in the MTF of auditory cortex voxels starting on the first day of training reflecting a clear selectivity for the target ripple. This selectivity improves during the course of learning, by continued differential response to the target ripple coupled with gradual drop in response to remaining ripple set, that is accompanied by a drop of global BOLD signal in auditory cortex

Conclusion

Our study demonstrates changes in spectrotemporal modulation tuning during learning that reflect the modulation content of the target sound. Preliminary analyses suggest a correspondence between cortical changes in tuning and behavioral changes in target

387 Understanding the Effects of Central and Peripheral Masking in Cochlear Implant Users

Carol Q. Pham^{1,2}, Peter Bremen^{2,3}, John C. Middlebrooks^{2,3}, Fan-Gang Zeng^{1,2}, Myles Mc Laughlin^{1,2}
¹Hearing and Speech Laboratory, University of California, Irvine, ²Center for Hearing Research, University of California, Irvine, ³Department of Otolaryngology-Head and Neck Surgery, University of California, Irvine

Background

Although cochlear implant (CI) users communicate relatively well in quiet, they have great difficulty understanding speech-in-noise. Previous studies in normal hearing (NH) subjects have demonstrated that both peripheral and central processes play a significant role in speech-in-noise perception. While it is known that wide peripheral filters in CI users contribute to poor speech-in-noise performance, the role of altered or degraded central processing has been less well studied. Here, by first measuring peripheral filters, we could use carefully controlled informational (IM) and energetic masking (EM) stimuli to study the roles of central versus peripheral processes, respectively, in electric hearing.

Methods

Four post-lingually deaf Nucleus 24 users were tested. Peripheral filter bandwidth was measured using standard electrically evoked compound action potential forward masking techniques. All stimuli were presented through a research interface (HEINRI) at a rate of 300 pulses per second. The signal was fixed on electrode 11. The masker was on four other electrodes placed either inside (EM) or outside (IM) of the peripheral filter. Both signal and masker were 40 ms bursts, pulsed 4 times at 5 Hz. Maskers with synchronous and asynchronous onset time re signal were tested as were maskers with varying (V) and constant (C) electrode position over time. Masker level was roved to avoid introducing any loudness cues. A two-interval,

forced-choice adaptive procedure was used to measure signal detection thresholds in the presence of maskers.

Results

Surprisingly, the amount of masking produced by stimulating electrodes outside of the peripheral filter (IM) tended to be greater than that produced by stimulating electrodes inside of the filter (EM). In agreement with previously reported data in NH listeners, CI data showed that (1) thresholds with synchronous maskers were higher than those obtained with asynchronous maskers, and (2) thresholds for C maskers were higher than thresholds for V maskers. In general, inter- and intra-subject variability was large for all masker types.

Conclusion

Results indicate that in electric hearing the effects of central masking can often be greater than peripheral masking. While spectral cues did improve signal detection for some CI subjects, the effect of temporal cues dominated and improved signal detection for all subjects tested.

388 A Spectrally Rippled Noise Mismatch Negativity Paradigm for Objectively Assessing Speech Perception in Cochlear Implant Users

Myles Mc Laughlin^{1,2}, Alejandro Lopez Valdes², Laura Viani³, Peter Walshe³, Jacklyn Smith³, Richard B. Reilly², Fan-Gang Zeng¹
¹Hearing and Speech Lab, UC Irvine, ²Trinity Centre for Bioengineering, Trinity College Dublin, ³National Cochlear Implant Programme, Beaumont Hospital, Dublin

Background

A number of recent studies suggest that cortical evoked potentials (CEPs) may provide a useful objective measure of speech perception in cochlear implant (CI) users. However, weak correlations with behavior and artifact cancellation issues have hampered the clinical impact of CEP based objective measures in CI users. Psychoacoustic studies have shown that a CI user's ability to discriminate spectrally rippled noise stimuli correlates reasonably well with their speech perception. Here, we have developed a clinically applicable single-channel artifact cancellation approach which allows the acquisition of artifact free CEPs using complex stimuli. Using this approach we demonstrate how CEPs to spectrally rippled noise may be used to estimate speech perception in CI users.

Methods

We developed a high bandwidth (0-100k Hz), high sample rate (125kHz) CEP acquisition system which allows us to clearly resolve the CI related artifact. When acquired with this system the artifact is completely high frequency (\geq CI stimulation rate) and can be removed using standard filtering techniques. Using this system we measured mismatch negativity (MMN) responses in 10 CI subjects and 10 normal hearing controls. The standard stimulus (90%) was spectrally rippled broadband noise; the deviant

(10%) was the inverted version, having an equal number of ripples per octave (RPO). To define a neural RPO detection threshold we increased the number of RPOs until the MMN response was no longer greater than a noise floor determined from the standard only responses using a boot-strap method. Behavioral RPO detection thresholds were also measured using a two alternative forced choice paradigm.

Results

The high bandwidth, high sample rate system provides robust, fully automatic, real-time, CI artifact removal. A significant correlation ($p=0.02, r^2=0.54$) was found between the neural RPO detection threshold and the behavioral RPO detection threshold.

Conclusion

Using a single-channel clinically applicable artifact removal technique it was shown that CEPs can be used to estimate the spectral processing abilities of CI users. Given the known correlation between speech perception and the behavioral RPO detection threshold, we expect to see a correlation with neural RPO detection threshold and this is currently being tested.

389 Temporal Processing Properties of the Auditory Evoked Potentials in Cochlear Implant Users

Fawen Zhang¹, Chelsea Benson¹, Dora M. Murphy-Courter¹, Michael Scott², Paul Abbas³

¹University of Cincinnati, ²Cincinnati Children's Hospital Medical Center, ³University of Iowa

Background

For perception purposes, the auditory system encodes temporal and spectral information of sounds. The primary purpose of this project is to investigate the temporal properties of auditory evoked potentials (AEPs) at the peripheral and cortical stage of the auditory system in cochlear implant (CI) users. This research may lead to future efforts toward improving the temporal representation of sounds, thereby maximizing CI performance. We expected the temporal properties of the late auditory evoked potential (LAEP) from the cortex to be related to that of the electrical compound action potential (ECAP) from the auditory nerve, given that the temporal properties may be kept and/or accumulated after multiple neural synapses along the auditory system.

Methods

A group of postlingual CI adults were recruited. A stimulus-train paradigm was used to examine how the AEPs change over time. The ECAP was recorded using NRT software (Custom Sound EP 2.0) installed on the clinical fitting system. Since the NRT software does not allow for ECAP recording in response to individual pulses within a pulse train, the approach described previously was used (Hay-McCutcheon et al., 2005). Specifically, the response to a probe that is preceded by a varying number of a series of masker pulses was measured. Offline subtraction was performed to extract the ECAP to each pulse in a pulse

train (1000 pps, 100 ms). The LAEP was recorded using the 40-channel Neuroscan system. Tone bursts at 1 kHz were presented according to the stimulus-train paradigm consisting of 30 trains (inter-stimulus-interval = 0.7 ms; inter-train-interval = 15 sec) via a loudspeaker placed at ear level, 50 cm from the test ear at 90° azimuth.

Results

Pilot results showed that, for both AEPs, the response was the largest in response to the first stimulus and declined fast until it reached asymptote, displaying adaptation. The adaptation index (AI) was calculated using the formula, $AI = A_{asympt}/A_1$. The adaptation index ranged from approximately 0.22-0.57 ($M=0.42, SD=0.16$) for ECAP and 0.19 to 0.72 ($M=0.45, SD=0.17$) for the N1-P2 complex of the LAEP.

Conclusion

This study is ongoing. Full results will show the correlation between LAEP and ECAP adaptation in CI users and LAEP data from normal hearing controls.

390 Behavioral Measures of Temporal Processing and Speech Perception in Normal Hearing and Cochlear Implant Listeners

Chelsea Benson¹, Fawen Zhang¹, Melissa Boian¹, Danielle Bronkema¹, Robert Keith¹

¹University of Cincinnati

Background

Although all cochlear implant (CI) users achieve some level of hearing sensitivity, post-implantation speech perception outcomes vary greatly. Previous studies reported a strong correlation between CI users' phoneme recognition scores and modulation detection thresholds using an electric pulse train directly presented via the electrode array, suggesting that temporal processing may largely contribute to speech perception (Fu, 2002). The purpose of this study was to examine the relationship between speech perception performance and behavioral measures of temporal processing using the Random Gap Detection Test (RGDT, Keith, 2000) presented in the sound field. The results can help improve understanding the large variability of speech perception performance.

Methods

A group of NH subjects ($n=10$) and postlingually deafened CI users ($n=5$, 2 bilaterally implanted) participated. Stimuli were presented monaurally via loudspeaker at the most comfortable loudness level (MCL) for CI subjects and insert earphones for NH subjects. The contralateral ear was plugged throughout the entire testing session. The stimuli consisted of the following: Speech Recognition Threshold test, Central Institute for the Deaf (CID) W-22 Word Discrimination test, Banford-Kowel-Banch Speech In Noise (BKB-SIN) test, and RGDT Test.

Results

Pilot results showed that the RGDT thresholds are significantly higher in cochlear implant users (26.67 ms, $SD = 3.33$) than in normal hearing (NH) listeners (7.11 ms,

SD = 4.37, $p < 0.01$). The SRT is significantly poorer in CI users (Median=30 dBHL) than in NH listeners (Median=0 dBHL, $p < 0.01$). Discrimination percent correct was significantly poorer in CI users (Median=68%, $p < 0.01$) than in NH listeners (Median=100%, $p < 0.01$). The SNR (signal-noise-ratio) for BKB-SIN test is significantly higher for CI users (M=11.69, SD=4.23) than for NH listeners (M=-4.38, SD=2.70), indicating that the CI subjects required a more favorable SNR in order to be able to repeat 50% of target words correctly. Regression analysis for CI data showed a nearly significant correlation between the mean gap detection threshold and the discrimination score ($R^2=0.56$, $p=0.05$). There was no significant correlation between the mean gap detection and SRT ($R^2=0.15$, $p>.05$), or the BKB-SIN results ($R^2=0.37$, $p>0.05$).

Conclusion

This study is ongoing. Pilot results suggest that cochlear implant users do have temporal processing limitation, which is the basis of poorer speech discrimination.

391 Processing of Coherent Temporal Level Fluctuations in Cochlear Implant Users

Stefan Zirn^{1,2}, John-Martin Hempel¹, Maria Schuster¹, Werner Hemmert²

¹LMU Munich, ²Technical University of Munich

Background

The normal hearing (NH) auditory system has elaborated strategies to segregate different sounds with overlapping spectra occurring at the same time – a usually unsolvable task for cochlear implant (CI) users. An important neural mechanism in this context is across-frequency processing: the comparison of temporal level fluctuations across auditory filters. Many natural sounds including speech provide such correlated patterns of intensity changes across-frequency that enable comodulation masking release (CMR) and affect auditory stream formation.

Methods

The experiment followed a flanking-band paradigm for CMR measurements using the Nucleus Implant Communicator: uncorrelated and comodulated biphasic pulse trains were addressed to selected intra cochlear electrode contacts (masker components). A steady state level variable pulse train was added to a medial channel (target signal). Masked detection thresholds (MDT) of the target signal were determined according to an adaptive 3-AFC paradigm.

Results

The measured mean CMR was strongly reduced in CI users (3.6 dB \pm 5.9, $p < 0.05$) compared to NH listeners (12.9 dB \pm 2.6, $p < 0.01$). However, results of CI users were heterogeneous: 66% of test subjects achieved no (0.1 dB \pm 2.7) and 33% a high CMR (10.7 dB \pm 3.2).

Conclusion

We looked for reasons and indicators for CMR in individual CI users. Additional masking as the main reason for the

effect is unlikely: the MDT in the comodulated test condition in test subjects with CMR decreased, while MDT in the uncorrelated test condition was not higher than the mean level across all test subjects. These findings point out to a centrally mediated CMR in our study with direct stimulation. Etiology revealed to be a good indicator for CMR: CI users with e.g. acute hearing loss or other sensorineural hearing impairment achieved much higher magnitudes than listeners with e.g. long-term progressive hearing loss or late-implanted congenital hearing loss. Also the duration of hearing loss pre-implantation seemed to be a good indicator for CMR.

The outcome that a subgroup of CI users benefits from amplitude comodulation inspires the development of new signal processing strategies for CI systems in terms of enabling across-frequency processing in everyday settings.

Funding: Bernstein Center for Computational Neuroscience (German Federal Ministry of Education and Research: 01GQ1004B) and Cochlear Ltd., Germany.

392 Recovery from Forward Masking in Cochlear Implant Listeners Depends on Stimulation Mode

Monita Chatterjee¹, Aditya Kulkarni¹

¹Boys Town National Research Hospital, Omaha, NE

Background

Bipolar and monopolar stimulation in cochlear implants result in different detection thresholds, suggesting that different groups of neurons may be activated by the two stimulation modes. It is likely that one group (ie that excited by bipolar stimulation) is a subset of the other. Given the recent interest in more focused stimulation of the auditory nerve in cochlear implants, it is important to quantify the response properties of more focused groups of neurons. The objective of this study is to compare the time course of recovery from forward masking in cochlear implant listeners using bipolar and monopolar stimulation modes.

Methods

The masker is a 300-ms long train of biphasic current pulses (100 microseconds/phase, 1000 pulses/s). The probe is a 20-ms long train of identical pulses. Recovery functions are measured under the following three conditions: A. Monopolar masker, monopolar probe; B. Monopolar masker, bipolar probe; C. Bipolar masker, bipolar probe. Stimuli are delivered using a custom research interface and directed to different electrodes across the device. Masker and probe are always directed to the same active electrode, regardless of stimulation mode. The masker is presented at a fixed level, and maskers on different electrodes are loudness-balanced to each other. Psychophysical detection thresholds for the probe were measured using a 2 interval forced choice adaptive procedure. Thresholds were obtained at masker-probe intervals ranging from 2 to 128 ms.

Results

Results suggest that in conditions B and C, recovery functions are nonmonotonic, consistent with previous results obtained with stimuli similar to those in condition C by previous investigators. Condition A seems to result in smoother and faster rates of recovery. Recovery functions for condition A appear to be fairly homogeneous across electrodes within the same subject, but recovery functions are more variable across electrodes for conditions B and C.

Conclusion

These results suggest that the response of smaller groups of neurons (presumably elicited by the use of a bipolar probe) recovers more slowly and nonmonotonically than the recovery of the aggregate response of the larger group of neurons excited by monopolar stimulation. Results of planned experiments with tripolar probes will be presented, and implications of these results for signal coding by the electrically stimulated auditory nerve will be discussed.

[Work supported by NIH/NIDCD grant no. R01 DC004786]

393 Sensitivity of Normally-Hearing and Cochlear-Implanted Children Raised in the US and Taiwan to Pitch-Related Cues

Mickael LD Deroche¹, Yung-Song Lin², Hui-Ping Lu³, Shu-Chen Peng⁴, Charles J Limb¹, Monita Chatterjee⁵

¹Johns Hopkins University School of Medicine, Baltimore, MD, ²Taipei Medical University, Chimei Medical Center, Tainan, Taiwan, ³Chimei Medical Center, Tainan, Taiwan,

⁴US Food and Drug Administration, Silver Spring, MD, ⁵Boys Town National Research Hospital, Omaha, NE

Background

The ability of children to hear subtle changes in pitch is potentially critical for their acquisition of the native language and yet has been little investigated. For children speaking a tonal language, rapid changes in voice pitch carry linguistic information. We hypothesize that these children might have a finer sensitivity to pitch than English-speaking children. Pitch perception by cochlear-implanted (CI) listeners is notoriously poor. However, children who are implanted very early in life may be able to maximize the benefits of brain plasticity. Our second hypothesis is that these children might overcome to some extent their device limitations and process purely temporal pitch more effectively than their normal-hearing (NH) peers.

Methods

Participants were NH children and CI children tested in the US and Taiwan. Percentage correct was measured in a 3-interval 3-alternative forced choice task, for the discrimination of fundamental frequency (F0) of broadband sine-phase harmonic complexes, and for the discrimination of sinusoidal amplitude modulation rate (AMR) of broadband noise. The reference F0 was 100 and 200 Hz, as was the reference AMR. Stimuli were presented via loudspeakers and CI children listened through their speech processors. Data were fitted using a maximum-likelihood technique that extracted threshold and slope.

Results

Preliminary results indicate that in all four groups of listeners, there were large individual differences in threshold and slope, but they did not vary systematically with age. In the NH population, Taiwanese children had lower thresholds and steeper slopes than American children for F0 discrimination but not for AMR discrimination. In the CI population, there was no obvious difference in threshold or slope between Taiwanese and American children.

Conclusion

Based on these preliminary results, our first hypothesis is validated. Speakers of a tonal language seem to display a finer sensitivity to subtle changes in F0. This benefit however does not transfer to purely temporal pitch. Our second hypothesis is rejected: whether one considers the child's age, the implantation age or the age of use, threshold does not significantly correlate with age. Children who were implanted earlier did not display a better sensitivity to F0 or AMR than children who were implanted later in life. [Work supported by NIH/NIDCD grant no. R21 DC011905 to MC]

394 Cochlear Implant Use Causes Changes in the Cochleotopic Organisation of Auditory Cortex in Deaf Animals

Dexter Irvine¹, Samuel Irving¹, Robert Shepherd^{1,2}, James Fallon^{1,2}

¹Bionics Institute, ²University of Melbourne

Background

Neonatal deafness results in the loss of the normal cochleotopic organisation of primary auditory cortex (AI). Environmentally-derived chronic electrical stimulation, via a cochlear implant (CI), can restore that organisation (Fallon et al. 2009, J Comp Neurol). This study explores the time course of the changes in cochleotopic organisation by using chronic recordings of neural activity in auditory cortex of both normal hearing (NH, n=2) and neonatally deafened cats receiving auditory input via a CI (DCI, n=2).

Methods

All animals had 6x10 'Utah' planar silicon substrate recording electrode arrays (Blackrock Microsystems) implanted into putative AI as young adults. Multi-unit cortical responses to acoustic or electric stimulation were obtained under ketamine-xylazine anaesthesia at least monthly for approximately six months.

Results

In the NH animals, well characterised acoustic response areas were initially obtained on 67% of the recording channels, which decreased to 52% in the final recording session. In contrast, in DCI animals, well characterised electrical response areas were initially obtained on 22% of the recording channels, which increased to 69% of channels in the final recording session. There was no significant change in cochleotopic (tonotopic) organisation in NH animals over the 6-month recording period (paired t-

test on characteristic frequency; p 's > 0.1). However, DCI animals exhibited a significant change in cochleotopic organisation over the 6-month recording period (paired t -tests on best electrode; p 's < 0.01). The first statistically significant changes in cortical organisation (paired t -tests; p < 0.05) occurred after 4-5 months.

Conclusion

These results demonstrate that auditory cortex can undergo changes in cochleotopic organisation (over several months) as a result of CI use. They also suggest chronic CI use increases cortical responsiveness.

This work was funded by the NIDCD (HHS-N-263-2007-00053-C). The Bionics Institute acknowledges the support it receives from the Victorian Government through its Operational Infrastructure Support Program.

395 Bilateral Effects of Chronic Unilateral Intra-Cochlear Electrical Stimulation on the Central Auditory Pathway

Sebastian Jansen¹, Moritz Gröschel^{1,2}, Patrick Boyle³, Arne Ernst², Dietmar Basta^{1,2}

¹Humboldt University of Berlin, ²Dept. of ENT at Unfallkrankenhaus Berlin, ³Advanced Bionics Clinical Research

Background

Little is known about binaural interactions induced by simultaneous acoustic and electric stimulation of the auditory system in patients with unilateral deafness. Since large differences are known between the loudness coding in electric and acoustic hearing, plastic changes would be expected in structures which receive acoustic and electric input in binaural hearing. This study therefore aims to investigate the structural consequences of unilateral chronic intra-cochlear electrical stimulation within the ascending auditory pathway in an animal model.

Methods

Normal-hearing guinea pigs were single-side deafened by the insertion of a standard HiRes 90k® cochlear implant with a HiFocus1j electrode array into the first turn of the cochlea. Four to five electrode contacts were used for the stimulation. Six weeks after surgery, the speech processor (Auria®) was programmed based on tNRI-values and mounted on the animal's back.

The three experimental groups were stimulated with a HiRes strategy based on different stimulation rates. Group 1: lowest feasible stimulation rate (275 imp/s). Group 2: medium stimulation rate (1500 imp/s), group 3: highest feasible stimulation rate (5000 imp/s). The experimental groups were compared to group 4: unilateral deafened control (implanted but not stimulated). Experimental groups and controls experienced a standardised free field auditory environment (16 h/day). After 90 Days of stimulation cell density was determined in the medial geniculate body and in the inferior colliculus.

Results

Group 1 (275 imp/s) showed a significantly higher cell density bilaterally in the inferior colliculus (IC) and on the normal hearing side of the medial geniculate body (MGB) compared to the unilateral deaf control. Group 2 (1500 imp/s) showed a significantly higher cell density bilaterally in the MGB and the IC compared to the unilateral deaf control. Group 3 (5000 imp/s) showed a significantly higher cell density bilaterally in the MGB and on the normal hearing side of the IC compared to the unilateral deaf control.

Conclusion

The data of the present study shows that electrical intra-cochlear stimulation has a bilateral and rate independent conservational effect on key structures of the auditory midbrain. The decreased cell density in the control group seems to be induced by the sensory deprivation, which was prevented or reduced by the electrical stimulation of auditory nerve fibres. Based on the present data, an early implantation could be recommended in single sided deaf patients.

396 Growth-Function of Electrically Evoked Brainstem Responses in Cochlear Implant Patients

Xiaoge Chong¹, Michele Nicoletti¹, Hans-Joachim Steinhoff², Cora Giesse³, Christina Lackner³, Sonja Karg¹, Armin Giebel³, Werner Hemmert¹

¹Technische Universität München, ²Klinikum rechts der Isar, ³Munich University of Applied Sciences

Background

Objective methods are not only important for the fitting process of cochlear implants (CIs) e.g. in babies but can also provide insight about the response of the auditory nerve. Here we measure electrically evoked brainstem responses (eBERA) with single pulse stimuli, study their amplitude-growth function and relate them to the perceived loudness.

Methods

This study was conducted with CI patients with monopolar electrode configuration. Implants were controlled with a research interface box (RIB II). Biosignals were recorded with three electrodes on vertex and neck to measure eBERA responses (ground: contralateral cheek), amplified and digitized. Patients scored loudness with a stylus on a tablet. The tablet was covered with a form which showed five coarse loudness categories but read out was conducted with high resolution.

Results

Because of the huge artifact of the electrical stimulus, the first 1.25 ms of the responses were deleted completely, then responses to anodic and cathodic pulses were subtracted. The remaining stimulation artifact was eliminated by fitting and subtracting an exponential decay function. We then analyzed the amplitude of the wave V peak and identified significant amplitudes with the binominal average method at a confidence level of 99.7%.

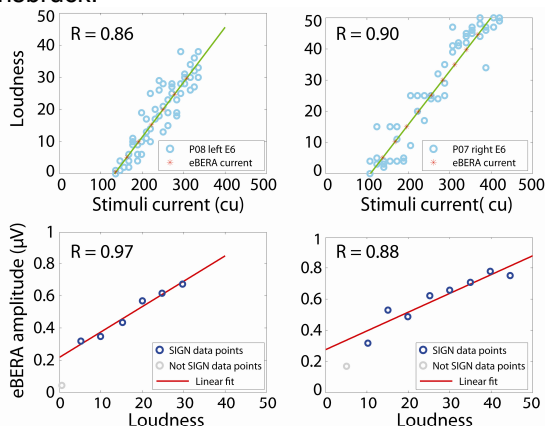
eBERA amplitudes increased linearly with the stimulation current. We excluded cases with muscle artifacts at high currents, which were probably caused by stimulation of the facial nerve. The figure (see supporting files) show the relation between stimulation strength, wave V amplitude and loudness. Results show significant eBERA responses already at very small loudness categories. The high correlation coefficient indicates a close relation between eBERA amplitude and loudness.

Conclusion

eBERA measurements require stringent data quality evaluations to exclude artifacts. Doing so, we were able to measure significant (99.7%) eBERA responses almost down to perception threshold. eBERA amplitudes grew linearly with stimulus current and also the relationship between loudness and current was well fitted with a linear model. Therefore also loudness grew linearly with eBERA amplitudes. This finding indicates that perceived loudness - at least for single pulse stimulation - is proportional to the number of excited nerve fibers.

Acknowledgement

This work was funded by a grant within the Munich Bernstein Center for Computational Neuroscience by the German Federal Ministry of Education and Research (reference number 01GQ1004B) and from MED-EL Innsbruck.



Loudness growth as a function of stimulus current (upper row) and eBERA growth with loudness (lower row) for two CI patients. For loudness categorization, 5 coarse categories were shown on a paper sheet, but read-out was fine-grained. Values <0 were below threshold and >50 too loud.

397 Whole-Nerve Responses to Pulse Trains in the Intact and the Degenerating Auditory Nerve in Guinea Pigs

Dyan Ramekers^{1,2}, Huib Versnel^{1,2}, Stefan Strahl³, Wilko Grolman^{1,2}, Sjaak Klis^{1,2}

¹University Medical Center Utrecht, ²Rudolf Magnus Institute of Neuroscience, ³MED-EL GmbH, R&D

Background

Effective functioning of cochlear implants (CIs) depends on the integrity of the auditory nerve, and its ability to transduce electrical signals to the central nervous system. Traditional measures such as threshold and amplitude of the electrically evoked compound action potential (eCAP) can be indicative of the nerve's viability. However, the

information that is conveyed by CIs ultimately lies in patterns of pulse trains rather than in its constituting individual pulses. Therefore, by means of eCAP recording, we have characterized the auditory nerve's behavior under various multiple-pulse conditions.

Methods

Guinea pigs were deafened by co-administration of kanamycin (400 mg/kg) and furosemide (100 mg/kg) two or six weeks before acute experiments. Untreated guinea pigs were used as normal-hearing controls. eCAPs were recorded using a MED-EL PULSAR cochlear implant. Pulse trains consisted of alternating biphasic current pulses, and had a duration of 10 or 100 ms; pulse rate was increased from 62.5 Hz to 2.5 kHz in ten steps. Amplitude and latency of the last ten eCAPs in the pulse train were measured. Immediately after the acute experiments, the animals were sacrificed for histological analysis of the spiral ganglion cells.

Results

The eCAP amplitude to the first pulse of the pulse train decreased with duration of deafness, which correlates with the decrease in number of spiral ganglion cells. The eCAP amplitude to later pulses decreased with higher pulse rates. This decay was more pronounced with longer pulse train duration, and also more pronounced for normal-hearing animals. In each animal we observed an oscillating effect in eCAP amplitude for pulse rates around 1.5 kHz. The average oscillating frequency was between 600 and 800 Hz. The amplitude of this oscillation was significantly smaller for normal-hearing than for deafened animals. Finally, the eCAP latency increased with increasing pulse rate, but only significantly so for the normal-hearing animals.

Conclusion

The slower decay and shorter latency of eCAPs in deafened animals may be a result of degeneration of the organ of Corti, creating a simpler neural interface. Higher oscillation amplitudes in these animals could indicate increased synchrony of the population of nerve fibers.

398 Recognition of Complex Frequency-Modulation Patterns Based on Recovered Envelope Cues in Cochlear Implant Users: Effects of Modulation Depth and Peripheral Filtering

Ward R. Drennan¹, D. Timothy Ives², Elyse M. Jameyson¹, Jong Ho Won^{1,3}, Elizabeth S. Anderson¹, Jay T. Rubinstein¹, Christian Lorenzi²

¹VM Bloedel Hearing Research Center, University of Washington, ²Equipe Audition, CNRS, Universite Paris Descartes, Ecole normale superieure, ³University of Tennessee

Background

Frequency-modulation (FM) patterns convey crucial information for sound identification. FM is encoded into both temporal-envelope and temporal fine-structure cues (TFS) via cochlear filtering and neural phase locking in the

auditory periphery. Cochlear implant (CI) users provide a unique opportunity to assess the ability to use the envelope cues reconstructed from FM after peripheral filtering with minimal contribution of TFS. This study also aims at assessing the effect of the clinical processor on the transmission of FM via the envelope reconstruction mechanism.

Methods

The sensitivity of CI users and normal-hearing (NH) listeners was measured in a discrimination task using complex FM patterns applied to a 930-Hz sine carrier. Two factors assumed to affect envelope reconstruction were tested: (i) the extent of frequency excursion in FM stimuli, and (ii) the characteristics of peripheral filtering. Three sets of FM stimuli were created using a low, medium or high modulation index. The FM stimuli were then passed either through a model of the normal cochlear filter (gammatone) or the corresponding broader clinical filter of the CI. In each case, the stimuli were presented through one electrode of the CI at the same level.

Results

For most conditions, CI users had better sensitivity to FM patterns on the basis of reconstructed envelopes than NH listeners. This might result from the use of a linear input-output function for the CI processor. Sensitivity increased substantially with frequency excursion and the effect was larger for CI users. However, CI users were not able to benefit from the use of filters narrower than clinical filters to recover envelope cues: only NH listeners showed better sensitivity with the gammatone filter compared to the clinical filter.

Conclusion

The results indicate that discrimination of complex FM patterns can be achieved on the sole basis of reconstructed envelope cues. The fact that peripheral filtering, which simulated normal cochlear filtering, provided no benefit over standard clinical filters suggests that current clinical filters are sufficiently selective to promote efficient envelope reconstruction.

399 Cortical Hemodynamic Response to Speech Stimuli in Adult Cochlear Implant Users by Functional Near-Infrared Spectroscopy

Cristen Olds¹, Luca Pollonini², Homer Abaya¹, Richard Gurgel³, Michael S. Beauchamp⁴, Heather Bortfeld⁵, John S. Oghalai¹

¹Department of Otolaryngology - Head and Neck Surgery, Stanford University, ²Department of Engineering Technology - University of Houston, ³Department of Otolaryngology - Head and Neck Surgery, University of Utah, ⁴Department of Neurobiology and Anatomy, University of Texas Health Science Center at Houston, ⁵Department of Psychology, University of Connecticut

Background

Cochlear implants (CIs) are a therapeutic option to restore hearing in people with profound sensorineural hearing

loss. Objective measures of a CI's function are needed, especially in the pediatric population where optimal CI programming is essential for normal speech and language development and patient feedback during programming is more difficult to obtain. Functional near-infrared spectroscopy (fNIRS) is a non-invasive, CI-compatible imaging method used to monitor cortical hemodynamic changes. In our previous work using an instrument with 2 light sources and 4 detectors, we showed that acoustic speech stimuli elicit cortical responses in adults and children with normal hearing, as well as pediatric CI users. With this project, we aimed to demonstrate that a response to acoustic speech stimuli by auditory cortex is present with the CI turned on, but not with the CI turned off.

Methods

We collected fNIRS data using 16 light sources and 24 detectors to permit spatial localization of the cortical responses. We tested this approach by using fNIRS to assess for hemodynamic responses in the auditory cortex to acoustic speech stimuli in adult CI users both with their device turned on and with it turned off.

Results

Most participants demonstrated speech-evoked cortical activity only when their CI was turned on and not when it was turned off, as well as substantially larger cortical volume of activation when their CI was turned on compared to when it was turned off. A bilateral cortical response was the most commonly observed finding, regardless of the side of implantation. Participants who showed equivalent cortical responses and volumes of activation with their CI active and inactive were those with recently activated CIs.

Conclusion

Our findings show that fNIRS is a valid tool for measuring cortical hemodynamic responses in adult CI users and hence assessing CI functionality. This method holds potential to provide an objective measure of speech perception among CI users, and may be useful during CI programming.

400 Electrical Stimulation of the Cochlear Nucleus: Effects of Location and Pulse Rate on Inferior Colliculus Responses

Michael Slama^{1,2}, Rohit U. Verma^{1,3}, Amélie Guex^{1,4}, Kenneth E. Hancock^{1,2}, Pierre Joris⁴, Nicolas Grandjean⁴, Philippe Renaud⁴, Stéphanie Lacour⁴, M. Christian Brown^{1,2}, Daniel J. Lee^{1,2}

¹Eaton-Peabody Laboratories, Massachusetts Eye and Ear Infirmary, Boston, MA, ²Harvard Medical School, Boston, MA, ³University of Manchester Medical School, UK, ⁴Ecole Polytechnique Fédérale de Lausanne, Switzerland

Background

Auditory brainstem implants (ABIs) help provide some hearing to patients with non-functional auditory nerves or ossified cochleae. Yet, performance of ABI users in speech reception tasks is usually worse than for cochlear implant users. ABIs bypass the cochlea and auditory

nerve and electrically stimulate the surface of the cochlear nuclear complex. Two of the possible reasons for their limited performance are: (1) the relative imprecision of device placement, making it difficult to specifically target frequency regions important for speech understanding, and (2) the poor spatial selectivity of electrical stimulation, which limits frequency resolution. Our goal is to evaluate the effects of electrode placement and pulse rate on spatial selectivity and stimulation threshold in the hope of improving ABI performance.

Methods

The surface of the dorsal cochlear nucleus (DCN) of anesthetized rats was stimulated with either commercially available parylene-insulated platinum-iridium twisted electrodes or with novel, flexible micro-electrode arrays integrated into a polyimide polymer pad. Multiunit activity was recorded with a 16-micro-electrode array in the inferior colliculus (IC).

Results

Consistent with the tonotopic organization of the DCN and IC, we found that DCN surface stimulation laterally (low frequencies) to medially (high frequencies) led to lower threshold activation dorsally to ventrally in the IC. Spatial selectivity of electrical stimulation, although somewhat narrower in the rostral-most or caudal-most portions of the DCN, was usually poor. Lower stimulation thresholds were found on the medial side of the DCN. Pulse rate (11 – 513 Hz) did not have a significant effect on these measures across animals.

Conclusion

Our results point to the need for new stimulation strategies and devices to improve frequency representation in the auditory system of ABI users. Ongoing work in our laboratory is investigating whether electrode arrays that conform to the surface of the CN may help in this regard.

401 Are Amplitude-Dependent Changes in Temporal Resolution in Deaf Cat Inferior Colliculus Affected by Electric Hearing History?

Maike Vollmer¹, Ralph Beitel², Patricia Leake²
¹Comprehensive Hearing Center Wuerzburg, Germany,
²UCSF

Background

In previous studies we have reported that temporal resolution of central auditory neurons can be altered by deafness and by experience with intracochlear electric stimulation (ICES). In deaf animals, degradations in the ability of neurons to follow repetitive electric signals and response latencies can be improved by chronic ICES or even restored to normal levels by behavioral training. The present study investigates whether temporal processing in animals with different deafness histories and electric hearing experience is differentially affected by the electric stimulus amplitude used in the electrophysiological experiments.

Methods

Kittens were neonatally deafened by injection of ototoxic drugs. Animals were implanted unilaterally with a feline prosthesis either as juveniles or as adults after long-term deafness (≥ 3.5 yr), and a regimen of continuous ICES was initiated (~4 h/day, 5 day/wk). Animals were studied after several weeks to months of ICES. Acutely deafened adult animals served as controls. Pulse trains (~10 to 300 pps) were presented at stimulus amplitudes between 2 and 6 dB above neuronal threshold. Neuronal responses were recorded in the external (ICX) and central nucleus (ICC) of the inferior colliculus. Temporal response parameters of isolated single units were quantitatively evaluated, including: 1) maximum stimulus rates that neurons followed in a phase-locked manner (Fmax) and 2) minimum neuronal response latencies.

Results

In all groups, increases in stimulus amplitude resulted in a significant decrease in response latencies in both ICX and ICC neurons. With respect to Fmax, only ICC neurons in juvenile animals showed a significant increase in frequency following with increasing stimulus amplitude. Otherwise increases in stimulus amplitude had no effect on frequency following of neurons in either the ICX or the ICC.

Conclusion

Electric hearing history had no differential effect on amplitude-dependent changes in response latencies in the ICX or the ICC. With the exception of ICC neurons in juvenile animals, hearing history, likewise, had no differential effect on amplitude-dependent changes in Fmax.

Supported by NIH Contract # HHS-N-263-2007-00054-C.

402 Temporal Responses to Regular-Interval and Alternating-Interval Electric Pulse Trains in the Inferior Colliculus

Steven Bierer¹, Arkadiusz Stasiak², Julie Bierer¹, Robert Carlyon³, Ian Winter²

¹Speech and Hearing Sciences, University of Washington,
²Physiological Laboratory, University of Cambridge, ³MRC
Cognition and Brain Sciences Unit, Cambridge

Background

With cochlear implants, the fundamental frequency and other temporal aspects of a sound can be conveyed by the temporal pattern of evoked neural activity. In previous work, Carlyon et al (2008) used acoustic click trains, bandpass filtered to remove “place of excitation” cues, in order to simulate several aspects of a “purely temporal” pitch code. For example, a click train in which the inter-pulse intervals alternated between 4 and 6 ms produced a pitch equal to that of a regular-interval (isochronous) train with IPI=5.7 ms. A similar result was observed for cochlear implant listeners when presented with a train of biphasic electrical pulses. Additionally, in a guinea pig model, Carlyon and colleagues measured smaller compound action potential (CAP) amplitudes following the shorter interval of a “4-6” acoustic click train, suggesting a

potential neural basis of the observed perceptual effect. To obtain a more complete account of the neural representation of pitch in CI users we have recorded the responses of single units from the inferior colliculus of the guinea pig to similar electrical pulse trains.

Methods

In urethane-anesthetized adult guinea pigs, the inferior colliculus (IC) was exposed following a craniotomy and aspiration of the overlying cortex. A tungsten microelectrode was lowered into the brainstem, and responses to acoustic tones were obtained to verify placement. After deafening with neomycin, a PtIr ball electrode was secured inside the scala tympani. A series of single pulse and pulse train stimuli were presented in blocks at several current intensities. Unit data were processed offline to remove electrical artifacts, classify action potentials, and analyze spike timings.

Results

The majority of units had sustained or build-up temporal response patterns at current levels within ~10 dB of threshold, and 85% of these responded synchronously to the 10 ms period of the 4-6 alternating-interval pulse trains. The remaining units responded only to the onset or offset of the trains. At relatively low current levels, the spiking probability of synchronized units following the 4 ms intervals was usually smaller than that following the 6 ms intervals, similar to the CAP results. At higher levels, however, this difference was less pronounced.

Conclusion

In general, the diverse response patterns to alternating-interval pulse trains were reflected in the responses to isochronous pulse trains and pulse pairs presented at corresponding inter-pulse intervals. How these temporal response patterns relate to pitch perception remains to be elucidated.

403 Completely Implantable Artificial Organ of Corti

Katherine Knisely¹, Karl Grosh¹, Yehoash Raphael¹, Cameron Budenz¹, Angeliqne Johnson¹

¹University of Michigan

Background

Present commercial cochlear implants are limited by power consumption, latency, and physical unwieldiness. Efforts to develop smaller and more efficient implants have focused on the use of microelectromechanical systems (MEMS) technology to build small, passive, frequency-filtering artificial basilar membranes (ABMs) to replace signal processing. We present a piezoelectric cantilever array that is designed to replace the function of the organ of Corti. Fluid motion in the ST deflects an array of piezoelectric cantilevers; this deflection produces an electric potential on the outer electrodes of each cantilever that is transmitted into the surrounding perilymph. When implanted, this device would function as a low power, completely implantable artificial organ of Corti.

Methods

An implant was fabricated using batch MEMS processing techniques. A silicon backbone supports five 400µm wide, 5µm thick bimorph (Platinum/aluminum nitride (AlN) stack) cantilevers, each of which is designed to have a resonance corresponding to its tonotopic location in the guinea pig scala tympani (ST) (20-40kHz). A 1mm wide, 10µm thick parylene and gold ribbon cable extends 3cm from the probe to an electrode bay, where electrical connections to each cantilever are accessed. Actuation responses of the fabricated devices were measured using laser vibrometry.

Results

A model predicting the resonant behavior of cantilevers in a viscous fluid was used to determine the geometry of the array. Further modeling predicts the current output of the device in the guinea pig cochlea ST; this model predicts the device will produce 90dB SPL ABR thresholds when actuated by a 1Pa sound source. Fabrication challenges such as film stress passivation and selective etching have been identified and the next generation prototypes are designed to overcome them. First generation devices have been fabricated and are electrically addressable through the ribbon cable and a MEMS electrode bay (developed to monitor/control the output). Individually actuated cantilevers show good agreement with model predictions. *In vivo* implantation of inactive devices in the guinea pig for a week produced no infection but some granulation tissue surrounding the device.

Conclusion

A novel, completely implantable artificial organ of Corti was designed to passively restore hearing using a piezoelectric cantilever array. Initial *in vitro* electromechanical array element testing shows good agreement between predicted and measured actuated cantilever frequency response. Future work includes *in vitro* device response testing in water and ionic fluid to fully characterize the array behavior, as well as *in vivo* testing to measure ABR thresholds.

404 Correlation Between Intracranial Pressure and Skull Vibration in Bone Conduction of Cadaveric Human Whole Heads

Christof Röösl¹, Jae Hoon Sim¹, Xie Youzhou¹, Alex Huber¹

¹ENT Clinic, University Hospital Zurich, Zurich, Switzerland

Background

Several pathways including ear canal radiation, inertia of the ossicles and cochlear fluid, compression and expansion of the skull, and pressure transmission through soft tissues are considered to contribute to bone conduction hearing. The importance and frequency dependency of these pathways have not been comprehensively understood. Especially, the contribution of pathway via non-osseous skull contents such as brain content and CSF are controversially discussed. The aim of this study is to assess the correlation between intracranial

pressure and skull vibration on the promontory for bone conduction stimulation.

Methods

The measurements were performed on 3 human cadaver heads. The bone conductive stimuli of 100 dB SPL in the frequency range of 0.1 – 10 kHz were delivered to the cadaver heads via bone anchored hearing aid (BAHA). The BAHA was held in place with a 5-N steel headband at mastoid, forehead, eye, and neck. Additionally, it was percutaneously implanted at the mastoid and forehead. With the bone conductive stimulation, the motion of the cochlear promontory and intracranial pressure at the center of the head were measured simultaneously using a Laser Doppler Vibrometer and a hydrophone. An absolute static pressure sensor placed in the middle of the head during the measurement to monitor intracranial static pressure.

Results

Frequency dependency of the intracranial sound pressure differed from the corresponding dependency of the skull bone vibration measured at the cochlear promontory on the ipsilateral and contralateral sides. Further, the intracranial attenuation could be estimated from the difference of skull bone vibration between the ipsilateral and contralateral sides.

Conclusion

The presence of variation of intracranial sound pressure indicates that non-osseous skull contents may contribute to bone conduction hearing in some frequencies.

405 Functional and Morphological Effects of Variable Laser Stimulation Parameters at the Ear Drum Level

Gentiana I. Wenzel¹, Marc Kannengießer², Martin R. Sanger³, Dietmar J. Hecker¹, Cathleen Schreiter¹, Hubert H. Lim⁴, Hans-Jochen Foth³, Achim Langenbacher², Bernhard Schick¹

¹Saarland University Medical Center, Department of Otorhinolaryngology, ²University of Saarland, Institute of Experimental Ophthalmology, ³Technical University of Kaiserslautern, Department of Physics, ⁴University of Minnesota, Department of Biomedical Engineering

Background

Visible light can be used to activate the peripheral hearing organ when applied at the ear drum level (Wenzel et al. 2010). However, to enable the detection of complex sounds and intelligible speech perception, controlled frequency-specific activation spanning the audible frequency range is necessary. Using current laser technology, it is not possible to switch effectively between different laser sources, with different wave lengths, within the duration of a word. Therefore, the overall objective of our project is to establish methods for achieving frequency specific activation of the complete audible spectrum using monochrome laser pulses. As a first step, we analysed the electrophysiological and morphological effects of varying laser-pulse repetition rates in an animal model.

Methods

Click-Auditory Brainstem Responses (ABR) were recorded preoperatively in anesthetized guinea pigs to confirm normal hearing. A 100 µm diameter optic fiber was inserted into the outer ear canal and directed towards the ear drum. Optically-induced ABRs were recorded in response to laser stimulation with Q-switched 10 ns, 532 nm laser pulses from a diode-pumped solid state Nd:YAG laser (Xiton Photonics GmbH, Kaiserslautern, Germany). The animals were then sacrificed immediately after laser irradiation and the temporal bones were rapidly explanted and processed for histological analysis.

Results

Optical stimulation of the ear was possible with pulse energies from 0-17 µJ/pulse and repetition rates from 10 Hz - 20 kHz. Increasing the laser-repetition rate led to a superposition of the optically-induced ABRs. The morphological changes were dependent on the applied energy level, time of exposure, and pulse repetition rate.

Conclusion

These findings suggest that laser-pulse shaping based on variable temporal pulse distributions, a process that is well known in physics, applies for biological systems as well. Further studies investigating optimal pulse shaping strategies for the activation of the complete auditory spectrum as well as the biocompatibility of green light irradiation of the auditory system are under investigation.

406 Fabrication of Biomimetic Shaped Ceramic Ossicles and Evaluation of Their Vibration Performance Using Finite Element Method

Jeong-Hoon Oh¹, Jung-Seob Lee², Dong-Woo Cho², Sung Won Kim¹

¹The Catholic University of Korea, ²POSTECH

Background

Many three-dimensional geometric models of the human ossicles have been proposed and finite element modeling has distinct advantages in modeling the middle ear over circuit models that correspond indirectly with its structure and geometry. The object of this study was to evaluate vibration performance of synthetic ossicular chain fabricated by projection-based microstereolithography (pMSTL) and to compare its vibration characteristics with those of human ossicles. We also investigated the characteristics of the fabricated ossicular chain using finite element analysis method.

Methods

Synthetic ossicular scaffolds, which have same configuration of human ossicular chain, were created from hydroxyapatite, porogen and SK-cytec using pMSTL and CAD/CAM technology. Their vibration performances resulting from piezo-electric and signal analyzer were measured with laser vibrometer. Vibration characteristics of the ossicles were also measured by finite element analysis.

Results

Fabricated ossicles showed output resonance frequency of 528, 1344, 1921, 3584, 5505, 6060, 7168, 7894, 11488 and 17302 Hz with input resonance frequency of 5520 and 6849 Hz, which was comparable to known results of human ossicular chain. However, finite element analysis of the synthetic ossicular chain showed much lower resonance frequencies than the frequencies measured with vibrometer.

Conclusion

Fabricated ossicular chain using pMSTL and CAD/CAM technology may have similar vibration characteristics with those of human ossicular chain.

407 Design and Preliminary Testing of a Visually-Guided Hearing Aid

Gerald Kidd Jr.¹, Sylvain Favrot¹, Joseph Desloge², Timothy Streeter¹, Christine Mason¹
¹Boston University, ²Sensimetrics Corporation

Background

The defining complaint of listeners with sensorineural hearing loss (SNHL) is difficulty hearing in "noise." For most people with SNHL, hearing aids are the only effective treatment. Despite the many advances in hearing aid design over the past few decades the fundamental problem remains: how to selectively amplify the sounds the listener wishes to hear while excluding unwanted, interfering sounds. The goal of this work is to explore a new approach to amplification designed to facilitate sound source segregation and selection. This approach is based on the premise that only the listener can make the distinction between which sources deserve attention and which should be ignored, and therefore which sources should be amplified and which suppressed. In this study we describe initial efforts at designing a "visually-guided hearing aid" (VGHA) that senses where vision is directed and steers a beam of amplification in that direction.

Methods

The new prototype "hearing aid" couples an acoustic beam-forming microphone array to an eye-glasses-mounted eye-tracking device. The array consists of four pairs of cardioid microphones secured on the headband of a pair of earphones. The gaze angle sensed from the eye tracker is used to steer the acoustic look direction (ALD) of the array. Estimates of the benefit of the VGHA include acoustic measurements of array gain/attenuation as a function of azimuth surrounding the ALD and perceptual measurements of speech recognition under multitalker conditions. Furthermore, estimates were obtained of the time required for dynamic refocusing of the ALD during speech testing.

Results

Acoustic measurements conducted on the array in a mildly reverberant test environment indicate spatial tuning that varied with frequency but that provided a high degree of selectivity at frequencies above 2 kHz. Perceptual

measurements indicated that near-normal selectivity of a target talker may be achieved by the VGHA, as reflected in the magnitude of spatial release from speech-on-speech masking. The interface and components working together were able to reposition the ALD rapidly across a range of azimuths spanning roughly + 45°.

Conclusion

The approach embodied by the VGHA offers some advantages over current methods for amplification and sound source selection in uncertain and dynamic multitalker listening environments. The current prototype only tests the premise upon which the device depends and by no means comprises a wearable, useable device. However, as a platform for testing this new approach the VGHA appears to be useful.

408 Assessment of Temporal Resolution of Bone-Conducted Ultrasonic Hearing Using Psychophysical and Neuromagnetic Measurements

Seiji Nakagawa¹, Takuya Hotehama¹

¹National Institute of Advanced Industrial Science and Technology (AIST)

Background

Bone-conducted ultrasound (BCU) is perceived even by the profoundly sensorineural deaf. We have objectively proven the BCU perception by neurophysiological data and developed a novel hearing-aid using the BCU perception (BCU hearing aid: BCUHA) for the profoundly deaf, that transmits a 30-kHz bone-conducted carrier that is amplitude-modulated by speech or environmental sounds. In this study, the temporal resolution of the BCUHA hearing were assessed by psychophysical and neuromagnetic measurements in normal-hearing and profoundly deaf subjects.

Methods

To investigate the temporal resolution of the BCUHA hearing psychophysically, the temporal transfer modulation functions (TMTFs) were measured. TMTF shows the threshold of sinusoidal amplitude-modulation (SAM) detection as a function of modulation frequencies. The SAM detection threshold is determined systematically by measuring a detection of modulation depth. TMTF for 10-, 20-, and 30-kHz bone-conducted (BC) sounds were measured. Further, mismatch fields (MMFs) for changes of stimulus-duration were recorded. MMFs for 10-, 20-, and 30-kHz bone-conducted tone bursts amplitude-modulated by 1 kHz, and a 1-kHz air-conducted (AC) tone burst were measured in different sessions. Each session consisted of one standard stimulus (75-ms duration, 85%) and three types of deviant stimuli (52.5-, 37.5-, and 22.5-ms durations, 5 % each).

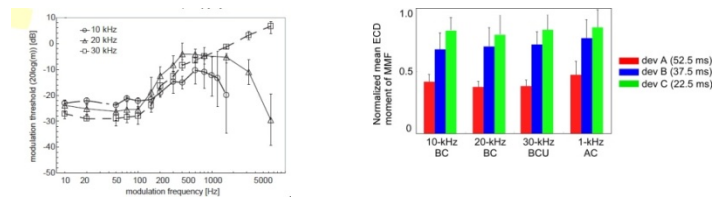
Results

The psychophysical detection threshold curves for all carriers commonly showed the low-pass characteristics at low modulation frequencies; the thresholds were roughly constant at modulation frequencies from 10 to about 100

Hz and then begin to increase at about 100-150 Hz as the modulation frequency increases. Meanwhile, clear MMFs were observed for all types of stimuli. Equivalent current dipoles (ECDs) moments of MMFs were significantly different between three types of BC and AC stimuli (10-kHz BC:20-kHz BC:30-kHz BC:1-kHz AC=0.95:0.92:0.91:1.0), however, ECD moments of BC stimuli were close to that of AC stimulus.

Conclusion

The both results obtained in the psychophysical and neuromagnetic measurements indicated that the BC/UA hearing has nearly equal temporal resolution to that of lower-frequency BC and AC sounds. These results also provide useful information for further developments of the BC/UA.



409 Development of a Bedside Gaze Stabilization Test

Choongheon Lee¹, Julie Honaker¹

¹University of Nebraska-Lincoln

Background

The gaze stabilization test (GST) is used not only in examining gaze stability required by daily life activities such as walking, running, and driving, but also in identifying unilateral or bilateral vestibular deficits. However, a computerized GST (CGST) is an expensive assessment which cannot be commonly used in most balance and vestibular clinics. Validation of low-cost and low-technical clinical bedside tests is required to decrease health care costs.

Methods

All twenty healthy volunteers were between the ages of 20-60 ears and had normal extra-ocular range-of-motion. This study measured the effect of a bedside GST (BGST) as a validated screening tool to accurately identify adults with normal inner ear balance function, as well as the test-retest reliability of BGST when re-assessed 5-7 days after the initial testing session. Subjects were instructed to identify a visual target placed at 0.2 logMAR increased from static visual acuity score while actively and passively performing head movements in the yaw plane at an initial screening velocity of 130 degs/sec.

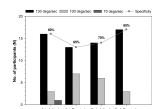
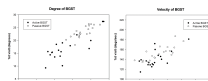
Results

The main outcome was a strong positive correlation in both active and passive BGST head movement amplitude degree and head movement velocity. Our finding showed that passive head movements had good specificity (85%) to identify healthy individuals with functioning peripheral vestibular systems. The BGST seems to be a reliable screening assessment to identify normal functional

performance of the peripheral vestibular system to maintain stable gaze while moving the head at a screening velocity of 130 degs/sec and has good test-retest reliability in head movement amplitude degree ($r = 0.795$) and head movement velocity ($r = 0.797$) of passive BGST within two testing sessions.

Conclusion

A low-cost, low-tech (bedside) version of the GST may not only play an essential part in reducing the burden of medical expenses for adults but may also be useful as an assessment tool to screen individuals with vestibular impairment. In this study, the BGST screening assessment was deemed to be a measure to identify individuals with normal reported peripheral vestibular function and it showed good test-retest reliability in degree and velocity of passive BGST. The aim of this future research is to establish a screening cut-point score in terms of the maximum head velocity that will identify individuals with both normal peripheral vestibular function and peripheral vestibular impairment.



410 Masking Effects in Patients with Auditory Neuropathy - Possible Involvement of Suppression Mechanism Caused by Normal Outer Hair Cell Function -

Kazuha Oda¹, Tetsuaki Kawase^{1,2}, Yusuke Takata¹, Hiromitsu Miyazaki¹, Hiroshi Hidaka¹, Toshimitsu Kobayashi¹

¹Department of Otolaryngology - Head and Neck Surgery, Tohoku University Graduate School of Medicine,

²Laboratory of Rehabilitative Auditory Science, Tohoku Univ. Grad School of Biomedical Engineering

Background

Masking is a phenomenon by which by the presentation of an interfering sound (masker) decreases a signal's audibility. Noise audiometry is a proposed method for assessing hearing acuity in noisy environments based on measurement of auditory thresholds in the presence of masking noise. Auditory neuropathy is a type of sensorineural hearing loss characterized by absence or marked abnormality of auditory brainstem responses beyond that expected for the degree of hearing loss, with preserved activity of the outer hair cells. Noise audiometry has not been examined extensively in patients with auditory neuropathy, although speech intelligibility in patients with retrocochlear lesion often deteriorates remarkably in the presence of masking noise. To investigate the possible mechanism of the characteristic masking feature of the disease, this study reviewed the

findings of noise audiometry and pathogenesis retrospectively in patients with auditory neuropathy.

Methods

Study Design: Retrospective chart review.

Patients: 55 ears of 30 patients with sensorineural hearing loss who underwent noise audiometry at our institute since 2010 in response to complaints of hearing difficulty in noisy environments.

Main Outcome Measures: Masked threshold for narrow band and white noise.

Results

Masking effects in patients with auditory neuropathy were significantly greater than in patients with hearing loss of other types. Specifically, masking effects of broad-band white noise were greater than those of narrow-band noise. With white noise, masking effects were observed even in the elevated threshold region, where little contribution of excitatory masking effect is expected.

Conclusion

This retrospective study of noise audiometry conducted at our institute revealed strong masking effects, especially in patients with auditory neuropathy. Fragility for the masker in patients with retrocochlear lesion is often explained as "easy fatigability" or "easy adaptability", known as a temporal threshold shift in Bekesy audiometry. However, such an explanation might be inappropriate to explain the masking phenomenon caused by the lower level masker, which presumably does not cause excitatory masking effects as a line busy or an adaptation mechanism. We speculate that other masking effects originating from cochlear nonlinearity caused by outer hair cells, such as "suppression mechanism", are involved in masking by a lower level broad-band masker because auditory neuropathy type hearing loss exhibits normal outer hair cell function.

411 Clinical Features and Prognosis of Hearing Impairment Due to Meningeal Carcinomatosis

Go Inokuchi¹, Hirokazu Komatsu¹, Naoki Sawada¹, Daisuke Yamashita², Kazuo Kumoi¹

¹Nishi-Kobe Medical Center, ²Kobe University Graduate School of Medicine

Background

Meningeal carcinomatosis is uncommon and characterized by multifocal spread of neoplastic cells in the leptomeninges. A variety of multiple neurological symptoms and known history of malignancy are usually the signs suggesting the diagnosis. Only a few reports of hearing impairment due to meningeal carcinomatosis have been reported. By reason of their poor vital prognosis, hearing impairment has not been evaluated and discussed enough. Here we presented four cases of progressive hearing impairment due to meningeal carcinomatosis.

Methods

We conducted a retrospective chart analysis of patients demographic, audiograms, and MRI findings from case series presenting hearing impairment due to meningeal carcinomatosis. Auditory brainstem response (ABR) and distortion product otoacoustic emission (DPOAE) were also tested.

Results

Primary lesions were two lung adenocarcinoma, one esophageal carcinoma and malignant lymphoma respectively. Diagnosis was made based on past history of malignancy, MRI findings, and the cytology in cerebrospinal fluid. Major complaining symptoms were rapidly progressed hearing impairment, unsteadiness, and tinnitus. Facial nerve palsy was not noted at first, but two cases presented in later stages. All cases showed enhancement of vestibule-cochlear nerves on gadolinium-weighted MRI. Two cases of internal auditory canal metastasis were revealed on high-resolution MRI focused on internal auditory canal. ABR obtained in two cases showed prolonged latency between wave I and III. The response of DPOAE was initially seen in lower frequencies, but finally lost completely. Hearing impairment rapidly progressed to deafness even in the patient with high-dose steroids treatment. Hearing improvement was not observed, except for the case with malignant lymphoma.

Conclusion

Hearing prognosis was poor in hearing impairment due to meningeal carcinomatosis. Steroids treatment had the least effect on preventing the progression of hearing impairment. Internal auditory canal metastasis often coexisted with meningeal carcinomatosis and suggested cochlear dysfunction. Both gadolinium enhancement and high-resolution MRI focused on internal auditory canal were recommended to diagnose the meningeal carcinomatosis as soon as possible. Clinical course and results of ABR and DPOAE suggested that cochlear nerve dysfunction preceded and cochlear dysfunction developed later.

412 Aided ASSR on a Cadaver: Relevance in the Clinic

Shruti Deshpande (Balvalli)¹, Peter Scheifele¹, Michael Scott¹, Aniruddha Deshpande¹, John Clark¹, Gloria Valencia¹, Robert Keith¹

¹University of Cincinnati

Background

Auditory Steady State Response (ASSR) is used to determine aided hearing thresholds, set hearing aid (HA) parameters and verify HA benefit. Aided auditory evoked potentials (AEPs) can be affected by electromagnetic interferences related to the HA (Croese et al, 2011). Most studies on aided ASSR, use an electrode montage with reference electrode physically distant from the HA (e.g. Shemesh et al., 2012); however studies (Picton et al., 1998; Stroebel et al., 2007) have used the mastoid ipsilateral to the HA for the reference electrode.

Additionally, braiding minimizes electrical interference (Stecker and Patterson, 1996). However, AEP studies, especially ones using devices like HAs, do not mention if electrode leads were braided. The purpose of this study was to investigate if the amplitude spectrum of the ASSR is affected by 1. HA-related interference based on the position of the reference electrode (ipsilateral vs. contralateral); 2. Braiding electrode leads.

Methods

An adult male cadaver was fitted monaurally with an Oticon Safari SuperPower HA to record “pure electrical interference” without interaction with physiological responses. HA specifications are listed in Table1 and the setup is described in Figure1. Recordings were made from the forehead (Fz) to 1. Ipsilateral mastoid; 2. Contralateral mastoid; with clavicle as ground and with electrode leads unbraided vs. braided. Before data collection, we recorded ASSR with the stimulus at 90 dB SPL but with the HA ‘OFF’ and the stimulus at 0 dB SPL but the HA ‘ON’ to ensure that possible interferences were from the HA. Multi-frequency ASSRs were recorded from 90- to 40 dB SPL in 10 dB decrements for each montage- unbraided and braided. Also, single frequency ASSRs were recorded at 90 dB SPL for each montage- unbraided and braided.

Results

A peak indicating electrical interference was observed in the amplitude spectrum of the multi-frequency ASSR at approximately 120 Hz for the ipsilateral-unbraided condition for all intensities tested and also for the single frequency stimulus, ipsilateral-unbraided condition at 90 dB SPL. Such interference can potentially affect the acquisition of a response clinically. However, this interference disappears for ipsilateral-braided, contralateral-unbraided and contra-braided conditions (Figure2).

Conclusion

Positioning the reference electrode away from the HA and braiding electrode leads is essential while recording AEPs, especially in the presence of a HA. This study is unique in nature because it highlights the possibility of electrical interference from a HA and emphasizes the utilization of simple techniques that can eliminate such interference.

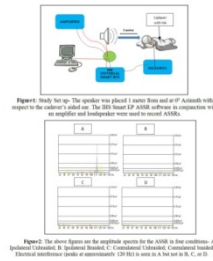


Figure 1: The setup for recording ASSR. The amplifier was placed 2 meters from the HA. The stimulus was presented to the subject's ear with the HA 'OFF' and the stimulus was presented to the subject's ear with the HA 'ON'. The stimulus was presented to the subject's ear with the HA 'OFF' and the stimulus was presented to the subject's ear with the HA 'ON'.

Specifications: Oticon Safari SuperPower

OSPL90	Peak
	1600 Hz
	Average
Full-on gain	Peak
	1600 Hz
	Average
Frequency Range	
Total Harmonic Distortion (input: 70 dB SPL)	500 Hz
	800 Hz
	1600 Hz
Equivalent Input Noise Level	Omni
	Dir

Table1: The Oticon Safari SuperPower hearing aid was used in the present study. The hearing aid specifications are listed in the table above.

413 Effect of Threshold Sound Conditioning on Pure-Tone Hearing Thresholds in Human Subjects with Sensorineural Hearing Loss

Eunye Kwak¹, Sangyeop Kwak²

¹Earlogic Auditory Research Institute, ²Earlogic Korea, Inc

Background

Sensorineural hearing loss has long been considered to be an irreversible phenomenon. Most likely for this reason, there has been little or no attempt to investigate the effect of sound conditioning on the hearing threshold in people with sensorineural hearing loss. Because we have observed the same phenomenon (i.e., a hearing threshold decrease due to sound conditioning) during research on tinnitus treatment, we decided to investigate the effect of sound conditioning on pure-tone hearing threshold in people with sensorineural hearing loss. Sound conditioning using a non-traumatic, moderate-level acoustic signal is a well-studied method to protect against age-related or noise-induced hearing loss in animals. In humans, acoustic signals provided at the hearing threshold level or slightly higher than the hearing threshold level have been studied for the treatment of hyperacusis and tinnitus and have been found to have positive effects. In this study, we adopted the term j° sound conditioning j_{\pm} instead of j° sound training j_{\pm} because the subjects were not asked to pay attention to the acoustic signals. In addition, because the subjects in the experimental group were instructed to listen to the acoustic signals at their hearing threshold levels (i.e., a barely audible level), we named the experimental method j° threshold sound conditioning (TSC) j_{\pm} .

Methods

We examined the changes in the pure-tone hearing threshold after 2~3 weeks of TSC (i.e., sound conditioning with a frequency-specific acoustic signal at the hearing threshold level) or music listening (i.e., listening to music at a comfortable listening level). In addition, we examined

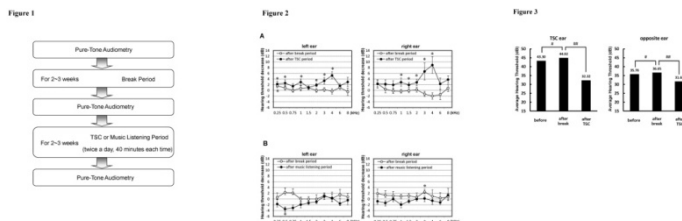
hearing threshold changes without TSC or music listening in both groups.

Results

After the music listening period in the control group, the only change observed was a hearing threshold increase at one frequency. In contrast, statistically significant decreases in the hearing threshold were observed at several frequencies after the TSC period. Clinically significant threshold decreases of 10 dB or more were observed at 9 subjects in the experimental group. In total, clinically significant threshold decreases were observed for 33 frequencies. The average hearing threshold of the 20 TSC frequencies before the break period, after the break period, and after the TSC period was analyzed. A hearing threshold decrease of 12.6 dB was observed for the TSC frequencies of the TSC ear ($P < 0.001$).

Conclusion

Threshold sound conditioning can decrease pure-tone hearing thresholds in people with sensorineural hearing loss.



414 Using the Cochlear Microphonic as a Clinical Diagnostic Procedure to Detect the Cochlear Location of Damage of Outer Hair Cells

Marcello Peppi^{1,2}, Mark Chertoff^{3,4}

¹University of Kansas Medical Center, ²Department of Hearing and Speech, ³University of Kansas Medical Center, ⁴Department of Hearing and Speech

Background

The progression of new medical treatments for curing sensorineural hearing loss requires the development of new diagnostic procedures that localize the damaged site/s within the cochlea, and/or auditory nerve. The goal of our research is to investigate the cochlear microphonic (CM) as a clinical diagnostic procedure to detect the location and amount of damage in hearing impaired ears.

The CM is an electrophysiological signal generated from receptor currents passing through outer hair cells (OHCs). We have recently shown that CM amplitude, in response to a low frequency tone embedded in filtered noise, increases as the high-frequency cutoff decreases (Chertoff, Earl, Diaz, and Sorensen, (in press)). When the CM amplitude is normalized relative to the unmasked response and plotted as a function of cochlear distance from the apex, the growth is defined as the cumulative amplitude function (CAF).

Methods

We have studied the CAFs in 6-week-old Mongolian gerbil by recording CM responses to a 762 Hz tone from 80 to 40 dB SPL levels embedded in 25 high-pass filtered noise conditions.

Results

We observed that the CAFs reached an asymptote at distances more apically than the CAF for high level signals. This suggests an apical shift in the contribution of OHCs to the CAF. An important question is the contribution of signals coming from other cochlear structures to the CAF. That is, at low frequencies, phase-locked action potentials may also contribute to the electrophysiological cochlear response.

Conclusion

Thus determining the contribution of neural potentials to the CAF will be important for determining the specificity of the CAF to OHCs.

Supported by NIH NIDCD R33DC011096-01

415 Steps Towards Untangling the Enigma of Auditory Processing Disorder

Johanna Barry¹, Sophie Richardson¹, David Moore¹

¹MRC Institute of Hearing Research

Background

Listening problems in children, despite apparently normal hearing, are common in a variety of developmental learning disorders. In paediatric audiology, these problems are often diagnosed as 'auditory processing disorder' (APD). The validity of APD as a diagnostic category is controversial since many children receiving a diagnosis of APD are, largely, indistinguishable from children with other disorders such as specific language impairment (SLI). It has been argued that the diagnostic label that children receive reflects referral route rather than valid differences in auditory or linguistic abilities. To counter this, we hypothesise that there are clear differences in presenting symptoms and that these determine the referral route a child is most likely to follow.

Testing this hypothesis requires three steps, two of which are addressed here.

Methods

First we developed a psychometrically robust tool for assessing the listening difficulties. Parents of 950 children indicated the extent to which they agreed with 84 possible presenting symptoms. Based on their responses, five factors were extracted: Online speech/nonspeech processing; Environmental sensitivity; Language & literacy; Pragmatic skills; and, Memory. Second, we compared the responses of parents of 3 groups of children commonly thought to have listening difficulties i.e., SLI (n=23); SLI/APD (n=18) and dyslexia (n=19).

Results

The 3 groups of children received significantly different parental evaluations [$F(2, 57) 4.58, p = .014$], and they

could be ordered hierarchically in terms of severity of listening difficulties, from least (dyslexics) to most (SLI/APD) severely affected on the latent traits gauged by this questionnaire. The dyslexics scored in the normal range on all factors except Language & literacy and Memory. The children with SLI/APD had difficulties across all latent traits except Environmental sensitivity.

Conclusion

The questionnaire developed suggests there are measurable differences between the different groups assessed here. In the final step towards answering our primary research question, we will use the questionnaire to compare children clinically referred for assessment for APD, with children clinically referred to speech and language therapists and to determine how and if these two groups of children differ in their presenting symptoms.

416 Crossed and Uncrossed Acoustic Reflex Growth Functions in Normal Hearing Children, Adults and Children with Auditory Processing Difficulties

Udit Saxena¹, Chris Allan¹, Prudence Allen¹

¹National Centre for Audiology

Background

Children who experience difficulty understanding sounds and learning through their hearing in spite of normal sensitivity are often considered for evaluation of auditory processing difficulties. Professional associations recommend a battery of tests that assess behavioral function, often in difficult listening situations, and the evaluation of underlying neural integrity of the auditory system using objective measures. But there is little agreement on what objective measures should be used. Acoustic reflex measurements may provide a sensitive objective measure of lower brainstem integrity, particularly when patterns of crossed and uncrossed reflexes are examined. Our previous work has noted a higher incidence of threshold elevations or absent acoustic reflexes in children with suspected Auditory Processing Disorder (APD), especially in the crossed reflex pathway. This study presents a more detailed description of acoustic reflex characteristics in children with suspected APD through the measurement of acoustic reflex growth functions. These functions describe the rate of change in middle ear impedance with changes in stimulus level. Evaluations of both crossed and uncrossed pathways were examined.

Methods

Uncrossed (ipsilateral stimulus and recording) and crossed (contralateral stimulus and recording) reflexes were recorded in normal hearing adults and children, and in children with suspected APD. Stimuli were pure tones of 500, 1000 and 2000 Hz. The impedance change in response to stimulation was recorded over a 15 dB range above threshold and data were fitted with a linear function. Because absolute magnitude of the reflexes varies with individual differences in static compliance, the ratios of slopes in uncrossed and crossed conditions were

calculated within individuals and conditions (right and left ears at 3 frequencies).

Results

Children with suspected APD showed larger slope ratios (uncrossed/crossed), on average exceeding 2. In contrast, slope ratios were smaller in the normal hearing adults and children, on average 1-1.5. There were no significant differences as a function of stimulus frequency or ear.

Conclusion

Larger slope ratios in the children with suspected APD resulted from shallower growth of the amplitude of the crossed reflex with increasing stimulus level when compared to that of the uncrossed reflex. This pattern may suggest reduced neural integrity in the auditory brainstem pathways of many children with APD. The relationship between acoustic reflex abnormalities and functional hearing, especially in noise, may be significant.

417 Interaction Between Cognition and Audibility in Speech-In-Noise Hearing in Middle Aged People

David Moore^{1,2}, Robert Pierzycki², Heather Fortnum², Abigail McCormack^{1,2}, Mark Edmundson-Jones², Oliver Zobay¹

¹MRC Institute of Hearing Research, ²NIHR Nottingham Hearing Biomedical Research Unit

Background

The launch of UK Biobank (www.ukbiobank.ac.uk) opened a major international opportunity to address an almost limitless range of issues in translational hearing research. Epidemiological data from the 1980s showed that 21% of the UK population aged 40-69 years had a hearing loss (Davis, Hearing in Adults, 1995), with a higher incidence predicted as the population ages. However, recent US evidence has found that as people live longer they retain sensitive hearing later in life (Zhan et al, Am J Epidemiol, 2010, 171, 260-6). No recent comprehensive UK data on the prevalence of hearing disability are available. There has never been a large scale, quasi-random sampling of performance on a speech-in-noise (SiN) test. By comparing self-reported hearing disability in the older (Davis, 1995) and current (Biobank) samples with objective measures of audiometry (older sample), SiN and cognitive performance (Biobank), we will test the hypothesis that a decline in cognition with age will be associated with a decline in SiN hearing that is greater than predicted by audiometry.

Methods

About 500,000 people from across England, Scotland and Wales aged between 40-69 years in 2006-2010 participated in Biobank. About 170,000 completed a specially developed version of the digit triplet test (DTT), an adaptive, high redundancy speech-in-(speech-shaped) noise (SiN) test. In addition to the hearing tests, participants provided data on a wide range of other markers, including age, sex, lifestyle, cognition, employment, socioeconomic, nutrition, medication and

other medical variables that have all been linked to hearing. Participants also provided biosamples (blood, saliva, urine) that can be used for testing relationships between hearing and its underlying biology (e.g. genomics and metabolomics). Cognitive tests were fluid intelligence, executive function, processing speed, and auditory (digit recall) working memory.

Results

25.6% reported in a touchscreen questionnaire that they have difficulty with their hearing and 37.5% found it difficult to follow a conversation if there was background noise. Other summary data (www.biobank.otsu.ox.ac.uk) show mean DTT response thresholds (-6.6 dB S/N) and cognitive test scores in line with expectations. Linking data for Biobank that will enable the hypothesis to be addressed are being released during October 2012.

Conclusion

In addition to the above data, we will present full UK Biobank data on the DTT that will show the detailed relationship between audibility, SiN perception and cognitive performance.

418 Test Performance of a Computer Version of the Digits-In-Noise Test for Adult Hearing Screening

M. Patrick Feeney^{1,2}, Robert L. Folmer^{1,2}, Jay Vachhani¹, Garnett P. McMillan^{1,3}, Charles S. Watson⁴, Gary R. Kidd⁵

¹VA National Center for Rehabilitative Auditory Research, Portland, OR, ²Dept. of Otolaryngology, Head and Neck Surgery, Oregon Health and Science University, ³Dept. of Public Health and Preventive Medicine, Oregon Health and Science University, ⁴Communication Disorders Technology, Inc., Bloomington, IN, ⁵Dept. of Speech and Hearing Sciences, Indiana University

Background

The telephone Digits-in-Noise (DIN) hearing screening test has been used in the Netherlands and other European countries since about 2005. Watson et al. (2012) developed an English version of the test with a Middle American dialect. The test uses spoken three-digit sequences presented in speech-spectrum background noise over the telephone. The signal-to-noise ratio for 50%-correct performance is obtained using an adaptive tracking procedure. The purpose of the present study was to evaluate the DIN test for use on a computer using a sound card and headphones. For the purposes of this study, the American English version of the telephone DIN test was modified for use with a computer interface by Watson and Kidd. We were interested in evaluating the use of the computer version of the DIN as a screening test for hearing loss in adults. It was expected that performance might differ somewhat from the telephone version of the test given the greater signal bandwidth available with the headphones used (Sennheiser HDA 200) compared to the telephone, and the new set of recorded sequences selected for this version.

Methods

Forty subjects were recruited for the study; 16 females and 24 males with mean age of 52.2 years. There were 32 ears with normal hearing and 48 ears with sensorineural hearing loss defined as having one or more pure-tone thresholds at 10 frequencies from 250 to 8000 Hz ≥ 30 dB HL. No subject had an audiometric air-bone gap >10 dB. Following pure-tone audiometric testing in a sound-treated booth, subjects were seated in a quiet room for computerized DIN testing. Subjects followed on-screen instructions for completing a few training trials and then started the test. The test was completed on the right ear and then the left.

Results

For a hearing loss criterion of 3-frequency pure-tone average (1, 2 and 4 kHz) ≥ 25 dB, the area under the ROC curve (AROC) was 0.95. When a criterion of hearing loss was set at two or more frequencies from 250 to 8000 Hz ≥ 30 dB HL, the AROC was 0.96.

Conclusion

The computer version of the DIN demonstrated excellent properties for our sample of 32 ears with normal hearing and 48 ears with sensorineural hearing loss. The excellent AROC results (≥ 0.950) suggest that this version of the DIN should be very useful for adult hearing screening.

419 Which Children Should Be Considered Candidates for Bilateral Cochlear Implantation?

Rosemary Lovett¹, Deborah Vickers¹, Quentin Summerfield²

¹University College London, ²University of York

Background

We are conducting a longitudinal comparison of outcomes for children with bilateral cochlear implants and children with bilateral acoustic hearing aids. The goal is to define a criterion of candidacy for pediatric bilateral cochlear implantation.

Methods

Twenty-seven of the participants use bilateral cochlear implants and have severe-to-profound hearing impairment. Forty-one of the participants use bilateral acoustic hearing aids and have hearing impairment ranging from moderate to profound. Children are assessed twice with an interval of a year between assessments. To date, all children have completed the first assessment, aged 4.3 years on average (range 3.0 to 6.3 years). Participants completed assessments of: 1) language skill; 2) sound-source localization; 3) speech perception in quiet, in random noise, and in babble.

Results

For each outcome measure, a regression function was used to characterize the relationship between unaided hearing level and performance for children with acoustic hearing aids. The distribution of scores for implanted children was used to calculate, for a newly-diagnosed child

with a known hearing level, the odds of better performance with implants than with hearing aids. A criterion of candidacy can be defined as the most advantageous hearing level for which the odds of better performance with implants exceed an acceptable ratio, such as 4 to 1.

As predicted, the results varied with the outcome measure. Based on the results of the first assessment, the four-frequency pure-tone average hearing level (PTA) associated with odds of 4 to 1 was 90 dB (speech perception in quiet) and 95 dB (language skills). The remaining outcome measures were not suitable for the proposed method of data analysis, because there was insufficient overlap of the ranges of scores shown by children with cochlear implants and children with hearing aids.

Conclusion

Based on the results of the first assessment, children with PTA greater than 90 dB should be considered candidates for bilateral cochlear implantation. We will present results from the second assessment at the conference. Supported by Action on Hearing Loss.

420 Speech Discrimination and Spatial Release from Masking in Toddlers with Cochlear Implants

Christi Hess¹, Jan Edwards¹, Ruth Litovsky¹
¹University of Wisconsin-Madison

Background

Bilateral cochlear implants (BiCIs) have been shown to promote the development of spatial hearing skills in children and adults, but little is known about the role of bilateral stimulation in enhancing language and speech reception in infants and toddlers. In addition, the difference in performance between toddlers with unilateral cochlear implants (UCIs) and BiCIs remains unexplored. We tested two hypotheses:

1. Toddlers with BiCIs will discriminate minimal pair contrasts that differ in voice and/or place of articulation with higher accuracy than toddlers with UCIs because they receive “two looks” at the speech signal.
2. Toddlers with BiCIs will show more spatial release from masking than toddlers with UCIs.

Methods

Toddlers with UCIs and BiCIs (24-36 mo.) were tested. Experiment 1: In a novel Reaching for Sound paradigm, Toddlers were trained to reach for an object whose location the correct stimulus, and were reinforced for correct responses (toy, snack, sticker, etc.). The stimulus consists of the carrier phrase “I’m hiding under” followed by one of the three test words (bee, pea, or key). The locations for the discrimination set are randomized within each group of toddlers (e.g., pea-Left vs. bee-Right), and percent correct was recorded. Experiment 2: Using a computerized 4 alternative forced choice (AFC) task, we adaptively measured speech reception thresholds (SRTs) in quiet and in the presence of a masker whose location was varied between 0° and 90°.

Results

Preliminary results indicate that in Experiment 1 NH toddlers have high %correct scores, i.e., clear discrimination of all speech contrasts, while toddlers with BiCI or UCI have low %correct scores. As hypothesized, toddlers with CIs discriminate voicing contrasts with higher accuracy than place contrasts, potentially due to temporal information being presented more reliably than spectral cues by CI processors. In Experiment 2 NH toddlers demonstrate a benefit when target and masker are spatially separated while toddlers with BiCIs and UCIs are highly variable in their performance on this task.

Conclusion

Speech discrimination results to date suggest that: (1) In implanted toddlers, speech discrimination abilities develop faster for temporally-based speech cues than spectrally-based cues, but thus far there is no measurable difference between UCI and BiCI users. (2) The rate of development in NH toddlers is unknown, because they perform equally well with all stimuli. NH toddlers show a benefit when target and masker are spatially separated while toddlers with BiCIs and UCIs have not.

421 Acoustic Evaluation of Ambient and Performance Noise in Georgia Aquarium

Aniruddha Deshpande¹, Whitney Brinker¹, Peter Scheifele¹

¹University of Cincinnati

Background

Many aquaria hold marine mammal shows for entertainment and educational purposes. Most of these performances are delivered over public announcement (PA) systems. The hearing safety of exhibits and audience is of utmost importance before, during and after the performances. Georgia Aquarium invited the FETCHLAB to ensure that their new dolphinarium met the regulated noise standards. FETCHLAB stands for Facility for Education and Testing of Canine Hearing & Laboratory for Animal Bioacoustics. In addition to testing canine hearing, the FETCHLAB performs noise assessments of animal housing facilities such as kennels and aquaria. We performed both underwater and in-air noise assessments of the dolphinarium; though the focus of this paper is the in-air acoustic evaluation as it relates to human hearing.

Methods

Sound intensity measurements were made at various locations throughout the dolphinarium theatre and stage. The places to be measured were selected in reference to where patrons of the show would be seated during a performance in the theatre. Sound intensity measures were taken using two calibrated sound level meters (SLMs) - Quest Diagnostics and B&K. Burst measurements (e.g. water effects) were collected using a ‘fast’ SLM response; and measurements of songs and theatrics were collected using a ‘slow’ response. Two sets of recordings were made – ambient and performance noise levels – at 15 locations in the theatre (Figure 1). In

addition, noise measurements were performed in the pump rooms to ensure hearing safety of workers and performers.

Results

The recordings revealed average ambient noise levels of 61.4dBA (range: 53-69dBA) and performance noise levels of 96.9dBA (range: 92.6-101.1dBA) for the story track and 98.1dBA (range: 92.3-104.7dBA) for the music track. Noise level in the main pump room was measured at 87.4dBA (range: 86.9-88dBA) and that in the supporting equipment room at 74.1dBA (range: 72.2-76.1dBA).

Conclusion

According to Occupational Safety and Health Administration (OSHA) guidelines, these levels, although high, are well within the safe noise exposure levels as long as the exposure time is limited to 8 hours/day. Use of hearing protective devices (e.g. ear muffs, ear plugs) is recommended for hearing conservation. Annual hearing screenings of workers and annual noise measurements at the dolphinarium are recommended. Future research may focus on the use of noise dosimeters worn by workers to measure the noise dose that they are exposed to in a typical work-day.

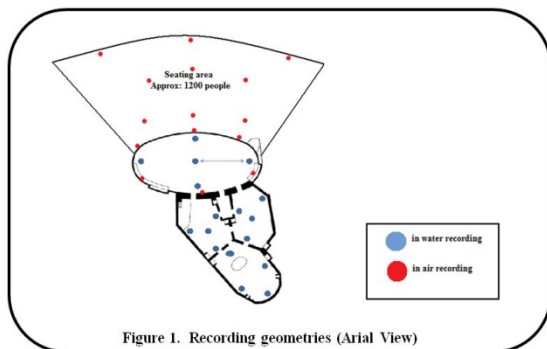


Figure 1. Recording geometries (Aerial View)

422 Reliability of the Reference Sound Pressure Level (RSPL) for Korean Speech Audiometry

Junghak Lee¹, Jinsook Kim²

¹Hallym University of Graduate Studies, ²Hallym University

Background

The reference sound pressure level (RSPL) for speech audiometry is established based on the speech recognition threshold (SRT) measured by standardized words and procedures (ISO 8253-3, IEC 60645-2). The purpose of this study was to examine the reliability of the RSPL for Korean speech audiometry using 36 bisyllabic words which were adopted as the Korean standard words for speech audiometry (KS I ISO 8253-3-2009).

Methods

Subjects were 230 normal hearing persons from 5 universities over the country aged between 18 years and 25 years. Criteria of subjects were type A tympanometry and pure tone thresholds less than 10 dB HL from 250 Hz to 8000 Hz. SRTs were measured by the descending method described in ISO 8253-3 only at the better ear

based on the PTA or right ear if PTAs were equal using 36 bisyllabic words which consist of 3 sets and each set has 12 test items. Retest of SRT was performed for the same subject about an hour after the first test. was based on mean difference, correlation, standard error of measurement (SEM) and 95 % confidence interval (CI) were calculated for test-retest reliability of the RSPL for Korean speech audiometry.

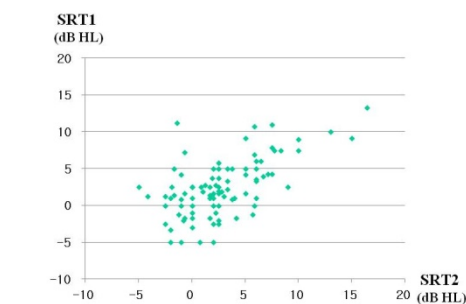
Results

Mean SRTs for the test and retest were 23.45 and 23.18 dB SPL with the standard deviations of 3.79 dB and 4.02 dB, respectively, which was not statistically significant (paired t-test, $p > .05$). Correlation between two tests was significant ($r=0.73$, $p=.000$) and SEM was 1.97 dB. Finally, CI of 95% was between 19.51 and 27.39 dB SPL for the RSPL of Korean speech audiometry.

Conclusion

The reliability of the RSPL for Korean speech audiometry is considerably high based on the mean difference, correlation and CI. Therefore, it is suggested that Korean RSPL be 23.45 dB SPL for speech audiometry, which is 3.45 dB greater than English RSPL.

Scattergram of Test-Retest Results



Hallym University of Graduate Studies

423 Measuring Cochlear Ischemia Using a Combined Dual-Wavelength Laser Speckle Contrast Imaging and Doppler Optical Microangiography System

Roberto Reif¹, Jia Qin¹, Lei Shi¹, Suzan Dziennis¹, Zhongwei Zhi¹, Alfred Nuttall², Ruikang Wang¹
¹University of Washington, ²OHSU

Background

Several hearing disorders such as noise-induced hearing loss, age related hearing loss, sudden sensorineural hearing loss, tinnitus and Ménière's disease, have been related to cochlear ischemia. Cochlear ischemia is an understudied area of research due to the lack of tools available. It has been difficult to obtain information regarding cochlea ischemia in humans given that the invasiveness of the existing techniques carries the risk of increasing the functional loss. Understanding the mechanisms underlying the pathophysiology of the cochlear microcirculation and oxygenation in a non-invasive manner and in vivo is of fundamental clinical

importance, and may enable more effective understanding and management of these disorders.

Methods

A synchronized dual-wavelength laser speckle contrast imaging (DWLSCI) system and a Doppler optical microangiography (DOMAG) system was developed, and used to determine several ischemic parameters in the cochlea due to a systemic hypoxic challenge. DWLSCI can obtain two-dimensional data (the system averages the signal within a small volume of tissue), and was used to determine the changes in cochlear blood flow, and the concentrations of oxyhemoglobin (HbO), deoxyhemoglobin (Hb) and total hemoglobin (HbT) in mice. DOMAG can obtain three-dimensional data, and was used to determine the changes in cochlear blood flow with single vessel resolution.

Results

The changes in the concentrations of Hb, HbO and HbT, as well as the changes in cochlear blood flow were monitored through time. During the hypoxic challenge there was an increase and decrease in Hb and HbO, respectively, and a slight decrease in HbT. The rate of change in the concentrations of Hb and HbO were quantified during and after the hypoxic challenge. The cochlear blood flow decreased during the challenge.

Conclusion

The ability to simultaneously measure these ischemic parameters with high spatio-temporal resolution will allow the detailed quantitative analysis of several hearing disorders, and will be useful for diagnosing and developing treatments.

424 Miami Otogenetic Program: Implementing Genomic Medicine in Clinical Care of Deaf Patients

Xue Zhong Liu^{1,2}, Susan Blanton², Zhongmin Lu³, Denise Yan¹, M'hamed Grati¹, Simon Angeli¹, Mustafa Tekin²

¹University of Miami Miller School of Medicine, Dept of Otolaryngology, ²University of Miami Miller School of Medicine, Dr. John T. Macdonald, Dept of Human Genetics, ³University of Miami, Dept of Biology

Background

The identification of numerous genes causing NSHL (nonsyndromic hearing loss) along with recent technological advances in "target-enrichment" methods and next generation sequencing (NGS) is now making possible molecular epidemiological studies of genetic deafness. The translation of this knowledge to patient care is, however, lagging. There is an urgent need to bring comprehensive genomic information of individual patients into the "real world" clinical environment. The Miami Otogenetic Program is providing a unique platform to translate laboratory studies to deaf patient care.

Methods

We have collected a unique cohort of multiplex families derived from three sources, the USA, China, and Turkey,

suitable for determination of molecular epidemiology of hereditary deafness and for new gene identification. Using target-enrichment/NGS, we are determining 1) the overall frequencies of different forms of genetic deafness in each of the three populations and identify ethnic differences in the distribution of genes for HL, 2) identifying new genes for ARSNHL (autosomal recessive nonsyndromic hearing loss) and ADNSHL using traditional and innovative technologies in the collected families, and 3) creating important Genomic Deafness Database (GDD) and Personalized Sequence Profile (PSP) for the clinical care of deaf patients where data is ranked based on its clinical validity and utility. Our interdisciplinary and collaborative team will conduct outcome evaluation of genetic service on deafness patient care in our diversity populations.

Results

We have established the Miami Otogenetic Program which includes both research and the clinical components. The infrastructure of our multidisciplinary otogenetics team will be presented along with our utilization of testing algorithms when evaluating patients with SNHL. We have collected DNA samples from over 800 probands from multiplex families with no mutations in the common deafness genes from three unique cohorts. In 60% of the small multiplex families, we have identified mutations in known deafness genes. The remaining 40% have mutations in other yet-unidentified deafness-causing genes. We have identified the genes for the DFNA41 and DFNB84 loci in large multi-generational families as well as three new deafness genes for NSHL in small multiplex families.

Conclusion

The combined target-enrichment/next generation sequencing (NGS) and WES (whole exome sequencing) is a powerful tool in the identification of new deafness genes in small multiplex families and large multi-generational families. The multidisciplinary team approach is an effective way to bring the sequencing data to clinical practice for the clinical diagnosis and management of deaf and hard-of-hearing families.

425 Otitis Media Impacts Hundreds of Middle and Inner Ear Genes

Carol MacArthur¹, Fran Hausman¹, Beth Kempton¹, Dongseok Choi¹, Dennis Trune¹
¹OHSU

Background

Otitis media is known to alter gene expression of selected cytokine, mucin and ion homeostasis middle ear (ME) and inner ear (IE) genes in the mouse model. However, whole mouse genome studies of the gene expression in a setting of otitis media have not previously been undertaken. Ninety-nine percent of genes in the mouse are shared in the human, so these studies are relevant to the human condition.

Methods

To assess inflammation-driven processes in the mouse ME and IE, gene chip analyses were conducted on mice

treated with trans-tympanic heat-killed *Hemophilus influenzae*. ME and IE tissues were harvested at 6 hours, RNA extracted, and 7-8 samples for each treatment processed on the Affymetrix 430 2.0 Gene Chip for expression of its 21,816 genes. This represents approximately 70% of the entire mouse genome.

Results

Results were statistically analyzed for expression of each gene against control (untreated) mice. Significant alteration of gene expression was seen in 2,355 genes, 11% of the genes tested and 8% of the mouse genome. Significant ME and IE upregulation (fold change >1.5, $p < 0.05$) was seen in 1,081 and 599 genes respectively. Significant ME and IE downregulation (fold change <0.67, $p < 0.05$) was seen in 978 and 287 genes respectively. Twenty-nine percent of IE genes upregulated were unique to the IE, while 60% were unique to the ME. Forty-two percent of the IE genes downregulated were unique to the IE, while 83% were unique to the ME. These studies show hundreds of ME and IE genes are affected by inflammation. While otitis media is widely believed to be an exclusively middle ear process with little impact on the inner ear, the IE gene changes noted in this study were numerous and discrete from the ME responses. This suggests that the IE does indeed respond to otitis media and that the IE response to ME inflammation is a distinctive process from that occurring in the ME. Numerous new genes, previously not studied, are found to be affected by inflammation in the ear.

Conclusion

Whole genome analysis via gene chip allows simultaneous examination of expression of hundreds of gene families influenced by inflammation in the ME. Discovery of new gene families affected by inflammation may lead to new approaches to the study and treatment of otitis media.

426 Biofilm Structures in Infants with Silent Otitis Media and Tympanogenic Meningitis

Sebahattin Cureoglu¹, Patricia Schachern¹, Vladimir Tsuprun¹, Steven Juhn¹, Michael Paparella¹
¹University of Minnesota

Background

Silent otitis media is defined as chronic pathologic conditions that are "undetected" behind an intact tympanic membrane. Because pathologies in the middle ear are undetected, there is a lack of clinical treatment increasing the risk of complications. Since the initial description of biofilms in chronic infections, there has been increasing evidence supporting the related role of biofilms on disease progression and persistence of inflammation in chronic otitis media. Our hypothesis is that there is an association between the presence and location of biofilms in the middle and inner ear of patients with silent otitis media and tympanogenic meningitis.

Methods

Thirty-one cases with meningitis were screened to select those with tympanogenic meningitis. Inclusion criteria for

tympanogenic meningitis were acute meningitis with histopathological evidence of chronic otitis media, and no other source of infection. Pathologic changes of the middle and inner ears were noted. We defined biofilm as bacterial aggregates encapsulated within a surface that were frequently associated with a fibrous matrix and contained inflammatory cells. In order to detect the bacteria in the specimens and their aggregates, gram staining, matrix as well as dead-bacteria staining has been performed.

Results

Seventeen temporal bones, from 9 cases (2 females and 7 males), ranging in age from 5 to 23 months, met our criteria of tympanogenic meningitis. Of these, 82% had biofilms that contained bacteria within fibrous matrix as well as the presence of polymorphonuclear leukocytes and mononuclear cells. Biofilm-like structures were located in 1 anatomical region in 1 ear and multiple regions in 16. Most common locations were the areas near the oval and round windows and the epitympanum, facial recess, and supratubal recess. Biofilms within the inner ear were observed in the scala tympani and modiolus in 9 ears. Labyrinthitis was seen in all ears as were intact tympanic membranes.

Conclusion

There is an association between the presence of biofilm in the ear and tympanogenic meningitis in infants. Chronic pathologic changes in the middle ear, behind an intact tympanic membrane and the lack of ear symptoms, may result in potentially serious sequelae and complications in infants. The clinician should, therefore, be aware that an intact tympanic membrane does not necessarily preclude the presence of pathologic changes such as granulation tissue, cholesterol granuloma, fibrosis and/or biofilm structures in the middle ear cleft, and that the clinical definition of chronic otitis media may not cover the majority of infants with this condition.

427 Limitations of Hearing Screening in Newborns with a Pendrin Mutation

Bo Gyung Kim¹, Joong-Wook Shin², Hong-Joon Park², Jung Min Kim¹, Un-Kyung Kim³, Jae Young Choi¹
¹Yonsei University, College of Medicine, ²Soree Ear Clinic, ³College of Natural Sciences, Kyungpook National University

Background

Pendrin gene mutations are the most common cause of congenital hearing loss in East Asia. Because hearing loss caused by the pendrin mutation tends to have a delayed presentation, universal newborn hearing screening (UNHS) examinations are poorly predictive of long-term hearing ability in these patients. We examined associations between UNHS and long-term hearing outcome in deaf patients with biallelic pendrin mutations.

Methods

Forty-three patients with severe to profound hearing loss were recruited. Patients had an enlarged vestibular aqueduct and biallelic PDS mutations. Seventeen deaf

patients without a PDS mutation were recruited as a comparison group. We reviewed children's hearing loss history using medical records and parent interviews.

Results

Fourteen of 43 children (32.6%) with a pendrin mutation received a UNHS test. Four of these 14 children (28.6%) passed in both ears, while six (42.9%) passed in one ear, and four (28.6%) were referred in both ears. In contrast, 15 of 17 children (88.2%) without a PDS mutation were referred bilaterally. The age at confirmation of bilateral hearing loss in bilateral pass children was 31.5 \pm 17.9 months, which was significantly later than the age for bilateral refer children (1.75 \pm 0.96 months) ($p=0.045$).

Conclusion

The UNHS is not an accurate tool for predicting long-term hearing loss in patients with a pendrin mutation. We recommend that genetic screening be combined with UNHS, particularly in communities with a high prevalence of pendrin mutations, to better identify children in need of early habilitation.

Table 1. Clinical characteristics of patients with PDS mutation

Patient number	Gender	Age at which hearing loss was confirmed (months)	Pendrin mutation type	Screening device	Type of UNHS	Setting threshold
1	F	54	H723R/Val306Glyfs	NATUS ALGO _{3i}	AABR	35
2	F	12	H723R/H723R	VIASYS	AABR	35
3*	F	24	H723R/H723R	GSI-Audera	ABR	
4	M	36	IVS7-2 A>G/IVS7-2 A>G	NATUS ALGO _{3i}	AABR	35
5	M	3	IVS7-2 A>G/H723R	NATUS ALGO _{3i}	AABR	35
6	M	4	H723R/H723R	NATUS ALGO _{3i}	AABR	35
7	M	1	H723R/IVS7-2A>G	NATUS ALGO _{3i}	AABR	30
8*	M	16	IVS7-2 A>G/H723R	GSI-Audera	ABR	
9	F	24	IVS7-2 A>G/H723R	NATUS ALGO _{3i}	AABR	35
10	M	27	T410M/H723R	ILO 88	TEOAE	30
11	F	3	H723R/H723R	NATUS ALGO ₅	AABR	35
12	F	2	H723R/IVS7-2A>G	NATUS ALGO _{3i}	AABR	35
13	F	1	H723R/H722R	ILO v6	TEOAE	35
14	M	1	IVS7-2 A>G/H723R	GSI AUDIO screener	AABR	35

*The patient 3 performed the ABR at age 18 months and was confirmed with normal at age 24 months. The patient 8 performed the ABR at age 2 months and was confirmed with one side hearing loss at age 16 months.

428 Otology in the Classical World -- 500 BCE to 200 CE

Robert Ruben¹

¹Albert Einstein College of Medicine

Background

This presentation is part of a history of otology using a uniform subject matter framework across time. Information is accessible through hypertext based upon the subject.

Methods

Original source material is searched using uniform criteria for subject categories.

Results

The Hippocratic corpus (ca 460BCE -- 377BCE) describes conditions interpretable as otitis media which appears as a

lethal disorder, without interventions. Deafness is cited among sequelae of other disorders in which there is recovery. Celsus (25BCE -- ca 50CE) emphasizes the seriousness of ear infections, especially for young and old. Serous Otitis Media: Hippocratic writings note conditions interpretable as SOM, associated with southerly winds and/or dampness, causing a fullness of the head and deafness. Acute onset deafness associated with apparent systematic infection is mentioned. These cases do not indicate initial ear infections but the ear is affected in the illness's course. SOM is not recognized as an entity.

Barotrauma: Aristotle (384 BCE -- 322BCE) appreciates the relationship of middle ear pressure to external pressures, noting that tympanic membrane rupture in deep sea diving is preventable by attaching a sponge to the external ear. He attributes the protection to blocking of sea water, although the sponge's evident effect is lessening pressure on the tympanic membrane caused by lower pressure in the middle ear cleft.

Deafness: Greeks and Romans provide no etiologies for congenital deafness. Aristotle recognizes hearing's essential role in spoken language development, and notes greater morbidity of congenital and early onset deafness compared with blindness. Mutism is attributed to inability to use the tongue. Plato (ca 360BCE) describes the use of sign language by the deaf

Ear Surgery: Celsus describes hearing restoration in congenital or acquired external canal stenosis using caustic and/or incision with stenting. His techniques for repairing pinnae injuries are much like contemporary practice.

Medical providers: The general population received medical care from general physicians, some paid, in part, by their communities. The wealthy had personal physicians. Rome and Alexandria had otologic specialists adept at removing external canal foreign bodies and caring for pinnae injuries.

Conclusion

The seriousness of ear infection was recognized, with no available interventions. Care existed for external canal stenosis, pinnae injuries and external canal foreign bodies. Hearing's essential role in spoken language acquisition was known, with lack of speech attributed to tongue dysfunction. Sign language of the deaf was recognized.

429 Ototoxicity of Burow's Solution on the Guinea Pig Cochlea

Mayumi Sugamura¹, Takafumi Yamano¹, Hitomi Higuchi¹, Takashi Nakagawa¹, Tetsuo Morizono²

¹Department of Otorinolaryngology, Fukuoka University, school of Medicine, ²Nishi Fukuoka Hospital

Background

The main ingredient of Burow's solution is 13% aluminum acetate and it has been topically used worldwide for the treatment of chronic discharging ears. However, ototoxicity of this solution is not well understood.

The aim of the present study is to evaluate the ototoxicity and the bacteriostatic activity of Burow solution, with different concentration.

Methods

Using guinea pigs, compound action potentials (CAPs) of the eighth nerve were measured before and 30 minutes and 24 hours after the application of the Burow's solution in the middle ear cavity.

The bacteriostatic activity of Burow's solution was studied using a disk diffusion assay.

Results

Use of the original Burow's solution (pH 3.5) for 30 minutes caused a significant reduction of CAP threshold to click sounds. A 2-fold diluted Burow solution (pH 4.4) for 30 minutes caused no reduction in CAP threshold. Burow's solution, pH adjusted to 4.5, caused no changes in CAP threshold at 30 minutes. At 24 hours, original Burow's solution (pH 3.5) caused complete abolition of CAP.

Both the original concentration and the 2-fold diluted Burow's solution showed bacteriostatic activity against all bacteriae.

Conclusion

Burow's solution is ototoxic in the guinea pig when applied in the middle ear cavity for 30 minutes or longer. In the clinical settings, it is advisable to avoid allowing the solution to contact the round window membrane for extended duration. We should be aware of anatomical differences of the round window membrane in rodents and human.

References

- 1) Serin GM, Ciprut A, Balancicek S, Sari M, Acdas F, Tutkum A. Ototoxic effect of Burow's solution applied to the guinea pig middle ear. *Otol Neurotol* 2007;28:605-8.
- 2) Suzuki M, Kashio A, Sakamoto T, Yamasoba T. Effect of Burow's solution on the guinea pig inner ear. *Ann Otol Rhinol Laryngol* 2010;19:495-500.
- 3) Sugamura M, Yamano T, Higuchi H, Takase H, Yoshimura H, Nakagawa T, Morizono T. Ototoxicity of Burow solution on the guinea pig cochlea. *Am J Otolaryngol*. 2012 Sep;33(5):595-9.

430 Postoperative Outcome of Cochlear Implantation in Children with Cochleovestibular Malformations

Teru Kamogashira¹, Akinori Kashio¹, Erika Ogata¹, Yusuke Akamatsu¹, Shotaro Karino¹, Takashi Sakamoto¹, Akinobu Kakigi¹, Shinichi Iwasaki¹, Tatsuya Yamasoba¹
¹Department of Otolaryngology, Faculty of Medicine, University of Tokyo

Background

Malformations of the inner ear were initially considered to be a contraindication to cochlear implantation (CI). However, most cases with inner ear malformations have demonstrated significant improvements in speech recognition skill after CI. Recently, Sennaroglu proposed a new classification system for inner ear malformations on the basis of radiological findings. In this study, we aimed to assess the outcomes after CI in children with a variety of

inner ear malformations classified according to the Sennaroglu's classification.

Methods

Data of children who underwent CI at The University of Tokyo Hospital from May 1999 to April 2012 were collected. The cochleovestibular malformation in each case was evaluated using computed tomography and magnetic resonance imaging. Subjects were divided into 7 groups according to Sennaroglu's classification. The Meaningful Auditory Integration Scale (MAIS) scores and the Meaningful Use of Speech Scale (MUSS) scores were analyzed before and 12 months after CI. The incidence of CSF gusher and facial nerve stimulation as well as the number of inserted electrodes were also compared among groups.

Results

Of the 164 children that received CI, 28 had cochleovestibular malformations that were classified as follows: incomplete partition type I (IP-I) (n = 4); incomplete partition type II (IP-II) (n = 15); enlarged vestibular aqueduct (EVA) (n = 2); and common cavity (CC) (n = 3). Other cases that did not match with Sennaroglu's classification included the following: enlarged internal acoustic meatus (n = 2); narrowed internal acoustic meatus (n = 1); and lateral semicircular canal aplasia (n = 1). Three children with IP-II had other complications, including Waardenburg syndrome, Goldenhar syndrome, and CHARGE syndrome, respectively. The average MAIS scores before and after the CI were 11 and 30 in cases of CC, 27 and 37 in those of EVA, 9 and 23 in those of IP-I, and 11 and 24 in those of IP-II. The corresponding MUSS scores were 10 and 26 in cases of CC, 28 and 34 in those of EVA, 7 and 19 in those of IP-I, and 9 and 21 in those of IP-II. Cerebrospinal gusher occurred in 1 CC case and 5 IP-II cases. All electrodes were successfully inserted in all cases except in 1 IP-II case.

Conclusion

The Sennaroglu's classification does not impact the outcome of MAIS and MUSS. However, the risk of CI complications is high in patients with cochleovestibular malformations.

431 Computed Tomography-Based Preoperative Evaluation of Round Window Niche Visualization from Facial Recess

Akinori Kashio¹, Akinobu Kakigi¹, Shotaro Karino¹, Takashi Sakamoto¹, Shinichi Iwasaki¹, Tatsuya Yamasoba¹

¹University of Tokyo

Background

The introduction of new electrode array designs and the increased emphasis on preserving residual hearing for lector-acoustic stimulation has recently focused attention on the use of the round window membrane (RWM) approach or extended-RWM approach for cochlear implant (CI) electrode insertion. The visualization of round window niche (RWN) from the facial recess would be an important

factor for evaluating accessibility of RWM at the CI surgery. In this study, we aim to preoperatively evaluate RWN visibility by using high resolution computed tomography (HRCT).

Methods

We retrospectively reviewed data from 46 CI patients who underwent HRCT of the temporal bone and whose surgical video was recorded. The axial slice showing RWN was selected and a line was drawn along the posterior wall of the bony external auditory canal (line A). Another line was drawn parallel to line A that made contact with the vertical segment of the facial nerve (line B). The band within line A and B was extended toward the RWN and the relation between the band and the RWN was classified into 3 types: [1] almost no contact with the band, [2] fully included in the band, and [3] partially included in the band. In this procedure, we eliminated 3 cases owing to tortuous external auditory canals. Next, the visibility of the RWN was evaluated and classified into 3 types: (A) almost impossible to visualize, (B) fully visible, and (C) Partially visible.

Results

Ten cases were classified as [1] by CT and all of them were classified as (A) by the surgery video record; 14 out of 16 cases classified as [2] by CT were classified as (B) by the surgery video record. The rest of 2 cases were classified as (C); 16 out of 17 cases classified as [3] by CT were classified as (C) by the surgery video record and the remaining 1 case was classified as (A).

Conclusion

RWN visibility and the preoperative HRCT findings have showed high correlation. Our method for the preoperative evaluation of the RWN has the potential to become a useful tool for CI surgery.

432 Eustachian Cushion Features Do Not Correlate with Otitis Media

N. Wendell Todd¹, Mina Tran¹

¹Emory

Background

Diminutive inferiorly positioned Eustachian cushions, as viewed with fiberoptic nasopharyngoscopy, have been associated with otitis media. Our objectives are to describe Eustachian cushion position and features in clinically normal cadaver specimens, and address the hypotheses that bilateral symmetry exists and that Eustachian cushion position and features are unrelated to the small mastoid size indicator of otitis media in childhood.

Methods

From 41 adult cranial specimens without clinical otitis, rectilinear digital photographs were made of the lateral nasopharyngeal walls, both en face directly laterally and viewing 45 degrees posterior-lateral. Features were categorized, and distances measured. Mastoid sizes were quantified on radiographs.

Results

Though good repeatability of assessments and bilateral symmetry of Eustachian cushion features and positions were found, there was no relation of any of the studied Eustachian cushion parameters with mastoid size.

Conclusion

No difference in Eustachian cushion architecture was found to correlate, in these clinically normal crania, with the small mastoid size indicator of childhood otitis media.

433 Ear-Canal Reflectance as a Screening Tool for the Diagnosis of Superior Semicircular Canal Dehiscence

Gabrielle R. Merchant^{1,2}, Christof Röösl^{2,3}, Marlien E. F. Niesten⁴, Mohamad A. Hamade^{2,3}, Daniel J. Lee^{2,3}, John J. Rosowski^{2,3}, Saumil N. Merchant^{2,3}, Hugh D. Curtin⁵, Hideko H. Nakajima^{2,3}

¹Speech and Hearing Bioscience and Technology, Harvard-MIT Division of Health Sciences and Technology, ²Eaton-Peabody Laboratory, Massachusetts Eye and Ear Infirmary, Boston, MA, USA, ³Department of Otolaryngology and Laryngology, Harvard Medical School, Boston, MA, USA, ⁴Department of Otorhinolaryngology - Head and Neck Surgery, University Medical Center, Utrecht, ⁵Department of Radiology, Massachusetts Eye and Ear Infirmary, Boston, MA, USA

Background

Ear-canal-reflectance (ECR) was measured in patients with superior semicircular canal dehiscence (SCD) to determine whether ECR coupled with an appropriate detection algorithm can be used as a non-invasive, fast, and easy screening test for SCD. The aim of such screening is to determine if the diagnosis of SCD (and other third-window lesions) should be considered for a patient with vestibular and/or auditory symptom(s) and whether a further workup (such as computed tomographic (CT) imaging and balance testing) should be pursued.

Methods

We measured ECR in 32 ears diagnosed with SCD by high-resolution CT imaging, utilizing specialized methods for measuring size and location of the dehiscence, and compared these measurements to ECR measurements made in normal ears. An analysis algorithm was introduced that detects possible SCD using unique features of ECR measurements that are common in ears with SCD and less common in normal ears. We: 1) evaluated sensitivity and specificity of ECR and our algorithm in the diagnosis of patients with SCD regardless of symptomatology (i.e. with or without hearing loss, dizziness, or abnormal auditory sensations), 2) compared ECR to another non-invasive mechanical measurement – umbo velocity measurements by laser Doppler vibrometry – which has been shown to aid in differentiating various pathologies associated with conductive hearing loss (Rosowski et al. 2008, Nakajima et al. 2011) and 3) correlated specific parameters of ECR measurements to

SCD size and location and the air-bone gap seen on the audiogram.

Results

SCD was commonly associated with a notch in ECR near 1 kHz. We assessed the ability of our algorithm to detect SCD based on this ECR notch; various detection thresholds yielded sensitivities of 0.926–0.852, specificities of 0.690–0.724, negative predictive value of 0.925–0.913 and positive predictive value of 0.581–0.589. There was no similar stereotypic feature visible in umbo velocities measured in ears with SCD cases. Statistical analysis showed that there were significant correlations between air-bone gap and ECR notch size, as well as between air-bone gap and an increase in low-frequency umbo velocity magnitude, but no correlations were found between notch size and the size and/or location of the dehiscence.

Conclusion

Our findings suggest that notches in ECR measurements can be used to screen patients for third-window lesions such as SCD in the early stages of a diagnostic workup.

434 Development of Head and Neck Cancer Xenograft Animal Model for in Vivo Anti-Cancer Drug Screening

In Seok Moon¹, Mee Hyun Song², Jae Young Choi¹
¹Yonsei University College of Medicine, ²Kwandong University College of Medicine

Background

The development of a relatively simple, reliant and cost-effective animal test will greatly facilitate drug development. In this study, our goal was the establishment of a rapid, simple, reproducible, and live zebrafish head and neck squamous cancer cell (HNSC) and thyroid cancer cell xenograft model for anti-cancer drug screening.

Methods

We optimized the conditions for the cancer cell xenograft in terms of injected cell numbers, incubation temperature and time. We used cell lines as follows: HNSC (Cal27, FaDu) & Thyroid cancer (FTC33, TPC1). Cancer cells were stained with a mCherry fluorescent protein prior to injection into the 30hpf zebrafish larvae. Cancer cells were counted by microscopy, suspended in 10% FBS and 200 cells were injected into the center of yolk sac using a micro-injecting system. Injected embryos were transferred to E3 media and subsequent tumor formation and cancer cell dissemination was observed under fluorescent microscopy for 5 days. To test our new model, we carried out further validation. Xenografted embryos were transferred in a 24 well plate (3 embryos/well) and treated with several known anti-cancer drugs (RAD001 and others).

Results

MFP-tagged cancer cells were successfully grafted into the yolk sac of zebrafish embryo without immunosuppressant treatment. 2 days after injection, xenografted cell formed tumor mass in all cell lines. 4 days after injection, dissemination from the yolk sac to the tail can be observed

from in FaDu line under fluorescent microscope. Differences in injected cell numbers were reflected in the speed of tumor formation and rate of dissemination from the xenograft site. The preliminary test was performed using 1 μ M of RAD001 and others. RAD001 produced > 20% reduction in the cancer cell number of embryos.

Conclusion

Our in vivo animal model system should greatly facilitate drug development for cancer therapy because of its speed, simplicity, reproducibility and live imaging.

435 p75NTR-Mediated Apoptosis in Vestibular Schwannoma (VS) Cells Depends on Subcellular Localization of the Intracellular Domain

Nathan Schularick¹, Augusta Fernando¹, Iram Ahmad¹, Jason Clarke¹, Marlan Hansen¹

¹University of Iowa Department of Otolaryngology

Background

Our work focuses on p75NTR signaling in neoplastic and non-neoplastic Schwann cells (SC). Post-activation cleavage of p75NTR yields an intracellular domain (ICD) in the cytoplasm that induces apoptosis in non-neoplastic SCs. We recently showed that the ICD of p75NTR localizes to the nucleus in auditory SCs that have re-entered the cell cycle following deafness. Further, work in PC12 cells demonstrated that nuclear-localized p75NTR-ICD regulates cyclin E1 expression. These observations suggest that subcellular localization of p75NTR-ICD regulates SC cell cycle entry and survival.

Methods

p75NTR expression in VS tissue, relative to normal nerve, was quantified by qRT-PCR and western blot. To explore the contribution of p75NTR signaling in VS cell proliferation and death, we generated adenoviral vectors that express full-length (FL) p75NTR, p75NTR-ICD, p75NTR-ICD targeted to the cytoplasm with a nuclear export signal (NES) peptide, or p75NTR-ICD targeted to the nucleus with a nuclear localization signal (NLS) peptide. Primary human VS cultures derived from acutely resected tumors were transduced with these viral vectors or treated with proNGF, a high affinity p75NTR ligand. TUNEL staining and caspase-3 cleavage were used to demonstrate apoptosis. Proliferation was determined by EdU uptake. Finally, transcriptome analysis of VS cultures treated with proNGF was performed using Nimblegen microarrays.

Results

Compared to normal nerve, VSs express a ~3-fold increase in p75NTR. Based on immunostaining, the ICD of p75NTR localizes to the nucleus in EdU-positive VS cells in vitro as in non-neoplastic SCs. Treatment of VS cultures with proNGF resulted in an anti-apoptotic response in VS cells while non-neoplastic SCs responded with increased apoptosis. Expression of FL p75NTR and NES-p75NTR-ICD both increased the percent of TUNEL-positive VS cells compared with cultures transduced with an empty vector. By contrast, expression of NLS-p75NTR-ICD failed to

induce VS cell apoptosis. Treatment of VS cultures with proNGF or transduction with the various p75NTR isoforms did not alter the percent of EdU-positive VS cells. Microarray data are currently being analyzed.

Conclusion

VS cells express high levels of p75NTR yet are resistant to proNGF-mediated apoptosis. The ability of p75NTR to induce VS apoptosis appears to depend on the subcellular localization of the ICD. Activation of p75NTR with proNGF altered expression levels of several genes potentially related to neoplasia in VS cells.

436 Endolymphatic Hydrops in Histopathologic Otosclerosis and Surgery Effect

Christina Forshell Hederstierna¹, Sebahattin Cureoglu², Vladimir Tsuprun², Michael Paparella²

¹Karolinska University Hospital, ²University of Minnesota

Background

Otosclerosis is a disease of the bony labyrinth and stapes, causing a remodeling of the bone structure. In clinical cases, the affected motility of the stapes causes a conductive hearing loss, in one or both ears. However, patients with otosclerosis often experience other symptoms that are not typical of the disease, e.g. symptoms of tinnitus, fullness of the ear, vertigo and dizziness. These symptoms are more often characteristics of Meniere's disease and related conditions, where the basis for the symptoms is considered to be endolymphatic hydrops.

Methods

We studied the complete collection of temporal bones with histological otosclerosis at the University of Minnesota Otopathology laboratory. 188 ears from 104 subjects with histologic otosclerosis were examined for the degree of cochlear and saccular hydrops and correlated with presence or absence of surgical intervention.

Results

In 4 of these cases only one ear was available for examination. 84 of the remaining 100 cases were bilateral and 16 were unilateral; 6 in the left and 10 in the right ear. In total, 167 ears with otosclerosis had quantifiable cochlear hydrops and 150 ears had quantifiable saccular hydrops according to our specified rationales for grading.

Conclusion

We found that histological otosclerosis is associated with a notable prevalence of both cochlear and saccular hydrops. The number of otosclerotic foci correlates strongly with the degree of cochlear and/or saccular hydrops; the prevalence of both types of hydrops appears lower in ears that have had otosclerotic surgery.

437 Contribution of the Incudo-Malleolar Joint to Middle-Ear Sound Transmission

Rahel Gerig¹, Jae Hoon Sim¹, Christof Rösli¹, You-zhou Xie¹, Sebastian Ihrle², Alexander M. Huber¹

¹University Hospital Zurich, ²University of Stuttgart

Background

The incudo-malleolar joint (IMJ) in human middle ears is considered to be the diarthrodial joint binding the malleus and the incus. Investigations on measurement of IMJ mobility have been conducted during the last several decades, and the IMJ in human is generally accepted to be mobile, especially at high frequencies. However, the behavior of the IMJ has not been fully characterized, and its roles in sound transmission are still questionable. Furthermore, the supporting band apparatus of the IMJ may have a relation to age-related hearing loss, but this has not been demonstrated. Characterizing IMJ motions systematically and developing a comprehensive mechanical model of the IMJ can answer questions about its anatomical features and function, and serve as a base for the development and optimization of middle-ear implants.

Methods

Spatial motion of the middle-ear ossicles in fresh temporal bones (TB) was measured using a scanning laser Doppler interferometry (LDI) system. Three-dimensional (3-D) motion components of each middle-ear bone were calculated from the measurements, using a custom-made algorithm. The measurement and calculation were repeated with the IMJ experimentally fixed, in order to quantify the transmission losses caused by the immobility of this joint. The spatial motion components were registered into an anatomical frame, which was obtained from micro-CT images. Four pieces of reference wires were attached to the TB close to the measurement site, and their outlines were used as references to obtain the relation between the LDI measurement frame and the anatomical frame.

Results

While the malleus and the incus moved as one rigid body with the fixed IMJ, relative motion between the two middle-ear bones was observed with the non-fixed IMJ, especially at high frequencies above 2 kHz. The pattern of the stapes spatial motion also showed differences between the non-fixed and fixed conditions of the IMJ.

Conclusion

The spatial modes of the middle-ear ossicles are affected by the IMJ condition, especially at high frequencies. Therefore, the IMJ is presumed to contribute to the middle-ear sound transmission and thus air-conductive (AC) hearing.

438 Alternative Lever Arms for Mobile and Fused Ossicular Chains

Ryan Jackson¹, Allison Zemek¹, Hongxue Cai¹, Charles Steele¹, Sunil Puria¹

¹Stanford University

Background

Several publications have argued that morphometric properties of the ossicular chain play an important role in determining force gains, inertial impedance, and, consequently, the frequency range of hearing in mammals. More recently, Puria and Steele (2010) proposed that at high frequencies the vibration of the ossicles should be predominantly rotational about their individual principal moment-of-inertia axes, rather than their anatomical axis, which is defined by the malleal anterior and incudal posterior ligaments. Such vibrations could significantly reduce the mechanical impedance of the ossicular chain and enable efficient sound transmission to the cochlea. Here the first, second, and third principal axes (PA1, PA2, and PA3 respectively) were compared to the anatomical axis (ANA) and another axis of interest, the malleus-incus complex center-of-mass axis (COMA). Lever arms were calculated for each axis to estimate primary motions that should be observed experimentally if rotation occurs about each of these axes, provided the ossicles behave primarily as rigid bodies. Further, the ratio of the malleus-lever-arm to incus-lever-arm was calculated to estimate middle ear gain as an ideal transformer ratio.

Methods

Cadaveric temporal bones from three species with mobile malleus-incus joints (MMIJ): gerbil (n=6), cat (n=2), and human (n=1), and two species with fused malleus-incus joints (FMIJ): guinea pig (n=6), chinchilla (n=2) were scanned and segmented to analyze ossicular chain morphology. Analysis of lever arms, moments-of-inertia, and tangential linear velocity directions for each animal was performed.

Results

For species with MMIJ, the average values of malleus-to-incus lever arm ratios were increased when the incus rotated about its PA1 for any malleus axis of rotation (increases of 5x for gerbil, 2.5x for cat, and 3.5x for human). A similar maximization was found for species with FMIJ, when the malleus and incus rotated about their combined PA1 (increases of 2x for guinea pig and 1.3x for chinchilla). It was also found that for either MMIJ or FMIJ, rotation of the incus about PA1 imparts force to the stapes approximately in the piston direction.

Conclusion

Examination of the lever arm ratios indicated that in the mammals studied, rotation of the incus about its PA1 is significantly greater than is possible with rotation strictly about ANA (or COMA). This could indicate a novel mechanism for increased middle ear gain.

[Work supported in part by NIDCD/NIH Grant R01 DC005960.]

439 Estimation of the Orthotropic Elastic Properties of the Eardrum Using a Pressurization Technique

Ehsan Salamati¹, S. Alireza Rohani¹, Sumit K. Agrawal², Abbas Samani¹, Hanif M. Ladak¹

¹Western University, ²London Health Sciences Centre

Background

Previously, we reported a method based on indentation testing and optimization of a finite-element (FE) model to estimate the orthotropic elastic parameters of the pars tensa in situ. This approach is challenging to use because of the curved shape of the pars tensa which requires special care during experimentation to keep the indenter perpendicular to the local surface at the point of contact. In addition, FE simulations involve complicated contact modeling. A new method is presented here in which pressurization is used instead of indentation.

Methods

Measurements were made on three rat eardrums with immobilized ossicular chains. A pressurization system was used to apply quasi-static pressures up to 4 kPa to each eardrum. The resting and deformed shapes of each eardrum were measured using a Fourier transform profilometer, a non-contacting optical device for shape measurements. To simulate the pressurization experiment, an FE model was constructed for each eardrum from the resting shape data. The orthotropic parameters of each model pars tensa were optimized so that simulated deformed shapes matched measured ones. A variant of the Nelder-Mead simplex method that is formulated to handle constrained multivariable optimization was used, and the optimal values were taken to be estimates for the actual orthotropic parameters.

Results

The estimated parameter values are circumferential elasticity of 37.9 ± 0.12 MPa, radial elasticity of 48.0 ± 0.01 MPa and in-plane shear modulus of 22.0 ± 0.01 MPa. The average estimated values for the radial and circumferential elasticities are within the range reported in the published literature on tensile testing of tissue strips cut from the pars tensa; however, tensile testing cannot be used to estimate the in-plane shear modulus.

Conclusion

The new pressurization-based approach is simpler to use than the indentation-based method both in terms of measurement and modeling, and yields estimates for circumferential and radial elasticities that are comparable to those published by other groups. Moreover, the results are highly repeatable as indicated by the low standard deviations.

440 Characterization of Ear Canal Sound Field in Forward and Reverse Transmission

Jeffrey Cheng¹, Michael Ravicz¹, Cosme Furlong^{1,2}, John Rosowski^{1,3}

¹Massachusetts Eye and Ear Infirmary, Harvard Medical School, ²Worcester Polytechnic Institute, ³Speech and

Background

Sound propagation from the external environment through the human ear canal (EC) to the tympanic membrane (TM) can be described fairly well in terms of plane wave propagation at least at frequencies below 15 kHz (Stinson 1985). However, the sound field generated inside the EC by motion of the TM in reverse transmission (for instance, by otoacoustic emissions) has not been well studied. We have reported preliminary measurements showing that (1) the relationship between TM displacement and ear canal pressure differs in both magnitude and phase between forward and reverse transmission (Cheng et al., 2011), and (2) there is little correspondence between the nonuniform TM surface motion in forward transmission and the nearly uniform pressure distribution inside the EC below 15 kHz (Cheng et al., 2012).

Methods

In this study, we compare the distribution of sound pressure inside the EC for both forward and reverse sound transmission. For forward transmission, sound was delivered from an earphone to the opening of an artificial EC (with dimensions similar to the human ear) that was coupled to the tympanic ring of a temporal bone at a 45-degree angle to mimic sound propagation inside the actual human EC; for reverse transmission, the incus body near the long process was stimulated by a piezoelectric actuator (the EC entrance was open). Sound pressure was measured in a 1-mm grid in a plane parallel to and within 1 mm of the tympanic ring with a probe tube microphone. Sound pressure was also measured in a set of planes normal to the EC axis but more distant from the TM ring.

Results

In forward sound transmission the sound pressure was approximately uniform over both the EC normal and the tympanic ring planes at frequencies up to 15 kHz. In reverse transmission the sound pressure varied within the tympanic ring plane at frequencies as low as 1 kHz, but was uniform throughout the EC normal planes. The pressure variations along the tympani ring plane in reverse transmission tend to be frequency dependent, and the pressure from reverse transmission is significant lower than those from the forward case with the open EC.

Conclusion

Our results suggest the presence of evanescent waves from TM motions in reverse transmission which may influence assessment of oto-acoustic emissions measurements in real ear canals.

441 Imaging the Human Tympanic Membrane Motion Using Scanning Laser Vibrometry and Finite Element Model

Xiangming Zhang¹, Xiying guan¹, Mario Pineda², Vikrant Palan², Rong Gan¹

¹University of Oklahoma, ²Polytec, Inc

Background

Sound-induced tympanic membrane (TM) vibration has been studied through the motion of the umbo which was measured by laser Doppler vibrometry or analyzed using finite element (FE) models for decades. Recently, some preliminary studies were conducted to measure the full-field TM surface motion using stroboscopic holographic interferometry and optical coherence tomography. The technology of imaging human TM motion has the potential to be a clinical diagnosis tool for middle ear diseases. However, how is the TM surface motion related with the middle ear transfer function in normal and disordered ears is still not clear.

Methods

In this study, a scanning laser vibrometer (PSV-400, Polytec) was used to measure and image the full-field surface motion of the TM sample from six fresh human temporal bones. Both displacement amplitude and phase were measured under the normal and disordered conditions with different middle ear pressure or fluid levels across 200 to 8,000 Hz. A completed FE model of the human ear, including the ear canal, middle ear and spiral cochlea, which was published recently by our group (Zhang and Gan, 2011) was used to simulate the measurement and derive the holographic images of TM motion.

Results

The mode shape and displacement phase of the TM at low (below 1,000 Hz), medium (between 1,000 and 4,000 Hz) and high frequency ranges (above 4,000 Hz) under normal and disordered conditions were acquired from the temporal bone experiments and predicted by the FE model. The complex mode shape and standing wave were observed on TM at high frequencies. The relationship between the mode shape of the TM and the middle ear transfer function was analyzed.

Conclusion

The scanning laser vibrometry is capable to measure and image the full-field motion of the human TM. The holographic images of TM can be clearly distinguished between the normal ear and the middle ear with effusion at high frequencies. The data reported in this study may help better understand the complex TM motion in relation to its acoustic transfer function. (Work supported by NIH R01DC011585)

442 The Effect of Static Force During Stimulation of the Round Window with the Floating Mass Transducer

Rolf B. Salcher¹, Burkard Schwab¹, Thomas Lenarz¹, Hannes Maier¹

¹Medical School Hanover, Germany

Background

The round window (RW) stimulation has developed to a standard procedure in the treatment of sensor neural hearing losses in combination with middle ear pathologies since Colletti et al. successfully implanted the first series of patients in 2005. Despite encouraging clinical results there is still a high variability in hearing improvement results. Two key requirements seem to play an important role for obtained sufficient sound transmission. First the FMT must be centered onto the round window membrane and secondly the back of the FMT must be supported elastically in the hypotympanic area to apply the necessary contact pressure.

The goal of our study was to investigate the influence of a controlled axial static force on transmission efficiency and variability

Methods

We investigated experimentally the effect of the Round Window Coupler (RWC) and the interposition of an artificial material (TUTOPATCH®) in fresh human temporal bones at constant contact force of ~2mN. The equivalent sound pressure output was determined by comparison of sound evoked to RW stimulation evoked stapes footplate displacement. Results were compared to direct attachment of the FMT to the RW membrane without the interposition.

Results

The obtained mean equivalent sound pressure for all four conditions was not significantly altered at frequencies ≥ 3 kHz. Compared to the direct FMT stimulation the coupler in combination with TUTOPATCH® lead to a statistically insignificant decrease of approx. 5 dB, whereas the use of TUTOPATCH® or the coupler alone resulted in smaller changes. At low frequencies (≤ 2 kHz) the effect of the coupler in combination with the interposition material was more pronounced, leading to an average increase in output of 12.2 dB (500 Hz – 2kHz). The improvement in the output was statistically significant at 500 Hz ($p < 0.1$ %, Mann-Whitney-Rank-Sum-Test) and 1 kHz ($p < 5$ %, Student t-Test).

Beside the increase in obtained output amplitude the variability at low frequencies was decreased by the coupler / TUTOPATCH® combination. By using TUTOPATCH® and the coupler a major reduction the output variability (SD = 2.4 dB) compared to the “naked” FMT situation (SD = 9.2 dB) was found at 500 Hz

Conclusion

Applying the FMT with pre-defined force in combination with TUTOPATCH® and the RWC to the RW, leads to higher output and lower variability in sound transmission at low frequencies.

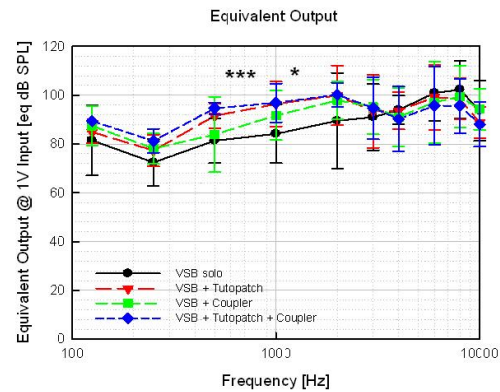


Figure 1 Average equivalent sound pressure output for the four conditions (MV \pm SD). At 500 Hz and 1 kHz the obtained output is significantly higher with the RWC in combination with TUTOPATCH® compared to the FMT alone, *** $p < 0.1$ % * $p < 5$ %

443 Fiber Arrangement in the Rat Tympanic Membrane

Jian Liu¹, Hanif M. Ladak², Sumit Agrawal³, Wankei Wan¹

¹Dept. of Chemical and Biochemical Engineering, Western University, London, ON, Canada, ²Dept. of Medical Biophysics, Western University, London, ON, Canada,

³Dept. of Otolaryngology - Head and Neck Surgery, London Health Sciences Centre, London, ON, Canada

Background

It is well known that the arrangement of fibers (radial and circular) in the pars tensa plays an important role in the mechanical properties of the tympanic membrane (TM). Scanning electron microscopy (SEM) images of the fiber arrangement of the TM have previously been reported. However, due to the limitations of available scanning electron microscopes at the time, those images were not able to resolve the detailed structure of the TM fiber network. Here we report the fiber arrangement of the rat TM observed under a high-resolution field emission SEM.

Methods

The TMs were dissected from adult rats and were fixed in 2.5% glutaraldehyde in phosphate buffer solution overnight. After decalcification in 5% EDTA for 24 hours, the TMs were soaked in 10% NaOH for 3-4 days and conductive-stained with 1% tannic acid followed by 1% OsO₄. The specimens were then dehydrated in a series of graded ethanol solutions and critical point-dried using liquid CO₂. The dried specimens were coated with 5 nm osmium and the fiber arrangement of the TM was observed under SEM from both the external ear canal side and the middle ear cavity side.

Results

The TM is composed of individual fibers with diameters around 20 nm. From the external ear canal side, radial and parabolic fibers can be observed. In the middle region between the manubrium and tympanic ring (TR), the orientation of the radial and parabolic fibers is highly ordered. Close to the TR, the radial fibers become intertwined into a random fiber network, and then attach to the TR. Similarly, the radial fibers become random near the manubrium and cover it. Observing from the middle ear

cavity side, the radial fibers converge onto the manubrium in an orderly way. Circular fibers can be seen starting at a distance of one-tenth of the radius from the manubrium. They are woven into a plexus in the middle region and grouped into bundles close to the TR.

Conclusion

With state-of-the-art SEM available today, the fiber morphology and arrangement of the TM can be clearly observed.

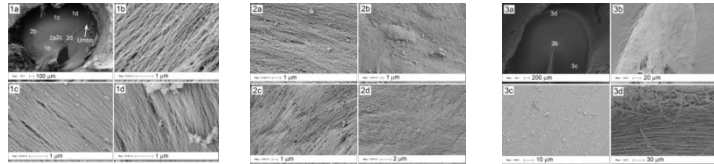


Figure 1. 1a, SEM image of rat TM observed from external ear canal; 1b–1d, high magnification images of the spots labeled in 1a.

Figure 2. 2a–2d, high magnification SEM images of the spots labeled in Fig. 1a.

Figure 3. 3a, SEM image of rat TM observed from middle ear cavity; 3b–3d, high magnification images of the spots labeled in 3a.

444 Experimental Study of Effects of Opening Middle-Ear Cavity on Vibrations of Gerbil Tympanic Membrane

Nima Maftoon¹, Robert Funnell¹, Sam Daniel¹
¹McGill University

Background

Opening the middle-ear air cavity strongly affects the behaviour of the middle ear. This study extends previous observations by examining the effects of different sizes of the opening, and the effects of the opening on vibrations at multiple points on the tympanic membrane and manubrium.

Methods

A laser Doppler vibrometer at the Montréal Children's Hospital is used to measure the vibration at multiple locations on the tympanic membrane and manubrium. After making measurements with a closed cavity, the cavity is opened to varying extents, starting with a hole approximately 1 mm in diameter and ending with the largest possible opening. At each intermediate stage measurements are taken several times at the umbo, and at the final stage measurements are taken at multiple locations.

Results

Opening the cavity with even a small hole causes an increase in the low-frequency magnitude and a shift of the main middle-ear resonance to lower frequencies, and introduces an anti-resonance. When the opening is progressively widened the anti-resonance progressively moves from about 2 kHz to about 9.5 kHz. With a closed cavity, a normal flat pars flaccida causes a magnitude minimum in the manubrium and pars-tensa responses at a frequency between 400 and 700 Hz. This minimum becomes progressively more shallow as the opening is progressively enlarged. When the cavity is opened, the ratio of the displacement magnitude of the umbo to that of the short process changes little from its closed-cavity value. Although the low-frequency magnitudes of points on the pars tensa increase with even the smallest opening, they are practically unchanged when the opening is

subsequently enlarged. Opening of the middle-ear cavity does not change the break-up frequency of the pars tensa.

Conclusion

Our multi-point measurements show that, although the middle-ear resonance moves to a lower frequency, the mode of vibration of the manubrium does not change appreciably when the cavity is opened. Opening the cavity introduces an anti-resonance which shifts to higher frequencies as the opening is enlarged. There is also a progressive diminishing of the effect of the pars flaccida on the responses. The presence or absence of the cavity has no effect on the break-up frequency of the pars tensa. These results have implications for both experimental and modelling studies.

445 Finite-Element Modelling of the Newborn Ear Canal and Middle Ear

Hamid Motallebzadeh¹, Brian Gariepy¹, Nima Maftoon¹, Robert Funnell¹, Sam Daniel¹
¹McGill University

Background

There exist several techniques for early hearing screening and diagnosis but the available screening procedures cannot distinguish clearly between conductive and sensorineural hearing loss in newborns, and the results of available diagnostic tests in very young infants are difficult to interpret. Admittance measurements can help to detect conductive losses but do not provide reliable results for newborns. The newborn ear is anatomically very different from the adult one; for example, the newborn's canal wall is not yet fully ossified and has a much lower stiffness than that of the adult.

Methods

Finite-element models of the newborn ear canal and middle ear were developed and their responses were studied for frequencies up to 2000 Hz. Material properties were taken from previous measurements and estimates, and the sensitivities of the models to these different parameters were examined. The simulation results were validated through comparison with previous experimental measures.

Results

Simulations indicate that at frequencies up to 250 Hz the admittance of the canal wall is comparable to that of the middle ear in the newborn. Above 250 Hz the admittance of the canal wall remains almost constant. For the middle ear, however, there is a clearly defined resonance peak in the vicinity of 1100 Hz that produces an admittance much larger than that of the canal wall. Above this frequency, the middle-ear admittance gradually decreases, reaching a value approximately twice that of the canal wall at 2000 Hz. Overall, the middle-ear admittance only dominates that of the canal wall in a narrow band around the middle-ear resonance.

Conclusion

Our model predicts that at the conventional tympanometric frequency of 226 Hz the newborn canal-wall admittance is comparable to that of the middle ear, so the canal-wall admittance is not negligible as it is in adults. In addition, this model suggests that tympanometry with probe tones in the vicinity of the middle-ear resonance frequency, where the middle-ear admittance dominates, improves the chance that the measured admittance will give useful information about the middle ear.

446 Negative Middle Ear Pressure Versus Ear Canal Pressure Variations: Effects on Wideband Energy Absorbance Measurements in Humans

Xiao-Ming Sun¹, Mark D. Shaver¹

¹Wichita State University

Background

A recent study reported the effects of negative middle ear pressure (-MEP) and positive/negative ear canal pressure (\pm ECP) on the middle ear function using otoacoustic emissions (Sun, 2012). Wideband energy absorbance (EA) has been proposed to characterize the forward middle ear transfer function. It is determined by the ratio of absorbed to incident sound energy. This technique offers larger SNRs than otoacoustic emissions thus preventing underestimation by way of noise floor effects.

Methods

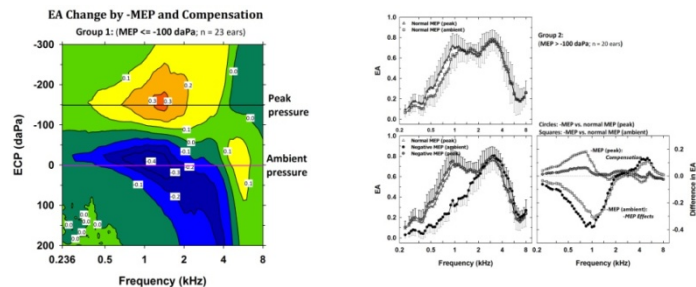
Data were collected from 34 adults with normal hearing using an Interacoustics wideband tympanometer. EA measurements were analyzed from 0.236 to 8 kHz with ECP swept from +200 to -300 daPa under normal and -MEP conditions. MEP was estimated by the bandpass tympanogram peak pressure (BTTP). Subjects produced -MEP by performing a Toynbee maneuver. Data were grouped into two MEP ranges: > -100 daPa (20 ears) and ≤ -100 daPa (23 ears). EA under normal MEP (at BTTP) was subtracted from EA with pressure manipulations to define four effects: (1) -MEP effect (EA under -MEP at the ambient pressure); (2) compensation effect (EA under -MEP at BTTP); and (3, 4) +ECP and -ECP effects (EA under normal MEP at ECP = \pm (-MEP), respectively).

Results

Under normal MEP (mean = -15 daPa), mean ambient EA was ~ 0.07 and ~ 0.09 lower than EA at BTTP for the two groups. Under -MEP for Group 1, EA decreased for frequencies below 2 kHz (~ 0.38 at 1 kHz) and increased (up to ~ 0.13) above 2 kHz. For Group 2, the transition frequency for EA decrease and increase moved upward to 4 kHz with a maximal reduction of ~ 0.43 and enhancement of ~ 0.19 . Difference in EA between compensated and normal MEP conditions was small (~ 0.05). The EA change by +ECP and -MEP was similar. In contrast, -ECP resulted in less reduction (~ 0.05) for low frequencies and less enhancement (~ 0.1) for high frequencies.

Conclusion

Negative MEP substantially alters EA in a frequency-specific pattern. This effect is clinically important even in ears undergoing everyday MEP variations. These findings should be considered when establishing clinical norms. Application of an equivalent ECP in ears with -MEP effectively corrects the altered EA. This procedure may improve diagnosis of middle ear diseases with coexistent MEP. The effects of +ECP and -MEP are comparable while the -ECP effect is smaller. Positive ECP may be utilized to research -MEP effects on middle ear physiology.



447 Assessment of Tympanic Membrane-Coupled Ossicular Integrity on Mechanical and Physiologic Responses in a Middle Ear Effusion Model

R.Alex Harbison¹, Jennifer L. Thornton¹, Kanthiah Koka¹, J. Eric Lupo¹, Daniel J. Tollin¹

¹University of Colorado Denver

Background

Middle ear effusions (MEE) arising as a result of otitis media or Eustachian tube dysfunction are characterized by impaired mobility of the tympanic membrane (TM) and ossicular chain often resulting in a conductive hearing loss. The contribution of diminished ossicular mobility to the hearing loss seen in MEE, however, remains to be further characterized. We hypothesized that if ossicular coupling is interrupted during a MEE, there would be a reduced umbo velocity magnitude ($[V_U]$) and an increased cochlear microphonic (CM) threshold.

Methods

V_U and CM responses were measured in response to tone pips ranging in frequency from 0.25 – 8 kHz and in intensity from 10-100 dB in chinchilla ears (N=5). $[V_U]$ and CM thresholds were recorded in normal ears (baseline) and fluid-filled bullae (fluid) simulating a MEE (2.0cc, 0.5 Poise silicone oil). Responses were then observed in two additional conditions: 1) after disarticulating the incudostapedial joint in baseline ears (baseline without chain) and 2) after filling the disarticulated middle ear with fluid (fluid without chain).

Results

Results showed reduced $[V_U]$ at all frequencies in simulated MEE with the ossicular chain intact. With introduction of ossicular chain disruption, $[V_U]$ in the fluid without chain versus fluid condition decreased significantly

at low and medium but not high frequencies (~4, 5, and 2 dB, respectively). Elevated CM thresholds were greatest in conditions without an intact chain (re: normal). A 6 dB increase in CM threshold was observed during the fluid without chain versus the baseline without chain state at low frequencies. The slope (a) of the linear regression relating $[V_U]$ and CM threshold changes shows proportional change with MEE, however, the proportionality is lost with disarticulation in baseline and fluid states ($a = 0.94, 0.07, \text{ and } 0.69 \text{ dB/dB}$, respectively).

Conclusion

During MEE with interrupted ossicular coupling 1) changes in $[V_U]$ are consistent with reduced summative TM input to umbo (re: fluid) and 2) changes in CM threshold suggest attenuated difference in sound pressure between the oval and round windows (re: baseline without chain). Moreover, CM and $[V_U]$ relations may be of potential clinical utility providing a sensitive test to differentiate MEE from MEE with ossicular pathology [supported by: NIH NIDCD R01-DC01155].

448 Development of Cartilage Conduction Hearing Aid (3) -Monosyllable Intelligibility in the Noisy Condition-

Ryota Shimokura¹, Hiroshi Hosoi¹, Toshie Matsui¹, Tadashi Nishimura¹

¹Nara Medical University

Background

In 2004, professor Hosoi found that clear sound can be heard when a transducer touches softly on an aural cartilage. From the basis for the idea, a trial model of the cartilage conduction hearing aid has been completed (Figure 1b). The ring-shaped fitting part attached to the transducer is put in the entrance of the external auditory canal, and the vibrated cartilage around the fitting part transmit sound information. Since the cartilage conduction hearing aid does not occlude the external auditory canal, it can be used as an alternative to an open-fitting hearing aid. Our previous study reported that the vibration of aural cartilage generates sound in an external auditory canal especially in the low frequency range (< 3 kHz), and the amplified sound is hard to leak from the canal, regardless of the opening. So conversely, is the cartilage conduction hearing aid sensitive to inflow of environmental noise through the opening? To answer this question, monosyllable intelligibilities of open-fitting and cartilage conduction are compared in noisy conditions.

Methods

First, a sound pressure level (SPL) to present monosyllable is determined. Three subjects with normal hearing took speech audiogram tests in a silent condition. The presentation methods were open-fitting and cartilage conduction (Figure 1). In each presentation, the SPL to obtain maximum discrimination score (SPLmax) was measured for each subject, and the presentation SPL was determined by SPLmax + 10 dB.

Second, the speech audiogram tests were carried out presenting a white noise. A loudspeaker to present the white noise was put on the left side of the subject (the distance: 3 m). The SPL of noise changed in 55, 58, 61, 64, and 67 dB. The presentation methods of the monosyllables were open-fitting and cartilage conduction at the left ear, and the presentation SPL was constant. The unused right ear was occluded by an earplug.

Results

Figure 2 compared the monosyllable intelligibilities for the open-fitting and cartilage conduction presentations in the noisy conditions. The monosyllable intelligibility for the cartilage conduction was higher than that for the open-fitting.

Conclusion

Although the both open-fitting earplug and cartilage conduction transducer keeps the external auditory canal opened, the cartilage conduction transducer is more robust against the coming noise. The open-fitting earplug is hard to amplify sound in the low frequency range, while the cartilage conduction transducer does not leak the low frequency sound, which is important to discriminate speech.

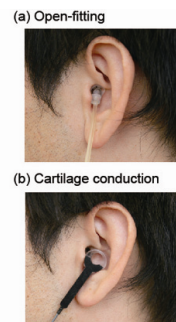


Figure 1. Presentation methods

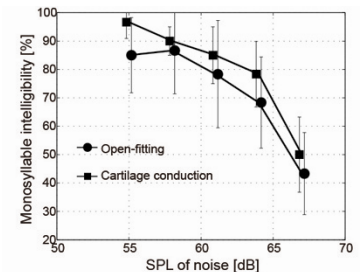


Figure 2. Monosyllable intelligibilities in the noisy conditions for each presentation method (error bar: standard deviation)

449 Investigating the Emergence of Binaural Processing Strategies After Surgical Correction of Congenital Unilateral Conductive Hearing Loss

Brian Gartrell^{1,2}, Alan Kan², Shelly Godar², Samuel Gubbels¹, Ruth Litovsky²

¹University of Wisconsin Hospital and Clinics, ²Binaural Hearing and Speech Laboratory, Waisman Center, University of Wisconsin-Madison

Background

Long-term improvement in performance on binaural processing tasks has not been observed after surgical correction of congenital unilateral conductive hearing loss (CUCHL). Previous investigations have evaluated subjects only over the short-term (< 6 months after surgery). However, animal studies investigating auditory development and research on human subjects receiving bilateral cochlear implants indicate that auditory plasticity may exist after critical periods have passed.

Methods

Subjects underwent surgery at least 1.5 years before free-field testing (range 1.5 – 7 years). Pure-tone audiometry was performed before and after surgery.

Sound localization was tested while each listener sat in the center of an arc of 19 loudspeakers spaced 10° apart, positioned at 0° azimuth. A train of four bursts of pink noise at 50 dB sound pressure level (SPL) with a +/- 4 dB level rove was emitted from each loudspeaker, with twenty repetitions per location. Listeners indicated the perceived sound location on a touch-screen, and the difference between reported and actual locations was calculated as root mean square (RMS) error.

Speech-in-noise testing involved listening to a male target voice consisting of CNC words presented from 0° azimuth. Two female maskers were presented at 50 dB SPL in the following configurations: 0°, + 90°, - 90°, or +/- 90°. Testing was conducted at signal-to-noise ratios (SNR) ranging from 0 to -30 dB SPL. Listeners were asked to select the heard word from a closed list of words. Spatial release from masking (SRM) was computed as the difference in performance with maskers at 0° vs. either +90°, -90°, or +/- 90°.

Results

Preliminary results suggest that listeners demonstrate SRM within the range of values of normal-hearing controls (range 4-9 dB). Localization accuracy may be slightly worse in subjects tested to date (RMS range 8.37-12.99°) than in normal-hearing controls (range 5.29-9.2°), but is within the range of performance observed in normal-hearing children, and better than performance seen in bilateral cochlear implant users.

Conclusion

In listeners with CUCHL performance on binaural hearing tasks falls within the range observed in normal-hearing listeners, which has not been reported in patients with short-term follow-up. This may be a result of auditory plasticity. These findings suggest that binaural processing strategies may mature with continued auditory stimulation over long-term follow-up after repair of CUCHL.

Work funded by NIH-NIDCD (R01DC8083 and R01DC8365) and NIH-NICHD P30HD03352

450 HB-EGF Stimulates Hyperplasia of the Middle Ear Mucosa in Bacterial Otitis Media

Keigo Suzukawa¹, Julia Tomlin², Grace Luu², Eduard Chavez², Kwang Pak², Stephen Wasserman², Allen Ryan,²

¹University of Tokyo, ²University of California San Diego

Background

Otitis media is one of the most common pediatric diseases. While it is usually treated without difficulty, up to 20% of children may progress to long-term complications that include hearing loss, impaired speech and language development, academic underachievement, and irreversible disease. Hyperplasia of middle ear mucosa contributes to the sequelae of acute otitis media and is of

important clinical significance. Understanding the role of growth factors in the mediation of mucosal hyperplasia could lead to the development of new therapeutic interventions for this disease and its sequelae.

Methods

To explore growth factors that may regulate mucosal hyperplasia, a whole genome gene array analysis of mRNA expression of mice during acute otitis media induced by nontypable *Haemophilus influenzae* was performed. We identified growth factors with expression kinetics temporally related to mucosal hyperplasia. We then tested the factors for their ability to stimulate mucosal growth in vitro with mucosal explant model of rat middle ear mucosa.

Results

From the gene array analysis, we discovered seven candidate growth factors with up-regulation of mRNA expression related to mucosal hyperplasia; Amphiregulin, Epiregulin, HB-EGF, GDF-15, LIF, Activin A, Cxcl1. Each factor was then applied in vitro to middle ear mucosal explants in three different concentrations. Of the seven, only HB-EGF induced significant mucosal hyperplasia. Subsequent quantification of HB-EGF protein expression in vivo via Western blot analysis with anti-HB-EGF antibody confirmed that the protein is highly expressed from 6 to 24 hours after bacterial inoculation, while immunohistochemistry revealed production by middle ear epithelial cells and infiltrated lymphocytes.

Conclusion

HB-EGF is expressed during the course of acute otitis media and can stimulate mucosal growth, suggesting an active role in the disease process. These results imply that therapies which target HB-EGF may have the ability to ameliorate mucosal hyperplasia during otitis media, and thereby reduce the detrimental sequelae of this childhood disease.

451 High-Throughput Screening of Kinases Regulating Mucosal Growth in Bacterial Otitis Media

Julia Tomlin¹, Keigo Suzukawa², Eduard Chavez¹, Kwang Pak¹, Stephen Wasserman¹, Allen Ryan,¹

¹University of California San Diego, ²University of Tokyo

Background

Hyperplasia is a phenomenon unique to the mucosa of the middle ear. In the setting of otitis media it can contribute to the numerous detrimental sequelae of this common pediatric disease, including hearing loss, speech and language delay, and learning impediments. Understanding the mechanism of mucosal growth during infection is, therefore, of clinical significance. Though it is known that mucosal cell proliferation is regulated by intracellular signal transduction, the role of various signalling pathways in the middle ear remains poorly understood. We developed a novel high-throughput screening model to identify signaling cascades integral to

mucosal hyperplasia, and used the model to evaluate the inhibition of kinase inhibitors.

Methods

In 48 well plates, we plated 0.25mm² explants of middle ear mucosa from bacterially infected rat ears. The mucosa was allowed 48 hours to attach. Kinase inhibitors from a 160 compound commercial library that covered the mammalian kinome were added to the culture media. The growth of each explant was monitored for 6 days and the surface area was measured on the final day.

Results

Middle ear mucosal explants were cultured successfully and demonstrated consistent growth. Each inhibitor was applied at three concentrations to groups of three explants per concentration to develop a dose response function. The screening yielded compounds with the potential to regulate mucosal hyperplasia in bacterial otitis media. Elements of several different kinome families were found to contribute to mucosal hyperplasia.

Conclusion

We have established a high-throughput screening technique to identify kinase inhibitors that play a role in mucosal growth in the middle ear. This method proved to be repeatable and consistent, and may be useful in screening other compound libraries in the future. Most importantly, it facilitates greater understanding of the intracellular signaling pathways involved in middle ear infection and introduces potential targets for the amelioration of otitis media sequelae.

452 Development of Cartilage Conduction Hearing Aid (2) –Benefits in Patients with Continuous Otorrhea or Acquired Aural Atresia

Tadashi Nishimura¹, Hiroshi Hosoi¹, Osamu Saito¹, Ryosuke Miyamae¹, Ryota Shimokura¹, Toshie Matsui¹, Takashi Iwakura²

¹Nara Medical University, ²Rion Co., Ltd

Background

Sound was effectively transmitted by attaching a transducer to the aural cartilage even without fixation pressure. This new method for sound transmission was termed cartilage conduction (CC). CC can be utilized even in hearing-impaired patients who cannot use air-conduction hearing aids due to continuous otorrhea or aural atresia. Although we develop a hearing aid employing CC, the benefits of the prototype hearing aid have not yet been assessed. In this study, the CC hearing aid was fitted in patients, and its benefits were investigated.

Methods

Four patients with conditions such as continuous otorrhea and acquired aural atresia after surgery participated in this study. The benefits were assessed by audiometric tests and interview.

Results

Thresholds and speech recognition scores improved in all subjects. Below 2 kHz, the functional gains in the patients with acquired aural atresia were larger than those with continuous otorrhea. However, at 4 kHz, the functional gain at 4 kHz could not reach a sufficient level in the patients with aural atresia. The large gains below 2 kHz in the patients with aural atresia were probably caused by a soft tissue transmission pathway in the postoperative space. Sound at 4 kHz may be transmitted via direct air-conduction pathway. No subjects complained of pain associated with the attachment of the transducer, although such problems are usually observed for a bone-conduction hearing aid. This feature is considered one of the advantages of the CC hearing aid.

Conclusion

These results indicate that the CC hearing aid has potential as a useful amplification device for patients with hearing disability.



Cartilage conduction hearing aid

453 The Effect of Visual Information on Intelligibility in Bone-Conducted Ultrasound Perception

Akinori Yamashita¹, Tadashi Nishimura¹, Yoshiki Nagatani², Hiroshi Hosoi¹

¹Nara Medical University, ²Kobe city college of Technology

Background

Since Gavreau reported that ultrasound could be heard by bone-conduction, many interesting characteristics have been reported about bone-conducted ultrasonic perception. Especially, recent studies indicated that Bone-conducted ultrasound (BCU) modulated by different speech sounds can be discriminated by some profoundly deaf subjects as well as the normal-hearing. Recently, a bone-conducted ultrasonic hearing-aid (BCUHA) for profoundly deaf individuals have been developed and its utility has been evaluated. However, previous studies using BCUHA revealed intelligibility only with the use of acoustic media in transmitting language information. In this study, we investigated the effects of visual information (lip-reading information) on intelligibility in bone-conducted ultrasound perception of normal-hearing individuals.

Methods

Speech discrimination tests were performed in three conditions: (1) audio-alone condition, (2) audio-visual condition, (3) visual alone condition. The results of three speech discrimination tests were compared.

Results

The results of speech discrimination tests in this study revealed that lip-reading information strongly affected bone-conducted ultrasound speech perception. The speech intelligibility of bone-conducted ultrasound with visual information was significantly higher than that without visual information.

Conclusion

We found that lip-reading information had clear effects on bone-conducted ultrasound perception, showing that simultaneous presentation of audio and visual information improved intelligibility to levels sufficient for speech perception. Our findings also suggested the efficacy of use of signal processing techniques in improving the intelligibility of prior consonants.

454 Identification of Conductive Hearing Loss in CBA/CaJ Mice Using Bone Conduction

David Chhan^{1,2}, Melissa McKinnon^{2,3}, John Rosowski^{1,3}

¹Harvard-MIT program in Speech and Hearing Bioscience and Technology, ²MEEI Eaton Peabody Laboratory,

³Massachusetts Eye and Ear Infirmary

Background

We explored the use of bone conduction to identify conductive hearing loss in mice.

Methods

Auditory brainstem responses (ABR) were recorded from two dozen 7 to 8-week old CBA mice with both acoustic and bone conduction stimuli. For bone conduction stimulation, a flat head metal screw was implanted near the vertex of the skull, and the screw was glued to a Bruel & Kjaer minishaker. Brief tone pip stimuli were presented either by air conduction (AC) or by activating the shaker (BC). ABR thresholds, the lowest stimulus levels to produce response peaks, were determined by visual detection. Conductive hearing pathology was introduced by two ways: 1. removal of the tympanic membrane (TM) and malleus of the tested ear, 2. filling the middle ear cavity (MEC) with saline. Removal of the TM and malleus decouples the ossicular chain that is required to efficiently transfer acoustic energy into the cochlea. With the fluid filled middle ear cavity, the middle system now becomes stiffer making it harder for the TM and ossicles to move in response to AC sound.

Results

Both of these manipulations produced significant increases (30- 50 dB) in ABR thresholds in response to acoustic stimulation. Since bone conduction involves different pathways, we expected that these manipulations would

have little effect on the hearing sensitivity. Our results show that the threshold stimulus levels with bone conduction stimulation remained unchanged at frequencies above 10 kHz, and at lower frequencies, were increased by 5-10 dB.

Conclusion

These results suggest that the combination of air and bone conduction testing can distinguish sensorineural hearing loss from conductive hearing loss in mice. This technique can be a useful tool in evaluating the onset and development of hearing loss in various strains of mice.

455 Finding of Characteristic DFNA9 Cochlin-Staining Eosinophilic Deposits in the Middle Ear: Comparison of Wild-Type (WT), Coch Knock-In (KI) and Knock-Out (KO) Mouse Models and DFNA9-Affected and Unaffected Individuals

Nahid Robertson¹, Cheng Ong², Jennifer O'Malley², Anne Giersch¹, Konstantina Stankovic², Cynthia Morton¹

¹Brigham & Women's Hospital, Harvard Medical School,

²Massachusetts Eye & Ear Infirmary, Harvard Medical School

Background

Mutations in *COCH*, encoding cochlin, the most abundant protein detected in the inner ear, cause the midlife-onset, progressive sensorineural hearing loss and vestibular disorder, DFNA9. To date, 14 missense *COCH* mutations have been found throughout four continents. A pathognomonic DFNA9 finding is presence of cochlin-staining, eosinophilic deposits throughout the spiral ligament and limbus, and the stroma in the vestibular system, and reduction in number of fibrocytes, which normally express cochlin. A recent study (McCall AA *et al.*, *JARO*, 2011, 12(2):141-9) reported presence of acellular deposits in middle ear structures in DFNA9. We have investigated more thoroughly the nature of these deposits and the role of cochlin by characterizing 1) middle ear histology in wild-type (WT), *Coch*^{G88E/G88E} knock-in (KI) and *Coch*^{-/-} knock-out (KO) mouse models, 2) cochlin localization in unaffected human and WT mouse middle ears, and 3) cochlin immunostaining in human DFNA9 and *Coch* KI mouse middle ears.

Methods

H&E staining of celloidin-embedded DFNA9 and age-matched control middle ear sections, and paraffin-embedded WT, *Coch* KI, and *Coch* KO mouse sections were performed. Immunohistochemistry of adjacent sections were performed using an anti-cochlin antibody.

Results

Eosinophilic deposits were detected in the *Coch* KI middle ears, most notably in the inter-ossicular joints. These aggregates were absent in the WT and *Coch* KO mouse, consistent with our hypothesis that DFNA9 pathology is gain of deleterious function of mutant cochlin, rather than haploinsufficiency, or absence of cochlin. Immunostaining

revealed specific and prominent cochlin localization in inter-ossicular joints and pars flaccida of the tympanic membrane (TM) in both WT and *Coch* KI mice, including areas of aggregates. Deposit formation in the TM of 1-year-old KI mice was not appreciable, in contrast to prominent deposits in the incudo-malleal joint, suggesting that abnormal aggregates in TM occur later than in the inter-ossicular joints. Mice at different ages are being evaluated to assess initial formation and progression of this pathology. Immunostaining of DFNA9-affected and age-matched control middle ears revealed cochlin localization in the same structures as seen in the mouse, as well as in the aggregates. Proteomic studies underway may further identify composition of the aggregates, pointing toward cochlin interactors and other proteins involved in cochlin functional pathways.

Conclusion

Our DFNA9 and *Coch* KI findings provide further insight into cochlin function and its role in progression of the disease process.

456 Therapeutic Potential of Adenovirus-Mediated Induction of β -Defensin 2 for Otitis Media

Sung Moon¹, Jeong-Im Woo¹, Yoojin Lee¹, Okjin Ahn¹, Douglas Brough², David Lim¹

¹House Research Institute, ²GenVec Inc.

Background

In our prior studies, we demonstrated that β -defensins inhibit viability of the common otitis media pathogens. We also showed that the middle ear epithelial cells induce β -defensin 2 in response to nontypeable *H. influenzae* (NTHi) via TLR2-dependent signaling, suggesting therapeutic potential of a β -defensin 2 inducer. Here, we aim to determine if an adenoviral vector containing the human β -defensin 2 gene (DEFB4) can serve as a β -defensin 2 inducer of the middle ear epithelial cells.

Methods

Regulation of β -defensin 2 expression was determined with qRT-PCR analysis and ELISA analysis. Confocal microscopy was performed to determine an inhibitory effect of β -defensin 2 on bacterial adhesion. For bacterial clearance, NTHi colonies were counted after culturing of the murine middle ear lavage.

Results

We found that transtympanic inoculation of the recombinant β -defensin 2 enhances NTHi clearance from the middle ear cavity. The adenoviral vector expressing β -defensin 2 (Ad-DEFB4) was found to up-regulate β -defensin 2 expression in the epithelial cells in a time- and dose-dependent manner, compared to Ad-null. Infection with Ad-DEFB4 appeared to inhibit adhesion of NTHi to the epithelial cells. Transtympanic inoculation of Ad- β -gal appeared to induce β -galactosidase without inflammatory response in the rat middle ear. Moreover, Ad-DEFB4 was found to improve clearance of NTHi from the murine middle ear cavity.

Conclusion

Taken together, our results suggest that induction of β -defensin 2 by an adenoviral vector may be considered as an alternative strategy for the management of middle ear infection. [Supported by NIH grants: DC005025, DC006276 and DC011862]

457 Influence of Target Tissue on Survival and Differentiation of Neurons Derived from HES Cells

Suvarna Dash-Wagh¹, Rouknuddin Ali², Lars Ärhlund-Richter³, Mats Ulfendahl⁴

¹Karolinska Institutet, ²Department of Neuroscience,

³Center for Cancer Research, ⁴Department of Neuroscience

Background

Cell replacement therapy is a potentially powerful approach to replace degenerated or severely damaged hair cells and spiral ganglion neurons in the inner ear. Cell therapy has been proposed to be a promising strategy to restore hearing either by replacing degenerated neurons or via improving the efficacy of cochlear implants which rely on functional neurons. Neurons derived from embryonic and adult neural tissue or stem cells have been successfully transplanted into the inner ear. It remains to identify how the auditory tissue influence these implanted cells. During development and regeneration, a plethora of growth factors are secreted from the target tissue including neurotrophins. These factors promote the survival, migration and integration of the approaching cells. Currently, we are investigating how the secreted factors from the auditory tissue influence the growth and differentiation of neural progenitors generated from human embryonic stem (hES) cells.

Methods

Organotypic culture from different tissue (brainstem, organ of Corti, spiral ganglion neurons) were prepared from early postnatal rat. Conditioned media which contains all the secreted factors were collected. The activity of the medium from the different auditory system tissues was tested on neurons derived from human neuroblastoma SHSY5Y or hES cells cultures. Different parameters using molecular biology, immunohistochemistry and cytotoxicity and other techniques are tested.

Results

The preliminary results of the testing of the effects of secreted factors on the neural progenitor derived from hES cells exhibit interesting trends. The measurement of the cell migration distance in these progenitors shows that medium from SGNs and organ of Corti induced higher migration while brainstem derived medium was similar to control. The neurite outgrowth is parameter to check the different of progenitor into neurons. Again we observed that the medium from SGN induce higher neurite outgrowth in the hES cells derived neural progenitors than control.

Conclusion

Our preliminary data shows that there are factors secreted from the auditory tissue which influence the differentiation of the neurons derived from hES cells. Identification of these factors would be very helpful in developing cell therapy for inner ear.

458 Localization of Kainate Receptors in Inner and Outer Hair Cell Synapses

Taro Fujikawa¹, Ronald S. Petralia¹, Ya-Xian Wang¹, Bechara Kachar¹
¹NIDCD/NIH

Background

Glutamate and its receptors mediate inner hair cell (IHC) afferent transmission. Recent physiological data show that glutamate also plays a role in outer hair cell (OHC)/type II afferent transmission, but the glutamate receptors that are involved are not well defined. A previous study using in situ hybridization showed that several kainate-type glutamate receptor subunits (GluR5, GluR6, KA1, KA2) are expressed in cochlea ganglion neurons (Niedzielski & Wenthold, 1995, *J Neurosci* 15: 2338). Another group reported that kainate receptors are expressed in IHC afferent synapses and contribute to hair cell acoustic transmission (Peppi et al., 2012, *J Assoc Res Otolaryngol* 13: 199).

Methods

X-gal staining was performed on whole-mount cochlea and cryostat sections of KA2-KO mice (P8, P14, 1.5 months and 1 year old), which have a Lac Z cassette for the reporter gene. Type I and type II ganglion neurons were discriminated by different labeling patterns of neurofilament-H. Immunocytochemistry was performed on rat whole-mount cochlea using commercial antibodies against all kainate receptor subunits. Slight paraformaldehyde fixation combined with microwave-mediated antigen-retrieval or pure methanol fixation was essential for labeling. Also, electron microscopy of postembedding immunogold labeling was performed in guinea pigs.

Results

X-gal staining was found in both type I and type II ganglion neurons in adults. Also, staining was seen only in OHCs and spiral limbus region at 1.5 months or older, although staining may be more widespread at younger ages.

GluR6 immunolabeling colocalized with CtBP2 at IHC and OHC synapses. Also, labeling was contiguous with postsynaptic PSD-93 at OHC synapses; these patterns matched those with the AMPA glutamate receptor subunit, GluR2. GluR5 mainly labeled OHC efferent synapses - shown by double labeling of VAMP2 or Na⁺/K⁺-ATPase α 3. No distinct labeling was found in IHC and OHC afferent synapses. KA2 labeled IHC afferent synapses definitively, but labeling in OHC synapses was less definitive. KA1 appeared to label OHC afferent synapses but not IHC ones. No immunoreactivity for GluR7 was detected in the cochlea.

Conclusion

OHC afferent synapses contain at least GluR6 and possibly KA1 and KA2 that could form various combinations on the presynaptic and postsynaptic membrane. GluR6 and KA2 are expressed in IHC afferent synapses. These results suggest that kainate receptors are involved in synaptic transmission in both IHCs and OHCs. Also, GluR5-containing receptors may modulate OHC efferent inhibition.

459 Exocytosis of Protons Blocks Ca²⁺ Currents in Auditory Hair Cells

Soyoun Cho¹, Henrique von Gersdorff¹
¹Vollum Institute, OHSU

Background

Ca²⁺ influx across the plasma membrane of hair cells triggers neurotransmitter release at ribbon type active zones. To manage an uninterrupted flow of transmission, this synapse continuously releases glutamate, the neurotransmitter stored in synaptic vesicles. The pH inside vesicles is thought to be about 5.7 and the exchange of protons for glutamate allows the vesicular glutamate transporter to fill synaptic vesicles with glutamate. The exocytosis of synaptic vesicles transiently acidifies the synaptic cleft of bipolar cell synapses, which are also ribbon type synapses. This leads to a transient acidification of the synaptic cleft and block of the Ca²⁺ channels located near the sites of exocytosis. We studied an analogous process in the hair cell ribbon synapse.

Methods

Amphibian papillae were carefully dissected from adult bullfrogs that had been sedated in ice water bath and double-pithed. Semi-intact preparations of hair cells and their connecting afferent fibers were obtained as described by previous studies. Whole-cell patch-clamp recordings were performed with an EPC-10/2 patch-clamp amplifier (HEKA).

Results

We have found that the shapes of Ca²⁺ currents are different depending on the membrane holding potential of hair cells. When hair cells were depolarized from -60 mV, a potential close to the physiological resting membrane potential of in vivo hair cells, to -30 mV, the Ca²⁺ currents showed "outward" transient components in contrast with Ca²⁺ currents of hair cells that were held at -90 mV. The average size of outward component was 22.9 ± 2.6% of the peak Ca²⁺ current. We also examined how much time is required to for a detectable outward component to develop. We depolarized hair cells from -90 mV to -60 mV for various durations as a pre-pulse and then depolarized to -30 mV for 20 ms. The outward component required about 50 ms to 100 ms at -60 mV to start showing, and the size of this component increased as hair cells were held longer at -60 mV. To confirm whether protons co-released with glutamate from fused vesicles cause the outward components in Ca²⁺ currents, we applied methylamine, a weak base. This abolished the outward component. The outward component was also significantly decreased when

the concentration of external HEPES was increased to 50 mM.

Conclusion

The transient outward components in Ca^{2+} currents of frog auditory hair cells results from a block of Ca^{2+} channels by protons released from fused synaptic vesicles.

460 Evidence for K⁺ Accumulation Around Mammalian Vestibular Type I Hair Cells: An Electrophysiological Study

Donatella Contini¹, Valeria Zampini¹, Elisa Tavazzani¹, Jacopo Magistretti¹, Giancarlo Russo¹, Sergio Masetto¹, Ivo Prigioni¹

¹University of Pavia

Background

Mammalian vestibular organs contain two types of sensory receptors, named Type I and Type II hair cells. While Type II hair cells are contacted by several small afferent nerve terminals, the basolateral surface of Type I hair cells is almost entirely enveloped by a single large afferent nerve terminal, called calyx. Moreover Type I, but not Type II hair cells, express a low-voltage activated outward K⁺ current, IK,L, which is responsible for their much lower input resistance (R_m) at rest as compared to Type II hair cells. The functional meaning of IK,L and associated calyx is still enigmatic.

Methods

Experiments were performed on mice (C57 and Swiss CD1) obtained from Harlan Italy. Mouse age ranged between postnatal day (P) 7 and P25. The roof of the isolated SCC ampulla was gently torn to expose the crista ampullaris, which was then immobilized at the bottom of a glass Petri dish by means of a weighted nylon mesh. Hair cells in the crista were viewed and photographed by using an upright microscope equipped with differential interference contrast optics (Zeiss Axioskop, Germany), 63x water immersion objective. By using the patch-clamp whole-cell technique we have recorded the current- and voltage responses from in situ hair cells.

Results

Outward K⁺ current activation resulted in K⁺ accumulation around Type I hair cells, since it induced a rightward shift of the K⁺ reversal potential, the magnitude of which depended on the amplitude and duration of K⁺ current flow. Since this phenomenon was never observed for Type II hair cells, we ascribed it to the presence of a residual calyx limiting K⁺ efflux from the synaptic cleft. Intercellular K⁺ accumulation added a slow ($\tau > 100$ ms) depolarizing component to the cell voltage response. In a few cases we were able to record from the calyx and found evidence for intercellular K⁺ accumulation as well. The resulting depolarization could trigger a discharge of action potentials in the afferent nerve fiber.

Conclusion

Our results support a model where pre- and postsynaptic depolarization produced by intercellular K⁺ accumulation

cooperates with the conventional neurotransmitter release in sustaining afferent transmission arising from Type I hair cells. While vesicular transmission together with the low R_m of Type I hair cells appears best suited for signaling fast head movements, depolarization produced by intercellular K⁺ accumulation could enhance signal transmission during slow head movements.

461 Spatio-Temporal Pattern of Action Potential Firing in Mouse Inner Hair Cells

Gaston Sendin¹, Jérôme Bourien¹, Jean-Luc Puel¹, Régis Nouvian¹

¹INSERM

Background

Inner hair cells (IHCs) are the primary transducer for sound encoding in the cochlea. In contrast to the graded receptor potential of adult IHCs, immature hair cells fire spontaneous calcium action potentials during the first postnatal week.

Methods

Here, we investigate the pattern of spontaneous action potential firing in mammalian IHCs during development. We recorded action potentials from neonatal mouse IHCs (P1 to P7) of apical or basal cochlear coils using the perforated patch-clamp technique in the current-clamp mode (I_{inj}=0pA).

Results

We show that IHCs fire burst of action potential and that pattern is undistinguishable between basal and apical hair cells. However, the bursting behavior became more salient during development, i.e, from a broad structure right after birth to a sharp and stereotyped motif at the end of the first postnatal week.

Conclusion

The IHCs spiking activity has been proposed to shape the tonotopic map along the ascending auditory pathway. We suggest that in addition to carrying place information to the ascending auditory nuclei, the firing pattern conveys temporal information of the cochlear development.

462 Analysis of Fluorescently-Labeled Protein Puncta in Hair Cells: Synaptic Strength & Systematic Artifacts

Mark Rutherford¹, Tzu-Lun Wang¹, Gerhard Hoch¹, Carolin Wichman¹, Tobias Moser¹

¹Inner Ear Lab

Background

Immuno-fluorescence microscopy promises to provide high-throughput assessment of antigen abundance in the organ of Corti, at the level of individual synapses. However, semi-quantitative measurements of protein levels may be significantly biased by artifacts introduced during image acquisition. We estimated and corrected for artifacts of (1) bleaching and (2) attenuation in the optical axis so that molecular determinants of relative synaptic strength can be ascertained with confidence.

Methods

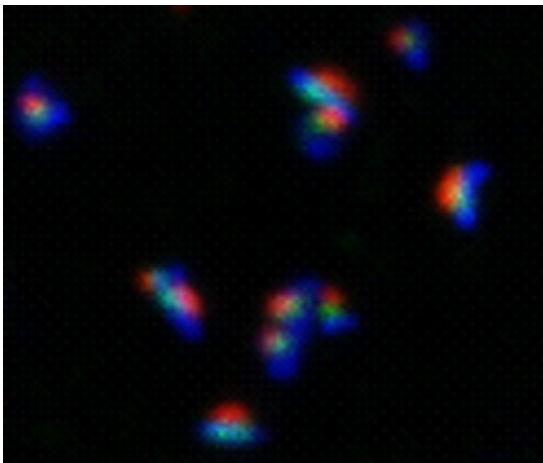
Synapses were triple-labeled for glutamate receptors, calcium channels, and synaptic ribbons. (1) The effect of bleaching was assessed by acquiring two Z-stacks on the same volume of tissue and changing the order-of-acquisition in Z, from top-down to bottom-up. (2) The effect of attenuation was assessed by mounting the organ between two cover slips and imaging the same region of interest from both sides. Puncta were identified by thresholding and then quantified by integrating the voxel intensities within iso-intensity surfaces after background subtraction. Standard microscope settings: 10% laser power, 0.33 μ m step size, 4 scans averaged per XY-section, 400Hz scan rate, 50nm pixels, 25x50 μ m field of view).

Results

(1) The rate of bleaching varied amongst the 3 labels in a stack, ranging from 1-37% when measured as the mean reduction of punctum intensity between two 20 μ m Z-stacks acquired one after another on the same volume (20x3x4=240 XY-scans per channel per stack). Thus the order in which a Z-stack was acquired resulted in as much as ~37% difference in measured intensity of an individual punctum, depending upon whether it was imaged in the first or the final XY-section of the stack. (2) Signal attenuation as a function of tissue depth produced a systematic intensity gradient in the optical axis when using conventional mounting media. When a special mounting medium (TDE) was used to match the refractive index of tissue, attenuation and the resulting spatial gradient artifact were relatively small.

Conclusion

Intensity correlations between labels and spatial gradients of label intensity can be artificially created, augmented, or obscured by systematic artifacts of image acquisition. They can be averaged-out by varying the order-of-acquisition and the preparation's orientation. Before correlations can be interpreted and cells reconstructed with cell-centric coordinates, these Z-axis artifacts must be corrected for. We present a strategy for estimation and compensation to minimize these artifacts of bleaching and attenuation.



463 Evolutionary Changes of the Efferent Hair Cell Receptor

Marcelo Moglie¹, Marcela Lipovsek¹, Ana Belen Elgoyhen¹

¹Instituto de Investigaciones en Ingenieria Genetica y Biologia Molecular (CONICET), Argentina

Background

The α 9 and α 10 nicotinic acetylcholine receptor (nAChR) subunits are expressed in cochlear hair cells, where they form the receptor that participates in the efferent control of auditory function. This nAChR mediates the inhibitory synapse between efferent fibers and outer hair cells in mammals, or short hair cells in birds. This cholinergic efferent feedback to hair cells is a common feature among all vertebrates. Accordingly, one would expect the evolutionary history of the genes coding for the α 9 and α 10 subunits to be similar throughout the whole Subphylum. However, a detailed analysis of the phylogeny and sequences showed signatures of positive selective pressure only for the mammalian α 10 subunits. These differences in the evolutionary history correlate with the divergent biophysical properties of rat and chicken α 9 α 10 nAChRs, such as calcium permeability. Here, we compared the pharmacology of chicken and rat receptors looking for a better understanding of the effects of the non-synonymous substitutions accumulated on mammalian α 10 subunits.

Methods

Recombinant α 9 and α 10 subunit cRNAs were synthesized in vitro and injected in *Xenopus laevis* oocytes. Responses to drugs were measured using the two microelectrode voltage-clamp technique.

Results

The effects of the classical nicotinic agonists choline and DMPP and the antagonist serotonin on chicken receptors differed from those on rat α 9 α 10 receptors and resembled those on rat α 9. Above all, choline showed higher efficacy on chicken α 9 α 10 receptors (88 \pm 8% max response to ACh, n=5) compared to rat α 9 α 10 receptors (34 \pm 4% max response to ACh, n=4). Moreover, in a Rat α 9Chick α 10 hybrid receptor, responses to choline were 86 \pm 4% (n=3) of the maximal response to ACh, resembling chicken receptors and strongly suggesting that the sites involved have been altered in mammalian α 10 subunits.

Conclusion

The aminoacid changes that accumulated on mammalian α 10 subunits resulted in a mammalian α 9 α 10 nAChR with reduced efficacy to the neurotransmitter metabolite choline. We propose that differential sensitivity to choline might result in differences in efferent synaptic kinetics and strength across species.

464 Miniature Post Synaptic Currents Are Entrained by Infrared Pulses

Qiang Liu¹, Erik Jorgensen¹, Holly Holman¹, Micah Frerck¹, Richard Rabbitt^{1,2}

¹University of Utah, ²Marine Biological Laboratory

Background

Inner ear hair cells are exquisitely sensitive to pulsed infrared radiation (IR) and often modulate neurotransmitter release in response to each optical pulse. Four distinct endogenous mechanisms of IR sensitivity have been demonstrated: optoacoustic gating of the mechano-electrical transduction (MET) channels, thermal modulation of plasma membrane ion channels, thermal modulation of plasma membrane capacitance, and thermal modulation of intracellular Ca²⁺ signaling. In the present work we examined thermal modulation of synaptic vesicle release by single IR pulses at wavelengths where IR absorption by water converts the IR optical energy into rapid, but small, heat pulses.

Methods

The neuro-muscular junction of *Caenorhabditis elegans* was used as the model system to facilitate genetic manipulations and reveal molecular targets of IR energy. Conventional whole cell voltage clamp was used to record spontaneous and laser-pulse evoked miniature post-synaptic currents (mPSCs). IR pulses were delivered via a 200-400 μ m diameter optical fiber positioned approximately one fiber diameter away from the cell. Laser diodes tuned to 1862nm or 1550nm were gated at 0-500 μ s pulse to deliver 0-20 μ J/pulse over an area of 100-300nm².

Results

Post-laser-stimulus histograms revealed momentary silencing of mPSCs (zero probability at 0-1.5ms) followed by a doubling of the mPSC rate (peak probability ~2x spontaneous at ~2.6ms). Recovery to the background mPSC rate followed two time courses, a rapid component ~1ms accounting for nearly half of the peak response, followed by a slow component correlating with thermal relaxation. Increased mPSC rates occurred in zero extracellular Ca²⁺ as well as calcium channel knock outs (*nca-1*; *nca-2*) showing that voltage activated plasma membrane Ca²⁺ currents were not required and that IR acted primarily through a voltage independent synaptic vesicle release mechanism.

Conclusion

Pulsed IR rapidly alters the capacitance of the membrane through charge redistribution, and evokes mitochondrial Ca²⁺ currents through non-equilibrium thermodynamics. Although causality has not been shown, present results are consistent with the hypothesis that these biophysical events underlie IR entrainment of mPSCs reported here and IR-evoked synaptic transmission reported previously in vestibular hair cells.

Support was provided by NIH DC011481 (Rabbitt), NIH NS034307 & HHMI (Jorgensen), and NSF DGE-0903715 (Frerck).

465 Protocadherin-15 (PCDH15) Interacts with Integrin α 8 (Itga8) in the Inner Ear. Implications for a Signaling Mechanism Involving Usher Proteins

Marisa Zallocchi¹, Dan Meehan¹, Duane Delimont¹, Linda Cheung¹, Oluwatobi Ogun¹, Dominic Cosgrove^{1,2}

¹Boys Town National Research Hospital, ²University of Nebraska Medical Center

Background

In the inner ear PCDH15 is expressed at the apical and basal aspects of hair cells and neuronal terminals, with multiples isoforms playing different roles, from the kinociliary and tip links formation, to cell polarity and synapse maturation. Mutations in the PCDH15 gene result in Usher syndrome type 1F (USH1F) and sometimes non-syndromic deafness. Itga8 is an integral membrane protein that, upon dimerization with integrin β 1, forms an active membrane receptor that binds extracellular matrix ligands and signals mainly through the small GTPase, RhoA. Expression of itga8 has been demonstrated in the mouse apical hair cell surface and a possible association with focal adhesion kinase has been suggested.

Methods

We employed dual confocal immunohistochemistry, siRNA knockdown technology in the mouse embryonic hair cell line UB/OC-1, and co-immunoprecipitation studies to address whether a possible association between itga8 and PCDH15 exists.

Results

We observed basal and apical expression of itga8 in P1 mouse cochlea. In zebrafish ITGA8 is expressed at the apical and basal aspects of neuromast hair cells, where it co-localizes with Pcdh15a and Pcdh15b and the pre-synaptic marker SV2. UB/OC-1 cells transfected with siRNAs directed to itga8 showed a modification in the distribution pattern for PCDH15 compared with the scrambled controls, suggesting a key role for itga8 in PCDH15 trafficking and/or protein stabilization. PCDH15 knockdown cells did not show any effect in itga8 expression or distribution. In agreement with this last result, the expression analysis in the PCDH15 mutant mouse model, av-3J, show the characteristic distribution pattern and protein abundance for ITGA8 compare with wild type animals. These results reinforce the idea of itga8 playing a central role in complex formation. Co-immunoprecipitation studies from P1 mouse inner ear demonstrated the existence of this complex in vivo.

Conclusion

Our results demonstrate protein interactions between specific PCDH15 variants and itga8. This is the first evidence linking Usher protein function to an integrin-mediated signaling cascade. Because both proteins are expressed early in the immature inner ear they may function in hair cell stereocilia and synaptic maturation. Their expression in zebrafish during hair cell development

provides evidence of a highly conserved function for these two proteins.

This work was supported by NIH grants R01 DC004844 and 5 P20 RR018788-08.

466 Stereocilia Tenting Is Present in Live Hair Cells and Involves Remodeling of the Actin Core

A. Catalina Vélez-Ortega¹, Artur A. Indzhukulian¹, Gregory I Frolenkov¹

¹University of Kentucky

Background

Tenting refers to the “conical” or “wedge-like” shape at the stereocilia tips of the auditory and vestibular hair cells. It has been repeatedly imaged using scanning (SEM) and transmission (TEM) electron microscopy. Some TEM images show actin filaments filling the tented stereocilia tips while other TEM images depict membrane tenting only. The prevailing model proposes that tenting is caused by the tension that tip links exert on the plasma membrane. This model is mainly supported by SEM data of chemically-fixed tissue showing the loss of tenting after the disruption of tip links via chemical or genetic manipulations. However, specimen preparation artifacts (such as tissue shrinkage) could result in an exaggerated tented appearance of the stereocilia when the tip links are present.

Methods

We imaged the stereocilia bundles of live rat inner hair cells using hopping probe scanning ion conductance microscopy (HPSICM). Using conventional SEM, we studied the dynamic changes in stereocilia tenting after the disruption of tip links with BAPTA-buffered Ca²⁺-free medium.

Results

HPSICM imaging showed, for the first time in live cells, the presence of tenting in the second and third rows of inner hair cell stereocilia. We were not able to find any differences between the shape of the stereocilia tips observed with HPSICM and SEM. Using SEM, we observed that the degree of tenting is different in outer versus inner hair cells. Moreover, the degree of tenting in inner hair cells showed a gradual increase from base to apex. Immediately after BAPTA treatment the tip links were not observed but, interestingly, tenting was still present. Tenting did disappear by 20 min post-BAPTA and the time course of its recovery correlated with the re-appearance of the tip links during the following 5 hours.

Conclusion

Our results demonstrate that stereocilia tenting is not an artifact of tissue fixation but is likely to be a tip link-mediated and mechanically-driven phenomenon that involves the remodeling of the stereocilia actin core.

Supported by NIDCD/NIH (R01DC008861)

467 Eps8L2 Knockout Mice Show Progressive Hearing Loss and Hair Bundle Defects in Auditory Hair Cells

David N Furness¹, Stuart L Johnson², Uri Manor³, Lukas Rüttiger⁴, Jennifer Olt², Richard Goodyear⁵, Carole M Hackney², Andrea Disanza⁶, Giorgio Scita⁶, Marlies Knipper⁴, Matthew C Holley², Guy P Richardson⁵, Bechara Kachar³, **Walter Marcotti**²

¹Keele University, ²University of Sheffield, ³NIDCD,

⁴University of Tübingen, ⁵University of Sussex, ⁶IFOM

Background

The mammalian auditory system is able to detect and process a wide range of sound frequencies and intensities. Central to this process is the transduction of sound waves into electrical signals by cochlear hair cells, which depends upon mechanosensitive stereociliary bundles (Fettiplace and Hackney, 2000 *Nat Rev Neurosci* 7: 19-29). The growth and maintenance of the stereociliary actin core is dynamically regulated via a treadmill mechanism with actin polymerization at the tip and depolymerisation at the base (Manor and Kachar 2008 *Semin Cell Dev Biol* 19: 502-510). Actin capping (e.g. twinfilin 2, gelsolin, Eps8) and cross-linking (e.g. espin, plastin) proteins are crucial for the elongation and thickening of the stereocilia actin core.

Methods

We used a combination of immunolabelling, overexpression of GFT-tagged proteins, single-cell electrophysiology, electron microscopy and in vivo physiology to investigate the role of Eps8-L2, an Eps8-related protein endowed with actin binding activity (Offenhauser et al. 2004 *Mol Biol Cell* 15: 91-98).

Results

Using control and Eps8-L2 knockout mice we show that this protein is a novel component of the hair-cell hair bundle. Eps8L2 localized at the tip of the stereocilia of hair cells from the cochlear and vestibular system and is essential for their maintenance. Eps8L2 knockout mice exhibited progressive hearing loss, which was directly linked to a gradual deterioration of hair-bundle morphology. We found that Eps8-L2 regulates the maintenance of stereocilia height and thickness in hair cells.

Conclusion

Our results indicate that Eps8-L2 directly regulates actin dynamics in hair-cell stereocilia and that it is critical in maintaining the normal functionality of hair cells and hearing in mammals.

Supported by the Wellcome Trust, Westfield Health, The Royal Society, the National Institutes of Health Intramural Research Fund.

468 Mechanotransduction Defects in Sensory Hair Cells of USH1C Knock-In Mice

Charles Askew^{1,2}, Yukako Asai², Jennifer J. Lentz³,
Gwenaelle S.G. Geleoc²

¹Neuroscience Graduate Program, University of Virginia,
²Kirby Center for Neurobiology and Dpt of Otolaryngology,
Boston Children's Hospital, ³Dpt of Otorhinolaryngology &
Biocommunications and Neuroscience Center, LSU Health
Sciences Center

Background

Numerous mouse models of Usher Syndrome (USH) have been identified or engineered over the past decade. Interestingly from over seven models that target harmonin (USH1C), only one reproduces both auditory and retinal deficits. The *Ush1c.216G>A* (Lentz et al. 2007, 2009) is a knock-in model with the cryptic splice site mutation found in French-Acadian USH1C patients. The mutation results in the complete absence of ABR responses in homozygous mutant mice at one month indicating the mice are deaf. Cochlear histology at P30 shows disorganized hair cell rows, abnormal bundles, and loss of both inner and outer hair cells along the organ (Lentz et al. 2012).

Methods

To assess the development of hair cells in the *Ush1c.216G>A* mutant mouse, we analyzed hair bundle morphology, the developmental expression of voltage dependent channels as well as the presence of functional mechanosensitive ion channels in outer hair cells (OHCs) of wild type, heterozygous and homozygous littermates during the first postnatal week.

Results

Disorganized hair bundles were evident in homozygous mice along the entire organ of Corti. Normal voltage-dependent currents and resting potentials were observed for all genotypes. Analysis of FM1-43 uptake in control and heterozygous mutant mice revealed a gradual developmental increase base to apex during the first postnatal week as described previously (Lelli et al. 2009). While the developmental pattern was maintained in the organ of homozygous mutant mice, weaker FM1-43 fluorescence was observed with some sensory cells showing strong dye uptake and others showing no uptake. Direct measurement of transduction currents evoked by stiff-probe deflections of OHC bundles mice revealed similar properties in heterozygous *Ush1c.216G>A* and wild type littermates with maximal currents (I_{max}) of 468 ± 53pA (n=8 het +/- S.D., Apical half P4-P6) at a holding potential of -64mV. In contrast but consistent with the decreased FM1-43 fluorescence, OHCs from homozygous mutants with moderately disrupted hair bundles had smaller (range: 66pA to 296pA) or no transduction current with a mean I_{max} of 220 +/- 70pA (n=9 cells excluding non-transducing cells, Apical half, P3-P6). Adaptation was always present but with a slower fast component in homozygous mutants, similar to that described for other harmonin mutants. More complete adaptation was also occasionally observed.

Conclusion

We conclude that mechanosensitivity is partially preserved in developing OHCs of *Ush1c.216G>A* mutant mice.

(Support: Manton Center for Orphan Disease Pilot Award 2011 to GSGG)

469 Localization of PDZD7 to the Stereocilia Ankle-Link Associates This Scaffolding Protein with the Usher Syndrome Protein Network

M'hamed Grati^{1,2}, Jung-Bum Shin^{3,4}, Michael D. Weston⁵, James Green⁶, Henry Adler^{1,7}, Manzoor A. Bhat⁶, Peter G. Gillespie³, Bechara Kachar¹

¹The National Institute on Deafness and other
Communication Disorders, National Institutes of Health,

²University of Miami Miller School of Medicine, ³Oregon
Hearing Research Center, Oregon Health & Science
University, ⁴Department of Neuroscience, University of
Virginia, ⁵Department of Oral Biology, Creighton University
School of Dentistry, Omaha, NE, ⁶University of North
Carolina, ⁷National Technical Institute for the Deaf,
Rochester Institute of Technology

Background

Usher syndrome is the leading cause of genetic deaf-blindness. Monoallelic mutations in PDZD7 increase the severity of Usher type II syndrome caused by mutations in USH2A and GPR98, which respectively encode for plasma membrane proteins usherin and GPR98. PDZ domain-containing 7 protein (PDZD7) is a paralog of the scaffolding proteins harmonin and whirlin, which are implicated in Usher type 1 and 2 syndromes, respectively. While usherin and GPR98 have been reported to form ankle links in hair-cell stereocilia, harmonin localizes to the stereocilia upper tip-link density and whirlin localizes to both the stereocilia tip and ankle-link regions. Moreover, PDZD7 has been shown to co-immunoprecipitate with USH1 proteins that make up the upper tip-link insertion density, i.e., harmonin (USH1C) and sans (USH1G), as well as with the cytosolic tails of usherin and GPR98. These interactions have not been corroborated by structural evidence. We wanted to investigate the subcellular localization of PDZD7 in hair cells, and to understand its potential role in the development and function of their mechanosensory stereocilia.

Methods

We used mass spectrometry to examine the presence of PDZD7 amongst chicken purified hair bundle proteins. We used immunopurified PDZD7 antibodies to examine its subcellular localization in mammalian sensory hair cells stereocilia bundle and compare it to that of USH1 and USH2 proteins complexes. We also used ballistic transfection of explant rat hair cells to examine the subcellular localization of Cherry-tagged PDZD7. Finally, we used immunocytochemistry on LLC-PK1 epithelial cells to investigate the interactions of PDZD7 with proteins of the ankle-link complex.

Results

We show that PDZD7 is expressed in chick stereocilia at a comparable molecular abundance to GPR98. We also show by immunofluorescence and by overexpression of tagged proteins in rat hair cells that PDZD7 localizes to the ankle-link region of developing organ of Corti and vestibular hair cells and of only mature vestibular hair cells, overlapping with usherin, whirlin, and GPR98. Finally, we expressed in LLC-PK1 cells fusions of the cytosolic domains of both usherin and GPR98 and the interleukin- α subunit, which targets the plasma membrane, and show that both whirlin and PDZD7 can bind to both tails.

Conclusion

Our observations are consistent with PDZD7 being a modifier and candidate gene for USH2, and suggest that PDZD7 is a second scaffolding component of the ankle-link complex that positions and stabilizes GPR98 at hair cells ankle-link region.

470 Can Side Links Mediate Hair Cell Mechanotransduction?

Stephanie Edelmann¹, Artur Indzhykulia¹, Ghanshyam Sinha¹, Gregory Frolenkov¹

¹University of Kentucky

Background

The tip links are thought to be the tethers that open the mechanotransduction channels on the tops of the shorter row stereocilia. Two molecular components of the tip link have been identified: protocadherin 15 (PCDH15) at the lower end of the link and cadherin 23 (CDH23) at the upper end of the link. Both PCDH15 and CDH23 have been shown to be necessary for mechanotransduction in hair cells.

The asymmetric PCDH15/CDH23 composition of the tip link may be disrupted in Shaker 2 and Whirler mice. The inner hair cell bundles in these mutant mice do not form a characteristic staircase. Instead, their stereocilia are interconnected with "top-to-top" links that still mediate mechanotransduction responses but in both positive and negative directions.

Methods

PCDH15 and CDH23 were immune-localized using immuno-gold scanning electron microscopy (Immuno-SEM). The directional sensitivity of the mechanotransduction responses was studied with conventional whole cell patch clamp technique.

Results

In Shaker 2 and Whirler inner hair cells, stereocilia are packed in a hexagonal pattern with the links running in 6 predominant directions from each stereocilium, along 3 axes. We found that the links connecting stereocilia aligned in the axis of normal mechanosensitivity (presumably tip link equivalent) have the same amount of PCDH15 and CDH23 as the side links between neighboring stereocilia.

Conclusion

Our data suggests an apparently identical molecular composition of the tip link equivalent and side links in Shaker 2 and Whirler inner hair cells. Therefore it is very likely that side links could mediate similar mechanotransduction responses. The experiments studying the directionality of mechanotransduction responses in these bundles are underway.

471 Weak Lateral Coupling Between Stereocilia of Inner and Outer Hair-Cell Bundles

K. Domenica Karavitaki¹, Paul D. Nixsch^{1,2}, David P. Corey^{1,2}

¹Harvard Medical School, ²Howard Hughes Medical Institute

Background

The forces felt by different transduction channels in a bundle depend critically on how well stereocilia remain cohesive during deflection. In the bullfrog sacculus, sliding adhesion mediated by horizontal top connectors confers coherent motion to hair cell stereocilia and parallel gating to all transduction channels (Karavitaki and Corey, 2010). Is this true for cochlear bundles? In cochlear inner and outer hair cells (IHCs and OHCs), the mature complement of horizontal top connectors is established by postnatal day 12 (P12); they extend between adjacent stereocilia of both rows and columns (Goodyear et al, 2005). We therefore expect that bundle cohesion should be maintained in both directions. However in neonatal (P4) bundles, lateral coupling of OHC stereocilia appears low (Langer, Fink et al., 2001). Does this improve with development or are cochlear bundles fundamentally different from frog?

Methods

We cultured organs of Corti from P4 to P12 gerbils. A stiff probe with a blunt, $\sim 0.5 \mu\text{m}$ tip was used to push IHC and OHC stereocilia in the excitatory direction. Stimuli were slow sinusoids of 120, 240, and 480 nm, corresponding (depending on bundle height) to 1-14 degrees. Stimuli were delivered at multiple locations along the tallest stereociliary row, and along the stereociliary height. Displacements of individual stereocilia were recorded with a CCD camera and analyzed with cross-correlation methods (Karavitaki and Corey, 2010).

Results

With data from 111 cells, we found that lateral coupling among stereocilia of the tallest row is weak. Movement in the excitatory direction propagated laterally by only a few stereocilia and the bundle did not move coherently. This was true for IHC and all three rows of OHC stereocilia, for all developmental ages, all cochlear turns and all stimulus positions and amplitudes tested.

Conclusion

The lateral coupling within the stereocilia of the tallest row is weak, suggesting that the function and molecular composition of horizontal top connectors are different from

those in bullfrog hair cells. This also raises concern for current stimulus methods, which involve glass probes that are often small compared to the bundle width. Our data suggest that only stereocilia in contact with the probe will be stimulated, and delivery of the stimulus to the remaining stereocilia will be weak and therefore not homogeneous. To mimic the simultaneous and equal OHC stimulus delivered by the overlying tectorial membrane to stereocilia of the tallest row *in vivo*, better stimulation methods must be developed.

472 Electrical Coupling of Mouse Adult Inner Hair Cells Measured *in Situ*

Antonio M. Garcia de Diego¹, Jonathan Ashmore^{1,2}

¹*UCL Ear Institute*, ²*UCL NPP*

Background

Inner hair cells (IHCs) of the mammalian cochlea use ribbon synapses to signal rapidly to the afferent dendrite. Although much functional information has been obtained from relatively immature rodent cochlear coils, it has proved more difficult to record from adult hair cells as isolation of the cells can be problematic. We have overcome this issue by patch-clamp recording from adult hair cells of the mouse in the isolated temporal bone. We have used fluorescent probes to investigate calcium signalling at the synapse using simultaneous imaging with a multiphoton confocal laser scanning microscope (2PCLSM).

Methods

Cochlear inner and outer hair cells were visualised in the intact isolated temporal bones of mice aged P25 to 10 mo. The cochlea was opened to reveal the 10-15 kHz cochlear region with the cells in identifiable positions and orientation. The chamber was superfused with (in mM): Na, 142; Ca, 1.3; K, 4; Cl 147; 0.7 phosphate; hepes 10, to pH 7.3 at 24°C. Cells were recorded in the whole cell tight seal mode, the pipette including 0.5, 5 or 10mM EGTA and 0.25 mM OGB-5N (excited at 935 nm by the 2PCLSM beam). Intracellular cesium was used to reduce large outward currents to less than 1.5nA at 0 mV.

Results

Distinct calcium entry sites, 'hotspots', could be observed on depolarizing the IHC from -60 mV. With frame rates of 80 Hz, z-sectioning of the cell showed a basal pole distribution of hotspots with the largest calcium rises on the modiolar side of the cell. The precise kinetics and amplitude of the responses depended upon the pipette buffer concentration. In the apical region it was often found that cells were both dye and electrically coupled with up to 9 cells sometimes be found filled with OGB-5N. Calcium responses in the coupled cells could be observed on pipette depolarization; the kinetics generally differed from that of the recorded cell. The electrical input capacitance scaled with the number of coupled cells. Modelling the system suggests that the coupling resistance was less than 10MΩ.

Conclusion

Adult IHCs can be coupled. Comparison of the calcium signal in groups of coupled IHCs indicates that the endogenous buffer is excluded by the coupling pores. The approach allows visualization of the calcium kinetics of an unperturbed adult ribbon synapse.

473 The Properties of Short Hair Cells in the Avian Basilar Papilla

Xiaodong Tan¹, Maryline Beurg², Shanthini

Mahendrasingam³, Carole Hackney⁴, Robert Fettiplace¹

¹*University of Wisconsin*, ²*INSERM U587, Université Victor Segalen Bordeaux 2, Bordeaux, France*, ³*Keele University, UK*, ⁴*Sheffield University, UK*

Background

The origin of frequency selectivity in the avian basilar papilla is incompletely understood. The tall hair cells (THCs) are electrically tuned over part of the frequency range but little is known about the short hair cells (SHCs).

Methods

To address this problem, we made patch clamp recordings from SHCs in an isolated chicken basilar papilla preparation (E18 to P5; T = 33 degrees C) at fractional distances along the papilla from the apex, $d = 0.1-0.6$. SHCs were identified by lower surface density and location less than 10 rows from abneural edge.

Results

SHCs are analogous to mammalian outer hair cells in having a large efferent but sparse afferent innervation and are distinguished by possessing an A-type inactivating K⁺ current (Murrow 1994). We found that SHCs are also electrically tuned by a BK Ca-activated K⁺ conductance, but such tuning is optimal only at resting potentials positive to -40 mV where the A-current is inactivated. The depolarized resting potential stems from a standing inward current through the mechanotransducer (MT) channels, whose resting open probability, Pr, is about 0.35. Two factors produce the high Pr: a low endolymph calcium (0.24 mM) and high intracellular calcium buffering. With perforated patch recordings using the MT current Pr as an assay, we estimated the intracellular calcium buffer as equivalent to 0.5 mM BAPTA ($d = 0.4$). To confirm the high levels of buffer, the distribution of calcium binding proteins in SHCs was examined with post-embedding immunogold labeling in transmission electron micrographs. Heavy stereociliary labeling was seen with antibodies to both calbindinD-28K and parvalbumin-3 and displayed an apex to base gradient matching the tonotopic gradient in the MT current amplitude. The stereociliary concentrations of both calcium-binding proteins were estimated by calibrating immunogold counts against gels containing defined amounts of the proteins (Hackney et al. 2003).

Conclusion

We conclude that avian SHCs resemble mammalian outer hair cells in their large calcium buffer content, high resting open probability for MT channels and depolarized resting potential. However, the dichotomy between SHCs and

THCs is less marked than between mammalian inner and outer hair cells. Funded by RO1 DC01362 from NIDCD to RF

474 Pitch Perception in Cochlear Implant Users with Square Wave Iterated Rippled Noise

Richard T Penninger^{1,2}, Eugen Kludt¹, Charles J Limb³, Andreas Büchner¹, Marc Leman², Ingeborg Dhooge⁴
¹Medical University Hannover (MHH), ²University Ghent,
³The Johns Hopkins University School of Medicine,
⁴University Hospital Ghent

Background

Manipulation of temporal (rate) pitch mechanisms in cochlear implant (CI) users through carrier rate modulation may expand the potential number of distinct pitch percepts available beyond that which is available through place pitch coding alone. Rate pitch has the advantage of being able to provide a continuum of pitches on a single electrode up to approximately 300 Hz. However, this limit varies greatly between subjects and within subjects (for different electrodes), with a few exceptional performers being able to distinguish rate pitch cues up to at least 1000 Hz. Square wave iterated rippled noise (SWIRN) can be created by delaying white noise and adding it back to the original signal and transmitting it to a CI user by direct electrical stimulation.

Methods

Ten CI subjects were asked to identify the higher tone of two tones presented with direct electrical stimulation using SWIRN. The base SWIRN rates ranged from 100 Hz to 500 Hz; target SWIRN rates were 35% higher. The carrier stimulation rate was 15 kHz. Using loudness-balanced stimuli, pitch ranking was measured for three base modulation rates on groups of 3 (one basal, middle and apical electrode), 6 (two basal, middle and apical electrodes) and 11 (every other electrode) for several subjects using Cochlear Nucleus CI512 and CI24R devices. The order of the electrodes and the current level on each electrode was randomized in each block.

Results

Preliminary results demonstrate little variability across subjects, frequencies and electrode groups. Subjects seem to be able to accurately rank SWIRN stimuli in all three groups of electrodes in the tested frequency range. Midpoint comparison shows that the perceived pitch increases linearly as the modulation rate is increased from 100 to 500 Hz.

Conclusion

These results suggest that sound processing strategies that utilize SWIRN-based stimuli may lead to improved pitch and music perception in CI users.

475 Investigating the Effect of Training with Amplitude Modulated (AM) Tones on Tone-Vocoded Speech Perception

Sygal Amitay¹, Ediz Sohoglu^{1,2}, Christian Füllgrabe¹, Katharine Molloy¹, David Moore¹
¹MRC Institute of Hearing Research, ²MRC Cognition and Brain Sciences Unit

Background

In vocoded speech, temporal-envelopes are extracted from broad frequency regions and used to modulate tone- or band-limited noise carriers. Such a manipulation removes temporal fine-structure and degrades spectral content whilst preserving temporal-envelope cues and, if a sufficient number of frequency channels are used (usually ≥ 6), retaining intelligibility. We asked here whether training on a task requiring the explicit use of temporal-envelope cues but no speech content will transfer to 4-channel vocoded speech, which is unintelligible when initially heard.

Methods

Identification of vocoded vowel-consonant-vowel (VCV) stimuli was assessed before (pre-test) and after (post-test) two sessions of training on amplitude-modulation (AM) tasks. In order to reduce any interaction between experimental effects arising from AM-based training and the rapid learning that occurs when listeners are first exposed to vocoded speech, participants were trained on vocoded VCV-identification prior to the pre-test session. During the training phase, one group (N = 18) practiced an AM-detection task, a second group (N = 18) practiced an AM-rate discrimination task, and a third group (N = 13) served as untrained Control.

Results

Although there was no significant group difference, both AM-training groups (but not Controls) showed significant improvement (~4%) on vocoded VCV identification. Analysis of the confusion matrices showed differences in the specific groups of consonants indexing training-induced changes.

Conclusion

This preliminary demonstration that training on temporal-envelope cues can transfer to the identification of vocoded speech is now being investigated using a more extended AM training regimen.

476 Frequency Shifts Enhance Tones Within Chords, in a Special Way

Laurent Demany¹, Samuele Carcagno¹, Catherine Semal¹
¹CNRS and Université de Bordeaux

Background

In a chord of equal-SPL pure tones, one of the tones can be made to pop out perceptually by presenting, before this chord, a copy of it in which the target of the pop-out effect is attenuated, thus producing a spectral notch. A subjectively similar pop-out or "enhancement" effect is obtained when the target tone is shifted in frequency rather than in SPL. Erviti et al. (J. Acoust. Soc. Am., 2011)

reported evidence that the mechanism of enhancement is not the same for these two types of change. Here, we report other findings supporting that view.

Methods

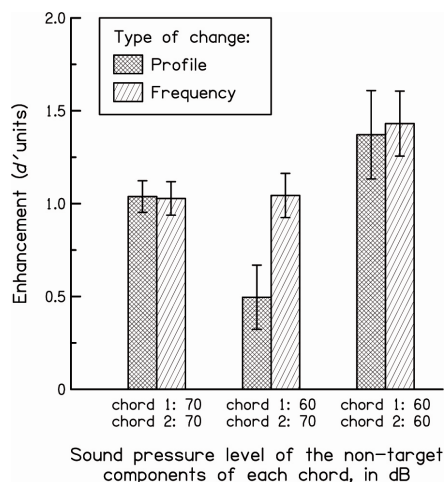
Enhancement was measured using short-duration (at most 100 ms) inharmonic chords varying randomly in frequency content across trials and a "present/absent" task assessing the audibility of their individual components (see, e.g., Erviti et al., 2011). The second of the two successive chords presented on each trial always had a flat spectral profile. Its components were either matched in SPL to the non-target components of the first chord, or 10 dB louder than them. Enhancement was elicited either by filling a spectral notch existing in the first chord ("Profile change" condition) or by a 1-semitone shift in one tone ("Frequency change" condition); for each listener, the depth of the spectral notches (in dB) was initially adjusted so as to obtain the same enhancement magnitude in these two conditions, when the non-target tones had a constant SPL within trials.

Results

The main result (see the Figure) is that changing the SPL of the non-target tones within trials disrupted enhancement to a larger extent in the "Profile change" condition than in the "Frequency change" condition. It is also noteworthy that, when the non-target tones did not change within trials, the notch depth needed to match the enhancement produced by 1-semitone frequency shifts was as large as 11.5 dB, on average. According to the excitation-pattern model of Moore et al. (J. Audio Eng. Soc., 1997), this implies that, for a given change in the excitation of auditory filters, enhancement is stronger when it is elicited by a frequency shift than when it is elicited by filling a spectral notch.

Conclusion

While the enhancement effects resulting from changes in spectral profile are usually explained in terms of neural adaptation, this does not seem to be a sufficient explanation for the enhancement effects resulting from frequency shifts.



477 Using Training to Overcome the Switch Cost Induced by Stimulus Randomization on Auditory Temporal-Interval Discrimination

Karen Banai¹, Beverly A. Wright²

¹University of Haifa, ²Northwestern University

Background

Alternating between two simple cognitive tasks is difficult and comes at a cost (the switch cost). In auditory perception, an example of a switch cost is the significant elevation in temporal-interval discrimination thresholds when two distinct standard temporal intervals are presented randomly trial-by-trial (roving) compared to separately in different blocks of trials (consecutive). Our goal was to determine if the cost of roving could be alleviated with practice, either with the randomized stimuli or with each stimulus in isolation.

Methods

Naïve normal-hearing adults practiced temporal-interval discrimination of two base intervals (100 and 350 ms, marked with 15-ms 1-kHz or 4-kHz tones), 720 total trials per session for six sessions in either a roving (n=16) or a consecutive (n=16) regimen. In the roving regimen, the two temporal intervals were randomly presented throughout each training session for a total of 360 trials each. In the consecutive regimen, in each session, all 360 trials of one interval were completed before training on the other interval began. A control group (n=16) completed pre- and post-training sessions only. We compared learning (on the trained intervals in the trained regimen) and generalization (to the other regimen and to untrained stimuli) between the two regimens.

Results

Both regimens yielded significantly greater improvement compared with controls on at least one of the two trained intervals, and generated similar patterns of generalization to untrained stimuli. However, the amount of learning on the consecutive regimen (estimated with effect size) was greater than on the roving regimen. Most importantly, learning did not generalize across regimens. Training on the consecutive regimen did not improve roving thresholds or vice versa. Although training on the roving regimen brought roving thresholds in line with naïve consecutive thresholds, it did not lead to improvement on consecutive thresholds.

Conclusion

The performance cost of randomly switching between two auditory temporal intervals can be overcome with multi-session training with that randomization (roving), but not with training without randomization (consecutive). Further, training with randomization does not aid performance without it. Thus, it appears that presumed improvements in stimulus encoding (after consecutive training) do not reduce the cost of switching between stimuli, and that reductions in the switch cost (after roving training) do not improve stimulus encoding. Rather, these results suggest that the switch cost between stimuli is mediated by

processes separate from those that affect basic stimulus encoding.

478 Frequency-Modulation Vowel Maps in Normal-Hearing and Hearing-Impaired Listeners

Sébastien Santurette¹, Marianna Vatti^{1,2}, Niels Henrik Pontoppidan², Torsten Dau¹

¹Technical University of Denmark, ²Eriksholm Research Centre, Oticon A/S

Background

Human singing voices are not steady in pitch but typically contain coherent frequency fluctuations over time. The perception of natural voice vibrato thus relies on the presence of coherent frequency modulation (CFM). Sensorineural hearing loss is known to affect the ability to detect changes in frequency, presumably leading to degraded voice perception. This study investigated the ability of normal-hearing (NH) and hearing-impaired (HI) listeners to perceive a sung vowel by adding CFM to a steady complex tone. The aim was to determine the extent of the “vowel map” along the FM-rate and FM-excursion dimensions in NH listeners, and whether this area for FM-based singing-voice perception is affected by hearing impairment.

Methods

The ranges of CFM rates and excursions leading to voice formation were determined in a group of NH listeners and a group of HI listeners with moderate to severe sensorineural hearing loss. The listeners adjusted either the FM rate or the FM excursion applied to the synthesized vowel /oh/ in an adaptive “yes/no” procedure, while the other FM parameter remained fixed. In each presentation, the listeners were asked to judge whether the sound corresponded to a natural singing voice. The lower and upper FM-excursion thresholds were determined for fixed FM-rates between 3 and 8 Hz, and the lower and upper FM-rate thresholds for fixed FM-excursions between 21 and 91 cents.

Results

In NH listeners, adding CFM to an unmodulated complex tone was sufficient to evoke the perception of a singing voice for FM rates between 4.3 and 7.4 Hz and FM excursions between 15 and 64 cents on average. In contrast, HI listeners typically exhibited broader vowel maps than NH listeners, whereby their maps were shifted towards higher FM excursions and extended towards lower FM rates than those of NH listeners. The large across-subject variability in the HI group was not fully explained by the listeners’ audiograms or auditory-filter bandwidths at the vowel’s fundamental frequency.

Conclusion

Hearing loss was found to affect the formation of a sung vowel based on FM-rate and FM-excursion cues. It remains unclear to what extent this is attributable to deficits in FM detection or discrimination, reduced frequency selectivity, or difficulties in following the rate of

frequency changes. The vowel maps determined in NH listeners may provide reference values when constructing synthetic-vowel stimuli with realistic sung vibrato.

479 The Ability of Hearing-Impaired Listeners to Use Temporal-Envelope Cues Recovered from Speech Frequency Modulation

Christian Lorenzi¹, Nicolas Wallaert¹, Jayaganesh Swaminathan², Dan Gnansia³, Agnes Leger¹, David Ives¹, Andre Chays⁴, Yves Cazals⁵

¹Ecole normale supérieure, Paris, France, ²Massachusetts Institute of Technology, Cambridge, MA, USA, ³Neurelec, Vallauris, France., ⁴Hôpital Robert Debré, Reims, France, ⁵Université Paul Cézanne, UMR CNRS 6231, Marseille, France

Background

Recent studies suggest that normal-hearing listeners maintain robust speech intelligibility despite severe degradations of amplitude-modulation (AM) cues, by using temporal-envelope information recovered from broadband frequency-modulation (FM) speech cues at the output of cochlear filters. This psychophysical study aimed to assess whether cochlear damage alters this capacity to reconstruct temporal-envelope information from FM.

Methods

This was achieved by measuring the ability of normal-hearing listeners and listeners with mild-to-moderate hearing loss to identify nonsense syllables processed to degrade AM cues while leaving FM cues intact within three broad frequency bands.

Results

Hearing-impaired listeners showed significantly poorer identification scores than normal-hearing listeners. However, the deficit shown by hearing-impaired listeners was relatively modest. Overall, hearing-impaired data and the results of simulation studies were consistent with a poorer-than-normal ability to reconstruct temporal-envelope information resulting from a broadening of cochlear filters by a factor ranging from 2 to 4.

Conclusion

These results indicate that temporal-envelope reconstruction from broadband FM is an important, early auditory mechanism contributing to the robust perception of speech sounds in degraded listening conditions. These results also suggest that most people suffering from mild to moderate cochlear hearing loss can make efficient use of reconstructed envelope cues despite degradations in frequency selectivity. Still, these results suggest that poorer-than-normal frequency selectivity impairs somewhat temporal-envelope reconstruction mechanisms.

480 Hearing Speech in Noise from a Single Source Before and After Surgical Improvement of Congenital Conductive Hearing Loss

Bradley Kesser¹, Erika Cole², Lincoln Gray³

¹University of Virginia, ²Metropolitan ENT and Facial Plastic Surgery, ³James Madison University

Background

Patients with congenital aural atresia are born with a conductive hearing loss due to malformations of the external and middle ears. Surgery can improve hearing in the atretic ear to within normal limits. Atresia is thus an opportunity to evaluate roles of early conductive hearing loss on binaural processing. Here we investigate post-operative emergence of summation (binaural redundancy), the advantage of hearing with two ears rather than one when an identical signal arrives at both ears simultaneously. This simple benefit has been estimated at about 3 dB in normal listeners.

Methods

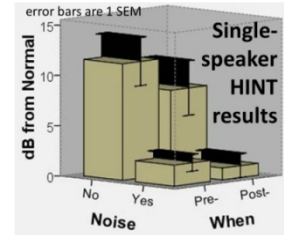
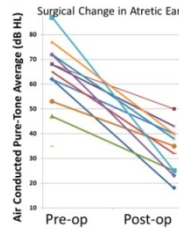
We tested 12 patients between the ages of 6 and 53 years with an average 64 dB (± 14 dB sd) unilateral conductive hearing loss, normal hearing in the non-atretic ear, and normal bone conduction in the atretic ear. Surgery improved pure-tone averages by 30 dB to post-operative PTA of 34 (± 10) dB. Before surgery and 5 weeks later, single speaker HINT tests evaluated speech reception in quiet and noise. Patients faced one central speaker. Levels of sentences were adaptively varied to determine a reception threshold. This was done first in the quiet and then with simultaneous multi-talker babble at 65 dB from the same speaker.

Results

After surgery, thresholds for speech in quiet improved 3.4 dB, and thresholds in noise improved 0.8 dB, both statistically insignificant (1-tailed p values of .1 and .2 respectively). Patients performed worse than normal in quiet and in noise (1-tailed p values of .001 and .037 respectively). There was a significant effect of age on performance in noise ($r^2=.58$) but not in quiet ($r^2=.01$). Pooling pre- and post-op results in quiet across ages, the patients were 10 (± 2.2) dB worse than normal. Converting results to dB-worse-than normal, atresia patients did better in noise (relative to normal) than in quiet ($p=.008$).

Conclusion

We see the expected summation effect (3 dB) in quiet but not in noise. Better performance in noise than quiet (relative to normal) might arise because these patients likely developed skills attending to threshold-level speech in noise without any binaural benefit. Since both signal and noise came from the same speaker, we don't understand why performance in quiet remains worse than normal (by an effect size > 4). A bold speculation might be that having two ears somehow helps you learn to hear out of one ear.



481 Behavioral Discrimination of Ultrasonic Vocalizations in CBA/CaJ Mice

Erikson Neilans¹, David Holfoth¹, Kelly E. Radziwon¹, Christine V. Portfors², Micheal L. Dent¹

¹University at Buffalo, SUNY, ²Washington State University

Background

Previous studies have attempted to categorize ultrasonic vocalizations (USVs) from mice using spectrographic analysis and human-based classification (e.g. Grimsley et al., 2011; Portfors, 2007). However, relatively little research has focused on the perception of these different call types. Results from Holmstrom et al. (2010) illustrate that neurons in the inferior colliculus respond differently to an array of USV categories, suggesting that the auditory system uses specific patterns for encoding different call types. However, until now, no study has examined how well different USVs are discriminated by awake, behaving mice.

Methods

Both the perceptual saliency of USV categories and the impact of different call manipulations were measured here. CBA/CaJ mice were trained to discriminate target USVs from a different USV presented in a repeating background. The repeating background signal in a session was one of five different call types that were previously used by Holmstrom et al., 2010: two frequency modulated up-sweeps, one produced by a male and the other by a female, as well as harmonic jump calls that varied in the number (0-2) of jumps found within the call. The discrimination targets in a session included the four non-background USVs and spectrotemporal manipulations of the background call. The spectrotemporal manipulations were removing the frequency modulation, shifting the frequency up and down ten and twenty percent, shortening and lengthening the call by a factor of two, and reversing the signal.

Results

Interestingly, many calls within human-created 'categories' were easily discriminated from one another while the mice were unable to discriminate other between-category calls, suggesting that current conceptions of USV categories may not be accurate for awake, behaving mice. The discrimination performance on the spectrotemporal manipulations indicates that some call parameters are more important than others for USV perception. For most calls, large frequency shifts ($\pm 20\%$) resulted in high discrimination performance, suggesting that frequency information may be important for ultrasonic communication. Manipulating the duration of the USV appears to have disparate impacts among harmonic jump

calls and up-sweep USVs, suggesting that the role of temporal cues may differ between call types. Surprisingly, reversing the call and removing the frequency modulation had a substantial reduction in discrimination performance for most USVs.

Conclusion

These results suggest that frequency modulation and contour have little impact on how USVs are perceived, and imply that categories emphasizing these differences (e.g. upsweeps vs. downsweeps) are not relevant for USV perception.

482 The Pitch of the Broadband Temporal Envelope: Effects of Modulation Rate and Shape

Mickael L. D. DEROCHE¹, Monita CHATTERJEE²
¹Johns Hopkins University School of Medicine, ²Boys Town National Research Hospital

Background

Pitch perception of an amplitude modulated (AM) signal depends on the modulation rate, the carrier bandwidth and the modulation shape. While much attention has been paid to the effects of rate and bandwidth of the carrier, fewer studies have investigated effects of modulation shape. Moreover, cochlear implants (CI) users rely primarily on temporal envelope cues for complex pitch perception. Attempts to improve coding of the fundamental frequency (F0) for CI listeners have used peakier modulation envelopes. In the present study we examined the temporal pitch percept conveyed by such envelopes in normally hearing (NH) listeners.

Methods

We investigated NH listeners' sensitivity to rate and shape of the broadband temporal envelope of noise stimuli. The stimuli were either sinusoidally amplitude modulated (SAM) noise or noise that received the broadband temporal envelope of sine-phase harmonic complexes based on a fundamental frequency equal to the rate of SAM. These harmonic envelope modulations (HEM) varied in peakiness depending on the number of partials in the complex modulator.

Results

Experiment 1 showed that both shape and rate had some influence on loudness, which could be released by a level roving ranging over 3 dB. Experiment 2 measured discrimination of the shape of noise stimuli modulated at the same rate. Sensitivity worsened at higher rate and at higher peak factor. Experiments 3 and 4 showed that even though rate dominated the sensation of temporal pitch, shape had an influence: peaky modulations tended to sound lower in pitch than sinusoidal ones. Experiments 5 and 6 measured listeners' sensitivity to discriminate modulation rates keeping a constant shape. Difference limens were lower for the HEM than for the SAM stimuli at both 100 and 200 Hz, but remained much larger than those obtained with full harmonic complexes.

Conclusion

First, the sensitivity of NH listeners to temporal pitch can be improved by using modulations peakier than sinusoidal. Second, temporal pitch is not entirely governed by modulation rate: modulations peakier than sinusoidal tend to sound lower in pitch. Third, NH listeners are able to discriminate temporal envelopes that are modulated at the same rate with different shapes. Thus, CI users might well use both rate and shape of modulation to perform a pitch discrimination task. A larger focus on modulation shape might help to improve F0-coding in CIs.

483 Phase Effects in Speech Recognition Masked by Harmonic Complexes

Mickael L. D. DEROCHE¹, Monita CHATTERJEE²
¹Johns Hopkins University School of Medicine, ²Boys Town National Research Hospital

Background

Compression by the basilar membrane (BM) helps to listen in extremely short temporal dips and facilitates tone detection in masker waveforms that are deeply modulated. Its role for speech understanding in a background of other voices remains however unclear.

Methods

Experiment 1 measured speech reception thresholds (SRTs) for an unprocessed male and a female voice masked by broadband or speech-shaped harmonic complexes with partials either in sine phase (SP) or in random phase (RP). The masker's fundamental frequency (F0) was 50, 100 or 200 Hz. Experiment 2 measured masked thresholds (MTs) for speech-shaped noise that was restricted to the regions of resolved or unresolved partials of the same maskers used in experiment 1.

Results

In experiment 1, SRTs were lower for SP than for RP maskers only at 50-Hz F0. This masking release (MR) was absent at 100-Hz F0 and was negative at 200-Hz F0. The results were similar whether the maskers were broadband or speech-shaped and whether the target talker was male or female. In experiment 2, MTs were similar for SP and RP maskers in the region of resolved partials, and lower for SP than RP maskers in the region of unresolved partials at both 50- and 100-Hz F0. It appears that the MR observed at 100-Hz F0 did not transfer from MT to SRT because the SRT was lower than the range of target-to-masker ratios where compression is potentially beneficial. In other words, speech can often be understood at 50% intelligibility without the information located in unresolved regions of the masker. Compression can play a critical role but only at supra-threshold performance. Psychometric functions were reconstructed from the adaptive tracks of experiment 1 to extract thresholds at 65% and 80% intelligibility. Only at 80% intelligibility, was a MR observed at 100-Hz F0.

Conclusion

Overall, these results suggest that BM compression contributes weakly to listening in extremely short temporal

dips present in steady-state speech-shaped periodic maskers at 65 dB SPL.

484 Interactions of Pitch and Timbre: How Changes in One Dimension Affect Discrimination of the Other

Emily Allen¹, Andrew Oxenham¹

¹University of Minnesota

Background

Variations in spectral shape, perceived as timbre changes, can lead to poorer fundamental frequency (F0) or pitch discrimination. Less is known about the effects of F0 variations on the discrimination of spectral shape. The present study used bandpass-filtered complex tones to examine both the effect of changes in spectral centroid on pitch discrimination, and the effect of F0 changes on timbre discrimination. Variations in the two dimensions were equated for salience by normalizing changes relative to individual subjects' difference limens (DLs). The two aims of the study were 1) to determine whether the interactions between pitch and timbre were symmetric, and 2) to assess the effects of musical training on listeners' ability to ignore variations in irrelevant perceptual dimensions.

Methods

The thirty subjects were divided into two equal groups of musicians and non-musicians. In Experiment 1, the subjects' task was to compare sequentially presented tone pairs that differed in either pitch or timbre and to judge which was higher. The DLs obtained for both tasks were used in subsequent experiments. In Experiment 2, F0DLs were measured as a function of the size of random variations in spectral centroid, and vice versa. In Experiment 3, sensitivity was measured as the target parameter and the interfering parameter varied by the same amount, in terms of individual DLs.

Results

Both pitch and timbre DLs were affected by random variations in the non-target dimension. The amount of interference observed was similar for both pitch and timbre dimensions. Although musicians had lower (better) F0DLs than non-musicians on average, the amount of interference produced by random spectral variations was similar for the two groups. In addition, there was no significant difference in spectral centroid (timbre) DLs between musicians and non-musicians with or without random variations in pitch. Overall, performance was better when the random non-target variation was in the same direction as the target variation (e.g., when an upward movement in timbre was paired with an upward movement in pitch).

Conclusion

Difference limens for both pitch and timbre are strongly, and similarly, affected by random variations in the non-target dimension, and extensive musical training does not seem to reduce this interference. The results confirm that pitch and timbre are not easily separable as perceptual

dimensions of hearing, and that directional changes can be confused across the two dimensions.

[Work supported by NIH grant R01 DC 05216.]

485 Masker Profiling Yields Insights Into Mechanisms of Masking

Suyash Joshi¹, Walt Jesteadt¹

¹Boys Town National Research Hospital

Background

Signal detection in noise is assumed to be a function of signal-to-noise ratio in the frequency region of the signal, but there is little consensus regarding specific decision strategies.

Methods

Thresholds were determined for eight normally hearing listeners for detection of a signal (2000-Hz sinusoid, 100 ms long, and 20 ms ramps) centered in an 8-ERB wide broadband noise (1219-3200 Hz, 300 ms long, 5 ms ramps) presented at 47, 62, and 77 dB SPL. An independent level rove of +/- 8 dB in 1 dB steps was then applied to individual half-ERB wide bands of the masker while the signal was fixed at either +4 or +8 dB above threshold. In each condition, listeners ran 1000 trials in a Yes-No paradigm. Perceptual weights for masker bands were obtained using a reverse correlation method, separately for signal and no-signal trials, such that a positive weight indicates a tendency to vote "Yes" when the level of the masker band is higher. In a new masker profiling analysis based on the overall framework of signal detection theory, trial-by-trial data were divided into four categories of responses namely, Hits, Misses, False Alarms, and Correct Rejections and the mean level of each masker band within each response category was calculated.

Results

Perceptual weighting patterns reflect auditory filter shapes and indicate that listeners respond "Yes" on signal trials when the level of masker bands near the signal is low, but respond "Yes" on no-signal trials when the level of those bands is high. The four-category masker profiling analysis provides a basis for the interpretation of perceptual weights by showing the average masker levels resulting in the "Yes" and "No" decisions that contribute to each weight.

Conclusion

Lower mean levels of masker bands near the signal in Hits and higher levels for those bands in Misses suggest that detection is based on signal-to-noise ratio. On no-signal trials, however, listeners vote "Yes" when the level of the masker in bands near the signal is higher, consistent with an energy detector. Since signal and no-signal trials are presented randomly and listeners are blind to this information a priori, it is generally assumed that listeners' decision strategies are similar on signal and no-signal trials, but this is clearly not the case. Use of masker profiling may provide significant information to improve models of masking.

486 Behavioral Paradigm to Measure the Lower Limit of Pitch for Complex Harmonic Sounds in Macaques

Olivier Joly¹, Simon Baumann¹, Colline Poirier¹, Alexander Thiele¹, Timothy Griffiths¹

¹*Institute of Neuroscience, Newcastle University Medical School, Newcastle Upon Tyne, United Kingdom*

Background

Pitch is an auditory percept related to the repetition rate of sounds but with a complex relationship to the physical attributes of sounds. To study the neural correlates associated to pitch perception using non-human primate models, behavioral measurements of pitch perception in these animals are critical. In humans, the range for pitch perception is approximately 30-5000 Hz but this range is currently unknown in monkeys partly because of the difficulty to train monkeys for auditory tasks (Brosch et al., 2004). In this study, we developed and applied a behavioral paradigm to measure the lower limit of pitch for complex harmonic sounds in macaques based on changes in the discrimination threshold across the values of repetition rate (Krumbholz et al, 2000).

Methods

We trained three rhesus monkeys (*Macaca mulatta*) using a "go/no-go" procedure to release a touch bar sensor at each detection of a change in repetition rate. Stimuli were harmonic complexes (cosine and alternating phase) with repetition rates in the range of 8 to 128 Hz. The sounds were played diotically through earphones. A trial began with an initiation interval during which a trial could be initiated by contacting the touch bar. Upon contact, a holding period (1-3 sec) began. During this period, the standard harmonic complex sound was played and followed by a stimulus change interval during which a comparison sound with a higher rate was presented. The monkeys responded with bar release to detected changes in rate (test trials) and were rewarded for hits and for correct rejections (holding the bar during catch trials). We used an adaptive staircase procedure with 3 trials (2 test trials and 1 catch trial) per step (Moore and Fallah, 2004) to determine the thresholds.

Results

Our paradigm was used to estimate the lower limit of pitch in the 3 animals who successfully learnt to detect a change in repetition rates. We found that each animal shows a lower threshold (<5%) for higher rates (≥ 32 Hz).

Conclusion

The lower limit of pitch in rhesus monkeys (~ 30Hz) seems very similar to that of humans. This work allows the behavioral definition of a pitch threshold against which BOLD responses to pitch-associated stimuli at different rates can be compared (Baumann et al., 2012): a predicted property of a neural correlate of pitch is an existence region only above lower limit.

487 Effects of Noise Reduction on AM Discrimination for Hearing-Impaired

Listeners

David Ives¹, Sridhar Kalluri², Olaf Strelcyk², Stanley Sheft³, Christian Lorenzi¹

¹*Ecole Normale Supérieure*, ²*Starkey Hearing Research Center*, ³*Communication Disorders & Sciences, Rush University Medical Center*

Background

Noise-reduction (NR) algorithms are employed in digital hearing-aid devices to improve the listening experience of the user in noisy backgrounds. Although these algorithms may increase the signal-to-noise ratio (SNR) in an ideal case, they generally fail to improve speech intelligibility. However, due to the complex nature of speech, it is difficult to disentangle the numerous effects of noise reduction which may underlie the lack of speech benefits.

Ives et al (2012) examined the effect of a NR algorithm on the ability of normally-hearing (NH) listeners to discriminate a basic acoustic feature known to be crucial for speech identification, namely amplitude modulation (AM). They found that NR slightly improved discrimination at higher SNRs. The goal of the present study was to assess whether the benefit of NR on AM discrimination was present for hearing-impaired (HI) listeners.

Methods

The discrimination of complex AM patterns was measured for 10 HI listeners and 10 NH listeners using a same-different discrimination task. The stimuli were generated by modulating a pure-tone carrier by a two-component AM modulator with modulation rates centered around 3 Hz. The carrier tone was either 500 Hz or 2 kHz and fixed within a block. Discrimination was measured for both groups of listeners (NH and HI) at 500 Hz and 2 kHz in the presence of a band-pass filtered Gaussian white noise at an SNR of 12dB. Stimuli were left as such or processed via a NR algorithm based on the spectral subtraction method. The HI listeners had normal hearing (≤ 20 dB HL) at 500 Hz and moderate-severe hearing loss (≥ 40 dB HL) at 2 kHz.

Results

NR was found to: (i) improve AM discrimination at both 500 Hz and 2 kHz for the NH listeners; (ii) improve AM discrimination at 500 Hz for HI listeners; (iii) have no effect on AM discrimination at 2 kHz for HI listeners.

The stimuli were passed through a computational model of the peripheral auditory system. The simulation results suggest that the lack of benefit of NR for the HI listeners at 2 kHz may arise from the combined effects of higher absolute thresholds and reduced cochlear compression. Auditory filter width did not affect performance.

Conclusion

HI listeners do not benefit from NR for AM discrimination. The results suggest that this lack of benefit may arise from a poor matching between the compression stage and NR algorithm in hearing aids.

488 Effects of Noise on Detection of Vowels by Nonhuman Primates

Jason Grigsby¹, Peter Bohlen¹, Maggie Dylla¹, Ramnarayan Ramachandran¹

¹Vanderbilt University Medical Center

Background

Vowel detection in noisy conditions can help understand detection of general complex signals. In macaques, the thresholds for pure tone detection increase by 1 dB per dB of broadband noise added, maintaining the signal to noise ratio. In humans, vowel detection has been shown to depend on the signal to noise ratio of the most intense formant peak, but it is not clear that these mechanisms are in play in macaques which attach no semantic significance to and have no previous experience with vowels.

Methods

To investigate some of the underlying principles of detection of complex sounds, we examined detection of vowels in various kinds of noise. Three macaques (*Macaca mulatta*) were trained in a reaction time lever release task with interleaved catch trials to report detection of vowels presented alone and in continuous noise. We manipulated the bandwidth and the frequency range of the noise in order to evaluate the signals and noise components that influence detection. Signal detection theoretic analysis was used to determine behavioral accuracy from hit rates and false alarm rates.

Results

We studied the effect of noise on reaction times as well as detection thresholds, but found that noise only influenced thresholds. Detection of vowels shows the classic sigmoid relationship with sound pressure level. Broadband noise shifted the thresholds of vowel detection by +1 dB for 1 dB of noise. The pattern of incremental threshold shift did not change significantly when a mixture of vowels was used as background. When the bandwidth of the noise was restricted to 4000Hz, the frequency range of the vowel signal itself, it still caused a shift rate of 1 dB/dB, not significantly different from broadband noise. When the 4000 Hz noise band was translated in frequency, the shift rate decreased as the overlap between the vowel and the noise band decreased. When the noise components corresponding to the formant peaks were individually notched, no single formant was found to have predominance in vowel detection. When the bandwidth of noise was increased, the effect increased continuously but saturated beyond the second formant; increasing bandwidth while fixing the high frequency end caused small changes until both first and second formants were encompassed by the noise.

Conclusion

These results suggest that detection of vowel signals may relate to the total pressure over a partial band of the signal rather than the individual formant peak or the total pressure over the whole signal band. (NIH_R01_DC_11092)

489 Perception and Neural Representation of Tones in Conditions of Masking Release

Katharina Egger¹, Bastian Epp¹

¹Technical University of Denmark

Background

The audibility of sounds in natural acoustic environments is often hampered due to the presence of other masking sounds. The amount of masking can be reduced due to the presence of beneficial signal properties. Psychoacoustical experiments showed that a masking release can be found in the presence of coherent intensity fluctuations across frequency (comodulation masking release, CMR) or interaural signal phase disparities (binaural masking level difference, BMLD) compared to a condition where those properties are absent. It was shown (Epp et al., ARO 2012) that a release from masking is reflected in auditory evoked potentials evaluated at constant stimulus levels and that the P2 amplitude reflects the level above masked threshold better than the physical level of the stimulus. It is hypothesized that a psychoacoustical measure of the audibility of the signal also correlates with the auditory evoked potentials when evaluated at the same level above masked threshold.

Methods

To assess the psychoacoustical measure of audibility, thresholds were measured for masked tones. Masked threshold was varied with the introduction of comodulation, interaural signal phase disparity or a combination of both. Based on the individual data, the listeners were asked to rate the audibility of a masked tone at individually adjusted physical levels corresponding to constant levels above threshold. To assess the neural activity, auditory evoked potentials were measured for the same stimuli as used in the rating experiment within the same listeners.

Results

Psychoacoustical results indicate a growth of audibility that is increasing with increased level above masked threshold. Conditions without a release from masking show a tendency for higher audibility than conditions with a masking release. Auditory evoked potentials show an increase in amplitude with increased level above masked threshold. The analysis of the evoked potential shows differences in sensitivity between N1 and P2 to comodulation and interaural signal phase. The electrophysiological data with constant level above masked threshold are in agreement with data of Epp et al. (ARO 2012) with constant physical stimulus levels.

Conclusion

The psychoacoustical data show that audibility is mainly determined by the level above masked threshold rather than the physical level of the stimulus. The higher audibility for conditions with a masking release might be some residual influence of the overall level of the stimulus on the audibility rating. The electrophysiological data support the hypothesis that the P2 component of auditory evoked potentials correlates closely with levels above masked threshold rather than with physical stimulus levels.

490 Frequency Difference Limens and Cue Trading in CBA/CaJ Mice

Kelly Radziwon¹, Micheal Dent¹

¹SUNY University at Buffalo

Background

Although much is known about the genetic makeup and physiology of the laboratory mouse, far less is known about mouse auditory behavior. Using behavioral approaches, previous researchers have examined the frequency and intensity discrimination abilities of the NMRI mouse, feral house mice, and other strains of mice with known hearing impairments. The present experiments examine the hearing of the CBA/CaJ mouse strain using operant conditioning procedures.

Methods

Seven adult CBA/CaJ mice were used in these experiments. The test stimuli used in the frequency difference limens (FDL) experiment were pure tones at 12, 16, 24, and 42 kHz presented at both 10 and 30 dB (SL). The mice were trained to discriminate a comparison tone (target) from a reference tone (repeating background). The target tones were higher in frequency than the reference stimulus. The cue trading experiment used an identification paradigm where the mice had to place tones into one of two categories. For example, if a mouse heard a 70 kHz tone with a 25 ms duration it had to respond to the left response hole, and if it heard a 30 kHz tone with a 120 ms duration, it had to respond to the right response hole. Once the mouse was able to identify these two stimulus categories accurately, a 70 kHz tone with a 120 ms duration was presented. If the mouse was using frequency to identify the tones then it should choose the left hole; however, if duration was the more important cue, then it should choose the right hole. Using this paradigm it was possible to determine whether frequency or duration was the more salient cue for mice when identifying tones.

Results

In the FDL experiment, the mice had a mean just-noticeable-difference (JND) of 3.5% Weber fraction across all four frequencies and sound levels. In the cue trading task, the mice overwhelmingly identified tones based on their frequencies rather than their durations.

Conclusion

Results from the FDL test showed that CBA/CaJ mice had similar Weber fractions as wild mice and guinea pigs but had much poorer frequency resolution compared to humans and cats. Despite this poorer resolving power, the mice used frequency cues over duration information in the cue trading task, suggesting that frequency might be the dominant cue that mice use to discriminate among various mouse vocalizations.

491 Matching of the Dominant Pitch of Scale Alternating Wavelet Sequences Against Complex Tones with Odd Harmonics

Attenuation: Decision Statistics on the Stabilized Auditory Images

Minoru Tsuzaki¹, Chihiro Takeshima², Toshie Matsui³, Toshio Irino⁴

¹Kyoto City University of Arts, ²J. F. Oberlin University,

³Nara Medical University, ⁴Wakayama University

Background

Scale alternating wavelet sequences (SAWSs) has been introduced where a certain wavelet and its scaled version alternate every other cycle of the overlap-and-adding. It has been reported that the pitch of the SAWS tended to shift downwards by an octave when the differences in scaling became large. The observed pitch shift could be matched to the harmonic complex tones whose odd harmonics were attenuated. The purpose of the current study was to inquire a better decision statistics to predict the observed pitch shift.

Methods

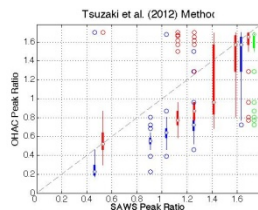
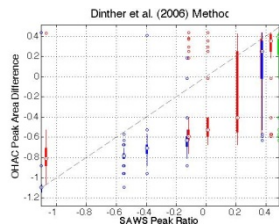
The SAWSs were generated based on the wavelet of the impulse responses of three Japanese vowels. The original wavelet and its scaled version were overlap-and-added alternately at an cycle of 8 ms. The scaling factor ranged from 0.50 to 2.00. Odd harmonics attenuated complexes (OHAC) were used as comparison stimuli. The OHACs were harmonic complexes with a 16 ms fundamental period and with each vowel's spectrum envelope. When the attenuation level is infinite, the OHAC becomes a harmonic complex whose fundamental frequency raises by an octave. The listeners' task was to adjust the attenuation level until the perceived pitch became equivalent to that of the SAWS.

Results

The matched attenuation level varied systematically with the divergence in the scaling factor. Tsuzaki et al. (2012) demonstrated that the ratios between two major peaks in the summary stabilized auditory images (SAIs) were good indicators to explain the dominating pitch, while Dinther et al. (2006) reported that the difference between the area under the two dominant peaks worked well to explain the pitch saliency for the OHAC. Two scatter plots using the two decision statistics can be obtained where the points on the plane corresponds pairs of the SAWSs and their matched OHACs. If the prediction were complete, all the points should be on the line whose slope is a unit. The RMS errors from this line were 0.269, and 0.299, respectively for Tsuzaki's, and for Dinther's decision statistics. This suggests that the peak ratios could be a better indicator for the saliency of the dominant pitch.

Conclusion

Based on the results of the pitch matching task between the SAWSs and OHACs, the simulations using the SAIs demonstrated that the ratio between the height of two peaks in the summary SAI could provide a better prediction than the difference between the area under the two peaks.



492 On the Nature of Rhythm and Memory for Time

Sundeep Teki¹, Timothy Griffiths^{1,2}

¹University College London, ²Newcastle University

Background

Internal clock models ascribe a working memory component which serves as an intermediate module between the accumulator and the comparator (Church, 1984). Previous work on temporal memory was limited and did not consider sequences with different rhythmic structures and memory loads as occurs in natural stimuli like speech and music.

Methods

Here, we developed a novel paradigm to analyze working memory for single time intervals in the context of sequences with different: (1) rhythmic structures: jitter ranging from 5-50%, (2) memory loads: 1-4 intervals, and, (3) inter-onset intervals – sub-second (500-600ms) and supra-second (1000-1200ms).

Participants listened to intervals in a sequence of clicks and were probed on their memory for a random interval after a variable delay. Response was initiated by a programmed click and participants matched the duration of the probed interval by terminating the response interval with a button press. Feedback, defined as the difference between the duration of the probed and the reproduced interval was provided.

Time matching responses were analyzed in terms of precision, or the inverse of the standard distribution of the error responses. Consistent with distributed resource models of working memory which posit that memory can be dynamically shared between one or more items (Bays and Husain, 2008), precision provides a measure of the variability of the memory for an item around its true value.

Results

Results from experiment 1 indicate that the decay of precision with decreasing temporal regularity can be best modelled as a quadratic function ($n=10$) and showed a significant main effect of jitter ($p=0.011$). Experiment 2 showed a significant effect of working memory load ($p < 0.05$) and a linear decay of precision with memory load ($n=9$). Experiment 3 did not show a main effect of jitter ($p = 0.65$) suggesting that sensitivity to temporal regularity is lost at supra-second intervals and also revealed a linear decay of precision with temporal regularity ($n=10$).

Conclusion

These results suggest for the first time that the memory for time intervals between auditory stimuli depends crucially on the context and varies with temporal structure and working memory demands. Results from these and ongoing experiments will be discussed in terms of mechanisms of timing that consider the rhythmic structure of time intervals (Grube et al., 2010; Teki et al., 2011), models of time perception (Meck, 2005; Teki et al., 2012), as well as working memory.

493 The Role of Auditory Feedback on Vocal Pitch Production in Cochlear Implant Users

Juan Huang¹, Patpong Jiradejvong¹, Courtney Carver¹, Xiaoqin Wang¹, Charles J. Limb¹

¹Johns Hopkins University

Background

Cochlear implantation (CI) has been highly successful in improving speech perception and production in people with profoundly hearing loss. However, how CI users perceive pitch cues in speech and how these cues affect speech production remains poorly understood. In this study, we investigated two questions. First, how does vocal pitch production in CI users differ from that of normal hearing (NH) listeners? Second, how does CI-mediated auditory feedback influence vocal pitch production in CI users?

Methods

We recorded the vocal production of consonants (in the form of a+C+a words) and vowels (in the form of h+V+d and s+V+t words), the vocal pitch simulation of the word “Ma” in the pitches of seven musical notes, as well as melody singing in postlingually-deafened CI users and NH listeners. We evaluated the vocal pitch of CI users by asking NH listeners judging the pitch contour that CI users produced and related the results to their pitch contour perception data. To assess the influence of auditory feedback through the CI on vocal pitch production, we compared speech production and singing in two conditions in CI users, CI on or CI off.

Results

Results show that pitch production by CI users is significantly less accurate than by NH controls. CI users typically produced lower pitch with greater variations in comparison to NH controls. However, the performance of pitch contour produced by CI users as judged by NH listeners is relatively accurate and is significantly correlated to their pitch contour perception. Vocal pitch production with CI off was generally less stable than when the CI was on. When the CI was turned off, CI user’s vocal production was typically louder than when the CI was on. In addition, the fundamental frequency and harmonics of vowels shifted towards higher frequencies in CI off comparing with CI on condition in most CI subjects.

Conclusion

These findings show that vocal production of CI users captures the contour but not the absolute pitch of the target sounds, indicating that vocal production of CI users

is affected by the impoverished auditory feedback received and the poor pitch perceived through their CIs. Furthermore, these findings suggest that optimizing auditory feedback in CI users should improve both vocal pitch production and speech intelligibility.

494 A Model of Bi-Modal Localization in Young Children

Karen Ann Martin¹, Patti Johnstone¹, Mark Hedrick¹

¹*University of Tennessee*

Background

The Duplex theory of localization has long been the main explanation of localization. However, given the varying developmental rates of different sensory modalities in humans, it is possible that factors such as task comprehension, vision, and attention contribute to auditory localization capabilities in young children. Visual development is complete before the end of the first year of life but auditory development is more complex anatomically and continues to develop up to and beyond age twelve. Spatial attention in children is stimuli-directed up until approximately twelve years of age. Beyond twelve years old, spatial attention becomes more goal-directed. A model for the study of visual and auditory development influences on localization was designed. Localization acuity was then tested in these two sensory modalities to separate non-auditory attention and task comprehension factors from the developmental central auditory processing factors affecting sound localization in young children.

Methods

Localization testing was conducted using visual and auditory stimuli with a group of 12 adults and 3 groups of young children aged 3-, 4- and 5-years old respectively. Testing occurred in a sound-treated booth containing a semicircular array of 15 loudspeakers. Each loudspeaker had a tiny light bulb and a picture fastened underneath. Seven of the loudspeakers were used to randomly test sound and light source identification. The sound stimulus was the word "baseball". The light stimulus was a flashing of the light bulb triggered by the digital signal of the word "baseball." Each participant was asked to indicate the location of test stimuli upon presentation.

Results

Localization acuity was significantly better for light than sound stimuli for children and adults. When compared to adults, children showed significantly greater localization error for both sensory modalities. 3-year-old children had significantly greater sound localization error compared to that of 4- and 5-year-olds. Adults performed better on the sound localization task when the light localization task occurred first.

Conclusion

Young children can understand and attend to localization tasks. When the central processing burden is lessened, children and adults show improved localization acuity to visual stimuli over auditory stimuli. Children show poorer localization acuity than adults across sensory modalities,

which may reflect differences in both attention and central processes in young children. Young children, like adults, do not rely exclusively on level cues to localize sounds. Adults can infer the location of sound sources based on prior experience localizing light sources.

495 How Do Cognitive Factors Interact with Speech-In-Noise Segregation in Normal Hearing Children and Adults?

Sara M Misurelli¹, Sara R Bernstein¹, Ingrid S Johnsrude², Ruth Y Litovsky¹

¹*University of Wisconsin-Madison*, ²*Queen's University*

Background

In noisy environments, it is difficult to attend to a talker while simultaneously ignoring background speech and noise. Compared to adults, children have more difficulty extracting target speech from interfering noise, and demonstrate greater variability in performance on source segregation tasks. Little is known about auditory or non-auditory factors accounting for this variability. This study tested the following novel hypotheses: semantic content of target speech influences speech intelligibility for children; measures of cognitive assessment predict performance on speech-in-noise tasks; and cognitive measures are inversely correlated with informational masking.

Methods

Four groups of normal hearing (NH) listeners were tested: Elementary school (7-10yrs), Middle school (11-14yrs), High school (15-17yrs) and Post-Secondary (18-22yrs). The auditory task consists of subjects repeating target sentences that are either semantically coherent or anomalous. Target speech is presented in quiet and with interfering speech or noise at four signal-to-noise ratios (SNRs) (-16, -8, 0, 8dB), representing the target level relative to the interferer. The target and interferers are either collocated or spatially separated. Cognitive tests assess working memory (WM) and attention, and are administered through computer-interactive methods. WM is assessed using a List Sorting Test requiring recall and sequencing. Attention is assessed using the Flanker Test, involving focusing on one stimulus while inhibiting another, and the Dimensional Change Card Sort Test, measuring flexibility by matching pictures according to various dimensions (e.g. color, shape).

Results

Preliminary results indicate the percentage of words correctly identified at each SNR, in each spatial configuration, is greater for target sentences that are semantically coherent than those that are anomalous. Percent correct decreases at lower SNRs, especially when both the target and interferers are speech and sources are collocated. Data from cognitive measures will be reported to determine whether the hypotheses are confirmed.

Conclusion

This is the first study to evaluate how children's WM and attention predict individual differences in ability to hear speech in noisy environments. Consistent with adult data,

semantically coherent sentences are more accurately reported, indicating semantic content influences intelligibility of target speech. Performance on these tests improves with age, suggesting they might provide a useful tool for tracking the developmental trajectory of source segregation in NH listeners. The tests used in this study may be informative in assessing individuals with hearing impairment and who use assistive listening devices.

Funded by NIH-NIDCD (R01DC8083 and R01DC8365) and NIH-NICHHD (P30HD03352)

[496] Hearing the Elephant in the Scene: A Computational Model of Bottom-Up Auditory Attention for Auditory Scene Analysis

Emine Merve Kaya¹, Mounya Elhilali¹

¹*Johns Hopkins University*

Background

As we listen to our environment in our daily lives, our brains are constantly extracting information from the incoming sound waveforms. One aspect of this mechanism is the detection of sounds that appear to be outliers within the context of their surrounding sounds. We hypothesize that as the sound statistics change over time, variance from these statistics drive bottom-up attention processes that direct our focus to certain events in a scene.

Methods

Here, we propose a model of bottom-up attention around a predictive coding framework. We use a rich high dimensional feature space that aims to capture the various characteristics of sounds that can steal the spotlight of attention. Among each feature axis, the statistics of the signal is learned; leading to a prediction for the next time instance. We obtain an estimate of saliency across time for every feature as a result of how well the real signal matches the predictions. The streams are fed to an interaction mechanism which brings the information across different features together in accordance with human experiment results. The result is a prediction of the times when an event occurs that is likely to grab the attention of a listening person.

Results

We present both human experiment results and computational model results using the same set of stimuli, and discuss the strengths and weaknesses of the attention model in matching the human experiment results.

Conclusion

We have presented a computational model of bottom-up auditory attention, introducing a predictive coding framework for the first time. Our model provides an efficient way to computationally find deviants in sound signals, and lays the foundation for investigating more sophisticated aspects of auditory attention.

[497] Psychophysiological Analyses of the Effects of Phase Information on Perceptual Outcomes for Normal-Hearing Listeners

Il Joon Moon^{1,2}, Jong Ho Won³, Michael Heinz^{4,5}, Jay Rubinstein¹

¹*V.M. Bloedel Hearing Research Center, University of Washington, Seattle, WA 98195, USA*, ²*Dept. of Otorhinolaryngology-Head and Neck Surgery, Samsung Medical Center, Seoul 135-710, Korea*, ³*Dept. of Audiology & Speech Pathology, Univ of Tennessee Health Science Center, Knoxville, TN 37996*, ⁴*Dept of Speech, Language, and Hearing Sciences Purdue University, West Lafayette, IN 47907, USA*, ⁵*Weldon School of Biomedical Engineering, Purdue University, West Lafayette, IN 47907, USA*

Background

Previous studies have demonstrated the importance of encoding phase cues for speech perception, and it is generally agreed that deficits in encoding phase cues result in degraded speech perception, particularly in noise. However, it is still not clear to what extent disrupted phase encoding is related to a reduction in processing of complex stimuli. The goal of this study was to understand the systematic relationship between the degree of accurate phase information available for listeners and perceptual outcomes. The encoding of such phase cues in the auditory nerve was investigated using a computational auditory model.

Methods

A phase randomization vocoder was used to systematically vary the degree of phase information available for listeners from 0 to 100%. To determine the effect of phase randomization upon speech perception, sentence recognition was measured for normal-hearing listeners in the presence of a steady or modulated masker. To further understand the nature of the effect of phase randomization, psychoacoustic performance was also evaluated. Spectral-ripple discrimination was used to evaluate spectral processing and Schroeder-phase discrimination was used to evaluate temporal processing as a function of the degree of phase randomization. Neural cross-correlation coefficients were computed to quantify neural envelope and temporal fine structure (TFS) coding in model auditory nerve spike trains.

Results

The phase randomization vocoder successfully varied the degree of phase cues available in the signal as well as in the auditory nerve. An almost linear relationship was observed between the broadband TFS of original and vocoded speech signals as a function of the degree of phase randomization. Results from the computational auditory model showed that neural TFS coding was systematically degraded as the phase was disrupted in the acoustic speech signals. A change in neural envelope coding was also observed, but these changes in neural envelope and TFS coding were independent from the effect of the number of vocoder bands. The perceptual outcomes utilizing the randomized phase information were

shown to be different for different tasks. In general, performance improved as more accurate phase information was provided, but the pattern of improvement was dependent on testing conditions (masker type or number of bands).

Conclusion

The present study demonstrated that disrupted phase in the acoustic signal leads to the disrupted representation of neural coding of those cues, and this disrupted neural coding results in a reduction in perceptual performance. [Supported by NIH T32-DC000033 and an educational fellowship from Advanced Bionics Corporation.]

498 Asynchronous Glimpsing of Speech in Natural and Simulated Hearing Loss

Erol J. Ozmeral¹, Emily Buss¹, Joseph W. Hall, III¹
¹University of North Carolina at Chapel Hill

Background

Howard-Jones and Rosen (1993) investigated the ability of normal-hearing adults to integrate glimpses of masked speech that are separated in time and frequency by applying asynchronous amplitude modulation (AM) to neighboring masker bands. A recent study in our lab tested the hypothesis that performance in Howard-Jones and Rosen's study was limited by peripheral spread of masking (Ozmeral et al., 2012). In some conditions, the even- and odd-numbered bands of the target speech and asynchronous AM masker were presented to opposite ears, minimizing the deleterious effects of spread of masking. Consistent with the hypothesis related to spread of masking, we found greater evidence for asynchronous glimpsing in dichotic conditions than in corresponding monaural conditions. [Work supported by NIH NIDCD R01 DC00418 & F31 DC012694]

Methods

In the present study, hearing-impaired listeners and normal-hearing listeners with simulated hearing loss discriminated consonants in several different AM maskers, including monaural and dichotic asynchronous conditions. Simulations of reduced audibility and poorer frequency resolution were achieved through attenuating and spectrally smearing the stimulus, respectively.

Results

Listeners with either hearing impairment or simulated impairment experienced comparable benefit of dichotic presentation as normal-hearing listeners without a simulated loss. Asynchronous glimpsing was evident in all listening groups, indicating an ability to integrate dichotic speech information across time, frequency, and the two ears.

Conclusion

By varying levels of spectral smearing, the present experiment explored the impact of impaired frequency resolution on noise-masked speech perception. Preliminary results indicate that hearing impaired listeners can benefit from dichotic presentations in an asynchronous

glimpsing task, and therefore, may provide impetus for new processing strategies in bilateral auditory prostheses.

499 Learning to Understand Degraded Speech: Effects of Age, Masker Configuration, and Training Procedure

Daniel E. Shub¹, Emma Gore¹

¹School of Psychology, University of Nottingham

Background

This work represents a first step towards developing a game-based educational curriculum for improving communication. The experiments were designed to evaluate how training with an audio-game compares to training with videogame and testing-based regimes. Speech reception thresholds (SRTs) were measured before and after training under a variety of different masker configurations. The masker configuration used during training was systematically manipulated to investigate the transfer of training.

Methods

Two experiments consisting of three stages (pre-test, training, and post-test) were conducted. During the pre- and post-tests, SRTs were measured with vocoded speech targets and vocoded (1) on-frequency speech, (2) on-frequency noise, and (3) off-frequency speech maskers that were either co-located or spatially separated from the target. In Experiment I, there were five groups. One group of younger listeners trained with a videogame. The other four groups (two older and two younger) trained with an on-frequency speech masker that was spatially separated from the target with the training being either audio-testing or audio-game based. In Experiment II, three groups trained with the audio-game and the masker configuration used during training varied amongst the groups.

Results

All groups demonstrated statistically reliable improvements in SRTs. The younger groups had a lower overall SRT, however, the pattern and amount of learning was independent of age. There was no difference in the pattern of learning between the audio-testing and audio-game groups. There was a statistically reliable difference in the pattern of learning between the videogame and audio-game groups. The overall trend was towards greater learning in the audio-game group, however, in some conditions the trend was towards greater learning in the video-game group. Further, the maximal amount of learning was not reliably observed in the trained stimulus condition and there was no obvious relationship between the pattern of learning and the training condition.

Conclusion

Audio-game based training can be just as effective as audio-testing based training. Further, the amount of learning is independent of age. This suggests that audio-game based training may present a viable means of alleviating some of the burdens of hearing impairment. The complexity of the learning patterns and their dependence on the masker configuration used during training suggests

that optimizing a training-based intervention will be non-trivial. [This work was supported by the NIHR and Royal Society.]

500 Modeling Speech Intelligibility Performance with Spatially Separated Interferers in Normal Hearing and Hearing Impaired Listeners

Nathaniel Spencer¹, Steven Colburn¹

¹*Boston University, Biomedical Engineering and Hearing Research Center*

Background

The Equalization-Cancellation (EC) model (Durlach 1963, JASA) has been used extensively to predict the outcomes of various binaural processing experiments. In an ongoing experimental study, speech reception thresholds (SRTs) were measured monaurally and binaurally in NH and HI listeners with monotonic speech stimuli, with a target in front and two maskers laterally displaced either with one in each hemisphere (symmetric) or both in the same hemisphere (anti-symmetric). The purpose of this work is to see how model predictions relate to the experimental data, including the effects of various model parameters.

Methods

Speech sentences were bandpass-filtered into 1/3-octave narrow bands and jittered in time and intensity. These jittered narrow bands comprise monaural channels to the model's decision stage. For each filter band, a binaural channel is created consistent with the EC model modified to process short time-sections of the stimuli separately, each with its own equalization and cancellation processing to minimize masker energy. The resulting processed time sections were combined to form a signal with an improved signal-to-noise ratio (SNR). It was assumed that the speech intelligibility index (SII) could be calculated using the channels with the best SNR in each frequency bin. In this study, the time-slice window duration and the time- and intensity-jitter standard deviations were varied to see how the threshold predictions changed.

Results

Experimentally measured binaural SRTs were variable, up to about 8 dB lower than the monaural SRTs. Symmetric binaural model predictions with normal jitter parameters varied between 1.5 and 9 dB below monaural predictions, depending on window length (between 10 and 1600 ms). Anti-symmetric binaural predictions were 6 dB below monaural. When the jitter was decreased by a factor of four, symmetric predictions were relatively insensitive, while anti-symmetric SNRs decreased by 3 dB. Increasing the jitter made the predictions equal to the monaural predictions.

Conclusion

Binaural advantage data could be fit by the model for either masker configuration. The nature of the parameters that varied the predicted SNRs differed between the two cases. Anti-symmetric predicted SNRs depended more on the amount of jitter applied, and the symmetric predicted

SNRs depended more on the time-window. The next step is to use this information, combined with information on subject performances in other tasks, to define how to most appropriately model the data for the individual subjects. [Research supported by NIH/NIDCD: grant RO1 DC00100.]

501 Harmonicity and Spectral Sparsity in Speech Segregation

Josh McDermott¹, Michael Schemitsch², Hideki Kawahara³, Dan Ellis⁴

¹*Massachusetts Institute of Technology*, ²*New York University*, ³*Wakayama University*, ⁴*Columbia University*

Background

Sound created by a periodic process, as in speech and other natural signals, has harmonic structure – Fourier components at multiples of a fundamental frequency (f_0). Harmonicity is closely related to the perception of pitch and is believed to provide an important acoustic grouping cue underlying sound segregation. Here we use a novel speech synthesis method to manipulate the harmonicity of otherwise natural-sounding speech tokens, and report the results of speech segregation experiments with such tokens.

Methods

We utilized elements of the STRAIGHT framework for speech manipulation and synthesis [Kawahara (2006), *Acoustical Sci. and Tech.*], in which a recorded speech utterance is decomposed into voiced and unvoiced vocal excitation and vocal tract filtering. Unlike the conventional STRAIGHT method, we modeled voiced excitation as a combination of time-varying sinusoids. By individually modifying the frequency of each sinusoid (shifting each component by a fraction of the f_0 , or jittering each component by a random fraction of the f_0), we introduced inharmonic excitation without changing other aspects of the speech signal. We also re-synthesized speech using noise excitation, to simulate the effects of whispering. To assess the effect of these manipulations on speech segregation, we presented listeners with individual words or pairs of concurrent words spoken by different speakers, and asked them to report as many words as they could.

Results

Performance for isolated words was high for both harmonic and inharmonic speech, and somewhat worse for whispered speech. For pairs of concurrent words, we observed a small performance decrement for inharmonic speech relative to harmonic speech. However, this effect was substantially smaller than the decrement for whispered speech relative to harmonic speech. Surprisingly, the deleterious effect of inharmonicity on speech segregation was significantly larger in musicians than nonmusicians, despite the nonmusical nature of the task.

Conclusion

Harmonic speech excitation aids the comprehension of speech amid concurrent talkers, but the benefit of

harmonicity is modest, and seems to be most pronounced in listeners with musical experience. The cost of whispering relative to inharmonic speech indicates that an equally important consequence of voiced speech excitation may be spectral sparsity – the presence of discrete frequency components, as are absent in whispering. By reducing spectral overlap between concurrent signals, sparsity may facilitate segregation via other acoustic grouping cues or top-down lexical matching.

502 Speech Enhancement Effects Robust to Changes in Spatial Position Within a Room

Eugene Brandewie¹, Pavel Zahorik¹

¹*University of Louisville*

Background

Previous studies have shown that speech intelligibility in a reverberant room is enhanced by prior listening exposure to that room. Here, this speech enhancement effect is examined under conditions where a carrier phrase and target are presented at different spatial positions in a reverberant room environment that was simulated using virtual auditory space techniques. If the speech enhancement effect relies primarily on the decay pattern of later reverberant energy and not on the specific spatial/temporal patterns of the early reflections, then the effect should be minimally affected by spatial position changes within the room.

Methods

The carrier phrase and target were convolved with separate binaural room impulse responses from different spatial positions in the same room environment. This manipulation altered the temporal positioning of the early reflections but maintained similar patterns of decay in the late reverberation. Intelligibility enhancement data are compared to previous work in which the late reverberation patterns were altered between the carrier phrase and the speech target.

Results

A consistent speech enhancement effect was observed even when spatial position was changed between carrier and target, which suggests that the effect is robust to the resulting changes in the spatial/temporal patterns of early reflections. Consistent with previous work, the magnitude of the effect varies with the amount of room reverberation.

Conclusion

The speech enhancement effect is independent of the specific positioning of the speech source and its carrier phrase in a reverberant room environment.

503 Remote-Frequency Masking in School-Aged Children and Adults: Effects of Spectral Proximity and Masker Bandwidth

Lori Leibold¹, Emily Buss¹

¹*The University of North Carolina at Chapel Hill*

Background

Previous studies have shown that infants (Werner & Bargones, 1991) and 4- to 6-year-old children (Leibold &

Neff, 2011) are susceptible to masking in the presence of a remote-frequency band of noise. In these studies, a 4000-10000 Hz noise band produced significant masking of a 1000-Hz signal in younger listeners, but not in older children or adults. This study examined the influence of envelope modulation rate, masker bandwidth, and spectral separation of the signal and masker on child-adult differences in remote-frequency masking.

Methods

Listeners were 5- to 6-year-olds, 7- to 9-year-olds, and 19- to 30-year-olds (adults). Detection thresholds were measured for a 500-ms, 2000-Hz pure-tone signal in quiet or presented simultaneously with a band of noise, filtered in one of four frequency configurations: 425-500 Hz, 4000-4075 Hz, 8000-8075 Hz, or 4000-10000 Hz. Maskers were played at an overall level of 60 dB SPL, gated on in each interval of a 3IFC adaptive procedure. Two or three estimates were obtained in each condition for each listener. Masking was computed for each listener in each condition, by subtracting the quiet threshold from the masked threshold.

Results

Masking was positive on average for all listener groups in all maskers. However, significantly greater masking was observed for the 4000-4075 Hz masker than for the other three maskers. Remote-frequency masking was comparable for narrowband maskers two octaves above (8000-8075 Hz) and below (425-500Hz) the signal. There was a modest trend for greater masking in the younger group of children than in the older group of children or in the group of adults, although there were substantial individual differences within listener age groups. Supplemental data were obtained from five additional adults with psychoacoustic listening experience. Following practice, five to seven estimates of threshold were obtained in each condition. In contrast to data obtained from children and naïve adults, results for experienced adult listeners showed little or no masking for any of the four masker conditions.

Conclusion

These results are consistent with those of other studies, showing a reduced ability of children to listen in a frequency-selective manner. These findings also suggest that spectral proximity of the signal and masker plays an important role in masking, even when the signal and masker do not overlap in the auditory periphery.

Support from the NIDCD (R01 DC011038)

504 Assessing Relative Sound Localization Abilities of Human Listeners in Noise

Katherine Wood¹, Jennifer Bizley¹

¹*University College London*

Background

The 'hemifield code' proposes that the perceived location of a sound source is a consequence of the relative activity of two populations of neurons tuned to contralateral and

ipsilateral space respectively. In contrast, the topographic model proposes that neurons exist tuned throughout auditory space. Attempts to disambiguate these two models using brain imaging found that sounds moving away from the midline elicit a greater neural response than those moving toward the midline for broadband and ITD-only stimuli, supporting the hemifield model (Salminen et al 2009, Magezi & Krumbholz, 2010). However, it remains unknown whether these neural response differences result in a behavioural difference in discriminating a change in sound location for outward- versus inward-moving stimuli. We performed a human psychophysics experiment using free-field stimuli to investigate this.

Methods

Subjects made a relative sound localization judgment of stimuli composed of 6 15 ms, white-noise pulses, presented at 10 Hz. Subjects sat within a ring of 18 speakers arranged at 15° intervals spanning 255°. On each trial, the first 3 pulses (reference) were presented from one of 10 locations and the second 3 pulses (target) from an adjacent speaker. The subject made a left/right response to indicate the position of the target relative to the reference. This pulse-train was embedded in noisy background, with independently varying noise being presented from each speaker location. An ITD paradigm with low-pass filtered pulses and an adaptation paradigm with 8-13 pulses at the reference were also tested.

Results

The accuracy of relative sound localization varied throughout auditory space. Relative sound localization abilities were substantially worse in the periphery compared to frontal space, with subjects' best localization performance for judging the relative location of a target sound occurring close to, but not across, the midline. The accuracy of relative sound localization also varied with SNR, with a lower SNR decreasing accuracy. Statistical analysis demonstrated that target location and SNR significantly influenced accuracy, but whether the target sound moved inward or outward did not. The pattern of results observed was very similar in the ITD condition and in the adaptation condition. We compared our experimental data to modeled data based on the models of sound localization outlined above. Relative sound localization abilities were most closely predicted by the two-channel model.

Conclusion

Relative sound localization abilities are affected by reference and target sound locations and signal to noise ratio.

505 Stimulus Burst Duration Influences

Audiovisual Spatial Binding

Adam Bosen¹, Emily Clark¹, Paul Allen¹, William O'Neill¹, Gary Paige¹

¹University of Rochester

Background

Binding, the process by which information from multiple senses is combined to form a unified percept, occurs with a likelihood that is influenced by the spatial discrepancy between auditory and visual stimuli. Previous studies have reported conflicting results indicating that binding likelihood is 50% for audio-visual stimulus discrepancies from as low as 4 degrees, to greater than 15 degrees. One potential source of the disagreement between these studies is differences in burst duration of audio-visual stimuli; studies reporting smaller binding windows used longer stimulus bursts.

Methods

Young adult subjects were asked to localize the source of a continuous train of broadband noise bursts in the presence of a punctate visual distractor that was temporally synchronized, but spatially disparate. Spatial discrepancies ranged from 0° to 20° visual angle, and burst duration was either 50 ms or 200 ms for each trial, with a constant 2 Hz stimulus presentation rate. Auditory localization was measured for each subject and binary logistic regression was used to estimate the audio-visual spatial discrepancy at which binding likelihood was 50%. This metric provides a reliable estimate of the spatial range over which audio-visual binding is likely to occur, since it does not rely on oversampling particular spatial discrepancies or auditory stimulus locations in a manner that could bias subject responses.

Results

Our results demonstrate that increasing audio-visual stimulus burst duration from 50ms to 200ms reduces the audio-visual spatial discrepancy at which binding likelihood was 50%. Additionally, we discovered considerable variability between subjects, suggesting that there are broad individual differences or unidentified factors contributing to audio-visual spatial binding.

Conclusion

Increasing stimulus burst duration reduces the range of audio-visual spatial discrepancies over which stimuli are bound, suggesting that multisensory binding improves with integration over time. These results help explain differences across previous studies.

506 Individual Differences in Sound

Localization Performance : Role of HRTFs

Spectral-Richness

Guillaume Andeol¹, Jean Christophe Bouy¹, Lionel Pellieux¹

¹Institut de Recherche Biomédicale des Armées

Background

Studies of sound localization often show substantial differences in performance across participants. Previous

studies have suggested that interindividual variability could be related to acoustical differences in localization cues such as the “spectral richness” of the HRTFs (Head Related Transfer Functions). A low spectral richness would limit sound localization performance. In the current study, we investigated the hypothesis that spectral richness can account for interindividual variability in sound-localization performance.

Methods

In this study, 25 young (<35 years old) normal-hearing listeners performed an absolute sound-localization task with individual and non-individual HRTFs. The task involved localizing 119 targets distributed uniformly on the surface of a 1.40 m virtual sphere. Participants gave their responses by pointing on a smaller-scale replica of the virtual sphere (God Eye Localization Pointing technique). To reduce procedural-learning effects, participants received procedural training prior to the localization tests. Unsigned left/right and up/down errors, and front/back and up/down reversals rates, were measured as well as the spectral richness of the HRTFs.

Results

Large interindividual variability was observed for each of these measured variables. No correlation was observed between the spectral richness and the measured variables. However, the results suggest that interindividual variability in localization performance in the left-right dimension could stem from interindividual variability in the use of the different types of cues available for sound localization in this dimension (binaural/spectral cues). Besides, interindividual variability in sound-localization performance in the up-down and front-back dimensions could be linked primarily to spatial attention and to its variation across the area of space.

Conclusion

Interindividual variability in sound localization performance appeared to be more likely related to perceptual origins than acoustical origins.

[507] Effect of Head Movement on Sound Localization Accuracy in the European Starling (*Sturnus Vulgaris*)

Arne Feinkohl¹, Georg Klump¹

¹Carl von Ossietzky University Oldenburg

Background

In sound localization experiments, long stimulus durations represent closed-loop conditions that allow the sensory feedback to modify the orientation response of the subject during stimulus presentation. This may yield better thresholds compared to short stimulus durations that represent open-loop conditions and do not allow for orientation responses during stimulus presentation. A previous Go/NoGo experiment on the Minimum Audible Angle (MAA) in the European starling (*Sturnus vulgaris*) showed that the starlings reach a better MAA for stimulus durations of 1s compared to 100ms in broadband noise conditions (Feinkohl & Klump 2012). For 2-kHz tones, the

improvement was not significant. In the present study, we evaluated whether head movements of the starlings during the stimulus presentation in the MAA experiment affect the localization accuracy

Methods

We recorded videos of the MAA experiment from top view for broadband noise (BBN) and 2-kHz tone (2kT) conditions. For each standard (range 1-5 stimuli) and test signal in a trial, we determined the starling's head orientation in 9 video frames for the 1s conditions and in 5 video frames for the 100ms conditions, respectively, and calculated the head movement. For occasionally appearing blurry frames that were a result of fast head movement, we only determined the direction of the head movement. Based on these data, we analyzed the effect of the number of head movements on the probability of correct response in relation to stimulus type (100ms BBN, 1s BBN, 100ms 2kT, 1s 2kT). An additional analysis evaluated the role of head movements during the test stimulus presentation only.

Results

Generally, the probability of a correct response increased with the number of head movements. Preliminary data on the analysis of head movements during the test stimuli indicate differences between the stimulus conditions. For stimulus conditions with a duration of 1s, the probability of a correct response increased with the number of head movements, while we found a contrary effect for stimuli with a duration of 100ms.

Conclusion

Head movements allowed the starlings to improve sound localization accuracy in the MAA experiment. While Stimulus durations of 100ms were too short to provide effective head orientation responses, stimulus durations of 1s allowed orientation responses and therefore improved sound localization accuracy.

[508] Rat Cortical Units Display Sharp Hemifield Tuning

Justin D. Yao¹, Peter Bremen¹, John C. Middlebrooks¹

¹University of California, Irvine

Background

We wish to examine the cortical mechanisms of spatial hearing, specifically of localization and spatial stream segregation. While the cat is a popular model for spatial hearing research, the rodent is a more appropriate model for conducting the in vivo intracellular recordings and pharmacological techniques we envisage. Thus, as a first step, we have developed an anesthetized rat preparation for spatial hearing experiments. Here, we evaluate the spatial tuning of rat primary auditory cortex (A1) to sound-source azimuth with broad-brand noise.

Methods

Extracellular responses were recorded simultaneously from 16 channels of a silicon-substrate probe in field A1 of urethane/xylazine-anesthetized Sprague Dawley rats.

Stimuli were 80-ms broad band noise bursts, varying in sound level, and presented from an array of 18 free-field loudspeakers spaced 20 degrees apart throughout 360 deg in the horizontal plane (azimuth). For all cortical units, spatial tuning was characterized by rate-azimuth functions, widths of Equivalent Rectangular Receptive Fields, depths of azimuth-dependent spike-rate modulation, and locations of steepest tuning slopes. Current Source Density (CSD) was used as a functional indicator of the depth of thalamic input layers.

Results

Rat A1 units demonstrated exclusively “hemifield” spatial tuning, with strong responses to contralateral sounds, little or no response to ipsilateral sounds, and a sharp cutoff across the frontal midline leaving little dynamic range to convey information within each hemifield. Moreover, spatial tuning showed surprisingly little variation across sound levels from 20 to 40 dB above threshold. CSD analysis revealed that relative to the putative thalamic input layer, spatial tuning displayed little variation across cortical depth, suggesting that spatial tuning characteristics in rat A1 are already apparent at the level of thalamic input.

Conclusion

In contrast to results from anesthetized cats, primates, and ferrets, which display a mixture of contralateral, ipsilateral, and omni-directional tuned neuronal units that expand to increasing suprathreshold sound levels, A1 in anesthetized rats is dominated by neurons that show sharply delimited contralateral tuning with remarkably little variation across increasing suprathreshold sound levels. Previous behavioral investigations have shown that spatial discrimination in rats is excellent across the frontal midline, but that rats cannot discriminate between locations within the lateral fields (Kavanagh & Kelly, 1986). This is in accordance with our results, suggesting that rat A1 units typically signal left or right and do not distinguish among locations away from the frontal midline.

509 Sound Localization in Sagittal Planes: Modeling the Level Dependence

Piotr Majdak¹, Robert Baumgartner¹, Thibaud Necciarì¹, Bernhard Laback¹

¹Austrian Academy of Sciences

Background

Sound localization in sagittal planes (SPs), including front-back discrimination, relies on spectral cues resulting from the filtering of incoming sounds by the human body. For short sounds, the vertical range of perceived sound direction depends on the sensation level (SL), an effect often described by the polar gain (linear fit between target and response angles). Data on the polar gain for setups involving both frontal and rear targets seem to be rather limited. Furthermore, models considering the level-dependency are available only as a conceptual description.

Methods

Localization responses to brief (3-ms) noise bursts, distributed around normal-hearing listeners both horizontally and vertically in the upper hemisphere, were collected at various SLs from 5 dB to 75 dB in a virtual binaural environment using listener-specific head-related transfer functions. Responses to 300-ms noise bursts presented at an SL of 50 dB were also collected. Localization performance was evaluated in terms of quadrant errors (QE, hemifield confusions), polar angle errors (PE, local root-mean-square errors in the SPs), and polar gain. Performance was also modeled with a localization model based on the comparison of internal sound representation with a template. It consisted of a nonlinear filterbank, a probabilistic decision stage, and a stage retrieving the psychophysical performance parameters. Two template level (TL) conditions were tested: varying with the SL and fixed to 40 dB.

Results

For short stimuli, QEs and PEs were lowest at an SL of 40 dB and increased at other SLs. The goodness of fit of the polar gain was overall low, with R^2 of 0.058 for SLs \geq 50 dB. The polar response variability was largely level dependent. The psychoacoustic results were accurately predicted by the model with TL fixed to 40 dB and inaccurately predicted by the model with varying TL. For long stimuli, both models were unsuccessful.

Conclusion

The level-dependency was confirmed in terms of best performance at an SL of 40 dB. The polar gain did, however, not well describe the effect of SL. Our model was successful in predicting the results for the short stimuli. It failed for longer stimuli, indicating that additional stages such as the MOCR or temporal integration are required. Good results were obtained for the TL fixed to 40 dB, suggesting that the spectro-to-spatial mapping is tuned to a fixed level at the neural level. Funded by the Austrian Science Fund (FWF, P24124-N13).

510 Smooth Pursuit Eye Movements During Tracking of Auditory Targets Suggest Motion-Specific Processing in the Auditory System

Christina Cloninger¹, Emily Clark¹, Paul Allen¹, William O'Neill¹, Gary Paige¹

¹University of Rochester

Background

Two conflicting theories address how the perception of auditory motion is perceived: dedicated motion-specific processing, and a strictly position-oriented ‘snapshot theory’. Motion-specific processing posits specialized motion detecting circuits within the CNS, specifically responsive to auditory object velocity. Alternatively, the snapshot theory assumes sound motion perception is based on periodic sampling of spatial position cues as the target moves through space. Eye movements (saccades and smooth pursuit) may be informative regarding these opposing, though not mutually exclusive, views of auditory motion perception. Smooth pursuit maintains foveal

fixation on a moving visual target by smoothly moving the eyes to match target velocity, while saccades ballistically shift foveal fixation from one point to another. Saccades are often employed during visual smooth pursuit when the eyes fall behind and must catch-up to the now peripheral (non-foveal) target. A saccadic strategy of catch-up movements when tracking moving auditory targets argues for the snapshot theory, while smooth pursuit would suggest true motion detection and behavioral tracking. Previous studies have shown little, if any, smooth pursuit of moving auditory targets, but most studies have used high or low velocities that are not ecologically relevant in daily life.

Methods

We presented audio-visual or auditory-only moving targets over a range of realistic velocities (<50°/s) using a concealed loudspeaker/LED target carried on a robotic arm. Eye movements of head-fixed subjects were recorded using electrooculography.

Results

We found that at modest target velocities (20 and 33°/s) smooth pursuit of auditory motion routinely occurs, but with a lower gain (half or less) than for visual targets.

Conclusion

Smooth pursuit of auditory targets occurs, providing strong evidence for a motion-specific auditory processing mechanism. Catch-up saccades are intermingled with pursuit. This suggests that the gain of auditory-driven ocular pursuit is inadequate to accurately track sound objects, requiring a position-dependent correction process co-existing with a true motion processing system.

511 The Acoustical Cues to Sound Location in the Adult Guinea Pig: Measurements of Directional Transfer Functions (DTFs)

Kelsey Anbuhl¹, Alexander Ferber¹, Kanthaiha Koka², Whitney Williams², Jennifer Thornton², Daniel Tollin³

¹Neuroscience Training Program, ²Department of Physiology and Biophysics, ³Department of Otolaryngology, University of Colorado- Anschutz Medical Campus, Aurora, CO 80045 USA

Background

There are three main acoustical cues to sound location, each of which is generated by the spatial-and frequency-dependent filtering of the propagating sound waves with the outer ears: Interaural differences in time (ITD) and level (ILD) as well as monaural spectral shape cues. The guinea pig has been a common model for studying the anatomy, physiology, and psychophysics of binaural and spatial hearing, yet little is known about their acoustical cues.

Methods

Here, we measured the directional transfer functions (DTFs), the directional components of the head-related transfer functions, for 4 adult guinea pigs. DTFs were measured at both ears from 325 locations, with steps of

7.5° in both azimuth and elevation. The resultant localization cues were computed from the DTFs.

Results

The mean weight, head diameter, and the length and width of the pinnae for the guinea pigs were 797 ± 138 g, 30.7 ± 3.5 mm, 32.7 ± 2.9 mm and 10.9 ± 2.5 mm, respectively. In the frontal hemisphere, spectral notches were present for frequencies from ~11-19 kHz; in general, the frequency corresponding to the notch increased with increases in source elevation and in azimuth towards the ipsilateral ear. The mean maximum ITD observed across the guinea pigs was 215 ± 5.8 μs. Interaural level differences (ILD) depended strongly on source azimuth and frequency. In general, maximum ILDs were < 12.2 dB for frequencies < 4 kHz, and ranged from 12.2 dB - 40 dB for the frequencies from 4-16 kHz. ILDs for frequencies > ~15 kHz varied with azimuth in complicated ways. Pinna removal eliminated the spectral notches and reduced both ILD and ITD cues.

Conclusion

The acoustical cues to sound location for the guinea pig are consistent with other mammals that have been studied, with respect to their head and pinna size. These results also emphasize the pinna's role in generating these acoustical cues.

Support: NIDCD R01-DC011555

512 Frequency Dependent Directionality in the Mechanical Response of the Gray Treefrog Ear

Michael Caldwell¹, Norman Lee¹, Katrina Schrode¹, Jakob Christensen-Dalsgaard², Mark Bee¹

¹University of Minnesota, ²Syddansk University

Background

The amphibian ear is inherently directional. Mechanical coupling of the two tympana via the Eustachian tubes and mouth cavity allows each ear to function as a pressure difference receiver. We investigated the frequency and amplitude dependence of this directionality in Cope's gray treefrog (*Hyla chrysoscelis*), a species for which there is now a wealth of behavioral data on sound source segregation.

Methods

We measured tympanum vibration with a laser vibrometer in response to short tones (0.60 kHz, 1.25 kHz, 1.625 kHz, 2.50 kHz, and 3.20 kHz) and FM sweeps presented at twelve azimuthal angles (every 30°).

Results

The response of the tympanum to variation in sound source location was frequency dependent. Directionality was most pronounced at frequencies between the two spectral peaks present of the frog's sexual advertisement call (1.25 kHz and 2.5 kHz), with a mean directionality of 6 dB for the 1.625 kHz tone. This frequency dependence was further affected by the volume of air occupying the lungs, with response to lower frequencies most strongly

affected by lung air volume. Tympanum response to variation in sound location was sex dependent. Males showed on average 4 dB greater directionality at 1.625 kHz than did females, but tympanum vibration velocities were 3 dB lower across frequencies. Additionally, individuals housed in the laboratory for one year showed similar directionality to frogs recently collected from breeding ponds in the wild, but were less sensitive to high frequency sound (-13 dB at 3.2 kHz).

Conclusion

Our results are congruent with those of previous studies, and represent one of the most thorough investigations to date of the mechanical response of the frog ear. [This work supported by NIDCD R01 5R01DC009582.]

513 Comparing Two Measures of Absolute Sound Localization Performance in Cats

Amy Hong¹, Janet Ruhland¹, John Cress¹, Yan Gai¹, Tom Yin¹

¹University of Wisconsin

Background

Behavioral studies measuring absolute sound localization ability generally implement either an approach-to-target or a pointing task. The approach-to-target task requires the subject to move toward a sound source from a fixed location, while the pointing task typically requires head and/or eye movements toward an auditory target. The fact that subjects usually initiate a head and gaze movement towards the target during the approach-to-target task enables us to measure the accuracy of the initial head and gaze movement and compare it with subsequent speaker selections.

Methods

Cats were trained to localize a broadband noise presented randomly from one of four speaker locations ($\pm 30^\circ$ and $\pm 60^\circ$) along the horizontal plane. Trials were self-initiated when the cat's body and head were centered and she was fixating on a central LED. Cats indicated their response by walking to and pressing a lever at the perceived location to obtain a food reward. Reward was delivered only if the first attempt was correct. Trials without a response were classified as "no-go" trials while first selections at the wrong location were "incorrect". A non-categorized measurement of localization accuracy was ascertained by recording the initial head and eye movements immediately following target onset prior to walking to its perceived location. To provide variations in performance, we varied the stimulus duration from 25 to 1000 msec.

Results

Localization performance under both speaker selection and initial gaze movement was very high for long duration sounds but decreased as stimulus duration was reduced. Interestingly, for many of the incorrect and no-go responses, the head and eye oriented to the correct sound source, even when the cat did not approach the correct target. Importantly the eye was significantly more accurate than the head in indicating target location, as the head

undershot the eye by as much as 15-20 degrees. At times, the eyes oriented to the targets but the head did not.

Conclusion

Reducing stimulus duration resulted in a systematic decline in both measurements of localization performance. Our data suggest that the head or gaze-orienting response provides a better measure of localization accuracy, especially when the task is difficult and may minimize bias to specific targets. Apparently, a higher degree of certainty is required to walk to the target, suggesting more involvement in higher-order cognitive processing in this task as compared to gaze orienting.

514 Effect of Reverberation on Acoustic Measures Relevant for Localization (Where) and Recognition (What) of Sounds Located at Various Azimuths and Distances: A Study of Humans and Rabbits

Duck O. Kim¹, Pavel Zahorik², Brian Bishop¹, Shigeyuki Kuwada¹

¹University of Connecticut Health Center, ²University of Louisville

Background

Binaural room impulse responses (BRIRs) describe how a sound source is transformed into signals in the two ears of a listener located in a reverberant environment. Measures such as reverberation time (T60), direct-to-reverberant (D/R) energy ratio, interaural correlation coefficient (IACC) and acoustic modulation transfer functions (MTFs) can be derived from BRIRs (for MTF, see Schroeder, 1981). Acoustic MTFs have been shown to predict speech intelligibility (Houtgast and Steeneken, 1985). Although BRIRs have been reported in the literature, descriptions of the above acoustic measures are sparse. The goal here is to provide BRIRs of humans and rabbits with a sound source at various locations in two different reverberant environments and to derive the above measures that are relevant for localization and recognition of sounds. This will delineate acoustic conditions that the auditory system faces to accomplish the tasks of localization and recognition in reverberant environments.

Methods

We measured BRIRs in an anechoic, moderately- and highly-reverberant environments with a sound source at 0° elevation over a range of azimuths ($\pm 180^\circ$) and distances (10 cm or 14 cm to 160 cm; Kim et al., 2010; Kuwada et al., 2010). The above acoustic measures were derived from BRIRs for octave-band noise sources with center frequencies of 0.25 ~ 10 kHz.

Results

Results for human and rabbit were qualitatively similar. The T60 was a nonmonotonic function of frequency. The values of T60 averaged across frequency were 0.91 and 2.3 sec in the two reverberant environments. With decreasing distance, the D/R increased because the reverberant energy remained approximately constant while direct energy increased. The D/R also depended on

azimuth and frequency. The IACC decreased with increasing distance and frequency. Across azimuth, the IACC was large and interaural time difference (ITD) was small when the sound was in the front or back whereas the IACC was small and the ITD large when the sound was lateral. Modulation loss increased monotonically with increasing modulation frequency and distance. When the sound was in the front, modulation loss was large for low carrier frequencies. When the sound was lateral, modulation loss in the ear facing the sound was large for low carrier frequencies whereas, in the opposite ear, the dependence of modulation loss on the carrier frequency was complex.

Conclusion

This study delineates acoustic conditions that the auditory system faces to localize ("where") and recognize ("what") sounds in two different reverberant environments.

515 Effect of Reverberation on Neural Coding of Sound Location (Where) and Pattern (What) in the Inferior Colliculus (IC)

Shigeyuki Kuwada¹, Brian Bishop¹, Duck Kim¹

¹Univ. Connecticut Health Center

Background

The major functions of the auditory system are to localize and recognize a sound. Traditionally, neural and behavioral studies have examined these two functions separately using artificial conditions that do not represent transformations created by the head and body and environmental reverberations at different sound distances. Furthermore, it is rare to find a study that examined the differences between binaural and monaural stimulation. The goal here is to study simultaneously neural coding of sound location and pattern to binaural and monaural stimulation in environments with different degrees of reverberation.

Methods

We measured binaural room impulse responses (BRIRs) in anechoic, moderately- (T60 = 0.91 s) and highly-reverberant (T60 = 2.3 s) environments with a sound source over a range of azimuths ($\pm 180^\circ$) and distances (10 -160 cm). Our sound source was an octave-band noise with center frequencies between 0.25 and 14 kHz that were sinusoidally amplitude modulated (2 - 512 Hz). We created virtual auditory space (VAS) stimuli by convolving these sound sources with the individual animal's BRIRs. We applied these VAS sounds while recording from neurons in the IC of the unanesthetized rabbit. The center of the noise band was based on the neuron's best frequency.

Results

In all three environments, we found 4 types of neurons: 1) those that code both azimuth and envelope, 2) those that code only azimuth, 3) those that code only envelope, 4) those that code neither. In all environments, to binaural stimulation, ~25% of the neurons coded only envelope, ~17% coded only azimuth. In anechoic ~55% coded both

azimuth and envelope whereas this decreased to ~32% in reverberation. Compared to binaural stimulation, the proportion of neurons that coded envelope to monaural stimulation decreased slightly whereas those that coded azimuth decreased substantially. In general, reverberation tended to degrade azimuth and envelope coding, especially at far distances. This degradation could be almost eliminated by decreasing the sound source distance. In contrast, some neurons were resistant to reverberation even at far distances. Such neurons showed high neural modulation gain.

Conclusion

The IC contains different types of neurons that code azimuth and envelope in combination or separately. The neurons that coded only azimuth or envelope may be the basis for the prominent specialization seen in the non-primary regions of the auditory cortex (Malhotra and Lomber, 2007). The mechanisms that underlie azimuth coding generally require binaural processing whereas the mechanisms that underlie envelope coding generally do not.

516 Investigating Adaptation in the Barn Owl with a Double-Stimulus Paradigm: A

Behavioral Approach

Lutz Kettler¹, Sandra Brill¹, Dana Zähringer¹, Hermann Wagner¹

¹RWTH Aachen University - Institute for Biology 2

Background

During hunting barn owls attend to sounds - as for example rustling generated by prey. The birds typically do not attack upon hearing the first sound, but wait for a second sound. This situation was mimicked with a double-stimulus paradigm.

Methods

It was tested behaviorally whether and how a first or reference sound influenced the head turning of the birds toward a second sound or probe. The inter-stimulus interval between reference and probe was varied between 100 ms and 3200 ms on a log₂ scale. Additionally, the owls were stimulated with single stimuli.

Results

Preliminary data collected with three adult barn owls indicate a reduction in precision of head-turning responses when two successive stimuli were presented compared with a situation where only a single sound was presented. Furthermore, head-turning latencies were increased in the double-stimulus condition. This indicated response adaptation. Latencies as well as head-turning precision returned to the level of the single-sound condition if the duration of the inter-stimulus interval was increased. The time constant of recovery from adaptation coarsely matched time constants that were determined in electrophysiological experiments.

Conclusion

Thus, a first stimulus rather lowers than facilitates the response to a second stimulus under the conditions examined.

517 Efficient Binaural Sound Localization Model for Mobile Agents in Reverberant Environments

Tom Goeckel¹, Hermann Wagner¹, Gerhard Lakemeyer¹

¹RWTH Aachen University

Background

Binaural sound source localization in home environments is encumbered in the presence of strong reverberations. Our goal was to develop an efficient real-time algorithm that improves the localization performance in echoic environments and is able to track sound sources through time and space. In our case, efficiency is required because of the limited processing power of mobile agents.

Methods

As localization cues we used a combination of interaural time differences (ITD) and level differences (ILD), which were analyzed for their reliability using interaural coherence (IC), or the normalized cross-correlation coefficients. A pair of ITD and ILD values is determined for each sample of the digital input signal in each frequency band, and subsumed in a probability density function (PDF) weighted with the corresponding IC values. To merge ITD cues across frequencies we used a summed average in combination with the frequency-specific reliability index. Peaks in the ILD PDFs are matched with our reference ILD values, and the related sound source directions are compared to the peaks in the ITD PDFs to find the most likely sound source locations. The results are integrated over time, to emphasize consistent sound sources and to take gaps in the signal into account.

Results

To evaluate the performance of our algorithm, tests with noise and speech signals in different echoic conditions, and with several degrees of background noise, have been performed. We could show a significant increase of localization accuracy in reverberant environments in comparison to algorithms purely relying on ITD and ILD values.

Conclusion

We combined several simple methods to extract sound source directions with the least possible computational costs and show that this algorithm is still able to extract usable localization information in reverberant, and other adverse acoustical conditions.

518 Rapid Recalibration of Auditory Distance Perception in Reverberant Environments

Lubos Hladek¹, Beata Tomoriova², Aaron Seitz³, Norbert Kopco¹

¹Safarik University, Kosice, Slovakia, ²Technical University of Kosice, ³University of California, Riverside

Background

Reverberation and the received sound level provide the most robust cues for auditory distance perception. Specifically, both the direct-to-reverberant energy ratio and the received level increase as the source-to-listener distance decreases. However, the relationship between reverberation, level, and distance varies from room to room. Thus, the auditory system must recalibrate in order to correctly map the cues to distance. Previous experiments showed that listeners are able to "learn" reverberation in a fixed room over the course of multiple hours and days [Kopco et al. (2004) "Learning to Judge Distance of Nearby Sounds in Reverberant and Anechoic Environments." Congress CFA/DAGA; Kopco et al. (2011). "Learning of reverberation cues for auditory distance perception," 161st ASA meeting].

Methods

Current experiments examined the process of rapid adaptation of distance judgments in a small reverberant room during a single 1-hour session. Each session consisted of 8 runs of 80 trials. Presentation level was either fixed during a run, resulting in natural variations in received level with the source distance, or roved by 12 dB for each trial in a run, eliminating the received level as a distance cue. The runs with fixed and roved level alternated during a session. Two groups of subjects participated, differing only by whether they started with a fixed-level or a roved-level run. No feedback was provided. Performance was evaluated in terms of correlation coefficients, means, and variance in responses. Only subjects whose performance was not correlated with presentation level during the roved-level trials were considered in the analysis.

Results

Results depended on whether the level cue was available during the initial run. Correlation coefficients improved over time only if the initial run was performed with roved level. Most of this improvement occurred immediately after the first run. In contrast, subjects who initially had both reverberation and level cues available did not improve over time, and their performance remained inferior compared to the initial-roved-level group throughout the whole session.

Conclusion

These results confirm that rapid recalibration processes occur in spatial perception when listeners enter a new acoustic environment, resulting in improved performance over time. However, the adaptation processes are not triggered automatically, and their occurrence might be conditioned on various factors. For example, distance recalibration occurs only if the level cue is unavailable

during the initial exposure to sounds in the new environment.

[Supported by NIH, the European Community, and VEGA]

519 Accommodating to New Ears: The Effects of Sensory and Sensory-Motor Training

Simon Carlile¹, Kapilesh Balachandar¹, Heather Kelly¹

¹University of Sydney

Background

The auditory system of adult listeners has been shown to re-calibrate to spectral cues altered using in-ear molds (Hofman et al.1998 NatNeuro 1:417-421). Molds initially degraded localization performance but significant improvement followed chronic exposure of 10-60 days (Carlile et al, 2007 ProclCA:221-218). While the functional plasticity of the mature auditory system is itself remarkable, individual differences in the extent and rate of accommodation suggest a number of factors driving accommodation. Prompted by work on cross-modal learning, we hypothesized that it would be possible to facilitate this process by providing multi-modal and sensory-motor feedback during accommodation.

Methods

Using head pointing, 15 subjects localized broadband noise bursts (150 ms) or monosyllabic words from 58 locations roughly equally distributed about an imaginary sphere in a darkened, anechoic environment (5 repeats - baseline). Silicone molds were then fitted, filling approximately 40% of the concha, and localization performance retested (3 repeats). Molds were worn for nearly all waking hours over a period of 10-11 days and performance was tested daily (except weekends) using broadband noise. Subjects were divided into three groups: (1) Control group received no feedback; (2) Visual feedback group: An LED collocated with the sound source, indicated location following each trial; (3) Audio-Visual Sensory-Motor (AVSM) feedback group: In addition to the LED, the sound source pulsed at a rate proportional to the localization error. Subjects were encouraged to explore the stimulus location to minimize localization error. On the final day of accommodation subjects localized broadband sound and speech stimuli (5 repeats each) with molds and without molds (post-accom).

Results

Performance was assessed using the spherical correlation (SC) between actual and perceived stimulus locations and front-back confusion (FBC) rate. Initial mold insertion produced a significant performance reduction. Following accommodation, the FBC rate reduced somewhat for the control group with little change in the SC. Significant improvements were seen for both parameters with both experimental groups, with the largest improvement in SC demonstrated by the AVSM group. Accommodation using the noise stimuli generalized to the speech stimuli.

Conclusion

In addition to the accommodation provided by chronic wear, relatively short periods of training involving sensory-motor feedback significantly improved performance that generalized across different stimuli. This has implications for adaptive training to altered auditory inputs.

520 Measuring Binaural Sensitivity in Normal Hearing Children Using Headphones

Erica Ehlers¹, Kristi Ward¹, Corey Stoelb¹, Alan Kan¹,

Ruth Litovsky¹

¹University of Wisconsin-Madison

Background

Motivated by the fact that children with bilateral cochlear implants (CI) show significantly worse sound localization skills than their normal hearing (NH) peers; we investigate whether this can be attributed to poor binaural sensitivity, or other factors. When locating sounds, NH listeners use interaural level differences (ILDs), and interaural time differences (ITDs) in the low-frequency fine structure and high frequency envelopes. The challenge when comparing NH and CI listeners is to use comparably degraded binaural cues. This study is the first to systematically test binaural sensitivity in NH children using CI simulations, and to demonstrate that binaural sensitivity is task-dependent.

Methods

Ten NH children (ages 8-10) participated in two experiments. In Experiment 1, intra-cranial lateralization was measured for three stimuli: (1) Spondaic words, (2) Transposed tones (4 kHz carrier modulated at 125 Hz), and (3) vocoder using 500 ms Gaussian-enveloped tone (GET) pulse train (4 kHz center frequency, 100 pulses per second). ITDs (0, ± 50 , ± 100 , ± 200 , ± 400 , and $\pm 800\mu s$) and ILDs (0, ± 1.5 , ± 3 , ± 6 , ± 9 , and $\pm 15dB$) were imposed on the stimuli and tested in separate blocks of trials. Prior to beginning Experiment 1, children were trained on the task for each set of stimuli. In Experiment 2, just noticeable differences (JNDs) were measured for the transposed tone and GET.

Results

When using binaurally degraded stimuli, preliminary results show children have JNDs ranging from ~ 10 -70 μs for ITDs, and ~ 0.5 -2 dB for ILDs. This is comparable to the range of JNDs found in adults. In contrast, on the lateralization task, children perform significantly worse than adults. Although children tend to use the same range of ITD and ILD values to indicated perceived stimulus location, their responses have greater variability across trials, suggesting either task difficulty or spatially ill-defined perception of sound images.

Conclusion

The novel finding in this study is that NH children showed binaural discrimination JNDs comparable to adults, suggesting that binaural sensitivity is mature by 8 years of age, even with degraded stimuli. However, the ability to utilize binaural cues for identifying perceived intracranial locations is immature in NH children. Because

lateralization is proving to be a more challenging task than discrimination, it may be a better task for assessing binaural maturity. This work offers a benchmark for future studies on binaural sensitivity in children with bilateral CIs.

Work funded by NIH-NIDCD(R01DC8365)and NIH-NICHD (P30HD03352)

521 Effects of Target and Masker Spatial Continuity on Speech Intelligibility

Nandini Iyer¹, Eric Thompson², Griffin Romigh¹, Douglas Brungart³, Brian Simpson¹

¹Air Force Research Laboratory, ²Ball Aerospace, ³Walter Reed National Military Medical Center

Background

In a digit recall task, listeners showed improvement for listening conditions in which a target talker remained stationary and the voice remained unchanged, relative to the case in which the target location and target voice were varied across successive digit presentations (Best et al., 2008). Moreover, recall improved with each successive digit in a sequence. This pattern of performance was attributed a listener's ability to establish, and refine, a spatial filter over time when continuous auditory stimulation occurred at the filter location. However, it was not clear if changing the spatial locations of the interfering talkers would have a similar impact performance as had been seen with the nonstationary target. The current experiment was designed to address the effect of changing masker and/or target location and pitch on a speech intelligibility task.

Methods

Eight listeners (19-26 years) participated in the experiment. On each trial, listeners seated in quiet rooms heard a target phrase that was created by concatenating 2, 3, 4 or 5 monosyllabic words (Kidd et al., 2008). Two same-sex interfering talkers, also comprising of the same number of monosyllabic words as the target talker, were presented along with the target phrase. The target and two interferers were presented at three of seven possible spatial locations using individualized head-related transfer functions. The spatial location and/or pitch of the target and masker phrases remained fixed or varied word-by-word, resulting in 10 unique listening conditions; all listening conditions remained fixed within a block of trials.

Results

As in Best et al., 2008, word intelligibility improved as a function of number of words contained in the target phrase when the target was stationary and fixed in pitch, and changing either target location or target voice counteracted those improvements. The decline in performance was observed even in conditions when the maskers were stationary and fixed in pitch, suggesting that listeners were unable to utilize masker information to improve performance in the task. And while changing the pitch of the masking talkers did not lead to any further decline in performance, there was a further decline in performance

when the maskers changed in spatial locations and varied in pitch.

Conclusion

Data from the current study mostly supports a Listener-Max strategy because performance improved over time when the target was fixed in location or voice. A simple weighted model accounted for the results obtained in the current experiment.

522 The Effects of Interaural Frequency Mismatch on Spatial Release from Masking

Corey Stoelb¹, Alan Kan¹, Matthew Goupell², Ruth Litovsky¹

¹University of Wisconsin - Madison, ²University of Maryland - College Park

Background

In normal hearing (NH), binaural benefits occur when frequency-matched inputs from the two ears arrive at the brainstem. Many profoundly deaf individuals receive bilateral cochlear implants (BiCIs) in an attempt to restore the benefits of binaural hearing, but their performance in noisy environments and ability to localize sound sources is still worse than that of NH individuals. This may be caused by mismatched frequency information between the ears, due to a difference in the insertion depths of the two electrode arrays. Previous studies in which binaural mismatch was deliberately introduced in NH listeners with band-limited acoustical pulse trains, or BiCI users with binaural electrical stimulation, resulted in degraded interaural time and level sensitivity. Without reliable localization cues, it is unlikely that these listeners would be able to make optimal use of the spatial separation from multiple sound sources. The aim of the present study was to investigate the effects of interaural frequency mismatch on speech understanding in a simulated noisy environment.

Methods

Fifteen NH listeners participated in this study. Subjects listened over headphones to five-word sentences spoken by a frontal female target, in the presence of two male maskers speaking IEEA sentences. Maskers were either collocated or 90° to the right of the target. Spatial separation was simulated by filtering stimuli through head-related transfer functions prior to vocoding with an eight-channel sine vocoder. Interaural frequency mismatch was introduced by changing the sine carriers. Listeners responded by identifying the five-word sentence from a closed set. Percent correct scores were calculated at four signal-to-noise ratios (SNRs) in the two spatial conditions and spatial release from masking (SRM) was calculated by subtracting the percent correct in the separated condition from the corresponding collocated condition.

Results

Percent correct scores decreased significantly with increasing mismatch and SRM increased with decreasing SNR. However, there was no interaction between SRM and mismatch.

Conclusion

Mismatch reduced speech understanding, but had little effect on SRM. This may be due to access to ILD information at mismatched conditions, which has been shown to be fairly robust to interaural mismatch. It is also possible that limited experience of NH listeners to vocoded speech may have rendered the effects of spatial cues less significant. In contrast, most BiCI users have a prolonged period of adaptation to electrical stimulation, whereby speech understanding improves, and interaural frequency mismatch might still be an important factor for SRM

523 Word Recognition Benefit from Attention Systems in Older Adults with Hearing Loss

Stefanie Kuchinsky¹, Kenneth Vaden¹, Stephanie Cute¹, Jayne Ahlstrom¹, Judy Dubno¹, Mark Eckert¹

¹Medical University of South Carolina

Background

Speech recognition in noise depends on the integrity of auditory and attention systems to adapt to adverse listening environments. The engagement of the cingulo-opercular error-monitoring system appears to support task performance (Dosenbach et al., 2007; Weissman et al., 2006) and predicts the likelihood of correct word recognition on trials following an error (Vaden et al., 2012). Because the engagement of error-monitoring (Harris et al., 2009) and cross-modal neural systems increases with age (Kuchinsky et al., 2012), we examined the extent to which activity in cingulo-opercular and visual cortices supports correct word recognition for older adults with hearing loss.

Methods

In a functional MRI study, 29 older adults (M =67 years; 9 male) with mild to moderately severe sloping sensorineural hearing loss (HL) listened to and repeated 120 consonant-vowel-consonant words presented in multi-talker babble (82 dB SPL) at +3 and +10 dB signal-to-noise ratios (SNRs). Sparse sampling allowed for word presentation and response between image acquisitions. The percent of phonemes correctly reported for each word was tallied. The degree of high and low frequency (HF, LF) HL for each participant was calculated based on weights derived from a normative sample (Eckert et al., 2012) and were independent for these participants.

Results

Elevated cingulo-opercular activity associated with incorrect responses predicted better performance on the next trial in the more challenging + 3 dB SNR condition (peak threshold $p < .01$ uncorrected, cluster extent $p < .05$ corrected). However, this benefit was reduced with increasing HFHL or LFHL. Whole-brain analyses revealed that visual cortex engagement following an error predicted better subsequent performance only for individuals with greater HFHL.

Conclusion

The results demonstrate that older adults engage the cingulo-opercular error-monitoring system, but its efficacy for adapting to error in challenging listening conditions is diminished with increasing hearing loss. For individuals with HFHL, visual cortex activity associated with making an error predicted subsequent correct word recognition, suggesting these individuals employ a cross-modal system to support word recognition. These findings highlight the importance of attention systems that support word recognition and suggest they may be used as biomarkers of hearing loss intervention outcomes.

Work supported by NIH.

524 Developmental Trends in Listening to Adult and Child Speech in the Presence of Another Talker

Stuart Rosen¹, Leila Ball¹

¹UCL Speech, Hearing & Phonetic Sciences

Background

An interesting and important question concerns the extent to which children and adults differ in their abilities to hear speech in the background of other sounds, and how children's abilities change as they develop. In this study we investigated the impact of child and adult interfering talkers on children's ability to focus on child and adult target talkers.

Methods

Target stimuli were of the form 'Show the dog where the [colour] [number] is' with the listener required to select the corresponding coloured number from an on-screen response grid. In the conditions with speech maskers, sentences were of the same form as the targets but with a different animal, colour and number. Speech Reception Thresholds (SRTs) were measured adaptively for four conditions: target child speech with masking adult speech, target adult speech with masking child speech, and the same two target speakers in the presence of speech-spectrum-shaped noise matched to the talker. Participants consisted of adults (17 to 51 years) and primary-school-aged children (6 to 11 years).

Results

On the whole, performance for children was very similar to that of adults, except when listening to adult targets in the presence of a child talker. Here, children performed significantly worse than adults, and also showed rapid improvement with age, approaching adult-like levels by age 11. SRTs in the other 3 conditions were close to those of the adults, and showed only small changes across age. The fact that children showed no significant difference in performance from adults for the two target talkers with noise masker suggests it is not the case that children simply find other children's voices more intelligible than those of adults.

Conclusion

Children, especially those of early school age, find it more difficult to understand an adult talker when the competing sound consists of a single child speaker than when they are listening to a child with an interfering adult talker. In our view, this happens because children are more likely to be distracted by speech from another child than from an adult, and is consistent with the protracted maturation of frontal lobe networks responsible for executive functions related to attention. Such a result has clear implications for listening in the classroom, and unusual distractibility to other children's voices may be a factor in determining if a child is suspected of auditory processing disorder (APD).

525 Preparatory and Selective Attention in Children During Multi-Talker Listening

Emma Holmes¹, Padraig Kitterick², A. Quentin Summerfield¹

¹University of York, UK, ²NIHR Nottingham Hearing Biomedical Research Unit

Background

When differences in the accuracy of multi-talker listening are found between groups of participants, it may be difficult to determine whether the difference results from impaired central attentional control or from a distorted input from the ear. The current project explored a technique for dissociating attentional from peripheral processes that is suitable for use with both adults and children. The technique is based on one established with normal-hearing adults by Hill and Miller (2010, *Cereb Cortex* 20: 583-590). On each trial, they presented three simultaneous talkers who differed in pitch and spatial location. Importantly, before the acoustic stimuli were presented, participants were cued visually to either the location or the pitch of one of the three talkers. Functional magnetic resonance imaging revealed distinct networks active in preparation for the acoustic stimuli and during the acoustic stimuli. Activity in both networks was influenced by whether participants were cued to the location or pitch of the target voice. Potentially, therefore, brain activity recorded before acoustic stimuli are presented could reveal deficiencies in the control of attention without being confounded by a distorted input from the periphery.

Methods

The current experiment employed a similar paradigm, but recorded the time-course of brain activity using 64-channel electroencephalography. Participants were 22 children 7-12 years of age and 16 young adults 18-27 years of age, all with normal hearing. On each trial, two simultaneous sentences spoken by different adult talkers (one male and one female) were presented from loudspeakers in two spatial locations (one left and one right of fixation). Participants were cued, in advance of the acoustic stimuli, to either the location (left/right) or the gender (male/female) of the target talker. The task was to report key words spoken by that talker.

Results

Event-related potentials (ERPs) differed between trials where participants were cued to the location compared to the gender of the target talker. Differences arose both during preparation for, and during the presentation of, the acoustic stimuli. Children and adults displayed similar ERPs during acoustic stimuli, but showed differences in the preparatory phase.

Conclusion

We conclude that the technique could be used to distinguish preparatory attention from the response to the acoustic input. Ultimately, this paradigm could further our understanding of the contribution of central and peripheral impairments to difficulties with multi-talker listening both in children and in adults.

Supported by the Goodricke Appeal Fund.

526 Auditory and Working Memory Training for Adults with Hearing Loss: Addressing Key Considerations of Outcome Measure Selection and Mechanisms of Benefit

Helen Henshaw^{1,2}, Melanie A. Ferguson^{1,3}, David R. Moore⁴

¹NIHR Nottingham Hearing Biomedical Research Unit, ²University of Nottingham, ³Nottingham University Hospitals NHS Trust, ⁴MRC Institute of Hearing Research

Background

For auditory training (AT) to be an effective intervention for people with hearing loss (PHL), any task-specific learning needs to transfer to functional benefits in real-world listening. This issue has been examined in two auditory training (AT) studies and an ongoing working memory (WM) training study.

Methods

(i) A randomised controlled trial (RCT) of 44 adults with mild sensorineural hearing loss (SNHL) examined the benefits of AT. Participants trained using a phonetic discrimination task in quiet. Measures of speech intelligibility, cognition and self-report of hearing disability were assessed for trained and control participants.

(ii) A repeated measures study identified optimal outcome measures to assess the benefits of AT in 33 hearing aid (HA) users with mild-moderate SNHL. Participants trained on a phonetic discrimination task in noise, thus increasing task difficulty and content validity. Complex measures of cognition (divided and sustained attention, WM and dual-task listening effort [LE]) were assessed pre and post-training. Functional listening benefit was examined using an adaptive two-competing-speaker task (CCRM).

Results

(i) Significant post-training improvements were shown for self-report of hearing, with the largest improvement for a challenging listening situation ($p < .05$). No improvements were shown for sentences in 8Hz modulated noise (SiMN). Significant improvements were shown for complex

measures of cognition (divided attention, $p < .01$ and WM, $p < .05$), with no improvements for control participants, nor for simple cognitive tasks.

(ii) Baseline CCRM scores correlated with self-report of hearing ($r = .49$, $p < .01$), divided attention ($r = .46$, $p < .05$), LE ($r = .57$, $p < .001$) and WM ($r = .59$, $p < .01$). This supports the contention that competing speech is a more cognitively demanding task than SiMN, which was significantly associated with hearing sensitivity only ($r = .39$, $p < .001$). Significant post-training improvements were shown for CCRM ($p < .05$) and LE ($p < .01$), with the largest improvements in challenging but achievable task conditions.

Conclusion

Findings suggest outcomes to assess the benefits of AT should be appropriately challenging, yet achievable. Furthermore, benefits of AT may share a greater association with the development of cognitive abilities than the refinement of sensory skills.

A third study directly trains cognition. A double-blind RCT aims to examine benefits of WM training in 54 HA users. Training is performed at an adaptive or a fixed practice-level (active-control). Findings will help inform the most effective training modality (auditory vs. cognitive) for PHL.

527 Decoding Auditory Attention (In Real Time) with EEG

Edmund Lalor¹, Nima Mesgarani², Siddharth Rajaram³, Adam O'Donovan⁴, James Wright⁵, Inyong Choi³, Jonathan Brumberg^{3,6}, Nai Ding⁷, Adrian KC Lee⁸, Nils Peters⁹, Sudarshan Ramenahalli¹⁰, Jeffrey Pompe¹⁰, Barbara Shinn-Cunningham³, Malcolm Slaney^{11,12}, Shihab Shamma⁷

¹Trinity College Dublin, ²University of California, San Francisco, ³Boston University, ⁴University of Maryland, ⁵University of Western Sydney, ⁶University of Kansas, ⁷University of Maryland, College Park, ⁸University of Washington, ⁹University of California, Berkeley, ¹⁰Johns Hopkins University, ¹¹Microsoft Research, ¹²Stanford CCRMA

Background

Both magnetoencephalography and electrocorticography recordings have been used to decode which of two competing sources a listener is attending. However, it is not clear whether these techniques might work with Electroencephalography (EEG), particularly in a real-time system. We therefore set out to decode a listener's attentional focus from EEG signals in real time, knowledge that could be incorporated into next-generation assistive listening devices.

Methods

Offline, we acquired EEG data when a subject listened to a single speech source, from which we estimated a mapping from the EEG data to the perceived speech. The subject then attended to one of two simultaneous speech streams, presented dichotically. The previously estimated system

transfer function from the single-source presentation was used to estimate the attended stream in real time. Whichever input speech stream more closely resembled the estimated input was deemed to be the attended stream.

Three decoding methods were tested. The first approach, canonical correlation analysis (CCA), is based on measuring the correlation between audio streams and the EEG signals. The second two approaches estimate the mapping from the EEG to the input stimulus. This can be done using a single channel at a time and summing the result, or by finding a single multi-channel filter that represents all the signals.

Results

We found the best results by estimating a multivariate linear filter that incorporates the channel covariance structure in the least-squares estimation of the impulse response, similar to the approach described by Mesgarani & Chang (2012). Using this approach we could estimate single-speaker data with high accuracy. Notably this approach yielded estimates of the speech envelope that were better correlated with the original speech ($r \sim 0.08$) than the other two methods. Applying this to the attention paradigm (after training on single-speaker data), we could predict the focus of attention with 95% accuracy for a one-minute-long sample of dichotic speech. As we shortened the amount of data used to decode, our accuracy fell almost linearly to about 65% for 10 seconds. Other presentation conditions (i.e., diotic and HRTF) were decoded with lower accuracy than dichotic.

Conclusion

EEG signals can be decoded in real time to determine what natural speech stream a listener is attending with relatively high accuracy.

528 The Effect of an Enhanced Acoustic Environment on Noise-Induced Tinnitus in Rats

Ross Mayerhoff¹, Gregory Kruper¹, Gulrez Mahmood¹, Jinsheng Zhang¹

¹Wayne State University School of Medicine

Background

Noise-induced tinnitus may result from maladaptive plasticity in the brain. Recent studies indicate that enhanced acoustic environments (EAE) can mitigate acoustic trauma-induced hearing loss and tonotopic map reorganization. We aimed to investigate whether an EAE suppresses tinnitus in a rat model.

Methods

Following intense tone exposure (10 kHz, 120 dB SPL, 3 hrs), 12 Sprague-Dawley rats were placed in an EAE consisting of tone pips of random frequency (0.625-20 kHz) and intensity (60-80 dB SPL) for approximately 16 hrs daily over a period of 18 weeks. Another 12 exposed rats were placed in a quiet sound attenuation booth and served as controls. Gap detection (GAP), prepulse inhibition (PPI)

acoustic startle reflex behavior, and auditory brainstem response (ABR) were tested on a weekly basis.

Results

Following intense tone exposure, GAP and PPI significantly worsened, indicating behavioral evidence of tinnitus and hearing loss. During the first four weeks, we found gradual improvement in both GAP and PPI data in rats with and without EAE treatments, indicating improved tinnitus. However, continued EAE treatment up to 18 weeks did not improve GAP and PPI results, which was in contrast to the improved GAP and PPI results found in rats without EAE treatment. In addition, the EAE treatment did not induce significant difference in the intense tone-induced ABR threshold shift compared to rats without EAE treatment.

Conclusion

The currently used EAE induced temporary rather than permanent improvement of behavioral evidence of tinnitus in rats. It remains to be investigated whether higher intensity EAE sounds at particular frequency bands will effectively ameliorate acoustic trauma-induced tinnitus.

529 Noise Induced Hearing Loss on Glutamatergic and GABAergic Gene Expression Changes in Rat Cochlear Nucleus

Senthilvelan Manohar¹, Brandon Decker¹, Dalian Ding¹, Richard Salvi¹

¹University at Buffalo

Background

Noise-induced damage to the inner ear reduces the neural activity flowing from auditory nerve into the cochlear nucleus. Paradoxically, this leads to a significant increase in spontaneous activity in cochlear nucleus (CN); one of the putative mechanisms for tinnitus. The biological mechanisms that lead to increased spontaneous hyperactivity are largely unknown, but arise from changes in glutamatergic or GABAergic neurotransmission.

Methods

To explore this hypothesis, we unilaterally exposed rats to an intense narrow band noise that caused significant cochlear damage and hearing loss to the exposed ear, but no damage to opposite. Hearing loss was confirmed by auditory brainstem response measurements obtained 14 and 28 days post-exposure. The CN on the exposed and unexposed side of the brainstem were harvested separately at 14 or 28 days post-exposure for qRT-PCR analysis of 84 genes related to glutamatergic and GABAergic neurotransmission.

Results

Unexpectedly, three genes (Gabrg1, Grik4 and Slc17a8) from CN on the unexposed side were significantly up-regulated at 14 days post-exposure. In contrast, two genes (Slc17a6 and Gabrg3) were significantly up-regulated in the CN on the exposed side at 28 days post-exposure. Slc17a6 codes for vesicular glutamate transporter 2 (Vglut2) which is involved in non-auditory

glutamatergic synaptic transmission, results consistent with recent work showing increased somatosensory inputs to the CN following cochlear damage. Surprisingly, the CN on the unexposed side showed up-regulation of Slc17a8 which codes for vesicular glutamate transporter 3 (Vglut3), results consistent with recent studies significant changes in Vglut3 in the CN following deafening. Gabrg3, which codes for a subunit of the GABA_A receptor gamma 3, also increased in the exposed CN suggesting changes in GABA-mediated inhibition.

Conclusion

Slc17a6 (Vglut2) mRNA expression increased in the ipsilateral CN; this increase may be linked to the invasion of axons from trigeminal nerve. Increased expression of Gabrg3 suggests a compensatory increase of inhibitory, may be occurring to counteract the increases in spontaneous hyperactivity occurring in the CN following cochlear damage.

Acknowledgement: Research supported in part by grants from NIH (R01DC009091 and R01DC009219) and ONR (N000141210731)

530 Cholinergic Modulation of Tinnitus Related Hyperactivity in the Dorsal Cochlear Nucleus

Nauman Manzoor¹, James Kaltenbach¹

¹Department of Neurosciences, Lerner Research Institute/Head and Neck Institute, Cleveland Clinic.

Background

Increased spontaneous firing rate (hyperactivity) is observed in various auditory structures in animal models of noise-induced tinnitus. We have previously shown hyperactivity in the DCN (dorsal cochlear nucleus) which undergoes plastic changes and is prominent at frequency loci higher than the frequency of the exposure tone. Previous work has shown that spontaneous firing rate (SFR) in the DCN can be modulated by cholinergic agonists (Chen et al. 1998; Kaltenbach and Zhang 2007). There is also ultra structural evidence of plasticity of the descending cholinergic system after cochlear lesion (Meidinger et al. 2006) which is supported by increased ChAT (choline acetyltransferase) expression in the cochlear nucleus (Jin et al. 2006). In the present study, we sought to examine the functional significance of plasticity of descending cholinergic system in the DCN following noise trauma.

Methods

Adult Syrian golden hamsters were divided in 2 groups, a control group that was not exposed to sound and a sound exposed group (10 kHz, 115 dB SPL for 4 hours). Multi-unit SFR was recorded from the fusiform cell layer (150-250 μm deep from surface) using micropipette electrodes. Effects of the cholinergic agonist carbachol were studied by direct application on the DCN surface. ACSF (artificial cerebrospinal fluid) acted as an internal control and was applied before carbachol application at every recording locus. Long term plots of SFR versus time were obtained

from each locus during ACSF and carbachol application respectively. The effect of carbachol on SFR was quantified as mean rate change (mean SFR during carbachol- mean SFR during ACSF / mean SFR during ACSF).

Results

In controls, carbachol had a powerful excitatory effect on SFR at both high (10 and >10 kHz) and low (<10 kHz) frequency loci. This excitatory effect was abolished by atropine. In contrast, carbachol had only a modest effect on thresholds at characteristic frequency in control animals. In exposed animals (short -2-3 weeks and long -6-7 weeks recovery), carbachol had a slight excitatory effect in the low frequency region (short recovery only), but a powerful suppressive effect was observed in the high frequency region. This suppressive effect was blocked by atropine.

Conclusion

Our findings reveal that activation of the cholinergic system can suppress SFR in the high frequency region of the DCN of sound exposed animals. Activation of the granule cell - parallel fiber - cartwheel cell pathway may be a possible route through which the suppressive effect is mediated.

531 Auditory Brain Stem Responses After Noise Damage Predict Tinnitus

Seth Koehler¹, Malav Parikh², Susan Shore¹

¹University of Michigan, ²Wayne State University

Background

Tinnitus is the phantom perception of a ringing sound in the absence of external auditory stimuli. While startle based gap-detection testing is an objective, behavioral method developed to determine the presence and quality of tinnitus in animal models, objective physiological testing methods are needed to evaluate tinnitus. Following temporary threshold shifts in the auditory brainstem response (ABR) induced by over-exposure to a narrowband noise, guinea pigs show diminished gap-induced reduction of startle response suggesting the development of tinnitus. After recovery of ABR thresholds, there is mounting evidence for loss of auditory nerve drive and compensatory central plasticity, reflected in changes in ABR peak amplitudes and latencies. Here, we extend these studies to provide input-output functions for both left and right ears immediately and several weeks after noise exposure.

Methods

Gap detection and ABRs were recorded in 17 guinea pigs. Nine were unilaterally exposed to a 97 dB, ¼ octave noise band centered at 7 kHz for two hours and eight were sham exposed under Ketamine and Xylazine. Tone-evoked ABRs at frequencies at and outside the exposure band were recorded at baseline, immediately and one week after each noise-exposure procedure, and several weeks after the 2nd noise exposure. Gap detection was assessed biweekly. ABRs were grouped by exposure and evidence for tinnitus.

Results

Five of eight noise-exposed guinea pigs showed impaired gap detection indicative of tinnitus in at least one frequency band. ABR thresholds were elevated near the exposure frequency band immediately after the each noise exposure but recovered to normal within 1 week. In the exposed ear, one week after the noise exposure, P1 amplitudes were reduced but later peak amplitudes were maintained or enhanced. By the final ABR measurement (6-8 weeks after exposure), P1 amplitudes in the exposed ear remained suppressed while P3 and P4 amplitudes were significantly enhanced, more so in animals showing evidence of tinnitus. In the unexposed ear, P3 and P4 were suppressed in animals without evidence of tinnitus but enhanced in animals with evidence of tinnitus.

Conclusion

Reduced P1, but enhanced P3 and P4 ABR amplitudes, correlate with behavioral evidence of tinnitus revealing compensatory changes in central pathways, likely from the VCN, that may play a role in tinnitus. Parallel changes in ABR and gap-detection responses over time suggest the potential of the ABR as an objective physiological measure of tinnitus.

Supported by NIH RO1-DC004825 and P30-DC05188.

532 Acute Tinnitus Perception Is Characterized by Altered Oscillatory Activity in Rat Auditory Cortex

Daniel Stolzberg¹, Sarah H Hayes¹, Nina Kashanian¹, Richard J Salvi¹, Brian L Allman²

¹Center for Hearing & Deafness, University at Buffalo, SUNY, ²Dept. Anatomy and Cell Biology, Schulich School of Medicine, University of Western Ontario

Background

Subjective tinnitus is characterized by the perception of a sound without an acoustic source. Magnetoencephalographic studies comparing people with and without tinnitus have identified specific changes in the spectrum of ongoing activity in auditory cortex. The vast majority of investigations into neurophysiological mechanisms underlying tinnitus-related activity in animals have been carried out in anesthetized preps which abolish perception or in passive animals without confirmation of tinnitus perception and without control for attention. In order to investigate the neural correlates of tinnitus perception in individual attending rats, we developed a novel two-alternative forced choice appetitive behavioral paradigm optimized for the simultaneous recording of neural activity.

Methods

A two-alternative forced choice task was developed to minimize head movement within the acoustic field while permitting several seconds of neural activity to be sampled. Briefly, Sprague-Dawley rats self-initiated a trial by nose-poking in a center hole and waiting between 4 and 8 seconds for a bright light serving as a GO cue. Rats

were trained to respond to a right or left feeder depending on the background sound played from an overhead speaker. Correct feeder choices were reinforced with a food pellet: left for steady narrow-band noises (NBN, 1/8th octave bandwidth) of randomized center frequency, right for amplitude modulated broadband noise (modulated 100% at 5 Hz) or Quiet (speaker off). Microwire electrode arrays were implanted in auditory cortex of trained rats. Neural activity was recorded during the behavior on testing days and filtered offline for local field potentials which were subjected to a multi-tapered spectral analysis. Differences between conditions were evaluated using a Jackknife estimated test statistic.

Results

Following salicylate (200 mg/kg IP), but not saline control, rats changed feeders only on Quiet trials indicating a steady phantom sound was present. During tinnitus, significant changes in oscillatory activity were measured as a decrease in alpha (10 – 14 Hz) and an increase in gamma (40 – 55 Hz) bands.

Conclusion

Changes observed in alpha and gamma bands following salicylate corroborate results from several studies of tinnitus perception in humans. Furthermore, oscillatory activity present during NBN but not Quiet trials indicate that aberrant oscillatory activity during tinnitus perception may not be equivalent to true sound perception and that acute tinnitus perception may be generated cortically. We hope to extend this approach to better characterize the neural mechanisms of phantom sound perception in the brain.

533 Biofeedback as a Potential Prophylactic Treatment for Blast-Induced Tinnitus

Gregory Mlynarczyk¹, Diana Peterson¹
¹Iowa State University

Background

The American Tinnitus Association has estimated that over 50 million Americans experience tinnitus. Currently the only known effective treatment is the use of biofeedback techniques. Because tinnitus is thought to be perpetuated via a hyper-excitation of the amygdalo-auditory cortex circuits, biofeedback therapy may act to increase GABAergic inhibition of these circuits.

Previous experiments in our laboratory have shown that GABAergic neurons are disproportionately damaged during blast-exposure. We hypothesize that flooding the amygdalo-auditory cortex circuit with GABA prior to the blast trauma may decrease the excitation in these circuits and increase the threshold of activity necessary for tinnitus formation.

Methods

To test our hypothesis, animals were tested for tinnitus using acoustic startle responses (i.e., startle, pre-pulse, and gap detection tests). They were then exposed to blast sounds (90 dB SPL; 1 hour/day). During this sound exposure, animals became accustomed to the sounds and

started to sleep during the exposures. After 2 weeks of sound exposure, animals were exposed to a 20 psi blast pressure wave, and then subsequently tested for tinnitus twice per week post-blast-exposure. The incidence of tinnitus was then compared in the sound-exposed group of animals versus blasted non-sound-exposed animals.

Results

The incidence of tinnitus with sound-exposure (i.e., biofeedback treatment) was substantially decreased when compared to similar animals that did not receive the biofeedback treatment.

Conclusion

We hypothesize that biofeedback therapy may be a simple and cost-effective prophylactic treatment for individuals that are at risk for blast-exposure.

534 Functional Changes in Amygdala and Striatum in Rats with Noise-Induced Hearing Loss

Guang-Di Chen¹, Brandon Decker¹, Wei Sun¹,
Senthilvelan Manohar¹, Richard Salvi¹
¹SUNY at Buffalo

Background

Most studies of noise-induced hearing loss (NIHL) have focused on functional and structural changes within the classical auditory pathway. However, other regions outside the classical auditory pathway may also respond to acoustic stimulation, for example the striatum which is involved in vocal motor control and the amygdala which play a role in auditory fear conditioning and can modulate the acoustic startle reflex. To determine how acoustic overstimulation affected these non-classical auditory regions, we measured neural firing patterns in the lateral amygdala (LA) and the overlying striatum area of rat after inducing a high-frequency NIHL.

Methods

Rats were exposed to a narrowband noise (16-20 kHz) at 102 dB SPL. Afterwards, auditory brainstem response (ABR) was measured to determine the degree of NIHL. Multiunit recordings were obtained from the LA and striatum using 16 channel electrodes. Then, the cochleograms were prepared to characterize the location and degree of IHC and OHC loss.

Results

The noise exposure resulted in ABR threshold shifts of 30-40 dB at the high frequencies. This was associated with varying amounts of IHC and OHC loss in the basal turn of the cochlea. Neural thresholds in the LA and striatum of the noise-exposed rats were normal at low frequencies, but elevated at the high frequencies, consistent with the ABR data and cochlear lesions. In 2 of the 4 noise-exposed rats, neural responses to suprathreshold stimuli decreased with increasing frequency, i.e., high frequency hypoactivity. However, in the other 2 rats, suprathreshold neuronal responses in the LA, but not the striatum, were hyperactive (enhanced) at the low-frequencies bordering

the hearing loss region and hypoactive at the high frequencies within the NIHL. The 2 rats with edge-frequency hyperactivity had fewer missing OHC than those with strictly high-frequency hypoactivity.

Conclusion

The frequency-dependent loss of auditory sensitivity in the amygdala and striatum following noise exposure was consistent with the ABR threshold shifts and cochlear lesion. In some noise exposed rats, neural responses in the LA were hyperactive at the transition from normal hearing to impaired hearing region; the hyperactivity at the transition region appears to be related to the survival of OHCs at the edge of the cochlear lesion. In a broader context, the hypoactivity seen in the striatum would likely impair vocal motor control whereas the hyperactivity seen in the amygdala might be related to hyperacusis or emotional reaction to sound.

535 Corticosterone Increases Significantly During Salicylate Induced Tinnitus

Brandon Decker¹, Senthilvelan Manohar¹, Adam Sheppard¹, Richard Salvi¹

¹University at Buffalo

Background

Previous reports suggest that the onset or increase in tinnitus in patients with hearing loss is often associated with periods of high stress. Since high levels of stress could conceivably play a critical role in the development of tinnitus, we hypothesized that the onset of tinnitus might be linked to an increase in the circulating stress hormones. To test this hypothesis, we treated rats with a high dose of sodium salicylate, an extremely reliable method for inducing tinnitus.

Methods

Male Sprague-Dawley rats were treated with saline or 50, 150 or 250 mg /kg of sodium salicylate. Blood was sampled at 48 h before and 2, 24 and 48 h post-salicylate. Blood serum corticosterone levels were measured using a competitive ELISA assay kit. Corticosterone measurements were obtained from both anesthetized and un-anesthetized animals treated with salicylate.

Results

The 250 mg/kg dose of salicylate produced a massive increase in corticosterone levels at 2 h post-salicylate (614 ng/ml serum) compared to saline controls (25 ng/ml serum). Corticosterone levels decreased as the salicylate dose was lowered. The 50 mg/kg dose had no effect on corticosterone levels whereas the 150 mg/kg dose produced a modest increase in corticosterone. Corticosterone levels were highest 2 h post-treatment and then gradually declined over the next 24-48 h. Corticosterone levels increased in both anesthetized and un-anesthetized animals; however the increases were substantially less in anesthetized animals.

Conclusion

High doses of salicylate increased corticosterone levels in a dose and time dependent manner. The 50 mg/kg salicylate dose, which does not induce tinnitus, did not increase corticosterone levels whereas the 150 mg/kg salicylate dose, the lowest dose that induces tinnitus, produced a modest increase in corticosterone. The decrease in corticosterone levels following the 250 mg/kg salicylate dose decreased over time but was still elevated in some rats at 48 h post-treatment. Thus, the recovery of corticosterone levels over time parallels the behavioral recovery of tinnitus. These results are consistent with the hypothesis that the stress response induced by high doses of salicylate contributes to the induction of tinnitus.

Acknowledgement: Research supported in part by grants from NIH (R01DC009091; and R01DC009219) and ONR (N000141210731)

536 Histological Analysis of Vestibular Organs in Caspase 3 Deficient Mice

Mckay Moline¹, Rebecca Cook¹, Tomoko Makishima¹

¹University of Texas Medical Branch

Background

Caspase 3 deficient (Casp3 KO) mice exhibit circling behavior suggestive of vestibular dysfunction. In previous studies we have shown that Casp3 KO mice have absent horizontal vestibulo-ocular responses (angular acceleration), but have normal otolith-ocular responses (linear acceleration). Our goal was to identify histological characteristics which correlate with the behavioral functional analysis results, in order to determine the mechanism of the vestibular dysfunction in these mice.

Methods

Whole mount vestibular organs of Casp3 KO, Casp3 heterozygous and WT mice, were labeled with hair cell markers (phalloidin, calretinin) and observed at different ages. Younger (0-6 months) and older (7-24 months) age groups were compared. The following metrics were measured in the anterior-, lateral-, posterior ampullae, utricle and saccule: hair cell number, sensory epithelia area, hair cell density, striolar/extrastriolar hair cell density. Two-tailed t-tests and analyses of variance were used for statistical analysis.

Results

In younger ages, the vestibular organs were smaller in Casp3 KO mice, especially in the anterior- and lateral ampullae and utricle ($p < 0.05$), while those of heterozygous and WT mice were normal in size and shape. In Casp3 KO mice, hypomorphisms in the vestibular organs varied in degree, ranging from unilateral, bilateral or normal. Occasionally the anterior-, and lateral ampullae were found to be fused together, or the utricle in narrower shape.

In older ages, we observed fewer hair cells in all vestibular organs and in all genotypes ($p < 0.05$). The most striking observation was that in older Casp3 KO mice (>6 months), the saccular hair cells were almost completely degenerated, while heterozygotes and WT type mice did

not have hair cell loss even in older ages. On the other hand, there was no significant hair cell loss in the utricle of older Casp3 KO mice ($p>0.05$).

Younger heterozygotes had higher hair cell count and density in all organs, but both decreased significantly with age. Heterozygote utricles and saccules both increased in size with age.

There was a trend that hair cell loss occurred mainly in the striolar area rather than the extrastriolar area in all genotypes.

Conclusion

In Casp3 KO mice, the hypomorphic shape and fewer hair cell numbers of the lateral ampulla correlate well with the hypofunctional horizontal VOR. The complete loss of saccular hair cells in Casp3 KO mice may be used as a unique model to differentiate individual otolith organ function.

537 Distributions of the cVEMPs Along the Sternocleidomastoid Muscles During Neck Rotation and Flexion in Normal Human Subjects

Subjects

Alex Ashford¹, Wei Wei¹, William Mustain¹, Hong Zhu¹, Thomas Eby¹, Wu Zhou^{1,2}

¹Department of Otolaryngology and Communicative Sciences, University of Mississippi Medical Center, ²Depts Neurology, Neurobiology and Anatomical Science, University of Mississippi Medical Center

Background

Tone burst-evoked myogenic potentials recorded from the sternocleidomastoid (SCM) muscle (cervical VEMP or cVEMP) are commonly used clinically to assess the vestibular function. The SCM is not only one of the largest muscles in the neck, running from the sternum and clavicle to the mastoid and occipital bone, but also has multiple functions. When the pair of SCMs contract together, the neck is flexed and the chin is led downward. When a single SCM acts alone, the head is rotated to the opposite side. The cVEMP is commonly recorded at the upper third of the SCM during head rotation or neck flexion. In a previous study, we examined the distributions of cVEMPs along the SCM during head rotation. In the present study, we further compared the cVEMP distributions along the SCM during neck rotation and flexion.

Methods

Surface electrodes overlying the SCM muscles were used to record cVEMPs in 12 healthy adult subjects evoked by tone bursts delivered to the ipsilateral or the contralateral ear (tone burst, 8ms plateau, 1ms rise/fall, 130 dB SPL, 50-4000Hz). Tonic contractions of the SCMs were achieved by turning the head to the right or flexing the head downward.

Results

Preliminary analysis revealed that cVEMPs exhibited differences in amplitude, latency and morphology during neck rotation and flexion. The differences were tone frequency-dependent.

Conclusion

Neck rotation and flexion recruit different innervations patterns along the SCM, which may influence the cVEMPs recorded at different sites along the SCM. Future studies are to characterize these responses and explore their clinical implications.

538 The Neural Basis of Clinical Vestibular Responses to Bone Conducted Vibration (BCV) and Air-Conducted Sound (ACS)

Ian Curthoys¹, Vedran Vulovic¹, Ljiljana Sokolic¹, Jacob Pogson¹, Mike Robins¹, Ann Burgess¹

¹University of Sydney

Background

New clinical tests of human otolithic function use 500Hz BCV and ACS stimuli and measure vestibular evoked myogenic potentials from surface EMG electrodes beneath the eyes (oVEMPs) or over neck muscles (cVEMPs). A different clinical indicator uses intense 50Hz or 100Hz vibration of the mastoid to induce vibration induced nystagmus (VIN) in patients with unilateral vestibular loss. This study asked are some utricular and saccular afferents activated by both 500Hz BCV and ACS? do these stimuli activate semicircular canal neurons? Is 100Hz BCV also specific for otolithic afferents or are semicircular canal afferents also activated by intense low frequency vibration?

Methods

Single primary vestibular neurons were recorded extracellularly in guinea pigs anesthetized with Ketamine and Xylazine or rats anesthetized with pentobarbital. The neurons were identified by their location and their response to angular and linear accelerations. BCV stimulation was delivered either by a Radioear B-71 bone oscillator cemented to the skull or a Bruel and Kjaer 4810 Minishaker held against the stereotaxic frame. ACS stimulation of up to 140dB SPL was delivered by a TDH-49 headphone. Juxtacellular neurobiotin injections were used to identify whether the receptors synapsing on the recorded afferent, originated from the otoliths.

Results

Many otolithic irregular neurons were activated at low threshold by 500Hz BCV. Many of these were also activated by high intensity 500Hz ACS. Neurobiotin labelling showed that in both guinea pigs and rats these afferents originated from the utricular macula and also from the saccular macula, usually from presumed Type I receptors at the region of the striola. Semicircular canal neurons were not activated by 500Hz BCV or ACS up to the maximum intensity we delivered. At 100Hz otolithic afferents were strongly activated and synchronized with the stimulus, but with 100Hz high intensity vibration stimulation, irregular semicircular canal neurons and even some regular canal afferents were activated and synchronized to the stimulus.

Conclusion

The wide presumption in clinical vestibular testing - that ACS only activates saccular afferents in the inferior vestibular nerve - is not correct: these results show that 500Hz BCV and ACS selectively activate otolithic but not canal neurons. So 500Hz BCV and ACS are effective specific otolithic stimuli for testing oVEMPs and cVEMPs. However at low frequency this specificity is lost; high intensity 100Hz BCV activates **both** otolithic and semicircular canal neurons. The activation of these canal neurons is likely mainly responsible for vibration induced nystagmus in human patients.

539 Updating Alexander's Law and the Oculomotor Neural Integrator

Stefan Hegemann¹, Elham Khojasteh¹, Christopher Bockisch¹

¹Zurich University Hospital

Background

Alexander's law (AL) states that the nystagmus slow phase velocity in patients with peripheral vestibular lesions is lower when looking in the slow compared to the fast phase direction. It has been hypothesized to arise either due to adaptive changes in the velocity-to-position neural integrator (NI), or as a consequence of processing of the vestibulo-ocular reflex. It has also been reported to develop with a latency of 20-30 s after start of nystagmus, and proposed that only an abnormal stimulus evokes AL.

Methods

We tested AL in healthy volunteers during unilateral warm and cold caloric stimulation, as well as simultaneous bilateral bithermal stimulation. The latter condition simulates the normal push-pull stimulation of natural head movements. We also tested subjects during long duration, constant angular acceleration, which produced constant nystagmus for > 35 seconds, in order to stimulate the vestibular system with real head rotations.

Results

All caloric stimuli evoked AL, although in < 10% it was inverted. On average, the development of AL did not lag nystagmus. During constant acceleration, i.e. an almost natural stimulus, all volunteers developed a strong and stable AL, corresponding to integrator time constants of < 3 seconds which are much less than normal time constants (~25 seconds) and similar to those observed in patients with acute unilateral vestibular lesions showing AL. Alexander's law also developed, on average, in less than 10 seconds.

Conclusion

We conclude from these experiments, that AL is not an adaptive reaction and that it occurs immediately with natural vestibular stimulation. We propose a model of processing of vestibular and eye position signals in the vestibular nuclei, that explains the immediate start of AL.

540 Functional Dissection of the Neural Circuitry Responsible for the Vestibuloocular Reflex in Larval Zebrafish

David Schoppik¹, Isaac Bianco¹, Leung-Hang Ma², Drew Robson¹, Jennifer Li¹, Florian Engert¹, Robert Baker², Alexander Schier¹

¹Harvard University, ²NYU School of Medicine

Background

We have combined a systems-level behavioral characterization with molecular neuroscience to identify and characterize the neural circuitry underlying the vestibuloocular reflex (VOR) in the larval zebrafish. Young zebrafish develop excellent compensatory ocular rotations following body tilts over the first week of life, after which the larval zebrafish can reach mammalian levels of performance. This behavior is mediated by the utricle only, as the semicircular canals are not yet functional. We have shown that a classic three neuron circuit (primary vestibular afferents, central processing neurons, and ocular motoneurons) is necessary for gaze stabilization following body rotations.

Methods

We developed a novel transgenic line which expresses in vestibular afferent neurons and second-order central neurons. We used this line to perform laser ablations, optogenetic excitation, single-cell fills, and electrophysiology to characterize the role these neurons play during the VOR.

Results

By targeted photoablation, we found that the neurons in this line are necessary for the VOR. Using optogenetics, we can elicit stereotyped eye movements comparable to those observed during body rotation, suggesting sufficiency. To understand how these neurons function as a population, we sought to identify subgroups of neurons likely to subserve specific aspects of the VOR. We build a model of the larval zebrafish VOR circuit, using previous insights from mammalian preparations, and known projection patterns in teleost fish. Our model predicts anatomically distinct classes of second-order central vestibular neurons. We labelled individual neurons in our transgenic line, traced their morphology, and showed that the predicted classes of neurons are indeed present. We are currently using ablation and activation to test the functional role of these specific subpopulations. Finally, we report on the basic electrical properties of central vestibular neurons, identifying both mature and immature classes.

Conclusion

Our transgenic line of fish offers molecular-level control over the population of neurons responsible for a dynamic sensorimotor transformation. The anatomical and electrophysiological properties of labelled neurons are compatible with a simple model using stereotyped wiring to link the sensation of gravity to muscle activation to stabilize gaze.

541 Magnetic Field-Induced Eye Movements in Mice

Bryan K Ward¹, Dale C Roberts¹, Lani Swarouth¹, John P Carey¹, Charles C Della Santina¹

¹Johns Hopkins School of Medicine

Background

Roberts et al. demonstrated that static magnetic fields induce nystagmus in humans by peripheral vestibular stimulation and that this effect may be mediated by a magnetohydrodynamic force (1). This hypothesis can be tested by changing head orientation within static magnetic fields, but MRI magnet bore dimensions limit the ability to do this with humans. A mouse model would allow greater flexibility in assessing multiple head orientations. The aim of this study was to demonstrate magnetic field-induced nystagmus in mice.

Methods

Wild-type C57BL/6J mice were exposed to a 4.7T Earth-horizontal magnetic field. Prior to exposure, the mouse's head was secured to a non-ferromagnetic post and positioned so the horizontal semicircular canals were earth-horizontal. Monocular eye movements of the mouse's right eye were recorded via video-oculography in darkness with infrared illumination. Mice were positioned in the center of the magnet bore for at least 1 minute in each of several head orientations. Slow-phase nystagmus velocity (SPV) was calculated and an exponential decay was fit to the peak SPV over time.

Results

When placed in the bore nose-first, all mice demonstrated robust left-beating nystagmus lasting approximately 20 seconds on first entry. Mean peak SPV of six mice was 282°/s and the time constant was 3.62 s (SD 0.39) over the initial interval within the bore. Beats of nystagmus direction reversal were seen on a few trials after exiting the bore. When placed in the bore tail-first, nystagmus direction reversed from the nose-first orientation. When placed in the bore left-ear-first or right-ear-first, few eye movements were observed.

Conclusion

Mice exposed to high-strength magnetic fields demonstrate robust magnetic field-induced nystagmus that depends on magnetic field orientation. These findings support the hypothesis that static magnetic fields induce peripheral vestibular stimulation through a Lorentz force created by resting ionic currents within the labyrinth. The peak SPV and decay are both faster than in human subjects and may reflect poor velocity storage and relatively weak velocity-to-position integrator in the mouse.

1. Roberts DC, Marcelli V, Gillen JSet al. MRI Magnetic Field Stimulates Rotational Sensors of the Brain. *Curr Biol* 2011.

542 Glycine Receptor Deficiency and Its Effect on the Vestibulo-Ocular Reflex: A Study on the SPD1J Mouse

Patrick Huebner^{1,2}, Rebecca Lim³, Alan Brichta³, Americo Migliaccio^{1,2}

¹Neuroscience Research Australia, Sydney, Australia,

²University of New South Wales, Sydney, Australia, ³The University of Newcastle, Callaghan, Australia

Background

Our recent study in three strains of mice with naturally occurring glycine receptor (GlyR) mutations identified a difference in MVN neuronal action potential (AP) and discharge properties. When compared to wildtype mice, this difference in spastic, spasmodic, and oscillator mice manifested itself as a reduction in background discharge rates, larger AP after-hyperpolarizations (AHP), and lower sensitivity to current steps. We hypothesized that these differences, particularly the reduced excitability of MVN neurons in mutant strains, would impair the slow-phase VOR response. In addition, because glycine is also used by the omnipause neurons (OPN) of the saccadic and quick-phase system we predicted that the quick-phase amplitudes and peak velocities would be altered.

Methods

To study the effects of GlyR deficiency we tested the three dimensional angular vestibulo-ocular reflex (3D VOR) of homozygous (affected) and heterozygous (control) spasmodic mice (13-15 weeks). Slow-phase and quick-phase velocity of the VOR response was analysed for sinusoidal head rotations between 0.1 to 12 Hz reaching peak-velocities of 20, 50 or 100 °/s and for transient acceleration steps of 3000 or 6000 °/s² reaching a velocity plateau of 150 °/s (for 3000 °/s²), 300 and 600 °/s (for 6000 °/s²).

Results

The slow-phase VOR of affected mice was significantly lower during the constant velocity plateau of the transient acceleration step stimuli and at low-frequency (0.1 – 0.5 Hz) high-velocity (100 °/s) sinusoidal stimuli. Compared to control mice, quick-phases in affected mice were reduced in number (30 – 70 % less per cycle, depending on stimulus) and had considerably smaller peak-velocities (38% ± 5% less) and amplitudes (55 ± 5% less).

Conclusion

Glycinergic transmission deficiency in homozygous spasmodic mice predominantly affects the quick-phase system of the VOR. Our results support the notion that glycinergic OPNs in the saccadic/quick-phase system act as a regulator of quick-phase gain rather than as a gate for quick-phases.

543 Partial Restoration of the VOR in Humans by Motion-Modulated Electrical Stimulation of the Vestibular System

Angelica Perez Fornos¹, Nils Guinand¹, Marco Pelizzone¹, Jean-Philippe Guyot¹
¹Geneva University Hospitals

Background

Patients with a bilateral vestibular loss (BVL) suffer from imbalance and oscillopsia. Currently there is no treatment. We explored whether the vestibulo-ocular reflex (VOR) can be artificially restored in BVL patients using motion-modulated electrical stimulation of the vestibular system.

Methods

A unilaterally deaf BVL subject (male, 50 years old) was fitted with a modified cochlear implant (Med-EL®; Innsbruck, Austria) providing an extracochlear “vestibular” electrode positioned in the vicinity of the posterior ampullary nerve. After adaptation to steady-state suprathreshold electrical stimulation, motion sensors were fixed on the subject’s head and used to modulate stimulation currents delivered to the “vestibular” electrode. Eye movements were recorded with a video-oculography system incorporating 6 DOF head motion sensors (EyeSeeCam VOG; Munich, Germany) during whole body rotations about an earth-vertical axis (sinusoidal, 1Hz, 30°/s peak velocity).

The VOR response was tested in two conditions: a) without any electrical stimulation (**SYSTEM OFF**), and b) with motion-modulated electrical stimulation of the vestibular pathways (**SYSTEM ON**). Electrical stimuli consisted in charge-balanced biphasic current pulse trains (200µs/phase at 400 pulses-per-second), amplitude modulated via the yaw signal captured by the head-fixed motion sensor (gains: 1.7µA/°/s–3.4µA/°/s).

Recordings were analyzed on a cycle-by-cycle basis; mean (±SD) responses were calculated over all cycles. VOR gains were computed using sinusoidal fits to raw data.

Results

Control subjects with normal vestibular function presented VOR gains ranging 0.7-1.0 (Fig. 1a). For the BVL subject in the SYSTEM OFF condition, VOR gain was consistently ≤0.1 and eye movements were not correlated to yaw motion data (Pearson’s correlation: $r=0.07$, $p<0.05$; Fig. 1b). In the SYSTEM ON condition, the VOR gain of the BVL subject increased progressively as stimulation strength increased and eye movements were highly correlated to yaw motion data (Pearson’s correlation: $r=0.69$, $p<0.0001$). The maximum gain observed was $0.36(\pm 0.18)$, a substantial recovery towards normal function (Fig.1c).

Conclusion

This is the first demonstration that the VOR can be partially restored in a human BVL patient via motion-modulated electrical stimulation of a vestibular nerve branch. This is a fundamental first step towards the demonstration that such devices could help rehabilitate patients with BVL. Our next

step will be to extend these results to other patients implanted with similar devices.

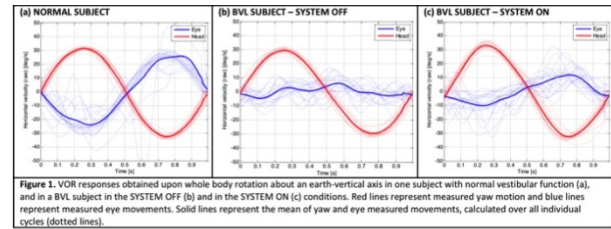


Figure 1. VOR responses obtained upon whole body rotation about an earth-vertical axis in one subject with normal vestibular function (a), and in a BVL subject in the SYSTEM OFF (b) and in the SYSTEM ON (c) conditions. Red lines represent measured yaw motion and blue lines represent measured eye movements. Solid lines represent the mean of yaw and eye measured movements, calculated over all individual cycles (dotted lines).

544 Bilateral Stimulation of the Vestibular Labyrinth in Rhesus Monkeys Using a Multichannel Vestibular Prosthesis

Chenkai Dai¹, Mehdi Rahman¹, Charles Della Santina¹
¹Johns Hopkins University, School of Medicine

Background

Maximizing efficacy of vestibular nerve branch stimulation is a key goal in development of a multichannel vestibular prosthesis (MVP) intended to restore sensation of 3-dimensional head movement in individuals disabled by chronic bilateral loss of labyrinthine hair cell function. Unilateral prosthetic stimulation in bilaterally vestibular-deficient (BVD) rhesus monkeys elicits vestibulo-ocular reflex (VOR) responses with marked asymmetry in gain during rapid head rotations. VOR gain is lower for head rotations toward the non-implanted side (away from the prosthesis side) than for rotations in the opposite direction. Reducing this gain asymmetry by enhancing contralateral responses would be an important step toward improving gaze stability in BVD individuals using a MVP. Noting that an individual with two normal labyrinths has a much more symmetric VOR than an individual with a single normal labyrinth (e.g., after unilateral labyrinthectomy), we hypothesized that bilateral, complementary prosthetic stimulation of the vestibular labyrinths will elicit responses with less asymmetry than observed with unilateral stimulation.

Methods

We implanted MVP electrodes in semicircular canals of both ears in one rhesus monkey previously rendered bilaterally vestibular-deficient via intratympanic gentamicin administration. We characterized horizontal VOR responses using scleral coils in darkness during unilateral and bilateral prosthetic electrical stimulation.

Results

Bilateral complementary stimulation produced significantly higher VOR gain and improved symmetry compared with unilateral stimulation.

Conclusion

Consistent with a prior study characterizing horizontal VOR performance during bilateral stimulation of the lateral semicircular canals in squirrel monkeys, our results support the hypothesis that bilateral vestibular prosthetic stimulation can achieve better 3D VOR performance in rhesus monkeys than possible with unilateral stimulation.

However, this improvement comes at the expense of twice the surgical risk and, barring implant designs with a single processor driving electrode arrays in both ears, approximately twice the cost per patient once this technology becomes a part of routine clinical practice. The relative risks, costs and benefits between bilateral and unilateral stimulation will ultimately depend on the extent to which changes in stimulation timing and waveforms can achieve good symmetry with unilateral implantation.

545 System Integration of an Application Specific Integrated Circuit to Advance Toward a Fully Implantable Multichannel Vestibular Prosthesis

Kristin N. Hageman¹, Zaven Kalayjian², Mehdi A. Rahman¹, Bryce Chiang¹, Francisco Tejada², Gene Y. Fridman³, Chenkai Dai¹, Andreas G. Andreou², Charles C. Della Santina^{1,3}

¹*Johns Hopkins University Department of Biomedical Engineering*, ²*Johns Hopkins University Department of Electrical and Computer Engineering*, ³*Johns Hopkins University Department of Otolaryngology - Head & Neck Surgery*

Background

The Johns Hopkins Multichannel Vestibular Prosthesis (MVP) has demonstrated success in modulating vestibular afferent fiber firing rates to encode rotational head movements for those with profound bilateral vestibular hypofunction. Current implementation of the MVP follows a semi-implantable approach, with implanted electrodes coupled to an external component including motion sensors, processing circuitry, and the power source. Decoupling of the external component would cause loss of power for the prosthesis and sudden onset of vertigo. To avoid the issue of decoupling, development of the next generation MVP (MVP3) aims for a fully implantable system, where device size becomes a key consideration. The development of a complementary metal-oxide semiconductors (CMOS) application specific integrated circuit (ASIC) provides the ability to greatly reduce size of the device. The goal of this experiment was to determine whether integration of the CMOS ASIC would offer the same clinical benefits as the existing MVP architecture (MVP2).

Methods

We developed a CMOS ASIC to replace most of the circuitry for the output of the prosthesis, leaving three main components that make up the MVP3: motion sensors, a microcontroller and the ASIC. Integration of the ASIC into the existing MVP architecture required modification of existing software for the microcontroller to supply correct commands to the ASIC based on the motion sensor input to the system. The ASIC was designed to efficiently organize commanded signals from the microcontroller with regard to current amplitude, timing, and polarity. After bench testing of ASIC integration, the MVP3 system was verified in a rhesus monkey rendered bilaterally vestibular-deficient via intratympanic gentamicin. We rotated the monkey sinusoidally in darkness at 0.1-5 Hz, at 50-200 °/s

peak. The 3-dimensional vestibular ocular reflex (3D VOR) responses were recorded and compared to eye movements evoked by the MVP2.

Results

Bench testing of the ASIC with custom microprocessor software allowed for correct encoding of motion to frequency modulation of pulses. Physiological tests produced 3D VOR eye velocity movements that are statistically similar to the MVP2.

Conclusion

Comparison of the MVP3 with the MVP2 showed no significant difference, thereby verifying physiological implementation of the ASIC interface between the microcontroller and electrodes. With these initial tests of feasibility for the ASIC, future development will further integrate circuitry for the microcontroller into the ASIC. This continued miniaturization and reduction of power consumption will provide a solution for a fully implantable prosthesis.

Supported by NIH-R01DC9255

546 Heterogeneity in the Population of Vestibular Neurons That Are Activated by Sinusoidal Galvanic Vestibular Stimulation (sGVs) and Send Projections to Pre-Sympathetic Neurons in the Ventrolateral Medulla

Giorgio P. Martinelli¹, Victor L. Friedrich, Jr.¹, Bernard Cohen¹, **Gay Holstein**¹

¹*Mount Sinai School of Medicine*

Background

Vestibulo-sympathetic pathways mediate rapid changes in blood pressure in response to movement and adjustments in head and body position. We previously demonstrated that there are direct projections from the caudal vestibular nuclei to the rostral and caudal ventrolateral medullary cell groups (RVLM and CVLM, respectively), the key pre-sympathetic sites for integration of cardiovascular signals. We have also shown that neurons in this pathway are activated by sGVs. The goal of the present study was to identify the topography and chemical anatomy of these projections.

Methods

Unilateral iontophoretic injections of the retrograde tracer FluoroGold (FG) were placed in the RVLM or CVLM of rats. After 7-10 days, the animals were anesthetized and received sGVs while changes in blood pressure were recorded using photoplethysmography. Animals were perfused 90 min after the stimulation. The brains were harvested and the brainstems were sectioned serially. Sets of sections were used to map the tracer injection sites, and other series of sections were used for multiple label immunofluorescence studies of the caudal vestibular nuclei. These latter experiments used c-Fos protein accumulation as a marker for neurons activated by sGVs,

as well as immunolabels to identify the tracer, glutamate, GABA, and imidazoleacetic acid-ribotide (IAA-RP), a neuromodulator involved in blood pressure regulation, in vestibular neuronal somata.

Results

FG was present bilaterally in cell bodies of the inferior and caudal medial vestibular nuclei (IVN and MVNc, respectively) that had c-Fos protein accumulation in response to sGVS. The sGVS-activated vestibular neurons with projections to RVLM or CVLM were distributed approximately equally in MVNc and IVN (101 vs 90 cells observed with co-localization of FG and cFos in MVNc and IVN, respectively). Within MVN and IVN, approximately equal numbers of cells projected to CVLM and to RVLM. However, almost twice as many cells in each vestibular region sent ipsilateral as opposed to contralateral projections. These studies also revealed differential localization of glutamate, GABA and IAA-RP immunofluorescence in the MVNc and IVN projections to ipsilateral and contralateral RVLM and CVLM.

Conclusion

We conclude that there are multiple topographical and chemoanatomical components of the vestibulo-sympathetic pathway.

Supported by NIH/NIDCD grant R01 DC008846 and NIA grant R21 AG035389.

547 Double Oscillations in Blood Pressure and Heart Rate from Monaural Sinusoidal Galvanic Vestibular Stimulation (SGVS) in the Rat

Sergei B. Yakushin¹, Giorgio P. Martinelli¹, Theodore Raphan², Gay R. Holstein¹, Bernard Cohen¹

¹Mount Sinai School of Medicine, ²Brooklyn College, CUNY

Background

Binaural sinusoidal galvanic vestibular stimulation (sGVS) induces oscillatory changes in blood pressure (BP) and heart rate (HR) in anesthetized rats that are associated with vasovagal responses (VVR). sGVS also induces similar oscillations in muscle sympathetic nerve activity (MSNA) in alert humans. There are generally two oscillations of BP and HR in rats and two cycles of MSNA in humans for each cycle of low frequency sGVS. We questioned whether these double oscillations were related to known vestibular mechanisms and could shed light on the processing of sGVS signals from the vestibular nerve to the autonomic system.

Methods

BP and HR were measured with intra-aortic sensors in three rats anesthetized with 2% isoflurane. The labyrinths were stimulated at frequencies of 0.025-0.5 Hz with currents of 3 mA through Ag/AgCl needle electrodes inserted over the external auditory meati on both sides (binaural stimulation) or in front and behind the external auditory meatus of one ear (monaural stimulation). Single

sinusoids were also given monaurally and binaurally at 2 minute intervals. In addition, rats were also oscillated in pitch $\pm 50^\circ$ at 0.025-0.1Hz.

Results

Double oscillations of BP and HR were induced by both binaural and monaural stimulation in each rat. The double oscillations were commonly induced by stimulus frequencies ≤ 0.1 Hz. Stimulation at higher frequencies commonly induced only single oscillations. Single sinusoids produced increases in BP that slowly declined over several minutes whether given monaurally or binaurally. Double oscillations in BP were similarly induced by tilting rats $\pm 50^\circ$ at low frequencies.

Conclusion

The facts that sGVS induces both MSNA in humans and VVRs in rats and that single sinusoids induce increases in BP are consistent with the hypothesis that sGVS is channeled through the vestibulo-sympathetic reflex and induces VVRs when appropriately activated. We posit that sGVS sinusoidally activates orientation sensitive central otolith neurons with polarization vectors close to the spatial vertical to produce double oscillations in their firing rates in a manner similar to that induced by pitch and roll tilt. Such otolith neurons have low frequency characteristics. When coupled with the low frequency characteristics of the cardiovascular/baroreflex rhythm, these neurons could drive the large amplitude, low frequency oscillations in BP known as Mayer waves that are commonly associated with VVRs.

Supported by NIH Grants DC008846, AG035389, DC004996 and DC05204

548 Fluctuating Hyper-G Acceleration Induces Body Temperature Drop in Normal But Not Circling Mice

Donald L. Swiderski¹, Hideto Fukui¹, Yohei Takada¹, Dwayne Vaillencourt¹, Chris Ellinger¹, Yehoash Raphael¹
¹University of Michigan

Background

Balance disorders are increasingly prevalent and may be due to aging or drug treatments. Diagnosis and treatment of these symptoms is complicated because they may stem from neuromuscular disorders rather than a specific vestibular lesion. The potential to learn compensatory behaviors also interferes with evaluation and treatment, in the clinic and in the lab. Recent studies showing vestibular influence of autonomic functions suggests a new avenue of diagnosing vestibular organ defects: measurement of short-term body temperature changes after controlled fluctuations of centrifugal acceleration. Here, we present a device for producing varying accelerations and show it induces short-term depression of body temperature in intact wild-type mice, but not in mutants or chemically lesioned mice with overt vestibular phenotypes.

Methods

Mice were placed in a 50 ml conical tube and accelerated by a rotating arm, with the tube and mouse held perpendicular to the plane of rotation. An automated controller accelerated the 25.4 cm arm to 1.4 cps, then alternated arm speed between 1.4 and 2.4 cps (2 G and 6 G), maintaining each speed for 10 seconds. After a preset number of cycles, the arm slowly decelerated and the mouse was removed from the tube.

Core body temperature was measured just prior to acceleration, immediately after, and at specified subsequent times.

Mutant mice (*Pou4f3*, *Grxcr1*) with circling and head bobbing, associated wild-types, and wild-types lesioned bilaterally with streptomycin were tested.

Results

Wild-types of all strains exhibited a 2-3° C drop in body temperature within 10 minutes of stimulation, and all returned to baseline within 30 minutes. Most mutant mice exhibited no temperature change; none decreased >0.5°. Streptomycin-lesioned mice also showed little or no drop in temperature.

Conclusion

Brief exposure to controlled fluctuation of hyper-G acceleration produces a repeatable and substantial temporary drop of body temperature in mice with normal vestibular organs. In contrast, mice with vestibular phenotypes due to mutations or ototoxic lesions show no such temperature change. This acceleration protocol is a safe, non-invasive method of testing for peripheral vestibular dysfunction, and free of errors due to the subject 'learning' the testing protocol. These characteristics allow this technique to be used to diagnose naïve subjects and those with less overt symptoms, and also to assess the efficacy of therapeutic regimens.

Acknowledgments: The Williams Professorship, The Hirschfield Foundation, and NIH/NIDCD grants P30 DC-05188, and DC-001634.

549 Summation of Vestibular, Proprioceptive, and Visual Signals in the Parieto-Insular Vestibular Cortex

Michael Shinder¹, Shawn Newlands²

¹Dartmouth College, ²University of Rochester Medical Center

Background

Vestibular signals are pervasive throughout the central nervous system, including the cortex, where they likely play different roles than they do in the better studied brainstem. Little is known about the function of the parieto-insular vestibular cortex (PIVC). This brain region is not well defined by anatomical boundaries, but is the largest cortical region with physiological responses to vestibular stimulation and projects to the rostral vestibular and y-group nuclei.

Methods

Single unit neural activity was recorded in the PIVC of 2 rhesus macaques during combinations of rotation in the horizontal plane at 0.2 Hz of the head (vestibular), body (twisting of body relative to head to stimulate the neck), and visual targets. The head was controlled by a head-fixed motor independent from the rotator moving the primate chair. Both passive and active head movements were utilized. The animals were trained to follow visual targets with either their eye or their head. In this way, complex combinations of visual, vestibular, and proprioceptive stimuli were applied while recording.

Results

We report on the responses of 75 PIVC neurons. The activity of these PIVC neurons correlated with the rotation of the head-in-space (vestibular), the twist of the neck (proprioceptive), and/or the motion of visual targets. Visual target sensitivity was not associated with eye movement, but with target motion itself. Most neurons responded to more than one stimulus. The pattern of visual, vestibular and somatic sensitivities on PIVC neurons displayed a continuous range with some cells more strongly responding to one or two of the stimulus modalities while other cells responded to any type of motion with relative equivalence. The responses to combinations of stimuli were often roughly predicted by summing the expected responses to the component head, neck, and target movements. However, this was not always the case. Responses to vestibular and neck rotation stimuli were almost always similar whether motion was passively applied or the result of a volitional movement of the head.

Conclusion

We found that the PIVC neurons respond to convergent, multisensory inputs related to movement of the animal and external visual objects. PIVC neurons may be involved in keeping track of the motion of external objects and the animal's own movements. This comparison of self and external movement in the PIVC is consistent with insular cortex functions related to monitoring, and explains many disparate findings of previous studies.

550 The Influence of Tilt and Inter-Stimulus Interval on the Roll Aftereffect

Benjamin Crane¹

¹University of Rochester

Background

Exposure to a stimulus often biases subsequent stimulus perception in the opposite direction. As a result of this aftereffect a neutral stimulus may be perceived as opposite the adapter. One such aftereffect is the post-roll or "Gillingham" illusion in which after making an abrupt roll pilots erroneously perceive a roll in the opposite direction. The potential influence of gravity in the roll aftereffect has not previously been examined.

Methods

Stimuli were delivered using a 6-degree-of-freedom motion platform. In three trial blocks the test stimulus alone was

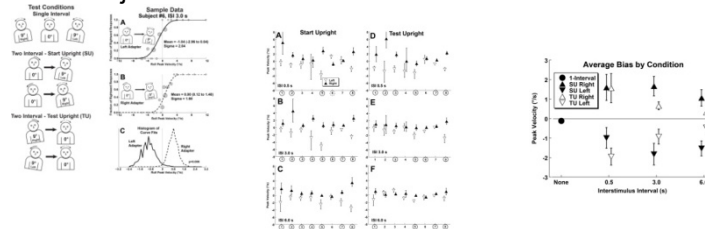
tested at starting tilts of 9° right/left and upright. The maximum test stimulus amplitude was 3° over 0.5 s (peak velocity 12°/s, peak acceleration 75°/s/s). A two-interval procedure was used to measure aftereffects. The adapting (first interval) stimulus was always 9° of roll over 1.5 s (peak velocity 12°/s, peak acceleration 25°/s/s) with right and left interleaved. Blocks of trials included ISI of 0.5, 3, or 6s. For each ISI, subjects started upright (SU), thus the test stimulus occurred when tilted. In other blocks subjects started at ±9° such that the test stimulus occurred when upright-test upright (TU). Eight human subjects participated (42±18 years). A cumulative Gaussian function was determined from each subject's responses.

Results

The baseline bias was near zero in every subject and in all cases < 0.8°/s. The starting position had no significant influence on the bias (p=0.49). The addition of an adapting stimulus often produced an aftereffect. This aftereffect was observed in 4/8 subjects with the SU at an ISI of 0.5s, in all subjects at an ISI of 3, and 7/8 subjects at an ISI of 6. For the TU condition the aftereffects were less consistently observed. The size of the roll aftereffect was similar between TU and SU conditions. At 0.5 ISI the difference between leftward and rightward adapters was 3.0±2.7°/s (TU and SU similar). The aftereffect was smaller in TU relative to SU at ISIs of 3s (p=0.04) and 6s (p=0.01). This is consistent with aftereffect persisting longer when the subject remains tilted after delivery of the adapting stimulus.

Conclusion

The roll aftereffect causes a perceptual bias even after modest low amplitude roll and persist for long durations when subject remains tilted.



551 Perceived Tilt and Translation During Periodic Versus Non-Predictable Motion

Scott Wood¹, Jerome Jeevarajan², Jan Holly³
¹NASA Johnson Space Center, ²USRA, ³Colby College

Background

The ability to accurately separate out the effects of tilt relative to gravity from those of translation is essential to maintaining accurate spatial orientation awareness. Previous studies have often characterized motion perception with periodic oscillations or non-predictable steps and pseudorandom stimuli. The purpose of this study was to compare motion perception during periodic sinusoidal motion (0.11 Hz, ±5°), non-predictable sum-of-sinusoidal motion (0.02 – 0.17 Hz, <±7°) and non-predictable random step motion (<±7°).

Methods

Thirteen subjects were either tilted in the pitch plane about their interaural axis or translated in the fore-aft direction along a 4 m air-bearing linear track using an equivalent acceleration as the tilt stimuli. Subjects were trained to use a joystick to continuously record both the magnitude and direction of perceived motion using a visual display of actual motion during step stimuli of various amplitudes. Subjects then reported perceived position of either tilt or translation in darkness with eyes closed.

Results

During tilt motion, phase errors were smallest during sinusoidal motion and increased during both random step and sum-of-sinusoid stimuli. During translation motion, phase errors were smallest during random step motion and increased during both sinusoidal and sum-of-sinusoid stimuli. Joystick responses were more variable during translation motion, with subjects often losing awareness of their position along the linear track during translation trials.

Conclusion

Our results are consistent with perception becoming predictive during tilt motion that can utilize the gravitational vector as a corrective anchor. The absence of a similar reference during translation in darkness without tilting increases the perceptual uncertainty during either periodic or non-predictable oscillations. We hypothesize that during natural lower frequency stimuli, phase-linking of translation movements with tilt motion and non-vestibular references is important to construct a perception of one's overall motion path.

552 Assessing Misperception of Rotation in BPPV

Jan E. Holly¹, Helen S. Cohen², M. Arjumand Masood¹
¹Colby College, ²Baylor College of Medicine

Background

Perception of illusory motion is often the most disturbing symptom of a vestibular disorder. However, these misperceptions of motion are difficult to measure, even though they may be a useful indicator of vestibular function. A classic example of illusory motion is the vertigo of benign paroxysmal positional vertigo (BPPV), in which perceived rotation arises especially during the Dix-Hallpike maneuver. Therefore, BPPV provides a good example in which to study patients' perceptions of illusory motion. We introduce a method of using cartoon videos to assist in subjects' reporting of misperceived motion, and investigate whether or how the reported misperceptions of motion vary between subjects.

Methods

Patients were identified with unilateral BPPV of the posterior canal only. The patients were instructed to pay attention to any perceived rotation while undergoing the Dix-Hallpike maneuver. After the Dix-Hallpike maneuver, the patients indicated the direction of perceived rotation by choosing between cartoon videos of possible perceptions. The videos showed a subject in the Dix-Hallpike supine

position, and had stripes on the head that rotated in a certain direction in each video. Each patient was instructed to choose one of more videos to indicate the rotation perceived during testing.

Results

Most patients chose the video with backward rotation about the posterior canal axis of the affected ear, but the majority also chose at least one additional video with rotation about an orthogonal axis. The most-selected videos were backward rotation about the posterior canal axis, ipsilateral rotation about an axis aligned with the body (yaw relative to the body), and ipsilateral rotation about an earth-vertical axis (roll relative to the body). Every combination of one, two, or three of these motions was selected by at least one patient. Nevertheless, the results showed test-retest reliability within subjects.

Conclusion

Patients with posterior canal BPPV report perception of rotation that is not necessarily aligned with the affected posterior canal axis. In addition, the direction of rotation differs between subjects. These results show that perception and eye movements must be studied independently in order to gain a full understanding of vestibular disorders.

553 Insights Into Prestin Function from Knock-Out/Knock-In Mice

Mary Ann Cheatham¹, Kazuaki Homma¹, Jing Zheng¹, Peter Dallos¹

¹Northwestern University

The discovery of outer hair cell (OHC) somatic electromotility was followed by a flurry of experiments designed to document this voltage-dependent behavior and to evaluate its role in cochlear amplification. The subsequent discovery of the OHC motor protein, prestin, resulted in the development of knockout mice lacking prestin and showing threshold shift and lack of tuning. In order to obtain a better model to test prestin's functional significance, knockin (KI) mice were developed to overcome the reduced stiffness and length of OHCs in prestin knockout (KO) mice. For C1 KIs (K233Q, K235Q, R236Q; Oliver et al., 2001; Gao et al., 2007), the peak of the nonlinear capacitance (NLC) function was shifted in the hyperpolarizing direction but the mice showed no change in phenotype. In contrast, 499 KIs (V499G/Y501H; Dallos et al., 2008) showed threshold shift and no frequency selectivity due to the fact that NLC and electromotility were vastly reduced at negative potentials. It was also anticipated that prestin KI mice would not suffer the premature OHC death associated with removal of prestin protein. Although the C1 KI met this expectation, the 499 KI mouse demonstrated an aggressive OHC death even before weaning. Other approaches included development of the chimeric mouse in which OHCs lacking prestin interleaved with normal OHCs to produce a mosaic and a hypomorph where various amounts of prestin protein are expressed in a given cochlea. Experimental results using these mouse models raise challenging questions about the

processes by which sensitivity and frequency selectivity are established in the peripheral auditory system. Even with a thorough characterization of each prestin mutation, it may be difficult to extrapolate from *in vitro* results on isolated OHCs or on cell lines to *in vivo* performance when the OHC is housed within its normal organ of Corti environment. (Work supported by NIDCD Grants DC00089 and DC010633, and The Knowles Hearing Center).

554 Voltage-Dependent Hair Bundle Motion of Chicken Auditory Hair Cells

Xiaodong Tan¹, Maryline Beurg², Robert Fettiplace¹

¹University of Wisconsin, ²INSERM U587, Université Victor Segalen Bordeaux 2, Bordeaux, France

Active hair bundle motion of auditory hair cells has been proposed to be the driving force of cochlear amplification in chickens but there is little direct evidence for this notion. The aim of the experiments was to search for active bundle movements in chicken hair cells and investigate their origin. We made patch clamp recordings, mainly from short hair cells (SHCs), in isolated chicken basilar papilla (E18 – P0; 33 degrees C), and monitored hair bundle motion with dual-photodiode imaging. Hair bundle deflections evoked by a fluid jet generated a mechano-transducer (MT) current with maximum amplitude increasing from 0.3 to 1.6 nA from apex to base of the papilla. The MT current encoded hair bundle displacements with a 10 to 90 percent working range of 30 to 60 nm. The current was blocked by dihydrostreptomycin or FM1-43 but was unaffected by 10 mM Na-salicylate. Depolarizing voltage steps induced a negative displacement of the hair bundle (away from the kinocilium) of 10 to 40 nm, sometimes followed by a positive overshoot after the voltage step. The voltage-evoked bundle motion consisted of two components of opposite polarity. Blocking the MT current with FM1-43 enhanced the negative motion indicating a positive component linked to gating of MT channels, whereas 10 mM salicylate reversibly blocked the negative movement. A non-linear capacitance change could also be measured in SHCs, also blocked by salicylate, with a peak voltage around +6 mV. Similar results were obtained in tall hair cells. Depolarizing one SHC in preparations lacking a tectorial membrane (TM) induced a displacement in bundles of adjacent hair cells, suggesting a movement of the cell body or cuticular plate. With the TM still present, its radial motion, assayed by imaging attached silica beads, could be produced by extracellular current stimulation. This TM motion was also blocked by salicylate and was of similar size (up to 20 nm) to evoked movements of hair bundles beneath the beads. Our results reveal a novel movement in chicken hair cells which might originate from their cell bodies instead of hair bundles. Movements of the same size for the TM and hair bundle beneath indicate that the active bundle force can be transmitted via the TM to the tall hair cells. The voltage-dependence, non-linear capacitance and sensitivity to salicylate suggest the involvement of chicken prestin in active hair bundle motion.

555 New Insights Into the Structure-Function Relationship of Prestin

David He¹, Kirk Beisel¹, Jason Pecka¹, Huizhan Liu¹, Jie Tang¹, Xiaodong Tan¹, Sandor Lovas¹
¹Creighton University

Prestin is a member of the family of solute carrier 26 (SLC26A) anion transporter proteins. It is the motor protein of the cochlear outer hair cells and uniquely functions as a direct voltage-to-force transducer. Although intracellular anions are known to be critical for voltage sensing and conformational change of prestin, the structure-function relationships of prestin remain to be elucidated. In this presentation, we will review recent work from comparative, evolutionary studies using site-mutagenesis, domain swapping and voltage-clamp techniques. On the basis of our new studies using a combination of *ab initio* structure prediction, 3D folding recognition by threading, homology modeling, molecular dynamics simulations and site-mutagenesis, we propose a new mechanism of how prestin interacts with intracellular anions to generate gating current. (Supported by NIH grant R01 DC 004696 from the NIDCD).

556 Prestin Structural Biology – Evidence for Oligomerization and Co-Operativity

Richard Hallworth¹
¹Creighton University

Since the identification of prestin as the motor protein of the outer hair cell, much progress has been made in elucidating its structure and mechanism, although much more remains to be understood. Recent attention has focused on its oligomeric nature and the possibility that the subunits work cooperatively. The presentation will review the contradictory nature of the evidence and will attempt a consensus view.

557 The Structural Basis of Electromotility and Anion Transport by Prestin and SLC26 Anion Transporters

Dominik Oliver¹, Dmitry Gorbunov¹, Florian Nies¹, Mattia Sturlese², Roberto Battistutta^{2,3}
¹Philipps University Marburg, ²University of Padua, ³Venetian Institute of Molecular Medicine

Despite the substantial efforts since the identification of prestin (SLC25A5), the molecular mechanisms that generate its electromechanical ('piezoelectric') activity have remained elusive. Similarly, little is known about the mechanisms that underlie anion transport by the close homologs within the SLC26 anion transporter family. Progress in understanding the molecular basis of SLC26 function has been hampered mainly by the lack of structural information on SLC26 proteins.

We have previously found that non-mammalian orthologs of prestin are electrogenic anion transporters. Generation of chimeras between electromotile prestin and its transporting non-mammalian orthologs enabled us to identify two domains within the transmembrane core region that cooperate in the generation of electromotile activity.

This finding defined functional domains of prestin for the first time and demonstrated an overlap in the protein structures that mediate piezoelectric activity in prestin and anion translocation in SLC26 transporters. Moreover, the results pointed to mechanistic similarities between electromotility and transport. However, how both domains function in the generation of electromotility and anion transport remained unknown.

Here we present a 3D structural homology model of prestin. Using a bioinformatic approach to search protein databases we identified a recent crystal structure as the appropriate template for homology modeling. Molecular dynamics simulations showed that the obtained structure is energetically favorable and stable, strongly supporting the suitability of the template used for modeling and confirming the quality of the derived structure.

Interestingly, the transmembrane architecture of the model differs from previously suggested topologies, and thus allowed for an experimental test of its validity. We therefore performed a substituted cysteine accessibility scan to determine the location of all predicted TM-TM linkers. The accessibility data are entirely consistent with the structural model but disagree with previously proposed 10 or 12 TM topologies.

The proposed model further pinpoints a central substrate binding site. Point mutations at this site affected anion selectivity both in prestin and its transporting orthologs and strongly altered the efficacy of the competitive inhibitor, salicylate. We conclude that the binding site that confers the anion dependence of electromotility corresponds to the central substrate binding site for anion translocation in other SLC26 transporters.

In conclusion, we present an experimentally validated structural model of prestin that will be highly useful for addressing the molecular mechanisms underlying electromotility and anion transport.

558 Prestin the Atypical Slc26 Transporter

Christoph Fahlke¹, Michael Schänzler²
¹FZ Jülich, ²MH Hannover

Prestin is a member of the SLC26 solute carrier family and functions as motor protein in cochlear outer hair cells. Whereas other SLC26 homologs transport as anion exchangers or channels a wide variety of anions, prestin is the only member of this family with piezoelectric properties. For many years, it was unclear whether mammalian prestin can mediate anion transport. The pseudohalide thiocyanate (SCN⁻) has been shown to uncouple many anion exchangers, and we thus used SCN⁻ to study whether prestin can also assume "slippage" modes of anion conduction. Mammalian cells heterologously expressing rat prestin exhibit SCN⁻ currents above background levels. The amplitudes of these anion currents are proportional to the number of prestin molecules per cell. Variation of the SCN⁻ concentration resulted in changes of the current reversal potential that obey the Nernst equation indicating that SCN⁻ transport is not stoichiometrically coupled to other anions. Application

of external SCN causes large increases of anion currents, but only minor changes in non-linear charge movements. We conclude that prestin can assume an anion transport mode that is promoted by SCN. However, only a very small percentage of prestin molecules functions as SCN-transporter under these conditions whereas the majority still functions as motor protein. Unitary current amplitudes are below the resolution limit of noise analysis and thus much smaller than expected for pore-mediated anion transport. We conclude that mammalian prestin is capable of mediating electrogenic anion transport and suggest that SLC26 proteins converting membrane voltage oscillations into conformational changes and those functioning as channels or transporters share certain transport capabilities.

559 The Relevance of Basic Research on Perceptual Learning to Clinical Auditory Rehabilitation

Beverly Wright¹

¹*Northwestern University*

Human adults can improve their auditory perceptual skills through practice, making perceptual training a promising tool to treat communication disorders. Our premise is that a greater understanding of the basic kinetics and mechanisms of skill learning in humans will lead to more effective training strategies. A general model holds that learning occurs over two phases, acquisition and consolidation. The acquisition phase is the actual period of training. The consolidation phase is the period after training ends during which the memories that were formed during acquisition are transformed from a fragile to a more stable state. The consolidation period can last for hours to days and behavioral improvements are often revealed only after consolidation has occurred. Thus, it is thought that the hour during which you are taking a tennis lesson is the period during which you are acquiring the experiences necessary to improve your serve, but it is during the hours after that lesson, when you are engaged in other activities including sleep, that those experiences are consolidated in long-term memory, yielding lasting improvements in performance. We have been addressing these principles in auditory learning by characterizing the circumstances that are necessary for acquisition to occur and by determining the vulnerability of the learning process to intervening events during the acquisition and consolidation phases. For example, we have evidence that (1) for improvement to occur across days requires a sufficient amount of training per day, and that additional daily training can be superfluous, (2) a combination of practice with relevant auditory stimuli and additional stimulus exposures without practice can enhance learning, and (3) the same intervening event (practice on a non-target condition) can have opposite effects depending on whether it occurs during acquisition or consolidation. We also have begun investigating how these characteristics change with age and are affected by sensory and cognitive disorders. For instance, we have identified a training regimen that is effective for adults, but not for most adolescents nor for most adults with dyslexia. Conclusions drawn from

learning on fine-grained discrimination tasks have held for speech learning, suggesting that common principles are at play in both domains. Application of these principles could improve clinical training strategies. Further, an individual's response to perceptual training could be used as an objective, clinical measure to guide diagnosis and treatment of a cognitive disorder. [Work supported, in part, by NIH/NIDCD RO1-DC04453]

560 Auditory Training: What the Brain Gets Versus What It Does with It

Arthur Boothroyd¹

¹*San Diego State University*

Background

What the brain gets is auditory (and/or visual) sensory evidence about spoken language plus information from the immediate physical, social, and language context. What the brain does with this evidence is to determine its most likely source. The listener's knowledge (cognitive, social-cognitive, and linguistic) determines both the possible decisions and the value of the context. The listener's skill determines success - defined, here, as making decisions at high speed (set by the talker) while maintaining an acceptably low probability of error. As in reading, speed is optimized by taking maximum advantage of context and using only enough sensory evidence to confirm predictions "beyond a reasonable doubt". For this reason, effective communication is possible in spite of stimulus degradation by noise, distance, reverberation, and poor or deviant articulation. An acquired hearing loss further degrades sensory evidence and reduces the range of conditions over which effective communication is possible, with serious implications for quality of life. A first, and essential, step in addressing hearing loss is to optimize auditory function with hearing aids and/or cochlear implants...in other words, to increase what the brain gets. To deal with the inevitable residual sensory deficit, the listener must adapt to changed and/or diminished sensory evidence by modifying knowledge and skills. Formal auditory training may speed and optimize this adaptation...in other words, it may help improve what the brain does with what it gets. There is evidence of benefit from auditory training but it is not clear: a) what aspects of knowledge and skill change, b) which aspects of training are responsible, c) how listener characteristics affect answers to these two questions, d) whether improvements affect quality of life.

Methods

San Diego State University student Stephanie Bigler, provided three experienced hearing aid users with 5 to 10 hours of story-level training in noise, using a software package developed by the author under a grant to Gallaudet University. Carry-over was measured using a talker and materials not involved in training.

Results

Improvements were found in the recognition of monosyllables in isolation and words in sentences but these were small. The improvements were not likely to be of practical significance...a conclusion supported by self-report.

Conclusions

These experienced hearing aid users may already have been performing as well as they could. Further research will include new aid and implant users. [supported in part by NIDRR H133E080006].

561 The Application of Hearing Aid Technology to Cognitive Rehabilitation

Brent Edwards¹

¹*Starkey Hearing Technologies*

Hearing aid development has focused primarily on audibility and signal-to-noise ratio improvements for the vast history of its existence. The impact of hearing aid technology on higher-level processing has largely been ignored in the development, prescription, and assessment of hearing aids. While the impact of top-down processing on auditory function has been well documented, only recently has the impact of cognition on hearing aid benefit been demonstrated. Similarly, the impact of hearing loss and hearing aids has only recently been demonstrated to have an effect on cognitive function. Our laboratories, in collaboration with several partners, have investigated the impact that hearing aids have on higher level function. This research includes the development of new higher-level focused outcome measures, demonstrations of the impact of hearing aids on listening effort, measures of a hearing aid's effect on auditory scene analysis, and diagnostic correlates with cognitive benefit from hearing aids. This talk will review our laboratories' research projects in these areas, including the motivation for each, and will speculate on the impact of this research on the future of the hearing aid field.

562 Training the Older Brain to Understand Speech in Noise

Larry Humes¹

¹*Indiana University*

The following facts have been established regarding age-related hearing loss and speech communication. Approximately 40% of older adults have a peripheral hearing loss sufficient to cause speech-understanding difficulties. For those who seek help, typically 10 years have passed from the time a hearing loss is first suspected to the onset of intervention. The most frequent complaint of older adults is that they can hear speech, but can't understand it, especially in backgrounds of noise. Despite significant technological advances in recent years, contemporary hearing aids still fall short in fully addressing the speech-in-noise difficulties for many older adults. Hearing aid use alone (also known as "acclimatization") does not appear to offer significant improvements in speech-in-noise performance through extended periods of use (at least out to 3 years of hearing-aid use).

In addition to these "auditory facts" regarding aging and speech communication, some additional and potentially relevant facts have been established regarding age-related changes in cognition and linguistic processing. In general, in normal healthy aging and for process-related cognitive measures, cognitive function declines steadily for the average adult beginning at about an age of 30 years. On

the other hand, product-related cognitive function, such as vocabulary, verbal comprehension and use of context, increases throughout much of adulthood, only declining at or beyond an age of about 75 years.

With this background in mind, we have been investigating an auditory-training regimen designed specifically to improve the ability of older adults to understand amplified speech in noise. The focus of this presentation, after reviewing briefly the evidence supporting the facts outlined above, will be on the conceptual framework underlying our auditory-training regimen and the evidence gathered to date in support of its efficacy. (Work supported, in part, by NIA R01 AG008293 and NIDCD R01 DC010135.)

563 Outcome Measures in Children Fit with Hearing Aids and Cochlear Implants

Lisa Davidson¹, Jamie Cadieux², Jill Firszt¹

¹*Washington University School of Medicine, ²St. Louis Children's Hospital*

Background: Speech recognition measures are the primary outcome used to validate the effects of sensory devices for children with hearing loss. Clinicians use these measures to determine candidacy (i.e. cochlear implant [CI] vs. hearing aid [HA]), to document progress in speech, language and auditory development and to assess the effects of device parameter selection. As technology improves and CI candidacy expands to include children with more residual hearing, there is a need to incorporate a variety of measures that better reflect real-life listening environments and have applications for clinical practice. Current clinical practice includes fitting and evaluating children who have different device configurations, for example a CI and a HA (i.e., bimodal). The fitting of both the HA and CI are critical variables that contribute to outcomes and specifically bimodal benefit. We present data from our lab where several speech recognition measures were incorporated to evaluate the effects of HA frequency response (FR) on bimodal benefit in children.

Method: Bimodal fittings with three different FRs were compared to the CI alone condition to assess benefit. Three FRs were evaluated: 1) baseline bimodal fitting with a traditional wide band FR, 2) restricted high frequency gain based on residual hearing and real ear gain, and 3) activated frequency compression. A baseline (A-wide band FR) and two experimental (B1-restricted response, B2-frequency compression) FRs were evaluated in an alternating research design (AB1AB2). Fourteen children (ages 7-21 years) were assessed with measures of speech recognition in quiet and noise, talker variability and localization. Subjective questionnaires were completed by parents and children for all conditions and each child was asked which of the FRs they preferred.

Results: Group data revealed no significant differences between mean scores for the three FR conditions in the bimodal condition compared to the CI alone condition across most measures. Group analysis using the FR that resulted in the highest individual bimodal scores revealed that the bimodal condition was significantly better than the CI alone condition across all measures. The best bimodal

condition varied across individuals and outcome measures, and the preferred FR varied across individuals.

Conclusions: Individual results support consideration of both restricted bandwidth and frequency compression, in addition to the traditional wideband frequency response, for HA settings used in bimodal fittings.

564 Pediatric Assessment and Rehabilitation of Hearing Loss

Karen Gordon¹

¹*The Hospital for Sick Children*

Sub-title: Defining and treating hearing loss in children

Hearing loss is one of the most common congenital anomalies and, when left untreated, results in significant deficits in oral communication. Despite clear effects on the immature auditory pathways during infancy and childhood, it is easy to overlook often subtle signs of hearing problems in young children until speech and language development are already delayed. The use of physiological measures of auditory function have revolutionized the diagnosis of hearing impairment in infants, making it possible to determine how much hearing sensitivity has been lost across the range of frequencies important for understanding speech. Clinically useful measures include otoacoustic emissions, which assess outer hair cell function, and evoked potentials, which measure electrical fields of neural activity at discrete areas of the auditory pathways. Many countries use these tests to screen for hearing loss in newborns. Treatment of permanent sensorineural hearing loss through auditory prostheses can be initiated based on these measures and refined once the child learns to respond to sound. Current research indicates that childhood hearing loss is heterogeneous with multiple associated genetic mutations affecting specific structures in the cochlea and/or auditory pathways. Advances in treatments must thus both account for the particular deficit involved and the degree of abnormal change suffered. It is clear that we can limit degenerative changes to the auditory system by restricting the time children are left without hearing and we continue to work on how best to restore hearing to each child.

565 Wrapping It Up - What Do We Know and Where Do We Need to Go?

Kelly Tremblay¹

¹*University of Washington*

Understanding the effects of sensory experience on the brain is a long-standing theme of research, crossing all modalities, in the field of neuroscience. In the auditory domain, motivation comes from at least two streams of scientific inquiry: 1) defining normal processes associated with auditory learning; including, but not limited to speech, language, and music; and 2) using the proposed models of learning to develop effective ways of (re)habilitating impaired perception. Here we wrap up this special session by reviewing what is known about the importance of access to sound, as well as the various ways humans are able to make use of this sound. In attempt to translate this

knowledge into clinical practice, this summary will emphasize gaps in knowledge where basic and applied scientists can work to improve the hearing health of people with communication disorders.

[Work supported, in part, by NIH/NIDCD R01-DC007705]

566 An Approach to Drug Discovery: Screening for Survival and Neurite Promoting Activity on Spiral Ganglion Neurons

Donna S. Whitlon^{1,2}, Mary Grover¹, Sara Fernandez Dunne^{3,4}, Chi-Hao Luan^{3,4}

¹*Department of Otolaryngology, Feinberg School of Medicine, Northwestern University*, ²*Hugh Knowles Center, Northwestern University*, ³*High Throughput Analysis Laboratory, Northwestern University*, ⁴*Department of Molecular Biosciences, Northwestern University*

Background

One key goal in hearing medicine is to develop interventions that will maintain survival and promote neurite regeneration from spiral ganglion neurons. Given the importance of spiral ganglion neurons for normal hearing and for the function of cochlear implants, one would assume that thousands of drugs and chemicals had already been evaluated for survival and neurite promoting activity in the cochlea. This has not happened, however, for a logical reason: Evaluating just one drug or chemical in the ear at multiple concentrations and time points, for effects on hearing and cochlear anatomy is so labor intensive that it is simply not possible to test thousands of drugs or chemicals in hearing loss animal models. Rather than push forward with unique or unknown compounds in the ear, the field has thus far mainly been occupied with factors that were first vetted in other regions of the nervous system. To focus in on interventions aimed at cochlear neurons, a new approach is required to speed up the process and strike a productive balance between discovery and *in vivo* evaluation. To this end, we have developed a novel prescreening procedure to evaluate thousands of compounds in a semi-unbiased manner. The goal is to narrow down a huge field of potential chemicals to a handful of the most promising to promote to *in vivo* evaluation

Methods

Our approach uses a well-characterized and quantified primary culture system of dissociated spiral ganglion from newborn mice. From 8 mouse pups, 192 cultures are generated in 384 well plates, tested, immunolabeled, automatically imaged and quantified. Forty four chemicals and 16 controls can be assayed in quadruplicate using the material generated from 8 mouse pups.

Results

In initial studies we demonstrated that the Rho Kinase inhibitor H-1152 stimulates neurite growth in spiral ganglion cultures. We further demonstrated that other Rho Kinase inhibitors, Fasudil and hydroxyfasudil also stimulated neurite growth, albeit at a higher concentration.

Conclusion

As an example of the utility of our approach, we will demonstrate results acquired in our screen of the NCC clinical collection, a library of over 400 known bioactive compounds. (Supported by ONR grant#N00014-12-1-0173)

567 Generation of Human Inner Ear Prosensory-Like Cells Via Epithelial-To-Mesenchymal Transition

Zhengqing Hu¹, Xuemei Luo^{1,2}, Lei Zhang¹, Fengqing Lu¹, Fengping Dong¹, Edwin Monsell¹, Hui Jiang^{1,3}

¹Wayne State University, ²Fudan University Zhongshan Hospital, ³Fudan University Jinshan Hospital

Background

Mammalian sensory hair cells are vulnerable to numerous insults, such as overstimulation, aging, genetic orders, and ototoxic drugs. Damage to mammalian sensory hair cell is usually irreversible; therefore, degeneration of hair cells generally causes permanent hearing loss, tinnitus, and other inner ear disorders. Generation of hair cell progenitors with the capability of proliferation and differentiation has been suggested as one of the critical steps in hair cell regeneration. It has been documented that mouse inner ear sensory epithelia possess stem/progenitor cells, which show the ability to proliferate and differentiate *in vitro*. However, it remains undetermined: (a) how do adult human utricular cells respond when dissociated and cultured *in vitro*; and (b) whether stem/progenitor cells exist in adult human inner ear sensory epithelia.

Methods

We collected discarded utricles from translabyrinthine surgery and isolated human utricular sensory epithelial cells (HUCs) to explore whether HUCs can proliferate and obtain features of stem/progenitor cells *in vitro* using reverse transcription polymerase chain reaction (RT-PCR) and immunofluorescence.

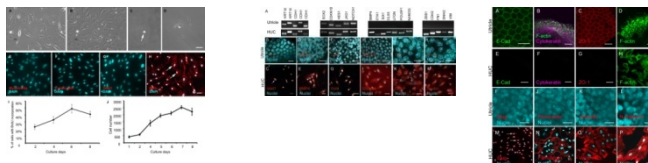
Results

When cultured *in vitro*, dissociated HUCs started to expand on the substrates and express genes and proteins that are widely shown in mesenchymal cells, such as ZEB1, CDH2 (N-Cadherin), FN1 (fibronectin), SNAI2, and VIM (vimentin). Furthermore, HUCs expressed genes and proteins that are usually present in prosensory cells and stem cells, including BMP4, EYA1, SIX1, DLX5, HES1, JAG1, CDKN1B (P27kip1), LFNG, NOTCH1, POU5F1 (Oct4), NANOG, SOX2, GFAP, and SSEA4. HUCs were observed to proliferate for up to 25 passages.

Conclusion

These results reveal that sensory epithelial cells from the adult human inner ear can undergo EMT to re-enter the cell cycle and express genes and proteins that are usually shown in the prosensory cells, which develop into sensory hair cells during development. The outcomes of this study may open avenues for human sensory hair cell generation, which will provide a novel stem cell-based replacement for

inner ear disorders, such as hearing loss, tinnitus, and other inner ear disorders.



568 Dose Response of Hair Cell Damage and Regeneration in the Neonatal Mouse Cochlea

Brandon C. Cox¹, Jian Zuo¹

¹St. Jude Children's Research Hospital

Background

Regeneration of β cells in the pancreas has been well studied and different mechanisms of regeneration occur depending on the amount of initial β cell loss (Nir et al., 2007 *J Clin Invest*; Thorel et al., 2010 *Nature*). We have previously shown that the neonatal mouse cochlea has the capacity to regenerate hair cells (HCs) after damage *in vivo* (Cox et al., 2012 ARO abstract #1066). After ablation of ~80% of neonatal HCs, we observed direct transdifferentiation of supporting cells (SCs) into HCs, as well as a new mechanism of HC regeneration where SCs changed cell fate, expressed early HC markers, and divided. We are now investigating the HC regenerative response that occurs after different amounts of initial HC death.

Methods

We used the HC-specific CreER line, Atoh1-CreERTM, to drive expression of diphtheria toxin, fragment A (DTA) with the ROSA26-loxP-stop-loxP-DTA allele. Tamoxifen injections at postnatal day (P) 0 and P1 achieves ablation of ~80% of HCs, while a single tamoxifen injection at P0 results in ~50% HC loss. We used a second CreER line, Atoh1-CreER^{T2}, with tamoxifen injections at P0/P1 to decrease the amount of HC loss to ~20%. HC regeneration mechanisms were then probed using the Hes5-nlsLacZ allele for fate mapping of SCs and BrdU injections to label cells in S phase.

Results

Both direct transdifferentiation and the new mechanism of HC regeneration were observed with the two smaller amounts of HC damage. We are currently creating a model to decrease the amount of HC loss further.

Conclusion

The neonatal mouse cochlea is able to respond to even a 20% HC loss and maintain the capacity to regenerate HCs using both direct transdifferentiation and mitotic mechanisms.

This work was supported in part by grants from the National Institute of Health (DC006471, DC008800, DC010310, and CA21765 the Office of Naval Research (N000140911014, N000141210191, and N000141210775), and the American Lebanese Syrian Associated Charities (ALSAC) of St. Jude Children's

Research Hospital. J. Zuo is a recipient of The Hartwell Individual Biomedical Research Award.

569 Lineage Tracing Reveals Supporting Cells Contributing to Hair Cell Regeneration in the Neonatal Mouse Cochlea in Vivo

Renjie Chai¹, Ling Tong², Brandon C. Cox³, Kavita Chalasani¹, Tian Wang¹, Angela Xue¹, Vikas Nookala¹, Genevieve Huang¹, Xuan-Phien Pham¹, Jian Zuo³, Edwin Rubel², Alan Cheng¹

¹Department of Otolaryngology-Head and Neck Surgery, Stanford University School of Medicine, ²Department of Otolaryngology-Head and Neck Surgery, University of Washington, ³Department of Developmental Neurobiology, St. Jude Children's Research Hospital

Background

Mammalian hair cell (HC) loss which leads to permanent hearing loss is long considered irreversible. The discovery of HC regeneration in the avian cochlea provided impetus to readdress this assumption. Several important studies have shown that neonatal cochlear supporting cells (SC), unlike those from older ages, displayed limited progenitor cell characteristics including the ability to proliferate and differentiate into HC-like cells in vitro. The relative paucity of efficient models for eliminating cochlear HC in vivo in both neonatal and adult mammals has limited analysis of the regenerative capacity of these SCs.

Methods

Here, we used the Pou4f3DTR transgenic mice where the human diphtheria toxin receptor is expressed specifically in HCs. HCs were ablated on postnatal day (P) 1 or 6 with toxin injection and tissues examined 1-9 days later. In parallel, we fate-mapped Lgr5+ SCs prior to HC loss using the Cre-loxP approach in Pou4f3DTR;Lgr5creERT2;ROSA26RtdTomato mice.

Results

After diphtheria toxin injection at P1, we observed an initial decrease of myosin7a+ HCs between P2-P5 (23% of control at P5) followed by a small but significant increase at P6-P7 (51% at P7) in the apex. This recovery in HC number was transient and most pronounced in the apex, and decreased towards the base. At P7 many myosin7a+ HCs expressed the prosensory/SC marker Sox2 (apex: 36±8; middle: 9±4; base: 0±0), when none were observed in undamaged, time-matched controls. To investigate whether SCs contribute to these potentially regenerated HCs, we fate-mapped Lgr5+ SCs prior to HC ablation in Pou4f3DTR;Lgr5creERT2;ROSA26RtdTomato mice after toxin injection at P1. Compared to controls (Lgr5creERT2;ROSA26RtdTomato), HC loss significantly increased traced tdTomato+/myosin7a+ cells at P7 (99±5, 23±7, 2±1, respectively), many of which also expressed Sox2 (19±6, 3±2, 0±0, respectively). HC damage induced at P6 led to a progressive HC loss without any regeneration. At P9 when cochleae have lost 20-40% of HCs, we did not detect any myosin7a+/Sox2+ cells or increase of tdTomato+/myosin7a+ cells in comparison to controls.

Conclusion

During the early postnatal period, mice have a limited capacity to replenish lost cochlear hair cells in vivo. Regeneration is most evident in the apex and diminishes toward the base. Lineage tracing experiments showed that Lgr5+ SCs contribute to the pool of replacement HCs. Ongoing work will characterize the functionality of fate-mapped, "regenerated" HCs in older cochlea.

570 Ablation of P27^{kip1} in Mouse Auditory Hair Cells Results in Cell Proliferation and Long Term Survival of Postnatally Produced Hair Cells

Bradley Walters¹, Zhiyong Liu¹, Mark Crabtree^{1,2}, Brandon Cox¹, Jian Zuo¹

¹St. Jude Children's Research Hospital, ²University of Bath

Background

p27^{kip1} has a well-established role in the quiescence of supporting cells within the mouse cochlea. However, whether or not p27^{kip1} is expressed, or plays a similar role, in hair cells (HCs) remains unclear.

Methods

To test the role of p27^{kip1} in postnatal HC quiescence, a tamoxifen inducible Cre recombinase transgene driven by a HC-specific Atoh1 enhancer element (Atoh1-CreERTM) was bred into mice homozygous for a p27^{kip1} floxed allele. As a comparator, the Atoh1-CreERTM transgene was also bred into mice homozygous for an Rb floxed allele. Experimental mice from both lines were induced with tamoxifen at postnatal days zero and one, while control animals received vehicle only. To assess proliferation, animals were injected with the thymidine analogs EdU and/or BrdU and cochlear whole mounts were immunostained for these compounds as well as for the mitosis marker phospho-Histone 3. Hearing function was tested via auditory brainstem responses (ABRs).

Results

Cre mediated disruption of p27^{kip1} in cochlear HCs resulted in robust proliferation of inner and outer HCs (IHCs and OHCs, respectively), with many cells progressing through, and completing the cell cycle. Interestingly, there were proportionally more EdU positive IHCs than OHCs, and more EdU positive cells were detected in the apical turns of the cochleae than in middle and basal turns. Additionally, following p27^{kip1} disruption, numerous HCs survived to at least 6 weeks of age, where supernumary HCs were still readily observed in apical turns, and animals retained ABR threshold levels similar to uninduced controls. By comparison, HCs in Atoh1-CreERTM;Rb(floxed) mice also demonstrated robust proliferation, where IHCs appeared more proliferative than OHCs, apical turns were more affected than middle and basal turns, and many cells progressed through the cell cycle. By contrast, however, very few HCs survived to 6 weeks of age after Rb disruption, and these mice exhibited profound hearing loss as measured by ABRs.

Conclusion

Together, the current data suggest that p27^{kip1} is expressed in cochlear HCs and that it contributes to their quiescence. Furthermore, p27^{kip1} presents a significant advantage over Rb as a potential therapeutic target for HC regeneration since the disruption of Rb in HCs adversely affects HC survival and hearing function, while ablation of p27^{kip1} does not.

This work was supported in part by the NIH, the Office of Naval Research, the Hearing Health Foundation, the National Organization for Hearing Research, and the American Lebanese Syrian Associated Charities.

571 MYC Gene Delivery to Adult Mouse Utricles Stimulates Proliferation of Postmitotic Supporting Cells in Vitro

Joseph Burns¹, James Yoo¹, Anthony Atala¹, John Jackson¹

¹Wake Forest Institute for Regenerative Medicine

Background

The inner ears of adult humans and other mammals possess a limited capacity for regenerating sensory hair cells, which can lead to permanent sensory deficits. During development and regeneration, undifferentiated supporting cells within inner ear sensory epithelia can self-renew and give rise to new hair cells; however, these otic progenitors become depleted postnatally. Therefore, reprogramming differentiated supporting cells into otic progenitors is a potential strategy for restoring regenerative potential to the ear. Transient expression of the induced pluripotency transcription factors, Oct3/4, Klf4, Sox2, and c-Myc reprograms fibroblasts into neural progenitors under neural-promoting culture conditions, so as a first step, we explored whether ectopic expression of these factors can reverse supporting cell quiescence in whole organ cultures of adult mouse utricles.

Methods

Utricles were dissected from adult Swiss Webster mice, adhered to glass-bottom dishes, and infected with adenoviruses encoding Oct3/4, Klf4, Sox2, the degradation-resistant T58A mutant of c-Myc (c-MycT58A), or GFP under the control of a cytomegalovirus promoter. Following adenovirus washout, utricles were cultured in growth medium (5% FBS). BrdU was included to label cells in S-phase. To promote differentiation, growth medium was replaced with serum-free differentiation medium containing N2 supplement. The cultures were fixed in 4% paraformaldehyde at the indicated timepoints, labeled with appropriate antibodies, and imaged on a Zeiss LSM 510 microscope.

Results

Co-infection of utricles with adenoviral vectors separately encoding Oct3/4, Klf4, Sox2, or c-MycT58A triggered significant levels of supporting cell S-phase entry as assessed by continuous BrdU labeling. Of the four factors, c-MycT58A alone was both necessary and sufficient for the proliferative response (Fig. 1A). The number of BrdU-

labeled cells plateaued between 5-7 days after infection, and then decreased ~60% by 3 weeks, as many cycling cells appeared to enter apoptosis. Switching to differentiation-promoting culture medium at 5 days after ectopic expression of c-MycT58A temporarily attenuated the loss of BrdU-labeled cells and accompanied a very modest but significant expansion of the sensory epithelium. A small number of the proliferating cells in these cultures labeled for the hair cell marker, myosin VIIA (Fig. 1B), suggesting they had begun differentiating towards a hair cell fate.

Conclusion

The results indicate that ectopic expression of c-MycT58A, in combination with methods for promoting cell survival and differentiation, may restore regenerative potential to supporting cells within the adult mammalian inner ear.

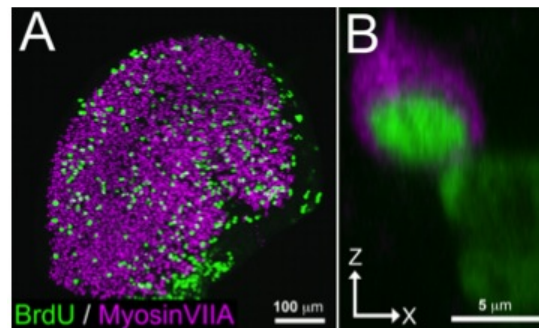


Figure 1: c-MycT58A induces robust proliferation of postmitotic supporting cells in adult mouse utricles (assessed with BrdU labeling, green, A), and some proliferating cells appear to become hair-cell-like cells (myosin VIIA, purple, B).

572 A Comparison of the Effects of BDNF and NT3 Gene Therapy on Peripheral Auditory Fibers and Spiral Ganglion Survival in the Deafened Guinea Pig Inner Ear

Cameron Budenz¹, Hiu Tung Wong¹, Donald Swiderski¹, Yehoash Raphael¹

¹University of Michigan, Kresge Hearing Research Institute

Background

Hair cell loss usually leads to secondary regression of peripheral auditory fibers (PAFs) from the basilar membrane area. Spiral ganglion neurons (SGNs) have a variable survival rate in the deafened ear. Cochlear implants (CI) rehabilitate hearing by bypassing the missing hair cells and directly stimulating the remnant auditory neural structures. Treatment strategies to enhance the survival and health of these remnant auditory neural structures may lead to improved CI outcomes. Prior work has demonstrated that BDNF and NT3 enhance SGN survival and induce PAF regrowth following deafening. To determine which of these neurotrophins performs better in bestowing long term SGN survival and inducing PAF regeneration, we compared the effects of BDNF and NT3 on ears deafened systemically or unilaterally.

Methods

Adult guinea pigs were deafened by either local administration of neomycin into the cochlea or systemic administration of kanamycin and furosemide. BDNF and NT3 were delivered to the adult guinea pig inner ear via adeno-associated viral vectors one week following deafening, and all animals were sacrificed three months following treatment. The extent and pattern of PAF regrowth was assessed on whole mount dissections of the cochlea, and SGN survival was assessed on plastic sections through Rosenthal's canal.

Results

Both BDNF and NT3 promote regrowth of PAFs and enhance survival of SGNs. Ears deafened with neomycin have a complete loss of hair cells and supporting cells in the basal turn, whereas ears systemically deafened have patches of surviving supporting cells. There is no significant difference in the number of PAFs in the basilar membrane area of animals based on the method of deafening; however, in animals systemically deafened there was a negative correlation between the presence of regrown PAFs and the presence of supporting cells.

Conclusion

Gene therapy with either BDNF or NT3 leads to PAF regrowth and enhanced SGN survival, which may in turn lead to improved CI outcomes. Presence of supporting cells may inhibit PAF regeneration into the basilar membrane area.

This work is supported by The Williams Professorship, and NIH/NIDCD grants DC-010412, DC-007634, T32 DC-005356, and P30 DC-05188.

573 Lithium Alters the Morphology of Neurites Regenerating from Cultured Adult Spiral Ganglion Neurons

Samit Shah¹, Chirag Patel¹, Albert Feng¹, Richard Kollmar^{1,2}

¹University of Illinois at Urbana-Champaign, ²SUNY Downstate Medical Center

Background

The small-molecule drug lithium (as a monovalent ion) promotes neurite regeneration and functional recovery, is easy to administer, and is approved for human use to treat bipolar disorder. Lithium exerts its neuritogenic effect mainly by inhibiting glycogen synthase kinase 3, a constitutively-active serine/threonine kinase that is regulated by neurotrophin and "wingless-related MMTV integration site" (Wnt) signaling. In spiral ganglion neurons of the cochlea, the effects of lithium or the function of glycogen synthase kinase 3 have not been investigated. We, therefore, tested whether lithium modulates neuritogenesis from adult spiral ganglion neurons.

Methods

Primary cultures of dissociated spiral ganglion neurons from adult mice were exposed to lithium at concentrations

between 0 and 12.5 mM. The resulting neurite morphology and growth-cone appearance were measured in detail by using immunofluorescence microscopy and image analysis.

Results

We found that lithium altered the morphology of regenerating neurites and their growth cones in a differential, concentration-dependent fashion. Low concentrations of 0.5 to 2.5 mM (around the half-maximal inhibitory concentration for glycogen synthase kinase 3 and the recommended therapeutic concentration for bipolar disorder) enhanced neurite sprouting and branching. A high concentration of 12 mM, in contrast, slowed elongation. As the lithium concentration rose from low to high, the microtubules became increasingly disarranged and the growth cones more arborized.

Conclusion

Our results demonstrate that lithium selectively stimulates phases of neuritogenesis that are driven by microtubule reorganization. In contrast, most other drugs that have previously been tested on spiral ganglion neurons inhibit neurite outgrowth or affect only elongation. Our results are qualitatively and quantitatively consistent with lithium inhibiting glycogen synthase kinase 3 activity in spiral ganglion neurons. Experiments with additional drugs and molecular-genetic tools will be necessary to confirm that glycogen synthase kinase 3 regulates neurite regeneration from spiral ganglion neurons, possibly by integrating neurotrophin and Wnt signals at the growth cone.

574 Derailing Organ of Corti Development: Uncoupling Topology from Cell Type Specification Reveals Causality of Signaling

Bernd Fritsch¹, Israt Jahan¹, Ning Pan¹, Jennifer Kersigo¹

¹University of Iowa

Neurosensory precursor cells differentiate as hair cells and neurons through progressive restriction of their developmental potential. Proneural basic Helix-loop-Helix transcription factors consolidate this decision to differentiate as neurons (Neurogenin1) or hair cells (Atoh1). Atoh1 has been claimed to be both necessary and sufficient to generate hair cells. However, Atoh1 expression in the brain generates cerebellar or cochlear nucleus neurons, indicating that the ear provides the context for Atoh1 to differentiate hair cells. Even in the ear, Atoh1 expression occurs in cells that do not differentiate as hair cells such as inner pillar cells or sensory neurons. Understanding this complexity requires a better appreciation of intra and intercellular signals in the developing organ of Corti. Current data suggest that three neurosensory precursor types exist in the ear: one pure neuronal, one pure hair cell and a mixed type with the possibility to differentiate as either hair cells or neurons. This switching is apparently mediated by a neurogenic transcription factor, Neurod1. Neurod1 is known to regulate neuronal differentiation, but is also expressed in hair cells. Neurod1 null mutants transform some neurons

into hair cells inside the remaining ganglia through de-repression of Atoh1. Likewise, hair cell fate in the apex of the cochlea is influenced by the absence of Neurod1, resulting in premature expression of Atoh1 with a change in hair cell fate: some outer hair cells differentiate to appear more like inner hair cells. Premature and more profound expression of Atoh1 in these mutants can be corrected using haploinsufficiency of Atoh1. This ability of Neurod1 to alter differentiation of hair cells is not possible with Neurog1 knocked into the Atoh1 locus suggesting that at the time Atoh1 is expressed in undifferentiated hair cell precursors these cells are committed to differentiate as hair cells and this fate decision cannot be changed. However, combining 'self-terminating' Atoh1 conditional deletion with knockin replacement of Atoh1 by Neurog1 shows that under these conditions, Neurog1 is able to differentiate hair cells surprisingly normal, indicating that with the exception of an initial early phase for which Atoh1 is essential, other transcription factors might be able to replace Atoh1. Our data suggest that Atoh1 is a differentiation factor needed to drive a specific step in early hair cell development, Hair cell fate decision happens before that step, Atoh1 expression reflects that decision and other transcription factors can partially replace Atoh1 in later steps.

575 Notch Signaling in Cochlear Development: Puzzles and Pathways

Martin Basch¹, Yalda Moayedi-Esfahani¹, Juan Maass¹,
Andrew Groves¹

¹*Baylor College of Medicine*

The Notch signaling pathway has been implicated in the development of sensory tissue in the inner ear, and in regulating the proportion of hair cells and supporting cells that develop in each sensory organ. However, the precise contribution of Notch signaling in the development of the cochlea remains unclear. Although lateral inhibitory Notch signaling through the Notch1 receptor can regulate hair cell and supporting cell differentiation, canonical Notch signaling is not necessary for the development of the prosensory domain from which the organ of Corti derives.

We propose a model in which low levels of Notch signaling are required to establish the neural boundary of the organ of Corti through lateral inductive processes, and higher levels of Notch signaling are required to regulate the proportion of hair cells and supporting cells through lateral inhibition. This model is based on the analysis of a series of Notch pathway mutants of varying severity, and on the blockade of Notch signaling with a variety of inhibitory compounds of varying strength and specificity.

576 Mechanisms of Hair Cell Regeneration in the Zebrafish Lateral Line System

David Raible¹, Ivan Cruz¹, Heather Brignull¹, Eva Ma¹,
Edwin Rubel¹

¹*University of Washington*

BACKGROUND

The mechanosensory lateral line system is used by aquatic vertebrates to detect water flow. Hair cells are located in clusters on the surface of the body called neuromasts. Like hair cells of the inner ear, lateral line hair cells are susceptible to damage from ototoxic compounds such as aminoglycoside antibiotics. We are using the zebrafish lateral line system to study mechanisms controlling the regeneration process.

METHODS

Zebrafish were treated with the aminoglycoside antibiotic neomycin to kill lateral line hair cells. Transgenic zebrafish were used to monitor hair cell replacement. To identify mutations involved in hair cell regeneration, animals were mutagenized with ethylnitrosourea and offspring screened in the F3 generation.

RESULTS

After aminoglycoside exposure, regeneration is rapid with complete hair cell renewal seen by 72 hours. Timelapse analysis demonstrates that new hair cells are derived from symmetrically dividing precursors. Regeneration can occur after repeated damage in adult zebrafish with no loss in potential for recovery. Labeling hair cells with a genetically encoded photoconvertible tag demonstrates that hair cells undergo continuous turnover. Label retention reveals distinct regions of the neuromast have different kinetics of turnover. A screen for mutations that alter regeneration has revealed those that block hair cell replacement. Initial development of neuromasts is normal, suggesting that defects are regeneration specific. Identification of genes that regulate regeneration in zebrafish is underway.

CONCLUSIONS

Taken together our studies suggest that precursors must be continuously generated to replace hair cells lost to damage or turnover.

577 Cell-Cell Interactions That Underlie Cochlear Innervation

Noah Druckenbrod¹, **Lisa Goodrich¹**

¹*Harvard Medical School*

The sense of hearing is mediated by precisely wired connections between hair cells and spiral ganglion neurons (SGN) in the cochlea. Hair cells are organized by optimal frequency along the length of the cochlea, with low frequencies in the apex and high frequencies in the base. Tonotopic information is preserved by the SGNs, which send a single process radially from the ganglion and into the cochlear duct, innervating one inner hair cell. SGNs generally connect with nearby hair cells, only rarely extending processes tangentially within the cochlea. Hence, processes from SGNs in a small sector of the ganglion fasciculate to form radial bundles, thereby creating spokes that radiate along the length of the cochlea. The physical arrangement of SGN processes

therefore reflects the logic of how sound information is encoded.

To create the mature cochlear wiring diagram, SGN processes navigate a complex environment that contains a wide variety of cell types. We have been using genetic tools to label and visualize SGNs, efferents, and glia in the developing cochlea. During the earliest stages of differentiation, SGN neurites grow through the mesenchyme to reach the cochlear duct. Once in the cochlear duct, SGN processes encounter support cells and eventually reach the hair cells. In addition, neural crest-derived glia migrate in from the central nervous system and become tightly associated with SGNs and their processes. All of these events occur in parallel for the cochlear efferents, which originate in the brainstem and grow along the eighth nerve and into the cochlea, extending together with SGN processes in the radial bundles. We find that SGN processes are preceded by a wave of glia. Efferents, on the other hand, follow the afferents, spiraling towards the apex upon reaching the cochlea, and then eventually sending processes into the radial bundles and towards the hair cells. To characterize the interactions between SGNs and surrounding cells, we have established a method for live imaging in embryonic cochlear explants. This has allowed us to analyze the pattern of SGN outgrowth and cell-cell interactions in wild-type cochlea and in mutants with abnormal cochlear wiring patterns. By ablating specific cell types and blocking critical signaling pathways, we have begun to elucidate the rules that govern cochlear wiring.

578 ATP-Dependent Signaling in Supporting Cells of the Developing Cochlea

Han Chin Wang¹, Nicolas X. Tritsch^{1,2}, Ying Xin Zhang¹, Dwight E. Bergles¹

¹Johns Hopkins University, ²Harvard University

Neural circuits that process sensory information exhibit spontaneous, sensory-independent, electrical activity during early development, which has been shown to promote neuronal survival, sculpt electrophysiological properties, and induce refinement of synaptic connections. In the auditory system, neurons fire discrete bursts of action potentials separated by long periods of quiescence prior to hearing onset, events that are initiated by periodic depolarization of hair cells in the developing cochlea. Our studies have focused on understanding the mechanisms responsible for initiating this spontaneous activity, and the effects of this activity on the maturation of cochlea and auditory circuits in the CNS. Studies performed on both acutely isolated and cultured cochleae from prehearing rodents indicate that supporting cells within a developmentally transient expanse of columnar epithelial cells known as Kölliker's organ (also termed the greater epithelial ridge, GER), play a crucial role in triggering hair cell depolarization by periodically releasing ATP. The release of ATP from these cells sets in motion a cascade of events that results in generation of bursts of action potentials in spiral ganglion neurons. Pharmacological and physiological manipulations in excised cochleae indicate

that extracellular ATP binds to purinergic autoreceptors (primarily P2Y receptors), causing elevation of intracellular Ca^{2+} and opening Ca^{2+} -activated Cl^- channels. The resulting efflux of Cl^- has two main consequences: (1) it induces cell shrinkage (crenation) due to the concomitant movement of water to maintain osmotic balance, and (2) it forces efflux of K^+ to maintain ionic balance. K^+ that is released into the extracellular space accumulates around inner hair cells, inducing depolarization, Ca^{2+} action potentials, glutamate release and eventual excitation of spiral ganglion neurons. In addition, the depolarizing shift in the equilibrium potential for K^+ that occurs around inner hair cells during ATP-evoked events enhances the release probability of cholinergic efferent fibers. This spontaneous activity declines abruptly after the ear canal is drained of fluid and normal hearing thresholds are established, due to a cessation of ATP release from inner supporting cells. Together, these results suggest that ATP signaling in supporting cells of the cochlea plays a crucial role in initiating spontaneous electrical activity in the auditory system during early development.

579 Expression of Human Pendrin Rescues Hearing in Mice Lacking Mouse Pendrin

Philine Wangemann¹, Xiangming Li¹, Fei Zhou¹, Joel Sanneman¹, Donald Harbidge¹, Dominique Eladari², Daniel C. Marcus¹

¹Kansas State University, ²INSERM U872, Équipe 3, 15 Rue de l'École de Médecine, Esc. E RDC, F-75006 Paris, France

Background

Mutations of *SLC26A4*, the gene coding for pendrin, are a common cause for deafness associated with an enlargement of the vestibular aqueduct (EVA). *Slc26a4*^{-/-} mice, a model for EVA, develop an abnormal enlargement of the membranous labyrinth and fail to develop hearing and balance. The goal of this study was to determine whether limited expression of human pendrin can prevent enlargement of the membranous labyrinth and rescue hearing and balance.

Methods

A transgene was generated to express human pendrin under the promoter of the B1-subunit of the V-H⁺ ATPase, *Atp6v1b1*. This transgene was crossed into *Slc26a4*^{-/-} mice to generate Tg(+)*Slc26a4*^{-/-} and Tg(-)*Slc26a4*^{-/-} as well as Tg(+)*Slc26a4*^{+/+} and Tg(+)*Slc26a4*^{+/-} mice. Auditory brain stem recordings were used to determine hearing thresholds and RotoRod was used to test balance. RT-PCR was used to determine the expression of *Atp6v1b1* mRNA during cochlear development and to differentiate between expression of human and mouse *Slc26a4* mRNA. Immunocytochemistry was used to evaluate pendrin protein expression without distinction of species origin.

Results

Between embryonic day (E) 14.5 and postnatal day (P) 8 *Slc26a4*^{+/-} and *Slc26a4*^{-/-} mice expressed similar levels of *Atp6v1b1* mRNA in the cochlea. This finding makes it likely that mRNA for human pendrin is expressed at similar levels in Tg(+)*Slc26a4*^{-/-} and Tg(+)*Slc26a4*^{+/-} mice.

Tg(+)Slc26a4^{-/-} mice expressed human Slc26a4 mRNA in the cochlea, however, there was no evidence for significant pendrin protein expression. In particular, there was no evidence for pendrin protein expression in the lateral wall or in the spiral limbus, the site that is known to express *Atp6v1b1* mRNA (Karet et al., 1999). Most interestingly, Tg(+)Slc26a4^{-/-} mice developed normal hearing and balance. Hearing thresholds in Tg(+)Slc26a4^{-/-} mice were similar to thresholds in Tg(+)Slc26a4^{+/+} and Tg(+)Slc26a4^{+/-} mice and RotaRod tests revealed no difference between Tg(+)Slc26a4^{-/-} and Tg(+)Slc26a4^{+/-} mice. In contrast, Tg(-)Slc26a4^{-/-} failed to develop hearing and balance thereby resembling the established phenotype (Everett et al., 2001; Wangemann et al., 2007).
Conclusions

Limited expression of human pendrin protein in the membranous labyrinth of Tg(+)Slc26a4^{-/-} mice is sufficient to rescue the development of normal hearing. This finding in conjunction with the fact that pendrin expression is required for the development but not for the maintenance of hearing (Choi et al., 2011) opens the prospect that a spatially and temporally limited therapy may be sufficient to restore a life-time of normal hearing in mice and possibly in human patients carrying mutations of *SLC26A4*.

NIH-R01-DC012151, KCALSI, KINBRE and NIH-P20-RR017686

580 Overview of Sound Sensitivity

Brian Moore¹

¹University of Cambridge

Hyperacusis refers to abnormally sensitive hearing, such that normally tolerable sounds are perceived as excessively loud and/or as unpleasant. It is not associated with unusually low (good) thresholds for detecting sounds. Rather, hyperacusis is manifested by aversive reactions to sounds that are clearly audible but would not normally lead to such reactions. It is useful to distinguish between cases where sounds are perceived as louder than normal, and cases where sounds are not abnormally loud but are nevertheless aversive.

Greater than normal loudness can occur via several mechanisms: (1) Defective operation of the stapedius reflex can lead to greater loudness of low-frequency sounds. (2) Loudness recruitment associated with cochlear hearing loss involves a more rapid than usual growth of loudness with increase in stimulus level once the elevated detection threshold is exceeded. Although loudness often approaches "normal" values for high input levels, sometimes "over-recruitment" occurs, such that high-level sounds appear louder than normal. This effect can be predicted by a loudness model (Moore and Glasberg 2004). It seems to be a consequence of loss of amplitude compression in the cochlea and reduced frequency selectivity. (3) The gain of the central auditory system may be increased following peripheral hearing loss. (4) The functioning of the efferent system may be impaired. This system serves to regulate the gain of the active mechanism in the cochlea. If a signal is sent from the brain to the cochlea with "instructions" to reduce the gain, but

the actual gain reduction is less than it should be, the mismatch may be interpreted as excessive loudness.

In other cases, loudness is not the dominant factor. When fear is the dominant factor, the term phonophobia is often used. Dislike of a sound is described as misophonia. These negative emotions sometimes arise as a result of an unpleasant event or experience occurring at the same time as or associated with sound, but such an event cannot always be identified. Once an association is set up, exposure to the "trigger" sounds can result in an over-activation of the limbic and autonomic nervous systems, causing a "fight or flight" response which is itself unpleasant and reinforces the negative associations with sound.

In conclusion, hyperacusis can occur via a variety of mechanisms, both peripheral and central.

MOORE BCJ, GLASBERG BR. A revised model of loudness perception applied to cochlear hearing loss. *Hear. Res.* 188:70-88, 2004.

581 The Impact of Hyperacusis on an Individual's Life

Monica Weinberg¹

¹New York School of Medicine

The impact of hyperacusis on an individual's life: Monica Weinberg MD, New York School of Medicine. Dr. Weinberg suffers from hyperacusis

Hyperacusis typically has a significant impact on every part of a person's life, from their work, their home environment, and virtually every social setting. Depending on the severity of one's symptoms, hyperacusis patients can develop symptoms of ear pain and worsening tinnitus when exposed to certain sounds greater than ~60-75 dB HL. Hyperacusis patients frequently focus on escaping these pain-inducing sound sources. For some patients, the cycle of pain typically induced from a single new exposure can last from hours to days or weeks. As patients stabilize they are often confused about how to determine the risk level to various social settings. For example how can a person determine if a new cycle of pain may be created from a sporting event or child's musical performance? Should they wear ear protection to be safe? What can they do if an old filling needs to be drilled out? Can additional damage be done? The anticipation and subsequent impact can be very disabling yet hyperacusis is not classified as a disability, and few in the general population or healthcare professions are aware of hyperacusis.

The impact on the hyperacusis patient's family and social involvement is also significant as friends see a very different person. The joy that came from seeing a favorite performance or movie is replaced with anxiety and ear pain if the patient risks exposing their ears to the event. There is isolation and loneliness if the patient drops all effort to participate in the key social activities that made up

their pre-hyperacusis life. Additional tension and frustration can be added to many relationships unless the friend or family member takes an active role in understanding and supporting the unique challenges the hyperacusis patient now experiences on a regular basis.

It is important for auditory researchers and clinicians to hear from someone who lives with the negative impact of hyperacusis and has found positive ways to cope. Additionally, this presentation will help health care professionals better understand what a patient is experiencing, which will allow them to have a more educated approach in dealing with the patient's symptoms.

582 The Epidemiology and Etiology of Hyperacusis

David Baguley¹

¹*Cambridge University Hospitals*

The epidemiology and etiology of hyperacusis: David Baguley PhD, Audiology, Cambridge University Hospitals, Cambridge UK

Data regarding the epidemiology of hyperacusis is sparse. Indications are that 40% of individuals with clinically-significant tinnitus experience reduced sound tolerance. Regarding the general population, there are few population studies available, but the distinction between dislike of intense sound and decreased sound tolerance in general is not clearly made, and an overestimate of prevalence is possible. Baguley and McFerran (2011) derived an estimate of the prevalence of significant hyperacusis at 2% of the adult population. If correct, this indicates a public health problem of some significance.

There are a number of medical conditions which can involve hyperacusis, including Lyme Disease, Addison's Disease, head injury, migraine and depression. In many cases, however, the sound tolerance issues remain idiopathic. Associations between Autistic Spectrum Disorders and hyperacusis have been reported, but much further work is required.

This presentation will report what is presently known about the epidemiology and etiology of hyperacusis, and where there are significant gaps in our knowledge. The need for information about the mechanisms of hyperacusis to guide treatment interventions will be discussed.

583 Diagnosing Hyperacusis and Measuring Hyperacusis Severity

James Henry^{1,2}

¹*VA National Center for Rehabilitative Auditory Research,*

²*Oregon Health & Science Dept. of Otolaryngology*

A key challenge to diagnosing hyperacusis is that we do not have specific physical exam findings or imaging tests that provide a standard to accurately diagnose and assess hyperacusis. Loudness Discomfort Level (LDL) diagnostic testing currently performed by audiologists has a high degree of subjectivity. Additionally, LDL testing can induce anxiety in patients with hyperacusis, as they are required

to listen to sounds that push their limits of sound tolerance. There is currently no measure of overall hyperacusis impact that combines both psychological and functional impact. We have developed a brief assessment tool, the Tinnitus and Hearing Survey (THS), which includes questions designed to determine if a patient has any degree of a sound tolerance problem. Using the THS, patients with severe sound intolerance are scheduled for a full assessment using primarily the Sound Tolerance Interview to diagnose the extent of the problem and to determine treatment options. Further testing may include in-clinic trials of ear-level sound generators to determine their potential utility in mitigating the condition. The development of a Hypersensitivity Severity Index would be useful in clinical practice to measure improvement rates of hyperacusis patients. Furthermore, no etiology or underlying mechanism in the auditory pathway has been demonstrated to cause hyperacusis. Possible mechanisms include the following: biochemical changes in the peripheral auditory system, auditory efferent dysfunction, a change in central auditory gain, and alterations in the limbic response systems to loud sounds. This presentation will explore current diagnostic methods and offer suggestions for potential approaches for researchers to explore.

584 Hyperacusis Treatment Options

William Martin¹

¹*Oregon Health & Science University*

Hyperacusis treatment options: William Martin PhD, Oregon Health & Science University.

Currently, primary treatment approaches have centered on sound therapy to desensitize the patients' responses to certain sounds. A popular approach is a habituation training process based on the Tinnitus Retraining Therapy (TRT) methodology which was established by Jastreboff & Hazel for improving tinnitus patients' condition. There are numerous approaches that are similar from pink noise for music players to neuromonics. Another aspect is that the etiology of hyperacusis can vary, and therefore it is important to recognize that each hyperacusis patient is different. There may be variability in optimal treatment from patient to patient. This presentation will review the current approaches and the evidence associated with their success.

585 Comparison of Hair Cells and Supporting Cells by DeepCAGE Sequencing

Judith Kempfle^{1,2}, Shannan Ho Sui³, Winston Hide³, Albert Edge¹

¹*Massachusetts Eye and Ear Infirmary, Harvard Medical School, Boston,*

²*University of Tuebingen, Dept of Otolaryngology,*

³*Harvard School of Public Health, Boston*

Background

Although supporting cells and hair cells have a common embryologic origin, their phenotypes become fixed in the mature, post-mitotic cochlea, and hair cells do not regenerate in adult mammals. A subset of Sox2-Lgr5-double positive supporting cells can divide and differentiate

into hair cells after isolation from neonatal mice and are thought to harbor stem cell potential.

Methods

We isolated inner ear stem cells as neurospheres from neonatal ears and subjected them to differentiating conditions that generate hair cells. We also sorted Atoh1-GFP positive hair cells and Sox2-GFP positive supporting cells from neonatal organ of Corti. We used deepCAGE sequencing in collaboration with the FANTOM5 project to gain further information about expression patterns. Bioinformatics tools such as DAVID and Opossum were used for analysis. Genes related to signaling pathways of hair cell differentiation were confirmed by quantitative RT-PCR analysis of the different cell types.

Results

We compared transcription factor expression in supporting cells and hair cells and assessed inner ear neurospheres for changes in pathway activity and transcription factor expression during differentiation. Several genes expressed in other stem cells in the FANTOM database, HMGA2 and *lrx1*, were highly expressed in proliferating inner ear stem cells, and several genes expressed after differentiation of inner ear stem cells, such as *Twist2* and *Hlx*, were also higher in hair cells than in supporting cells. Genes such as *Foxd3*, which maintains progenitor status and is important for stem cell self-renewal, were expressed more in supporting cells than in hair cells. In addition, pathway imprinting technology and changes in transcriptional start sites yielded further insight into differentiation of inner ear progenitors. Wnt, Notch and retinoic acid pathways were active during differentiation. Quantitative RT-PCR analysis of the different cell types confirmed the expression patterns in our bioinformatics screen.

Conclusion

Comparison of hair cells and supporting cells indicated progenitor properties of supporting cells, and inner ear stem cells during proliferation used pathways of other progenitor cells. They converted to a more hair cell-like phenotype upon differentiation. A better knowledge and understanding of transcription factor expression in the conversion of inner ear stem cell to hair cell will provide important insights for regeneration of hair cells.

586 Investigating Hair Cell Regeneration Through Integrated Genomic Datasets

Nicole Renaud¹, Yuan-Chieh Ku¹, Rose Veile¹, Cynthia Helms¹, Mark Warchol¹, Michael Lovett¹

¹Washington University School of Medicine

Background

Lower vertebrates are capable of inner ear hair cell (HC) regeneration, but mammals have little capacity to replace these essential mechano-electrical transducers. We seek to understand the regenerative process by comparing the genetic and regulatory architecture of the regenerating avian utricle and cochlea, and by directly modifying specific pathways during avian regeneration.

Methods

We employed next generation nucleic acid sequencing (RNA-seq) to derive complete transcriptome information from regenerating avian utricle and cochlea organotypic cultures. Pure SE were collected at 24 hour intervals over a 168 hour time course following aminoglycoside ablation of HCs. Transcriptomes were computationally assembled from biological replicate samples and were compared to untreated control samples that were cultured in parallel.

Results

The utricular and cochlear regeneration time courses share ~2,300 differentially expressed genes. Both datasets contain remarkably dynamic patterns of gene expression that correlate with the onset of the phenotypic conversion of supporting cells (SC) to HCs. There are also major differences in the temporal regulation and specific components of Notch signaling, Hedgehog signaling, and apoptosis pathways between utricle and cochlea regeneration. In particular, *Atoh1*, *Notch*, and *Hes* gene expression profiles and gene family members, differ significantly between the two SE.

The statistically significant up and down regulation of transcription factors (TFs) in the databases—647 and 217 differentially expressed in the cochlea and utricle respectively—suggest complex, and possibly different, regulatory networks are working in the two SE. The overwhelming majority of these TFs have never been investigated in HC regeneration.

Our datasets are a valuable new resource for identifying new HC and SC markers. By statistical clustering methods we have identified a set of ~500 new HC-specific genes (and have validated a subset of these by immunohistochemistry). Several of these are novel HC-specific TFs shared between the two SE.

Conclusion

We have derived comprehensive measurements of the transcriptome changes that occur in organotypic cultures during avian utricular and cochlear HC regeneration. The insights gained from these databases suggest that there are a core set of ~2,000 transcriptional changes that overlap between the two SE. These most probably encompass the core signals for HC regeneration. There are also several hundred differences in TF programs between the two SE that may point at pathways for cochlea and utricle SE functional specialization.

587 High-Frequency Human Middle-Ear Model with Compound Eardrum and Airway Branching in Mastoid Air Cells

Douglas Keefe¹

¹Boys Town National Research Hospital

Background

The goal is to construct a high-frequency acoustical/mechanical model of human middle-ear function and validate it against published measurements. The

model has novel eardrum and middle-ear cleft elements. The eardrum is represented by two components, one component bounded along the manubrium and the other multi-modal component bounded by the tympanic cavity. The eardrum components are additionally coupled to one another by a time-delayed impedance. The middle-ear cleft is an acoustically coupled system of the tympanic cavity, aditus, antrum, and mastoid air cell system (MACS).

Methods

Modeling of ossicular, cochlear, and oval- and round-window function based on a one-dimensional transfer-matrix approach generally follows past studies. The two eardrum components are coupled by a compliant, lossy impedance. Each middle-ear cleft component is represented by a viscothermal acoustic transmission line. A symmetrical binary airway model with 12 generations of airway branchings is constructed for the MACS, in which airway radius and length decrease to 0.2 mm. The MACS input impedance is efficiently calculated over all airways using recursion. Model parameters are fitted to published measurements in human subject ear canals of energy reflectance (0.25-13 kHz) and eardrum input admittance (0.25-11 kHz), and to published temporal-bone measurements of sound pressure in scala vestibuli and scala tympani (0.1-11 kHz). Intracochlear pressure measurements with middle-ear cavities open are modeled using a radiation impedance as the terminating impedance.

Results

The MACS model has total volume of 6.4 ml and surface area of 107 cm², similar to mean dimensions from CT scan analyses of temporal bones. The middle-ear model optimization produced an adequate fit to all data. The two-component eardrum with time delay helps fit intracochlear pressure responses. A multi-modal representation of the eardrum and the high-frequency transmission-line model of the middle-ear cleft help fit ear-canal responses. The eardrum input reactance is small at high frequencies (i.e., not mass controlled). The high-frequency eardrum resonances and the MACS model are critically important in explaining this, and in predicting the frequency dependence of energy reflectance. The ability to accurately explain intracochlear pressure data also explains the input pressure difference acting on the cochlea.

Conclusion

The model accurately fits middle-ear responses to high frequencies, and is well suited for the study of middle-ear dysfunction and for integration into models of cochlear mechanics.

588 High-Speed Video Analysis of Ossicular Chain of Near-Intact Guinea Pig Middle Ear

Tetsuro Yasui¹, Mitsuru Ohashi¹, Nozomu Matsumoto¹, Shizuo Komune¹

¹Kyushu University

Background

The actual, acoustic vibration of ossicular chain in the middle ear has not been easy to analyze.

Methods

We investigated ossicular movement in the intact middle ear in response to acoustic stimulation using a high-speed videocamera and video analysis software. The high-speed videocamera could record analyzable ossicular motion up to 1kHz. We made visual access to the middle ear of deeply anesthetized guinea pig by opening ventral wall of otic capsule without injuring sound conductive structures from external auditory canal to oval window.

Results

The stapes showed reciprocal movement in the same frequency with the stimulating tone, and with amplitude partially proportional to the stimulating sound intensity. Injury to the tympanic membrane or round window influenced the mechanical properties of the stapedia motion. When the middle ear was stimulated with multiple tones, the stapes showed complex waveforms whose original stimulating frequencies could be later analyzed and recovered after Fourier transformation.

Conclusion

Our experimental setup was capable of evaluating the conductive hearing regardless of the status of sensorineural hearing or even life. The video analysis may become a powerful tool to investigate middle ear physiology.

589 Biomechanical Properties of Human and Porcine Auricular Cartilage

David Zopf¹, Colleen Flanagan¹, Annie Mitsak¹, Vishnu Rajendran¹, Glenn Green¹, Scott Hollister¹

¹University of Michigan

Background

Genetic defects involving mutations of collagen subtypes often result in phenotypic abnormalities of the external cartilaginous auricle as well as hearing. Several studies have detailed the biomechanical properties for septal, costal, and articular cartilages. However, the biomechanical properties of auricular cartilage are largely undescribed. Therefore, it is of interest to determine the biomechanical properties of the cartilage of the external ear.

Methods

Auricular cartilage specimens were harvested from six fresh porcine and six fresh human cadaveric ears. Mechanic properties were determined with an Alliance RT/30 MTS material testing machine. For porcine cartilage two punch biopsies were taken from each ear at a proximal (adjacent to the mastoid), mid, and distal site

along the cartilaginous framework. Duplicate specimens were taken and placed in Lactated Ringers solution.

The first test that was run on each porcine punch biopsy specimen was a stress relaxation confined compression test. The parameters for this test included confined compression in a compression chamber 6 mm in diameter, to 10% strain, 500N load cell, a preload hold time of 10 min, test speed of 300 um/sec, and a test temperature of 37 C. After overnight relaxation, they were then subjected to a 60% strain unconfined compression test, also carried out using the 500N load cell. The preload was maintained for 3 minutes duration.

For human cartilage, the ear was first subjected to a whole ear helix down unconfined compression test in order to determine overall flexibility/stiffness of the specimen – a method previously unreported in literature. Afterwards, punch biopsies were taken from each ear and subjected to both 10% strain confined compression test as well as the 60% unconfined compression test as described above.

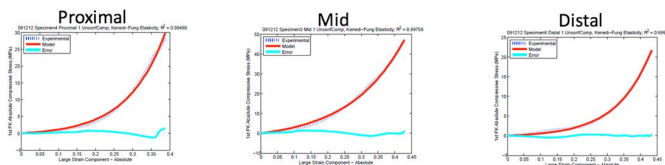
To assess for regional differences in the complex conformation of the human auricle, biopsies were obtained from standardized locations: root of the helix, posterosuperior helix, triangular fossa, conchal bowl, and tragus.

Results

Aggregate modulus and offset yields are provided for porcine and human auricular cartilage. A quasilinear viscoelastic model from stress relaxation data and nonlinear elastic curve using Kenedi-Fung model from unconfined compression data are proposed with graphic representative fits.

Conclusion

Defining robust auricular cartilage biomechanical data allows for comparative indices in analysis of genetic defects affecting collagen subtypes that may have phenotypic biomechanical variation of the external cartilaginous auricle. Both human and porcine auricular cartilage is characterized.



590 Simulator and Mechanical Model Development for Middle Ear Surgery

Guillaume Kazmitcheff^{1,2}, Mathieu Miroir¹, Christian Duriez², Yann Nguyen^{1,3}, Evelyne Ferrary^{1,3}, Olivier Sterkers^{1,3}, Stephane Cotin², Alexis Bozorg Grayeli^{1,3}
¹INSERM, UMR-S 867, Univ. Paris Diderot, Sorbonne Paris Cite, France, ²Shacra Inria Lille Nord Europe, Univ. Lille 1, France, ³Otolaryngology-Head and Neck Surgery department, Beaujon Hospital AP-HP, Clichy, France

Background

Otologic surgical simulators currently available do not allow interaction with the ossicular chain. To improve

teaching interest of these tools, a simulator based on a finite element mechanical model of the ossicles as well as their ligaments and muscles was developed. The objective of this study was to evaluate the mechanical behavior of this model with sound transfer function and sound pressure (tympanometry) simulations.

Methods

A surface model of the ossicular chain and muscles of the tympanic cavity was created from a three-dimensional anatomical data published. Ligaments and muscles were implemented according to the anatomical and physical characteristics reported in literature with Blender (Amsterdam, Netherlands). The model was integrated into the medical simulation software, SOFA (INRIA, France).

Mechanical parameters (Young's modulus, density, Poisson's ratio ...) of the ossicles were defined based on the literature's data. The experimental results of the transfer function and forces pressures were compared to results from studies on temporal bones and other finite element models.

Results

A sine wave was applied to malleus and the vibration of the stapes was measured. At 250 Hz and 90 dB SPL, the peak-to-peak displacement of the stapes footplate was 22.4 nm. It increased slightly to 53.8 nm at 1000 Hz before falling sharply to 0.54 nm to 8000 Hz. These measures were in good agreement with measurements on human temporal bones. The evaluation by simulated tympanometry consisted to apply a force to the umbo corresponding to the variation of the pressure in the external ear meatus and to observe the motion of the umbo. These tests showed displacements similar to temporal bones measurements. In case of simulation of annular ligament ankylosis, the displacement decreased slightly whereas a removal stapes yielded to higher motion for high pressure.

Conclusion

Tests have shown that the mechanical behavior of our model was compatible with the experimental data. The mechanical model combined with our surgery simulator was in accordance with the published data on the temporal bones. This model will be used as a training tool for residents on various surgical pathologies.

591 Motion of the Tympanic Membrane in Acute Otitis Media Model of Chinchilla

Measured with Scanning Laser Vibrometry
Rong Gan¹, Xiyang Guan¹, Xiangming Zhang¹, Vikrant Palan², Mario Pineda²

¹University of Oklahoma, ²Polytec, Inc.

Background

Acute otitis media (AOM) arises from acute infection of the middle ear and is caused in about 70% of cases by bacteria. Haemophilus influenzae, a bacterium found in the human nasopharynx, is an opportunistic pathogen that now is the most common cause of human otitis media. There are no reports describing middle ear biomechanical

function changes in AOM induced by this Gram-negative bacterium.

Methods

Sound-induced motion of the tympanic membrane (TM) in eight chinchillas with AOM was measured using a scanning laser vibrometer (PSV-400, Polytec). AOM was produced by transbullar injection of H. influenzae strain 86-028NP into the left ear and the right ear served as the uninfected control. Four days after challenge, the auditory brainstem response (ABR) and wideband tympanometry were conducted in the animals. The full view of displacement of the TM was acquired by PSV system when a multi-tone stimulus was applied on the TM at the ear canal from 0.2 to 10 kHz.

Results

The wideband tympanograms show that all AOM ears had negative middle ear pressure, and the energy absorbance in AOM ears was lower than that in control ears. ABR thresholds in AOM ears were increased compared with control ears. This finding indicated that hearing loss was associated with AOM even at this early time post challenge of the chinchilla ear with bacteria. The displacements at the umbo and four quadrants of the TM show that there was a significant reduction in the superior-posterior and inferior-posterior quadrants of the TM at frequency below 2 kHz in AOM ears compared to controls. At higher frequencies (2-10 kHz), the reduction was observed only in the superior-posterior quadrant.

Conclusion

3D motion of the entire TM in H. influenzae-induced AOM ears of chinchillas was characterized using the scanning laser vibrometer with the measurements of ABR and wideband tympanometry. The results suggest that there probably exists a correlation between 3D motion of the TM and sound energy transmission into the middle ear as measured in control and AOM ears. (Supported by NIH R01DC011585)

592 Department of Defense Hearing Center of Excellence: Providing Facilitation of Translational Research in Auditory Injuries

Mark Packer^{1,2}, Tanisha Hammill¹

¹Department of Defense Hearing Center of Excellence,

²United States Air Force

Background

Military service members are routinely exposed to hazardous environments leading to auditory injuries which diminish quality of life and affect the war fighters' ability to hear and communicate safely on the battlefield. The US Department of Veteran's Affairs has documented that impairment of the auditory system currently affects over 1,500,000 individuals, accounting for the two most prevalent disabilities, tinnitus and hearing loss, claimed among all veterans.

In 2009, Congress established the Department of Defense Hearing Center of Excellence (HCE) to address

prevention, diagnosis, mitigation, treatment and rehabilitation of hearing loss and auditory system injury for the DOD and the VA. The Air Force was designated as the Lead Component with the goal of ensuring optimal DOD and VA collaboration.

Methods

The HCE research mission is "to facilitate a DoD- and Veteran-wide practice-based research network which will coordinate the identification of and solutions to unsolved problems related to the prevention, diagnosis, mitigation, rehabilitation, treatment, and restoration of hearing loss and auditory injury among US military and Veteran populations." Focus areas include:

Provide research tools that promote, and encourage involvement, and remote partnerships among a collaborative network of clinicians, scientists, and cohorts. Longitudinal tracking database to identify injury patterns and best clinical practices.

Prioritized translational strategies for research outcomes.

Scientific steering and review of auditory research projects and programs.

Streamlined administrative processes

Results

The HCE has established the DoD Auditory Research Working Group, and expanded it to include technical experts across the VA and NIH, to include a Scientific Advisory Board capacity. The HCE will work with portfolio managers to identify all Federal hearing and balance projects, as well as to serve as a central coordinator for academic/industry collaboration. The HCE has organized several work streams through this networked effort. The Hearing Center of Excellence has identified potential value in integrating research efforts with sister DoD CoEs and has developed a model and initiated discussion with other CoEs to develop a roadmap based on this common model.

Conclusion

The intent of organizing a transparent, coordinated practice-based research network is to encourage and facilitate the conduct of research, and the development of best practices. Based on the foundation of information management, outreach and allied research, the ultimate measures of HCE success will be the effect of this networked system on the prevention of hearing loss, and the outcomes of the health care delivered to those that suffer auditory injury.

593 The Public Health Importance of Noise-Induced Hearing Loss

William Clark¹

¹Washington University School of Medicine

Although cochlear physiologists and anatomists had used excessive noise in their labs as a tool to study the effects of damage to the cochlea or auditory nervous system for decades, the general problem of noise-induced hearing loss as a medical condition that required assessment and rehabilitation awaited the end of World War II, and the resultant need to treat the "casualties" who were returning

from combat. In his memoirs, Hallowell Davis detailed the development of this new field, which he and his colleagues coined "Audiology" because the military personnel used the term "Auricular Training", which sounded like teaching them to wiggle their ears! In the 1950's and 1960's the basic science work of Bekesy, Davis, Wever, Lawrence, Kiang, Zwislocki, Schuknecht, Hawkins, Tonndorf, and others provided important, new information about cochlear function, anatomical correlates of noise injury, and behavioral effects of excessive noise exposure. In industry, state worker's compensation laws were introduced to compensate individuals whose hearing was damaged by occupational noise exposure, and increasing efforts to reduce NIHL in the military were introduced. This combination of events led to the implementation of federal regulations governing exposure to noise in the workplace, first established as the Walsh Healey Act in 1969, and then promulgated by OSHA as the Noise Control Act of 1972. This act has not been substantively changed since its inception, except by an amendment establishing hearing conservation programs in 1983.

But what we know about auditory physiology and noise induced hearing loss has exploded since 1975. This session, honoring Barbara Bohne and Don Henderson, reflects what we have learned since they joined the field, and features seven individuals whose efforts have helped to define our current state of knowledge about noise induced hearing loss and possible mechanisms to prevent or treat it. My presentation summarizes our current knowledge about the public health importance of NIHL: how many people are affected; the contributions of occupational and leisure noise; are children more at risk than previously thought; what are other effects of noise besides NIHL, and how does or should our current knowledge inform the regulatory agenda?

The inaugural Midwinter Meeting of the ARO was in January, 1978, at the Happy Dolphin in St. Pete Beach. Barbara and I were presenters, and Don Henderson was, as well. The hotel rate was \$15/night. Certainly, a lot has changed since 1978, but not the regulations. Should they?

594 Noise-Related Hair Cell Death and Preservation of Endolymph/Perilymph Boundaries in the Bohne Labyrinth

Kevin K. Ohlemiller¹

¹*Washington University School of Medicine*

Cochlear hair cell injury and loss are the best predictors of noise-induced permanent threshold shifts (NIPTS) in animal models. Hair cell cuticular plates form part of the boundary of the endolymphatic space. Thus, large or prolonged openings (or gaps) in the reticular lamina may lead to a decrease in the endocochlear potential (EP) and elevate potassium levels in the organ of Corti, potentially amplifying injury. Such openings might take the form of 'holes' left by degenerating hair cells or reticular lamina 'ruptures' caused by direct mechanical trauma. Selective pressure to save what can be saved, and to preserve as much hearing as possible, might be expected to favor efficient closure of holes and ruptures and quick restoration of endolymphatic boundaries. Some causes of

hair-cell loss (aging, inflammation) are evolutionarily old, while damaging noise is 'new'. It is unclear whether noise, aging, inflammation, and ototoxins engage the same processes for disposal of damaged hair cells, or how the mode of cell death (necrotic/apoptotic/'3rd pathway') modifies death processes (Bohne et al., HR 2007; Lee et al., *Open Otorhinolaryngol. J.* 2008; Bohne & Harding, ARO 2012). Few studies have been designed to detect holes or ruptures, or to distinguish the exposure conditions or models that favor one form of injury over another. In chinchillas and guinea pigs, holes may form after even moderate noise exposure (Bohne & Rabbitt, HR 1983; Fredelius et al., *Acta Otolaryngol.* 1988; Ahmad et al., HR 2003), while ruptures require much higher levels (Bohne, *Effects of Noise on Hearing* 1976; Henderson et al., HR 1994; Wang et al., JARO 2002). I will consider evidence for holes versus ruptures as distinct processes, and the implications for cochlear damage and protection.

595 You Say "Toughening", I Say "Conditioning", Let's Call the Whole Thing Off

Barbara Canlon¹, Inna Meltser¹

¹*Karolinska Institutet*

 You say toughening and I say conditioning.
Toughening, conditioning, toughening, conditioning.
Let's call the whole thing off! Both toughening and conditioning are active processes induced by low-level, non-damaging acoustic stimulation that creates long-term protection to subsequent detrimental forms of noise trauma. This phenomenon is now shown to occur in a variety of mammals, including gerbils, chinchillas, guinea pigs, rabbits, rats, mice and human subjects. Different paradigms have been proven successful in preventing a variety of pathological changes to the auditory system. Even though toughening and conditioning experiments are well-documented methods of protecting against hearing loss, the underlying mechanisms have not been well characterized. Several mechanisms have been suggested to play a role in auditory protection by sound conditioning including the activation of antioxidant enzymes, inhibition of apoptosis, increased efferent activity and glucocorticoid activation. This review will discuss these different mechanisms.

596 What Otoacoustic Emissions Have Told Us About Noise-Induced Hearing Loss

Brenda Lonsbury-Martin^{1,2}, Glen Martin^{1,2}, Barden Stagner¹

¹*Research Service, VA Loma Linda Healthcare System,*

²*Dept of Otolaryngology--Head & Neck Surgery, Loma Linda University Medical Center*

Soon after the discovery of otoacoustic emissions (OAEs), early reports described their general properties in normal ears in terms of their spontaneity, or their production with various types of acoustic stimuli. The next phase of articles illustrated the effects of various hearing impairments on the assorted OAEs. This presentation will provide an overview of prior studies that used OAEs to investigate NIHL. Such investigations utilized research in

experimental models, attempts to detect occupational NIHL, or clinical case-study descriptions of emissions in patients with NIHL symptoms. Given that the initial pathology underlying NIHL entails damage to, or destruction of, the organ of Corti's outer hair cells (OHCs), it was expected that OAEs, which are generated by OHCs, would faithfully describe the behavioral audiogram in humans and/or the underlying cochlear pathology in experimental models. On a population basis, this expectation was usually born out. However, in general, using OAE tests, it is difficult to predict either the pattern of behavioral hearing or the underlying cochlear pathology on an individual basis. Among the reasons for explaining disagreements between the various response measures is the field's present knowledge about distinct and complex sources that contribute to the generation of OAEs. Nevertheless, current research findings will be discussed that hold promise for the ability of future OAE tests to detect early NIHL, and to accurately predict its associated hearing pattern and/or cochlear pathology.

597 Tinnitus and Hyperacusis: Involvement of Auditory and Nonauditory Structures

Richard Salvi¹, Guang-Di Chen¹, Daniel Stolzberg¹, Ed Lobarinas²

¹University at Buffalo, ²University of Florida

Background: Exposure to intense noise or ototoxic drugs not only results in hearing loss, but often leads to tinnitus and hyperacusis. The aberrant neural activity responsible for tinnitus and hyperacusis was believed to originate within the classical auditory pathway; however, more recent data suggest the potential involvement of nonauditory structures in the CNS. Here we review some of the neurophysiological changes seen in the cochlea and CNS when rats are treated with a dose of salicylate that induces tinnitus and hyperacusis-like behavior.

Methods: Operant conditioning techniques and the startle reflex were used to identify doses of salicylate that produce tinnitus and hyperacusis-like behavior in rats. Afterwards, we characterized the aberrant patterns of neural activity in the cochlea, auditory pathway and nonauditory sites.

Results: High-dose salicylate (i.p.) caused a frequency-dependent loss in DPOAE and reductions in CAP amplitude; losses were greatest at low and high frequencies and least in the mid-frequencies (10-20 kHz). Salicylate induced threshold shifts in the central auditory pathway that mirrored the cochlear losses, but did not significantly alter spontaneous activity. Despite the threshold shifts and reduced cochlear output (hypoactivity), sound-evoked responses in auditory cortex, medial geniculate, amygdala, striatum and hippocampus were larger than normal at suprathreshold intensities (hyperactivity). Moreover, many low-CF and high-CF neurons in auditory cortex and amygdala shifted their CF into the mid-frequencies. These up-shifts and down-shifts resulted in an over-representation of mid-CF neurons; the expanded mid-CF region lies near the tinnitus pitch induced by salicylate. To eliminate peripheral drug effects, salicylate was applied to the amygdala or auditory cortex,

while recording from the auditory cortex. In both cases, salicylate increased sound-evoked activity in auditory cortex at suprathreshold levels, but did not alter threshold. **Conclusion:** Salicylate exerts potent effects on the cochlea, central auditory pathway and non-auditory regions of the CNS. Salicylate-induced thresholds shifts originate in the cochlea whereas sound-evoked hyperactivity, a possible correlate of hyperacusis, likely originates at auditory and nonauditory sites in the CNS. The salicylate-induced tonotopic shifts seen in auditory cortex, which may underlie tinnitus, likely results from both peripheral and central changes.

Research supported by NIH (R01DC009091; R01DC009219, F31DC010931) and ONR (N0001412107).

598 Translating Data Into Knowledge and Action: Challenges in Evidence-Based Hearing Loss Prevention

Thais Morata¹

¹National Institute for Occupational Safety and Health

Background: Evidence-based practices seek to ensure that the best available scientific evidence is used in clinical decision making. Such approach requires assessing all scientific evidence available on the risks and benefits of interventions and diagnostic procedures. Evidence quality is assessed based on the source type (from meta-analyses and systematic reviews of randomized clinical trials as high-quality sources, down to conventional wisdom as low-quality ones), currency, statistical validity, clinical relevance, and peer-review acceptance. The 2009 American Recovery and Reinvestment Act included a provision for federal funding to investigate how different interventions compare to each other. The Act called on the Institute of Medicine to recommend comparative effectiveness research priority topics. Their recommendations are in the report Initial National Priorities for Comparative Effectiveness Research (<http://www.nap.edu/catalog/12648.html>). The need for research on hearing loss interventions was placed in the highest priority group. This recommendation underscores the human and societal costs of the condition. The risk of hearing impairment increases with age and is exacerbated by exposure to noise, particularly at work. This risk can be minimized by reducing noise levels to 85 dB(A) or less. Many countries have mandated hearing loss prevention programs when noise exposures cannot be reduced to this level. However, the continuing high rate of noise-induced hearing loss raises concerns on the effectiveness of these programs.

Methods: Recent Cochrane Reviews investigated various initiatives and mechanisms (e.g., legislation, proper hearing protector usage, etc.) to determine which work best to either promote the use of hearing protections, and/or reduce noise exposure or hearing loss among workers.

Results: Results from intervention effectiveness studies on hearing loss prevention do not provide evidence to support current practices. There is consensus in the literature that some interventions improve the use of hearing protection devices compared to non-intervention; there is low quality

evidence that legislation can reduce noise levels in workplaces, and contradictory evidence that prevention programs are effective in the long-term. Most reported interventions focus on the use of hearing protectors, and effectiveness depends on the quality of the implementation of prevention programs. Substantial noise control can be achieved in the workplace, with no evidence of this practice in the literature.

Conclusions: Better and large scale implementation of technical interventions and evaluation of their long-term effects are necessary to identify the most effective strategies for reducing occupational hearing loss.

599 Frequency Discrimination Through Phase Locking

Tobias Reichenbach¹, A. J. Hudspeth¹

¹The Rockefeller University

Background

Humans can discriminate frequencies that are only about 0.2% apart when the frequencies are below 4 kHz. For comparison, a semitone in Western music represents a frequency step of about 6%. Frequencies higher than 4 kHz are increasingly hard to differentiate; as an example, the frequency-discrimination threshold at 6 kHz is about 1.5%. This contrasts with tuning curves of auditory-nerve fibers, which are considerably sharper for high-frequency than for low-frequency fibers. The enhanced frequency discrimination below 4 kHz has been hypothesized to involve the phase locking of specialized neurons in the auditory brain stem that fire at a preferred phase of stimulation.

Methods

We performed psychoacoustic experiments to directly measure the effect of phase locking on frequency discrimination. We generated tones based on a single frequency but in which a random phase change occurred every few cycles. These tones were presented to subjects who performed a frequency-discrimination task. In a theoretical work we then investigated how the frequency information contained in phase locking might be read out in neural networks. We specifically used numerical and analytical techniques to study a class of random neural networks in which signal propagation from one neuron to another induces a time delay and in which the neurons perform coincidence detection.

Results

Our psychophysical experiments showed that random phase changes systematically impede our ability to discriminate frequencies. The frequency resolution in the presence of phase changes is bad as that for short tones whose duration is limited to the time between two subsequent phase changes. We found that the neural networks can perform sharp frequency discrimination when stimulated with phase-locked input: different frequencies induce different neural activity patterns. The frequency resolution achieved by this means depends on the noise in the phase locking and can, for realistic values, reach the

minute frequency differences of around 0.2% that have been measured in humans.

Conclusion

Our psychophysical experiments provide direct evidence that phase locking is employed for frequency discrimination. Our theoretical study on a class of random neural networks with temporal delay and coincidence detection offers a framework for how the brain can read out the temporal information contained in phase locking.

600 Spectral Ripple Discrimination in Infants: Effect of Ripple Depth and Envelope Phase Randomization

David Horn^{1,2}, Lynne Werner^{2,3}, Jay Rubinstein^{1,2}, JongHo Won⁴

¹Department of Otolaryngology - Head and Neck Surgery, University of Washington School of Medicine, ²Virginia Merrill Bloedel Hearing Research Institute, Seattle, WA, ³Department of Speech and Hearing Sciences, University of Washington, ⁴Department of Audiology and Speech Pathology, University of Tennessee Health Science Center

Background

Spectral ripple discrimination (SRD) measures sensitivity to spectral change across a broad frequency range. In infants, SRD might be affected by developmental differences in non-spectral factors, such as intensity resolution, attention, or listening strategy. In Experiment 1, we measured infants' and adults' SRD thresholds at various ripple depths to determine the spectral modulation transfer function (SMTF). It was predicted that SMTF height would be lower in infants due to immature intensity resolution and/or attention, while SMTF slopes would be equivalent between age groups due to mature spectral resolution. In Experiment 2, two stimulus conditions were used to determine whether either age group relied on within channel listening strategies. It was predicted that availability of within-channel intensity cues would not affect SRD in either age group.

Methods

Participants were normal-hearing 7-month-olds and young adults. Stimuli were broad-band noise bursts filtered by a full-wave rectified sinusoidal spectral envelope with logarithmically-spaced peaks. The Observer-based Psychoacoustical Procedure was used to determine the highest ripple density at which a participant could detect a 90° phase shift in the spectral envelope. In experiment 1, ripple depth was varied between subjects and SRD threshold in ripple density was assessed. In experiment 2, two stimulus conditions were created based on the starting phase of the spectral envelope: Constant (starting phase was always 0°) and Randomized (starting phase varied from 0° to 270°). Stimulus condition was varied between subjects and SRD threshold assessed.

Results

In experiment 1 the effect of ripple depth and age group on SRD threshold was measured using ANOVA. Main effects of age-group (adults with better thresholds than infants)

and ripple depth (better thresholds at higher ripple depths) both reached significance. The interaction between age-group and ripple depth did not reach significance, suggesting that SMTF slope was similar between age groups. Results from Experiment 2 preliminarily suggest no significant main effect of stimulus condition on SRD thresholds in either age group.

Conclusion

As expected, SMTF slopes were similar between infants and adults, reflecting mature spectral resolution by 7 months old. Differences in SMTF height between age groups, possibly reflecting immature intensity resolution, illustrate that SMTF slope is a better measure of spectral resolution in infants than SRD threshold at a single ripple depth. Preliminary data from Experiment 2 suggest that neither infants nor adults rely heavily on within-channel intensity cues in an SRD task.

601 Comparative Measures of Temporal Coherence

Erikson Neilans¹, Micheal L. Dent¹

¹University at Buffalo, SUNY

Background

Being able to hear and isolate communication signals in the environment is important for both humans and animals. In humans, we know that basic acoustic parameters such as frequency, loudness, and timing, from different sound sources are important in the perceptual isolation or streaming of multiple auditory objects (Bregman, 1990). Relative to humans, however, little work has been devoted to how animals isolate sound sources to create auditory objects and even less is known about the comparative psychology of auditory stream segregation. Frequency separation of sounds is arguably the most common parameter studied in auditory scene analysis and has been shown to be an important feature for streaming auditory objects in both humans and birds. However, frequency separation of sounds is not the only factor influencing auditory scene analysis, as the relative timing of sounds in the acoustic environment appears important as well (Elhilali, et al., 2009, van Noorden, 1975). Elhilali et al. (2009) found that in humans, synchronous tones are heard as a single auditory stream, even at large frequency separations, compared to asynchronous tones with the same frequency separations, which are perceived as two sounds. These findings demonstrate how both timing and frequency separation of sounds are important for auditory scene analysis. It is unclear how animals such as budgerigars (*Melopsittacus undulatus*) would perceive synchronous and asynchronous sounds.

Methods

In the present study, both budgerigars and humans were trained and tested using the same operant conditioning procedures to investigate the perception of synchronous, asynchronous, and partially overlapping pure tones and budgerigar contact calls.

Results

Results illustrate that budgerigars segregate partially overlapping sounds in a manner predicted by computational models of streaming. Additionally, both budgerigars and human listeners have trouble segregating harmonic stimuli compared to non-harmonic stimuli of the same duration. These results support previous research illustrating that harmonic sounds most often originate from the same sound source and are more likely to be perceived as one stream (Carylon, 2004; Alain, 2007). Interestingly, for both budgerigars and humans listeners, overlapping budgerigar contact calls and sine-wave bird calls are more likely to be segregated than pure tone stimuli with the same temporal overlap.

Conclusion

These results further support the idea that frequency separation has little influence in how overlapping complex, communication stimuli are segregated, considering the two sets of stimuli fall within the same spectral range.

602 Auditory Streaming of Syllables: Words Fuse More Readily Than Non-Words

Robert Carlyon¹, Alex Billig¹, John Deeks¹, Jolijn

Monstrey¹, Matthew Davis¹

¹Medical Research Council

Background

The extent to which auditory streaming is influenced by high-level cognitive processes remains a matter of debate. We investigated whether streaming is influenced by linguistic processes, by studying whether streaming of a repeated syllable depends on whether it is a word or a non-word.

Methods

We presented listeners with single spoken syllables (a real word, “stem”, “stone” or a non-word, “stome”, “sten”) repeated every 673 ms for 150 sec. Listeners continuously judged whether they heard the syllables as fused or whether the initial /s/ of each syllable formed a separate stream. We obtained an objective measure of streaming by asking listeners to detect an occasional silent gap of between 20-50 ms long, inserted after the initial /s/ of some “target” syllables.

Results

After a few seconds the initial /s/ was reported to stream apart from the remainder of the sound and the percept then fluctuated in a bi-stable manner between the veridical syllable and a two-stream percept of an isolated fricative /s/ plus the remainder of the syllable. This is an instance of the “Verbal Transformation Effect” (VTE); the lack of aspiration when a /t/ is preceded by /s/, leads to a streamed percept containing the words (“den”, “dome”) or non-words (“dem”, “dohne”). Note that this streaming effect transforms words (“stem” and “stone”) into non-words (“dem” and “dohne”), and vice-versa (for “sten” and “stome”). Performance on the gap-detection task was better at times when the listener reported hearing a single stream than when the /s/ was streamed off. Importantly, it

was also better when the fused percept corresponded to a word than when it corresponded to a non-word. This provides evidence that the segregation of the sequence into two streams, or, conversely, its integration into a single stream, was influenced by the lexical status of the repeated syllables. Note that this finding cannot be attributed to low-level acoustic-phonetic factors, since the vowel (/o/ or /e/) and final consonant (/m/ or /n/) occurred equally in lexical and non-lexical stimuli.

Conclusion

Our results are consistent with the following conclusions: a) auditory streaming of speech sounds is affected by lexicality, b) the verbal transformation effect can be driven by streaming, and c) perceptual organisation of speech is sensitive to lexical status. These findings illustrate how high-level cognitive processes influence auditory and speech perception.

603 Rhythm Perception in Macaque Monkeys

Elena Selezneva¹, Susann Deike¹, Henning Scheich¹, Andre Brechmann¹, Stanislava Knyazeva¹, Michael Brosch¹

¹Leibniz Institut

Background

The capacity to rhythmically organize isochronous series of external stimuli is found in all humans. It requires that a subject extracts periodicities from isochronous stimuli and makes periodic temporal anticipation of future events. Concomitant with these operation, the sensory processing and the speed of perception of stimuli concurrent with the regular temporal grid is facilitated. It is unknown whether nonhuman primates are also endowed with this perceptual ability.

Methods

We constructed a tone sequence that was composed of repeating triplets of two short (50 ms) tones and one long (200 ms) tone and that was presented at a constant pulse of 150 tones per minute. This sequence was contrasted with an irregular sequence of the same number of short and long tones and the same pulse. Human listeners perceptually organize the regular sequence into triplets with two weak beats followed by a strong beat.

Results

In a first study on humans we show that the different perceptual organizations of regular and irregular sequences are reflected in different abilities of subjects to detect tones of intermediate duration (100 ms) that are occasionally presented in place of a long tone. We then show that monkeys that are passively exposed to the same sequences more frequently changed their facial expressions or their gaze during deviant presentation when the deviants were embedded in a regular sequence. We also show that approximately one quarter of 175 multiunits recorded from primary auditory cortex of monkeys fired more spikes, in a particular time range, to

regularly presented tones than to irregularly presented tones.

Conclusion

These results suggests that monkeys are capable to hold external stimuli in memory over several seconds. Monkeys are able to extract periodicities from isochronous stimuli and to make periodic temporal anticipation of future events. Thus the cognitive ability to hierarchically organize a stimulus sequence appears to be part of the 'natural' and innate behavior of monkeys. It also implies that some of the characteristics of the music and language faculty in humans may be based on sensory mechanisms and sensory-motor transformations already present in the last common ancestor of nonhuman primates and humans.

604 Concurrent Speech Segregation Based on the Pitch Strength of Iterated Rippled Noise

Marjorie R. Leek^{1,2}, Frederick J. Gallun^{1,2}, Michelle R. Molis^{1,2}, Heather M. Belding^{1,2}

¹Portland VA Medical Center, ²Oregon Health & Science University

Background

In a sound environment with overlapping talkers, voice pitch provides a strong cue to segregation of one speaker among others. We investigated the role of pitch strength in speech-in-background identification for normal-hearing (NH) and hearing-impaired (HI) listeners. Iterated Rippled Noises (IRNs) were created by delaying a noise, applying a gain, and adding this copied noise to the original noise. IRNs produce a pitch that varies in strength with the number of iterations (successive delayed copies added together) as well as with the gain applied to each copy before addition to the original.

Methods

Speech from the Coordinate Response Measure corpus was processed into a series of 16-ms overlapping time windows from which the frequency spectrum was extracted through Fourier analysis. The amplitude spectrum of each window was combined with the phase spectrum of similarly-windowed IRNs and converted back to the time-domain via an inverse Fourier transform. The resulting time waveform contained the frequency contours of speech but the temporal patterns of the IRNs. Target speech was developed with an IRN delay of 10 ms (100 Hz - a voice pitch common for male talkers). Masker speech was generated using two independently generated IRNs, each with a delay of 4.45 ms (224.5 Hz pitch - typical of female speech). Target and masker IRNs were generated with the same number of iterations (2, 4, or 8) and a range of gain factors. The task of the listener was to identify keywords in sentences spoken by the male talker in the presence of the female talker maskers.

Results

For all IRN conditions, identification performance was considerably worse for hearing-impaired subjects than for normal-hearing subjects. However, for both listener

groups, better target speech identification was observed for the greater number of iterations, and, to a lesser extent, as the gain increased. Nearly all listeners showed improvements as the pitch strength increased.

Conclusion

Increases in pitch strength of target speech sounds overlapping in time with other talkers results in a consistent and beneficial effect on speech identification for both NH and HI listeners. However, listeners with hearing impairment have great difficulty overall using pitch of IRN to support speech-in-background identification. This is likely a result of the generally weaker pitches produced by IRNs in the impaired auditory system, which may in turn be related to an inability to perceive temporal fine structure. [Work supported by NIDCD]

605 Molecular Mechanisms of Deafness Mutations Disrupting Tip-Link Function and Hair-Cell Transduction

Marcos Sotomayor¹, Wilhelm A Weihofen², Rachelle Gaudet³, David P Corey⁴

¹Harvard Medical School, ²Harvard University / Novartis, ³Harvard University, ⁴HHMI / Harvard Medical School

Background

Mechanical force from sound waves or head movements is directly conveyed to hair-cell transduction channels by tip links, fine filaments thought to be formed by two atypical cadherins: protocadherin-15 and cadherin-23. These two proteins are essential for inner-ear mechanotransduction, they are products of deafness genes, and they feature long extracellular domains that interact tip-to-tip in a calcium-dependent manner. However, the molecular architecture of the complex is unknown, and the molecular mechanisms leading to cadherin-related deafness remain largely unexplored.

Methods

Here we combine X-ray crystallography, molecular dynamics simulations, and binding experiments to characterize the cadherin-23/protocadherin-15 bond and to understand molecular mechanisms by which deafness mutations disrupt tip-link function.

Results

X-ray crystallography revealed a stable and unique overlapped antiparallel heterodimer comprising the two most N-terminal cadherin repeats (EC1+2) of each protein. This "handshake"-like interaction was found to be mechanically stronger than that of classical cadherins, based on molecular dynamics simulations and binding experiments. We suggest that it might be specially adapted to withstand large mechanical forces produced by loud sound. We also find that deafness mutations within the handshake may disrupt tip-link function through impaired complex formation (PCDH15-R113G), impaired calcium binding (CDH23-D101G), subtle weakening of structural stability (CDH23-S47P), or impaired folding (PCDH15-D157G). Interestingly, the different effects of the

deafness mutations, studied with biochemistry, correlate with the severity of the reported inner-ear phenotype.

Conclusion

Our results shed light on the molecular mechanics of hair-cell sensory transduction and may help develop tailored treatments for cadherin-mediated deafness.

606 Noddy, a New Mouse Model for Hereditary Deafness, Illuminates the Function of Protocadherin-15 in Inner Ear Hair-Cell Tip Link

Ruishuang Geng¹, Marcos Sotomayor², Kimberly Kinder¹, Suhasini R. Gopal¹, John Gerka-Stuyt¹, Daniel H.-C. Chen¹, Rachel E. Hardisty-Hughes³, Greg Ball³, Andrew J. Parker³, Rachelle Gaudet⁴, David N. Furness⁵, Steve D. M. Brown³, David P. Corey², **Kumar N. Alagramam¹**

¹Case Western Reserve University, ²Howard Hughes Medical Institute, Harvard University, ³MRC Mammalian Genetics Unit, ⁴Harvard University, ⁵Keele University

Background

Considerable evidence now indicates that tip links, structures thought to gate the mechanotransducer channels of the inner ear hair cells, are formed by a tetramer of two cadherin proteins: protocadherin 15 (PCDH15) and cadherin 23 (CDH23), which have 11 and 27 extracellular cadherin (EC) repeats, respectively. Mutations in either PCDH15 or CDH23 often cause inner ear disorders in mice and humans. Using in vitro approaches, we recently showed that PCDH15 and CDH23 bind tip-to-tip in a "handshake" mode that involves EC1 and EC2 repeats of both proteins. However, a paucity of appropriate animal models has slowed our understanding both of the interaction and of how mutations of residues within the predicted interface compromise the integrity of the tip link and consequence of disabling the handshake in vivo. Here, we present noddy, a new mouse model for hereditary deafness and vestibular dysfunction.

Methods

From a recessive N-ethyl-N-nitrosourea (ENU) mutagenesis screen, we identified mice with hearing impairment and abnormal balance. One such line showed lack of an auditory startle response and head-bobbing, and so was named noddy. Various in vivo and in vitro approaches were used to characterize the phenotype and mutation in the noddy mutant mice.

Results

Here we report on a new ENU-induced mouse mutant, noddy, which harbors a missense mutation (I108N) in PCDH15 EC1-the first reported missense mutation in the mouse Pcdh15. Binding of PCDH15-CDH23 fragments is impaired by this mutation in vitro, as indicated by isothermal titration calorimetry experiments. Thus, noddy mutant mice allowed us to test the functional consequences of blocking the handshake interaction in vivo: Noddy homozygotes are completely deaf, mechanotransduction is absent, and hair bundles are fragmented and misoriented. Yet the PCDH15 protein

appears to localize normally to the tips of stereocilia. These studies confirm the critical importance of a residue within the putative handshake interface, illustrate, in vivo, how a subtle missense mutation in the tip link can produce deafness and balance disorders, and introduce the first mouse model for this kind of tip-link missense mutation

Conclusion

The data presented here offer new insights into the interaction between PCDH15 and CDH23, and help explain the etiology of human deafness linked to mutations in the tip-link interface.

607 TMHS Is an Integral Component of the Mechanotransduction Machinery of Cochlear Hair Cells

Ulrich Mueller¹, Wei Xiong¹, Nicolas Grillet¹, Heather Elledge¹, Thomas Wagner¹, Bo Zhao¹, Kenneth Johnson², Piotr Kazmierczak¹

¹The Scripps Research Institute, ²Jackson Laboratory

Background

Hair cells are mechanosensors for the perception of sound, acceleration and fluid motion. Mechanotransduction channels in hair cells are gated by tip links, which connect the stereocilia of a hair cell in the direction of their mechanical sensitivity. The molecular constituents of the mechanotransduction channels of hair cells are not known.

Methods

To identify components of the mechanotransduction machinery of hair cells, including ion channel subunits, we have analyzed mechanotransduction currents in mouse lines afflicted with hearing impairment. We have also studied the function of the affected proteins by biochemical, cell biological and physiological means.

Results

Here we show that mechanotransduction is impaired in mice lacking the tetraspan TMHS. TMHS binds to the tip-link component PCDH15 and regulates tip-link assembly, a process that is disrupted by deafness-causing Tmhs mutations. TMHS also regulates transducer channel conductance and is required for fast channel adaptation.

Conclusion

TMHS therefore resembles other ion channel regulatory subunits such as the TARPs of AMPA receptors that facilitate channel transport and regulate the properties of pore-forming channel subunits. We conclude that TMHS is an integral component of the hair cells mechanotransduction machinery that functionally couples PCDH15 to the transduction channel.

608 Activated Radixin Is the Major Actin-To-Membrane Connector of Stereocilia

Matthew Avenarius¹, Jocelyn Krey¹, Hongyu Zhao¹, Clive Morgan¹, Manfred Auer², Peter Gillespie¹

¹Oregon Health & Science University, ²Lawrence Berkeley National Laboratory

Background

Radixin (RDX) is a member of the ezrin-radixin-moesin (ERM) family, which serves to organize cell-cortex membrane domains by coupling membrane proteins to actin filaments. Hair-cell stereocilia apparently require at least one ERM member for development. RDX can be activated by sequential binding to phosphatidylinositol 4,5-bisphosphate (PIP2) and phosphorylation; activation unfolds RDX, allowing the C-terminus to bind to actin and the N-terminus to bind to membrane proteins or adapters like SLC9A3R2 (NHERF2).

Methods

We used mass spectrometry to identify and quantify proteins of hair bundles purified from P0 chicken utricles and P21-P25 mouse utricles. We identified and quantified stereocilia structures using electron tomography. We transfected mouse hair cells with in utero electroporation at E12.5, and localized proteins in chicken, mouse, and frog hair cells with immunocytochemistry and confocal microscopy. Protein abundance was assessed with immunoblotting.

Results

RDX was abundant in vestibular stereocilia, present at ~7,000 molecules per stereocilium in chicken and ~4,000 molecules in mouse. By electron tomography, chicken stereocilia had ~7,000 actin-to-membrane connectors. SLC9A3R2 was present at ~30% that level in each species' stereocilia. In frog hair cells, RDX was found at the periphery of the stereocilia core; in the longitudinal axis, RDX decreased from tapers to tips. An antibody that recognizes activated ERM proteins only recognized RDX above the tapers. The lower edge of the reactivity corresponded exactly to the boundary between the glycosphingolipid (taper) and PIP2 (shaft) membrane domains. In chicken utricle stereocilia, SLC9A3R2 was located in a pattern that was overlapping but not identical to that of RDX. SLC9A3R2 co-immunoprecipitated with RDX extracted from partially-purified mouse stereocilia; binding selectivity of the SLC9A3R2 PDZ domains suggests that it could bind to GPR98 and USH2A, as well as to CDH23 and PCDH15. In mouse cochlear hair cells at P6.5, GFP-RDX was absent from tapers but present in stereocilia shafts, which was confirmed using immunocytochemistry with an anti-RDX antibody.

Conclusion

That localization of GFP-RDX was identical to that of wild-type RDX indicates that we will be able to use mutant RDX constructs to further dissect the role of this protein in stereocilia function. RDX is the only protein present in stereocilia that is present at a high enough concentration,

and is in the right place, to be the principal actin-to-membrane connector of stereocilia.

609 Developmental Changes in the Mechanotransducer Channels of Cochlear Hair Cells and Their Regulation by Transmembrane Channel-Like Proteins

Kyunghee X. Kim¹, Robert Fettiplace¹

¹*University of Wisconsin*

Background

The first step in sound detection is vibration of the stereociliary bundles of cochlear hair cells to activate calcium selective mechanotransducer (MT) channels. Although the molecular identity of the MT channels is still uncertain, recent evidence indicates that Tmc1 and Tmc2, isoforms of the transmembrane channel like family, play a key role in transduction (Kawashima et al 2011). We have followed these findings by investigating the effects of Tmc knockouts on MT channel properties.

Methods

We examined variations in the hair cell mechanotransducer (MT) channels along the cochlea's tonotopic axis in wild-type, Tmc1^{-/-} and Tmc2^{-/-} mice between post natal day (P)0 and P10. Patch clamp recordings were made from inner hair cells (IHC) and outer hair cells (OHC) in apical, middle and basal regions of isolated organs of Corti and hair bundles were stimulated with a fluid jet to determine the maximum current. The relative calcium permeability of the MT channel, P_{Ca}, in different hair cells was inferred from measurements of reversal potentials in 100 mM external calcium.

Results

MT amplitudes OHCs increased about 1.5-fold from cochlear apex to base but there was little change in IHCs. Similar values were obtained in wild type and mutant mice in the first post-natal week, but after P7, the OHC MT current in the Tmc1^{-/-} (dn) declined to zero, which may account for the deafness phenotype (Steel & Bock 1980). The calcium permeability of the MT channel, P_{Ca}, in different hair cells showed a small but significant decrease from apex to base in OHCs but not in IHCs of wild-type mice up to P6. In Tmc1^{-/-}, P_{Ca} in basal OHCs increased to equal that of apical OHCs whereas in Tmc2^{-/-}, P_{Ca} was reduced in both apical and basal OHCs. In older mice after P7, P_{Ca} in apical OHCs decreased to equal that at the base, but P_{Ca} in IHCs was unaltered. In Tmc2^{-/-}, P_{Ca} was reduced in IHCs at all ages.

Conclusion

We suggest that differences in calcium permeability reflect different subunit compositions of the MT channel which are determined by expression of Tmc1 and Tmc2, the latter conferring higher P_{Ca} in apical OHCs and IHCs. Changes in P_{Ca} with maturation are consistent with a later down-regulation of Tmc2 in OHCs but not in IHCs. The significance of the transition at about P7, though not understood, is accompanied by other developmental changes in the hair cells. Supported by RO1DC01362

610 Cochlear Adaptation Is Not Driven by Calcium Entry

Anthony Peng¹, Thomas Effertz¹, Anthony Ricci¹

¹*Stanford University*

Background

To hear, animals rely on specialized mechanosensory hair cells. All hair cells feature a mechanosensory organelle called a hair bundle that is comprised of actin-filled microvilli, termed stereocilia, arranged in a staircase pattern. Deflection of the hair bundle causes activation of mechano-electrical transduction (MET) channels. MET currents decrease in the face of a constant hair bundle deflection by a process called adaptation, where additional stimulation recovers lost current. Though significant controversy exists over the mechanisms of adaptation, it is universally found that calcium drives adaptation. This data largely comes from frog saccule, turtle auditory papilla, and chick cochlea, with some supporting data from mammalian vestibular and cochlear cells.

Methods

Whole-cell patch clamp recording of rat inner and outer hair cells was performed. Hair bundles were stimulated using stiff probes driven by a macroscale piezo actuator.

Results

While further studying the effects of calcium in mammalian cochlear hair cells, we find that rat IHCs and OHCs show robust adaptation at depolarized potentials, when there is no calcium entry. To confirm this result, we performed experiments using different internal calcium buffering conditions and find robust adaptation both when intracellular calcium levels are high or low. Finally, we lowered extracellular calcium with different internal calcium buffering, and again, we find robust adaptation. Shifts observed in activation curves in the presence of low external calcium are independent of internal buffering therefore appear to be due to an extracellular effect.

Conclusion

Overall, contrary to accepted adaptation mechanisms, we find that calcium entry is not required for adaptation in mammalian cochlear hair cells.

This work was supported by RO1 DC0003896 to AJR, F32 DC010975 to AWP, DAAD Fellowship to TE and NIDCD Core Grant P30-44992.

611 Audio-Visual Interactions in Modulation Discrimination Are Modality Specific

Adrian Rees¹, Anjana Prabhu¹, Quoc Vuong¹

¹*Institute of Neuroscience, Newcastle University,*

Newcastle upon Tyne, NE2 4HH, UK

Background

The McGurk and ventriloquist effects attest to the power of cross modal interactions between seeing and hearing. Studies with more abstract stimuli than lips and speech demonstrate that visual information influences sound position, but we know little about how visual stimuli

influence the hearing of temporal features in sound and vice versa. We report a unidirectional cross modal influence on participants' ability to discriminate the modulation depths of sounds and shapes.

Methods

In Experiment 1, participants were sequentially presented with pairs of sinusoidally amplitude-modulated sounds and responded whether the modulation depth of each pair was the same or different. Sounds were 250-Hz pure tones modulated at 2 Hz with depths between 20% and 58% and duration 1.5s. The modulation depth of each sound pair could differ by 0% to 32% in 8% steps. Sounds were presented alone and in two audio-visual conditions. In the latter conditions, the sound in one interval was accompanied by a cuboid that was modulated about its long axis (rate 2Hz, depth 70%) in phase with the sound modulation. The cuboid was presented with either the least or the most modulated sound.

In Experiment 2, new participants discriminated the modulation depth of cuboid pairs with depths between 10% and 18%. The modulation depth of each pair differed by 0% to 8% in 2% steps. Stimuli were presented alone, or with one interval accompanied by an amplitude-modulated sound (rate 2Hz, depth 70%). The sound was paired with either the least or most modulated visual stimulus on each trial.

Results

When participants judged the modulation of the two sounds in Experiment 1, the presence of the amplitude-modulated cuboid significantly impaired their ability to discriminate sound modulation depth, relative to the sound-only condition, when the shape was paired with the least modulated sound. There was a trend towards enhanced discrimination when the shape was paired with the most modulated sound. This finding suggests that the visual stimulus enhanced the perceived modulation of the accompanying sound so that participants found it more or less difficult to discriminate sound pairs depending on the interval in which the shape was presented. The presence of the modulated sound in Experiment 2 had no impact on the discrimination of visual shape modulation.

Conclusion

We conclude that the discrimination of modulated sounds is influenced by shape modulation, but that the discrimination of modulated shapes is not influenced by modulated sounds.

612 Children with Cochlear Implants Demonstrate Working Memory Deficits in Storage, Not Processing

Susan Nittrouer¹, Joanna Lowenstein¹, Amanda Caldwell¹
¹The Ohio State University

Background

There is growing consensus that hearing loss and consequent amplification likely interact with cognitive systems. A phenomenon often considered in regards to these potential interactions is working memory, modeled

as consisting of one mechanism responsible for storage of information in a short-term buffer and another mechanism responsible for processing of that information in some manner. The capability to explore potential interactions between hearing loss/amplification and the operations of this cognitive system has been hindered because there has been no way to index separately the performance of storage and processing. That distinction is important because signal degradation as occurs with a cochlear implant should selectively inhibit the ability to store words in a memory buffer, without affecting processing. The goal of this study was to examine two related hypotheses: (1) Recall accuracy indexes storage while speed of recall indexes processing efficiency; (2) Storage is negatively impacted for children with CIs, but not processing.

Methods

124 children who had just completed second grade participated in this study: 49 with NH, 19 with HAs and 56 with CIs. Listeners heard multiple lists consisting of the same six words (either non-rhyming or rhyming) in different orders, and recalled the order of presentation by tapping pictures on a touch-screen monitor representing each word. Recall accuracy and time required to recall all items were measured.

Results

Three results supported the hypotheses: Recall accuracy for the non-rhyming words was poorer for children with CIs than for those in the other two groups, but was similar across groups for the rhyming words. This outcome suggests that children with CIs are hindered in their abilities to recover phonemic structure from speech signals and use it to store words in a memory buffer. Speed of recall was similar for all children, for both kinds of materials. This finding suggests that the processing abilities of children with hearing loss are not affected by their losses. Recall accuracy and speed were not correlated, reflecting independence of these mechanisms.

Conclusion

It seems possible to measure the operations of storage and processing mechanisms in working memory separately, and that only storage is impaired for children with CIs. This finding could be used in empirical studies to enhance our understanding of the direction and nature of interactions between hearing loss/amplification and cognitive operations by examination of each component of working memory separately.

613 Investigating Phase Effects in On- And Off-Frequency Masking by Schroeder-Phase Complexes

Jordan A. Beim¹, Magdalena Wojtczak¹, Andrew J. Oxenham¹

¹University of Minnesota

Background

Phase effects in forward masking by Schroeder-phase complexes are thought to be mediated by the interaction of the phase curvature of stimulus with that of the basilar-

membrane (BM) filter tuned to the signal frequency, and by BM compression. Although the two factors account well for the phase effects in on-frequency masking, they cannot explain phase effects in off-frequency masking, where the BM should respond linearly. To account for off-frequency phase effects, the activation of the medial olivocochlear reflex (MOCR) has been invoked. Here, the role of the MOCR was tested in two experiments. The first experiment utilized the fact that MOCR activation is stronger for binaural than monaural elicitors to test the prediction that diotic maskers should produce higher masked thresholds, and possibly stronger phase effects, than monaural maskers. The second experiment provided direct measurements of MOCR activation using stimulus-frequency otoacoustic emissions (SFOAEs) with Schroeder-phase complexes as elicitors. A third experiment tested the hypothesis that off-frequency masker phase effects are due to residual BM compression by comparing forward masking produced by on- and off-frequency amplitude-modulated (AM) tones with that produced by unmodulated tones.

Methods

Psychophysical masked thresholds were measured for a 10-ms, 6-kHz signal. The maskers were centered on 6 kHz (on-frequency) and on 3 kHz (off-frequency). The effect of efferent activation on SFOAEs was measured using a continuous fixed-level 6-kHz probe and on- and off-frequency Schroeder-phase MOCR elicitors. Changes in SFOAE due to elicitors were calculated from a heterodyned ear-canal pressure measured in the presence and absence of the elicitor.

Results

Phase effects observed with diotic Schroeder-phase maskers were smaller than those for monaural maskers. The effects of efferent activation by Schroeder-phase elicitors on SFOAEs did not show a systematic dependence on the elicitor phase curvature. Forward masked thresholds measured with an off-frequency AM masker were consistently lower than those for an unmodulated pure-tone masker with the same rms amplitude.

Conclusion

Results from psychophysical and SFOAE measurements do not support the hypothesis that efferent activation contributes to phase effects observed in masking by Schroeder-phase complexes. Results from forward masking by AM and unmodulated tonal maskers are not consistent with phase effects being due to residual compression. Thus, the off-frequency effects of Schroeder-phase maskers remains a phenomenon with no clear explanation.

[Supported by NIH grant R01DC010374.]

614 Characteristics of Learning an Invented Auditory Non-Linguistic Rule

Liat Kishon-Rabin¹, Shira Cohen¹, Sara Ferman¹, Daphne Ari-Even Roth¹

¹Communication Disorders Department, Tel-Aviv University

Background

Learning of a language involves both implicit and explicit processes that are considered memory-based learning mechanisms. Implicit learning assumes automatic identification of patterns of regularities among similar experiences. Although it does not require conscious effort to discover the underlying rules or structure of the task, it necessitates a critical amount of time and repetition. In contrast, explicit learning involves intentional learning and conscious use of knowledge about events and facts that can occur even after a single exposure. One interesting question is whether these processes are specific to language learning or are they part of a common mechanism that underlie learning of rules with nonlinguistic stimuli. Thus, the goal of the present study was to investigate the characteristics of learning an invented rule using non-linguistic auditory stimuli.

Methods

Ten young adults participated in learning an invented 'Dolphin language' in 5 sessions. In each session, each subject listened twice to a modeling list of 16 sequences that consisted each of the same four different sounds (pure-tones and narrow bands) but in a different order according to an invented rule. Then listeners were presented with 16 sequences, half from the modeling list and half were incorrect. Listeners were asked to judge the correctness of these sequences. Listeners were also required to complete sequences. To test transfer of learning, listeners were presented with new sequences and were asked to judge their appropriateness. Dependent variables included percent correct, reaction time (RT) and verbal reports.

Results

Results showed that 50% of the listeners were able to judge correctly the sequences but only a third showed transfer of learning. This suggests that for some listeners implicit learning was involved via memory (and not by discovering the rule). The finding that for some subjects improvement in percent correct was associated with a decrease in RT (supporting implicit learning) while for others with an increase in RT (supporting explicit learning) is in keeping with the notion of variable use of learning processes among subjects.

Conclusion

Although the results of the present study are limited to specific learning conditions, these preliminary data support a common mechanism that underlies learning of linguistic and nonlinguistic grammar. Such information has theoretical as well as practical implications for the diagnosis and intervention of individuals who have difficulties acquiring a language, such as, children with

specific language impairment and learners of a second language.

615 The Spatial Pattern of Cochlear Amplification

Jonathan Fisher¹, Fumiaki Nin², Tobias Reichenbach¹, Revethy Uthaiyah¹, A. J. Hudspeth^{1,3}

¹The Rockefeller University, ²Graduate School of Medical and Dental Sciences, Niigata University, ³Howard Hughes Medical Institute

Background

Sensorineural hearing loss, which stems primarily from the failure of mechanosensory hair cells, is associated with changes in the traveling waves that transmit acoustic signals along the cochlea. However, the connection between cochlear mechanics and the amplificatory function of hair cells remains unclear.

Experiments involving isolated hair cells have identified two force-generating mechanisms. The mechanoreceptive hair bundles of many tetrapods are capable of generating forces that can be entrained by an external stimulus. Another force-generating mechanism specific to the outer hair cell of mammals is somatic motility or electromotility: changes in membrane potential rapidly alter the cylindrical cell's length. This behavior is mediated by voltage-dependent conformational changes in the membrane protein prestin.

Although a wealth of evidence suggests that hair-cell forces influence movement of the cochlear partition and vice versa, it has not been possible heretofore to locally separate the contributions of active hair-bundle motility and somatic motility.

Methods

By applying a scanned-beam laser interferometer in the chinchilla's cochlea, we recorded the two-dimensional profiles of the traveling waves elicited by pure tones.

We developed an optical technique that locally and significantly perturbs electromotility. Our technique uses 4-azidosalicylate, the azide group of which forms covalent bonds with prestin upon activation by ultraviolet light.

To guide our experiments, we developed a mathematical technique that computed a spatial map of cochlear-partition impedance based on measurements of active traveling waves.

Results

We found that a 500 μm -long segment of the cochlear partition that extended roughly one cycle basal from a wave's peak, depending on the location of the hole, encompassed most of the expected region of gain.

We then probed two narrow segments that extended roughly 50 μm along the cochlear partition: one region lying a full cycle basal to the traveling wave's peak and another situated just an eighth of a cycle before the peak.

Inactivation of the more basal segment elicited a more gradual accumulation of gain; this caused a small decrement in gain that persisted, but did not increase, up to the wave's peak.

Conclusion

These results demonstrate that an active process overcomes viscous damping to locally amplify the cochlear traveling wave, and that this locally accrued gain accumulates spatially up to the wave's peak. The results further demonstrate that prestin plays a crucial role in establishing this gain.

616 Transduction Channels' Gating Produces Friction Forces That Dominate Viscous Drag on Vibrating Hair-Cell Bundles

Volker Bormuth¹, Jérémie Barral¹, Frank Jülicher², **Pascal Martin**¹

¹CNRS - Institut Curie - UPMC, ²MPIPKS

Background

Hearing begins when sound-evoked vibrations of the hair-cell bundle change the open probability of mechanosensitive transduction channels. A dynamic interplay between channel gating and Ca^{2+} -dependent adaptation can give rise to spontaneous hair-bundle oscillations and frequency-selective amplification of sinusoidal inputs. As for any micromechanical device, friction is critical to the performance of the hair bundle. Here we performed dynamic force measurements to decipher the different contributions to hair-bundle friction.

Methods

We used flexible glass fibers to deflect single oscillatory hair bundles from the bullfrog's sacculus. In response to a symmetric triangular waveform of motion, the force-displacement relation followed a hysteretic cycle; friction forces were deduced from the cycle width along the force axis. Velocity of the bundle's tip was varied (0.5-15 $\mu\text{m/s}$), while the amplitude of motion was fixed (± 100 nm). In addition, we studied how the waveform and frequency of spontaneous oscillations were affected by increasing the viscosity of the endolymph that bathed the hair bundles.

Results

At low velocities of bundle motion, friction could be negative, a signature of the active process that drives spontaneous hair-bundle oscillations. When moving at velocities high enough to outrun adaptation, however, we found that friction became positive and displayed a maximum within the narrow region of displacements where the bundle manifested gating compliance, the elastic correlate of transduction channels' gating. Strikingly, friction was significantly reduced in the presence of a channel blocker (gentamicin). From this reduction, we estimated that channel gating contribute frictional forces 3-5 fold larger than those of hydrodynamic origin. The later were measured after the tip links were severed by applying a Ca^{2+} chelator (BAPTA). In accordance with these measurements, increasing endolymph viscosity η by thirty-fold had only a mild effect on active hair-bundle

movements: oscillation frequencies decreased by only 20% and the speed of the fast transitions within a bundle's rectangular waveform of oscillation varied like $\eta^{-0.25}$. A physical description of active hair-bundle mechanics that accounts for the finite activation kinetics of the transduction channels ($\tau \approx 1$ ms in frog) could quantitatively reproduce the data from both experiments.

Conclusion

We conclude that transduction channels provide a major contribution to hair-bundle friction. Channel properties, but not endolymph viscosity, control damping of hair-bundle movements. Channel friction in turn helps setting the sensitivity and the characteristic frequency of the hair-bundle amplifier.

617 The High-Frequency Response of an Active Outer Hair Cell Is Enhanced by Cochlear Inertia

Daibhid O Maoileidigh¹, A. J. Hudspeth¹

¹Rockefeller University

Background

Our ears employ an active process that endows them with heightened sensitivity and frequency discrimination. This process results from the action of outer hair cells that amplify the sound-induced motion of the cochlear partition. Outer hair cells perform two forms of movement that potentially contribute to cochlear amplification: active hair-bundle motility and somatic motility. It is unclear, however, how these processes function effectively at high frequencies.

Amplification by active hair bundles has been observed only at low frequencies; moreover, the speed of hair-bundle motion is limited by mechanical loading. High-frequency somatic motility by isolated outer hair cells is severely attenuated by low-pass filtering of the receptor potential driving it, whereas the mechanical load imposed by the cochlear environment inhibits low-frequency somatic length changes.

Methods

To examine the effects of the cochlear environment on the response of outer hair cells at high frequencies, we introduce a model of active outer hair cells. The descriptions of hair-bundle motility and somatic mechanics accord with published observations of movement by isolated outer hair cells. We then use this model to predict the response of an active outer hair cell to sinusoidal forcing.

Results

The model confirms that significant high-frequency motility by an isolated active outer hair cell is unlikely owing to damping and low-pass filtering of the receptor potential. Loading an active outer hair cell with additional damping and stiffness corresponding to that of the surrounding cochlear structures reduces its response even further.

When the masses of the basilar and tectorial membranes are taken into account, however, the system displays high-frequency resonance near the cell's characteristic frequency. The magnitude and sharpness of this response are enhanced when the parameters controlling the activity of the hair bundle are chosen such that the system operates near a Hopf bifurcation, the operating point at which the unforced system transitions from quiescence to spontaneous oscillation. This enhancement by the active hair bundle is possible only when the mass of the tectorial membrane is sufficiently great. Low-pass filtering of the somatic response is counteracted by the activity of the hair bundle.

Conclusion

High-frequency amplification by active outer hair cells is possible owing to a combination of inertial components in the cochlea and the activity of the hair bundle. Somatic motility and active hair-bundle motility collude to create an active amplifier that enhances the motion of the cochlear partition.

618 Identification of the Voltage Sensing Mechanism in Prestin

Kirk Beisel¹, Sandor Lovas¹, Jie Tang¹, Huizhan Liu¹, Pecka Jason¹, David He¹

¹Creighton University

Background

Among the SLC26A proteins mammalian prestin uniquely functions as a direct voltage-to-force transducer of cochlear outer hair cells and the underlying molecule for cochlear amplification. The mechanism of the voltage sensitivity of prestin is still unresolved. So far, two mechanisms are proposed: (1) The extrinsic voltage sensor mechanism is elicited by the intracellular anions, chloride and bicarbonate, that facilitate the voltage-sensor charge movement manifested as nonlinear capacitance (NLC). (2) Positively charged residues within the transporter channel provide the chloride binding site(s) and serve as the intrinsic voltage sensor. We have developed a three dimensional (3D) model of the SulP domain (Lovas et al., Proceedings of 22nd American Peptide Symposium, 2011, pp 120-121). The major structural features are 8 transmembrane (TM) spanning domains, two helical pin (HP) re-entry loops and the intracellular finger (ICF). A variant of prestin in which the ICF was removed had substantially reduced NLC. Furthermore, specific residues within the internal anion gating structure and adjacent to the intracellular channel entrance participate in the voltage sensor mechanism of prestin are predicted. These sites were examined to test their contribution to voltage sensitivity.

Methods

Using our 3D structure of the SulP domain of rat prestin, chloride binding sites were established and then tested for structure/function relationships in gerbil prestin. Mutations were generated using a QuikChange Lightning site-directed mutagenesis kit and the resulting nucleotide changes were verified by DNA sequencing. cDNA clones,

containing normal and mutated modified gerbil prestin sequences with a C-terminal EGFP tag, were expressed in HEK293 cells. After 24-48 hours of transfection, cells with robust, membrane-associated EGFP expression was used to measure the NLC using whole cell patch clamp technique.

Results

Four tyrosine (Tyr) residues were targeted for substitution with alanine (Ala), phenylalanine (Phe), tryptophan (Trp) and arginine (Arg). All substitutes resulted in a diminished NLC with Tyr>Phe=Trp>>Ala>Arg. Replacement by the positively charged Arg generally caused loss of NLC.

Conclusion

Our observations suggest that a series of Tyr residues, through anion- π interactions, function as intrinsic voltage sensors. These sites are associated with the transporter gating structure and adjacent to the intracellular opening of the transporter pore. These data further suggest that anion- π interactions provide a novel non-covalent binding mechanism by which chloride and bicarbonate anion bind to prestin.

619 The Slc26 Family Proteins in Membranes Are All Tetramers

Richard Hallworth¹, Kelsey Stark², Lyandysha Zholudeva¹, Benjamin Currall³, Michael Nichols¹
¹Creighton University, ²Doane College, ³Brigham and Women's Hospital

Background

Mammalian prestin, the motor protein of the cochlea outer hair cell, is an oligomer that has recently been shown to be a homotetramer when incorporated into membranes. Prestin is also a member of a large family of membrane proteins, the Slc(Solute Carrier)26 family, which are anion transporters. Although prestin does not transport anions, it requires anions for function, and non-mammalian prestins, transport anions. The sequence similarities of the Slc26 proteins suggest the existence of common underlying mechanisms, including oligomerization. We therefore extended the prior study of prestin oligomerization to determine the stoichiometry of other Slc26 family proteins in membranes.

Methods

We determined the stoichiometry of other Slc26 family proteins, including two non-mammalian prestins and three evolutionarily disparate proteins of the Slc26 family, using the bleach step counting method as previously applied to prestin. Plasmids expressing fusions of Slc26 proteins with enhanced Green Fluorescent Protein (eGFP) were expressed in Human Embryonic Kidney cells. Membrane fragments containing fluorescent Slc26-eGFP molecules were prepared by osmotic lysis. Single fluorescent molecules were isolated and imaged under continuous U-V excitation using an electron-multiplying CCD camera. Bleach step counts were obtained using off-line analysis. A known dimer, Orai1, was studied and analyzed in a similar fashion as a control.

Results

All Slc26 proteins studied were found to be tetramers in membranes.

Conclusion

The existence of tetrameric configurations common to the Slc26 proteins suggests a functional requirement for tetramerization and the existence of conserved oligomerization motifs.

620 FLIM-FRET Measurements of Voltage Dependent Conformational Changes in Prestin

Shinji Strain¹, Guillaume Duret¹, Chance Mooney¹, Robert M. Raphael¹

¹Rice University

Background

Cochlear sensory cells, outer hairs cells (OHCs), elongate and contract in response to changes in transmembrane potential. This electromotility is important for auditory frequency selectivity and sensitivity and is believed to be driven by a motor protein, prestin, which is highly expressed within the membrane of OHCs. While the electrical aspects of prestin function can be studied by measuring the nonlinear capacitance (NLC), there is currently no method to study the mechanical aspects of prestin function.

Methods

We have previously utilized acceptor photobleach fluorescence resonance energy transfer (FRET) to study prestin-prestin interactions in living cells. However, traditional FRET, based upon detection of fluorescence intensity, is inherently subjected to artifacts that arise from variations in excitation intensity, photobleaching, and fluorophore concentration. We have recently implemented fluorescence lifetime imaging microscopy (FLIM) to perform robust FRET experiments in HEK cells cotransfected with prestin-TFP and prestin-YFP. FLIM-FRET measurements were performed in patch-clamped HEK cells on the stage of an inverted confocal microscope equipped with a multiphoton laser and time correlated single photon counting electronics.

Results

NLC measurements confirmed that labeled prestin proteins were functional and comparable to wild-type prestin. FRET efficiency was calculated by fitting the lifetime decay of prestin-TFP in cells clamped at various holding potentials. High FRET efficiencies were measured at hyperpolarized potentials, and low FRET efficiencies were measured at depolarized potentials.

Conclusion

The results indicated that changes in the transmembrane potential induce a conformational change in prestin that can be detected by FLIM-FRET. Thus, FLIM-FRET can provide a sensitive assay for the mechanical correlate of prestin function.

Supported by NIDCD grants (DC009622 and R2Z960 to R.M.R.) and a by a training fellowship from the Keck Center of the Gulf Coast Consortia, on the Nanobiology Interdisciplinary Graduate Training Program, National Institute of Biomedical Imaging and Bioengineering (NIBIB) T32EB009379.

621 MiRNA183 and MiRNA34a Are Involved in the Onset and Progression of Age Related Hearing Loss

Qian Zhang¹, Huizhan Liu¹, Joann McGee², Edward J. Walsh², Garret Soukup¹, Zhizhou He¹

¹Creighton University, Omaha, Nebraska, ²Boys Town National Research Hospital, Omaha, Nebraska

Background

MicroRNAs (miRNAs), a class of short non-coding RNAs that regulate the expression of mRNA targets, are important regulators of cellular senescence and aging. Our microarray analyses of the organ of Corti from C57 and CBA mice showed that approximately 98 miRNAs exhibited differential expression and that downregulated miRNAs significantly outnumbered upregulated miRNAs during aging. Among these differentially expressed miRNAs, miR34a, a known regulator in the pro-apoptotic pathways, was significantly up-regulated while miR183, known to be important for differentiation and proliferation, was drastically down-regulated. The goal of current study was to examine the temporal and spatial distribution of these two miRNAs during onset and progression of age-related hearing loss (ARHL) and to explore their potential regulatory pathways in the organ of Corti.

Methods

C57BL/6J and CBA/J mice at different time points during aging were used for the studies. Auditory brainstem responses (ABR) thresholds and hair cell morphology were examined to monitor the onset and progression of ARHL. Q-PCR and in situ hybridization were used to quantify and localize the expression of these two miRNAs. Apoptosis qPCR arrays were used to explore target genes of the two miRNAs in the organ of Corti.

Results

Q-PCR analyses showed miR183 was downregulated more than two fold while miR34a was upregulated two fold in both strains of mice during degeneration of the organ of Corti. The changes of expression levels of both miRNAs preceded the decline of ABR thresholds and hair cell loss. In situ hybridization revealed that miR183 was specifically expressed in hair cells, while miR34a expression in the cochlea was more extensive, in both hair cells and supporting cells. Apoptotic qPCR array analyses showed that many apoptotic genes, such as p53 family, caspase family, Bcl2 family and death domain receptor family members, were drastically altered during degeneration of the organ of Corti in both strains.

Conclusion

miR-183 and miR-34a are differentially expressed during the course of ARHL in both mouse models. Significant up/down-regulation of several major apoptotic gene families suggests these genes might be direct or indirect targets for miR-34a and miR-183. Our study suggests that changes in miRNA expression patterns precede morphological and functional changes and that up-regulation of pro-apoptotic miRNAs and down-regulation of miRNAs important for differentiation and proliferation are both involved in the age-related degeneration of the organ of Corti.

622 Age Effects in Discrimination of Temporal Cues Within and Between Interval Groupings of Accented Tone Sequences

Peter Fitzgibbons¹, Sandra Gordon-Salant²

¹University of Maryland, ²University of Maryland, College Park

Background

Older persons exhibit difficulty understanding speech that is spoken with an accent and altered timing patterns that differ from their own native language. One change in speech timing results from an elongation of one or more inter-word pause intervals, an outcome that both enhances the perception of accent and creates groupings of longer and shorter sequence intervals. These timing changes could be problematic for older listeners, as age-related deficits in temporal processing are commonly reported. We examine potential age effects on temporal discrimination by using non-speech stimulus sequences that feature some timing attributes of accented speech.

Methods

Reference stimulus sequences consisted of six 50-ms 1000-Hz tone bursts, each separated equally by silent intervals to produce tonal inter-onset intervals (IOI) of 200ms ("Short" or S). Other sequences featured an accent, produced by a lengthening of one or more IOIs to 400ms ("Long" or L). For each of 12 sequence patterns, adaptive forced-choice discrimination procedures were used to measure a duration DL for increments of one targeted sequence IOI (S or L). Listeners included a group of younger normal-hearing adults and two groups of older adults with and without high-frequency hearing loss (N = 15/group). Stimuli were presented monaurally via earphone at 85 dB SPL.

Results

The duration DLs of the two older listener groups were equivalent, indicating that hearing loss did not influence discrimination performance. Younger listeners exhibited better interval discrimination than older listeners for each stimulus sequence. The magnitude of the age-related discrimination deficits was smaller for sequences with the target IOI embedded within similar interval groups (e.g. all Ls or Ss), and substantially larger for a target located between interval groups (e.g., L target between S interval groups).

Conclusion

Comparative discrimination data collected for target intervals within unaccented stimulus sequences indicate that the detrimental influence of sequential accent is much greater for older listeners compared to younger listeners. Diminished temporal sensitivity is evident for target intervals at and adjacent to accent locations within stimulus sequences. Outcomes from these measurements with non-speech stimulus sequences can serve our understanding of the problems experienced by many older listeners when processing the altered temporal cues found in accented speech.

623 BERA in Aging Grey Mouse Lemurs (*Microcebus Murinus*)

Christian Schopf¹, Elke Zimmermann¹, Julia Tünsmeier², Sabine Kästner², Andrej Kral³

¹*Inst. of Zoology, University of Veterinary Medicine Hannover, Foundation,* ²*Dep. of Small Animal Medicine and Surgery, University of Veterinary Medicine Hannover, Foundation,* ³*Inst. of Audioneurotechnology & Dep. of Experimental Otolology, Medical University Hannover*

Background

Mouse lemurs are small, gerbil-sized, nocturnal primates, communicating in the high-frequency and ultrasonic range. They are discussed as an emerging new primate model for aging research. The aim of this study was to gain first empirical information on auditory thresholds and hearing sensitivity in mouse lemurs during aging.

Methods

We applied brainstem evoked response audiometry (BERA) a cost-efficient method traditionally used for screening hearing sensitivity in human babies and animal models in hearing research such as cats. Animals were anesthetized using sevoflurane. To assess the effect of age in grey mouse lemurs, we determined frequency dependent auditory thresholds using tone pips in the range between 500 Hz and 95 kHz of two age groups of mouse lemurs (young animals: 1 to 5 years of age; old animals: 6 years or older). Altogether 19 animals were tested.

Results

Audiograms were established individually based on visually determined auditory thresholds. Findings indicate that mouse lemurs show broadband frequency sensitivity from 800 Hz to 40 kHz. Although they exhibit better hearing in the ultrasonic range than most primates, their best frequency of hearing is about 8 kHz. A significant decreased hearing sensitivity over the complete tested frequency range was revealed in aged animals. Furthermore the eldest tested individual was found to be completely deaf.

Conclusion

Long-term measurements will characterize the progress of that possible hearing loss more exactly. Thus, BERA is a promising, cost- and time-efficient technique to estimate hearing capabilities and deficiencies in small primates, such as mouse lemurs.

624 Age Related Changes in Inhibition in Mouse Auditory Cortex

Kevin A Stebbings¹, Don Caspary², Jeremy G Turner^{2,3}, Dan A Llano¹

¹*UIUC,* ²*SIU,* ³*Illinois College*

Background

Studies attempting to examine age related cortical changes in vivo are often confounded by the dependence of cortical responses upon altered input from the auditory periphery. To obviate this problem, we have employed a slice preparation in which afferents from the auditory thalamus are preserved and can be stimulated in isolation by an electrode to produce responses in the auditory cortex (AC).

Methods

Hearing was measured by ABR at several frequencies (4, 8, 16, 32 and 45KHz) and with Gaussian noise in both young (mean age =7.1 months , n=11) and old (mean age =23.0 months , n=9) CBA/J mice. Auditory thalamocortical slices were cut and cortical responses generated by stimulation of the thalamocortical afferents. These responses were imaged by flavoprotein autofluorescence which utilizes FAD+ as an indicator of metabolic changes induced by neuronal activation. A series of stimulation amplitudes ranging from 5- 500 μ A were used, and a 4 - parameter sigmoidal dose -response model was used to fit activation signal in the AC to both an untreated condition and a condition of 150nm GABA_A, a GABA_A-receptor blocker. Basic parameters of the curve in both conditions were extracted and used to evaluate the sensitivity of AC to disinhibition.

Results

The maximum fluorescence above baseline was found to decline linearly with age and hearing threshold in both the normal and GABA_A conditions. Sensitivity to GABA_A was measured as the ratio of maximum fluorescence in the AC during the GABA_A condition, divided by the maximum in the normal condition. Older animals showed a lower sensitivity to GABA_A as indicated by a smaller proportional increase in maximum in the GABA_A condition, which may indicate an age-related decrease in cortical GABAergic inhibition. The differences in old vs. young animals do not appear to be dependent on differences in slice viability, as assessed via AC FAD/NAD ratio, an indicator of metabolic stress.

Conclusion

These data suggest that auditory cortical inhibition in the thalamocortical system may diminish with age and/or hearing loss. More studies are needed to separate out the effects of age and hearing on cortical inhibition.

625 Dendritic Extent in Aged Auditory

Thalamus

Emily Tignor¹, Ben Richardson¹, Lynne Ling¹, Evgeny Sametskiy¹, Donald Caspary¹

¹*Southern Illinois University School of Medicine*

Background

Age related hearing loss is highly prevalent, occurring in 33% of those over the age of 70 years. Associated with poor central auditory processing, social withdrawal and depression, presbycusis has a major impact on psychological as well as overall physical health. Presbycusis has a multi-factorial etiology, including peripheral deafferentation leading to mal-adaptive changes to the central auditory pathway. The medial geniculate body (MGB) is an obligate auditory brain center in a unique position to gate and code acoustic information. Examining dendritic extent as a measure of neuronal function and processing capacity may be a way to quantify age-related changes in MGB. Early studies found age-related changes in neuronal dendritic extent in neocortex, while more recent studies have not found reduced dendritic extent in aged rat hippocampus.

Methods

Neuroleucida imaging and neuron tracing were performed to compare dendritic extent of neurobiotin-filled young and aged Fischer Brown Norway (FBN) rat MGB neurons.

Results

Preliminary result from 12 young and 14 age filled MGB neurons showed only small non-significant changes in dendritic extent. The density of the dendrites and the capacitance of the neurons showed no significant age-related changes between MGB neurons: mean dendritic length (young: 4096±317.5 length units; aged: 3948.9±459.6 length units, p=0.80). Surface area also showed no difference between the two groups (young: 14,732.9±1136.7 units, aged: 15,449.5±1895.1 units, p=0.76). Capacitance showed no difference between the two groups (young: 103.1 ± 33.2pF, n=29; aged: 104.6 ± 28.0pF, n=32; p= 0.38).

Conclusion

Initial findings suggest small non-significant age-related changes in dendritic extent and whole cell capacitance. Previous studies have shown inconsistent results regarding age-related changes of synaptic structures, dendritic spines and dendritic extent. Fast Golgi Cox studies are underway in order to confirm or reject the present findings.

This study is supported by NIH DC000151

626 Morphometric Analysis and DTI of the Auditory Cortex in Man – Changes with Aging

Oliver Profant¹, Antonin Skoch², Jaroslav Tintera², Ibrahim Ibrahim², Zuzana Balogova¹, Josef Syka¹

¹*Institute of Experimental Medicine ASCR, Prague,*

²*Institute of Clinical and Experimental Medicine, Prague, Czech Republic*

Background

Presbycusis is accompanied in man with changes in the inner ear as well in the central auditory system. The aim of our work was to find out what are the age-related changes in the auditory cortex. Therefore parameters of hearing function were assessed in a group of healthy young controls (YC), a group of elderly with normal presbycusis (EC) and a group of elderly with expressed presbycusis (EP) and then their auditory system was examined using Siemens Trio 3T magnetic resonance.

Methods

Diffusion tensor imaging (DTI) was performed using EPI sequence. For morphometric analysis and for determination of seed ROI for tractography, 3D structural image was acquired using MPRAGE sequence. Morphometry of the auditory cortex (Heschl's gyrus – HG and planum temporale –PT) and of the primary visual cortex (V1) was done by means of Freesurfer image analysis suite. Gray matter volume (GrayVol), area of gyral surface (SurfArea) and average thickness of gray matter (ThickAvg) were computed. Probabilistic tractography of auditory pathway from the inferior colliculus (IC) to HG and subsequent DTI analysis was done in FSL environment. Masks of white matter under HG were generated by Freesurfer; masks of IC at both sides of brainstem were defined manually.

Results

Significant decrease of ThickAvg in groups EC, EP with respect to YC was found for HG and PT. The analysis showed significantly higher SurfArea on the left side with respect to the right side in HG and PT in all groups. The decrease of the GrayVol for groups EC, EP with respect to YC and higher GrayVol on the left side was in accordance with the ThickAvg and SurfArea results. Visual cortex showed only a non-significant trend in a decrease of the thickness in both EC and EP. The results from DTI indicated a tendency for increasing L1 in EC and EP with respect to YC in auditory pathway, observable to a greater extent on the right side. No differences between EC and EP were observed in any of the morphological or diffusion parameters.

Conclusion

The results demonstrate typical left-right asymmetry of the primary auditory cortex and planum temporale and indicate the degree of the age-related atrophy of these structures that does not depend on the level of hearing dysfunction and is not present to such extent in the primary visual cortex.

Supported by grants 00023001 IKEM and GACR P304/10/1872

627 Age-Related Changes in Sox10 Expression in the Cochlear Lateral Wall

Xinping Hao¹, Nancy Smythe¹, Yazhi Xing¹, Bradley A. Schulte¹, Judy R. Dubno¹, Hainan Lang¹

¹Medical University of South Carolina

Background

Age-related auditory function deficits may result from a loss of non-sensory cells in the cochlear lateral wall and a decline in the endocochlear potential (EP). Despite the importance of these non-sensory cells, the mechanisms underlying their degeneration remain poorly understood. Sox10 transcription factor is required for the regulation of neural crest-derived cells including several types of non-sensory cells in the inner ear. Mutation of the Sox10 gene causes varying combinations of hearing loss and pigmentation defects in humans. Here, we investigated age-related changes of Sox10 expression in the cochlear tissues of CBA/CaJ mice and human temporal bones.

Methods

Young adult (1-3 month old) and aged (2-2.5 year old) CBA/CaJ mice were used because these mice show a greater EP decline at 12 months of age compared to most other mouse strains (Ohlemiller et al., 2010). Sox10 expression patterns were examined in the lateral wall of young adult and aged cochlear tissues obtained from CBA/CaJ mice and human temporal bones using quantitative immunohistochemistry. Ultrastructural changes with age in the cochlear lateral wall also were examined in mouse inner ears using transmission electron microscopy.

Results

Nuclear expression of Sox10 protein was present in strial marginal and intermediate cells in both young adult and aged CBA/CaJ mice. Outer sulcus cells and root cells of the spiral ligament also stained positively for Sox10, whereas none of the five types of fibrocytes in spiral ligament reacted positively. Quantitative analysis of Sox10 immunostaining indicated a significant decrease of Sox10+ cells in both the stria vascularis and spiral ligament of aged mice compared to young adult controls. Ultrastructural observations also indicated several signs of lateral wall degeneration in aged mice, which involved multiple cell types in the stria vascularis and spiral ligament. Sox10 immunostaining on the cochlear tissues of human temporal bones are ongoing.

Conclusion

Age-dependent morphological and cytochemical changes were seen in multiple cell types in the lateral wall of aged CBA/CaJ mice, an aging animal model with a pronounced EP decline. An age-dependent change in Sox10 gene regulation in the non-sensory cells may contribute the functional decline of cochlear lateral wall and hearing loss in aged mice and humans. This study was supported by NIH R01 DC7506 (H.L.), NIH P50 DC00422 (HL and JRD), NCRRL UL1RR029882 and a research grant from the South

Carolina Clinical and Translational Research Institute (JRD).

628 Age-Associated Changes of Na, K-ATPase Subunit Isoform Distribution and Expression in the CBA/CaJ Mouse Cochlea

Xiaoxia Zhu¹, Bo Ding¹, Joseph P. Walton¹, Robert D. Frisina¹

¹Univ. South Florida

Background

Presbycusis- aging related hearing loss is the number one communication and neurodegenerative disorder of our aged population, and has multi-faceted etiologies. One prominent cause involves declines in the cochlear endolymphatic potential (EP), the cochlear "battery" which is linked to dysfunction of the stria vascularis, The high potassium concentration in the endolymph is maintained by sodium-potassium pumps, such as Na, K-ATPase. It has been reported that Na, K-ATPase isoforms (subunits) including α 1, β 1 and β 2 are present in the cochlea of young adults, but it is not clear whether their protein expression change with age.

Methods

Cochlea were dissected from CBA/CaJ mice: young adults (2-4 months old) and old mice (>30 months). Immunocytochemistry staining with Na, K-ATPase antibodies for α 1, β 1 and β 2 was performed on frozen serial sections of the cochlea.

Results

The young adult group displayed strong α 1 expression in stria vascularis (SV) marginal cells. The Na, K-ATPase β 1 subunit was expressed in SV, spiral ligament, organ of Corti, spiral limbus and spiral ganglion neurons. The Na, K-ATPase β 2 staining was observed in SV, organ of Corti and in the spiral ganglion. Comparison of these Na, K-ATPase subunit isoform's for the two age groups revealed *down-regulation* of protein expression of all subunits in old mice. It was also noted that atrophies in the aged group, which included a 30-50% shrinkage in cytoarchitectonic area when compared to the young adult group for SV, was confined to the basal part of SV.

Conclusion

The main finding of this study is that Na, K-ATPase subunit declines with age and likely plays an important role in age-related hearing loss. Further investigation is needed to clarify the temporal sequence of events for the anatomical atrophy of SV, discharge of the cochlear "battery" and the down-regulation of Na, K-ATPase isoforms. Prevention of these age-related cochlear degenerative events could halt the progression of peripheral elements of presbycusis, leading to novel biomedical interventions to treat age-related hearing loss.

629 Age Related Na⁺/K⁺-ATPase Isoform Gene and Protein Expression Changes in the Cochlear Stria Vascularis

Bo Ding¹, Xiaoxia Zhu¹, Robert Frisina¹, Joseph P. Walton¹

¹Univ. South Florida

Background

Na⁺/K⁺-ATPase in cochlear marginal cells plays an important role in the stria vascularis' (SV) function for generation of the endocochlear potential (EP) and maintenance of the ionic composition of endolymph. Isoforms of this ion channel have been reported to localize inside SV including Na⁺/K⁺-ATPase α 1, β 1 and β 2 subunits. The effects of aging on these isoforms in SV are not clear. Previously we found that post-translational modification of NKCC1 by Aldosterone may contribute to age-related hearing loss (Ding et al. ARO Abstr. 2012). Since the similarities and functional cooperation between these two ion transport mediators are responsible for generating and maintaining K⁺ levels in cochlear endolymph, we hypothesize that aging may change Na⁺/K⁺-ATPase expression in SV.

Methods

Cochleae from CBA/CaJ mice and the cell line SV-K1 (mouse cochlear marginal cells) were used for RT-PCR and Western Blot assays.

Results

New RT-PCR experiments revealed that the Na⁺/K⁺-ATPase β 2 subunit mRNA levels are hardly detected in the cochlea from young adult or aged mice. But relative to young adult mice, Na⁺/K⁺-ATPase α 1 and β 1 subunits' mRNA levels are *down-regulated* with age. We then investigated the Na⁺/K⁺-ATPase mRNA levels in the marginal cell line. The results were similar to our *in vivo* studies of mRNA expression levels from cochleae of young adult mice. We then extended our investigation to Na⁺/K⁺-ATPase protein expression *in vivo* and in the cultured cells. Na⁺/K⁺-ATPase protein expression is *down-regulated* in the cochlea of aged mice (30 months old) compared to young mice (2-3 months old). Interestingly, ouabain-treated (an antagonist of Na⁺/K⁺-ATPase) SV-K1 cells showed no Na⁺/K⁺-ATPase expression changes, suggesting that down regulated Na⁺/K⁺-ATPase expression in the aged mouse cochlea may be associated with some so far unknown mechanisms or pathways.

Conclusion

To better understand the role of aging on Na⁺/K⁺-ATPase down regulation *in vivo*, further studies are required using Na⁺/K⁺-ATPase transgenic mice, along with *in vivo* measurement of the EP endolymph potential, and measurements of Na⁺/K⁺-ATPase promoter regulation assay (Dual-Luciferase® Reporter Assay System) would be helpful to determine if increases in Na⁺/K⁺-ATPase expression might lead to ion channel activation, moving

towards novel biomedical therapies targeted to prevent age-related hearing loss.

Supported by NIH Grant P01 AG009524

630 ABR Gap Responses Start to Decline in Middle Age Mice

Tanika T. Williamson¹, Xiaoxia Zhu¹, Bo Ding¹, Joseph P. Walton¹, Robert D. Frisina¹

¹Univ. South Florida

Background

The CBA/CaJ mouse strain's auditory function is normal during the early phases of life and gradually declines over its lifespan, much like human age related hearing loss (ARHL), but on a mouse life cycle "time frame". This pattern of ARHL is relatively similar to most humans, and currently is not treatable medically. For this reason, CBA mice were used for the present study to analyze the beginning stages and functional onset markers of ARHL. The results from Auditory Brainstem Response (ABR) and Gap-in-Noise (GIN) ABR tests were compared between two groups of mice of different ages, young and middle aged as well.

Methods

For this study, CBA/CaJ mice were used; 10 female and 20 male, and classified into two groups: young adult (Y, N=18, 3 to 4 months old) or middle aged (MA, N=12, 15 to 18 months old). After being anesthetized, ABR GIN ABRs were measured at 80 dB SPL, using wide band noise bursts with gap durations ranging from 0.1 ms to 48.1 msec. ABR tests included an ABR audiogram on each mouse.

Results

For long gap durations the response amplitudes for peak 1 (P1) and peak 4 (P4) to the initial noise burst (NB1) were significantly larger for the Y group. Similarly, P1 and P4 amplitudes to the second noise burst (NB2) were also larger for Y as compared to MA group. P1 amplitudes to NB1 were higher when compared to the NB2 response for the MA group. For NB2, there was a systematic decrease in P1 latency with increases in gap duration for both age groups; however, the NB2 P1 latency was longer for the MA group, particularly for the shorter gap intervals.

Conclusion

At 15 to 18 months old, mice start to show temporal deficits in the GIN test as observed by prolongation of the NB2 P1 latency for shorter gap durations. Effects of ARHL for the MA group were also seen in that the P1 amplitude did not fully recover compared to Y. These findings indicate that age-linked degeneration of the auditory is just beginning in middle age, allowing for biomedical preventative measures to still be a possibility for attenuating further damage due to ARHL.

631 Modulation of Mcl-1 Expression Reduces Age-Related Cochlear Degeneration

Weiping Yang¹, Yang Xu¹, Wei-Wei Guo¹, Hui-Zhan Lui¹, Bo Hua Hu²

¹Chinese PLA General Hospital, ²State University of New York at Buffalo

Background

Sensory cell degeneration in the cochlea is a major pathology contributing to age-related hearing loss in the adult population. Previous investigations have implicated the apoptotic pathway in age-related sensory cell death. Mcl-1 is an anti-apoptotic member of Bcl-2 family genes that modulates apoptosis-related signaling pathways and promotes cell survival. We have documented the reduction in Mcl-1 expression in aging rat cochleae. Importantly, this reduction in Mcl-1 expression is spatially correlated to the cells undergoing apoptosis. The current study was designed to investigate whether restoration of Mcl-1 expression could reduce aging-related sensory cell degeneration.

Methods

Fischer rats (male and female, 24-25 months) and Sprague Dawley rats (male and female, 2-3 months) were used. Human Mcl-1/enhanced green fluorescent protein plasmid was locally applied to the round window of the rat cochlea. The effect of Mcl-1 transfection on Mcl-1 expression in the cochleae was examined using qRT-PCR, Western blotting, and immunolabeling assays. The auditory function of the animals was assessed using the measurement of auditory brainstem responses. Sensory cell apoptotic activity was assessed with the morphological analysis of the nuclei. The release of cytochrome c from mitochondria, a mitochondrial event of apoptosis, was evaluated using immunohistology.

Results

Strong Mcl-1/enhanced green fluorescence was observed in both sensory and supporting cell regions 15 days after the treatment, suggesting that the *in vivo* treatment of Human Mcl-1/enhanced green fluorescent protein plasmid transfected both sensory and supporting cells of the cochlear sensory epithelium. Mcl-1 transfection increased both the transcriptional and protein expression levels of Mcl-1 in aging cochleae. The upregulation of Mcl-1 expression reduced the progression of age-related cochlear dysfunction and sensory cell death. We further demonstrated that the protective effect of Mcl-1 transfection was mediated by the suppression of cochlear apoptotic activity and that the reduction in apoptosis was associated with the suppression of the mitochondrial event of the apoptosis.

Conclusion

The genetic modulation of Mcl-1 expression reduces the progression of age-related cochlear degeneration. Mcl-1 may serve as a potential target for future therapeutic

intervention of age-related sensory cell degeneration in the cochlea.

(This study was supported by National Natural Science Foundation of China No.30973304 and in part by NIDCD 1R01DC010154)

632 Age-Related Hearing Loss: Gamma-Amino Butyric Acid, Nicotinic Acetylcholine and N-Methyl-D-Aspartate Receptor Expression Changes in Spiral Ganglion Neurons of the Mouse Cochlea

Xiaolan Tang¹, Xiaoxia Zhu¹, Bo Ding¹, Joseph P. Walton¹, Robert Frisina¹

¹Univ. South Florida

Background

Age-related hearing loss – presbycusis – is the number one communication and neurodegenerative disorder of our aged population. Although speech understanding in background noise is quite difficult for those with presbycusis, there are currently no biomedical treatments to prevent or reverse this condition. A better understanding of the cochlear mechanisms underlying peripheral presbycusis will help lead to future treatments. Objectives of the present study were to investigate gamma-amino butyric acid A (GABA-A) receptor subunit $\alpha 1$, nicotinic acetylcholine (nACh) receptor subunit $\beta 2$, and N-methyl-D-aspartate (NMDA) receptor subunit NR1 protein expression changes in spiral ganglion neurons of the mouse cochlea, that occur in age-related hearing loss, utilizing quantitative immunohistochemistry techniques.

Methods

Frozen serial sections were prepared from young adult (n=6, 2-6 months, 3 males, 3 females) and old (n=6, 28-33 months, 3 males, 3 females) CBA/CaJ mice. The distribution of GABA-AR $\alpha 1$, nAChR $\beta 2$ and NMDARNR1 were assayed immunohistochemically. The labeling was measured quantitatively with densitometry using Image J. ABR audiograms confirmed the degree of age-related hearing loss.

Results

GABA-AR $\alpha 1$ protein expression decreased with age in spiral ganglion neurons (P<0.05). Surprisingly, the expression of NMDANR1 *increased* in spiral ganglion neurons of the aged mice compared with the young adult mice (P<0.01). The nAChR $\beta 2$ study is ongoing.

Conclusion

These findings demonstrated that there are age-related changes of GABA-A and NMDA receptor expression in CBA mouse spiral ganglion neurons, which may be related to functional changes in cochlear synaptic transmission as a function of age. This study leads to more insights into the function of GABA-A $\alpha 1$, nACh $\beta 2$ and NMDANR1 receptor protein regulation in the aging mammalian auditory system, paving the way for novel biomedical interventions to prevent or slow down the progression of age-related hearing loss, as well as other types of hearing impairment.

633 Noise Exposure and Male–Female Hearing Impairment Differences in Years Lived with Disability in Norway

Howard J. Hoffman¹, Chuan-Ming Li¹, Kristian Tambs², Bo Engdahl²

¹NIDCD, NIH, Bethesda, MD, ²Norwegian Institute of Public Health (NIPH), Oslo, Norway

Background

Many studies show hearing impairment (HI) as a major contributor to years lived with disability (YLD), yet few are focused specifically on the relative contribution by HI etiology. The Nord-Trøndelag Hearing Loss Study (NTHLS), 1996–1998, affords the opportunity to analyze HI-YLD by sex and etiology based on screening criteria. A population-based sample of 51,574 adults (20–101 years) completed audiometric exams and questionnaires on noise exposure, tinnitus, and hearing health. Engdahl et al. 2005 published audiometric findings contrasting the unscreened and audiotologically-screened population, after exclusions based on screening criteria.

Methods

YLD distributions are calculated using World Health Organization (WHO) recommended procedures by 10-year age groups and HI severity: mild, moderate, moderately-severe, severe, profound, and complete. Severity weights are based on AMA-AAO recommendations (JAMA 1979). Subjects are classified by the questionnaire-based screening criteria, including noise exposure history, ear-related disorders, conductive losses, symptoms (tinnitus), and known hearing loss. Noise exposure history included loud occupational exposure, daily exposure from known sources, and frequent exposure to impulse noise. Audiometric criteria associated with noise exposure (Dobie 2005; Hoffman et al. 2006) were used to identify subjects with bilateral audiometric bulges or notches. These two methods were used as proxy measures for the harmful impact of noise exposure.

Results

Age-specific YLD distributions demonstrate that Norwegian men have a steep increase beginning about age 50 and continuing high levels for each subsequent decade of life. Women have a 21% reduction in total YLD due to a delay in the steep increase until age 60. After screening out subjects with noise exposure history, only 49% remain in the sample (males, 25%; females, 75%), which no longer has a sex disparity in HI-YLD. The other screening criteria do not affect the male-female disparity in HI-YLD. If only subjects with bilateral bulges/notches are screened out, then 80% of the sample remains (males, 69%; females, 89%). Screening out these subjects reduces by 60% the excess YLD of males compared to females. Both noise exposure history and bilateral notch/bulge criteria affect primarily HI-YLD of males, with negligible effect on females.

Conclusion

Noise exposure is the major contributor to male-female differences in HI-YLD. For HI and other age-related conditions, delay in age at onset is a preventive measure. Reductions in noise exposure not only reduce total YLD but also diminish age-related sex disparity.

634 Age-Related Changes in Neural Population Representation of Amplitude-Modulation in the Presence of Overlapping Maskers

Aravindakshan Parthasarathy¹, Jesyin Lai¹, Edward Bartlett^{1,2}

¹Biological Sciences, Purdue University, ²Weldon School of Biomedical Engineering, Purdue University

Background

Age related auditory processing deficits in the central auditory pathway primarily manifest as temporal processing difficulties. Elderly listeners are especially deficient in processing multiple concurrent sound stimuli, or sound stimuli in the presence of partial or complete masking sounds. This study aims to further understand the age related deficits in the neural processing of these sounds in a rodent model of aging.

Methods

Frequency following responses were obtained from young (3-5 months old) and aged (20-22 months old) Fischer-344 rats using subdermal needle electrodes. The target sound stimuli used were sinusoidally amplitude modulated tones (sAM), in the presence of completely or partially overlapping maskers. The maskers used were either broadband noise or sAM tones with the same carrier frequency but a different modulation frequency. The sound levels of the maskers were also systematically varied, to ascertain the growth of masking with level.

Results

As seen in our previous studies, the young exhibited higher FFR amplitudes for the faster modulation frequencies (128, 256 Hz AM) compared to the aged. However, in the presence of other competing sAM tones or broadband noise, the young animals showed a greater degree of relative masking compared to the aged. The masking increased with the degree of overlap, and was the greatest when the maskers were presented concurrently. The decrease in masking with age increased with AM frequency of the target.

Conclusion

This study exhibits the differences in segregation of concurrent sound stimuli, as well as stimuli overlapping with masking noise, with age. The decrease in masking seen with age could, in part, explain the difficulties in processing sounds in the presence of maskers. The decrease in the degree of masking with increase in AM frequency is in concurrence with our previous studies that indicate a decrease in auditory temporal processing with age selectively for faster modulation frequencies. Various explanations for this decrease in masking are consistent

with age-related compensatory increases in neural excitability.

635 Age-Related Changes in the Capillary Basement Membrane of the Stria Vascularis

Mitsuya Suzuki¹, Takashi Sakamoto², Akinori Kashio², Tatsuya Yamasoba²

¹Toho University, ²University of Tokyo

Background

Strial presbycusis is one of the 4 predominant pathologic types of presbycusis. Previous studies have shown failure of the basement membrane (BM) structure of strial capillaries in 6- and 12-month-old C57BL/6 mice. The purpose of this study is to examine the cause of age-related changes in the capillary BM of the stria vascularis.

Methods

C57BL/6 mice were grouped according to age as follows: 3 days, 8 weeks, 12 months, and 15 months. Cationic polyethyleneimine (PEI) was used to examine age-related changes in the anionic sites of the BM of the strial vessels. In 3-day-old, 8-week-old, and 12-month-old mice, the bony labyrinths were removed and immersed in a 0.5% PEI solution. Next, they were immersed in 2% phosphotungstic acid and 2.5% glutaraldehyde and embedded in epoxy resin. Ultrathin sections of the cochlear lateral wall were examined using a transmission electron microscope. In 3-day-old, 8-week-old, and 12- and 15-month-old mice, the bony labyrinths were extirpated and immersed in 10% paraformaldehyde and then embedded in paraffin. Serial mid-modiolar 5- μ m-thick sections were incubated with either anti-mouse IgG antibody or anti-mouse heparan sulfate proteoglycan (HSPG) antibody.

Results

In 3-day-old mice, PEI particles were evenly distributed on the capillary BM of the stria vascularis and spiral ligament. The area of distribution of PEI particles in the capillary BM of the stria vascularis in 8-week-old mice was smaller than that in 3-day-old mice. In 12-month-old mice, PEI particles were barely detected on the BM capillaries. A statistically significant difference was observed in the distribution of PEI particles between 3-day-old mice and mice in the other groups. Three-day-old mice barely showed any anti-immunoglobulin G (IgG) staining either in the stria vascularis or in the spiral ligament. In 8-week-old mice, anti-IgG staining was localized in the marginal cells. Further, IgG deposition was detected in the strial capillary BM in 12- and 15-month-old mice. Marked anti-HSPG staining was observed in the spiral ligament, unlike that in the stria vascularis. In the 12- and 15-month-old mice, anti-HSPG staining markedly reduced in the spiral ligament.

Conclusion

An appearance of IgG deposition in the stria vascularis may reduce the anionic sites on the BM of strial capillaries.

636 Differences in the Processing of Spoken Sentences Between Young and Elderly Normal-Hearing Adults

Anastasios Sarampalis¹, Mareike Alisch¹, Katharina Böhmen¹, Tobias Böske¹, Maraike Coenen¹, Enja Jung¹, Deniz Baskent^{2,3}

¹University of Groningen, Dept of Experimental Psychology, Netherlands, ²University of Groningen, UMCG, Dept of Otorhinolaryngology/Head and Neck Surgery, Netherlands, ³University of Groningen, Research School of Behavioral and Cognitive Neurosciences, Netherlands

Background

Elderly adults experience greater difficulty understanding speech in challenging listening conditions, compared to young adults. This is partially attributed to changes in the auditory periphery which result in loss of audibility. However, even when audibility factors are taken into account, significant ageing effects are still observed. This suggests that changes beyond those in the auditory periphery are also responsible for the challenges faced by elderly listeners. In this project, we investigate the hypothesis that cognitive changes due to ageing also contribute to differences in using context information of spoken sentences.

Methods

Young ($M_{age} = 19.5$ years) and elderly ($M_{age} = 66.5$ years) participants listened to sentences where the subject either preceded or followed (and was thus semantically constrained by) the verb. Their task was to decide which of four pictures presented on a computer screen was the target, that is, the subject in the sentence they heard. The remaining three pictures represented nouns that were either phonetically or semantically related to the target, or unrelated to it. A desktop eye-tracker recorded the size of the participants' pupils and the direction of their gaze. Changes in the size of the pupil are used as a measure of changes in the effortfulness of the task, while the participants' gazes serve as a window to the online processing of speech. The sentences were presented either in quiet or with background, speech-shaped noise.

Results

The two groups showed no significant differences in their scores in the vocabulary and reading span tests, but the elderly participants were significantly slower in a visual speed-of-processing task. Word recognition scores were very high for both groups, with averages ranging between 90% and 98% correct. Semantically constrained nouns were slightly easier to recognize for both groups, but this difference was not significant. The background noise did not have a significant effect on recognition performance, either. The similarities in recognition performance between the two groups ensure that the differences in the way the two groups scan the visual scene are indicative of differences in the way they process spoken sentences.

Conclusion

Based on the preliminary results of this study, we can conclude that eye gazes in this type of paradigm (typically termed “the visual world” paradigm) can be used to shed light on the differences in processing between young and elderly adults. In this study, differences in eye gazes may be attributable to age-related changes in cognitive performance.

637 Synaptic Aging in the Mouse Cochlea: New Views and Functional Clues

Sharon G. Kujawa¹, Kumud Lall², M. Charles Liberman¹, Yevgeniya Sergeyenko²

¹Harvard Medical School, Massachusetts Eye and Ear Infirmary, ²Massachusetts Eye and Ear Infirmary

Background

Studies of sensorineural hearing loss and cochlear compromise have historically concentrated on thresholds and hair cell damage. Although important metrics, recent work has identified widespread loss of IHC-afferent synapses and progressive cochlear nerve degeneration after “reversible” noise-induced hearing loss, i.e. in the absence of hair cell loss or permanent threshold shift (Kujawa and Liberman 2009). Here we ask if these degenerative changes also appear, with age, in CBA/CaJ mice that are never purposely exposed to noise.

Methods

DPOAEs and ABRs were recorded (5.6 – 44.07 kHz) from an age-graded series (4 to 144 wk) of male CBA/CaJ mice. Immunostained cochlear whole mounts and osmium-stained, plastic-embedded sections (10 µm) were studied at 3 cochlear locations (5.6, 11.3, 32 kHz) by confocal and conventional light microscopy, respectively, to quantify hair cells, ganglion cells and synaptic structures: i.e. synaptic ribbons (CtBP2), glutamate receptors (GluR2) and cochlear-nerve terminals (Na/K ATPase).

Results

Age-related sensitivity loss grows nonlinearly in CBA/CaJ. Threshold elevation is minimal, and confined primarily to mid to high frequencies, out to ~2 yrs. Thereafter, thresholds rise rapidly at all frequencies, particularly for ABR. DPOAE suprathreshold amplitudes are maintained throughout much of the lifespan; in contrast, ABR amplitude declines begin early and progress steadily, even when threshold sensitivity is little changed. Hair cell numbers are maintained until advanced age: OHCs in all rows decline precipitously beyond 2 yrs, first in the apex; whereas, IHC counts change little, even in very old animals. Spiral ganglion losses are modest and slow. In comparison, synaptic changes are dramatic. Ribbons decline throughout life, and throughout the cochlea, falling ultimately to ~50% of young ears. Virtually all surviving ribbons are paired with a glutamate receptor and terminal; thus, the ribbon appears to be a good proxy for the afferent synaptic complex. Moreover, ribbon counts and ABR wave I amplitudes are highly correlated; thus, ABR amplitude is a good proxy for synaptic counts, as long as OHC loss is minimal.

Conclusion

Thus, we document dramatic synaptic aging in the mouse cochlea. Even at ages where threshold sensitivity and hair cells are well preserved, loss of synapses is robust, presumably altering inputs to the aging brain. Results underscore the importance of understanding peripheral status when studying central contributions to auditory aging. Results also suggest that ABR amplitudes may provide non-invasive clues to cochlear synaptopathy, enhancing the possibilities for translation to human clinical characterization. Research supported by NIDCD: R01 DC008577

638 Effects of Age on the Perception and Neural Representation of Frequency

Modulation

Christopher Clinard¹

¹James Madison University

Background

Older adults, even with clinically normal hearing sensitivity, have difficulty understanding speech in the presence of background noise. This difficulty may be partly due to age-related declines in the neural representation of sounds.

Methods

Adults with clinically normal hearing sensitivity (thresholds < 25 dB HL at octave frequencies 0.5 – 8.0 kHz) between the ages of 22 and 69 participated in this study. Perception of frequency was tested by obtaining modulation detection limens (FMDLs) at 500 and 1000 Hz using an adaptive procedure. Stimuli were frequency modulated at a rate of 2 Hz. To examine the neural representation of frequency modulation, frequency-following responses (FFRs), which are dependent on phase-locked neural activity, were elicited by FM tones with carrier frequencies of 500 and 1000 Hz. FFR stimuli for each carrier frequency had modulation depths of 0.4 and 2 %. All stimuli were presented at 80 dB SPL. Analysis of FFRs included stimulus-to-response correlations, signal-to-noise ratios, and autocorrelograms. Speech-in-noise understanding was tested using the QuickSIN.

Results

Behavioral FMDLs declined at both 500 and 1000 Hz as age increased. FFR stimulus-to-response correlations and autocorrelograms showed greater age-related declines at 1000 Hz than at 500 Hz. FMDLs and FFR measures were correlated with speech-in-noise understanding.

Conclusion

These results suggest that the perception and neural representation of frequency modulation is negatively affected by age, even in the absence of significant hearing loss. [Supported by the National Organization for Hearing Research Foundation]

639 Single Unit Recordings in the Cochlear Nucleus of the Anesthetized Rat

Yaneri A. Ayala¹, Douglas Oliver², Nell Cant³, Manuel Malmierca^{1,4}

¹Lab of Auditory Neurophysiology, Institute of Neuroscience of Castilla y León, Salamanca, Spain, ²Department of Neuroscience, University of Connecticut Health Center, Farmington, Connecticut, USA, ³Duke University Medical Center, Durham, North Carolina, USA, ⁴The Medical School, University of Salamanca, Spain

Background

Neuronal types in the cochlear nuclei can be distinguished on the basis of both physiological and morphological criteria. The neuronal types participate in a complex neural circuitry with both excitatory and inhibitory components and project to higher auditory nuclei. Frequency response areas (FRA) and peri-stimulus time histograms (PSTH) have been used to characterize different neuronal populations in several species, but response types in the rat have not been described. Here, we describe FRA and PSTH patterns recorded in the same neurons in the DCN of the anesthetized rat.

Methods

Experiments were performed on 17 female Long-Evans rats anesthetized with urethane (1.5 g/kg, i.p.). Glass micropipettes filled with 2 M NaCl (15–25 M Ω) or tungsten electrodes (1–2 M Ω) were used to make extracellular recordings of neural responses in well-isolated single units. Electrolytic lesions (10–15 μ A for 10–15 s) were made after recording and used for subsequent histological verification of the recording sites. Auditory stimuli consisted of 35ms long pure tones with a 5 ms rise/fall ramp at a repetition rate of 4 Hz.

Results

The present data set includes the response profiles of 45 single units in the cochlear nuclei. Twenty-seven of these were localized to the DCN and will be described here. (Eleven units were localized to the VCN and 7 could not be assigned a location.) The recorded neurons include a wide variety of firing patterns and rate-level functions, as have been described in detail for other species. More than the half of the neurons in the DCN (17/27) displayed non-monotonic rate-level functions. Based on the PSTHs, DCN neurons were classified as, primary-like (n = 12), pause/build (n = 6) and onset (n = 9) firing patterns. According to FRAs, neurons were identified as type II (n = 3), III (n = 16) and II/III (n = 8). We found the 3 PSTH types for type III FRA, primary-like and onset firing pattern for type II/III, and primary-like was found to be only type II FRA. In the VCN, our small sample included the primary like, n = 5; pause/build, n = 2; onset, n = 3 and chopper, n = 1.

Conclusion

Our study describes basic temporal and spectral properties of unit responses in the DCN of the anaesthetized rat.

Supported by BFU2009-07286 & EUI2009-04083 to MSM and NIH DC00135 to NBC and R01 DC000189 to DLO.

640 Synergistic Action of GABA and Glycine Provides Powerful Inhibition to Spherical Bushy Cells in the Cochlear Nucleus of Gerbil

Jana Nerlich¹, Thomas Künzel², Christian Keine¹, Andrej Korenic³, Rudolf Rübsamen¹, Ivan Milenkovic¹

¹Faculty of Biosciences, Pharmacy and Psychology, University of Leipzig, Germany, ²Department of Zoology and Animal Physiology, RWTH Aachen University, Germany, ³Faculty of Biology, University of Belgrade, Serbia

Background

In the auditory brainstem nuclei of mature rodents, precisely timed inhibition is predominantly mediated by the fast glycinergic neurotransmission which contributes to accurate timing of action potentials. GABA is transiently released from inhibitory terminals during early postnatal development (LSO), but in the mature system it mainly plays a modulatory role through presynaptic GABA_B receptors (MSO, AVCN) or postsynaptic glycine receptors (MNTB). In the AVCN, presynaptic terminals containing glycine and/or GABA and respective postsynaptic receptors are present not only during development, but also in maturity. Although in vivo recordings with iontophoretic drug applications consistently suggested a contribution of both transmitters to the inhibition on spherical bushy cells (SBCs), our understanding of their action and the advantage of such a two-transmitter based system beyond development are still inconclusive.

Methods

Physiological effects of inhibition were assessed by means of in vivo extracellular recordings of SBCs, conducted in P20-30 Mongolian gerbils using either a sole inhibitory stimulation (stimulus within the unit's inhibitory sideband) or a two-tone stimulation protocol (additional excitatory stimulus at unit's CF). In slices containing AVCN, pharmacologically isolated, evoked inhibitory postsynaptic currents (eIPSCs) and potentials (eIPSPs) were recorded in SBCs at postnatal days P22-30. The contribution of glycine- and GABA-mediated synaptic transmission was measured following application of GABA_A- and glycine-receptor antagonists. Amplitudes and waveform kinetics of inhibitory currents (glycinergic, GABAergic and synergistic) measured in vitro were used to constrain a conductance based model of synaptic interaction in SBCs.

Results

Acoustically evoked inhibition changes the ratio of isolated EPSP/APs and prolongs the EPSP-AP transition. In slice recordings, eIPSCs exhibit slow synaptic decays causing a stimulus number- and frequency-dependent conductance plateaus. Glycinergic transmission largely determines the amplitude and the kinetic of eIPSCs and eIPSPs, while the contribution of GABA_A receptors potentiates the AP inhibition. The amplitude of eIPSCs is larger than the sum

of pharmacologically isolated glycinergic and GABAergic components. Physiological significance of synergistic action is suggested by the modeling results, showing the increased inhibitory potency at a wider range of excitatory conductances and longer duration of inhibition.

Conclusion

Efficient synaptic inhibition of SBCs is mediated by a synergistic action of glycine and GABA. The joint action of transmitters causes a supra-additive increase of the dynamic range in which the inhibitory conductance prevents the AP generation by the excitatory synaptic input. Still, the physiological mechanism underlying a possible interaction remains to be elucidated.

641 Neural Correlates of Tone Detection in the Cochlear Nucleus of Nonhuman Primates

Maggie Dylla¹, Peter Bohlen¹, Jason Grigsby¹, Ramnarayan Ramachandran¹

¹Vanderbilt University

Background

Detection of sounds is a critical and fundamental function of the auditory system. Our behavioral studies showed that thresholds to detect a tone displayed a characteristic U-shaped relationship with frequency. Reaction times to detect tones decreased as the tone sound pressure levels increased beyond threshold. To evaluate the neuronal correlates, we measured the responses of neurons in the inferior colliculus (IC) to tones. Signal detection theoretic analysis revealed that neuronal thresholds and slope of neurometric functions in IC matched behavioral thresholds and slope of psychometric functions. The responses of single units were different on correct trials relative to incorrect trials at the same signal sound pressure level. The behavioral reaction times could be related to the magnitude of IC neuronal responses. These results suggest that IC neuronal response strengths were strongly correlated with behavior. To test the hypothesis that the response correlations were derived in the IC and were not inherited from the responses of the cochlear nucleus (CN), we simultaneously measured behavioral responses and neuronal responses in the CN, to evaluate the role of the CN in detection.

Methods

Two macaques (*Macaca mulatta*) were trained in a reaction time lever release task to report the detection of tones. Appropriate catch trials were interleaved to make sure the monkeys were actually reporting tone detection. Single units were simultaneously recorded from the CN (n=60). The characteristic frequency of these units ranged up to 32.5 kHz. Most of the units were classified as type I or type I/III or type III, based on the distribution of excitation and inhibition in frequency response maps. Signal detection theory and Receiver Operating Characteristic (ROC) analyses were used to create psychometric (behavioral), and neurometric functions. Neurometric functions reveal the probability of correct response based on the distribution of the number of spikes fired by the CN neuron on tone trials and catch trials.

Results

On the average, CN neuronal thresholds were larger than behavioral thresholds by about 19 dB. In addition, the slopes of the neurometric functions were shallower than those of the simultaneously measured psychometric functions. The responses of some neurons were different based on the behavioral outcome of the trial, but the number of these was smaller than in the IC.

Conclusion

These results suggest that the magnitude of CN responses are only weakly correlated with behavior, and a model is suggested to transform CN responses into IC responses. Supported by R01 DC11092.

642 Modulation of Temporal Coding in the Superior Paraolivary Nucleus

David Sloan¹, Albert Berrebi¹

¹Sensory Neuroscience Research Center, West Virginia University, Dept of Otolaryngology

Background

Precise temporal coding by auditory system neurons is essential to accurate hearing. The superior paraolivary nucleus (SPON) is a GABAergic nucleus of the superior olive whose neurons are particularly sensitive to discontinuities in auditory stimuli. It is known that the characteristic offset spikes of SPON neurons result from a post-inhibitory rebound mediated by strong glycinergic inputs from the medial nucleus of the trapezoid body. However, less is known about the modulatory effects of excitatory inputs (originating from the cochlear nucleus) or GABAergic inputs (arising from collateral innervation from other SPON units) that also impinge on SPON cells.

Methods

SPON neurons were manipulated pharmacologically in vivo in anesthetized adult female rats. "Piggyback" electrodes, in which a recording electrode was glued to a multibarrel glass pipette, were loaded with either the glycine antagonist strychnine, the GABA antagonist Gabazine, the AMPA receptor antagonist NBQX or the NMDA receptor antagonist CPP. Single SPON units were isolated and characterized using a battery of auditory stimuli, including stimuli designed to measure the response of the units to sound gaps and sinusoidally amplitude-modulated tones. Drugs were then administered iontophoretically, either separately or in combination, and the units were monitored to detect differences in firing patterns.

Results

As previously reported, only blockade of glycine receptors greatly diminished the typical offset spiking patterns to pure tones. Moreover, when glycine neurotransmission was blocked SPON neurons showed both increased spike rates and decreased synchronicity to amplitude modulated tones, as well as altered responses to sound gaps. Blockade of glutamate receptors reduced the ability of SPON neurons to synchronize with modulation rates

above 200 Hz, whereas blockade of GABAergic inhibition showed little effect on temporal processing. We are currently investigating the functional role of glycine, GABA and excitatory neurotransmitters in modulating other aspects of SPON response properties.

Conclusion

Preliminary data suggests that blockade of glycine, GABA-A or glutamate receptors caused changes in the ability of SPON neurons to phase lock to increasing rates of amplitude modulations. This finding indicates that each of these neurotransmitters has a role in modulating aspects of the temporal response properties of SPON neurons.

643 Contribution of NMDA and AMPA Receptors to Response Properties of Neurons in the Medial Nucleus of the Trapezoid Body of the Rat

Fei Gao¹, Albert Berrebi¹

¹Sensory Neuroscience Research Center, West Virginia University, Dept of Otolaryngology

Background

The medial nucleus of the trapezoid body (MNTB) is a prominent cell group of the superior olivary complex that plays a critical role in sound localization circuitry. MNTB principal cells, the dominant cell type in the nucleus, receive their excitatory input from globular bushy cells of the contralateral cochlear nucleus via large calyces of Held. While the excitatory input to MNTB neurons carried via the calyx of Held is mediated by fast-acting AMPA receptors (Banks and Smith, 1992), NMDA-mediated excitation with a slower time course has also been documented in rats younger than postnatal day 16 (Forsythe and Barnes-Davies, 1993; Hamann et al., 2003) and mice (Joshi and Wang, 2002).

Methods

In present study, single units in the MNTB were manipulated pharmacologically using "piggyback" electrodes in vivo in anesthetized adult rats. We compared contributions of NMDA and AMPA/kainate receptors to auditory evoked responses in MNTB. We examined response magnitude, temporal patterning, gap detection threshold (GDT) and responses to sinusoidally amplitude modulated (SAM) tones before, during and after local micro-iontophoretic application of the NMDA receptor antagonist CPP [(±)3-(2-carboxypiperazin-4-yl)-propyl-1-phosphonic acid], the AMPA receptor antagonist NBQX [(1,2,3,4-tetrahydro-6-nitro-2,3-dioxo-benzo[f]quinoxaline-7-sulfonamide)], or both drugs applied simultaneously.

Results

CPP and NBQX reduced spontaneous and evoked firing rates, and resulted in longer first-spike latencies and increased jitter in the timing of the first spike. The effects of NBQX and the NBQX/ CPP cocktail were much stronger than CPP administered alone. For some neurons, GDTs were markedly increased by application of NBQX. Each drug also reduced the firing rate and entrainment of MNTB

neurons in response to SAM tones, but did not change vector strengths.

Conclusion

Overall, blockade of AMPA receptors was more effective in modulating response properties of MNTB neurons than blockade of NMDA receptors. However, the results obtained under pharmacological blockade of the NMDA receptor suggest that NMDA-mediated excitation at the calyx-MNTB synapse persists into adulthood.

644 The Temporal Responses of Single Units in the Ventral Cochlear Nucleus to Conspecific Vocalisations

Arkadiusz Stasiak¹, Jean-Marc Edeline², Quentin Gaucher², Christian Lorenzi³, Ian Winter¹

¹University of Cambridge, England, ²Paris-Sud, France,

³Ecole Normale Supérieure, France

Background

The neural mechanisms responsible for the difficulties in understanding vocalisations in adverse listening conditions are still debated. Here we compare the representation of temporal fine structure (TFS) and envelope (E) cues of complex sounds, including conspecific vocalisations, in the responses of single units from the ventral cochlear nucleus of normal-hearing guinea pigs with the responses from guinea-pigs with a mild sensorineural hearing loss.

Methods

Single units have been recorded from the ventral cochlear nucleus (VCN) of 7, normal-hearing, urethane anaesthetised guinea pigs. For a further 7 animals we produced a moderate sensorineural hearing loss by exposing the guinea pigs to a 2 kHz sinusoid at 120 dB for 1 hour. The 2-kHz region was selected to lie within the phase-locking limits of the guinea pig. This exposure resulted in a threshold loss of about 20 dB between 0.1 and 3 kHz and less than 10dB loss between 3 and 7 kHz. Recordings from animals with a hearing impairment commenced around 30 days post-exposure. The stimuli were pure tones (for comparison with previous studies) and both conspecific and non-conspecific animal vocalisations. We selected signals to provide a variation in temporal envelope and spectral range. Four guinea pig vocalisations were studied; the chirp, purr, chatter and whistle. All vocalisations were randomly presented for a total of 50 repeats.

Results

We have recorded from 80 units in animals with normal hearing and 81 units from animals with a mild sensorineural hearing loss. As expected many units in the VCN produced a good temporal response to the waveform of conspecific sounds. This response was correlated with unit type with primary-like units showing the best response to the temporal aspects of the sound although the onset units showed a strong response to the peaks of the temporal envelope. In animals with a mild sensorineural hearing loss the thresholds of fibres in the 1-3 kHz region were raised by approximately 20 dB re: thresholds in our

normal hearing population. Although thresholds were elevated we found no significant difference in the tuning between normal and hearing impaired animals.

Conclusion

A preliminary analysis of the data suggests there is little change in the temporal discharge properties to conspecific vocalisations following a mild sensorineural threshold loss. This is consistent with the small shift in unit thresholds and corresponding lack of significant changes in tuning.

645 Stability and Plasticity of Brainstem Function Across the Lifespan

Erika Skoe¹, Jennifer Krizman¹, Samira Anderson^{1,2}, Nina Kraus¹

¹Northwestern University, ²University of Maryland

Background

The general consensus is that the human auditory brainstem undergoes rapid developmental changes early in life (until age ~2) followed by a prolonged period of stability that terminates when aging-related changes in brainstem function emerge. However, earlier work on human brainstem development was limited by inadequate sampling across the lifespan and/or averaging across children and adults. Using a larger dataset than past investigations, we aimed to trace more subtle variations in brainstem function that occur normally from infancy to the 7th decade of life.

Methods

We recorded auditory brainstem responses (ABRs) to a click and the speech syllable "da" in normal-hearing healthy individuals between the ages 0.25 to 70 years. Suprathreshold stimuli were presented monaurally to the right ear. Analyses were performed on a dataset of 580 subjects, divided into 13 sex-matched age groups. We measured the latency of each prominent peak in the speech- and click-ABR. For the speech-evoked ABR, we also measured frequency encoding across the response spectrum, in addition to gauging the trial-by-trial consistency of the response.

Results

Although each family of measures (latency, frequency encoding, response consistency) has a distinct developmental profile, there is a common trend for developmental changes to continue well past age 2. In the case of timing and frequency encoding, the developmental profile is characterized by a relatively transient developmental apex around ages 8-10. That is, latencies become progressively earlier and frequency encoding becomes progressively more robust until the apex, after which latencies become longer and frequency encoding declines until early adulthood where the developmental trajectory stabilizes. In the case of response consistency, the developmental apex is more prolonged, with trial-by-trial consistency increasing from infancy to age 8 and then staying relatively stable into early adulthood. Across all measures, aging-related changes begin to emerge in the fifth decade of life.

Conclusion

This study provides the first comprehensive assay of how the ABR changes over the human lifespan. The outcomes of this research provide new insight into auditory development. It establishes that developmental plasticity continues well into the second decade of life, which challenges conventional wisdom that the auditory brainstem is mature by age ~2. We interpret the developmental apex as reflecting a sensitive period in development when experience, including auditory remediation and deprivation, may be most influential.

Supported by: Northwestern University Knowles Hearing Center, NIH RO1DC10016, NSF 0921275

www.brainvolts.northwestern.edu

646 The Mouse Anteroventral Cochlear Nucleus (AVCN): Regional Differences in Synaptic Organization of Bushy Cells

Amanda Lauer¹, Catherine Connelly², Heather Graham³, Katanyu Pongstaporn², David Ryugo^{1,2}

¹Johns Hopkins University, ²Garvan Institute of Medical Research, ³University of Maryland Baltimore County

Background

Spherical and globular bushy cells (SBCs and GBCs) of the AVCN receive huge auditory nerve endings, the endbulbs of Held and modified endbulbs, which are specialized for precise representation of acoustic information. These high fidelity synapses are essential for locking neural activity to acoustic events to encode features such as interaural level and timing differences used to compute sound location. Recent physiological studies in mice and other species have called into question the clear distinction between SBCs and GBCs, suggesting instead a sort of continuum of response properties determined by the inputs to the cell with exemplars of both response types at either end of the spectrum. We conducted a systematic investigation of mouse bushy cells along the rostral-caudal axis in an effort to more completely understand the morphological variation that gives rise to reported response properties in mice.

Methods

We combined quantitative light and electron microscopy to investigate regional differences in the AVCN of CBA/CAJ mice. Cell morphology, immunostaining, and the distribution of primary and non-primary synaptic inputs along the rostral-caudal axis were characterized. Morphometric analysis was accomplished using ImageJ.

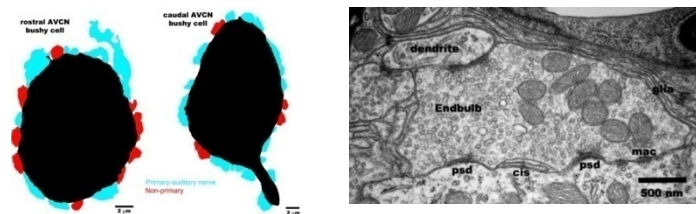
Results

Overall, large regional differences in postsynaptic cell characteristics were not found. In contrast, bushy cells of the rostral AVCN received a greater proportion of axosomatic input than bushy cells of the caudal AVCN. The percentage of terminals displaying primary auditory nerve morphology was larger in caudal AVCN, while non-primary excitatory and inhibitory inputs were more

common in rostral bushy cells (Figure 1). The ultrastructural characteristics of primary auditory nerve inputs revealed many similar characteristics in rostral and caudal AVCN (Figure 2). Primary terminals were large, replete with synaptic vesicles, and often displayed multiple postsynaptic densities and structures associated with ultrafast auditory synapses (mitochondrion adherens complexes, extended extracellular spaces). Cross sectional area, postsynaptic density length and curvature, and percent mitochondrial area were not different in axosomatic auditory nerve terminals in rostral and caudal AVCN; however, rostral auditory nerve terminals contained more synaptic vesicles near the postsynaptic densities. Primary axosomatic auditory nerve terminals also formed synapses with adjoining dendrites.

Conclusion

Regional differences in physiological responses of mouse bushy cells likely depend mainly on the pattern of inputs rather than morphological characteristic of the cells themselves. These findings suggest that rostral bushy cells may display greater postsynaptic synaptic integration than caudal bushy cells, but further characterization is needed.



647 Microglial Cells Participate in Reshaping Neuronal Circuitry of the Rat Auditory Brainstem After Cochlear Ablation

Robert Illing¹, Philipp Janz¹

¹University of Freiburg

Background

Cochlear ablation triggers a wealth of cellular and molecular responses in the central auditory system of adult rats. Axonal degeneration, neuronal shrinkage, astrocyte hypertrophy, and axonal growth related to the expression of the growth-associated protein GAP-43, lead to complex rearrangements in auditory brainstem circuitry. Microglia are known to phagocytose cellular debris, secrete cytokines and growth factors, and remodel the extracellular matrix in neuropathological conditions. Although previous work has shown a reaction of microglia following the intracerebral injection of heat-killed bacteria, visual-experience, axotomy, and cochlear ablation, only little is known about their participation in synaptic plasticity. We here asked whether microglia respond to sensory deafferentation with identifiable actions on central neuronal circuitry.

Methods

Young adult Wistar rats were unilaterally deprived from primary auditory input by cochlear ablation. After survival times of one to seven days, immunocytochemistry for light and electron microscopy was performed. Double-labeling was done for several combinations of cytological markers,

signaling molecules, and second messengers. This approach allowed us to study the spatial relationship between microglia identified by CD11b and neuronal compartments before and after sensory deafferentation.

Results

By one to seven days post-lesion, activated microglia have developed intense immunoreactivity for MAP kinases p-ERK1/2 and p-p38 in ventral cochlear nucleus (VCN), lateral superior olive (LSO), and central inferior colliculus (CIC). Labeling for p-ERK1/2 and p-p38 was largely absent outside microglial profiles, with the exception of selected presynaptic endings. Remarkably, these microglia were found in close apposition to neuronal somata, often engulfing presynaptic endings. Most of these endings contained either vGluT1 or GAD65. Microglial processes showed morphological signs for phagocytotic actions on synapses, suggesting that they participate actively in altering the architecture of neuronal networks. This was apparent not only in VCN directly affected by axonal degeneration, but also in LSO and CIC where modification of the pattern of synaptic contacts must be invoked by secondary causes. Furthermore, the microglial reaction was seen in AVCN and LSO to precede astroglial hypertrophy, supporting the concept of microglia-derived cytokines activating astrocytes.

Conclusion

In central auditory pathways, microglia displaying MAPK-signaling appear to contribute to an adaptive response to sensory deafferentation. This response occurred in regions that were directly affected by axonal degeneration as well as in others only indirectly affected, and appears to include two ways of action: (1) activation of astrocytes, and (2) synaptic rearrangement of neuronal networks.

648 Synaptic Organization of Posterior Ventral Cochlear Nucleus (PVCN)

Magnocellular Core in the CBA/CaJ Mouse

Brian McGuire¹, Heather Graham², Amanda Lauer¹

¹Johns Hopkins University, ²University of Maryland Baltimore County

Background

Large cells of the PVCN are thought to be essential for many fundamental auditory processing tasks such as loudness perception, listening in noisy backgrounds, spectral and temporal integration, and modulation of the contralateral cochlear nucleus. Much of what we know about the hypothesized roles of PVCN cells comes from studies performed in mice, yet most of what we know about the ultrastructure of PVCN synapses comes from studies performed in cats and rats. A detailed characterization of synaptic organization of PVCN in mice is needed to enhance our understanding of the role of synaptic organization in generating specific physiological responses and to accurately identify age-related, environmental, and genetic contributors to hearing loss that may affect auditory processing in PVCN in mouse models.

Methods

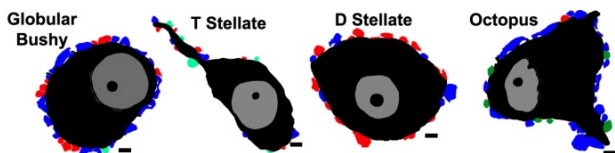
We used electron microscopy, immunohistochemistry, light microscopy, and unbiased stereological methods to reveal qualitative and quantitative details regarding the baseline state of synaptic organization of the PVCN magnocellular core in young adult CBA/CaJ mice.

Results

The CBA/CaJ PVCN magnocellular core contains approximately 110,000 to 120,000 VGLUT1-positive auditory nerve puncta within approximately 110 to 120 million μm^3 as measured using stereological probes. Prototypical PVCN neurons are depicted in the figure (scale bars = 2 μm). Globular bushy cells with oblong or round somata resembled those of the AVCN with auditory nerve (blue), inhibitory (red) and non-primary excitatory inputs (light green) contacting most of the soma. T stellate cells received few axosomatic terminals, and much of their somata were ensheathed in glia. Many small auditory nerve boutons, inhibitory terminals, and nonprimary excitatory terminals contacted their dendrites. T stellate cells were often adjacent to other T stellate cells, but membranous specializations suggestive of junctions were not obvious. D stellate cells with variable soma shapes received numerous, mostly inhibitory axosomatic terminals. Small auditory nerve boutons and non-primary excitatory terminals were also observed. D stellate dendrites also received many inputs. Auditory nerve terminals of varying size covered much of the octopus cell somata and dendrites. Specializations common to other fast auditory synapses were observed in some of these terminals. Non-primary excitatory terminals were also observed (dark green), possibly originating from axon collaterals from other octopus cells.

Conclusion

The general synaptic organization of the PVCN magnocellular core is similar to other species. These data will form the basis for future quantitative studies of PVCN neural plasticity and degeneration in response to genetic and environmental manipulations and aging.



649 Laminar and Cellular Organization of the Human Dorsal Cochlear Nucleus

Joan Baizer¹, Nadav Weinstock¹, Nicholas Paolone¹

¹University at Buffalo

Background

Tinnitus, the perception of a phantom sound, or “ringing in the ears” is a debilitating condition affecting as many as 10% of the US population. It is usually, but not always, associated with hearing loss. In some patients, tinnitus may be modulated by somatosensory input (somatic tinnitus), suggesting somatosensory-auditory interactions. Much work has been devoted to determining the CNS site

of tinnitus generation. Especially useful have been studies using behavioral animal models of tinnitus, usually rodents. Data from these studies have implicated the dorsal cochlear nucleus (DCN) as a key site in tinnitus generation. In nonprimate mammals, the DCN has a distinct laminar organization and several anatomically and neurochemically defined neuronal types. The circuitry in the nonprimate DCN has been well-characterized. Studies of rodent models of tinnitus have shown an increase in spontaneous activity in the projection neurons (fusiform or pyramidal cells) of the DCN. Further, anatomical data in rodent have shown that the DCN receives both auditory and somatosensory information, suggesting it as a mediator of somatic tinnitus. However, there is a major problem in extending the findings from the rodent DCN to humans. Classic studies of human DCN suggest that its structure is substantially different from that of the rodent, with an erosion of laminar organization, and the loss of several cell types, including granule cells. These results suggest major differences in circuitry in human DCN compared to that in rodents and question the usefulness of data from rodents in understanding tinnitus in humans.

Methods

We have reexamined the organization of the human DCN using cases from the Witelson Normal Brain Collection. We used Nissl-staining and immunohistochemistry for several markers including nNOS (nitric oxide synthase), calretinin, calbindin, nonphosphorylated neurofilament protein and VGLUT2 and VGLUT1, markers that label axon terminals of somatosensory and auditory afferents in the rodent DCN.

Results

Our data show that the human DCN has three distinct layers, an outer molecular layer, a layer of large projection neurons and a deeper layer with multiple cell types. We also found axon terminals immunoreactive to VGLUT2 and VGLUT1, suggesting both somatosensory and auditory inputs to the human DCN.

Conclusion

Contrary to earlier studies, our results suggest that the organization and inputs of the human DCN are not that different from the rodent DCN and support the usefulness of rodent models in studying the role of the DCN in the generation of tinnitus.

650 3D Reconstructions of Dorsal Cochlear Nucleus Neurons and Their Synapses Using Serial Block Face Scanning Electron Microscopy

Guoyou Chen¹, Nauman Manzoor¹, Grahame Kidd¹,

James Kaltenbach¹, Lily Velet¹

¹Cleveland Clinic

Background

Serial Block Face Scanning Electron Microscopy (SBFSEM) provides a rapid, reproducible means of viewing ultrastructural features from biological samples in 3D. Using SBFSEM for reconstructing ultrastructural

details of synapses and synaptic circuitry in the dorsal cochlear nucleus (DCN), we sought to reconstruct and map synaptic terminals on different regions of fusiform cells, the principal output neurons of the DCN.

Methods

Fixed and stained samples of the DCN were embedded in epon then sliced and imaged on a Zeiss Sigma VP scanning electron microscope equipped with a Gatan 3View stage/knife system. The sections were cut at 75 nm thickness in the transverse plane at a level where the DCN reaches its maximal dorsoventral dimension. Images were obtained in 6 adjacent fields, which together, spanned the molecular, fusiform cell and outermost part of the deep layers of the DCN. In each field, a stack of over 600 sections was cut and imaged such that the total thickness of each stack was approximately 50 μm . After image acquisition, the resulting stacks were stitched together into a montage that measured 160 x 240 μm . Within this montage, the outlines of fusiform cells and their dendrites and inputting synapses were traced.

Results

The cells were classified as fusiform cells if they met the following criteria: soma measured approximately 25-30 μm in diameter, dendritic arbors extended toward both the ependymal surface (apical dendrite) and deep layer (basal dendrite), an axon extended toward the dorsal acoustic stria and the apical dendritic arbors were studded with spines. To obtain insight into how synapses are spatially distributed over the fusiform cells, we mapped the terminals over the somal surface and on selected segments of their primary and secondary dendrites. We also obtained measures of the number and sizes of dendritic spines on the apical dendrites. In selected subsets of terminals, the number of neurotransmitter vesicles and dimensions of synaptic densities were quantified. Lastly, we attempted to trace axons from their synaptic ending to determine whether axons can be traced to their cells of origin and to assess whether different synaptic terminals arise from different branches of the same axon.

Conclusion

We are using this data to establish normative values that can be used for comparison with similar measures obtained from animals that have been exposed to intense sound. (Supported by NIH R01 DC009097).

651 Suppression of Neural Firing in the Inferior Colliculus Induced by Focal Electrical Stimulation of Auditory Cortex: Implications for the Treatment of Tinnitus

Craig Markovitz¹, Kyle Wesen¹, Patrick Hogan¹, Henisha Dhandhusaria¹, Hubert Lim¹

¹University of Minnesota

Background

One potential treatment option for tinnitus suppression utilizes cortical electrical stimulation to reverse abnormal neural changes causing the tinnitus percept. Although

initial clinical trials have been encouraging, cortical stimulation results have varied dramatically across patients. In order to improve clinical results, we sought to determine the neurophysiological effects of focal electrical stimulation of auditory cortex (AC) on the auditory pathway. Particularly, we assessed whether AC stimulation can suppress neural firing within the inferior colliculus (IC), a region that has shown hyperactivity in tinnitus animals and patients. Since primary auditory cortex (A1) is difficult to surgically access in humans (hidden within Heschl's gyrus), we focused the majority of our investigation on secondary auditory cortex (A2).

Methods

We positioned multi-site electrode arrays into AC and the IC of ketamine-anesthetized guinea pigs. After characterizing the acoustic-driven responses on each site to confirm its location (i.e., frequency region and sub-nuclei of AC or IC), we electrically stimulated the deeper output layers of AC and recorded the corresponding changes in spontaneous and acoustic-driven responses throughout the IC.

Results

Stimulation of deeper A1 output layers suppressed acoustic-driven activity in the IC. The amount of suppression depended on a number of factors, including the relative time between the acoustic and electrical stimuli, the best frequency of the A1 and IC electrode sites, and the location of the IC site along an isofrequency lamina. Stimulation of deeper A2 output layers elicited a variety of interesting suppressive results, including direct suppression from stimulation, residual suppression affecting acoustic-driven spiking after stimulation had ceased, and suppression of spontaneous activity.

Conclusion

Cortical stimulation can suppress acoustic-driven and spontaneous neural firing in the IC, demonstrating its potential for the treatment of tinnitus. Further work must be performed to characterize the optimal locations and stimulation strategies for eliminating the phantom percept, including counteracting the hyperactivity and hypersynchrony associated with the tinnitus percept.

This work was supported by NIH NIDCD R03-DC011589, NIH NIDA T32-DA022616, the University of Minnesota Institute for Engineering in Medicine Walter Barnes Lange Memorial Award, and start-up funds from the University of Minnesota (Institute for Translational Neuroscience and College of Science and Engineering).

652 Extensive Areas of the Cortex Are Evoked by Stimulation from the Newly Implanted Ear in Children Who Were Long-Term Unilateral Cochlear Implant Users

Salima Jiwani^{1,2}, Blake C. Papsin^{1,3}, Karen A. Gordon^{1,2}

¹Archie's Cochlear Implant Laboratory, Department of Otolaryngology, The Hospital for Sick Children, ²Institute of Medical Sciences, Faculty of Medicine, University of

Toronto, ^{3b} Departments of Otolaryngology - Head and Neck surgery, Faculty of Medicine, University of Toronto
Background

We recently showed that the development of cortical responses follows a normal-like trajectory with time-in-sound over long-term unilateral cochlear implant use when the duration of bilateral auditory deprivation in childhood is limited. We know from normal hearing data that the temporal lobe is the principal region of auditory processing in the brain. However, the sources of cortical activation in cochlear implant users remain unknown. In the present study, we investigate the areas of the brain that are activated by sound in cochlear implant users. Specifically, we ask whether cortical areas of the brain which normally respond to sound are activated by auditory input in adolescents who grow up using one cochlear implant; and whether activity in the deprived pathways is compromised by the long-term use of only one implant.

Methods

Electrically-evoked cortical responses were recorded within the first week of bilateral cochlear implant activation in 12 adolescents who had over 10 years of unilateral cochlear implant experience at the time of the test. Responses were recorded from 64-cephalic electrodes, using 250Hz biphasic pulse trains presented at a rate of 1Hz and evoked by electrical pulses delivered from cochlear implants on the experienced and naïve sides separately. Cortical activation underlying the peaks of the evoked cortical response was localized to different areas of the brain (i.e., temporal, frontal, parietal and occipital lobes) on both hemispheres (ipsilateral and contralateral to stimulation), using our unique beamforming method.

Results

Consistent with previous reports, responses from the experienced ear contained amplitude peaks similar to those expected in same aged peers with normal hearing. These peaks were found to come predominantly from the temporal (i.e., auditory) cortex. By contrast, responses from the naïve ear had completely different peaks occurring with larger amplitudes. Neural activity underlying these peaks was more widely distributed, occurring in temporal, frontal, parietal and occipital areas.

Conclusion

Long-term unilateral cochlear implant use promotes maturation of the auditory cortex in children. However, diffuse activation of the temporo-fronto-parietal regions from stimulation of the naïve side suggests that the deprived auditory pathways may recruit more attentional resources to process the novel input.

653 Auditory Cortex Structure and Metabolite Findings in Older Adults with High-Frequency Hearing Loss

Kelly C. Harris¹, Mark A. Eckert¹, Judy R. Dubno¹
¹Medical University of South Carolina

Background

Age-related differences in auditory function in older adults with normal hearing may be attributed to central auditory system declines and to changes in the auditory periphery not reflected in pure-tone thresholds. Although thresholds for these individuals may be equivalent to normal at lower and mid-frequencies, most older adults exhibit varying degrees of higher frequency hearing loss. The effects of hearing loss and the sensitivity of pure tone thresholds as they relate to changes in the structures of the central auditory system remain unclear.

Methods

To better understand the effects of high frequency hearing loss on the aging central auditory system, we examined the extent to which variation in high frequency hearing was associated with variation in auditory cortex structure and metabolism in 15 older adults whose pure-tone thresholds were ≤ 25 dB HL from 0.5 kHz to 3.0 kHz and ranged from 15 to 70 dB HL at 8.0 kHz. Diffusion imaging (DTI), magnetic resonance spectroscopy (H-MRS) (NAA), and T1-weighted images were compared to thresholds at 8.0 kHz, where individual differences were largest. Right and left Heschl's gyri were selected as regions of interest (ROI).

Results

Pure-tone thresholds at 8.0 kHz were positively correlated with DTI mean diffusivity (MD) in the right HG, suggesting that changes in high frequency hearing occur with changes in white matter microstructure. Similarly, elevated thresholds at 8.0 kHz occurred with lower NAA values, suggesting reduced neuronal viability with high frequency hearing loss. Results from linear regression suggest that the association between high-frequency hearing loss, MD, and NAA remained significant after controlling for differences in brain volume and age.

Conclusion

Our measurements were obtained from large ROIs, which encompass regions associated with encoding of both low and high frequency stimuli, and did not have the spatial resolution of voxel-based analyses in which gray matter associations with pronounced high frequency hearing loss have been observed. These results suggest that (1) diffusion and H-MRS metrics are sensitive to auditory cortex changes that may occur with age-related declines in high frequency hearing and (2) widespread central auditory system changes may occur with age-related changes to the auditory periphery that do not result in hearing loss typically considered clinically significant. These changes in white matter integrity and metabolism may contribute to suprathreshold processing deficits observed in older adults with normal hearing.

654 Corticofugal Slow Effects of Auditory Cortex Electrical Microstimulation on Cochlear Responses in the Chinchilla

Constantino Dragicevic¹, Natalia Jara¹, Gonzalo Terreros¹, Paul H Delano^{1,2}

¹*Fisiología y Biofísica, ICBM, Universidad de Chile,*

²*Servicio Otorrinolaringología, Universidad de Chile*

Background

The auditory efferent system comprises descending pathways from the auditory cortex to the cochlea, including the cortico-collicular and the olivocochlear system. The electrical stimulation of the medial olivocochlear fibers produces two types of effects with different time scales: (i) fast (tens of milliseconds) and (ii) slow effects (tens of seconds). Whether these two types of effects could also be obtained by electrical stimulation of the auditory cortex is unknown. Here, we recorded cochlear microphonics (CM) and auditory-nerve compound action potentials (CAP) previous, during and after auditory cortex microstimulation and found slow but not fast corticofugal modulations.

Methods

CAP and CM responses were recorded using a right round-window electrode. Cortical evoked potentials were obtained from a Nichrome® electrode positioned in the left auditory cortex of nine anesthetized chinchillas (ketamine/xylazine). Trains of four electrical pulses (0.25 ms each, separated by 2.2 ms) were delivered to the auditory cortex at different rates (1-33 Hz) and current intensities (1-100 µA), during one to five minutes, using an isolated pulse generator (2100, AM-Systems®). Tone bursts were presented at different frequencies (0.5-8 kHz) and intensities (20-90 dB SPL) using a Tucker-Davis-Technologies® system III hardware and ER-2 (Etymotic Research®). Data was acquired using a National Instruments® Board (NI-6071E).

Results

Auditory-cortex microstimulation produced significant changes in the amplitude of CAP and CM in five experiments. Of these, three (two) showed decrements (increments) of both potentials, 2.3 (2.7) and 2.6 (0.9) dB on average for CM and CAP, respectively. Only one showed modulations going in opposite directions, 1.5 and -8.6 dB for CM and CAP, respectively. These corticofugal modulations appeared only after three to five minutes of electrical stimulation. In addition, these effects were obtained only using microstimulation rates higher than 30 Hz.

Conclusion

Different to olivocochlear electrical stimulation, auditory-cortex electrical microstimulation in the chinchilla produced only a slow modulation of cochlear responses that builds up after three to five minutes. These results suggest that fast olivocochlear modulations are restricted to brainstem circuits, while slow efferent modulations are present from the auditory cortex to the cochlea.

Supported by FONDECYT 1120256 and Fundación Guillermo Puelma.

655 Functional Reorganization in Area DZ of Congenitally Deaf Cats

Rüdiger Land¹, Christiane Sprenger¹, Peter Baumhoff¹, Peter Hubka¹, Jochen Tillein², Andrej Kral¹

¹*Medical School Hannover,* ²*Johann Wolfgang Goethe-University Frankfurt*

Background

Sensory deprivation during development can induce functional reorganization of cortical sensory areas. Areas deprived from their natural sensory input may take part in processing of other inputs. In congenitally deaf cats - a model of sensory deprivation - possible visual reorganization of the auditory dorsal zone (DZ) has been demonstrated indirectly in behavioral studies (Lomber et al., Nat Neurosci 2010).

Methods

Here we studied extracellular unit activity in the auditory area DZ and the adjacent visual areas AMLS/PMLS of cochlear-implanted congenitally deaf cats (n=4) and hearing controls (n=4). We measured neuronal responses to visual, electrical auditory and bimodal stimulation simultaneously in AMLS/PMLS and DZ using two 16-channel linear multi electrode arrays (MEA). Recording positions were reconstructed histologically after the experiment.

Results

Modality, distribution and relative frequencies of sensory responsive sites were generally similar in hearing and congenitally deaf cats, in area DZ as well as AMLS/PMLS. Although visual responsive sites in area DZ were sparsely distributed in both groups, the total number of visually modulated sites was increased in congenitally deaf cats.

Conclusion

The results demonstrate that area DZ of congenitally deaf cats remains responsive to input from the cochlea, however, also shows that area DZ of congenitally deaf cats receives increased visual input.

656 Cortical Auditory Processing in Individuals with Long-Term Symptoms Following Mild TBI

Kathy Vander Werff¹, Brian Rieger²

¹*Syracuse University,* ²*SUNY Upstate Medical University*

Background

While many individuals recover rapidly from concussion or mild traumatic brain injury (mTBI), a significant number of these individuals continue to experience debilitating problems for months and years after injury. Auditory processing problems, including disproportionate difficulty understanding speech in competing noise, are among these common long-term problems. The goals of the current study were to examine neural correlates of auditory processing in this population at both sensory/obligatory

and cognitive levels of the central auditory system using cortical auditory evoked potentials and to compare these measures with functional performance on behavioral auditory processing and cognitive test batteries.

Methods

Electrophysiological measures were conducted in a group of individuals who sought rehabilitation in a concussion management program due to on-going symptoms 3-18 months post mTBI (n =21) and un-injured age and gender-matched controls. Both obligatory cortical auditory evoked potentials (P1-N1-P2) and cognitive event-related potentials (P300) were recorded to speech syllables in quiet and in a background of multi-talker babble. A neuropsychological cognitive test battery and a battery of behavioral tests of central auditory processing were also completed.

Results

Preliminary results showed that over 50% of the mild TBI participants performed abnormally on 2 or more behavioral tests of central auditory processing. Overall, there were few significant group differences in peak latency or amplitude for the P1-N1-P2 or the P300, although P300 behavioral reaction time was significantly prolonged and percent correct discrimination significantly poorer in noise for the mTBI group compared to controls. Within the mTBI group, P1-N1-P2 responses tended to differ more from controls in those who performed abnormally on auditory processing tests but had normal performance on most cognitive tests, while P300 responses tended to differ from controls more in those who performed poorly on *both* auditory processing and cognitive tests.

Conclusion

A significant number of individuals still symptomatic in the long-term following mTBI showed abnormal performance on behavioral tests of central auditory processing. As a group, there was evidence of slowed processing and reduced discrimination in background noise. Patterns of results from cortical auditory evoked potential and behavioral tests may suggest primarily sensory level auditory processing deficits following mTBI in some individuals, while others have evidence of more global cognitive processing problems that include difficulty processing auditory information. These results could have important implications for rehabilitation planning. This research was supported by NIH R03DC010246.

657 Development of a Rodent Model of Chronic Stress-Induced Auditory Dysfunction

Sarah H. Hayes¹, Daniel Stolzberg¹, Richard Salvi¹, Brian L. Allman²

¹Center for Hearing and Deafness, University at Buffalo, SUNY, ²Dept. Anatomy and Cell Biology, Schulich School of Medicine, University of Western Ontario

Background

Tinnitus and hearing loss are two of the most prevalent auditory impairments. Recent studies have correlated the presence of hearing loss and tinnitus with high levels of life

stress. Importantly, the relationship between stress and auditory dysfunction appears multifaceted; not only does hearing loss and tinnitus increase stress, but stress itself may contribute to the development of these auditory disorders. At present, the underlying mechanisms by which chronic stress contributes to auditory dysfunction are unknown; however, chronic stress has been shown to alter GABAergic neurotransmission in the brain. Stress-induced alterations in GABAergic neurotransmission along the auditory pathway represents one possible route by which chronic stress could contribute to auditory disorders. In order to investigate this possibility, we developed a rodent model to characterize changes in auditory brain regions following chronic stress and hearing loss.

Methods

Male Sprague Dawley rats were divided into 4 groups: (1) restraint stress (6 hours/day for 21 days), (2) noise exposure (1h,16-20kHz, 123dB, bilateral), (3) chronic stress plus noise exposure, and (4) control. Tone-evoked auditory brainstem responses (ABRs) were performed at baseline and following stress and noise exposure. Restraint stress was confirmed by monitoring changes in body weight as well as performance on elevated plus maze and open field tests. Standard immunohistochemical techniques are being used to profile the changes in expression of the GABAergic marker GAD67 in the brain.

Results

As predicted, chronic restraint stress resulted in reduced body weight, as well as less time spent in the open arms of the elevated plus maze and in the center of the open field. Restraint stress alone did not affect ABR thresholds. Noise exposure alone significantly elevated ABR thresholds; however, ABR thresholds of rats exposed to chronic restraint plus noise were not significantly different from rats exposed to noise alone. Assessment of changes in expression of GABAergic markers is in progress.

Conclusion

Our rodent model will allow us to investigate the underlying mechanisms by which chronic stress contributes to auditory dysfunction. Understanding the contribution of stress to auditory dysfunction may help identify individuals at increased risk for developing hearing loss and/or tinnitus and may lead to novel treatment and prevention strategies.

658 Acoustically-Evoked Auditory Change Complex in Children with Auditory Neuropathy Spectrum Disorder: A Potential Objective Tool for Identifying Cochlear Implant Candidates

Shuman He¹, John Grose¹, Craig Buchman¹

¹University of North Carolina at Chapel Hill

Background

Children with Auditory Neuropathy Spectrum Disorder (ANSD) present a challenge for early intervention and habilitation because of the diversity of the disorder and the current lack of robust indicators to guide in management of

this population. This project investigates the utility of the acoustic change complex (ACC) for predicting hearing aid success in ANSD children. It tests the hypothesis that speech perception performance of ANSD children fit with hearing aids can be predicted using the ACC elicited by stimuli containing temporal gaps.

Methods

To date, eight ANSD children ranging in age between 1.9 to 14.2 years have been tested. These ANSD children had mild to moderately severe hearing loss between 250-2000 Hz. All subjects had a minimum of 12 months experience with their hearing aids. The stimulus was an 800-ms Gaussian noise presented at 35 dB SL re. pure tone average through ER-3A insert earphones. Two stimulation conditions were tested: (1) In the standard condition, an 800-ms Gaussian noise was presented to the test ear without any interruption; (2) In the gap condition, a silent period (i.e. temporal gap) was inserted after 400 ms of stimulation. The gap duration was fixed at 5, 10, 20, 50, or 100 ms. The ACC was differentially recorded from high forehead (Fz, active) to contralateral mastoid (A1/2, reference) relative to body ground at low forehead (Fpz). For each gap duration, two replicates of 100 artifact-free sweeps were recorded. These replicates were averaged together for data analysis. Presence of an ACC response required two criteria to be met: (1) identification of a repeatable response complex within the expected latency window; and (2) a root mean square (RMS) amplitude within this window that was at least 50% higher than the noise floor. The shortest gap that could reliably evoke the ACC response was defined as the gap detection threshold.

Results

Robust onset cortical auditory evoked responses were recorded from all ANSD subjects. ACC responses elicited by gap stimuli were also recorded from all ANSD subjects. However, subjects who exhibited limited benefit from their hearing aids had longer gap detection thresholds than subjects who received substantial benefit from their listening devices.

Conclusion

These preliminary data suggest that the ACC elicited by temporally interrupted stimuli might be predictive of hearing aid outcomes. If so, this objective measure could play an important role in the assessment of ANSD children for cochlear implant candidature.

659 Automated Fibertracking of the Acoustic Radiation Tract in Normal and Hearing-Impaired Adults

Muwei Li¹, Andreia V. Faria¹, Kenichi Oishi¹, Susumu Mori¹, **J. Tilak Ratnanather¹**

¹*Johns Hopkins University, Baltimore, MD, USA.*

Background

The acoustic radiation (AR) tract is the penultimate stage of the auditory pathway. It consists of white matter fibers coursing from the medial geniculate body (MGB) of the thalamus to the Heschl's gyrus (HG) which contains the

primary auditory cortex. However the AR presents a challenge to automated methods for tracking white matter fibers in diffusion tensor images (DTI) as it is partly obscured by the optic radiation tract running from the lateral geniculate body (LGB) of the thalamus to the visual cortex. Only probabilistic tracking methods can deal with crossing fibers. One such method is dynamic programming (DP) tracking of single fibers between specified regions of interest (ROIs) and is shown here to reliably generate AR from DTI scans.

Methods

DP uses a quadratic cost based on the Gaussian model of diffusion at the DTI voxel. The HG and MGB were parcellated automatically via the LDDMM registration algorithm in MRI Studio. With the HG and MGB respectively as the start and terminal ROI, DP was used to generate the AR in the left hemisphere in DTI scans of 5 normal and 5 hearing-impaired (HI) subjects.

Results

3D visualization reveals that the fibers are initially bunched together and then begin to spread out like a fan as the AR approaches the HG. Further there is little difference in the fractional anisotropy and spatial topology of the AR in normal and HI subjects.

Conclusion

While DP requires accurate parcellation of ROIs, it is less computationally intensive than other probabilistic tracking methods. The spreading pattern of AR appears to be consistent with published post-mortem staining at least in the coronal view and suggests a structural basis for the HG to be tonotopic. The macroscopic structural integrity of the AR appears to be maintained in HI subjects due to early intervention and may be a contributing factor in positive outcomes in the 4 subjects who subsequently got a cochlear implant. Generation of additional tracts in both hemispheres from the MGB and non-MGB parts of the thalamus to the whole superior temporal gyrus as well as from the LGB to the visual cortex will also be presented. Research supported by P41-EB015909, R01-AG020012 and National Organisation for Hearing Research Foundation.

660 Nerve Survival in CI Patients, and Its Functional Consequences: Psychophysical Measures and Cortical Recordings

Lendra Friesen¹, Monita Chatterjee², Aditya Kulkarni², Samidha Joglekar³, Arthri Srinivasan⁴

¹*Sunnybrook Health Sciences Centre, University of Toronto,* ²*Boystown,* ³*Sunnybrook Health Sciences Centre,* ⁴*SUNY Downstate Medical Center*

Background

The objective of the present study is to examine cochlear implant (CI) patients' sensitivity to pulse phase duration (PPD) as a potential index of nerve survival. We take two approaches to the question: In one approach (Chatterjee lab) we are measuring i) detection threshold for different

PPDs and ii) supra-threshold sensitivity to PPD modulation with bipolar (BP), tripolar (TP) and monopolar (MP) stimuli.

In the second approach (Friesen lab) we are conducting parallel measurements of supra-threshold psychophysical PPD discrimination and CAEP responses to changes in PPD, in patients who have had a “softer” surgical implantation with the MEDEL flex soft electrode and those who were implanted with the same electrode but did not have the soft surgery. We hypothesize that the soft surgery will result in improved nerve survival and improved sensitivity to PPD changes in both sets of measures, particularly in apical cochlear regions.

Methods

All stimuli are delivered using custom research interfaces. Detection and discrimination thresholds are measured using forced choice adaptive procedures. We are recording the N1-P2 and ACC on the same CI electrodes for both the low and high range of phase durations to determine the relationship to the behavioral jnd.

Results

Consistent with previous results, results suggest that MP stimulation results in more consistent, efficient charge integration (~ 6 dB/doubling) at threshold than BP stimulation. Strong level-dependence in the across-site pattern of sensitivity to PPD modulation was observed with focused stimuli.

Generally, results show reduced discrimination JNDs and ACC latencies for the longer PPDs. Discrimination JNDs are also smaller for the shorter PPD on the apical electrodes compared to basal electrodes. In the individuals with the “soft” surgery, JNDs are smaller for shorter PPDs on the apical electrodes compared to those not having the soft surgery; reduced ACC latencies were observed for these shorter PPDs on the apical electrodes as well.

Conclusion

Results are consistent with greater dominance of small-diameter peripheral processes in the response, at least at threshold. Sensitivity to PPD modulation likely reveals an increased contribution of central axons at increasing current levels.

With the second approach, it appears that for individuals having the “soft” surgery, PPD JNDs for short duration PPDs are smaller on the apical electrodes, indicating better neural survival. This increased neural survival appears to lead to increased neural synchrony, reflected at the level of the auditory cortex as indicated by the shorter ACC latencies.

661 Resting Cortical Oscillations Predict Hyperacusis: A Hyperresponsiveness

Network with Inactive Auditory Cortex at Rest
Jae-Jin Song^{1,2}, Dirk De Ridder^{1,3}, Nathan Weisz⁴, Winfried Schlee⁵, Paul Van de Heyning^{6,7}, Sven Vanneste^{1,7}

¹Brai©+n, TRI & Department of Neurosurgery, University Hospital Antwerp, Belgium., ²Seoul National University Hospital, ³Department of Surgical Sciences, Dunedin School of Medicine, University of Otago, New Zealand, ⁴Center for Mind/Brain Sciences, University of Trento, Trento, Italy., ⁵Department of Clinical and Biological Psychology, University of Ulm, Germany., ⁶Brai©+n, TRI & ENT, University Hospital Antwerp, Belgium., ⁷Department of Translational Neuroscience, Faculty of Medicine, University of Antwerp, Belgium.

Background

Hyperacusis is a hyperresponsiveness to non-noxious auditory stimuli, analogous to allodynia in neuropathic pain, but the neural substrates of hyperacusis are not well understood. By comparing tinnitus participants with hyperacusis (T+H+ group) with those without hyperacusis (T+H- group), we aimed to explore characteristic resting-state cortical activity of hyperacusis.

Methods

The T+H+ and T+H- groups were comprised of 17 participants each and were strictly matched for all tinnitus characteristics (tinnitus intensity and distress, laterality and type, gender, onset age and duration) to exclude cortical activity changes due to tinnitus characteristics. We compared differences in cortical activity between the 2 groups using resting state electroencephalography (EEG) source-localized activity complemented by functional connectivity analyses. Also, EEGs of 17 normal controls, matched for sex and age, were utilized for further comparison.

Results

Compared to the T+H- group, the T+H+ group demonstrated increased beta power in the dorsal anterior cingulate cortex (dACC), orbitofrontal cortex (OFC) and supplementary motor area (SMA) and increased alpha power in the right auditory cortex (AC). Region of interest analyses including normal controls further confirmed that these differences originated solely from relatively increased power of the T+H+ group, while power was not increased relative to the normal hearing controls. Functional connectivity analysis revealed increased connectivity between the OFC/dACC and the AC in the T+H+ group in comparison to the T+H- group. The beta power increase in the OFC/dACC/SMA may indicate increased vigilance leading to increased startle reflex in hyperacusis participants. Additionally, increased resting-state alpha power in the AC may reflect an adaptive top-down inhibition against environmental sound stimuli probably mediated by the increased beta power of the OFC.

Conclusion

The OFC and the dACC may compose a hyperresponsiveness network as these areas have also frequently been found to be activated in allodynia/hyperalgesia studies, and the results may be applicable for developing future treatment strategy in patients with hyperacusis or allodynia/hyperalgesia.

662 The Role of GABAergic and Glycinergic Inputs in Shaping SSA in the Inferior Colliculus of the Anesthetized Rat

Yaneri A. Ayala¹, David Perez-Gonzalez¹, Manuel Malmierca^{1,2}

¹Lab of Auditory Neurophysiology, Institute of Neuroscience of Castilla y León, Salamanca, Spain, ²The Medical School, University of Salamanca, Spain

Background

Stimulus-specific adaptation (SSA) is a reduction in the responsiveness of a neuron to a common or repetitive sound while the neuron remains highly sensitive to a deviant sound (Ulanovsky et al., 2003). This single-neuron level phenomenon could enhance the saliency of unexpected stimuli against a background of repetitive signals. Previous work from our laboratory has shown that adaptation to the repetitive stimulus still occurred in the absence of GABAA function and that the GABAA-mediated inhibition acts as a gain control mechanism that enhances SSA by controlling the neuron's gain and responsiveness (Pérez-González et al., 2012). Here, we test whether inhibitory mechanisms other than those GABAA-mediated contribute to the generation and/or modulation of SSA in the inferior colliculus (IC).

Methods

Antagonists of GABA_A-, GABA_B- and glycinergic receptors (gabazine, CGP-35348 and strychnine, respectively) were applied microiontophoretically while recording single units in the IC of rats, using an oddball paradigm. The responses to high- and low- probability tones were recorded before, during and after the drug injection using an assembly of microelectrodes in a 'piggy-back' configuration. The experimental stimuli were pure tones in the range 0.5–40 kHz, with a 75 ms duration and presented at a repetition rate of 4 Hz. The frequency response area (FRA) of the neuron, i.e., the combination of frequencies and intensities capable of evoking a response, was also recorded before and during the blockade of the inhibitory inputs.

Results

So far, we have recorded the extracellular activity of 30 single units. The application of gabazine and CGP-35348 increased spontaneous activity and altered the tuning of the FRAs and the rate-level functions at the best frequency, although the magnitude of the effect was higher under gabazine. The blockade of the three different receptors independently increased the response magnitude to high and low probability stimuli and caused a reduction of the first spike latency. Application of CGP-35348 alone had only a weak effect on SSA. However,

when combined with gabazine and/or strychnine the effects were more profound than each drug alone and resulted in a significant reduction of SSA.

Conclusion

Our data indicates a synergic action of GABAergic and glycinergic inhibition in shaping SSA at the IC level. Furthermore, it suggests that the SSA observed in the IC is generated locally.

Supported by the Spanish MICINN (BFU2009-07286), (EUI2009-04083) to MSM.

663 Response to Complex Patterns of Regularity in the Inferior Colliculus of the Anesthetized Rat

Blanca N. Aguillon¹, Javier Nieto¹, Carles Escera^{2,3}, Manuel S. Malmierca^{1,4}

¹Lab of Auditory Neurophysiology, Institute of Neuroscience of Castilla y León, Salamanca, Spain, ²Institute for Brain, Cognition and Behavior (IR3C), University of Barcelona, Catalonia-Spain, ³Cognitive Neuroscience Research Group, Department of Psychiatry and Clinical Psychobiology, Univers, ⁴The Medical School, University of Salamanca, Spain

Background

Single neurons in the inferior colliculus (IC) of the rat show a specific decrement of response to simple repetitive stimuli. This ability to encode the complex auditory past in multiple time scales would enable the auditory system to generate expectations about the incoming stimuli.

So far, stimulus-specific adaptation (SSA) has been studied in animal models using the simple repetition suppression effect of the classical oddball paradigm. Yet it remains to be determined whether violations of more complex regularities can also be detected at single neuron level in the form of expectation suppression, as they are in humans at population level through EEG and MEG.

Methods

Experiments were performed on female Long-Evans rats anesthetized with urethane (1.5 g/kg, i.p.). Tungsten electrodes (1–2 M Ω) were used to make extracellular recordings of neural responses in well-isolated single units in the IC. Auditory stimuli were sequences of 75 ms long pure tones with a 5 ms rise/fall ramp and constant stimulus-onset asynchrony (SOA) of 250 ms. Sound sequences consisted of two alternating pure tones selected from the frequency response area (FRA) of the neuron, following an alternation-repetition paradigm similar to those used in human studies. The average response to each stimulus when it was embedded in a regular pattern (expected), was compared to the average response to that same stimulus when it was breaking the regularity (unexpected). We presented each stimulus as repeated-expected and repeated-unexpected in order to control for repetition suppression, and we tested omission trials as well to look for true pattern regularity violation sensitivity.

Results

Among the recorded neurons, a significant number of them were considered strongly adapted neurons, showing much higher response to deviant tones than to the same tones being standard within a classical oddball paradigm. By contrast, other units showed little or no SSA, i.e., similar response profiles to standard and deviant stimuli. Remarkably, we have found signs of pattern violation sensitivity in both classes of neurons, in the form of a differential response to expected and unexpected tones, regardless of its repetition.

Conclusion

Our preliminary results show that at the level of the midbrain, there is not only repetition suppression (SSA) but may be also expectation suppression. These properties may occur independently to a different extent in different neurons, but this question awaits future experiments. Supported by (BFU2009-07286 & EUI2009-04083) to MSM; EUI2009-4086 to CE

664 Stimulus Specific Adaptation in the Inferior Colliculus of the Awake Marmoset

Troy Rubin¹, Eric Young¹

¹Johns Hopkins University

Background

Neural mechanisms to detect novel stimuli in perceptually complex environments are fundamental to our survival. In sensory systems, these mechanisms exist at a cellular level in the phenomenon known as stimulus specific adaptation (SSA) where single neurons can be seen to adapt to repetitive (standard) stimuli while remaining highly responsive to rare stimuli. While SSA has been observed in the auditory system at the level of the cortex, thalamus and the inferior colliculus, there remains debate as to its origin particularly given the paucity of data from unanaesthetized preparations with unmodified inhibitory circuits.

Methods

To further elucidate this system, single neurons were recorded from the inferior colliculi of awake head-fixed marmoset monkeys with tungsten microelectrodes. SSA was assessed with five free-field presentations of three consecutive streams containing repeated tones of two frequencies, f_1 and f_2 chosen from either side of the best frequency of each neuron. In the first stream, f_1 was presented with high probability (90%), and f_2 at low probability (10%), these probabilities were inverted in the second stream and presented at equal probability in the third stream.

Results

The majority of neurons within the central (ICC) and external (ICX) nuclei showed some degree of SSA. These effects were observed in both sustained and onset neurons although the latter were less frequently observed. This phenomenon was frequency specific such that SSA was greatly affected by the position of the tone within the receptive field of the neuron. Indeed latency was also

observed to vary throughout the stream in a manner dependent on frequency. This phenomenon was most striking in a number of ICX units that showed a progressive increase in latency over the duration of the stream with a concomitantly large degree of adaptation that did not affect the deviant.

Conclusion

The majority of units recorded with SSA demonstrated sustained discharges throughout tone presentation while some of these showed pauser or attenuated responses after the first 10-15ms. These data convincingly demonstrate that SSA is seen in the central nucleus of the unanaesthetized IC albeit at reduced levels relative to the external nucleus. Many presentation frequencies delivered to ICX units with broad receptive fields induced progressively increased latencies over each stream in a manner dependent on the position of this frequency in the receptive field of the neuron.

665 Spectral Receptive Field Plasticity May Underlie Stimulus-Specific Adaptation in Rat Inferior Colliculus

Li Shen¹, Lingyun Zhao^{1,2}, Bo Hong¹

¹Dept. of Biomedical Engineering, Tsinghua University,

²Dept. of Biomedical Engineering, Johns Hopkins University

Background

Neuron can change its coding strategy dynamically according to its stimulus context. One example in auditory system is stimulus-specific adaptation (SSA), in which rare stimuli elicit higher responses than common stimuli. SSA to frequency was observed at single neuron level in both cortical (Ulanovsky et al., 2003) and subcortical areas (Malmierca et al., 2009; Zhao et al., 2011). However, SSA can only reveal the adaptive change of responses to two specific frequency probes. It remains unknown how frequency selectivity changes in repetitive context and how much these changes relate to SSA. We explored this question by comparing frequency tuning curves of neurons in rat inferior colliculus (IC) in an adapted condition and a normal condition.

Methods

Normal frequency tuning curves were measured at random frequency points centered at neuron i 's best frequency (BF) while adapted tuning curve was measured by the same set of probes except they were randomly interspersed in a repeating tone sequence with a fixed frequency. The repeating tones acted as common stimuli and accounted for 90% of the tone sequence. The frequency of the repeating stimulus was selected similar to the standard frequency in the oddball paradigm (Ulanovsky et al., 2003; Zhao et al., 2011).

Results

We found that in adapted condition, the responses to frequencies very close to the repeated one were significantly decreased while to frequencies at farther vicinities showed enhancement. The

suppressed/enhanced pattern was frequency specific with radically center-surround pattern relative to the repeating frequency and depended on both inter-stimulus interval (ISI) and the segregation between the common stimuli and BF of the neuron. Moreover, we stimulated neurons using oddball paradigm with the same common stimuli and found the responses to rare ones can be largely predicted by the adapted tuning curve. Finally, a channel-based adaptation model was proposed, which can qualitatively predict the observed change in adapted condition. It revealed that adaptation induced frequency specific suppression of input to IC through the underlying center-surround connection pattern inter- and intra- IC neurons.

Conclusion

This result suggests that neurons' receptive fields undergo elaborate dynamics during adaptation to the ongoing sound stream, which may increase the frequency discriminability to facilitate novelty detection. Furthermore, it provided evidence of the neural mechanism of SSA and suggested more properties of adaptation, which were not shown by current SSA experiments.

666 Temporal Modulation Tuning in the Auditory Midbrain Provides Distributed Neural Representation for Coding Vowel-Like Sounds

Tianhao Li¹, Laurel H. Carney¹

¹University of Rochester

Background

Many auditory midbrain neurons are tuned to amplitude modulation frequencies between from 50 to 500 Hz. It is reasonable to ask whether these neurons play a particular role in coding speech information and if so, how? It has been hypothesized that midbrain neurons that are periodicity-tuned to voice pitch will have decreased rates when the neuron's best frequency (BF) is near a formant frequency and increased rates when BF is between formants (Carney and McDonough, 2012, *JASA* 131:3309). The present study tests this hypothesis across a wide range of best frequencies using synthesized vowel-like sounds to explore the role of temporal modulation tuning of neurons in speech coding.

Methods

Responses of single neurons in the inferior colliculus (IC) were recorded in the awake rabbit. Response maps and modulation transfer functions (MTFs) were measured to characterize neurons. Stimuli were presented to the contralateral ear. The stimuli were synthesized harmonic complexes with vowel-like spectra having two formants. The two formants were shifted with respect to the BF of the neuron to test the above-mentioned hypothesis. The fundamental frequency of the stimulus was matched to the best modulation frequency of the neuron. Two phase relationships (random and sine phase) across the harmonics were used to generate two sets of stimuli with similar spectra but different temporal envelopes. The average discharge rate and synchronization coefficient were used to quantify the neural responses.

Results

For the neurons with narrowband MTFs the responses to the vowel-like harmonic complexes with sine phase were significantly stronger and more synchronized to the stimulus than responses to random phase complexes. For onset neurons with broad MTFs, the responses to the vowel-like harmonics complexes with sine phase were also significantly stronger and synchronized to the stimulus. For sustained neurons with broad MTFs, the difference in the responses to the two sets of stimuli diminished. Some neurons had decreased discharge rates when a simulated formant was near the BF of the neuron, supporting the formant-coding hypothesis.

Conclusion

The present study provides evidence to support the hypothesis for coding vowels at the level of the auditory midbrain. The results also show that IC neurons with different modulation transfer functions may encode stimuli with similar spectra but different temporal envelopes in different manners, suggesting a distributed neural representation for temporal information in speech in the auditory midbrain.

Supported by NIH DC001641

667 Serotonin Reduces Noise-Evoked Suppression of Vocalization Responses in Inferior Colliculus

Laura Hurley¹, Adam Smith¹

¹Indiana University

Background

One of the ways the neuromodulator serotonin influences the excitatory-inhibitory circuitry of the inferior colliculus (IC) is by decreasing the strength of the GABAergic inhibitory surround.

Methods

To explore a functional consequence of this interaction in CBA/J mice, we used a stimulus consisting of a vocalization alone or one paired with a broadband noise. For a given neuron, vocalizations eliciting a strong excitatory response were chosen from a range of sample vocalizations and played at levels from just below threshold to 20 dB above threshold to generate a limited rate-intensity function. Noise was presented at a level for each neuron that evoked a minimal response alone while influencing the response to the vocalization.

Results

Many neurons in the sample showed effects similar to those previously reported in the IC for the influence of noise on tone responses, including an increase in threshold and a shift in the rate-intensity function to higher intensities. Noise suppressed the spike counts in response to vocalizations near threshold by an average of 41%. Serotonin reduced the effect of noise, so that noise only decreased the spike count by 25% on average in the presence of serotonin in the same group of neurons.

However, neurons varied widely; serotonin almost entirely removed the effects of noise in some, but even facilitated the effects of noise in others. Noise also altered the timing of spike trains in some neurons, an effect that could be abolished by serotonin.

Conclusion

These results are consistent with multiple mechanisms of serotonergic action, including a decrease in the surround inhibition leading to a reduced influence of broadband noise for a limited range of vocalization-noise intensity pairs.

668 Responses to Acoustic Stimuli Vary Along the Isofrequency Laminae of the Inferior Colliculus Consistent with Spatially Segregated Sub-Lemniscal Auditory Pathways

Malgorzata Straka¹, Samuel Schmitz¹, Patrick Lee¹, Melissa McMahon¹, Hubert Lim¹

¹University of Minnesota

Background

The central auditory system has traditionally been divided into the lemniscal and non-lemniscal pathways. The lemniscal pathway transmits high-fidelity auditory information and maintains a precise tonotopic organization. In contrast, the non-lemniscal pathway codes for multi-modal information and is involved with modulation of the lemniscal pathway and limbic interactions. The central nucleus of the inferior colliculus (ICC) is the main auditory midbrain nucleus of the lemniscal system. Based on previous anatomical and neurophysiological studies, we hypothesize that the ICC should be further divided into at least two sub-regions along the isofrequency laminae, a rostral and a caudal region, that exhibit different coding properties to sound.

Methods

Short tone pips were presented to ketamine-anesthetized guinea pigs. Multi-site electrode arrays were used to record local field potentials (LFPs) and spikes simultaneously in up to four regions along an ICC lamina. Multiple array placements were made for each animal. Three-dimensional histological reconstructions of the placements were performed for six animals to identify all the recording locations across a given ICC lamina. The responses were then compared across locations.

Results

We observed that both LFP and spike response patterns differed between rostral versus caudal regions along an ICC lamina. The rostral region exhibited more temporally-precise spiking, shorter first spike latencies, less jitter in first spike latencies, and shorter response durations. The rostral region also exhibited LFPs with shorter peak latencies as well as activity with greater growth and temporal synchrony.

Conclusion

These results support previous histological and electrophysiological studies suggesting that the lemniscal pathway should be divided into at least two sub-projection pathways. Specifically, the rostral region appears to have properties more consistent with the lemniscal pathway (e.g., excitatory discharge patterns, short latencies, and precise time-locking) and may serve to reliably and synchronously transmit sound information from the auditory nerve up to the auditory cortex. Based on additional studies from our lab, the caudal pathway may be more involved with modulating sound information ascending through the lemniscal pathway. Identifying the spatial coding pattern across the isofrequency laminae of the ICC has major implications not only for understanding central auditory processing but also for improving auditory midbrain implants, in which the rostral area of the ICC may be a better stimulation target for restoring intelligible hearing.

This research was funded by University of Minnesota start-up funds and NIH NIDCD R03DC011589.

669 Progressive Recovery of Acoustic Sensitivity in the Inferior Colliculus of Adult Mice Following Near-Complete Primary Cochlear Neuronal Degeneration

Daniel Polley^{1,2}, Yasheng Yuan^{1,3}, Albert Edge^{1,2}, Charles Liberman^{1,2}

¹Eaton-Peabody Laboratory, Massachusetts Eye & Ear Infirmary, ²Harvard Medical School, ³Department of Otolaryngology, EENT Hospital, Fu Dan University

Background

Spiral ganglion neuron (SGN) survival declines as a normal consequence of aging and in pathological conditions such as auditory neuropathy spectrum disorder and acoustic trauma.

Methods

To better understand how SGN loss affects the central auditory system, we performed electrophysiological recordings from the central nucleus of the inferior colliculus (ICC) of adult mice following specific depletion of Type I SGNs in the contralateral cochlea. For each individual mouse, in vivo multiunit recordings were compared to the auditory brainstem response (ABR), distortion product otoacoustic emissions (DPOAE), histological quantification of inner hair cell synaptic complexes or the spiral ganglion, and acoustic startle reflex behavior.

Results

Unilateral application of ouabain to the round window membrane eliminated ~90% of Type I SGN synapses onto inner hair cells without affecting hair cell function or Type II SGN survival, as determined by quantitative histopathology and otoacoustic emission measurements. As expected, the amplitudes of the auditory brainstem response and acoustic startle reflex elicited from the ouabain-treated ear were substantially reduced. Despite the profound deafferentation and apparent hearing loss, a substantial minority of ICC units exhibited low-threshold,

non-adapting, and tonotopically organized sound-evoked responses one month – but not one week – following ouabain treatment. By contrast to the recovery of responses to simple sounds such as tones in silence, the representations of tones presented in broadband masking noise or the accurate synchronization of spike times to the modulation rate of the sound pressure envelope were similarly impaired at both recovery times.

Conclusion

The persistence of robust responses evoked from the ouabain-treated ear could not be attributed to the fraction of surviving inner hair cell synapses, but rather appeared to represent a slowly developing compensatory plasticity that was evident at the level of midbrain unit responses, but not in the gross electrical potential or startle reflex generated by brainstem circuitry. These findings imply a readjustment of synaptic gain in the ascending auditory pathway, which may have relevance to the development of tinnitus, hyperacusis or other complex behavioral sequelae of peripheral damage.

670 Masking Release Due to Coherent Envelope Fluctuations Across Frequency at the Level of the Inferior Colliculus

Jan Diepenbrock^{1,2}, Frank Ohl¹, Jesko Verhey²

¹Leibniz Institute for Neurobiology (LIN), Magdeburg, Germany, ²Department of Experimental Audiology, University of Magdeburg, Germany

Background

Many natural sounds including speech contain coherent level fluctuations in different frequency bands. A psychoacoustical phenomenon associated with the ability of the auditory system to use this characteristic is comodulation masking release (CMR). The physiological mechanisms underlying CMR are still unclear.

Methods

The present study used a typical CMR paradigm, in which a tonal signal is embedded in a masker with a spectral component at the signal frequency and one or more off-frequency components. The psychoacoustical CMR describes the effect of a reduced masking when the masker components showed coherent level fluctuations (comodulated condition, CM) compared to a condition in which the level fluctuations were incoherent (codeviant condition, CD) or to a condition where the masker consisted of the on-frequency component only (the so called reference condition, RF). The present study used sinusoidally modulated tones as masker components, one centred at the best frequency of the unit and the other positioned into the inhibitory sidebands of the unit. The recording was done in the inferior colliculus of the Mongolian gerbil; 53 units in 17 animals were tested.

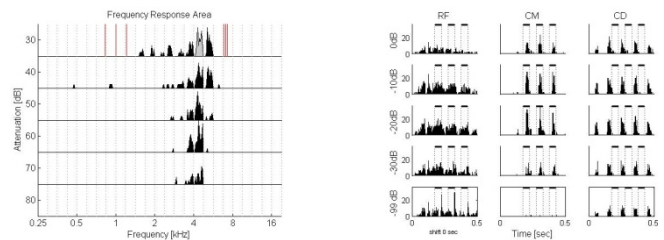
Results

Preliminary analysis on the current data base showed that 33 out of 53 units were able to follow the amplitude modulation. Out of these ca. 25% displayed response properties that were consistent with the hypothesis of

wideband inhibition, the hypothesized physiological mechanism underlying CMR from previous studies at the level of the cochlear nucleus. Approximately 20% of the units also showed a reduction of the representation of the masker modulation due to the presence of the signal, i.e., envelope locking suppression which is another hypothesized physiological mechanism. This mechanism was proposed on the basis of cortical recordings. Since both effects were found at the level of the IC, it is possible that the auditory system uses a combination of both, leading to a further enhancement of signal detectability.

Conclusion

Wideband inhibition is a mechanism that may account for a physiological correlate of CMR at the level of the IC, and additionally envelope locking suppression could also play a role.



671 Auditory Stream Segregation Abolishes Informational Masking

Lena-Vanessa Dollezel¹, Sandra Tolnai¹, Rainer Beutelmann¹, Georg M. Klump¹

¹Animal Physiology and Behaviour Group, Oldenburg University, Germany

Background

Informational masking describes a common phenomenon observed in everyday life. Important acoustic information, like an alarming sound, can be masked by surrounding acoustic events, even up to the point in which the important information is below detection threshold although the sound is well represented in the auditory periphery. This non-energetic masking is thought to originate in the central auditory system and can be measured and defined as an increase in detection threshold caused by stimulus uncertainty (e.g., Durlach et al. 2003). Most studies have concentrated on analyzing the effect of simultaneous informational masking (e.g. target and masker sequences are presented simultaneously, see Kidd et al. 2007). In an EEG study of auditory stream segregation Winkler et al. (2003) used the mismatch negativity (MMN) response to evaluate the ability of the brain to detect a deviant (76 dB SPL) in a series of standards (61 dB SPL) and intervening signals (66, 71, 81 and 86 dB SPL). Large differences in MMN response were observed as a function of frequency difference between the standards/deviants and intervening signals.

Methods

We adopted Winkler's paradigm and applied it in a psychophysical (humans and gerbils) and neurophysiological approach (extracellular recording in the inferior colliculus (IC) and auditory cortex (AC) of

anesthetized gerbils). Psychophysical thresholds were obtained with the method of operant conditioning using positive reinforcement in a Go/NoGo procedure.

Results

Similar to other objective tasks of auditory stream segregation (e.g., Micheyl and Oxenham, 2010) the intensity increment thresholds derived with Winkler's paradigm, providing sequential informational masking, varied depending on the frequency difference between the tones. In both humans and gerbils thresholds were considerably larger in the condition of small frequency differences representing a 1-stream percept than in the condition of a large frequency differences representing a 2-stream percept. No difference between species was observed.

Using the same types of stimuli as in the behavioral study, neuronal rate responses were analyzed using the receiver operating characteristic (ROC) functions and d_a - values were calculated and compared to the psychophysical results. The observed change in the d_a - values with stimulation condition could explain the behavioral observations.

Conclusion

The similarity between the neurophysiological and the psychophysical response measures in the gerbil renders it suitable as a model revealing the relation between auditory stream segregation and informational masking that may also apply to human perception.

672 Neural Discrimination of Vocoded Consonants

Mark Steadman¹, Chris Sumner¹

¹MRC Institute of Hearing Research

Background

Cochlear implants provide an input to the auditory system that is both spectrally and temporally degraded. Despite this, many cochlear implant users are able to discriminate between speech sounds with a performance comparable to normal hearing listeners. Vocoders have been used to acoustically simulate this degraded input in many psychophysical studies, but the neural bases of this robust phonemic discrimination are not yet clear. Understanding the aspects of the neural representation of speech sounds that are used for discrimination and that are robust to degradation of the input signal could have implications for both cochlear implant design and automatic speech recognition systems.

Methods

A set of 16 medial consonants (a/C/a) produced by 3 male speakers were processed using a noise-band vocoder. The number of noise bands was varied between 1, 2, 4 and 8 and temporal modulation bandwidth was limited to 16 and 500 Hz. Multi and single unit responses to the processed and unprocessed stimuli were recorded in the inferior colliculus of anaesthetised guinea pigs. A nearest neighbour classifier was then trained on the average spatio-temporal neural representation of each consonant.

Novel activity patterns were classified according to the closest of the training set given any possible relative onset time.

Results

The classifier was able to correctly identify unprocessed phoneme sequences based on neural activity patterns with a success rate of 93%. For the single channel, 16 Hz envelope bandwidth condition, performance dropped to 51% and increased monotonically with increasing numbers of noise bands to 84% for the eight channel condition. For the 500 Hz envelope bandwidth condition, performance was greater than 90% for any number of noise bands.

Conclusion

When envelope modulation bandwidth is restricted to 16 Hz, the distinguishability of neural activity patterns closely matches human psychophysical data for the same task. However, there is sufficient information encoded in the guinea pig auditory midbrain to facilitate near-perfect discrimination of vocoded vowel-consonant-vowel phoneme sequences when temporal modulations of up to 500 Hz are conserved in the input signal. This suggests that although the auditory midbrain preserves temporal information about speech which can distinguish between different speech sounds, that this is not used for speech recognition. One explanation for this might be that generalized representations built on finer temporal information are not robust across environmental variations, such as inter-speaker differences, background noise or reverberation. However, the cause of this is still being investigated.

673 Mathematical Modeling of Gap Detection

Gevorg Grigoryan¹, Abigail Fellows², Frank Musiek³, Robert Chambers⁴, Odile Clavier⁴, Jay Buckley²

¹Dartmouth College, ²Geisel School of Medicine at Dartmouth, ³University of Connecticut, ⁴Creare, Inc.

Background

As part of a study of hearing loss in HIV-positive individuals, we have collected gap detection thresholds on 350 HIV-positive and HIV-negative individuals. For each subject, at each gap length, the percentage of time the subject correctly identifies the gap is measured.

Methods

The dependence of correct identification rate on gap length is sigmoidal, showing a threshold below which no gaps are detected, a rapid rise in detection percentage as gap length increases, and then a plateau. The dataset was systematically analyzed via curve fitting to provide a simple two-parameter characterization of each subject's gap response. A simple neural network model for gap-sensing was also developed, incorporating a population of neurons, where each neuron has its own sigmoidal response to gap detection (and different gap detection performance).

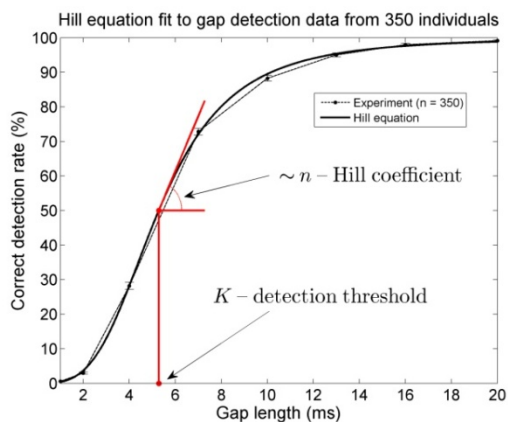
Results

The gap detection curves fit extremely well to the Hill equation (see figure), which is often used to describe the

cooperative binding of multiple ligands to a macromolecule, such as the binding of oxygen to hemoglobin. The equation provides a Hill coefficient, which captures the degree of cooperativity of the binding reaction (i.e. how much the binding of one ligand is enhanced by the presence of others). The Hill equation also naturally emerges from the simple neural-network model for gap sensing, enabling us to ascribe meaning to the equation's two parameters, where "n" or cooperativity, is a measure of the number of neurons, and "K" represents the effective gap detection threshold.

Conclusion

The Hill equation provides a simple mathematical description of central nervous system gap detection. This process involves multiple neurons tuned to detect particular gap lengths, with the ensemble response providing the overall gap encoding. The concept of cooperativity lends itself to a particularly intuitive interpretation in this setting, which is explored in this study. We show that the Hill coefficient is directly related to the number of neurons involved in our neural network model, whereas the binding constant from the Hill equation corresponds to the gap detection threshold. Although these findings are preliminary, they indicate that the shape of the percent correct vs. gap length curve may reflect neuronal loss in the gap detection pathways. Cooperativity in gap detection may serve to reduce noise in signal detection, similar to the effects of cooperativity in cellular signal processing.



674 Neural Correlates of the Detection of Tones in Noise in the Inferior Colliculus of Nonhuman Primates

Peter Bohlen¹, Maggie Dylla¹, Jason Grigsby¹, Troy Hackett¹, Ramnarayan Ramachandran¹
¹Vanderbilt University

Background

Detection of sounds in noise is a fundamental function of the auditory system. The thresholds of macaques for tone detection displayed a characteristic U-shaped relationship with frequency. Reaction times to detect tones decreased as the tone sound pressure levels increased beyond threshold. Noise modified the responses by shifting thresholds to higher sound pressure levels at the rate of 1

dB per dB of noise, but reaction times were not significantly different in the presence of noise. The response magnitude of inferior colliculus (IC) neurons was more strongly related to detection of tone alone than those of cochlear nucleus (CN) neurons. Studies in decerebrate and anesthetized cats have shown that the dynamic range of some IC neurons were shifted at the rate of 1 dB per dB of noise, but most CN units showed smaller shifts. In addition, neurons in decerebrate and anesthetized cats showed a compromised representation of signal. Here we report results of experiments designed to evaluate the role of the neurons in the IC of awake and behaving animals in detecting tones in noise.

Methods

Two macaques (*Macaca mulatta*) were trained in a reaction time lever release task with appropriate catch trials to report the detection of tones in noise. Single units were recorded from the IC (n=70) during behavior. The characteristic frequency of these units ranged up to 25 kHz. Most of the units were classified as type V or type I, based on the distribution of excitation and inhibition in frequency response maps. Signal detection theory and Receiver Operating Characteristic (ROC) analyses were used to create psychometric (behavioral), and neurometric functions. Neurometric functions reveal the probability of correct response based on the distribution of the number of spikes fired by the IC neuron on tone trials and catch trials.

Results

Background noise increased the average firing rate of IC neurons. The dynamic range of the neurometric functions shifted to higher sound pressure levels in the presence of noise. On average, with the addition of noise, IC neurometric thresholds showed shift rates of 1 dB per dB noise, and were strongly correlated with behavioral thresholds in noise. The relationship between reaction times and spike counts was not significantly different with the addition of noise.

Conclusion

These results, that the neuron-behavior correlations were not altered in the presence of noise, suggest an important role for the IC in processing signals in noise. Supported by R01 DC11092.

675 Glycinergic and GABAergic Input Provide Excitatory Drive in the Inferior Colliculus

Anthony Williams¹, Zoltan Fuzessery¹
¹University of Wyoming

Background

Glutamate is the dominant excitatory neurotransmitter in the auditory system, but there is growing evidence that glycine can provide the sole excitatory input to inferior colliculus neurons through an excitatory rebound from inhibition. This study of the pallid bat inferior colliculus shows that either glycine or GABA can provide excitatory drive to a population of highly selective neurons that

respond only to downward FM sweeps, and whose selectivity is shaped by an asymmetrical facilitation when presented with two tones in a spectrotemporal sequence approximating their occurrence in an excitatory downward FM sweep.

Methods

Five-barrel microelectrodes were used to record single neurons, and iontophoretically apply blockers of AMPA (NBQX) and NMDA (CPP) glutamate, glycine (strychnine) and GABA_A (gabazine) receptors. Iontophoretic currents were gradually increased to maximize effect, but minimize response saturation.

Results

As expected, the blockade of glutamate receptors suppressed responses in the majority of neurons, and the blockade of glycine and/or GABA_A receptors disinhibited responses and altered response selectivity in terms of FM sweep direction or sweep rate. Neurons that previously responded only to downward sweeps now responded to tones as well. However, in 33% of neurons in which glycine receptors were blocked, their response was eliminated. The same effect was observed in 20% of neurons in which GABA_A receptors were blocked. In some of these neurons, the blockade of glutamate receptors had no effect on their response, suggesting these inhibitory transmitters provided the sole excitatory drive.

Conclusion

The excitatory effect of glycine and GABA is thought to be the result of a rebound from inhibition, in some cases in coincidence with excitatory input, and has been observed in avian and mammalian thalamic and cortical circuits. In the mammalian auditory system, the excitatory effect of glycinergic input has been documented in both the midbrain and brainstem, and is thought to be a source of temporally precise interneuron communication. Present results indicate that both GABA and glycine, most likely through inhibitory rebound, can contribute to the submillisecond temporal resolution observed in inferior colliculus neurons in which asymmetrical facilitation shapes their selectivity for FM sweep direction and rate.

676 Identification of Three Classes of Excitatory Synapses in the Inferior Colliculus

Kyle Nakamoto¹, Jeffrey Mellott¹, Jeanette Killius¹, Megan Storey-Workley¹, Colleen Sowick¹, Brett Schofield¹
¹Northeast Ohio Medical University

Background

The inferior colliculus (IC) integrates ascending auditory input from the lower brainstem and descending input from auditory cortex. Understanding how IC cells integrate these inputs requires identification of their synaptic arrangements. Here, we provide the first description of excitatory synapses in the main IC subdivisions (dorsal cortex, central nucleus, and external cortex) in guinea pigs. We describe characteristics that allow distinction between excitatory and inhibitory synapses as well as differentiation of 3 classes of excitatory boutons.

Methods

We used electron microscopy (EM) on aldehyde-fixed tissue from 6 pigmented adult guinea pigs. We stained the ultrathin sections with post-embedding anti-GABA immunogold histochemistry to identify GABAergic cells. We analyzed 450 synapses (150 from each IC subdivision). Excitatory synapses were identified by round vesicles, asymmetric synaptic junctions, and GABA-immunonegative presynaptic boutons. Presumptive inhibitory synapses had non-round vesicles, symmetric junctions, and GABA-positive (GABA+) or GABA-negative presynaptic boutons.

Results

Excitatory synapses constitute ~ 60% of the synapses in each IC subdivision. Three subtypes can be distinguished by presynaptic profile area and number of mitochondrial profiles. Large excitatory (LE) boutons are more than 2 μm^2 in area and usually contain 4 or more mitochondria. Small excitatory (SE) boutons are less than 0.7 μm^2 in area and usually contain 1 or no mitochondria. Medium Excitatory (ME) boutons are intermediate in size and usually contain 2 to 4 mitochondria. A k-means cluster analysis confirmed that the 3 types of boutons could be distinguished by presynaptic area and the number of mitochondrial profiles. LE boutons are mostly confined to the ICC, while the other two types are present throughout the IC. SE boutons target spines more frequently than dendritic shafts, while the ME and LE types target dendritic shafts more frequently. Finally, each bouton type terminates on both GABA+ and GABA-negative (i.e., glutamatergic) targets, with targets on GABA-negative profiles being much more frequent.

Conclusion

Excitatory boutons give rise to about 60% of the synapses in each IC subdivision. Excitatory boutons comprise 3 subtypes that are distinguishable by profile size and mitochondrial content. SE boutons include boutons that arise from auditory cortex. Most or all LE boutons and many ME boutons likely arise from lower brainstem auditory nuclei. The data suggest that each of these inputs are likely to contact both GABAergic and non-GABAergic IC cells, and thus likely to activate both excitatory and inhibitory IC circuits.

677 Inhibitory Projections and GABAergic "Cross-Talk" Between Parallel Pathways in the Projections from Inferior Colliculus to the Medial Geniculate Body in Guinea Pigs

Jeffrey Mellott¹, Nichole Foster^{1,2}, Brett Schofield^{1,2}

¹Northeast Ohio Medical University, ²Kent State University

Background

Classic studies in cats identified 3 parallel streams in the projections from the inferior colliculus (IC) to the medial geniculate body (MG) (Calford and Aitkin, 1983, J Neurosci 11:2365). The streams are reflected in subdivision-specific connections: 1) a "lemniscal" pathway is formed primarily by projections from central IC to ventral MG (ICc-MGv); 2)

a “diffuse” pathway involves projections from IC dorsal cortex to dorsal MG (ICd-MGd); and, 3) a “polysensory” pathway involves projections from IC external cortex to medial MG (ICx-MGm). Smaller numbers of cells in each pathway terminate in the “wrong” MG subdivision, providing an opportunity for interactions, or “cross-talk”, between the parallel pathways. More recent studies have identified a substantial GABAergic projection from the IC to the MG, but whether these projections follow the parallel organization is not known.

Methods

We combined retrograde tracing with immunocytochemistry in guinea pigs to identify GABAergic cells that project to MGv, MGd or MGm. We injected Fast Blue, FluoroGold or red or green fluorescent microspheres into individual MG subdivisions and stained the IC with anti-glutamic acid decarboxylase (GAD) to identify GABAergic cells. We quantified tracer- and immuno-labeled (double-labeled) cells in the IC ipsilateral to the MG injection. The present analysis is based 4 cases (1 for each MG subdivision) and >5,800 retrogradely-labeled cells.

Results

After MGv injection, 58% of the GABAergic tectothalamic cells were in ICc. After MGd injection, 60% of the GABAergic tectothalamic cells were in ICd. After MGm injection, ICx contained 69% of the GABAergic tectothalamic that project to MGm. Thus, the bulk of GABAergic tectothalamic cells are located in IC subdivisions predicted by the classic parallel pathways. However, in each case a substantial percentage of GABAergic tectothalamic cells were located in “other” subdivisions. For example, MGv injections labeled GABAergic cells in ICx and ICd; MGd injections labeled GABAergic cells in ICx; and MGm injections labeled GABAergic cells in ICc.

Conclusion

We conclude that the bulk of GABAergic tectothalamic cells project in a pattern that reflects the classic lemniscal, diffuse and polysensory pathways. However, additional GABAergic IC cells project “across” the pathways, providing an opportunity for inhibitory crosstalk between the parallel pathways in the tectothalamic projection. Supported by NIH DC04391 and DC012450.

678 c-Fos Immunolabeling Reveals Changes in Sound Frequency Representation in Inferior Colliculus Following Chronic Low-Level Neonatal Sound Exposure

Lisa M. D'Alessandro^{1,2}, Robert V. Harrison^{1,2}

¹University of Toronto, ²The Hospital for Sick Children, Toronto, Canada

Background

Sensory areas of the brain have the remarkable ability to reorganize as a result of significant changes in peripheral sensory input, especially during early development. While cortex is often investigated as the primary site of developmental plasticity, our study provides evidence for

midbrain plasticity. Our working hypothesis is that the development of auditory pathways is influenced in large part by patterns of sensory activation experienced during early development. Specifically, we hypothesize that post-natal exposure to an unusual sound environment modifies the neural representation of the exposure sound frequency in inferior colliculus (IC).

Methods

Newborn chinchillas were reared in the presence of a chronic, moderately-intense (c. 70 dB SPL) narrowband sound signal (centered at 2 kHz) for 4 weeks. We estimated hearing thresholds using auditory brainstem responses (ABRs). We then observed neural activation patterns in IC using c-fos labeling (protocol optimization for chinchilla developed in-house, using commercially-available reagents).

Results

Hearing thresholds were similar between control and sound-exposed subjects, suggesting that sound-exposure does not affect normal hearing. We observed a statistically-significant increase in the number of labeled cells both in the 2-kHz region (corresponding to the sound-exposure frequency) as well as throughout the IC of sound-exposed subjects, compared with controls.

Conclusion

These results support the hypothesis that abnormal sound patterns at the periphery during a neonatal period can induce changes in neural activation patterns in sub-cortical auditory structures. We also discuss some plausible interpretations. Studying the effect of sound on the developmental plasticity of the auditory brain is important for our general understanding of how the auditory system develops. The work also has some relevance for the rehabilitation of the hearing impaired, for example with hearing aids and cochlear implants.

679 Reciprocal Connections Between the Inferior Colliculus and Dorsal Cochlear Nucleus

Michael Muniak^{1,2}, Vikas Kodali², Makoto Tanigawa², Catherine Connelly^{1,2}, Tan Pongstaporn^{1,2}, David Ryugo^{1,2}

¹Garvan Institute of Medical Research, ²Johns Hopkins University

Background

Descending pathways are an essential element of sensory systems, and may facilitate realtime modification of neural responses to external stimuli at any stage from periphery to cortex. In the auditory system, the cochlear nucleus is a key site for descending influence because it initiates all ascending pathways. Studies of descending projections in rat and guinea pig suggest that colliculo-cochlear nucleus projections originating in the central nucleus of the inferior colliculus (CNIC) terminate bilaterally and topographically in the dorsal cochlear nucleus (DCN; Caicedo & Herbert, 1993; Malmierca et al., 1996). We recently quantified and confirmed this projection in the mouse, and furthermore suggested that this pathway is reciprocal (Muniak et al.,

2011). We now present ultrastructural evidence that these descending terminals from the CNIC form excitatory axodendritic and axosomatic synapses on the principal projecting cells of the DCN.

Methods

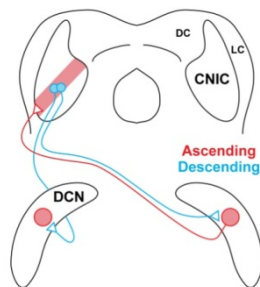
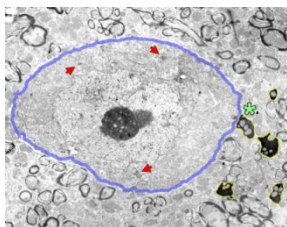
Adult CBA/CaJ mice received an injection of biotinylated dextran-amine (BDA) and cholera toxin subunit-B (CTB) in the CNIC through a recording micropipette following electrophysiological characterization. Brains were sectioned and histochemically reacted to reveal both retrogradely labeled projection neurons in the DCN and anterogradely labeled descending projections from the IC. Contralateral reciprocal connections were examined between the labeled neurons via light and electron microscopy.

Results

Retrograde (CTB) and anterograde (BDA) label were readily identified at the injection site. CTB was found contralaterally in the DCN, whereas BDA was distributed bilaterally. Based on size and location, retrogradely labeled neurons comprise both pyramidal and giant cells. In the contralateral DCN, the close proximity of anterogradely labeled axonal swellings to retrogradely labeled cell bodies was highly suggestive of direct contact. Under electron microscopy, labeled axons were darkly stained and easily identified. Labeled soma were discernable due to accumulations of label within the Golgi apparatus and lysosomes. Synapses from descending projections were noted by the presence of a postsynaptic density on the retrogradely labeled cell adjacent to an anterogradely labeled terminal filled with synaptic vesicles. All labeled endings examined to date were filled with large round vesicles, suggesting the synapses are excitatory.

Conclusion

Our results demonstrate a direct tonotopic pathway by which the CNIC can bilaterally modulate activity in the DCN. Furthermore, our findings indicate that the contralateral descending projections are excitatory to the principal projecting neurons of the DCN. This point-to-point reciprocity provides a physical substrate for modulating ascending auditory information, and could be involved in "egocentric feedback" to enhance signal discrimination and/or selective attention.



680 Projections from the Dorsal Cochlear Nucleus to the Ipsilateral and Contralateral

Inferior Colliculi: Single Fiber

Reconstructions

M. Christian Brown¹, Thane Benson¹, Kristen Babicz², Keith Darrow³

¹Massachusetts Eye and Ear Infirmary, ²University of Massachusetts - Boston, ³Worcester State University

Background

Neurons of the dorsal cochlear nucleus (DCN) form a large projection to the contralateral inferior colliculus (IC) and a smaller projection to the ipsilateral IC. These projections are important because they may mediate sound localization based on spectral cues.

Methods

We labeled the projections to both the ipsilateral and contralateral IC by injecting the anterograde tracer, biotinylated dextran amine, in the DCN of mice. The trajectory, branching pattern, and synapses were studied.

Results

Injections resulted in many labeled fibers to the IC contralateral to the injected side and, in some cases, a few fibers to the ipsilateral IC. On the contralateral side, some fibers branched at the ventral edge of the IC, with a thicker branch innervating the central nucleus and dorsal cortex and a thinner branch innervating the lateral cortex. Some fibers only innervated the central nucleus and dorsal cortex. The few fibers that could be reconstructed to all their terminations demonstrated that a single fiber forms numerous branches with terminal and en passant swellings. On the ipsilateral side, the smaller number of labeled fibers (0-12 per case) made it easier to reconstruct fibers. Some of these fibers traveled mainly within the central nucleus along a presumed iso-frequency lamina. Other fibers formed terminations only in the lateral cortex. Tracing these ipsilateral fibers in the retrograde direction indicated that some of them were from bilaterally projecting axons. One terminal in the ipsilateral central nucleus formed an asymmetric synapse with round synaptic vesicles, characteristics of excitatory synaptic transmission.

Conclusion

Projections from the DCN to the contralateral and ipsilateral IC exhibited a variety of patterns, with some fibers innervating most of the IC and others targeting just one of its sub-regions. These diverse projections may indicate specialized patterns for specific aspects of sound localization as well as other functions. Support: NIDCD grant DC01089.

681 Perineuronal Nets on GABAergic Cells in the Inferior Colliculus That Project to the Medial Geniculate Body

Nichole Foster^{1,2}, Jeffrey Mellott¹, Brett Schofield^{1,2}

¹Northeast Ohio Medical University, ²Kent State University

Background

Perineuronal nets are aggregates of extracellular matrix that can inhibit structural plasticity, promote synaptic plasticity, and protect neurons from oxidative stress

(Karetko et al. 2009, *Acta Neurobiol Exp* 69:564). In many brain areas, perineuronal nets are preferentially associated with GABAergic neurons. In guinea pigs, nets in the inferior colliculus (IC) are most numerous in the central nucleus (ICc), though they also occur in dorsal cortex and external cortex. Most nets surround GABAergic cells, forming a population of “netted” GABAergic cells and a population of GABAergic cells without nets (Foster et al. 2012, *Soc. Neurosci. Abst.* 365.10). GABAergic IC cells project to a number of extrinsic targets; we test here whether nets are associated with GABAergic cells that project to the medial geniculate body (MG).

Methods

We injected red or green fluorescent beads or Fast Blue into the MG to label IC cells by retrograde transport. We stained GABAergic cells with antibodies to glutamic acid decarboxylase (GAD) and perineuronal nets with fluorescent-labeled *Wisteria floribunda* agglutinin. We identified retrogradely-labeled cells and determined whether they were GAD-immunopositive (i.e., GABAergic) and whether they were surrounded by a perineuronal net.

Results

A large injection in MG labeled GAD+ and GAD-negative cells in all IC subdivisions. Roughly 10-35% of the projecting GAD+ cells were surrounded by perineuronal nets. Small tracer injections demonstrated perineuronal nets surrounding IC GABAergic cells that project to each MG subdivision, with very few projecting to supragenulate MG but a surprising number projecting to medial MG. While our focus was on GABAergic cells, we also observed IC-MG cells that were GAD-immunonegative (i.e., presumptive glutamatergic) and surrounded by perineuronal nets.

Conclusion

We conclude that perineuronal nets surround a subset of GABAergic IC-MG cells. These GABAergic projections terminate in multiple MG subdivisions. Nets also surround some glutamatergic tectothalamic cells. The proposed functional roles of perineuronal nets suggest that “netted” cells may react differently than other cells with regard to plasticity and oxidative stress. Future study of these topics in the IC may benefit from distinguishing not only GABAergic vs. non-GABAergic projecting cells, but also cells that have nets vs. those that do not. Supported by NIH DC04391 and DC012450.

682 Expression of the GABA_BR1 and GABA_BR2 Subunits in the Rat’s Inferior Colliculus

Lena Jamal¹, Aziz Khan¹, Sehrish Butt¹, Chirag Patel¹, Huiming Zhang¹

¹University of Windsor

Background

The type B γ -aminobutyric acid receptor (GABA_B receptor) is an important GABAergic neurotransmitter receptor in the inferior colliculus (IC). GABA_BR1 and GABA_BR2 are two subunits of the GABA_B receptor. One of our previous

studies has revealed that the GABA_BR2 subunit is expressed at a higher level in the dorsal cortex (ICd) than the external cortex and the central nucleus (ICx and ICc) of the IC. The present study was conducted in the rat’s IC to examine: 1) whether the GABA_BR1 subunit had a similar area distribution; 2) how the overall level of the GABA_B receptor in a specific IC region was dependent on the density of cell bodies expressing the receptor and the abundance of the receptor in the neuropil in the region; 3) morphological features of cells expressing the receptor.

Methods

Immunohistochemical experiments were conducted by using antibodies specific for the GABA_BR1 and GABA_BR2 subunits. Immunoreactivity was visualized using 3,3-Diaminobenzidine tetrahydrochloride reaction product and was quantified using optic density.

Results

GABA_BR1 and GABA_BR2 subunits were expressed in cell bodies and the neuropil throughout the IC. Regional distributions of the two subunits were similar to each other. For both subunits, the combined level of cell body and neuropil expression was higher in the ICd than the other subdivisions; and the area distribution of the expression in the neuropil was parallel to that of combined neuropil and cell body expression. The density of immunoreactive cell bodies tended to be higher but sizes of cell bodies tended to be smaller in the ICd than in the other subdivisions. No systematic regional changes existed in the level of cell body labeling, except that GABA_BR2-immunoreactive cell bodies had slightly higher intensity of labeling in the ICd than in other regions. Elongated cell bodies existed throughout the IC. No strong tendency of orientation existed in immunoreactive cell bodies in ICc.

Conclusion

GABA_BR1 and GABA_BR2 subunits have similar area distributions in the IC, supporting that a functional GABA_B receptor is a heterodimer. The contrast in the level of neuropil immunoreactivity among different subdivisions is consistent with the fact that the GABA_B receptor has different pre- and postsynaptic functions in these different subdivisions. The lack of trend in the orientation of immunoreactive cell bodies in the ICc likely suggests that these cells are outside fibrodendritic lamiae in the structure, although this suggestion has yet to be verified by further experiments.

683 Non-Invasive Measures of the Health of the Implanted Cochlea

Bryan Pfingst¹, Cameron Budenz¹, Deborah Colesa¹, Elizabeth Hyde¹, Lisa Kabara¹, Gina Su¹, Yehoash Raphael¹, Melissa Watts¹

¹University of Michigan

Background

The hypothesis that cochlear implant function depends on the health of the cochlea has motivated research and clinical efforts aimed at preservation and restoration of the normal cochlear biology. To help test the hypothesis we

are examining several non-invasive, clinically applicable measures of implant function across animals that have a large range of cochlear pathology. Such measures are needed to assess the efficacy and stability over time of treatments designed to preserve or restore the health of the cochlea following implantation and to identify the healthiest stimulation sites when programming a patient's processor MAP.

Methods

We define 'cochlear health' in terms of the percentage of surviving inner hair cells (IHCs), the density of spiral ganglion neurons (SGNs) in Rosenthal's canal, and the level of ensemble spontaneous neural activity (ESA). We evaluated four potential monitors of cochlear health: electrically-evoked compound action potentials (ECAPs) and auditory brainstem responses (EABRs); and psychophysical temporal and multipulse integration functions. To create a variety of conditions in the implanted cochleae, four different treatment procedures were used in adult male guinea pigs. 1. Hearing group: implanted in a hearing ear, typically has retained IHCs. 2. AAV.NTF-3 treated group: deafened with neomycin, inoculated with an adeno-associated viral vector containing an active neurotrophin gene to promote SGN survival and neurite regeneration. 3. AAV.Empty group: deafened with neomycin, inoculated with an empty AAV. 4. Deaf group: deafened with neomycin with no further procedures.

Results

ECAP data exhibited significant differences in slope steepness and level between animals with low versus moderate SGN densities. EABR data exhibited differentiation across all levels of SGN density. Both psychophysical monitors exhibited steep slopes and low thresholds only in animals that had >50% SGN density, moderate to good ESA levels, and surviving IHCs. Animals with no IHCs had shallow slopes (<1dB/doubling) and high thresholds, but some animals with surviving IHCs and ESA also had shallow slopes and high thresholds.

Conclusion

Cochlear health is reflected in the levels and slopes of the functions of these various non-invasive measures in guinea pigs. The psychophysical functions are good for differentiating between high and moderate to poor levels of cochlear health while the electrophysiological measures are sensitive to cochlear conditions across a large range of neural survival.

684 Listening Effort with Simulated Cochlear Implant Hearing and Electric Acoustic Stimulation – Effects of Noise on Response Time

Carina Pals^{1,2}, Mart van Dijk², Anastasios Sarampalis³, Deniz Baskent^{1,2}

¹Department of Otorhinolaryngology, University Medical Center Groningen, The Netherlands, ²Research School of Behavioral and Cognitive Neurosciences, University of

Groningen, The Netherlands, ³Department of Experimental Psychology, University of Groningen, The Netherlands

Background

Cochlear implant (CI) fit is commonly assessed using speech intelligibility measures and self-report. However, these measures may not reflect listening effort. Prior research [1] has shown that, when presenting normal-hearing listeners with CI-simulated speech, a dual-task paradigm can capture improvements in listening effort that are not reflected in speech intelligibility nor in subjective measures. These effects, however, were recorded near ceiling for speech intelligibility. The current study aimed to examine listening effort with simulated electric acoustic stimulation (EAS, combined CI and ipsilateral/contralateral acoustic hearing) compared to simulated CI alone, with intelligibility fixed at equal levels, below ceiling.

Methods

Normal-hearing listeners participated in one of three experiments. In experiment 1, intelligibility was fixed at 50% sentence recognition (SRT50) and in experiment 2 at 79% (SRT79) by presenting the speech stimuli at the appropriate signal-to-noise ratios (SNRs) in continuously present noise. In experiment 3 the stimuli were presented without noise, in alignment with the previous study [1]. All three experiments used the same procedure, a dual-task paradigm proposed by Pals et al. [1]. The participants listened to speech recordings processed to simulate CI hearing, residual low-frequency hearing, and EAS, and repeated back what was heard. Response times (RTs) on a simultaneous, visually-presented rhyme-judgement task served as a measure of listening effort.

Results

Preliminary results show no significant difference in RTs between simulated CI and EAS conditions presented at SRT50 or at SRT79. Average RTs for the CI and EAS conditions were about equal for both SRT50 and SRT79 and RTs recorded during listening to an auditory stimulus were shorter than RTs recorded between auditory stimuli. Preliminary results for experiment 3, without noise, show the reversed effect, in line with the previous study [1].

Conclusion

Noise affects the dual-task results in several ways; the difference in duration of RTs between and during listening is reversed compared to speech in silence, and the presence of noise may limit best performance on the response-time task. Other research has shown clear differences in listening effort between different intelligibility levels, yet the best RTs show no difference for SRT50 and SRT79. Preliminary results show no benefit in listening effort for simulated EAS compared to CI alone. However, effects of noise and listening effort need to be untangled before drawing final conclusions.

[1] Pals, C., Sarampalis, A., Baskent, D., Listening Effort with Cochlear Implant Simulations, in revision.

685 Factors That Influence the Integration of Acoustic and Electric Stimulation in Bimodal Cochlear Implant Users

Joseph Crew^{1,2}, John Galvin III¹, Qian-Jie Fu^{1,2}

¹House Research Institute, ²University of Southern California

Background

For cochlear implant (CI) users, effective combination of acoustic (A) and electric (E) stimulation may be limited by patient-related factors (e.g., residual hearing, performance in either ear), device-related factors (e.g., frequency overlap between devices), and/or listening condition (e.g., speech-in-noise, music). Likewise, optimization of combined electro-acoustic stimulation (EAS) may involve changing one or both device settings to address different concerns. This project aims to identify factors/conditions that limit the integration of electric and acoustic information for CI users' speech and music perception.

Methods

Bimodal CI subjects, hearing aid (HA) in one ear and CI in the other, were tested using their clinical settings for both devices. Subjects were tested with the HA only (A), the CI only (E), and with both devices (EAS). Speech reception thresholds (SRTs) were adaptively measured for HINT sentences in speech babble. Melodic contour identification (MCI) was measured with and without a competing instrument. The pitch of target contour and the competing masker was varied to test integration/segregation with E, A, and EAS.

Results

Preliminary results showed great inter-subject variability in terms of integration of EAS. A strong difference across speech and music was observed with EAS offering a greater benefit for speech, but little benefit or even interference for music. For most subjects, HINT SRTs were poorest with A-only, better with E-only, and best with EAS. Most subjects had difficulty with the MCI task with E-only (<50% correct), and most had no difficulty (>90%) with A-only at low frequencies. For music, some subjects attended to the better ear (EAS = A) while others had difficulty combining information across ears (EAS < A). For most subjects, performance was better when the pitch of the masker and target contours did not overlap; segregation using pitch cues was generally better with the A-only and EAS conditions than with E-only.

Conclusion

Acoustic hearing greatly allows for the perception of low frequency pitch cues which can be utilized in both speech and music. However, the present data suggest that the benefit of adding A to E depends on the listening condition, as well as patient-related factors such as the amount of aided hearing and the performance of the acoustic hearing ear. Such factors should be considered when optimizing the CIs and HAs for bimodal patients.

686 Influence of Insertion Site and Sealing Technique on Hearing Thresholds and Tissue Formation After Cochlear Implantation

Alice Burghard¹, Andrej Kral¹, Thomas Lenarz¹, Gerrit Paasche¹

¹Hannover Medical School

Background

Nowadays severely hearing impaired people and patients suffering from profound hearing loss are treated with a cochlear implant (CI). Even though many of these patients benefit from receiving the implant, some challenges still remain.

The development of a fibrous tissue sheath around the electrode carrier and/or new bone formation after implantation has an influence on the increase in impedance after surgery as well as on the hearing performance of the patients. Factors influencing the formation of connective tissue are the implant materials and surface properties as well as any trauma induced during surgery. As there is indication that the fastest and strongest growth of fibrous tissue and/or new bone formation is found always in the basal turn of the cochlea, the insertion site might have an influence on its formation.

The aim of this study was to investigate the influence of the insertion site, round window membrane (RWM) vs. cochleostomy, and of different sealing techniques, no additional seal vs. muscle graft seal vs. bone cement seal.

Methods

Dunkin Hartely guinea pigs were implanted for 28 days with a silicone covered platinum-wire. All animals underwent frequency specific auditory brainstem response measurements (ABR) prior to surgery and at the end of the experiment to detect their hearing thresholds. Three groups were implanted through an incision of the RWM. The remaining groups received their implants via a drilled cochleostomy. Each implantation procedure was combined with three different sealing techniques (no additional seal, muscle graft seal, bone cement seal).

At the end of the experiment the cochleae were harvested and prepared for histology. Cochleae were embedded in epoxy and then a grinding procedure was performed (40 μ m steps). After measuring the area filled with fibrous tissue/new bone formation, we calculated its volume. Additionally the ABR measurements were analysed to determine the threshold shift after implantation.

Results

In all animals a threshold shift after implantation was detected. In 1/3 of the animals implanted through the RWM the hearing threshold after surgery was above 90 dB SPL. In the groups implanted via a cochleostomy this occurred in 2/3 of the animals. Comparing the different sealing techniques, the groups with a bone cement sealing showed the largest threshold shifts as well as massive new bone formation.

Conclusion

According to our data, both, insertion site and sealing technique have an influence on the outcome after cochlear implantation.

687 Pre- And Post-Operative Binaural Masking Level Differences for Bimodal Cochlear-Implant Listeners

Benjamin Sheffield¹, Gerald Schuchman¹, Joshua Bernstein¹

¹Walter Reed National Military Medical Center

Background

Cochlear implants (CIs) are increasingly recommended to individuals with bilateral acoustic hearing sensitivity that approaches or exceeds current clinical guidelines because of the documented benefits of combined electric and acoustic hearing. Although new electrode designs and surgical approaches are being developed to promote hearing preservation, most current patients will lose much of the acoustic hearing in the ear implanted. Consequently, there might be aspects of binaural hearing which they are sacrificing. While speech perception is generally improved from the combination of a CI with residual acoustic hearing, bimodal listeners have difficulty taking advantage of binaural squelch to improve speech understanding in noise. This study aimed to examine the potential trade-off between the benefits of a CI and the loss of binaural squelch for speech perception in noise as a result of cochlear implantation for individuals with limited bilateral acoustic hearing.

Methods

Binaural Masking Level Differences (BMLDs) were measured prior to unilateral cochlear implantation for 10 severely hearing-impaired subjects with some bilateral acoustic hearing (<80 dB HL at 500 Hz). Six of these subjects (to date) were also tested at least six months post-activation. IEEE sentences were presented audiovisually (including a video of the talker's face) because auditory-alone performance was often too poor to reliably measure at signal-to-noise ratios (SNRs) where a BMLD would be expected. Speech signals were presented in speech-shaped noise for SNRs between -15 and +15 dB in 5-dB steps. The noise was always correlated between the two ears, while the speech signal was either correlated (N_0S_0) or inversely correlated (N_0S_π). Signals were delivered via headphones (95 dB SPL speech level) to the unaided ear(s) and/or via direct connection to the CI processor at MCL. BMLDs were calculated for each subject as the greatest dB difference between the N_0S_0 and N_0S_π psychometric functions.

Results

Four of 10 subjects showed evidence of a BMLD preoperatively (range: 2–8 dB). Of these four subjects, three have been tested postoperatively and none showed a measurable BMLD. However, all six subjects tested postoperatively showed N_0S_0 performance equal to or better than their preoperative N_0S_π performance.

Conclusion

Binaural sensitivity is diminished for some individuals with bilateral acoustic hearing who receive a CI, reducing binaural unmasking when the source of interest is spatially separated from the background noise. However, this deficit is likely overcome by the overall benefit to speech understanding provided by the CI.

688 Binaural Spectral Fusion in Hearing Aid and Cochlear Implant Users

Lina Reiss¹, Rindy Ito^{1,2}, Jessica Eggleston¹, David Wozny^{1,3}

¹Oregon Health & Science University, ²VA Pacific Islands Health Care System, ³Carnegie Mellon University

Background

Many hearing-impaired individuals receive little additional speech perception benefit or even interference from combining two hearing devices bilaterally, whether the devices are bilateral hearing aids (HAs), bilateral cochlear implants (CIs), or a CI worn with a HA in the contralateral ear (bimodal CI+HA). One contributing factor may be a change in the central processing of binaural inputs. Interaural pitch mismatches are often introduced by hearing loss, i.e. diplacusis, or CI programming, where real-world frequencies allocated to the electrodes differ from the electrically stimulated cochlear frequencies. Previous studies have shown that pitch perception adapts to reduce this discrepancy in some, but not all CI+HA users (Reiss et al., 2007). We hypothesize that some individuals instead adapt by increasing binaural fusion to reduce the perception of pitch discrepancy and, as in other sensory modalities, this fusion leads to averaging of information between ears.

Methods

Subjects were tested on three tasks: 1) *Interaural pitch matching*, in which a reference stimulus, a pure tone for a bilateral HA subject or a single electrode for a CI+HA subject, was pitch-matched to sequentially presented pure tones in the contralateral ear; 2) *Dichotic fusion range measurement*, in which a reference stimulus was presented simultaneously with a pure tone in the contralateral ear, and the contralateral frequency varied to find the frequency range that fused with the reference; 3) *Fusion pitch matching*, in which a fused reference-contralateral stimulus pair was pitch-matched to sequentially presented tones in the contralateral ear. All stimuli were loudness balanced before testing.

Results

Seventeen CI+HA users and three bilateral HA users showed increased dichotic fusion frequency ranges of up to 2-3 octaves, compared to <0.03 octaves in normal-hearing listeners (van den Brink, 1976). The size of the fusion range was significantly correlated with the interaural pitch mismatch in both groups. In addition, averaging of dichotic pitch was observed, i.e. simultaneous presentation of two different pitches to the two ears resulted in the perception of a new binaural pitch intermediate between the original pitches.

Conclusion

The increased fusion frequency ranges and correlation of fusion frequency range with interaural pitch mismatch suggest that binaural fusion increases in some individuals as a compensation mechanism to reduce perceived interaural discrepancy. The increased fusion and associated spectral averaging between ears may account for speech perception interference effects observed with binaural compared to monaural hearing device use.

689 Residual Hearing Changes with Electrical Stimulation in Cochlear Implanted Guinea Pigs

Lina Reiss¹, Chiemi Tanaka^{1,2}, Anh Nguyen-Huynh¹, Katherine Loera¹, Gemaine Stark¹

¹Oregon Health & Science University, ²University of Hawaii at Manoa

Background

Hybrid cochlear implants (CIs) are designed to preserve low-frequency (LF) hearing and allow combined acoustic-electric stimulation in the same ear. However, ~30% of these CI patients have >30 dB of LF hearing loss (HL) post-operatively between 3-36 months after CI activation (Gantz et al., 2010). The slow time course suggests that in addition to surgical trauma, electrical stimulation from the CI also contributes to HL. The goal of this study was to directly investigate the effects of electrical stimulation on residual hearing in a guinea pig CI model.

Methods

Twelve 2-month-old normal-hearing guinea pigs were implanted with an 8-ring animal electrode (Cochlear Limited, Australia) in the left cochlea via a cochleostomy. These animals were divided into two groups: chronic acoustic and electric stimulation (CAES; n=6) and no stimulation (NS; n=6). Non-implanted animals served as chronic acoustic stimulation controls (CAS; n=6). Auditory brainstem responses (ABRs) at 1, 2, 6, and 16 kHz and electrically-evoked ABRs (EABRs) were recorded biweekly to monitor changes in acoustic and electric hearing. In CAES animals, CIs were activated 5 weeks after surgery. EABR thresholds and behavioral responses were used to program T- and C- levels, respectively. CAES and CAS animals were stimulated 3 hours/day, 5 days/week for 10 weeks with modulated white noise. At the conclusion of the study, cochleae were processed and embedded in JB-4 resin for sectioning. Hair cell counts, stria vascularis vascular density, and spiral ganglion density were quantified.

Results

The majority of animals in the CAES and NS groups had significant post-surgical HL at 6 and 16 kHz. After 10 weeks of stimulation, four out of six animals in the CAES group had additional LF HL at 1 kHz. One out of six animals in the NS group had additional HL at 1 kHz; blood was observed in the apex of the cochlea for this animal. No additional HL was seen in the CAS group. Fibrosis, ossification, and changes in vascular density at the

electrode region were seen in animals with post-surgical HL.

Conclusion

The greater incidence of increased HL at 1 kHz in the CAES group after electrical stimulation compared to the NS group suggests that electrical stimulation can contribute to HL with CI use over time. The results indicate that further study is needed to determine the effects of electrical stimulation on residual hearing.

690 Real-Time Impedance Measurement Feedback for Intracochlear Electrode Insertion

Chin-Tuan Tan¹, Mario Svirsky¹, Abbas Anwar¹, Shaun Kumar², Bernie Caessens², Claudiu Treaba², Paul Carter², J. Thomas Roland Jr.¹

¹New York University, School of Medicine, ²Cochlear Ltd., Sydney, NSW, Australia

Background

This pilot study details the use of a software tool that measures electrode impedance continuously during intracochlear electrode insertion, with the eventual potential to assess and optimize electrode placement and reduce insertional trauma.

Methods

A prototype software program for measuring electrode impedance and displaying it graphically in real time has been developed. The software was evaluated in both human cadaveric temporal bones and two live surgeries during intracochlear electrode insertion. Electrode positions were cross-evaluated in time alignment with the impedance measurements using real time fluoroscopic analysis.

Results

Several electrode designs were evaluated with the new software system and data were obtained during electrode insertion with fluoroscopic guidance. Impedance changes were observed with various scalar positions. Using Contour Advance™ electrodes, impedance values increased after stylet removal, particularly when the electrodes are stimulated in the monopolar mode.

Conclusion

Impedance values seem to vary systematically with electrode position in scala; higher impedance values being associated with proximity to the cochlear wall. The new software is capable of acquiring impedance measurements during electrode insertion and this data may be useful to guide surgeons to achieve optimal and atraumatic electrode insertion, to guide robotic electrode insertion, and to provide insights about electrode position in the cochlea.

This study was supported by Cochlear Ltd. (PI: Roland). Dr. Tan's participation in the study was supported by NIH grant K25-DC010834 (PI: Tan), and Dr. Svirsky's participation was supported by NIH grant R01-DC003937(PI: Svirsky).

691 Hyaluronic Acid Perfusion Enhances Cochlear Implant Insertion While Preserving Some Degree of Hearing Function

Sushrut Kale¹, Mailing Wu¹, Elizabeth Olson¹

¹Columbia University

Background

Hyaluronic acid (Healon or HA) is frequently used as a substrate for the delivery of therapeutic drugs into the inner ear via the round window (RW) membrane. HA is also used as a lubricant in cochlear implant surgeries to facilitate a safer implantation. However, the effects of acute intra-cochlear exposure of HA on hearing are not well understood. HA is a highly viscous glycosaminoglycan polysaccharide that is widely present in human body and is bio-degradable. We have devised a novel cochlear implant insertion technique that entails perfusion of the cochlea with HA and takes advantage of its viscous nature. In present work we report (1) further developments in previously proposed implantation technique and (2) evaluate hearing function after perfusing the cochlea with HA.

Methods

A small cochleostomy was performed in the scala vestibuli (SV) of anesthetized, young adult Mongolian gerbils. RW membrane was removed to view the entrance to the tunnel of scala tympani (ST). RW was filled with 1% HA and a mock-silicone implant was positioned directly above the entrance to the tunnel of ST with the help of a microcapillary. Another microcapillary was snugly inserted into the SV hole and a steady flow of HA was set up from RW to SV outlet. With the aid of the HA flow an implant was pulled into the cochlea. The effect of implantation and HA perfusion on hearing was assessed by comparing compound action potential (CAP) input-output functions and distortion-product otoacoustic emissions (DPOAEs) measured before and after the implant insertion. Perfusion with artificial perilymph using the same set up served as a control.

Results

Following artificial perilymph perfusion, CAP thresholds were comparable to pre-perfusion level. HA perfusion resulted in CAP threshold elevation that ranged from 30-60 dB across animals. However, none of the animals showed complete loss of hearing function following HA perfusion, which suggests that HA is not inherently ototoxic to hair cells and auditory-nerve fibers. The CAP threshold elevations might have resulted from changes in mechanical function within the cochlea, which will be explored further. The new implantation technique resulted in the implant insertion all the way to the apex. Following HA perfusion, the DPOAEs were either reduced or in the noise floor with large variability across animals.

Conclusion

The new technique that flows an implant into the cochlea seems like a good alternative to traditional implant insertion methods.

692 Long-Term Neurotrophic and Functional Effects of BDNF and Intracochlear Electrical Stimulation in Neonatally Deafened Animals

Patricia Leake¹, Olga Stakhovskaya^{1,2}, Stephen

Rebscher¹, Ben Bonham¹

¹Epstein Laboratory, University of California San

Francisco, ²Department of Hearing and Speech Sciences, University of Maryland, College Park

Background

Postnatal development and survival of cochlear spiral ganglion (SG) neurons depend upon both neurotrophic support and neural activity. Our studies in cats deafened prior to hearing onset have shown that intracochlear electrical stimulation (ES) from a cochlear implant (CI) can help prevent SG degeneration, and intracochlear infusion of BDNF can further improve neural survival.

Methods

Kittens were deafened as neonates (systemic neomycin) and implanted at \approx 1 month of age with custom-designed scala tympani electrodes with a drug-delivery cannula connected to a mini-osmotic pump. BDNF (94 μ g/ml; 0.25 μ l/hr) was infused for 10 weeks, and ES delivered for \approx 5 months.

Results

Combined BDNF+ES elicited marked improvement in SG survival (>50% increase) and larger cell areas in the implanted ears as compared to contralateral. Moreover, SG survival after combined BDNF+ES was significantly better than after ES alone over these prolonged durations. BDNF+ES also resulted in angiogenesis in the SG, increased peri-implant fibrosis, higher density/larger size of radial nerve fibers within the osseous spiral lamina, and ectopic sprouting of these fibers into scala tympani. EABR thresholds improved relative to initial thresholds on chronically stimulated channels of the CI, but not on a control unstimulated channel.

In a separate study we asked whether neurotrophic effects would persist after cessation of BDNF infusion, *without ES*. After identical deafening and BDNF infusion procedures, animals were studied at ages similar to the BDNF+ES group (mean, 26 weeks). SG density data indicated that neurotrophic effects persisted for >3 months after terminating BDNF (38% increase). Substantial ectopic sprouting of radial nerve fibers again occurred.

Electrophysiological recordings in the inferior colliculus (IC) showed maintenance of the normal cochleotopic organization after BDNF+/-ES. IC thresholds were well-correlated with EABR thresholds. Lower IC thresholds were correlated with more selective central activation in all other groups, but *not in BDNF-treated subjects* where variability was much greater, perhaps due to the disorganized ectopic fiber sprouting.

Conclusion

BDNF promotes improved long-term survival of SG neurons and radial nerve fibers. These neurotrophic effects persist for ≥ 3 months after terminating BDNF delivery and withstand the additional stress of ES. Lower EABR thresholds and higher radial fiber density may be beneficial for CI function. However, the disorganized ectopic radial nerve fiber sprouting may be deleterious to optimized CI function.

Research supported by NIDCD Contract #HHS-N-263-2007-00054-C. BDNF donated by Amgen Inc, Thousand Oaks, CA.

693 Target Structures for Infrared Neural Stimulation (INS)

Hunter Young¹, Agnella Matic¹, Sama Kadakia², Claus-Peter Richter¹

¹Department of Otolaryngology, Feinberg Medical School, Northwestern University, ²Northwestern University

Background

Pulsed mid-infrared lasers have been used as a method for neural stimulation, including cochlear stimulation. The use of lasers is appealing for many reasons, namely the spatial selectivity and non-contact method of stimulation. The mechanism of INS is believed to be involved with local heating of discrete neuron populations. In cochlear INS, some of the heat is absorbed in the cochlear fluid proximal to the stimulation site, resulting in measurable stress relaxation waves. These waves may vibrate the basilar membrane or directly stimulate hair cells, causing a stimulation by-product. Hair cell stimulation due to INS-created stress relaxation waves has been observed in vestibular system optical stimulation. The goal of the present study was to determine the contributions of hair cells to the recorded cochlear INS response.

Methods

In normal hearing animals, auditory responses can be masked with a noise stimulus. In the present experiments the INS was masked in hearing animals with an auditory stimulus. The optical fiber was inserted through a cochleostomy in the basal turn. After recording the effect of the masking using CAP measurements taken at the round window, the animals were deafened by 30mM Neomycin, which was injected directly in the scala tympani via the cochleostomy. After deafening was confirmed by testing for auditory-evoked CAPs, the masking experiment was repeated. If INS occurs through direct neural interaction, and not from hair cell stimulation, then the masking effect should disappear. Chronic deaf animals lacking hair cells were used in a second series of experiment, in which recordings from the central nucleus of the inferior colliculus (ICC) were used to determine whether stimulation of a cochlea lacking hair cells is possible.

Results

Preliminary data show that the masking effect is present in normal hearing animals and disappears after deafening with Neomycin. Animals that showed no hair cells in

histologic sections revealed a neural response recorded from the ICC.

Conclusion

The effects of hair cells on INS can be seen through masking noise over optical stimulation. However, when hair cells are damaged or no longer present, INS still generates a neural response. These findings lead to the conclusion that although INS-induced stress relaxation waves may have some interaction with hair cells INS occurs through the direct interaction of the radiation and the neuron.

694 Optogenetic Stimulation of the Auditory Nerve: Toward an Optical Cochlear Prosthetic

Victor H. Hernandez^{1,2}, Gerhard Hoch¹, Kirsten Reuter^{1,2}, Zhizi Jing³, Matthias Bartels⁴, Gerhard Vogl⁵, Carolyn W. Garnham⁵, George J. Augustine^{6,7}, Sebastian Kügler⁸, Tim Salditt⁴, Nicola Strenzke³, Tobias Moser^{1,2}

¹InnerEarLab, Department of Otolaryngology, University of Goettingen School of Medicine, ²Bernstein Focus for Neurotechnology, University of Göttingen, Germany, ³Auditory Systems Physiology Group, Dept. of Otolaryngology, University of Göttingen Medical Center, ⁴Department of Physics, University of Goettingen, Germany, ⁵MED-EL Company, Innsbruck, Austria & MED-EL Germany, Starnberg, Germany, ⁶Program in Neuroscience and Behavioral Disorders, Duke-NUS Graduate Medical School, Singapore, ⁷Center for Functional Connectomics, Korea Institute of Science and Technology, ⁸Viral Vectors Laboratory, Dept. of Neurology, University of Goettingen Medical School

Background

When hearing fails, electrical stimulation of spiral ganglion neurons (SGNs) by cochlear implants (CIs) enables open speech comprehension in a majority of deaf subjects. Still, while healthy listeners encode a wide range of sound pressures (10^6) and frequencies (10^3 in 2400 steps), CIs typically employ only a narrow range of electrical currents to encode sound intensity and no more than 22 channels for frequency coding. The later limitation is caused by widespread current flow from each stimulating electrode, activating a large number of SGNs that represent many different sound frequencies. Optical SGN stimulation may improve CI coding by enabling more independent information channels to the CNS.

Methods

Here we employed channelrhodopsin-2 (ChR2), to render SGNs sensitive to blue light.

We used transgenic mice expressing ChR2 under the Thy-1 promoter and virus-mediated expression of the ChR2 variant CatCh employing transuterine injection of AAV into the embryonic otocyst. Coupling blue light emitted by LED, into a cochleostomy or blue laser inserted through the round window, caused large compound potentials in scalp recordings. Activation of the ascending auditory pathway was corroborated by light on tone masking and

optogenetically evoked single neuron activity in the auditory nerve/cochlear nucleus and midbrain.

Results

Light stimulation caused compound potentials in scalp recordings (oABR) of hearing mice and in mouse models of acute and chronic human deafness. oABRs were absent in WT mice or in ChR2 mice when light was projected onto their intact cochlea. oABR generation was inhibited by lidocaine or TTX. Activation of the auditory pathway was corroborated by single neuron action potentials in the auditory nerve, cochlear nucleus and inferior colliculus. Light-on-tone masking corroborated specific activation of the ascending auditory pathway and coincided with the position of the cochleostomy relative to the tonotopic map of the cochlea as identified by high resolution X-ray tomography. Transuterine injections of CatCh-AAV into the otocyst effectively transduced SGN showing expression in SGN somata and neurites. oABRs and AP in the auditory nerve could be elicited in ears expressing CatCh.

Conclusion

- Optical stimulation of SGNs is feasible
- Specific activation of the auditory pathway was demonstrated by single neuron action potential from the auditory nerve/cochlear nucleus and inferior colliculus and by tone and light compound responses.
- AAV6-mediated expression of ChR2 constructs in murine SGNs is feasible.

Outlook

- Improve temporal bandwidth of stimulation by appropriate constructs.
- Study behavioral responses
- Develop mouse chronic intracochlear implants

695 Optogenetic Control of Central Auditory Neurons

Keith N. Darrow^{1,2}, Michael Slama², Judith Kempfle², Edward Boyden³, Daniel Polley², M. Christian Brown², Daniel J. Lee²

¹Worcester State University, ²Massachusetts Eye and Ear Infirmary, ³Massachusetts Institute of Technology

Background

Electric current spread limits the performance in users of central auditory prostheses by reducing the number of independent acoustic channels and increasing side effects from the activation of non-auditory pathways. Optogenetic stimulation of neuronal circuits has been proposed to improve the specificity of stimulation and has been demonstrated in a number of systems.

Methods

The left cochlear nucleus (CN) of CBA/J mice was transfected with AAV2/8-Channelrhodopsin-2 (ChR2) following posterior craniotomy in vivo. Following an incubation period of two to four weeks, mice were reanesthetized and blue light stimulation was delivered via an optical fiber placed near the surface of the transfected cochlear nucleus. Multi-channel recordings of neural

activity were made in the inferior colliculus (IC) and in auditory cortex (Actx).

Results

A significant increase in neural firing rate was observed in the IC and Actx during blue light stimulation. Optical stimulation of the CN evoked spiking activity throughout the tonotopically organized central nucleus of the IC. This spread of activity was consistent with histological verification of transfection across the tonotopic gradient of CN. Varying pulse rate between 5 and 320Hz did not significantly affect threshold or bandwidth of the IC population response across animals. The spatial spread and magnitude of IC activity elicited by optical stimulation was comparable to that obtained with an acoustic click stimulus presented at 50 dB SPL. In contrast, no significant increase in neural firing rate was observed in response to optical stimulation in those cases with no ChR2 expression and in control cases. No acoustic artifact was measured when using the blue light laser.

Conclusion

These data suggest that optogenetic excitation of central auditory neurons is feasible and may provide the basis for a new generation of optically based neuroprosthetic devices.

696 Wavelength Dependency of Inner Ear Responses to Pulsed Laser Stimulation

Peter Baumhoff¹, Michael Schultz², Hannes Maier³, Ingo U. Teudt¹, Alexander Krüger², Thomas Lenarz^{1,4}, Andrej Kral¹

¹VIANNA, Hannover Medical School, ²Laser Zentrum Hannover e.V., ³Department of Experimental Otology, Hannover Medical School, ⁴ENT Clinics, Hannover Medical School

Background

Current research investigates the potential of optical stimulation of the inner ear to improve dynamic range and frequency resolution compared with stimulation via a conventional, electric cochlear implant. In addition to a potential for neural stimulation, laser radiation has been shown to cause pressure waves in the audible range along the axis of the laser beam in different media. In the current study we show cochlear sensitivity to nanosecond laser pulses at wavelengths ranging from ultraviolet to near infrared and for different pulse energies in vivo.

Methods

Cochlear responses to laser pulses were investigated by recording compound action potentials (CAPs) in seven normal hearing, anesthetized guinea pigs. The wavelength of the laser pulses were varied between 420 nm and 2150 nm for pulse energies between 3 µJ and 12 µJ. The stimulation site was located at the boundary between the basilar membrane and the spiral lamina seen through the round window. Both extra- and intracochlear stimulation approaches were investigated.

Results

We found a positive correlation between the energy level and the peak-to-peak CAP amplitude at all wavelengths investigated, with maximum CAP amplitudes comparable to ones evoked by acoustic stimuli at sound levels of 65 dB above threshold. These results could be shown for extra- and intra-cochlear stimulation. Stimulation between 420 nm and 2150 nm at constant energy levels led to a reproducible wavelength dependent CAP amplitude function. Below 1370 nm CAP amplitudes are significantly correlated to the absorption of either one of two main absorbers in the cochlea: hemoglobin and water respectively. Interestingly, the correlation with water absorption becomes negative for high absorption coefficients. We saw no CAP responses to laser irradiation following a Neomycin induced total hearing loss.

Conclusion

Overall laser evoked CAP characteristics are very similar to those of auditory evoked CAP. This is a good indication that laser stimulation can induce a substantial optoacoustic response in the cochlea. The strength of the response depends on pulse energy as well as the absorption coefficients of the media for the respective wavelengths. We see evidence for a change in the shape and extend of the absorbing volume at height absorption coefficients, leading to more localized optoacoustic effects and thus smaller CAP amplitudes than would be expected from the absorption strength alone. The extent of the observed optoacoustic effects demonstrates the importance of complete deafening in the investigation of neuronal laser stimulation.

Support: Cluster of Excellence Hearing4All / SFB Transregio 37

[697] Response Patterns to Infrared Neural Stimulation of the Cochlea Recorded from the Inferior Colliculus

Claus-Peter Richter^{1,2}, Agnella Matic¹

¹Northwestern University, ²Biomedical Engineering

Background

Cochlear spiral ganglion neurons can be stimulated with infrared radiation. While the stimulation is spatially selective and can be achieved over weeks without notable damages of the cochlea, it has to be demonstrated that infrared neural stimulation (INS) has the dynamics to encode the temporal structure of speech. In the present study, we further characterize the patterns of neuronal activity to irradiation of the cochlea with infrared pulses.

Methods

Single Tungsten electrodes and multichannel electrodes were placed in the central nucleus of the inferior colliculus (ICC) to recorded neural activity in response to INS of spiral ganglion neurons, both in normal hearing and deafened guinea pigs. Aculight tabletop diode infrared lasers (wavelength: 1844-1878nm) were used generate the optical pulses. The pulse length was between 10 and 200µs, the pulse repetition rate was between 1 and 250Hz,

and the radiant energy was 0 to ~126µJ/pulse. A 200µm optical fiber was inserted into the cochlea and was coupled to the laser to deliver the radiant energy to the target neurons. Optical stimuli included simple optical square pulses, triangular pulses, ramps up, ramps down, and amplitude modulated pulse sequences.

Results

Peri-stimulus histograms showed a single maximum with a latency of ~5.4 ms after the presentation of stimulus. Increasing the stimulus intensity shortened the latency of the first maximum to ~5.1 ms. Changing the stimulus pulse duration did not affect the response pattern. The maximum repetition rate for the neurons was lower for activity obtained with single Tungsten electrodes. For multi channel electrodes repetition rates of 200 pps could be seen.

Conclusion

The results for INS are similar to most of the data obtained with electrical stimulation. The data suggest that cochlear INS could provide stimulation with the appropriate temporal resolution to encode speech in future optical cochlear implants.

This work was supported with federal funds from the National Institute on Deafness and Other Communication Disorders, National Institutes of Health, Department of Health and Human Services, under Contract No. HHSN260-2006-00006-C / NIH No. N01-DC-6-0006, DC011855-01A1, DC011481-01A1 and by Lockheed Martin Aculight.

[698] Modeling Performance of Optical Stimulation for Use in Cochlear Implants

Alexander Thompson¹, Scott Wade¹, Paul Stoddart¹

¹Swinburne University of Technology

Background

Infrared neural stimulation (INS) has been demonstrated as an alternative to conventional electrical techniques for the stimulation of nerves. Based on the absorption of short pulses of infrared light, INS has the potential for higher spatial selectivity compared to standard electrical stimulation. There is interest in using INS to replace or complement electrical stimulation in bionic devices, specifically the cochlear implant where the increase in spatial selectivity would be advantageous. The majority of reports on INS have presented experimental results, whereas theoretical modeling of the processes involved can complement this work. Herein a detailed simulation of the localization of infrared stimulation, the potential for interference between multiple channels and the potential heat build up at high repetition rates is reported.

Methods

The model presented consists of a Monte Carlo model and finite element analysis (FEA) of the heat equation. Monte Carlo methods are utilized to simulate light transmission and absorption in tissue and provide spatial localization of an instantaneous laser pulse. The FEA solution of the heat

equation reveals the temporal behavior of heat flow and allows repetitive pulses to be considered. The energy of the laser pulses and constants of the relevant media have been taken from the literature.

Results

The model predicts the temperature rise from single pulses can be as low as 0.01°C, depending on the wavelength and pulse duration, with the temperature decaying to the baseline temperature after ~250 ms. When a repetition rate of 10 Hz is used, the temperature peaks due to successive pulses overlap and the baseline temperature stabilizes at a value of 50% of an individual pulse's peak temperature. Faster repetitions result in greater temperature superpositions, a repetition rate of 100 Hz stabilizes at 760% of an individual pulse's peak temperature. When an array of spatially separated pulses are used, no increase in peak temperature is observed. However with a separation of less than 500 μm, the decay to baseline temperatures takes longer and an increase in the temperature superposition is observed over multiple pulse repetitions.

Conclusion

Results of INS modeling show that a significant increase in temperature is present in tissue when using a repetition rate similar to that used in current implants (> 100 Hz). The results show the need for further chronic experimentation to evaluate the effect of the increased temperature and show the potential advantage of a hybrid optical/electrical stimulation technique.

699 Water Transport in the Rat Inner Ear; Translational Research of Meniere's Disease

Masahiko Nishimura¹, Akinobu Kakigi², Taizo Takeda³, Setsuko Takeda³, Teruhiko Okada³, Junko Murata¹, Katsuhisa Ikeda¹

¹Juntendo University Faculty of Medicine, ²University of Tokyo Faculty of Medicine, ³Kochi Medical School

Background

In order to develop new treatments of Meniere's disease, we investigated a time course of changes of the stria vascularis after vasopressin (VP) injection and the influence of OPC-31260 on experimentally induced enlargement of the intrastrial space caused by VP injection.

Methods

In the time course study, Wistar rats were injected with 50 mg/kg of VP subcutaneously. The stria vascularis specimens were harvested at 10, 20, 30, and 60 min after VP injection. For OPC-31260 administration, animals were administered 100 mg/kg of OPC-31260 orally 1 h before receiving 50 mg/kg of VP subcutaneously. The specimens were harvested 20 min after VP injection. These specimens were observed using transmission electron microscopy.

Results

In the time course study, the incidence of intrastrial space enlargement was 50%, 100%, 25%, and 0% for 10, 20, 30, and 60 min, respectively. In the study with OPC-31260 administration, the enlargement of the intrastrial space was reduced.

Conclusion

The intrastrial space was enlarged remarkably at 20 min after VP injection, and this enlargement of the intrastrial space was reduced by administration of OPC-31260 before VP injection. These results suggest that VP increases the influx of water from the perilymph to the basal cells via aquaporin (AQP) 2 and causes the formation of endolymphatic hydrops.

700 A Biodegradable Drug Delivery Microdevice for Tinnitus

Jane Wang^{1,2}, Tara Campbell², Avi Chad-Friedman², Robert Langer³, Sharon Kujawa^{4,5}, Jeffrey Borenstein²

¹Department of Materials Science and Engineering, Massachusetts Institute of Technology, ²Biomedical Engineering Center, Charles Stark Draper Laboratory, ³Department of Chemical Engineering, Massachusetts Institute of Technology, ⁴Eaton-Peabody Laboratory, Massachusetts Eye and Ear Infirmary, ⁵Department of Otolaryngology, Harvard Medical School

Background

Tinnitus is the leading cause of disability in troops returning from Iraq and Afghanistan. It is often associated with blast injury and traumatic brain injury, and affects more than 13 million people in the US and Western Europe. Current treatment includes antidepressants and glutamate receptor antagonists. Here we report on a prototype biodegradable microdevice designed to deliver drugs to the cochlea for the treatment of tinnitus and other diseases of the inner ear. It is constructed from a recently developed class of biodegradable elastomeric poly(ester amide)s, poly(1,3-diamino-2-hydroxypropane-co-polyol sebacate)s (APS), showing a much longer and highly tunable in vivo degradation half-life compared with other commonly used biodegradable polymers.

Methods

A prototype implantable medical device fabricated from elastomeric scaffolds with tunable degradation properties is being developed for long-term drug delivery to the inner ear. Lidocaine is chosen as a surrogate for the early stage development of the device, which will be designed to be compatible with emerging therapeutic compounds for the treatment of tinnitus. The microdevice is built by casting APS into porous Teflon molds, curing and assembling for the encapsulation of a therapeutic compound. The polymer degradation rate in vitro is measured compared to acceleration via enzyme degradation. Drug permeation properties of lidocaine through APS have been examined by performing Franz cell diffusion tests and simulated with MATLAB to predict release profiles.

Results

A prototype of the microdevice has been fabricated and tested in vitro. Lidocaine diffusion test shows that the diffusion coefficient of lidocaine through standard silicone is 10-fold higher than that of lidocaine through APS, allowing APS to better encapsulate lidocaine. Two different ratios of diamine:glycerol in the APS have been explored: 2:1 (diamine:glycerol) and 1:2, in order to establish optimal selectivity of the enzymatic triggering process relative to baseline degradation.

Conclusion

We report on a fully biodegradable drug delivery microdevice built using a fast, inexpensive, reproducible, and scalable fabrication process. The low diffusion coefficient of a small molecule surrogate (lidocaine), tunability in degradation rate, and selective degradation via lipase administration renders APS a suitable substrate for the delivery microdevice. When combined with emerging therapeutic compounds for tinnitus, this device will enable patient-controlled drug release via enzymatic degradation mechanisms at the desired time.

701 Pharmacokinetics of Perilymph Assessed with Fluorescent Markers

Alec N. Salt¹, Jared J. Hartsock¹, Ruth M. Gill¹

¹Washington University School of Medicine, St. Louis, MO

Background

Understanding drug kinetics in the ear requires the use of quantitative procedures for drug delivery and fluid sampling and requires validated models for the interpretation of data. In the present study we have used sodium fluorescein and fluorescent dextran as markers to evaluate pharmacokinetic procedures.

Methods

Artificial perilymph containing 1 mM sodium fluorescein (NaF) or 1 - 2.5 mM fluorescein isothiocyanate conjugated dextran; FW 3000-5000 (F-dextran) was injected from pipettes sealed into the basal turn of scala tympani (ST), the cochlear apex, or the lateral semi-circular canal. As the cochlear aqueduct provides the outlet for injected volume, each procedure fills different regions of the ear. Either immediately after injection or after varying delay times, multiple fluid samples were taken sequentially from the cochlear apex or from the lateral canal. Each sample also represents perilymph from a different region of the ear. Perilymph sample concentrations were interpreted with the aid of a computer model.

Results

Previous studies have shown that NaF is a valuable marker as it is only slowly lost from perilymph. However, we found that following injection into the basal turn of ST, NaF was rapidly lost from ST to the middle ear through the round window membrane. Efflux was reduced when the round window membrane (RWM) was occluded with adhesive (Tissuemend) but was not blocked by inclusion of 5 mM probenecid, an organic anion transport inhibitor, in the injected solution. F-dextran applied into perilymph was

consistently retained better than NaF but results with F-dextran applied into the basal turn of ST remain difficult to interpret. Perilymph concentrations were found to be dependent on the orientation of the animal, as a consequence of isosmotic F-dextran solution having a higher density than perilymph and "falling" along ST. Occlusion of the RWM also increased the retention of F-dextran.

Conclusion

Results with F-dextran show that pharmacokinetics of the basal turn of ST is more complex than previously appreciated. Distribution of F-dextran is affected by animal orientation, losses through the RWM, a sustained, slow entry of CSF via the cochlear aqueduct, distribution to adjacent compartments, distribution along the length of ST, and the elimination to blood. The data allow the parameters representing these kinetic processes in the computer model to be refined so that the model better represents the distribution of applied substances in perilymph of the inner ear.

This study supported by NIH/NIDCD R01 DC001368

702 Inner Ear Gene Delivery with an EIAV-Based Lentiviral Vector

Hideto Fukui^{1,2}, Pratik Nataraj¹, Yatish Lad³, Kyriacos Mitrophanous³, Katie Binley³, Yehoash Raphael¹

¹Kresge Hearing Research Institute, University of

Michigan, ²Department of Otolaryngology, Kansai Medical University, ³Oxford BioMedica

Background

Gene transfer into the cochlea provides a new opportunity for both research and future therapy for long-term protection, repair and regeneration. To date, a number of viral vectors have been evaluated for cochlear and vestibular gene delivery including adeno-associated virus (AAV), adenovirus (AV) and lentivirus. Lentiviral vectors have several advantages for cochlear gene therapy, including an ability to transduce terminally differentiated cells, long-term gene expression, large insert capacity (8-9 kb) and relatively early onset of gene expression following transduction. In this study, we evaluated the transduction efficiency of an equine infectious anaemia virus (EIAV)-based lentiviral vector carrying the green fluorescent protein (GFP) as a reporter gene (EIAV-GFP) in the inner ear of normal hearing mice.

Methods

We investigated several routes of administration including the posterior semicircular canal (PSC) via canalostomy, scala tympani (ST) through the round window and scala media (SM) via cochleostomy. Under general anesthesia, we administered EIAV-GFP (1µl) into the left ear via PSC, ST or SM. Two or 4 weeks after the surgery, cochlear and vestibular whole-mounts were stained for F-actin to identify the types of cells in the cochlea and examined by epifluorescence to determine the distribution of transgene expression.

Results

Two weeks after PSC administration, many cells in the non-sensory epithelium of the saccule expressed GFP, as did interdental cells in the cochlear basal turn. After ST administration, mesothelial cells showed GFP expression. SM administration resulted in GFP expression in several cochlear cell types, including fibrocytes in the osseous spiral lamina, pillar and Deiters' cells, other non-sensory epithelial cells and the stria vascularis. Four weeks after administration, GFP expression was still present in all 3 treatment groups (PSC, ST and SM administration), although qualitative observation suggested the intensity of the green fluorescence was weaker than at 2-weeks.

Conclusion

EIAV-GFP transduces several different cell-types when administered via PSC, ST and SM inoculation. These data indicate that the EIAV-based lentiviral vector may be potentially useful for future clinical applications.

This work is supported by The Williams Professorship, The Hirschfield Foundation, Oxford BioMedica (UK) Ltd and NIH/NIDCD P30 grant DC05188.

703 Using Gene Therapy Approach to Rescue Hearing in Connexin30 Null Mice by AAV1-Mediated Connexin Expressions in the Scala Media

Jianjun Wang¹, Yunfeng Wang², Shoeb Ahmad¹, Qing Chang¹, Binfei Zhou¹, Huawei Li², Xi Lin¹

¹Emory University, ²Fudan University

Background

Non-sensory cells in the sensory epithelium of the cochlea are connected extensively by gap junctions (GJs) that facilitate intercellular ionic and biochemical coupling. Mutations in the genes coding for connexin 26 (Cx26) and Cx30 are the most common causes of human nonsyndromic hereditary deafness. Currently no mechanism-based therapy is available for treatment. We have previously identified a method to completely preserve hearing after directly inoculating viral vectors into the scala media when the surgeries were done in mice younger than postnatal day 5 (P5). In this study we performed gene-therapy studies using the Gjb6 null (Cx30 knockout) mice as the model.

Methods

GFP-tagged Cx30 (Cx30-GFP) or Cx30 without any tag was inserted into an adeno-associated virus (AAV) vector. These vectors were packaged into AAV2/1 viruses with the titers of 1.0×10^{13} and 1.5×10^{13} , respectively. The recombinant viruses were injected into the scala media of one side of the cochlea of Cx30 null mice (P0 or P1). The contralateral side of the cochlea was not injected and used as a control.

Results

Without antibody labeling and beginning from 3 days after injections, we observed extensive green fluorescent punctas in the cell membrane of the claudius, outer sulcus and Hensen's cells. Strong ectopic expressions in the

cytoplasm of marginal cells, spindle-shaped cells were also observed. Weaker viral-mediated Cx30-GFP signal were detected in other types of cochlear non-sensory cells as well. In Cx30 null mice expressed Cx30 without any tag, we observed similar pattern of expressions after labeling with the Cx30 antibody. Stronger expression was observed over time and the viral-mediated Cx30 expression lasted for at least 3 months, which was the longest time period we have observed so far. Exogenous Cx30 colocalized with endogenous Cx26. The normal function of these GJs was confirmed by fluorescence recovery after photobleaching assay. Dye transfer between GFP-positive cells showed more rapid fluorescence recovery than GFP-negative cells, although the rate of recovery was quantitatively slower than that measured from wild type mice.

Conclusion

Viral-mediated expressions of Cx30 with or without the GFP tag in Cx30 null mice were able to partially restore the intercellular communication mediated by gap junctions in the cochlea. Currently we are examining auditory brainstem responses to determine whether the viral-mediated expressions of Cx30 in the deaf Cx30 null mice were enough to rescue hearing

704 Development and System Integration of a Micro-Actuator for Controlled Intracochlear Drug Delivery

Ernest Kim¹, Jason Fiering¹, Mitchell Hansberry¹, Mark Mescher¹, Erin Pararas¹, Abigail Spencer¹, Jeffrey Borenstein¹

¹Draper Laboratory

Background

Controlled, programmable intracochlear drug delivery may be necessary to treat certain hearing and vestibular disorders. Delivery directly to the inner ear using our system enables accurate dosing and sequencing of multiple compounds and overcomes obstacles such as the blood-cochlear barrier and the round window membrane. We have previously reported on our reciprocating system and in vivo testing for short and long-term experiments. In our design, a volume of solution (perilymph and concentrated drug) is repeatedly infused and then withdrawn, resulting in zero net volume transfer to the scala tympani while allowing drug transport by diffusion and mixing within the perilymph. Further miniaturization and functionality is required for an implantable device targeted for human therapeutic use.

Methods

A custom micro-actuator drives a reciprocating pump and reservoir refresh pump. It has been developed to replace the larger, heavier commercial actuator and pump currently in the system. We are prototyping low-power electromagnetic assemblies which are surface-mounted to our planar, laminated fluidic manifolds. The assemblies interface to membranes which are part of either pumping chambers or valve structures. The actuators are electronically controlled to provide variable pumping rates

and valve sequence control. We are also integrating fluidic check valves as part of our pump development effort. Parallel development of the reciprocating pump and reservoir refresh system proceeds toward long-term bench testing and sustained *in vivo* drug delivery.

Results

The actuator (with a volume of less than 0.2 cc) is sized to fit the form-factor constraints of the human implantable device. It is designed with dual electromagnetic and permanent magnetic control to achieve low-power operation. It can produce up to 1 N of force over a displacement of several hundred microns, generating fluid displacements between 0.1 and 1.0 microliter per cycle. The actuator requires very little power, using approximately 1 mJ of energy or less per actuation cycle. Additionally, the actuator is utilized, in combination with in-line valves, to drive the positive-displacement reservoir pump. Integration of the actuator with fluidic components and test results at the system level have been obtained.

Conclusion

Low-power, miniature electromagnetic actuators will be required for reciprocation and reservoir refresh in order to meet the size requirements of clinical systems. These results represent an advance in miniaturization and enhanced functionality towards the goal of a fully implantable drug delivery system for treatment of SensoriNeural Hearing Loss and other diseases.

705 Intracochlear Tamoxifen Distribution Visualized by a Cre-Lox System

Kunio Mizutani^{1,2}, William Sewell^{1,2}, Albert Edge^{1,2}

¹Department of Otolaryngology, Harvard Medical School, ²Eaton-Peabody Laboratory, Massachusetts Eye and Ear Infirmary

Background

Local delivery to the cochlea has the potential to avoid systemic side effects of drugs such as steroids, and has resulted in widespread use of transtympanic approaches to drug delivery in the clinic. Detailed pharmacokinetic studies of drugs applied to the inner ear have relied on the determination of drug concentration in perilymph, which is technically challenging in animal models and does not reveal whether drug gains access to individual tissues or cells. We have developed a novel approach to the determination of drug distribution at the cellular level using a Cre-Lox system in which we can visualize exposure of individual cells to tamoxifen, a synthetic steroid analogue.

Methods

We used two Cre-reporter strains to perform cell tracing. To assess exposure to cochlear supporting cells we used a Cre strain driven by the Sox2 promoter and for visualization of all exposed cells we used a Cre strain driven by the CMV promoter, which is ubiquitously expressed and labeled the cochlear lateral wall, spiral limbus, and spiral ganglion cells. The Cre strains contained fusion proteins with the estrogen receptor rendering them sensitive to tamoxifen. The mice were crossed to a

reporter strain that converts from expression of tdTomato, a red fluorescent protein, to expression of GFP upon Cre activity. We used several doses of intraperitoneal tamoxifen as the systemic treatment, and delivery of drug via the round window niche or lateral semicircular canal for local delivery. The number of GFP-positive cells was counted in ears dissected 1 week after drug treatment.

Results

A clear dose-dependent response to systemic tamoxifen injection was observed in all cochlear tissues. Tamoxifen showed a gradient of distribution from the basal to apical turns of the cochlea after delivery by the round window niche approach. No significant differences in the location of GFP-positive cells along the cochlear spiral were observed by the posterior semicircular canal approach.

Conclusion

We could visualize tamoxifen distribution in cochlear tissue with the use of a novel reporter system. Since cells retained GFP expression after exposure to tamoxifen, timing and distribution of tamoxifen could be monitored in the cochlear tissue. This reporter system could be a valuable strategy for the visualization of drug distribution in any organ.

706 Microparticle Characterization for Cochlear Drug Delivery

Astin Ross¹, Sahar Rahmani¹, Diane Prieskorn¹, Josef Miller¹, Joerg Lahann¹, Richard Altschuler¹

¹University of Michigan

Background

Cochlear implants are the treatment of choice for patients with moderate to profound sensorineural hearing loss, however increasing numbers of cochlear implant recipients have remaining hearing that needs protection from insertion trauma. Local delivery of therapeutic agents could potentially protect remaining sensory cells and neuronal connections. The ideal carrier for local delivery would have the ability to be functionalized to attach to the cochlear implant and/or cochlear cells, deliver multiple drugs with distinct pharmacokinetics, and sustain factor release over a defined period of time. It would also be useful to be able to monitor carrier distribution in the cochlea via fluorescent probes incorporated into/onto the carrier in test studies. To that end, fluorescent multicompartamental microparticles appear to be excellent candidates for use as carriers for drugs aimed at reducing cochlear implant trauma. Specifically, we characterize the feasibility of intrascalar delivery, detection of multicompartamental microparticles in the cochlea, and the controlled drug release from the particles.

Methods

Particles were fabricated from an FDA approved biodegradable polymer and a polysaccharide via a process called electrohydrodynamic co-jetting. For *in vivo* assessment, 5 μ L of 15mg/mL microparticle solutions were infused via cochleostomy into the scala tympani of a guinea pig animal model at a rate of 1 μ L/min. For *in vitro*

experiments, Piribedil, an anti-excitotoxic drug, was incorporated into the polymer matrix at 2% w/w (drug to polymer in one compartment) prior to jetting. Confocal laser scanning microscopy (CLSM) was used to confirm particle composition and tricompartmental nature, scanning electron microscopy to determine particle size, shape and surface topology, and 2 photon CLSM to delineate *in vivo* particle distribution within the 3D volume of the cochlea. *In vitro* drug release was assessed with UV spectrophotometry. After *in vivo* infusion, cochleae were harvested, decalcified, and sectioned to enable visualization of particles within the scala tympani and cochlear tissue via CLSM.

Results

Microparticles composed of distinct compartments were present in the cochlea up to 24 hrs post-infusion. The majority of the particles were found in the basal turn near the site of the cochleostomy. Piribedil was successfully incorporated into the microparticles and the release profile over a period of 14 days was determined.

Conclusion

Multicompartmental microparticles have demonstrated promise as intracochlear drug carriers as they exhibit controlled drug release and the ability to persist in the cochlea.

707 Sustained Release Glucocorticoid Formulation for Long Term Intracochlear Drug Delivery

Erik Pierstorff¹, Wanwan Yang¹, Yen-Jung Angel Chen², Federico Kalinec², William Slattery¹

¹O-Ray Pharma, Inc, ²House Research Institute

Background

Previously we reported our short term data on extended release glucocorticoid (GC) formulations using various dose-ranges. Our work demonstrated very good short term sustained release profiles *in vitro* and *in vivo* and studies in animal models demonstrated excellent safety. One major advantage of the O-Ray drug delivery system is the ability to deliver consistent amounts of therapeutics over very long periods of time.

Methods

To show this *in vivo*, O-Ray extended release GC formulations (predicted 100 day release) were implanted into guinea pig cochleae. Pre- and post- treatment otoacoustic emissions and ABRs were performed and excellent hearing preservation was observed. Pharmacokinetic studies were performed testing GC presence in the perilymph at 90, 120, and 180 days.

Results

Interestingly, superior hearing was observed in ears administered extended release steroids at four and six months after implantation, possibly suggesting a rescue of age dependent hearing loss. As expected, all ears containing an implant showed significant GC levels in the perilymph at 90 days (5/5). Some animals still had

detectable GC in the perilymph at 120 days (2/4) and 180 days (1/4) showing the potential for even longer sustained release durations.

Conclusion

In otology, GCs are routinely used to treat sudden hearing loss, Meniere's disease, autoimmune inner ear diseases, and certain vestibular disorders. Despite their widespread use, GCs can cause serious systemic side effects and a localized sustained release formulation of GCs is expected to be more effective and safer for use in the ear. The ultimate goal of this study is to develop a tunable system for the delivery of glucocorticoids to the ear for the treatment of myriad diseases of the inner ear.

708 Rescue of Cisplatin Dependent Hearing Loss by an Intracochlear Drug Delivery Implant

Erik Pierstorff¹, Wanwan Yang¹, Yen-Jung Angel Chen², Federico Kalinec², William Slattery¹

¹O-Ray Pharma, Inc, ²House Research Institute

Background

Chemotherapy induced ototoxicity is damage to the inner ear caused by side effects of administered drugs. This can lead to permanent hearing loss and/or tinnitus in the patient. Some of the most common drug classes causing ototoxicity are anti-cancer therapeutics such as cisplatin. Cisplatin is considered one of the most ototoxic drugs in use, with monitored ototoxicity frequencies commonly ranging from 20-100% depending on the dosage used. The development of an otoprotective treatment to combat chemotherapy induced hearing loss would have significant impacts on patient quality of life. Various compounds have been studied and tested in animal models for protection against cisplatin mediated hearing loss. Among those with some ototoxic activities include antioxidants, sulfur containing nucleophiles, and steroids. Steroids remain attractive candidates as they are well characterized, and have been used extensively for various inner ear indications.

Methods

We previously reported our extended release steroid formulations in various dose-ranges utilizing a sustained release polymer formulation. To test their activity, sustained release steroid formulations were implanted directly into the cochleae of guinea pigs followed by a cisplatin challenge sufficient to induce hearing loss.

Results

Pre- and post- treatment otoacoustic emissions and ABRs were performed to assess hearing. In all cases, significant hearing improvement was observed in ears administered steroid implants.

Conclusion

These results demonstrate otoprotection from cisplatin ototoxicity and form the foundation for the initiation of clinical trials.

709 Administration of Glucocorticoid Attenuates Trauma-Induced Hearing Loss Associated with Intracochlear Cell Transplantation

Yi-Tsen Lin¹, Ying-Chang Lu², Chuan-Jen Hsu²
¹National Taiwan University, Yun-Lin Branch, ²National Taiwan University

Background

One of the greatest challenges in the treatment of inner ear diseases is to find a cure for hearing loss caused by the loss of cochlear hair cells or spiral ganglion neurons. Development of stem cell transplantation raises the hope for future regeneration therapy in the inner ear. However, residual hearing usually deteriorates after intracochlear cell transplantation. Application of glucocorticoid has been shown to ameliorate hearing loss resulting from the trauma of cochlear implantation in experimental animals. The purpose of this study is to investigate whether administration of glucocorticoid can protect inner ear from hearing loss resulting from the trauma associated with intracochlear cell transplantation.

Methods

Embryonic stem cells were delivered into the cochlear via the round window membrane of B6 mice. Betamethasone of either 200 µg/ml or 800 µg/ml was injected into the cochlea with the transplanted stem cells simultaneously. Auditory brainstem responses (ABRs) were measured immediately, 1 week, and 2 weeks after the cell transplantation. After 2 weeks, the distribution and survival of the embryonic stem cells were investigated by immunohistochemistry study. Terminal deoxynucleotidyl transferase dUTP nick end labeling (TUNEL) assay was used to detect the possible apoptotic event in the treated inner ears.

Results

The ABR thresholds increased immediately after the cell transplantation in both the control group and the betamethasone-treated groups, and the hearing partially recovered in the treated groups at 1 week and 2 weeks after the surgery. Simultaneous injection of 800 µg/ml betamethasone with the transplanted significantly attenuated the hearing loss resulting from the trauma associated with intracochlear cell transplantation.

Conclusion

Simultaneous administration of glucocorticoid diminishes the trauma caused by intracochlear cell transplantation. These findings might provide insight into a novel strategy for preserving the residual hearing when stem cell therapy is to be applied via the intracochlear route.

710 Identification of COCH Gene Mutation in Exon 5 of the LCCL Domain in Archived DFNA9 Temporal Bone

Joni Doherty¹, Jamie Treadway¹, Jose Fayad¹, Robert Gellibolian², Fred Linthicum, Jr.¹
¹House Research Institute, ²N-Abl Therapeutics, Inc.

Background

DFNA9 is an autosomal dominant nonsyndromic hereditary hearing loss due to heterozygous mutation in the COCH gene, encoding cochlin. Manifestations of DFNA9 include adult onset progressive sensorineural hearing loss and vestibular dysfunction. Cochlin is the most abundant protein in the inner ear. Our laboratory and others have previously described the histopathology of DFNA9 at the otopathological level. Interestingly, the late manifestations of DFNA9 include cartilage deposits in the tympanic membrane, mucosa, and ossicular joints. However, anacusis precedes the dysfunction of the ossicular chain or tympanic mobility, and patients do not typically present with a mixed hearing loss.

Methods

Extraction of genomic DNA from archived celloidin-embedded temporal bone was performed. This temporal bone was previously identified as having an LCCL domain mutation via proteomic analysis in our laboratory. Temporal bone DNA and control DNA (commercial human genomic DNA) were amplified using PCR with primers designed to flank exon 5 of the LCCL domain, spanning the region corresponding to the suspected mutation. PCR products of 396 bp amplicon length were gel purified and sequenced.

Results

Sequencing of PCR products from the DFNA9 temporal bone revealed a heterozygous single nucleotide G->A transition at residue 6328 within exon 5, which was predicted to result in an A119T (Ala to Thr) amino acid change in the cochlin protein product.

Conclusion

We have verified a mutation in the COCH gene that we previously identified at the protein level via proteomic analysis from an archived formalin fixed celloidin-embedded temporal bone. At the time this temporal bone was received, our laboratory was not routinely collecting another DNA source from donors; whereas, we now collect buccal swab samples. To our knowledge, this is the first report of an hereditary hearing loss mutation identified in archived temporal bone tissue.

711 Diagnostic Application of Targeted Exome Sequencing for Familial Nonsyndromic Hearing Loss

Byung Yoon Choi¹, Gibeum Park², Jungsoo Gim^{3,4}, Ah Reum Kim⁵, Bong Jik Kim⁵, Juyong Chung⁵, Tae-Sung Park³, Sun O Chang⁵, Seung-Ha Oh⁵, Kyu-Hee Han⁵, Woong-Yang Park²

¹Seoul National University Bundang Hospital, ²Department of Biomedical Sciences, College of Medicine, Seoul National University, ³Interdisciplinary Program for Bioinformatics, Seoul National University, ⁴Department of Statistics, College of Natural Science, Seoul National University, ⁵Department of Otolaryngology, Seoul National University

Background

Identification of causative genes for hereditary nonsyndromic hearing loss (NSHL) is important to decide treatment modalities and to counsel the patients. Because the genetic heterogeneity is extraordinarily huge in sensorineural disorders, we need to develop high-throughput diagnostic tools. To this end, we designed molecular genetic diagnosis based on targeted exome sequencing (TES) to screen all the candidate genes for NSHL.

Methods

Targeted exome capture of 80 known deafness genes and massively paralleled sequencing were done in 20 probands from families with two or more members with variable degree of hearing loss. To identify the causative mutations among variants found in TES, we filtered out the variant that were not compatible with the inheritance pattern of the family. Finally we validated all the candidate variants by Sanger sequencing. We further checked the variants if they are detected among normal hearing 80 control subjects. Genotype-phenotype correlation including configurations of audiogram and the progression pattern of hearing loss was also used.

Results

Critical mutations were identified in 11 of 20 probands of these multiplex families through NSHL80-TES. We identified damaging mutations in nine genes such as WFS1, COCH, EYA4, MYO6, GJB3, MYO6, COL11A2, MYO3A and MYO7A. Most of them are private, again confirming etiologic heterogeneity of hereditary deafness in this population. In this study, we suggested the NGS-based new diagnostic flow to identify mutations responsible for familial NSHL, which detected mutations in 55% of multiplex families with hearing loss.

Conclusion

We suggested a diagnostic flow to identify a causative mutation responsible for hearing loss. This genomic analysis procedure will enable us to evaluate causative mutation with more efficiency.

712 Differences in the Pathogenicity of the P.H723R Mutation of the Common Deafness-Associated SLC26A4 Gene in Humans and Mice

Ying-chang lu^{1,2}, Chen-Chi Wu², Ting-Hua Yang², Ying-Hung Lin², I-Shing Yu³, Shu-Wha Lin³, Qing Chang⁴, Xi Lin⁴, Jau-Min Wong¹, Chuan-Jen Hsu²

¹Institute of Biomedical Engineering, National Taiwan University, Taipei, 100, Taiwan, ²Department of Otolaryngology, National Taiwan University Hospital, Taipei, 100, Taiwan, ³Transgenic Mouse Models Core (TMMC), Division of Genomic Medicine, Research Center For Medical Excel, ⁴Department of Otolaryngology, Emory University School of Medicine, Atlanta, GA, USA

Background

Recessive SLC26A4 mutations contribute to both Pendred syndrome (PS) and nonsyndromic hearing loss (DFNB4), constituting a common cause of hereditary hearing impairment worldwide. In recent years, the understanding of the pathogenesis of PS and DFNB4 has been accelerated by various mouse models with mutations in the Slc26a4 gene, including knock-out Slc26a4^{-/-} mice, Slc26a4loop/loop mice with the p.S408F mutation, Slc26a4tm1Dontuh/tm1Dontuh mice with the c.919-A>G mutation, and conditional knock-out Tg[E];Tg[R];Slc26a4^{ΔG/ΔG} mice. However, none of these mouse models could perfectly simulate the progressive or fluctuating hearing loss in humans. In the present study, we established a knock-in mouse model with the p.H723R (c.2168A>G) mutation, a common SLC26A4 mutation in the Asian population, and then, we characterized the associated audiovestibular phenotypes as well as the inner ear pathology.

Methods

Mice homozygous for the p.H723R mutation (i.e., Slc26a4tm2Dontuh/tm2Dontuh) were generated and maintained in the C57BL/6 background. Corresponding to the human genotypes, mice with compound heterozygous mutations for p.H723R and c.919-2A>G (i.e., Slc26a4tm1Dontuh/tm2Dontuh) were also obtained. Mice were then subjected to audiological assessments, a battery of vestibular evaluations, inner ear morphological studies, and noise exposure experiments. The expression of pendrin was examined using immunolocalization; whereas the expression of Kcnj10, a gene regulated by Slc26a4 and involved in the pathogenesis of Slc26a4 mutations, was investigated using real-time PCR and Western blotting.

Results

Both Slc26a4tm2Dontuh/tm2Dontuh and Slc26a4tm1Dontuh/tm2Dontuh mice showed normal audiovestibular phenotypes and inner ear morphology, and they did not show significantly higher shifts in hearing thresholds after noise exposure than the wild-type mice. The expression of pendrin and Kcnj10 was not affected in Slc26a4tm2Dontuh/tm2Dontuh and Slc26a4tm1Dontuh/tm2Dontuh mice as compared to the wild-type mice. The results indicated that the p.H723R

allele was non-pathogenic in mice because a single p.H723R allele was sufficient to maintain normal inner ear physiology.

Conclusion

Using a genotype-driven approach, we generated a knock-in mouse model segregating the common deafness-associated SLC26A4 p.H723R mutation in humans. To our surprise, mice with the Slc26a4 p.H723R mutation had a normal audiovestibular phenotype and inner ear morphology. Because there might be differences in the pathogenicity of specific SLC26A4 mutations in humans and mice, precaution should be taken when extrapolating the results of animal studies to humans.

713 Large-Scale Application of Next Generation Sequencing Approach in Screening Mutations of Currently-Known and Candidate Human Deafness Genes in Multiple Ethnic Populations

Yongyi Yuan¹, Jingqiao Lu², Wenxue Tang², Shoeb Ahmad², Yeunjung Kim², Basilide Tea³, David Okou², N.Wendell Todd², Charles Moore², Douglas Mattox², Dai Pu¹, Xi Lin²

¹Chinese PLA General hospital, ²Emory Univ School of Medicine, ³Department of Otolaryngology, Service de otorhino-laryngologie, CHU de Cocody, BP 582 Abidjan cedex

Background

Targeted capture and sequencing of all reported human genes linked to deafness by the next-generation sequencing (NGS) method may provide a powerful tool for studying the spectrum of genetic mutations in different human ethnic populations. The uses of the NGS technology for mutation screening of deafness genes on an epidemiological scale have been hindered by (1) a bottleneck in streamlined samples processing; (2) a high per-sample cost; (3) difficulties in bioinformatic data analyses.

Methods

In order to solve these three major problems we have developed: (1) a flexible robotic process for NGS library preparation based on the Hamilton robotic liquid handling system; (2) a low-cost hybridization-based gene capture method for enriching exons of >120 genes that have been reported to cause deafness in humans and mice; (3) a bioinformatic pipeline for automatic identification of disease-causing mutations from large numbers of samples and generation of reports.

Results

The automatic library preparation has the flexibility of processing 1 to 96 samples in one run, and generated quality of Illumina libraries similar to that done manually. Our hybridization-based gene capture method achieved specificity, multiplexicity, uniformity and depth of coverage in exon captures suitable for downstream Illumina sequencing. The high coverage depth and cost benefits of our approach is applied for genetic screening of close to one thousand samples so far, including samples collected

from Asia (Han and Tibetan Chinese, Korean), Africa (Ivory Coast and Cameroon) and the United States. Samples from confirmed cases of genetic deafness, from unknown etiology but with genetic suspicion and from clinically-confirmed normal hearing subjects were tested. Preliminary data obtained found a spectrum of mutations in GJB2, SLC26A4, WFS1, DFNB59, GJB4, CDH23, KCNE1, MYO15A, KCNJ10, MYO1F, GJB3, and POU3F4 genes. Further bioinformatic data analysis is ongoing.

Conclusion

We are approaching the milestone of developing an automatic pipeline for the large-scale application of NGS for genetic screening of about 120 deafness genes for clinical applications. We will report our findings from these multi-ethnic populations in terms of the rank of most prevalent genetic mutations found, the error rates in terms of both false negatives and false positives, and confirmation studies with Sanger sequencing.

714 Loss of FGF23 Signaling Results in Mixed Hearing Loss and Middle Ear Malformation

Andrew Lysaght^{1,2}, Neil Kalwani³, Quan Yuan⁴, Paul Caruso², MeryBeth Cunnane², Beate Lanske⁴, Konstantina Stankovic^{2,3}

¹Harvard - MIT, ²Massachusetts Eye and Ear Infirmary,

³Harvard Medical School, ⁴Harvard School of Dental Medicine

Background

Fibroblast Growth Factor 23 (FGF23), a member of the FGF19 subfamily, is a circulating hormone, secreted by osteoblasts and osteocytes, which regulates renal phosphate handling. KLOTHO is a single-pass transmembrane protein that acts as a critical cofactor for FGF23 mediated signaling by increasing FGF Receptor (FGFR) affinity for FGF23, and is believed to account for FGF23's tissue specific function. KLOTHO expression has been observed in the cochlea, specifically in the stria vascularis, spiral ligament, OHCs, IHCs and SG cells. KLOTHO^{-/-} mice exhibit hearing loss, and are used as a model of age-related hearing loss. Cochlear histology in KLOTHO^{-/-} mice demonstrates no obvious morphological abnormalities and normal SG neuron densities.

Multiple hypotheses exist concerning the mechanism of hearing loss in KLOTHO^{-/-} mice; it is unclear whether or not the KLOTHO^{-/-} phenotype is independent of FGF23 signaling. Motivated by the critical role that several FGFs play in the developing auditory organ, and the potential implications of the KLOTHO^{-/-} mouse, this work sought to uncover the role FGF23 plays in the auditory system.

Methods

The physiological performance of the auditory system in FGF23^{-/-} and FGF23^{+/-} mice was assessed using ABR and DPOAE measurements. Anatomical differences were assessed via histological and morphological characterization of the bulla, ossicles and cochlea using

light microscopy and high-voltage X-ray computed tomography (micro CT).

Results

ABR measurements from FGF23^{-/-} mice demonstrated profound hearing loss across the physiological frequency range, while FGF23^{+/-} mice had statistically normal hearing below 20 kHz, and losses of up to 25 dB above 20 kHz. Similar to ABR results, DPOAE assessment of FGF23^{-/-} mice demonstrated nearly complete hearing loss, while FGF23^{+/-} mice had severe loss at the highest frequencies, and nearly normal hearing below 30 kHz.

Morphological assessment of middle ears in FGF23^{-/-} mice demonstrated cartilaginous bone and malformation of the bulla and ossicles; FGF23^{+/-} mice had near-normal morphology. The cochleae and vestibular organs of FGF23^{-/-} and FGF23^{+/-} mice appeared normal grossly, and on microscopic analysis of midmodiolar sections.

Conclusion

FGF23^{-/-} mice have profound hearing loss, and extensive middle ear malformations. FGF23^{+/-} mice have mixed hearing loss. The observed hearing phenotype does not match observations in KLOTHO^{-/-} mice, and suggests that loss of FGF23 signaling impacts the cochlea via different mechanisms than KLOTHO.

715 Interaction Between Adiponectin and Adiponectin Receptor 1 Is Associated with Age-Related Hearing Impairment

Chen-Chi Wu^{1,2}, Ching-Hui Tsai³, Juen-Haur Hwang⁴, Ying-Chang Lu^{1,5}, Yin-Hung Lin^{1,6}, Yungling Leo Lee³, Tien-Chen Liu¹, Chuan-Jen Hsu¹

¹Department of Otolaryngology, National Taiwan University Hospital, ²Department of Medical Genetics, National Taiwan University Hospital, ³Institute of Epidemiology, National Taiwan University College of Public Health, ⁴Department of Otolaryngology, Buddhist Dalin Tzu-Chi General Hospital, ⁵Institute of Biomedical Engineering, National Taiwan University, ⁶Graduate Institute of Molecular Medicine, National Taiwan University College of Medicine

Background

Age-related hearing impairment (ARHI) is a complex disease caused by an interaction between environmental and genetic factors. Recently, several studies confirmed obesity as an independent risk factor for ARHI. In our previous study investigating the underlying mechanisms, we demonstrated that plasma adiponectin might protect peripheral hearing function. It has been revealed that polymorphisms of the adiponectin gene, ADIPOQ, might affect plasma adiponectin levels; and polymorphisms of both ADIPOQ and its type 1 receptor gene, ADIPOR1, have been related to obesity-related morbidities. Hence, we postulated that genotypes of ADIPOQ and ADIPOR1 might be associated with the development of ARHI.

Methods

A total of 1682 volunteers (Han Chinese, aged 40 to 80 y) were included in the clinical analyses, and their audiological phenotypes were determined according to the Z scores converted from their original frequency-specific hearing thresholds. By using the database of Chinese Han haplotypes in International HapMap Project and NIEHS, followed by analyses with the Haploview software, 9 tagSNPs and 4 tagSNPs in ADIPOQ and ADIPOR1, respectively, were selected for genotyping. The genotypes were then correlated to the audiological phenotypes under the assumption of various inheritance models.

Results

The rs2241767 [G] allele and the rs1063539 [C] allele of ADIPOQ were significantly associated with low-tone Z scores under dominant, additive, and co-dominant models; whereas no association was identified between the ADIPOR1 variant alleles and Z scores. To explore the interaction between ADIPOQ and ADIPOR1 concerning the contribution to ARHI, we stratified the subjects according to their genotypes of the ADIPOR1 tagSNPs, and then correlated ADIPOQ genotypes with the Z scores in each stratification of subjects. Of note, the association between rs2241767 and rs1063539 of ADIPOQ and Z scores appeared to exist in subjects with certain ADIPOR1 genotypes only. These findings were then validated on haplotype analyses.

Conclusion

ADIPOQ variant alleles were associated with ARHI. In contrast, although ADIPOR1 variant alleles were not directly associated with Z scores, the association between ADIPOQ and hearing thresholds seemed to be modulated by the ADIPOR1 genotypes. In other words, the development of ARHI might result from an interaction between adiponectin and type 1 adiponectin receptor.

716 Novel Pathological Model of SYM-1 and Conductive Hearing Loss Revealed by Docking Simulation of Noggin and Heparin

Kazunori Namba¹, Sawako Masuda², Hideki Mutai¹, Hiroki Kaneko³, Tatsuo Matsunaga¹

¹National Institute of Sensory Organs, National Tokyo Medical Center, ²National Mie Hospital, ³College of Humanities and Sciences, Nihon University

Background

The access of bone morphogenetic protein (BMP) to the BMP receptors on the cell surface is regulated by its antagonist Noggin. Noggin-BMP complex associates with heparan-sulfate proteoglycans (HSPGs), a major proteoglycan on the cell surface and in extracellular matrices, and is regulated by sulfatases to control the local activity of BMPs. Mutations in NOG are associated with various autosomal dominant syndromes that are characterized by a spectrum of skeletal defects and synostoses, such as multiple synostoses syndrome (SYNS1), Teunissen-Cremers syndrome (TCS), and tarsal-carpal coalition syndrome (TCC). Proximal symphalangism (SYM1), SYNS1, and TCS are usually

associated with conductive hearing loss. It is not yet understood how different *NOG* mutations can produce this wide range of symptoms.

Methods

Genetic analysis of *NOG* gene of a family with SYM1 and conductive hearing loss was performed. To compare normal and R136C mutant Noggin structure, we generated modeling structures using crystal structure as a template. To analyze the effect of R136C on the function of Noggin, we conducted docking simulation of the Noggin and pentasaccharide analogue of heparin (used as the ligand) using AutoDock4.2.

Results

A pedigree diagnosed as SYM-1 was found to have a novel heterozygous missense mutation (p.R136C) associated with the symptoms. The position 136 was the heparin-binding site of Noggin, raising the possibility that R136C would change the binding affinity. No mutations of the heparin-binding site of Noggin have previously been reported to associate with diseases. We utilized the crystal structure of wild-type Noggin and investigated whether the p.R136C mutation altered its structure that could lead to some pathogenic effect. An *in silico* docking analysis showed that the heparin analogue appeared to associate with the putative heparin-binding site (K133-K144) of wild-type Noggin. However, one of the salt bridges between Noggin and heparin pentasaccharide disappeared following the replacement of the arginine at position 136 with a non-charged cysteine.

Conclusion

Based on our computational analyses, we predicted that the number of mutant Noggin-BMP complexes that are tethered to HSPGs on the cell surface are decreased because of the low binding affinity of the Noggin with R136C mutation to HSPGs. Reduced binding ability of the mutant Noggin to HSPGs is likely to be the cause of excess BMP signaling that ultimately resulted in PIP joint fusion and conductive hearing loss.

717 *Mcp1*-Deficient Mice Are a Model for Heritable Otitis Media

Jing Chen^{1,2}, Neil Ingham^{1,2}, Simon Clare², Claire Raisen², Ozama Ismail², Rebecca McIntyre², Gordon Dougan², David Adams², Jacqueline White², Karen Steel^{1,2}
¹King's College London, ²Wellcome Trust Sanger Institute

Background

Otitis media is a common reason for hearing loss, especially in children. Otitis media is a multifactorial disease and its pathogenesis includes environmental factors, anatomic dysmorphology and genetic predisposition. However, the reasons for the variable susceptibility to otitis media are elusive. *MCPH1* mutations cause primary microcephaly in humans. So far, no hearing impairment has been reported either in the *MCPH1* patients or mouse models with *Mcp1* deficiency.

Methods

Mcp1-deficient (*Mcp1*^{tm1a/tm1a}) mice were produced using embryonic stem cells with a targeted mutation by the Sanger Institute's Mouse Genetics Project. Auditory brainstem response (ABR) measurements were used to test the hearing. Anatomic and histological examinations were carried out to investigate the change in the middle ears. Expression of *Mcp1* was detected by using immunohistochemistry. Other phenotypes of *Mcp1*^{tm1a/tm1a} mice were examined in the standard screening of Mouse Genetics Project.

Results

Auditory brainstem response measurements revealed that *Mcp1*^{tm1a/tm1a} mice had mild to moderate hearing impairment with around 70% penetrance. We found otitis media with effusion in the hearing-impaired *Mcp1*^{tm1a/tm1a} mice. Expression of *Mcp1* in the epithelial cells of middle ear cavities supported its involvement in the development of otitis media. Other defects of *Mcp1*^{tm1a/tm1a} mice included small skull sizes, increased micronuclei in red blood cells, increased B cells and ocular abnormalities.

Conclusion

These findings not only recapitulated the defects found in other *Mcp1*-deficient mice or *MCPH1* patients, but also revealed an unexpected phenotype, otitis media with hearing impairment, which suggests *Mcp1* is a new gene underlying genetic predisposition to otitis media.

718 Targeted Exome Capture and Paired-End Massively Parallel Sequencing Reveals New Mutations for Human Hereditary Deafness in the Middle East

Zippora Brownstein¹, Amal Abu Rayyan², Daphne Karfunkel¹, Dima Dweik², Yoni Bhonker¹, Orly Yaron³, Nitzan Kol³, Adva Yehekel⁴, Lilach M. Friedman¹, Varda Oron-Karni³, Moshe Frydman^{1,5}, Noam Shomron^{3,6}, Moien Kanaan², Karen B. Avraham^{1,3}

¹Dept. of Human Molecular Genetics, Sackler Faculty Medicine, Tel Aviv Univ., Tel Aviv, Israel, ²Dept. of Biological Sciences, Bethlehem University, Bethlehem, Palestinian Authority, ³Functional Genomics Laboratory, Tel Aviv Univ., Tel Aviv, Israel, ⁴Bioinformatics Unit, Faculty of Life Sciences, Tel Aviv Univ., Tel Aviv, Israel, ⁵Sheba Medical Center, Tel Hashomer, Israel, ⁶Dept. of Cell and Developmental Biology, Sackler Faculty Medicine, Tel Aviv Univ., Tel Aviv, Israel

Background

Classic techniques such as linkage analysis and Sanger sequencing have led to the discovery of over 100 genes for deafness, a highly genetically heterogeneous disease. Nevertheless, a significant portion of hereditary hearing loss remain unsolved and many more genes remain to be discovered. This is particularly true of the Middle Eastern population, with many different ethnic groups and high rates of consanguinity. Exome capture and massively parallel sequencing can be exploited to address this challenge.

Methods

A targeted capture pool was used for identifying mutations in 284 genes, including 118 human genes, three human microRNAs, and 163 human orthologues of mouse deafness genes. The Agilent SureSelect Target Enrichment system was used for a final capture design targeting 4,475 exons of 1.86Mb. The multiplexed libraries, representing 96 Israeli Jewish and Palestinian Arab patients, were analyzed with paired-end sequencing at a read length of 2x101 bp, using the Illumina HiSeq 2000. Coordination with homozygosity mapping in consanguineous families optimized bioinformatics analysis.

Results

This method resulted in doubling the number of deafness genes in the Middle East population. Protein structure predictions were made to provide insight into deafness mechanisms. Mutations and the genes identified will be presented.

Conclusion

The discovery of novel genes will have implications not only for the Middle East, but worldwide, as many mutations first found in this region have turned out to be present in other populations. This strategy allows for improved diagnostics, in an economically and temporally feasible manner, and establishing etiologically-based genetic counseling and hearing loss management. Further gene discovery will allow for a better understanding of the mechanisms of deafness, facilitating therapeutic development.

Supported by The Hedrich Charitable Trust and NIH/NIDCD grant R01-DC011835.

719 Wbp2-Deficient Mice Show a Progressive Pattern of High-Frequency Hearing Loss

Annalisa Buniello^{1,2}, Andreea Huma², Raquel Martinez-Vega², Johanna Pass^{1,2}, Neil Ingham^{1,2}, Karen Steel^{1,2}

¹King's College London, ²Wellcome Trust Sanger Institute

Background

The *WBP2* gene encodes the WW domain-binding protein 2. *WBP2* is phosphorylated before translocating into the nucleus, where it specifically binds to the estrogen receptor α , working as a transcriptional coactivator (Dhananjayan et al., 2006). *Wbp2* knockout mice (*Wbp2^fm1a^{(EUCOMM)Wtsi}*) were screened for hearing impairment as part of the Wellcome Trust Sanger Institute Mouse Genetics Programme.

Methods

ABRs were recorded from ketamine / xylazine anaesthetised mice, aged 4, 14, 28 and 44 weeks. Immunohistochemistry on paraffin sections from five days and four weeks old mice was performed to study *Wbp2* expression in the inner ear. Middle ear dissection, inner ear clearing and scanning electron microscopy were performed on four and thirty weeks old mice to characterize the gross structure of the inner ear. For the

innervation study, we are using confocal imaging of the sensory epithelium in *Wbp2^{KO/KO}* and littermate controls at four weeks, using antibodies to CtBP2 to label pre-synaptic ribbons, to GluR2 and GluR3 AMPA subunits to label post-synaptic densities and to Neurofilament to label unmyelinated nerve fibers in the sensory epithelium.

Results

Auditory Brainstem Response measurements in *Wbp2*-deficient mice showed high-frequency hearing impairment as early as 4 weeks old at frequencies from 24 kHz and above. This hearing loss was progressive, with these thresholds becoming higher by 14 weeks and hearing impairment becoming increasingly pronounced at lower frequencies (down to 12kHz) from 28 to 44 weeks. Immunohistochemistry detected *Wbp2* expression in inner and outer hair cells of the organ of Corti and in cells of the stria vascularis, spiral ligament and spiral ganglion in control mice. No anomalies were found in the gross structure of the inner ear and the middle ear of *Wbp2^{KO/KO}* compared to controls, and Scanning Electron Microscopy showed no sign of hair cell degeneration in the organ of Corti.

We are investigating whether the *Wbp2^{KO/KO}* high frequency loss is due to a problem in the innervation to the basal turn of the cochlea that normally responds best to high frequencies. Preliminary data show swelling of afferent nerve terminals contacting the IHCs as well as an abnormal organisation of ribbon synapses at the inner hair cell membrane in *Wbp2^{KO/KO}*, and this phenotype is more pronounced in the basal region of the cochlea.

Conclusion

These experiments will help us to understand the role of *Wbp2* in ear function and to gain more insights on progressive age-related hearing loss.

720 Mislocalization of POU3F4 in the Nucleus Due to Novel Mutations in Humans and Mice

Shaked Shivatzki¹, Thomas Parzefall¹, Danielle R. Lenz¹, Daphne Karfunkel¹, Birgit Rathkolb^{2,3}, Eckhard Wolf², Sybille Sabrautski³, Martin Hrabé de Angelis³, Moshe Frydman^{1,4}, Zippora Brownstein¹, Karen B. Avraham¹

¹Dept. of Human Molecular Genetics, Sackler Faculty Medicine, Tel Aviv Univ., Tel Aviv, Israel, ²Ludwig-Maximilians-Universität, München, Germany, ³Helmholtz Zentrum München, German Research Center Environmental Health, Neuherberg, Germany, ⁴Sheba Medical Center, Tel Hashomer, Israel

Background

POU3F4 is a POU domain transcription factor that is required for hearing. In the ear, POU3F4 is essential for the mesenchymal remodeling of the bony labyrinth, and is the causative gene for DFNX2 human deafness. Ear abnormalities underlie this form of deafness and include hypoplasia of cochlear regions, reduced coiling of the cochlea, and stapes malformations. A male child of Israeli Jewish Ashkenazi descent presented with congenital profound bilateral hearing loss with a Mondini

malformation, one of the hallmarks of X-linked *POU3F4* deafness. An ENU screen led to the recovery of a mutant mouse line, *schwindel (sdl)*, exhibiting deafness and circling. Both were further studied to identify the causative mutation responsible for their hearing loss.

Methods

The patient's DNA was included in a targeted capture and exome sequencing study. Exons of 284 human genes were captured and sequenced using a 101-bp paired-end recipe to sequence 48 captured library/human DNA samples multiplexed on one lane on an Illumina HiSeq 2000 Analyzer. SNP, indel, and CNV calls were made for all samples. The founder mouse *sdl* was generated in a large-scale ENU mutagenesis program. After defining linkage to chromosome X using microsatellite markers, Sanger sequencing was used to sequence the candidate *Pou3f4* gene. Inner ears were analyzed by paint-fill, histology, scanning electron microscopy, and immunohistochemistry. COS-7 cells were transfected with the mouse mutation.

Results

Targeted capture and massively parallel sequencing identified a nonsense mutation in the human *POU3F4* gene in the child. Sanger sequencing confirmed the presence of c.C235T, predicted to lead to a stop codon, p.Q79X. Analysis of the mouse colony mating data provided evidence that the *sdl* phenotype is linked to the X chromosome, confirmed in a genome scan. Sequencing of the *Pou3f4* gene revealed c.T900A, predicted to cause a stop codon, p.C300X. The subcellular localization of the mouse mutation is damaged and the protein does not appear to be in the nucleus, as seen in transfected cells and *Pou3f4^{sdl/sdl}* ears.

Conclusion

We report novel *POU3F4* mutations in human and mouse. Massively parallel sequencing is shown to be a valid approach for identifying a mutation in a single affected child, with no family history. This approach will continue to speed up the discovery of genes and mutations involved in inner ear pathologies.

Supported by EC Eumodic 037188, The Hedrich Charitable Trust, and NIH/NIDCD R01-DC011835.

721 Gene Discovery Approaches to Characterize Molecular Mechanisms Underlying the *Brn4/Pou3f4* Mutant Phenotype

Jason Brant¹, Kyung Ahn², E Bryan Crenshaw III^{1,2}

¹Perelman School of Medicine at the University of Pennsylvania, ²Children's Hospital of Philadelphia

Background

Targeted mutagenesis of the mouse *Brn4/Pou3f4* gene generates an animal model for X linked deafness, DFNX2, that accurately recapitulates much of the phenotype observed in DFNX2 patients, including enlarged internal auditory meatus, hypoplastic cochlea and auditory nerve

anomalies (Phippard et al., J. Neurosci. 19:5980, 1999; Coate et al., Neuron, 73:49, 2012). Further characterization of the mouse mutant demonstrates that much of the *Brn4* phenotype results from dysmorphogenesis during inner ear development.

Methods

To assess the molecular changes that give rise to the mutant phenotype, we have undertaken expression profiling using microarray technology.

Results

We and our collaborators have characterized the molecular mechanisms underlying the enlarged internal auditory meatus (Ahn et al., ARO, 2009) and the auditory nerve anomalies (Coate et al., 2012). Additional gene discovery approaches are directed towards uncovering the molecular mechanisms regulating other aspects of inner ear development that are disrupted in the *Brn4* mutants. We will present our analyses of genes whose expression is altered in the mutants, as well as a more in depth analysis of the changes in the TGF β signaling pathway that affect temporal bone development.

Conclusion

These gene discovery approaches should provide additional insights into the underlying molecular mechanisms that direct the development of the inner ear.

722 Evaluation of the Pathogenicity of GJB3 and GJB6 Variants Associated with Nonsyndromic Hearing Loss

Se-Kyung Oh¹, Soo-Young Choi², Song Hee Yu¹, Chang-Jin Jeon¹, Kyu-Yup Lee³, Sang-Heun Lee³, Un-Kyung Kim¹

¹Department of Biology, Kyungpook National University, Daegu 702-701, South Korea, ²Department of Medicine, University of Pennsylvania, Philadelphia, PA, 19104, USA,

³Department of Otolaryngology, Kyungpook National University, Daegu 700-721, South Korea

Background

A number of genes responsible for hearing loss (HL) are related to ion recycling and homeostasis in the inner ear. Connexins (Cx26, Cx31 and Cx30, respectively encoded by the GJB2, GJB3 and GJB6 genes) are core components of gap junctions (GJs) in the inner ear. GJs are intercellular communication channels and an important factor that are associated with HL. To date, a molecular genetics study of GJB3 and GJB6 as a causative gene for hearing loss has not been performed in Korea. This study was therefore performed to elucidate the genetic characteristics of Korean patients with nonsyndromic sensorineural hearing loss and to determine the pathological mechanism of HL by checking for intercellular communication function of Cx30 and Cx31 variants.

Methods

The GJB3 and GJB6 coding regions were amplified by polymerase chain reaction. An ABI 3130XL DNA sequencer was used to assay the products. GJ biochemical coupling was measured using a single cell dye

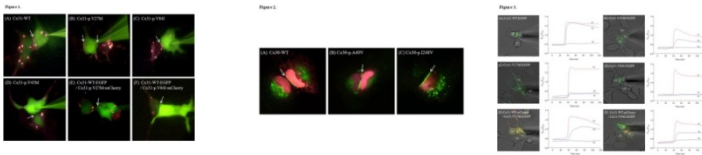
transfer assay. One of the two adjoining cells forming a GJ was performed patch-clamp using a micro electrode filled with a 1% Lucifer Yellow solution or with 0.15 mM Propidium Iodide. GJ ionic coupling was measured using a Ca²⁺ transfer assay. Transfected cells grown on cover glasses were loaded with the calcium indicator dye, fura-2 acetoxymethyl ester, and pluronic F-127. Mechanical stimulation was performed by lightly touching one cell membrane, and calcium image was analyzed using Axon Imaging Workbench software.

Results

Sequencing analysis of the GJB3 and GJB6 genes in our population revealed a total of nine variants, including four novel variants in the two genes. Three of the novel variants (Cx31-p.V27M, Cx31-p.V43M and Cx-30-p.I248V) and two previously reported variants (Cx31-p.V84I and Cx30-p.A40V) were selected for functional studies using pathogenicity prediction program and assessing for whether the mutation was located in a conserved region of the protein. The results of biochemical and ionic coupling tests showed that both the Cx31-p.V27M and Cx31-p.V84I variants did not function normally when each was expressed as a heterozygote with the wild-type Cx31.

Conclusion

This study demonstrated that two variants of Cx31 were the pathogenic mutations with dominant negative effect. This information will be valuable in understanding the pathogenic role of GJB3 and GJB6 mutations associated with HL.



723 Gap Junction Mediated miRNA Intercellular Communication

Hong-Bo Zhao¹, Yan Zhu¹, Liang Zong¹, Ru-Qiang Liang¹
¹University of Kentucky Medical Center

Background

Gap junction is an intercellular channel and possesses a relatively large pore size (1.0-1.5 nm) allowing passage of ions, cell signaling molecules, and small molecules up to 1.5 kDa. miRNAs are small in size (<1.0 nm in diameter and 3.5-8 nm in length) and are able to survive and function for several hours and even days. In this study, we investigated whether miRNA can pass through gap junction to function.

Methods

Connexin-defined cell lines, fluorescent-activated cell sorting (FACS), quantitative real-time PCR (qRT-PCR), and scrape-loading were used to measure miRNA intercellular transfer.

Results

We found that miRNA had transfer between cells in the connexin-defined cell lines but had no intercellular transfer in the connexin-null HeLa cell line. This intercellular transfer of miRNA was eliminated by gap junction channel blockers. Connexin mutations also disrupted such miRNA intercellular transfer. We also used scrape-loading of fluorescence-tagged miRNA to directly show miRNA intercellular passage through gap junctions. miRNA had good intercellular diffusion in the connexin cell lines but had no diffusion in connexin-null cell line and Cx26R75W mutant cell line. The diffusion was also blocked by gap junction channel blockers. The functional assay by miRNA reporter further shows that the transferred miRNA in neighboring cells is functional.

Conclusion

miRNA can pass through gap junctions directly. These studies also indicate that gap junction channels not only play an important role in metabolic communications but also in genetic communications between cells.

724 A Japanese Family with Autosomal Dominant Auditory Neuropathy Spectrum Disorder

Yoshihiro Noguchi¹, Ayako Nishio¹, Noriaki Takeda², Aki Shimada², Izumi Chida², Taeko Naruse³, Akinori Kimura³, Ken Kitamura¹

¹Tokyo Medical and Dental University, ²University of Tokushima School of Medicine, ³Medical Research Institute, Tokyo Medical and Dental University

Background

Auditory neuropathy spectrum disorder (ANSD) is a disorder where outer hair cell function shows normal as revealed by otoacoustic emissions (OAEs) and/or electrocochleography, but auditory brainstem responses (ABRs) is absent or severely impaired. Although the etiology of ANSD is extremely variable, approximately 40% of cases have a genetic background. Non-syndromic ANSD most commonly occurs as a sporadic or recessive pattern. In the present study, we report the clinical features of a Japanese family with autosomal dominant ANSD and the result of next-generation sequencing for the proband.

Methods

A three-generation Japanese family with autosomal dominant sensorineural hearing loss (SNHL) was studied. In 4 of the 10 family members, audiometric examinations including pure-tone audiometry, distortion product OAEs (DPOAEs), and ABRs were performed. For the measurement of ABRs, alternatively polarity clicks at the intensity of 90 and 105 dB nHL were presented as the acoustic stimuli. Whole exome sequencing was performed on the proband using the Agilent SureSelectXT Human All Exon V4+UTRs+LincRNA and HiSeq 1000 system (Illumina).

Results

The proband was a 29-year-old female who had suffered from gradually progressive, bilateral hearing loss (HL)

since the age of 20. Pure-tone audiogram showed bilateral moderate SNHL with normal DPOAEs and absent ABRs. Speech discrimination scores were 90% in the right ear and 70% in the left ear. The proband's sister (25-year-old) and mother (48-year-old) became aware of HL at the ages of 20 and 32, respectively. Audiograms showed bilateral moderate SNHL in the sister but bilateral profound SNHL in the mother. The sister showed normal DPOAEs but the mother had decreased DPOAEs. Both the two members showed absent ABRs. The proband's grandmother (71-year-old) had been aware of slight HL during the last few years. She had bilateral mild SNHL, decreased DPOAE, but normal ABRs, suggesting presbycusis. The proband's grandfather who died at the age of 62 had bilateral profound HL by the age of 60. All the affected members had no symptoms other than HL. The result of next-generation sequencing for the proband showed no variants in OTOF, PJKV and DIAPH3 genes.

Conclusion

A Japanese family with late onset, gradually progressive, autosomal dominant ANSD was shown. Further genetic studies for the other family members are needed to know the etiology of the ANSD.

725 Environmental and Lifestyle Factors Involved in Normal Hearing Function and Age-Related Hearing Loss

Giorgia Giotto¹, Dragana Vuckovic¹, Ginevra Biino², Francesco Panu³, Mario Pirastu⁴, Paolo Gasparini¹
¹Med Genet, IRCCS-Burlo Garofolo Children Hospital, Trieste Univ, Trieste, Italy, ²Institute of Molecular Genetics, Pavia, CNR, ³Unità Operativa di Otorinolaringoiatria Ospedale Brotzu, Cagliari, ⁴Institution of Population Genetics, CNR, Sassari, Italy

Background

Until now, little is known about environmental/lifestyle factors underlying normal hearing function and age-related hearing loss (ARHL). To reach this goal we decided to run an epidemiological study on hearing quantitative and qualitative traits (analysing the low, medium and high Pure Tone Average-PTA) on subjects coming from several isolated populations from Europe, Caucasus and Central Asia.

Methods

4401 subjects coming from Europe (Italy, Croatia and Ukraine), Caucasus (Armenia, Azerbaijan, Georgia) and Central Asia (Uzbekistan, Kazakhstan, Tajikistan and Kirghizstan) and ranging from 4 to 95 years were included in the analysis. Different thresholds (0.25, 0.5, 1, 2, 4, 8 kHz) as well as PTAs have been considered in the study. A medical examination has been performed in order to exclude pathological conditions related to the hearing impairment. A series of lifestyle/environmental factors have been tested including habits (smoking, drinking, etc.), diet (several foods and beverages intakes), level of education, etc. A model based on linear/logistic regression was used to fit PTAs to all the covariates (smoking, chocolate,

coffee, tea, wine, beer, dairy products, hard-liquor) including sex and age.

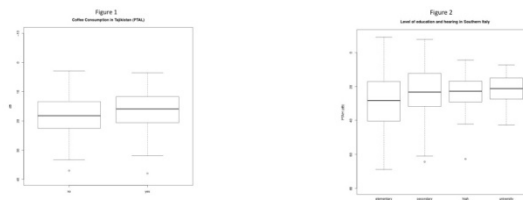
Results

As regards hearing function, our results show, for the first time, that among eight analyzed variables only coffee consumption (but not the coffee intake) was strongly associated with better normal hearing function in particular at low and high frequencies in four out of ten countries investigated ($p=0.038$ in Sardinia, 0.006 in Southern Italy, 0.017 in Azerbaijan, 0.016 in Tajikistan). As represented in the Figure 1, in the coffee-drinkers, the hearing function improves on average of 5.01 dB in Tajikistan. No association was found in the other populations, neither with other substances or coffee intake. In this light, we might suppose a connection between specific populations/communities, genes and environment.

As regards ARHL phenotype, we found an association in two Italian isolated populations ($p=0.02$ for Sardinia, and $p=0.05$ for Southern Italy), in which a lower level of education is associated to an increased susceptibility to ARHL (Figure 2).

Conclusion

These data demonstrate, for the first time, a relationship between coffee consumption and a better hearing function, and confirm the relevance of a higher education in protecting against ARHL. The understanding of lifestyle/environmental risk factors will help us in developing new preventive strategies for ARHL.



726 Linkage Studies and Whole Exome Sequencing Analysis Aimed at the Identification of New Deafness Genes

giorgia giotto¹, Flavio Faletra¹, Danilo Licastro², Diego Vozzi¹, Khalid Abdulhadi³, Savina Dipresa¹, Emmanouil Athanasakis¹, Moza Khalifa Alkowiari⁴, Ramin Badii⁴, Paolo Gasparini¹

¹Med Genet, IRCCS-Burlo Garofolo Children Hospital, Trieste Univ, Trieste, Italy, ²CBM S.c.r.l. Trieste, Italy, ³Audiology and Balance Unit, National Program for Early Detection of Hearing Loss, WH, Hamad Medical, ⁴Molecular Genetics Laboratory; Laboratory of Medicine and Pathology, Hamad Medical Corporation (HMC)

Background

Nonsyndromic Hereditary Hearing loss is a common disorder accounting for at least 60% of prelingual deafness. Despite GJB2, GJB6 and A1555G mitochondrial mutations play a major role worldwide still there is a need to search for new causative mutations/gene underlying the disease in several populations such as Italy as well as countries from the Gulf region

Methods

A combined strategy has been developed based on linkage analysis and whole exome sequencing. In particular, high density SNPs arrays (OmniExpress 700K from Illumina, Usa) have been utilized to get linkage data (even the so called "sniff" considering that families in some cases are not large enough to lead to the identification of only one locus). By this approach it is possible to define a given number of candidate loci for each family to be applied in the exome sequencing filtering phase. As regards exome sequencing they have been carried both on SOLID4 or Illumina platforms after the enrichment step carried out using Agilent technology. After library construction and sample running, single nucleotide variants (SNVs) were called by Samtools V0.1.8 and filtered comparing with dbSNP database v132 and our in-house database. Selected variants were then confirmed by direct Sanger sequencing and a complete functional prediction analysis was done using a series of tools such as PolyPhen-2, MutationTester, SIFT, ConSurf, and Condel

Results

Six Italian families (showing a dominant pattern of inheritance) and 5 Qatari ones (showing a recessive pattern of inheritance), all negatives for the presence of mutations in the most common HHL genes (i.e. GJB2, GJB6 and A1555G mitochondrial mutation) have been selected. In the Italian families our approach led to the identification of 5 new loci/gens for which Sanger sequencing confirmation is now in progress. Moreover, 4 new loci and one new possible HHL gene have been identified in Qatari families. In particular a causative mutation (c.7873 t>g leading to p.*2625Gluext*11) in BDP1 gene has been found in one family. The mutation disrupts the termination codon of the transcript resulting in an elongation of 11 residues of the BDP1 protein. Immunohistochemistry analysis carried out in the mouse inner ear showed Bdp1 expression in the mouse cochlea

Conclusion

These findings definitely increase our knowledge of new HHL genes, further confirming the importance of the combination of both strategies for disease gene identification and may suggest new targets for hearing impairment treatment and prevention

727 Auditory Rehabilitation and Genetic Analysis in Patients with BO/BOR Syndrome Showing Mixed Hearing Loss

Mee Hyun Song¹, Hwi Ram Kim², Tae Jun Kwon², In Seok Moon³, Un-Kyung Kim², Jae Young Choi³

¹Kwandong University College of Medicine, ²Kyungpook National University, ³Yonsei University College of Medicine

Background

BO/BOR syndrome is one of the most common forms of autosomal dominant syndromic hearing loss. The EYA1 gene has been identified as the causative gene of BO/BOR syndrome, and association with mutations in

SIX1 and SIX5 genes has also been reported. In this study, we have focused on the auditory manifestations and rehabilitation in patients with BO/BOR syndrome, and also performed genetic analysis for EYA1, SIX1, and SIX5 genes.

Methods

Seven families (10 patients) including one multiplex family showing hearing loss and one or more of the typical features of BOR syndrome were included. Pure tone audiometry was serially performed, and the type, onset, progressiveness of hearing loss were evaluated in each patient. The history and outcome of middle ear surgeries, hearing aids, and cochlear implantation were analyzed. The temporal bone CT and temporal MRI were analyzed. For genetic analysis, direct sequencing and deletion analysis of the EYA1 gene were performed. If mutation was not identified in the EYA1 gene, mutations in the SIX1 and SIX5 genes were subsequently analyzed. For splice site mutations, exon trapping analysis was performed.

Results

All patients presented with mixed type of hearing loss ranging from moderate to profound degree. The onset was mostly perilingual or postlingual, and five of 10 patients presented variable degrees of progressive hearing loss. All patients exhibited enlarged vestibular aqueduct of tubular type, cochlear hypoplasia, facial nerve anomaly, and ossicular abnormalities on temporal bone CT. Five of 10 patients underwent middle ear surgeries after which none of the patients experienced significant hearing gain. All of the patients used hearing aids. Cochlear implantation was performed in two patients with severe to profound hearing loss, which improved their hearing and language ability significantly. Five of 7 families presented with mutations in the EYA1 gene including 3 splice-site and 1 missense mutations as well as a whole gene deletion found in one patient. No significant genotype-phenotype correlation was demonstrated concerning auditory manifestations. No mutations in the SIX1 or SIX5 gene were found in patients without EYA1 gene mutation.

Conclusion

Four novel mutations of the EYA1 gene and one whole gene deletion were identified in patients with BO/BOR syndrome showing mixed hearing loss and inner ear anomalies. Various auditory manifestations were demonstrated but no genotype-phenotype correlation could be found. Middle ear surgeries failed to improve hearing in these patients, while cochlear implantation provided successful auditory outcome in selected patients.

728 Functional Studies of the Mouse Deafness Gene *Grxcr2*

Matthew Avenarius¹, David Kohrman¹

¹University of Michigan Medical School

Background

Mice carrying a targeted mutation of *Grxcr2* exhibit severe hearing loss that is associated with developmental defects in stereocilia bundle orientation and organization, similar to

those previously observed in mouse models of Usher Syndrome. The localization of GRXCR2 protein within stereocilia suggests that it plays an intrinsic role in influencing normal orientation, organization and cohesion of the bundles. Based on sequence analysis suggesting a putative chaperone activity of GRXCR2, together with the similarity in bundle defects observed in mouse Usher and *Grxcr2* mutants, we hypothesize that GRXCR2 normally acts to assist in appropriate folding and/or complex formation of Usher proteins and thereby regulates their localization and function.

Methods

Predicted protein structure of GRXCR2 was evaluated using the Phyre2 (Nature Protocols 4:363-371, 2009) and I-TASSER (Nature Protocols 5:725-738, 2010) platforms. Localization of Usher proteins was determined by immunocytochemistry of fixed cochlear tissue derived from *Grxcr2* mutants and controls using specific antibodies.

Results

We identified significant similarity in the predicted structure of the Cys-rich, C-terminal region of GRXCR2 and the known secondary structures of several dnaJ-related proteins, including *E. coli* dnaJ/Hsp40 and human DNAJ3. This family of proteins act as co-chaperones and provide functional specificity for heat shock protein 70 (HSP70) to control protein conformation in a variety of contexts, including proper folding of newly translated proteins, refolding of proteins after cellular stress, and modulation of protein-protein interactions (Nature Reviews-Mol. Cell Biol. 11:579-592, 2010).

In early postnatal *Grxcr2* mutants, we observed a broad stereocilia distribution of the Usher protein harmonin rather than the precise tip localization found in bundles of normal control mice. This is unlikely to be a general effect on stereocilia proteins, as in previous studies we have demonstrated intact transduction currents in OHC bundles in early postnatal *Grxcr2* mutants, indicating that assembly of the apparatus necessary for mechanotransduction such as tip links initiates normally.

Conclusion

The similarity of the C-terminal domain of GRXCR2 with Cys-rich domains present in dnaJ-related co-chaperone proteins suggests a role in regulating protein folding and/or complex formation in stereocilia. Consistent with this model, we have observed mislocalization of harmonin early in bundle development in *Grxcr2* mutant mice. We are currently testing for direct interactions of GRXCR2 with harmonin and the localization of other Usher proteins in mutant stereocilia.

729 Intra-Familial Locus Heterogeneity Confounds Deafness Gene Identification

Atteeq Rehman¹, Shaheen Khan², Meghan Drummond¹, Robert Morell¹, Zubair Ahmed³, Rachel Fisher⁴, Karen Friderici⁴, Sheikh Riazuddin², Thomas Friedman¹, Ellen Wilch⁴

¹Laboratory of Molecular Genetics, NIDCD, Rockville, Maryland, ²Allama Iqbal Medical College, Lahore 53700, Pakistan, ³Division of Pediatric Ophthalmology, Cincinnati Children's Hospital Medical Center, Cincinnati, Ohio, ⁴Department of Microbiology & Molecular Genetics, Michigan State University, East Lansing, Michigan

Background

Pedigree-based linkage analysis and homozygosity mapping have been used to genetically map the chromosomal locations of human hereditary recessive deafness loci in consanguineous pedigrees and community isolates. Recessive nonsyndromic deafness is both highly genetically heterogeneous and not rare. Although most, if not all, DFNB loci have been identified in pedigrees where deafness segregates as a monogenic trait, the population incidence and extreme heterogeneity suggest that some pedigrees may be segregating mutant alleles of more than one deafness gene. Pedigrees that fail to yield statistically significant evidence of genetic linkage may do so because two or more non-allelic pathogenic mutations are segregating within the same pedigree.

Methods

We reanalyzed consanguineous pedigrees from Pakistan in which recessive nonsyndromic deafness was segregating in multiple sibships. Each of these pedigrees failed to show evidence of linkage to a single locus in genome-wide screens with 388 STR markers. To address the possibility of locus heterogeneity, we Sanger-sequenced several known deafness genes in at least one affected individual from each sibship. Also, in a large North American kindred with multiple sibships segregating deafness, we used Sanger-sequencing, genotyping by restriction enzyme assay, or array CGH to identify multiple non-allelic mutations.

Results

Intra-familial locus heterogeneity was documented in six deafness pedigrees. In five of the pedigrees, two non-allelic pathogenic mutations are segregating. All affected siblings in each sibship are homozygous by virtue of identity by descent for one of these two mutations; however, closely related sibships in each pedigree are segregating pathogenic alleles of different genes. In each pedigree, homozygous pathogenic alleles of *GJB2* are responsible for deafness of some individuals while other deaf individuals in the same pedigree are homozygous for pathogenic alleles of *SLC26A4*, *HGF*, or *MYO7A*. In the North American pedigree, two recessive DFNB1 mutations, two recessive mutations of *SLC26A4*, and a novel deletion of *POU3F4* segregate in this community isolate.

Conclusion

Intra-familial locus heterogeneity in hearing loss is uncommon or perhaps largely unpublished, but should no longer be surprising, because congenital hearing loss is not rare, a significant proportion is genetic, and many genes cause monogenic hearing loss. Unrecognized locus heterogeneity can confound deafness gene identification by linkage analysis or homozygosity mapping when all affected and unaffected individuals in different sibships are included in the analysis. As whole-exome sequencing becomes established in clinical practice, it is important to consider the potential for genetic heterogeneity in extended families.

730 Foxo3 Protects Hearing Through Synapse Maintenance

Felicia Gilels¹, Irfan Rahman¹, Patricia White¹

¹University of Rochester School of Medicine and Dentistry

Background

Foxo3 is a member of the Foxo winged-helix transcription factor family. Foxo3 mediates oxidative stress responses, apoptosis, and cell cycle withdrawal in many systems. Foxo3 can be activated by excitotoxicity or mechanical stress. Human Foxo3 alleles are associated with extreme longevity and with female infertility. We have discovered that Foxo3 is expressed in cochlear cells, and we hypothesize that it functions to preserve hearing. Previously, we showed that loss of Foxo3 causes high-frequency hearing dysfunction with age, and here we have characterized the mechanism of this hearing loss.

Methods

All experiments were conducted on Foxo3 wild-type and knock-out littermates, derived from FVB/n, at two and four months of age. Immunohistochemistry was used to analyze Foxo3 expression in the sensory region of the ear and to detect hair cells and neurons for subsequent quantification. Auditory function was assessed with Auditory Brainstem Responses (ABR) and Distortion Product Otoacoustic Emissions (DPOAE). Ultrastructural analysis was performed on the 32-kHz cochlear turn isolated from both wild-type and Foxo3-KO animals at four months of age.

Results

Foxo3-KO mice develop hearing loss at 24 and 32 kHz by four months of age, compared to their wild-type counterparts. Outer hair cell function, assessed by DPOAE amplitudes at the same frequencies, appears unaffected. Foxo3-KOs also have similar numbers of hair cells compared to wild-type littermates. Moreover, spiral ganglion neurons are still present in the Foxo3-KO in the 32-kHz cochlear turn. We find, however, that synapses between spiral ganglion neurons and inner hair cells are dysmorphic, with increased gaps, reduced post-synaptic densities and neurite beading.

Conclusion

We conclude that Foxo3 preserves hearing with age by maintaining synapse integrity. We speculate that the

synapse disruption exhibited in the four month-old Foxo3-KO mouse is due to an intrinsic sensitivity to excitotoxicity. Future research will address the mechanism of Foxo3's role in noise damage to the cochlea.

731 Mapping of an Otitis Media Gene Within an Indigenous Population

Regie Lyn Santos-Cortez¹, Ma. Rina Reyes-Quintos², Eva Maria Cutiongco-de la Paz³, John Belmont¹, Suzanne Leal¹, Charlotte Chiong², Generoso Abes²

¹Baylor College of Medicine, ²Philippine National Ear Institute, ³Institute of Human Genetics, UP Manila - NIH

Background

Otitis media (OM) affects a large proportion of the global population, causing significant mortality and morbidity, and is a major cause of hearing loss across all age groups. It incurs a huge cost to health systems from repeated consults and antibiotic prescription. Despite vaccination regimens and specific treatment guidelines for different forms of OM, due to changes in pathogen patterns and increased antibiotic resistance, OM remains an important public health problem. Chronic OM or recurrent/persistent OM/middle ear effusion may require surgical intervention and can result in permanent hearing impairment which influences a person's communicative skills, cognitive abilities and psychosocial well-being. Strong evidence for a genetic basis of OM susceptibility exists, but only a few genes have been associated with OM in humans, and the causal variants are yet to be identified.

Methods

A single large pedigree from an indigenous, intermarried population with a high prevalence of OM has been ascertained. Out of 49 pedigree members who provided DNA, 42 DNA samples were successfully genotyped using the exome chip. Minimal pedigree errors were detected using PedCheck for Mendelian inconsistencies and MERLIN for possible genotyping errors. Two-point and multipoint linkage analyses were performed using Superlink, and haplotypes were reconstructed using Allegro software.

Results

For the initial linkage analyses, we used 7,601 common variants from the exome chip which were informative for the pedigree. Based on an autosomal dominant model of inheritance with reduced penetrance (70%), the maximum two-point LOD score for the entire pedigree was 1.54 at chromosome 5p, and 1.43 at the 10q region. When affecteds-only analysis was performed at equal allele frequencies, the maximum LOD scores slightly increased to 1.58 at 5p and 1.56 at 10q. For multipoint analysis, rare variants within the 5p and 10q regions that are informative for the pedigree were included. Using affecteds-only, the maximum multipoint LOD score at 5p is lower at 2.77, while at the 10q region the maximum multipoint LOD score is statistically significant at 3.56. Linkage heterogeneity within the pedigree was detected.

Conclusion

DNA samples from affected individuals have been submitted for exome sequencing, which will lead us to identification of genetic variants that cause OM susceptibility. The identification of genetic variants that confer susceptibility to OM has the potential to increase our understanding of pathophysiology, which can then lead to improvements in preventive and therapeutic strategies for OM.

732 Cell Type-Specific Studies of the Mouse Inner Ear – Challenges and Solutions

Lorna Silipino¹, Manan Shah¹, Manoj Racherla¹, Rani Elkon², David Eisenman¹, Scott Strome¹, **Ronna Hertzano¹**

¹University of Maryland, ²The Netherlands Cancer Institute

Background

The auditory and vestibular sensory organs consist of complex epithelia that are composed of multiple cell types. Fluorescent Activated Cell Sorting (FACS) has become an increasingly popular tool to study the development of the mouse inner ear, isolate specific cell populations for subsequent applications, or study the downstream effects of cell type-specific mutations. In this presentation we describe OTO-SORT, a protocol that can be used to isolate the sensory epithelium, neurons, vascular endothelium and mesenchyme from the auditory and vestibular systems, as well as combinations of OTO-SORT with transgenic mice expressing cell type-specific fluorescent proteins. We address the technical aspects of the process in a stepwise fashion, starting from the cell dissociation to challenges and solutions for downstream applications.

Methods

Tissue is dissected from mice up to postnatal day 5, incubated in thermolysin and then dissociated in Accutase enzyme cell detachment medium, followed by a mechanical disruption using a 23G blunt ended needle connected to a 1ml syringe. The reaction is stopped by adding an equal volume of complete media. Cells are passed through a 40- μ m cell strainer and washed in FACS buffer. The dissociated cells are then stained with CD326-APC, CD49f-alexa488 and CD34-PE prior to sorting.

Results

The auditory and vestibular epithelia can be dissociated with minimal induction of cell death. As little as one ear can be used for isolation of hair cells, for example, with a yield that can reach up to 1000 cells per auditory or vestibular epithelium. Tissue can be dissected and successfully sorted up to 2 days following dissection. Cell type-specific gene expression analysis can identify transcription factors and miRNAs that determine cell fate.

Conclusion

FACS can be applied to study inner ear development in embryonic and early postnatal stages even when starting from single epithelia. Using a combination of antibodies for cell surface markers and mice that express fluorescent

molecules in a cell type-specific pattern can enhance the ability to sort unique cell populations. Generating antibodies for the extracellular domain of cell type-specific transmembrane proteins will simplify FACS of the inner ear and obviate the need to use mice expressing cell type-specific markers.

733 Molecular Network Analysis of Hearing Loss and Hypogonadism

Eleni Asimacopoulos^{1,2}, Joseph Adams^{1,2}, Peter Sadow³, Konstantina Stankovic^{1,2}

¹Eaton-Peabody Laboratory, Massachusetts Eye and Ear Infirmary, ²Department of Otolaryngology, Harvard Medical School, ³Massachusetts General Hospital, Department of Pathology

Background

Hypogonadism and hearing loss are conditions that have significant clinical burdens. They represent a diverse range of clinical presentations and pathological processes. While they are both functionally distinct entities, the gonadal axis and auditory pathway have similar embryological origins. Syndromic forms of hypogonadism with hearing loss are well documented. However, identification of specific genes involved in both non-syndromic hearing loss and hypogonadism have yet to be elucidated. The aim of this study is to identify key molecular regulators of hypogonadism and hearing loss through a comprehensive bioinformatic analysis of genes common to both diseases.

Methods

A search of the Online Mendelian Inheritance in Man (OMIM) database was performed to identify genes associated with hypogonadism. All entries including the term *hearing loss* were compiled into a dataset. Two network analyses were performed using Ingenuity Pathway Analysis software (IPA; Ingenuity Systems, Redwood City, California) – one focused on direct connections among genes, and another, inclusive of direct and indirect connection. The most interconnected, i.e. nodal molecules, of each networks were identified. Bioinformatic results were validated by immunohistochemistry applied to cross-sections from human cochleae and gonadal tissue (male and female).

Results

The OMIM search identified a total of 59 genes associated with both hypogonadism and hearing loss. The IPA analyses yielded five highly statistically significant networks. The transcription factor hepatocyte nuclear factor-4 α (HNF4 α) emerged as a key nodal molecule in both networks. This bioinformatic result was validated by identifying, via immunohistochemistry, specific expression of HNF4 α in the human reproductive tract and inner ear.

Conclusion

This study identifies key nodal molecules that are likely to play significant roles in both hypogonadism and hearing loss. We highlight HNF4 α ; as a potential novel regulator of both the gonadal axis and the auditory system. The

precise role of HNF4 α ; in these tissues requires further study.

734 Acoustic Trauma Changes the Expression of Serotonergic Receptors in the Inferior Colliculus

Adam Smith¹, Jae Hyun Kwon¹, Marco Navarro², Laura Hurley¹

¹Indiana University, ²Saint Louis University

Background

Multiple studies have demonstrated that an important neuromodulatory network in the inferior colliculus (IC) is the serotonergic system, which modulates neural activity in response to acoustic stimuli. In this work, we studied the effects of acoustic trauma on the expression of serotonergic and GABAergic receptor genes in order to determine how acoustic insult to the inferior colliculus impacts the neuromodulatory network.

Methods

Individual male mice (CBA/J strain) at 11-15 weeks of age were used for these experiments. The auditory brainstem response (ABR) was measured at four frequencies (8, 12, 16, and 20 kHz) to establish hearing thresholds. Sham surgical controls were then left under anesthesia for three hours while trauma individuals were anesthetized and exposed to a 10 kHz pure tone at 116 dB for three hours. After a one month recovery period, the auditory brainstem response was measured again to determine hearing loss and the individual was sacrificed. The IC was then dissected and processed for real-time quantitative PCR (RT-qPCR). The expression of the following genes was measured relative to β -actin: 5Htr1B, 5Htr1A, 5Htr2A, 5Htr3A, and GABArA.

Results

ABR measures indicated that the trauma paradigm used caused severe hearing loss at frequencies above the trauma stimulus in individuals after a month of recovery time (threshold shifts of 40dB or greater at 12, 16 and 20 kHz). Significant changes between sham surgical controls and traumatized individuals were found in the expression of two genes following acoustic trauma. As other researchers have reported, expression of the GABArA gene was downregulated 60% on average. In contrast, the 5Htr1B gene was upregulated 3-6 fold in traumatized individuals. This results in a mean 4.6-fold relative shift of GABArA to 5Htr1B between control and trauma individuals. The other genes measured were not significantly different between sham controls and trauma.

Conclusion

Since the 5-HT1B receptor may act in the IC by decreasing GABA release, our gene expression results suggest that increased 5-HT1B expression contributes to a general downregulation of inhibitory mechanisms following acoustic trauma.

735 Conditional Expression of Microbial Rhodopsins in Mouse Cochlear Hair Cells and Supporting Cells

*Marcia Mellado Lagarde^{1,2}, Victoria Lukashkina², Ian Russell², Jian Zuo¹

¹St Jude Children's Research Hospital, ²University of Brighton

Microbial rhodopsins are light-gated ion channels that can be expressed in excitable mammalian cells to modify their activity. ChR2(H134R) is a channel rhodopsin variant that produces reversible membrane depolarization due to cation influx in presence of blue light and can activate neurons. Archaelhodopsin-3, an outward proton pump, and Halorhodopsin, an inward chloride pump, under yellow light produce membrane hyperpolarization and neuronal silencing. Recently, the Allen Institute for Brain Sciences has created floxed mice of these three variants. Cre-mediated deletion of a stop cassette in these mice produces expression in specific neuronal populations and successful modulation of their activity. We have crossed these floxed rhodopsin mice with CreER mouse lines that are specifically expressed in different cell types of the postnatal cochlea. PrestinCreERT2 and Fgfr3iCreER drive specific expression of rhodopsins in outer hair cells and supporting cells, respectively, when induced with tamoxifen (3mg/40g bodyweight) once a day at postnatal day (P) 6 and P7. Auditory brainstem responses measured in these mice show that hearing is largely not affected by microbial rhodopsin expression in cochlear cells. The models driven by PrestinCreERT2 can be used to alter (silence or augment) electromotility of isolated outer hair cells with light, overriding the membrane potential changes that trigger this response. In vivo, light stimulation may be used to modulate outer hair cell-dependent amplification at specific locations along the cochlea to determine the place of generation of the peak of sound-driven travelling waves. Supported by: Wellcome Trust Fellowship (MML), NIH, ALSAC and Hartwell Foundation.

736 In Vivo Visualization of Endolymphatic Hydrops Using Optical Coherence Tomography (OCT)

Tatsunori Sakamoto¹, Yosuke Tona¹, Takayuki Nakagawa¹, Juichi Ito¹

¹Kyoto University

Background

Endolymphatic hydrops has been believed as the most important feature for the pathogenesis of Meniere's disease. However, its dynamic pathology is not well understood due to the lack of in vivo non-invasive testing tools for the inside morphology of inner ears in animals and humans.

Optical Coherence Tomography (OCT) is a relatively new imaging modality that utilizes near infra-red light to obtain cross sectional images of opaque biological tissues. OCT has already been used as a diagnostic imaging tool in ophthalmology and coronary vessels.

In this study, we demonstrate that OCT is capable to visualize inner ear structure of endolymphatic hydrops

model mice in vivo, and discuss the possibility of OCT as an in vivo diagnostic tool for inner ear disorders.

Methods

Eleven week-old mice with targeted disruption of *Slc26a4* (formerly known as *Pendrin* or *Pds*) and their littermates were used as experimental animals, because homozygotes for that gene are known to develop extensive dilatation of the scala media (Everett, 2001; Wangemann, 2009). To test the hearing function, auditory brainstem responses (ABRs) were recorded at 8, 16, 32 kHz. On the following day, each animal was anesthetized and the left bulla was removed to expose bony contour of the left cochlea. The animal was placed to obtain the optical sections that include the apex and the round window niche, then a series of cross sectional images was obtained by the OCT (OCS-1300SS, Thorlabs Inc., NJ). Then, animals were intracardially perfused with PBS followed by 4% paraformaldehyde (PFA), temporal bones were excised, inner ears were re-fixed by cochlear perfusion, and postfixed for more than 4 h. Hematoxylin and eosin staining of 10 μm -thick frozen sections were used for morphological evaluations.

Results

Homo mice showed profound hearing impairment, and hetero and wild type (wt) mice were normal in hearing. OCT images of hetero and wt mice cochlea revealed the Reissner's membrane at normal position. While, OCT images of homo mice revealed limited number of cochlear turns, and the Reissner's membrane close to the inner wall of the cochlea indicating severe dilatation of the scala media. These findings were consistent with histological study.

Conclusion

OCT is capable to visualize morphological features in the inner ear of live animals. OCT should provide diagnostic information of inner ear diseases in vivo.

737 Evaluation of the Internal Structure of the Normal and Pathological Guinea Pig Cochleae Using Optical Coherence

Tomography

Akinobu Kakigi¹, Yuya Takubo¹, Naoya Egami¹, Akinori Kashio¹, Munetaka Ushio¹, Takashi Sakamoto¹, Shinji Yamashita¹, Tatsuya Yamasoba¹

¹The University of Tokyo

Background

Structural observation of cochlea has primarily been limited to histological methods, which require chemical fixation followed by dissection of the tissues or embedment in mold such as paraffin and sectioning. It is, however, well known that these preparations of tissue samples introduce significant changes in tissue integrity and organization, which thus may induce misinterpretation, limiting the generality and overall value of the results. To innovate the approaches to visualize the internal structure of the cochlea, an emerging noninvasive imaging modality of optical coherence tomography (OCT) has been applied.

Methods

20 Hartley guinea pigs were used and allocated into the following four groups, each consisting of five animals. 1) Normal control group. 2) Endolymphatic hydrops group: ears with the electro-cauterization of the endolymphatic sac and 4-week feeding. 3) Kanamycin sulfate-ethacrynic acid group: administration in combination of kanamycin sulfate and ethacrynic acid and 2-day feeding. 4) Streptomycin sulfate group: ears with perilymphatic perfusion with 20% streptomycin sulfate and 4-month feeding.

To observe the cochleae with OCT, we obtained the both temporal bones immediately following fixation and kept them in 10% formalin solution for 1 week. Subsequently, the specimens underwent decalcification in EDTA for 14 days. Then we obtained images of the cochleae by using Santec OCT system (Santec Co., Aichi, Japan). After obtaining OCT images, the temporal bones were dehydrated in increasing concentrations of alcohol, embedded in paraffin, and cut serially at 6 μm in the plane parallel to the modiolus. The sections were stained with hematoxylin and eosin and observed under a light microscope.

Results

In this OCT study, we visualized the internal structures of the organ of Corti, Reissner's membrane, and lateral wall in the normal and pathological ear. OCT images of normal and pathological cochleae did not exhibit artifacts observed in HE specimens that were induced during histological preparations. OCT could demonstrate endolymphatic hydrops, striae atrophy, and the damage of the organ of Corti, shown as the distention of the Reissner's membrane, thinning of the lateral wall, and flattening of the organ of Corti, respectively.

Conclusion

By decalcifying the bony wall of the cochlea, we could clearly and widely visualize the internal structures of the normal and pathological cochleae. These OCT images did not exhibit artifacts observed in HE specimens. These results indicate that observing the decalcified cochlea by using OCT would be of great value of examining the cochlear pathology, prior to or without histological examination.

738 The Limited Use of Micro-CT in Cochlear Imaging of Rat

Chul-Hee Choi¹

¹Catholic University of Daegu

Background

After the clinical computed tomography (CT) was first developed in 1967 by G. Hounsfield, x-ray CT has been widely used for diagnosis in biomedical fields. X-ray CT is a medical imaging method using tomography created by digital geometry processing to generate a three dimensional image of the inside of an object. The use of x-ray CT has increased dramatically over the last two decades in many countries and has been applied to

various organs such as brain, lungs, pulmonary angiogram, cardiac, abdominal and pelvic, and extremities. The use of x-ray micro CT on the ear has been mainly focused on the outer and middle ears. The objective of this study is to investigate the degree of visualization for the macro-, micro-, and nano- structures of the cochlea with x-ray micro-CT based on a cone-beam geometry for rats.

Methods

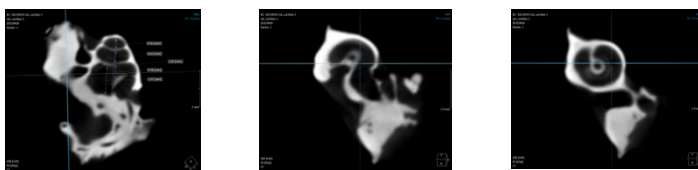
Before obtaining the visual images, the hearing thresholds were obtained with auditory brainstem responses (ABR). The entire experiments for visual images with x-ray micro CT were performed at Wonkwang University. X-ray micro-CT based on a cone-beam geometry for a small animal was used for examining cochlear image of rats. The micro-CT was mainly composed of an x-ray tube with tungsten target, a sample holder made from plastic of 2 mm thick, and a digital detector of CMOS (Complementary Metal Oxide Semiconductor)

Results

X-ray micro CT provided a clear depiction of the basal, middle, and apical cochlear turns. X-ray micro CT allows visualizing the macro-structures of the cochlea. However, it did not well depict the micro- and nano-structures of the cochlea.

Conclusion

X-ray micro CT provided a clear depiction of the basal, middle, and apical cochlear turns. X-ray micro CT allows visualizing the macro-structures of the cochlea. However, it did not well depict the micro- and nano-structures of the cochlea. To visualize the micro- and nano-structures of the cochlea, optimal parameter values of x-ray micro CT should be identified. In addition, many factors such as signal-to-noise-ratio, resolution, image averaging, pixel, pixel number, pixel value, exposure time, and binning should be properly considered.



739 Two Photon Microscopy of the Mouse Cochlea in Situ for Cellular Diagnosis

Xin Yang¹, Ye Pu¹, Chia-Lung Hsieh¹, Cheng Ai Ong², Demetri Psaltis¹, **Konstantina Stankovic**²

¹École Polytechnique Fédérale de Lausanne,

²Massachusetts Eye and Ear Infirmary, Harvard Medical School

Background

Sensorineural hearing loss is the most common type of hearing loss worldwide yet the underlying cause is typically unknown because the inner ear cannot be biopsied today without destroying hearing, and intracochlear cells have not been imaged with resolution sufficient to establish diagnosis. Intracochlear imaging has been technologically

challenging because of the cochlea's small size and encasement in bone.

Methods

Six week old CBA/CaJ mice were exposed to an octave band noise of 8-16 kHz at 106 dB SPL for 2h, which produced permanent cellular damage. Unexposed age- and sex-matched mice served as controls. The cochleae were extracted 3 weeks after noise exposure, and imaged in situ, through the intact round window, after intracaradiac perfusion with 4% paraformaldehyde. A separate group of unfixed cochleae were also imaged. Cochlear imaging was performed with two-photon excitation fluorescence (TPEF) microscopy, one-photon excitation fluorescence (OPEF) microscopy, and wide-field transmission microscopy.

Results

We found that the TPEF yielded clear advantages over OPEF and wide-field transmission microscopy. Our experiments revealed fine cellular structure of the hair cells, and allowed morphological distinction between healthy and noise-damaged organs of Corti. Furthermore, cochlear neurons were imaged through the intact bone. The intensity of TPEF signal was brighter in the freshly harvested, unfixed samples than in the fixed samples. The detected TPEF signal coincided with the peak of emission of flavin adenine dinucleotide (FAD), which is a major endogenous fluorophore in the inner ear. Our results, combined with the fact that the sensory epithelium of the inner ear has one of the highest tissue concentrations of FAD known, strongly motivate future development of TPEF-based microendoscopy for cellular diagnosis of sensorineural hearing loss.

Conclusion

Our results demonstrate that the round window provides a useful access to the cochlea through the middle ear, and they motivate future development of new and efficient diagnostic tool based on two-photon micro-endoscopy. The use of TPEF eliminates the need for exogenous labeling and provides the maximum non-invasiveness in the process.

740 Variations in Microanatomy of the Human Cochlea

Ersin Avci¹, Tim Nauwelaers², Thomas Lenarz¹, Volkmar Hamacher², Andrej Kral¹

¹Medizinische Hochschule Hannover, ²Advanced Bionics

Background

The human cochlea shows considerable interindividual variability in size and morphology. For development of atraumatic CI electrodes details of variability of human anatomy are required with high precision. For this purpose, X-ray microtomography (μ CT) was used. This imaging technique allows for non-invasive high resolution visualization with almost histological quality of the cochlear structure. The obtained data were imaged and dimensions of the scala tympani were determined.

Methods

From fresh frozen temporal bones, blocks of approximately 3, 5 x 3, 5 cm were cut out around the cochlea. In order to visualize the soft tissues in the cochlea, the cochlear fluid was gently removed. The bones were scanned using a Skyscan 1173 machine (40-130kV source, 5Mp, 12 bit CCD sensor), resulting in images with pixel size varying from 8 -17 μm .

Materialise MIMICS software was used to segment out the scala tympani (ST) and Rosenthal's canal from the obtained μCT images. A 3-D model of the segmented area was generated. To compare multiple cochlear dimensions, the centers of the round window were merged, and the cochlear coordinate system was applied for all cochleae. Cross sectional images were taken perpendicular to the centerline of the ST. The 2-D images were exported to Matlab and analyzed by a custom-made software.

Results

Comparison of different ST showed a large variability in the cross sectional diameter (CSD), vertical layout, and the width and height of the ST. The CSD of the ST reaches a maximum within the first 2 mm and then overall decreases towards the apex. Relative standard deviation of the CSD are between 7.5 and 16.5 %. In general, the mid-scala and modialar region of the ST contain largest surface area, laterally, the ST surface area diminishes due to the decrease in height.

There was significant variability in wrapping and vertical lay-out between the ST: in Z direction, dips were observed regularly between 95 and 130 degrees. A typical incline was observed between 245 and 285 degrees. The Rosenthal's canal extended up till 460 to 585 degrees.

Conclusion

We segmented the ST and measured the internal dimensions using micro-computed tomography. We observed a large dimensional variability between different ST. These differences could have large implications in the design approach of CI arrays especially towards their capability to preserve residual hearing during insertion of the CI electrode array.

[741] Quantitative Polarized Light Microscopy of Unstained Mammalian Cochlear Sections

Neil Kalwani^{1,2}, Cheng Ai Ong^{1,2}, Andrew Lysaght^{2,3}, Simon Haward^{3,4}, Gareth McKinley³, Konstantina Stankovic^{1,2}

¹Harvard Medical School, ²Massachusetts Eye and Ear Infirmary, ³Massachusetts Institute of Technology,

⁴Universidade do Porto

Background

Hearing loss is the most common sensory deficit in the world, and it most frequently originates in the inner ear. Yet, the inner ear has been difficult to access for diagnosis because of its small size, delicate nature, complex 3D anatomy, and encasement in the densest bone in the body. Evolving optical methods are promising to afford cellular diagnosis of pathologic changes in the inner ear. To appropriately interpret results from these emerging

technologies, it is important to characterize optical properties of cochlear tissues. Quantitative polarized light microscopy (qPLM), a technique that allows for quantitative determination of sample retardance and optic axis orientations, has not been applied to the cochlea before.

Methods

Unstained cochlear sections from C57BL/6J (n=3) and CBA/CaJ (n=3) mice, common animal models of human hearing loss, were prepared. Pseudocolor retardance magnitude and orientation images of the sections were captured using the Abrio Birefringence Imaging System. Additional sections were immunolabeled for collagen type II and myelin basic protein.

Results

qPLM of cochlear sections reveals intricately detailed networks of fiber tracts that correspond to collagen fibrils and myelinated neuronal processes. The retardance of the otic capsule (C57BL/6J = 1.36 ± 0.10 nm, CBA/CaJ = 1.56 ± 0.38 nm), the spiral ligament (C57BL/6J = 0.88 ± 0.11 nm, CBA/CaJ = 1.54 ± 0.07 nm), and the basilar membrane (C57BL/6J = 5.03 ± 0.47 nm, CBA/CaJ = 5.07 ± 0.26 nm) is substantially higher than the retardance of other cochlear structures. The retardance of the spiral ligament and the basilar membrane decreases from the cochlear base to the apex, compared to the more uniform retardance of other structures.

Conclusion

qPLM has important advantages over immunohistochemistry in evaluating the organization of collagen fibrils and myelinated neuronal processes because qPLM provides detailed qualitative and quantitative information on unstained fiber networks. Our results strongly motivate the future application of polarization-sensitive optical coherence tomography and similar imaging technologies to the human inner ear in vivo.

[742] Intravital Calcium Imaging of Cochlear Hair Cells

Yu Matsumoto^{1,2}, Shotaro Karino¹, Shigeyuki Namiki³, Kenzo Hirose³, Kazunori Kataoka^{2,4}, Tatsuya Yamasoba¹

¹Department of Otorhinolaryngology and Head and Neck Surgery, The University of Tokyo, ²Division of Clinical Biotechnology, Graduate School of Medicine, The

University of Tokyo, ³Department of Neurobiology, Graduate School of Medicine, The University of Tokyo,

⁴Department of Materials Engineering, Graduate School of Engineering, The University of Tokyo

Background

In vivo imaging has drawn much attention in recent years, as it can elucidate the complex biological and pathological events within a living animal. Although histological examination of excised tissues has long served as a fundamental approach for tissue analysis, intravital confocal microscopy provides instant histopathology at the cellular and subcellular level. Therefore, it is considered

ideal for investigating dynamic events involved. In this study, we examine the development and application of intravital confocal microscopy for calcium imaging of cochlear hair cells upon sound stimulation.

Methods

Adult guinea pig was anesthetized, and apical turn of the cochlea was surgically exposed via ventral approach, leaving tympanic membrane and auditory ossicles intact. A membrane-permeant green-fluorescent calcium indicator, Fluo-4 AM, was applied for 20 minutes, and then removed to fill the middle ear with air. Fluorescent images were obtained before, during, and after sound stimulation. All picture/movie acquisitions were performed using a Nikon A1R confocal laser scanning microscope system attached to an upright ECLIPSE Ni equipped with a x10, 0.3 numerical aperture, 17.3 mm working distance objective. The A1R incorporates both a conventional galvano scanner and a high-speed resonant scanner together. The resonant scanner allows an acquisition speed of 30 frames per second while maintaining high resolution of 512 x 512 scanned points. Fluo4-AM was excited with a 488 nm argon laser, and emission was detected through a 525/50 nm band pass filter.

Results

Inner hair cells, outer hair cells, and supporting cells were all clearly identified, indicating successful loading of Fluo-4 AM dye. Increased fluorescence intensity of the hair cells was observed upon sound stimulation.

Conclusion

We have demonstrated a technique to capture the image of dynamic fluorescent changes in the sound-stimulated cochlear hair cells in living guinea pigs. Although apical opening is necessary for visualization, the preparation well preserves physiological hearing functions and conditions such as sound conduction, innervation, blood supply, and body temperature. Our technique offers opportunities to investigate hair cell transduction of living and hearing animals in both spatial and temporal resolution.

[743] Phosphatidylcholine Species Localization in the Mouse Inner Ear by Mass Microscopy

Yoshinori Takizawa¹, Kunihiro Mizuta¹, Kenichi Sugiyama¹, Takahiro Hayasaka¹, Hiroshi Nakanishi¹, Jun Okamura¹, Hiroyuki Mineta¹, Mitsutoshi Setou¹
¹Hamamatsu University School of Medicine

Background

We recently developed a mass microscope consisting of a mass spectrometry imager with high spatial resolution equipped with an atmospheric pressure matrix-assisted laser desorption/ionization and quadrupole ion trap time-of-flight analyzer. Phosphatidylcholine (PC), a phospholipid, is a basic structural component of cell membranes. PC species exhibit various binding patterns with fatty acids and were analyzed in the brain, eye, and others; however, the distributions of PC species in the inner ear have not been fully understood. We have previously reported the

localization of PC species in the guinea pig cochlea by this microscope. In this study, we extended the use of our mass microscope to the mouse inner ear with special attention to the vestibular organ.

Methods

Three-week-old male DBA2J mouse were anesthetized with pentobarbital and decapitated in accordance with an animal study protocol approved by the Hamamatsu University School of Medicine Animal Care and Use Committee. The temporal bone was isolated and the inner ear was dissected. The inner ear was immediately frozen in liquid-nitrogen-cooled isopentane without fixation. The frozen section was then immersed in a 2% sodium carboxymethylcellulose solution for embedding and stored at -80°C. Before sectioning, the inner ear was held for 20 min at -20°C. Consecutive 15µm sections of the frozen inner ear was prepared using a cryostat. The section was mounted on indium-tin-oxide (ITO)-coated glass slides.

A mass microscope (Shimadzu Corporation, Kyoto, Japan) is a high-resolution IMS instrument with MALDI-QIT-TOF combined with an optical microscope under atmospheric pressure.

Matrix was prepared 50 mg/ml 2,5-Dihydroxybenzoic acid (DHB). After the DHB matrix was allowed to dry, the ITO-coated glass slide was placed on the mass microscope target plate. The mass microscope was operated in the range of m/z 400 - 1000 to detect the ion signals of the PC species.

Results

The mouse specimens are smaller than those of the guinea pig, we clearly localized some PC species in the vestibular organ and cochlea. PC(16:0/20:4) was observed mainly in the vestibular sensory cells and PC(16:0/18:1) was highly localized in the nerve fiber under sensory cells. PC(16:0/16:1) was found primarily in the organ of Corti.

Conclusion

These distributional differences may be associated with the cellular architecture of these inner ear regions.

[744] Assessment of Methods for the Preservation of Inner Ear Tissue by High Pressure Freezing

Anwen Bullen¹, Carolyn Moores², Roland Fleck³, Andrew Forge¹

¹University College London, ²Institute of Structural and Molecular Biology, Birkbeck College, ³National Institute for Biological Standards and Control

Background

Electron tomography can provide detailed three-dimensional reconstructions of cellular structures at nanoscale resolution. To make the most effective use of this technique, sample preparation must preserve structures in as 'close to life' a state as possible with minimal artefact formation. Cryo-preparation techniques such as high pressure freezing (HPF) aim to preserve samples by freezing them rapidly at high pressure, promoting formation of vitreous water and minimising ice

crystal formation. However artefacts from freezing and tissue preparation can often still be seen in these samples. Previous work has suggested that fragile tissues, such as the mammalian organ of Corti, may benefit from prefixation before HPF to improve tissue preservation for tomographic reconstruction. We have explored conditions necessary to preserve inner ear tissue for high resolution structural analysis.

Methods

For HPF, tissue was obtained from mice, gerbils and guinea pigs and mounted in aluminium planchettes with one of a variety of cryoprotectants. Some samples were chemically fixed in glutaraldehyde before HPF. Frozen samples were freeze substituted in acetone with secondary fixation and staining by osmium tetroxide, uranyl acetate and tannic acid. Warming to ambient temperature took place over 36 hours before embedding in plastic. Standard thin sections (80nm) were examined in an electron microscope operating at 80kV. Thicker sections (200nm) for electron tomography were examined in a microscope operating at 200kV. Images were collected using SerialEM software. Tomograms were reconstructed and visualised using the IMOD suite of programmes.

Results

Multiple freezing artefacts were observed in both organ of Corti and utricles that had been prepared by HPF and freeze substitution. Optimisation of cryoprotectants showed that hexadecene reduced freezing artefacts, but that no change in cryoprotectant improved the disordered actin in stereocilia that was observed. Prefixation with glutaraldehyde dramatically improved the preservation of parallel actin in stereocilia in samples frozen with hexadecene. Further improvement in preservation was observed when prefixed samples were frozen with a yeast paste cryoprotectant. Electron tomography of samples frozen under optimised conditions revealed structural details of the interstereociliary links in a sample of guinea pig organ of Corti.

Conclusion

A chemical fixation step before HPF was found to preserve the ordered structure of actin filaments in the stereocilia far better than freezing alone. Combined with optimisation of the cryoprotectant used, this method produced samples with little evidence of freezing damage and excellent structural preservation. Electron tomography of the HPF frozen samples revealed high resolution structural details of the stereocilia bundle.

745 L- N-Acetylcysteine: A Promising Antioxidant for Prevention of TNF α Ototoxicity in Vitro

Chhavi Gupta¹, Dustin Lang¹, Joshua Tillinger¹, Espernza Bas¹, Thomas Van De Water¹, Adrien Eshraghi¹

¹Department of Otolaryngology, University of Miami

Background

Tumor necrosis factor α (TNF α) has been suggested to play a significant role in hearing loss following: acoustic trauma; vibration-trauma; bacterial meningitis; cisplatin exposure; and autoimmune mediated sensorineural hearing loss. Our previous work demonstrated oxidative stress in TNF α -challenged organ of Corti (OC) explants. L- N-acetylcysteine (L-NAC), an acetylated variant of L-cysteine and an excellent source of sulfhydryl (SH) groups, is converted into metabolites capable of stimulating glutathione (GSH) synthesis and acting directly as a free radical scavenger. Earlier studies have shown L-NAC to be an effective protectant against noise-induced hearing loss. The present study tests the antioxidant capability of L-NAC for protecting against TNF α -induced oxidative stress and hair cell (HC) loss.

Methods

OC explants were dissected from P-3 rats and placed in serum-free media. Explants were divided into five groups: 1) untreated controls; 2) TNF α ; (2 μ g/ml); 3) TNF α +L-NAC (5mM); 4) TNF α +L-NAC (10mM); and 5) L-NAC (10mM). All explants were stained for HCs after 96hrs in vitro. After determining with HC counts that 5mM was the most effective concentration, four groups of explants were used for additional studies: 1) untreated controls; 2) TNF α ; (2 μ g/ml); 3) TNF α +L-NAC (5mM) and 4) L-NAC (5mM) only. Levels of: total reactive oxygen species (ROS) with CellROX®; superoxide dismutase; catalase; 4-Hydroxy-2-noneal (HNE);and total glutathione were studied after 24hrs in vitro .

Results

We observed protection of HCs from the ototoxic effects of TNF α in the L-NAC treated explants. There was no evidence of either ROS (CellROX®) or HNE immunolabeling in TNF α + L-NAC (5mM) explants compared to TNF α -challenged explants. Superoxide dismutase and catalase activities were both significantly reduced in TNF α -challenged explants compared to levels for these antioxidant enzymes present in control explants. Total glutathione levels were low in TNF α -challenged explants compared to levels for this antioxidant molecule measured in control and TNF α + L-NAC treated groups of explants.

Conclusion

Treatment of OC explants with L-NAC significantly decreases the TNF α -initiated level of oxidative stress and protected the HCs against TNF α -initiated loss. L-NAC is a promising treatment for protection of the auditory HCs undergoing inflammation-induced oxidative stress.

746 Action of Substance P on the Recovery from the Intense Noise Exposure

Eijju Kanagawa¹, Kazuma Sugahara¹, Yoshinobu Hirose¹, Takefumi Mikuriya¹, Hiroaki Shimogori¹, Hiroshi Yamashita¹

¹*Yamaguchi University Otolaryngology*

Background

Substance P is a polypeptide composed of 11 amino acids, and it is known as a perception neurotransmitter. We have already reported that the VOR gain increased after the administration of substance P into the inner ear. In addition, the nystagmus after the vestibular disorder was suppressed. In the last meeting, we have reported the role of substance P on the recovery from the temporary threshold shift after the intense noise exposure. And we have also reported that substance P affected synaptic ribbons of inner hair cells. In the present study, we administered substance P to the inner ear after TTS, and evaluated the synaptic ribbon beneath the inner hair cells.

Methods

Hartley male guinea pigs (350 - 400 g) with the normal tympanic membranes and the normal Preyer's reflexes were used in this study. Animals were divided into 2 groups (TTS group, Substance P+TTS group). After the post-auricular incision, gelatin sponge which included substance P (10⁻² M) (Substance P + TTS group) or saline (TTS group) was placed on round window membrane. The mastoid bulla was closed with the dental cement. The ABR threshold was measured immediately after this operation to confirm that the hearing function did not change. The animals were exposed to the intense band noise (110 dB SPL for three hours as the TTS model). 3 hours, 12 hours, 24 hours, 3 days, 7 days later, the temporal bone was removed to evaluate the synaptic ribbon count. To reveal the synaptic ribbon, the immunohistochemistry was performed using the anti-CtBP2 antibody. These samples were observed with the fluorescence microscope.

Results

Three hours, 12 hours later, in the Substance P+TTS group, the significantly higher density of signals for synaptic ribbon were observed than those in TTS group. Twenty-four hours later, in the Substance P+TTS group, the lower density of signals for synaptic ribbon were observed than those in TTS group. There is no significant difference in the count number of a synaptic ribbon in the two groups.

Conclusion

The previous reports assumed that substance P has amplified the cochlea nerve compound action potential and that substance P protected the spiral ganglion. In the present study, we showed that the administration of substance P inhibited the change of synaptic ribbon after the intense noise exposure. The result suggests that the polypeptide promotes the recovery of the cochlear function after noise trauma.

747 Screening for Protective Effect in Supplement Drugs Using the Zebrafish Lateral Line

Yoshinobu Hirose¹, Kazuma Sugahara¹, Eijyu Kanagawa¹, Hiroshi Yamashita¹

¹*Yamaguchi University Graduate School of Medicine*

Background

The zebrafish lateral line is a powerful system for studying hair cells and hair cell death. Hair cells can be easily labeled and imaged in vivo with fluorescence microscopy. We have previously described a screening system to rapidly assess drugs for possible ototoxic effects in anti-cancer drugs (Hirose et al., 2011). Also it is possible to screen protective effect against some ototoxicity drugs. There are many kind of supplement in USA, Europe, and Japan, etc. Supplement can be a prophylactic treatment especially against age-related hearing loss. Some countries have trouble against medical expenses, so it can be useful to such countries.

Methods

We have screened the supplement drugs for protective effects against aminoglycoside. 5-7 dpf Zebrafish (*Danio rerio*) embryos of the AB wild type strain were used in this study. Zebrafish larvae were exposed to supplement drugs (0, 1, 10, 100, 1000 uM) for 1 and 24 hours before 100 uM Neomycine for 1 hour. After that, they were fixed in 4% paraformaldehyde, incubated with anti-parvalbumin, and hair cell damage was assessed by fluorescent microscope. We made dose-response curve to evaluate protective effect against Neomycine. Then we confirm whether screened drug can protect inner ear hair cell on noise-induced hearing loss in guinea pigs. The ABR threshold was examined under anesthesia. The sound stimuli consisted of 2-, 4 -and 8-kHz tone bursts. ABR threshold was defined as the lowest stimulus intensity to produce a reliable waveform of 3-5 peaks.

Results

Dose-response curve show some of drugs show (e.g. Quercetin) protective effect against neomycin. In the guinea pigs study, we observed that the ABR threshold shift was significantly less in the Quercetin group than in control group. In addition, missing outer hair cells was lower in the Quercetin group than in the control group.

Conclusion

We show that some of supplement drugs show protective effect against neomycin, further more, screened drugs by zebrafish lateral line show protective effect against sound exposure. It is useful to screen drugs on zebrafish hair cell damage model, because zebrafish hair cell is similar not only to morphologically but also biochemically.

748 Cholesterol Homeostasis and Auditory Function

Michelle Seymour¹, Frederick Pereira¹

¹Baylor College of Medicine

Background

Animal models and human studies support a link between altered cholesterol homeostasis and sensorineural hearing loss, implicating pathologies that affect the cochlea, auditory nerve and/or central auditory pathways. However, knowledge of the relative quantities and species of lipids in the cochlea, as well as how circulating lipids modulate cochlear cellular activities, is currently lacking. The rising prevalence of obesity and hypercholesterolemia demands a better understanding of how systemic cholesterol homeostasis influences cochlear cholesterol homeostasis and hearing function. We hypothesize that cholesterol homeostasis is essential for hearing function and maintenance, and that changes in cholesterol levels lead to decreased cochlear and hearing function.

Methods

Auditory function was assessed by measuring auditory brainstem responses (ABRs) as described previously by our group. Total cholesterol levels in cochlear tissues were quantified using the Amplex Red cholesterol assay (Invitrogen, Carlsbad, CA) and compared to serum lipid panels. *Stria vascularis* capillary organization and perivascular-resident macrophage-like melanocytes (PVM/Ms) were visualized by whole-mount staining and fluorescence confocal microscopy.

Results

We have demonstrated that cochlear levels of total cholesterol and serum lipid panels change significantly during normal maturation of cochlear and auditory function. Interestingly, we have shown that the sensory epithelium (SE) contains higher levels of cholesterol than the vascular compartment. Current studies focus on how systemic hypercholesterolemia affects the hearing system by using the Low-Density Lipoprotein Receptor (LDLR) KO mouse model. LDLR KO mice display elevated hearing thresholds, indicative of hearing loss. In addition, LDLR KO mice have altered organization of the vasculature within the *stria vascularis*, the metabolic engine of the cochlea. We are also exploring how these changes develop with age, as well as the contribution of PVM/Ms to maintenance of the structural integrity of the blood-labyrinth-barrier (BLB) in the *stria vascularis* capillaries.

Conclusion

Preliminary results not only suggest that serum cholesterol levels influence cochlear cholesterol homeostasis, but also the existence of a mechanism for concentrating cholesterol in the SE or endogenous synthesis of cholesterol by hair cells, supporting cells or other cells of the organ of Corti. Hypercholesterolemic LDLR KO mice have impaired auditory function, which may result from altered *stria vascularis* structure or altered cochlear cholesterol homeostasis.

749 Activation of Endoplasmic Reticulum Stress in an Inner-Ear Immortomouse Cell Line

Tae Su Kim¹, Jong Woo Chung¹, Hong Ju Park¹, Woo Seok Kang¹, Jin Kyung Suh¹, Seung-Hyo Choi²

¹Asan Medical Center, ²Je-Ju National University Hospital

Background

Induction of mild endoplasmic reticulum (ER) stress has been associated with an increased tolerance to cellular toxins. But under severe ER stress, specific stress-associated apoptotic pathways are activated. We investigated the alteration of HEI-OC1 cell under activation of ER stress.

Methods

ER stress was induced after exposure to tunicamycin and thapsigargin. We examined the unfolded protein response (UPR) by measuring the protein levels of specific genes such as glucose-regulated protein of 78kDa (GRP78) and GRP94 in HEI-OC1 cell.

Results

ER stress inducers resulted in a dose-dependent increase of cell death, but the magnitude of cytotoxicity was inducer-dependent. Cytotoxicity was not increased by mild ER stress. GRP78 and GRP98 expression were statistically increased after activation of ER stress.

Conclusion

Our results indicate UPR and cytotoxicity are dependent on the ER stress inducer in HEI-OC1 cell. These results suggest that the ER stress may play diverse roles in ototoxicity of HEI-OC1 cell.

750 Evaluation of the Ototoxicity of Gentian Violet Solution

Taro Takanami¹, Makoto Kinoshita², Takashi Sakamoto², Tatsuya Yamasoba², Mitsuya Suzuki¹

¹Department of Otolaryngology, Toho University,

²Department of Otolaryngology, University of Tokyo

Background

Antibiotic abuse can lead to an increase in the incidence of multiple antibiotic resistance among organisms. Non-antibiotic solutions such as Burow's solution and Gentian violet solution have been reported to be effective in treating refractory otorrhea caused by multiple drug-resistant bacteria or fungi. Burow's solution has astringent and antibacterial properties while Gentian violet solution has a strong sterilizing effects.

Recent studies have demonstrated that intratympanic application of Burow's solution causes degeneration of the outer epithelium and outer hair cell loss in the basal turn in guinea pigs. Although Gentian violet solution is also known to show ototoxicity, there is very little data regarding the physiological and morphological changes following intratympanic application of Gentian violet solution. We aimed to examine the effects of Gentian violet solution

Methods

Albino guinea pigs with normal Preyer's reflex were used. All animals were anesthetized with an intramuscular injection of xylazine and ketamine. ABR and DPOAE were recorded at 4, 8, 16, 32 kHz. Under aseptic conditions, an incision was made in the left postauricular region, and a small hole was made in the tympanic bulla to allow direct visualization of the RWM. In control animals, 0.05 ml of physiological saline was directly dropped onto the RWM. In experimental animals, 0.05 ml of 1% Gentian violet solution was directly dropped onto the RWM. Seven days later, ABR and DPOAE were recorded, and the left temporal bone was removed. In half of the experimental animals, the cochleae were dissected using the surface preparation technique, stained with rhodamine-phalloidin, and examined under a fluorescence microscope. In the remaining experimental animals, the cochleae were embedded in paraffin and section in the radial plane at 4-7µm using a microtome.

Results

In the control animals, no marked ABR threshold shifts were observed at any frequency. No hair cell loss was observed anywhere in the organ of Corti. In the experimental animals, the ABR thresholds shifts at all frequencies were significantly higher than those in the controls. On the other hand, DPOAE showed normal responses at all frequencies. Many phalangeal scars were observed in the region of outer hair cells in the lower half of the basal turn.

Conclusion

Gentian violet solution applied onto RWM may cause marked hearing impairment. This hearing impairment may be induced not only by outer hair cell loss but also by damage to the spiral bundle and/or spiral ganglion.

751 CCR2 Expression Defines Cochlear Response to LPS Preconditioning

Song-Zhe Li¹, Keiko Hirose¹

¹Department of Otolaryngology, Washington University School of Medicine

Background

Lipopolysaccharide (LPS) at low doses has been widely used as a preconditioning stimulus to prime the immune system before a subsequent injury. In ototoxicity, LPS pretreatment worsens hair cell loss and exacerbates threshold shift caused by kanamycin/furosemide combination therapy. This LPS induced exacerbation of hearing loss is reversed, and LPS pretreatment is protective against threshold shift in mice that are deficient for CC-chemokine receptor 2, CCR2, which is expressed in inflammatory monocytes that enter the inner ear after exposure to LPS.

Methods

8 weeks old C57Bl6 mice were injected with saline or LPS (0.5mg/kg/day for two consecutive days) and then injected with kanamycin/furosemide (1000mg/kg and 180 mg/kg

respectively) on the third day. ABR thresholds were obtained at day five after kanamycin/furosemide, and cochleas were harvested and analyzed for hair cell survival and numbers of monocyte/macrophage entry and chemokine receptor expression.

Results

Threshold shift after LPS priming is about 40 dB greater than threshold shift in mice injected with saline prior ototoxic injury in CCR2+/+ mice. CCR2 expressing monocytes are recruited in abundance to the cochlea with LPS pretreatment, but few CCR2 expressing monocytes are present in the inner ear after ototoxic exposure alone. Threshold shift in LPS-pretreated mice was about 20 dB lower compared to saline-pretreated mice exposed to the same kanamycin/furosemide treatment when CCR2-/- mice were studied. Thus, LPS in CCR2 wild-type mice has the effect of exacerbating ototoxicity, while in CCR2 null mice, LPS is protective.

Conclusion

CCR2 expression in peripheral monocytes is critical in defining whether LPS pretreatment causes exacerbation of ototoxic injury or mediates protection. This finding represents an important example of where mononuclear phagocytes, recruited into the inner ear can play an important role in determining hearing function after hair cell injury.

752 Selective Hair Cell Ablation Recruits Macrophages Into the Cochlea and Activates Microglia in the Cochlear Nucleus

Tejbeer Kaur¹, Melissa Strong², Darius Zamani¹, Ling Tong², Edwin Rubel², Keiko Hirose¹, Mark Warchol¹

¹Washington University School of Medicine, ²University of Washington School of Medicine

Background

Prior studies have demonstrated that macrophages are recruited into the cochlea after acoustic trauma or aminoglycoside ototoxicity. However, the signals that initiate macrophage recruitment, as well as the contribution of macrophages to cochlear pathology and/or repair, have not been determined. Injury to the cochlea also activates microglia within the cochlear nucleus, but the role of those cells in brainstem pathology or plasticity is also unclear. We have used a novel mouse model to characterize the response of both cochlear macrophages and microglia in the cochlear nucleus to selective elimination of hair cells.

Methods

Mice expressing diphtheria toxin receptor under control of the Pou4f3 promoter were crossed to CX3CR1-GFP mice, which express GFP in all macrophages and microglia. Mice 6-8 weeks of age were given single IM injection of diphtheria toxin (DTX, 25ng/20gm), which caused an extensive loss of both inner and outer hair cells. At 1-12 days after DTX treatment, mice were euthanized and perfused with 4% paraformaldehyde. Cochleae and brainstems were isolated and processed for immunohistochemical labeling of neurons and hair cells.

Results

Hair cell loss was first evident at 3 days after DTX injections. At 7 and 12 days post-injection, we observed nearly complete ablation of both inner and outer hair cells. This was accompanied by recruitment of numerous GFP-expressing macrophages into the cochlea. Notably, such macrophages were abundant in the scala tympani, immediately below the basilar membrane. Those cells often extended processes into the injured outer hair cell region. Macrophages are also observed in close contact with dendrites of the spiral ganglion neurons within the habenula perforata and with neurons crossing the tunnel of Corti and extending towards outer hair cells. Also, macrophages in the DTX injected mice are amoeboid compared to the ramified cells in DTX injected wild-type mice. We also observed many GFP-expressing microglia within the cochlear nucleus of mice status post hair cell ablation. Increased numbers of microglia were present in the ventral cochlear nucleus at 12 days after DTX injection. Finally, injection of diphtheria toxin into wild type mice did not induce an inflammatory response in the cochlea or auditory brainstem.

Conclusion

The mouse model employed in these studies permits the selective complete elimination of hair cells, without any other evident pathology. Our data indicate that the loss of cochlear hair cells is sufficient to recruit macrophages into the cochlea and microglial activation within the cochlear nucleus.

753 Inflammation Mobilizes Vestibular Perivascular Resident Macrophage-Like Melanocytes

Fei Zhang¹, Lingling Neng¹, Allan Kachelmeier¹, Xiaorui Shi¹

¹Oregon Hearing Research Center

Background

A large number of perivascular cells expressing both macrophage and melanocyte characteristics (named perivascular resident macrophage-like melanocytes, PVM/M) were previously found in the intra-strial fluid-blood barrier.

Methods

In this study, we used confocal microscopy combined with fluorescence immunohistochemistry approach.

Results

The PVM/Ms were found to also locate in the area of the blood-labyrinth barrier of the vestibular system in normal adult cochlea, including in the three ampullae of the semicircular canals (posterior, superior and horizontal), utricle, and saccule. The cells were identified as PVM/Ms, as they were positive for the macrophage and melanocyte marker proteins F4/80 and MIFT. Similar to the PVM/Ms present in the stria vascularis, the PVM/Ms in the vestibular system are closely associated with microvessels and structurally intertwined with endothelial cells and

pericytes. The density of PVM/Ms in normal, unstimulated tissue is $225 \pm 43/\text{mm}^2$ in the utricle, $191 \pm 25/\text{mm}^2$ in the saccule, $212 \pm 36/\text{mm}^2$ in horizontal ampullae, $238 \pm 36/\text{mm}^2$ in anterior ampullae, and $223 \pm 64/\text{mm}^2$ in posterior ampullae. Injection of bacterial lipopolysaccharide (LPS, 5 mg/ml) into the middle ear through the tympanic membrane dramatically increases the presence of PVM/Ms irregularly situated along capillary walls in all regions within a 48 hour period. PVM/M foot processes were notably detached from some of the capillaries. The inflammatory response significantly increased vascular permeability and leakage.

Conclusion

The results indicate PVM/Ms in the vascular wall of the blood-labyrinth barrier are contributing factors in the local inflammatory response. This work was supported by National Institutes of Health grants NIH NIDCD R01-DC010844 (XS), DC R21DC1239801 (XS), and NIHP30-DC005983.

754 Pigment Epithelium-Derived Growth Factor Protects Against Noise-Induced Hearing Loss

Fei Zhang¹, Min Dai¹, Lingling Neng¹, Jin Hui Zhang¹, Xiaorui Shi¹

¹Oregon Hearing Research Center

Background

Acoustic trauma not only directly damages sensory hair cells, but it also disrupts the cochlear intra-strial fluid-blood barrier in the stria vascularis. An intact intra-strial fluid-blood barrier is critical for sustaining the ionic gradients and endolymphatic potential (EP) essential for hearing function.

Methods

In this study, animals were exposed to broadband noise at 1170 dB SPL in a sound exposure booth for three hours and for an additional three hours the following day. An auditory brain-stem response audiometry to pure tones was used to evaluate hearing function in control, noise-exposed, noise-exposed + pigment epithelium-derived growth factor (PEDF), a potent endogenous inhibitor of vasopermeability, treated groups. Endocochlear potential (EP) was recorded. Expression of tight junctions were detected with immunohistochemistry combined with confocal microscopy.

Results

We found that PEDF protects against noise-caused hearing loss. Animals pre-treated with PEDF show substantially reduced EP drop with noise exposure. The PEDF promotes expression of tight junction-associated proteins such as ZO-1 and VE-cadherin between endothelial cells and stabilizes accessory perivascular-resident macrophage-like melanocytes by increasing expression of neural cell adhesion molecule (NCAM, CD56).

Conclusion

Our results demonstrate the critical role of PEDF in maintaining cochlear homeostasis and suggest its potential therapeutic role in protecting against noise-induced vascular permeability and hearing loss. This work was supported by National Institutes of Health grants NIH NIDCD R01-DC010844 (XS), DC R21DC1239801 (XS), and NIHP30-DC005983.

755 IL-10 Inhibits Otitis Media-Induced Cochlear Inflammation Via HMOX1-Dependent NF- κ B Inactivation

Jeong-Im Woo¹, Sejo Oh¹, Yoojin Lee¹, Okjin Ahn¹, Raekil Park², David Lim^{1,3}, Sung Moon¹

¹House Research Institute, ²Wonkwang University,

³University of Southern California

Background

Recently, we have demonstrated that the spiral ligament fibrocytes (SLFs) play a pivotal role in the cochlear inflammation secondary to otitis media (OM). However, considering that the middle ear infection is one of the most common infectious diseases in children, clinical evidence of the cochlear symptoms secondary to OM is less than our expectation. This suggests that cochlear inflammation is tightly regulated to prevent tissue damage by excessive inflammatory response. In this study, we aim to determine the molecular mechanism involved in IL-10-mediated inhibition of OM-induced cochlear inflammation.

Methods

To localize IL-10-expressing cells, immunolabeling and RT-PCR analysis were conducted. To determine MCP-1 regulation, we performed qRT-PCR analysis and luciferase assays. HMOX1 was activated by CoPP and CORM and was inhibited using the specific siRNA. Chromatin immunoprecipitation (ChIP) analysis was performed to determine binding of NF- κ B to the enhancer of the MCP-1 gene.

Results

The SLFs appeared not to produce IL-10, but we found that IL-10-expressing cells are localized in the spiral ligament. The SLFs were shown to inhibit NTHi-induced MCP-1 expression upon exposure to IL-10, which was suppressed by silencing of IL-10RA. The inhibitory effect of IL-10 was mimicked by treatment of CoPP and CORM but was blocked by silencing of HMOX1. The SLFs were found to activate NRF2 in response to IL-10, resulting in up-regulation of HMOX1. Luciferase assays showed that IL-10 inhibits NTHi-induced NF- κ B activation. Furthermore, ChIP analysis demonstrated that IL-10 inhibits NTHi-induced binding of p65 to the NF- κ B binding motif of the MCP-1 gene.

Conclusion

Taken together, our results suggest that IL-10 modulates OM-induced cochlear inflammation through HMOX1-mediated negative regulation of MCP-1 expression in the SLFs. [Supported by NIH grants: DC005025, DC006276 and DC011862]

756 Interaction of IFN-Gamma and TNF-Alpha in Cisplatin Ototoxicity

Jeong-Im Woo¹, Yoojin Lee¹, Okjin Ahn¹, Raekil Park², David Lim¹, Sung Moon¹

¹House Research Institute, ²Wonkwang University

Background

Inflammatory response is known to be involved in cisplatin cytotoxicity. Previously, we have demonstrated that the auditory hair cells induce pro-inflammatory cytokines in response to cisplatin. Moreover, inhibition of cytokines was shown to ameliorate cisplatin ototoxicity. However, we poorly understand interactions of cytokines in cisplatin ototoxicity. In this study, we aim to determine a role of IFN- γ and TNF- α in cisplatin ototoxicity.

Methods

To determine cell viability, we performed MTT assays and cytometric analysis with trypan blue staining. For the *ex vivo* model of ototoxicity, the organ of Corti was isolated from the Math-1-EGFP mice and explanted on the PCTE membrane. Superoxide generation was monitored using flow cytometric analysis with hydroethidine staining. qRT-PCR analysis was conducted to determine NOX1 regulation.

Results

TNF- α appeared to augment cisplatin-induced ototoxicity *in vitro* and *ex vivo*, which was blocked by a small molecule inhibitor of TNF- α activity. IFN- γ alone appeared to insignificantly enhance cisplatin-induced cytotoxicity in the HEI-OC1 cells. However, pretreatment of IFN- γ was found to highly potentiate TNF- α -mediated enhancement of cisplatin cytotoxicity. In addition, IFN- γ -mediated enhancement of TNF- α -induced cytotoxicity was inhibited by Epigallocatechin-3-gallate, indicating the involvement of STAT1 signaling. The HEI-OC1 cells appeared to up-regulate superoxide generation and NOX1 expression in response to TNF- α , which was enhanced by the pretreatment of IFN- γ . Cisplatin-induced caspase-3 activation was enhanced upon exposure to TNF- α in the HEI-OC1 cells. Pharmacological inhibition of caspases was found to ameliorate TNF- α -induced enhancement of cisplatin cytotoxicity.

Conclusion

Taken together, our results suggest that interaction of IFN- γ and TNF- α augments cisplatin ototoxicity, which involves superoxide generation. [Supported by NIH grants: DC005025, DC006276 and DC011862]

757 Rescue of Hearing and Vestibular Defects in Usher Syndrome Using Antisense Oligonucleotides: Histological and Scanning EM Analysis

Jennifer Lentz¹, Francine Jodelka², Anthony Hinrich², Kate McCaffrey², Hamilton Farris¹, Matthew Spallita¹, Nicolas Bazan¹, Dominik Duelli², Frank Rigo³, Michelle Hastings²

¹LSU HSC, ²Rosalind Franklin Chicago Medical School,

³Isis Pharmaceuticals

Background

Usher syndrome (Usher) is the most common cause of hereditary deaf-blindness, characterized by sensorineural hearing impairment combined with retinitis pigmentosa, and in some cases, vestibular dysfunction. The only treatment for Usher is the use of prosthetics, such as hearing aids and cochlear implants, and the feasibility of curing deafness at the cellular level is uncertain. A mouse model for Usher has been developed based on the Acadian Usher mutation, in which the USH1C.216G>A mutation (216A) has been knocked into the mouse Ush1c gene. The 216AA mice have profound deafness, vestibular dysfunction and develop retinal degeneration characteristic of Usher patients. The 216A mutation introduces a cryptic splice site that is used preferentially over the authentic site producing a truncated mRNA and protein product. We hypothesize that blocking the mutant splice site with antisense oligonucleotides (ASOs) will activate the authentic site, rescue protein expression and be therapeutic for mice and ultimately Usher patients.

Methods

ASO activity was optimized using a cell-free splicing system, an ASO-tiling screen and cell lines isolated from the 216AA mice and an Usher patient with the 216AA mutation. 216AA mice were injected with ASOs and correction of splicing and protein expression was quantitated by rt-pcr and western blot, respectively. Harmonin b expression and localization was examined by immunohistochemistry. Outer hair cell (OHC) bundle morphology was evaluated by scanning electron microscopy. Hearing was evaluated by auditory-evoked brainstem response (ABR) analysis.

Results

Treatment to neonatal 216AA mice with a single systemic dose of ASOs partially corrects splicing and protein expression in the cochlea, improves OHC stereocilia organization and rescues cochlear hair cells, vestibular function and hearing function.

Conclusion

Our results demonstrate the therapeutic potential of ASOs in Usher syndrome and other diseases caused by mutations that disrupt splicing.

758 Trafficking Deficiency of KCNQ4 Channels Associated with Progressive

Sensorineural Hearing Loss Can Be Corrected by Molecular Chaperone HSP90 β

Yanhong Gao¹, Sergey Yechikov¹, Ana E. Vazquez¹, Dongyang Chen¹, Liping Nie¹

¹University of California, Davis

Background

The inner ear KCNQ4 channel plays crucial roles in maintaining cochlear ion homeostasis and regulating hair cell membrane potential that are essential for normal auditory functions. Dysfunction of the KCNQ4 channel leads to the autosomal dominant non-syndromic deafness DFNA2, characterized by progressive sensorineural hearing loss. At younger ages, hearing loss in DFNA2 patients is moderate and predominantly at high frequencies. At older age, however, all affected individuals have severe to profound hearing impairment with all frequencies involved. Genetic studies have identified numerous KCNQ4 mutations in DFNA2 patients. However, the molecular etiology of DFNA2 is elusive.

Methods

Using immunofluorescent, biochemical, and electrophysiological approaches, we investigated functional consequences of seven DFNA2 mutations.

Results

Dramatic decrease in cell surface expression of KCNQ4 channels was detected by immunofluorescent microscopy and confirmed by Western blot for all mutations tested, while the cellular levels of these mutant channels remained normal. In addition, none of these mutations interrupt subunit interaction, consistent with their dominant-negative effects on the wild type KCNQ4 trafficking. Moreover, we found that upregulation of HSP90 β , a major molecular chaperone that controls the KCNQ4 biosynthesis, significantly improved cell surface expression of DFNA2 mutants; KCNQ4 expression in the plasma membrane was restored in cells mimicking heterozygous conditions of DFNA2 patients. However, no significant changes in KCNQ4 currents was observed after restoration of KCNQ4 surface expression.

Conclusion

Trafficking deficiency and impaired KCNQ channel function are two underlying mechanisms for hearing loss in DFNA2.

759 Oral Capsaicin Consumption Protected Against Noise Induced Hearing Loss (NIHL)

Puspanjali Bhatta¹, Debashree Mukherjee¹, Kelly Sheehan¹, Leonard P Rybak¹, Vickram Ramkumar¹

¹SIU School of Medicine, Springfield IL

Background

Exposure to high levels of noise is the most common cause of hearing loss in adults. Noise exposure leads to cellular stress in the cochlea by activating and increasing a cochlear specific NADPH oxidase, NOX3 and transient receptor potential vanilloid 1 (TRPV1) channel. Increased NOX3 and TRPV1 expression lead to increased inflammation as evidenced by increases in proinflammatory mediators such as tumor necrosis factor- α

(TNF- α), inducible nitric oxide synthase (iNOS) and cyclooxygenase-2 (COX-2). This mechanism of reactive oxygen species (ROS)-induced inflammation leading to hearing loss is similar to that underlying cisplatin ototoxicity, previously delineated in our laboratory. We have previously shown that direct activation of TRPV1 by capsaicin reduced cisplatin ototoxicity in the rat. Therefore, in this study, we assessed the effectiveness of capsaicin against noise-induced hearing loss (NIHL).

Methods

Baseline auditory brainstem responses (ABRs) of male Wistar rats were recorded. This was followed by intratympanic (IT) (50 μ l of 0.1 μ M capsaicin) or the oral (0.01 to 2% in water) capsaicin administration and noise exposures (122dB octave band noise centered at 16kHz for 1h). Post-treatment ABRs were recorded 21 days following noise exposures. Rat cochleae were extracted and used for various assays. Functional assessments include ABRs and scanning electron microscopy (SEM). Gene expression studies were conducted using real time real time PCR and by immunohistochemistry (IHC) of the mid-modiolar sections of the rat cochleae.

Results

Our data indicate that noise exposure produces a 45-60dB shift in ABR thresholds. Rats administered oral capsaicin demonstrated significantly reduced ABR threshold shifts of <10dB. Significant decreases in ABR threshold shifts following noise exposures were also observed following IT capsaicin to <30 dB. Capsaicin-mediated otoprotection was co-related with preservation of outer hair cells, decreased expression of NOX3 and TRPV1 genes and inflammatory mediators such as TNF- α , iNOS and COX-2.

Conclusion

We conclude that noise trauma increases cochlear ROS generation and pro-inflammatory genes in the cochlea. In addition, pretreatment with capsaicin (either orally or IT) reduced the responses to noise trauma and protected against NIHL. Our study suggests that the consumption of capsaicin in spicy food could offer protection against NIHL.

760 Oral Epigallocatechin Gallate (EGCG) Protects Against Cisplatin-Induced Ototoxicity in Rats

Tejbeer Kaur¹, Vikrant Borse¹, Kelly Sheehan¹, Debashree Mukherjee¹, Sarvesh Jajoo¹, Leonard P Rybak¹, Vickram Ramkumar¹

¹SIU School of Medicine, Springfield, IL

Background

Cisplatin is an anticancer drug used to treat various solid tumors. Patients treated with cisplatin develop significant ototoxicity and nephrotoxicity. Various drugs are under investigation for the alleviation of cisplatin-induced ototoxicity and nephrotoxicity. In previous studies, we reported that the cisplatin triggers reactive oxygen species (ROS) generation, activation of signal transducer and activator of transcription-1 (STAT-1) and inflammation in the cochlea, which ultimately leads to damage and death

of outer hair cells (OHCs) and hearing loss. Accordingly, inhibition of STAT-1 by siRNA or inflammation by tumor necrosis factor (TNF- α) antagonist, etanercept, protected against death of OHCs and preserved hearing. In this study, we test the ability of the green tea extract, epigallocatechin gallate (EGCG), a known inhibitor of STAT1, to protect against cisplatin-induced cell death in vitro and against hearing loss in Wistar rats.

Methods

Organ of Corti-derived cells (UB/OC-1) were cultured and treated with cisplatin in the absence and presence of EGCG to determine effects on STAT1 activity and cell apoptosis. Male Wistar rats (200-250g) were treated with oral EGCG (100mg/kg), followed by cisplatin (11mg/kg, i.p.). Auditory brainstem responses (ABRs) and scanning electron microscopy (SEM) studies were performed to assess hearing loss and OHC morphology. University of Michigan squamous cell carcinoma (UMSCC) 10b cells were used to test for potential antitumor interference by EGCG.

Results

Western blot studies indicated that EGCG inhibited cisplatin-induced STAT1 phosphorylation and activation. EGCG also inhibited cisplatin-induced p53 expression and increased the levels of anti-apoptotic proteins, Bcl-2 and Bcl-xl. In vivo studies indicated that EGCG protected against cisplatin-induced loss of OHCs. Current studies are testing the effects of EGCG against cisplatin-induced loss of outer hair cells. Studies in UMSCC 10b cells demonstrated that EGCG augmented cisplatin-induced cell killing, indicating a potential lack of anti-tumor interference.

Conclusion

We propose that EGCG could serve as an important treatment for cisplatin-induced hearing loss by inhibiting a STAT-1 dependent apoptotic pathway. Furthermore, EGCG did not interfere with cisplatin-induced killing of squamous cell carcinoma cells. These studies would support the use of oral EGCG for the treatment of cisplatin ototoxicity. (Supported by NIH grants R01Dco2396 and R15DC011412 and funds from SIU SOM).

761 Effect of Non-Steroidal Anti-Inflammatory Drugs (NSAIDs) on Prestin

Guillaume Duret¹, Robert Raphael¹

¹Rice University

Background

High doses of salicylate can cause reversible hearing loss and tinnitus. According a classification of ototoxicity-inducing drugs by to Cianfrone and colleagues, other NSAIDs can trigger side effects related with hearing and cause tinnitus. Although ototoxicity can be due to the interaction of these medicines with any sensitive part of the hearing system, we are investigating a possible prestin-related mechanism for these adverse reactions.

Methods

To measure the non linear capacitance of prestin, we used HEK-cells stably transfected with a plasmid containing the prestin gene. The NLC was measured from these cells after 48 hours of induction. For each cell, a control NLC in the absence of drug was obtained. The appropriate NSAID was then perfused in the recording chamber and a second NLC was measured. We also investigated the impact of NSAIDs when present only outside or only inside the cell to address a possible sidedness of the effect.

Results

We assessed the effect on prestin of the widely used ibuprofen, acetaminophen and naproxen, all of which have ototoxic side effects. We also report the impact of salicylate-derivatives diflusalin and piroxicam whose side effects on hearing are stronger than with most NSAIDs. All NSAIDs tested, except piroxicam, triggered a voltage shift of the NLC. The stronger shift in was observed with diflusalin, which triggered a 46mV shift at 2 mM. Moreover, a change in charge density was observed when ibuprofen or diflusalin were perfused. The presence of 2 mM diflusalin decreased the charge density by over 50% which could suggest a competition with Cl⁻ ions. The perfusion of 6mM ibuprofen, on the other hand, increased the charge density by 20%, suggesting a decrease in membrane lateral pressure.

Conclusion

NSAIDs induce alterations in the function of prestin which could impact hearing. The NSAID-induced shift in the NLC could modify the function of the OHC at resting potential and alter cochlear amplification. We also witnessed a correlation between the V_{1/2}-shift and the pK_as of the NSAIDs. The drug that shows no effect was the least charged (piroxicam), the ones that trigger hyperpolarization were positively charged (ibuprofen, naproxen and diflusalin) while the negatively charged molecule (acetaminophen) had a depolarizing effect. This suggests that the charges brought to the membrane by the NSAIDs are responsible for the alteration in V_{1/2}.

762 Mechanical Tuning in the Hearing System of Bushcrickets

Jennifer Hummel¹, Manfred Koessl¹, Manuela Nowotny¹
¹Goethe University

Background

The high-frequency hearing organ (crista acustica, CA) of bushcrickets is located within the tibiae of the forelegs. Earlier studies revealed a tonotopical representation of sound-induced amplitude maxima along the organ when stimulated with 80 dB SPL. The anatomical basis for tonotopy, however, is unknown. It has been assumed that the varying mass of supporting cells on top of each dendrite, called cap cells, might influence sensory cell tuning by acting as mechanical resonators. To investigate the influence of possible mechanical resonances, we analyzed the sound-induced mechanical tuning of the CA as well as the anatomy of the hearing system.

Methods

The tropical bushcricket *Mecopoda elongata* was used to investigate mechanical vibration thresholds. For this purpose, pure-tone stimuli (2-77 kHz, 10-80 dB SPL) were applied and the mechanical vibration response of the CA was measured by a laser-Doppler-vibrometer. Additionally, we examined the anatomical features of the hearing system by analyzing the hearing organ structures on cross sections through the CA.

Results

In a first series of experiments the mechanical response to a set of different frequencies and levels was determined at three different locations along the hearing organ (proximal, medial and distal). According to the predicted tonotopical preference of the sensory cells, low frequencies elicited the most sensitive response in the proximal region and high frequencies in the distal region. The tuning curves from the proximal and medial locations revealed distinct characteristic frequencies at stimulus frequencies of 7 and 17 kHz, respectively. In contrast, in the distal region no distinct characteristic frequency could be identified. Anatomical investigations of the CA revealed a steady decrease in size of all relevant hearing-organ structures from the proximal to the distal end supporting the tonotopical distribution of displacement amplitude maxima.

Conclusion

Mechanical threshold curves measured at a proximal and medial location along the CA revealed a tonotopical tuning of sensory cells supported by the anatomical gradient along the CA. Nevertheless, the fine tuning of mechanical CA vibration, especially the broad tuning curve with no distinct characteristic frequency measured at the distal region, seems to be influenced by unknown additional factors.

763 Phase-Locking of Individual and Coupled Hair Bundles of the Bullfrog Sacculus

Yuttana Roongthumskul¹, C. Elliott Strimbu¹, Dolores Bozovic¹

¹Department of Physics and Astronomy, UCLA

Background

Bullfrog sacculus has been shown to detect subnanometer-level mechanical signals. This exquisite sensitivity potentially arises from the synchronization between hair bundles, mechanically coupled via the otholithic membrane under *in vivo* conditions. In this work, we study the phase-locking behavior of single and coupled hair bundles to external stimulations.

Methods

Calibrated glass fibers are attached either to individual hair bundles, or positioned to couple to two bundles simultaneously. The fibers are then used to deliver sinusoidal mechanical stimulation. The phase of the oscillations is extracted from the phase portrait of displacement and velocity.

Results

At low stimulus amplitudes, the phase of hair bundle oscillation exhibits diffusive behavior, with a decrease in variance with increasing stimulus level. As the stimulus becomes stronger, phase-locking can be observed with the appearance of phase slips. We observe that phase-locking occurs at ~ 10 nm stimulus, the level which corresponds to the threshold of compressive nonlinearity. In the absence of external stimulation, mechanically coupled hair bundles exhibit synchronization.

Conclusion

Individual hair bundles exhibit signatures of entrainment, evidenced by peaks in their phase histograms, at stimuli as small as ~ 2 nm. With increasing stimulus amplitude, phase-locking occurs and phase slips can be observed; a behavior that is indicative of a saddle node on invariant circle (SNIC) bifurcation. We also find strong correlation between the occurrence of phase slips and the regime of compressive nonlinearity.

764 Statistical Properties of Spontaneous Hair Bundle Oscillations

Sebastian W.F. Meenderink¹, C. Elliott Strimbu¹, Roie Shlomovitz¹, Dolores Bozovic¹

¹University of California, Los Angeles

Background

Under *in vitro* conditions, hair bundles in the turtle papilla and the bullfrog sacculus have been shown to oscillate spontaneously when decoupled from the overlying membrane. This spontaneous motility results from the interaction of two mechanisms that affect the bundle's position and which act on different time scales. Here we analyze long, multi-minute recordings of the position of freely oscillating hair bundles to extract statistics on their variation.

Methods

Spontaneously oscillating hair bundles in freshly dissected sacculi of the American bullfrog (*R. catesbeiana*) were filmed continuously at a high frame rate (500 fps) for several minutes. The position of a hair bundle was extracted from each image in these recordings by fitting a Gaussian distribution to its intensity profile. We developed an automated routine which examined the local variation in amplitude and its derivative to detect bundle oscillations within each trace.

Based on the detected oscillations, several of their parameters were extracted: duration, amplitude, and inter-oscillation interval. Owing to the length of the recordings, over 2000 oscillations were present in any given trace. This results in rigorous statistical characterization of the oscillation's properties, allowing us to investigate the role of noise.

Results

Histograms of inter-oscillation intervals are either uni- or bimodal, resulting from "regular" and "bursting-type" oscillation patterns, respectively. For individual oscillations,

we found that their duration increases with the quiescent interval immediately preceding them. This is most evident in bursting-type oscillations, where the first oscillation in a burst (group of closely spaced oscillations) takes longer than the rest.

The length of the recordings also permitted the calculation of their correlation dimension, which can be used to determine whether the underlying system exhibits chaos. Preliminary calculations indicate that the correlation dimension grows with the embedding dimension, M .

Conclusion

The long recordings of spontaneously oscillating hair bundles facilitate a rigorous statistical quantification of their properties. Based on an automated detection of individual oscillations we are able to identify two types of behavior for the cell: "regular" vs. "bursting" oscillations. The latter display a Poisson-like distribution in the number of oscillations per burst. The long recordings also facilitate the calculation of the trace's correlation dimension, which is used to test for chaotic behavior in a system. The preliminary observation that this dimension grows with the embedding dimension implies that fluctuations in the bundle's position are stochastic. Supported by NIH grant RO1 DC011380.

765 IHC Stereocilia Are Excited by at Least Four Mechanical Drives That, in Combination, Explain Formerly Anomalous Auditory-Nerve Data

John Guinan^{1,2}

¹Mass. Eye & Ear, ²Harvard Medical School

Background

The bending of inner-hair-cell (IHC) stereocilia controls cochlear output, but the mechanisms that produce this bending are poorly understood. The common conception that IHC excitation is due only to shearing between the reticular lamina (RL) and the tectorial membrane (TM) does not explain auditory-nerve (AN) data. Two key new concepts are: (1) for low-frequency sounds, the RL-TM gap varies cyclically and produces fluid flow within the gap that bends IHC stereocilia (Nowotny and Gummer 2006, PNAS 103:2120), and (2) outer hair cell (OHC) stereocilia length can change (Hakizimana et al. 2011, ARO Abstr. #355) so the RL-TM gap over OHCs is not fixed.

Methods

We hypothesize how fluid flows drive IHC stereocilia, and show that these drives explain AN data.

Results

Last year we postulated that, in addition to classic SHEAR, there are two other IHC drives: (1) TM-PUSH: For upward BM motion, the force that moves the TM compresses the RL-TM gap over OHCs causing inward radial flow past IHCs. (2) OHC-MOTILITY: Upward basilar-membrane (BM) motion causes OHC somatic contraction which tilts the RL, compresses the RL-TM gap over IHCs and expands the RL-TM gap over OHCs, thereby producing an

outward radial fluid flow. For upward BM motion these drives deflect IHC stereocilia in the inhibitory and excitatory directions, respectively. We now add a second drive that is inhibitory for upward BM motion, the CILIA-SLANT drive: Motions that produce large tilting of OHC stereocilia squeeze the supra-OHC RL-TM gap and cause inward radial flow past IHCs. Combinations of these drives explain: (1) the reversal at high sound levels of AN initial peak (ANIP) responses to clicks, and medial olivocochlear (MOC) inhibition of ANIP responses below, but not above, the ANIP reversal, (2) dips and phase reversals in AN responses to tones in cats and chinchillas, (3) hypersensitivity and phase reversals in tuning-curve tails after OHC ablation, and (4) MOC inhibition of tail-frequency AN responses.

Conclusion

The ability of these IHC drives to explain previously anomalous AN data provides strong, although indirect, evidence that these drives are significant. The OHC-MOTILITY drive is another mechanism, along with BM motion amplification, that uses active processes to enhance cochlear output. Overall, the success of the hypotheses presented here argues for a new view of how the cochlea works at frequencies below 3 kHz. Supported by RO1DC00235, P30DC005209

766 The Effect of Noise-Clicks on IHC Bundle Mechanics

Sonya Smith^{1,2}, Pierre Hakizimana³, Richard Chadwick², Anders Fridberger³

¹Howard University, ²NIDCD, ³Karolinska Institute

Background

Mechanotransduction, the process by which the hair cells convert mechanical stimuli into a electrical response, is managed by transduction (ion) channels located at the attachment points of the tip links. The transduction channels are opened by elastic elements, i.e. gating springs, and are stretched when the hair bundle is deflected toward its tall edge. A molecular gate that opens and closes based on the tensioning in the spring controls each channel. Noise-induced damage the hair bundles of the inner ear appears as disarray, fusion, or collapsing of the stereocilia. This damage may result from breakage of side links and tip links.

Methods

The effects of noise clicks on IHC stereocilia bundle mechanics were investigated at several frequencies in the apical turn of a guinea pig temporal bone preparation using time-resolved confocal imaging and optical flow algorithms. The experimental data was used with the Smith-Chadwick computational model to investigate the effect of the noise-clicks on stereocilia tip link tensioning and bundle mechanics.

Results

Preliminary data show that the noise clicks reduced the stereocilia bundle motion amplitude and this effect was

also consistent with a decrease in the cochlear microphonics.

Conclusion

The results of this study will show that the noise-click exposure may affect mechanotransduction through disruption of stereocilia mechanics.

767 Prolonged Deflections Suppress Active Hair Bundle Motion

Albert Kao¹, Sebastiaan Meenderink¹, Dolores Bozovic¹
¹UCLA, Department of Physics and Astronomy

Background

Active hair bundle motility is one of the signatures of the amplification mechanism in non-mammalian hair cells. Here we impose high-amplitude deflections on the hair bundle for 0.1-50 seconds. Due to incompleteness of the adaptation mechanism, this is expected to change the opening probability of the transduction channels, thus mechanically bringing the bundle out of its equilibrium state. Recovery of hair bundle motion was characterized, and the effects of calcium on the feedback mechanism were investigated.

Methods

Adult bullfrogs (*Rana Catesbiana*) were anesthetized and decapitated following the UCLA DLAM protocol to extract the sacculus in the inner ear. The epithelium was then placed in a two-compartment chamber to separate the solutions bathing the apical and basal side, artificial endolymph and perilymph respectively. Mechanical stimuli were applied using two techniques. For one set of experiments, a glass probe, made with a micropipette puller, was used to deflect the bundles. In another set of measurements, magnetic beads of ~ 1 micron diameter were attached to the stereociliary bundles, and a magnetic probe was used to impose deflections. To study the influx of calcium, hair cells were dissociated after incubation of protease XXIV for 10 minutes and papain for 20 minutes, and loaded with Fluo-4 AM.

Results

Traces of hair bundle motility recorded immediately post stimulation show a slow drift towards the equilibrium position, without oscillatory motion. Bundles recover their innate oscillation between 0.1 – 1 second after cessation of the stimuli, and the quiescent time (T_q) shows a strong dependence on stimulus duration. Decreased calcium concentration leads to a slower spontaneous oscillation, consistent with prior results in the field. The quiescent interval induced by deflection of hair bundles in a low-calcium environment is shorter, recovering more rapidly post stimulus cessation.

Conclusion

High-amplitude stimulus induces a quiescent interval in hair bundles, with a slow relaxation that exhibits two characteristic time scales. The two time constants of the recovery show a correlation coefficient of 0.47, indicating that the mechanisms are dependent of each other.

Calcium was found to play a significant role in modulating the effects of stimulus on active hair bundle motility. Blockage of the extrusion pumps that regulate its concentration inside the stereocilia was likewise seen to prolong the induced quiescence, indicating that calcium accumulation may underlie the suppression of spontaneous motility. Research was supported by NIH Grant No. 1R01DC011380.

768 Open and Closed-Loop Gain of the Mammalian Cochlear Amplifier

Sripriya Ramamoorthy¹, Alfred Nuttall¹

¹Oregon Hearing Research Center

Background

The cochlear amplifier is a hypothesized positive feedback process responsible for our exquisite hearing sensitivity. However, experimental evidence for or against the positive feedback hypothesis is still lacking.

Methods

In this study, we apply linear control theory to investigate the cochlear amplifier.

Results

We determine the open-loop gain and the closed-loop sensitivity of the cochlear amplifier from available measurements of basilar membrane vibration in sensitive mammalian cochleae.

Conclusion

We show that the frequency of peak closed-loop sensitivity is independent of the stimulus level and close to the characteristic frequency. This implies that the half-octave shift in mammalian hearing is an epiphenomenon of the cochlear amplifier. The open-loop gain is consistent with positive feedback and suggests that the high-frequency cut-off of the outer hair cell transmembrane potential in vivo may be necessary for cochlear amplification. Acknowledgment: This work is supported by NIH/NIDCD grant R01 DC000141.

769 In Vivo Measurement of Organ of Corti Vibrations Near the Mouse Round-Window Using Phase-Sensitive Fourier Domain Optical Coherence Tomography

Sripriya Ramamoorthy¹, Yuan Zhang¹, Tracy Petrie², Hrebesh Molly Subhash², Niloy Choudhury², Fangyi Chen¹, Ruikang Wang³, Steven Jacques², Alfred Nuttall¹

¹Oregon Hearing Research Center, ²Department of Biomedical Engineering, Oregon Health & Science University, ³Bioengineering & Ophthalmology, University of Washington

Background

Hearing loss often has its origin in pathological processes that alter the normal vibratory patterns of the organ of Corti inside the cochlea. Being a mammal and amenable to genetic manipulations, mouse is an excellent animal model to study human hearing and its pathology. However, it has been very challenging to measure the vibration response

of the mouse cochlea as the available technology is limited.

Methods

We have developed the phase-sensitive Fourier domain optical coherence tomography (PSFDOCT) and interferometry to image and simultaneously measure the in vivo vibrations of the mouse cochlea.

Results

In this work, we will present the image and in vivo measurements of the mouse organ of Corti vibration at high frequencies (> 50 kHz) viewed through the round-window. Basilar membrane (BM) vibration tuning curve and radial pattern along the BM for high sound levels will be presented.

Conclusion

Simultaneous in vivo measurement of imaging and vibration of organ of Corti in mouse near round window is possible using the PSFDOCT technique. This preliminary study will be improved to study mouse auditory physiology along with genetic modifications. Acknowledgments: This work is supported by NIH/NIDCD grants R01 DC010399 and R01 DC000141.

770 Evidence Against Power Amplification of the Cochlear Traveling Wave

Marcel van der Heijden¹, Corstiaan P.C. Versteegh²

¹Erasmus MC, ²Erasmus MC, Rotterdam, Netherlands

Background

The inner ear of mammals mediates sound-induced traveling waves that peak at a frequency-dependent location. It is widely assumed that active processes inject extra power into this wave, thereby enhancing sensitivity, but the power delivered by this cochlear amplification is unknown.

Methods

We determined the power carried by the traveling wave by combining two datasets: (1) We performed two-point interferometric recordings of the gerbil basilar membrane (16-kHz region) in response to tone complexes and derived group delay from the point-to-point phase curves. (2) A recent study by Ren et al. [Nature Commun. 2:216] reported the radial and longitudinal profiles of basilar membrane motion in the 16-kHz region. Using generic wave-physics techniques, we derived from those data the energy density of the traveling wave.

Results

(1) Group velocity increased from 0.9 m/s to 2.1 m/s with sound intensity (10-90 dB SPL). (2) The time average energy per length unit grew from 55 aJ/m to 1.4 pJ/m with sound intensity. (1+2) The power carried by the traveling wave grew from 51 aW to 3.0 pW with sound intensity. For intensities up to 40 dB SPL, the power of the traveling wave at its peak was 1 dB less than the acoustic power entering the middle ear. For higher intensities, the difference grew to 34 dB.

Conclusion

Our findings show that there is no net power gain from middle ear to the peaking traveling wave, and suggest that the nonlinear, compressive response of the cochlea may be realized by variable dissipation rather than saturating amplification.

771 Cochlear Nonlinearity: The Benefits of Logarithmic Compression

David Mountain¹

¹*Boston University*

Background

It has been hypothesized that the medial efferent reflex decreases the cochlear amplifier gain by just the right amount so that the nonlinearity in the basilar membrane response lines up perfectly with the inner hair cell nonlinear transduction process to produce a hair cell receptor potential that is proportional to the logarithm of the sound pressure level (Mountain, AIP Conf. Proc. 1403:238-243.). In this study it is shown that this logarithmic compression provides benefits for coding signals such as speech that have exponential amplitude distributions and also facilitates binaural processing.

Methods

Two theoretical approaches were used. The first approach was to analyze biologically important sounds (e.g. animal vocalizations) for their time-domain statistics and examine the effect of logarithmic compression on coding efficiency. The second approach was to represent signals in the frequency domain using Fourier transforms statistics and examine the effect of logarithmic compression on features related to sound-source localization.

Results

Animal vocalizations (e.g. human speech) often have a probability distribution for amplitude values that is exponential in nature. Logarithmic compression produces a probability distribution that is uniform, a distribution that is optimal for noisy communication channels such as the auditory nerve. The frequency-domain analysis shows that logarithmic compression facilitates the separation of interaural phase and intensity cues. Furthermore it shows that there can be a unique mapping between these interaural cues and the spatial location of a sound source.

Conclusion

The logarithmic compression that is hypothesized to be present at moderate and high sound levels facilitates coding in the auditory nerve and subsequent coding in the medial superior olive complex that contributes to sound-source localization.

772 Experimental Evidence for Cochlear Amplification and Its Basis in OHC Somatic Forces

Wei Dong¹, Elizabeth Olson¹

¹*Columbia University*

Background

Normal mammalian hearing relies on outer-hair-cell (OHC) based electromechanical forces that augment the cochlea's mechanical response to sound, known as cochlear amplification. Cochlear amplification is frequency- and level-dependent. It amplifies low level sounds more than high level sounds, and the amplification occurs at frequencies close to the local best frequency (BF). Cochlear amplification has been explored theoretically and experimentally. However, the coupling between the OHC electromechanical activity and mechanical responses along the cochlear partition is not well understood.

Methods

We probed cochlear electromechanics with spatially and temporally coincident voltage and pressure measurements using a novel hybrid-sensor positioned close to the sensory tissue. Experiments were performed in anesthetized young adult gerbils. The left pinna was removed and the bulla was widely opened. The basilar membrane (BM) was accessed through a hand-drilled hole in scala tympani (ST) in the basal turn of the cochlea. Compound action potential (CAP) responses to tone pips were recorded at different stages of the experiment to monitor cochlear condition. The hybrid-sensor was constructed in the lab, and was composed of our lab's standard micro-pressure sensor (OD 125 microns) with a 28 micron diameter, isonel-insulated platinum electrode adhered to its side.

Results

With simultaneous mapping of the intracochlear pressure and extracellular voltage at a series of distances from the BM, BM displacement was derived, resulting in a trio of coincident pressure, voltage, and displacement measurements. We found a phase shift between voltage and displacement, approximately half an octave beneath the peak frequency, which would allow power injection from OHC somatic forces. Moreover, at low SPL the phase between pressure and displacement indicated negative resistance, signifying that biomechanical elements within the sensory tissue were amplifying the power in the traveling wave.

Conclusion

These results are the most concrete evidence for intracochlear power amplification to-date and support OHC somatic forces as its source.

773 Power Flow Calculation in the Cochlea by Estimation of the Spatial Patterns of Intracochlear Pressure and Basilar Membrane Response

Yizeng Li¹, Tianying Ren², Karl Grosh¹

¹University of Michigan - Ann Arbor, ²Oregon Health and Science University

Background

Power flow in the cochlea is an important indicator of the presence (or absence) of energy generation from active process, the so-called cochlear amplifier. Calculation of spatial power flow requires the knowledge of both the basilar membrane (BM) velocity and the intracochlear pressure in the spatial domain. However, due to technical difficulties, direct measurements of these two quantities with fine spatial resolution are not available. The purpose of this study is to calculate the power flow in the cochlea based on available experimental data.

Methods

The spatial pattern of the BM velocity is estimated from the BM spectrum response by using the frequency-location mapping. Measured BM spatial response around a best-frequency (BF) place is used to adjust the transformation by using the traditional frequency-location mapping. The intracochlear pressure is estimated from both the WKB method and the finite element method (FEM) as a postprocessing step, using the measured (near the BF place) or estimated (over a larger spatial range) BM velocity as the input. The accuracy of the pressure estimation is checked by comparing the application of the algorithm to the self-consistent FEM data, using FEM predicted BM velocity as the input. The power flow in the cochlea is calculated at each cross section along the longitudinal direction.

Results

The developed algorithm predicts the wavenumber as a function of the longitudinal coordinate near the BF place. The accuracy of predicted pressure depends on the spatial extent of the known BM velocity. Knowledge of the BM velocity basal to the BF place is found to be required for accurate power estimation.

Conclusion

The power flow in the cochlea decays longitudinally if the cochlea is passive. In an active cochlea, the power flow increases significantly around the BF place.

774 Intracochlear Pressures with Bone Conduction Stimulation in Human Temporal Bones

Christof Stieger^{1,2}, Nakajima Hideko¹, John Rosowski^{1,3}

¹Massachusetts Eye and Ear Infirmary, Harvard Medical School, ²University Hospital Basel, ³Speech and Hearing Bioscience and Technology, MIT-Harvard Division of Health Sciences and Technology

Background

Experimental studies on bone conduction on temporal bones or anatomical whole heads have often measured the velocity or acceleration of the promontory as an estimate for the cochlear input. The aim of this study is to measure pressures in cochlear scalae to investigate the mechanism of bone conduction on temporal bones. Measurements of intracochlear pressures during sound stimulation and round-window stimulation have provided important information. Similarly, the differential pressure across the partition – which estimates the cochlear drive at the base of the cochlea – can be measured during bone conduction, providing information not previously available.

Methods

Custom-made fiberoptic pressure sensors (diameter of 200 μm) were used to simultaneously measure the intracochlear pressures of the scala vestibuli and the scala tympani in human temporal bones. After insertion of the sensors (100 μm deep) through cochleostomies, the sensors were sealed to the surrounding bone with dental impression material (Jeltrate) followed by dental cement to firmly fix the sensors to the cochlear promontory, minimizing relative movement of the sensors with respect to the bone. Holders for the fiberoptic cables were released to remove significant friction along the cable to allow them to vibrate freely. The bone was stimulated with pure tones between 100-20000 Hz using a commercially available bone anchored hearing system at a constant electrical voltage (1 V peak).

Results

During bone conduction stimulation, the relative movement of the fiberoptic sensors near the cochleostomies versus bone was generally below 5 dB, thus the sensors were vibrating similarly to the cochlea. Intracochlear pressures with signal to noise ratios of more than 10 dB and linear were recorded for frequencies between 300 and 8000 Hz. In the same frequency band, the magnitude of the differential pressure during bone conduction stimulation was in the same order of magnitude as the differential pressure obtained with ear-canal sound stimulation of 1 Pa.

Conclusion

With modifications of our method for intracochlear pressure measurements, we can now understand the effect of bone conduction on scalae pressures and the cochlear drive in human temporal bones.

775 Intracochlear Pressure Measurement Using Commercially Available Sensors

J. Eric Lupo¹, Kanthaiah Koka², Daniel Tollin^{1,2}, James Easter^{1,3}

¹Department of Otolaryngology, University of Colorado School of Medicine, Aurora, Colorado, USA, ²Department of Physiology and Biophysics, University of Colorado School of Medicine, Aurora, Colorado, ³Cochlear Boulder LLC, Boulder, Colorado, USA

Background

Measurement of differential intracochlear pressure has proven to be a useful technique for the exploration of normal and pathological processes of ossicular transmission and the effectiveness of stimulation through bone conduction and the round window. Previous studies have employed custom-fabricated micro-optical pressure sensors with special purpose signal-conditioning circuitry, or have taken measurements at two different sound pressure levels so as to overcome the dynamic range limitations of commercially available sensors.

Methods

In this study, a system using off-the-shelf fiber optic pressure sensors and signal conditioners was used for measurement of intracochlear pressures in human cadaveric temporal bones concurrently with laser Doppler vibrometry (LDV) measurement of ossicular and round window velocities at the same sound pressure levels. Measurements of pressures in the scala vestibuli (SV), scala tympani (ST) and external auditory canal (EAC) were made concurrently with LDV measurement of either stapes or round window velocity.

Results

Experimentally obtained estimates of SV/EAC and ST/EAC transfer functions, middle ear gain and group delay, cochlear fluid volume velocity and cochlear impedance were taken for a sample of normal human temporal bones and found to be consistent with previously published results.

Conclusion

The technique of using off-the-shelf fiber optic pressure sensors and signal conditioners offers a significant reduction in the cost and difficulty of intracochlear pressure measurement and may prove useful in the further exploration of normal and pathological auditory mechanics, assessment of performance in acoustic implants, and modeling of acoustic trauma.

776 Local Transfer Characteristics of the Basilar Membrane

Corstiaen Versteegh¹, Marcel van der Heijden¹

¹Department of Neuroscience, Erasmus MC, Rotterdam, The Netherlands

Background

Studies on cochlear mechanics mainly report motion of single basilar membrane (BM) locations. However, comparison of responses from two locations in the same preparation can give much additional information on the

propagation of the traveling wave. In a recent study, Ren et al. [2011, PlosOne 6:e20149] reported two-point BM recordings and introduced "local transfer functions," obtained by dividing the complex spectra of the responses at the two points to identical stimuli. This cancels out any irregularities in calibration and/or middle-ear transfer. In this study, we used local transfer functions to analyze the propagation of the traveling wave.

Methods

A single-point laser vibrometer measured the motion of two beads placed (typically <400 μm apart) on the BM in anesthetized Mongolian gerbil. We stimulated with irregularly-spaced, equal-amplitude tone complexes of varying sound intensity. The responses of the two beads to identical stimuli were used to construct local transfer functions.

Results

(1) Phase velocity and wavelength of the traveling wave were strongly intensity dependent, confirming the findings of Ren et al. (2) Phase velocity was minimal for frequencies just below the characteristic frequency (CF) and did not decrease further with increasing frequency. (3) Above CF, bead-to-bead amplitude and bead-to-bead phase both steadily decreased with frequency; their relative rate was approximately 54 dB/cycle.

Conclusion

(1) The strong dependence of phase velocity on intensity suggests that damping is not the only mechanical property of the cochlear partition that changes with intensity. Most likely, the effective stiffness of the BM changes with intensity, too. (2) The absence of a continued decrease of phase velocity with frequency, even for frequencies well above CF, indicates that resonance does not play a role in the frequency selectivity of the BM. (3) The ratio of amplitude and phase decrease observed above CF contradicts the mass dominated motion expected from resonance, and is consistent with a damping dominated motion expected from the assumption that the cochlear partition has negligible fixed mass.

777 Transmission of Distortion Products in the Mammalian Cochlea

Wei Dong¹, Elizabeth Olson¹

¹Columbia University

Background

Otoacoustic emissions (OAEs) are sounds originating in active cochlear mechanics that travel back out to the ear canal (EC). The mechanism by which OAEs are transported out through the cochlea is not certain. In most cochlear models, the cochlea was assumed to operate similarly in forward and reverse propagation and the OAE was supposed to travel out of the cochlea via a reverse traveling wave along the cochlear partition. Another possibility is that reverse transmission is mediated via a compression pressure in the cochlear fluid. Past experimental observations have implicated both these reverse transmission modes. To probe the role of cochlear

fluid in reverse transmission, two-tone stimulation was used and the distortion products (DPs) generated in the cochlea were considered to be the intracochlear sound sources. The DPs drove the stapes in reverse and were detected in the EC as distortion product otoacoustic emissions (DPOAEs). Reverse transmission was characterized by comparing intracochlear pressure responses at the basilar membrane (BM) and at the stapes.

Methods

Experiments were performed in anesthetized young adult gerbils. The left pinna was removed and the bulla was widely opened. The BM was accessed through a hand-drilled hole in scala tympani (ST) ~ 2.2 mm from the base (~20% of the cochlear length). Simultaneously, the intracochlear pressure responses were measured in scala vestibuli (SV) at the very base, next to the stapes. Compound action potential (CAP) responses to tone pips were recorded at different stages of the experiment to monitor the cochlear condition.

Results

Comparison between the ST and SV pressures at primary and DP frequencies allowed us to characterize sound transmission in the forward and reverse directions. By comparing the phases of the ST and SV pressure the travel delay between the two locations was determined, and reverse transmission was found to be consistent with a reverse traveling wave. In addition, transverse spatial variations in ST pressure were similar at primary and DP frequencies. Because the spatial variation reflects traveling wave wavelength, this similarity reinforced the notion that reverse propagation was mainly via a traveling wave mode along the cochlear partition, rather than via a compression pressure through the cochlear fluid.

Conclusion

Sound reverse propagation is primarily via a reverse traveling wave, rather than the cochlear fluid.

778 Making Waves in the Tunnel of Corti

Aleks Zosuls¹, Laura Rupprecht¹, David Mountain¹

¹Boston University

Background

Evidence of fluid flow in the tunnel of Corti (ToC) was demonstrated by Karavitaki (Biophysical Journal, vol.92, p.3284-3293). Experiments by Chen et. Al. (Nature Neuroscience, vol.14, p.770-774) show that the basilar membrane (BM) and reticular lamina don't always move in phase. This differential motion could create a local pressure in the fluid filled ToC. These results indicate that fluid flow in the ToC may be significant for tuning and coupling in the hearing organ.

Methods

Experiments were performed on fresh excised gerbil cochleae. The scala vestibuli and tympani were opened to access and image the organ of Corti (OC). A blunted micropipette pushed on the BM under the outer pillar cell

to create a point pressure. The pipette was driven by a piezoelectric stack. Radial motion of the inner hair cell stereocilia hair bundles (IHCSS) and lateral motion of the tunnel crossing fibers (TCF) in the ToC was observed by stroboscopic imaging under high magnification. The motion of IHCSS and TCF bundles was quantified using a cross correlation algorithm.

Results

When the probe was indenting the BM, the TCF fibers moved longitudinally (basal or apical) away from the probe. Assuming the TCF's move with the flow of fluid in the ToC, the TCF motion can be interpreted as flow in the tunnel. There was a 180 degree transition at the probe location signifying the fibers moving in opposite directions (figure1). When moving away from the probe basal or apical there was a building phase delay in the fiber motion that is evidence of traveling wave propagation (figure1). The propagation velocity was estimated via curve fitting to be 2.3 m/s. The fit ignored data points near the probe to eliminate the transition region.

When the probe was indenting the BM the IHCSS moved toward the modiolus due to motion of the OC. Similar to the TCF phase, the phase of the IHCSS had a building delay moving away from the probe (figure1). This is evidence of a travelling wave with a propagation velocity estimated to be 2.2 m/s.

Conclusion

There is no evidence that the pillar cells move longitudinally during the probe stimulation which indicates that the TCF's are driven by fluid flow, not movement of their anchor points. The similar traveling wave velocities in both structures indicate that there is coupling between IHCSS motion and fluid flow in the ToC.

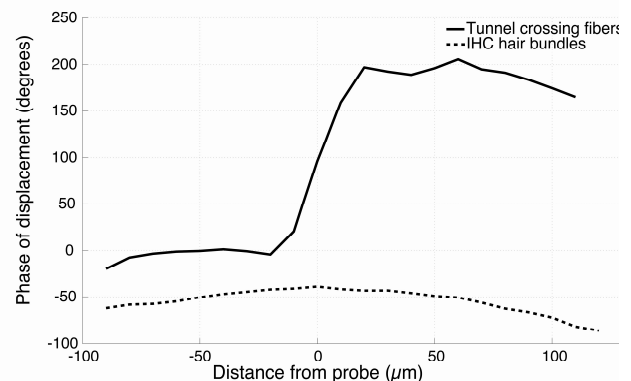


Figure 1. Solid line is phase response of lateral displacement of tunnel crossing fibers. Dashed line is phase response of radial motion of inner hair cell stereocilia bundles. Negative distances from the probe are basal, positive distances are apical.

779 Assessment of Superior Canal Dehiscence Location and Size on Intracochlear Sound Pressures

Marlien Niesten^{1,2}, Daniel Lee¹, Christof Stieger^{1,3}, John Rosowski^{1,4}, Wilko Grolman², Heidi Nakajima¹

¹Massachusetts Eye and Ear Infirmary, Harvard Medical School, ²University Medical Center Utrecht, the

Netherlands, ³University Hospital Basel, ⁴Speech and Hearing Bioscience and Technology, MIT-Harvard Division of Health Sciences and Technology

Background

Superior canal dehiscence (SCD) is a defect in the bony covering of the superior semicircular canal. Patients with SCD syndrome present with a wide range of hearing loss. Some clinical studies have suggested that an increase in SCD size is associated with increased hearing loss, while others have observed no association. Our previous human cadaveric temporal bone study showed that increase in dehiscence size (up to 2 mm long and 0.7 mm wide) causes a low-frequency monotonic decrease in the cochlear drive across the partition, consistent with increased hearing loss. At stimulus frequencies of more than 1 kHz, a small dehiscence (0.5 mm diameter) sometimes produced a larger decrease in cochlear drive than larger dehiscences. But the effects of larger SCDs (> 2mm long) were not studied, although most SCD patients have larger than 2 mm-long SCDs. Furthermore, it is unknown whether hearing is affected by the location of the SCD. In this study we assess the effect of SCD location and the effect of large sized SCD on intracochlear pressures.

Methods

We used simultaneous measurements of intracochlear sound pressures in scala vestibuli and scala tympani to determine the sound-pressure difference across the cochlear partition, which is a measure of hearing loss in a temporal bone preparation. We measured the pressure difference before and after SCDs at different locations (e.g. closer to the ampulla of the superior semicircular canal or closer to the common crus), and for different dehiscent sizes (including larger than 2 mm long and 0.7 mm wide).

Results

Our measurements suggest: 1) Changes in SCD location do not affect the intracochlear pressure difference. 2) Larger SCDs produce larger decreases in the pressure difference at low frequencies. However, the effect of SCD size seemed to saturate as the size increased above 2-3 mm long and 0.7 mm wide. Although these trends were generally consistent across ears, the amount of pressure change due to dehiscence varied across ears.

Conclusion

These findings show that SCD size can help explain some of the variability of hearing loss in patients and that the location of the SCD does not influence the amount of hearing loss. However, different ears varied in the extent of hearing loss for similar SCD sizes.

780 Decreasing Stiffness Reduces Spread of Excitation Via Tectorial Membrane Waves

Shirin Farrahi^{1,2}, Roozbeh Ghaffari¹, Dennis Freeman^{1,2}

¹MIT Research Laboratory of Electronics, ²MIT Department of Electrical Engineering and Computer Science

Background

Classical models have treated the tectorial membrane (TM) as a resonant system that can increase sensitivity and sharpen cochlear tuning (Allen, 1980). Recently, it has been shown that the TM supports longitudinal traveling waves (Ghaffari et al, 2007) and that the spatial extent of these waves is strongly correlated with cochlear tuning (Ghaffari et al, 2010). Here we investigate the relationship between stiffness and tuning for TM waves and compare this relation to predictions from resonance models.

Methods

We measured wave and material properties of isolated mouse TMs equilibrated at pH 7 and 4. Wave decay constants and speeds were measured by stimulating suspended TM samples at acoustic frequencies (Ghaffari et al, 2007). TM stiffness and viscosity were measured using microfabricated shear impedance probes (Gu et al, 2008).

Results

Reducing bath pH from 7 to 4 decreased shear stiffness (45% change) but had a minor effect on shear damping, as predicted by gel models of the TM (Freeman et al, 1997). Wave measurements at normal and acidic pH showed that the spatial extent of TM waves decreased by 42% but wave speed changed relatively little (<12%). These findings suggest that decreasing shear stiffness (without changing viscosity) reduces spread of excitation via TM waves.

Conclusion

Our results show that decreasing stiffness reduces spread of excitation in TM waves. By scaling symmetry, this change would tend to sharpen cochlear tuning. In contrast to previous models, this sharpening occurs without changes in viscous damping in the subtectorial space (Allen, 1980) or changes in outer hair cell motility (Neely, 1993). These findings show that TM wave and resonance theories differ significantly. While both suggest that the TM plays an important role in determining cochlear tuning, the underlying mechanisms are completely different.

781 In Vivo Vibrometry at the Apex of the Unopened Mouse Cochlea

Simon Gao^{1,2}, Patrick Raphael², Rosalie Wang², Brian Applegate³, John Oghalai²

¹Rice University, ²Stanford University, ³Texas A&M University

Background

The study of cochlear mechanics has provided important insights into cochlear function. Previous experiments from the base of the opened, mammalian cochlea have shown frequency selectivity and non-linear compression. However, in vivo measurements of cochlear mechanics

have traditionally been difficult to obtain at the apex of the mammalian cochlea. Recent advancements in imaging technology provide the opportunity to make such measurements. Herein, we present in vivo images and measurements from the apex of unopened mouse cochlea using spectral domain optical coherence tomography (OCT).

Methods

Spectral domain OCT is a non-invasive interferometric imaging technique that generates images based on depth-resolved sample reflectivity through the use of a fast Fourier transform. By analyzing the phase of the reflected signal at each depth, OCT can also be used as a vibrometer. Using OCT, we were able to visualize and measure organ of Corti vibrations approximately a half turn from the mouse cochlear apex. At the lowest stimulus intensity, we averaged to ensure a noise threshold <1nm, defined as the mean of the noise plus three times the standard deviation of the noise.

Results

The characteristic frequency (CF) of the locations we recorded from was between 7 to 10 kHz. We found that compression was highest at the CF with growth rates of ~0.2 dB/dB. The Q10-dB value at a stimulus level of 50 dB SPL was ~2. These values are similar to previously measured values from the cochlear base in other species with CFs of between 6 to 18 kHz.

Conclusion

Our results suggest that the cochlear amplifier functions in the mouse apex much like it does in the base of larger mammals.

782 Handling of Experimental Data on the Cochlea Obtained with Optical Coherence Tomography (OCT)

Egbert de Boer¹, Alfred L. Nuttall²

¹AMC-OHSU, ²Oregon Health & Science University

Background

With the technique of Optical Coherence Tomography (OCT) it is possible to measure movements of the basilar membrane (BM) and the Reticular Lamina (RL) separately. In the dead animal these movements were found to be nearly identical. In the living animal, in a viable cochlea, the RL moves in the region of maximum response with an amplitude about three times larger and a phase difference less than 90 degrees.

Methods

This implies that for the intact cochlea we have to take into account a definite oscillatory movement of the fluid inside the Organ of Corti (OoC) and the Internal Spiral Sulcus (ISS). In a most simplified and perhaps exaggerated way it can be stated that 'activity' of Outer Hair Cells (OHCs) operates on this mass of fluid.

Results

It will be shown how this problem can be treated in cochlear modeling. Specific experimental evidence on lateral fluid motion lacking, we have to follow paths defined by assumptions about the movements of the fluid contained in those two spaces.

Conclusion

The consequences of various sets of assumptions will be demonstrated.

With the technique of Optical Coherence Tomography (OCT) it is possible to measure movements of the basilar membrane (BM) and the Reticular Lamina (RL) separately. In the dead animal these movements were found to be nearly identical. In the living animal, in a viable cochlea, the RL moves in the region of maximum response with an amplitude about three times larger and a phase difference less than 90 degrees. This implies that for the intact cochlea we have to take into account a definite oscillatory movement of the fluid inside the Organ of Corti (OoC) and the Internal Spiral Sulcus (ISS). In a most simplified and perhaps exaggerated way it can be stated that 'activity' of Outer Hair Cells (OHCs) operates on this mass of fluid. It will be shown how this problem can be treated in cochlear modeling. Specific experimental evidence on lateral fluid motion lacking, we have to follow paths defined by assumptions about the movements of the fluid contained in those two spaces. The consequences of various sets of assumptions will be demonstrated.

783 Lgr5-Positive Cells Contribute to Hair Cell Regeneration in the Damaged Mouse Utricle

Tian Wang¹, Renjie Chai¹, Xuan-Phien Pham¹, Lindsey May², Vikas Nookala¹, Genevieve Huang¹, Lisa L. Cunningham², Alan G. Cheng¹

¹Department of Otolaryngology-Head and Neck Surgery, Stanford University School of Medicine, ²National Institute on Deafness and Other Communication Disorders, National Institutes of Health

Background

Hearing loss and balance disturbance are sensory disorders affecting millions of patients, with sensory hair cell (HC) loss being a primary pathology in both disorders. Previous studies illustrated that the postnatal mouse utricles contain cells capable of regenerating HCs after pathologic HC loss, yet our understanding of their exact identity and regulatory mechanisms is limited. Wnt signaling regulates cellular repair in several organ systems. Here, we hypothesize that the Wnt target gene Lgr5 marks HC precursors in the damaged mouse utricle.

Methods

Utricles from embryonic (E) and postnatal (P) mice were examined for Lgr5 expression. To induce HC loss, P3 mice were cultured with neomycin (1.0mMx24hr) and then in drug-free media for 2 to 13 days. Lgr5EGFP-CreERT2/+ transgenic mice or quantitative PCR were used to determine Lgr5 expression. To fate-map Lgr5+ cells, a cre-loxP approach using the Lgr5EGFP-CreERT2/+;

Rosa26RtdTomato/+ mice was taken. Time-lapse imaging of fate-mapped cells in cultured utricles using spinning disk confocal microscopy was performed. After culture, tissues were fixed and immunostained for markers of HCs (Myosin7a), supporting cells (Sox2 and Plp1), and cell death (TUNEL).

Results

In the Lgr5EGFP-CreERT2/+ mice, EGFP expression was found in HCs and supporting cells at E15.5 and 18.5, then became undetectable by P3. After neomycin treatment, Lgr5-EGFP was upregulated in supporting cells in the striolar region, where HC loss concentrated, and subsequently persisted for at least 6 days. Quantitative RT-PCR also found Lgr5 upregulation in neomycin-treated wildtype utricles. Two days after damage, myosin7a+ HCs decreased by 56% and Lgr5+ cells (70.3±9.2 per 20,000 μm²) were 99.8% Myosin7a-, 99.4% Sox2-, 100% Plp1+, and 97% TUNEL-. Five days after damage, lineage tracing of Lgr5+ cells showed that 84.7% of traced, tdTomato+ cells (48.0 per organ) were myosin7a- residing in the supporting cell layer. tdTomato+, myosin7a+ cells significantly increased from 5 to 12 days after damage (7.3±2.5 to 17.7±7.0 per organ). Time-lapse imaging from 2.5-6 days after damage demonstrated that tdTomato+ cells underwent dynamic morphological changes, a subset of which was reminiscent of nascent HCs.

Conclusion

We found Lgr5 expressed in the embryonic utricles and downregulated at birth. HC loss reactivates Lgr5-EGFP expression among supporting cells that were fate-mapped to regenerated HC-like cells. Together our data suggest that Lgr5+ cells behave as facultative HC precursors.

784 Regeneration of Mammalian Cochlear and Vestibular Hair Cells Through Hes1/Hes5 Modulation with siRNA

Xiaoping Du¹, Wei Li¹, Xinsheng Gao¹, W. Mark Saltzman², Christopher J. Cheng², Matthew West¹, Richard Kopke^{1,3}

¹Hough Ear Institute, Oklahoma City, OK 73112, ²Dept. of Biomedical Engineering, Yale University, ³Oklahoma Medical Research Foundation, Oklahoma City, OK 73014

Background

The Notch pathway is a cell signaling pathway determining initial specification and subsequent cell fate in the inner ear. Previous studies have suggested that new hair cells (HCs) can be regenerated in the inner ear by manipulating the Notch pathway.

Methods

The organ of Corti and vestibular maculae of postnatal day 3 (P3) mouse pups were harvested and cultured in vitro. siRNA to Hes1 and Hes5 using a transfection reagent or siRNA to Hes1 encapsulated within poly(lactide-co-glycolide acid) (PLGA) nanoparticles were added to cultures.

Results

Increased HC numbers were observed in the cultured and untreated cochleae and maculae, and in the cultured cochleae and maculae pre-conditioned with a HC toxin (4-hydroxy-2-nonenal or neomycin) and then treated with the various siRNA formulations. A decrease of Jagged1 positive supporting cells (SCs) was observed in cultured cochleae of mouse pups treated with Hes1 siRNA and transfection reagent. Treating cochleae with siRNA to Hes1 associated with a transfection reagent or siRNA to Hes1 delivered by PLGA nanoparticles decreased Hes1 mRNA and up-regulated Atoh1 expression allowing SCs to acquire a HC fate. Experiments using cochleae and maculae of p27kip1-GFP transgenic mouse pups demonstrated that newly generated HCs trans-differentiated from SCs. PLGA nanoparticles are non-toxic to inner ear tissue, readily taken up by the tissues, and present a synthetic delivery system that is a safe alternative to viral vectors.

Conclusion

These results indicate that when delivered using a suitable vehicle, Hes siRNAs are potential therapeutic molecules that have the capacity to regenerate new HCs in the inner ear and possible restore human hearing and balance function.

785 Preparing the Cochlea for Stem Cell Implantation

Yong-Ho Park^{1,2}, Yehoash Raphael¹

¹Kresge Hearing Research Institute, Department of Otolaryngology, University of Michigan, ²Department of Otolaryngology, Chungnam National University, Daejeon, South Korea

Background

Technology for growing hair cells from stem cells (SCs) in vitro is rapidly advancing. In parallel, it is necessary to design methods for inserting SCs into the auditory epithelium (AE) of deaf ears devoid of hair cells (HCs), in vivo. Inserting cells into an epithelial cell layer is complicated in any organ, and is even more complex in the hostile, high potassium environment of the scala media (SM). The robust junctional complexes between cells in the AE present an additional obstacle to SC integration. A successful therapy will require methods that optimize survival of exogenous cells injected into SM and their integration into the AE by making the cochlear environment more tolerable and relaxing intercellular junctions. To that end, we evaluated the survival of cells in artificial cochlear fluids in vitro and then manipulated the cochlear environment in vivo to open intercellular junctions and increase its hospitable to exogenous cells.

Methods

Cell survival in cochlear fluids was evaluated by monitoring fluorescence of mCherry labeled HeLa cells after adding artificial fluids (endolymph, perilymph or endolymph+perilymph) to the culture. In vivo experiments used neomycin-deafened guinea pigs. To render SM more hospitable to exogenous cells, we reduced potassium

levels by (a) injecting furosemide, and (b) replaced the endolymph with artificial perilymph. To disrupt the adherens junctions in the AE we injected sodium caprate via a cochleostomy. We then injected HeLa cells into the SM. Changes of the AE junctions were evaluated in whole-mounts of the AE stained for ZO-1. Presence of HeLa cells in the cochlea was evaluated by fluorescence stereomicroscopy followed by epi-fluorescence on whole-mounts of AE.

Results

Cells exposed to artificial endolymph detached from the dish and became spherical promptly. Most cells died within six hours. Cells cultured in perilymph or in the endolymph-perilymph mixture survived. In the AE of sodium caprate-treated ears, gaps appeared between cells, suggesting deterioration of apical junctions. One day after the injection, implanted exogenous HeLa cells were observed in the AE and other areas in ears treated with sodium caprate and furosemide.

Conclusion

Transient manipulations of the cochlear environment facilitate survival of exogenous cells for at least one day. Further refinements are needed to prepare the deaf cochlea for SC therapy.

Acknowledgments: Supported by NIH/NIDCD grants R21-DC011631 and P30-DC05188.

786 Age-Related Alterations in Neural Crest-Derived Cells of the Mouse Inner Ear

Hainan Lang¹, Shawn M. Stevens¹, Yazhi Xing¹, Luke T. Havens¹, Xinping Hao¹, John E. Baatz¹, Edward L. Krug¹, Jeremy L Barth¹

¹Medical University of South Carolina

Background

Glial cells in the auditory nerve and cells in the cochlear lateral wall undergo turnover in response to several stress conditions, although their ability to repopulate themselves declines with age. The neural crest is a transient embryonic structure that gives rise to a wide variety of cell types including glial cells, some neurons of the peripheral nervous system and mesenchymal cells. Multi-potent neural crest-derived stem cells (NCSCs) have been found in several adult tissues and organs suggesting an important role of the neural crest-derived cells in the maintenance of adult tissue homeostasis and self-repair after injury. This study seeks to correlate the effects of aging on the self-renewal of neural crest-derived cells in the adult inner ear with age-related alterations in gene expression profile.

Methods

The sphere formation assay was used to determine the relative numbers of NCSCs in the auditory nerves and cochlear lateral wall of young adult (1-3 mo) vs. aged (18-30 mo) CBA/CAJ mice. Gene expression profiles of cochlea from young adult vs. middle to early old aged (12-16 mo) mice were examined using gene microarray,

proteomic analysis, western blot and quantitative immunohistochemistry. Twelve to 16 month old mice were used to determine changes in gene expression that might precede significant cell loss that occurs in old age.

Results

Our data show that cells isolated from the auditory nerves and cochlear lateral wall tissues of both young and old adult mice formed spheres in culture that displayed extensive self-renewal capacity and contained cells that express p75 and Sox10, markers of a neural crest lineage. Application of ouabain, an inhibitor of Na⁺/K⁺-ATPase, into the cochlea significantly increased the number of NCSCs from the auditory nerves of young adult mice. This was not the case with auditory nerves of older mice. Gene expression profiles of cochlea from young adult vs. middle to early old aged mice revealed age-related changes in expression of more than 40 genes associated with the regulation/differentiation of neural crest-derived cells.

Conclusion

Age-dependent hearing loss and pathological changes in the inner ear may be due to a decline in the number of neural crest-derived cells suggesting an age-related loss of self-renewal capacity. Expression profiling studies revealed potential targets for restoring cell renewal in the adult inner ear. This study was supported by NIDCD R01DC7506, P50DC00422 and NCRR P20RR16434.

787 Molecular Characteristics of Severely Damaged Organ of Corti

Elizabeth Oesterle¹, Stefan Heller², Albert Edge³, Ling Tong¹, Sean Campbell¹

¹University of Washington, ²Stanford University, ³Harvard University

Background

Humans with severe or profound hearing loss have cochlear regions where putative support cells remain despite total hair cell loss, as well as regions where the organ is replaced with a flat unspecialized epithelium (Teufert et al., 2006; Hoa et al., 2010 ARO). Understanding the characteristics of the cells that remain after hair cell loss will be crucial to identifying feasible regenerative procedures.

Methods

Adult C57BL/6J mice were damaged by kanamycin/furosemide injection (Oesterle et al., 2008), and transgenic mice that express diphtheria toxin (DT) receptor under control of the HC-specific promoter pou4f3 were injected with DT to kill hair cells. Mice were killed 8 days or 2 months later, and whole-mount preparations of the organ of Corti were immunohistochemically processed using support cell (acetylated tubulin, Kir 4.1, monocarboxylate transporter 2 (MCT2), Sox2) and sulcus cell markers (CD44).

Results

With both damage paradigms, regions are seen where putative support cells remain despite total hair cell loss.

Sox2, MCT2, and acetylated tubulin immunolabeled cells in these regions, and CD44 was expressed in cells in the flanking inner and outer sulcus. Regions of flat epithelium were seen in the C57BL/6J mice 2 months after kanamycin/furosemide administration. In the apical and middle turns of these animals, patches of flat epithelium were interspersed between segments of damaged epithelium containing pillar and Deiters' cells (acetylated tubulin+/Sox2+ cells). Fewer nuclei are present in the flat epithelium and these cells express CD44, but not Sox2 or acetylated tubulin.

Conclusion

1) Differentiated support cells can survive despite total hair cell loss and retain at least some cellular identity, and 2) Sulcus cells may migrate into the region formerly occupied by the organ of Corti.

Supported by the Hearing Health Foundation and NIDCD grants R01 DC03944 and P30 DC04661.

788 Deciphering the Strategy of Hair Cell Regeneration in Zebrafish Lateral Lines

Xiaoxiao Mi¹, Huihui Liu¹, Yuting Wu¹, Hong Guo¹, Yingxing Li¹, Dong Liu¹

¹State Key Laboratory of Biological Membrane and Membrane Biotechnology, School of Life Sciences, PKU

Background

The capacity and capability of hearing restoration upon hair cell impairments in the ear are apparently species dependent, even though the hair cells are killed essentially in the same way. For instance, cisplatin, an anti-cancer drug, frequently induces hearing loss in patients and kills zebrafish hair cells of inner ear and lateral lines; however, only fish can regenerate the hair cells after the treatment is terminated. Therefore, we ask why and how regeneration program is triggered in the neuromasts, which cells within the neuromasts become the nascent hair cells, and how these cells decide to undergo proliferation vs. differentiation.

Methods

Transgenesis in zebrafish; in situ hybridization; immunohistochemistry; small chemical screen; live imaging.

Results

We have observed that neuromast hair cells undergo apoptosis during the cisplatin treatment, and the damaged neuromasts start a slow and steady regeneration meanwhile. Interestingly, when the cell death, induced by other reagent(s), is not apoptotic, the hair cell regeneration process is quicker; suggesting different types of hair cell death may result in different ways to regenerate. Molecularly, the cisplatin treatment enables higher expression of Atoh1 and Sox21 in the sensory and periphery support cells, respectively, and a rapid proliferation in a group of periphery non-hair cells. Furthermore, through small chemical compound screens of hair cell regeneration regulators, we've obtained 4

inhibitors and determined in which step(s) these compounds act.

Conclusion

Our study has laid a ground to explore the mechanism(s) underlying zebrafish lateral line hair cell regeneration.

789 The Role of Planar Cell Polarity Pathway in the Ectopic Regenerated Hair Cells

Regulated by the Dynamic ADF/destrin

Expression

Dong-Dong Ren¹, Kai Jin¹, Rui Ma¹, Fang-Lu Chi¹

¹eye, Ear, Nose And Throat Hospital, Fudan University

Background

Planar cell polarity (PCP) signaling regulates cochlear extension and coordinated orientation of sensory hair cells in the inner ear. Studies have shown retrovirally-mediated introduction of Atoh1 transcription factor is capable of causing some mature supporting cells to transdifferentiate into hair cells. ADF/Destrin is one important factor in actin depolymerization families, which is essential for several cellular processes including cell survival, shaping, cytokinesis and migration. However, the role of PCP pathway in ectopic regenerated hair cells regulated by dynamic ADF/destrin expression is still unknown.

Methods

Ad5-EGFP-math1 was used to over-express math1 in the cochlea of neonatal mice in vitro. We compared dynamic distribution of ADF/destrin between developing cochlear and the ectopic regenerated hair cells, investigated the establishment of ectopic hair cell polarity and the relationship with ADF/destrin expression. We also observed the proliferation, differentiation and epithelial PCP in the lesser epithelial ridge (LER) down-regulated ADF/destrin after testosterone-BSA treatment in vitro.

Results

It showed that ADF/destrin distributed in some cuticular plate's border of both hair cells and supporting cells at E14.5, then expressed in the whole cuticular plate of hair cells and supporting cells at E18.5 and P1, there were no ADF/destrin in the hair cells after P4. Some ectopic regenerated Myo7a(+) cells expressed ADF/destrin within one week and disappeared 10 days after over-expressing Atoh1, which is compared with the high level differentiated ectopic hair cells. After ectopic regenerated Myo7a(+) cells developed actin-rich stereocilia, their basal body moved from center to the distal side, suggesting the underlying PCP establishment in ectopic regenerated myo(+) cells. The level of ADF/destrin decreased after testosterone-BSA treatment 12-24h in vitro, more Brdu(+) cells and Myo7a(+) cells were observed in LER, however, the CE and cell polarity of Ad5-EGFP-math1 infected LER is not affected obviously.

Conclusion

Our results indicate that ADF/destrin participate in the development of sensory epithelia in mammalian cochlear and ectopic hair cells induced by over-expressing Atoh1.

PCP signaling exists in the development of ectopic hair cells. Together, these data suggest that ADF/destrin dependent actin depolymerization maybe not essential for hair cell polarity while it is required for cell proliferation and differentiation of cochlear LER regions.

Supported by NSFC81028003, 81000413£-81271084; Shanghai Rising-Star Program 11QA1401100; The Research Fund for the Doctoral Program of Higher Education 20110071120086; 973 Program(2011CB504500£-2011CB504506).

790 Characterization of Human Pluripotent Stem Cell Derived Otic Progenitor-Like Cells

Cynthia Chow¹, Parul Trivedi¹, Megan Duffey¹, Su-Chun Zhang¹, Samuel Gubbels¹

¹University of Wisconsin-Madison

Background

Hearing loss is primarily caused by loss of sensory hair cells (HCs) in the organ of Corti within the cochlea. Although human pluripotent stem cells are a promising source for cell therapy, there are few reports of the efficient generation of otic progenitor or HC-like cells from human pluripotent stem cells. The auditory system develops alongside the central nervous system and is dependent for proper formation upon the signaling from the developing adjacent neural ectoderm. This study tested the hypothesis that when directing human pluripotent stem cells towards a neural fate, a sub-population of the cells will become otic progenitor cells. This work is a continuation of prior investigations using a well-characterized neural differentiation paradigm to direct human embryonic and induced pluripotent stem cells towards an otic progenitor cell fate.

Methods

Human H9 ES cells and IMR90-4 iPS cells were differentiated using a well established neural differentiation paradigm. An otic progenitor-like population of cells was characterized using immunocytochemistry, RT-PCR and qPCR analysis.

Results

Neural differentiation of human pluripotent stem cells identified a distinct subpopulation of cells expressing markers of an otic progenitor fate. The gene transcript and the protein expression profile were consistent with that seen during early mammalian inner ear development. Furthermore, the sequence and expression pattern of marker transcripts during differentiation of human pluripotent stem cells towards an inner ear lineage in vitro appears similar to that seen during normal mammalian inner ear development. In addition, we have found that modification of the neural differentiation protocol guided by knowledge of early mammalian inner ear developmental signaling mechanisms reliably leads to an enrichment of this otic progenitor-like population. Ongoing studies aim to further optimize the culture paradigm to generate a more robust otic progenitor cell population for use in

development and disease modeling as well as transplantation-based studies.

Conclusion

Neural differentiation of both embryonic stem cells and induced pluripotent stem cells leads to the expression of a panel of marker transcripts characteristic of developing otic progenitor cells as analyzed by immunocytochemistry, RT-PCR and qPCR analysis.

791 Characterization of Canonical Wnt/ β -Catenin Signaling Activity in the Developing and Adult Mouse Cochlea

Bonnie Jacques^{1,2}, Zhiyong Wang¹, Chin-Chun Lu¹, Florin Vranceanu¹, Alain Dabdoub^{2,3}, Scott Thies¹

¹Fate Therapeutics, ²University of California San Diego School of Medicine Dept. of Surgery, Div. of Otolaryngology, ³Department of Otolaryngology, University of Toronto

Background

During development canonical Wnt/ β -catenin signaling plays important roles in organogenesis by regulating proliferation and differentiation. In more mature tissues this pathway functions in progenitor and stem cell maintenance. Lgr5, a downstream target of Wnt/ β -catenin signaling, is expressed in the embryonic and mature organ of Corti, and recent studies have identified a role for canonical Wnt signaling during cochlear sensory epithelium development. However, the pattern of direct Wnt/ β -catenin activity had yet to be characterized in adult cochleae, thus we utilized a transgenic reporter mouse which provides highly specific single-cell-resolution readouts of canonical Wnt activity to compare signaling in developing and adult cochleae.

Methods

We analyzed Wnt/ β -catenin activity patterns using cochleae from TCF/Lef:H2B-GFP reporter mice which possess six copies of a TCF/Lef responsive element linked to an hsp68 promoter that drives expression of a nuclear H2B-GFP fusion protein. Embryonic cochleae from stages E12-E17.5 and adult cochleae from 8-10-week-old mice were collected, and analyzed by immunohistochemistry (n>4 cochleae analyzed per stage). Tissue was co-immunostained with antibodies against the support cell/progenitor cell marker Sox2, and either the proliferation indicator Ki-67 or the hair cell marker MyosinVI.

Results

During the early proliferative phase of development, nuclear GFP activity was observed throughout the floor of the cochlear duct where in some cells it was co-expressed with the prosensory marker Sox2 and/or the mitotic marker Ki-67. At E14.5, during the onset of hair cell differentiation, the level of GFP expression was significantly reduced. By E17.5, when HC differentiation is mostly complete, low levels of GFP were detected within support cells of the organ of Corti, and within the GER. In adult cochleae, GFP

expression could still be detected within a subset of cells within the organ of Corti.

Conclusion

In cochleae from TCF/Lef:H2B-GFP reporter mice, Wnt/ β -catenin activity appeared highest in younger prosensory cells and diminished with the onset of differentiation, with some activity being maintained through adulthood. The early pattern of activity was similar to that previously described in the Lgr5 reporter mice, demonstrating the cochlear specificity of the TCF/Lef:H2B-GFP reporter. A solid understanding of the progressive changes in Wnt/ β -catenin signaling may provide valuable insight for identifying cells which may serve as targets for inducing regeneration in damaged adult cochleae.

792 Bone Morphogenetic Protein and Inhibitor of Differentiation Antagonize Hair Cell Differentiation During Avian Hair Cell Regeneration in Post-Hatch Chickens

Jesse Keller¹, Rebecca Lewis¹, Jennifer Stone¹
¹University of Washington

Background

The transcription factor *Atoh1* is both necessary and sufficient to induce hair cell production during development. During avian hair cell regeneration, however, neither endogenous *Atoh1* activity nor overexpression of *Atoh1* fully predict hair cell fate. In developing auditory epithelia, bone morphogenetic proteins (BMPs) antagonize the expression of *Atoh1* via another set of transcription factors, Inhibitors of Differentiation (IDs).

Methods

To begin to explore the role of BMPs and IDs in auditory hair cell regeneration, we performed *in situ* hybridization to examine expression of these genes in normal and Streptomycin-damaged basilar papillae (BPs). We also tested the effect of inhibiting or activating BMP signaling in damaged BPs on 1) the levels of *Atoh1* and *Id* transcripts and 2) the numbers of regenerated hair cells. Additionally, in order to test the hypothesis that IDs antagonize hair cell differentiation, we electroporated full-length *Id3* or control plasmid into supporting cells in cultured BPs and examined effects on the numbers of supporting cells that transdifferentiated as hair cells.

Results

In situ hybridization showed that control basilar papillae have high expression of *Id2*, *Id3*, and *Bmp4* transcripts and very low levels of *Atoh1* and *Bmpr1a* (*Bmp2/4* receptor) transcripts. By 1 day post-Streptomycin, *Atoh1* and *Bmpr1a* are upregulated in the damaged area, whereas *Id2*, *Id3*, and *Bmp4* are downregulated. Treating tissue with BMP2 results in decreased *Atoh1* transcript, and decreased *Id2* and *Id3* transcripts. Conversely, treating with noggin, a BMP inhibitor, results in decreased *Id2* and *Id3* transcripts. Accordingly, the number of hair cells that differentiate increases with noggin treatment, while the number of hair cells that differentiate decreases with BMP4 treatment. Preliminary analysis indicates that

overexpression of *Id3* in supporting cells results in significant reduction of supporting cell transdifferentiation into hair cells ($p < 0.05$).

Conclusion

Id2, *Id3*, and *Bmp4* transcripts are elevated in normal, undamaged BPs but decreased after damage. Addition of BMP4 or overexpression of *Id3* after damage antagonizes *Atoh1* expression and/or hair cell regeneration. These results suggest that BMPs and IDs may maintain supporting cell quiescence in undamaged tissue, and their downregulation upon hair cell loss may allow *Atoh1* to drive hair cell differentiation. Future studies may focus on the manipulation of these additional factors to increase the efficiency of stimulating hair cell regeneration in the mammalian inner ear.

793 Capacity of Consonant Recognition in Normal Hearing and Cochlear Implant Users

Bomjun Kwon¹, Trevor Perry¹
¹Gallaudet University

Background

The present study sought to measure listeners' capacity for processing multiple speech sounds, using information theory (Miller; *Amer. Psychol.*, 1953). Normal hearing (NH) listeners are generally able to recognize more than one speech sound when two are presented, albeit with limited accuracy. We hypothesized that, if cochlear implant (CI) users' disadvantages are limited to the periphery, their capacity (a relative assessment between the single-presentation and concurrent-presentation conditions) would be similar, although their absolute performance might be poorer than the NH group. A contrasting hypothesis was raised that, due to the severely impoverished spectral resolution in the periphery, CI users would fail to segregate concurrent sounds, resulting in drastically lower capacity.

Methods

Consonant identification (16 consonants in /aCa/ format) was tested in eight NH listeners and four bilateral CI users, who were considered good users. After establishing baseline performance with one target sound, subjects were presented with two targets and asked to identify both. The two stimuli were presented monaurally or dichotically, and with a time delay of 0, 100 or 200 milliseconds. The relative information transmitted (RIT) for the baseline condition and composite RITs for the concurrent presentations were calculated, as defined by the sum of RITs for two target consonants, which would be 2.0 if both targets were always correctly identified.

Results

For the NH group, the mean baseline RIT was 0.93. The composite RIT for the condition of 0-ms delay was 1.22, a 32% increase from the single RIT, for the monaural condition, and 1.51, a 62% increase from the single RIT, for the dichotic condition. These results were consistent with preliminary findings reported earlier (Kwon, 2001; ASA meeting abstract 1pSC27). The composite RITs

improved as the inter-stimulus delay increased, indicating listener's ability to utilize the temporal separation between stimuli. For the CI group, the mean baseline RIT was 0.75, slightly lower than the NH counterpart. The composite RIT for 0-ms delay was 0.83 and 0.88, a 10% and 17% increase from the single RIT, for monaural and dichotic conditions, respectively. Furthermore, they did not demonstrate an improvement of RIT with an interstimulus delay of 100-ms.

Conclusion

CI users' ability to recognize multiple sounds presented concurrently is marginal, even for good CI users. They do not appear to take advantage of dichotic presentations or temporal delays between stimuli, as much as shown in the NH group.

794 Vocoder Simulations of Focused Cochlear Stimulation with Limited Dynamic Range and Discriminable Steps

Ryan Stafford¹, Jim Stafford¹, Jonathon Wells¹, Philip Loizou², Matthew Keller¹

¹Lockheed Martin Aculight, ²University of Texas at Dallas

Background

There is recent interest in focused stimulation of the cochlea via modalities such as tripolar electrical and infrared neural stimulation (INS). Previous experiments have examined the effect of excitation spread on speech recognition, but these were limited to models representing monopolar and bipolar stimulation, with attenuations of -2dB/mm and -8dB/mm, respectively. Focused stimulation can provide narrow-extent excitation of spiral ganglion cells with spatial attenuation of -10 to -17 dB/mm. Additionally, stimulation dynamic range and minimum discriminable steps can vary among patients, and many have looked at recognition scores as a function of these parameters. There is a void in the literature, however, regarding potential benefits of focused stimulation in cases of low signal to noise ratios (SNR), limited dynamic range, and/or few discriminable steps. The purpose of this work was to employ vocoder-based experiments to investigate speech recognition under the above conditions with synthesis filter slopes representative of both standard monopolar electrical and narrower extent excitation.

Methods

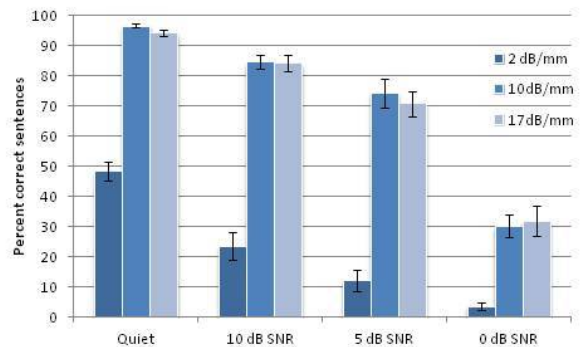
Vocoder simulations were used to assess the intelligibility of sentences, consonants, and vowels that were vocoded and presented to normal-hearing listeners for identification. Slopes of the vocoder synthesis filters were chosen to reflect the spatial spread of the stimulus longitudinally along the scala tympani. Comparisons were made between simulations representing standard monopolar electrical stimulation and the more focused approaches. Intelligibility was assessed for the different filter slopes under a variety of SNR levels, dynamic ranges, and numbers of discriminable steps.

Results

Speech processed via vocoder simulations representing focused stimulation was found to be substantially more intelligible than speech processed via a monopolar electric vocoder simulation. In noisy conditions, differences as large as 60 percentage points were noted (Figure 1). The data from Fig. 1 also indicate that there were no significant differences between the two filter slopes for focused stimulation. Speech processed via the focused vocoder was robust to constraints on small envelope dynamic range and small number of discriminable steps within the dynamic range. High performance was maintained with a 5-dB dynamic range and 8 or more discriminable steps. Significant drops in intelligibility were noted when the number of steps fell below 8.

Conclusion

Focused stimulation – tripolar electrical and INS - has potential for increased performance in noise compared to monopolar stimulation. INS holds additional value because it can achieve selective activation at each channel independently, which may lead to other benefits as well, including in music perception.



795 The Contribution of Room Exposure and Semantic Context to Speech Intelligibility in Cochlear Implant Users

Nirmal Srinivasan¹, Oldooz Hazrati¹, Philip Loizou¹

¹University of Texas - Dallas

Background

Speech is often embedded in environmental noise and is distorted in a variety of ways such as reverberation. Previous studies on speech intelligibility in reverberant listening environments on normal-hearing (NH) listeners found facilitative effect of semantic context on increased intelligibility and prior exposure to the reverberant listening environment improved intelligibility. However, there have been no studies that investigate the effect of prior room exposure and semantic context on speech intelligibility in cochlear implant (CI) users. The current study investigates the cumulative effect of reverberation, noise, and semantic context on speech intelligibility in CI users.

Methods

Virtual acoustic techniques were used to simulate two listening environments – low reverberant (LR) room (T60 = 0.1s) and high reverberant (MR) room T60 = 0.25 s). CI users were presented with Speech Perception in Noise

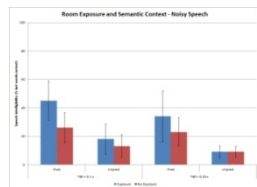
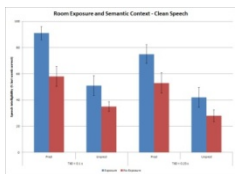
(SPIN) test sentences in quiet and in +15 dB signal-to-noise ratio. The carrier phrase and the target word of the speech stimuli were manipulated to be either in the same room or different rooms. Stimuli in congruent condition enhanced prior room exposure by having the carrier phrase and the target word in the same room. Stimuli in incongruent condition limited the prior room exposure by having the carrier phrase and the target word in different rooms. Listeners were instructed to repeat the last word of every sentence. Speech intelligibility was measured as the proportion of final words correctly identified by the CI users.

Results

Predictable sentences had higher speech intelligibility as compared to unpredictable sentences (context effect) in both congruent and incongruent conditions. This was true for both silent and noisy presentation conditions. The context effect was higher in LR listening environment as compared to MR listening environment. Increased intelligibility due to prior exposure (adaptation effect) was higher predictable sentences compared to unpredictable sentences in both congruent and incongruent conditions.

Conclusion

Semantic context of speech has a facilitative effect on speech intelligibility for CI users. This effect was larger in LR condition as compared to MR condition. Also, prior exposure to the reverberant listening environment helps in improving the speech intelligibility of CI users. Overall, semantic effect has a greater effect on speech intelligibility as compared to prior exposure to the reverberant environment.



796 Preliminary Estimates of F2 Formant Discrimination Thresholds in Cochlear Implant Users

Benjamin Russell¹, Gail Donaldson¹, Amanda Cooley¹, Catherine Rogers¹

¹University of South Florida

Background

Formant discrimination thresholds (FDTs) reflect the smallest change in formant center frequency a listener can perceive. As a measure of spectral acuity obtained with a speech-like stimulus, FDTs may provide useful insights concerning the factors that limit vowel perception by cochlear implant (CI) users. FDTs have been studied extensively in young normal-hearing (YNH) listeners, but have not yet been studied systematically in CI users.

Methods

Second formant (F2) FDTs were obtained from three CI users and three YNH listeners. Procedures and stimuli

were modeled after the low-uncertainty procedures used by Kewley-Port and Watson (1994, JASA 95, 485-96) but with shorter durations of testing and an expanded range of F2 values. Stimuli were Klatt-synthesized versions of three target vowels ("uh", "ae", "ih") with 29 F2 frequency values per vowel. FDTs were measured for both increments and decrements in F2 using an adaptive 3AFC task with feedback. Each FDT was based on threshold estimates for six consecutive 80-trial stimulus blocks.

Results

FDTs for the three YNH listeners were comparable to those reported by Kewley-Port and Watson in highly trained listeners: average FDTs were 2.4% of reference frequency in the present study compared to 1.5% in the earlier study. FDTs were successfully obtained in all three of the CI users. Two of the CI users exhibited FDTs that were relatively consistent across F2 frequency, but were about 70% larger than mean FDTs for the YNH listeners. The third CI user demonstrated more variable FDTs that approached the YNH values in one frequency region but were enlarged substantially in another region. FDTs in this subject could not be explained by place-pitch thresholds obtained in an earlier study, suggesting that spectral acuity for complex stimuli may not be directly predictable from measures of spectral acuity for simple stimuli.

Conclusion

1) Our reduced-duration protocol (about 1 hour per FDT) produces FDTs in YNH listeners that are comparable to those reported for highly-trained listeners. 2) It is feasible to measure F2 FDTs in CI users by employing an expanded range of F2 increments. 3) As expected, CI users demonstrate FDTs that are larger than corresponding FDTs in YNH listeners. Future studies will determine whether variations in FDTs among CI users can be predicted by pure tone frequency DLs and whether formant discrimination predicts vowel perception in these listeners.

797 Phonemic Restoration and Continuity Illusion of Speech in Users of Cochlear Implants

Pranesh Bhargava^{1,2}, Deniz Baskent^{1,2}

¹University Medical Center Groningen, The Netherlands,

²University of Groningen, School of Behavioural and Cognitive Neurosciences, The Netherlands

Background

Understanding speech in noisy environments is more difficult for cochlear implant (CI) users than normal hearing (NH) listeners. This may partially be because NH listeners are better at using the mechanism of phonemic restoration (PR) to their benefit than CI users. PR is perceptual restoration of speech sounds obliterated by noise using top-down processes. In NH, PR is accompanied by continuity illusion, which makes listeners perceive the speech stream to be continuous behind the noise despite inaudible parts. In the present study, we explored the hypothesis that typical CI users may not benefit from PR

as much as NH listeners and the continuity illusion of interrupted speech may also work differently.

Methods

Dutch CI users listened to the context-rich sentences. Some sentences were temporally interrupted with silence, while in others the temporal interruptions were filled with noise at various signal to noise ratios. The participants listened to and repeated the processed stimuli. Percent correct of the repeated words was measured as the intelligibility score. Benefit from PR was measured as the increase in intelligibility score with addition of noise in the silent gaps. For a given condition, continuity illusion was measured as the percent of interrupted sentences reported to be perceived as continuous.

Results

In the preliminary data obtained, the participants generally performed worse in identifying the sentences with noise filled gaps than silent gaps. Only two CI users (out of five tested) showed some restoration effect at a small number of test conditions. However, in general, as the level of the filler noise increased the speech intelligibility became worse. Sentences interrupted with noise were not always reported to be continuous.

Conclusion

Except a small number of conditions for a subset of participants, the CI users seemed to show no systematic benefit of PR in general. In contrast with the results found with the NH listeners in the previous studies, the filler noise seemed to hinder the intelligibility of interrupted speech for the CI users. As opposed to NH listeners, CI users also did not provide a clear indication of continuity illusion induced by filler noise.

798 Factors That Predict the Perception of Brief Prosodic Features by Postlingual Cochlear Implant Patients

David Morris¹, Lennart Magnusson², Radoslava Jönsson², Holger Juul¹

¹University of Copenhagen, ²Sahlgrenska University Hospital

Background

While the perception of prosody has received some research attention only a limited number of studies have reported on the abilities of Cochlear Implant (CI) listeners to perceive brief prosodic cues. In Scandinavian languages these cues can fulfill a semantic role.

Methods

Testing of the perception of brief prosodic features was undertaken with Danish (n=18) and Swedish cohorts (n=22) of CI listeners. A normal hearing control group from both languages was also tested. Closed set minimal pair testing of lexical stress, vowel quantity, compound word/phrase discrimination and stød. With the Swedish listeners a noise condition was also included. The results from these tests were used as the dependent variable in a regression model. The factors in the regression model

also included speech reception threshold results from a speech in noise test, demographic and psychoacoustic variables. The psychoacoustic variables tested with both groups included the Difference Limens for F0, intensity, duration and F1, which were measured with manipulation of a synthetically produced phoneme [ba].

Results

CI participants could not identify brief prosodic cues as well as normal hearing participants and their performance decreased significantly with the addition of noise. With the Danish CI listeners the SRT from a sentence test in noise emerged as a strong predictor. In the Swedish CI listeners age and noise condition emerged as predictors. In both languages the Difference Limen for intensity emerged as a predictor of performance on the minimal pair tasks. Analysis of the error patterns observed and the stimulation delivered by a common processing strategy reveals that electrical over-representation of the lower formants may be detrimental to perception.

Conclusion

This study shows that CI listeners are not able to perceive brief prosodic cues in natural utterances as well as normal hearing listeners.

799 Effects of Context on Speech Recognition by Cochlear Implants Users

Bomjun Kwon¹, Trevor Perry¹

¹Gallaudet University

Background

The process of speech perception is invariably affected by the context available to the listener. The relationship between speech recognition scores in conditions with and without contextual information was modeled by the equation: $p_c = 1 - (1 - p_i)^k$, where p_c and p_i were the scores with and without context, respectively (Boothroyd and Nittrouer, 1988). The exponent k ("k-factor") indicates the degree to which a listener utilizes contextual information. It is unclear how much contextual information is utilized in speech recognition by successful cochlear implant (CI) users. We hypothesized that CI users would rely on context to a greater degree than NH listeners to compensate for severely impoverished information from the periphery. In the present study, speech recognition scores were controlled by either adding background noise or reducing the presentation level of speech. While these two methods are considered conceptually equivalent in the calculation of articulation index, we hypothesized that they might address different implications in speech perception in CI. The noise might have a more detrimental impact because it might interfere with segmentation of the sentence into smaller linguistic units.

Methods

Ten young, NH listeners and ten "good" CI users participated in the study. 100 sentences with 4 target words were prepared and presented either with noise at several signal-to-noise ratios (SNRs) or without noise but at several reduced presentation levels. Additionally, 4

words were randomly extracted from the sentence sound files and presented as a sequence of words. Of 400 unique words, each was presented twice—once in a sentence and once in a random word string, in random order, with identical SNRs or presentation levels between presentations. The scores in the two conditions were used to calculate k-factors.

Results

While the k-factors were similar (2.3 and 2.2) for NH listeners, they were significantly different (2.9 and 2.5) for CI listeners, for the level-adjusted and noise conditions, respectively.

Conclusion

Successful CI users who perform well in daily listening tasks in the quiet condition (but with varied presentation levels) use contextual information to a greater degree than NH listeners. The well-known phenomenon of good CI users' performance worsening sharply in noise might be attributed to the deprivation, or less use, of contextual information. Thus, more emphasis ought to be made in future studies on speech perception regarding the interference of noise with segmentation, rather than audibility per se.

800 Can Interrupted Speech Be Used as Training Stimuli for Cochlear-Implant Users?

Michel Ruben Benard^{1,2}, Deniz Baskent^{2,3}

¹Pento Audiology Center Zwolle, The Netherlands,

²University Medical Center Groningen, Department of Otorhinolaryngology / Head and Neck Surgery, ³School of Behavioral and Cognitive Neuroscience, University of Groningen, The Netherlands

Background

Normal-hearing (NH) listeners use several mechanisms that increase speech intelligibility in difficult listening environments. In phonemic restoration (PR), the listener uses context and speech redundancy to perceptually restore inaudible or masked portions of temporally interrupted speech. Previous research has shown that this benefit is greatly reduced in untrained cochlear-implant (CI) users.

CI-users commonly complain about difficulties understanding speech in noise. Several training studies have focused on improving intelligibility, although none of them have used complex stimuli like interrupted speech. We investigated if CI-users can learn to use high-level cognitive repair mechanisms more effectively to understand interrupted speech, as well as derive a PR-benefit (i.e. increase in intelligibility between sentences interrupted by silence and interrupted sentences with filler noise).

Methods

The first experiment was spread over three days with 3 sessions per day, each session comprising of 26 Dutch sentences. The NH-participants (N=30) were tested on the perception of speech interrupted by silence with or without filler noise at the start and the end of the experiment. In-

between these baseline measurements, the participants were trained on interrupted speech. Feedback was provided during these training sessions by playing back the sentence stimulus, as well as showing the sentence on the screen.

In the second experiment, with an equal design to the first, different listeners (N=24) were trained with CI-simulations of interrupted speech, by means of an 8-channel noiseband vocoder.

Results

First experiment: Training participants with interrupted speech without CI-simulations showed an increase in intelligibility of 9.6%. The PR-benefit was shown before training by an increase of 9.2% in correctly repeated words after the filler noise was added, and of 8.7% after training.

Second experiment: Training with CI-simulations of interrupted speech increased the performance from 17% to 37%. Consistent with previous studies, no significant PR-benefit was observed before training, and even after intensive training, such benefit was not present.

Conclusion

CI sound transmission degrades the quality of the bottom-up speech signal, withholding high-level cognitive repair mechanisms initially to benefit from the filler noise. Even though intensive training with interrupted speech did not revive the PR-benefit in CI-simulations, overall there was a significant improvement of intelligibility of interrupted speech. This finding indicates that listeners (and potentially CI-users) can be taught to use the top-down mechanisms more efficiently to restore interrupted speech.

801 Unilateral Adaptation of the Normal Human Angular Vestibulo-Ocular Reflex

Americo Migliaccio^{1,2}, Michael Schubert³

¹Neuroscience Research Australia, ²University of New South Wales, ³Johns Hopkins University

Background

A recent study showed that the angular vestibulo-ocular reflex (VOR) can be better adaptively increased using an incremental retinal image velocity error signal compared with a conventional constant large velocity-gain demand (x2). This finding has important implications for vestibular rehabilitation that seeks to improve the VOR response after injury. However, a large portion of vestibular patients have unilateral vestibular hypofunction, and training that raises their VOR response during rotations to both the ipsi and contralesional side is not usually ideal. We sought to determine if the vestibular response to one side could selectively be increased without affecting the contralateral response.

Methods

We tested 9 subjects with normal vestibular function. Using the scleral search coil and head impulse techniques, we measured the active and passive VOR gain (eye velocity / head velocity) before and after unilateral incremental VOR adaptation training, consisting of self-generated (active) head impulses, which lasted ~15 mins. The head impulses

consisted of rapid, horizontal head rotations with peak-amplitude 15°, peak-velocity 150°/s and peak-acceleration 3000°/s².

Results

The VOR gain towards the adapting side increased after training from 0.92 ± 0.18 to 1.11 ± 0.22 (+22.7 ± 20.2%) during active head impulses, and 0.91 ± 0.15 to 1.01 ± 0.17 (+11.3 ± 7.5%) during passive head impulses. During active impulses the VOR gain towards the non-adapting side also increased by ~8%, though this increase was ~70% less than to the adapting side. A similar increase did not occur during passive impulses.

Conclusion

This study shows that unilateral vestibular adaptation is possible in humans with a normal VOR; unilateral incremental VOR adaptation may have a role in vestibular rehabilitation. The increase in passive VOR gain after active head impulse adaptation suggests that the training effect is robust.

802 VOR Gain and Time Course During Head Impulses in Patients with Bilateral Vestibulopathy According to Etiology

Olympia Kremmyda^{1,2}, Erich Schneider², Stanislav Bardins², Tatiana Bremova², Michael Strupp^{1,2}, Yuri Agrawal³

¹Department of Neurology, University of Munich, ²German Dizziness Centre, Munich, ³Johns Hopkins

Background

Vestibular dysfunction may involve loss of the phasic Type I vestibular hair cells and/or of the tonic Type II hair cells. We investigated the differential effect of Type I vs. II hair cell loss on vestibulo-ocular reflex (VOR) dynamics by evaluating two groups of patients with bilateral vestibulopathy: 1) secondary to systemic aminoglycoside therapy (AG; causing mostly Type I hair cell damage) and 2) bilateral Meniere's disease (MD; associated with Type II hair cell damage).

Methods

We recorded manually-induced head impulse tests (HITs) from 19 patients with bilateral vestibulopathy using video-oculography. Eight patients had aminoglycoside therapy (AG group) and 11 patients had bilateral Meniere's disease (MD group). Since hair cell groups respond at different rotational frequencies, we recorded HITs with low (<200deg/s) and high (>200deg/s) head velocities. We also considered HIT gains (eye velocity/head velocity) at different time points during the head impulse to assess whether eye velocities were associated with particular head movement parameters.

Results

MD patients had higher, near-normal gains in the high and low velocity paradigms compared to the AG group (p<0.001 for both paradigms). MD patients had peak gains at the point of maximal head velocity. AG patients had a peak VOR gain (0.58 ± 0.30) at the time of maximal head

acceleration in the high velocity paradigm, which was followed by an abrupt drop in gain value (referred to as a 'bump'). Gains reached a minimum value at the time of zero head acceleration (AG: 0.10 ± 0.17). Regression analysis showed that, whereas in the MD group eye velocity linearly correlated with head velocity, in the AG eye velocity followed head acceleration.

Conclusion

These differences in the VOR-generated eye movements during the HIT could be explained by a differential hair cell loss and compensation pattern in these two groups BV patients.

803 Analysis of Eye Tracking Test and Optokinetic Nystagmus Test by Original Video-Oculography, HI-VOG

Makoto Hashimoto¹, Hironori Fuji¹, Kazuma Sugahara¹, Hiroaki Shimogori¹, Takuo Ikeda¹, Hiroshi Yamashita¹
¹Yamaguchi University Graduate School of Medicine

Background

It is essential to use an infrared CCD camera in clinical examination of the vestibular system. Devices are currently available that can quite accurately record human eye movements, based on the principle of video-oculography (VOG). We devised an original video-oculography (HI-VOG) system using a commercialized infrared CCD camera, a personal computer and public domain software program (ImageJ) for the data analysis.

Methods

The video image from the infrared CCD camera was captured at 30 frames per second at a resolution of 640*480 pl.. For analysis of the horizontal and vertical components, the X-Y center of the pupil was calculated using the original macro. For analysis of torsional components, the whole iris pattern, which was rotated by 0.1 degree, was overlaid with the same area of the next iris pattern, and the angle at which both iris patterns showed the greatest match was calculated.

Results

For quantitative analysis, the slow phase velocity of each occurrence of nystagmus, the average value of the slow phase velocity and the visual suppression value, were analyzed automatically. Analyses of the eye tracking test, as well as the test for optokinetic nystagmus were also applied in this system.

Conclusion

Using the HI-VOG system, it was possible to inexpensively perform analysis from video images recorded with an infrared CCD camera, including eye tracking test and optokinetic nystagmus test.

804 Modulation of OVERTM Amplitudes by Lateral Head Tilts

Robert Gürkoy^{1,2}, Claudia Kantner^{1,2}

¹University of Munich, ²German Dizziness Centre

Background

Recently, the ocular vestibular evoked myogenic potentials (oVEMP) have emerged as a tool for assessment of utricular function. However, there is still a lack of unequivocal evidence in humans for either the sacculus or the utricle being the origin of the ACS oVEMP. To overcome this problem, we sought to alter the baseline activity of utricular afferents by lateral head tilts in order to achieve a modulation of the ACS oVEMP response.

Methods

In 20 healthy subjects, oVEMP were recorded in three positions: supine, right lateral (right ear down), left lateral (left ear down). The stimulus was delivered at intensities of 100 dB nHL using a tone burst stimulus at 500 Hz, with the parameters 2/2/2 ms rise/plateau/fall time at a repetition rate of 5/s.

Results

There is a large and highly significant decrease in amplitudes in the ear-down position compared to the supine position. The derived lateral tilt modulation index (LATIMO-Index) of the ACS oVEMP in this group of subjects was 0.71 +/- 0.27 (mean/STDV) for the ear-down position.

There is a small not-significant increase in amplitude in the ear-up position compared to the supine position.

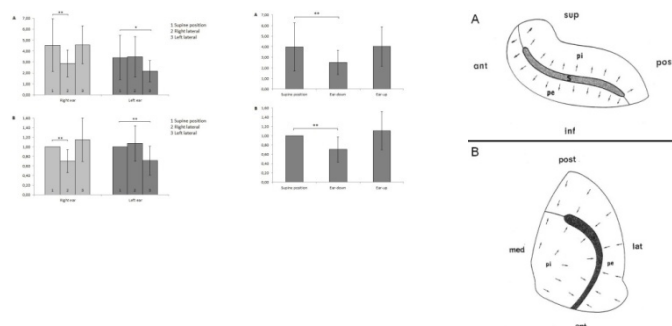
oVEMP amplitudes

	Supine	Ear-up	Ear-down
Mean	3,97	2,51	4,02
SD	2,27	1,15	1,85
p value	0,000	0,914	
	(vs. supine)		

Table 1: oVEMP amplitudes (mean/SD) in supine vs. ear-up and ear-down lateral positions.

Conclusion

The effects of the lateral tilts observed in our study correspond well to the effects of gravity on the utricular macula. The ear-down position has the opposite gravitational effect compared to the ear-up position, which is in line with the functional anatomy of the utricular macula. Likewise, the ear-down position markedly decreased the oVEMP amplitude, whereas the ear-up position slightly increased the oVEMP amplitude. We propose that this new parameter is a part of the ACS oVEMP response that is dependent on utricular function. Therefore, it is a promising new candidate for the specific evaluation of utricular function in humans.



805 Development of Accelerometer Based Device for Treatment of Benign Paroxysmal Positional Vertigo

Kyu-Sung Kim^{1,2}, Wookje Park², Wookey Lee³, Ki Hwan Hong², Hyeon-min Shim², Eunjin Park^{2,4}, Sangmin Lee²

¹Department of Otolaryngology, Inha University Hospital,

²Institute for Information and Electronics Research at Department of Electronic Engineering, ³Department of Industrial Engineering, Inha University, ⁴Department of Biological Science, Incheon, Korea

Background

Purpose: Benign Paroxysmal Positional Vertigo (BPPV) is well treated by proper diagnosis and otolith repositioning maneuver. On the other hand, high recurrence rate of 15 to 50 % causing timely, economic burdens as well as psychosocial burden in daily life. We introduce current work for development of accelerometer-based medical device to assist BPPV treatment.

Methods

Method: We developed head-fixed lightweight accelerometer sensor which transmit positional information of head to the device by using short-range wireless communication. The device has the application program with diagnostic and treatment algorithms for BPPV. It was designed to support patient to assist self-reposition or support physician to apply proper procedure of repositioning maneuver.

Results

Result: We developed device under the protocol of Inha Medical Device Development Center, and confirmed proper function of sensors, device-sensor interworking and interface of application.

Conclusion

Conclusion: We expect accelerometer-based medical device contribute the patient and physician for proper management of BPPV.

806 Efficacy of Vibrotactile Vestibular Neurofeedback Training Based on Objective Body Sway Measures in Everyday Life Conditions

Dietmar Basta¹, Marcos Rossi-Izquierdo², Andres Soto-Varela³, Mario Edwin Greters⁴, Tatsuhiko Harada⁵, Fumiyuki Goto⁶, Arne Ernst¹

¹*Department of ENT at ukb, University of Berlin, Charité Medical School, Germany,* ²*Department of Otolaryngology, University Hospital Lucus Augusti, Lugo, Spain,* ³*University Hospital of Santiago de Compostela, Santiago de Compostela, Spain,* ⁴*Department of Otolaryngology, Faculdade de Medicina, Universidade de Sa'õ Paulo, Sa'õ Paulo, Brazil,* ⁵*Department of Otolaryngology, International University of Health and Welfare, Atami, Japan,* ⁶*Department of Otolaryngology, Hino Municipal Hospital, Tokyo, Japan*

Background

Vestibular rehabilitation strategies mostly require a long-lasting training, which is finally not often successful. An individualized neurofeedback training which is based on a body sway analysis in everyday life conditions seems to be a more promising approach.

Hence, the present study was aimed at investigating the efficacy of an individualized vibrotactile neurofeedback training for vestibular rehabilitation.

Methods

One hundred five patients who experience one of the following balance disorders for more than 12 months were included in the study: canal paresis, otolith disorder, removal of an acoustic neuroma, microvascular compression syndrome, Parkinson's disease, and presbyvertigo. Vibrotactile neurofeedback training was performed in a double-blinded placebo controlled study design daily (15 min) over 2 weeks with the Vertiguard[®] system in those 6 tasks of the Standard Balance Deficit Test with the most prominent deviations from the normative values.

Trunk and ankle sway, dizziness handicap inventory, and vestibular symptom score were measured in the verum and placebo group before the training, on the last training day and 3 months later.

Results

A significant reduction in trunk and ankle sway as well as in the subjective symptom scores were observed in the verum group. Such an effect could not be found in any of the outcome parameters of the placebo group.

Conclusion

The vibrotactile neurofeedback training applied in the present study is a highly efficient method for the reduction of body sway in different balance disorders. Since the rehabilitation program is easy to perform, not exhausting, and time saving, elderly patients and those with serious, long-lasting balance problems also can participate successfully.

807 An Enhanced Safe Direct Current Stimulation System to Improve Vestibular Prosthesis Performance

Gene Fridman¹, Charles Della Santina¹

¹*Johns Hopkins University*

Background

In previous acute vestibular prosthetic stimulation experiments in chinchillas, we showed that the range of head velocities accurately encoded by a pulse-frequency-based vestibular prosthesis can be nearly doubled by suppressing spontaneous vestibular afferent activity in the implanted labyrinth using low-amplitude anodic direct current (DC). To overcome the safety concerns associated with direct current stimulation, we developed a safe DC stimulator prototype (SDCS1). This device delivers alternating current across the metal-saline interface for each of two metal electrodes but effectively delivers DC to the tissue using synchronously switched valves arranged in a bridge circuit. The fidelity of the SDCS1 output was degraded by periodic interruptions in current flow due to non-ideal behavior of the mechanical valves used in that device. In the present study, we sought to develop a next generation safe DC stimulation system, SDCS2, which solves the problems with the current flow interruptions of SDCS1 and miniaturizes the system sufficiently to enable chronic experiments of this technology in rodents.

Methods

Conceptually, the SDCS2 uses two SDCS1 subsystems attached in a dual H bridge to prevent current flow interruptions by sequentially alternating control from one SDCS1 subsystem to the other. At any time, one SDCS1 controls stimulation current flow, while the second (non-stimulating) SDCS1 switches its valves. We tested the ability of this two-system design to eliminate current flow interruptions by constructing a bench prototype using laboratory tubing, two isolated current sources and manually operated clamps in place of the mechanical valves. The current sources alternated control in 20s intervals to allow time to manually operate the valves. Subsequently, we designed a miniaturized 3x3x1.5 cm³ SDCS2 using layered construction compatible with MEMS processes.

Results

Experiments with the bench prototype SDCS2 show that this enhanced design completely eliminates the DC flow interruptions seen with a single SDCS1. The first miniaturized prototype of the SDCS2 was built using a 3D printer and NITINOL "muscle" wires to actuate the valves. We verified that the activated valves can be operated at 0.5 Hz as expected. When a valve is closed, its impedance is over 20x greater than when it is open.

Conclusion

These results indicate that the SDCS2 should be effective at chronically delivering uninterrupted yet biologically safe DC current. Using the SDCS2, we anticipate that we can markedly expand the range head velocities that can be encoded by a vestibular prosthesis.

808 Electrocochleography and ABR Variability Are Associated with Postsurgical Hearing Outcomes in Superior Semicircular Canal Dehiscence

Angela Wenzel¹, Bryan K. Ward¹, Eva K. Ritzl², Sergio Gutierrez-Hernandez², Charles C. Della Santina¹, Lloyd B. Minor³, John P. Carey¹

¹Johns Hopkins School of Medicine – Department of Otolaryngology-Head and Neck Surgery, ²Johns Hopkins School of Medicine – Department of Neurology, ³Stanford University School of Medicine

Background

Recent findings in patients with superior canal dehiscence (SCD) have shown an elevated ratio of summing potential (SP) to action potential (AP) as measured by ECoChG. Changes in this ratio can be seen during surgical intervention. The objective of this study was to evaluate the utility of intraoperative ECoChG and ABR as predictive tools for post-operative hearing outcomes following surgical plugging via middle cranial fossa approach for superior semicircular canal dehiscence syndrome (SCDS).

Methods

This was a review of 23 cases (22 patients) in which good, reproducible intraoperative ECoChG recordings were obtained during surgery. Diagnosis of SCDS was based on history, physical examination, vestibular function testing, and computed tomography imaging. Simultaneous intraoperative ECoChG and ABR were performed. Pure tone audiometry was performed pre-operatively and at least 1 month post-operatively. Changes in SP/AP ratio, SP amplitude and ABR wave I latency were compared to changes in pure tone average (PTA) before and after surgery.

Results

SP amplitude and SP/AP ratios were reliably obtained in the affected ears in these cases. Reproducible ABR recordings were found in 19 affected ears. Mean pre-plugging SP/AP ratio was 0.64 (SD 0.33) and decreased to 0.48 (SD 0.40) immediately after plugging ($p=0.015$). Mean pre-plugging SP amplitude was 0.25 μV (SD 0.22 μV) and decreased after surgery to 0.17 μV (SD 0.22 μV) ($p=0.033$). Mean ABR wave I latency was 2.54 ms (SD 0.26 ms) and was unchanged after surgery (mean 2.48 ms (SD 0.32ms), $p=0.48$). Before surgery, mean air-conduction PTA was 17.6 dB (SD 8.9dB) and increased to 20.9 dB (SD 17.3 dB) at least 1 month post-operatively. Pre-operative bone-conduction PTA was 9.1 dB (SD 9.8dB) before plugging and 16.5 dB (SD 21.2dB) at least 1 month after surgery. A significant correlation was found between ABR wave I variability and change in postoperative PTA ($p=0.03$). Intraoperative change in SP amplitude was also associated with worse PTA ($p=0.02$).

Conclusion

This study confirmed the presence of an elevated SP/AP ratio in ears with SCD. Intraoperative ECoChG and ABR

variability may predict hearing outcomes in patients with SCDS.

809 Reducing Sound Exposure During Ocular Vestibular Evoked Myogenic Potential Testing for Superior Semicircular Canal Dehiscence Syndrome

M. Geraldine Zuniga¹, Angela Wenzel¹, Carolina Trevino^{1,2}, John Carey¹

¹Johns Hopkins University, ²Escuela de Medicina Ignacio A Santos Instituto Tecnológico de Estudios Superiores de Monterrey Mex.

Background

Ocular vestibular evoked myogenic potentials (oVEMP) testing in response to air-conducted sound (ACS) has demonstrated excellent sensitivity and specificity for the diagnosis of superior semicircular canal dehiscence syndrome (SCDS). However, some patients experience oscillopsia while undergoing the test. Purpose: To develop an oVEMP testing protocol that may reduce the discomfort of the test and still serve for the diagnosis of SCDS.

Methods

Subjects: Five (ears= 10) healthy volunteers without history of neurotological complaints and ten (affected ears= 10) patients with a diagnosis of SCDS based on clinical presentation, audiometry and CT imaging.

VEMP recordings: OVEMPs were recorded in response to ACS (clicks and 500 Hz tone-bursts) delivered at the standard repetition rate of 5 pulses per second (pps) during 20s. Additional experimental recordings consisted of ACS delivered at a repetition rate of 2pps during 20s and 10s. Receiver operator characteristic analysis, evaluated the effectiveness of these different oVEMP protocols.

Results

OVEMP amplitudes from the three different protocols showed excellent (>90%) sensitivity and specificity for the segregation of patients with SCDS from controls. For controls, the experimental recordings with minimized sound exposure showed oVEMP amplitudes that were reduced (absent in 3 cases) relative to the standard oVEMP protocol. In contrast, in the SCD group oVEMP amplitudes showed no difference between protocols [$F(2,27)= 0.04$, $p = 0.98$].

Conclusion

Reducing the amount of sound delivered during oVEMP testing results in a more comfortable and tolerable test without compromising its effectiveness for the diagnosis of SCDS.

810 Body Sway Analysis in Patients with Superior Canal Dehiscence

Carolina Trevino^{1,2}, Kara Beaton¹, M Geraldine Zuniga¹, Angela Wenzel¹, Marcela Davalos¹, Michael Schubert¹, Yuri Agrawal¹, John Carey¹

¹Johns Hopkins University, ²Escuela de Medicina Ignacio A. Santos, Instituto Tecnológico y de Estudios Superiores de Monterrey

Background

The principal aim of this study was to determine if patients with superior canal dehiscence syndrome (SCDS) have increased body sway, especially when exposed to loud sound.

Methods

Subjects: Groups were patients with SCDS (N=5) and healthy (non-age-matched) controls (N=4). The diagnosis of SCDS was based on clinical presentation, audiogram, vestibular evoked myogenic potentials, and high-resolution CT imaging.

Methods: Small, wireless motion sensors, positioned at the hip and ankle, measured angular body sway at 100Hz in the anteroposterior (AP) and mediolateral (ML) directions. Subjects stood with eyes open (EO) or eyes closed (EC) on firm support, with and without exposure to air conducted sound (ACS, 105 dB nHL clicks at 5Hz), during 20s trials. Center of mass excursions in AP and ML planes were analyzed.

Results

ML and AP sway was increased in the SCDS group for both conditions, and overall sway tended to align with the affected superior canal (SC). However, upon sound stimulation, SCDS patients showed a surprising decrease in sway amplitudes, especially in the ML direction during the EC trials.

Conclusion

SCDS patients have greater body sway amplitudes than controls, and sway direction corresponds to the affected SC. Loud clicks surprisingly decreased the amount of body sway excursion in this group of unselected SCDS patients. Future work will examine whether sound increases body sway in SCDS patients with sound-induced vertigo.

811 Dynamic Visual Acuity for Screening Patients with Vestibular Disorders

Helen S Cohen¹, Brian T Peters², Ajitkumar P Mulavara³, Christopher Miller², Haleh Sangi-Haghepeykar¹, Jacob J Bloomberg⁴

¹Baylor College of Medicine, ²Wyle Integrated Sciences and Engineering, ³Universities Space Research Association, ⁴NASA/Johnson Space Center

Background

Several versions of dynamic visual acuity tests have been developed for use in testing patients with vestibular disorders. Many of these tests involve active head movements, which could allow the patient to perform the test with predictive saccades. We have developed a new

test that passively moves the patient vertically while viewing a simple image on a computer screen.

Methods

Patients with known vestibular disorders and normals sat in a custom-designed chair that oscillates vertically. Each subject performed two trials with the chair motionless and two trials with the chair oscillating at 2 Hz. During each trial, the subjects identified the orientations of a series of Landholdt-C optotypes presented briefly (75 ms or 500 ms) on a computer screen positioned 4 m away. A technician recorded each answer with a numeric keypad, which then prompted the showing of the next optotype. The C varied in orientation and size based on an algorithm that accounts for the number of correct and incorrect answers.

Results

Preliminary data show significant differences between patients and normals in the difference score between stationary and moving conditions.

Conclusion

This test may be useful for clinical screening, at remote locations such as future landing sites for astronauts after space missions, and in future epidemiologic tests.

Supported by NIH/NIDCD grant 1R01DC009031 to HSC and by a grant from the National Space Biomedical Research Institute through NASA NCC 9-58 (SA02001) to APM.

812 Gaze Stabilization Test Asymmetry Score as an Indicator of Previously Reported Head Injury in a Cohort of Collegiate Football Players

Julie Honaker¹, Robin Criter¹, Jessie Patterson¹, Sherri Jones¹

¹University of Nebraska-Lincoln

Background

The awareness and incidence of TBI due to contact sports is rising. Sport-related concussion is a complex pathophysiological process that can have lasting effects on brain function, balance, and behavior. Thus, there is a critical need to provide valid, reliable injury assessment measures to minimize the risk of recurrent injuries. It is therefore strongly recommended that a multi-faceted assessment protocol be used in the identification of concussion and the inclusion of more objective, sensitive measures are warranted. Vestibular function is currently not included in concussion management. Vestibular dysfunction may lead to decreased visual acuity with head movements, which may impede athletic performance and result in further injury. The Gaze Stabilization Test (GST) determines the maximum rightward and leftward head velocities in degrees/second that the athlete can perform and correctly identify a target on a computer screen. An asymmetry score denotes differences in the average head velocity between rightward and leftward head movements expressed as a percentage. The purpose of this investigation was to determine differences in the gaze

stabilization test for collegiate football players reporting a previous history of head injury.

Methods

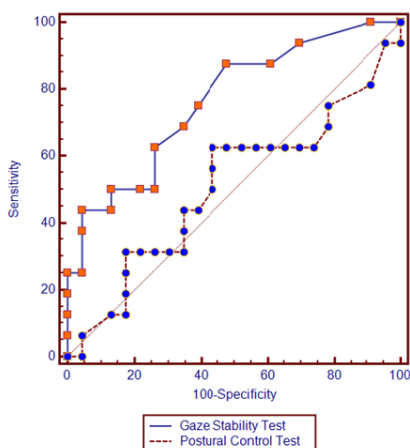
Forty collegiate football players, aged 18-22 years, from the University of Nebraska-Lincoln (14 with previously reported concussion) completed GST in the yaw plane. GST velocity scores for leftward and rightward head movements were measured and compared to participants' report of previous head injury and compared to a more widely accepted postural control measure for concussion management - NeuroCom® Stability Evaluation Test (SET).

Results

Our findings revealed that athletes with a previous history of head injury had a larger asymmetry score ($M = 11.94$, $SD = 8.97$) than those without head injury ($M = 4.91$, $SD = 4.77$; $t_{20.94} = -2.863$, $p = 0.009$). This finding suggests that those with previous history of concussion may have asymmetrical VOR performance that results in reduced gaze stability. Moreover, the GST asymmetry score was found to be the superior measure for identifying previous history of head injury when compared to the Stability Evaluation Test (SET). Receiver Operator Characteristic Curves (ROC) identified an area under the curve (AUC) of 0.76 for GST asymmetry suggesting good performance and AUC of 0.50 (ROC curve line closest to chance performance line) for SET indicating poor test performance.

Conclusion

Conclusions: Overall, these preliminary data provide evidence to support the use of the GST in concussion identification and management. This work may shift the traditional paradigm for concussion assessment to include objective vestibular measures.



813 Gait Characteristics of Patients with Vestibular Hypofunction

Chung-Lan Kao^{1,2}, Tzu-Hui Huang³, Po-Yin Chen^{1,3}, Shun-Hwa Wei³

¹Department of Physical Medicine & Rehabilitation, Taipei Veterans General Hospital, ²School of Medicine, National

Yang-Ming University, ³Department of Physical Therapy and Assistive Technology, National Yang-Ming University

Background

One of the most important functions of vestibular system is to maintain postural stability during head movements. Patients with vestibular hypofunction often complain of gait instability. Dynamic gait index (DGI) is a measurement tool frequently used to evaluate functional stability of gait for individuals with vestibular deficits. The purposes of this study were to: 1) Analyze the gait characteristics of patients with vestibular hypofunction during walking with active head movements, 2) Compare the differences of gait characteristics between healthy adults and patients with vestibular hypofunction.

Methods

Nine individuals with vestibular hypofunction (experimental group) and 10 healthy subjects (control group) performed DGI (items 1, 3, 4). Gait characteristics were captured by markers of the Vicon motion analysis system (Vicon Oxford, UK). Data was analyzed by NEXUS 1.7.1. Matlab 2010 was used to calculate gait parameters including step length, cadence, velocity, path deviation angles, and center of mass (COM) deviation for forward walking in the experimental and control groups.

Results

The step length and velocity decreased in the experimental group, especially during walking with horizontal ($p = 0.037$) and vertical head movements ($p = 0.048$). The experimental group showed larger mean path deviation angle ($p = 0.013$). The experimental group demonstrated lesser head rotation/flexion-extension angles and trunk rotation during walking ($p = 0.026$). The medio-lateral deviation ratio of COM of experimental group is greater than control group ($p < 0.01$).

Conclusion

The vestibular hypofunction patients walk with lower efficiency than normal subjects. The differences were more pronounced during walking with vertical head rotation at 90 and 120 degrees/second, and horizontal head movements at 120 degrees/second. The path deviation angle of walking as well as medio-lateral deviation ratio of COM were the most sensitive parameters to show the differences of gait and balance performances between patients and normal subjects.

814 Rotary Vestibulo-Ocular Reflex Suppression and Slow Phase Velocity Differences in Autism

Tana Bleser¹, Bradley Wilkes¹, Keith White¹
¹University of Florida

Background

Vestibular processing and oculomotor control deficits are commonly reported in children with autism spectrum disorder (ASD), yet only a few studies have investigated vestibulo-ocular reflexes (VOR). Healthy and lesioned VORs have been well studied in humans as well as animal models and serve as the optimal focus for studying the

neural mechanisms of vestibular and oculomotor deficits in ASD. The presence of a functioning VOR occurs early in development so deficits may be identifiable prior to onset of core social and communication ASD symptoms.

Methods

Typically developing (TD) children and children with ASD ages 6-12 participated in velocity step tests and sinusoidal harmonic acceleration (SHA) tests in three conditions: (1) Light (2) Dark and (3) Visual Suppression - dark except for a single LED visible. All tests conducted using a NeuroKinetics VOG system and rotary chair customized by the authors for pediatric use.

Results

Preliminary data indicate differences in rotational VOR (rVOR) between groups during visual suppression conditions. First, phase lag was reduced during suppression but not dark SHA tests at 0.05 Hz and 0.10 Hz in ASD compared to TD children. Second, the children with ASD had a longer time constant during velocity step tests with suppression relative to both the light and dark conditions, compared with TD children. Finally, in the dark the ASD group exhibited greater occurrence of episodes where slow phase is followed by a failure to generate a quick phase prior to subsequent nystagmus beats.

Conclusion

Our results suggest that children with ASD respond differently to visual stimuli during continuous and sinusoidal rotation and exhibit abnormal compensatory eye movements in the absence of visual stimuli compared with TD children. These novel findings will serve to improve our understanding of VOR function in ASD. Furthermore, this information will help to shed light on three important issues in ASD including: (1) identification of neurobiological loci for sensory motor processing differences in ASD, (2) provision of a potential behavioral marker for study as an early identification of risk for ASD and (3) improved clinical assessment, patient-treatment matching and treatment outcome measures for sensory processing deficits in ASD. Future studies will aim to evaluate the specificity of these findings to ASD as well as potential perceptual differences resulting from rVOR deficits in ASD such as dynamic visual acuity and subjective visual vertical/horizontal.

815 Functional Brain Imaging of Multi-Sensory Vestibular Processing During Computerized Dynamic Posturography Using Near-Infrared Spectroscopy

Helmet Karim¹, Susan Fuhrman¹, Patrick Sparto¹, Joseph Furman¹, Theodore Huppert¹

¹University of Pittsburgh

Background

Functional near-infrared spectroscopy (fNIRS) is a non-invasive brain imaging method that uses light to determine regional changes in cerebral cortex blood flow in the cortex. In this study, fNIRS was used to investigate how the brain processes information from multiple sensory modalities during computerized dynamic posturography.

Methods

Subjects included fifteen healthy volunteers (9M/6F; ages 28 +/- 9 yrs). fNIRS testing was performed during sensory organization test (SOT) conditions I, II, IV, and V. Due to the nature of the functional NIRS paradigm (as is done in fMRI and other functional testing paradigms), four pairs of two SOT conditions were created. Each pair consisted of a baseline condition-test condition-baseline condition comparison where the condition had one fewer sensory system (vision or proprioception) than the baseline. A bilateral fNIRS probe was used to examine cortical brain activation from the frontal, temporal, and parietal regions.

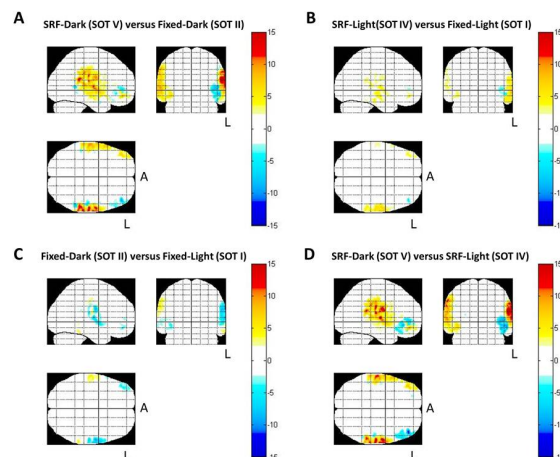
Results

The figure shows the reconstructed image of brain activation during each four of the pairwise comparisons. Conditions that forced vestibular reliance by dropping out both vision and proprioceptive information (Figure 1A and Figure 1D) caused significant bilateral temporo-parietal activations (specifically in the STG and SMG). Conditions that only dropped out either vision or proprioception (Figure 1B and Figure 1C) caused significantly less STG/SMG activation. Thus we found that there was bilateral activation in the temporal-parietal area including the superior temporal gyrus (STG) and supramarginal gyrus (SMG) when both vision and proprioceptive information were degraded thereby forcing reliance on primarily vestibular information in the control of balance.

Figure Legend. Estimated spatial maps (T-test) of the oxy-hemoglobin data collected using functional near-infrared spectroscopy (fNIRS) to detect the change in brain activity during the test condition compared to the baseline conditions.

Conclusion

Our result is consistent with previous reports of the role of these regions in vestibular processing. This study demonstrates the potential utility of fNIRS in the assessment of cortical activity during standing balance tasks.



816 VOR Gain and Compensatory Saccades Immediately After Unilateral Deafferentation: A Prospective Longitudinal Study

Michael Schubert¹, Georgios Mantokoudis¹, Yuri Agrawal¹, Aaron Wong¹

¹Johns Hopkins University

Background

The time course of changes in vestibular neurophysiologic function that occur immediately following unilateral deafferentation has not been well characterized in humans. We evaluated ipsilesional and contralesional vestibulo-ocular reflex (VOR) gain and metrics of compensatory saccade pre-operatively and for six consecutive days following vestibular schwannoma resection.

Methods

Vestibular schwannoma resection occurred via retrosigmoid approach at a tertiary academic medical center. Bedside video-oculography with a portable lightweight goggle system (EyeSeeCam) recorded eye and head rotations at a 250 Hz frame rate. Pre-operatively and then for six consecutive post-operative days (POD), we measured the horizontal VOR during head impulse testing and the latency of compensatory saccades.

Results

To date, we have evaluated 2 out of a projected 10 patients. On POD 1, mean ipsilesional horizontal VOR gain was $0.11 \pm .008$ (range 0.10 and 0.12). VOR gain on the contralesional side was reduced about 50% (mean 0.58 ± 0.03 , range 0.55 and 0.60). Over the inpatient stay, ipsilesional gain remained low while the contralesional gain returned to baseline by POD 3 or 4. Ipsilesional head impulses elicited compensatory saccades that occurred after the head stopped moving (overt) during the early days of recovery (POD 1 – 4). Compensatory saccades that occurred during the head rotation (covert) emerged at POD 5. On POD 2, mean compensatory saccade latency was $214.6\text{ms} \pm 35.0\text{ms}$, which reduced to $160.7 \pm 62.5\text{ms}$ by POD 5 – 6. Compensatory saccades occurred for contralesional head impulses as well.

Conclusion

Our data provide evidence of significant compensation beginning in the first days following unilateral deafferentation. This appears to occur via 2 primary means: normalization of the contralesional VOR gain, and a reduction in the latency of the compensatory saccades. We are continuing to explore the clinical and functional correlates of these changes in VOR gain and saccade metrics.

817 Does Aging Impact the Response to Vibrotactile Feedback (VTF) During Balance Tasks?

Chia-Cheng Lin¹, Susan Whitney², Patrick Loughlin³, Joseph Furman⁴, Kethleen Sienko⁵, Mark Redfern⁶, Patrick Sparto¹

¹Department of Physical Therapy, University of Pittsburgh, ²Department of Physical Therapy and Otolaryngology, University of Pittsburgh, ³Depts. of Bioengineering, and Electrical & Computer Engineering, University of Pittsburgh, ⁴Departments of Otolaryngology, University of Pittsburgh, ⁵Department of Biomedical Engineering and Mechanical Engineering, University of Michigan, ⁶Swanson School of Engineering, Univeristy of Pittsburgh

Background

Human balance relies on the integration of vision, somatosensation and vestibular inputs. Vibrotactile feedback (VTF) applied to the torso provides an additional sensory input to augment postural control. The purpose of this study was to examine short-term and long-term learning while using VTF during conditions of reduced sensory input. We also examined the effect of age on learning during VTF.

Methods

Eighteen young (age: $24.7 \pm 2\text{y}$; 8 males) and twenty older (age: $75.4 \pm 6\text{y}$; 10 males) healthy adults participated. Each subject completed three study visits including one training visit and two experimental visits. The standing balance task required subjects to stand for 120 s during different reduced sensory feedback conditions using a Smart Equitest™ platform. During the second and third visit, three sensory conditions with VTF were tested in random order after a short re-training period. The conditions included: eyes open with darkened goggles on a fixed platform (EOD/FIX), eyes open in light on a sway-referenced platform (EO/SR), and EOD/SR. The root-mean-square (RMS) of the center of pressure (COP) in the anterior-posterior direction was calculated during different time-periods (1: 0-30 s, 2: 30-60 s, 3: 60-90 s and 4: 90-120 s). A repeated measures ANOVA was conducted to investigate the effect of age (Young/Older), and the effect of short-term learning (Periods 1-4) and long-term learning (Visit 2/3), as well as the interactions on the RMS COP.

Results

In the condition of EO/SR, there were significant main effects of Period ($p = 0.012$) and Group ($p = 0.002$, RMS greater in older adults). In the conditions of EOD/FIX and EOD/SR, there were significant main effects of Period ($p < 0.001$), Visit ($p < 0.02$, RMS reduced on last visit), and Group ($p = 0.001$, RMS greater in older adults). Generally, the post-hoc analyses showed that the RMS of Period 1 was significantly greater than the RMS of other periods. No significant interactions were found in the three different conditions.

Conclusion

The reduced RMS COP after period 1 and during visit 3 suggests that young and older adults are able to learn to

use VTF over short and long-term periods. The lack of an interaction of Period and Visit with Group indicates that older adults are able to utilize the VTF as well as young adults.

818 Blast Exposure Is Associated with Unilateral Vestibular Damage in US Veterans

Jorge Serrador¹, Melissa Blatt¹, Amanda Acosta¹, Bemín Ghobreal¹, Scott Wood²

¹Veterans Administration, ²NASA

Background

Blast exposure and mild traumatic brain injury are significant problems for the current and recent conflicts, however, data remains limited on the effects of a blast on the vestibular system. The goal of this work was to determine if veterans with a blast exposure demonstrate impaired vestibular function.

Methods

Ten veterans (males, 41.8 ±8.5 years, 7 endorsed blast exposure) participated. Ocular counter-roll was measured during two different protocols. To assess bilateral response, subjects were tilted ±20 degrees at 0.03125 Hz (32 sec cycle) in the dark. To assess unilateral response from each ear, subjects were rotated in the dark at 400°/sec for 5 min after which there were translated 5 cm off center to the right and left for 30 sec, repeated 3 times. This allowed for unilateral stimulation of each otolith. Infrared images of both eyes were recorded continuously and analyzed using commercial software (SMI). Translation was not performed until subjects reported no sense of rotation.

Results

Examination of the tilt protocol demonstrated that bilateral ocular counter-roll was not different between groups (Controls: 0.108 ±0.021; Blast: 0.140 ±0.014). However, while unilateral values between sides did not differ in the control group (Max Response: 0.070 ±0.020; Other side: 0.067 ±0.016), they were significantly different in the group with Blast Exposure (Max Response: 0.124 ±0.013; Impaired side: 0.070 ±0.010).

Conclusion

These data indicate that veterans with blast exposure appear to have increased risk of unilateral otolith damage. In addition, this unilateral damage is masked when tested using stimuli that affects both ears. Further work is needed using a larger sample to determine the prevalence of this unilateral dysfunction. Supported by the War Related Illness & Injury Study Center, Veterans Administration and NIH grant R21DC009900 (Serrador).

819 The Effect of External Sound on Maintaining Balance

Madelyn Stevens¹, Rachael Mangiore¹, Rosalie Uchanski¹, Dennis Barbour¹, Timothy Hullar¹

¹Washington University in St. Louis

Background

Maintaining balance and reducing postural sway is critical in the prevention of falls, particularly among the elderly and those with vestibular impairments. Although enhancing haptic and visual cues has been shown to facilitate improvements in balance, little research has examined the contribution of auditory cues as a mechanism for maintaining balance. What work has been done has focused on modulation of auditory cues to provide a feedback signal to reduce sway. The present study demonstrates how stationary auditory stimuli provide useful external reference cues to maintain balance in patients with sensory deficits affecting balance.

Methods

12 subjects with hearing or vestibular deficits stood while their center of pressure was measured for four conditions consisting of three 20-second trials each: (1) visual and auditory cues absent (2) visual cues only (3) auditory cues only and (4) visual and auditory cues present. Visual cues were provided by a high contrast abstract landscape and auditory cues were provided by four speakers at ear height emitting a broadband sound stimulus at 55 dB SPL. The speakers were placed at ear height and 50 cm in front of each subject, to each side, and behind. Pressure was measured at 100 samples/second. Sway was quantified as the 95% level on the cumulative distribution of pressure measurements for each 60-second trial condition.

Results

Sway with sound or vision added was linearly related to baseline sway. Sound reduced sway by 51% over the baseline condition. The improvement in sway with the addition of sound was linearly related to the improvement with addition of vision only; the addition of sound represented 55% of the addition of vision.

Conclusion

These results indicate that auditory input provides sensory information that is remarkably important for maintaining balance, particularly in low-light conditions. This is particularly important for patients with poor baseline balance performance. These findings indicate that auditory input is included in the rich multisensory combination of visual, proprioceptive, and visual cues responsible for maintaining balance. They also suggest that optimized auditory input could be used as a tool to improve balance in those with sensory deficits, including in elderly subjects at an elevated risk for falling. These auditory inputs could include environmental cues or improvements in hearing aids or cochlear implants.

820 Psychology of Dizziness

Brian Blakley¹, Alice Kam²

¹U of Manitoba, ²Univ of Toronto

Background

Dizziness is a complex symptom resulting from an interplay of physiological and psychological factors. One potentially relevant psychological factor is called Locus of Control (LOC). LOC is a well-established psychological concept that reflects the extent to which an individual believes that he/she is controlled by either external or internal factors. LOC has not been studied in vestibular patients with and without caloric test abnormalities. The original LOC has been extended to assess the extent to which internal control, powerful others and chance play in controlling our symptoms.

Methods

Patients who presented for electronystagmography testing filled out a standardized, validated questionnaire to establish their LOC in three domains – INTERNAL, POWERFUL OTHERS, and CHANCE. Eight weeks later the subjects were contacted to see what treatments they had used, if they had improved, and what treatment(s) they thought had helped. Using IBM SPSS statistics v19.0, analysis of variance was used to assess the relationship between LOC, improvement, and treatment. Single sample t-tests were used to determine whether or not the scores differed from published normal values.

Results

Our response rate was 80.5%. Ninety-four percent reported that their symptoms had either not changed or were better. Only 6% were worse. There were no differences in improvements rates due to treatment or diagnosis or ENG testing results. There was a significantly lower INTERNAL locus of control in our sample ($p=0.042$) but not for POWERFUL OTHERS ($p=0.705$) or CHANCE ($p=0.816$). Patients who scored high in the POWERFUL OTHERS domain had a statistically significant greater chance of showing improvement ($p=0.019$) but neither INTERNAL nor CHANCE scores were significantly associated with improvement.

Conclusion

Patients with dizziness may feel that outside forces control their situation to a greater extent than the general population. LOC is not useful to guide treatment for dizzy patients.

821 ATP Response of P2X2 Receptor Deafness Mutation and Association with Prestin Activity

Yan Zhu¹, Hong-Bo Zhao¹

¹University of Kentucky Medical Center

Background

ATP is an important extracellular signaling molecule and can influence cellular function in many aspects through the activation of purinergic (P2) receptors. P2 receptors have ATP-gated ionotropic (P2X) and G protein-coupled metabotropic (P2Y) subgroups. P2X2 is a predominant

isoform and extensively expressed in the cochlea, including hair cells and supporting cells. Recently, it has been found that P2X2 mutation can induce human nonsyndromic hearing loss DFNA41. However, the deafness mechanisms remain unclear. We previously demonstrated that ATP can activate P2X receptors to mediate outer hair cell (OHC) electromotility and K⁺-sinking and recycling in the cochlea. In this study, we investigated whether P2X2 deficiency can affect ATP activation and prestin activity.

Methods

Prestin and P2X2 wild-type (WT) and V60L mutant were cloned and transfected into HEK 293 cells. ATP-evoked responses and prestin electromotility associated nonlinear capacitance (NLC) were recorded by patch clamp. We also used P2X2 knockout (KO) mice to assess whether P2X2 deficiency can diminish OHC response to ATP.

Results

Both P2X2 WT and V60L mutant targeted to plasma membrane. However, P2X2 V60L deafness mutation diminished ATP responses. The ATP-evoked inward current was eliminated in P2X2 V60L mutant transfected cells. We also found that ATP lacked the effect on prestin activity in prestin-transfected cells. However, the ATP effect was restored after co-transfection with P2X2 receptors. NLC was right-shift as we previously reported in native OHCs to ATP stimulation. P2X2 deficiency also eliminated the effect of ATP on prestin activity. OHCs in P2X2 KO mice retained NLC but lacked the response to ATP.

Conclusion

These data demonstrate that P2X2 V60L deafness mutation diminishes ATP responses. These studies also indicate that P2X2 deficiency compromises OHC electromotility regulation, which may result in over-activity of active cochlear mechanics under noise stress to induce hearing loss.

822 Tumor Necrosis Factor-Alpha-Mutant Mice Exhibit High Frequency Hearing Loss

Jun Chen¹, Naoki Oishi², Hong-Wei Zheng¹, Kayla Hill¹, Jochen Schacht², Su-Hua Sha¹

¹Department of Pathology, Medical University of South Carolina, ²Kresge Hearing Research Institute, University of Michigan

Background

Exogenous tumor necrosis factor-alpha (TNF α) modulates hair cell death by altering the expression of apoptosis-related genes in response to noxious stimuli. However, little is known on the function of TNF α in normal hair cell physiology. In this study, we investigated cochlear morphology and auditory function of TNF α -deficient mice.

Methods

Auditory brainstem responses and distortion product otoacoustic emissions (DPOAE) to measure hearing function - Plastic sections to determine cochlear

morphology and anatomical structure - Myosin VII and DAB staining on surface preparations of the cochlear epithelium for hair cell counts - Immunolabeling with anti-CtBP2 to determine synaptic ribbon counts - Scanning electron microscopy to analyze stereocilia morphology - Light microscopic inspection of auditory ossicles.

Results

At one month of age TNF α -mutant mice exhibited significant hearing loss, especially at higher frequencies, which was more profound in TNF α ^{-/-} mice compared to TNF α ^{+/-} and wild-type (WT) mice. Hearing loss did not progress any further from 1 to 4 months of age. DPOAE measurements (24 kHz) indicated outer hair cell dysfunction in TNF α ^{-/-} mice, but surface preparations showed no outer hair cell loss. However, stereocilia were lost in the basal turn and had collapsed in the middle turn of TNF α ^{-/-} mice. The synaptic ribbon counts of TNF α ^{-/-} and WT mice at four months of age were similar. There was also no difference in the morphology of the organ of Corti, lateral wall, and spiral ganglion cells in TNF α ^{-/-} mice compared to WT mice, nor were there differences in the morphology of the ossicles.

Conclusion

TNF α ^{-/-} mice show loss or malformation of stereocilia of outer hair cells. The otherwise normal cochlear and ossicular morphology and normal synaptic ribbon counts support the notion that stereociliary dysfunction is a major contributor to the observed threshold shifts.

The research project described was supported by R01 grants DC009222 (to SHS) and DC-03685 (to JS) from the National Institute on Deafness and Other Communication Disorders, National Institutes of Health.

823 Mice Deficient in the H⁺-ATPase A4 Subunit Have Severe Hearing Impairment Associated with Enlarged Endolymphatic Compartments Within the Inner Ear

Beatriz Lorente-Canovas^{1,2}, Neil J Ingham^{1,2}, Elizabeth E Norgett³, Zoe J Golder³, Fiona E Karet Frankl³, Karen P Steel^{1,2}

¹King's College London, ²Wellcome Trust Sanger Institute,

³University of Cambridge

Background

Mutations in the *ATP6V0A4* gene lead to autosomal recessive distal renal tubular acidosis in patients who often show sensorineural hearing impairment. A first *Atp6v0a4* knockout mouse model that recapitulates the loss of H⁺-ATPase function seen in humans has been generated and recently published (Norgett et al., 2012). Here we present the first detailed description of the structure and function of the auditory system in these *Atp6v0a4*^{-/-} mice.

Methods

Auditory brainstem responses (ABR) were recorded in mice at 14 and 20 days and endocochlear potentials were measured in mice at 19-21 days.

Gross morphology of the inner ears at P20 was examined after clearing with glycerol and paint-filling was used for inner ears at P0 and E16.5.

for histological examination samples were sectioned and stained with Haematoxylin & Eosin (HE). We selected sections for immunohistochemistry to test different markers.

We examined inner ears at P20 by scanning electron microscopy (SEM) to check the integrity of hair cell bundles in mutants and controls.

Results

Measurements of the auditory brainstem response (ABR) showed significantly elevated thresholds in mutant mice at 14 and 20 days old, which indicate a severe hearing impairment. In addition, analysis of paint-filled ears and sections from E16.5 embryos revealed a severe expansion of cochlear and endolymphatic ducts in *Atp6v0a4*^{-/-} mice. A regulatory link between *Atp6v0a4*, *Foxi1* and *Pendrin* has been reported and we find that the endolymphatic sac of *Atp6v0a4*^{-/-} mice expresses both *Foxi1* and *Pds*, which suggests a downstream position of *Atp6v0a4*.

These mutants also showed a lack of endocochlear potential which suggests a defect in function of the stria vascularis on the lateral wall of the cochlear duct. However the main K⁺ channels involved in the generation of endocochlear potential, *Kcnj10* and *Kcnq1*, are strongly expressed in *Atp6v0a4*^{-/-} mice.

Conclusion

Our results lead to a better understanding of the role of H⁺-ATPase a4 subunit in hearing function.

824 Cochlear Enlargement in Mice Lacking *Slc26a4* Is a Consequence of Disrupted NaCl Absorption

Xiangming Li¹, Fei Zhou¹, Daniel C. Marcus¹, Philine Wangemann¹

¹Kansas State University

Background

Enlargement of the vestibular aqueduct (EVA), commonly found in children with sensorineural hearing loss, is frequently associated with mutations of *SLC26A4* which codes for pendrin. A mouse model of EVA, *Slc26a4*^{-/-}, develops an abnormal enlargement of the membranous labyrinth, and fails to develop hearing. The goal of this study was to determine the ionic composition of endolymph at the time at which the enlargement develops.

Methods

K⁺ and Na⁺ concentrations in endolymph of *Slc26a4*^{+/-} and *Slc26a4*^{-/-} mice were measured with double-barrel ion-selective electrodes. The K⁺ concentration and transepithelial voltage were measured from embryonic day (E) 14.5 onward and the Na⁺ concentration was measured between E16.5 and postnatal day (P) 0. Expression of mRNA and protein of genes associated with K⁺ and Na⁺

transport in the inner ear were examined by quantitative RT-PCR and/or immunohistochemistry.

Results

Between E14.5 and E17.5, the K^+ concentration in cochlear endolymph remained low at ~10 mM and began to rise at E19.5. The rise of the endolymphatic K^+ concentration was delayed in the cochlea and the utricle of *Slc26a4*^{-/-} mice. Between E14.5 and P8, the cochlear expression of *Kcnq1*, *Slc12a2* and *Atp1a1* increased by ~4, ~8 and ~10 fold, respectively. Expression was similar in *Slc26a4*^{+/-} and *Slc26a4*^{-/-} mice. A surge in the mRNA expression of *Kcnq1* and *Slc12a2* was observed at the time of birth. The onset of *Kcnq1* and *Slc12a2* protein expression in the inner ear was observed at E19.5 in both *Slc26a4*^{+/-} and *Slc26a4*^{-/-} mice. At E16.5, cochlear Na^+ concentration in endolymph was ~140 mM, which dropped drastically at P0. The drop in the Na^+ concentration was delayed in *Slc26a4*^{-/-} mice. Cochlear expression of *Scnn1b* and *Scnn1g* was increased but no difference of *Scnn1a* expression was found in *Slc26a4*^{+/-} and *Slc26a4*^{-/-} mice at ages E14.5 to P8.

Conclusion

These data demonstrate that endolymph in the phase of cochlear growth during embryonic development of the mouse inner ear is a NaCl-rich fluid, which is modified into a KCl-rich fluid just prior to birth. Further, the data suggest that endolymphatic enlargement caused by a loss of *Slc26a4* is a consequence of disrupted NaCl absorption. Supported by NIH-R01-DC012151, KCALSI, KINBRE and NIH-P20-RR017686

825 Mechanical Filters in Rbl2 Null Mice: The Influence of Supernumerary Inner Ear Sensory And/or Support Cells

JoAnn McGee^{1,2}, Katyarina E. Brunette¹, Sarah Stimmler¹, Kaitlyn Filippini¹, Sonia Rocha-Sanchez³, Edward J. Walsh^{1,2}

¹Boys Town National Research Hospital, ²Creighton University School of Medicine, ³Creighton University School of Dentistry

Background

Numerous animal models that are characterized by the presence of supernumerary inner ear sensory and support cells have been generated by inactivating or partially inactivating genes that negatively regulate the cell cycle. This includes the *Rbl2* null mouse strain that stands as a unique animal model of inner ear cell proliferation in that sensitivity to sound and distortion product otoacoustic emission (DPOAE) suppression tuning curves appear normal in spite of the presence of an extra row of inner hair cells and extra row(s) of outer hair cells in the apical half of the cochlea (Rocha-Sanchez et al., 2011; Brunette et al., 2012). In this study, the shape and properties of inner ear mechanical filters in *Rbl2* null and wild-type (WT) mice were compared in an effort to determine if the presence of supernumerary sensory and/or support cells alters filter characteristics at suprathreshold levels.

Methods

To address this question, DPOAE “ratio series” were obtained in WT and *Rbl2* null mice. The separation between primary stimulus frequencies was varied in an orderly manner while holding f_2 constant ($f_1 < f_2$), and levels of the $2f_1 - f_2$ component were plotted as a function of distortion product (DP) frequency. This manipulation produces DPOAE filter functions that represent mechanical events underlying spatial interactions between two tones in the inner ear. The level of primaries used to generate responses varied from an f_1 level of 20 to 70 dB SPL, in 10 dB steps, and the level of f_1 was always 10 dB higher than that of f_2 .

Results

The center frequency of DP level versus DP ($2f_1 - f_2$) frequency curves predictably shifted in the direction of lower DP frequencies as stimulus levels increased in both WT and *Rbl2* null mice; however, DP peak frequency tended to be slightly lower in *Rbl2* null mice than in WT cohorts. In addition, broader mechanical filter envelopes were observed in *Rbl2* null mice when compared with WT mice, and DP levels produced by *Rbl2* null mice were lower than in WT mice when higher level primary tones were considered.

Conclusion

Mechanical filters of the inner ears of *Rbl2* deficient mice are qualitatively similar to those representing WT mice; however, extra sensory and/or supporting cells in *Rbl2*^{-/-} mice appear to influence the ratio between primary stimulus frequencies producing the peak DP, and reduce filter sharpness at moderate and higher primary stimulus levels for conditions studied thus far.

826 Autophagy Is Essential for the Maintenance of Cochlear Outer Hair Cells and Hearing in Vivo

Masato Fujioka^{1,2}, Sho Kanzaki¹, Yuto Baba³, Nana Tsuchihashi^{1,4}, Ken Hayashi⁵, Mitsuhiro Kawaura², Kaoru Ogawa¹

¹Dpt of Otolaryngology, School of Medicine, Keio Univrsitiy,

²Dpt of Otolaryngology, Keiyu Hospital, ³School of Medicine, Keio Univrsitiy, ⁴Dpt of Otolaryngology, Graduate School of Med, Kyushu Univ, ⁵Shinkawa Clinic

Background

Auditory hair cells are responsible for the transduction of sound-evoked mechanical energy to the nerve impulses throughout the life without replacement. We here investigated the role of autophagy, an evolutionary conserved intercellular recycle pathway via lysosome, in the maintenance of homeostasis in the auditory hair cells.

Methods

1) An autophagy reporter mouse line, *GFP-LC3* was examined by immunostaining for GFP using antibody. The mice has robust expression of GFP-LC3 fusion protein on the autophagosome, which is a fundamental structure of autophagy. Paraffin sections of the inner ear were investigated. 2) A mouse line disrupting autophagy

specifically in the inner ear hair cells was generated by crossing *Pou4f3-Cre*, an hair cell-specific Cre mouse, with *flox-Atg7*. *Atg7* is an essential gene for the formation of autophagosome and its genetic depletion results in the complete abolishment of autophagy. Tone-burst ABR at 2, 4, 8, 16, 32kHz and histological examinations were performed at 8 and 32 week old of the conditional knock-outs and their littermate controls.

Pou4f3-Cre is a kind gift from Dr. Vetter (Univ. Mississippi Medical Center). *GFP-LC3* (Tg(CAG-EGFP/Map11c3b)53Nmz: RBRC00806) and *flox-Atg7* (B6.Cg-Atg7tm1.1Tch: RBRC02759), were generated by Dr. Mizushima and Dr. Komatsu (Tokyo Medical Dental Univ), respectfully, and both were supplied via RIKEN BRC under their permissions.

Results

Reporter expression was observed in outer hair cells and supporting cells of *GFP-LC3* but was not seen in inner hair cells. Conditional knock-outs of *Atg7* suffered an accelerated hearing impairment from high frequency to the lower as their ages developed. ABR threshold was significantly elevated compared to the control. Histology showed missing outer hair cells at 32 week of age.

Conclusion

The results suggest that the autophagy is required especially for the maintenance of outer hair cells but is, interestingly, not necessarily required in inner hair cells. Further studies elucidating the precise role of autophagy in the outer hair cells, especially which protein and/or organelle is degraded by autophagy, will be investigated.

827 New Function for Connexin26 (Cx26) in the Cochlea and New Mechanism for Deafness Induced by Deficiency in Cx26

Jin Chen¹, Yan Zhu¹, Arya Parsa², Chun Liang¹, Liang Zong¹, Federico Kalinec², Hong-Bo Zhao¹

¹University of Kentucky Medical Center, ²House Research Institute

Background

Connexin 26 (Cx26, GJB2) mutations can induce a high incidence of nonsyndromic hearing loss. The deafness-inducing mechanism, however, remains largely undetermined. Hair cells have no gap junctions and connexins are only expressed in supporting cells with Cx26 being the predominant isoform in the cochlea. Recently, we have reported that cell degeneration is not a primary cause for Cx26 deficiency-induced hearing loss (Liang et al., 2012). We have also reported that supporting cells can modify active cochlear amplification, probably by influencing outer hair cell (OHC) electromotility (Yu and Zhao, 2009). However, the molecular and cellular mechanism underlying this modification remains unclear. In this study we investigate morphological changes in cochlear supporting cells induced by Cx26 deficiency.

Methods

Cx26 deficient mice were created by loxP-Cre technique. Auditory function was measured with ABR and DPOAE

techniques, and confocal and electron microscopy (EM) techniques were used to assess morphological changes in the cochlea. OHC nonlinear capacitance (NLC) was measured by patch clamp recording.

Results

Deletion of Cx26 in Deiters cells and outer pillar cells reduced DPOAE and increased ABR thresholds. However, the cochlea had normal development and the tunnel of Corti was open. Patch clamp recording showed that NLC was shifted to right in depolarization direction. In EM images Deiters cells appeared fat, with plasma membrane of adjacent cells sticking together in a way rarely observed in control animals. The microtubules in DCs and outer pillar cells also appeared to be less abundant.

Conclusion

Cx26 deficiency induces morphological changes in cochlear supporting cells, probably altering their mechanical properties. These changes might influence OHC electromotility and eventually lead to hearing loss. This study also suggests a new non-channel function of Cx26 in the cochlea.

828 Deiters Cells' Attachment to the Basilar Membrane Is Structurally Similar, and Mediated by the Same Adhesion Molecules, in Mice, Rats and Guinea Pigs

Pru Thein¹, Arya Parsa¹, Gilda Kalinec¹, Federico Kalinec^{1,2}

¹Section on Cell Structure & Function, Division on Cell Biology & Genetics, House Research Institute,

²Departments of Cell & Neurobiology and Otolaryngology, University of Southern California

Background

Deiters cells extend from the basilar membrane to the reticular lamina and, together with pillar cells and outer hair cells, structurally define the micro-architecture of the organ of Corti. We have recently described that mouse Deiters cells possess a morphologically distinct infranuclear region, and their very basal portion, known as Deiters' feet, contact the basilar membrane in a narrow stripe extending all along the length of the organ of Corti.

Methods

Using confocal laser and electron scanning microscopy we have now continued our studies in mice and extended them to two additional species, guinea pigs and rats.

Results

We found that, just like in mice, in rats and guinea pigs the basal pole of every Deiters cell was attached to the basilar membrane within an approximately 15 μ m-wide stripe adjacent to the row of outer pillar cells running all the length of the cochlear spiral. Also, as described in mice, complete detachment of Deiters cells in these other two species revealed an elliptical imprint on the top surface of the basilar membrane consisting of a smaller central structure with a very smooth surface surrounded by a rougher area, suggesting the presence of two different

anchoring junctions. Immunofluorescence studies with specific antibodies suggested that the adhesion molecules in the central region would be mostly integrins, whereas the peripheric region would contain laminins and the discoidin domain receptor tyrosine kinase 1 (DDR1).

Conclusion

These results indicate that Deiters cells follow the same pattern of organization, and use the same mechanisms of adhesion to the basilar membrane, in three different species, suggesting a high degree of evolutionary conservation.

Supported by NIH Grant DC010146

829 Metabolome Analysis of Inner Ear Fluid in Guinea Pigs Cochlea

Daisuke Yamashita¹, Takeshi Fujita¹, Yuriko Hashimoto¹, Hitomi Shinomiya¹, Shingo Hasegawa¹, Ken-ichi Nibu¹

¹Kobe University

Background

The metabolome analysis is to analyze metabolites resulting from all cellular activity to have of the organism cyclopedically. The intracellular dynamics which are not understood by expression of mRNA and proteome analysis are found by the profile of the metabolome analysis. Various clinical conditions such as cancer and immune disease have been recently apparent by metabolome analysis with many organs and tissues. This time we examined metabolome analysis of inner ear fluid in guinea pigs cochlea using gas-chromatography/mass-spectrometry (GC/MS).

Methods

Eighteen pigmented guinea pigs (250-300g; Hartley male) with normal Preyer's reflex were used in this study. The experimental protocol was approved by the Animal Care and Use Committee at the University of Kobe. After animals were deeply anesthetized decapitated, the temporal bones were immediately removed. Under a dissecting microscope, the round and oval windows were opened and the lymphatic fluids were taken. At the same time decapitating, plasma fluid were also taken. We extracted water-soluble metabolite from the inner ear lymphatic and plasma fluids. After freeze dry and a process of derivatizing, metabolites were measured with GC/MS-QP2010. The obtained data examined the metabolite by principal component analysis.

Results

As for the metabolite which was specific for inner ear fluid of guinea pig cochlea, it was detected 29 kinds in total. Also, the metabolite, which was significantly frequent in inner ear fluid compared to plasma, was detected totally seven kinds.

Conclusion

The present study reports for the first time that metabolome analysis of the inner ear. As results, it was detected 29 kinds in total, for the metabolite which was

specific for inner ear fluid of cochlea. Also, the metabolite, which was significantly frequent in inner ear fluid compared to plasma, was detected totally seven kinds. It seems that these results lead to clinical condition elucidation of the sensorineural hearing loss including noise-, drug- aging-induced hearing loss for a diagnostic tool and treatment therapy.

830 Defining the Role of Integrins in the Repair and Regeneration of Hair Cells in the Human Vestibular System

Kiran Hussain¹, Sally. J. Dawson¹, Andrew Forge¹, Shakeel Saeed¹, Ruth. R. Taylor¹

¹UCL Ear Institute

Background

Integrins are cell adhesion receptors that play important roles in physiological and pathological processes throughout the body. Integrins comprise alpha and beta subunits and the 24 $\alpha\beta$ heterodimeric members mediate the interaction of cell-cell signalling and communication between the cell and extracellular matrix.

Lesions created by the death of a hair cell is closed by supporting cells in a manner that maintains the permeability barrier at the luminal surface of the epithelium. This controlled process relies on cell shape changes and spreading that likely involves integrins. Furthermore, the supporting cells are thought to remove these dead hair cells by a phagocytic process. Certain integrin receptors recognise apoptotic cells mediating phagocytosis of the apoptotic body.

Following hair cell loss in the vestibular system of mammals there is limited regeneration possibly via the direct phenotypic conversion of supporting cell into hair cells without an intervening mitotic event. We hypothesise that integrins play an integral role in the repair and recovery process. We are able to test this hypothesis with human vestibular tissue obtained from patients undergoing trans-labyrinthine procedures for acoustic neuromas. In this first part of the work we identify which integrins are normally expressed in human vestibular tissues.

Methods

qPCR was used to screen for the integrin m-RNAs specifically expressed in human vestibular explants. Upon harvesting from the patient, the tissue was immediately transferred to RNAlater for transport to the laboratory. RNA was subsequently prepared using RNeasy (Qiagen) and reverse transcribed into cDNA. Each array was performed with cDNA from the vestibular tissue explanted from a single patient. Data was collated from individual arrays and relative expression was quantified by qPCR using the ddCT method.

Directed by the results of the qPCR analysis, the expression pattern of specific integrin proteins was localised using immunohistochemistry. Human vestibular tissue was transported in Minimal Essential Medium, subsequently fixed and labelled using antibodies with human specific reactivity.

Results

qPCR array demonstrated integrin subunit mRNAs ITA5, ITA6, ITA8, ITAV, ITB1 and ITB5 were expressed above background levels suggesting their presence in human vestibular tissue. Previous work in our laboratory has identified these integrins in adult mouse vestibular tissue.

Conclusion

The integrin profiles of human and mouse vestibular systems are similar but not identical. On-going work will continue to examine integrin protein expression and location and further elucidate their role in the repair of the sensory epithelia of the inner ear and regeneration of hair cells.

831 Expression Changes of Endothelin 1, Endothelin Receptor a and B in Noise Induced Cochlea

Jin Woong Choi¹, Ah-Ra Lyu¹, Yong-Ho Park¹

¹Department of Otolaryngology, Chungnam National University, Daejeon, South Korea

Background

After noise exposure, impairment of cochlear blood flow has been considered to be one of the factors of hearing loss. Although there were several evidences of reducing blood flow in the cochlea after noise exposure, the pathophysiology of blood flow change is still obscure. Endothelins are proteins that constrict blood vessels and have a key role in vascular homeostasis and works through its receptors. Recent research has shown that endothelin and its receptors were present in the cochlea and these things were regarded to have a role in regulation of cochlear blood flow. In this study, we investigated the expression changes of endothelin 1 (ET-1), endothelin receptor A (ETAR) and B (ETBR) according to auditory threshold change after noise exposure.

Methods

Mice were exposed to noise to generate transient threshold shift (TTS) and permanent threshold shift (PTS) respectively. Auditory threshold shifts were evaluated with auditory brainstem response and expression changes of ET-1, ETAR and ETBR after noise exposure were evaluated by RT-PCR.

Results

Expressions of endothelin 1, endothelin receptor A and B were changed after noise exposure in both TTS and PTS group. After noise exposure, expression of ET-1 was increased in TTS group compared to control and PTS group. Expression of ETAR was decreased just after noise exposure but increased 2 weeks after noise exposure in PTS group. Little changes of ETAR expression were noted in TTS group. Expressions of ETBR were increased in both TTS and PTS group just after noise exposure but it was sustained in PTS group after 2 week after noise exposure compared to TTS group.

Conclusion

These results suggest that expression changes of ET-1, ETAR and ETBR might be associated with hearing threshold shift and recovery after noise exposure in the cochlea.

832 Vascular Diameter of the Spiral Modiolar Artery Is Regulated by Ca²⁺ Sparks, K⁺ Channels and Ca²⁺ Sensitivity

Gayathri Krishnamoorthy¹, Katrin Reimann¹, Philine Wangemann¹

¹Kansas State University

Background

The combined action of Ca²⁺ sparks and Ca²⁺-activated K⁺ (BK) channels lowers smooth muscle global Ca²⁺ concentration leading to relaxation of vascular smooth muscle cells and vasodilation. Loss of Ca²⁺ sparks or uncoupling of BK channels from Ca²⁺ sparks leads to increase in global Ca²⁺ concentration and vasoconstriction. Here, we investigated whether Ca²⁺ sparks and BK channels regulate smooth muscle global Ca²⁺ and the vascular diameter of the spiral modiolar artery (SMA) and control cochlear blood flow.

Methods

SMAs from female gerbils were cannulated with a motorized concentric pipette system, pressurized at 40 or 60 cmH₂O and loaded with the fluorescent Ca²⁺ indicator dye, fluo4. Ca²⁺ sparks and Ca²⁺ waves were recorded in line scans and frame scans. Smooth muscle global Ca²⁺ and vascular diameter was recorded simultaneously using confocal microfluorometry.

Results

Ca²⁺ sparks and Ca²⁺ waves were observed in pressurized SMAs at 40 and 60 cmH₂O. At 40 cmH₂O, ryanodine abolished Ca²⁺ sparks and waves, increased the global Ca²⁺ and caused a vasoconstriction. In comparison, at 60 cmH₂O, ryanodine-induced increase in the global Ca²⁺ was smaller and vasoconstriction was suppressed. The pressure-dependence of the ryanodine-induced vasoconstriction was consistent with the pressure-dependence of the Ca²⁺ sensitivity, which was greater at 40 than at 60 cmH₂O. Treatment with 1nM endothelin-1 increased ryanodine-induced vasoconstriction at 60 cmH₂O. Iberiotoxin, an inhibitor of BK channels, had no effect on either global Ca²⁺ or vascular diameter, although in the presence of iberiotoxin, ryanodine-induced effects were greatly diminished. Iberiotoxin increased global Ca²⁺ and caused a vasoconstriction in the presence of apamin, an inhibitor of Ca²⁺-sensitive small-conductance K⁺ (SK) channels.

Conclusion

The results indicate that, in the SMA, regulation of global Ca²⁺ and vascular diameter by Ca²⁺ sparks and BK channels is modulated by SK channels and the Ca²⁺ sensitivity. SK channels are critical for the control of global Ca²⁺ whereas the Ca²⁺ sensitivity is critical for the control of vascular diameter.

This study was funded by NIH R01-DC04280 to PW.

833 The Functional Modification of pRb During the Early Development of Chicken Inner Ear

Wenyan Li^{1,2}, Yan Chen¹, Qin Lin³, Huiqian Yu¹, Zheng-Yi Chen², Huawei Li¹

¹Eye Ear Nose and Throat Hospital of Shanghai medical school, Fudan University, ²Eaton-Peabody Laboratory, Massachusetts Eye and Ear Infirmary, Harvard Medical School, ³Department of Otolaryngology, The First Affiliated Hospital of Fujian Medical University

Background

The retinoblastoma protein pRb plays a vital role in regulating mammalian cell cycle progression, and inactivation of pRb is necessary for S phase re-entry. Further, pRb plays a crucial role in cell survival. Therefore, modulation of pRb function transiently instead of permanent deletion, is an attractive route by which proliferation and survival can be achieved for hair cell regeneration.

Methods

pRb function is regulated by different types of phosphorylation: cyclin dependent that is mediated by Ras/Raf/Mek/MAPK cascade or cyclin independent that is mediated by the physical interaction between C-Raf and pRb. Using a culture system for chicken otocysts, we investigated how two small molecules U0126 and RRD 251, inhibitor of MAPK cascade or Rb-Raf-1 interaction, affect progenitor cells proliferation and differentiation during the early inner ear development.

Results

Inhibition by both U0126 and RRD 251 in the progenitor cells led to cell cycle arrest and increased apoptosis. Further, inhibition of MAPK cascade mediated pRb phosphorylation significantly reduced the number of proliferating pro-sensory progenitors; whereas inhibition of C-Raf-mediated phosphorylation significantly reduced the number of proliferating ganglion progenitors.

Conclusion

We concluded that different pathway of pRb phosphorylation play distinct roles during the early inner ear development, with implication in modulating pRb function according their cell type specificities.

834 Acute Ischemic Hypoxia Affects Distinct Channels in Smooth Muscle and Endothelial Cells in the Spiral Modiolar Artery

Yu-Qin Yang¹, Zhi-Gen Jiang¹

¹Oregon Health & Science University

Background

Acute ischemia generally induces a compensatory vasodilation in the most vascular beds including the cochlear arterioles but the underlying cellular mechanism remains controversial.

Methods

Using conventional intracellular and whole-cell recording from smooth muscle (SMC) and endothelial cells (EC) in situ of and dispersed from segments of guinea pigs cochlear spiral modiolar artery, we analyzed the membrane actions of acute ischemic treatment (AIT, hypercapnic hypoxia, pO₂ = 0 mmHg, pH = 6.5).

Results

The AIT for 2 to 30 min caused a reversible and partially repeatable vasodilation and hyperpolarization in the majority of cells. ACh- and 10 mM K⁺-induced dilation was significantly reduced, lost or reversed to a constriction during and after the AIT. Holding at -40 mV, AIT induced a reversible 10-60 pA outward current within 1-2 min in the majority of SMCs and ECs. During the AIT, the whole-cell I/V curve became stronger outwardly rectifying at voltages > -40 mV. The AIT-induced net current in isolated SMCs exhibited a voltage and time dependence and sensitivity to 1-10 mM TEA or 4-AP similar to those of voltage-gated (KV) and big conductance Ca-activated (BK) K⁺-channels. AIT also reduced gap junction coupling current in in situ SMCs. In contrast, the AIT-induced current in isolated ECs was blocked by 100 μM niflumic acid but not by TEA and 4-AP; the net current showed a voltage and time dependence typical of Ca²⁺-activated Cl⁻-channels (CaCC): slowly activating outwardly rectifying with a reversal potential near -30 mV.

Conclusion

We conclude that the acute ischemia in the cochlear arteriole induces hyperpolarization, dilation and loss of EDHF function by implicating activation of KV and BK, inhibition of gap junction coupling in the smooth muscle cells whereas in endothelial cells, AIT mainly activates CaCCs. Supported by NIH NIDCD DC 004716, P30 05983.

835 Acute Ischemia Activates Outward Rectifier Currents in Cochlear Lateral Wall Capillary Cells

Yuqin Yang¹, Alfred Nuttall¹, Zhi-Gen Jiang¹

¹Oregon Health & Science University

Background

Microcirculation in spiral ligament (SL) and strial vascularis (SV) of the cochlear lateral wall are critical for cochlear health, especially the highly energy-demanding auditory transduction, but the physio-pathology of the local capillary cells remains poorly understood.

Methods

Using acutely isolated capillary segments and whole-cell recording techniques, we characterized the main membrane currents and the responses to acute ischemic treatment (AIT, hypercapnic pH 6.5, pO₂ = 0 mmHg) of the endothelial cells (EC) and pericytes (PC) in the SL and SV.

Results

We found: 1) Within physiological solutions, the PCs, but not ECs, showed a [K⁺]_o-facilitated and Ba²⁺-sensitive

inward rectifier current. 2) ECs, but PCs rarely, showed a significant outward rectifier current, which was inhibited by 1 mM 4-AP, 100 μ M niflumic acid (NFA) but not TEA. 3) When recorded in situ of a vessel segment, both types of cells showed variable electrical coupling that can be blocked by 30 μ M 18 β -glycyrrhetic acid or 100 μ M 2-APB. 4) AIT (3 – 24 min) caused a partially reversible and repeatable outward current at holding potential -20 mV in isolated ECs and PCs. The AIT-activated net current had I-V curves and kinetics which mostly resemble to those of Ca²⁺-activated Cl⁻ channels: strong outward rectification with quick or slow time course to reach steady-state within 0.5 - 2 s voltage steps. This AIT-induced current was inhibited by niflumic acid and 1 mM TEA but not 4-AP. 5) AIT (>3 min) also inhibited gap junction coupling current.

Conclusion

We conclude that the capillary EC and PC in the SV and SL express different K⁺-channels, suggesting a role of PCs as the K⁺-sensor for blood flow regulation, and the acute ischemia activates chloride channels and BK channels likely via elevation of cytosolic Ca²⁺ in both ECs and PCs. Supported by NIH grants DC004716 (ZGJ) and DC005983, DC 00105 (ALN).

836 The Involvement of ROCK Pathway in the Apical Cell Contraction in Murine Organ of Corti

Tomoki Fujita¹, Hirofumi Sakaguchi¹, Shigenobu Yonemura², Yasuo Hisa¹

¹Department of Otolaryngology-Head and Neck Surgery, Kyoto Prefectural University of Medicine, Kyoto, ²RIKEN Center for Developmental Biology, Kobe, Japan

Background

We previously reported the morphological changes and plasticity of hair cells and supporting cells by inhibition of myosin II. In the current study, we report the contribution of ROCK and MLCK pathways to the activation of myosin II on the regulation of cell shaping using ROCK inhibitor (Y27632) and MLCK inhibitor (ML7).

Methods

By using explant cultures dissected from murine organ of corti, we compared the morphological changes of hair cells and supporting cells after the treatment with blebbistatin, Y27632 or ML7.

Results

Using Y27632, we observed morphological change less than but similar to one observed in blebbistatin treatment. After Y27632 treatment, the surface area was remarkably enlarged in supporting cells, although it was slightly but significantly enlarged in hair cells. This morphological change is recovered after two more hours of culture in the medium without Y27632. These morphological changes were not observed in ML7-treated samples.

Conclusion

Our data demonstrate that ROCK pathway is involved in the contraction of apical surface in hair cells and

supporting cells through the activation of myosin II. On the contrary, the involvement of MLCK in this process seems to be minimal.

837 Transfection of Therapeutic Genes by Hydroxyapatite Nanoparticle Complexes in Organotypic Cultures of the Inner Ear

Hong Sun¹, Hong Liu¹, Dalian Ding², Xuewen Wu¹, Richard Salvi²

¹Xiangya Hospital, ²University at Buffalo

Background

Gene therapy is a powerful technique for specific treatment of inner ear diseases. Hydroxyapatite nanoparticle (nHAT) is an ideal gene carrier without potential side-effects in comparison with viral vectors, such as oncogenicity, cytotoxic effect, immunogenicity, or non-specific inflammation. Therefore, nHAT has received increasing attention in gene therapy. Our previous studies demonstrated that transfection of nHAT through round window membrane in vivo was mainly ingested by dark cells in the inner ear via endocytosis. However, the transfection efficiency of nHAT to the inner ear in vitro is unknown. In current study, the explants of cochlear and vestibular organs from adult rats and neonatal rats were examined after PEI-nHAT-pEGFPC2-NT3 transfection.

Methods

Adult SASCO sprague dawley rats and post-natal day 3 rats were decapitated. The cochlear organs, macula of utricle and saccule, and crista of ampullaris were cultured in serum-free culture medium or treated with or without 1mM gentamicin. nHAT-pEGFPC2 was mixed into the culture medium with a final concentration of 500 μ g/ml cultured for various period. The explants were fixed with 10% formalin and then stained with TRITC-conjugated phalloidin, which preferentially labels filamentous actin in hair cell stereocilia. Specimens were also stained with Topro-3 to label nucleus. The whole mount specimens were examined under a confocal laser scanning microscope using appropriate filters to detect red fluorescein of phalloidin on the hair cells, green fluorescein of EGFP in transfected cells and blue fluorescein of Topro-3 in the nucleus.

Results

In adult organotypic culture system, EGFP were hardly detected in organs 3 hours after transfection. However, EGFP were clearly visible in vestibular hair cells, spiral ganglion neurons, epithelium of stria vascularis, and also in some damaged cochlear hair cells 30 hours after transfection. Differing from adult cultures, EGFP in neonatal cochlear culture system were not detectable 48 h after transfection. However, when cochlear organotypic cultures were pre-treated with 1mM gentamicin for 10 h, and then cultured with PEI-nHAT-pEGFPC2-NT3 material, EGFP was strongly expressed in many hair cells, spiral ganglion neurons, and epithelium of stria vascularis.

Conclusion

PEI-nHAT can easily transfect therapeutic genes into hair cells, spiral ganglion neurons and stria vascularis in the inner ear in adult rat in vitro. However, PEI-nHAT is difficult to transfect developing cochlear organs at the age of postnatal day 3 in culture condition, unless the barrier of cochlear tissue was damaged by gentamicin.

838 A Protocol for Isolation and Culture of Endothelial Cells, Pericytes, and Perivascular Resident Macrophage-Like Melanocytes from the Young Mouse Ear

Lingling Neng¹, Wenjing Zhang^{1,2}, Ahmed Hassan³, Marcin Zemla³, Allan Kachelmeier¹, Anders Fridberger⁴, Manfred Auer³, Xiaorui Shi¹

¹Oregon Hearing Research Center, ²Department of Otolaryngology/Head & Neck Surgery, Zhengzhou University, ³Life Sciences Division, Lawrence Berkeley National Laboratory, ⁴Karolinska Institute

Background

The cochlear blood-labyrinth barrier tightly regulates the cochlear microenvironment for auditory function. Pericytes (PCs), perivascular resident macrophages-like melanocytes (PVM/Ms), and endothelial cells (ECs) are critical components of the blood-labyrinth barrier essential for maintaining blood-labyrinth barrier integrity. However, investigation of these cell types has been hindered by lack of a method for isolating and culturing them.

Methods

Here we describe a novel growth medium-based method for obtaining cochlear ECs, PCs, and PVM/Ms from the stria vascularis of young mice (p10 - p15). The procedure does not involve mechanical or enzymatic digestion of the sample tissue. Explants of stria vascularis, "mini-chips", are selectively cultured in growth media.

Results

Primary cell lines are obtained in 7 - 10 days. The method is simple and reliable, and provides high quality ECs, PVMs, and PCs with a purity > 90% after two passages.

Conclusion

The newly established method is suitable for producing primary culture cells from organs and tissues of small volume and high anatomical complexity, such as the inner ear capillaries. The highly purified primary cell lines enable cell culture-based in vitro modeling of cell-cell interactions, barrier control function, and drug screening. This work was supported by National Institutes of Health grants NIH NIDCD R01-DC010844 (XS), NIH NIDCD DC R21DC1239801 (XS), and NIHP30-DC005983.

839 Endothelial Cell, Pericyte, and Perivascular Resident Macrophage-Type Melanocyte Interactions

Lingling Neng¹, Fei Zhang¹, Jinhui Zhang¹, Xiaorui Shi¹
¹Oregon Hearing Research Center

Background

The integrity of the fluid-blood barrier in the stria vascularis is critical for maintaining inner ear homeostasis, especially for sustaining the endocochlear potential, an essential driving force for hearing function. However, the mechanisms that control intra-strial fluid-blood barrier permeability are largely unknown. At the cellular level, the intra-strial fluid-blood barrier comprises cochlear microvascular endothelial cells connected to each other by tight junctions (TJs), an underlying basement membrane, and a second line of support consisting of cochlear pericytes and perivascular resident macrophage-type melanocytes.

Methods

In this study, we used a newly established primary cell culture-based in vitro model to show that endothelial cells, pericytes, and perivascular resident macrophage-type melanocytes interact to control intra-strial fluid-blood barrier permeability.

Results

When the endothelial cell monolayer is treated with pericyte— or perivascular resident macrophage-type melanocyte-conditioned media, the permeability of the endothelial cell monolayer is significantly reduced relative to an untreated endothelial cell monolayer. Further study has shown the pericytes and perivascular resident macrophage-type melanocytes to regulate TJ expression in the endothelial cell monolayer.

Conclusion

The new cell culture-based in vitro model offers a unique opportunity to obtain information on the organ-specific characteristics of the cochlear blood/tissue barrier. Our finding demonstrates the importance of signaling between pericytes, endothelial cells, and perivascular resident macrophage-type melanocytes to the integrity of the intra-strial fluid-blood barrier. This work was supported by National Institutes of Health/National Institute on Deafness and Other Communication Disorders Grants DC008888-02A1 (to X.S.), DC008888-02S1 (to X.S.), R01-DC010844 (to X.S.), and NIHP30-DC005983.

840 Robust Extracellular Matrix Production with Recombinant Tectorin Constructs in Mouse Cochlear Cultures

Julia Korchagina¹, Kevin Legan¹, Richard Goodyear¹, Jolanda Witteveen¹, Nicola Allen¹, Omar Risk¹, Andrew Forge², Guy Richardson¹

¹University of Sussex, School of Life Sciences, ²University College London, Ear Institute

Background

Alpha- and beta-tectorin (Tecta and Tectb) are major non-collagenous components of the tectorial membrane (TM). Tecta is a large modular glycoprotein composed of several modules; an entactin domain, a zonadhesin-like domain comprising three full and two partial vWF type D repeats, and a zona pellucida (ZP) domain. Tectb is much smaller and consists of a single ZP domain. The presence of a ZP domain in both tectorins suggests that Tecta and Tectb can form hetero- or homopolymers. It is still unclear, however, how these proteins assemble to form the TM matrix. The mechanisms of apical targeting, secretion and processing of the tectorins are also largely unexplored.

Methods

Fluorescently-tagged tectorin constructs were transiently expressed in polarised epithelial cell lines (CL4 and MDCK) to explore apical targeting, and MDCK derived cell lines stably expressing these constructs were used to study secretion and processing. Polarised epithelial spheres were generated from stable cell lines by growing cells in a mixture of collagen and Matrigel. Gene gun transfection was used to transfect the tectorin constructs into various cell types in mouse cochlear cultures. Site directed mutagenesis was used to introduce mutations that are known to cause human hereditary hearing loss.

Results

Tectorins were shown to be effectively targeted to the apical surface of CL4 cells, and the targeting of both proteins was shown to depend on the presence of a C-terminal GPI anchor sequence. With MDCK-based stable cell lines expressing Tecta or Tectb, the tectorins were detected in the media, within the cells, and on their apical cellular surface.

Significant amounts of matrix were, however, not observed with either stable or transient tectorin expression in monolayer cultures of polarised epithelial cell lines. With polarised epithelial spheres there was some evidence for the production of filamentous extracellular matrix. In contrast, substantial amounts of dense extracellular matrix were observed on the apical surfaces of outgrowth zone cells when cochlear cultures were transiently transfected with either Tecta or Tectb. When expressed in hair cells, Tecta and Tectb locate to the distal tips of the hair bundle.

Conclusion

The results reveal that (i) the GPI-anchor acts as a signal for the apical targeting of Tecta and Tectb, and (ii) epithelial cells in primary cultures of the early postnatal cochlea are the best suited for studying tectorin-based extracellular matrix production.

841 Thinking of Supporting Cells as Glia, Lessons for Studying Their Functions

Gabriel Corfas¹

¹Boston Children's Hospital

There is growing evidence that supporting cells of the inner ear sensory epithelia share significant similarities with glial cells elsewhere in the nervous system, and that these cell types also have common biological roles. I will introduce some of the similarities and differences between supporting cells and glia as well as discuss our studies on the roles of supporting cell-derived trophic factors in the development, function and maintenance of the inner ear.

842 Müller Glia as Retinal Stem Cells

Thomas Reh¹

¹University of Washington

The retina is a complex neural circuit, with sensory receptors, interneurons and projection neurons to the brain. Degeneration of one or more of these different types of neurons can lead to visual impairment and blindness. In non-mammalian vertebrates, regeneration of new neurons from supporting cells, like the Muller glia, can restore normal neuronal numbers and function, but this process is very limited in mammals. Recent work from our lab has shown the feasibility of stimulating neurogenesis from the Muller glia in mice, using reprogramming factors. This talk will review current progress and future prospects for repairing the damaged retina.

843 Supporting Cells as Mediators of Hair Cell Survival

Lindsey May¹, Inga Kramarenko², Carlene Brandon², Christina Voelkel-Johnson², Soumen Roy¹, Shimon Francis^{2,3}, Kristy Truong^{1,4}, Elyssa Monzack¹, Jonathan Gale⁵, Lisa Cunningham¹

¹NIDCD, ²Medical University of South Carolina, ³University of Virginia, ⁴University of Iowa, ⁵University College London
Cellular stress causes induction of both pro-apoptotic and pro-survival signals. The balance of these death and survival signals often determines whether the stressed cell lives or dies. Induction of heat shock proteins (HSPs) in response to cellular stress is a ubiquitous and highly-conserved response that can inhibit apoptosis in many systems. We recently showed that HSP induction inhibits both aminoglycoside- and cisplatin-induced hair cell death. HSP70 is required for this protective effect, and constitutive expression of HSP70 inhibits aminoglycoside-induced cochlear hair cell death and hearing loss. These data indicate that HSP70 induction is a critical stress response in the inner ear that can protect hair cells exposed to major stressors.

We utilized whole-organ cultures of utricles from adult mice to examine the mechanisms underlying the protective effect of HSP70. In response to heat shock, HSP70 was induced in glia-like supporting cells with little (or no) induction in hair cells. We developed a method of infecting supporting cells using adenovirus, and we utilized this technique to drive expression of HSP70 in supporting cells

alone. Ad-HSP70 inhibited aminoglycoside-induced hair cell death, indicating that supporting cells are the primary mediators of the protective effect of HSP70. We hypothesized that HSP70 is secreted by supporting cells and internalized by hair cells. To test this, we performed a series of co-culture experiments using Transwell culture inserts. Co-culture of heat-shocked utricles with non-heat shocked utricles inhibited hair cell death in all utricles. Experiments using utricles from HSP70 knockout mice showed that the protective effect of co-culturing requires HSP70. In addition, depletion of HSP70 from the media using a function-blocking antibody abolished the protective effect in both heat-shocked and non-heat shocked utricles. These data support our prior data on HSP70 as a mediator of hair cell survival and suggest that HSP70 is secreted by supporting cells.

We propose that supporting cells can promote the survival of damaged hair cells. Taken together with recent data indicating that supporting cells may mediate hair cell death (Lahne and Gale 2008 *J Neurosci* 28, 4918; Bird et al., 2010 *J Neurosci* 30, 12545), our data suggest a major role for supporting cells in determining whether a hair cell under stress ultimately survives or dies.

This work was supported by the NIDCD Division of Intramural Research. Additional support was from NIH/NIDCD R01 DC007613.

844 Damage-Induced Responses in Cochlear and Vestibular Supporting Cells: A Jekyll and Hyde Story in Which ERK1/2 Is Necessary and Sufficient?

Gregory Ball¹, Lindsey May², Lisa Cunningham², Jonathan Gale^{1,3}

¹*UCL Ear Institute*, ²*NIDCD, NIH, 5 Research Court, Rockville, MD 20850, USA*, ³*Dept. of Cell & Developmental Biology, UCL, London, UK*

Aside from certain cell types in the cochlea, the roles of inner ear supporting cells are not well defined. We know that during normal inner ear function supporting cells provide important structural support, but are also thought to provide critical trophic and homeostatic support for hair cells in both cochlear and vestibular systems. Work from a number of laboratories has shown that, under pathophysiological conditions, supporting cells are involved in repair of the epithelium and, in those systems that recover, supporting cells are the source of any replacement hair cells, whether it be by phenotypic conversion or a proliferative response. We have been studying the response of supporting cells during inner ear damage.

The extracellular regulated kinases 1 and 2 (ERK1/2) are activated in supporting cells surrounding an acute damage (laser/mechanical) site and also surrounding hair cells damaged by ototoxic aminoglycosides. Inhibition of MEK, the upstream kinase of ERK1/2, prevents ERK1/2 activation and affords some protection of inner hair cells in early postnatal cochlear cultures (Lahne & Gale 2008). In the chick utricle we have provided definitive evidence that

nearest neighbour supporting cells are triggered to act as professional phagocytes. Moreover, the data suggested that supporting cells act not just as scavengers, but as potential mediators of hair cell death.

We now show that, in both neonatal and adult mouse utricles, ERK1/2 activation is also localized to the nearest neighbouring supporting cells during laser-targeted and aminoglycoside-induced hair cell damage. MEK inhibition (using U0126) in adult utricles resulted in a small but significant protection of hair cells after 24 hours of aminoglycoside treatment. The MEK inhibitor is not an ideal approach because long term application (24 hours) may well have negative effects on the hair cells themselves. Therefore, in order to determine the function of ERK1/2 activation in supporting cells we used an adenoviral infection protocol (Brandon, Voelkel-Johnson et al. 2012) to specifically infect supporting cells with a constitutively active (CA-) MEK1 construct. Using this to maximally activate endogenous ERK1/2 in supporting cells resulted in significant changes in cell behavior and a reduction in the number of hair cells compared to Ad-RFP infected controls. Moreover, live imaging revealed supporting cells expressing CA-MEK1 could be caught in the act of phagocytosing apparently healthy hair cells, indicating that ERK activation is sufficient to switch those cells from Dr Jekylls to Mr Hydes.

845 The Enigmatic Function of Inner Ear Macrophages: Insights from Studies of Birds and Mammals

Mark Warchol¹, Keiko Hirose¹

¹*Washington University School of Medicine*

Macrophages are the first responders of the immune system and play essential roles in tissue maintenance and injury response. The sensory organs of the inner ear all contain resident populations of macrophages, which become activated and increase in number after hair cell injury. The avian cochlea contains numerous resident macrophages, which are mainly confined to the connective tissues and to the hyaline/cuboidal cell region. After hair cell injury, some macrophages migrate toward the damaged region, but they remain below the basilar membrane and do not enter the sensory epithelium. Experimental depletion of resident macrophages from the chick cochlea does not inhibit the removal of hair cell debris after ototoxic injury, and does not affect hair cell regeneration. However, macrophage depletion reduces the proliferation of cells immediately below the basilar membrane (the so-called mesothelial or tympanic border cells), suggesting that macrophages may serve a role in the maintenance of the basilar membrane.

In the mouse, the normal cochlea contains a small population of resident macrophages. Recruited monocytes from the vascular endothelium constitute the large majority of mononuclear phagocytes that populate the cochlea after sensory cell injury. Studies of Pou4f3-DTR mice suggest that the death of hair cells alone provides a sufficient stimulus to induce monocyte migration into the ear. As in

the avian cochlea, the essential function of murine cochlear macrophages remains unknown. Macrophages and monocytes are abundant in non-sensory structures of the cochlea, and inflammatory cells are rarely observed interacting with hair cells or the sensory epithelium in animal studies. However, time-lapse imaging of mouse cochlear cultures have revealed that cochlear macrophages are intimately associated with spiral ganglion dendrites and can recognize and phagocytose apoptotic hair cells. Hair cell injury *in vivo* leads to increased macrophage numbers within the osseous spiral lamina adjacent to the dendrites of afferent fibers as well as within the spiral ligament and limbus. The possible interaction between macrophages and afferent neurons is currently under investigation.

The vestibular maculae of chicks and mice also contain resident macrophages, which populate the stromal tissue below the sensory epithelium. Increased numbers of macrophages are recruited into the stroma of the chick utricle after aminoglycoside ototoxicity. Such cells often extend pseudopodia into the injured sensory epithelium, but they do not appear to play a key role in the removal of hair cell debris. As such, the function of vestibular macrophages remains a mystery.

846 Using Binaural Detection to Measure How Precision of Coding of Interaural Delay Varies with Both Magnitude of Interaural Delay and Center Frequency

Leslie Bernstein¹, Constantine Trahiotis¹
¹*University of Connecticut Health Center*

Background

Explanations of binaural processing postulate that “internal delays” compensate for external interaural temporal delays (ITDs). Additionally, sound-field and earphone-based ITD-discrimination studies have consistently demonstrated that sensitivity to changes in ITD declines with increases in magnitude of reference ITD. Recently, we discovered a way to measure, quite directly, precision of ITD-coding as a joint function of magnitude of ITD and center frequency.

Methods

Binaural detection thresholds were measured in three conditions. The first consisted of transforming the classic $NoS\pi$ stimulus into an “ $(NoS\pi)\tau$ ” stimulus by imposing an ITD on the entire signal-plus-masker waveform. With that stimulus, perfect internal compensation of external ITDs would yield thresholds both independent of ITD and equal to those obtained under $NoS\pi$. Such compensation would transform $(NoS\pi)\tau$ conditions back into $NoS\pi$. Alternatively, if precision of ITD-coding declines with ITD, that type of transformation could not occur and thresholds would increase with ITD. The second condition capitalizes on the “double-delay” condition of van der Heijden and Trahiotis [(1999). *J. Acoust. Soc. Am.* 105, 388-399]. It is a variant of the $(NoS\pi)\tau$ condition in which the masker is the sum of two independent noises, one interaurally delayed toward the left ear, one interaurally delayed equally toward the right ear. We call this $(No)\pm\tau(S\pi)\tau$. For

any τ , a double-delayed noise has the same interaural correlation as its “single-delayed” counterpart. There is, however, no internal delay that can be employed by the listener to transform $(No)\pm\tau(S\pi)\tau$ back to $NoS\pi$ and no value of internal delay expected to yield thresholds lower than could be achieved by imposing no internal delay. Thus, the difference, at any value of τ , between $(No)\pm\tau(S\pi)\tau$ and $(NoS\pi)\tau$ thresholds reveals the detection advantage achieved by imposing a compensating interaural delay. The third condition employed is called $(NoSo)\tau$ and is a “monaural” control condition in which adding the signal to the masker produces no interaural cues and, thus, no binaural advantage.

Results

Data revealed that thresholds obtained using $(NoS\pi)\tau$ stimuli centered at 500 Hz or 4 kHz increased with ITD and did so more rapidly at 4 kHz than at 500 Hz. The ordering of thresholds from low to high across τ was $(NoS\pi)\tau$, $(No)\pm\tau(S\pi)\tau$, $(NoSo)\tau$.

Conclusion

The data suggest strongly that precision of ITD-coding does, indeed, decline with ITDs up to, at least, 3 ms and does so more rapidly at 4 kHz than at 500 Hz.

847 Changes in Auditory Spatial Mapping Can Explain the Audiogravic Illusion

David Magezi¹, Tim Hahn¹, Levi van Iersel¹, Marc van Wanrooij¹, John van Opstal¹

¹*Donders Institute, Radboud University Nijmegen*

Background

Lateralization of sound sources is influenced by the observer’s orientation relative to gravity. When passively rolled about the naso-occipital axis in darkness, the perceived auditory median plane (AMP) is displaced towards the upper ear. This “audiogravic illusion” suggests that sound lateralization depends not only on the perceived spatial location of the sound, which may be based on mapping binaural acoustic cues to some internal auditory spatial representation, but also on the perceived head orientation. Previously, authors have proposed that the audiogravic illusion is due to either perceived head orientation (PHO), or auditory spatial mapping (ASM) changing as a function of roll angle. The aim of the current study was to distinguish between these two hypotheses.

Methods

Four participants were kept stationary at various roll angles of up to 120 degrees, where they lateralized noise bursts (150 ms, 0.3 – 12 kHz) presented simultaneously from two speakers. The speakers rolled with the participants and were near the interaural plane at azimuths of ± 37 degrees. A range of speaker level differences were employed to obtain psychometric functions and derive the speaker level difference corresponding to the AMP. No feedback was given. Simple equations for the PHO and ASM hypotheses were used to qualitatively model the results.

Results

The modelling data show that PHO and ASM vary linearly or sinusoidally, respectively, with roll angle. They also confirm that PHO, but not ASM, changes with the elevation of the sound source; for sounds along the interaural plane (zero elevation), PHO will not vary with roll angle. These modelling results suggest that experimental data from previous studies could not distinguish between the two hypotheses because head roll was limited to 90 degrees or less, and free-field sound sources were in the coronal plane. The current experimental data are consistent with the ASM-change hypothesis because AMP varies sinusoidally with roll angle, and the sounds were presented near the interaural plane. The experiment is currently being repeated with headphones, with sounds being perceived inside the head along the interaural plane. Preliminary results confirm that the direction of the audiographic illusion is the same, further supporting the ASM hypothesis.

Conclusion

For free-field sounds, the audiographic illusion can be explained by systematic changes in auditory spatial mapping (ASM). This would suggest that multisensory cues, predominantly vestibular otolith signals, directly influence the interpretation of binaural acoustic cues.

848 High Frequency Audibility and Spatial Release from Informational Masking

Frederick Gallun^{1,2}, Sean Kampel^{1,2}, Sara Blankenship³, Marjorie Leek^{1,2}

¹Portland VA Medical Center, ²Oregon Health & Science University, ³Vanderbilt University

Background

Previous work has shown that older and/or hearing-impaired listeners obtain less benefit of spatial separation in a multitalker informational masking experiment than do younger listeners with normal hearing. The goal of this study was to examine the role of high frequency speech information, which is often rendered inaudible by age-related hearing loss, in supporting spatial release.

Methods

A 20-dB range of target-to-masker ratios was examined in a brief test session, using the Coordinate Response Measure corpus. Two male masking talkers were presented across a range of levels and the task of the listener was to identify the color and number keywords spoken by a target male talker. Stimuli were adjusted for each listener to approximate the level above detection threshold that would be present for an ideal listener with no hearing loss (0 dB HL at all audiometric frequencies). Performance in this “broadband” condition was compared with a “lowpass” condition, in which the levels were adjusted to match the levels that would be present for an idealized hearing-impaired listener with a sloping high-frequency hearing loss (0 dB HL for .25, .5, and 1 kHz; -20 dB HL for 2 kHz; -40 dB HL for 4 and 8 kHz). Both the broadband and lowpass conditions were run at an RMS (before lowpass filtering) of 10 dB or 30 dB SL. SL was

calculated relative to each listener’s speech detection threshold as estimated from that listener’s audiogram. A group of more than twenty listeners varying in age and hearing ability participated in the testing.

Results

Raising the target level from 10 to 30 dB SL generally improved performance, but, surprisingly, many of the hearing-impaired participants performed better in the lowpass condition than in the broadband condition. Many of the normal hearing listeners, on the other hand, performed better in the broadband condition, as would have been expected due to the increased information present. This was true at both sensation levels.

Conclusion

These data are not consistent with the hypothesis that older and/or hearing impaired listeners obtain less spatial benefit due to reduced audibility in the high frequencies. On the contrary, the data suggest that for some listeners with impaired hearing there may be a disadvantage to high frequency energy, perhaps due to binaural interference or other types of distraction associated with the presence of energy in regions of impaired auditory function.

849 Modeling Sound Localization for Normal and Binaural CI-Listeners

Christian Wirtz¹, Michele Nicoletti², Werner Hemmert²
¹MED-EL, ²Technische Universität München

Background

Although modern cochlear implants (CI) provide good speech intelligibility, their performance in a “cocktail party” situation with multiple simultaneous sound sources is not satisfactory. It is well known that sound localization provides important cues to separate sources which enhance speech intelligibility in noisy environments. Since CIs were initially designed for monaural implantation only, there is room to optimize coding of binaural information.

Methods

Within a simulated listening setup the binaural Lindemann model can provide a metric to predict source localization abilities. After reviewing the model’s basic setup, we extended the model to work with action potentials. These were generated by physiologically inspired models which replicated auditory nerve responses for both intact ears and ears with CIs and different coding strategies.

The simulated listening setup consisted of a loudspeaker, which was circling around the listener’s head. The distance between the ears was 15 cm. An emitted wavefront reached both ears at different times and invoked interaural time differences (ITD). Furthermore, the simulation assumed linear air-attenuation and also generated interaural level differences (ILD).

The binaural Lindemann model extends the correlation delay line of the Jeffress model by inhibitory elements, thus adding ILD-sensitivity. A positive Lindemann correlation time-delay indicates a sound source right hand side. A sound source with 1 Hz circling frequency will lead to a deviation of max. 0.441 ms.

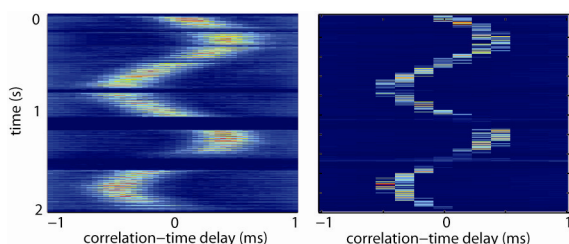
Results

For a normal hearing model the Lindemann correlation easily tracked the sound source (supplement). When we tested MED-EL's FS4 strategy, which conveys the temporal fine-structure in its four lowest frequency channels, we could also observe that the tracking of a moving source is possible, albeit with reduced precision (0.2 ms). When we analyzed the electrically induced spike trains, we found a much weaker Lindemann correlation due to the effects of channel crosstalk.

Conclusion

To improve sound localization of CI-listeners, coding strategies must convey ILDs and especially ITDs. We extended the Lindemann model to process input from spiking auditory models and used it for quantitative evaluations of localization cues of auditory models (normal hearing) and CI coding strategies. Whereas the CIS strategy did not provide useful fine-structure ITD cues, today's latest coding strategies, the FS4 by MED-EL, was already able to convey viable fine-structure cues for sound source localization.

Funding: Bernstein Center for Computational Neuroscience (German Federal Ministry of Education and Research: 01GQ1004B, 01GQ1004D) and MED-EL.



Lindemann correlation derived from spike trains generated by a normal hearing inner ear model (200 Hz channel, left) and from the stimulation signal of electrode 2 for a MED-EL FS4 coding strategy (right). We used a virtual speaker articulating a sentence while circling around the head (1 rotation/s).

850 Direction Selectivity Mediated by Response Adaptation in the Owl's Inferior Colliculus

Yunyan Wang¹, Jose Luis Pena¹

¹Albert Einstein College of Medicine

Background

Direction-selectivity has been shown in the auditory system for frequency modulations and motion in space. The underlying mechanisms have been attributed to nonuniform topography in sensory representations and lateral connections. We investigated this issue in space-specific neurons of the owl's external nucleus of the inferior colliculus (ICx).

Methods

We recorded single units in the ICx of anesthetized barn owls. Moving sounds were simulated in a hemispherical free-field speaker array with 10° resolution in space. The owl was turned so that the RF of each cell was centered at 0° azimuth. We synthesized auditory drifting gratings,

where the initial and final array configuration was constant at the beginning and end, irrespective of motion direction. The simulated moving sound started at one end of the array and moved around the owl's head at different velocities, in randomized directions. Spatial receptive fields (RFs) were measured in free field with randomized stimulation.

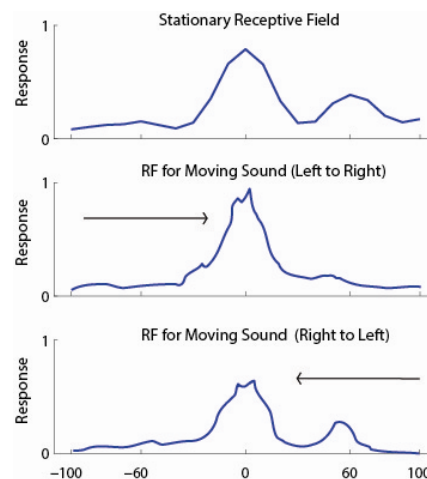
Results

Spatial RFs, as previously described, showed a main peak flanked by side peaks at 50-60° to each side. However, the sizes of the side peaks were often asymmetrical. The asymmetry can be caused by the convergence of ITD channels or by HRTF effects that attenuate the sound at certain locations.

Surprisingly, most cells showed direction selectivity using the method described above. Direction selectivity calculated from RFs during simulated moving sounds strongly correlated with the size of the side peaks. Neurons preferred sounds coming from the side where the side peak was smaller. We found that the size of side peaks was correlated with their suppressive effects on the response to the center. Response to the side peaks also depended on the direction of motion. In addition, direction selectivity varied with velocity. These data are consistent with rapid excitation-induced response adaptation as the underlying mechanism.

Conclusion

Spatial receptive fields of direction-selective ICx cells can be strongly modulated by the direction of sound motion. Response adaptation acting on asymmetric spatial tuning can explain this selectivity.



851 Psychophysical Analogies to Auditory Source Width in Hearing-Impaired Adults

William Whitmer¹, Michael Akeroyd¹

¹MRC Institute of Hearing Research

Background

In a previous study, we demonstrated that older hearing-impaired (HI) listeners produced visual sketches of headphone-presented noises that were insensitive to changes in coherence. The current study further explores this insensitivity by presenting stimuli in the free field to HI

and normal-hearing (NH) participants, and examines potential links in their perception of auditory source width to (a) binaural temporal fine-structure (TFS) resolution and (b) precision in absolute sound localization.

Methods

The stimuli for the sketching task were low-pass, high-pass and speech-spectrum noises. On each trial, a noise was presented from a center (0°) loudspeaker in a sound dampened room with two independent flanking noises that are simultaneously presented from loudspeakers at ±45° to act as arbitrary reflections. The flanking noises were attenuated 0-20 dB from the center signal level to generate partially coherent noises. HI and NH participants sketched the width of each stimulus presented repeatedly in random order. For the localization precision task, participants located 500-ms speech-spectrum filtered click trains presented from -30 to +30° in quiet. For the binaural TFS task, participants discriminated interaurally phase-shifted tones from diotic tones presented over headphones.

Results

The binaural TFS and localization precision data were in accord with previous studies showing the deleterious effects of age and impairment on these two measures, except that a portion of older participants could not perform the TFS task at all. When participants are parsed by their ability to do the TFS task, the sketching data showed a decreasing sensitivity to width with age and impairment that was not apparent in the headphone-presentation study: the worse one's binaural TFS threshold – which was correlated with age – the less the perceived width changed with interaural coherence.

Conclusion

These results suggest that perceiving changes in the width of sound sources is related to the ability to hear changes in low-frequency temporal information. For those HI participants with binaural TFS data, the perception of sound sources was not wider, despite having decreased localization precision. This finding indicates that senescent changes to the auditory system do not necessarily lead to perceptions of broader, more diffuse sound images based on interaural coherence. Thus, the use of interaural coherence to predict sound-source perception, as often assumed in architectural acoustics, may not hold for older hearing-impaired individuals.

852 On the Integration of Binaural Spatial Auditory Cues and Self-Motion (Idiothetic) Cues

W. Owen Brimijoin¹, Michael A. Akeroyd¹
¹MRC Institute of Hearing Research

Background

Our acoustic world is in constant motion because the ears are attached to the head and the head is never perfectly still; we tend, however, not to notice this movement. Here we summarize experiments examining phenomena that appear to be related in that they each require an ongoing and highly accurate comparison of binaural spatial cues

with 'idiothetic' cues (information on self motion derived from e.g. vestibular, proprioceptive, motor, or visual input). We will argue that these and related spatial phenomena are evidence of an auditory spatial processing mechanism that compensates for self motion.

Methods

We designed a system to move real and virtual sound sources as a function of head movements using a combination of a Vicon motion-tracking system (or Nintendo wii remotes) and real time digital signal processing. In the free field, we moved physical sound sources in a ring of loudspeakers, allowing us to create noises with illusory positions. In the free field and over headphones we moved sound sources in synchrony with head movements to examine the role of self motion in the externalization and internalization of sound sources. Finally, we used virtual sound sources that either moved with head movements or moved independently to examine whether there exists a fundamental difference between the processing of self motion and 'real' motion.

Results

We found that (1) signals that move predictably as a function of head movements can differ in perceived location from those that either remain static or move along arbitrary paths. (2) For noises, these illusory positions can affect their masking strength in a spatial release from masking paradigm. (3) Signals with fixed positions relative to the world are more likely to be perceived as being out in the world, whereas (4) those that move with the head tend to be internalized. Finally, (5) we found that self-generated auditory motion may be to some extent compensated for during moving spatial auditory tasks.

Conclusion

The results from each experiment suggest that auditory spatial perception is continually informed by self motion; that is, listeners constantly compare their own movement with the movement of the auditory world. All are consistent with the hypothesis that there exists a low-level integrative mechanism, not unlike the vestibulo-ocular reflex, whose function is to use ideothetic cues to adjust and stabilize auditory spatial representation in order to compensate for self motion.

853 Evaluation of a Missing Source Identification Paradigm for the Assessment of Spatial Hearing Ability in Hearing Aid Users

Julie Cohen¹, Mary Cord¹, Sridhar Kalluri², Bill Woods², Douglas Brungart¹

¹Walter Reed National Military Medical Center, ²Starkey

Background

When a sound source in a complicated auditory environment suddenly turns off, listeners with normal hearing often have the subjective impression that they can tell what the sound was and where it was coming from even in cases where they clearly were not paying any attention to the sound before it was removed from the

scene. However, little is known about the extent to which hearing impaired listeners may be able to maintain awareness of multiple sounds in their environment, or the impact that hearing aids might have on this capability. In this study, we conducted a preliminary evaluation of a spatial awareness paradigm that required listeners to detect the addition or deletion of a realistic environmental sound from the auditory scene. The study was conducted with hearing-impaired bilateral hearing aid users under three listening conditions: bilaterally aided, monaurally aided, and unaided.

Methods

Isolated environmental sounds were presented from an array of 30 loudspeakers located in a cylindrical pattern spanning +/- 135 degrees in azimuth and +/- 30 degrees in elevation. Listeners were first asked to listen to a 2-s environmental sound and determine the identity of the sound and its spatial location. They then participated in additional blocks that required them to identify a source that was either added or deleted from the scene after a listening interval where two, four, or six environmental sounds were presented for 6 seconds from speakers at different azimuth locations. Each block was administered twice for each of the three hearing aid conditions over two sessions.

Results

Preliminary results revealed that hearing impaired listeners (n=7) had the most difficulty localizing the sound source in the unilateral-aided condition. Localization accuracy in azimuth was comparable in the un-aided and bilaterally-aided conditions, but source identification accuracy and localization accuracy in elevation were slightly better in the unaided condition than in the bilaterally-aided condition.

Conclusion

Preliminary results show a localization benefit for bilateral amplification over unilateral amplification, but no significant benefit for bilateral amplification over unaided listening. In the future, it may be possible to develop more advanced hearing aid algorithms that use binaural processing to enhance auditory awareness in hearing impaired listeners. The result of this experiment suggest that the missing source identification paradigm may provide a useful tool for evaluating changes in spatial awareness in associated with these new binaural hearing aid processing systems.

854 The Sound of Danger: Rapid Transmission of Auditory Stimuli to the Amygdala

JOSEPH E LEDOUX¹

¹New York University

In the process of exploring the neural pathways through which the brain comes to associate auditory stimuli with aversive events we found evidence for direct inputs to the amygdala from the auditory thalamus. Behavioral studies demonstrated that these pathways are utilized in auditory threat (fear) conditioning. Physiological and molecular studies identified cellular and molecular mechanisms that

underlie the learning. It is likely that thalamic inputs to the amygdala are allow for the creation of rapid but imprecise representations which are then refined via cortical inputs.

855 Morphological, Neurochemical and Connectional Organization of the Non-Lemniscal Thalamocortical Pathways

Charles Lee¹

¹Louisiana State University School of Veterinary Medicine
The function of the medial geniculate body (MGB) in normal hearing still remains largely enigmatic, in part due to the relatively unexplored properties of the non-lemniscal MGB nuclei. Indeed, the canonical view of the thalamus as a simple relay for transmitting ascending information to the cortex belies a role in higher-order forebrain processes. However, recent anatomical and physiological findings now suggest widespread roles for the non-primary auditory thalamic nuclei beyond that of a simple relay. Neurons in the non-lemniscal nuclei have distinct dendritic and somatic morphologies and unique expression of calcium-binding proteins. Furthermore, the non-lemniscal nuclei send and receive feedforward and feedback projections among a wide constellation of midbrain, cortical, and limbic-related sites. Combined, these neuroanatomical features support roles for the non-lemniscal nuclei as conduits for auditory information flow to higher auditory cortical areas, mediators for transitioning among arousal states, and synchronizers of activity across expansive cortical territories.

856 Ascending Projections to the Non-Lemniscal Auditory Thalamus

Enrique Saldaña^{1,2}

¹University of Salamanca, Spain, ²Institute of Biomedical Research of Salamanca (IBSAL), Spain

The so-called non-lemniscal auditory thalamus of mammals consists of various structures that surround the purely auditory ventral division of the medial geniculate body (MGBv). These structures, which include the dorsal and medial division of the MGB (MGBd and MGBm), the supragenulate nucleus, the posterior intralaminar nucleus (PIN), the marginal zone, the posterior limitans nucleus (PLi), and the subparafascicular nucleus, differ in their cytoarchitecture and neural connections and may subserve different functions. Using anterograde and retrograde tracers, we are currently investigating systematically the ascending projections to the auditory thalamus of the rat, with emphasis on the non-lemniscal nuclei.

The (PLi), which extends for considerable rostrocaudal and dorsoventral distances as a narrow sheet along the lateral border of the anterior pretectal nucleus, receives very dense ipsilateral projections from the external cortex of the inferior colliculus (ECIC) and from the nucleus of the brachium of the IC. The collicular input arises selectively from small, presumably GABAergic neurons located in the modules or patches of layer 2 of the ECIC (Mugnaini and Oertel, 1985; Chernock et al., 2004). The PLi in turn is a source of descending projections whose targets include several motor related structures.

Our results also indicate that the auditory thalamus receives direct projections from an unexpectedly large number of neurons in subcollicular centers, including the contralateral dorsal and ventral cochlear nuclei, lateral superior olive and dorsal periolivary region, the ipsilateral medial superior olive, superior paraolivary nucleus (SPON), dorsomedial wedge of the superior olivary complex (and ill-defined territory wedged between the dorsal border of the medial nucleus of the trapezoid body and the SPON), ventral nucleus of the lateral lemniscus, and from the dorsal nucleus of the lateral lemniscus, the nucleus sagulum and the horizontal cell group of both sides. In some of these nuclei, the percentage of neurons that contribute to the innervation of the thalamus is surprisingly high. Multivariate analysis of the distribution of the neurons retrogradely labeled from the thalamus suggests that different thalamic nuclei receive different combinations of ascending inputs.

Our results suggest that a high degree of convergence of ascending auditory inputs takes place at thalamic levels and provide an anatomical framework for future studies of the specific functions of the non-lemniscal auditory nuclei.

Funding: Instituto de Salud "Carlos III" PI10/01803.

857 Response Properties of Non-Lemniscal MGB Neurons to Auditory Stimuli in Vivo

Lucy Anderson¹

¹*UCL Ear Institute, 332 Gray's Inn Road, London, WC1X 8EE, UK*

The principal nucleus of the auditory thalamus, the medial geniculate body (MGB), can be divided into ventral, medial, and dorsal subdivisions. Traditionally, the ventral division is the only subdivision considered to be part of the lemniscal or primary auditory pathway, while the medial and dorsal subdivisions are assigned to the non-lemniscal or secondary pathway. Based on physiological properties of neurons recorded from histologically identified subdivisions within the MGB of anaesthetised rodents, I suggest medial MGB neurons do not fit simply into the conventional functional dichotomy of high-fidelity lemniscal, and context-dependent non-lemniscal pathways. For example, while a high proportion of medial MGB neurons display change sensitivity (a property typical of non-lemniscal areas), neurons in the medial MGB also possess response fidelity (short latencies, high response probability, and an ability to follow sounds with high rates of temporal modulation) that frequently exceeds that of neurons present in the (lemniscal) ventral MGB. This enhanced reliability may be inherited from direct inputs from the auditory brainstem – a pathway unique to the medial MGB. Taken together, these results argue in favour of a distinct role for medial MGB in central auditory processing.

858 Computational, Physiological and Anatomical Findings That Distinguish MGBm Processing

Edward Bartlett¹, Cal Rabang¹, Yamini Venkataraman¹, Stephanie Gardner¹

¹*Purdue University*

BACKGROUND: The medial region of the medial geniculate body (MGBm), broadly defined to include the medial division of MGB, the suprageniculate and the posterior intralaminar nuclei, surrounds the ventral (MGBv) and dorsal (MGBd) divisions of the MGB on their ventral and medial aspects. MGBm is the most heterogeneous region of the MGB, in terms of connectivity, anatomy and physiology. Unlike MGBv and MGBd, MGBm projections mainly avoid middle cortical layers or they project to subcortical regions, where they have been shown to be critical for the formation of auditory-based associative memories. Here some salient differences in anatomy and physiology will be reviewed, along with new computational and anatomical data demonstrating how those differences are likely to influence auditory processing.

METHODS: Single compartment models of MGBm neurons are created using NEURON software. These models incorporated physiological data obtained from rat brain slice studies, including membrane properties, excitatory synaptic properties, and inhibitory synaptic properties. In addition, the distributions of ascending axon terminals from the IC are estimated using vesicular glutamate transporter 2 (vGluT2) immunohistochemistry.

RESULTS: Physiological results have shown that MGBm neurons often lack a low-threshold calcium current, a hallmark of standard thalamocortical neurons. In addition, many of these neurons have an apamin-sensitive calcium-activated potassium channel that causes MGBm neurons to adapt to sustained current injections. These properties are incorporated to compare model responses to collicular inputs in MGBm versus MGBv neurons.

CONCLUSIONS: Many MGBm neurons should not be grouped with MGBv and MGBd neurons when considering their physiology or their participation in thalamocortical sensory processing.

859 Dynamic Sound Representations in the Lemniscal and Extra-Lemniscal Divisions of the Medial Geniculate Body

Amanda Clause^{1,2}, Masaaki Torii³, Daniel Polley^{1,2}

¹*Massachusetts Eye & Ear Infirmary*, ²*Harvard Medical School*, ³*Center for Neuroscience Research, Children's National Medical Center*

The medial geniculate body (MGB) of the thalamus occupies a critical node between corticopetal, corticofugal and limbic processing networks. The corticothalamic (CT) projection from layers 5 and 6 (L5 and L6, respectively) represents the largest component of the auditory corticofugal network, and one of the largest projection systems in the brain. CT feedback has been implicated in

a diverse range of cognitive functions ranging from memory consolidation to dynamic sensory filtering, yet a detailed understanding of its functions and mechanisms has remained elusive due to the technical difficulties associated with selectively manipulating CT neurons without disrupting thalamocortical (TC) or intracortical processing. We found that CT axon terminals were restricted to a circumscribed zone within the dorsal subdivision of the MGB (MGBd) shortly after birth but had invaded surrounding regions in the ventral and medial subdivisions (MGBv and MGBm, respectively) by the time of hearing onset. Using in utero gene electroporation, we over-expressed EphA7, a receptor tyrosine kinase, in the auditory cortex, and were able to forestall the developmental elaboration of CT axonal projections into the MGBd and MGBm without disrupting TC projections. Electrophysiological recordings from the MGBv of adult mice with chronically reduced CT feedback revealed lower baseline spike rates compared to controls yet surprisingly subtle effects on sound-evoked response properties. Our most recent experiments explore the effects of acutely reducing CT feedback. Using a chemical-genetic approach, we were able to selectively and reversibly inactivate CT neurons in a single cortical layer while recording from ensembles of neurons in lemniscal and extra-lemniscal divisions of the MGB. We found that activating the inhibitory DREADD, hM4d, eliminated tonal receptive fields and strongly reduced firing rates in genetically targeted cortical neurons within 15 minutes and lasted for several hours. In contrast to the modest effects of chronic CT reduction, our ongoing experiments suggest that acute silencing of L6 cortical neurons via hM4D can strongly modulate sound-evoked responses in the MGB of awake, passively listening mice.

860 Interactions Between Auditory and Cognitive Aging

Kathy Pichora-Fuller^{1,2}

¹University of Toronto, ²Linköping University

Background: Auditory-cognitive interactions are important because the mutual influences of bottom-up and top-down processing shift depending on the listener, signal, task and context, and also because there can be brain re-organization to compensate for sensory and/or cognitive impairments. In cognitive aging, knowledge and use of context is preserved, but processing (working memory, attention/inhibition, speed of processing) declines. There are at least three sub-types of age-related hearing loss, including neural-type with little audiometric loss.

The trio of working memory, attentional control and speed of perceptual processing are inter-related. This trio operates differentially depending on bottom-up factors, including the quality of the speech signal and the nature of hearing loss.

Methods: Auditory-cognitive interactions will be illustrated with an overview of experiments in younger and older adults where the speed and/or accuracy of speech understanding is altered by manipulating the signal quality, contextual cues that enhance attention (semantics, emotion, location, timing, talker voice), or task demands

with varying cognitive processing loads. Context is manipulated in experiments in which 1. materials vary in the congruency of semantic context to facilitate or inhibit the speed of lexical decision; 2. the vocal emotion of the talker modulates word recognition accuracy in noise; 3. word recognition accuracy in a multi-talker scene varies depending on whether the location of the target is likely or unlikely; 4. vowel recognition in noise depends on the relationship between the timing of speech and expectancy based on musical stress patterns; 5. word recognition accuracy in noise develops with streaming based on talker voice. Cognitive load post word recognition is varied in terms of how the listener must manipulate the words and/or how many words are to be recalled.

Results: The illustrations demonstrate that there are both auditory effects on cognition and cognitive effects on audition. Age-related and individual differences suggest that there are short- and long-term, and inter- and intra-individual variations in auditory-cognitive interactions. Unifying themes across phenomena will be proposed.

Conclusions: Implications for research and practice will be suggested, including a new perspective on the possible short- and long-term benefits to both hearing and cognition of a rehabilitative approach that marries improving signal quality and training to increase active engagement in listening. This overview talk will set the stage for the following presentations in the session.

861 Individualization of Hearing Aid Signal Processing Based on Cognitive Measures

Thomas Lunner^{1,2}, Mary Rudner²

¹Eriksholm Research Centre, Oticon A/S, Denmark,

²Linneaus Centre HEAD, Department of Behavioural Sciences and Learning, Linköping University, Sweden

Hearing instruments use complex processing anticipated to improve speech understanding. While many listeners benefit from such processing, others do not and these differences are potentiated by adverse listening conditions. Unwanted artefacts of hearing aid signal processing may contribute to adverse listening conditions (Mattys et al., 2012). Under such conditions cognitive processing resources are allocated to the recovery of degraded information at the auditory periphery, leaving fewer resources for understanding the message.

Working memory refers to the capacity to hold and manipulate a set of items in mind, such as speech fragments. A number of recent studies indicate that individual working memory capacity influences the individual benefit of hearing aid signal processing. Ng et al., (under revision) examined the effects of binary masking noise reduction (Wang et al., 2009) in hearing aids on memory processing of speech perceived in a competing speech background, using a sentence-final word identification and recall test. The reading span test was also administered. The reading span test assesses the simultaneous processing and memory aspects of working memory. Noise reduction lowered the negative effect of noise on memory performance. Participants with good working memory capacity obtained a further benefit.

Lunner and Sundewall-Thorén (2007), among others, showed that the individual benefit of fast wide dynamic range compression was associated with individual working memory capacity. Persons with high working memory capacity benefited most from fast acting compression while the persons with low working memory capacity benefited most from slow acting compression. Arehart, Souza, Baca and Kates (in press) showed that elderly individuals with low working memory capacity were more disadvantaged by frequency compression processing during speech recognition in noise than elderly individuals with high working memory capacity. It is possible that the negative effects of fast acting wide dynamic compression and frequency compression for persons with low working memory are due to unwanted artefacts of signal processing.

In conclusion, the benefits of certain given implementations of complex processing in hearing aids have to be weighed against the extra cognitive load that such processing seems to engender, possibly as a result of unwanted artefacts. Although complex processing may aid speech understanding in noise for individuals with hearing impairment and especially those with good working memory capacity, it seems that for some individuals with lower working memory capacity, the drawbacks may outweigh the benefits. This should be taken into account when hearing aids are fitted.

862 Processing Load During Speech Perception in Noise – Insights from Pupillometry

Adriana Zekveld^{1,2}, Thomas Koelewijn¹, Sophia Kramer¹

¹*Dept. ENT/Audiology, VU University Medical Center,*

²*Linnaeus Center HEAD, Linköping University*

Title: Processing load during speech perception in noise – insights from pupillometry

Authors: Adriana A. Zekveld, Thomas Koelewijn, Sophia E. Kramer.

Background

Pupillometry provides an objective method for measuring cognitive load (listening effort) during speech perception in adverse listening conditions. We assessed the influence of individual factors like age, hearing loss, and cognitive ability and external factors like stimulus type, stimulus modality, intelligibility level, and masker type on the pupil response.

Methods

Combining and comparing the results of 4 studies allowed us to assess the influence of speech intelligibility level and masker type on cognitive processing load during listening and how this relates to cognitive ability. Five groups of young ($n_{\text{tot}} = 123$), two groups of middle-aged normal-hearing subjects ($n_{\text{tot}} = 62$) and one group of middle-aged hearing-impaired subjects ($n_{\text{tot}} = 38$) participated. Pupil dilation was recorded during speech perception in noise and during the text reception threshold (TRT) test. Sentences and words were presented over a wide range of sentence intelligibility levels (1% - 99% correct), masked

by different masker types (steady-state, fluctuating, single-talker) and in quiet.

Results

The results show consistently larger pupil responses in less intelligible or more complex listening conditions. The pupil response increases with decreasing speech intelligibility level. However, when speech perception is very difficult and subjects start to give up trying to perceive the speech, the pupil response decreases relative to less difficult conditions. This inverse-U shaped function of the pupil response across intelligibility levels supports the validity of the pupil response as measure of cognitive processing load. Middle-aged and hearing-impaired adults show a smaller decrease in pupil response with increasing intelligibility. Independent of intelligibility level, masker type affects cognitive processing load. Processing load is highest for speech masked by an interfering speaker. The TRT test is associated with cognitive load during listening, especially in relatively difficult listening conditions. The data suggest that an individual's cognitive abilities modulate the relation between speech intelligibility and processing load. The pupil response furthermore reflects processing load differences caused by different stimulus types (word versus sentence perception), task characteristics (detection versus identification) and stimulus modality.

Conclusions

The pupil response and speech perception performance data reflect different aspects of processing load during listening. The impact of several factors and individual differences that affect the complexity of the listening task and cognitive processing load are quantifiable by assessment of the pupil response during listening.

863 Listening Effort and Cochlear Implants

Deniz Baskent^{1,2}, Carina Pals^{1,2}, Anastasios Sarampalis³

¹*Department of Otorhinolaryngology, University Medical Center Groningen, The Netherlands,* ²*Research School of Behavioral and Cognitive Neurosciences, University of Groningen, The Netherlands,* ³*Department of Experimental Psychology, University of Groningen, The Netherlands*

Background

Sound transmission through cochlear implants (CIs), although restoring hearing for deaf individuals, is far from perfect. Typically, speech transmitted through the device maintains coarse spectral and temporal information but lacks temporal fine structure. Interpreting this degraded auditory signal can be effortful, and CI users do anecdotally report fatigue. Therefore, in addition to increasing speech intelligibility, a purpose of CIs could be to reduce listening effort. However, to be able to do so, a reliable measure of effort is needed. In this study, we proposed to use a dual-task paradigm to quantify listening effort with CIs. We hypothesized that listening effort may change differently than intelligibility for different CI programs, which may not be reliably captured with traditional speech intelligibility tests.

Methods

The dual-task paradigm is based on the idea that cognitive resources are limited and effort of the first task can be

quantified by changes in performance on the secondary task. In the present study, the primary task measured the intelligibility of sentences processed with a noiseband vocoder simulation of CIs. The secondary task, rhyme judgment, measured the response times (RTs). In the first experiment, using this paradigm, intelligibility and RTs were measured for a varying number of spectral channels of CI simulations with normal-hearing native Dutch speakers. In the second experiment, with a similar population, intelligibility and RTs were measured for a number of simulated CI configurations, such as a single CI and bimodal hearing of a CI combined with a hearing aid.

Results

Experiment 1 showed that speech perception, measured in percent correct, plateaued at 6 channels while listening effort, measured in RTs, further decreased up to 8 channels. Preliminary results from Experiment 2 did not show a significant reduction in effort with simulated bimodal hearing over a simulated single CI.

Conclusions

Results from the first experiment have shown that listening effort may be further optimized even after seemingly perfect speech perception is achieved, confirming our hypothesis. Preliminary results from the second experiment have not yet indicated an improvement in effort with bimodal hearing simulations, however this may have also been caused by not selecting the right parameters in the dual-task paradigm. Further research is conducted to pursue listening effort with new paradigms using cochlear implant simulations, as well as actual implants, and different implant configurations.

864 Measuring Listening Effort with Reaction Time to Digits in Noise

Rolph Houben¹, Maj Haverkate¹, Maaïke van Doorn-Bierman¹, Inge Brons¹, Wouter A. Dreschler¹

¹Academic Medical Center Amsterdam

Background: Audiological rehabilitation can be beneficial for speech communication even if it does not have a measurable effect on speech intelligibility. For example, single-channel noise reduction is often preferred by hearing-aid wearers, while it does not improve speech intelligibility. We hypothesized that this is caused by an improvement in listening effort. Unfortunately, there is no easy method for the measurement of listening effort. The purpose of the current study is to determine if the measurement of the reaction time to spoken digits in noise can be used to measure listening effort at signal to noise ratios (SNRs) that are high enough to render the speech completely intelligible. Additionally we want to determine if the reaction time to spoken digits can be improved by noise reduction processing.

Methods: We added various amounts of stationary noise to spoken digit triplets to obtain different SNRs (-10 dB, -5 dB, 0 dB, quiet). In addition to these “unprocessed” speech-in-noise stimuli we also included stimuli that were processed with two noise reduction schemes (an ideal binary mask and a Wiener algorithm with MCRA-noise estimator). All stimuli were used in a reaction time experiment with two different tasks. In the first task,

participants had to quickly identify the last digit of a triplet (‘identification’). In the second task they had to quickly add the first and the last digit (‘arithmetic’). Twelve normal-hearing participants participated in this study.

Results: At all SNRs the response time was increased significantly for lower (i.e. worse) SNRs for both the identification and the arithmetic tasks. The response time on the arithmetic task was more influenced by the noise than the response time on the identification task, but the arithmetic task led to a higher variance. Measurement of the effect of noise reduction on reaction time is ongoing.

Conclusions: The significant effect of SNR on reaction time implies that it is possible to measure listening effort with spoken digits at SNRs at which speech is highly intelligible. The optimal task may depend on the SNR that is of interest. A potential audiological application is the evaluation of noise reduction and data investigating this application are currently being gathered. If positive, this listening effort test would fill a gap in the evaluation of assistive hearing devices.

865 Seeing in the Dark: MEMRI of the Neuroretina

Bruce Berkowitz¹

¹Wayne State University School of Medicine

Functional MRI (fMRI) is usually based on detectable hemodynamic changes during a stimulus (BOLD). This endogenous contrast mechanism has greatly facilitated fMRI’s wide application; however, the information about neuronal activity generated by BOLD studies is indirect and limited to identifying the spatial location and spatial extent of activity. Here, I describe our studies using the neuroretina as a model system for evaluating another functional imaging approach, manganese-enhanced MRI (MEMRI). Importantly, MEMRI not only pinpoints functionally active regions but also allows for an analytical assessment of the degree of neuronal activity (based on calcium ion influx pathways like L-type voltage gated calcium channels) in that localized region-of-interest. The potential of applying MEMRI to translate studies between bench and bedside and back will also be discussed.

866 Detecting Laminar Specific Neural Plasticity in the Rodent Brain with MEMRI

Alan Koretsky¹

¹Laboratory of Functional and Molecular Imaging
NINDS, NIH, Bethesda MD.

Functional MRI techniques have found widespread use to measure brain neural circuits that are used for a large number of behaviors. When circuit activity changes due to plasticity, it remains a challenge to identify sites of synaptic changes responsible for the circuit level changes measured. Of particular interest are the cases of long range cortical rearrangements that have been detected in the human brain after injury. Rodent models that mimic some of these cortical rearrangements have been developed and are being used to determine the synaptic basis for the plasticity detected. We have developed a model of adult cortical plasticity due to peripheral

somatosensory nerve damage that is being used to develop MRI tools that can pinpoint sites of synaptic changes. Two weeks after peripheral denervation of one side of the forepaw, hindpaw, or whisker pathway there is a large up-regulation of cortical activity from the spared side and a large up-regulation of callosal inputs from the spared cortex to the cortical representation of the denervated area. A combination of functional MRI and laminar specific neural track tracing using manganese enhanced MRI predicted changes in thalamo-cortical inputs to layer IV that contribute to the up-regulation of cortical activity along the spared whisker barrel pathway. Slice electrophysiology confirmed that the thalamic inputs on layer IV stellate cells were strengthened by a post-synaptic mechanism. Sites of plasticity that explain the up-regulation of the callosal communication have also been studied with MRI. High temporal-spatial resolution fMRI demonstrates that up-regulation of the communication between the spared and denervated cortices likely occur through callosal inputs. These fMRI results were consistent with manganese enhanced MRI that predicts a strengthening of inputs into layer 2/3 and 5. Taken together these results demonstrate that MRI is positioned to begin to give laminar specific information about mechanisms of cortical plasticity.

867 Studying Development and Plasticity of Auditory Function with MEMRI

Dan Sanes¹, Xin Yu², Daniel Turnbull³

¹New York University, ²NIH/NINDS, ³New York University School of Medicine

There are several challenges to studying the emergence of central auditory processing. The sound-driven responses of juvenile neurons are small in magnitude and adapt rapidly. Furthermore, these characteristics can be exacerbated by the anesthetics the permit stable recordings. As a consequence, studies of functional development are usually based on a relatively sparse sample of neurons, and the effect of developmental manipulations, such as hearing loss or abnormal stimulation, are usually assessed in adulthood when robust recordings can be more easily obtained. In this presentation, I will review the strengths and limitations of Manganese-enhanced magnetic resonance imaging (MEMRI) for the purpose of studying auditory processing in control and experimentally reared animals.

Mice were raised either under normal laboratory conditions, or with conductive hearing loss, or in a specific acoustic environment. Each animal was then injected with MnCl₂, and Mn²⁺ uptake was induced by exposure to either a broadband noise or a single pure tone while awake. Animals were imaged in an anesthetized state using a 7-Tesla horizontal magnet and 25mm head coil. A 3D gradient echo pulse sequence was used to acquire T1-weighted brain images, with an isotropic spatial resolution of 100 μm. Volumetric image data from each brain was registered to a 3D template, and the inferior colliculus (IC) was extracted using a mask segmented from the template. 3D images were analyzed statistically with a

voxel-wise multiple-comparison method in Matlab (see Yu et al. 2005, 2007, 2008).

Three sets of developmental findings were obtained with MEMRI. First, the 3D map of sound frequency in IC displays significant refinement during the week after hearing onset. Second, developmental exposure to sound frequencies that are ordinarily represented in IC by non-overlapping volumes, causes a significant reorganization of the 3D map. Third, the effect of conductive hearing loss on IC activity depends on the age of hearing loss onset and duration of deprivation.

MEMRI offers certain advantages for studying functional development. Stimulus-specific activity patterns can be induced in awake animals, and the measurement obtained subsequently from all brain regions with a high spatial resolution. Furthermore, this activity pattern can be obtained, noninvasively, from the same animal at a later age. However, MEMRI activity patterns provide no information about neuron discharge patterns that encode specific sound cues. Therefore, MEMRI is best employed when whole brain mapping and assessment points are required to address a hypothesis.

868 Noise-Induced Calcium-Dependent Activity in the Central Auditory Pathway: A Manganese-Enhanced MRI Study

Dietmar Basta¹, Susanne Müller¹, Arne Ernst¹, Moritz Gröschel¹

¹Department of ENT at ukb, University of Berlin, Charité Medical School, Germany

Background

Noise exposure at high intensities leads to a temporary shift of hearing thresholds (TTS) and is followed by a permanent threshold shift (PTS). Permanent threshold shift is not only associated with cochlear damage as the primary site-of-lesion, but also with subsequent structural and functional changes within the central auditory pathway. The aim of the present study was to monitor neuronal activity within central auditory structures in mice after noise exposure at different time intervals using manganese-enhanced magnetic resonance imaging (MEMRI).

Methods

Young adult mice were noise exposed for 3 hours with a broad-band white noise (5–20 kHz) at 115 dB SPL. Twenty-four hours before the MRI-scanning was performed using a 7-Tesla rodent scanner, a 0.4 mM/kg dose of MnCl₂ was injected. Mice were investigated immediately after the noise exposure, or were kept in their cages for one or two weeks to be investigated at 7 or 14 days after noise exposure. Another group was noise-exposed for a second time at one week after the first exposure. These animals were investigated 7 days after the second exposure.

One additional group was exposed to sound intensities of 90 dB SPL (moderate noise exposure) and investigated 7 days later. Unexposed animals were used as controls.

Results

Calcium-dependent activity patterns were modified in several structures of the central auditory system as the result of noise-induced hearing loss (NIHL). The MEMRI data demonstrate that temporary threshold shift is correlated with an activity increase in hierarchically lower structures of the auditory pathway. This seems to be indicative of a direct noise impact at the first stage of central auditory processing. However, noise-dependent changes of higher auditory structures were found as well in the phase of PTS. Repeated noise exposure was found to induce an additional elevation of calcium-dependent activity in all investigated auditory structures — without a significant shift in auditory thresholds.

Sustained manganese accumulation was present in the auditory brainstem after moderate acoustic stimulation as well without PTS induction.

Conclusions

The long-lasting enhancement of MEMRI signals suggests a noise-induced activity increase of various calcium-dependent processes of different origin. The present findings could be helpful to better understand the time-course of different symptoms in NIHL and the individual susceptibility to noise.

869 Manganese Enhanced MRI (MEMRI) to Assess Axonal Transport Deficits and Improvements in Mouse Models of Alzheimer's Disease

Karen Smith¹, Cynthia Massaad¹, Robia Pautler¹

¹Baylor College of Medicine

Title: Manganese Enhanced MRI (MEMRI) to Assess Axonal Transport Deficits and Improvements in Mouse Models of Alzheimer's Disease

Background: Axonopathy is observed in many neurodegenerative diseases. In Alzheimer's disease (AD), axonal swellings and degeneration are prevalent and are thought to contribute to AD pathology. Current limitations in identifying the contribution of axonal damage to AD include the inability to detect when this damage occurs in relation to other identifiers of AD because of the invasiveness of existing methods. To overcome this, we used the MRI methodology Manganese Enhanced MRI (MEMRI) to assess *in vivo* axonal transport rates in the Tg2576 mouse model of AD and in Tg2576 mice crossed with superoxide dismutase 2 (SOD2) overexpressing animals.

Methods: Mice were imaged using a 9.4T, 21 cm bore horizontal scanner with a 35 mm volume resonator (Bruker, BioSpin). Mice were anesthetized with 5% isoflurane mixed with oxygen and maintained on 1.5 – 2 % isoflurane during imaging. The imaging parameters to acquire olfactory multi-spin/multi-echo MEMRI images were as follows: TR=500 ms; TE=10.2 ms; FOV=3.0 cm; slice thickness= 1 mm; matrix=128°—128; NEX=2; number of cycles=15; using Paravision 5.0 software (Bruker

BioSpin, Billerica, MA). The core temperature was maintained at 37 °C during scanning. The region of interest (ROI) was identified and placed on an axial slice 1 mm in front of the posterior of the olfactory bulb (OB). The ROI was determined by measuring the length of the olfactory bulb, locating the midpoint of this line, then extending this midpoint out to the ONL.

Results: Our results demonstrate that axonal transport deficits are present in the Tg2576 mouse during amyloid beta accumulation and also before plaque formation. Furthermore, our results demonstrate that by reducing oxidative stress by overexpressing SOD2 in the Tg2576 mouse rescues axonal transport deficits.

Conclusions: MEMRI can be used to measure axonal transport deficits and improvements in mouse models. We have shown that axonal transport deficits are present in mouse models of AD before plaque formation occurs. We also show that this axonal transport deficit can be rescued by reducing oxidative stress through SOD-2 overexpression. The use of MEMRI to assess transport deficits and improvements should be applicable to additional mouse models of neurodegeneration.

870 New Approaches for Studying Tinnitus: Bridging the Gap Between Basic Science and Current Clinical Concerns

Anthony Cacace¹

¹Wayne State University

Within the last decade, advancements in the study of tinnitus have been made by combining non-invasive neuroimaging modalities (anatomical and physiological) with non-invasive treatment paradigms. One such treatment paradigm involves the use of repetitive transcranial magnetic stimulation (*rTMS*) as a strategy for tinnitus abatement. Voxel-based morphometry (VBM) has been used as an anatomical outcome measure to evaluate plastic changes in the brain following treatment. Magnetic resonance spectroscopy (MRS) has also been used as a physiological outcome measure to evaluate changes in metabolites following *rTMS* treatment.

Recent experimental work has shown that manganese enhanced MRI (MEMRI) can identify tinnitus related neural activity in the nervous system in animals with behavioral evidence of tinnitus. To extend this exciting work, we now propose that manganese encapsulated nanoparticles may be the next advancement in tinnitus research when considered under the rubric of “nanotheranostics;” a new area of research that focuses on the combination of diagnostic detection with therapeutic drug delivery carriers. It is hypothesized that nanoparticles capable of housing manganese ions for MRI contrast enhancement, binding target-specific receptors, and releasing appropriate therapeutic agents in tinnitus positive brain areas, will improve treatment efficacy and ultimately lead to the best possible outcomes for individuals with tinnitus. Indeed, it is the *functionality* of nanoparticles that has inspired the use of this theranostic platform. In

addition, because many current methods used for tinnitus abatement are either ineffective or produce inconsistent and sometimes disappointing results, new and innovative approaches are needed. Developing unique nanotechnology provides the platform and opportunity to attack the issue of tinnitus suppression head on. If successful, we can bridge the gap between basic science and the translational clinical potential to humans in order to make new in roads for novel drug treatments. In combination with other technology and imaging techniques, we are on the road to a cure for abating this often debilitating condition.

871 In Vivo Identification of Hyperactive Neural Activity in Rats with Behavioral Evidence of Tinnitus Using MEMRI

Avril Genene Holt¹, David Bissig¹, Najab Mirza¹, Gary Rajah¹, Bruce Berkowitz¹

¹Wayne State University School of Medicine

Currently, there are no drugs that are broadly effective in the treatment of tinnitus. Crucial for development and testing of pharmacological interventions is a biomarker that is **a.** reliably correlated with the perception of tinnitus **b.** apparent regardless of hearing status or method of tinnitus generation and **c.** persistent, present as long as tinnitus percepts remain. Many tinnitus studies have suggested that changes in spontaneous neuronal activity may be one such biomarker. A novel non-invasive method for assessment of neuronal activity is manganese enhanced MRI (MEMRI). In this study our group has used MEMRI to evaluate neuronal activity in auditory related nuclei. Two complementary methods were combined to evaluate established tinnitus models: inhibition of acoustic startle and manganese-enhanced MRI. In order to induce tinnitus, adult male rats were either administered salicylate once daily for three days or exposed to a single noise event (10 kHz, 118 dB one-third octave band tone, four hours). Salicylate-induced tinnitus (as determined with acoustic startle) resulted in wide spread manganese uptake that was significantly elevated when compared to uptake levels in both non-tinnitus rats and rats with acute noise-induced tinnitus sustained. Only in the inferior colliculus (IC) did both tinnitus models exhibit manganese uptake that was significantly elevated when compared to non-tinnitus animals. Therefore, abnormal neuronal activity levels in the IC appear to be important in tinnitus-mediated activity. Our results suggest that increased spontaneous neuronal activity in the IC is an indicator of tinnitus perception and that modulation of spontaneous neuronal activity may be used as a method for evaluation of proposed therapeutic intervention. These studies provide the foundation for future studies correlating the longevity of tinnitus with hearing loss and neuronal activity in specific brain regions resulting in tools for evaluating treatment efficacy across tinnitus paradigms.

872 Biofabricated Manganese Encapsulated Nanoparticles: Novel Theranostic Applications to Identify and Treat Tinnitus

James Castracane¹, Magnus Bergkvist¹, Avril Genene Holt², Anthony Cacace²

¹College of Nanoscale Science and Engineering-UAlbany,

²Wayne State University

One challenge associated with targeted imaging and theranostic nanotechnology is the packaging and site-specific delivery of therapeutic/imaging agents to the tissue of interest. One route to a multifunctional nanoparticle platform is to leverage existing biological systems capable of self-assembly and multivalent display. Bacteria and plant virus capsids are ideal candidates in this respect, where entrapment of dyes/drugs inside the capsid combined with external capsid modification offer a novel concept for nanoscale packaging and site-specific targeting. The icosahedral MS2 bacteriophage is a potential candidate for such a system, having an exterior diameter of ~28 nm with large pores, where small molecules to enter the capsid interior. MS2 also has several lysines available on the exterior for conjugation of targeting ligands. We have previously demonstrated RNA-based self-packaging of a heterocyclic photoactive agent (meso-tetrakis(para-N-trimethylanilinium)porphine, TMAP) into the MS2 capsid and used this system for targeted delivery of drugs to cancer cells. In the current work, we investigate the potential of the MS2 capsid for use in a similar fashion to encapsulate Mn-chelating agents applied to MRI imaging. Extended functionality by modifying the capsid exterior with targeting moieties will be discussed to allow targeted imaging/treatment for tinnitus research.

873 Impact of Short-Term Auditory Training on Subcortical Processing of Sounds

Judy Song¹, Katharina von Kriegstein¹, Erika Skoe², Karen Banai³, Nina Kraus²

¹Max Planck Institute for Human Cognitive and Brain Sciences, ²Northwestern University, ³University of Haifa

Background: Auditory thalamus and brainstem structures play an important role in auditory learning. However, our understanding of the extent to which subcortical contribution is experience-dependent has been limited, particularly in healthy young adults. The purpose of our studies was to further our understanding of the neural impact of training on the subcortical processing of sound.

Method: In several studies, we investigated the impact of cognitive-based auditory training programs on perceptual ability and subcortical processing of speech via EEG and fMRI.

Results: Our findings show training-related perceptual improvement. In addition, neural recordings demonstrate continued malleability of subcortical encoding of speech in adulthood. Predictive relationships were also found between pre-training neural activity and amount of perceptual improvement, thus offering a useful metric to help identify individuals who would benefit most from auditory training.

Conclusions: Our studies offer empirical evidence that auditory training involving active engagement of cognitive

processes can alter the neural encoding of sound by enhancing the processing of acoustic cues that are important in speech perception. Also, by demonstrating training-related improvements in normal hearing, young adults, we were able to better delineate the capacity for change as well as limitations of the central auditory system.

Supported by NIDCD R01 DC01510, T32 NS047987 and the Knowles Hearing Center (N.K.) and Max Planck Society (KvK).

874 Circuit Organization and Synaptic Plasticity of Neurons in the Top-Down Auditory Brainstem Projecting Pathway

Jason W. Middleton¹, Charles T. Anderson¹, Gordon M. G. Shepherd², Thanos Tzounopoulos¹

¹Department of Otolaryngology, University of Pittsburgh,

²Department of Physiology, Northwestern University

Top-down corticofugal pathways exert significant influence on auditory stimulus processing in the brainstem. The inferior colliculus (IC) is a site of synaptic convergence from other auditory brainstem nuclei; its role in transmitting this convergent information to the thalamus makes it an important target of top-down modulation. The function of top-down pathways targeting the IC have been studied using behavioral assays and by characterizing physiology at the level of the IC. However, little is known about how cortical networks at the origin of this top-down pathway are structured and activated. To better understand this aspect of top-down auditory pathways we studied the microcircuit architecture and synaptic dynamics of IC projecting (cortico-collicular) neurons in the auditory cortex. Cortico-collicular neurons were labeled by injecting retrograde fluorescent tracers in the IC. We used laser-scanning photostimulation (LSPS) with glutamate uncaging to characterize the microcircuit architecture of monosynaptic inputs to IC-projecting neurons in layer 5B (L5B). To assess the specialization of top-down circuits we injected fluorescent tracers in the contralateral auditory cortex and characterized synaptic input maps of L5B cortico-cortical neurons. We demonstrate that cortico-collicular and cortico-cortical networks form the basis of two functionally distinct auditory projection pathways. For example, cortico-collicular neurons receive stronger inputs from L2/3 than do cortico-cortical neurons. To understand the synaptic dynamics of this pathway we performed dual whole cell recordings on connected L2/3 and L5B neurons. We found that L2/3->L5B cortico-cortical synapses obeyed conventional short-term plasticity rules: stronger synapses depress with repetitive activation and weaker synapses facilitate. In contrast, we observed a different form of plasticity at L2/3 synapses projecting to cortico-collicular L5B neurons: weaker synapses depress more than stronger ones. Computational models of an auditory cortical column allowed us to test the functional implications of these differential forms of plasticity. Short-term synaptic plasticity in the cortico-cortical column effectively shuts down the L2/3->L5 pathway, and by consequence L5 cortico-cortical output. Short-term synaptic plasticity maintains large-amplitude L2/3->L5

synapses thus keeping the cortico-collicular pathway open after short term sensory activation. Our findings establish that cortico-collicular and cortico-cortical networks form distinct parallel functional pathways in the cortex and we expect our findings will establish a new framework for the study of top-down networks in the auditory system.

875 The Disadvantaged Brain: Auditory Function and Socio-Economic Standing

Erika Skoe¹, Jennifer Krizman¹, Douglas Savitsky², Nina Kraus¹

¹Northwestern University, ²Cornell University

Background:

Studies of auditory deprivation in humans typically focus on the effects of deafness. However, deprivation can occur when hearing thresholds are intact. For instance, children from families of low socioeconomic standing (SES) hear fewer words per hour, receive less cognitive stimulation, and face greater noise exposure than their high SES counterparts. Despite the prevalence of poverty in the United States, little is known about how this early adversity affects the human brain. What is known, however, is that parental SES is a strong predictor of a person's life trajectory and that environmental factors, including auditory deprivation, can have lifelong repercussions. From this, we propose that auditory function and SES interact reciprocally.

Methods:

To characterize how SES affects auditory brain function, we compared two groups of normal-hearing adolescents that attended the same schools and were matched in age, sex, and ethnicity, but differed in their maternal education level (11.43 vs. 15.00 years), a correlate of socioeconomic status. We recorded auditory brainstem responses (ABRs) to the speech syllable "da" in addition to measuring neural noise in the absence of stimulation. From the speech-evoked ABR, we measured the fidelity of the response to the vowel (spectral power within 284-655 Hz) and computed within-session response consistency by comparing the first and second halves of the recording.

Results:

Adolescents from low-maternal education backgrounds have noisier responses, as reflected by greater spontaneous brainstem activity. Additionally, their response to the speech stimulus is less consistent over time with lower fidelity to the input signal.

Conclusions:

Noisier, more variable, and weaker brainstem responses are telltale signs of an inefficient auditory system. Consistent with work from laboratory animals, we interpret our findings as evidence that impoverished environments impinge upon the brainstem's ability to translate sounds into meaningful signals. We further suggest that disparate brain acuity may drive the achievement gap, effectively limiting social mobility for impoverished children. By studying SES within a neuroscientific framework, we have the potential to expand our understanding of how

experience shapes the brain, in addition to informing intervention strategies.

Supported by: Northwestern University Knowles Hearing Center, NIH RO1 DC10016, NSF 0921275

www.brainvolts.northwestern.edu

876 Human Brainstem Plasticity: Effects of Auditory Context and Training

Bharath Chandrasekaran¹

¹*The University of Texas at Austin*

While it is well established that the auditory brainstem undergoes experience-dependent plasticity even in adulthood, mechanistic aspects of such plasticity are poorly understood in humans. Invasive studies on animal models show two forms of brainstem plasticity— a stimulus probability-based plasticity, and a second form of plasticity that is training-dependent. Whether these kinds of plasticity have manifestations in humans is still unanswered. Here we examine the frequency-following responses (FFR), which reflect ensemble neural phase-locking, to non-native pitch patterns using a passive oddball design. Participants listened to pitch patterns presented at a high probability of occurrence (standards) or a low probability of occurrence (deviants). They then underwent a 2-week sound-to-meaning training program during which they learned to use these pitch patterns to distinguish words. Post-training, the pitch patterns were presented again using the same passive oddball design. Results demonstrate the existence of two distinct forms of plasticity in the human auditory brainstem: a stimulus probability-driven plasticity that is present even before training and a training-dependent plasticity that alters the brainstem representation of pitch patterns. FFRs to 'deviants' were poorer than FFRs to 'standards' before training; post-training differences between standards and deviants are less salient. These results establish multiple, distinct forms of plasticity concurrently operational in the adult auditory brainstem.

877 Predictive Coding in the Human Auditory Brainstem: Implications for Neural Plasticity

Daniel Abrams¹, Blair Kaneshiro¹, Jonathan Berger¹, Vinod Menon¹

¹*Stanford University*

Background: A basic function of the human nervous system is to detect regularities in the sensory environment to predict future events. Neural models describing active prediction in the auditory system focus exclusively on cortical structures. Here we examined whether predictive coding is solely the domain of auditory cortical structures or if this coding represents a more systemic phenomenon that extends to subcortical structures.

Methods: We measured auditory brainstem potentials in adult subjects in response to an oddball paradigm in which the frequent stimulus was a complete and recognizable melody and infrequent stimuli consisted of the same

melody with the final note either omitted or replaced with an unexpected note.

Results: Preliminary results show brainstem phase-locking for the final note of the melody for both the frequent and omitted stimulus conditions but not for a control condition. Moreover, the unexpected stimulus condition produces signals in the brainstem response at frequencies which are not present in the stimulus that correspond to the combination of the expected and unexpected notes.

Conclusions: Results indicate that anticipation of the final note of the melody is sufficient to drive phase-locked activity in the auditory brainstem, presumably through top-down, cortically mediated neural mechanisms.

878 Spatial Coding, Plasticity and Functional Asymmetries in the Human Auditory Brainstem

Marc Schoenwiesner¹

¹*University of Montreal*

The talk will explore interrelated themes of functional asymmetry, spatial coding, and plasticity in the human auditory brainstem. We report evidence for stimulus and context-dependent lateralization in the brainstem, measured with functional magnetic resonance imaging (fMRI). We found that speech, music, and noise stimuli are lateralized differently in the auditory thalamus. The lateralization of noise stimuli throughout the auditory pathway depends on the presence of other stimuli that are known to be preferentially processed in one hemisphere. A simple model in which the auditory cortices modulate their input from ipsi- and contralateral brainstem and thalamus via cortico-fugal projections accounts for these results.

We also present results on the encoding of interaural time differences (ITD) in the human brainstem. We presented binaural noises with different ITDs and recorded auditory brainstem evoked potentials using electroencephalography. We used an adaptation design to collect evidence for ITD encoding by two opponent neural populations, one tuned to the left and the other to the right acoustic hemifield. The results are consistent with models of ITD extraction in the auditory brainstem of other mammals. Lastly, we present results on plasticity in ITD coding in the brainstem from a study in which we shifted the correspondence between ITDs and sound locations by adding a constant time delay to one ear of test participants using small digital signal processing devices worn in the ear canal during several days. Most participants regained normal sound localization accuracy within 48 hours. ITD tuning in the cortex measured with fMRI changed in correspondence with the behavioral adaptation. Brainstem potentials recorded with EEG also showed a shift in directional tuning during the behavioral adaptation.

In summary, these results demonstrate an active role of the human auditory brainstem in perceptual and cognitive processes, such as context sensitivity, speech and music processing, and adaptation to modified sensory input.

879 Role of Cholinergic Modulation of the Auditory Cortex and Corticofugal Circuits in Spatial Learning in Adult Animals

Victoria M Bajo¹, Fernando R Nodal¹, Nicholas D Leach¹, Andrew J King¹

¹University of Oxford

Background

Mammals are able to maintain a stable sound localization percept thanks to the ability of the brain to adapt to changes in the spatial cues available. We have shown that ferrets trained by positive conditioning to localize broadband sounds in azimuth are able to recalibrate their behavioral responses by re-weighting monaural and binaural cues altered after reversibly plugging one ear. Here we aim to establish the role of cortical acetylcholine (ACh) release in this training-dependent plasticity and to identify the neural circuits within the auditory pathway that are responsible.

Methods

We tested adaptation to a unilateral earplug in two different experimental conditions: (1) when cholinergic input to the auditory cortex was removed by injecting the immunotoxin ME20.4-SAP, which specifically targets the p75 neurotrophin membrane-bound receptor (p75^{NTR}) expressed primarily by cholinergic neurons, in the nucleus basalis (NB) and (2) when pyramidal neurons from the primary auditory cortex that project to the inferior colliculus were selectively destroyed by chromophore-targeted laser photolysis.

Results

ME20.4-SAP injections in the NB produced a substantial loss of both p75^{NTR} positive cells in this region and of acetylcholinesterase positive fibers throughout the auditory cortex. The loss of cholinergic neurons impaired the ability of ferrets to adapt to altered spatial cues following unilateral ear occlusion. After training they exhibited less complete recovery of localization performance than control cases, with adaptation taking place at a significantly slower rate. Although their ability to localize the long-duration sounds used to investigate plasticity was unaffected under normal hearing conditions, these animals had longer response times than controls. When the stimulus duration was reduced (<500 ms), they became less accurate than controls, with a direct correlation between the number of cholinergic cells lost and the impairment in performance.

When the projection from the primary auditory cortex to the inferior colliculus was selectively destroyed by chromophore-targeted laser photolysis in a second group of ferrets, the animals were again unable to adapt to relearn to localize sound after plugging one ear, but this time sound localization under normal hearing conditions was not affected.

Conclusions

Together, these results show that cortical cholinergic inputs contribute to auditory spatial perception and provide evidence for a role for ACh in adult auditory spatial learning. The cortico-collicular pathway is a key element in

this adaptive plasticity, suggesting that collicular neurons can change their spatial response properties under cortical command.

880 The Effects of Music/language Expertise on Subcortical Plasticity, Auditory Perceptual Abilities, and Cognitive Transfer

Gavin Bidelman^{1,2}

¹School of Communication Sciences & Disorders, University of Memphis, ²Institute for Intelligent Systems, University of Memphis

The scalp-recorded frequency-following response (FFR), an evoked potential with putative generators in rostral brainstem, provides a detailed window into subcortical encoding of complex sound including speech and music. Studies demonstrating enhanced FFRs in tone-language speakers and musicians suggest: 1) long-term experience with complex acoustic scenes strengthens brainstem response properties; 2) neural plasticity can emerge peripheral to cortex, with nascent effects observable even in subcortical auditory structures. Cross-domain comparisons show overall enhancements in FFRs elicited by either musical or linguistic stimuli in musicians and tone-language speakers alike. Thus, experience-dependent effects act to improve the brain's initial registration of perceptually salient acoustic cues, a benefit which transfers across domains of expertise. Importantly, the fidelity (e.g., temporal precision and magnitude) of these sensory representations correspond with an individual's degree of training/experience and, assuming the stimuli and task are behaviorally relevant to the listener, their performance in speech and music perception. These findings collectively lead us to infer that both language and musical experience mutually benefit the subcortical extraction and subsequent perception of acoustic information. Yet, we also find that specific features of the auditory signal are highlighted in neurophysiological responses depending on their perceptual salience and function within a listener's domain of expertise.

881 Alterations of the CIB2 Calcium- And Integrin-Binding Protein Cause Usher Syndrome Type 1J and Nonsyndromic Deafness DFNB48

Saima Riazuddin^{1,2}, Inna Belyantseva³, Arnaud Giese^{1,2}, Kwanghyuk Lee⁴, Artur Indzhukulian⁵, Sri Pratima Nandamuri⁶, Rizwan Yousaf^{1,7}, Ghanshyam Sinha⁵, Sue Lee³, David Terrell², Rashmi Hegde⁸, Saima Anwar⁷, Paula B. Andrade-Elizondo⁴, Asli Sirmaci⁹, Sulman Basit¹⁰, Abdul Wali¹¹, Muhammad Ayub¹², Muhammad Ansar¹⁰, Wasim Ahmad¹⁰, Shaheen Khan⁷, Mustafa Tekin⁹, Sheikh Riazuddin¹³, Tiffany Cook², Elke Buschbeck⁶, Gregory Frolenkov⁵, Suzanne Leal⁴, Thomas Friedman³, **Zubair Ahmed**^{1,2}

¹Division of Pediatric Otolaryngology, Cincinnati Children's Hospital Medical Center, ²Division of Pediatric Ophthalmology, Cincinnati Children's Hospital Medical Center, ³Laboratory of Molecular Genetics, National

Institute on Deafness and Other Communication Disorders, ⁴*Department of Molecular and Human Genetics, Baylor College of Medicine*, ⁵*Department of Physiology, University of Kentucky*, ⁶*Department of Biological Sciences, University of Cincinnati*, ⁷*National Center for Excellence in Molecular Biology, University of the Punjab*, ⁸*Division of Developmental Biology, Cincinnati Children's Hospital Medical Center*, ⁹*Department of Human Genetics, University of Miami*, ¹⁰*Department of Biochemistry, Quaid-i-Azam University*, ¹¹*Institute of Biotechnology, Baluchistan University of Information Technology*, ¹²*Institute of Biochemistry, University of Baluchistan*, ¹³*Allama Iqbal Medical College*

Background

Many molecular components necessary for maintenance of vision and development of hearing have been discovered through identification of the genes underlying Usher syndrome. Usher syndrome (USH) is characterized by deafness and retinitis pigmentosa with variable age of onset and severity, sometimes accompanied by vestibular areflexia. We previously mapped a type I Usher syndrome locus segregating in two families and an autosomal recessive nonsyndromic hearing impairment (ARNSHI) locus (*DFNB48*) segregating in five families to chromosome 15q23-q25.1. Here, we report the identification of the gene causing USH1J/DFNB48 phenotype in humans.

Methods

We used genetic linkage analysis followed by a candidate gene screening strategy to identify the *USH1J/DFNB48* gene, *CIB2*. Molecular modeling, biochemical, cellular, histochemical and physiological techniques in mice, zebrafish and *Drosophila* were used to determine the expression, localization and function of *CIB2*.

Results

We found that mutations in a calcium- and integrin-binding protein *CIB2* are associated with nonsyndromic deafness *DFNB48* and Usher syndrome type 1J (*USH1J*). *CIB2* is a major cause of ARNSHI within the Pakistani population. In addition, a transition mutation of *CIB2* co-segregated with ARNSHI in a Turkish *DFNB48* family. In mice, *CIB2* is localized in mechanosensory stereocilia of inner ear hair cells and in retinal photoreceptor and pigmented epithelium cells. Consistent with molecular modeling predictions, *CIB2* significantly decreased the ATP-induced Ca^{2+} responses in heterologous cells, while *DFNB48* alleles altered *CIB2* effects on Ca^{2+} responses. Furthermore, in zebrafish and *Drosophila*, *CIB2* is essential for the function and proper development of lateral line hair cells and retinal photoreceptor cells. We also show that *CIB2* interacts with myosin VIIa and whirlin and thus is a new member of the vertebrate Usher interactome.

Conclusion

CIB2 mutations underlie Usher syndrome 1J and nonsyndromic deafness *DFNB48*. In *Drosophila*, *CIB2* is critical for proper photoreceptor maintenance and function due to its involvement in calcium homeostasis. Since *CIB2* is concentrated in stereocilia and interacts with myosin

VIIa and whirlin, and *Cib2* zebrafish morphants have reduced hair cell microphonic potential, we speculate that *CIB2* regulate Ca^{2+} in hair cell stereocilia.

882 From Pattern Generator to Sound Receptor, Hair Cells Adjust Ca^{2+} Signaling to Their Function During Development

Aaron Wong¹, Mark Rutherford¹, Zhizi Jing¹, Thomas Frank^{1,2}, Nicola Strenzke^{1,3}, Carolin Wichmann^{1,3}, Tobias Moser^{1,3}

¹*InnerEarLab, Department of Otolaryngology, University Medical Center Göttingen, Göttingen, Germany*, ²*Friedrich Miescher Institute for Biomedical Research, Basel, Switzerland*, ³*Collaborative Research Center 889, University of Göttingen, Göttingen, Germany*

Background

Ca^{2+} -triggered transmitter release from cochlear inner hair cells (IHCs) drives pre-sensory and sensory activity in spiral ganglion neurons (SGNs). Here, we studied the development of IHC Ca^{2+} signaling, afferent synaptic structure and SGN activity in mice.

Methods

We studied the changes of synaptic Ca^{2+} signal in mouse IHCs during development, using patch-clamp and fast confocal Ca^{2+} -imaging. Capacitance measurements and flash photolysis of caged calcium were used to investigate the apparent and intrinsic (biochemical) cooperativity of the hair cell ribbon synapse. Single unit recordings were performed in early postnatal mice to record activity of SGNs during the period of IHC maturation. Finally, immunofluorescence and electron microscopy were used to study molecular and morphological changes during development.

Results

Robust Ca^{2+} signals driven by spontaneous action potentials at IHC active zones (AZs) were observed before the onset of hearing. Concomitantly, we found bursting SGN activity *in vivo*, which markedly differed from the Poisson-like spontaneous activity in hearing animals. At each synapse, several small appositions of AZs and postsynaptic densities (PSDs) were initially formed, in contrast to the single AZ/PSD pair present after maturation. Coupling between Ca^{2+} influx and vesicle fusion progressively tightened in postnatal IHCs (decrease in apparent cooperativity). In parallel, immunohistochemistry reported a progressive loss of extrasynaptic Ca^{2+} channels. In contrast to the decreasing whole-cell Ca^{2+} current and total channel number, synaptic Ca^{2+} signals increased in strength and heterogeneity, reflecting the emergence of AZs with more Ca^{2+} channels. Computational modeling suggested that these stronger AZs may drive the activity of SGN sub-population with low thresholds and high spontaneous rates.

Conclusion

Here, we characterized the synaptic Ca^{2+} signal associated with naturalistic electric activity of IHCs before and after the onset of hearing, namely, spontaneous action

potentials and receptor potentials. We also demonstrated the presence of bursting activity in the postsynaptic SGNs *in vivo*. The change in IHC function from spiking driver of pre-sensory activity to faithful encoder of sound intensity is accompanied by a confinement synaptic organization and function. Moreover, we propose that maturing IHCs heterogeneously distribute their Ca²⁺ influx among AZs, in order to decompose auditory information to functionally diverse SGNs and encode a broad dynamic range of sound pressure.

883 Mechanisms Underlying Heterogeneity of Ca²⁺ signaling Among Hair Cell Active Zones

Tzu-Lun Wang¹, Mark Rutherford¹, Tobias Moser¹

¹*InnerEarLab, Department of Otolaryngology and SFB889, University Medical Center of Goettingen*

Background

Sound intensity is encoded as the firing rates of spiral ganglion neurons. These neurons show different rate-level functions and are thought to collectively encode the large dynamic range of the auditory stimuli. We investigated the heterogeneous properties of presynaptic Ca²⁺ microdomains and their relationship to synaptic ribbons. We tried to explain how hair cells decompose auditory information at their heterogeneous ribbon synapses driving neurons with different rate-level functions.

Methods

Postnatal (14-18 days) mouse inner hair cells from the apical half-turn of the organ of Corti were voltage clamped in whole-cell mode. A fluorescent Ca²⁺ indicator (Fluo-8FF) and a ribbon reporter (TAMRA-conjugated CtBP2-binding peptide) were perfused into the hair cells via the pipette solution. Step or ramp depolarization protocols were used to evoke Ca²⁺ influx and analyze the resulting Ca²⁺ microdomains. A spinning disk confocal microscope was used to image each cell in 3D, and to characterize each Ca²⁺ microdomain over time.

Results

Synaptic Ca²⁺ microdomains and ribbons exhibited strong heterogeneity, and their fluorescence intensities were positively correlated. Additionally, we assessed the spatial distribution of ribbon and Ca²⁺ hotspot intensities within individual inner hair cells. Larger ribbons and stronger Ca²⁺ microdomains tended to localize to the modiolar (neural) side.

Conclusion

Our results imply that larger synaptic ribbons are associated with more Ca²⁺ channels, which is expected to enhance neurotransmitter release at those synapses. Interestingly, previous studies (Merchan-Perez & Liberman, 1996) on cat cochlea suggested that high spontaneous rate auditory nerve fibers mainly innervate the pillar (abneural) face of inner hair cells. If conserved among species our finding of weaker Ca²⁺ microdomains on the pillar face seems in conflict with this view. Further

investigation is required to solve this apparent discrepancy.

884 Transmitter Release from Cochlear Hair Cells Is Phase-Locked to Cyclic Stimuli of Different Intensities and Frequencies

Juan Goutman¹

¹*Instituto de Investigaciones en Ingenieria Genetica y Biologia Molecular. Buenos Aires, Argentina*

Background

The auditory system analyzes time and intensity to code location of a sound source. These parameters are preferentially processed in different brainstem nuclei and so must be independently detected in the periphery and transmitted to the central nervous system. It is well-established that auditory nerve fibers are able to fire at a particular time within each cycle of a low-frequency periodic stimulus. Furthermore, this preferred phase can remain constant over a range of sound intensities at the characteristic frequency – phase constancy independent of intensity. We investigated this phenomenon at the first synapse of the hearing pathway, between inner hair cells and boutons of auditory nerve neurons.

Methods

Explants of the organ of Corti from neonatal rats were used for experiments (apical region). Simultaneous pre- and post-synaptic patch-clamp recordings at the inner hair cell-afferent synapse were performed. The series of differential equations corresponding to a model of the inner hair cell calcium sensor were solved numerically.

Results

Cyclic stimuli such as trains of depolarizations to different potentials were presynaptically applied, trying to mimic acoustic stimuli of different intensities. Synaptic responses elicited by these trains presented constant latencies (or phase) within each cycle, for a range of membrane potentials over which release probability varied significantly. Phase-locked release was observed with stimulating frequencies of 100, 250 and 500 Hz. In contrast, on single steps, synaptic responses proved to have a voltage-(calcium-) dependence on timing. Interestingly, short-term facilitation (only) partially compensated for changes in latencies (and also reduced jitter) in these single pulses. We also found that synaptic depression elicited longer 1st latencies events. Thus, during repetitive presynaptic stimulation, as hair cells are more strongly depolarized, increased calcium channel gating would speed up transmitter release, but the resulting vesicular depletion produced a compensatory slowing. Quantitative simulation of ribbon function showed that these two factors will vary reciprocally with hair cell depolarization (stimulus intensity) to produce constant synaptic phase.

Conclusion

We propose that equilibrium would be established between each stimuli level and the degree of synaptic depression. Stronger stimuli accelerate release kinetics but operate on

a smaller vesicular pool, which in contrast, slows down the release. Weaker pulses produce less depression determining a larger pool, which in turn, favors faster kinetics. This phenomenon helps determining that in trains of stimuli the average phase is conserved.

885 Otofelin Regulates Hair-Cell Receptoneural Secretion Through Novel Protein Interactions

Neeliyath Ramakrishnan¹, Marian Drescher¹, Barbara Morley², Phillip Kelley², Dennis Drescher¹
¹Wayne State University, ²Boys Town National Research Hospital

Background

Emerging evidence supports a pivotal role for otoferlin in the regulation of hair-cell secretion/exocytosis, where this protein may sense calcium in the process of SNARE-driven vesicle fusion.

Methods

These studies involved either purified, bacterially-expressed C2 domains and SNARE motifs, or full-length proteins as expressed in rat brain. In vitro binding was measured via surface plasmon resonance analysis, pull-down assays, and immunoprecipitation. Calcium binding of otoferlin C2 domains was detected by isothermal calorimetry. Proteomic analysis using mass spectrometry was carried out on immunoprecipitated proteins. Immunolabeling of rat organ of Corti was performed with anti-otoferlin and anti-Ca_v1.3 antibodies.

Results

Calorimetric measurements demonstrated Ca²⁺ binding to the otoferlin C2F domain. MS-proteomic analysis of otoferlin immunoprecipitation products showed that syntaxin 1B and SNAP-25 specifically interact with otoferlin. RT-PCR revealed expression of syntaxin 1B in rat organ of Corti. In vitro analysis by SPR and GST pull-down indicated that the SNARE motif of syntaxin 1 specifically interacts with otoferlin C2 domains, enhanced by addition of Ca²⁺ up to 200 μM. C2D, C2E, and C2F showed similar association-binding kinetics with the SNARE motif for increasing levels of Ca²⁺, but the dissociation rate at 20 μM Ca²⁺ was significantly reduced compared to dissociation rates at 0 μM and 10 μM Ca²⁺. There was no substantial further decrease in dissociation rate with Ca²⁺ increments up to 200 μM. We also demonstrated, for the first time, that C2 domains of otoferlin bind each other in vitro in the absence of Ca²⁺. Upon addition of Ca²⁺ to the binding buffer, this interaction was substantially *diminished*.

Conclusion

Our results indicate that otoferlin may be an unusual calcium sensor, playing an important role in vesicle fusion in hair cells. The otoferlin C2F domain binds calcium, and interacts with the syntaxin 1 SNARE motif in a calcium-dependent manner. Otoferlin selectively interacts with syntaxin 1B, which is a syntaxin form present in rat organ of Corti. The otoferlin C2-syntaxin 1B SNARE interaction

is possibly stabilized at 20 μM Ca²⁺ due to decreased dissociation at that Ca²⁺ level. Our finding that C2 domains engage in mutual C2-domain binding in the absence of calcium indicates a possible *intramolecular* mechanism involving closed otoferlin at low Ca²⁺ and open otoferlin at higher Ca²⁺ that may, in turn, regulate otoferlin's *intermolecular* interactions upon synaptic influx of Ca²⁺.

886 How Different Human Electrophysiology and Neuroimaging Methods Can Help Us Understand Auditory Processing

Ross Maddox¹, Eric Larson¹

¹University of Washington, Institute for Learning and Brain Sciences

Background

As organizers of this Young Investigator Symposium, we will use this talk to introduce the multiple methods described in this symposium's presentations to junior scientists as well as the interested but uninitiated.

Methods

We will discuss how non-invasive electrophysiological and neuroimaging methods (fMRI, ABR, EEG, and MEG) work, what types of experimental designs are used in conjunction with them, and how their varying spatial and temporal resolutions offer complementary information.

Results

We will provide a brief introduction to the talks in this symposium, highlighting different labs' approaches to answering questions of common interest.

Conclusion

Electrophysiology and neuroimaging, in concert with recent developments in data analysis methodology, provide new insights into how humans listen.

887 Bottom-Up and Top-Down Contributions to Individual Differences in Auditory Spatial Attention Task Performance

Hari Bharadwaj¹, Salwa Masud¹, Barbara Shinn-Cunningham¹

¹Boston University

Background

The ability to attend to a sound of interest amidst competing sounds is vital for navigating through the complex auditory scenes of everyday life. Even among "normal hearing" listeners, there is considerable variability in auditory spatial attention task performance. Our previous findings indicated that fidelity of brainstem phase locking to simple stimuli as measured using the brainstem frequency following response (FFR) is predictive of spatial attention task performance. Here, we extend the study of bottom-up coding using FFRs to understand the effect of sound level on envelope phase locking up to the brainstem, and use Magnetoencephalography (MEG) to study oscillatory synchronization in the cortex during top-down selective attention preparation.

Methods

MEG was recorded from normal-hearing listeners presented with three simultaneous streams of spoken letters, from distinct spatial locations using inter-aural time disparities (ITDs) or binaural room impulse responses (BRIRs). Subjects were visually cued to attend to either the left or the right location and count the occurrences of a target letter. MRI scans provided anatomical constraints for MEG source analysis. In a separate session, FFRs to a 100 Hz click-train at 3 different levels (60, 70 and 80 dB SPL) and both polarities were recorded using a 32 channel EEG cap. After optimally phase aligning the FFRs across channels, envelope phase-locking values (PLVs) were computed using a bootstrap procedure.

Results

FFR results indicate that PLVenv consistently increases when stimulus intensity increases from 60 to 70 dB SPL. However, there are large individual differences in the change in PLVenv from 70 to 80 dB SPL that correlate with performance on the spatial attention task. Preliminary MEG findings show subject-specific increase in beta-band activity in the right Intraparietal Sulcus (rIPS) in the preparatory period (post cue, before sound) in the attend trials and particularly in trials where the attended location is switched from the previous trial.

Conclusions

Subtle supra-threshold envelope spatial cues are important particularly in crowded and reverberant settings. Robustness of envelope coding at high levels, which can be investigated at the individual level using FFRs, may reflect the fidelity of integration of information from low and high threshold auditory nerve fibers. Sub-clinical effects of noise-exposure, aging etc. that compromise this may hence be objectively assessed. MEG correlates of top-down spatial selective attention along with FFRs help explain the large individual variability in spatial attention performance.

888 Neuromagnetic Signatures of Segregation in Complex Acoustic Scenes

Sundeep Teki¹, Christopher Payne¹, Sukhbinder Kumar², Timothy Griffiths^{1,2}, Maria Chait¹

¹University College London, ²Newcastle University

The natural auditory environment consists of multiple dynamically varying sound sources. In order to make sense of this complex mixture of sounds, we need to segregate individual sound sources. The brain has evolved specialized mechanisms for analyzing auditory scenes but the underlying mechanisms remain to be fully explained.

We improved upon earlier paradigms based on deterministic patterns of pure tones and modelled acoustic scenes using a stochastic figure-ground stimulus (SFG, Teki et al., 2011). The stimulus comprises a series of chords (25 ms long) containing random frequencies that vary from one chord to another in a range from 200 Hz to 2.5 kHz. To study segregation, we introduced a figure by randomly selecting a certain number of frequencies

(‘coherence’) and repeating them over a certain number of chords. This manipulation allows us to parametrically control the salience of the figure, which can only be extracted by binding across both time and frequency. We found that listeners are very sensitive to the emergence of these complex figures. We previously established a role for the intraparietal sulcus in stimulus-driven segregation of these figures (Teki et al., 2011) and ongoing work suggests a role for temporal coherence in mediating segregation (Shamma et al., 2011).

We used MEG to investigate mechanisms underlying the emergence of figures with different salience (coherence of 2, 4 or 8; 0.6s long) presented after statistically similar background segments (0.6 s). Listeners were engaged in an incidental visual task and were naive to the manipulations within the SFG stimulus. In another condition, we presented the same stimuli but interspersed with alternating white noise, as we previously found that this does not affect figure detection (Teki et al., 2012).

Analysis of time-locked activity in the auditory cortex shows an initial onset response to the emergence of the figure, followed by a sustained response which follows the figure. Source analysis is ongoing. The figure onset responses occur about 100 ms in the coherence=8 condition, and 150 ms for coherence values of 4 and 2. These latencies correspond to a duration of 4 (or 6) chords and parallel behavioural performance (obtained separately). Latencies from the ‘noise’ condition reveal the same threshold, suggesting that the segregation mechanism was not affected by the interspersed noise bursts. Time-frequency analysis is ongoing using a beamformer approach (Sedley et al., 2012) to identify sources of early and late oscillatory activity.

889 Cortical Encoding of Speech in Challenging Listening Environments

Nai Ding^{1,2}, Monita Chatterjee³, Jonathan Z Simon²

¹New York University, ²University of Maryland, College Park, ³Boys Town National Research Hospital

Normal hearing listeners are superb at understanding speech in noise. Here, we study the neural underpinnings of this phenomenon in human auditory cortex, by recording from subjects listening to spoken narratives using magnetoencephalography (MEG). In one experiment, the spoken narrative is mixed with spectrally matched stationary noise at different signal to noise ratios (SNR). We analyzed the auditory cortical response synchronized to the slow temporal modulations of speech (< 10 Hz). It is found that the cortical synchronization to the very slow temporal modulations of speech (< 4 Hz) is stable until the noise is far stronger than the speech. The cortical synchronization to faster modulations (> 4 Hz), however, is more susceptible to noise. In another experiment, the stimuli are processed by noise vocoders, to simulate listening with cochlear implants. The neural synchronization to vocoded speech is greatly reduced even when the background noise is only mildly weaker than speech, consistent with the behaviorally observed

noise susceptibility of vocoded speech. Taken together, these results suggest that the neural representation of very slow temporal modulations of speech is very robust to noise. This robustness, however, relies on the spectro-temporal fine structure of speech.

890 Using High-Field fMRI and Multivariate Methods to Study Neural Representations of Complex Sounds in Human Auditory Cortex

Annika C. Linke¹, Jacob Matthews¹, Joseph S. Gati², Rhodri Cusack¹

¹*Brain and Mind Institute, Western University, London, ON,*

²*Centre for Functional and Metabolic Mapping, Roberts Research Institute, London, ON*

Background:

Investigating auditory processing in the human brain remains a challenge due to the small size of auditory cortex, substantial individual differences in anatomy, and limitations of the methods for neural measurement. We used functional magnetic resonance imaging (fMRI) in combination with multivariate analyses methods to assess which acoustic and abstracted features of complex natural sounds are encoded in human auditory cortex during perception and cognitive tasks such as change detection and imagery.

Methods:

Structural and functional images were acquired on a 3T Siemens Tim Trio and a 7T Agilent/Siemens MRI scanner. We evaluated the benefits and drawbacks of ultra-high field 7T MRI to assess auditory cortex function at higher spatial resolution, used new acquisition sequences that reduce scanner noise and applied multivariate methods that are insensitive to individual differences in anatomy to make fMRI more suitable for auditory research. Participants listened to, performed change detection on and imagined simple and complex, natural sounds. Multivariate pattern analysis (MVPA) was conducted to assess feature tuning in human auditory cortex and to determine whether the acoustic and abstracted features of sounds encoded were task-dependent.

Results:

Our results show that the information encoded in spatially distributed patterns of activity in auditory cortex differs depending on the cognitive task being performed. During perception and short-term memory maintenance activity patterns in auditory cortex contained stimulus-specific information while abstracted, categorical information was encoded in the same region during auditory imagery. Furthermore, differences in activation magnitude and pattern distinctiveness were related to individuals' memory capacity and perceived imagery vividness. This indicates that auditory cortex is recruited for processes beyond analyzing simple feature information, playing an important role in maintaining sustained representations of sounds in short-term memory and encoding abstracted information during imagery. A comparison of data acquired on the 3T Siemens Tim Trio and 7T Agilent/Siemens MRI scanner

additionally indicates that ultra high-field MRI is particularly well suited for the assessment of human auditory cortex.

Conclusions:

Ultra-high field fMRI and multivariate methods are well suited for analyzing feature coding in human auditory cortex. They allow for the identification of much finer detail both structurally and functionally. In combination, these methods provide exciting opportunities to investigate how neural representations in auditory cortex vary within as well as between individuals.

891 What Musicians Reveal About the Aging Brain: Behavioral and Neural Indices

Alexandra Parbery-Clark¹, Samira Anderson¹, Nina Kraus¹

¹*Northwestern University*

Background: As the world's population ages, there is increased interest in identifying lifestyle factors that reduce aging's deteriorating effects. One marker of healthy aging is the ability to remain socially active, which requires intact communication skills. A major complaint of older adults, even those with normal hearing, is the inability to understand speech, especially in the presence of background noise. Defining the effects of age on auditory neurobiological processes is important as we seek to remediate this deficit. On a neural level, aging is associated with reduced temporal synchrony, evidenced by delayed neural timing and increased trial-by-trial response variability. Given recent evidence that older musicians have enhanced speech perception in noise, we asked whether musical experience offsets age-related declines for the neural processing of speech.

Methods: We recorded neural responses to a speech sound /da/ in 140 normal hearing younger (18-30) and older (45-65) normal hearing musicians and nonmusicians matched for age, IQ and sex, focusing on neural timing and response variability. Furthermore, we quantified both subjective and objective indices of speech-in-noise perception by administering a self-report questionnaire on which each individual rated themselves on their ability to hear in noise and the Hearing in Noise Test.

Results: Older nonmusicians have delayed neural responses and increased response variability relative to older musicians, who demonstrate resilience to these effects of aging and perform similarly to younger adults. Older musicians reported higher ratings on the scale of self-perceived hearing-in-noise ability, which was confirmed by better speech-in-noise perceptual thresholds, suggesting fewer communication difficulties relative to older nonmusicians.

Conclusions: Musical training strengthens aspects of neural processing that degrade with age, which may account for their enhanced ability to hear in noise. As such, we propose that older musicians may serve as a model of plasticity which can be used to further our

understanding of the aging process on the nervous system.

This work is supported by NSF 0842376 & BCS-1057556, NIH R01 DC010016 and the Knowles Hearing Center; www.brainvolts.northwestern.edu.

892 Hierarchical Neurocomputations Underlying Concurrent Sound Segregation: Connecting Periphery to Percept

Gavin Bidelman^{1,2}, **Claude Alain**^{3,4}

¹*School of Communication Sciences & Disorders, University of Memphis,* ²*Institute for Intelligent Systems, University of Memphis,* ³*Rotman Research Institute, Baycrest Centre for Geriatric Care,* ⁴*Department of Psychology, University of Toronto*

A critical process in auditory scene analysis is the ability to perceptually separate concurrently occurring sounds. When acoustic energy is harmonically related across the frequency spectrum, an auditory event is perceived as a single sound object; when there is additional energy not related to the same f_0 , listeners often report hearing two sound objects. Numerous studies have found that in human listeners, the perception of concurrent sounds is paralleled by complementary changes in cortical event-related potentials (ERPs). Although these studies provide a window into the neural mechanisms governing concurrent sound segregation, the neural architecture and hierarchy of neurocomputations supporting this robust perceptual process remain poorly understood. Here, we employ a coordinated blend of techniques including neurocomputational modeling, cortical/subcortical ERPs, and human psychophysics to assess the role of both peripheral and central neurophysiological responses in formulating concurrent sound segregation. Results suggest that the acoustic cues necessary for segregating auditory objects (e.g., inharmonicity) are adequately coded at the level of auditory nerve, are maintained with high fidelity within response properties of the upper brainstem, and are further transformed into a perceptual correlate by early auditory cortex. Our novel approach in studying multiple brain indices simultaneously helps illuminate the neural mechanisms underlying concurrent sound segregation and may lead to the further development and refinement of physiologically driven models of auditory scene analysis.

893 Investigating BOLD fMRI Tuning to Interaural Level and Time Differences in Human Auditory Cortex

Susan A. McLaughlin¹, **G. Christopher Stecker**²

¹*University of Washington,* ²*University of Washington*

Background: Interaural time and level differences (ITD and ILD) are binaural cues important in sound localization. At present, mechanisms underlying their cortical representation remain unclear. Responses from binaurally-tuned neurons suggest that a majority in each hemisphere respond more to earlier and more intense stimulation of the contralateral rather than ipsilateral ear. However, evidence for contralateral tuning in blood oxygenation

level-dependent (BOLD) fMRI of human auditory cortex (hAC) is more equivocal, possibly due to the nature of the measure, stimuli presented, and/or potential 'carryover' effects of stimulus history. The present study will therefore investigate binaural processing in hAC by measuring direct and carryover effects of parametric binaural cue modulation on the BOLD response.

Methods: In a series of experiments, the BOLD signal was measured in response to modulation of (Exp. 1) ILD (0, ± 5 , ± 10 , ± 20 , ± 30 dB) and (Exp. 2) ITD (0, ± 200 , ± 500 , ± 800 , $\pm 1500\mu$ s) imposed on narrowband click trains (4000 Hz carrier frequency, 1.8 kHz half-max bandwidth, 500 Hz click rate). Exp. 3 employed identical ITDs imposed on broadband stimuli (trains of 1ms Gaussian noise bursts repeating at 100 Hz). Across experiments, stimulus trains were presented for 1s (interstimulus intervals jittered from 1-5s), at 80 dB SPL, via insert earphones (Sensimetrics). Binaural cue order was counterbalanced, following a continuous carryover design [Aguirre, *NeuroImage* 35:1480-94, 2007]. The task involved pitch detection orthogonal to the experimental manipulation. Continuous event-related images were acquired (TR=2s, 42 slices, 2.75 x 2.75 x 3mm resolution, 3T). Data pre-processing and individual analyses were conducted using FSL; cross-subject analyses were conducted on the cortical surface using Freesurfer and Matlab.

Results: Consistent with the neural response data, a contralaterally-tuned non-monotonic ILD-response function was observed, with maximal responses at extreme contralateral ILDs. Responses declined at moderate contralateral and ipsilateral values but increased again at extreme ipsilateral ILDs. In contrast, ITD-response functions for both narrow and broadband sounds showed little to no contralateral tuning. Stimulus history effects also differed across cues, with preliminary ILD results suggesting attenuation of the response to ipsilateral stimulation with ipsilateral stimulus repetition.

Conclusions: Findings will be discussed in the context of binaural processing models, such as coding by excitatory/inhibitory "opponent" populations, by temporal spike patterns, and by distributed codes across populations of panoramic neurons. [Supported by R01-DC011548, R03-DC009482.]

894 Using fMRI to Study the Role of Attention in Speech Perception

Conor Wild^{1,2}, **Ingrid Johnsrude**^{1,3}

¹*Queen's University,* ²*Western University,* ³*Linköping University*

Background

The conditions of everyday life are such that people often hear speech that has been degraded (e.g., by background noise or electronic transmission) or when they are distracted by other tasks. However, it remains unclear what role attention plays in processing speech that is difficult to understand. Functional magnetic resonance imaging (fMRI) provides a valuable method to explore this

issue by allowing the comparison of brain responses to stimuli that are attended and unattended. In the current study, we used fMRI to assess the degree to which spoken sentences were processed under distraction, and whether this depended on the acoustic quality (i.e., the intelligibility) of the speech.

Methods

On every trial, participants were cued to attend to one of three simultaneously presented stimuli: a spoken sentence, an auditory distracter (a sequence of noise bursts that did not interfere with the speech signal), or a visual distracter (a series of rotating ellipses). Regardless of which stimulus was attended, the sentence on every trial was presented at one of four levels of intelligibility: clear speech, high- or low-intelligibility noise-vocoded speech, or rotated noise-vocoded (i.e., unintelligible) speech. After scanning, a surprise recognition test was administered to measure subjects' memory for the sentences.

Results

The post-test showed that attention did not affect the recognition of sentences presented in a clear or unintelligible form: clear sentences were always recognized at better than chance levels, regardless of whether or not they had been attended, and unintelligible sentences were never recognized. However, attention significantly enhanced the recognition of high- and low-intelligibility noise-vocoded speech.

Furthermore, the fMRI results demonstrated that speech-sensitive cortex could be parcellated according to how speech-evoked responses were modulated by attention. Responses in auditory cortex and areas along the superior temporal sulcus (STS) took the same form regardless of attention, although responses to distorted speech in portions of both posterior and anterior STS were enhanced under directed attention. In contrast, frontal regions, including left inferior frontal gyrus, were only engaged when listeners were attending to speech and these regions exhibited elevated responses to degraded, compared with clear, speech.

Conclusions

We suggest this pattern of fMRI responses is a neural marker of effortful listening. Together, our results suggest that attention enhances the processing of degraded speech by engaging frontal-cortex mediated mechanisms that modulate perceptual processing of speech.

895 Stereocilia Deflection Phase Is Frequency Dependent

Pierre Hakizimana¹, Anders Fridberger¹

¹Karolinska Institutet

Background

Mammalian hearing relies on the movements of cochlear stereocilia. Thanks to their attachment to the tectorial membrane (TM), outer hair cell (OHC) stereocilia bundles are deflected by sound-induced shearing motion between the TM and the cuticular plate. There is a consensus that such is not the case for the freestanding inner hair cell (IHC) stereocilia bundles whose deflection is driven by sound-induced viscous drag of the endolymph. Following these differences in stimulatory forces, the receptor

potential recorded in IHCs shows a phase lead of 90° relative to the basilar membrane motion. If the OHC stereocilia deflection depends only on the basilar membrane movement as generally assumed, then the stereocilia deflection in IHC would also have a 90° phase lead relative to OHC stereocilia. To investigate this hypothesis, direct measurement of the stereocilia deflection phase is required.

Methods

Using temporal bone preparations from guinea pigs, we measured the deflection phase at different frequencies and sound stimulus intensities by time-resolved confocal imaging and optical flow algorithms, a technical approach that we recently used to characterize nanometre-scale sound-evoked length changes in OHC stereocilia.

Results

IHC stereocilia bundles with respect to OHC stereocilia bundles exhibited a phase lead of about 60°, smaller than expected. In addition, this phase difference was maintained across a range frequencies and intensities. In both IHCs and OHCs, the phase increased with frequency but not with the stimulus intensity.

Conclusion

Taken together, these observations suggest that the mechanism for driving IHC bundles may be more complex than previously envisioned.

896 Synchronization of Active Hair Bundles by Artificial Membranes

Clark Elliott Strimbu^{1,2}, Yuttana Roongthumskul¹, Dolores Bozovic¹

¹University of California, Los Angeles, ²Center for Hearing and Communication Research, Karolinska Institutet

Background

In vitro, mechanically decoupled or free-standing hair bundles from the frog sacculus exhibit spontaneous mechanical oscillations. These active hair bundles show signs analogous to the "active process" seen in vivo in the auditory systems of all vertebrates, suggesting that hair bundle motility plays a role in active amplification. However, the spontaneous oscillations are uncorrelated and the performance of a single bundle does not match that of the auditory system in vivo. Several theoretical studies have suggested that mechanical coupling of active hair bundles can lead to an enhancement of the single-cell active process. We used artificial membranes to couple a small number of active hair bundles and recorded both spontaneous and entrained movements.

Methods

We used an in vitro preparation of the frog sacculus in which the sensory epithelium is mounted in a two-compartment chamber mimicking the native ionic environment. Artificial membranes were fabricated from poly(lactic-co-glycolic acid) (PLGA) microspheres. The microspheres were briefly melted to yield approximately hemispherical shapes, and the artificial membranes were

coated with concanavilin A to improve adhesion to the hair bundles. The artificial membranes were dispersed onto the preparation and typically coupled two to four hair bundles. In several experiments, the artificial membranes were mechanically stimulated with flexible glass fibers driven by a piezoelectric stack actuator. Bundle and artificial membrane motion were recorded with a high-speed CMOS camera as described previously.

Results

When coupled by artificial membranes, active hair bundles exhibited robust spontaneous oscillations. The motion of the hair bundles was strongly correlated (correlation coefficients of about 0.9) suggesting that direct mechanical coupling can lead to synchronized motion of a small number of active hair bundles.

Conclusion

When mechanically coupled, active hair bundles can exhibit synchronized spontaneous oscillations. The forces generated by a few hair bundles are sufficient to move overlying accessory structures. Preliminary data suggest that when driven sinusoidally, the bundles in this coupled system can exhibit sharpened frequency tuning relative to a single free-standing bundle. Further experiments on this hybrid system are ongoing.

This work was supported by grant 0920694 from the National Science Foundation and grant RO1 DC011380-01A1 from the National Institutes of Health.

897 Cable Property of OHC Lateral Membrane

Lei Song¹, Joseph Santos-Sacchi¹

¹Yale University

Background

The outer hair cell's (OHC) fast mechanical response is capable of following sinusoidal stimuli that go beyond 100 kHz. It remains puzzling that such a mechanical response can be achieved with the lateral membrane as low-pass filter. We hypothesize that the subsurface cisternae serve to overcome the restraining effect of lateral membrane's low-pass filter function therefore allowing the OHC's electromotility to respond to fast stimuli. We measured membrane time constants at various locations along the OHC lateral membrane by using a two electrode technique.

Methods

Isolated guinea pig OHCs are whole cell recorded with a perforated patch electrode near the supra-nucleus region. An electrical stimulus was generated by a roving electrode along the lateral membrane. Recordings were made with series resistance compensated to 10 Mohm under all conditions. Whole cell condition was then established and measurement repeated. Measurements were also made after OHCs were treated with 10 mM salicylate for 40 minutes. Membrane time constants were compared.

Results

The time constant for different positions along the lateral membrane showed little change when the OHC plasma membrane was intact (perforated patch) but showed a distance dependent change (re: stimulating electrode) when the membrane was ruptured (whole cell). We believe that the sub-plasma membrane space is destroyed in this case. Such changes can be reproduced by treating OHC with 10 mM salicylate even during perforated patch recording. Salicylate can also destroy the OHC's sub-plasma membrane space.

Conclusion

The intact subsurface cisternae helps to overcome the membrane filter that allows the OHC to respond to high frequency transduction current.

898 Optimal Electrical Properties of Outer Hair Cell Membrane for Cochlear Amplification

Jong-Hoon Nam¹, Robert Fettiplace²

¹University of Rochester, ²University of Wisconsin-Madison

Background

The organ of Corti (OC) is an auditory epithelium specific to the mammalian cochlea comprising sensory hair cells and supporting cells riding on the basilar membrane. The outer hair cells (OHCs) are cellular actuators that amplify small sound-induced vibrations for transmission to the inner hair cells. Two recent observations provide important insights to current debate on cochlear amplification by OHCs. First, OC with active OHCs was observed to vibrate with a characteristic mode such that the top and bottom surface of the OC have 90 degree phase difference (Chen, Zha et al., 2011). Secondly, the conductance of OHC membrane varies along the cochlear coil such that it is higher at high frequency location (Johnson, Beurg et al., 2011). We investigated the implications of these two findings through computational analyses of the OC.

Methods

Developed finite element model of the OC incorporates the sophisticated OC geometry such as pillar cells, tilted Deiters cell processes and OHCs, and longitudinal coupling (Nam & Fettiplace, 2010). The model also incorporates force generation by OHCs originating from active hair bundle motion due to gating of the transducer channels and somatic contractility due to the membrane protein prestin. It was a time-domain analysis with fully non-linear OHC mechano-transduction and electro-motility.

Results

The 90 degree phase difference between the top and the bottom surface vibrations of the OC appeared only when the OHC motility is prominent. Simulations of an individual OHC show that the OHC somatic motility lags the hair bundle displacement by ~90 degrees. Prestin-driven contractions of the OHCs cause the top and bottom surfaces of the OC to move in opposite directions. Combined with the OC mechanics, this results in ~90 degrees phase difference between the OC top and bottom

surface vibration. An appropriate electrical time constant for the OHC membrane was required to achieve the phase relationship between OC vibrations and OHC actuations. When the OHC membrane conductance is too high or too low, the OHCs do not exert force with the correct phase to the OC mechanics so that they cannot amplify. This optimal OHC membrane conductance is in nice agreement with the measured value of Johnson et al.'s (2011).

Conclusion

There exists an optimal range of OHC electrical property to set the correct phase relations needed for cochlear amplification.

899 Meno Presto, Prestin: Disparities Between Voltage-Sensor Charge and Electromotility Reveal Slow Chloride-Dependent Molecular State Transitions in SLC26a5

Joseph Santos-Sacchi¹, Lei Song¹

¹Yale University

Background

Outer hair cells (OHC) drive cochlear amplification, which enhances auditory detection and discrimination. The motor protein, prestin, which evolved from the SLC26 anion transporter family, underlies the OHC's electromotility.

Methods

Voltage clamp and video analysis of OHC NLC and motility.

Results

Here we report on simultaneous measures of prestin's voltage sensor charge movement (NLC) and electromotility that evidence disparities in their voltage dependence and magnitude as a function of intracellular chloride. A simple kinetic model, possessing fast anion binding transitions and fast voltage dependent transitions, coupled together by a much slower transition recapitulates these disparities and a host of other biophysical observations on the OHC. The intermediary slow transition probably relates to the transporter legacy of prestin, and this intermediary gateway which shuttles anion bound molecules into the voltage-enabled pool of motors, provides molecular delays that present as phase lags between membrane voltage and electromotility. Cochlear modelers find that phase lags are required to effectively inject energy at the appropriate moment to enhance basilar membrane motion.

Conclusion

Thus, slowing down prestin has its benefits.

900 Remodeling the Intracellular Distribution of DNA Repair Enzymes in Spiral Ganglion Neurons in Response to Noise Stress and Otoprotective Therapy

O'neil Guthrie^{1,2}, Jinwei Hu², Helen Xu²

¹Loma Linda Veterans Affairs Medical Center, ²Loma Linda University Medical Center

Background

Intracellular stress gradients drive the spatial distribution of DNA repair enzymes. In this study, we investigated if spiral ganglion neurons could remodel intracellular distributions of DNA repair enzymes in response to stress and otoprotective therapy.

Methods

The intracellular locations of DNA excision repair enzymes were determined within spiral ganglion neurons under normal conditions, after noise exposure, and following otoprotective treatment with carboxy alkyl esters (CAEs). Line scans were used to record immunoreactivity within the soma of each neuron to objectively profile the subcellular distribution of the enzymes.

Results

After noise stress at 105 dB for 4 hours, the enzymes aggregated in the cytoplasm and this effect was associated with a significant loss ($p < 0.001$) of neural sensitivity measured by compound action potential. After CAE therapy (160 mg/kg/28 days), the enzymes were enriched within multiple intracellular locations and this response had no significant change in neural sensitivity ($p > 0.05$). CAE therapy provided to noise exposed animals also resulted in the enrichment of repair enzymes in multiple intracellular compartments. This response was associated with significant preservation of neural sensitivity ($p < 0.05$).

Conclusion

In summary, the current study revealed that spiral ganglion neurons exhibit multiple compartmentalizing modes for excision repair enzymes and these modes exhibit plasticity following noise stress and otoprotective treatment. Furthermore, regulation of intracellular gradients of DNA excision repair enzymes may represent a novel approach to preserving neural function following stress.

901 Genetic/transgenic Conditional Expression of Nonmuscle Myosin-II in Auditory Neurons: Head Domain Regulates Assembly of the α -Helical Coiled-Coil Tail

O'neil Guthrie^{1,2}, Jinwei Hu², Helen Xu²

¹Loma Linda Veterans Affairs Medical Center, ²Loma Linda University Medical Center

Background

Nonmuscle myosin-II (MyoII) is an actin-binding protein that is involved in several motor functions including growth cone motility and neural migration, outgrowth and retraction. The molecule can be functionally divided into a head-domain and a α -helical coiled-coil tail. Self-assembly

of the MyoII α -helical coiled-coil tail with other MyoII molecules form bipolar filaments that power cell movements. This self-assembly of the tail is intrinsically regulated by intramolecular interactions of the tail with the head-domain as demonstrated by in vitro experiments. However, there is no in vivo evidence for this regulatory mechanism.

Methods

In this study, we further define whether the head-domain of MyoII regulates in vivo self-assembly of the α -helical coiled-coil tail in auditory neurons. A GAL4-UAS gene expression system was used to selectively express zip/MyoII full-length, zip/MyoII tail with and without isoleucine-glutamine (IQ) motifs in *Drosophila melanogaster* auditory (Johnston's organ) sensory neurons. The N-terminus of each construct was fused to green fluorescent protein (GFP) to follow the distributions of transgene expression.

Results

Our results reveal that the full-length molecule exhibited either globular or rod conformations in auditory neurons of Johnston's organ. In the absence of the head domain, the tail self-assembles into filament-like rods in both fixed and living preparations of Johnston's organ neurons. The tail+IQ motif failed to form rod conformations and instead filled the neuronal cell bodies with diffuse fluorescence.

Conclusion

The results suggest that the head-domain is critical for modulating the self-assembly of the tail in vivo. These findings may help to explain why human mutations in the head domain result in severe diseased phenotypes.

902 Are Species Differences in Dip Listening Predicted by Species Differences in Temporal Processing? An Evoked Potential Study in Treefrogs

Katrina M. Schrode¹, Mark A. Bee¹

¹University of Minnesota

Background

Acoustic communication in large social groups is made difficult by high noise levels, which can mask signals of interest. One solution for coping with this problem involves listening in the "dips" of fluctuating background noise, which requires the ability to track temporal envelope fluctuations. Acoustic communication in social groups is not a uniquely human problem, nor is dip listening a uniquely human solution. We have previously found that one species of treefrog, Cope's gray treefrog (*Hyla chrysoscelis*), is also able to exploit dips in background noise to recognize communication signals at lower thresholds, while a related species, the green treefrog (*Hyla cinerea*), appears incapable of doing so. Here, we tested the hypothesis that these species differences in dip listening are due to species differences in temporal processing.

Methods

To test our hypothesis, we used two measures of evoked potentials to assess temporal processing in gray treefrogs and green treefrogs. For the first measure, evoked potentials were recorded in response to double-click stimuli. Temporal integration time corresponds to the shortest inter-click interval at which distinct responses are evoked by both clicks. The second type of evoked potential, termed the auditory steady-state response (ASSR), measured phase locking by the auditory nerve to the envelope of amplitude-modulated tones. The magnitude of the fundamental frequency of the ASSR was used to construct modulation rate transfer functions (MRTF).

Results

Assessments of temporal processing using these two methods revealed very small differences between the two species. In both species, we observed two distinct responses to clicks with inter-click intervals averaging as low as 3-4 ms. The average inter-click interval at which two responses were present was slightly shorter in gray treefrogs than green treefrogs. The MRTFs for the two species were broadly similar in shape and did not differ greatly in absolute magnitude.

Conclusion

Our results indicate that temporal processing abilities at the level of the eighth nerve are conserved between the two species. While small species differences were observed, they are probably not great enough to account for species differences in dip listening. Our data do not rule out species differences in temporal processing at higher levels of the ascending auditory system. [This work was supported by NSF IOS 0842759.]

903 Encoding Temporal Fine-Structure at Different Sound Levels in the Barn Owl Auditory Nerve

Bertrand Fontaine¹, Christine Köppl², Jose Luis Pena¹

¹Department of Neuroscience, Albert Einstein College of Medicine, Bronx, NY, 10461, USA, ²Institut für Biologie und Umweltwissenschaft, Carl von Ossietzky Universität Oldenburg, Oldenburg, Germany

Background

Barn owls use interaural time difference (ITD) for sound localization. In order to do so their auditory system encodes the fine structure of sound up to 10 kHz. The level of ecologically relevant sounds can vary by tens of decibels and the effect on the monaural encoding of sound could have a great effect on ITD tuning. It is therefore important to understand time encoding at the first stage of the auditory pathway at different sound levels.

Methods

We recorded responses to noise of auditory nerve fibers with best frequency (BF) spanning the entire audible frequencies of owls. Unfrozen noise at three intensities was presented: one slightly above threshold, one in the middle of the dynamic range, and one at saturation. To

compute the AN impulse response, we used reverse correlation on the response to unfrozen noise, the spike triggered averaged (STA). Resulting STA were fitted to linear gamma chirps.

Results

While some properties of impulse responses were in concordance with studies in mammals and in the barn owl, some important differences were noticed. Unlike in mammals, the impulse responses showed frequency glides for fibers with BFs above 4 kHz. The glides were positively correlated with BF and had larger magnitude than previously measured in downstream nuclei. For lower BF the glide slopes were very small and independent of frequency. More importantly, the glide slopes were significantly dependent on level for BFs above 5 kHz. In this high frequency range the changes in slope could be as big as 1kHz/ms when level was varied across the dynamic range. In addition, the sign of the slope could change. We show that the outputs of the AN filters at different levels did not only have different envelopes but also different fine structures. Using cross-correlation of the analog filter outputs we predicted that the shape of the ITD curves derived from those neurons would be greatly dependent on interaural level difference (ILD).

Conclusion

While invariance on ILD would be desired to encode ITD our data suggest that, for BFs>5kHz, the fine structure of the responses at the first level of the monaural pathway is not level invariant. This casts additional constraints on the downstream pathway, in order to encode ITD independently of sound level, as it has been shown. More generally, level dependence of the spike train fine structure could be functionally useful in tasks such as distance or loudness perception.

904 Development of Spiral Ganglion Neuron Intrinsic Excitability and Modulation by NT-3 in CBA Mice

Robert A. Crozier¹, Robin L. Davis¹

¹Rutgers University

Background

The neurotrophins BDNF and NT3 have critical roles in promoting the survival, connectivity and function of spiral ganglion neurons (SGNs). In 1 week old mice the features of SGN intrinsic excitability are tonotopically organized with rapidly accommodating, high threshold neurons found in the base and slowly accommodating, low threshold neurons located in the mid-apical ganglion (Liu & Davis, J. Neurophysiol. 2007). Here we assess timing and excitability features including threshold, accommodation and action potential latency from P1 to P14 and have begun to determine the role of NT3 application in modulating these features during development.

Methods

Whole-cell current-clamp recordings were performed on SGN cultures obtained from postnatal day 1-14 (P1-P14) mice to ascertain the features described above. NT-3 (10

ng/ml) or vehicle was applied at time of plating. Step current injections (240 ms duration) were delivered to assess voltage threshold, action potential (AP) latency and accommodation.

Results

From P1 to P7, we find that base and apex neurons retain the aforementioned tonotopic profile for P6 and P7, with P5 being a transition period. However, base neurons from P1 to P4 manifest a prominently more excitable and immature phenotype relative to P7 base neurons: they display lower thresholds (P7 base vs. P4 base) -42.5 ± 0.9 mV, $n=25$ vs. -48.3 ± 1.1 mV, $n=15$; $P<0.01$), longer latencies (7.4 ± 0.4 ms vs. 15.8 ± 0.8 ms; $P<0.01$) and slow accommodation (1.24 ± 0.13 vs. 13.2 ± 2.7 ; $P<0.01$). From P7 to P14, both apex and base neurons become faster and rapidly accommodating such that tonotopic differences for these features are essentially indistinguishable by P14 (latency: base, 5.5 ± 0.2 ms, $n=12$; apex, 5.6 ± 0.2 ms, $n=15$ and accommodation (APmax: base, 1 ± 0 ; apex, 1.1 ± 0.07). However, tonotopic differences in threshold persist (base, -42.3 ± 1.2 mV; apex, -46.7 ± 0.9 mV; $P<0.05$). Finally, NT-3 application to base neuron cultures promotes lowering of voltage threshold, prolonged latencies and slow accommodation in P6 and P8 neurons. The effect of NT-3 on younger (P3) and older (P10 and P14) neurons is currently being investigated.

Conclusion

During the first 2 weeks of postnatal development, SGNs undergo rapid and considerable alterations in their intrinsic excitability, and NT-3 may play a central role in modulating SGN excitability as the animal matures. Funding: NIDCD RO1-DC01856.

905 MicroRNA-96 Is Required for the Postnatal Refinement of Auditory Nerve and the Survival of Type I Spiral Ganglion Neurons

Yazhi Xing¹, Nancy Smythe¹, Juhong Zhu¹, Karen Steel², Donna Fekete³, Hainan Lang¹

¹Medical University of South Carolina, ²Wellcome Trust Sanger Institute, ³Purdue University

Background

Mutations in the seed region of miR-96 cause progressive hearing loss in two DFNA50 families and Diminuendo (*Dmdo*) mice. Homozygous mutant (*Dmdo/Dmdo*) mice show profound hearing loss and have extensive sensory hair cell loss at one month of age (Lewis, et al. 2009). Using this animal model, Kuhn et al (2011) demonstrated that miR-96 is essential for morphological and physiological maturation of the sensory hair cells. Although it has been established that miR-96 is expressed in both sensory hair cells and spiral ganglia (Sacheli et al., 2009; Weston et al., 2011), the pathological alterations of the spiral ganglion neurons (SGNs) and their processes remain to be determined in *Dmdo* mice.

Methods

Wild type, *Dmdo/+* and *Dmdo/Dmdo* mice were examined at postnatal day (P) 3, P8, P14, P21, P23 and 1, 2 and 3 months of age. SGNs and their peripheral projections were examined using frozen sections and auditory nerve surface preparations. A battery of neuronal cell markers were employed to identify two populations (types I and II) of SGNs and their projections. Synaptic ribbons and the efferent component of the auditory nerve were labeled with antibodies for C-terminal binding protein (CtBP2) and choline acetyltransferase (ChAT), respectively. In addition, ultrastructural characteristics of neurons and fibers in the spiral ganglia of the *Dmdo* mice were examined by transmission electron microscopy.

Results

Disorganization and increased length (or density) of neurofilament 200 and ChAT positive fibers were seen under inner hair cells of both *Dmdo/+* and *Dmdo/Dmdo* mice aged P14 to P23. Ultrastructural observations indicated several signs of SGN degeneration in *Dmdo/+* and *Dmdo/Dmdo* mice including thinner myelin, loose myelin lamellae, vacuole-like inclusions in the cytoplasm of Schwann cells and “bracelet-like” processes around neuronal cell bodies. Quantitative analysis of cell density in two populations of SGNs shows a significant loss of type I SGNs in the basal turn of the one-month-old *Dmdo/Dmdo* mice.

Conclusion

MiR-96 is required for the postnatal refinement of the auditory nerve and the survival of type I SGNs. An early onset of type I SGN loss suggests that neuronal degeneration is one of the primary changes contributing to hearing impairment in *Dmdo* mice. This study was supported by NIH R01 DC7506 (H.L.), NIH P50 DC0422 (H.L.) and NOHR 206048 (D.M.F.).

906 A Viscoelastic Model of Adaptation in Mammalian Auditory-Nerve Fibers

Adam Peterson¹, Peter Heil¹

¹Leibniz Institute for Neurobiology, Magdeburg, Germany

Background

Responses of mammalian auditory-nerve fibers to acoustic stimuli show pronounced adaptation and recovery from adaptation. During a tone of constant amplitude, the spike rate declines markedly, particularly during the first tens of milliseconds following stimulus onset. Upon cessation of the tone, the spike rate drops to values below the spontaneous rate and gradually recovers. A variety of functions are ascribed to adaptation, including shifting the cell's sensitivity range. Most models of the adaptation behavior of mammalian auditory-nerve fibers assume the depletion of pools of synaptic vesicles in inner hair cells. However, recent research in mammalian systems suggests the presence of two alternative adaptation mechanisms, reflected in transducer currents and membrane potentials. A fast mechanism is thought to close transducer channels upon Ca²⁺ binding, whereas a slow mechanism is thought to relieve tension on the

channel through slippage of a myosin motor, both often modeled as exponential decays. Here, we examine whether a double exponential decay model with viscoelastic mechanics, inspired by the work of Howard and Hudspeth (PNAS 1987), can describe the responses of mammalian auditory-nerve fibers over the entire peristimulus time course.

Methods

Spike times were obtained from extracellular recordings of auditory-nerve fibers in barbiturate-anesthetized cats. Stimuli were 100-ms tones of different sound pressure levels at each frequency (mainly characteristic frequency), repeated at least 100 times at a rate of 4 Hz. Prior attempts to characterize adaptation have mainly involved fitting parametric models to poststimulus time histograms (PSTHs). However, such fits produce parameter estimates that depend on the chosen bin width. We instead fit our model to the cumulative spike count to avoid this problem. Cumulative spike count functions maintain maximal temporal precision and thus retain more information than most PSTHs, yet are smooth and allow precise fits.

Results

The viscoelastic model proposed here incorporates fast and slow exponential decay and recovery components, with a comparable number of parameters to classical models. We found that the viscoelastic mechanical model of adaptation can describe the data with small and unsystematic residual errors, throughout the entire peristimulus time interval. Furthermore, the parameters have simple physiological interpretations and seem to show meaningful relationships to stimulus parameters.

Conclusion

The viscoelastic description of adaptation may constitute a viable alternative to the assumption that vesicle depletion and re-supply are the prime factors underlying adaption in mammalian auditory-nerve fibers.

Supported by the Deutsche Forschungsgemeinschaft (SFB-TR 31).

907 Assessment of Neural Phase-Locking at the Round Window in Human

Eric Verschooten¹, Luis Robles², Christian Desloovere³, Philip X. Joris¹

¹Lab. of Auditory Neurophysiology, Leuven, Belgium,

²Program of Physiology and Biophysics, Universidad de

Chile, Santiago, Chile, ³Otorhinolaryngology, Head and

Neck Surgery, Univ. Hospitals Leuven, Univ. of Leuven, Belgium

Background

Phase-locking is a fundamental property of the peripheral auditory system. In single auditory nerve fibers, phase locking declines with frequency and becomes undetectable at an upper frequency limit which differs between species. This limit is unknown in humans, and widely differing values are assumed in the interpretation of psychophysical results. Our previous work in cat (Verschooten et al 2011)

suggested that mass-potentials at the cochlear round window allow an assessment of the limit of neural phase-locking. Here, we further test this assumption, and examine whether recordings through the middle ear can also be used in macaque monkey and human volunteers to assess phase-locking.

Methods

A minimally invasive transtympanic protocol was developed to record mass-potentials from the cochlear promontory or from the niche of the round window in macaque and human. This involved a custom made ear mold with openings for the transtympanic needle electrode and for acoustic stimulation (ER-2 earphone, calibrated in-situ with an ER-7 microphone). We used a forward masking paradigm to disambiguate contributions of receptor and neural origin: probe tones with alternating polarity were preceded by a forward masker of the same frequency to temporally mask the neural contribution in the response. The phase-locked neural contribution was estimated from the difference between the unmasked and the masked responses; the compound action potential was excluded by either filtering or by subtracting the results to stimuli of opposite polarity. To validate the applied method, we compared the results measured at the round window before and after administration of tetrodotoxin (10mM, round window) in cat.

Results

An adaptive, neural contribution could be measured on the cochlear promontory of macaque and human. Its magnitude and signal to noise ratio were much lower than in cat (Verschooten et al 2011). A neural, stimulus related phase-locked component could be detected for probe frequencies below 2 kHz in macaque and human. In human, spectral analysis sometimes revealed non-stimulus oscillatory components for probe frequencies above ~1 kHz. In cat, application of TTX showed that the adaptive part of the cochlear mass-potential was reduced by >90% over a wide frequency range, consistent with a neural origin.

Conclusion

Neural, phase-locked mass-potentials are recordable with a minimally invasive technique from awake, normal hearing subjects. We found evidence for stimulus-frequency phase-locking below 2 kHz in macaque and human. Supported by the Fund for Scientific Research – Flanders.

908 Examining the Effects of Vowel Training on Neural Response Sensitivity in Ferret Auditory Cortex

Huriye Atilgan¹, Kerry Walker², Andrew King², Jan Schnupp², Jennifer Bizley¹

¹Ear Institute, UCL, ²Department of Physiology, Anatomy and Genetics, University of Oxford

Background

Neurons in ferret auditory cortex are modulated by the pitch, spatial location and spectral timbre of artificial

vowels and found to be unable to represent either pitch, timbre or spatial location in a manner that was independent of changes in the other two dimensions. This study compared the responses of animals trained to discriminate artificial vowel sounds with our previous control data.

Methods

Three ferrets were trained to identify two of the vowel sounds (/u/ and /ɛ/) used in the previous study in a two-alternative forced-choice paradigm. Animals were anaesthetised and recordings were made from neurons located across five cortical fields. Our stimuli were all possible combinations of four vowel timbres (including the two trained vowels), four fundamental frequencies and four spatial locations (Bizley et al., 2009), as well as pure tone stimuli at varying sound intensities and noise bursts.

Results

We quantified to what extent neurons were sensitive to pitch, timbre or location with a variance decomposition approach and compared the neural responses from the trained animals with the control data we have previously published. As in our control data the majority of neurons were sensitive to more than one sound feature. Neurons in the trained dataset were significantly more informative about spatial location of the artificial vowels than responses from control animals and, over all, relatively less informative about the pitch and timbre of the sound. When we considered the responses recorded in each of the cortical fields individually, we observed that timbre sensitivity was significantly lowered in the primary auditory cortex (fields A1 and AAF), but was markedly increased in field PPF for trained animals versus controls.

Conclusion

These findings suggest that training elicits field-specific changes in the representation of vowel identity.

909 Determining the Relative Importance of Cues for Concurrent Vowel Identification

Ananthakrishna Chintanpalli¹, Jayne B. Ahlstrom¹, Judy R. Dubno¹

¹Medical University of South Carolina

Background

Listeners with normal hearing have the ability to understand one talker in the presence of other talkers. Difference in fundamental frequency (F0) is one important cue for talker segregation. When listening to two vowels simultaneously, identification of both vowels increases as the difference in F0 of the two vowels increases. Although vowel segregation clearly benefits from F0 differences, listeners' ability to segregate two vowels with identical F0 suggests that other cues are contributing, such as vowel spectral characteristics. To assess the relative importance and interaction of these and other cues, we measured concurrent vowel identification under conditions that limited the availability of certain cues. A computational model of responses of auditory-nerve fibers was used to predict the neural basis of these cues.

Methods

Younger adults with normal hearing listened to two synthetic concurrent vowels with and without F0 difference at vowel levels ranging from 25-85 dB SPL. Vowel pairs were selected from five vowels and included same and different pairs. In the computational model, F0 coding using a periodicity metric across various fibers, and formant coding using a synchronized rate metric, were predicted for vowel pairs at each level. These predictions assessed the extent to which (1) reduced salience of F0 difference cues at lower levels can be attributed to poorer phase locking of auditory-nerve fibers to harmonics of the two F0s and (2) changes in vowel identification with increasing level in the absence of F0 difference cues can be attributed to changes in phase locking of auditory-nerve fibers to vowel formants.

Results

Identification of both vowels improved as vowel level increased from low- to mid-levels and then declined at higher levels. The slope of the functions relating vowel identification to vowel level was differentially affected by vowel type and F0 difference. At most levels, identification of both vowels was better with than without an F0 difference. In contrast, scores for vowels with and without F0 difference were more similar at lower levels, suggesting a reduced contribution of this cue.

Conclusion

Younger adults with normal hearing use F0 difference, spectral, and other cues to identify two concurrent vowels. The relative importance of these cues for each vowel varies with vowel level and may relate to level-dependent changes in phase-locking of auditory-nerve fibers to vowel harmonics and formants.

[Work supported by NIH].

910 The Contribution of Low Spontaneous Rate, Auditory Nerve Fibers to Recognizing Speech in Noise

Christopher Boven¹, Robert Wickesberg¹

¹University of Illinois at Urbana-Champaign

Background

Humans are remarkably good at resolving speech in noise. While humans still perform well at -12 dB signal-to-noise (SNR) ratios and lower, even the best computer automatic speech recognition systems have significant performance decrements at around 0 dB SNR. How humans achieve this robust performance remains unclear. There is evidence that auditory nerve fibers with low spontaneous rates, which have been traditionally thought to be most important for encoding a large dynamic range, may play an important role (e.g. Silkes and Geisler, 1992). This proposal has been explored primarily for frequency cues, but not for the temporal cues that have been described recently (e.g. Clarey et al., 2004).

Methods

In this study, we presented speech consonants in quiet and with background noise to ketamine-anesthetized chinchillas while recording from individual auditory nerve fibers. A peristimulus time histogram (PSTH) was computed from the responses of each auditory nerve fiber to each consonant, and these PSTHs were averaged across all fibers to create the consonant's ensemble response.

Results

While this method produced an ensemble response which displayed a unique temporal pattern for each consonant in quiet, these temporal patterns were not apparent for consonants played in noise. Using only the responses from low spontaneous rate fibers, however, allowed for a reasonable recovery of these temporal patterns.

Conclusion

It appears that low spontaneous rate fibers are important for carrying the temporal cues when a consonant is heard in noise and would be crucial for robust speech recognition in noise.

This research was supported by the National Science Foundation.

911 Voltage-Gated Ionic Conductances Required for Action Potential Firing in Auditory Nerve Fibers

Christophe Michel¹, Régis Nouvian¹, Joseph Santos-Sacchi², Jean-Luc Puel¹, Jérôme Bourien¹

¹INSERM, ²Yale University School of Medicine

Background

Depolarization of the inner hair cell triggers glutamate release onto the dendrite-like processes of spiral ganglion neurons (SGNs) and drives action potentials, which are conveyed to the brain. Whereas knowledge of the transfer function at the ribbon synapse has considerably progressed, little is known about the voltage-gated ionic channels which shape the action potential firing. Here, we provide a comprehensive computational model bridging the gap between the voltage-dependent currents measured in vitro on fresh isolated SGNs and spikes (extracellular action potentials) recorded in vivo from guinea pig auditory nerve fibers.

Methods

Voltage-dependent currents (Na⁺ and K⁺) of SGNs somata patch-clamp recordings were fitted by a Hodgkin-Huxley model with a full-trace fitting Willms algorithm. Node of Ranvier model was designed from the hypothesis that channels expressed on soma were identical, but differ in density. Simulated spikes were adjusted in order to match in vivo single-unit recordings with gradient-descent algorithm.

Results

Computation of the data allows to the identification of: i) one fast inward Na⁺ current (GNa activation: $V_{1/2} = -33$

mV, $\tau = 0.5$ ms; inactivation: $V_{1/2} = -61$ mV, $\tau = 2$ ms); and ii) two K^+ delayed-rectifier conductances, a low voltage-activated component (GKL, activation: $V_{1/2} = -56$ mV; $\tau = 5$ ms) and a high voltage-activated component (GKH, activation: $V_{1/2} = -41$ mV; $\tau = 2.5$ ms). Node of Ranvier model generate spikes that fit with in vivo recordings. Interestingly, the different spike durations along the tonotopic axis measured in vivo (i.e. 450 ms peak-to-peak duration versus 250 ms for 1 to 20 kHz, respectively) was explained by a gradual change in Na and K channel densities along the cochlea (GNa ~ 78 nS, GKL ~ 9 nS, GKH ~ 3 nS at 1 kHz versus GNa ~ 90 nS, GKL ~ 12 nS, GKH ~ 6 nS at 20 kHz).

Conclusion

This study identifies the ionic conductances and densities, which shape the action potential waveform of auditory nerve fibers and suggests that the interplay of fast inward Na^+ current and the two K^+ delayed-rectifier enables the auditory nerve fibers to sustain high firing rates.

912 Merlin Is Expressed in Spiral Ganglion Neurons (SGNs) and Inhibits Neurite Growth

Joshua Tokita¹, Augusta Fernando¹, Bethany Harpole¹, Helal Shah¹, Marlan Hansen¹

¹University of Iowa Hospitals and Clinics

Background

Merlin, the product of the *nf2* tumor suppression gene, mediates cell-cell contact information to inhibit cell proliferation and motility. It does so by inhibiting several pro-growth intracellular signaling cascades such as Ras, Rac, phosphatidylinositol-3 kinase/Akt, extracellular regulated kinase, and c-Jun N-terminal kinase, which have also been implicated in neuritogenesis and neurite growth. We hypothesize that neuronally-expressed merlin regulates neurite growth by inhibiting these signals in response to cell-cell contact cues.

Methods

Immunostaining of cochlear organotypic explants with anti-merlin antibodies was used to verify merlin expression in SGNs and their peripheral neurites. We used a tamoxifen (Tx)-inducible Cre-mediated recombination system to knock out merlin in neonatal SGN, trigeminal ganglion (TGN), and cortical neuron cultures. Dissociated cultures were maintained in the presence or absence of Tx for 24h to induce Cre expression. Neurite length was measured after an additional 48h in culture. To distinguish between the effect of loss of merlin expression in SGNs and loss in Schwann cell (SCs), we plated neurons that had been treated or not treated with Tx onto a bed of SCs that had likewise been treated or not treated with Tx.

Results

We find that merlin is expressed in SGNs raising the possibility that merlin regulates SGN neurite growth in addition to its well-known role in SC tumorigenesis and cell motility. Reduction of merlin expression in neurons but not SCs increases both the number and length of neurites in SGNs and TGNs. Decreasing merlin expression via

simultaneous treatment of SCs and neurons with tamoxifen increased neurite length from $365 \pm 125 \mu\text{m}$ (mean \pm SE) to $522 \pm 165 \mu\text{m}$ in cultured neonatal SGNs and from $372 \pm 31 \mu\text{m}$ to $510 \pm 113 \mu\text{m}$ in TGNs. SGN and TGN neurite length in samples where SCs were treated with tamoxifen but not neurons was $388 \pm 122 \mu\text{m}$ and $391 \pm 101 \mu\text{m}$ respectively. SGN and TGN neurite length in samples where neurons were treated with tamoxifen but not SCs was $500 \pm 92 \mu\text{m}$ and $511 \pm 93 \mu\text{m}$ respectively.

Conclusion

Inhibition of neurite growth by merlin may be due to the effect of merlin expression in neurons rather than in SCs. Current studies examine the merlin-sensitive signaling pathways that contribute to SGN neurite growth and the influence of merlin status on synaptogenesis. This raises the possibility that merlin regulates neural development and/or regeneration, in addition to its role in suppressing tumor growth.

913 The Organ of Corti's Role in Regulating Spiral Ganglion Neuron Axonal Projection Length

Felicia L Smith¹, Robin L Davis¹

¹Rutgers University

Background

The distinct morphological features of a neuron can affect its signal transmission. Spiral ganglion neurons (SGNs) display a bipolar phenotype in which specific features are graded, such as soma area, axon diameter, and branching patterns. For example, the axon segment from the foramen nervosum to the Schwann glial border SGB (intracochlear axon) is longer for low frequency neurons (apex) relative to high frequency neurons (base) whereas, the segment from the SGB to the bifurcation (root branch) shows the opposite pattern. The length differences between these two regions compensate for each other to the extent that the total length from the organ of Corti (OC) to the bifurcation is the same for apical and basal neurons (Fekete D.M. et al., *JCompNeurol.*1984). This study examines the axon length that extends from the soma to the region of axon bifurcation when co-cultured with regions of the OC.

Methods

The preparation pairs the hair cells and their surrounding satellite cells (micro-isolates) with SGN explants (Flores-Otero et al., *JNeurosci.* 2007). Immunolabeling with α - β -tubulin antibody was utilized to identify the neurons; axon length was measured in IPlab (Scanalytics) from the soma to the first branch point.

Results

Here we examine the role that OC micro-isolates play in regulating axon length. Our in vitro data recapitulated the axon length relationship of the intracochlear axon measured in vivo. When apical hair cell micro-isolates were paired with apical neurons the measured axon length was significantly longer ($779 \pm 70 \mu\text{m}$, $n=17$) when compared to basal hair cell micro-isolates paired with

basal neurons ($462 \pm 82\mu\text{m}$, $n=10$; $p \leq 0.01$). The peripheral targets were identified to regulate this parameter when the OC micro-isolates taken from different tonotopic regions were mixed and matched with SGNs. The apical hair cell micro-isolates co-cultured with basal neurons increased axon length ($903 \pm 75\mu\text{m}$, $n=7$; $p \leq 0.01$) when compared to basal hair cell micro-isolates co-cultured with basal neurons. Conversely, basal hair cell micro-isolates co-cultured with apical neurons reduced axon length ($398 \pm 60\mu\text{m}$, $n=3$; $p \leq 0.05$) relative to apical hair cell micro-isolates co-cultured with apical neurons.

Conclusion

The intracochlear axon length relationship is reflected in our measurements. Thus, elements from the OC can regulate this parameter suggesting that the intracochlear axon and the root branch length are differentially regulated. NIH NIDCD R01 DC-0185.

914 Improved Parameters and Expanded Simulation Options for a Model of the Auditory Periphery

Muhammad S.A. Zilany¹, Ian C. Bruce², Rasha A. Ibrahim², Laurel H. Carney³

¹University of Malaya, ²McMaster University, ³University of Rochester

Background

The auditory periphery impacts the neural representation of speech and is the sole conduit for information to reach the higher auditory centers. A phenomenological model of auditory-nerve (AN) responses was developed to understand the staged transformations in the auditory periphery (Zilany *et al.*, 2009, *JASA*, 126:2390). This model incorporates most of the nonlinearities observed in AN responses; however, it does not accurately simulate data from Liberman (1978, *JASA* 63:442) describing the discharge rate at saturation as a function of characteristic frequency (CF) for higher CFs. The responses of higher-CF model fibers to low-frequency tones (e.g. 500 Hz) are also erroneously much higher than the responses of low-CF model fibers (Fig. 1A). This issue was addressed here, and the model was also extended to include a set of parameters for a human AN model.

Methods

It was determined that the source of the mismatch between the reported saturation-rate data from Liberman (1978) and the model responses lies in the parameters for the model stage that describes synaptic adaptation. With minimal effects to other response characteristics, the parameters of the synapse model were modified to solve the problem described above. Additionally, an analytical method was adopted from Vannucci and Teich (1978, *Optics Communications* 25:267) to compute the instantaneous mean discharge rate and variance from the model's synapse output that takes into account the effects of refractoriness. Finally, a set of parameters that describes estimates of human tuning is now included (Ibrahim and Bruce, 2010, *The Neurophysiological Bases*

of Auditory Perception, pp. 429) in addition to parameters for cat.

Results

The new model with the modified set of parameters has been extensively tested against the published and recorded data from the AN. The saturation rates, especially for high-CF model fibers, were corrected by the modification (Fig. 1B), whereas other response properties were largely unchanged. The forward-masking properties were affected to a small degree, as could be expected after modifying synaptic adaptation.

Conclusion

The revised AN model is a better candidate to examine realistic neural-encoding hypotheses, especially those involving high CFs. The changes made to the previous version correct the saturation rates as a function of CF without adversely affecting other response properties. The revised model also includes a set of parameters that describes the middle ear transfer functions and peripheral tuning in human.

Support: NIH DC010813 (LHC,MSAZ), NSERC DG 261736 (ICB,RAS)

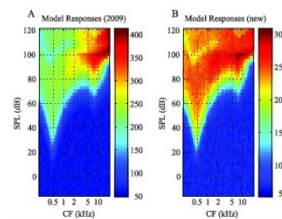


FIG 1. Response area to a 500 Hz tone (50-ms duration with 2.5 ms on/off ramp). Mean rate responses of the 100 AN fibers with CFs logarithmically spaced from 200 Hz to 20 kHz (along x-axis) are plotted for sound levels ranging from -15 to 120 dB SPL (along y-axis) in steps of 2.5 dB. A) Responses from the Zilany *et al.* (2009). B) Responses from the new model.

915 Amplitude of Masked Compound Action Potentials Indicates Location of Laser-Induced Lesions in the Auditory Periphery

Brian Earl¹, Mark Chertoff²

¹University of Cincinnati, ²University of Kansas Medical Center

Background

Auditory nerve degeneration is thought to lead to difficulties with understanding speech, especially in difficult listening situations. Recent research suggests that the presence of neural degeneration may be missed if threshold and latency are the only metrics used to assess auditory evoked potentials. Adding amplitude as a metric, overall nerve survival can be inferred from high-level compound action potentials (CAPs). However, the inherent variability in absolute amplitude measures may confound the prediction of the extent of nerve damage. Our recent experiments have focused on circumventing this confound and improving the location-specificity of damage predictions by tracking CAP amplitude growth while systematically limiting the region of synchronously firing auditory neurons with a high-pass masking paradigm.

The objective of this study was to determine if the pattern of CAP amplitude growth in animals with peripheral auditory nerve lesions indicates the corresponding cochlear location of the lesion.

Methods

Mongolian gerbils with laser-induced lesions in the auditory periphery were compared to normal-hearing gerbils. CAPs were evoked with broadband chirps at 90 dB SPL during simultaneous masking noise high-passed in 1/3 octave intervals between 0.4 and 50 kHz. Cumulative amplitude functions were constructed by plotting normalized CAP amplitudes as a function of distance from cochlear apex (inferred from masker cutoff frequencies). Animals were euthanized and the cochleae were fixed, decalcified, and sectioned into three turns. The cochlear turns were first stained with phalloidin to enable imaging of hair cells under confocal microscopy. The peripheral processes of the auditory nerve were then stained with osmium and imaged under light microscopy.

Results

Confocal images of laser-exposed cochlea revealed circular lesions through regions of the osseous spiral lamina and missing hair cells. Light micrographs of osmium-stained cochleae revealed regions of severed neurons and lighter staining consistent with myelin damage. Cumulative amplitude functions in normal-hearing gerbils were sigmoidal in shape and approached saturation at the basal end of the cochlea. In lesioned gerbils, the amplitude functions plateaued in regions that generally corresponded to the cochlear region at which the laser was directed.

Conclusion

These data indicate that the pattern of CAP amplitude growth may identify the cochlear location of auditory nerve damage. Future experiments gauging the reliability of amplitude growth functions and enhanced anatomical measures (e.g., dual-fluorescence labeling of hair cells and neurons) are needed to determine the predictive power of this technique.

Supported by Action on Hearing Loss, UK

[916] Heterogeneous Electrophysiological Properties from Murine Spiral Ganglion Neurons in Acutely Prepared Cochlear Slices

Qing Liu¹, Robert Crozier¹, Robin Davis¹

¹Rutgers University

Background

Type I spiral ganglion neurons (SGNs), composing most of the ganglion (90-95%), are responsible for conveying the acoustic signals that are encoded by the inner hair cell (IHC) receptors to the central auditory pathways in the form of action potentials. Although the initiation of action potential occurs at the synaptic terminal that innervates the IHC, the cell soma from acutely dissociated neurons is excitable and thus capable of shaping the signal during its propagation. Moreover, the timing and intrinsic excitability

features of cultured SGNs from one week old animals are distinctively organized along the tonotopic axis and may relate to coding separate sub-modalities of acoustic features (Liu and Davis, *J Neurophysiol*, 2007). To extend the studies in culture and facilitate our understanding of spiral ganglion function *ex vivo*, we have begun to characterize the electrophysiological properties from neurons in acutely prepared cochlear slices and have found evidence of the heterogeneity and firing features that are consistent with observations made *in vitro*.

Methods

After removing the cochlea, slices (Jagger et al., *J Neurosci Methods*, 2000) were prepared on a vibratome (Leica VT1200, ~200 μ m slice thickness) from postnatal day 4 (P4) to 8 (P8) CBA/CaJ mice. SGNs were visualized under infrared differential interference contrast (IR-DIC) microscopy (Olympus BX50WI) and recorded with the whole cell patch clamp technique.

Results

The SGNs from slices fire well formed action potentials (amplitude: 87 mV \pm 4 mV, n = 8). Both rapidly and slowly accommodating neurons were observed during a 240 ms step current stimulation: two cells fired a maximum of 13 and 16 action potentials, respectively, and the rest fired fewer than 7 (2.2 \pm 1.2, n = 5). A heterogeneous distribution was found for action potential latency at threshold (ranging from 4.1 to 9.9 ms; 7.8 \pm 1.4 ms, n = 8) and voltage threshold (-60.01 to -48.19 mV; -55.1 \pm 1.4 mV, n = 8); all features that are consistent with our culture recordings.

Conclusion

The basic firing features including accommodation, action potential latency at threshold and voltage threshold from spiral ganglion neurons in acutely prepared slices are heterogeneously distributed and similar to postnatal SGN recordings in culture. Future experiments will address whether the observed heterogeneity reflects tonotopic changes or developmental influences from P4 to P8. Supported by NIH NIDCD RO1-DC01856.

[917] Noise-Induced Hearing Loss Increases Sensitivity to Fast Temporal Modulations in the Auditory Nerve: Evidence from Wiener Kernel Analysis

Kenneth Henry¹, Sushrut Kale², Michael Heinz^{1,2}

¹Department of Speech, Language, and Hearing Sciences, Purdue University, West Lafayette, IN, ²Weldon School of Biomedical Engineering, Purdue University, West Lafayette, IN

Background

The increase in the bandwidth of cochlear filtering associated with many forms of hearing loss should theoretically extend temporal modulation sensitivity to higher modulation frequencies. However, both behavioral studies in humans and neurophysiological studies in animals have found little evidence of enhanced sensitivity to fast temporal modulations.

Methods

Here in anesthetized chinchillas, we estimated temporal modulation transfer functions (TMTFs) from auditory-nerve fiber responses to near-threshold Gaussian noise stimuli. TMTFs were computed from second-order Wiener kernels of the neural responses, and compared between control animals (N=12) and animals with noise-induced hearing impairment (N=16) to assess possible changes in sensitivity to fast temporal modulations. We studied temporal modulation tuning in 163 fibers with characteristic frequencies (CFs) between 0.25 and 10 kHz.

Results

The noise exposure caused a loss of sensitivity and increase in the bandwidth of the pure-tone tuning curve across the full range of CFs investigated. The corner frequency of the TMTF measured -3 dB and -6 dB from the peak of the function increased with CF in both the noise-exposed and control groups, as observed previously in studies using neural responses to sinusoidally amplitude modulated (SAM) tones. In contrast to previous studies however, the corner frequency of the TMTF was 20-30% higher in noise-exposed fibers than in control fibers at any given CF. Previous studies with SAM tones showed little effect of noise-induced hearing loss on TMTF corner frequency. The increase in TMTF corner frequency observed here was generally less than the increase in the bandwidth of the pure-tone tuning curve, which increased by 100-200% relative to controls in some cases.

Conclusion

The results suggest that noise-induced hearing loss does in fact increase neural sensitivity to fast temporal modulations in the auditory periphery. The discrepancy with previous neurophysiological results probably reflects differences in the choice of stimulus. Whereas previous work relied primarily on SAM tones, we estimated sensitivity to temporal modulation using a dynamic stimulus with broadband acoustic structure similar to many natural sounds including speech. Inasmuch as the results demonstrate a deviation from normal spatiotemporal neural coding of sound in the cochlea, they may help explain the basis of degraded speech perception in people with common forms of hearing loss. Furthermore, the results underscore the value of studying hearing loss with more natural, real-world acoustic signals.

Research supported by NIH (NIDCD) F32-DC012236 and R01-DC009838.

[918] Correlation and Temporal Properties of the Auditory Nerve

Brian Dougherty^{1,2}, Claus-Peter Richter¹
¹Northwestern University, ²Loyola University Medical Center

Background

Modeling of the spontaneous activity in auditory nerve fibers failed if an exponential (Poisson) or gamma distribution of the inter-spike time-intervals was assumed.

Nevertheless, the distribution may still be described by a stochastic process. Spontaneous and driven activity of pigeon auditory nerve fibers was tested for a renewal process. The experiments falsified mutually statistically independent lengths of time intervals between successive action potentials. The question for this study was if the generation of action potentials on the auditory nerve may be described by a doubly embedded stochastic model, the Hidden Markov Model (HMM), and whether the model parameters change for various inputs at different levels.

Methods

The analysis is an extension of the work by Richter et al., 1996. Spontaneous activity and responses to sinusoidal and white noise acoustic stimuli, which were recorded from single pigeon auditory nerve fibers, were used to estimate the transition and emission matrices of the HMM. Newly generated sequences of events (surrogate data) were generated and the autocorrelation functions of the original data and the surrogate data were compared.

Results

Autocorrelation functions of the original data and surrogate data were not significantly different. Although action potential repetition rate was below 100 Hz, fine structure of more than 1 kHz could be extracted from the spike trains. This fine structure was maintained in the surrogate data despite the fact that little correlation existed between the occurrence of the action potentials (recorded data) and the surrogate data. Fine structure of responses could be modeled with low event repetition rates.

Conclusion

The HMM provides a method to create sequences of events that contain similar high frequency structure as the original sequence of action potentials. The HMM might be used as a spike generator for auditory prostheses to stimulate the auditory system at low pulse repetition rates maintaining high frequency fine structure. This is particularly attractive for infrared neural stimulation.

[919] Unstable Representation of Sound: A Biological Marker of Dyslexia

Jane Hornickel¹, Nina Kraus¹
¹Northwestern University

Background

Learning to read proceeds smoothly for most children, yet others struggle to translate verbal language into its written form. Poor readers often have a host of auditory, linguistic, and attention deficits, including abnormal neural representation of speech and inconsistent performance on psychoacoustic tasks. We hypothesize that this constellation of reading-related deficits arises from the human auditory system failing to respond to sound in a consistent manner, and that this inconsistency impinges upon the ability to relate phonology and orthography during reading.

Methods

102 normal hearing children (ages 6-13) were classified as good (> 120), average (105-95), and poor (< 90) readers based on their scores on a test of reading fluency (Torgesen et al., 1999). We collected evoked auditory brainstem responses to [ba] and [ga] stimuli and calculated response consistency by correlating responses from the first 3000 repetitions of the stimuli to those from the last 3000 repetitions, with a higher r-value representing more consistency (conversely, less variability).

Results

Poor readers have significantly more variable auditory brainstem responses to speech than do good readers. The groups do not differ on prestimulus response amplitude, indicating differences in response consistency were independent of physiological noise levels.

Conclusion

Here we provide evidence that poor readers have less stable auditory nervous system function than do good readers. Although causality cannot be determined, heightened variability in nervous system function may underlie fluctuations in directed attention and impaired speech understanding due to inconsistent encoding. Our results suggest that good readers profit from a stable neural representation of sound, and that children who have inconsistent neural responses are at a disadvantage when learning to read.

920 Multichannel ABR

Alain de Cheveigné¹

¹CNRS / ENS / Université Paris Descartes

Background

The auditory brainstem response (ABR) is widely used clinically in humans, and in animal models, to assess the integrity of the peripheral auditory system. The signals are extremely small, embedded in environmental and physiological noise of much higher amplitude, and measurements require many repetitions and are time-consuming. Our hypothesis is that the method can be improved by increasing the number of recording electrodes, and processing the data with recent multichannel signal processing techniques.

Methods

Data are acquired using a standard 32-channel EEG system (Biosemi). Multiple electrode layouts are investigated in an attempt to (a) optimize sensitivity to brainstem components, and (b) optimize coverage of major noise sources, so that they can be factored out. Data are processed using the Denoising Source Separation (DSS) algorithm, that finds the optimal combination of channels to maximize repeatable activity. Data have also been acquired in mouse using multiple electrodes.

Results

Compared to standard ABR (two or three electrodes), multichannel ABR produces data with a better signal-to-noise ratio (SNR). In many instances multiple components

may be observed, with distinct time-course and spatial signature, suggesting that it may be possible to differentiate contributions from different processing stages within the brainstem.

Conclusion

Multichannel recording and processing techniques improve the signal-to-noise ratio and resolution power of ABR measurements.

921 Subcortical Pitch Encoding of Speech Sounds in the Normal and Impaired Auditory Systems

Saradha Ananthakrishnan¹, Ananthanarayan Krishnan¹

¹Purdue University

Background

Several perceptual studies have demonstrated that hearing impaired (HI) listeners have reduced access to temporal fine structure (TFS) information, which may possibly be due to reduced phase-locking ability. However, there are few electrophysiological studies examining phase-locking in HI listeners, particularly at the subcortical level using the frequency following response (FFR). The FFR is a scalp recorded sustained potential, reflecting phase-locked activity from a population of neural elements in the rostral brainstem. Previous FFR studies have found that the phase-locking ability to second formant transition in HI individuals is significantly reduced as compared to normal hearing (NH) listeners. Here we examine brainstem neural phase-locking (as measured by the FFR) to a synthetic steady state vowel in NH and HI (mild-moderate SNHL) listeners. First, we aim to characterize phase-locking to the envelope and TFS in both groups. Secondly, to determine if the difference between the two groups is related to audibility, we measured FFRs at multiple sound pressure levels (SPLs) to facilitate comparisons between the two groups at equal sensation levels (SLs) and equal SPLs.

Methods

FFRs were recorded from NH and HI listeners in response to a steady state synthetic vowel at multiple sound pressure levels. Temporal and spectral analyses were conducted to describe the FFRs. Pure tone audiograms, speech-in-noise testing and case-history information was obtained for all subjects.

Results

Preliminary results indicate statistically significant differences between the NH and HI groups for phase-locking to both envelope and TFS. Comparisons at equal SLs and SPLs continue to show differences between the two groups. Also notable is the variability noted within the HI group: a combination of clinical testing, demographic and case-history information collected seems to suggest a variety of factors (age, pure tone thresholds, use of amplification, etc.) could be contributing to the intra-group variability.

Conclusion

FFRs in NH are more robust in amplitude and phase-locking than those in HI listeners. Audibility does not appear to be the chief cause underlying the differences seen between the two groups. These results are consistent with those obtained in previous work by Plyler and Krishnan (2001). A multitude of other factors may be causing the intra group variability seen in the HI group. The results observed in the hearing impaired FFRs may be due to disruption in temporal synchronization of neural activity across a population of neural elements.

922 Context-Dependent Processing of Shepard Tones in the Human Auditory Brainstem and Cortex - An Electrophysiological Study

Sabine Grimm¹, Jordi Costa-Faidella¹, Carles Escera¹

¹Institute of Research for Brain, Cognition and Behaviour (IR3C), University Barcelona

Background

Recently, a series of studies using the frequency-following auditory brainstem response (FFR) have shown that the encoding in the human inferior colliculi is not merely determined by the acoustics of the incoming stimulus, but can be enhanced by short-term experience with specific auditory material, e.g. stimulus repetition. Here, we tested whether stimulus regularity, as in the case of regularly presented Shepard tones leading to the illusion of a continuously descending pitch, will lead to a modulation of the frequency representations in the brainstem.

Methods

23 healthy human subjects listened to sequences of tones presented monaurally through headphones to the right ear (75 dB SPL; SOA of 240 ms) while the left ear was masked with white noise. Sequences consisted of Shepard tones that were presented continuously either in a descending or in a random manner, the later with the restriction of keeping the step-size from one tone to the next identical to the one in the descending condition. EEG was recorded from Cz with an electrode at the left earlobe serving as reference, sampled at 20 kHz, and analyzed for the auditory brainstem response (ABR). Additionally, middle-latency responses (MLR) and long-latency responses (LLR) of the auditory evoked potential (AEP) were obtained to study later regularity-related effects.

Results

In the ABR time range, FFR to the prominent partials of the Shepard tones were smaller in amplitude in the descending than in the random condition ($p=0.029$). Results did not reveal an interaction between conditions and the amplitudes with which single partials were represented in the brainstem FFR. In the MLR time range, tones in the random condition elicited a smaller Pa-Nb complex than tones in the descending condition ($p=0.030$). LLR potentials in the time range from 130-180 ms were more negative in the random than in the descending condition ($p=0.001$).

Conclusion

In the long-latency range, results resemble a typical surprise-related negativity for randomly presented tones. In contrast, in the earlier latencies of the AEP, the pattern for regular descending Shepard tones (attenuated brainstem FFR, enhanced MLR) is opposite to the pattern observed for repetition regularities in previous studies (enhanced FFR, attenuated MLR). This could suggest that earlier processing stages are rather influenced by the higher local probability of tone repetitions in the random condition of the present study and not by the non-repetitive stimulus regularity.

923 Rapid Acquisition of Auditory Brainstem Frequency Following Responses

Hari Bharadwaj¹, Barbara Shinn-Cunningham¹

¹Boston University

Background

Auditory Brainstem Frequency Following Responses (FFRs) provide a non-invasive measure of encoding in the auditory pathway up to the Inferior Colliculus and have been used extensively both clinically and in basic neurophysiological investigation of auditory function. FFR data acquisition for simple stimuli such as click trains, tones, and speech tokens typically involves thousands of presentations of each stimulus type, sometimes in two polarities leading to acquisition times exceeding an hour per subject. Since the FFR sources are deep compared to the primary noise sources (i.e.) cortical activity, FFR varies more smoothly over the scalp than cortical noise. Additionally, since the FFR is a multi-source mixture, there are phase differences in the responses at different scalp locations. We present a novel approach to exploit the above properties using multichannel recordings and an eigendecomposition of the complex cross channel spectral density (CSD) matrix (i.e.) complex Principal Component Analysis or cPCA to extract FFRs efficiently.

Methods

First, we use simulations to validate the cPCA method. 32 channels, each containing a 200 ms burst of a 100 Hz sinusoid with a random phase, were added to 400 epochs of background EEG data to mimic SNR and between channel noise covariance of a real multichannel FFR recording. A multi-tapered estimate of the 32x32 normalized CSD matrix $C(f)$ (complex coherence matrix) was diagonalized using eigendecomposition. The function $d(f)$ of the highest eigenvalue in each frequency bin provides the inter-trial phase coherence of the first principal component (the extracted FFR) with the corresponding 1×32 eigenvector $v(f)$ providing the complex weighting function to combine the different channels with appropriate phase lags. An identical analysis is then applied on 32 channel EEG data acquired from human subjects stimulated with 400 trials of 200ms click-train bursts at 70 dB SPL in 2 polarities to extract FFR components phase locked to the envelope in the different cochlear channels.

Results

The cPCA eigenvector accurately estimated the phase lags needed to align the FFR across channels in the simulated data with $d(f)$ showing a very robust 100Hz peak compared to either an individual channel or traditional time-domain PCA. Preliminary results with real data suggest that a fifth of the trials can be combined to yield an SNR comparable to using all the trials with just the best electrode in the phase-locking measure.

Conclusion

The proposed method makes rapid acquisition of FFR data possible.

924 Hearing Threshold Estimation by Linear Regression on Auditory Brainstem

Parameters in Rats

José Miguel Ercolino¹, Jorge Hernandez-Rojas¹, Juan Chiossone^{1,2}, Stefania Gonçalves^{1,2}

¹Universidad Central de Venezuela, ²Fundación Venezolana de Otológica

Background

The hearing threshold is usually estimated by presenting a sequence of decreasing intensity auditory clicks with predetermined step size (4, 5 or 10 dB) until some or all the Auditory Brainstem Response (ABR) waves disappear within the physiological and electrical noise present in the system. This method is usually refined by further exploring the estimated threshold with a smaller intensity step size. These procedures exhibit the inconvenience that the noise level varies from one setup to another and with time.

Methods

20 Sprague Dawley rats weighing 300 ± 50 grams were used according to the local experimental animal research regulatory authority. The ABRs were obtained under xylazine-ketamine anesthesia (6-87 mg/Kg) administered intraperitoneally. The animal body temperature was kept at 37 ± 0.5 C. The stimuli, consisting in compression clicks 100 μ S in duration, were presented at a repetition rate of 50 Hz inside of a custom-made sound attenuated booth (50 x 30 x 30cm) exhibiting more than 35 dB attenuation above 1 kHz against the ambient noise. The stimulus sound intensity was varied in a predetermined pseudorandom sequence covering the hearing range of the rat, with two successive steps not differing more than 20 dB. The stimuli were presented binaurally by a commercial speaker placed 17cm right above the rat's head. A specially designed amplifier was used with 20K overall gain between 100 and 1500 Hz (-3 dB) and a 60 Hz notch filter.

The proposed method for the hearing threshold estimation is based on the linear regression of the stimulus intensity versus a calculated parameter of the ABR that conveys enough information related to the response to sound intensity and that exhibits an approximated linear relation with it. We used the RMS and total difference voltages of the ABR. The hearing threshold can be estimated as the stimulus intensity value at which the derived parameter

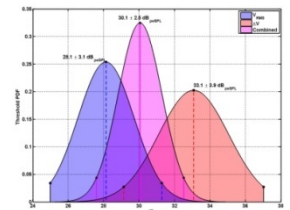
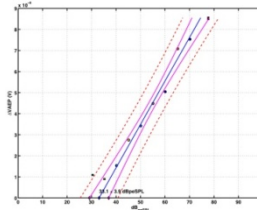
would be zero as if there was no noise. The two estimation results were combined by the weighted average method.

Results

The hearing threshold values obtained by the proposed method are consistently lower than those obtained by observing the extinction of the ABR waves. The difference between the measured values was 5 ± 2 dB (90% C.L.).

Conclusion

The proposed regression method represents an objective alternative, consistent with the conventional methods for hearing level threshold estimation in rats which requires no intervention by the operator or researcher and that can be easily automated.



925 High-Functioning Autistic Children Have Abnormal Stapedial Reflexes

Randy Kulesza¹, Richard Lukose², Carol Barber³, Kevin Brown⁴

¹LECOM Auditory Research Center, ²UPMC Hamot Dept of Neurology, ³Asheville Head, Neck and Ear, ⁴LECOM

Background

Autism is a neurodevelopmental disorder, characterized by social and communicative impairments, sensory abnormalities and restricted, repetitive behaviors. The incidence of autism is approximately 1:88 children and 1:54 in boys. Throughout the autistic brain, there is evidence of developmental dysregulation of neurogenesis, abnormal neuronal maturation, including aberrant neuronal migration, alterations in cell body size, number and dendritic morphology. Additionally, abnormalities in auditory processing are present, in most if not all autistic subjects and abnormal brainstem responses implicate dysfunction of the superior olive (SOC). Finally, we have provided evidence for significant and consistent dysmorphology in the SOC of the autistic brain. Thus, we hypothesize abnormalities in the acoustic stapedial reflex (ASR) in autistic subjects and further, that this objective measure of brainstem function can be used as an early screening tool to identify neonates at risk of carrying a diagnosis of autism.

Methods

The ASR utilizes a brainstem circuitry involving the auditory nerve, the ventral cochlear nucleus, SOC and stapedial motor neurons. Based on the known anatomical and functional auditory deficits in autism, we have compared the ASR in neuro-typical and autistic children. All control and autistic subjects in this study had normal hearing sensitivity. Control subjects were only included if:

they had no family members diagnosed with autism, normal hearing sensitivity, no upper respiratory disorders affecting middle ear function and satisfactory speech/language development. ASRs were measured ipsilateral and contralaterally at 500, 1000 and 2000 Hz, using .02ml negative deflection as threshold. ASR thresholds, amplitudes and latencies were compared using JMP10.

Results

Overall, autistic subjects have lower ipsilateral ASR thresholds than neuro-typical controls. Contralateral threshold differences are not statistically significant and there are no differences in ASR amplitude between autistic and control subjects. However, we observe significant differences in ASR response latencies. Overall in control subjects, ipsilateral latencies are shorter than contralateral responses, but we observed no such contrast in autistic subjects. Further, we observed significantly longer latencies in autistic subjects and significant asymmetry between responses in the left and right ears.

Conclusion

Our previous reports of dysmorphology in the autistic auditory brainstem along with reported auditory dysfunction and our current report of dysfunction in the ASR provide clear evidence of disruption of auditory pathways in the autistic brain. Based on this study, we believe that non-invasive, objective measures of auditory function have utility as a neonatal screening tool to identify patients with a high risk of autism.

926 Predicting Hearing Status from Auditory Brainstem Responses Differs in Term and Preterm Infants

Beth Prieve¹, Linda Hood²

¹Syracuse University, ²Vanderbilt University

Background

Because all newborns are now screened for hearing loss, diagnostic auditory brainstem response (ABR) testing is performed on more infants than ever before. Broadband and frequency specific stimuli are used to obtain information about auditory neural integrity and sensitivity, respectively. ABR latencies are compared to normative data from decades-old research comprised primarily of neurologically normal preterm infants or term infants with presumed normal hearing. The population of infants undergoing hearing testing today, especially preterm infants, is vastly different than that tested in previous decades. To better understand infant ABRs, a comprehensive model that includes middle ear measures, otoacoustic emissions and outcome measures is needed. The purpose of this study was to take an initial step towards that goal by modeling retrospectively collected ABR data in preterm and term infants with normal hearing (NH), conductive hearing loss (CHL) or sensorineural hearing loss (SNHL). Two hypotheses were tested: (1) Do ABR Wave V latency and Waves I-V interwave latency for infants with NH, CHL or SNHL have different trends as a

function of post-conceptual age (PCA)? (2) Is regression different for preterm and term infants?

Methods

Two data sets were combined: cross-sectional data from 84 ears of 71 infants who underwent a clinical research protocol; data from 83 ears of 44 infants with 1-3 clinical ABR tests following newborn hearing screening failure. ABR latencies as a function of PCA were modeled using simple, linear regression. Mean data from Eggermont and Salamy (1988) were used as a comparison.

Results

In term infants, the y-intercepts for Wave V latency were different for infants with NH, CHL and SNHL, as expected from previous literature. The slope and y-intercept of Wave V regressions for preterm infants differed from term infants. Waves I-V interwave latencies tended to be longer for preterm infants, which differs from Eggermont and Salamy (1988).

Conclusion

The results suggest that ABR latency as a function of post-conceptual age can be modeled using regression for ears with NH, CHL and SNHL. Moreover, regression may be different for preterm and term infants. These results provide a basis for further refinement of a model in which middle ear measures, otoacoustic emissions and outcome measures are included. [Research funded by the March of Dimes Birth Defects Foundation (BP), internal research funds (LH), and Vanderbilt University Summer Research Program.]

927 Envelope Coding in Humans Measured with Frequency Following Responses

Jayaganesh Swaminathan¹, Hari Bharadwaj¹, Lengshi Dai¹, Barbara Shinn-Cunningham¹

¹Boston University

Background

The scalp recorded human frequency following response (FFR) represents sustained phase-locked neural activity among a population of neurons in the rostral brainstem. The present study examined the robustness of envelope coding with increasing sound levels as reflected in the FFR component corresponding to the stimulus envelope.

Methods

FFRs were recorded from normal-hearing listeners to sinusoidally amplitude-modulated (SAM) tones, transposed tones, and tone complexes of different sound intensities. The SAM tones were 100% modulated; the transposed tone envelopes were half-wave rectified sinusoids. Both SAM and transposed tones had a modulation frequency (fm) of 200 Hz and a carrier frequency (fc) was of 4 kHz. The tone-complexes had frequency components ranging from 3400 Hz to 4600 Hz with an f0 of 200 Hz. Sound intensity was varied from 50 dB to 90 dB SPL in 10 dB steps. Phase-locking-value (PLV), a measure of the consistency of the evoked signals phase at the envelope

frequency, was estimated from the FFR component corresponding to the stimulus envelope.

Results

Preliminary results indicate that at moderate sound levels, envelope coding (as reflected in PLV measures) was strongest for transposed tones, second best for tone-complexes, and worst for SAM tones. Envelope coding across all three stimuli first improved with increases in sound level, but dropped from 80 to 90 dB SPL.

Conclusion

Previous single-unit neurophysiology studies in animals have reported that the envelope coding at the auditory nerve is strongest near threshold and falls dramatically with increasing sound levels. In contrast, these preliminary results suggest that the envelope coding measured from a population of neurons (as reflected in FFRs) remains fairly stable over a broad range of increasing sound levels.

928 Crossmodal Interactions Between Audition and Nociception

Alexandre Lehmann^{1,2}, Pierre Rainville², Marc Schönwiesner³

¹CRBLM, BRAMS U. Montreal, ²CRIUGM U. Montreal,

³BRAMS U. Montreal

Background

Research in perception has largely focused on bottom-up processing. Interest in the contribution of efferent pathways is relatively recent and these pathways are poorly understood. Refuting the traditional view that subcortical processing is purely automatic, plasticity has been demonstrated in human auditory brainstem. Such efferent modulation may play a key role in cognitive strategies of pain reduction, such as music-induced analgesia. To date, the underlying mechanism of such modulations is largely unknown.

Methods

We investigated crossmodal interactions between audition and nociception. We anticipated that an auditory task would modulate pain perception, and expected that pain would interfere with auditory processing. Like pain, audition can under certain circumstances serve as a 'danger detection' mechanism. We predicted that the earliest component of this crossmodal modulation is mediated by a low-level pathway, subserving a combined auditory-nociceptive 'danger detection' system. Sixteen subjects executed a three-oddball auditory task, while receiving either painful or non-painful thermal stimulations. Speech vowels (standard, target) or white noise (distracter) of 60ms were presented through shielded insert earphones (Etymotic) at 1.4Hz (Slow task) or 8Hz (Fast task). Thermal stimuli were produced by a 3x3cm contact thermode (Medoc) applied to the forearm. Stimulation consisted in plateaus of 15s. After each thermal block, subjects rated intensity and unpleasantness of the sensation using a visual analog scale. Skin conductance response (SCR) was measured throughout the experiment. Using a 64-channel EEG system

(Biosemi), with a sampling rate of 16kHz, auditory evoked potentials (AEPs) of several timescales were recorded: from auditory brainstem response (ABR) to the auditory P3a/b complex.

Results

The auditory task had a significant effect on pain ratings, with pain judged as less intense and unpleasant during the Slow task. A similar pattern was found in the SCR. Comparing the effect of painful and non-painful stimulations on AEPs revealed a distinct pattern of modulation, both in terms of temporal dynamics and topographic maps. In the presence of pain, early auditory responses are enhanced whereas later components such as the P3b are reduced.

Conclusion

By combining several methods and measuring AEPs at different timescales, we were able to assess both high-level and direct low-level interactions, between audition and nociception. Our results support the existence of a pain specific modulatory mechanism that affects early auditory processing. Results on auditory-nociceptive interactions also contribute to better characterize the human efferent system.

929 Effects of Unilateral Conductive Hearing Loss on Auditory Brainstem Responses in Rats

Cheryl Clarkson¹, Hongning Wang¹, Maria Rubio¹

¹University of Pittsburgh

Background

Listeners with unilateral conductive hearing loss (UHL) have reduced their ability to localize sound. The effects of UHL along the central auditory pathway are still poorly understood. Currently, most available information focuses on the ipsilateral effects of UHL. However, due to the extensive crosstalk along the entire central auditory pathway, we hypothesize that UHL will also affect the contralateral side of the central auditory pathway. Another important but still unresolved aspect is whether the effects of UHL are reversible, indicating the existence of experience dependent plasticity in the central auditory pathway.

Methods

To test this we used an animal model of UHL by earplugging. Earplugs were inserted in the right external canal of young adult Sprague-Dawley rats. Neuronal electrical activity was measured in both plugged (ipsilateral) and unplugged sides (contralateral) by auditory brainstem response (ABR) tests, in response to clicks and pure tones before, during (10 days), and 10 days after earplug removal.

Results

Our results from clicks in the plugged-side showed a threshold increase of 40 dB and smaller wave I, II and III amplitudes. In the unplugged-side, we found no change in the thresholds, but interestingly wave II and III amplitudes

were significantly smaller. The analyses of the latencies (peak and interpeak) showed an increase only in the plugged-side. We also analyzed the ratio of amplitude waves III/I. Data showed an increase in the ratio in the plugged-side, whereas there was a decrease in the unplugged-side. After earplug removal the threshold and latencies recovered in the ipsilateral side, whereas the amplitude was only recovered for waves II and III, not for wave I. In the contralateral-side the amplitude waves were fully recovered.

Conclusion

Our results suggest that UCHL alters reversibly and bilaterally the firing rates and/or synchrony of firing neurons in the auditory brainstem. The decreases in amplitude after UCHL might also reflect an imbalance between excitation and inhibition in the lower auditory brainstem.

930 Impact of Kv3 Channel Modulator AUT3 on in Vivo Auditory Processing in Mice

Lara Li Hesse¹, Lucy A. Anderson², David McAlpine², Charles Large³, Jennifer F. Linden²

¹Medical Faculty, University of Luebeck, Germany, ²Ear Institute, University College London, London, UK, ³Autifony Therapeutics, Imperial College Incubator, London, UK

Background

Voltage-gated K⁺ channels of the Kv3 subfamily activate at strongly depolarised membrane potentials to drive quick repolarisation after an action potential, and also rapidly deactivate to enable fast re-initiation of action potentials. Kv3 channels are strongly expressed in the central auditory system, at levels that can be modulated by auditory experience (such as noise exposure). These channels are therefore potential targets for drug treatments aimed at ameliorating central auditory pathologies arising from noise exposure. The aim of this study was to determine whether a novel modulator of Kv3 channel activity, AUT3, alters auditory brainstem responses (ABRs) in normal mice or in mice exposed to mild acoustic trauma.

Methods

ABRs were recorded from anaesthetised naïve or noise-exposed CBA/Ca mice. Noise-exposed mice had been subjected to 105 dB SPL, 8-16kHz noise under anaesthesia, 1 day prior to ABR measurements. ABRs were recorded 30 minutes before and 2, 32, 62, 92 and 122 minutes after intraperitoneal administration of either AUT3 (60mg/ml) or vehicle solution. Auditory stimuli were presented free-field, and included 0-80 dB SPL clicks, as well as broadband noises followed by clicks. Analysis involved calculation of ABR thresholds, peak-to-trough wave amplitudes, wave peak latencies, inter-peak latencies and root-mean-square overall amplitudes.

Results

In both naïve and noise-exposed mice, there was a small but significant increase ($p < 0.02$) in the inter-peak latency of ABR wave I to IV following AUT3 but not vehicle injections. The latency shift in wave IV was evident in

absolute as well as inter-peak latency analysis, whilst the absolute latency of ABR wave I was not significantly altered. No significant effect of AUT3 injections (relative to vehicle injections) was observed for ABR thresholds, wave amplitudes, or overall root-mean-square amplitudes in either group of animals.

Conclusion

AUT3, a Kv3 channel modulator, caused a small but significant increase in the latency of ABR wave IV in both noise-exposed and naïve mice, but no detectable change in either the latency of ABR wave I, ABR thresholds, peak-to-trough wave amplitudes, or overall root-mean-square amplitudes. These findings indicate that AUT3 causes no gross abnormalities in the ABR, but does have a subtle effect on the timing of late ABR waves, which may reflect an impact on auditory processing in higher central auditory structures such as the inferior colliculus.

931 Musical Training Strengthens the Subcortical-Cortical Encoding and Categorical Perception of Speech

Gavin Bidelman^{1,2}, Michael Weiss³, Sylvain Moreno⁴, Claude Alain^{3,4}

¹School of Communication Sciences & Disorders, University of Memphis, ²Institute for Intelligent Systems, University of Memphis, ³Department of Psychology, University of Toronto, Toronto, ON, ⁴Rotman Research Institute, Baycrest Centre for Geriatric Care, Toronto, ON

Background

There is increasing evidence suggesting that musical training alters the psychophysiological processing of complex sound, including speech. Given that speech sounds are typically perceived in a categorical manner, we reasoned that musicianship might also enhance the categorization/classification of speech and corresponding phonemic-level neural representations.

Methods

To this end, we compared cortical and brainstem event-related potentials (ERPs) elicited by a speech sound continuum in musician and nonmusician listeners.

Results

Behaviorally, musicians obtained steeper identification functions and classified speech sounds more rapidly (i.e., shorter reaction times) than their nonmusician counterparts. Analysis of the underlying neuroelectric activity revealed that relative to nonmusicians, musicians showed more robust and coherent phase-locking to speech formant energy in brainstem ERPs coupled with complementary increased magnitude (N1-P2 component) in cortical evoked responses. Identification functions derived from cortical potentials showed that neuronal activity could accurately predict listeners' perceptual boundary and phonetic classification of the speech continuum for both groups. While neural indices (e.g., magnitude) extracted from brainstem and cortical ERPs were correlated with behavioral measures across the

board, these brain-behavior associations were generally stronger in musically trained individuals

Conclusion

Results suggest that in addition to enhancing the overall salience of speech encoding at multiple tiers of the auditory pathway, musical training strengthens the coordination of processing between sensory and perceptual levels of the auditory brain. We infer that extensive musical training acts to refine a hierarchy of internalized representations for auditory objects thus supplying more faithful phonemic templates to the decision processes subserving speech sound identification.

932 Individual Differences in the Perception of Musical Consonance

Oliver Bones¹, Chris Plack¹, Kathryn Hopkins¹

¹University of Manchester

Background

A consonant sound is perceived as 'resolved', 'stable' and 'pleasant'. When two tones are played simultaneously (to produce a dyad), the frequency ratio between them determines the musical interval. Different intervals evoke differing degrees of consonance. Individual listeners have different preferences for consonant dyads over dissonant dyads. Individual preference for consonance correlates with preference for sounds with frequency components that closely fit a single harmonic series (McDermott et al 2010) suggesting that the perception of consonance may be related to the perception of harmonicity.

Neurons in the auditory pathway tend to synchronise their firing to periodic sounds, suggesting that pitch may be coded in the inter-spike intervals (ISIs) of neuronal firing patterns. Consonant musical intervals produce stronger representations of harmonically relevant periodicities in the ISI distribution of the auditory nerve than dissonant intervals, suggesting that this may be a sub-cortical mechanism contributing to the perception of consonance (Ebeling 2008; Bidelman and Krishnan 2009). It is therefore possible that individual differences in consonance correlate with individual differences in the neural representation of dyads.

Methods

We compared consonance ratings for both diotic and dichotic intervals to measures of the frequency-following response (FFR). The FFR is an electrophysiological measure of phase locking in the brainstem.

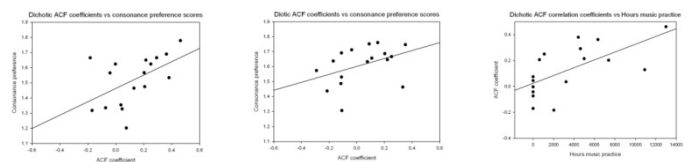
We used the procedure of McDermott et al (2010): individual preference for consonance for 19 normal hearing listeners with a range of musical experience was calculated by subtracting their average pleasantness rating of three dissonant dyads from their average rating of three consonant dyads. We then measured the FFR to a Perfect 5th musical dyad (a consonant interval) in order to assess individual sub-cortical temporal coding acuity. An autocorrelation function of each FFR was used to extract the strength of coding of stimulus periodicity.

Results

Individuals with a stronger preference for consonant musical dyads show a stronger representation of stimulus periodicity in the FFR for both diotic and dichotic dyads.

Conclusion

The results of this study demonstrate that more robust neural coding of pitch relevant periodicity at a subcortical level corresponds to a greater preference for consonance. The correlation was significant for both diotic and dichotic stimuli, providing support for models in which consonance is the consequence of increased neural synchronisation (Ebeling, 2008; Shapira Lots and Stone, 2008). The findings suggest that individual behavioural differences are driven in part by individual differences in how precisely populations of neurons are able to phase-lock to pitch-relevant periodicities.



933 Attention-Modulated Responses in the Cortex and Brainstem to Ongoing Speech Streams

Lenny Varghese¹, Barbara Shinn-Cunningham¹

¹Boston University

Background

Selective attention modulates neural activity recorded in the auditory cortex. However, little evidence exists that attention modulates activity in the auditory brainstem, despite the presence of efferent connections from auditory cortex to sub-cortical structures. To probe the effects of attention in both the cortex and the brainstem simultaneously, we recorded high-frequency EEG from listeners during a dichotic listening task using speech stimuli.

Methods

We recorded 32-channel EEG at 16,384 Hz from listeners selectively attending to one of two speech streams. Each speech stream consisted of a random string of digits (1-5). Listeners monitored one of the two streams for any occurrence of two back-to-back, consecutive digits within the ~60 s long stimuli. Onsets of digits within each stream were separated by 500 ms, and the mixture was presented such that the to-be-attended stream started 250 ms prior to the to-be-ignored stream (i.e., digits in the two streams alternated temporally, although they overlapped). To allow separation of the brainstem frequency following response (FFR) to each stream, stimuli were presented dichotically (one stream in each ear) and were each vocoded using pulse train carriers of differing repetition rates (97 and 113 Hz) and different frequency bands (so that each stream excited a distinct set of peripheral auditory filters). Half of all stimuli were reversed in polarity to enable analysis of the neural envelope and carrier FFRs. Responses to the

onset of each digit were examined in the time domain for the cortical response, and in the frequency domain for the FFRs.

Results

Cortical responses to attended and ignored digits showed large differences at most scalp electrode sites, although response morphologies varied across subjects. Applying a combination of PCA and SVM resulted in classification of attended and ignored responses at above-chance levels when small numbers of individual responses were averaged together. In contrast, brainstem envelope FFRs exhibited phase locking to the fundamental frequency of each stream for all subjects, but there were no systemic differences in the FFR strength in response to the streams depending on how attention was directed. No phase locking was observed in the carrier FFRs.

Conclusion

Despite inter-subject differences in response morphology, cortical responses were clearly modulated by selective attention. No such effects were seen in the brainstem response despite the care taken in designing stimuli to maximize the separability of the subcortical responses to the two streams.

934 The Role of Subcortical Encoding in Accounting for Speech Perception in Steady-State and Amplitude-Modulated Noise

Tim Schoof¹, Stuart Rosen¹

¹University College London

Background

One important factor that makes young normal-hearing listeners able to understand speech in a considerable amount of noise is the fact that they can 'listen in the dips' of time-varying maskers. This benefit has been hypothesised to depend upon accurate neural phase locking to the temporal fine structure to exploit periodicity in the target and/or masker, and upon the ability to track slower envelope fluctuations.

However, speech perception in noise not only depends on bottom-up auditory processing. The success of speech perception in both steady-state and amplitude-modulated noise also depends on higher order cognitive processes.

This study examines the relative contribution of both low level auditory processes and higher level cognitive processes to the perception of speech in noise. In particular, the role of subcortical encoding of speech in different types of maskers is assessed.

Methods

Auditory brainstem responses were measured in normal-hearing listeners to a steady-state vowel in quiet, steady-state speech-shaped noise (SSN), and amplitude-modulated speech-shaped noise (AMN). In addition, temporal processing abilities were assessed by measuring thresholds for gap detection, amplitude modulation detection, and frequency modulation detection. To assess

the contribution of cognitive factors, measures of processing speed, attention, and working memory were also obtained. Furthermore, a visual analogue of the speech perception in noise task was conducted (Text Reception Threshold). Of primary interest is the extent to which the various measures, both low and high level, correlate with listeners' abilities to perceive speech in SSN, AMN, and two-talker babble.

Results

Our pilot data indicate that voice pitch is less robustly encoded at the brainstem in background noise. Furthermore, in AMN the pitch may be more robustly encoded at the amplitude dip of the masker.

Conclusion

We expect to find that both low level auditory and higher level cognitive processes contribute to listeners' abilities to understand speech in noise. However, we expect that the robustness of subcortical encoding of speech will be the primary predictor for people's abilities to understand speech, especially in AMN. Subcortical encoding of speech is expected to be more robust in the dips of AMN. Furthermore, temporal processing abilities are expected to correlate highly with both subcortical encoding and speech understanding, particularly in AMN.

935 Hyperexcitability of Inferior Colliculus Neurons Caused by Acute Noise Exposure

Wei Sun¹, Yuguang Niu¹, Anand Kumaraguru¹

¹University at Buffalo

Background

Noise exposure is one of the most common causes of hearing loss. Recent studies found that noise exposure induced cochlear damage may change the excitability and tonotopic organization of the central auditory system (CAS). This plasticity was suspected to be related with tinnitus and hyperacusis. However, how cochlear damage affects CAS function and causes these neurologic diseases is still not clear. Since CAS function is activity dependent, we hypothesize that a restricted cochlear lesion might disrupt the balance of excitation and inhibition in the CAS, and therefore affect its neural activity.

Methods

Extracellular recording from the inferior colliculus (IC) neurons was recorded using a 16-channel microelectrode (NeuroNexus, A1x16-5mm-100-177) in anesthetized rats before and after the noise exposure. The multiunit discharges were recorded using OpenEx (TDT) software and the peri-stimulus time histograms (PSTH), frequency response areas (FRAs) and spiking rate level function were reconstructed using custom software. A narrow band noise (105 dB SPL, 20 kHz, 1000 Hz bandwidth) was presented by a high frequency speaker (FT28D) for 30 minutes to produce a restricted lesion in the cochlea.

Results

The noise exposure caused a dramatic decrease of the characteristic frequency (CF) in about 2/3 of the high

frequency neurons with/without causing a significant threshold shift. The noise exposure also caused an increase in firing rate of the low frequency neurons at super-threshold levels whereas it dramatically decreased the firing rate of the high frequency neurons. These results demonstrated that the hyperexcitability caused by noise exposure only occurred in the IC neurons tuned to frequencies lower than the noise exposure frequency; whereas the CF shift and tuning curve widening mainly happened in IC neurons tuned above the noise exposure frequency.

Conclusion

Our results suggest that noise exposure caused different plastic changes in IC neurons in different frequency regions. The reduced peripheral input following noise exposure may affect both the excitatory and the inhibitory circuits, especially the side-band inhibition at the lower edge of the noise exposure frequency, and affects the excitability and CF of IC neurons.

936 Pharmacological Activators and Inhibitors of Kv3.1 Potassium Currents

Maile Brown¹, Charles Large², Giuseppe Alvaro², Leonard Kaczmarek¹

¹Department of Pharmacology, Yale School of Medicine, New Haven, CT, ²Autifony Therapeutics, Imperial College Incubator, Level 1 Bessemer Building, London, UK

Background

Kv3 potassium channels are expressed in the auditory brainstem and in rapidly spiking neurons throughout the brain, where firing at high rates with high temporal accuracy is required for sensory processing. Kv3.1 channels typically activate at positive potentials and have a very rapid rate of activation and deactivation in response to transient depolarization.

Methods

We now report the first compounds to specifically modulate Kv3 channels. These compounds are imidazolidinedione derivatives, Compound 1 (AUT1) and Compound 2 (AUT2). We have performed whole cell patch clamp recordings of Kv3.1 channels.

Results

Using CHO cells stably expressing Kv3.1 channels, we have found that 10 μ M AUT1 shifts the voltage of activation of Kv3.1 currents towards negative potentials such that currents are activated around -20 mV and produce a 131% increase in current at test potentials of -10mV. Numerical simulations of the firing properties of auditory brainstem neurons, predict that increasing concentrations of AUT1 would be expected to decrease firing rate in response to high frequency stimulation (400 Hz), but to increase the temporal accuracy with which actions potentials are phase-locked to the stimuli. In contrast, 10 μ M AUT2 produced a sustained shift in voltage-dependence of inactivation to more negative potentials after three minutes of incubation, as well as altering voltage-dependence of activation. Although Kv3.1 channels usually inactivate only very

slowly during sustained depolarization, the rate of channel inactivation is also markedly increased in the presence of AUT2. Thus the net effect of this compound is to suppress Kv3.1 currents in the physiological range of membrane potentials. In numerical simulations, AUT2 had a biphasic effect on excitability. Low concentrations increased the rate of firing in response to 400 Hz stimulation whereas higher concentrations prevented neurons from responding to high-frequency stimulation, as is found in mice in which Kv3.1 has been deleted.

Conclusion

Pharmaceutical modulation of Kv3.1 currents represents a novel avenue for manipulation of neuronal excitability, and has the potential for therapeutic benefit in the treatment of hearing disorders associated with central auditory deficits.

937 Distribution of Vesicular Glutamate Transporters in the Cochlear Nucleus of C57

Mice

Chunhua Zeng¹, Mahfuzur Miah¹, Susan Shore¹

¹University of Michigan

Background

The cochlear nucleus (CN) is a multisensory integration center in the auditory pathway, receiving innervation from auditory and somatosensory structures. Vesicular glutamate transporters, VGLUT1 and VGLUT2, have distinct distributions in the CN in guinea pigs and rats: VGLUT1 is highly expressed in the magnocellular area of the ventral CN (VCN), whereas VGLUT2 is predominantly expressed in the granular cell domain (GCD), which includes DCN2 and shell region of the VCN. The GCD receives non-auditory inputs from somatosensory nuclei, including spinal trigeminal nucleus (Sp5) and cuneate nucleus (Cu). VGLUT1 and VGLUT2 have been used as the excellent markers to examine auditory nerve degeneration and somatosensory compensation after unilateral deafness in guinea pigs (Zeng et al., J. Neuroscience, 2009). C57 mice are prime candidates for genetic mutations in hearing system. However, the distributions of VGLUT1 and VGLUT2 have not yet been reported.

Methods

Here we examined the distributions of VGLUT1 and VGLUT2 in C57 mice in comparison with that in guinea pigs. Cresyl violet nissl stain was used to confirm the different layers and cell types in the CN. Metamorph software was used for quantification of VGLUT1 and VGLUT2 immunoreactivity in each CN region.

Results

The cytoarchitecture in the CN of C57 mice is similar to that of guinea pigs except for a large interstitial region (INT) in anteroventral CN (AVCN) in the C57 mice. The most intense VGLUT1 labeling in C57 mice was in the molecular layer of dorsal CN (DCN), shell region and magnocellular area of ventral CN (VCN), in contrast to less intense VGLUT1 labeling in the shell regions of guinea pigs. Like the guinea pig, the most intense VGLUT2

labeling in C57 mice was in the GCD, but VGLUT2 in C57 mice was more intense than guinea pigs in DCN3 and VCN. Similar to guinea pig, VGLUT2 was more intense than VGLUT1 in the DCN2 and DCN3, whereas VGLUT1 was more intense than VGLUT2 in the VCN and DCN1.

Conclusion

When compared with guinea pigs, VGLUT1 and VGLUT2 in C57 mice shows similar distribution in the CN, however, some regions show different intensities. This study will lay the foundation for studies of VGLUT distribution changes after deafness.

This work was Supported by grant R01 DC DC004825 and a core center grant P30 DC-05188.

938 Assessing the Relation Between Auditory Nerve Fibre Deafferentation, Hearing Threshold Increase, and Spontaneous Neuronal Hyperactivity

Lara Li Hesse¹, Warren Bakay², David McAlpine², Jennifer Linden², Roland Schaette²

¹Medical Faculty, University of Luebeck, ²UCL Ear Institute

Background

A recent study in mice has shown that normal hearing thresholds do not necessarily indicate the absence of cochlear damage; following temporary threshold shifts induced by noise exposure, a permanent reduction in wave I of the auditory brainstem response (ABR) is observed, together with deafferentation of auditory nerve fibres (ANFs) [Kujawa and Liberman (2009), *J. Neurosci* 29:14077-14085]. A similar reduction of ABR wave I has been observed in tinnitus subjects with normal audiograms, also suggestive of ANF deafferentation [Schaette and McAlpine (2011), *J. Neurosci* 31:13452-13457]. The amplitude of the centrally-generated wave V, however, was not reduced in the tinnitus group, suggesting a compensatory increase in neuronal response gain that might underlie the generation of a neuronal correlate of tinnitus.

Methods

CBA/Ca mice were exposed to an octave-band noise (8-16kHz) at either 96dB or 105dB SPL for 2 hours under anesthesia. ABRs were recorded pre-trauma, 1 day post-trauma, and 4 weeks post-trauma. Extracellular multiunit recordings from the inferior colliculus were obtained 4 weeks post-trauma. All recordings were performed under ketamine/medetomidine anaesthesia.

Results

For all trauma groups, ABR thresholds were significantly increased, and ABR wave amplitudes strongly reduced, 1 day post trauma. 4 weeks later, thresholds had recovered fully in the 96dB group, whereas the 105dB group still showed threshold elevations. The amplitudes of ABR wave I remained decreased in both groups, suggesting deafferentation of ANFs. Amplitudes of ABR waves II-IV remained below pre-trauma values in the 96dB group. However, in the 105 dB group, amplitudes of wave IV

recovered and reached pre-trauma levels at high sound intensities, suggesting a compensatory increase in neuronal response gain.

Extracellular multiunit recordings were obtained from the inferior colliculus 4 weeks post trauma. In the 96dB group, there was no significant increase in spontaneous firing rates. However, in the 105dB group, spontaneous firing rates showed a significant increase for neurons with tuning in the trauma frequency range, which was correlated with increased response thresholds.

Conclusion

The development of spontaneous neuronal hyperactivity in the inferior colliculus seems to require a minimum level of cochlear damage, demonstrating a non-linear relation between damage, plasticity, and spontaneous neuronal activity.

Acknowledgements

Supported by Boehringer Ingelheim Fonds, Action on Hearing Loss, and the British Tinnitus Association

939 Temporal Coherence Patterns in Auditory Cortex Neuronal Activity During an Auditory Streaming Paradigm

Brandon Farley¹, Arnaud Norena¹

¹Aix-Marseille University

Background

Auditory scene analysis refers to grouping or segregating features of a complex acoustic input in order to identify and process the underlying objects. Auditory streaming is a simplified version of this problem, where two alternating rhythmic stimuli are perceived as two separate "streams" or fused into one, depending on a number of defined factors. However, the physiological mechanisms underlying streaming are not understood. We tested the hypothesis that objects (i.e. streams) may be represented in auditory cortex by neural assemblies with temporally coherent activity patterns, whereas multiple objects may arise from multiple non-coherent assemblies.

Methods

We employed voltage-sensitive dye imaging to record ongoing subthreshold neural activity across multiple fields of the auditory cortex in anesthetized guinea pigs. Imaging was performed at a 250 Hz sampling rate with 100x100 imaging pixels that covered 10x10 mm of cortex. Each experiment began with measuring responses to pure-tone stimuli ranging from 0.5 - 32 kHz, to define the best-frequency of individual pixels and the full tonotopic organization of cortex.

Results

We found that in the presence of a single rhythmic (4 Hz) pure-tone stimulus, membrane potentials from regions representing that stimulus reliably entrained to the rhythm. The phase coherence of this 4 Hz activity was increased relative to a silence condition, across a 4-octave region of cortex. We next addressed temporal coherence patterns

in the presence of two out-of-phase rhythmic stimulus trains of pure-tones, as a function of their frequency difference (ΔF , from 1 to 18 semi-tones). We found that temporal coherence was largely dependent on ΔF : as ΔF increased, the two tones were represented by increasingly distinct (non-coherent) neural assemblies within individual areas. Temporal coherence did not depend on spatial segregation in cortex, as high coherence was also observed between distant subregions from separate cortical areas that shared best-frequency tuning. Finally, even at relatively large ΔF when temporally-distinct neural assemblies were present, some cortical regions were still responsive to both tones.

Conclusion

Our findings support a model whereby bottom-up object segregation may be enhanced by the formation of temporally incoherent neural assemblies. More specifically, the probability that two features will be grouped or segregated may vary with the degree of temporal coherence between neural assemblies representing those features, and intermediate values of coherence may be permissive for bistability.

940 Switching Auditory Attention Using Spatial and Non-Spatial Features Recruits Different Cortical Networks

Eric Larson¹, Adrian KC Lee^{1,2}

¹University of Washington, Institute for Learning and Brain Sciences, ²Department of Speech and Hearing Sciences

Background

Attention is a selective process that allows us to tune into one of potentially several possible sound sources of interest. In vision, the ability to flexibly redirect attention based on task goals and stimulus properties has been shown to involve a distributed cortical network including the right temporal-parietal junction (RTPJ), as well as multiple frontal areas including the frontal eye fields, which are involved both in gaze control and deploying attention. However, the cortical network controlling auditory attention has been studied less, and in particular, how attention might be directed to non-spatial stimulus features (such as pitch) is not clear.

Methods

Subjects performed a task where they counted the occurrences of a specific letter ("E") from one of two simultaneous talkers, each saying streams of six consecutive letters. Talkers were either spatially separated with the same pitch, or spatially collocated with different pitches. Subjects were cued at the beginning of the trial to attend to one talker (left, right, high pitch, or low pitch) for either the whole trial (maintain-attention condition) or for only the first half of the trial, switching to the other talker after three letters for the remainder of the trial (during a 600 ms gap period; switch-attention condition). Using magneto- and electro-encephalography combined with structural MRI information, we performed a within-subjects contrast of cortical activation when subjects maintained versus switched attention on both space and pitch trials.

Results

When switching versus maintaining auditory attention, using spatial stimulus features more strongly engaged RTPJ, consistent with previous results. However, when using non-spatial stimulus features, a distributed network including left auditory cortex and right frontal areas was more active.

Conclusion

Switching attention using spatial and non-spatial features differentially engages separate cortical networks. This suggests that top-down control of auditory attention involves the deployment of different processing strategies based on the stimulus features available for stream segregation.

This work was supported by NIH R00 DC010196 for AKCL.

941 Induced Gamma-Band Synchronization for Auditory Stream Segregation in Auditory Cortex of the Awake Rat

Takahiro Noda¹, Ryohei Kanzaki¹, Hirokazu Takahashi¹

¹University of Tokyo

Background

Perceptual segregation of alternating tone sequence differing in frequency (ABA-ABA-...) depends on the frequency differences (ΔF s) between A and B tones and the inter-tone intervals (ITIs) between successive tones as indicated in the van Noorden's perceptual boundary.

In the auditory cortex, tonotopic separation and forward suppression has been considered as possible neural underpinnings of this psychophysical phenomenon, which, however, cannot completely explain the phenomenon.

Recent studies have proposed that synchronized ensemble activities contribute to formation of perceptual objects. To investigate whether such processing is also critical for auditory streaming, multichannel recording methods are effective which meet requirements of both covering a targeted functional structure and achieving higher spatial resolution capable of evaluating correlation between neural ensembles in each functional structure. Secondly, it is important to examine how synchronized or desynchronized activities based on functional structure contribute to stream formation.

Methods

The present study developed a method that can acquire multiunit activities (MUAs) and local field potentials (LFPs) from auditory cortex of the awake rats with microelectrode arrays capable of covering auditory cortical fields with relatively high spatial sampling resolution. We investigated the relationship between oscillatory synchronization of LFPs or spike - LFP phase coupling and acoustic condition in ABA-tone sequence.

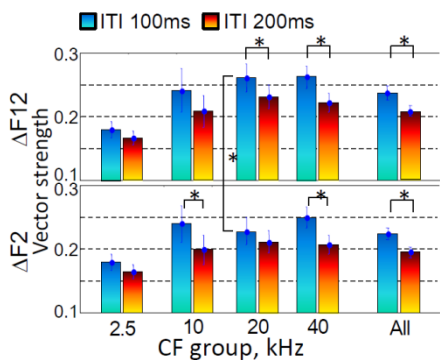
Results

Response magnitudes such as spike rate of MUA and amplitudes of raw / gamma-band LFP to A tone increased

with larger ΔF and longer ITI at recording sites selective to A-tone frequency, suggesting that tonotopic separation and forward suppression was most effective at the sites and not a correlate with the perceptual boundary. On the other hand, desynchronization across auditory cortical fields but tone selective synchrony was enhanced compared to those under anesthetized condition. Furthermore, different from evoked gamma-band oscillation, synchrony and power of induced gamma-band oscillation tended to be enhanced across neuronal ensembles selective to A tone under shorter ITI and larger ΔF . Especially spike - phase coupling significantly increased under those conditions, suggesting that these neuronal characteristics were closely correlated with the perceptual boundary.

Conclusion

Not transient but phase synchrony, spike-phase coupling or sustained power of induced gamma-band oscillation are possible neuronal representations of the perceptual boundary of auditory streaming.



942 Re-Examining the Evidence for a Neural Representation of Pitch in Human Auditory Cortex

Karima Susi¹, Deborah Hall², Andrew Dunn¹, Preethi Premkumar¹, Andrew Oxenham³

¹Nottingham Trent University, ²NIHR Nottingham Hearing Biomedical Research Unit, ³University of Minnesota

Background

A number of functional criteria have been proposed for defining a human pitch center including: (1) greater activation for a pitch-evoking stimulus than for a matched control, and (2) greater activation for a strong pitch percept than a weak one. Some human investigations using functional magnetic resonance imaging attribute such patterns of pitch-related activity to lateral Heschl's gyrus, but not all. In particular, Penagos and colleagues (2004) report sensitivity to pitch salience in this region, but used a small sample size ($n = 5$) that precluded group statistics.

Methods

The current replication reports a larger sample size, allowing group-level analysis and generalizability of results. Eighteen listeners (right-handed; 9 females) were scanned during passive listening. Four harmonic-complex

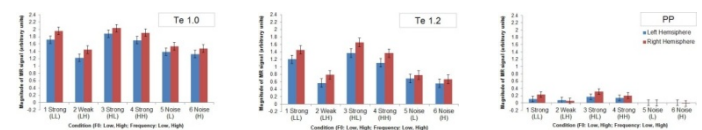
tone conditions (3 strong in pitch salience, 1 weak in pitch salience) were presented, plus two spectrally matched 'no pitch' noise controls and a silent baseline condition. Signals were presented in a noise background to reduce cochlear distortions. Each sound condition was a 32-s dynamic sequence where the pitch varied within a given narrow range. Image data were analysed using SPM8 and subjected to random-effects group analysis, incidence mapping and region-of-interest analysis.

Results

In the group analysis, pitch- and salience-related activity were defined by the contrasts 'pitch>noise' and 'strong>weak', respectively. Both these contrasts showed differential activity which was reliable across the group ($p < 0.001$, uncorrected) and widespread across auditory cortex. However incidence mapping revealed that this spatial distribution was not consistent in every listener (individual level $p < 0.01$, uncorrected), which highlights the risks of generalising from a few participants. Region-of-interest analysis confirmed that the resolved complex tone conditions (strong pitch) elicited much greater activity than unresolved (weak pitch) and matched noise controls. Although the response to the unresolved complex>noise was small, the incidence map did show that a differential effect was present in some listeners, thus confirming some degree of sensitivity to pitch salience within these regions. Interestingly, planum polare showed a significant right hemisphere preference for resolved complexes, which was not observed for the other sound conditions or brain regions.

Conclusion

Our findings broadly support Penagos, but extend current knowledge. (1) Neural representations of both pitch and pitch salience are co-localized within *multiple regions* of human auditory cortex. (2) Presenting pitch signals as a random melody sequence promotes right hemispheric involvement in planum polare. Not only do these results support pitch coding in auditory cortex, but also provide further evidence for a processing hierarchy.



943 Predicting the Attended Speech Stream from the Ongoing EEG Response in a Cocktail Party Paradigm

Siddharth Rajaram¹, Edmund Lalor², Barbara Shinn-Cunningham¹

¹Boston University, ²Trinity College Dublin

Background

In this study we aim to identify which of two ongoing speech streams a listener is attending using electroencephalography (EEG). The majority of work done in classification of auditory attention using EEG has used regular sequences of simple stimuli like noise or tone bursts, which evoke clear onset responses that are

modulated by attention. We classify the attended stimulus by correlating the EEG response to the known envelopes of the speech stimuli using time-lagged canonical correlation analysis (CCA).

Methods

Data were collected for a previous study [Power et al., *Eur. J. Neurosci.* 35(9), 2012] in which EEG was recorded while subjects attended to one of two audiobooks, presented dichotically (one to each ear) at equal intensities. EEG was recorded using a 128-channel cap (downsampled to 32) with a BioSemi ActiveTwo system, at a sampling rate of 512Hz. The stimuli were presented in approximately thirty 60s blocks. Subjects had to answer questions about both stories to confirm that they attended to the desired one. We projected out blink artifacts in the EEG using the signal space projection method and applied a high pass filter at 1Hz. We then performed CCA at all possible time lags on the training data, and picked the lag and spatial weighting that yielded the maximum canonical correlation with the speech envelope. The test data were then weighted with the spatial weights and correlated with the envelope of the two, competing speech streams in the test block at the optimal lag. The stimulus with the largest correlation value was classified as the attended speech stream. Performance for each of three classifiers was compared: trained to the attended stream, the unattended stream, or the sum of the two streams. A leave-one-out cross validation was used on the blocks.

Results

Preliminary results indicate that training the canonical correlation classifiers at longer lags (between 160-240ms) yields a more accurate classification of the attended stream (82.21% +/- 4.71% standard error across subjects) than at shorter lags in the 60-140ms range (65.57% +/- 4.99% standard error across subjects).

Conclusion

Prior EEG studies that classify which of multiple concurrent stream is being attended by a subject use attentional modulation of the N100 (which occurs 100ms after stimulus presentation). We show that for continuous speech, later evoked potentials (around 200ms) are better at differentiating which stream a listener attended.

944 Exploring the Perception and Neural Representation of Vowels in Ferrets

Stephen Town¹, Katherine Wood¹, Huriye Atilgan¹, Jennifer Bizley¹

¹UCL Ear Institute

Background

Object identification depends upon the exploitation of variation in object properties. In speech, vowels can be distinguished on the basis of formant frequencies – peaks in the spectral envelope introduced during articulation. Specifically, the location of first (F1) and second formants (F2) and distance between formants (F2-F1) offer cues for vowel identification across different talkers and voice pitches [Peterson GE, Barney HL (1952), Kewley-Port D,

et al. (1996)]. Vowel identification can be studied at behavioral and neuronal levels using animal models such as the ferret: Ferrets can identify vowels differing in F1 and F2 and the spectral envelope of such vowels modulate the responses of neurons across ferret auditory cortex [Bizley JK, et al. (2009); Walker KM, et al. (2011); Bizley JK et al. (In Press)].

Methods

Here, we describe results from behavioral and neurophysiological investigations of vowel discrimination in ferrets. In our behavioral study, ferrets (n = 4) were trained to associate water rewards at different locations with two artificial vowels that differed in F1 and F2 positions. Subjects were then presented with probe trials in which the F1, F2 or F2-F1 of training vowels were swapped. In our neurophysiological study, the same stimulus set of vowels and probes were presented to untrained anesthetized ferrets (n = 3) whilst multi-unit responses were recorded from auditory cortex.

Results

Trained ferrets responded to mismatch vowels more frequently at the location previously associated with F2 than F1. Discriminability (d') between vowel pairs was also positively correlated with F2 separation between vowels. Neither F1 separation nor F2-F1 separation was correlated with discriminability. Neural discriminability was measured as spike distance between PSTH responses to vowel pairs. Spike distance was well correlated with F1, F2 or F2-F1 separation between vowels in a subpopulation of vowel-sensitive units (29/84; 35%). However in the majority of vowel-sensitive units (55/84; 65%), discrimination was only weakly correlated with cue separation.

Conclusion

These findings suggest that F2 position may disproportionately influence the perception and discriminability of vowels in ferrets. The underlying physiological basis for such behavior may involve the contributions of cue separation sensitive units observed here; however this will require further examination in trained, behaving animals.

945 Electrophysiology and Perception of Speech in Noise: Effects of Age and Hearing Impairment

Curtis J. Billings^{1,2}, Tina Penman¹

¹National Center for Rehabilitative Auditory Research (NCRAR), Portland VA Medical Center, ²Department of Otolaryngology/Head & Neck Surgery, Oregon Health & Science University

Background

A common complaint of individuals with hearing impairment and older individuals is difficulty understanding speech in background noise. Despite being such a common problem, perception in noise difficulties are often not addressed clinically, leaving the affected population to suffer with decreased communication, additional stress,

decreased participation in social activities, and poorer quality of life. Our approach is to use a combination of brain and behavioral measures to better our understanding of performance variability across individuals as a means of improving diagnosis and individualizing treatment. By measuring the ability of the brain to encode speech in noise we can begin to determine what neural information is available to the listener to ultimately understand speech in a noisy environment. Recent electrophysiological studies demonstrate that signal-to-noise ratio (SNR) is an important factor contributing to the timing and amplitude of cortical auditory evoked potentials (CAEPs) in young, normal-hearing individuals. The purpose of this study was to extend those previous CAEP findings, by testing older, hearing-impaired individuals and to explore the relationship between CAEPs and behavioral responses.

Methods

CAEPs and behavior measures were collected from 15 younger normal-hearing individuals, 15 older normal-hearing individuals, and 15 older hearing-impaired individuals using signal-in-noise stimuli. CAEP measures included the passively elicited P1-N1-P2 complex, which was elicited by a 1000-Hz tone and the syllable /ba/. Behavioral measures included sentence-level and word-level stimuli presented in noise. Target signals were presented at four levels (50-80 dB in 10 dB increments) in steady-state speech spectrum noise that was also varied in level (40 to 90 dB) resulting in signal-to-noise ratios of -10 to 35 dB.

Results

Results from these studies demonstrate that key factors affecting neural coding and perception of speech in noise include signal type, signal-to-noise ratio, age, and hearing status. In addition, more robust and synchronous neural coding is associated with better understanding in noise. Significant correlations were found between CAEP measures and perception-in-noise measures. Differences in sensitivity between the two measures will also be discussed.

Conclusion

Further examination of the important factors affecting brain and behavior and investigation of the relationship between these two measures will improve our understanding of speech perception-in-noise difficulties and help us to improve diagnosis and treatment of individuals with these problems. [Research supported by VA/RR&D (C6971M, C4844C) and the NIH/NIDCD (R03DC010914)]

946 The Effect of Attention and Temporal Shift on the Build-Up of Auditory Streaming: A Concurrent EEG and Subjective Study

Anahita Mehta¹, Ifat Yasin¹

¹University College London

Background

Auditory streaming tends to “build-up” over time with a tendency for listeners to perceive two streams increasing with sequence duration (Anstis and Saida, 1985). In

addition, imposing a frequency or temporal shift mid-ABA sequence may influence stream segregation (Chakalov et al., 2012). The aim of the present study was to obtain a measure of the disruption to auditory streaming build-up by imposing a temporal shift near the beginning, or close to the end of, an ABA-sequence under different conditions of attention. The magnetoencephalographic negative wave N1m may be used as an indicator of auditory stream segregation (Gutschalk et al., 2005). When the repeating sequence of a pure-tone triplet (ABA-) is perceived as a single stream, the N1m amplitude is relatively small and consistent with the inter-stimulus-interval (ISI) between successive tones, when the sequence is perceived as segregated, the N1m amplitude is relatively large and consistent with the longer ISI between tones of each segregated stream. The present study used the electroencephalographic (EEG) equivalent, wave N1 to investigate stream segregation using a combined EEG and psychophysical test approach.

Methods

The stimuli were 9-sec sequences of repeating ABA triplets, where A= 1260 Hz, B=1000 Hz and $\Delta f = 4$ semitones. A temporal shift of 40 msec was imposed on the B tone in either the 4th triplet (early condition) or the 11th triplet (late condition). The control condition had no temporal shift imposed on the B tone. For each temporal shift condition, participants were instructed to focus on an integrated or segregated percept. Participants responded by button-press to indicate if one or two streams were perceived whilst EEG recordings were obtained using a 32-electrode array. Fifteen participants participated and EEG and subjective responses were recorded concurrently.

Results

Results indicate a difference in the N1 amplitude between the attention conditions, when the temporal shift is imposed early, rather than later, in the ABA sequence.

Conclusion

The EEG and subjective responses appear to concur; allocating attention to either an integrated or segregated percept affects the detection of a temporal shift imposed on and ABA sequence, particularly so early on in the sequence, rather than later in the sequence.

947 A Computational Model of Spatial Tuning in the Auditory Cortex in Response to Competing Sound Sources

Junzi Dong¹, Steven Colburn¹, Kamal Sen¹

¹Hearing Research Center and Biomedical Engineering Department, Boston University

Background

To better understand sound localization in the auditory system, much work has been done on the spatial tuning of single neurons along the auditory pathway. It has been established that single neurons in the midbrain are sharply tuned to preferred directions, while cortical neurons show much broader tuning. A recent experiment on cortical

responses in birds found evidence of spatial tuning to multiple competing sounds in the cortex (Maddox RK et al. Competing Sound Sources Reveal Spatial Effects in Cortical Processing. PLoS Biol. 2012). This study described situations in which cortical neurons show broad tuning to single location stimuli, but develop spatial preference in response to a second competing noise source. In the current study, we construct a computational model to explore how a cortical network can utilize sharp spatial tuning in its inputs to extract the locations of competing stimuli in a noisy environment.

Methods

The model cortical network receives inputs from spatially tuned neurons from an input layer. The spike rates of the input layer neurons are implemented using cross-correlation and time delay methods, followed by a spike generator. A mid-layer of interneurons receives inputs from input layer neurons, and synapses onto cortical neurons. Both interneurons and cortical neurons are implemented using integrate-and-fire models. The time course and magnitude of excitatory post-synaptic currents (EPSC) and inhibitory post-synaptic currents (IPSC) at the synapses were varied. The output of the model is the response of the cortical neurons to competing sounds.

Results

The model demonstrates broad tuning to single sounds, and develops spatial preference when a second competing noise is presented. Spatial tuning to masked stimuli is achieved by the suppression of neurons tuned to non-preferred directions by neurons tuned to preferred directions. The slower decay in IPSC relative to EPSC is important in order for response to the preferred direction to take dominance.

Conclusion

This study proposes a cortical mechanism of sound localization in noise. The model suggests that, in noisy environments, multi-neuron networks may be able “tune in” to their preferred source. This may be the functional basis of spatial location and noise separation in the auditory system, and could be a key component in understanding more complex behavioral phenomena such as the cocktail party effect.

Acknowledgement

Work supported by NIH/NIDCD; grant R01 DC00100

948 Cortical Pitch Regions Respond Primarily to Resolved Harmonics Once Distortion Products Are Masked

Sam Norman-Haignere^{1,2}, Nancy Kanwisher^{1,2}, Josh McDermott¹

¹Department of Brain and Cognitive Sciences, Massachusetts Institute of Technology, ²McGovern Institute for Brain Research, Massachusetts Institute of Technology

Background

Pitch is a defining perceptual property of many real-world sounds. Classically, theories of pitch perception have differentiated between temporal and spectral cues. These cues are rendered distinct by the frequency resolution of the ear, such that some frequencies produce “resolved” peaks of excitation in the cochlea, while others are “unresolved”, providing a pitch cue only via their temporal fluctuations. Behaviorally, unresolved harmonics on their own produce a weak pitch relative to resolved harmonics. Human neuroimaging studies, in contrast, have often reported strong responses to the temporal cues conveyed by unresolved pitch stimuli. One possibility is that many of these studies were influenced by ‘distortion products’ - frequency components introduced by nonlinearities in the ear that can effectively act as resolved harmonics. Here we use fMRI to test the relative contribution of resolved harmonics, unresolved harmonics, and distortion products to the response of cortical regions sensitive to pitch.

Methods

We first searched for brain regions in each subject that responded more to pitch stimuli compared with noise, irrespective of resolvability, and we then compared responses to resolved and unresolved harmonics using independent data from these same regions. Every condition was scanned with and without low-frequency noise designed to mask distortion products. This design allowed us to test whether masking noise enhances response differences between resolved and unresolved harmonics, as would be expected if distortion products generated by unresolved harmonics are effectively treated as resolved frequency components.

Results

We report: 1) Consistent with previous reports, all 23 subjects tested exhibited pitch-sensitive regions that responded more to harmonic tones than noise; these regions were predominantly localized to low-frequency and non-tonotopic regions of anterior auditory cortex. 2) These regions were driven primarily by spectrally resolved harmonics, although they also produced a weak but consistent response to unresolved harmonics relative to frequency-matched noise. 3) Notably, this response preference for resolved harmonics was only observed with concurrent noise designed to mask distortion products. Without masking noise, we observed strong responses to harmonic tones irrespective of resolvability, suggesting that distortion products have a surprisingly large effect on the cortical response, effectively acting as resolved frequency components and potentially explaining

previously observed responses to pitch in the absence of spectral cues.

Conclusion

Our results suggest that resolved spectral information is critical to the response of pitch-sensitive brain regions and that resolved distortion products substantially enhance cortical responses to unresolved pitch stimuli when not masked.

949 Neural Correlate of Time Shift Detection in an ABA- Streaming Paradigm in the European Starling

Naoya Itatani¹, Georg M. Klump¹

¹*Animal Physiology & Behavior Group, Carl-von-Ossietzky University Oldenburg, Germany*

Background

Segregating or integrating sounds from multiple sources is a crucial task of the auditory system for survival. For studying the mechanism of auditory scene analysis, sequences of two alternating tones are commonly used as stimuli (ABA-, A and B being different tones, - indicating a longer temporal gap). Using such stimuli, van Noorden (1975) reported that the temporal shift of the middle B tone in ABA- triplets was more easily detected when the consecutive sounds were perceived as one stream (fusion) compared to the situation where the sounds were heard as two streams (fission). The European starling (*Sturnus vulgaris*) showed a similar ability to detect the time shift of middle tones in a triplet depending on the frequency separation between consecutive tones suggesting a similar perception of stream segregation (Itatani, Cordes and Klump 2011). The change in neuronal representation in relation to fission or fusion, however, is still unclear. Here we combined the behavioral and physiological observations using the European starling to investigate the neural correlate of perceptual stream segregation.

Methods

Three European starlings were trained to respond to the time shift of B tones in ABA- tone triplets in an operant Go-NoGo task. Platinum-iridium electrodes were chronically implanted into the field L complex being homologous to the mammalian primary auditory cortex. During the behavioral experiment, spike responses were recorded using a radio telemetry system. The frequencies of the A and B tones were set so that their frequency separation was 0, 6 or 12 semitones. The amount of the time shift of the B tone was varied between 10 and 90%. For constructing neurometric functions, spike responses in each time shift condition were compared.

Results

The ongoing data collection suggests similar patterns of change of the d' values of the psychometric and neurometric functions, which increased as the amount of the time shift increased. In general, the d' values in neurometric function dropped if the frequency separation between two tones was increased.

Conclusion

The results suggest that in the European starling the representation of time shifts by the spike responses for different frequency separations of the tones are correlated with the behavioral observation of the accuracy of detecting a time shift.

950 Neuronal Representation of Temporal Regularity Associated with Pitch Perception in Macaque Auditory Cortex

Yukiko Kikuchi¹, Sukhbinder Kumar², Simon Baumann¹, Tobias Overath³, Timothy D. Griffiths^{1,2}, Christopher I. Petkov¹

¹*Inst. of Neurosci., Newcastle Univ. Med. Sch.*, ²*Wellcome Trust Ctr. for Neuroimaging, Univ. Col. London*, ³*Ear institute, Univ. Col. London*

Background

Pitch is an auditory percept that requires neural representations of both stimulus regularity and perceived pitch. Recent human studies using direct recordings of local field potentials (LFPs) in the auditory cortex along Heschl's gyrus show that time-locked responses correlate with the temporal regularity of the stimulus, whereas sustained gamma oscillations correlate with perceived pitch (Griffiths et al., 2010; Sedley et al., 2012). The present study in a primate model system examined temporal regularity associated with pitch at both the single-unit level and at the level of cell assemblies (LFPs).

Methods

Stimuli contained a transition between noise and either a noise with a regular repetitive structure in time, known as a regular interval noise (RIN), or a harmonic complex, at seven different rates (i.e., 8, 16, 32, 64, 128, 256, and 512 Hz). Comparing neuronal responses above and below the lower limit of pitch (approximately 30 Hz) allows differentiation of responses related to pitch as opposed to stimulus regularity. LFPs were analysed for evoked potentials and time-frequency analysis.

Results

Single-unit activity (116 neurons) and LFPs (82 sites) were recorded simultaneously from the core and the lateral belt (LB) of macaque auditory cortex identified using fMRI. Evoked responses time-locked to the stimulus regularity were observed both below and above the lower limit of pitch, whereas induced, non-time locked, high-gamma (> 70 Hz) responses associated with the transition from noise to RIN were observed particularly for rates above the lower limit of pitch. Neuronal tuning specific to the different rates of the RIN and harmonic complex stimuli was compared at the level of single-units and LFP. The tuning of single units was sharper compared to LFP, yet both types of neuronal responses exhibited tuning above the lower limit of pitch, associated with pitch perception. There were some stimulus specific differences: (i) the magnitude of responses was stronger to the RIN than to the harmonic complexes, and (ii) responses to the RIN were sustained compared to the transient nature of response to the harmonic complexes.

Conclusion

The results seem to be topographically distributed in that the stimulus-regularity related responses were observed mainly in the AI, whereas the induced high-gamma responses related to the pitch percept were observed lateral to this in the belt. These results complement those from the recordings of LFPs in humans and provide insights into how single neuronal responses might support pitch perception.

951 MEG Correlates of Pitch Perception in Human Auditory Cortex

Tobias Overath¹, Sukhbinder Kumar¹, Will Sedley², Sundeep Teki¹, Tim Griffiths²

¹University College London, ²Newcastle University

Background

Despite its ubiquity in speech and music, the cortical origins and neural mechanisms underlying pitch perception are still not well understood. While some researchers have shown cortical correlates of pitch in lateral Heschl's gyrus (HG) (Patterson et al., 2002; Penagos et al., 2005; Pushmann et al., 2010), others argue for a locus in planum temporale (PT) (Hall & Plack, 2009). A more distributed representation of pitch along the HG has also been argued (Griffiths et al., 2010), where different parts of HG have specific functions within a pitch system (Kumar et al., 2011). The predicted properties of such a 'pitch centre' (or higher-order 'predictive centre' in the pitch system) are that a) activity should be similar across different pitch types, e.g. harmonic complex (HC), clicktrain (CT), and regular-interval noise (RIN); and b) for each pitch type, activity will occur for a transition between a spectrally matched control stimulus (noise) and a pitch stimulus.

Methods

We used three different pitch types (HC, CT, RIN) and two different regularity rates (20 and 250 Hz), one below and one above the lower limit of pitch (Krumbholz et al., 2000). The stimuli used unresolved harmonics (including masking noise below the lowest harmonic) and spectra were 1-over-f shaped with a range between 15-3000 Hz. Participants listened passively to contiguous segments of either regular-noise-regular or noise-regular-noise stimuli.

Results

The results revealed a strong transition response from noise to pitch (250 Hz) for all three pitch types with a latency of ~130ms and an N100m-like topography. The opposite transition resulted in a P50m-N100m complex for transitions from HC and CT, while transitions from RIN did not yield any evoked response (see also Lütkenhöner et al., 2011). In contrast, transitions from noise to 20Hz regularity were generally much weaker (HC, CT) and non-existent for transitions to RIN. The opposite transition again resulted in a weaker P50m-N100m complex (HC, CT), with the exception of transitions from RIN.

Conclusion

The results confirm both of the predicted properties in that the response is similar for all three different pitch types used here and is specific to that transition, i.e. is different from the reverse transition. Analyses of the time-frequency response and beamforming algorithms are ongoing and will shed light on the cortical origins of these responses.

952 Cortical Pitch Response: Differential Sensitivity to Pitch Contour and Pitch Direction

Ananthanarayan Krishnan¹, Saradha Ananthakrishnan¹, Jackson Gandour¹

¹Purdue University

Background

Voice pitch is an important information-bearing component of language and music that is subject to experience-dependent plasticity at both cortical and subcortical stages of processing. The components of the scalp-recorded cortical pitch response (CPR), reflecting synchronized neural activity relevant to pitch in the lateral Heschl's gyrus (the presumed site of pitch processing), may provide a new and complementary window to examine experience-dependent enhancements in pitch encoding previously observed in musicians and tone language speakers at the level of the brainstem and to shed more light on the hierarchical nature of pitch processing along the auditory pathways. We recently demonstrated that the CPR is sensitive to both pitch and its salience. Here we examine the sensitivity of the CPR components to changes in pitch contour, and pitch direction that are characteristic of lexical mandarin tones.

Methods

Cortical pitch (CPR) responses were evoked from 10 Chinese listeners in response to three IRN stimuli with: (1) a flat steady state pitch (SS); (2) a rising pitch contour approximating Mandarin lexical tone 2 (T2); and (3) a falling pitch contour approximating Mandarin lexical tone 4 (T4). Pitch specific response components were isolated by preceding the 250 ms IRN (evoking a pitch response) stimuli by a 500 ms noise precursor (evoking only the obligatory onset responses). Stimuli were presented binaurally at 80 dB SPL at a repetition rate of 0.93/sec.

Results

CPR response amplitude systematically varied with pitch contour and pitch direction with T2 eliciting the largest pitch response followed by T4, and the steady state stimulus eliciting the smallest CPR component with poorly defined response morphology. In addition, response to T4 exhibited the shortest latency followed by T2, with the response latency for the steady state stimulus being the longest. These results suggest that the CPR is differentially sensitive to both pitch contour and pitch direction.

Conclusion

Results are consistent with the notion that the CPR reflects neural activity relevant to pitch that is differentially

sensitive to certain pitch attributes (steady state vs. dynamic pitch; and rising vs. falling contour of pitch). Thus, the CPR, along with the brainstem frequency following response, provides a physiologic window to evaluate the hierarchical organization of early sensory level pitch processing at the cortical and brainstem levels that is subject to experience-dependent plasticity.

953 Functional NIRS Measurements of Auditory, Visual and Somatosensory Responses in Normal-Hearing Individuals

Rebecca Dewey^{1,2}, Douglas Hartley^{1,3}

¹Division of Otorhinolaryngology, The University of Nottingham, ²Nottingham Hearing Biomedical Research Unit, ³MRC Institute of Hearing Research

Background

Deafness induces crossmodal reorganisation within the auditory cortex. Electrophysiology and functional neuroimaging studies suggest a link between cortical crossmodal activation patterns and cochlear implant performance. However, electrical artefacts and implant magnets confound EEG and fMRI recordings respectively. Near-infrared spectroscopy (NIRS) is suited to auditory neuroimaging following cochlear implantation since it is unaffected by electrical artefacts and the implant magnet. NIRS has been used successfully to assess auditory-evoked cortical responses in deaf children with cochlear implants. We present preliminary NIRS data from a study of multisensory responses (visual, auditory and somatosensory) in 10 normal-hearing adult participants (mean age 33±9 years, n=4 male).

Methods

Auditory stimuli consisted of sinusoidal amplitude-modulated (10Hz; 100% modulated) or unmodulated broadband noise at 80dB SPL. Visual stimuli consisted of 1000 white dots on a black background that were randomly flashing or coherently moving. Somatosensory stimuli were delivered to the palms of both hands via a custom-made vibrotactile stimulator. These consisted of 10Hz or 20Hz sinusoidal vibrations. Auditory, visual and somatosensory stimuli of duration 20s were presented five times each in a pseudorandom order, interleaved with rest periods (20s). NIRS data were acquired using a 24-channel Hitachi ETG4000 system. All data were preprocessed and statistically analysed using NIRS-SPM software and general-linear-modelling techniques.

Results

Cortical responses were successfully recorded in auditory (n=8), visual (n=9) and somatosensory (n=6) modalities. HbT changes in the temporal lobe, occipital lobe and post-central gyrus from a representative subject are shown (Fig1). Auditory stimuli: 6 of 8 subjects exhibited areas in the temporal lobe with significantly greater HbT responses to modulated, compared with unmodulated noise. Visual stimuli: 6 of 9 participants showed areas in the occipital lobe with greater cortical response to coherent-moving, compared with random dots. Somatosensory stimuli: 20Hz vibration, compared with 10Hz, produced significantly

greater responses in the region of the postcentral gyrus in 3 of 6 participants. Statistics significant to $p < 0.05$; expected EC correction.

Conclusion

We successfully recorded cortical responses in auditory, visual and somatosensory modalities. Our future studies will use a similar paradigm to assess crossmodal activity in the auditory cortex of profoundly deaf adult subjects with and without a cochlear implant. We hypothesise that crossmodal activity measured in deaf individuals using NIRS may provide a useful prognostic indicator of performance following cochlear implantation.

This work is supported by the University of Nottingham and the NIHR.

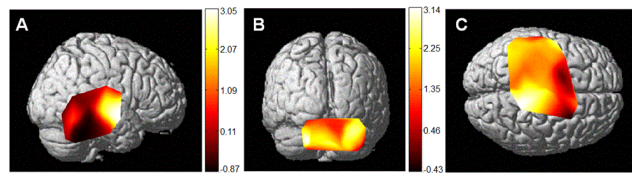


Figure 1: HbT changes: (A) temporal lobe response to auditory stimuli (10 Hz amplitude modulated noise > unmodulated noise), (B) occipital lobe response to visual stimuli (coherently moving > random dots), (C) post-central gyrus response to somatosensory stimuli (20 Hz > 10 Hz vibrotactile). Colour bars show values of T statistic.

954 Crossmodal Influences on Steady-State Responses in a Subjective Audio-Visual Binding Task

Ross Maddox¹, Adrian KC Lee^{1,2}

¹University of Washington Institute for Learning & Brain Sciences, ²University of Washington Speech & Hearing Sciences

Background

When faced with a crowded auditory scene, such as the canonical cocktail party, speech can be better understood when a listener is able to see the talker's face. In this situation, the talker's voice and moving mouth vary coherently in time and are often perceived as "bound" together into one crossmodal object, an important phenomenon for understanding the sensory world. Much of the behavioral work examining crossmodal effects has focused on illusions, such as the McGurk effect. Electrophysiology has shown a number of brain regions to respond to both auditory and visual stimuli, and a subset of those regions show crossmodal interactions. Here we investigated binding based crossmodal temporal correlations, using human neuroimaging and stimuli created to share some of speech's properties, but to be free of the linguistic confounds of the cocktail party.

Methods

Neural activity was recorded using magneto- and electroencephalography (M-EEG). Auditory stimuli consisted of an amplitude-modulated (AM) tone complex; visual stimuli consisted of a radius-modulated disc on a black background. The modulation envelopes were created by low-passing noise at 6 Hz. On each trial, the tone amplitude and the disc radius changed in one of three temporal relationships: larger amplitude, larger radius (0-phase); larger amplitude, smaller radius (pi-phase), and no

relationship (ind-phase). Listeners were asked to answer the question, "Did the visual and auditory stimuli change as one?" in order to determine if binding was perceived. Additionally, auditory stimuli were "tagged" by applying sinusoidal AM at 37 Hz and visual stimuli were tagged by sinusoidally modulating the intensity of the center of the disc at 10 Hz, facilitating steady-state analysis (e.g., phase-locking value, PLV). Anatomically-constrained inverse imaging was used to localize data on the cortical surface.

Results

Listeners perceived binding much more frequently in the 0-phase and pi-phase conditions than in the ind-phase condition. The 0-phase condition was reported to bind slightly more often than the pi-phase condition. Additionally, some cortical regions showed significant steady-state differences between bound and unbound conditions.

Conclusion

It is possible to create stimuli for which listeners report strong binding. By tagging different modalities with orthogonal frequencies and using inverse imaging, we are able to create a cortical map of the crossmodal effects of binding.

This work was supported by Grant No. R00 DC010196 for AKCL and T32 DC005361 for RKM from NIH.

955 Cross-Modal Alterations to Receptive Field Properties of the Auditory Cortex

Adam P Jones¹, Amal Isaiyah^{1,2}, Patrick O Kanold¹

¹Dept of Biology, University of Maryland College Park,

²Dept of Oto-HNS, University of Maryland Medical Center

Background

Sensory integration occurs across various sensory systems and is observed in primary sensory cortices. Such cross-modal inputs might provide substrates for cross-modal compensation in the event of losing one of the sensory modalities. For example, losing vision not only alters the functionality of the visual cortex, but is also known to affect other sensory systems. Prior in-vitro studies of circuit-level changes in auditory cortex (ACX) showed global changes in synaptic transmission following light deprivation (Goel et al., 2006).

Methods

We investigated the functional consequences of these synaptic changes by examining sound-evoked responses of ACX neurons in-vivo using electrophysiological recordings and 2-photon imaging in mice that had been light-deprived for 5-10 days.

Results

We found fundamental alterations of key metrics of sound-evoked neuronal activity in dark-reared (DR) mice with observed differences between cortical layers. Driven firing rates, signal-to-noise ratios and slopes of rate-level functions of ACX neurons were significantly increased.

Furthermore, there were significant alterations in frequency tuning properties of neurons within ACX.

Conclusion

We conclude that the functional alterations seen in the auditory cortex as a result of dark-rearing represents cross-modal compensation in the form of improved representation of auditory information. These changes may point towards potential for strategies such as visual deprivation that may be used for recovery of sensory function in other affected modalities, to possibly counter the effects of maladaptive changes in sensory processing.

956 Source Localization of the N1 Potential After Visual and Auditory Inhibition

Allison Bradley¹, Jun Yao¹, Jules Dewald¹, Claus-Peter Richter¹

¹Northwestern University

Background

In response to an auditory stimulus train, the N1 potential of the cortical auditory evoked potential in response to later stimuli of the train has been shown to reduce in amplitude as compared to the first one. This phenomenon has been related to lateral inhibition. The reduction in the amplitude of the N1 potential has also been shown if an auditory stimulus is preceded by a stimulus in another sensory modality, such as a visual stimulus. This indicates that the lateral inhibition may not be specific to the auditory system, but originates from a source or multiples sources that respond to multiple sensory modalities. This is of particular interest as the extent of adaptation of the N1 potential has been shown to correlate with cochlear implant patient speech perception ability. A non-auditory-specific source(s) of this adaptation may therefore indicate non-auditory specific deficits in poor performing CI users. However, these non-auditory-specific sources have not been identified yet.

Methods

Cortical auditory evoked potentials were recorded using a high-density array of 160 electrodes in 10 normal hearing individuals. Stimuli for auditory-inhibited responses were trains of five 1kHz tonebursts, with 1 second between tonebursts within a train, and 12 seconds between trains. Stimuli for visual-inhibited responses were a checkerboard pattern change, followed after 1 second by a 1kHz toneburst, with 12 seconds before the following visual stimulus. The topography of the auditory and visual- and auditory-inhibited potentials were compared, as different cortical generators produce different topographies at the scalp. Subject specific head model based current source density algorithms were used to reconstruct cortical activity.

Results

Preliminary data suggest that the N1 potential of the response to the first stimulus of a train of auditory stimuli (uninhibited response) has a different topography to the response to later stimuli in that train (auditory inhibited response).

Conclusion

Further experiments are ongoing to verify our hypothesis.

957 Multi-Sensory Integration in Primary Auditory Cortex Is Stimulus Timing Dependent and Alters Neural Synchrony

Gregory Basura¹, Seth Koehler¹, James Wiler¹, Susan Shore¹

¹University of Michigan

Background

Central auditory neurons are influenced by activity-dependent inputs from non-auditory systems. In addition to acoustic stimulation, primary auditory cortex (A1) receives somatosensory input to areas previously considered to be exclusively “unimodal” (Hackett et al., *J Comp Neurol*, 2007). A1 neurons are capable of multisensory integration since spinal trigeminal (Sp5)-auditory stimulation modulates early event-related field potentials that are supra-additive (Lakatos et al. *Neuron*, 2007; Kayser et al., *Neuron*, 2005). The mechanisms underlying activity-dependent and spontaneous neural changes in A1 response properties following multi-modal stimulation remain largely unexplored. The present study examined the effects of combined auditory-Sp5 (bimodal) stimulation on tone-evoked, spontaneous firing rates and neural synchrony in A1 neurons in response to varied order and timing of bimodal stimuli.

Methods

Four-shank, 32-channel silicon electrodes were placed in guinea pig A1 to record tone-evoked responses and spontaneous unit activity before and after bimodal stimulation with alternating pairing order (tone-Sp5 or Sp5-tone) at various pairing intervals (40, 20, 10 and 0ms). Synchrony between neuron pairs was measured using cross-correlations (Vos et al., *J Neurosci*, 1999).

Results

Bimodal stimulation induced both facilitation and suppression of tone-evoked firing rates in A1. Greater levels of suppression were observed when Sp5 stimulation preceded tones by 40 and 20ms, while preceding Sp5 activation with tones robustly facilitated neural firing at all pairing intervals. Increased neural synchrony in A1 was observed when Sp5 preceded sound, but decreased when the pairing order was reversed (tone-Sp5).

Conclusion

The changes in responses to bimodal stimulation order observed here may reflect spike-timing dependent plasticity (Dahmen et al., *J Neurosci*, 2008). Thus, neuronal multisensory integration of A1 neurons may be influenced by temporal relationships of converging auditory and non-auditory sensory systems, which may be important in normal sensory processing and in central pathway aberrancy as observed in tinnitus.

This work was supported by NIH grants R03DC009893 (GJB) and P30DC05188.

958 Dependence of Sensory Responses on Locomotion and Vigilance Along the Central Auditory Pathway in Awake-Behaving Mice

Matthew McGinley¹, David McCormick¹

¹Yale University

Background

The dynamics of cortical network activity is influenced by the state of the animal as well as the dynamics of input coming from the sensory periphery, which is itself state-dependent. Much less is known about sensory responses in the cortex of awake-behaving preparations than in anesthetized or quietly immobile and not alert animals, particularly in the auditory system. In the visual cortex, locomotion (walking) causes a strong enhancement of sensory responses (Niell and Stryker, *Neuron* 65:472-9, 2010). However, it is not known how this effect relates to vision, cortical network dynamics, locomotion, or the state of vigilance of the animal.

Methods

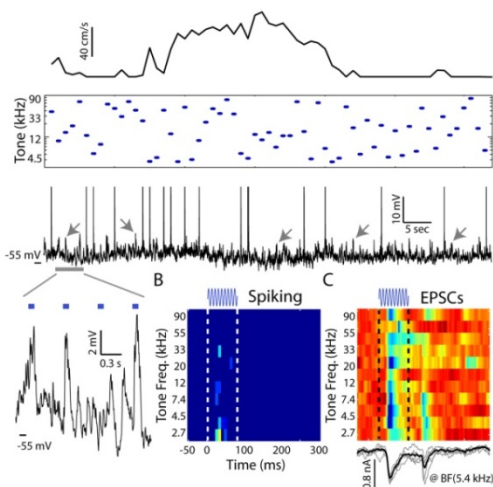
To address these issues, we have developed a head-fixed awake-behaving preparation in which mice are free to walk on a custom made cylindrical treadmill based on Wienisch et al. (*Springer protocols*, 2012). We record the local field potential (LFP) and multiunit activity (MUA) across layers with a 16-channel laminar probe, or whole-cell membrane potential in auditory cortex while mice are engaged in passive behaviors or perform a Go/No-Go auditory discrimination task. We simultaneously record activity in the CA1 field of hippocampus using a separate 16-channel laminar probe and monitor the movements of the animal with an optical sensor and high-speed video.

Results

We find that, in contrast to the visual system, walking causes a significant suppression (~40%) of evoked responses to tones that is apparent in the onset, sustained, offset, and rebound suppression components. Also in contrast to the visual system, where the locus of the locomotion effect is thought to be the cortex (Niell and Stryker, 2010), we find a similar suppression in the central nucleus of the inferior colliculus with or without bilateral silencing of the auditory cortices with muscimol. In the hippocampus, during walking we observe a strong and persistent theta rhythm (~8 Hz). During still periods we observe intermittent theta rhythmic activity as well as large amplitude irregular activity including intermittent fast ripples (~150 Hz) in the pyramidal layer often associated with sharp waves in other layers.

Conclusion

In ongoing experiments we are using this hippocampal rhythmic activity to define the state of vigilance of the animal, and exploring the dependence of sensory responses in auditory cortex on vigilance and behavioral task performance measures. In addition, we are further isolating the locus of the effect of locomotion on auditory responses with experiments in the auditory periphery.



959 Binaural Sensitivity in Human Auditory Cortex: Analyzing the Time Course and Spatial Pattern of Activity in fMRI

G. Christopher Stecker¹, Susan McLaughlin¹, Nathan Higgins¹

¹University of Washington

Background

Although the representation of auditory space within the auditory cortex (AC) remains poorly understood, contemporary studies have combined psychophysical, neuroimaging, and physiological approaches in human and animal models to explore that representation and its dependence on behavioral and stimulus context. To that end, recent studies in our lab have used functional magnetic resonance imaging (fMRI) to study the dependence of human AC blood-oxygenation-level-dependent (BOLD) responses on the binaural characteristics of sounds, namely interaural differences of level (ILD) and time (ITD). The results demonstrate clear modulation of AC responses by ILD due to inhibition of the BOLD response by the ipsilateral ear, but surprisingly weak modulation of responses by ITD. Here, we examine whether the stimulus-specific time courses or multi-voxel activation patterns of AC BOLD response exhibit greater modulation by ITD.

Methods

BOLD responses were measured from continuously-acquired images (whole-head echo-planar imaging at 3T [Philips Achieva], TR=2s, 2.75x2.75x3 mm resolution) using an “event-related” paradigm that presented trains of narrowband or broadband clicks carrying ILD or ITD that varied parametrically across 1-s trials. Sounds were presented via insert earphones (Sensimetrics), and listeners tasked with detecting infrequent (~1/13 s) pitch-change targets. BOLD activity was analyzed on each individual’s cortical surface using FSL, Freesurfer, and MATLAB. Three separate analyses were conducted: univariate tests employing the general linear model (GLM), BOLD timecourse estimation, and multivoxel pattern similarity analyses.

Results

Consistent with previous results, response-ILD functions obtained from GLM analyses indicated significant reductions of the BOLD response for moderate ipsilateral ILD compared either to large contralateral or ipsilateral values. Response-ITD functions for both narrowband and broadband modulated sounds revealed little modulation of the overall BOLD response by that cue. Time-course analyses revealed significant response adaptation for both cues. Finally, multivoxel pattern analysis was used to assess the degree to which ILD and ITD sensitivity varied systematically at smaller spatial scales than detectable with standard univariate measures.

Conclusion

Together with past work, the results support a role for binaural suppression (as opposed to facilitation) in shaping the ILD sensitivity of AC bold responses. The effects of ITD, in contrast, are more subtle; they suggest that careful attention should be paid to the pattern of excitatory and inhibitory binaural processing in AC, and to potential modulatory effects of the behavioral task. [Supported by R01-DC011548, R03-DC009482]

960 Intracranial Responses Representing Stop Consonant Voice Onset Time and Place of Articulation on the Human Posterior Lateral Superior Temporal Gyrus

Mitchell Steinschneider¹, Kirill Nourski², Hiroyuki Oya², Hiroto Kawasaki², Matthew Howard²

¹Albert Einstein College of Medicine, ²University of Iowa

Background

Intracranial recordings performed in patients undergoing electrocorticographic (ECoG) evaluation for surgical remediation of medically intractable epilepsy have greatly enhanced our understanding of how speech is represented in the brain. Recently, we demonstrated using averaged trials that both voice onset time (VOT) and place of articulation (POA) of stop consonants were represented by high gamma ECoG activity recorded from posterior lateral superior temporal gyrus (PLST) (Steinschneider et al., *Cereb Cortex*, 2011, 21:2332-47). It is unclear from these analyses, however, whether representations of POA and VOT are reliable at the more environmentally relevant single trial level.

Methods

Here, we examined the reliability of high gamma ECoG activity to represent stop consonant POA and VOT at the single trial level using a sparse logistic regression classification analysis. The study was IRB approved and followed patient informed consent. Stimuli were synthesized syllables /ba/, /ga/, /da/, /pa/, /ka/, and /ta/. They were constructed to have identical first and fourth formant center frequencies and overlapping second and third formant transitions (e.g., /ba/ and /ga/ shared the same third formant transition while /da/ and /ga/ shared the same second formant transition). Differences in POA were mainly based on varying the spectral content of frication within the first 5 ms of the sounds. Spectra were maximal

at 800 Hz for /ba/ and /pa/, 1600 Hz for /ga/ and /ka/, and 3000 Hz for /da/ and /ta/. VOT was 5 ms for /ba/, /ga/, /da/ (voiced stops) and 40 ms for /pa/, /ka/, and /ta/ (unvoiced stops).

Results

Classification analysis yielded highly reliable discrimination of VOT when comparing responses elicited by voiced and unvoiced stop consonants. In contrast, POA was not accurately represented in the ECoG when comparing the combined responses elicited by /ba/ and /pa/ versus those to /ga/ and /ka/, and /da/ and /ta/. There was also a poor and variable representation of POA when voiced and unvoiced stop consonants were analyzed separately. Additional correlational analysis indicated that responses to 800, 1600, and 3000 Hz pure tones could not reliably predict responses to syllables varying in their consonant POA.

Conclusion

VOT is a powerful cue for speech sound discrimination on PLST. In contrast, POA based primarily on spectral differences during frication are weak cues for neural discrimination in the same brain region. Discrimination of POA based on formant transition or combined cues may be more reliable. (KN and MS contributed equally to this work).

961 Neural Entrainment to Speech, a Matter of Time or Frequency?

Nai Ding^{1,2}, Jonathan Z. Simon¹

¹University of Maryland, College Park, ²New York University

Background

Spatially coherent neural activity measured by MEG, EEG, or LFP is entrained to the slow temporal modulations, i.e. envelope, of speech.

Methods

In the time domain, this entrainment is often decomposed into responses with different latencies, while in the frequency domain it is usually decomposed into neural oscillations in distinct frequency bands. Here, we compare time domain analysis and frequency domain analysis for the MEG responses to speech presented in a variety of auditory scenes.

Results

In the time domain, it is found that late (>~100 ms) auditory responses are robust to the acoustic background while early (<~50 ms) auditory responses are not. In the frequency domain, it is found that very low frequency activity (< 4 Hz, delta band) is robust to the acoustic background, while higher frequency activity (4-8 Hz, theta band) is not.

Conclusion

These results suggest that robust delta band activity reflects the audibility of speech while theta band activity reflects the intelligibility of speech.

962 Enhancement of the N1 Cortical Auditory Evoked Potential in Low-Level Background Noise

Melissa Papesh^{1,2}, Curtis Billings^{1,3}, Lucas Baltzell^{1,3}

¹National Center for Rehabilitative Auditory Research (NCRAR), Portland VA Medical Center, ²Department of Speech and Hearing Sciences, Indiana University,

³Department of Otolaryngology/Head & Neck Surgery, Oregon Health & Science University

Background

Though most people are familiar with the notion that background noise is detrimental to hearing, some reports indicate that low levels of background noise may actually enhance certain aspects of neural auditory stimulus encoding. These studies classify enhancement as an increase in the amplitude of the N1 cortical response in low levels of background noise relative to the N1 amplitude recorded in quiet. Because most cortical auditory evoked potential (CAEP) studies report an amplitude decrement with the addition of background noise, cases of enhancement are particularly intriguing and deserving of further investigation.

The present study sought to determine what conditions are required to elicit enhanced CAEPs in the presence of noise. Reports of N1 amplitude enhancement have thus far been confined to studies employing binaural listening conditions and relatively fast presentation rates. Therefore, we examined the effect of both signal presentation rate and differences in monaural vs. binaural mode of presentation.

Methods

CAEPs were recorded from sixteen young normally hearing listeners using a 64-channel electrode cap. The signal was a 450-ms naturally spoken /ba/ presented at a level of 80 dB with interstimulus intervals of 900 and 1900 ms. The signal was presented both in quiet and in the presence of a continuous speech-spectrum noise at +10 and at +30 dB signal-to-noise ratio (SNR).

Results

Binaural presentations using a fast stimulus rate elicited enhanced N1 amplitudes in background noise relative to the quiet condition. In contrast, slow presentation rates generally elicited decreasing N1 amplitudes with increasing background noise level. Thus, preliminary results suggest that both rapid presentation rates and binaural activity are crucial for the enhancement of N1 potentials in background noise. Further, the N1 enhancement was lost when low-frequency activity (i.e., <3 Hz) was filtered out, suggesting that the enhancement effect arises from low-frequency response activity.

Conclusion

Preliminary results indicate that background noise elicits enhanced N1 responses when stimuli are presented binaurally at a fast presentation rate. The enhancement appears to result from low-frequency activity in the CAEP

response. The implications of the importance of monaural/binaural mode and rate of presentation on N1 CAEP enhancement as well as the dependence of the enhancement effect on low frequency response activity will be discussed. [Supported by NIH-NIDCD (R03DC010914) and VA RR&D (CoEC4844C)]

963 Multiplexed Single-Unit Codes for Sensory-Cognitive Mapping in Ferret Frontal Cortex During an Auditory Reversal Task

Nikolas Francis¹, Jonathan Fritz¹, Shihab Shamma¹

¹University of Maryland

Background

During auditory-guided behavior, flexible sensory-cognitive associations are needed for sudden changes in the behavioral meaning of sounds. The plasticity of neural coding in frontal cortex (FC) is likely to contribute to such behavioral flexibility. Single-units in FC exhibit spike-rate codes that separately represent target and distractor tones during a two-tone discrimination task (Fritz et al., 2010). However, it is not known if single-units in the ferret FC change their spike-rate codes for two discriminated tones when the behavioral meaning of the two tones are suddenly reversed.

Methods

Two ferrets were trained on a conditioned avoidance frequency discrimination task. Exactly the same sounds were presented in each block of trials, but the behavioral meaning of the sounds was reversed in alternating blocks. Tones from either a high- or low-frequency region were selected as the target for a given block of trials. The animal quickly learned to identify the target stimulus, and to stop licking a waterspout during targets to avoid a mild tail shock. Thus, behavioral responses to the task sounds were reversed for each consecutive block. After training, we recorded from single-units in the dorsal FC of the behaving, head-fixed ferret to study the plasticity of neural representations for high- and low-frequency sounds during the reversal task.

Results

We found neurons in dorsal FC that responded most strongly to the targets and more weakly to distractors, independent of the absolute frequency of the sounds. In other words, when the task was reversed, spike-rate codes for the task sounds also reversed, following the behavioral meaning rather than sound frequency. In some of the same cells, the target's absolute frequency-range was tagged with characteristic spike-rate dynamics, allowing these neurons to encode both task meaning and absolute frequency of the stimulus.

Conclusion

Our results suggest that single-units in the dorsal FC of the ferret have multiplexed spike-rate codes representing orthogonal assignments of task meaning to sounds. This context-dependent plasticity may contribute to the behavioral flexibility required in a reversal task. We will also discuss our results on sensory (ie. tone frequency) vs.

cognitive (ie. behavioral meaning) target-class coding in dorsal FC, the dependence of single-unit-based stimulus classification on the time-course of learning during task-reversal, and the coding of long-term memories to task-relevant sounds during non-task as well as task conditions.

964 The Neural Mechanisms of the Phonemic Restoration in People with Normal Hearing

Kishiko Sunami¹, Hidefumi Yamamoto¹, Tetsushi Sakashita¹, Hideo Yamane¹, Satoshi Ishii¹, Masaaki Tanaka¹, Yasuyoshi Watanabe¹

¹OsakaCity University

Background

In our daily life, parts of speech are completely drowned out by noises; however, we can still hear the speech as if it has not been interrupted by noises. This is caused by the effect known for phonemic restoration. Impaired ability of phonemic restoration has been reported to be related to the difficulties in understanding speech in patients with hearing loss even when hearing level is corrected by hearing aids. However, the neural mechanism of the phonemic restoration is not clear. The aim of our study was to elucidate the neural mechanisms of the phonemic restoration in people with normal hearing.

Methods

Eight healthy male volunteers participated in our study. This study was approved by the Ethics Committee of Osaka City University, and all the participants gave written informed consent for participation. They were requested to carefully listen to and understand 3 stories with their eyes closed. The stories were constructed of recorded narratives in which several syllables were partly replaced by white noises for 300 ms. Although 2 of the stories were played forward (forward condition), 1 story was played in reverse to assess the neural responses caused by listening to the noises (reverse condition). The neural responses while listening to these stories were measured by using MEG with high temporal resolution. The MEG data were analyzed using dual-state adaptive spatial filtering methods. The oscillatory power in the forward condition relative to that in the reverse condition was analyzed using statistical parametric mapping to make inferences at a population level.

Results

The MEG data from 1 participant were excluded from our analysis because the participant experienced hearing loss. We focused on the MEG data in the time range of 100 to 300 ms and in the frequency range of 3 to 5 Hz, since the sensor-level time-frequency maps showed event-related synchronization in this time-frequency area. The group analysis showed that the oscillatory power in the forward condition was higher than that in the reverse condition in 2 brain regions ($P < 0.001$, uncorrected for multiple comparisons). One brain region extended from Brodmann area (BA) 32 and the other extended from BA6. The latter region seemed to overlap with Broca's area.

Conclusion

We found two brain regions were related to phonemic restoration. Our findings may help clarify the neural mechanisms of the phonemic restoration as well as develop innovative methods for patients suffering from hearing loss.

965 Interactions Between Areas in the Forebrain of Anaesthetized Guinea Pigs That Elicit Vocalizations

David Green¹, Mark Wallace¹, Alan Palmer¹

¹MRC Institute of Hearing Research

Background

Guinea pigs are gregarious animals with a well-characterized repertoire of 11 vocalizations. These are context dependent, communicating information about danger, identity and emotional state. In previous work guinea pig vocalizations were elicited by electrical stimulation of three brain areas, but the call types were not well classified. Here we investigate interactions between the areas that produce calls.

Methods

Five brain areas were electrically stimulated (60 Hz for 1.6 s) in anaesthetized animals: the anterior cingulate cortex, medio-dorsal thalamus, hypothalamus, amygdala and the midbrain periaqueductal grey substance. Spectral structure and pulse frequency of the evoked calls were analysed using SAS Lab Pro (Avisoft Bioacoustics).

Results

Eight distinct calls were classified. The structure of the calls was similar to those from spontaneously vocalizing animals. Five of the calls were produced only during electrical stimulation and three were produced after the end of the stimulation. Two of the post-stimulation calls were a series of "screams" gradually changing to "squeals" before fading away over a period of up to 30 s. These could be elicited from all five brain regions and showed a predictable response to changes in stimulation current. Concurrent bilateral stimulation of loci producing scream/squeal always had an additive effect, whereas stimulation of two loci giving during-stimulus calls was more complex. It appears that each post-stimulus vocalization area contributes to a shared system of excitatory re-entrant loops, that are involved in the generation of a call series.

Conclusion

Stimulation of the amygdala yielded two call types with contrasting emotional intent. To date, this has been reported only in primates. Our experimental protocol, therefore, provides a useful model for the investigation of the common mammalian vocalization pathways.

966 Alignment of Sound Localization Cues in the Nucleus of the Brachium of the Inferior Colliculus

Sean Slee¹, Eric Young²

¹Oregon Health and Science University, ²Johns Hopkins University

Background

Previous studies have demonstrated that although single neurons in the central nucleus of the inferior colliculus (ICC) are sensitive to multiple sound localization cues, they do not show a preference for spatially coherent cues. In the present study we measured the effects of misalignment of sound localization cues in the nucleus of the brachium of the IC (BIN) in unanesthetized marmoset monkeys. The BIN receives its predominant auditory input from the ICC and provides a major auditory projection to the superior colliculus, which contains a topographic map of auditory space.

Methods

Sound localization cues including interaural time differences (ITDs), interaural level differences (ILDs), and spectral shapes (SSs) were measured in each monkey. The results were used to impose aligned and misaligned combinations of cues on a set of broadband noise stimuli. The stimuli were presented to the same marmoset while recording spike responses in the BIN. We computed mutual information between the set of spike rates and stimuli containing either aligned or misaligned cues. In a subset of neurons noise ITD sensitivity and tone frequency response maps were also measured.

Results

The results can be summarized as follows: 1) A significantly larger number of BIN neurons encoded more information about auditory space when cues were aligned compared to misaligned. 2) This result holds in subsets of BIN neurons with or without ITD sensitivity. 3) In general tonal frequency tuning was broad (3-5 octaves). However, a subset of neurons that did not respond to tones below 2 kHz also had a preference for cue alignment.

Conclusion

The results suggest that ITD sensitivity is not necessary for cue alignment preferences in the BIN and posits an additional role for the interaction between ILD and SS cues. Alignment of sound localization cues in the BIN is hypothesized to play a role in the formation of the auditory space map found in the SC.

967 Spike-Rate Variance as the Detection Parameter for Interaural Incoherence

Torsten Marquardt¹, Simon Jones¹, David McAlpine¹

¹UCL

Background

It has been shown that Inter-Aural Correlation (IAC) is linked to the variance of Inter-aural Time Difference (ITD) and Inter-aural Level Difference (ILD) and whilst normalised IAC can account for behavioural IAC

discrimination performance so can models directly employing this variance.

The prevailing view, influenced by observations of binaural sluggishness, has been that this variance is too rapid for the binaural system to utilise. Attempts at identifying a neurometric correlate of IAC discrimination have consequently focused on changes in mean spike count, typically at the peak of ITD tuning curves.

We propose that IAC discrimination relies on variance spike rates on the slope of ITD tuning curves and compare computer simulations to midbrain neurons.

Methods

A physiologically-based hemispheric balance model was developed, where the fluctuations in the ratio between left and right brain activity served as the detection cue to a reduction in IAC from unity. Note that this ratio is stimulus power invariant (intrinsic normalisation). The analysis focused on neural populations with the same best ITD magnitude but opposite sign. Static changes in this ratio served as a cue to static changes in ITD. Comparisons were made with a model where changes in normalised mean spike rate at the ITD function peak served as the detection cue.

IC neural responses to binaurally presented noise stimuli of various IAC were recorded from anaesthetised Guinea pigs. Identical stimuli were presented twice, with ipsilateral and contralateral waveforms swapped so each neuron could serve as the model for a matching neuron with the same best ITD magnitude but in the opposite hemisphere aiding comparison to our models.

Results

Adjusting the model parameters to predict published behavioural ITD and IAC discrimination data, the hemispheric balance model required approximately 175 neurons in each hemisphere whilst two orders of magnitude more activity was needed to achieve the same performance with the model using mean group spike rate at the peak of their ITD functions. This adjustment also revealed a necessary neural time integration of 10ms, which is comparable with physiological estimates.

Conclusion

Hemispheric balance is invariant to stimulus power fluctuations but sensitive to interaural differences. Reduction in IAC leads to fluctuation in hemispheric balance and is a plausible IAC discrimination cue. Sensitivity to variance in ITD inherent in IAC stimuli supports recent evidence of a more rapid binaural neural system than suggested by "classic" behavioural binaural sluggishness.

968 In-Vivo Whole Cell Recordings Revealed Binaural Mechanism for the Facilitated Response in EI/F Neurons

Na Li¹, George Pollak¹

¹University of Texas at Austin

Background

Cells that receive excitation from one ear and inhibition from the other (EI cells) process interaural intensity disparities (IIDs), the cues for localizing high frequencies. EI cells in the inferior colliculus (IC) fire to contralateral stimulation, while ipsilateral stimulation at progressively higher intensities suppresses the spikes evoked by contralateral stimulation. Facilitated EI cells (EI/f) are a variation of EI cells in that facilitated spike-counts, more than those evoked by the contralateral signal, are evoked with binaural signals having low ipsilateral intensities.

Methods

To evaluate the binaural mechanism underlying the facilitated binaural response, we made whole cell patch-clamp recordings in 11 EI/f cells in the IC of awake Mexican free-tailed bats. Both spikes and postsynaptic potentials (PSPs) evoked by contralateral, ipsilateral and binaural signal were recorded. Moreover, excitatory and inhibitory synaptic conductances were derived from each response recorded in one cell.

Results

Based on both the PSPs and conductances, we propose the inputs that innervate these EI/f cells and show that the basic EI property was produced by innervation from a lower binaural nucleus, presumably the LSO. We then show that these cells also received an ipsilaterally evoked inhibition and an ipsilaterally evoked subthreshold excitation.

Conclusion

The facilitation resulted from two ways. 1) the ipsilaterally evoked excitation and a reduction in the ipsilaterally evoked inhibition due to contralateral stimulation. Thus, at small IIDs, with weak ipsilateral signals, the reduced inhibition allows the combined contralateral and ipsilateral excitatory inputs to generate a larger EPSP than would be evoked by the contralateral excitation alone, thereby generating the facilitated response. 2) only a reduction in the ipsilaterally evoked inhibition due to contralateral stimulation. This reduced inhibition produced a larger EPSP than that would be evoked by the contralateral excitation alone. Supported by NIH grant DC007856.

969 Establishing Optogenetics in the Auditory System of the Mongolian Gerbil

Stefan Keplinger¹, Fred Koch², Stylianos Michalakis², Martin Biel², Benedikt Grothe^{1,3}, Lars Kunz¹

¹Neurobiology, Dept. Biology II, University of Munich,

²Dept. Pharmacy, University of Munich, ³Bernstein Center for Computational Neuroscience Munich

Background

The rodent Mongolian gerbil (*Meriones unguiculatus*) has been established as model organism for human hearing

due to its similarly broad hearing range and the ability to localise low frequency sounds. However, by choosing the Mongolian gerbil as model organism we currently lack genetic tools and techniques already established in mouse or rat. Optogenetics is one example. Optogenetic techniques allow for specific targeting of individual brain nuclei and for control of electrical activity of neurons via light. Optical stimulation can circumvent off-target responses from passing fibres where electrical stimulation lacks precision.

Methods

Stereotactic injection of adeno-associated virus (AAVs) into auditory nuclei of anaesthetised gerbils was followed by an expression period of 2-3 weeks. Animals were sacrificed and brain slice preparations were performed. Whole-cell patch-clamp recordings from targeted auditory nuclei in acute brain slices were used to characterise kinetic parameters of the expressed channelrhodopsins. Immunohistochemistry and confocal scanning of paraformaldehyde-fixed brain slices served to measure the spread of the AAV-infection and to determine co-localisation of fluorescence-tagged channelrhodopsin with microtubule-associated protein 2 (MAP2).

Results

AAV mediated gene delivery reliably drove neuronal-specific expression of channelrhodopsins in the inferior colliculus (IC) and other auditory nuclei. Viral transduction of neurons in these nuclei with channelrhodopsin variants enabled us to control neuronal activity with light of appropriate wavelengths and characterise channelrhodopsins in the gerbil. Performing whole-cell patch-clamp recordings we determined maximum firing rates, firing reliability, and jitter of elicited action potentials in current-clamp as well as transition from peak to stationary current (τ_{in}), current kinetics after light-off (τ_{off}) and maximum photocurrents in voltage-clamp mode.

Conclusion

Our results are a first step to establish optogenetics in the auditory system of the Mongolian gerbil and might aid to decipher the intricate connectivity of auditory nuclei.

970 Does Visual Stimulation Influence Spatial Tuning in the Central Nucleus of the Inferior Colliculus?

Todd Jennings¹, Benedikt Grothe¹

¹Ludwig-Maximilians-Universität München

Background

The central nucleus of the inferior colliculus (ICC) is one of the key stages in the auditory pathway. It is one of the main areas of convergence for both afferent and efferent fibers passing between the auditory brainstem and auditory cortex. It has many cells sensitive to particular auditory features, such as sound localization cues. It also receives indirect projections from multimodal structures, including the superior colliculus (SC) and the primary sensory cortices. This suggests that multimodal information is likely reaching the ICC. Further, since many

ICC neurons are sensitive to sound direction cues, and vision is an inherently directional sense in most vertebrates, it would be natural for visual inputs to modulate responses to sound localization cues in the ICC. However, although its place in the auditory pathway is well-established, it has not been conclusively established that connections with other sensory modalities actually exist in the ICC.

Methods

The purpose of this study is to combine visual inputs with auditory inputs in order to look for any visual influences on ICC single-neuron responses in-vivo. To test for visual influences on ICC neurons responses from extracellular recordings in anesthetized Mongolian gerbils were analyzed.

Results

Paired directional visual inputs were combined with binaural sound inputs. A combinatorial analysis was carried out to look for synergistic, antagonistic, or non-selective visual influences on ITD and ILD response curves.

Conclusion

As the nexus of the auditory pathway, understanding the full range of influences on ICC neurons is critical to understanding how auditory information is processed and interpreted by the brain.

971 Sensory Responses to Ethologically Relevant Auditory Stimuli in the Superior Colliculus

Melville Wohlgenuth¹, Cynthia Moss¹

¹University of Maryland

Background

Selective processing of stimulus elements in a complex environment lays the foundation for natural scene perception; however, the underlying neural mechanisms are not well understood. We have studied neural responses to natural acoustic stimuli in the midbrain superior colliculus (SC) of the echolocating bat, an animal that actively probes its environment by emitting ultrasonic vocalizations and listening to echo returns. Previous research on the bat SC has examined auditory evoked activity in superficial/intermediate layers (Valentine and Moss, *J. Neurosci.*, 1997) and premotor activity in the intermediate/deep layers (Sinha and Moss, *J. Neurosci.*, 2007). What remains elusive in the bat, and more generally for all mammals, is how sensory information is integrated into motor commands for perceptually guided behaviors. The purpose of the current study was to provide a broad framework for understanding sensorimotor processes in the mammalian SC. Echolocating bats serve as an excellent model for this line of study, because bats are auditory specialists that represent their 3D environment with sound and adapt vocal-motor behaviors in response to acoustic input.

Methods

In the current study, we examined SC encoding of dynamic echolocation signals employed by the bat while tracking moving prey items. Electrodes were lowered into the SC as the bat listened to natural sound stimuli. Responses were later analyzed with respect to the depth of the recording site. By using this approach, it is possible to study how neurons in each layer of the bat SC respond to ethologically relevant auditory stimulation.

Results

Sensory responses to sonar vocalizations were elicited from SC neurons at superficial, intermediate and deep layers. Response latencies ranged from very short (<10 msec) to very long (>45 msec). We found selectivity in SC neurons to subsets of FM signals embedded in sound sequences over which call duration, interval, bandwidth and harmonic strength changed. Response selectivity was traced to correlated changes in acoustic features of sonar signals within the dynamic call sequences.

Conclusion

Sensory evoked responses were found across all depths of the bat SC, illuminating a process by which auditory information can affect ongoing motor planning in deeper layers. These results are novel in that they identify how auditory information is encoded in each of the layers of the SC, and they also provide a method to more broadly understand how sensory activity is represented in the SC of mammals.

972 Neural Coding of Interaural Level Differences with Bilateral Cochlear Implants
Yoojin Chung^{1,2}, Kenneth Hancock^{1,2}, Bertrand Delgutte^{1,2}
¹Massachusetts Eye & Ear Infirmary, ²Harvard Medical School

Background

Interaural level differences (ILD) are by far the most potent sound localization cues presently available to bilateral cochlear implant users. Although the neural representation of ILD has been well-studied in normal hearing, virtually nothing is known about how the brain encodes ILDs of electrical stimuli.

Methods

We compared ILD sensitivity of single units in the inferior colliculus (IC) of barbiturate-urethane anesthetized cats and awake rabbits with bilateral cochlear implants. The cats were deafened one week before neural recordings, while recordings in rabbits lasted up to 6 months after deafening and implantation. Stimuli were trains of biphasic current pulses presented at rates <100 pulses/s. Current levels were systematically varied in each ear starting just below threshold and spanning the dynamic range, yielding a matrix of firing rate as a function of stimulus level in each ear. Rate-ILD curves at different mean binaural levels (MBL) were extracted from each matrix.

Results

Neural ILD sensitivity evoked by electric stimulation was qualitatively similar to that previously observed in normal hearing animals. Stimulation of the contralateral ear evoked excitation in the vast majority of neurons. The predominant effect of ipsilateral stimulation could be excitatory ("EE" response), inhibitory ("EI"), or weak ("EO"). A few neurons responded nonmonotonically with increasing level to contralateral and/or ipsilateral stimulation.

EI neurons showed a monotonic dependence of firing rate on ILD that was relatively invariant with changes in MBL, thereby providing a robust code for ILD. In contrast, rate-ILD curves for EE neurons were nonmonotonic and highly dependent on MBL, providing an ambiguous code for ILD that degraded at high MBLs. Such neurons might still provide a distributed code for ILD if their ipsilateral and contralateral thresholds varied systematically across the neuron population.

The prevalence of the various binaural response types appeared to differ between the two preparations. EE was most common in cat, followed by EO and EI. Based on a small sample, the EO type predominated in rabbit, followed by EI and EE.

Conclusion

Our results suggest that the predominant code for ILD may differ in acutely-deafened, anesthetized cats vs. chronically-implanted, awake rabbits. Several factors may contribute to this difference, including effects of anesthesia, species differences, or sampling biases. Additionally, in the chronic rabbit preparation, the balance of excitation and inhibition may be influenced by prolonged deprivation of acoustic input and by electric stimulation during daily recording sessions.

Supported by NIH Grants R01DC005775, P30DC005209.

973 Investigating the Effect of Microphone Position on Sound Localization in Bilateral Cochlear Implant Users

Heath Jones¹, Alan Kan¹, Ruth Litovsky¹
¹Waisman Center - University of Wisconsin

Background

Bilateral cochlear implants (BiCIs) have become a standard of care in many clinics, in an effort to improve spatial hearing skills in profoundly deaf individuals. However, BiCI users demonstrate poorer sound localization accuracy compared to normal hearing (NH) listeners. One of the many factors that might contribute to poorer performance is the behind-the-ear microphone placement of these devices. Such placement does not maximize the ability to capture the natural filtering properties of the head/pinna known to be important cues for sound localization. Here, we evaluated the effect of microphone placement on sound localization performance in BiCI users. We hypothesized that the most natural position, in-the-ear placement of microphones, will capture spatial cues that are unavailable in standard CI fittings, improving performance.

Methods

Eight postlingually deafened BiCI users participated in this study. Virtual acoustic space (VAS) techniques were used to capture individualized acoustic transfer functions (ATFs) recorded for 19 loudspeaker locations, spaced 10° apart along the horizontal plane. Microphones were positioned to reflect those currently used by clinics: (1) in-the-ear (ITE); (2) behind-the-ear (BTE); or (3) on the shoulders (SHD). ATFs were used to generate VAS stimuli consisting of a pink noise train (four burst each 170 ms). Stimuli were delivered to the CI user's speech processors through direct connect cables. A sound localization task was conducted to evaluate performance for each microphone position condition. Free-field localization using the subject's clinical processors was also tested.

Results

Subjects were able to localize all VAS stimuli, except one who indicated that the stimuli did not sound externalized. Results demonstrate that placing the microphone in-the-ear resulted in improved localization accuracy compared to the free-field and other microphone conditions. Accuracy and sensitivity decreased substantially in the SHD condition. In all conditions, localization performance was still less accurate compared to NH listeners.

Conclusion

We found ITE microphone placement provides a small improvement in sound localization over BTE. However, the results also indicated that ITE placement is not enough to restore localization to NH performance. Additional factors need to be considered for improvement of sound localization in BiCI users, such as the restoration of binaural timing cues known to be important for accurate sound localization. Combining the preservation of acoustic temporal fine structure with bilateral synchronization between processors may provide these cues and improve BiCI sound localization. Supported by NIH-NIDCD (R01003083) and (P30 HD03352).

974 The Effect of Interaural Frequency Mismatch on Correlation Change Detection in Bilateral Cochlear-Implant Users

Matthew Goupell¹

¹University of Maryland - College Park

Background

The insertion depth of a cochlear implant (CI) may differ across the ears in the case of bilateral implantation. This will cause an interaural frequency mismatch of electrical stimulation that may affect binaural processing, which is thought to require matched frequency inputs. While previous studies have investigated the effects of interaural frequency mismatch on the perception of static interaural differences using constant-amplitude pulse trains, we extended that work to investigate interaural correlation change detection in modulated stimuli.

Methods

In experiment 1, correlation change discrimination just-noticeable differences (JNDs) were measured in six CI listeners. The stimuli began as a 50-Hz narrowband noise. The envelope was extracted, biphasic monopolar electrical pulses sampled the envelope at 1000 pulses per second (pps), and amplitudes were compressed as typically occurs in speech processing strategies. Starting from a pitch-matched pair of electrodes, interaural frequency mismatches of $\Delta = 0, 2, 4,$ and 8 electrodes were tested. JNDs were measured for correlated and uncorrelated reference stimuli. In experiment 2, the percentage of correct discriminations between correlated and anti-correlated (i.e., half-period phase shifted) stimuli was measured as a function of pulse rate. In experiment 3, a fusion experiment was performed to measure the subjective diffuseness of the correlated, uncorrelated, and anti-correlated stimuli. Parallel simulation experiments using acoustic pulse trains were performed in normal-hearing listeners.

Results

In experiment 1, all listeners were sensitive to changes in correlation from correlated reference stimuli for $\Delta = 0$. JNDs were relatively worse for changes from uncorrelated references. Increasing Δ caused increased JNDs; however, most listeners could tolerate a shift of four electrodes (3 mm) before JNDs increased. In experiment 2, listeners could almost perfectly discriminate correlated and anti-correlated pulse trains at 100 pps. However, performance dropped to chance by 500 pps. In experiment 3, uncorrelated and anti-correlated stimuli were perceived to be more diffuse than correlated stimuli.

Conclusion

An interaural frequency mismatch of more than 3 mm is detrimental to processing of changes in interaural correlation, consistent with previous mismatch studies using monopolar stimulation. Given that listeners were not sensitive to changes in phase of the electrical stimuli (correlated vs anti-correlated) at rates typically used in speech processing strategies, this demonstrates a significant hurdle in presenting binaurally-relevant fine-structure information to CI users.

975 Lateralization of Interaural Level Differences in Multi-Channel Electrical Stimulation

Olga Stakhovskaya¹, Tanvi Thakkar¹, Matthew Goupell¹

¹University of Maryland - College Park

Background

Improved sound localization is one of the benefits associated with use of bilateral cochlear implants (CIs). Modern speech processors cannot reliably encode all of the localization cues available to normal-hearing listeners. Therefore, CI listeners rely mostly on interaural level differences (ILDs) to produce a spatial impression of the surrounding environment. The thresholds (T) and the "most-comfortable" (C) levels obtained during the mapping procedures often differ across the electrodes within the ear

and across the ears, resulting in a different spread of excitation at different cochlear locations. Moreover, real world sounds can activate multiple electrodes simultaneously. It is unclear if multi-electrode stimulation with current spread can produce a centered and punctate auditory image in a CI user's head, which could be used as a baseline to create a consistent spatial map across frequencies.

Methods

We investigated the perceived intracranial location of direct electrical stimulation in a group of bilateral CI listeners. For five electrodes in each ear, T and C levels were obtained. Stimuli were monopolar, 1000 pulse/sec pulse trains that were 500 ms in duration. They were presented bilaterally at 70-80% of the dynamic range using single-electrode pairs and several multi-electrode combinations, including three widely-spaced pairs, three closely-spaced pairs, and five-electrode pairs. Listeners reported the position of the perceived intracranial image at ILDs of 0, ± 2 , ± 5 , and ± 10 current units (cus). Lateralization ability with inconsistent ILDs across frequencies was studied in normal-hearing listeners to simulate lateralization with multi-electrode stimulation in CI listeners.

Results

The shape of the lateralization curves was highly variable for single- and multi-electrode stimulation, both within and across listeners. This often resulted in an offset in the perception of a centered image for 0-cu ILD. Adjusting the levels of individual electrode-pairs within a multi-electrode combination with the offsets measured in the single-electrode pairs shifted the location of the perceived sound at 0-cu ILD. This shift resulted in a more centered image for 7/10 multi-electrode combinations in 4 listeners.

Conclusion

The results suggest that auditory spatial maps are distorted for single- and multi-electrode stimulation in bilateral CI users. The perception of a centered image for 0-cu ILD can be improved by adjusting the levels of individual electrodes within a multi-electrode combination based on the single-electrode data. These data have implications for bilateral clinical mapping strategies.

976 Place Coding in the Cochlear Apex

David Landsberger¹, Griet Mertens², Paul Van De Heyning²

¹House Research Institute, ²Antwerp University Hospital

Background

The majority of cochlear implant psychophysics has been conducted with users of electrodes that are typically inserted approximately 1.25 turns into the cochlea. From work with these devices, it is commonly accepted that a change in place of stimulation corresponds to a change in pitch.

Med-EI produces two long (31.5 mm) electrode arrays (the Standard and FLEXSoft), which are inserted deeper into the cochlea than traditional electrode arrays, providing an

opportunity to study the properties of the cochlear apex. Pitch scaling studies with the long Med-EI arrays show that some patients describe the most apical electrodes as having a similar pitch while others report that pitch lowers continuously across the array. One explanation is that as the electrodes approach the apex, more peripheral processes are stimulated and therefore the reported pitch change may not be of the same pitch quality as place changes elsewhere in the cochlea (similarly to how place and rate changes do not produce the same quality of pitch change). Therefore, we conducted an investigation into the perceptual quality of a change in place of stimulation across 31.5 mm electrode arrays using Multi-Dimensional Scaling.

Methods

Stimuli consisted of equally loud single electrode, 5000 pulse-per-second pulse trains. Nine stimuli represented electrodes numbered 1-9. Note, in the Med-EI system, 1 is the most apical electrode out of 12. In a given trial, a pair of stimuli was presented to the listener who had to scale how different the two sounds were. All pairs of stimuli were compared 10 times. Nine subjects were tested.

Results

An INDSCAL analysis shows that in two dimensions, each electrode is plotted in order in a horseshoe configuration, suggesting that even with a deep insertion, a change in place yields a change in place pitch throughout the array. However, the perceptual distances between the most apical electrodes are shorter than the perceptual distances between other electrodes. Analysis of individual subjects ALCSAL plots suggest that most patients results are typical of the INDSCAL analysis; however a number of patients show a perceptual clustering near the apex.

Conclusion

Deep insertions provide continuous place pitch throughout the cochlea. From a place pitch perspective, the extended length of the Med-EI Standard and FLEXSoft array provides additional benefit relative to shorter electrode arrays. However, the ideal electrode configuration might involve greater spacing between electrodes in the apex than the rest of the array.

977 Ipsilateral and Contralateral Masking in Bilateral Cochlear Implant Users

Justin Aronoff^{1,2}, Monica Padilla¹, Qian-Jie Fu¹, David Landsberger¹

¹House Research Institute, ²University of Southern California

Background

It has been proposed that cochlear implant (CI) users' spectral resolution can be improved by distributing adjacent spectral channels across ears, an approach referred to here as interleaved processors. However, the benefit of interleaved processors depends strongly on selecting truly independent channels within and across ears. Ipsilateral and contralateral masking may be used to measure the spread of excitation (SOE), which can be

used to identify independent spectral channels. For normal-hearing (NH) listeners, peak ipsilateral and contralateral masking occurs when the probe and the masker are approximately the same frequency, and the spread of masking is narrower with contralateral than with ipsilateral masking. Two factors may cause CI listeners' contralateral masking functions to differ from those of NH listeners. First, stimulating matched cochleotopic locations in each ear may not yield the same perceived pitch. Second, because CIs directly stimulate the auditory nerve, much of the cochlear mechanics that may be responsible for the greater spread of ipsilateral masking functions are circumvented. The goals of this study were to determine whether the peak of contralateral masking for CI listeners occurs when the probe and masker yield the same pitch percept and whether the SOE for CI listeners was reduced with contralateral maskers.

Methods

Pitch matching was performed by stimulating a reference stimulus in one ear and adjusting the stimulation site of an equally loud probe in the opposite ear until the pitch matched across ears. Contralateral and ipsilateral masking was measured using a modified Bekesy tracking procedure; a 20 ms probe was temporally embedded in a 500 ms masker. Maskers were presented at the most comfortable loudness level and loudness matched across ears. The ipsilateral masker was placed at the peak of the contralateral masking function.

Results

Preliminary data suggest that contralateral and ipsilateral masking functions differ considerably across patients and across stimulation sites. Despite that variability, the results indicated that the peak of contralateral masking occurred at approximately the same location as the perceived pitch matches. The results also indicated that, despite circumventing much of the cochlear mechanics, SOE was narrower with contralateral than with ipsilateral masking.

Conclusion

The relatively narrower contralateral SOE suggests that the number of independent channels can be increased by moving some stimulation sites to the opposite ear. The results also suggest that, whether using interleaved processors or standard clinical processors, pitch matching can provide an efficient method to optimally align stimulation across arrays.

978 Use of a Dual-Task Paradigm to Assess Listening Effort in a CI Simulation

Arlene Neuman¹, Keena Seward¹, Nandini Govil¹, Matthew Fitzgerald¹

¹New York University School of Medicine

Background

Many bilateral or bimodal users of cochlear implants (CIs) report that it is easier to listen when both devices are active than with only a single device, especially in noise. However, there is currently no method to quantify listening effort in these patients. Here we used a CI simulation to

test the feasibility of using a dual-task paradigm to measure listening effort. In a dual task paradigm, the listener divides attention between a primary and secondary task. As the primary task becomes more difficult, fewer cognitive resources are available for the secondary task, generally resulting in poorer performance. Our hypothesis was that when listeners perform a sentence-recognition task, as signal-to-noise ratio (SNR) decreases, performance on a secondary task will decrease due to an increase in listening effort.

Methods

Normal-hearing young adults participated. The primary task was to repeat sentences processed through an 8-channel CI simulation. AzBio Sentence Lists were presented in quiet and noise (+16, +12, and +8 dB SNR). The secondary task was to recall 7 digits presented visually before each set of 4 sentences. As a control, both the sentence-recognition and digit-recall tasks were tested singly. The NASA Task Load Indices for Effort, Mental Demand, and Performance were completed in each test condition.

Results

On the primary sentence-recognition task, performance did not differ between the single- and dual-task paradigms. Sentence-recognition scores decreased significantly as the SNR deteriorated. In contrast, the digit-recall scores were significantly lower in the dual-task paradigm, suggesting an increase in listening effort. However, no significant changes occurred in digit-recall as the SNR deteriorated. Finally, the NASA ratings indicated a significant perceived increase in listening effort and mental demand and decrease in performance as the SNR deteriorated.

Conclusion

A dual-task paradigm may be useful for quantifying listening effort because, when compared to the single-task control 1) performance on the primary sentence-recognition task was not affected, but 2) performance on the secondary digit-recall task decreased significantly. However, scores on the digit-recall task did not decrease as the SNR deteriorated. This may be due to the test parameters utilized here, or because the digit-recall task was suboptimal for observing smaller changes in listening effort, particularly within individual listeners. We are modifying our protocol to better understand these issues, and are testing the efficacy of the dual-task paradigm in CI recipients.

979 Self-Selected and Pitch-Matched Frequency Tables in Users of Bilateral Cochlear Implants

Matthew Fitzgerald¹, E. Katelyn Glassman¹, Chin-Tuan Tan¹, Mario Svirsky¹

¹New York University School of Medicine

Background

Bilateral cochlear implants (CIs) provide many benefits including improved speech-understanding abilities in noise and sound-localization. Currently, bilateral CIs are fit by

programming each ear independently, with minor adjustments to balance loudness between ears. While this procedure yields bilateral benefit in most patients, it cannot account for between-ear mismatches in insertion depth or neural survival. To address this issue, we have been exploring the use of real-time manipulations of the frequency table as a possible tool to aid the fitting of bilateral cochlear implants. Our previous data suggest that a subset of individuals select a frequency table in one ear that differs from the standard table worn in the contralateral ear. Our goal was to determine whether such selections are made because the listener is attempting to match the pitch percepts heard in each ear.

Methods

Participants included bilateral recipients of the Advanced Bionics (AB) device. All participants were initially presented speech via loudspeaker, and were instructed to adjust the frequency table until speech intelligibility was maximized. These selections were made both unilaterally, and with the contralateral CI active. All frequency-table selections were made in real time using custom software. Then, for each electrode in the array, a pure tone was presented via loudspeaker at the center frequency of the standard frequency table for one ear. In the contralateral ear, patients adjusted the frequency table until the pitch percepts were matched. These selections were then combined into a global pitch-matched table.

Results

Within a given listener, any shifts in the frequency table to bilaterally match the pitch percepts were largely consistent in the apical, mid, and basal end of the array. Taken together, the global pitch-matched table often differed from the table selected to maximize speech intelligibility. Generally, these pitch-matched tables were shifted higher in frequency than the self-selected table, which was usually shifted higher in frequency than the standard.

Conclusion

When listeners select a preferred frequency table that differs from the standard, they may be trying to select a signal that is as natural-sounding as possible without hindering speech intelligibility. Here, the pitch-matched tables rarely lined up perfectly with the self-selected tables for speech stimuli, especially in those cases where the self-selected speech table differed from the standard. We are currently investigating how performance on tests of speech intelligibility and sound-localization are affected by use of these frequency tables.

980 Absent Cortical ITD Representation in Congenital Single-Sided Deafness

Jochen Tillein^{1,2}, Peter Hubka¹, Andrej Kral¹

¹*Experimental Otology, ENT Clinics, Medical University Hannover, Germany,* ²*ENT Department, J.W.Goethe University Frankfurt, Germany and Medel Starnberg, Germany*

Background

Despite substantial reduction of ITD sensitivity in the cortex of congenitally deaf animals, cells sensitive to ITD changes were still observed (Tillein et al., 2010, *Cereb Cortex* 20:492-506). The auditory cortex of subjects with early single-sided deafness receives asymmetrical input leading to extensive reorganization of cortical aural dominance with aural preference for the hearing ear (Kral et al. 2012, *Brain*, in press). The recent study focuses on cortical ITD processing in this asymmetric hearing condition.

Methods

Two adult cats with congenitally unilateral deafness were compared to four adult deaf and four adult hearing control cats. Controls were acutely deafened by intracochlear application of neomycin. All animals were acutely stimulated with charge-balanced biphasic pulses (200µs/phase) in wide bipolar configuration through a custom made cochlear implant inserted into the scala tympani on either side. Cortical regions which were most responsive as defined by local field potential mapping were subjected to recordings of multi-unit activity using 16 channel electrode arrays (Neuronexus probes). Sensitivity to ITDs between -600 and +600 µs was tested with pulse trains (500 Hz, 3 pulses) at intensities of 0 – 10 dB above brainstem response thresholds. Template ITD functions (Tillein et al., 2010) were fitted to the data and the templates were statistically compared. ITD functions which did not fit significantly to the templates or had a modulation depth below 50 % were categorized as unclassified.

Results

Results demonstrate a significant increase in the number of unclassified but responsive cells with respect to deaf and hearing animals. These were found in more than 50% of all recording sites. However, when compared to deaf animals a significant increase in responsive sites was observed, so that with respect to responsiveness single-sided animals compared well to normal hearing controls. In consequence, cortical cells remained responsive to binaural stimulation, although the response was not ITD specific. Modulation depth of ITD functions in classified responses was additionally significantly smaller than in deaf and in hearing animals.

Conclusion

This study demonstrates that monaural deprivation leads to a distinct decrease of sensitivity to variation of binaural cues, whereas general responsiveness to binaural stimulation is comparable to hearing animals. This finding is in strong contrast to the situation in binaural deafness and demonstrates the detrimental influence of unilateral

deafness on binaural feature sensitivity and consequently on the localization ability.

Supported by DFG (Kr 3370/1-3 and Cluster of Excellence Hearing4All)

981 Comparison of Signal-Detection and Gap-Detection Thresholds with Focused Cochlear Implant Stimulation

Julie Arenberg Bierer¹, John M. Deeks², Alexander J. Billig², Robert P. Carlyon²

¹University of Washington, ²MRC- Cognition and Brain Sciences Unit

Background

With focused stimulation, such as with the tripolar electrode configuration, detection thresholds often vary substantially across electrodes for a given listener. In addition, we have previously shown that channels with high thresholds exhibit poorer frequency selectivity than those with low thresholds. These two findings could reflect variations in the health of auditory nerve fibers across the neural array, or, alternatively, variations in electrode distance from the modiolus. Differentiating the roles of electrode distance to nearby neurons and neural health (viability) is difficult for two reasons: 1) modern technology cannot image spiral ganglion neurons, and 2) imaging of the location of the electrode array is costly. Here we describe the measurement of gap detection thresholds, with the rationale that they might be elevated by the altered temporal discharge patterns associated with neural degeneration, but are less likely to be affected by the distance of the electrode from the modiolus.

Methods

Behavioral thresholds with focused stimulation were obtained for seven adult CI users to identify two channels with low and two channels with high thresholds for further testing. Gap detection threshold was then measured on the four test channels with the focused partial tripolar electrode configuration ($\sigma = 0.75$). A 2-interval forced choice, 2-down, 1-up adaptive procedure was used. Stimuli were 194 μ s/phase, 1031 pulses-per-second pulse trains lasting 200 ms. Both the train duration and level were varied. Gap detection thresholds were obtained at the most comfortable listening level for each channel unless that level could not be reached, in which case stimuli were presented at a medium-soft level that was loudness balanced across test channels. Thresholds were measured four or five times for each stimulus condition.

Results

The results showed a trend for channels with high thresholds to be basally located and to have longer gap detection thresholds, but there were clear exceptions to this relationship.

Conclusion

It is suggested that gap detection thresholds may help differentiate the effects of neural health and modiolus position on tripolar detection thresholds.

This work was funded by a Bloedel Hearing Research Travel Award (Bierer) and NIH DCR01-012142 (Bierer).

982 Assessing Spatial Channel Interactions in Cochlear Implants

Katrien Vermeire¹, Eddy De Vel¹, Idrick Akhoun², Ingeborg Dhooge¹

¹Ghent University Hospital, ²Advanced Bionics Research Centre

Background

The main drawback of modern multi-channel cochlear implants (CI) is that the spatial selectivity of the excitation pattern is severely limited by the widespread nature of electric fields in the extracellular tissue. Modern CIs have the flexibility to electrically stimulate the auditory nerve and to capture various electrical signals inside the cochlear lumen.

Methods

This study examines spatial channel interactions at the electrical and neural level in a group of Advanced Bionics HiRes90K users. All subjects were implanted with the Helix array. The EFI measurements were made with the EFIM research tool. EFI data were obtained for all electrodes. ECAP recordings were done using the RSPOM software. SOEs were obtained from 4 different electrodes (3-7-11-15) using a variable recording location paradigm. SOEs were collected with 4 different loudness levels.

Results

Width, slope and symmetry of spatial excitation patterns derived from these physical (EFI) and physiological (SOE) measures will be compared.

Conclusion

EFI recordings allow a finer interpretation of neural SOEs as it teases out the effects of electrical spread within the cochlea. Taken as a whole, this study serves as a direct comparison and identification of inter- and intra-subject variability in spatial profiles.

983 Current Focusing Improves Speech in Noise and Spectral Resolution in Cochlear Implant Users

David Landsberger¹, Arthi Srinivasan^{1,2}, Justin Aronoff^{1,3}, Bonnie Ong^{1,4}, Joseph Crew^{1,3}, Robert Shannon^{1,3}

¹House Research Institute, ²SUNY Downstate, ³University of Southern California, ⁴Emerson College

Background

Although each electrode in a cochlear implant provides independent information, the spreads of excitation from adjacent electrodes overlap such that multiple electrodes stimulate the same neural populations. To reduce channel interaction and spread of excitation, current focusing techniques have been proposed in which multiple electrodes provide simultaneous stimulation out of phase to restrict current spread. One current focusing technique, partial tripolar stimulation (PTP) involves stimulating on two flanking electrodes in the opposite phase of a central electrode. Previous work has shown that the spread of

excitation from PTP stimulation can be narrower than monopolar (MP) stimulation. In the present study, we implemented MP and PTP stimulation in novel speech processing strategies. Patients were tested on speech in noise and spectral resolution tasks to evaluate differences between the strategies.

Methods

Two novel sound coding strategies were implemented into an Advanced Bionics body worn speech processor. Each strategy consisted of 14-channel CIS to electrodes 2-15. The two strategies were identical in all parameters except for stimulation mode (MP stimulation for Exp-MP strategy and PTP for Exp-PTP strategy). M-levels for each electrode were carefully loudness balanced across the two strategies to ensure an equivalent spectral shape. Performance with each strategy was evaluated with HINT sentences, digits in noise and a new test to measure spectral resolution, the Spectral-temporally Modulated Ripple Test (SMRT). The SMRT consists of a spectral ripple whose phase drifts in time, eliminating potential loudness or edge effects of traditional spectral ripple tasks. Furthermore, the SMRT prevents the listener from performing the task by attending to a single electrode. Patients were evaluated on their spectral resolution with the SMRT test using both Exp-MP and Exp-PTP strategies.

Results

The average improvement in Speech Reception Thresholds (SRTs) with Exp-TP was 2.7 dB for HINT sentences in noise and 3 dB for digits in noise. All subjects performed better with Exp-TP with HINT sentences. One subject performed similarly with both strategies for the digits in noise task while all others performed better with the Exp-TP strategy. In pilot data, all subjects tested have shown better SMRT scores (i.e. better spectral resolution) with the Exp-TP strategy.

Conclusion

Current focusing (specifically PTP stimulation) provides better speech understanding in noise and better spectral resolution. Although further optimization of the strategies are needed, current focusing is a promising tool for better performance in future cochlear implant strategies.

984 Stimulation of the Cochlear Apex with Partial-Bipolar Asymmetric Pulses: Effects on Speech Intelligibility and Pitch Contour Identification by Cochlear Implant Listeners

Olivier Macherey^{1,2}, Jolijn Monstrey², John Deeks², Robert Carlyon²

¹LMA-CNRS, 31 Chemin Joseph Aiguier, 13402 Marseille Cedex 20, France, ²MRC Cognition and Brain Sciences Unit, 15 Chaucer Road, CB2 7EF Cambridge, UK

Background

Bipolar asymmetric pulses presented on the most apical channel of a cochlear implant (CI) can extend the range of both place and temporal pitch cues available to CI listeners (Macherey et al., JARO, 2011). Here, we investigate

whether the implementation of such pulses may improve the perception of speech and the ability to identify pitch contours of CI subjects.

Methods

Ten users of the Advanced Bionics CII/HiRes 90k device took part in two sets of experiments. In the first, we measured consonant identification in a vCv context and sentence recognition using low-pass filtered IHR sentences for two speech-processing strategies. The two strategies were identical in all respects except that the most apical channel delivered either monopolar symmetric or partial-bipolar asymmetric pulses. In the second set, subjects had to identify a five-note pitch contour in a five-alternative forced choice task. The spacing between notes was three semi-tones and several ranges of fundamental frequencies were tested. Performance was measured in three conditions: (1) for a subset of channels delivering high-rate monopolar pulse trains sinusoidally-amplitude modulated (SAM) at the fundamental frequency (F0); (2) for a partial-bipolar pulse train presented at the apex at a rate equal to F0; and (3) for a combination of (1) and (2). An additional condition presented pulses at the F0 rate to the apex, but, unlike condition (2), used monopolar stimulation.

Results

The results of the speech tests showed no difference in performance between the two strategies. The pitch contour test showed that a partial bipolar asymmetric pulse train presented at F0 on the apical channel can improve the identification of pitch contours, even when combined with monopolar SAM pulse trains on other channels. However, replacing the partial-bipolar asymmetric pulses by monopolar symmetric pulses on the apical channel yielded similar benefits.

Conclusion

The results of this acute study revealed no advantage of having partial bipolar asymmetric pulses instead of monopolar symmetric pulses on the apical channel of a CI. They also suggest that temporal pitch perception may be improved by an explicit representation of F0 delivered to a single channel (which in the present study was at the apex).

Macherey, Deeks and Carlyon (2011) J. Assoc. Res. Otolaryngol. 12: 233-251.

985 Refractory Properties of Cochlear Implant-Induced Spiking in Auditory Nerve Fibers Are Dependent on Location of Stimulation and Voltage-Gated Channel Type Distribution

Jason Boulet¹, Ian Bruce¹

¹McMaster University

Background

Experimental work has demonstrated that auditory nerve fibers (ANFs) of cats cannot fully respond to high rates of electrical stimulation, thus reducing the information transfer to the brain. Miller et al. (JARO 2001) have shown that a

limiting factor of the reduced spike information transfer can be attributed to the neuron's refractory period. A computational model of a node of Ranvier of the ANF (Negm and Bruce, EMBC 2008) suggested that low-threshold potassium (KLT) and hyperpolarization-activated cyclic nucleotide-gated cation (HCN) channels (Yi et al., J Neurophysiol 2010) might be responsible for a larger refractory period (Negm and Bruce, in prep.).

Methods

We extend that work with a simulation study taking into account ANF morphology (Woo et al., JARO 2010) to consider the differential spiking activity as a function of 1) the location of electrical stimulation and 2) nodal channel composition at important locations along the ANF. Specifically, we test three ANF models variants: A) only fast Nav and delayed-rectifier Kv at all nodes, B) with the addition of KLT & HCN channels (Yi et al., J Neurophysiol 2010) at the first peripheral node and on the nodes of Ranvier neighboring the soma and C) by expanding the distribution of KLT channels to all nodes (Bortone et al., Hearing Res 2006).

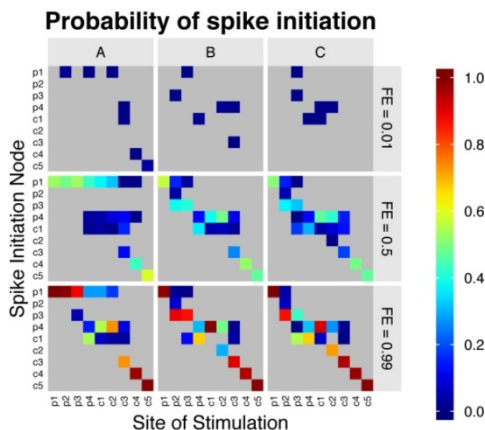
Results

In general, we observed the absolute refractory period of model C to be the greatest followed by model B, then by model A. Models B and C contrasted with model A by having a greater probability of spike initiation at the location of stimulation. Model A did not show a strong relative refractory period at its peripheral nodes. We argue that the washout of the relative refractory period in this region was dependent on the low correlation between the location of the stimulating electrode and the location of spike initiation.

Conclusion

Preliminary results indicate that model C is most consistent with the published physiological data. In addition to the KLT & HCN channels of model C, other ion channel types may be necessary to explain all aspects of refractory behavior observed *in vivo*.

This research was supported by the Natural Sciences and Engineering Research Council of Canada (Discovery Grant #261736).



986 Qualitative Ratings of Current Focusing by Cochlear Implant Users

Monica Padilla¹, David Landsberger¹

¹House Research Institute

Background

Channel interaction is believed to be a limiting factor in the number of effective spectral channels available to cochlear implant patients. Current focusing (determined by coefficient σ) is expected to reduce channel interactions, which could lead to better speech performance under difficult listening conditions. In a previous study (Landsberger et al., 2012) we related the reduction in spread of excitation from current focusing on one electrode with qualitative ratings of the tone perceived by CI users. We found a relationship between the reduction of spread of excitation and qualitative ratings. These results were exciting in that an adjective scaling task could be used as a quick (and possibly clinically implementable) test to predict who would benefit from current focusing. However in the previous study, only one location was tested in each of six patients. In this follow-up study, we measured qualitative ratings at many locations across the array on multiple subjects to determine the variability of qualitative ratings across the array within subjects. Furthermore we collected forward masked spread-of-excitation measures at a number of locations to verify if the relationship between spread of excitation and qualitative rating is maintained with more data points. If this is the case then qualitative ratings could be an easier and faster way to make these measurements reliably.

Methods

Seven users of the Advanced Bionics CII and HiRes 90k cochlear implants participated in this study. Spread of excitation for electrodes 4, 6, 10 and 12 was measured, using a 2IFC forward masking task. Qualitative ratings were measured for electrodes 2, 4, 6, 8, 9, 10, 12 and 14 using only two σ values (0 and 0.75). The same adjectives as in the previous study were used for ratings (clean/dirty, pure/noisy, high/low, full/thin, flute/kazoo).

Results

Preliminary results suggest that spread of excitation is related to the qualitative ratings used in most electrodes. As in the previous study, the Clean / Dirty Index, seems to be the most closely related to the reduction of spread of excitation.

Conclusion

It seems possible to quickly predict spread of excitation by using qualitative ratings. Of all of the tested adjective pairs, the clean/ dirty adjective pair best predict the amount of spread of excitation in that given electrode.

987 Musical Instrument Identification in Cochlear Implant Users: A Psychophysical Study of Acoustic Changes

Tanner Fulmer¹, Alison Crane¹, David Friedland¹, Christina Runge¹

¹Medical College of Wisconsin

Background

Cochlear implants (CIs) offer many deaf individuals greater opportunity to interact with their environment, but there are still shortcomings in the user's ability to perceive sound, particularly music. CI users perceive rhythm, but struggle distinguishing between instruments. This study examined CI users' ability to hear musical changes and explored the viability of using standard clinical equipment to measure auditory evoked potentials (AEP) in response to instrument changes.

Methods

Two same-different tests were designed to examine CI users' discrimination of instrument stimuli. Sample notes from 5 instruments (clarinet, flute, violin, saxophone, and trumpet) were trimmed to only include the center 500ms. The first test concatenated random combinations of these instrument samples and asked subjects to identify the sounds as same or different. The second test spaced the combinations by 500ms and again asked users to identify whether there were differences between sounds. Ten experienced adult CI users and four adult normal hearing (NH) subjects were administered both tests. Percent correct scores and sensitivity indices (D') were compared within and between groups. AEPs were measured on 4 NH subjects in response to clarinet-trumpet changes using clinical ABR equipment and a simple 3-4 electrode montage.

Results

CI subjects had lower discrimination scores on all tests and instrument combinations. However, both groups followed similar patterns in terms of which instruments seemed to be the easiest or most difficult to differentiate: clarinet-saxophone combinations were most difficult (NH $D'=1.70$, CI $D'=.85$), while both groups correctly identified flute-trumpet combinations over 99% of the time. Normal hearing D' scores for the spaced tests were .44 standard deviations lower than concatenate scores ($p=.03$), while CI D' scores were equal across the two tests. Statistically significant differences between NH and CI D' scores were observed for trumpet-violin, flute-saxophone, and clarinet-saxophone combinations. AEPs were successfully recorded in four NH individuals in response to clarinet-trumpet changes. The stimulus onset responses and acoustic change complexes were observed.

Conclusion

CI subjects have a baseline lower capacity than NH for instrument discrimination; however, both groups struggle with the same instrument combinations. Several CI subjects who scored poorly on instrument identification tasks had discrimination scores similar to NH, perhaps indicating these individuals may benefit from musical

training. Onset responses and acoustic change complexes can be recorded in response to instrument changes, although additional investigations need to be completed to correlate these responses with behavioral data.

988 Musical Instrument Identification in Cochlear Implant Users: The Effect of Attack and Decay on Perception

Alison Crane¹, Tanner Fullmer¹, Christina Runge¹, David Friedland¹

¹Medical College of Wisconsin

Background

Cochlear implants (CI) have revolutionized speech perception for patients who are severely hard-of-hearing; however, they have not provided good music perception. CI users have a near-normal ability to hear rhythm and tone duration but lack the ability to interpret timbre, a complex spectral and temporal perceptual attribute. It remains unclear which elements of timbre, if any, provide the most and the least information to CI users, specifically for the task of instrument identification.

Methods

Ten adult CI users were asked to identify instruments, a task that relies at least partly on timbre. CI-user performance was compared to normal hearing (NH) controls based upon a major scale and four modified versions. Five instruments were tested: clarinet, flute, alto saxophone, trumpet, and violin. The scale in the characteristic frequency range of each instrument was digitally manipulated to create four additional scales with varying acoustic properties: a G4-G5 scale, a G4-G5 scale with the decay removed, a G4-G5 scale with the attack removed, and a G4-G5 scale with the attack and decay removed. Subjects were presented with five separate tests consisting of randomly ordered instruments playing eight-note scales. Each instrument was presented four times per test, and after each scale, subjects were asked to identify the instrument.

Results

CI users performed at a level roughly 60% that of normal hearing participants for each scale, although scores were variable. Both CI users and NH participants performed progressively worse as the amount of information in the notes was decreased. Correct identification scores for each scale were as follows: characteristic scale (CI=57%, NH=95%), G4-G5 scale (CI=45%, NH=74%), G4-G5 scale with decay removed (CI=44%, NH=73%), G4-G5 scale attack removed (CI=36%, NH=64%), and G4-G5 scale with the attack and decay removed (CI=37%, NH=62%). Instrument identification using the characteristic scale in CI users was positively correlated with speech scores (CNC $R=0.260$; AZ Bio Quiet $R=.510$), although not as strongly as shown in previous studies.

Conclusion

The relative decline in performance when musical notes were manipulated was similar for CI users as for NH subjects. As such, information such as attack and decay

are important for instrument identification, but are not excluded by the processor or implant transmission. Instead, the data suggest that additional spectral elements of timbre are not being encoded.

989 Music Perception Associated with the Quality of Life in Post-Lingually Deafened Cochlear Implant Users

Christina Fuller^{1,2}, Rolien Free^{1,2}, Bert Maat¹, Deniz Baskent^{1,2}

¹University Medical Center Groningen, Department of Otorhinolaryngology / Head & Neck Surgery, NL,

²University of Groningen, Graduate School of Medical Sciences (Behavioural & Cognitive Neurosciences)

Background

The perception of music remains challenging for adult cochlear implant users. Nevertheless music is a pervasive art form, an environmental sound and a potent pleasurable stimulus that can be used to positively affect emotional state. As such, music therapies have shown to improve the quality of life for terminally-ill patients and older adults, an effect that could be relevant for CI users. Therefore in the present study we hypothesized that better enjoyment, quality, and perception of music in post-lingually deafened cochlear-implant users may be associated with higher health-related quality of life and better hearing ability.

Methods

Ninety-eight cochlear-implant users evaluated themselves on: 1) music enjoyment, quality, and perception (Dutch Musical Background Questionnaire), 2) health-related quality of life (Nijmegen Cochlear Implant Questionnaire) and 3) hearing ability (Speech, Spatial and Qualities of hearing Scale). In addition, percent-correct scores of word recognition in quiet were gathered.

Results

All music measures were correlated with the quality of life; only one music measure, the subjective perception of the elements of music, was correlated with the self-reported hearing ability. Furthermore, both quality of life and self-reported hearing ability were moderately correlated with the word perception in quiet. Multiple regression analyses showed the perception of elements of music and words to account for 34% of the variance in quality of life and the perception of elements of music and words and the music listening habits for 46% of the variance of the hearing ability.

Conclusion

In support of our hypothesis all music measures were correlated with the quality of life. In partial support of our hypothesis only one music measure, the subjective perception of the elements of music, and the speech perception measures were correlated with the hearing ability. An explanation for this finding may be that both the self-reported hearing-ability and the subjective perception of the elements of music are more pointed towards measuring performance and ability than the health-related quality of life, which covers more domains of daily life.

Concluding, a musical therapy program or new signal processing algorithms that enable CI users to enjoy music more may improve their quality of life and partially their hearing ability.

990 Comparing Enhancement of Signal Detection in Normal-Hearing, Hearing-Impaired, and Cochlear-Implant Listeners: Effects of Stimulus Level and Spectral Spacing

Matthew Goupell¹, Olga Stakhovskaya¹, Kia Griffith², Tanvi Thakkar¹, Sandra Gordon-Salant¹

¹University of Maryland - College Park, ²Howard University

Background

Improved signal detection (i.e., enhancement) of tones occurs when a component of a complex tone is originally absent from the signal and is inserted at some later time. While enhancement has been shown to occur in normal-hearing (NH) and cochlear-implant (CI) listeners, it has yet to be shown to occur in hearing-impaired (HI) listeners. We therefore compared enhancement in NH, HI, and CI listeners under conditions of varying stimulus level and spectral spacing.

Methods

Ten NH, six HI, and six unilateral CI listeners participated in the study. Detection thresholds were measured with an adaptive procedure for a component in a 100-ms complex tone (test stimulus). Enhancement was defined as the difference in the thresholds between the test stimulus preceded by a 1-s adapter and the test stimulus alone. NH and HI listeners were presented harmonic complexes with a fundamental frequency (F0) of 100 or 200 Hz. The target frequency (TF) was 1 or 2 kHz. Spectrum levels were varied between 23 and 63 dB SPL. CI listeners were presented constant-amplitude pulse trains over multiple electrodes via direct stimulation. Electrode spacing, number of background electrodes, and level were varied.

Results

All three types of listeners showed enhancement, i.e., lower detection thresholds of the target component/electrode with the adapter present. For NH listeners, enhancement was independent of overall level and was largest for F0 = 200 Hz and TF = 1000 Hz. HI listeners also showed enhancement, but it was less than that observed for NH listeners, particularly in regions of hearing loss. All CI listeners showed enhancement; individual tendencies were prevalent, though most showed larger enhancement for larger levels.

Conclusion

Stimulus parameters (e.g., spectral spacing) as well as subject factors (e.g., hearing loss) affect the magnitude of enhancement. Comparison of enhancement across listener groups might elucidate the mechanisms necessary for enhancement to occur. For CI listeners, conditions that show enhancement may inform future processing strategies on how to improve speech understanding in noise.

991 Assessing the Effects of Reverberation on Musical Sound Quality Perception in Cochlear Implant Users

Alexis Roy¹, Patpong Jiradejvong¹, Charles Limb^{1,2}
¹*Johns Hopkins University School of Medicine*, ²*Peabody Conservatory of Music*

Background

In previous studies, we designed a musical sound quality assessment method (called CI-MUSHRA) to quantify specific acoustic parameters that contribute to cochlear implant (CI)-mediated sound quality impairments. The purpose of this study was to assess the acoustic parameter, reverberation time (RT60; time for sound to decay by 60dB), using CI-MUSHRA. It is well established that acoustic reverberation plays an important role in the perceived sound quality of music by adding fullness and a sense of space; without reverberation, music sounds dry and lifeless. We hypothesized that the difficulty of CI users to perceive reverberation cues contributes to their overall musical sound quality impairments.

Methods

To determine the appropriate stimuli for the CI-MUSHRA evaluation, 6 classical musical pieces (solo and ensemble) that were originally recorded using an anechoic sound chamber were modulated with various RT60s (0, 1, 2, 3, 4, 5, or 6 seconds). 9 normal hearing (NH) listeners completed a two-alternative forced choice (2AFC) paradigm in which they were presented with two RT60 versions of a musical piece and asked to select the stimulus in the pair with the best sound quality.

For the CI-MUSHRA evaluation, five RT60 versions of a classical piece (0, 1, 2, 4, 6 second RT60 versions) were simultaneously presented in random order, along with a labeled-reference (2 second RT60; best sound quality version as rated by NH listeners). One CI participant listened to each version and provided sound quality ratings based on a 100-point scale that reflected perceived sound quality difference among versions. CI user data accrual is ongoing.

Results

For the 2AFC paradigm, NH listeners rated pieces with small amounts of reverberation (1-2 second RT60) as having better sound quality than anechoic versions (0 second RT60) and versions with greater than 2 second RT60 (Bradley-Terry Model). These results revealed that small amounts of reverberation play an important role in perceived sound quality. In comparison, for the CI-MUSHRA evaluation, the one CI user tested could not detect sound quality difference among most RT60 versions ($p > 0.05$; two-way ANOVA), suggesting that difficulties perceiving reverberation cues contributes to implant-mediated sound quality impairments.

Conclusion

These preliminary results indicate that the impaired ability of CI users to perceive reverberation cues may contribute

to musical sound quality limitations. Processing strategies that can enhance perception of acoustic reverberation have the potential to improve implant-mediated music listening.

992 Effect of Site-Specific Level Adjustments on Speech Recognition with Cochlear Implants

Ning Zhou¹, Bryan E. Pfingst¹
¹*University of Michigan*

Background

Modulation detection thresholds (MDTs) vary across stimulation sites in a cochlear implant electrode array in a manner that is ear specific. Previous studies have demonstrated that speech recognition with a cochlear implant can be improved by removing stimulation sites with poor modulation sensitivity from a subject's processor MAP. The objective of the current study was to test an alternative site-specific approach for improving speech recognition. Based on previous findings that modulation detection improves significantly with stimulus level, adjustments in level were made at stimulation sites with the poorest MDTs.

Methods

Nine postlingually-deafened ears implanted with the Nucleus cochlear implants were evaluated for MDTs, detection threshold levels (T levels) and the maximum-comfortable loudness levels (C levels) on each of the available stimulation sites. In six ears, these measures were compared to measurements taken on average 1.4 years prior to the study to test for stability over time. For each ear, the minimum stimulation level settings in the speech processor MAP were raised from true thresholds (i.e., Ts) on 5 stimulation sites with the poorest MDTs. Level increases of 5% and 10% of the dynamic range were tested. For comparison, a 5% level raise was applied to all stimulation sites. Speech reception thresholds using the level-adjusted processor MAPs were compared to a control MAP that utilized true threshold settings without level adjustment.

Results

In most cases, the across-site patterns of Ts, Cs, and MDTs were consistent with those measured 0.9 to 1.8 years earlier. On average, the 5% level increase on the 5 electrodes with the worst MDTs resulted in an across-ear mean improvement in speech reception thresholds of 2.36 dB relative to the control MAP. For individual ears, the 5% raise almost always produced better performance relative to the control. Performance with the 10% raise produced the best performance in 3 of the 9 ears but performance was equal to or less than that with the 5% raise in 4 ears and it was worse than the control in 2 ears. The 5% level increase on all stimulation sites, a parsimonious approach, was not effective compared to the site-specific level adjustments.

Conclusion

Across-site patterns of psychophysical measurements remained stable in experienced implant users over a test-retest period averaging 1.4 years. Level adjustment was an effective alternative to site selection for improving speech recognition in cochlear implant users.

993 Sound-Field Auditory Steady State Response (ASSR): Data from Normal-Hearing Adults, Cochlear Implant Recipients and Cochlear-Implanted Human Cadaveric Model

Shruti Deshpande (Balvalli)¹, Michael Scott^{1,2}, David Brown³, Ravi Samy¹, Jareen Meinzen-Derr², Jill Stephens⁴
¹University of Cincinnati, ²Cincinnati Children's Hospital Medical Center, ³Pacific University, ⁴The Listening Center at Johns Hopkins

Background

Objective sound-field (SF) techniques need to be explored for evaluating difficult-to-test cochlear-implant (CI) recipients as they may provide real-world information not provided by electrical pulses. The purpose of the present study was: Experiment 1: To determine if the SF-ASSR can be measured for adults with normal-hearing (NH) and CIs. To investigate if electrophysiologic ASSR thresholds (E-ASSR) obtained through SF correspond to the subject's behavioral thresholds to both narrow band noise (NBNthds) and ASSR stimulus (B-ASSR). Experiment 2: To evaluate E-ASSR data for artifact that may need to be controlled for in this and future studies.

Methods

Experiment 1: Subjects included 15 adults with NH and 6 adults with CI. ASSR measurements (IHS SmartEP) were made with a SF speaker located 1 meter from test-ear and at 90° Azimuth, with the non-test ear plugged. Recordings were made from two montages: forehead to contralateral-mastoid and forehead to nape, ground: contralateral clavicle. Thresholds were obtained for both groups in three conditions: NBNthds, B-ASSR, and E-ASSR for 0.5, 1, 2, 4.0 kHz. Experiment 2: The right ear of a human cadaver (CIHC) was implanted with a CI 6 hours post-mortem. Normal impedances indicated that the CI was placed in an electrically conductive environment, while Neural Response Telemetry was absent for all channels. ASSR was recorded with the same protocol outlined in experiment 1.

Results

Experiment 1: Statistically significant differences between NBNthds, B-ASSR and E-ASSR were present for the NH group. A subtraction factor could be applied to predict behavioral thresholds if E-ASSR is known. There were no significant differences between the three conditions for the CI group (Figure1) suggesting that E-ASSR may be a good predictor of behavioral thresholds.

Experiment 2: In the CIHC, ASSR was recorded despite nonexistent neural activity (Figure2), suggesting that the artifact "mimicked" the response. Across frequencies, as intensity of the stimulus increased from 40 to 70 dB SPL, the amplitude of the artifact increased irrespective of the

site of recording (contralateral mastoid vs. nape). Also, when the stimulus characteristics were held constant, amplitude of the artifact was greater when recorded from the contralateral mastoid compared to the nape of the neck.

Conclusion

Further data is needed to characterize and control the artifact, which will enhance the clinical applicability of SF-ASSR, especially in assessing difficult-to-test CI recipients.

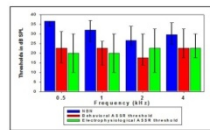


Figure 1: For the CI group, the Friedman test, Wilcoxon Signed Rank Test (post-hoc) and Bonferroni adjustments indicated that the thresholds were not significantly different between NBN, B-ASSR & E-ASSR across the four frequencies ($p > 0.05$).

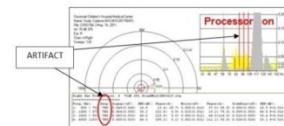


Figure 2: CI-Artifact recorded in the CIHC.

994 Speech Enhancement Using Sparse Coding in a Neural Space

Jessica Monaghan¹, Ian Winter², Matthew Wright¹, Stefan Bleack¹

¹University of Southampton, ²University of Cambridge

Background

In normal hearing, the ability to understand speech is remarkably robust even in the presence of high levels of noise and reverberation. In contrast, hearing-impaired listeners, including those with cochlear implants, have great difficulty understanding speech and following a conversation even when the speech is considerably more intense than the noise. Similarly, automatic speech recognition algorithms are highly susceptible to corruption by interfering noise of even moderate intensity. The superiority of human listening motivates a neural approach to speech processing. Sang et al (2011) proposed just such an approach, based on the hypothesis that the response of each class of neuron in the ventral cochlear nucleus can be modeled by fractional derivatives of order k , where $0 \leq k \leq 1$. This provides for a multi-dimensional neural space in which speech sounds can be represented. An efficient representation of speech such as this may be one factor contributing to the robustness of human speech perception.

Methods

Employing a sparse-coding strategy, we tested the potential of using a multi-dimensional neural space as a biologically-inspired basis for noise reduction and speech enhancement. Noisy speech was processed with an auditory model and the output of each frequency channel transformed into a neural space with ten k dimensions. Sparse coding was performed on the speech in the neural space and the enhanced speech signal was then reconstructed.

Results

Informal listening indicated that the level of the background noise had been reduced. The intelligibility of the reconstructed enhanced speech will be formally tested in normal hearing listeners using the BKB sentence corpus.

The results of these experiments will be reported at the conference.

Conclusion

Fractional derivatives enable transformation of speech signals into the neural space, and these can be resynthesized without loss of quality. De-noising can be performed by sparse coding on fractional derivatives and may assist noise reduction for hearing prostheses and automatic speech recognition.

995 Radiant Energy, Pulse Shape, and Power as Driving Parameters for Infrared Neural Stimulation in the Cat Cochlea

Ken Zhao¹, Suhrod Rajguru², Claus-Peter Richter¹
¹Northwestern University, ²University of Miami

Background

Infrared neural stimulation (INS) is a non-contact mode of spatially selective stimulation that shows promise for future applications in cochlear implants (CIs). Delivery of radiation pulses results in heat deposition. It is crucial to optimize the stimulation parameters to prevent tissue damage.

Methods

We conducted physiological studies of the stimulus parameters (radiant energy, pulse duration, and pulse shape) in cat cochleae using the Capella, Renoir, and RINS-Alpha lasers. The physiological response of auditory neurons was quantified by measuring evoked compound action potentials (CAPs) from the round window.

Results

Pulses of equivalent radiant energy but different pulse durations were used for INS. Shorter pulses were more effective. For pulses above approximately 100 μ s, the response scaled with power. Investigations of the effect of pulse shape showed that waveforms with a rapid onset to, or rapid offset from, peak power elicited the largest responses. At low values, further reductions in radiant energy decreased the CAP response.

Conclusion

The results suggest that short duration pulses of shapes with a rapid rise to, or fall from, peak power that delivered sufficient radiant energy were the most efficient form of INS and should be utilized in the development of CIs based on INS.

This work was supported by DC011855-01A1 and Lockheed Martin Aculight.

996 Optimization of Cochlear Implants Coding Strategies Using Spike Distance Metrics and Information Theory

Jonathan Laudanski¹, Teng Huang^{1,2}, Nicolas Veau¹, Dan Gnansia¹
¹Neurelec, ²EUROCOM

Background

Over the past 20 years, different cochlear implant coding strategies have been proposed to improve the patients' speech recognition performance. Frequently, vocoders are used on normal hearing listeners (NH) as a model to study the impact of specific psycho-acoustical effects (e.g. dip-listening in co-modulation masking release) or new coding strategy (e.g. strategies using both amplitude and frequency modulation). A major problem of this approach is to generate stimuli carrying identical information to NH and CI listeners: place coding (that corresponds to most common case of envelope coding by the cochlear implant) is accurately simulated, however fine temporal coding cannot be simulated through vocoder technique. In addition, the vocoded stimuli are ultimately re-analysed by the healthy ear with its distortion products and no peripheral degeneracy.

Methods

We use a computational model of electrical stimulation to simulate the responses of auditory nerve fibers (ANF) to electric stimulation. The model includes the CI pre-processing stages, computation of the intra-cochlear potential and its effect on a biophysical model of ANF. First, we fit the model to the results of Miller et al. (2001) before optimizing pre-processing parameters using two different cost functions. In both cases, the cost functions are related to the distance between spike trains produced by the ANF population. We use a two parameters bin-less spike distance metric (Aronov 2003) where the first parameter describes the cost of moving spikes in time while the second that of swapping discharge across cells.

Results

We present a first cost function which measures the distance between spike trains produced by electrical stimulation and normal responses to acoustic sounds. Responses are simulated following presentation of vowel-consonant-vowel (VCV) at different signal-to-noise ratio (SNR). The second cost function solely uses responses to electrical stimulation. The optimization is done by assessing the information carried by spike trains encoding the finite set of VCV sounds. We show that the temporal and spatial resolution at which distances are computed can have a major effect on the pre-processing parameters. We discuss the results in relation with tolerance to electrode placement and peripheral nerve survival.

Conclusion

This study provides a new quantitative method for improving coding strategies based on the peripheral information supplied by CI.

997 An Objective Criterion for Detecting Threshold of Evoked Potential Based on a Likelihood Ratio Test

Jonathan Laudanski¹, Kai Dang², Dan Gnansia¹, Nicolas Veau¹

¹Neurelec, ²EUROCOM, Sophia-antipolis, France

Background

Electrically evoked compound action potentials (ECAP) are routinely used in clinical audiology to set the threshold level of a patient's cochlear implant (CI) processor. In comparison to psychophysical experiments where threshold are usually estimated using an adaptive procedure, the estimation of threshold from evoked potentials is often left to the judgment of experts. Only a few statistical tests have been proposed to set objective criteria for the detection of an evoked potential. For instance, Hughes et al. (2000) propose to compare a template to the recorded response. Threshold is set when a minimal level of correlation with the template is obtained. More recently, Undurraga et al. (2012) proposed a criterion for threshold estimation based on the deviation from F-statistics between the signal and residual noise measured. In this study, we demonstrate the use of a threshold criterion based on a likelihood ratio test.

Methods

First, numerical simulations are carried to demonstrate the validity of the likelihood ratio test in setting a threshold for signal detection. The simulation use a template signal embedded into a Gaussian white noise of different levels. Second, electrically evoked compound action potential (ECAP) recorded from implanted guinea-pigs are analysed. Animals are implanted using miniaturized electrode array and stimulated by biphasic current pulses. A forward masking paradigm is used for artifact subtraction to obtain the ECAP.

Results

We demonstrate both analytically and using simulation that the likelihood ratio test is equivalent to the F-statistic in the case of a one-sample signal. We then show that prior knowledge of the signal shape can be used to decrease the minimal SNR for detection. We investigate the effect of filtering on the recordings and show how to derive optimal filter parameters for a signal-filter pair. Finally, we validate the approach on ECAP recordings obtained from anethetised guinea-pig and discuss existing drawbacks linked to partial artifact cancellation.

Conclusion

In conclusion, using a standard approach in signal detection theory, we can provide a statistical test allowing to decide on the presence or absence of an evoked response.

998 Enhanced Temporal Coding in Auditory Prostheses of Onsets in the Speech Envelope Can Lead to Improved Sound Perception in Adverse Listening Conditions

Raphael Koning¹, Jan Wouters¹

¹ExpORL, Dept. Neurosciences, University of Leuven, Belgium

Background

Speech intelligibility (SI) can be very good in quiet for users of hearing aids (HAs) or cochlear implants (CIs). In adverse listening conditions their speech understanding rapidly decreases.

Recent studies have confirmed that the most important parts of the speech signal for SI are the phoneme transitions and the rapid changes in temporal and spectral content. In this research a speech enhancement algorithm called enhanced envelope (EE) strategy has been developed that focuses on the enhancement of the onsets of the speech envelope. The strategy amplifies the onsets of the speech envelope in all frequency bands by deriving and introducing additional peak signals at the onsets.

Methods

The algorithm was evaluated with two groups of hearing impaired listeners: HA and CI users. The potential of the EE strategy was investigated in stationary speech shaped noise (SSN) and in an interfering talker. Keyword correct scores were collected for the Dutch LIST sentences in stationary SSN with six CI users at fixed signal-to-noise ratios (SNRs). Additionally, the speech reception threshold (SRT) was determined in an adaptive procedure in stationary SSN and in the competing talker scenario with 5 HA and 5 CI users, respectively. The presentation level of the speech was 65 dB SPL. For the HA users, the presentation level was fitted to the hearing loss using NAL-rules.

Results

All CI users showed an immediate benefit of the EE algorithm in comparison to the reference strategy that they were using in their clinical device. Overall, an SRT improvement of 2 dB was obtained in stationary SSN and around 3 dB in the competing talker condition when the onsets of the target speaker were enhanced. Furthermore, a benefit was obtained when the onsets of the noisy mixture were enhanced. The latter does not require a priori knowledge of the speech signal for the peak signal extraction. In HA listeners, an SRT improvement of 1.5 - 2.5 dB was obtained in stationary SSN.

Conclusion

The results suggest that SI can be improved in adverse listening conditions by an enhanced temporal coding of the onsets of the speech envelope in the signal processing path of auditory prostheses.

999 A Case Study of Optimized Cochlear Implant Stimulation in a Congenitally-Deaf Individual

Daniel Aguiar¹, Thomas Talavage^{1,2}, J. Brandon Lafren^{1,3}

¹School of Electrical and Computer Engineering, Purdue University, ²Weldon School of Biomedical Engineering, Purdue University, ³Departments of Otolaryngology, Physiology and Neuroscience, New York University School of Medicine

Background

In post-lingually deafened individuals, cochlear implants (CIs) are effectively intended to achieve the ideal condition of replicating excitation patterns in the auditory nerve produced under normal acoustic hearing conditions. Under this ideal, perception of external acoustic stimuli would be unchanged relative to performance prior to onset of deafness. However, few efforts have been directed at identifying the upper-bound of performance that is achievable with current CI hardware and signal processing. Rather, current stimulation patterns have often been developed in a phenomenological manner. We have developed a framework by which CI stimulation may be optimized for an individual, and documented substantial performance benefit in a vowel identification task.

Methods

In our framework (Figure 1), an acoustic source is passed through (top) a computational model of normal acoustic hearing (Heinz et al., ARLO, 2001) and (bottom) a cochlear implant electrode selection algorithm followed by a computational model of electric hearing (Bruce et al., IEEE TBME, 1999), yielding two neural activation patterns (NAPs). These NAPs are compared using an objective function to obtain a distance measure that is used to select electrodes to best match the NAP produced by the model of electrical hearing with the NAP produced by the model of normal acoustic hearing. This optimizes the electrical stimulation sequence against the nerve activity expected to be input to the central auditory pathway in the case of a healthy cochlea.

Optimized stimulation patterns were generated for a 23 y.o. congenitally-deaf user (14 years; Nucleus-24). Patterns were generated for nine /hVd/ vowel tokens, each presented in quiet (infinite SNR) or speech spectrum-shaped noise (20 and 10 dB SNR). The Nucleus MATLAB Toolbox drove the user's implant while performing a 9AFC vowel identification task under his preferred (real-time) and optimized (pre-generated) strategies, using an A-B-A-B (by day) test paradigm.

Results

Substantial benefit was evidenced for optimized stimuli (Figure 2) under conditions of speech in quiet and noise.

Conclusion

Appreciable improvement in a subject for whom this optimization is non-ideal (a congenitally-deaf user is not expected to better recognize "normal acoustic hearing" inputs) suggests that CI stimulation patterns can be

improved to increase speech perception performance, even in modest background noise. Use of this framework can provide a lower-bound on the ceiling for CI speech perception performance, against which future improvements in hardware and stimulation strategy may be measured.

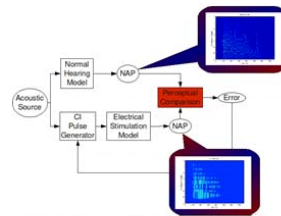


Figure 1: Framework for optimization of CI electrode stimulation, based on matching neural activation pattern produced by a model of electrical hearing (bottom) with that produced by a model of normal acoustic hearing (top).

Strategy	Quiet	20 dB SNR	10 dB SNR
Preferred	(25.6%/23.3%) 24.5%	(20.0%/24.4%) 22.2%	(24.4%/21.1%) 22.8%
Optimized	(51.1%/41.1%) 46.1%	(52.2%/42.2%) 47.2%	(32.2%/36.7%) 34.5%

Figure 2: 9AFC vowel identification task results for a 23 y.o. congenitally-deaf CI user (14 years; Nucleus-24), aggregated over an A-B-A-B (by day) paradigm. Tokens generated from sources in quiet or speech spectrum-shaped noise at 20 or 10 dB SNR. Session-level percent correct scores given for (1st/2nd day) and Average.

1000 Asymmetric Signal Degradation Causes Difficulty in Understanding Speech in Spatial Attention Tasks

Daniel Eisenberg¹, Matthew Goupell¹

¹University of Maryland - College Park

Background

Normal-hearing (NH) listeners can nearly perfectly recall words in an attended ear while ignoring the other ear when dichotic speech is presented over headphones. However, recent experiments have shown that this does not necessarily occur in people with asymmetrical hearing. People with asymmetrical hearing loss, bilateral cochlear implants, or single-sided deafness very likely have a relatively "good" ear (i.e., high-quality speech signals) and "bad" ear (i.e., low-quality speech signals). We simulated different levels of signal degradation by independently varying the signal quality in each ear, as would occur in users of one or two cochlear implants, in order to understand the effect of having a good and bad ear in spatial attention tasks.

Methods

Ten NH listeners participated in the study. Listeners reported keywords from five-word nonsense sentences in selective and divided attention tasks. Over headphones, a target talker was presented in one ear and an interferer was presented in the other, both at 65 dB SPL-A. In experiment 1, signal degradation was imposed by varying the number of channels in a noise vocoder. The signals were either unprocessed speech or had 4, 8, or 16 channels. In experiment 2, signal degradation was imposed by tonotopically shifting carrier frequencies in an eight-channel sine vocoder. Training was provided prior to testing for the shifted sine-vocoded sentences.

Results

For experiment 1, in conditions with symmetrical signal degradation, in the selective attention task, listener performance was near ceiling for all conditions; hence, there was no effect of the number of channels. In the divided attention task, performance was near 50% correct on average and gradually increased as the number of

channels increased. In conditions with asymmetrical signal degradation, in both the selective and divided tasks, listener performance was systematically lowest when there was poorer resolution in the attended ear compared to the ignored ear, and was highest when there was better resolution in the attended ear compared to the ignored ear. It was hypothesized that a similar trend would be seen in experiment 2 when tonotopic shift was imposed.

Conclusion

These data demonstrate that it is more difficult to attend to a poor-quality speech signal when trying to ignore a high-quality speech signal. This may adversely affect the advantage of spatial listening in certain spatial configurations for people with asymmetrical hearing, i.e., those with good and bad ears.

1001 Vertical Perception of Simple Stimuli in Normal-Hearing and Cochlear-Implant Listeners

Tanvi Thakkar¹, Olga Stakovskaya¹, Matthew Goupell¹
¹University of Maryland, College Park

Background

In normal-hearing (NH) listeners, elevation perception depends upon frequency-dependent peaks and notches imposed by filtering from the pinna. However, limited spectral resolution and current spread in cochlear-implants (CIs) make it difficult to encode spectral cues. Previous research has shown that elevation can be perceived from single tones. Sounds presented over headphones or with CIs lack filtering from the pinna and are perceived “within” the head. We examined the perceived intracranial elevation of tones in NH listeners and single-electrode stimulation in CI listeners. We hypothesized that post-lingually deafened CI users would show systematic changes in elevation with electrode number, while pre-lingually deafened CI users would not. The ultimate goal was to determine the importance of typical elevation perception development from acoustic stimulation.

Methods

NH listeners were presented monaural and diotic tones varying from 0.125 to 16 kHz (19 frequencies) using ear-insert headphones. Stimuli were calibrated to a comfortable and equal loudness (reference of 50 dB SPL-A at 1000 Hz). Unilateral and bilateral stimulation was presented to two bilateral CI listeners; unilateral stimulation was presented to three unilateral CI listeners. Stimuli were biphasic, monopolar pulse trains at one of 13 electrodes or electrode pairs, all presented at comfortable levels. The rate of pulse trains was 300 or 1000 pulses per second (pps); conditions with rate roving were also tested (50% randomization) to confound assigning elevation simply to pitch. On each trial, listeners indicated where they heard the auditory image by clicking on a face (horizontal and vertical position).

Results

Preliminary NH data showed that listeners perceive a change in elevation as frequency increases. Specifically,

sounds are perceived higher as the frequency increases between 0.25-12 kHz and does not change at higher frequencies. Most post-lingually deafened CI users showed that the basal electrodes were often perceived as higher in elevation and responses were unaffected by rate roving. No prelingually-deafened CI users showed a change in elevation that was unaffected by rate roving, implying that these listeners were simply assigning elevation to pitch.

Conclusion

These data highlight the association between place of stimulation and elevation perception in NH and CI listeners. Post-lingually deafened individuals may be making use of their spatial maps developed prior to hearing loss and may help us understand how the auditory system develops the perception of elevation. These data also demonstrate the potential to present elevation cues to CIs.

1002 Acoustic Models of Cochlear Implants: Evaluation in Single Sided Deafness Patients

Mario Svirsky¹, Arlene Neuman¹, Keena Seward¹, Katelyn Glassman¹, Nai Ding¹, Chin-Tuan Tan¹, Xiang Zhou¹, Matthew Fitzgerald¹, Elad Sagi¹
¹NYU School of Medicine

Background

Acoustic models of cochlear implants have been used in numerous published studies but the validity of these models has not been well established. A recent development presents a unique opportunity to validate and enhance these acoustic models: the implantation of “single-sided deafness” listeners, who have normal or near normal hearing in the ear contralateral to the implant. These listeners can compare what they hear with the implant to what they hear with an acoustic model in the normal hearing ear.

Methods

Three cochlear implant users with single sided deafness were presented the same sentence twice. First, the unprocessed sentence was sent through a direct connection to their cochlear implant speech processor (which had the microphone input deactivated). Then the sentence was processed through a cochlear implant acoustic model (a noise vocoder) and presented to the normal hearing ear through loudspeakers. The analysis filters used in the acoustic model had the same cutoff frequencies as those in the listener’s speech processor, but the noise bands of the vocoder were adjustable. Listeners used a graphical interface to determine a “self-selected model” by modifying the low- and high-frequency edge of the set of noise bands until the noise vocoder sounded as similar as possible to the percept provided by the implant. The process was then repeated for a sinewave vocoder. Lastly, listeners answered questionnaires about the similarity between the sentences as heard through the cochlear implant and through four different types of vocoders: noise vs. sinewave, and standard vs. self selected. The standard models (which

are the most commonly used in the literature) used noise bands or sinewaves whose center frequencies were identical to those of the analysis filters.

Results

Self-selected models tended to have higher frequency ranges than the standard models. On average, these self-selected models were deemed to produce sounds that were “very similar” to those heard through the implant (6.7 in a 9 point scale). Ratings for standard models were poorer on average, with a 4.7 score (where 5 corresponds to a “somewhat similar” rating). Some standard models received ratings of 3 (not very similar) and even 1 (not at all similar-completely different). Noise vocoders were better for two of the listeners and sinewave vocoders were better for the third one.

Conclusion

Results suggest that some of the acoustic models commonly used in the literature are inaccurate representations of the percepts actually heard by some cochlear implant users.

1003 Restriction of Wnt Signaling in the Dorsal Otocyst Determines Semicircular Canal Formation in the Mouse Embryo

Tepei NODA^{1,2}, Shizuo KOMUNE², Chikara MENO²

¹Hamanomachi Hospital, ²Kyushu University

Background

Inner ear develops from single epithelial sheet, otic placode. Whereas canonical Wnt signaling plays an important role in induction of the otic placode and its axial determination, its contribution to otic morphogenesis at later stages has remained unclear. We therefore have studied the role of Wnt signaling in that stage.

Methods

To investigate the expression pattern of Wnt signaling in the later stage of otic development (E10.5~E12.2), we used a Wnt reporter strain, BAT-gal. We next used a combination of whole-embryo culture and chemical compounds in order to evaluate the function of Wnt signaling.

Results

The activity of Wnt signaling was continuously observed, but gradually restricted in the dorsolateral otocyst. The genes for several Wnt ligands were expressed in the dorsal otocyst according to specific patterns, whereas those for secreted inhibitors of Wnt ligands were expressed exclusively in the ventral otocyst. With the use of whole-embryo culture in combination with potent modulators of canonical Wnt signaling, we found that forced persistence of such signaling resulted in impaired formation both of the lateral outpocketing and of the fusion plates of the dorsal outpocketing. Canonical Wnt signaling was found to suppress the expression of otic determinants, Netrin1 and Otx1.

Conclusion

Our stage-specific functional analysis suggests that strict regulation of canonical Wnt signaling in the dorsal otocyst is required for the process of semicircular canal formation.

1004 Effects of Small RNA Depletion on Development of Mammalian Inner Ear and Sensory Hair Cell Differentiation and Maintenance

Marsha L. Pierce¹, Heather C. Jensen-Smith¹, Sharalyn M. Steenson¹, Colby W. Bradfield¹, Isha Dewan¹, Garrett A. Soukup¹

¹Creighton University

Background

Small RNAs, namely endogenous siRNAs and miRNAs, are crucial regulators of transcriptional and post-transcriptional regulation in eukaryotic cells. Prior studies of *Dicer1* conditional knockout (CKO) effecting small RNA depletion and *Dgcr8* CKO effecting specifically canonical miRNA depletion have demonstrated differences regarding cell proliferation and differentiation. While *Dicer1* CKO in stem cells has effects on both proliferation and differentiation, *Dgcr8* CKO primarily effects differentiation. These results largely reflect specific roles for siRNAs in chromosomal maintenance and miRNAs in regulatory pathways effecting cell fate and function.

Methods

To compare loss of small RNAs vs. loss of canonical miRNAs in mouse inner ear, we generated *Dicer1* CKO and *Dgcr8* CKO in the otic placode using *Pax2-Cre* and in hair cells using *Atoh1-Cre*. In addition to gross morphological observation, in situ hybridization was used to confirm miRNA depletion, and immunohistochemical detection of Phalloidin and MyoVIIa was used to examine development and maintenance of hair cells in each of these models.

Results

Our study of *Dicer1* CKO in mouse inner ear has shown considerable defects in gross development and maintenance of sensory hair cells depending on the timing and tissue specificity of conditional deletion. We hypothesized that *Dgcr8* CKO would result in less severe outcomes. To the contrary, preliminary analysis of *Dgcr8* CKO demonstrates that depletion of only canonical miRNAs results in greater variability of developmental outcomes in the *Pax2-Cre* model and surprisingly more detrimental effects on sensory hair cell differentiation and maintenance in the *Atoh1-Cre* model.

Conclusion

Results are interpreted to reflect the role of miRNAs in canalization (i.e. reproducibility of developmental outcomes) and the importance of the balance of small RNA functions in cell differentiation and maintenance.

1005 Spatiotemporal Expression of Protochaderin-15 (PCDH15) Proteins in Zebrafish Hair Cells

Marisa Zallocchi¹, Oluwatobi Ogun¹

¹Boys Town National Research Hospital

Background

Mutations in PCDH15 gene can cause Usher syndrome type 1F (USH1F) in humans, characterized by congenital deafness, vestibular dysfunction and progressive retinal degeneration. Animal models harboring mutations in the PCDH15 gene (i.e. Ames waltzer and orbiter) show different degrees of splaying stereocilia reduce FM1-43 uptake and abnormal transducer currents, suggesting the involvement of PCDH15 in hair bundle development and function. A role in synaptic maturation has also been suggested for specific PCDH15 isoforms. Zebrafish have duplicate *pcdh15* genes, *pcdh15a* and *pcdh15b*. Previous observations from mRNA in situ hybridization studies suggested the existence of specific and unique roles for *Pcdh15a* and *Pcdh15b* in the ear and eye, respectively.

Methods

We developed antibodies directed to the more divergent intracellular tails of *Pcdh15a* and *Pcdh15b*. Western blot analysis and immunohistochemistry experiments demonstrated the expression of both *Pcdh15* proteins in ear hair cells from 1 day post-fertilization (dpf) to 5dpf.

Results

In hair cells *Pcdh15a* is restricted to the stereocilia hair cell bundle while *Pcdh15b* is also expressed at the hair cell bundle and below the cuticular plate. Neuromast hair cells show high expression of both *Pcdh15* proteins in the kinocilia, the hair cell bundle and in the cuticular plate. Modest expression is also observed at the basolateral membrane and hair cell body. In the zebrafish retina (4dpf) we observed expression of *Pcdh15b* only at the connecting cilia in photoreceptor cells. No expression was observed for *Pcdh15a* in zebrafish eye under our experimental conditions. These last observations are in agreement with previous published work showing only expression of *Pcdh15b* in fish retina.

Conclusion

Taken together, the results presented here show for the first time the spatiotemporal pattern of expression of both *Pcdh15* proteins in zebrafish and also may explain the mild splayed stereocilia phenotype and the normal planar polarity observed in orbiter mutants where only *Pcdh15a* is mutated.

This work was supported with NIH grant 5 P20 RR018788-08

1006 Ethanol Affects the Development of Sensory Hair Cells in Larval Zebrafish (*Danio Rerio*)

Phillip Uribe^{1,2}, James Asuncion¹, Jonathan Matsui¹

¹Department of Neuroscience, Pomona College, ²Graduate Program in Neuroscience, Washington State University

Background

Some children who are born to mothers who have consumed alcohol during pregnancy present a number of morphological, cognitive, and sensory abnormalities, including hearing deficits, collectively known as fetal alcohol syndrome (FAS). The goal of this study was to determine if the zebrafish lateral line could be used to study sensory hair cell abnormalities caused by exposure to ethanol during embryogenesis.

Methods

Lateral line hair cells are present at 2 days post-fertilization (dpf) and by 5 dpf sensory hair cells are functional. We treated a transgenic line of zebrafish that expresses membrane-targeted green fluorescent protein under control of the *Brn3c* promoter/enhancer with embryo medium supplemented with varying concentrations of ethanol (0.75%-1.75% by volume) from 2 dpf through 5 dpf. Age-matched, non-treated controls were also raised in parallel. The vital dye FM 1-43FX was used to detect the presence of functional mechanotransduction channels. Larval zebrafish were fixed, mounted, and imaged using a confocal microscope.

Results

As the concentration of ethanol increased, we observed some classical abnormalities associated with FAS; enlarged heart, small eye, and craniofacial defects. Moreover, the number of sensory hair cells decreased as the concentration of ethanol increased in a dose-dependent manner. Also, the percentage of FM 1-43-labeled hair cells decreased as the concentration of ethanol increased.

Conclusion

Ethanol treatment of zebrafish embryos during the time when hair cells are added to the lateral line not only results in fewer hair cells, but those hair cells that are formed do not function properly. Our results mirror data obtained by investigators who have analyzed the effect of ethanol on auditory function in developing mammals. Zebrafish may prove to be a useful model system to study the mechanisms underlying the development of FAS.

1007 Roles of Primary Cilia in Mammalian Inner Ear Development

HongKyung Kim¹, Jihyun Ma¹, Duyeol Han¹, Hyukwan Ko², Jinwoong Bok¹

¹Yonsei University College of Medicine, ²College of Pharmacy, Dongguk University

Background

Primary cilia are microtubule-based structures that extend from the surface of all mammalian cells. These non-motile cilia serve as a cellular signaling center for many pathways

including Sonic hedgehog (Shh), Wnt, FGF, and PDGF. Defects in the formation or function of primary cilia are shown to be associated with a range of genetic diseases collectively known as ciliopathy. Hearing loss is one of the well-characterized phenotypes found in human ciliopathy, yet the underlying pathological mechanisms remain unclear.

Methods

In order to understand the role of primary cilia in inner ear development, we analyzed the inner ears of a ciliopathy mouse model, in which ciliary morphology is defective due to a missense mutation in *Broad minded (Bromi)* encoding an uncharacterized TBC (Tre-2, Bub2, and Cdc16) domain-containing ciliary protein.

Results

We observed that inner ears of *Bromi* mutants exhibited diverse inner ear defects, some of which are attributed to defective Shh signaling. For example, the cochlear duct of *Bromi* mutants was severely shortened and lacked the expression of *Msx1*, an apical cochlear marker, suggesting a failure of apical cochlear specification that requires high levels of Shh signaling. Multiple extra rows of hair cells (HCs) were observed in the organ of Corti in the apical cochlea, suggestive of a failure of convergent extension of the prosensory domain. However, HC orientation appeared unaffected in *Bromi* mutants based on normal localization of the kinocilia at the abneural side of HCs. Interestingly, ectopic sensory patches containing vestibular-like HCs developed in the Kolliker's organ in *Bromi* mutants, similar to phenotypes reported in *Gli3*^{1699/1699} mutants, in which Shh signaling is compromised. Based on *Atoh1* expression and hair bundle morphologies, HCs were more mature in *Bromi* mutants, consistent with the in vitro results of Shh inhibiting HC formation. Additionally, formation of primary cilia was severely affected in most of the supporting cells of *Bromi* mutants but not in the HCs, consistent with a previous report that *Bromi* mutants display neural tube or limb defects associated with abnormal cellular responses to high levels of Shh signaling.

Conclusion

Our results suggest that the phenotypes observed in *Bromi* mutants are due to compromised Shh signaling and that Shh signaling in the mammalian cochlea is mediated through the primary cilia.

1008 Spontaneous Activity in Auditory Inner Hair Cells Drives Ribbon Synapse Maturation During a Critical Period

Stuart L. Johnson¹, Stephanie Kuhn¹, Christoph Franz², Neil Ingham³, David N Furness⁴, Marlies Knipper², Karen Steel³, John P. Adelman⁵, Matthew C Holley¹, Walter Marcotti¹

¹University of Sheffield, ²University of Tübingen,

³Wellcome Trust Sanger Institute, ⁴Keele University,

⁵Vollum Institute

Background

The maturation of neural circuits is thought to rely on spontaneous electrical activity that occurs during immature stages of development (Katz & Shatz, 1996 Science 274: 1133-8; Blankenship & Feller, 2010 Nat. Rev. Neurosci. 11: 18-29). In the developing mammalian auditory system, the sensory inner hair cells (IHCs) fire calcium action potentials (Tritsch et al 2007 Nature 450: 50-5; Johnson et al 2011 Nat. Neurosci. 14: 711-7). IHC action potentials are generated by the interplay between a depolarizing Ca²⁺ current and a repolarizing delayed rectifier K⁺ current (Marcotti et al. 2003 J. Physiol. 548:383-400). However, the ability to sustain repetitive firing activity depends largely upon the activation of the transiently expressed small conductance Ca²⁺-activated K⁺ current SK2 (Johnson et al 2007 J. Physiol. 583: 631-46).

Methods

Using a transgenic mouse in which the repolarizing potassium current, SK2, is normally over-expressed, but can be down regulated in vivo using doxycycline (Hammond et al 2006 J. Neurosci. 26: 1844-53), we investigated whether normal spiking activity is required for IHC development. Electrophysiological experiments were carried out using physiological conditions (body temperature and 1.3 mM extracellular Ca²⁺). Whole-cell patch clamp was used to measure current and voltage responses in immature and adult IHCs and their exocytotic properties, which were assessed by measuring changes in cell membrane capacitance (ΔC_m).

Results

We found that the larger SK2 current in immature IHCs of SK2 over-expresser (SK2-OE) mice made the action potential hyperpolarization phase more robust, which consequently reduced spike width and increased their frequency compared to controls. The consequence of abnormal immature spontaneous activity was that SK2-OE IHCs failed to develop the linear exocytotic Ca²⁺ dependence that is a characteristic of adult cells (Johnson et al. 2010 Nat. Neurosci. 13: 45-52), indicating a direct role for spontaneous Ca²⁺ action potentials in regulating IHC maturation. Using the ability to down-regulate the over-expression of SK2 channels in OE mice with doxycycline, we were able to define the "critical period" over which this regulation occurred.

Conclusion

Our results provide the first direct evidence that maturation of mammalian primary auditory receptors depends upon a

specific temporal pattern of spontaneous calcium signals that occurs during a critical period prior to the onset of sound-driven neuronal activity.

Supported by the Wellcome Trust; WM and SLJ are Royal Society University Research Fellows

1009 Conditional Deletion of *Pten* Leads to Defects in the Spiral Ganglion by Modulating Akt/GSK3 β Signaling in the Inner Ear

Hyung Jin Kim¹, Hae-Mi Woo¹, Jihee Rye¹, Jinwoong Bok², Jin Woo Kim³, Sang Beak Choi¹, Mi-Hyun Park¹, Hyun-Young Park⁴, Soo Kyung Koo¹

¹Division of Intractable Diseases, Center for Biomedical Sciences, Korea National Institute of Health, ²Department of Anatomy, BK21 Project for Medical Science, Yonsei University College of Medicine, ³Department of Biological Sciences, Korea Advanced Institute of Science and Technology, ⁴Division of Cardiovascular and Rare Diseases, Center for Biomedical Sciences, KNIH

Background

All cellular phenomena and developmental events, including inner ear development, are modulated through harmonized signaling networks. Phosphatase and tensin homolog deleted on chromosome 10 (PTEN), a tumor suppressor, is a major signaling component involved in crosstalk with key regulators of development, i.e., Wnt, Notch, and bone morphogenetic proteins. Although *Pten* function has been studied in various systems, its role in inner ear development is poorly understood.

Methods

Here, we used inner ear-specific *Pten* conditional knockout mice and examined the characteristics of the inner ear.

Results

In a detailed analysis of the phenotype, reduced cochlear turning and widened epithelia were observed. Phalloidin staining of sensory epithelium revealed that hair cell patterns were disturbed, i.e., additional rows of hair cells were discovered. The neural abnormality revealed a reduction in and disorganization of nerve fibers, including apoptosis at the neural precursor stage. *Pten* deficiency induced heightened phosphorylation of Akt at Ser473. The elevation of inhibitory glycogen synthase kinase 3 β Ser9-phosphorylation (pGSK3 β) was sustained until the neuronal differentiation stage at embryonic day 14.5, instead of pGSK3 β downregulation.

Conclusion

This is the first report of the influence of *Pten*/Akt/GSK3 β signaling on the development of spiral ganglia. These results suggest that *Pten* is required for the maintenance of neuroblast number, neural precursors, and differentiation in the inner ear.

1010 Tis21 Is Involved in Development of Spiral Ganglion Cells

Takao Yamada¹, Toru Miwa¹, Momoko Ise¹, Ryosei Minoda¹, Eiji Yumoto¹

¹Department of Otolaryngology-Head and Neck Surgery, Graduate School of Medicine, Kumamoto University

Background

Spiral ganglion cells (SGCs) play a very important role in auditory function to transmit sound signals from the cochlear hair cells to the brain. The molecular mechanism of development of SGCs has not been elucidated enough. As with other neurons, SGCs pass through mitotic proliferation, ceasing proliferation, and differentiation at a development. We focused on the Tis21/BTG2/PC3 (Tis21) gene. A Tis21 gene belongs to the member of BTG/Tob family with antiproliferative properties. Tis21 has function to induce the neuronal differentiation at cerebellum in mice (Canzoniere, Neurosci., 2004). We have already revealed that Tis21 expresses in the SGCs in embryonic stage (Hayashida, Neuroreport, 2010). We set out to perform further developmental analysis utilizing Tis21 knock-in mice.

Methods

Normal mice (Tis21(+/+) mice), heterozygous Tis21-GFP knock-in mice (Tis21(+/-GFP) mice) and homozygous Tis21-GFP knock-in mice (Tis21(-GFP/-GFP) mice) were used for this experiment. We performed histological analysis of GFP expression in Tis21(+/-GFP) mice and Tis21(-GFP/-GFP) mice, and we counted the number of SGCs of Tis21(-GFP/-GFP) mice and Tis21(+/+) mice.

Results

The GFP expression was detected in the cytoplasm of SGCs at Embryonic day15.5 (E15.5), E18.5 and Postnatal day4 (P4) in Tis21(+/-GFP) mice and Tis21(-GFP/-GFP) mice. The number of SGCs in Tis21(-GFP/-GFP) mice was significantly decreased when compared with that of Tis21(+/+) mice at E15.5, E18.5 and P4.

Conclusion

Tis21 (-GFP/-GFP) mice showed significant decrease of number of the SGCs. This finding suggested that Tis21 is involved in development of SGCs. Neurogenin1(Ngn1) deficient mice show complete absence of SGCs (Ma, Otolaryngol., 2000). NeuroD deficient mice show mostly complete absence of SGCs (Kim, Development, 2001). It is considered that Ngn1 acts upstream of NeuroD during development of SGNs (Liu, Genes Dev., 2000). In addition, Tis21 acts upstream of Math1 during cerebellum development (Canzoniere, J Neurosci., 2004). Considering these facts, Tis21 probably acts downstream of Ngn1 during development of SGCs.

1011 Conditional Deletion of Neurotrophins Indicate Their Essential Role in Postnatal Fiber Reorganization

Jennifer Kersigo¹, Qiong Wang¹, Bernd Fritschsch¹
¹University of Iowa

Background

Two neurotrophins (Bdnf, Ntf3) support developing spiral ganglion neurons (SGNs), which degenerate in their absence. Other aspects of each neurotrophin in patterning the embryonic innervation of the ear have been partially clarified: Ntf3 is essential for the normal innervation of the organ of Corti (OC) in the basal turn of the cochlea while Bdnf plays only a supporting role for SGNs, primarily in the apex. Suggestions of the role of each neurotrophin in sorting of afferents to the two types of OC hair cells (Ntf3 for type I fibers to inner hair cells [IHCs], Bdnf for type II fibers to outer hair cells [OHCs]) were refuted by subsequent work. Early lethality has blocked analysis of the role of neurotrophins in postnatal sorting of type afferents to the two types of hair cells of the OC, leaving room for interpretations mostly based on non-experimental data. For example, some *in vivo* and *in vitro* data suggest neurotrophins may be critical for synapse formation while others suggest only a limited influence of neurotrophins on postnatal synaptogenesis and viability of neurons.

Methods

To go beyond these suggestions, we have generated viable conditional single and double mutants of both neurotrophins using hair cell and ear specific cre lines (Atoh1-cre and Pax2-cre) in which we analyze the pattern of afferent and efferent innervation and formation of synaptic contacts.

Results

We show that loss of both neurotrophins in hair cells using Atoh1-cre has only a limited effect on afferent viability but completely eliminates afferent growth to outer hair cells without influencing inner hair cells. In contrast, complete loss of either neurotrophin using Pax2-cre results in topographical disorganization of both afferents and efferents with limited innervations and synapse formation in the base in Pax2-cre; Ntf3f/f mice. Finally, conditional elimination of all neurotrophins only in the ear results in delayed loss of all afferents in postnatal mice, followed by further delayed loss of efferents and an even further delayed loss of hair cells.

Conclusion

These data clarify for the first time in two distinct conditional deletion mouse models the role of neurotrophins in postnatal afferent sorting to various hair cells and the role of afferents for efferent innervation to inner and outer hair cells. We show that differential longitudinal, radial, and temporal distribution of neurotrophins define the postnatal afferent and efferent fiber sorting to the two hair cell types of the OC.

1012 Developmental Alterations of Hair Cell Types Help in Understanding the Pattern of Innervation

Israt Jahan¹, Ning Pan¹, Jennifer Kersigo¹, Yoko Nakano², Botond Banfi², Bernd Fritschsch¹

¹Department of Biology, College of Liberal Arts and Sciences, University of Iowa, Iowa city, IA, ²Department of Anatomy and Cell Biology, Carver College of Medicine, University of Iowa, Iowa city, IA

Background

The organ of Corti (OC) consists of a regular mosaic of two different types of hair cells (HCs; inner hair cells, IHCs and outer hair cells, OHCs) which are innervated in a stereotyped fashion by two types of afferents (type I to IHCs; type II to OHCs) and efferents. In sensorineural hearing loss, HCs are lost followed by progressive degeneration of neurons. Regaining complete hearing will require reconstituting the OC HCs with the precise sorting of their innervation. To achieve this goal, it is necessary to understand the molecular regulation of OC patterning. Beyond generalized HC differentiation, formation of specific types of HCs and their innervation must be understood at the molecular level.

Methods

We used different mouse models to assess the temporal and intensity variations of TF Atoh1 modulation to differentiate specific types of HCs: Atoh1 conditional null using Pax2-cre and Atoh1-cre, Neurog1 knockin (Atoh1KINeurog1/KINeurog1), combination of Atoh1 floxed and Neurog1 KI (Atoh1cre; Atoh1f/KINeurog1), Bronx Waltzer (bv/bv) and Pax2-cre; Neurod1f/f.

Results

The transient expression of Atoh1 in Atoh1-cre; Atoh1f/f mice result near complete loss of all IHCs. Similarly, bv/bv mutant mice also lose IHC, with reduced Atoh1 expression at birth. In contrast, loss of Neurod1 results in OHCs specification as ectopic IHCs due to premature and aberrant expression of Atoh1.

Molecular modifications of HCs affect innervation. In the absence of differentiated HCs in Pax2-cre; Atoh1f/f, the radial fibers fail to reach the OC. Atoh1 KINeurog1/KINeurog1 mice can attract more fibers to the partially differentiated OC, most likely by promoting Ntf3 expression by Neurog1. In the mutants with specific loss of IHCs display projection of type I fibers to the remaining OHCs. In contrast, mutants with ectopic conversion of IHCs in the region of OHCs attract type I fibers regardless of their ectopic topology.

Conclusion

We conclude that afferents can sort out IHC and OHC specific patterns if choices are possible in mutants with altered distribution of HC types. In the absence of IHC all fibers will innervate OHCs if they cannot divert to nearby IHCs due to increased distances to the nearest IHC. Understanding the dosage and cross-regulation of these above TFs, in regulating specific types of HCs development and their specific fiber sorting mechanism will

provide useful information for the future attempts to restore hearing.

1013 Countergradients and Modular Expression Patterns of Eph-Ephrin Signaling Proteins in the Developing Auditory Brainstem

Caitlyn Klotz¹, Matthew Wallace¹, J. Aaron Harris¹, Mark Gabriele¹

¹James Madison University

Background

A family of receptor tyrosine kinases, the Eph-ephrins, is involved in guiding topographic mapping and projection pattern formation in a variety of systems. We are interested in understanding their role in establishing the orderly arrangement of converging inputs to the inferior colliculus (IC) prior to hearing onset. Previously, we described the development of several layered projections to the central nucleus of the IC (CNIC), as well as a modular input to the lateral cortex of the IC (LCIC) arising from the lateral superior olive (LSO). Immunohistochemical studies revealed expression patterns for EphA4, ephrin-B2 and ephrin-B3 during this period of projection shaping that suggest their involvement in the mapping of these early connections. Recently, we showed in ephrin-B2 mutant mice that LSO inputs to the CNIC (bilaterally layered) and LCIC (ipsilaterally modular) lack a clear topography, despite maintaining their characteristic axonal patterns.

Methods

These results led to the present studies that build upon preliminary expression data from immunohistochemistry and X-Gal staining experiments utilizing lacZ mutants. Here, quantitative methods were used to confirm discernible CNIC gradients and LCIC expression modules, as well as to explore the possibility of similar gradients in the LSO.

Results

Sampling methods reveal gradients of EphA4 and ephrin-B2 across the tonotopic axis of the CNIC, with protein most concentrated in high-frequency regions. In addition, expression data reveals prominent modules for each throughout the LCIC. In contrast, the CNIC is devoid of ephrin-B3, although present in the LCIC and exhibiting a similar modular expression. Ephrin-B2 in the LSO is expressed in a complementary gradient, with protein most concentrated in low frequency regions. EphA4 is present in the LSO, while ephrin-B3 is absent.

Conclusion

The described countergradient between ephrin-B2 (LSO) and EphA4 (CNIC) that have known binding affinities for one another may provide insights for the establishment of topographic connections between these auditory brainstem nuclei. Further, it remains to be seen whether modular LCIC expression patterns for EphA4, ephrin-B2, and ephrin-B3 are superimposed, partially overlapping, or mutually exclusive of one another. Determining this, as well as which specific modules LSO targets, is paramount

for fully understanding the role of Eph-ephrins in guiding multiple converging inputs to the IC.

1014 The Calyx of Held as a Model System to Study Neural Development: Competition and Pruning to Mono-Innervation

Paul Holcomb¹, Dakota Jackson¹, Brian Hoffpauir¹, Tom Deerinck², Glen Marrs¹, Marlin Dehoff¹, Jonathan Wu¹, Mark Ellisman², George Spirou¹

¹West Virginia University School of Medicine, ²National Center for Microscopy and Imaging Research, UCSD

Background

Several neural systems, including the neuromuscular junction and climbing fiber innervation of Purkinje cells, are considered models to study neural development because they exhibit hallmark features of initial competition and pruning, they establish a recognizable endpoint of mono-innervation of their targets and their presynaptic terminals are large and easily monitored. Several studies, using physiological counting methods and serial-section EM of relatively small numbers of cells, show evidence for competition among developing calyces of Held (CH), but its prevalence has not been properly assessed. Also, although it is well-established that the CH grows rapidly over several days during the first postnatal week, this process has not been quantified.

Methods

In order to objectively assay the dynamics of CH formation and mono-innervation of medial nucleus of the trapezoid body (MNTB) neurons, we used a primarily anatomical approach because physiological counting techniques provide an underestimate of convergent synaptic inputs due to sectioning of axons in brain slice preparations and because independent inputs may share a stimulation threshold. Serial block-face scanning electron microscopy provides high resolution to identify neuronal contacts and the means to accurately register cellular ultrastructure through large tissue volumes.

Results

Here we make the first application of these technologies to the developing brain and study changes in neural connections across the age range critical for calyx growth (P2-P6). We establish that competition, defined as multiple large growing calyces forming synaptic contact with MNTB cells, is a common trait during this developmental period. By segmenting pre- and postsynaptic cellular structures and quantifying contact areas between nerve terminals and MNTB cells, we describe P3 as a uniquely active day in calyx growth during which cell apposition areas are added at a rate exceeding 200 $\mu\text{m}^2/\text{day}$.

Conclusion

These data define metrics for growth dynamics in this system, illustrate shared features with other neural systems considered as models of neural development and exemplify utility of the CH:MNTB system for studies of synaptogenesis and pruning with relevance to other neural systems throughout the brain.

1015 Reversal of Early Mild Hearing Loss Reveals a Discrete Critical Period for Maturation of Cortical Excitability

Todd Mowery¹, Vibhu Kotak¹, Dan Sanes¹

¹NYU

Background

Sensory systems are highly susceptible to changes in peripheral activity during developmental critical periods (CP). To reveal the onset and termination of critical periods, sensory input is typically diminished or restored as a function of age. Our unpublished results in gerbils have suggested that there are at least two CPs during which deprivation influences the maturation of auditory cortex cellular properties: ear plugging immediately after hearing onset, from postnatal (P) 11-13 delays intrinsic membrane property development, while ear plugging from P14-22 disrupts voltage-gated properties. Therefore, we asked whether hearing loss induced changes to active and passive membrane properties would recover when ear plugs were removed during or after the closure of the second CP.

Methods

At P11, gerbils (*Meriones unguiculatus*) were implanted bilaterally with malleable plugs that induced a behavioral threshold shift of ~20 dB at 4 kHz. The plugs were removed on either P17 or P23, followed by ~6 days of normal hearing. Whole-cell current clamp recordings were then obtained from L2/3 pyramidal neurons in thalamocortical slices at P21-35 and compared to age-matched controls.

Results

When ear plugs were implanted at P11 and removed on P17 or P23, certain membrane properties eventually reached normal age-specific values (e.g., V_{rest} : Age-matched control = $-32.5 \text{ mV} \pm 1.0$ vs P23 plug removal = $-32.4 \text{ mV} \pm 1.4$; $t = -3.6$, $p > 0.1$). Therefore, the CP for development of these properties remained open through at least P23. In contrast, specific membrane properties did not recover to normal values when earplugs were removed at P17 or P23 (e.g., AHP: Age-matched control = $-14.1 \text{ mV} \pm 0.7$ vs P17 plug removal = $-12.1 \text{ mV} \pm 0.7$; $t = 0.21$, $p < 0.05$). Therefore, the CP for normal development of these membrane properties closed before P17.

Conclusion

These findings strongly suggest that even mild hearing loss can delay the functional development in cortex, and the maturation of specific membrane properties are disproportionately affected by deprivation during at least two CPs that open and close abruptly after the onset of hearing. This suggests that the restoration of normal hearing does not necessarily restore normal neuronal processing (supported by NIH DC011284 DHS and VCK).

1016 Functional and Cellular Abnormalities in the Developing Auditory Cortex After Neonatal Cerebral Hypoxia-Ischemia

Jessica Wess¹, Aminah Sheikh¹, Patrick Kanold¹

¹University of Maryland, College Park

Background

Subplate neurons (SPns) are required for the formation and functional refinement of thalamocortical connections (Kanold & Luhmann 2010, Tolner et al. 2012). SPns are selectively vulnerable to neonatal hypoxic-ischemic (HI) insults (McQuillen et al. 2003). Such insults in human can give rise to auditory impairments, as well as a multitude of other developmental language disorders. Thus we investigated the consequences of HI on auditory cortex development in rodents.

Methods

HI was performed on rat pups on postnatal day (P) 1-2 and extracellular single-unit recordings were performed in anesthetized animals between P20-30 to assess the effects of HI on receptive field organization of auditory cortex neurons. Whole-cell patch clamp recordings were also performed in layer 4 of auditory cortex cells after HI on rat pups between P18-22, in order to get a more in-depth understanding of our results on a cell-specific level.

Results

We find that compared with normal controls, auditory cortex neurons in HI treated pups showed increased firing rates and abnormal tuning characteristics. Receptive fields were disrupted and thresholds were increased. Abnormal EEGs, reminiscent of seizure activity was also observed in 30 percent of the animals. After whole-cell recording we find that intrinsic properties of layer 4 cells and synaptic transmission are altered.

Conclusion

Our observations imply that SPns are necessary for normal development of the circuit and tuning properties in the auditory cortex. Thus, injury to these neurons results in widespread abnormalities of sensory processing.

1017 Silent Synapses on Subplate Neurons in Developing Auditory Cortex

Xiangying Meng¹, Patrick Kanold¹

¹Department of Biology, University of Maryland

Background

Functionally silent excitatory synapses exist in several systems during development. Little is known about the presynaptic spatial origin of silent synapses. Cortical cells receive input from multiple layers and connections between these layers develop at different ages. Since cells receive inputs from multiple presynaptic cells we hypothesized that functional and silent synapses might originate in different layers.

We investigated this hypothesis in the developing circuits in auditory cortex. Subplate neurons form one of the earliest maturing circuits in the cerebral cortex and crucial to cortical development. We recently found that subplate

neurons receive inputs from the developing cortical plate in the 2nd postnatal week.

Methods

We here use laser-scanning photostimulation in acute slices of auditory cortex during the 1st two postnatal weeks in mouse to study the spatial origin of silent synapses to subplate neurons.

Results

We find that silent synapses from the cortical plate can be present in subplate neurons before the emergence of functional synapses from the cortical plate. They are mostly located in the periphery of cells' response fields and are discerned into two broad classes based on their distinct spatial patterns.

Conclusion

Since subplate neurons can be activated at these young ages by thalamic inputs, cortical neurons at young ages have the ability to signal to subplate neurons depending on the activation state of subplate neurons.

These results suggest that subplate neurons are an integral part of the intracortical circuitry at the youngest ages.

1018 Age-Related Primary Neural Degeneration Is Aggravated in the Absence of Olivocochlear Efferents

M. Charles Liberman^{1,2}, Stéphane F. Maison^{1,2}
¹Harvard Medical School, ²Massachusetts Eye & Ear Infirmary

Background

Olivocochlear (OC) efferents can reduce threshold shift from noise exposures in excess of 100 dB SPL, but the significance of this effect has been questioned, since natural environments do not typically contain such high sound levels (Kirk and Smith, 2003). We recently showed that threshold recovery after moderate-level exposures (84 dB SPL) can hide massive degeneration of cochlear nerve fibers, and that this neuropathy is exacerbated by loss of OC innervation (Usubuchi et al., ARO 2012). Here, we ask whether OC feedback also minimizes neural degeneration in mice aged without any purposeful acoustic overexposure.

Methods

In one group of 6-wk old CBA/CaJ mice, OC efferents were lesioned unilaterally via stereotaxic injections of melittin into the LSO and/or the VNTB, where the lateral and/or medial OC fibers originate, respectively. In another group, the crossed OC bundle was cut via midline section at the floor of the IVth ventricle. A third (control) group had no brainstem surgery. ABRs and DPOAEs were measured in both ears at 8, 11, 16, 22, 32 and 45 wks of age. The strength of medial OC efferents was assessed by shocking the OC bundle while measuring DPOAE amplitudes. Cochlear nerve degeneration, and the degree of de-efferentation, were assessed by immunostaining cochlear

whole mounts for pre-synaptic ribbons (CtBP2), post-synaptic AMPA-receptor patches (GluR2) and OC terminals (VAT).

Results

At 45 wks, controls ears showed <15% loss of afferent synapses throughout the cochlea [8-32 kHz] and minimal (<8 dB) threshold shifts. In mice with partial or complete de-efferentation, threshold shifts were larger (10-30 dB) especially at the lowest and highest frequencies, and synaptic loss was significantly worse (by as much as 25%) especially in the apical and basal thirds of the cochlea. Analysis to date suggests that both MOC and LOC systems contribute to this effect.

Conclusion

These findings suggest that OC feedback may be essential for the long-term survival of cochlear nerve terminals in the face of a constant excitotoxic challenge from their highly active glutamatergic synapses with inner hair cells.

Research supported by a grant from the NIDCD: R01 DC0188

1019 Using the Auditory Steady-State Response to Measure Noise-Induced Auditory Nerve Degeneration

Luke Shaheen^{1,2}, Bertand Delgutte^{1,3}, M Charles Liberman^{1,4}

¹Eaton-Peabody Laboratories, Massachusetts Eye & Ear Infirmary, ²Harvard-MIT Division of Health Sciences and Technology, ³Research Laboratory of Electronics, MIT, ⁴Dept. of Otology & Laryngology, Harvard Medical School

Background

Moderate noise exposure can cause permanent loss of auditory nerve (AN) fibers, without causing hair cell loss or permanent threshold shifts (Kujawa & Liberman, JNeurosci 29:14077, 2009). This neuropathy is likely present in humans, but undetected by routine clinical examination. Reduction of suprathreshold auditory brainstem response (ABR) wave I amplitude has been used to quantify this primary neural degeneration in mice. However, ABR amplitudes are more variable in humans, and therefore may not be a useful diagnostic tool. This noise-induced neuropathy is selective for high-threshold ANs, i.e. those with low spontaneous rates (SRs) (Lin et al., ARO 2011, #400). Since low-SR fibers show greater phase locking to amplitude modulation than high-SR fibers (Joris & Yin, JAcoust Soc Am, 91:215, 1992), we hypothesized that the auditory steady-state response (ASSR), the gross electrical potential in response to amplitude-modulated tones, may be a useful metric of noise-induced AN loss.

Methods

8-wk mice were exposed to 98 dB SPL, 8-16 kHz noise for 2 hours. ASSRs and ABRs were recorded before, and 2 weeks after, exposure. ABRs were measured at tone pip frequencies of 11.3 and 32 kHz. ASSRs were evoked with carrier frequencies of either 11.3 or 32 kHz. Modulation frequencies were greater than 700 Hz so that ASSRs

would be dominated by more peripheral auditory structures. Cochlear neuropathy was assessed by confocal microscopy of whole mounts immunostained for pre- and post-synaptic markers.

Results

This noise exposure causes loss of up to 50% of AN synapses with inner hair cells throughout the basal turn, i.e. at cochlear frequencies from 16 – 45 kHz. While ABR and ASSR amplitudes in response to 11 kHz tone pips or carriers, respectively, were similar to controls, at 32 kHz both ABR and ASSR amplitudes were significantly lower in noise-exposed mice. The phase consistency of the ASSR response at 32 kHz was also significantly lower in noise-exposed mice. To simulate the amplitude variability in humans, we randomly attenuated the responses, while holding the noise level constant. This did not affect the group difference in ASSR phase consistency, but eliminated the group difference in ASSR and ABR amplitudes.

Conclusion

Loss of ANs reduces ABR amplitude, ASSR amplitude, and ASSR phase consistency. Only ASSR phase consistency is unaffected by amplitude variability, and therefore might be used to diagnose AN loss in humans. Supported by NIDCD R01DC002258, R01DC000188, & P30DC005209.

1020 Neurotrophin-Like Rescue of Spiral Ganglion Neurons After Noise

Kumud Lall¹, Katharine A. Belzner¹, Mingjie Tong¹, Albert S. Edge², Sharon G. Kujawa²

¹Massachusetts Eye and Ear Infirmary, ²Harvard Medical School, Massachusetts Eye and Ear Infirmary

Background

Neurotrophins can delay or prevent cochlear nerve degeneration secondary to hair cell loss and encourage dendritic sprouting in a denuded cochlear epithelium (Wise et al 2005). This raises the exciting possibility that, for noise exposures that damage neurons without destroying hair cells (Kujawa and Liberman 2009), delivery of neurotrophins or like-acting compounds could lead to hair cell reinnervation and functional recovery of IHC-afferent communications. Amitriptyline is a compound that mimics the neuroprotective effects of neurotrophins by Trk receptor agonist activity and has better bioavailability when delivered to the systemic circulation. Systemic amitriptyline suppresses neuronal apoptosis in a TrkA-dependent manner in hippocampus after glutamate agonist-induced neuro-excitotoxicity (Jang et al 2009). Here, we test whether acute and chronic neuro-excitotoxic consequences of noise exposure can be similarly suppressed by systemic amitriptyline.

Methods

Experiments were conducted on male, 16 wk old CBA/CaJ mice. Animals received once daily i.p. injections of amitriptyline (15 mg/kg) or an equal volume of vehicle (saline) for 5 days. Awake animals were noise exposed (8-

16 kHz OBN, 100 dB SPL, 2 h) on day 2 and were held for various post-exposure times (1 d to 1 yr) before physiologic testing (ABR, DPOAE). Tissues were retrieved and studied as immunostained (CtBP2, Na-K-ATPase) cochlear whole mounts and osmium-stained, plastic-embedded sections (10 µm). We counted hair cells, synaptic ribbons and spiral ganglion cells at cochlear places corresponding to 5.6, 11.3 and 32 kHz frequencies.

Results

Acute noise-induced threshold shifts were similar in amitriptyline- and saline-treated animals, they recovered to baseline by 2 wk post exposure and changed similarly with age throughout our period of monitoring. As expected, hair cells were not lost from this exposure and numbers were not altered by drug treatment. One year after noise, ribbon counts were ~20-40% greater and ganglion cell counts were ~25-40% greater, depending on frequency, in drug-treated ears vs. saline-treated controls. Although nerve survival appears enhanced in amitriptyline-treated ears, a corresponding functional preservation of suprathreshold ABR amplitudes was not observed using this treatment regimen.

Conclusion

Treatment with amitriptyline, which has neurotrophin-like activity at TrkA receptors, preserves spiral ganglion neurons in noise-exposed mice. Studies aimed at optimizing the dosing regimen and extending characterization of the functional status of these neurons are underway. In parallel, a cochlear explant preparation is in use to characterize drug effects on dendritic sprouting and afferent connections. Research supported by NIDCD: R01 DC008577

1021 Glutamate-Induced Neural Degenerations in Cochlear Organotypic Cultures

Haiyan Jiang¹, Dalian Ding¹, Weidong Qi², Richard Salvi¹

¹University at Buffalo, ²Huashan Hospital

Background

Glutamate is believed to be the excitatory amino acid neurotransmitters released by inner hair cells. When glutamate is released, it can bind to 2 classes of glutamate receptors (AMPA or Kainate) that are located on auditory nerve fiber synapses beneath the inner hair cell. During intense sound stimulation, excess glutamate release can lead to excitotoxicity. Excitotoxicity can be induced in vivo by infusing glutamic acid or kainic acid into the cochlea; this results in significant swelling at type I afferent synapses or death of type I spiral ganglion neurons. Little is currently known about glutamate and kainate excitotoxicity in developing afferent synapses of the postnatal ear. To address this question, we treated postnatal cochlear organotypic cultures with glutamic or kainic acid and determined their effects on the afferent terminals and spiral ganglion neurons (SGN).

Methods

Cochlear explants from postnatal day 3 rats were treated with glutamic acid (10-5000 μ M) or kainic acid (100-20000 μ M) for 24 h. Cochlear hair cells, auditory synapses, and spiral ganglion neurons (type I and type II) were labeled and evaluated by confocal microscopy.

Results

Treatment of rat cochlear cultures with glutamic acid resulted in damage that was confined to auditory nerve synapses and peripheral nerve fibers. In contrast, cochlear hair cells and SGN soma appeared normal. Surprisingly, kainic acid failed to induce obvious damage to hair cells, synapses, or SGN soma.

Conclusion

The lack of kainic acid-induced damage suggests that there is a paucity of functional kainate receptors on the afferent synapses and soma of SGN. Alternatively, glutamic acid only damaged the synaptic terminal of auditory nerve fibers. These results suggest that functional AMPA-type glutamate receptors are present mainly at the afferent synapse.

1022 Involvement of the Superoxide Radical in Salicylate-Induced Spiral Ganglion Degeneration

Lili Deng^{1,2}, Dalian Ding¹, Jiping Su², Senthilvelan Manohar¹, Richard Salvi¹

¹University at Buffalo, ²Guangxi Medical University

Background

Salicylate, the active component in aspirin, is a potent antioxidant that can protect against cochlear hearing loss. However, high doses of salicylate have long been known to cause transient tinnitus and hearing loss. Recent studies have shown that salicylate does not damage cochlear hair cells or supporting cells, but paradoxically selectively destroys spiral ganglion neurons (SGN) by mechanisms consistent with apoptosis. To gain insights into the processes that initiate SGN death, we monitored superoxide generation and characterized the early stages of caspase-mediated SGN death.

Methods

Cochlear organ cultures were prepared from postnatal day 3 rats and treated with different concentrations of salicylate. Superoxide, a reactive oxygen species, was detected with dihydroethidium, a fluorescent probe. Fluoregenic caspase-specific probes were used to detect initiator caspase 8 and caspase 9 and downstream executioner caspase 3.

Results

Salicylate caused a dose and time-dependent loss of SGN and nerve fibers. SGN degeneration was characterized by nerve fiber disintegration and nuclear shrinkage and fragmentation. Caspase 8 and caspase 9 were activated during the early stages of degeneration followed by activation of executioner caspase 3. Salicylate significantly increased superoxide labeling in SGN.

MnTMPyP pentachloride, a cell-permeable scavenger of superoxide, significantly attenuated salicylate-induced SGN degeneration.

Conclusion

One of the most puzzling aspects of salicylate ototoxicity is its selective damage of SGN. Our results suggest that SGN are preferentially damaged because of the increase of superoxide exclusively in SGN. This interpretation is supported by the fact that MnTMPyP, a superoxide scavenger, prevented salicylate-induced SGN degeneration.

Acknowledgments: Research supported by grants to RS from NIH/NIDCD(R01DC009091; R01DC009219), to JS from NSFC (30860098, 81060082) and to LD from China Scholarship Council (2011845025)

1023 Exogenous BDNF and NT-3 Have Distinct Biological Effects on Afferent Synaptogenesis on Inner Hair Cells (IHCs) Without Endogenous NT-3 *in Vitro*

Qiong Wang¹, Steven Green¹

¹Departments of Biology & Otolaryngology, University of Iowa

Background

Previous results (Wang & Green, J. Neurosci. 31: 7938-49, 2011) using neonatal rat organotypic cochlea explant cultures indicated that endogenous NT-3 in the postnatal organ of Corti has a distinctive role, not mimicked by BDNF, in promoting SGN synapse regeneration on IHCs. Here we ask directly whether BDNF and NT-3 are equivalent in their ability to promote SGN axon growth and synaptogenesis on IHCs.

Methods

We generated Atoh1-CreER^{T2}; NT-3^{flox/flox}; Z/EG mice and treated with tamoxifen on P0 to delete NT-3 from a random subset of cochlear IHCs and label the NT-3-lacking hair cells with GFP. Organotypic cochlear explant cultures were made from the mice three days after tamoxifen injection. IHC-SGN synapses were destroyed after 1 day *in vitro* (DIV) with the glutamate agonist kainate (0.5 mM, 30 min). Reinnervation of IHCs was assessed after 3 more DIV with or without presence of neurotrophins (NT-3 or BDNF). SGN fiber-IHC contacts and postsynaptic densities (PSDs) on individual IHCs were quantified in confocal image stacks. These counts were compared between NT-3-lacking IHCs and adjacent IHCs expressing NT-3.

Results

Although reinnervation after excitotoxic trauma is generally poor in mice, most NT-3-lacking IHCs were selectively bypassed by regrowing SGN axons, while adjacent NT-3-expressing IHCs were reinnervated and acquired new PSDs. Significantly ($p < 0.05$) fewer PSDs (0.06 ± 0.3 , $n = 87$) were associated with reinnervated IHCs lacking NT-3. Culturing with NT-3 enhanced both SGN fiber regrowth (1.4 ± 1.2 SGN fibers/IHC, $n = 111$) and synaptogenesis (1.3 ± 1.5 PSDs/ IHC, $n = 64$) on NT-3-lacking IHCs to a level

comparable to NT-3-expressing IHCs (1.2 ± 1.1 SGN fibers/IHC, $n=499$; 0.9 ± 1.4 PSDs/IHC, $n=342$). In contrast, culturing with BDNF had no significant effect on synaptogenesis on NT-3-lacking IHCs (0 PSDs/IHC, $n=30$) although BDNF did promote SGN fiber growth to a similar extent as did NT-3.

Conclusion

Endogenous NT-3 expressed in each IHC promotes SGN synapse regeneration on that IHC after synapse destruction by excitotoxic trauma. Addition of exogenous NT-3 or BDNF to the cultures during the three days over which reinnervation occurs results in comparably improved SGN fiber growth. However, only NT-3 addition, but not BDNF addition, enhances synaptogenesis on IHCs.

1024 Gene Expression Changes in the Spiral Ganglion (SG) After Deafening

Erin M. Bailey¹, J. Robert Manak¹, Steven H. Green^{1,2}

¹Department of Biology, University of Iowa, ²Department of Otolaryngology, University of Iowa

Background

Hair cells (HCs) are the sole afferent input to spiral ganglion neurons (SGNs). Following aminoglycoside exposure from postnatal day 8 (P8) to P16, SGNs degenerate and gradually die. In rats, this occurs over a period of ~3 months (Alam et al. JCN 503: 832-52, 2007). SGN death may be due to loss of HC-derived neurotrophic factors (NTFs). However, expression of NTFs other than NT-3 persists throughout the period during which most SGNs die. Possibly, SGN death is an indirect outcome of HC loss, due to degenerative changes in the cochlea initiated by HC loss. We used microarray-based gene expression profiling to identify changes in the SG during the SGN death period and gain insight into why SGNs die.

Methods

Rats were deafened as previously described (Alam et al., 2007) and euthanized at P32, when SGN loss has just become significant or at P60, a time at which ~50% of the SGNs remain. Spiral ganglia were removed and divided into apical and basal halves prior to extraction of RNA. cDNA was hybridized in triplicate to Nimblegen HD2 rat gene expression arrays. Three separate biological repetitions were performed. DNASTAR software was used for quantile normalization and DAVID for functional annotation.

Results

13,000-15,000 genes are expressed above background. In comparing expression changes between P32 and P60 (maturation-related) or between hearing and deaf, expression of most genes does not change significantly. This includes genes encoding most NTFs and their receptors and genes related to apoptosis/survival, implying that lack of NTFs is not a primary cause of SGN death. Expression of ~8% changes significantly in hearing rats between P32 and P60, implying significant changes due to maturation. Expression of ~5% changes significantly after deafening at P32; remarkably, most transcriptional

changes occurring after deafening also occur in maturation, implying accelerated maturation-related changes in the SG post-deafening. <3% of expression changes are deafness-specific. Many of these are indicative of infiltration of immune system-related cells into the spiral ganglion.

Conclusion

Gene expression profiling has provided significant insight into the question of why SGNs die after HCs are killed by aminoglycosides. The data do not support a hypothesis that SGNs die because of loss of HC-derived NTFs in spite of observations that NTF application can rescue SGNs. Rather, SGN death may be due more directly to changes in glia or other cell types in the deafened ganglion.

1025 Increased Presence of Cells of the Immune System in the Spiral Ganglion During Spiral Ganglion Neuron (SGN) Death Post-Deafening

Erin Bailey¹, Catherine J. Kane¹, Zarin Rehman¹, Michael E. Dailey¹, Steven H. Green¹

¹Dept. of Biology, University of Iowa

Background

Following hair cell (HC) death due to aminoglycoside exposure from postnatal day 8 (P8) to P16, rat SGNs degenerate and die over a period of ~3 months (Alam et al. JCN 503: 832-52, 2007). The reason for SGN death is not clear. Several neurotrophic factors remain expressed in the cochlea after HC loss and SGNs do not die in all types of HC death. Possibly, SGN death is an indirect outcome of HC loss, due to other degenerative changes in the cochlea. We used microarray-based gene expression profiling to identify changes in the spiral ganglion during the SGN death period and gain insight into why SGNs die.

Methods

Rats were deafened by daily kanamycin injection P8-P16 and euthanized at P32, when SGN loss is just becoming significant, or at P60, when ~50% of the SGNs have died. RNA was isolated from dissected spiral ganglia. cDNA was hybridized in triplicate to Nimblegen HD2 rat gene expression arrays with three separate biological repetitions. DNASTAR software was used for quantile normalization and DAVID for functional annotation. Expression of selected representative genes was verified by qPCR. Immunofluorescence was performed as previously described (Alam et al., 2007).

Results

For genes expressed in the spiral ganglion, expression of ~0.8% decreases by >2X and of ~2% increases by >2X in deafened P60 rats, relative to hearing littermates. Many of these are indicative of infiltration of immune system-related cells into the spiral ganglion. For example, C-C and C-X-C chemokines are upregulated (CCL3 verified by qPCR) and interferon-inducible genes, e.g., Mx1, Mx2, are upregulated. There is a resident population of macrophages in the ganglion and characteristic gene expression (e.g., IBA1/AIF1, CD14, CD11b/ITGAM,

CD45/PTPRC, CD68) is evident in the gene expression profiling data in hearing rats. Expression of several of these, including PTPRC and CD68 (verified by qPCR), as well as MHCII expression increases >2X by P60 after deafening, suggesting an increased number of activated macrophages. This was verified by detection, by immunofluorescence, of an increased number of CD68-positive cells in the deafened spiral ganglion at P60.

Conclusion

Gene expression profiling provides evidence for increased immune cell presence, including cells of the innate system, in the spiral ganglion at the time when SGNs are dying. While their presence may be related only to clearance of debris, the observations raise the possibility that they are involved in SGN death.

1026 Targeted Deletion of Oncomodulin Alters Efferent Innervation in the Cochlea

Dwayne Simmons^{1,2}, Vasily Rozenbaum¹, Joyce Tsang¹, Aubrey Hornak¹

¹UCLA, ²Brain Research Institute

Background

The tight regulation of Ca²⁺ is essential for cochlear function, and yet the role of Ca²⁺ binding proteins in hair cells remains elusive. Oncomodulin (Ocm), a member of the parvalbumin family, has a restricted expression pattern, and in the cochlea is found in the basolateral membrane and hair bundle of outer hair cells (OHCs). Oncomodulin may mediate efferent-induced OHC responses and other Ca²⁺ dependent mechanisms, and therefore in the absence of Ocm, OHC function and efferent-mediated responses may be disrupted. As an initial test of this hypothesis, we performed preliminary morphological studies on OHCs and their efferent innervation in both wild-type and Ocm^{-/-} mice.

Methods

To study the role of Ocm, we generated a conditional Cre-lox knockout line with Cre-recombinase driven by the β -actin promoter (*Ocm^{tm1.Ddsi}*). The absence of Ocm expression was confirmed by RT-PCR and immunocytochemistry. Hearing function was assessed by auditory brainstem responses (ABRs). Choline acetyltransferase (ChAT) was used to label efferent axons and terminals. Phalloidin labeling was used to assess hair cell loss.

Results

Preliminary analysis of *Ocm^{tm1.Ddsi}* mice reveals no obvious phenotypic abnormalities compared with controls. At 4 weeks, there is no difference in cochlear function between mutant and wild-type littermates. However by 8 - 10 weeks, Ocm^{-/-} mutants have ABR threshold shifts of as much as 60 dB in frequencies above 10 kHz. There is no significant hair cell loss prior to 8 weeks. However after 8 weeks, OHC loss is pronounced. Ocm^{-/-} mutants exhibit abnormal ChAT-labeled, efferent innervation patterns compared to controls. At 4 weeks, Ocm^{-/-} mutants also exhibit a dense innervation in the IHC region and a more

disorderly innervation below OHCs. We see a higher density of efferent terminals below OHCs at 1 month compared to 4 months and in the apex compared to the base. The number of terminal clusters in basal regions begins to decline precipitously around 2 months. Also efferent terminal clusters in the Ocm mutant are smaller as the animal ages. Finally, there is significant remodeling of efferent projections in the cochlea in the 3 and 4 month Ocm mutants.

Conclusion

In the absence of a major Ca²⁺ binding protein, efferent organization is disrupted and OHCs are more susceptible to damage. Our data suggest that calcium regulators such as Ocm may play a protective role in hearing and play a role in organizing efferent innervation.

1027 Human Spiral Ganglion Degeneration Is Independent of Hair Cell Loss

Karen Berliner¹, Joni Doherty¹, Jose Fayad¹, Fred Linthicum, Jr.¹

¹House Research Institute

Background

Human spiral ganglion cells, in contrast to those of experimentally deafened animals, do not degenerate shortly after the loss of the organ of Corti. In fact, regardless of the time interval following the loss of hair cells and the individual's death, there is not an associated degeneration of spiral ganglion neurons (SGN). Numerous investigations with animal models have shown that cochlear neurons degenerate following degeneration of hair cells induced by ototoxicity. The time interval from hair cell loss to neuron loss in animals varies from 25% of the animal's life expectancy in the guinea pig to 1% in the chinchilla. In contrast to animals, we have observed surviving SGN in human temporal bone specimens from congenitally deaf humans with no surviving hair cells.

Methods

Histopathological and clinical history investigation of 40 temporal bones in our laboratory that are from patients, deafened by various etiologies, with no surviving hair cells. The durations of the hearing losses ranged from 9 to 93 years.

Results

Ganglion cell counts varied from 360 to 28,262 (avg. 14,514; SD=7934.75); the normal range for humans is 13,918 to 36,918, depending on age. Duration of hearing loss ranged from 5 to 93 years with an average of 38 years (SD=22.8), and hearing thresholds were recorded for durations ranging from 2 to 39 years (avg. 15.6 years; SD=10.6). Statistical analysis demonstrated no relationship between SGN survival and years of hearing loss.

Conclusion

Eight temporal bones from individuals that were deaf for an average of 21.25 years had SGN counts within the normal range for their age. SGN survival ranging in absolute

number from 11,722 to 19,093 was demonstrated in congenitally deaf individuals who survived 89-93 years of age with no surviving hair cells. These numbers suggest that, unlike animals, human SGN do not undergo degeneration following loss of auditory hair cells. Further investigations are necessary to determine factors involved in human SGN survival after hair cell degeneration.

1028 Cochlear Uptake of Gentamicin in Neonatal Mice

Hongzhe Li¹, Jawon Koo^{2,3}, Joo Hyun Park^{2,3}, Peter Steyger¹

¹Oregon Health and Science University, ²Seoul National University Bundang Hospital, ³Seoul National University College of Medicine

Background

Unlike the functionally mature cochlea of human newborns, the murine cochlea becomes functionally mature around 2 weeks after birth. In mice, tight junctions between adjacent marginal cells, and between adjacent endothelial cells, within the stria vascularis are established during this postnatal period, with consequent enrichment of endolymph with potassium. This dynamic postnatal cochlear maturation in the mouse provides a unique opportunity to study how ototoxic reagents permeate the developing blood-labyrinth barrier to reach young sensory hair cells.

Methods

Neonatal C57Bl/6 mice were intraperitoneally injected with fluorescently-conjugated gentamicin (GTTR) for 30 or 60 minutes at various postnatal ages prior to in situ fixation. Harvested cochlear tissues were either whole-mounted or cryosectioned for confocal microscopy. The intensity and distribution of GTTR in all tissues were acquired at the same confocal settings in all experimental groups. The intensity of GTTR fluorescence in cochlear and renal proximal tubule tissues were quantified and compared between different age groups (p7, p21, p35, n=6, 3, 6 respectively).

Results

GTTR fluorescence in hair cells and the lateral wall (including marginal, intermediate and basal cells of the stria vascularis, and fibrocytes of the spiral ligament) was significantly higher at p7 than at p21 or p35 ($p < 0.01$). This is suggestive of paracellular permeation of GTTR through the premature blood-labyrinth barrier. Furthermore, hair cells exhibited a heterogeneous pattern of GTTR uptake between p7 to p10. That is, a subset of sensory and supporting epithelial cells presented increased GTTR fluorescence compared to adjacent cells of the same cell type. Animals treated with Texas Red only had negligible red fluorescence at all time points. Renal proximal tubules did not show significant differences in fluorescence intensity between different time points.

Conclusion

Prior to complete maturation of the cochlear blood-labyrinth barrier, GTTR readily permeates into stria cells,

fibrocytes and sensory hair cells. A heterogeneous pattern of GTTR uptake in the organ of Corti from p7 to p10 corresponds with a known wave of purinergic activation of sensory epithelial cells that precedes the onset of functional hearing. This suggests that purinergic ion channels, such as P2X2, may facilitate hair cell uptake of GTTR and aminoglycosides.

Funded by NIH-NIDCD grants R01 DC004555, R01 DC010588, R03 DC011622, P30 DC005983; and by a National Research Foundation of Korea Grant 2011-0010166.

1029 Identification of Cisplatin-Binding Proteins in the Cochlea

Takatoshi Karasawa¹, Martha Sibrian-Vazquez², Robert Strongin², Peter Steyger¹

¹Oregon Health & Science University, ²Portland State University

Background

Cisplatin is widely used as an antineoplastic drug, but its ototoxic and nephrotoxic side-effects, as well as the inherent or acquired resistance of some cancers to cisplatin, remain significant clinical problems. Cisplatin's selectivity in killing rapidly proliferating cancer cells is largely dependent on covalent binding to DNA via cisplatin's chloride sites that had been aquated. We hypothesized that cisplatin's toxicity in slowly proliferating or terminally differentiated cells is primarily due to drug-protein interactions, instead of drug-DNA binding.

Methods

To identify proteins that bind to cisplatin, we synthesized two different platinum-agarose conjugates, one with two amino groups and another with two chlorides attached to platinum that are available for protein binding, and conducted pull-down assays using cochlear and kidney cells, including the organ of Corti HEI-OC1 cells. The proteins that bound to the platinum-agarose were removed from platinum-agarose in SDS sample buffer, analyzed by SDS-gel electrophoresis and Coomassie blue staining, and identified by mass spectrometry.

Results

Platinum-agarose pull-down assay revealed that proteins poorly bound to cisplatin at the chloride site, while many proteins bound to the amino groups with high affinities. Comparison among different cell lines did not show significant differences in binding proteins, except for myosin IIA, which only appeared in HEI-OC1 cells. Mass spectrometric analysis on protein bands after gel electrophoresis and Coomassie blue staining identified several proteins, including myosin IIA, glucose-regulated protein 94 (GRP94), heat shock protein 90 (HSP90), calreticulin, valosin containing protein (VCP), and ribosomal protein L5, as cisplatin-binding proteins in HEI-OC1 cells. Previous reports suggested that some of these proteins are specifically expressed in the cochlea and most of them are overexpressed in cancer.

Conclusion

We have identified several cisplatin-binding proteins that are either specifically expressed in the cochlea or overexpressed in cancer. These proteins likely play a role in cisplatin-induced ototoxicity/nephrotoxicity or cisplatin resistance of cancer. Future studies on the cisplatin-binding proteins will elucidate whether these drug-protein interactions are involved in ototoxicity and nephrotoxicity, or contribute to tumor resistance to cisplatin treatment.

Supported by NIDCD R21 10231, P30 05983, and Medical Research Foundation of Oregon.

1030 Early Time Course of Gentamicin Uptake in Peripheral Vestibular Cells After Systemic Administration

Jianping Liu¹, Allan Kachelmeier¹, Chunfu Dai², Hongzhe Li¹, Peter Steyger¹

¹Oregon Health & Science University, ²Fudan University

Background

Systemic aminoglycoside therapy can induce vestibulotoxicity as well as cochleotoxicity, resulting in imbalance and visual dysfunction. The underlying trafficking routes and cytotoxicity mechanisms remain unknown. We investigated the early time course of gentamicin trafficking into the peripheral vestibular system after systemic administration of fluorescently-tagged gentamicin (GTTR).

Methods

C57BL/6 mice received GTTR 2 mg/kg via intraperitoneal injection; control mice received equivalent doses of Texas Red or PBS. Mice were sacrificed at 0.5, 1, 2, 3 or 4 hours, followed by transcardiac perfusion with PBS, and fixation with 4% paraformaldehyde. Excised vestibular tissues were permeabilized and subsequently counterlabeled with fluorescent phalloidin, and examined by sequential scanning laser confocal microscopy. Identical confocal settings were used for all experimental and control groups. Fluorescence pixel intensities in nonsensory and sensory cells (including dark, transitional, and supporting cells) from single optical sections were obtained after removal of extracellular pixels. Mean pixel intensity-time course plots were constructed.

Results

Vestibular cells of both ears of all animals exposed to GTTR exhibited changes in GTTR fluorescence over time. Low intensity fluorescence was detected at 0.5 hours, and increased in intensity to peak at 3 hours, before declining 4 hours after injection. The distribution of GTTR fluorescence differed in sensory and nonsensory cells. Sensory cells typically had only diffuse GTTR fluorescence, at all tested timepoints. In contrast, nonsensory cells displayed (i) an intensely fluorescent granular distribution (> 0.6 microns in diameter), as well as (ii) a diffuse pattern of fluorescence throughout the cytosol. The area of granular fluorescence in dark cells and transitional cells significantly increased over time. Control

vestibular tissues exposed to PBS or hydrolyzed Texas Red had negligible fluorescence at all tested timepoints.

Conclusion

Systemically-administered GTTR is rapidly taken up by murine peripheral vestibular sensory and nonsensory cells, peaking in fluorescence intensity 3 hours after a single injection. The intensity of GTTR in sensory and nonsensory cells share similar time courses. However, the distribution of GTTR within cells is very different. Diffuse fluorescence suggests entry via GTTR-permeant ion channels, while granular fluorescence suggest either endocytosis and/or compartmentalization of cytosolic GTTR. The difference in GTTR distribution within sensory and nonsensory cells suggests differential uptake mechanisms and/or subcellular GTTR targets in these cell types. The intra-vestibular trafficking routes of GTTR also remain to be elucidated.

Funded by NIH-NIDCD grants R01 DC04555 (PS), P30 DC05983 and NSFC 30600704 (JL).

1031 Is a Temporary Threshold Shift Required for Sound-Enhanced Uptake of Gentamicin?

Hongzhe Li¹, Peter Steyger¹

¹Oregon Health & Science University

Background

Animal studies have firmly demonstrated the ototoxic synergy between acoustic overstimulation and aminoglycoside antibiotics. We have previously reported that prior sound exposure, at moderate sound levels which induce temporary threshold shifts (TTS), also enhanced gentamicin uptake in the cochlea. We propose that sound-enhanced aminoglycoside uptake by the cochlear tissue is a candidate mechanism for ototoxic synergy. In order to determine whether correlation between TTS and sound-enhanced gentamicin uptake is present, we systemically varied the sound level of wideband noise, and examined its effect on cochlear uptake of gentamicin.

Methods

To induce temporary threshold shifts, adult C57Bl/6 mice were exposed to wideband noise (86-96 dB SPL) for 6 hours/day for 3 days. The degree of TTS was assessed by tonal ABR measurements (4, 8, 12, 16, 24 and 32 kHz) at multiple time points before and after sound exposure. Mice were also intraperitoneally injected with fluorescently-conjugated gentamicin (GTTR) after sound exposure. Thirty minutes later, fixed cochlear tissues were excised and processed for confocal microscopy. The intensity of GTTR fluorescence were acquired using identical confocal settings, quantified and statistically tested to determine the effect of sound exposure on GTTR uptake in the cochlea.

Results

Higher sound levels (91 and 96 dB SPL) produced evident TTS at higher (16, 24 and 32 kHz) frequencies, while no TTS was observed at lower frequencies (4 and 8 kHz). Sound levels that induced TTS also enhanced hair cell

uptake of GTTR. For cochleae with TTS, we examined multiple frequency locations along the organ of Corti. Enhanced hair cell uptake of GTTR was observed in basal high frequency regions with TTS, and also in more apical low frequency regions with normal ABRs thresholds. In cochleae without evident TTS, hair cells did not show the enhanced uptake of GTTR that is associated with TTS.

Conclusion

TTS is required for sound-enhanced uptake of gentamicin by hair cells in the cochlea. Sound-enhanced uptake of gentamicin by hair cells is not specific to the frequency regions with TTS, and also occurs at frequencies below the region of TTS. Thus, the mechanisms that induce sound-enhanced gentamicin uptake extend beyond the cochlear region associated with TTS and the mechanisms that induce TTS.

Funded by NIH-NIDCD R01 DC004555, R03 DC011622, and P30 DC005983.

1032 Bumetanide Hyperpolarizes Cells and Enhances Cellular Uptake of Gentamicin by Elevating Cytosolic Ca^{2+} and Facilitates Intermediate Conductance Ca^{2+} -Activated Potassium Channels

Tian Wang¹, Yu-qin Yang¹, Takatoshi Karasawa¹, Meiyuan Jiang¹, Peter Steyger¹, Zhi-Gen Jiang¹

¹Oregon Health & Science University

Background

Loop diuretics such as bumetanide and furosemide enhance aminoglycoside ototoxicity when co-administered to patients and animal models. The underlying mechanism(s) is poorly understood.

Methods

We investigated the effect of these diuretics on cellular uptake of aminoglycosides, using fluorescently-tagged gentamicin (GTTR), and the action of these diuretics on membrane potentials and specific channel currents using intracellular/whole-cell recordings of Madin-Darby Canine kidney (MDCK) cells. MDCK cells preloaded with the calcium indicator Fluo-4 were used to detect the effect of bumetanide on cytosolic Ca -level by image recording with a Yokogawa CSU10 spinning disk confocal system, and data quantitation and analysis with Fiji/ImageJ software.

Results

We found that bumetanide and furosemide concentration-dependently enhanced cytoplasmic GTTR fluorescence up to ~60%. This enhancement was suppressed by La^{3+} , a non-selective cation channel (NSCC) blocker, and by K^+ channel blockers Ba^{2+} and clotrimazole, but not by tetraethylammonium (TEA), 4-aminopyridine (4-AP) or glipizide, nor by Cl^- channel blockers diphenylamine-2-carboxylic acid (DPC), niflumic acid (NFA), and CFTR_{inh}-172. Bumetanide and furosemide hyperpolarized MDCK cells by ~14 mV, increased whole-cell I/V slope conductance; the bumetanide-induced net current I/V showed a reversal potential (V_r) ~-80 mV. Bumetanide-

induced hyperpolarization and I/V change was suppressed by Ba^{2+} or clotrimazole, and absent in elevated [Ca^{2+}]_i (2 μ M), but not affected by apamin, 4-AP, TEA, glipizide, DPC, NFA or CFTR_{inh}-172. Bumetanide and furosemide stimulated a surge of Fluo-4-indicated cytosolic Ca^{2+} . Ba^{2+} and clotrimazole alone depolarized cells by ~18 mV and reduced I/V slope with a net current V_r near -85 mV, and reduced GTTR uptake by ~20%. La^{3+} alone hyperpolarized the cells by ~-14 mV, reduced the I/V slope with a net current V_r near -10 mV, and inhibited GTTR uptake by ~50%. In the presence of La^{3+} , bumetanide caused negligible potential or I/V change.

Conclusion

We conclude that NSCCs constitute a major cell entry pathway for cationic aminoglycosides; bumetanide enhances aminoglycoside uptake by hyperpolarizing cells that increases cation influx driving force. Bumetanide-induced hyperpolarization is caused by elevating intracellular Ca^{2+} and thus enhances intermediate conductance Ca^{2+} -activated K^+ channels.

Funded by NIDCD R01 DC004716 (ZGJ), R01 DC004555 (PSS), F32 DC008465, R03 DC009501 (TK) and P30 DC005983.

1033 Protection of Hair Cells from Aminoglycoside Antibiotics in the Zebrafish *merovingian* Mutant

Tamara Stawicki¹, Kelly Owens¹, Tor Linbo¹, Brock Roberts^{1,2}, Katherine Reinhart¹, Edwin Rubel¹, David Raible¹

¹University of Washington, ²University of California, Berkeley

Background

A number of therapeutic agents, including aminoglycoside antibiotics and chemotherapeutics cause hair cell death. While progress has been made in delineating the cellular pathways responsible for toxicant induced hair cell death, our knowledge is still incomplete, and hearing loss remains a dose limiting side effect of multiple therapeutic drugs. Our lab uses the zebrafish lateral line system to identify novel genes involved in toxicant induced hair cell death.

Methods

5-6 days post fertilization zebrafish are used for all experiments. For experiments looking at neomycin toxicity, fish were exposed to varying doses of neomycin for 30 minutes, and then given 1 hour to recover. Hair cells were labeled using parvalbumin staining to quantify hair cell number after treatment. For measuring uptake of Texas Red-conjugated neomycin or FM1-43 fish were exposed to the compound for 15 minutes or 1 minute respectively and then imaged immediately.

Results

We have previously identified the *merovingian* (*mero*) mutant in a screen for zebrafish mutants where lateral line hair cells are protected from aminoglycoside hair cell death (Owens et al, PLOS Genetics, 2008). *merovingian*

mutants show complete protection against neomycin-induced hair cell death which appears to be due to a failure of the drug to enter hair cells. These mutants also show a decreased initial number of lateral line hair cells, vestibular defects, and decreased FM1-43 uptake suggesting impaired hair cell development and function. Through genetic mapping we have identified a mutation in transcription factor *gcm2*, a gene necessary for global pH and ion regulation in the *merovingian* mutants. This is of particular interest as we have previously identified a mutation in the chloride/bicarbonate exchanger, SLC4A1b, as also conferring resistance to aminoglycoside induced hair cell death (Hailey et al., PLOS Genetics 2012, Owens et al, PLOS Genetics, 2008).

Conclusion

Our results implicate a role for global ion and pH regulation in controlling hair cell function as well as susceptibility to aminoglycoside-induced hair cell death. We are continuing to study the *merovingian* mutant to elucidate the relevant ionic transporters affecting hair cell function and aminoglycoside susceptibility.

1034 Neutral Sphingomyelinase Is Involved in Hair Cell Death Induced by Gentamicin

Keiji Tabuchi¹, Le Chi¹, Mariko Nakamagoe¹, Bungo Nishimura¹, Masahiro Nakayama¹, Shuho Tanaka¹, Isao Uemaetomari¹, Hideki Okubo¹, Tetsuro Wada¹, Akira Hara¹
¹University of Tsukuba

Background

The sphingolipid metabolites ceramide, sphingosine, and sphingosine-1-phosphate (S1P) are known as a new class of lipid second messengers and reportedly play essential roles in the regulation of cell proliferation, survival, and death. Ceramide has been shown to regulate diverse cellular processes including apoptosis, cell senescence, the cell cycle, and cellular differentiation. Recently, we showed that exogenous ceramide increased hair cell death in gentamicin ototoxicity (Nishimura et al., 2010). Sphingomyelinase (SMase) converts sphingomyelin to ceramide. Several signaling molecules, such as tumor necrosis factor, Fas ligand, γ -interferon, interleukin 1, vitamin D, and stressful events including radiation and ischemia, reportedly activate SMase and promote ceramide-induced apoptosis. This study was designed to investigate the possible involvement of neutral SMase in hair cell death due to gentamicin.

Methods

The basal turn of the organ of Corti was dissected from Sprague–Dawley rats on postnatal days 3 (p3) to 5 (p5). Cochlear cultures were exposed to a medium containing 35 μ M gentamicin for 48 hours to assess the effects of GW4869, a neutral SMase inhibitor.

Results

One to 30 μ M GW4869 did not affect hair cell loss induced by gentamicin. However, hair cell loss significantly decreased in the presence of 35 to 50 μ M GW4869.

Conclusion

The present finding strongly suggests that GW4869 protected hair cells against gentamicin ototoxicity by inhibiting ceramide synthesis via the SMase pathway.

1035 Targeted Activation of ERK1/2 in Supporting Cells Is Sufficient to Promote Hair Cell Death in the Adult Utricle

Gregory Ball¹, Lindsey May², Lisa Cunningham², Jonathan Gale¹

¹UCL Ear Institute, 332 Gray's Inn Road, London, WC1X 8EE, UK, ²NIDCD, National Institutes of Health, 5 Research Court, Rockville, MD 20850, USA

Background

In the neonatal cochlea, extracellular regulated kinases 1 and 2 (ERK1/2) are activated in supporting cells surrounding an epithelial wound, and also around hair cells damaged by the aminoglycoside, neomycin. Inhibition of MEK1/2, the upstream kinase, prevents activation of ERK1/2 and affords some protection of inner hair cells (Lahne & Gale 2008). Given that supporting cells exhibited the phosphorylated-ERK1/2 signal, we concluded that supporting cells could be contributing to hair cell death. Direct evidence that supporting cells can phagocytose hair cells was obtained using live-imaging of ototoxically damaged avian utricles (Bird et al. 2010). Here we investigate whether a similar supporting cell and ERK1/2-dependent mechanism is present in the mature inner ear and whether activating ERK in supporting cells is sufficient to trigger phagocytic activity.

Methods

Adult and neonatal mouse utricle explant cultures were used to examine ERK1/2 activation following acute damage to hair cells using a multi-photon laser or using neomycin for 24 hours. The MEK1/2 inhibitor U0126 was used to probe the function of ERK1/2 activation. In order to determine the role of ERK1/2 in supporting cells, we used an adenoviral protocol (Brandon et al. 2012) to infect supporting cells with consecutively active MEK1 (CA-MEK1). Infected utricles were fixed and analysed using immunohistochemistry and confocal microscopy, or were subjected to live imaging using a spinning disk confocal microscope.

Results

Damaging hair cells using either the laser or neomycin resulted in the activation of ERK1/2 in the neighbouring supporting cells. Although we observed subtle differences in the spatiotemporal properties of ERK1/2-activation, the overall pattern was very similar in both mature and immature utricles. Pharmacological inhibition of MEK1/2 achieved a small but significant protection of hair cells during 24 hours aminoglycoside treatment in adult utricles. Constitutive activation of MEK1 in supporting cells using adenovirus was confirmed by phosphoERK staining. ERK1/2 activation resulted in changes in cell phenotype including expansion of cell surfaces, movement towards the surface of the epithelium, and suggested phagocytic behavior. These phenotypes were confirmed in live

imaging experiments. Finally, the activation of ERK1/2 in supporting cells resulted in a reduction in the number of hair cells in infected utricles.

Conclusion

This work provides evidence that supporting cells play a significant role in mediating hair cell death in adults, and that activation of the ERK1/2 signalling pathway is sufficient for this.

1036 Investigating Free Radical Production in the Cochlea During Ototoxicity

Paromita Majumder¹, Michael Duchen², Jonathan Gale^{1,2}
¹UCL Ear Institute, ²Department of Cell & Developmental Biology, UCL

Background

Research over the last decades has implicated reactive oxygen species (ROS) as major causative factors for both ototoxic and noise-induced hearing loss. Despite much research in this area the sites, sources and dynamics of ROS production have evaded thorough examination. We use live imaging to measure ROS production in the cochlea during neomycin exposure.

Methods

We use cochlear explant cultures from basal and middle turns of 4-7 day old mice with intact stria vascularis. ROS is measured using 5 μ M dihydroethidium (HET). In some experiments we also measured intracellular calcium using Oregon-GreenBAPTA. Confocal image-stacks containing inner sulcus (IS), inner hair cells (IHC), outer hair cells (OHC), Hensen's cells, outer sulcus (OS) and stria vascularis (SV) are recorded every 1 to 5 min over ~4 hours using a Zeiss 510NLO-META.

Results

HET fluorescence showed a steady increase indicating a basal rate of ROS production in different cells/regions. After 30 minutes of baseline measurement explants were exposed to 1mM neomycin. In the first hour of exposure the rates of ROS generation were generally increased (n = 5). By the second and third hours of neomycin exposure the ROS-production rates were reduced towards baseline values.

To investigate the role of mitochondria in neomycin-induced ROS production, explants were treated with a complex I inhibitor (rotenone 20 μ M, n = 4) prior to neomycin exposure. Rotenone pre-treatment reduced the neomycin-induced increase in ROS production in almost all cell types except for the IS cells suggesting mitochondria are a significant source of ROS produced in most cochlear cells after aminoglycosides but not the IS.

In addition we measured the dynamics of intracellular calcium and ROS. A proportion of hair cells die during the 4 hour experiment. Preliminary analysis of 6 different experiments revealed an increase in intracellular calcium that began 42 \pm 10 minutes before cell death. Approximately half of the cells analysed showed a second large calcium increase and an increase in ROS production, just prior to cell death.

Conclusion

Further experiments are ongoing to characterize the sites and mechanisms of ROS production during aminoglycoside treatment.

1037 A Novel Role of Cytosolic Protein Synthesis Inhibition in Aminoglycoside Ototoxicity

Shimon Francis¹, James Pagana¹, Jung-Bum Shin¹
¹University of Virginia

Background

In this project, we studied the role of cytosolic protein synthesis inhibition in aminoglycoside (AG)-induced hair cell degeneration. Most apoptosis-inducing compounds such as anisomycin and cycloheximide, also cause protein synthesis inhibition, suggesting a mechanistic connection between protein synthesis and apoptosis regulation. We therefore set out to test whether protein synthesis inhibition might be involved in AG-induced hair cell degeneration.

Methods

Protein synthesis activities in explant cultures from vestibular and auditory organs of the mouse and chick were detected using the bioorthogonal noncanonical amino acid tagging (BONCAT) method, which uses click-chemistry to visualize protein synthesis activity on a cell-by-cell basis. In combination with immunocytochemistry methods, BONCAT allows correlation of protein synthesis activity with markers of cellular signaling pathways.

Results

Using the BONCAT method, we discovered for the first time that AGs inhibit protein synthesis in hair cells. We found that protein synthesis inhibition is strictly correlated with the activation of the c-Jun kinase (JNK) pathway: shown by microscopy on a cell-by-cell basis, hair cells with arrested protein synthesis display strong JNK activation. In addition, we find that the ototoxic potency of a given aminoglycoside (tested were apramycin, kanamycin, gentamicin) correlated very well with its ability to cause cytosolic protein synthesis inhibition and JNK activation.

The observed stress response pattern (protein synthesis inhibition, JNK activation, caspase-3 mediated apoptosis) is characteristic for the so-called ribotoxic stress response, caused by a class of toxins that bind to and/or inactivate ribosomal RNA (rRNA). Indeed, AGs are known to bind to both mitochondrial and cytosolic rRNA. While the binding to mitochondrial rRNA has already been reported to contribute to AG ototoxicity, the affinity to cytosolic rRNA was believed to be too low to cause damage. Our data suggests the opposite, and we propose that a stress response similar to ribotoxic stress contributes to aminoglycoside ototoxicity. In agreement with this, we found that the FDA-approved anti-cancer drug sorafenib, known to inhibit ribotoxic stress response, also inhibits aminoglycoside-induced JNK activation and, to a limited degree, hair cell apoptosis.

Conclusion

In summary, we report the discovery of a novel stress pathway that contributes to aminoglycoside-induced hair cell degeneration. We demonstrate that aminoglycosides inhibit protein synthesis in hair cells and activate a stress pathway similar to ribotoxic stress response. A FDA-approved drug known to inhibit ribotoxic stress prevents JNK activation and improves hair cell survival.

1038 Effects of Dietary Nutrients on Amikacin Ototoxicity in Guinea Pigs: Reduced Hearing Loss and Increased Hair Cell Survival

Colleen Le Prell¹, Susan DeRemer², Eric Rudnick¹, Mark Nelson¹, Alamea Goldstein¹

¹University of Florida, ²University of Michigan

Background

Amikacin is an aminoglycoside antibiotic that is toxic to sensory cells in the inner ear, and produces hearing loss. Much of the damage to the sensory cells is the result of metabolic stress and related free radical production. Several agents that attenuate free radical production have been shown to attenuate amikacin and other aminoglycoside antibiotic induced ototoxicity. Here, we present data demonstrating protection from amikacin ototoxicity using a dietary supplement, composed of beta-carotene, vitamins C and E, and magnesium.

Methods

Albino guinea pigs were maintained on a nutritionally complete standard laboratory diet (2040 Teklad Global Guinea Pig Diet; n=10) or a custom-manufactured version of the 2040 diet (TD.08623) with increased levels of beta-carotene, vitamins C and E, and magnesium (n=8). Maintenance on the TD.08623 diet has previously been shown to reduce noise-induced and gentamicin-induced hearing loss in guinea pigs. Dietary manipulation was initiated 28-days prior to initiating daily amikacin injections. Subjects were maintained on the assigned diet during the daily amikacin injections (200 mg/kg/day amikacin x 28 days), and for the following 9 weeks after the last amikacin injection. Auditory brainstem response (ABR) thresholds were assessed at frequencies including 2, 4, 8, 16, and 24 kHz; tests were conducted at eight specific test times before, during, and after amikacin. At the end of the 9-week post-amikacin ABR assessment, subjects were euthanized, cochlear tissues were harvested, and hair cells were labeled and counted.

Results

Functional protection included a significant reduction in ABR threshold shift of ~10-20 dB across test frequencies and across test times. Inner hair cells (IHCs) were completely eliminated in amikacin-treated controls, whereas 80-90% were missing in animals receiving the supplemented diet plus amikacin. Outer hair cells (OHCs) were largely eliminated in the control group, except in the most apical 25% of the organ of Corti, where average OHC survival was ~10%. In animals receiving supplemented

diet, average OHC survival reached ~15% over the most apical 40% of the cochlea.

Conclusion

The small but reliable protective effects of our custom diet are striking given the virtually complete cell death and profound hearing loss observed in control animals. Additional studies are needed to optimize the protective effects observed here, and to further support the long-term goal of translating successful therapeutics from animal models to clinical trials.

1039 Cochlear Transfection of X-Linked Inhibitor of Apoptosis Protein Via Round Window Reduces Cisplatin Induced Hearing Loss in Guinea Pigs

Lijie Liu¹, Jian Wang²

¹Southeast University, China, ²Dalhousie University

Background

Previously, we demonstrated that over-expression of X-linked inhibitory of apoptosis protein (XIAP) can delay the development of presbycusis and mitigate noise induced cochlear damage by using transgenic mouse model. Later, we developed and optimized an approach that is minimal invasive for cochlear gene transfection. In this approach, transgene is carried by adeno-associated virus (AAV). The AAV vector is delivered to the cochlea across round window membrane (RWM) which is made permeable to AAV by using a digestive enzyme. In combination with the use of the new generation of AAV with this RWM approach, we fulfill a satisfactory gene transfection in most of the key cell types including outer hair cells.

Methods

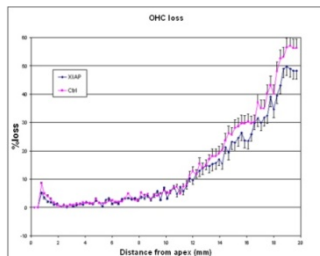
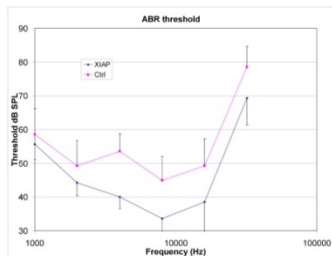
In the present study, we examine if the XIAP overexpression induced by cochlear gene transfection via RWM approach can effectively reduce the cochlear damage of a commonly used chemotherapeutic drug, cisplatin, which is applied 10 days after the transfection surgery and at the dose of 4 mg/kg in 3-6 consecutive days. The hearing threshold was tested in auditory brainstem responses (ABR) in closed field and compared in a self-control design between ears with and without XIAP gene transfection.

Results

Gene-transfection via RWM does not significantly damage cochlear function. After cisplatin treatment, both ABR threshold elevation and hair cell loss are significantly less in the ear transfected with XIAP gene. The exogenous XIAP is quantified and compared with endogenous XIAP in Western blotting.

Conclusion

XIAP gene transfection mediated with AAV vectors via RWM approach can effectively reduce the damage of cisplatin on various cell types in cochlea. The reduced cell damage is associated with functional preservation. RWM approach may be a method applicable in human subjects in hearing preservation against ototoxicity.



1040 Hydrogen Peroxide Production Can Be Measured in Lateral Line Hair Cells Using HyPer [Tg(Myosin6b:HyPer)] Expressing Zebrafish

Patricia Wu¹, Robert Esterberg², Henry Ou^{1,3}

¹University of Washington, VM Bloedel Hearing Research Center, ²University of Washington, Dept of Biological Structure, ³Seattle Children's Hospital

Background

Oxidative stress caused by reactive oxygen species (ROS) has been hypothesized to play a critical role in hair cell death, however its role in zebrafish lateral line hair cell death is not well described. Characterization of the timecourse of ROS production in response to ototoxic agents would offer insight on the role of ROS, and role of antioxidants in preventing cell death.

Methods

HyPer (Evrogen) is a hydrogen peroxide biosensor that has been used in vivo to detect low levels of intracellular hydrogen peroxide. We have generated a transgenic zebrafish line expressing cytoplasmic HyPer under the control of the hair cell-specific myosin6b promoter [Tg(myosin6b:HyPer)]. Transgenic zebrafish were then exposed to neomycin followed by in vivo imaging at 1 minute intervals using an inverted Marianas spinning disk system. Mitochondrial depolarization was simultaneously examined using tetramethylrhodamine ester (TMRE) labeling. HyPer signal was examined with and without cotreatment with the antioxidant glutathione.

Results

Hydrogen peroxide generation as measured by HyPer fluorescence increased rapidly in response to neomycin. This effect could be blocked by high (1000 μ M) but not low concentrations (250-500 μ M) of the antioxidant glutathione. Time courses of hydrogen peroxide generation and TMRE signal were measured in response to neomycin. Only high dose glutathione could protect against neomycin-induced hair cell death.

Conclusion

The Tg(myosin6b:HyPer) expressing zebrafish line can be effectively used to study hydrogen peroxide generation in neomycin-treated zebrafish lateral line hair cells. Neomycin-induced hydrogen peroxide generation and neomycin-induced hair cell death could only be blocked by high doses of the antioxidant glutathione in the zebrafish lateral line.

1041 Small Molecule Inhibitors of Cisplatin-Induced Hair Cell Death: Results of a 10,000 Compound Screen in the Zebrafish Lateral Line

Andrew Thomas¹, Patricia Wu¹, David Raible², Edwin Rubel¹, Julian Simon³, Kelly Owens¹, Henry Ou^{1,4}

¹University of Washington, VM Bloedel Hearing Research Center, ²University of Washington, Dept of Biological Structure, ³Fred Hutchinson Cancer Research Center, ⁴Seattle Children's Hospital

Background

Cisplatin is a commonly used anti-cancer drug which causes damage to inner ear hair cells and hearing loss. Because cisplatin treatment is given in planned doses, a compound that protects against cisplatin-induced hair cell damage would be useful for prophylaxis during cisplatin chemotherapy. We sought to identify such a compound using a zebrafish lateral line screening protocol we have successfully used in the past to identify compounds that protect against hair cell death.

Methods

We screened a library of 10,000 drug-like small molecules for protection against cisplatin-induced hair cell damage in the zebrafish lateral line. For compounds associated with reduced hair cell damage, dose-response relationships were determined in the zebrafish lateral line using immunocytochemistry. Hair cell counts were performed to quantify the number of hair cells remaining after cisplatin treatment with and without the potential protectant. To evaluate whether the protective compounds altered the chemotherapeutic efficacy of cisplatin, we tested the compounds with cisplatin in cancer cell culture using human lung adenocarcinoma cells from the A549 and NCI-H23 cell lines.

Results

Two compounds, CHCP1 and CHCP2, demonstrated dose-dependent protection against cisplatin-induced hair cell death. At the most optimal concentration, CHCP1 and CHCP2 increased hair cell survival (% control) after cisplatin treatment from $37.1 \pm 4.0\%$ to $65.4 \pm 11.6\%$, and from $29.7 \pm 5.3\%$ to $70.0 \pm 10.2\%$, respectively. The dose-dependent tumoricidal activity of cisplatin was retained in the presence of CHCP1 and CHCP2 when evaluated in tumor cell culture. We also evaluated 5 analogs of CHCP2, and found similar protection among compounds with minor structural modifications.

Conclusion

The finding of two small molecules that protect against cisplatin-induced hair cell death affirms the feasibility of screening using the zebrafish lateral line and provides 2 compounds that may have therapeutic benefit as protectants against cisplatin-induced hair cell damage. Further characterization of these compounds and structurally related analogs are being conducted.

1042 Copper-Induced Hair Cell Death in the Zebrafish Lateral Line Requires Functional Mechanotransduction

Andrew Thomas¹, Patricia Wu¹, Henry Ou^{1,2}

¹University of Washington, VM Bloedel Hearing Research Center, ²Seattle Children's Hospital

Background

Copper is known to induce rapid dose-dependent toxicity in zebrafish lateral line hair cells. The mechanism by which copper gains access to the hair cells is not known. Previous studies have suggested a possible role for the mechano-electrical transduction (MET) channel in copper toxicity. Olivari et al. (2008) found decreased copper toxicity in immature hair cells that do not yet have functional MET channels, and decreased toxicity in the presence of the MET inhibitor amiloride. We have examined the effects of chemical and genetic inhibition of mechanotransduction on copper damage in hair cells of the zebrafish lateral line.

Methods

Zebrafish larvae were exposed to a treatment condition then incubated in either normal fish embryo media or media with 1 micromolar CuSO₄. Tip link proteins, required for normal MET channel function, were disrupted by calcium chelation in calcium-free media with 5 mM EGTA. Quinine was used as a potent chemical inhibitor of the MET channel. Genetic disruption of MET function was assessed using the cadherin-23 mutant, sputnik. After treatment, zebrafish were fixed for immunohistochemistry and hair cell survival was quantified.

Results

Consistent with previous studies, we found that copper rapidly induced dose-dependent hair cell death. Tip link disruption with EGTA increased hair cell survival (% control) from 37.8 ± 5.9% to 99.5 ± 7.5%. The sputnik mutant demonstrated hair cell survival of 93.5 ± 8.3%. Quinine partially prevented hair cell death, increasing hair cell survival from 58.9 ± 8.6% to 79.2 ± 6.3%.

Conclusion

Chemical and genetic inhibition of mechanotransduction protected against copper-induced hair cell death. This suggests that functional mechanotransduction is important for copper-induced hair cell death in the zebrafish lateral line.

1043 p53 Plays a Key Role in Cisplatin-Induced Cochlear Cell Death: Toward the New Therapeutic Strategy

Julien Menardo¹, Jean-Luc Puel¹, Jing Wang¹

¹inserm

Background

In the therapeutic arsenal in the fight against cancer, chemotherapy has a place. Cisplatin (cis-diamine-dichloroplatinum II [N₂Cl₂PtH₆] or CDDP) is a widely used anti-cancer drug. Unfortunately, it presents a significant toxicity to both the kidney (nephrotoxicity) and the cochlea

or inner ear (ototoxicity). Nephrotoxicity of CDDP is circumvented by strategies of hydration, permitting use of increased doses of CDDP. In contrast, no protocol to protect the cochlea is currently available.

The mechanism of action underlying the cytotoxicity of CDDP is based on DNA alterations. In the cochlea, CDDP has been shown to induce an oxidative stress leading to the activation of the mitochondrial apoptotic pathway of the auditory sensory cells. However, very few is known about the upstream actors of the apoptotic events. Those actors could be therapeutic targets to prevent hearing loss in CDDP treated patients.

Methods

To investigate the signalling events between DNA damage and apoptotic death, we use an in vitro model of cochlear primary culture. This model mimics the mechanisms of degeneration observed in vivo after a CDDP treatment, i.e. a dose-dependant toxicity, a greater sensitivity of outer hair cells to CDDP ad a base to apex gradient of degeneration. We used 129/sv mice lacking p53 to understand the role of this transcription factor in vivo when treated with CDDP.

Results

We have shown that, in vitro, p53 expression is upregulated and that p53 is phosphorylated on its serine 15 after CDDP treatment. We also have demonstrated that p53 have a crucial role in the CDDP mediated hearing loss using p53 KO mice. Indeed, the absence of p53 protects from a severe ABR threshold elevation following a cumulative dose of CDDP of twice 8mg/kg.

Conclusion

These results show for the first time that, in vivo, p53 is potential therapeutic target to prevent CDDP-induced hearing loss.

1044 A Combination of Cilostazol and Ginkgo Biloba Extract Protects Against Cisplatin-Induced Cochleo-Vestibular Dysfunction by Inhibiting the Mitochondrial Apoptotic and ERK Pathways

Chunjie Tian¹, Yeon Ju Kim¹, Seung Won Kim¹, Hye Jin Lim¹, Young Sun Kim¹, Seong Jun Choi², Hun Yi Park¹, Yun-Hoon Choung¹

¹Ajou University School of Medicine, ²College of Medical Science, Konyang University

Background

Cisplatin (CDDP) is an anticancer drug that induces significant hearing loss and balance dysfunction as side effects. Cilostazol (CS) has neuroprotective and antioxidant effects, whereas Ginkgo biloba extract (GbE) has preventive effects on CDDP-induced hearing loss in rats, and GbE enhances the antiatherogenic effect of CS by inhibiting generation of reactive oxygen species (ROS). The purpose of this study was to investigate the effects of renexin (RXN), which contains GbE and CS, against CDDP-induced cochleo-vestibular dysfunction in rats and

to elucidate the mechanism underlying the protective effects of RXN on auditory cells.

Methods

The first study was to identify the optimal Renexin dose against cisplatin-induced ototoxicity using adult male Sprague-Dawley rats (n=21). In the second phase, 57 rats were divided into six groups; cisplatin-only, Renexin+cisplatin, Cilostazol+cisplatin, GbE+cisplatin, vehicle+cisplatin and normal control. Rats were intragastrically treated with Renexin during 7 days for pretreatment and 5 days for posttreatment. Cisplatin in dose of 16mg/kg was treated intraperitoneally just two hours after the 7th time of the otoprotective agents. After the 5-day follow-up, ABR test, tail hanging test, and swimming test were performed for hearing function and vestibular function evaluation, respectively. Cochleas and utricles/sacculi were harvested for morphological evaluation (SEM). In vitro study, the effect of Renexin on cisplatin-induced cytotoxicity was analyzed in the HEI-OC1 cells. The cell viability, apoptosis, reactive oxygen species generation as well as changes in the signal pathway related to apoptosis were investigated by western blot assay.

Results

Rats intraperitoneally injected with CDDP exhibited an increase in hearing threshold and vestibular dysfunction, which agreed with hair cell damage in the Organ of Corti and otoliths. However, these impairments were significantly prevented in a dose-dependent manner by pre- and co-treatment with RXN, and these preventive effects in RXN-treated rats were more prominent than those in GbE-treated rats. In a CDDP pharmacokinetic study, platinum concentration was very similar between CDDP-only treated and RXN+CDDP co-treated rats. RXN markedly attenuated CDDP-induced intracellular ROS and significantly reduced CDDP-activated expression of p-extracellular regulated kinase (ERK), BAX, cytochrome c, cleaved caspase-3, and cleaved poly (ADP-ribose) polymerase but increased BCL-XL expression.

Conclusion

These results show that RXN may have a synergistic effect by strongly protecting hearing and vestibular dysfunction induced by CDDP by inhibiting ROS production, mitochondrial pathways, and the ERK pathway, without interfering with CDDP pharmacokinetics. Therefore, RXN could potentially be used to reduce CDDP-related hearing loss and dizziness.

1045 The Role of Connexin 43 and 26 Hemichannels in Cisplatin-Induced Apoptosis

Yeon Ju Kim¹, Chunjie Tian¹, Seung Won Kim¹, Hye Jin Lim¹, Young Sun Kim¹, Yun-Hoon Choung¹

¹Ajou University School of Medicine

Background

Connexins are assembled into a hemichannel and two identical hemichannels form a gap junction, which play an

important role in K⁺ recycling, metabolic communication in the cochlea. Non-junctional hemichannels can gate open and pass molecules (<1 kDa) by depolarization, extracellular Ca²⁺, oxidative stress, and metabolic inhibition. The purpose of this study was to investigate the role of hemichannel, connexin 43 (Cx43) and 26 (Cx26) in cisplatin-induced apoptotic process using siRNA techniques.

Methods

We constructed recombinant plasmid of pcDNA 3.1 (-)-Cx43, Cx26 and Cx-pcDNA 3.1 (-) plasmid was transfected in Cx-deficient HeLa cells. The formation of functional hemichannels was tested by the transfer of Lucifer yellow (LY, m.w 457.25) from a Ca²⁺ free condition with/without hemichannel blockers (25µM Carbenoxolone; CBX, 25µM 18 alpha-glycyrrhetic acid; 18-AGA). To investigate the mechanism for cisplatin-induced regulation of hemichannels, we analyzed opening of hemichannels under 4 different conditions (Ca²⁺ condition, Ca²⁺ Free condition, Hydrogen peroxide (H₂O₂), potassium chloride (KCl) and cisplatin-induced stress condition).

Results

Cx43 and Cx26 are significantly expressed by transfection of pcDNA 3.1(-)-Cx43, Cx26 in the HeLa cells. LY uptake was observed in Cx43, Cx26-transfected cells, but was absent in Cx-deficient wild type HeLa cells and these uptake was inhibited by both CBX, 18-AGA. Under cisplatin toxicity, hemichannels opened in Cx43, Cx26-transfected cells. Cx-transfected cells significantly responded to Ca²⁺ free condition but little in H₂O₂ or KCl. Live/dead cell assay and western blot assay indicate that cisplatin-induced cell death in Cx43, Cx26-HeLa cells increased (89%, 66%) compared to wild type HeLa cells. CBX, 18-AGA prevented increase of cell death.

Conclusion

The hemichannel Cx 43 and 26 are opened by cisplatin resulting in apoptosis, which may be closely connected with the suppression of Ca²⁺.

1046 Protective Effect of Metformin Against Cisplatin Induced Ototoxicity in Auditory Cell Line

Jiwon Chang¹, Gi Jung Im¹, June Choi¹, Jae Jun Song², Sung Won Chae¹, Hak Hyun Jung¹

¹Korea University College of Medicine, ²Dongguk University Ilsan Hospital

Background

Metformin, an antidiabetic drug with a potent anticancer property, is known to prevent oxidative stress-induced cell death in several cell types through a mechanism dependent on the mitochondria. In the present study, we investigated the influence of metformin on cisplatin ototoxicity in auditory cell line.

Methods

Cell viability was determined by MTT, and oxidative stress and apoptosis were assessed by flow cytometry analysis,

Hoeschst 33258 staining, ROS measurement, and western blotting. Intracellular calcium concentration changes were detected with calcium imaging.

Results

Pretreatment with 100 μ M of metformin prior to application of 20 μ M of cisplatin significantly decreased the late apoptosis in HEI-OC1 cells and also, significantly attenuated the cisplatin-induced increase in reactive oxygen species (ROS). Metformin also inhibited the activation of caspase-3 and the expression of poly-ADP-ribose polymerase. Also, pretreatment with metformin prevented the elevation of intracellular calcium concentration induced by cisplatin. We propose that metformin has protective effects against cisplatin induced ototoxicity by inhibiting the increase of intracellular calcium and preventing apoptosis and ROS production.

Conclusion

This is the first study on auditory hair cells to investigate the protective effects of metformin against cisplatin induced ototoxicity. By using HEI-OC1 cells in calcium imaging, we found that metformin inhibited the increase of intracellular calcium, enhanced the cell viability and prevented ROS production.

1047 NAD Attenuates Mefloquine-Induced Cochlear Damage from Reactive Oxygen Species

Dalian Ding¹, Shinichi Someya², Masaru Tanokura³, Haiyan Jiang¹, Chul Han⁴, Richard Salvi¹

¹University at Buffalo, ²Univerisy of Florida, ³University of Tokyo, ⁴Univesity of Florida

Background

Mefloquine, an anti-malarial drug, is widely used for prophylactic or chemotherapeutic treatment of drug resistant malaria. However, there is growing concern among government agencies about its neurotoxic and ototoxic side effects. Our previous studies demonstrated that mefloquine causes a dose-dependent apoptosis to cochlear hair cells, spiral ganglion neurons and auditory nerve fibers. Nicotinamide adenine dinucleotide (NAD) is a key mediator of important biological processes including energy metabolism, mitochondrial function, calcium homeostasis, and anti-oxidation. Our recent in vitro studies have shown that NAD can protect cochlear hair cells and afferent axons against mefloquine ototoxicity. However, the mechanisms underlying NAD otoprotection are not fully understood. Previous reports indicate that mefloquine increases the production of free radicals leading to cellular damage and apoptosis. These results suggest that the antioxidant properties of NAD may prevent mefloquine-induced cochlear damage.

Methods

We tested this hypothesis by treating cochlear organotypic cultures with mefloquine, NAD or mefloquine plus NAD and measured the resulting cochlear damage and the expression of the superoxide radical in hair cells and neurons using dihydroethidium fluorescence.

Results

When cochlear cultures were treated for 24 h with 35 μ M mefloquine nearly all of the hair cells and auditory nerve fibers in the basal turn were destroyed; however, most hair cells and nerve fibers in apical turn were intact. In contrast, when cochlear cultures were treated for 24 h with 35 mM mefloquine plus 20 mM NAD the auditory nerve fibers throughout the cochlear remained intact. When cochlear cultures were treated for 24 h with 50 μ M mefloquine, all the hair cells and nerve fibers were completely destroyed in both basal and apical turns. However, many of the hair cells and nerve fibers in the basal and apical turn survived if the cultures were treated with 50 μ M mefloquine plus 20 mM NAD. Superoxide expression was assessed 12 h after mefloquine treatment when most cells were still present. Superoxide was heavily expressed in mefloquine treated cochlear explants whereas superoxide was low in cultures treated with NAD alone or mefloquine plus NAD.

Conclusion

NAD suppresses the production of the superoxide radical in mefloquine treated cochlear cultures and provides significant protection against mefloquine ototoxicity.

1048 Lateralization of Traveling Wave Energy in the Hearing Organs of Katydid

Arun Udayashankar¹, Manfred Koessl¹, Manuela Nowotny¹

¹Goethe University

Background

Mathematical models of the curved mammalian cochlea predict that traveling waves propagate along the cochlea by reflection off the lateral walls. Beyond a certain number of reflections, sound waves propagate close to the outer wall analogous to sound waves in whispering galleries due to the cochlea's graded curvature. This results in lateralization of traveling wave energy. Experimental evidence for this has been lacking as in-vivo measurements of traveling wave propagation in the mammalian cochlea are generally restricted to the basal part along one dimension (longitudinal) due to its poor accessibility. In a previous study it was discovered that traveling waves form the physical basis of frequency discrimination in the hearing organ of katydids, the crista acustica (CA) and that their longitudinal (proximal-distal) characteristics are comparable to those measured in mammals.

Methods

Here we studied in detail the radial (anterior-posterior) structure of traveling waves along the CA in-vivo using laser Doppler vibrometry for stimulus frequencies between 9 and 30 kHz.

Results

During their propagation, sound-induced traveling waves along the CA were reflected off the lateral walls. A clear lateralization of traveling wave energy towards the anterior

CA was found. Lateralization of energy had an inverse correlation with radius of curvature. Further, a dynamic rotation of the hearing organ about the longitudinal (proximal-distal) axis was seen during propagation.

Conclusion

Presumably the dynamic rotation and the consequent tilt in the magnitude response generate the input relevant for signal transduction in the auditory sensillum of the CA. Our results are consistent with the predictions made by mathematical models of the curved cochlea. This opens up exciting possibilities of using the CA as a model system to put to test theories of cochlear mechanics.

1049 Two-Tone Suppression Based on Somatic Motility of the Outer Hair Cell with a Cochlear Model

Yasuki Murakami¹, Shunsuke Ishimitsu¹

¹Hiroshima City University

Background

Half a century ago, it was found out that the auditory nerve (AN) firing was suppressed by the other tone. This phenomenon is called two-tone suppression (2TS) and observed in both the basilar membrane (BM) and inner hair cell (IHC). Our interest is mechanisms of the 2TS. However, the mechanisms of the 2TS have been unclear because of technical difficulties. Models can predict the mechanisms of the 2TS. A transmission-line model of the cochlea is much for this problem because of possible to describe internal mechanical and electronically dynamics in the cochlea.

Methods

A transmission-line model of the cochlea containing an outer hair cell (OHC) model was developed in accord with findings about the somatic motility of the OHC. This model was used to investigate how the somatic motility generates the 2TS in the BM.

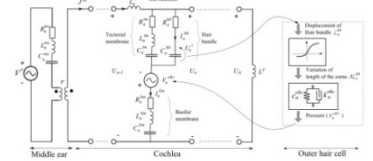
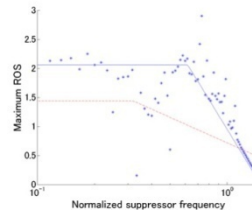
Results

The 2TS produced by the model was comparable with experimental results in the BM and the AN: (1) The maximum magnitude of suppression exceeded 40 dB around the characteristic frequency (CF) equaled to suppressor frequencies, (2) The distribution of maximum rates of suppression (ROS) was highly correlated with compression in the BM, (3) Maximum ROSs were approximately 2.0 dB/dB for low-frequency suppressors and (4) Maximum ROSs were reduced with increasing suppressor frequency near the CF. The third finding conflicts with BM data. However, the model indicated no filtering effect of the IHC. These results further indicate that the mechanisms of 2TS are based on the somatic motility of the OHC.

Conclusion

The basic mechanism of the 2TS appears to be a reduction in the output of the OHC in response to a probe when the variation in length of the OHC changes from

being linear to nonlinear, through an increase in the suppressor level.



1050 Reducing Boundary Reflection in Computational Models of the Cochlea

Samiya Alkhairy^{1,2}, Christopher Shera²

¹MIT, ²EPL - MEEI

Background

Both the efficiency with which cochlear model responses can be computed and the ease of their subsequent interpretation can often be substantially improved if unwanted reflections from the apical end of the cochlea can be reduced or eliminated.

Methods

We describe and compare several different schemes for reducing boundary reflections in box models of the cochlea. In one promising scheme, based on the concept of perfectly matched layers, the box representing the cochlea is supplemented with a thin boundary layer with modified governing equations or parameters and terminated with a boundary condition. The boundary layer is designed to be absorptive so that the solution decays substantially within the layer and no substantial reflections occur due to the boundary condition. The modified boundary layer is chosen to balance the conflicting needs of achieving a high spatial decay rate while avoiding reflections due to the rapid change.

Results

The modified boundary layer framework is applicable to most traveling wave models, and we illustrate it using passive and active 1D transmission-line models of the cochlea solved in the frequency and time domains. We compare the results with those of other methods, including specifying absorptive boundary conditions, such as terminating with the characteristic impedance.

Conclusion

The modified boundary layer method proves effective at reducing boundary reflections in computational cochlear models. The method is particularly appealing because of its simplicity and its extensibility to other cochlear models and simulation schemes.

1051 Two Effects of Viscosity Revealed by Tectorial Membrane Traveling Waves

Jonathan Sellon^{1,2}, Shirin Farrahi^{2,3}, Roozbeh Ghaffari², Dennis Freeman^{2,3}

¹Harvard-MIT Division of Health Sciences and Technology, ²MIT Research Laboratory of Electronics, ³MIT Department of Electrical Engineering and Computer Science

Background

The tectorial membrane (TM) is thought to play a critical role in stimulating hair cells as part of a resonant system (Allen, 1980). A key prediction of such models is that subtectorial space damping plays an important role in determining sharpness of tuning. Recently, however, it has been shown that TM traveling waves (Ghaffari et al., 2007) may contribute to cochlear tuning by longitudinally coupling radial cross sections. Here we test the relationship between viscosity and tuning for TM waves and compare that relation to results for wave and resonance models.

Methods

We measured wave properties of mouse TMs immersed in artificial endolymph solutions with poly-ethylene glycol (PEG) added to increase viscosity. Two PEGs with different molecular weights (MW) were used: one (8 kDa) chosen to penetrate TM pores (Masaki et al., 2006) while the other (400 kDa) could not.

Results

Our findings show that introducing small MW PEG increases TM wave speeds by ~40% and decreases wave decay constants by ~35%. Analysis of a lumped parameter model of the TM showed that these changes in wave parameters can be explained by a change in shear viscosity from 0.2 Pa*s to 0.65 Pa*s with no accompanying change in shear modulus. In contrast, introducing large MW PEG has little effect on wave speed (~2%) or decay (~9%), suggesting shear viscosity inside the TM is significantly more important compared to fluid viscosity.

Conclusion

Our results suggest that fluid surrounding the TM has two separate effects on TM motion. First, increasing fluid viscosity has the obvious effect of increasing drag on the surface of the TM. In addition, if high viscosity fluid penetrates the TM's porous structure then the TM's material properties are also directly affected. Of these two effects, we see that the latter has a much greater impact on TM waves.

Interestingly, these results counter a fundamental assumption in classical cochlear models: that increasing damping would broaden tuning. By contrast, scaling symmetry suggests that the decrease in wave decay constants caused by increased viscosity would sharpen tuning. These results highlight important differences between wave and resonance models of the TM and offer entirely new ways to think about cochlear tuning.

1052 Acoustic Emissions from Coupled Strings

Richard Chadwick¹, Jessica Lamb¹, Daphne Manoussaki²

¹NIDCD, ²Technical University of Crete

Background

Linear mode conversion is a phenomenon that has been studied for several decades and finds application in plasma physics, geophysics, and auditory mechanics. Typically, one propagating wave can excite another at a location where the wavelengths of the different modes become similar and energy can be exchanged. The slowly varying WKB approximation becomes singular at such a mode conversion point. Here we examine a simple mechanical system that illustrates that effect. Of particular interest is the understanding of how a reflection can occur when there are no discontinuities in physical properties. Originally, Rayleigh considered this problem on a single string with smoothly varying mass over a finite transition region. The reflected waves are an analog for stimulated emissions from the ear.

Methods

We consider traveling transverse waves on two identical uniform taut strings that are elastically coupled through springs that gradually decrease their stiffness over a region of finite length. The wave system can be decomposed into two modes: an in-phase mode (+) that is transparent to the coupling springs, and an out-of-phase mode (-) that engages the coupling springs. The system exhibits linear mode conversion whereby an incoming (+) wave is reflected back from the smooth transition both as a propagating (+) wave and an evanescent (-) wave, while both types emerge as propagating forward through the transition. We match a local transition layer expansion to the WKB expansion to obtain estimates of the reflection and transmission coefficients.

Results

The oscillatory behavior of the reflection coefficients with respect to the frequency parameter shows that even this simple system exhibits a stimulated emissions spectrum that is characteristic of the ear. In the present system the frequency spacing of the spectrum originates from the oscillatory nature of the Airy functions. Physically, it is due to the coupling stiffness gradient. In the mammalian ear there are numerous contributions to a decreasing coupling stiffness gradient in the organ of Corti. The increasing length of outer hair cells and their stereocilia from base to apex are an example. In contrast, the coherent reflection theory that Zweig and Shera developed for the ear argues that the incoming wave is scattered by local irregularities of any kind, and then coherently filtered by the incoming wave.

Conclusion

This work was supported by grant DC000033-17 from the Intramural Program of the National Institute of Deafness and Other Communication Disorders.

1053 High Sensitive Inertia Sensor Mimicking Stereocilia Array

Changwon Lee¹, Taegeun Song¹, Kang-Hun Ahn², Sukyung Park¹

¹Mechanical Engineering, Korea Advanced Institute of Science and Technology, ²Department of Physics, Chungnam National University

Background

Stereocilia could achieve high sensitivity over a broad dynamic range by the interplay of adaptation and negative stiffness mechanism, which is the limitation of conventional cantilever-type inertia sensors due to the mass and volume constraint. To overcome the conventional sensor design limitation, in this study, we proposed a high sensitive inertia sensor mimicking hair bundle's amplifying mechanism.

Methods

The proposed sensor consists of 10 sensing units of inverted pendulum array, pairs of magnet, which is controlled by stepping motor along the guide bar that mimics the readjustment of tip link tension by sliding molecular motors. The translation of magnets along the guide bar moves inverted pendulum to lean side way in a gradual manner. When the restoring force of the spring at the pivotal joint exceeds the maximum magnetic repulsive force, an abrupt change of the direction of pendulum lean occurs. Ten magnets on the guide-bar have slight phase differences, depending on the position of the magnet on the guide-bar and a moving direction, which would then induce differences in sensitivity among pendulum arrays. The count of abrupt change of pendulum position is measured by photo detector. To examine the characteristics of the proposed sensor, we measured the force-displacement relation and sensitivity when step and sinusoidal input is applied to the system.

Results

The inverted pendulum unit shows negative stiffness near the origin due to the magnetic repulsive force. The negative stiffness region is shifted when stepping motor moves the magnet on the guide-bar side-to-side. We observed the spontaneous oscillation which was induced by the interplay between the negative stiffness and adaptation mechanism. Experiment results showed that the count of abrupt change of pendulum position was proportional to applied force, implying the proposed biomimetic system could serve as an inertia sensor. Nonlinear compressive sensitivity was observed at the small force input compared to the conventional sensor.

Conclusion

We proposed a biomimetic inertia sensor which overcomes the limited sensitivity issue of conventional engineering sensors. The current system is limited in its range of measurable force due to constraints of the peak oscillation magnitude, which should be further resolved by biomimetic sequential resetting mechanism.

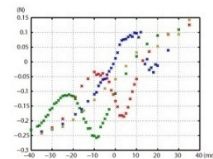


Fig2. Force-displacement curve



Fig1. Inverted Pendulum Unit

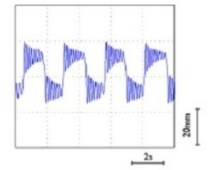


Fig3. Spontaneous oscillation

1054 Simulation of Tuberculoventral Inhibition in the Cochlear Nucleus and Its Role in Enhancing Tone Responses in the Cochlea Through the Olivocochlear Reflex Pathway

Lu-Ming Yu¹, Yi-Wen Liu¹

¹National Tsing Hua University

Background

Wickesberg and Oertel (1988) discovered that tuberculoventral (TUB) cells in the dorsal cochlear nucleus (DCN) provide inhibitory post-synaptic potentials to bushy and multipolar cells in the ventral cochlear nucleus (VCN). The inhibition was found to be delayed and frequency-specific (Wickesberg and Oertel, 1990) and may help achieve echo cancellation.

Methods

In the present work, a computer model is built to simulate the TUB inhibition of T-multipolar (TM) cells. The model allows both TUB and TM cells to be phase-locked to tonal stimuli at sufficiently low frequency. The model has also been integrated with models of the cochlear mechanics (Liu and Neely, 2010), the inner hair cells and the auditory nerves (Meddis 1986; Sumner et al., 2002), and the MOC efferents (Liu et al., 2012), so dynamics of the entire network can be calculated.

Results

Simulation shows that, if the delayed inhibition reaches its maximum strength at time $1/CF$ (characteristic frequency), the inhibition can reduce tone responses in the TM cells but not their noise responses.

Conclusion

Because the TM cells project to medial olivocochlear (MOC) interneurons, the TUB inhibition in the cochlear nucleus may work to enhance the cochlea's response to tones in noise by reducing the MOC reflex strength in a spatially confined manner.

1055 Stereocilia Lipid Membrane: Nonlinear Hair-Bundle Mechanics and Channel Activation

Jichul Kim¹, Peter Pinsky¹, Charles Steele¹, Sunil Puria¹, Anthony Ricci¹

¹Stanford University

Background

The Gating Spring Response, calculated from hair bundle force-displacement measurements, behaves in a non-linear manner. The measurement shows a region of

increased compliance that overlaps with mechanoelectric transduction (MET) channel gating. The presented computational work investigates the potential role of the lipid bilayer at the ciliary tip complex in providing the physical basis of: nonlinear mechanics in bundle activation; MET channel opening; and the correlation between them.

Methods

The first part of the biophysical model describes motion of the bundle by rigid body kinematics implementing pivot motion of a cilium with respect to its base and shear motion between adjacent cilia through the sliding mechanism of horizontal top connectors. The second key part of the model describes the elastic deformation of the lipid bilayer at the tip complex. The continuous lipid membrane of the cilia is partitioned into two regions with functionally distinct properties. The model describes the elastic flexure and stretching of the cap region under the action of the tip link force while accounting for lipid molecule diffusive transport between the cap and body regions. In this model, the body region acts as a lipid reservoir for the cap region and differential molecular diffusivities of these two regions are postulated to be crucial to the membrane tensioning response. Finally, using the lipid bilayer free energy density near the tip-link lower insertion, a Boltzmann function was used to calculate an open probability of the MET channel. With all components coupled, the model is capable of simulating the potential impact of the lipid at the tip complex for the MET channel opening.

Results

There are two key results from the model simulation. First, nonlinear bundle force-displacement can be generated by the lipid membrane tension without correlating contribution from the MET channel. The consistency of the simulation results to the experimental measurements suggests the existence of an isolated tip lipid compartment with a radial size of about 25nm, likely defined by membrane-skeleton-crosslinkers attachment. Second, MET channel can be activated by the free energy generated by the curvature on the tensioned membrane.

Conclusion

The proposed modeling framework demonstrates the plausibility of the lipid bilayer serving as the underlying mechanism responsible for the gating spring. It also indicates that the force transfer through the lipid can provide the gating energy needed to open the MET channel.

[Work supported in part by NIDCD/NIH Grants R01 DC007910 (SP) and DC003896 (AJR).]

1056 Estimation of Added Fluid Mass to Vibrating Cochlear Partition and Its Contribution to the Frequency-Place Relation of Mammalian Cochlea

Yanju Liu¹, Sheryl Gracewski¹, Jong-Hoon Nam^{1,2}

¹Department of Mechanical Engineering, University of Rochester, Rochester, NY, ²Department of Biomedical Engineering, University of Rochester, NY

Background

A pure tone vibration delivered to the oval window travels along the cochlear partition (CP) until it culminates at a location specific to the tone. The traveling wave has been explained with mechanical models represented by a series of spring-mass resonators interacting with the fluid of cochlear ducts. The frequency-dependent peak response locations are primarily determined by the stiffness and mass of the CP. The stiffness gradient of most cochlear models is about 11 dB/octave, which is greater than experimentally measured stiffness gradients (4-9 dB/octave: Naidu & Mountain, 1998; Emadi, Richter et al., 2004). We hypothesized that the added fluid mass of the CP due to its fluid interaction, increases toward the apex so that a broader frequency range can be encoded with a limited stiffness gradient.

Methods

A finite element (FE) model of the CP based on anatomical and mechanical measurement data of gerbil cochlea was used to estimate the mass of the CP. Its static responses were validated against experimental results (Nam & Fettiplace, 2010). From the dynamic response of the FE model without fluid-interaction, we obtained the effective mass of the CP that depends on the geometry and the vibrating mode. In order to evaluate the fluid mass, a Neely's 1D passive cochlear model (1981) was adopted with stiffness and mass of spring-mass resonators obtained from the FE analyses. Due to added fluid mass, the peak resonating frequency at a location was lower than the natural frequency of the CP spring-mass resonator. The fluid mass was obtained from the difference between those two frequencies.

Results

The stiffness of the CP ranged from 760 to 0.3 mN/m per 10 μ m section for 30 to 0.16 kHz frequency range (9 dB/oct). The mass of the CP per 10 μ m section ranged from 30 (base) to 60 ng (apex), while the fluid mass ranged from 5 (base) to 1000 ng (apex). The structural mass was dominant only at the most basal locations (< 2mm from the basal end).

Conclusion

Except at the most basal locations, the effect of added fluid mass is greater than the structural mass of CP which agrees with a previous study (Lim & Steele, 2000) and recent experimental measurement (Dong & Olson, 2009). The stiffness gradient dominates the frequency gradient near the base while fluid mass gradient explains the frequency gradient near the apex.

[Supported by NSF CMMI grant]

1057 Simulations of Two Tone Suppression and Distortion Products in a Physiologically-Based Computational Model of the Cochlea

Julien Meaud¹, Karl Grosh¹

¹University of Michigan

Background

Two tone suppression and distortion products are well known characteristics of the response of the cochlea to two tones. We have recently developed a nonlinear physiologically-based computational model of the cochlea (Biophys J., 2012, 102:1237-1246) and demonstrated that the model reproduces most aspects of the response of the cochlea to a single tone (frequency tuning, compressive nonlinearity, harmonic distortion and DC shift). We extend the previously developed model to the simulation of two tone interactions in cochlear mechanics.

Methods

In the model nonlinear hair bundle mechano-electrical transduction is coupled to outer hair cell somatic electromotility. The structural model includes degrees of freedom for the basilar membrane (BM) and tectorial membrane (TM) with longitudinal coupling and is coupled to a three-dimensional representation of the fluid. The nonlinear model is formulated in the frequency domain and is solved using an iterative alternative frequency-time scheme. The response of the cochlea to two tones is decomposed into carefully chosen harmonic components. Using forward and inverse Fourier transforms, the nonlinearity of the transduction current is introduced in the time-domain while the equations are solved in the frequency domain.

Results

Model simulations of two suppression and distortion products on the BM are compared to experimental data. Simulations reproduce the effect of a suppressor tone on the magnitude and phase of the BM response. The spatial extent of suppression on the BM response is analyzed. For distortion products simulations, the spectrum of the response of the BM to two tones is presented. The dependence of the cubic distortion product on the level and frequencies of the primaries is compared to measurements.

Conclusion

The physiologically-based computational model reproduces many aspects of the nonlinear response of the cochlea to two tones. These simulations support the theory that cochlear amplification is mainly due to somatic electromotility and that cochlear nonlinearity arises from the nonlinearity of hair bundle mechano-electrical transduction.

1058 Carhart's Notch: A Window Into Compressional and Inertial Mechanisms of Bone-Conducted Hearing

Namkeun Kim¹, Charles Steele¹, Sunil Puria¹

¹Stanford University

Background

It is well known that otosclerosis is accompanied by a sensitivity decrease in the 1-2 kHz range for bone-conducted (BC) hearing. This is now clinically referred to as Carhart's notch because of its importance in the clinical assessment of this pathological condition. However, the mechanism for Carhart's notch remains to be poorly understood. We developed a computational framework to address this question.

Methods

A three-dimensional finite element (FE) model of a human middle ear coupled to a cochlea was formulated. The geometry of the middle ear and cochlea, including semicircular canals, was obtained from micro-computed tomography (μ CT) images. In this study, BC hearing was simulated by: (1) applying rigid-body vibrations for the inertial mechanism; and (2) pressure on the outer bony shell to investigate the effects of bone compression mechanism. The stapes annular ligament was stiffened to simulate otosclerosis in the model. The change in hearing by the BC route was calculated by the difference in the maximum basilar membrane (BM) velocity between the normal and the otosclerotic conditions.

Results

Applying only inertia to the FE model caused about 20 dB hearing loss at low frequencies (below 0.5 kHz) which is not consistent with the clinical measurements. The inertia caused 30 dB hearing loss at 1.3 kHz, which decreased to 0 dB as frequency increased to 10 kHz. On the other hand, applying only bone compression caused no hearing loss at all calculated frequencies (0.2 kHz - 10 kHz) such that there was no notch in the 1 - 2 kHz frequency range. Applying both inertia and bone compression stimulation removed the hearing loss at low frequencies (0.2 - 0.3 kHz) returning to normal BC hearing. Applying both conditions also showed a 25 - 35 dB hearing loss in the 1 - 2 frequency range which was qualitatively consistent with clinical measurements.

Conclusion

The compressional mechanism of BC is dominant at 0.5 kHz and below and is unaffected by fixation of the footplate to the bony wall. At frequencies above 2 kHz, the inertial component of BC is dominant. Between 0.5 to 2 kHz, the dominant factor can be either inertia or bone compression depending on the magnitude ratio between two components. The magnitude ratio can differ between individuals due to the different outer bony shell thickness, degree of stapes fixation, or mass of middle-ear ossicles (or fluid in the cochlea).

1059 Directional Inertia at the Base of the Cochlea and Bone-Conduction Hearing

Namkeun Kim¹, Charles Steele¹, Sunil Puria¹

¹Stanford University

Background

For the most part, analytical and numerical models have not demonstrated any functional importance for the coil shape of the cochlea for air-conducted (AC) hearing. We hypothesize that this coiled shape affects the bone-conducted (BC) route of hearing by inertial forces of the middle ear and cochlear fluid which can be tested by stimulation from different directions.

Methods

A three-dimensional finite element (FE) model of a human middle ear coupled to the inner ear was formulated. The geometry of the middle ear and cochlea, including semicircular canals, was obtained from micro-computed tomography (μ CT) images. BC excitations were simulated by applying rigid-body vibrations normal (in the orthogonal direction) to the BM at 0.8 (d^1), 5.8 (d^2), 15.6 (d^3) and 33.1 (d^4) mm from the stapes such that relative motions of the fluid within the cochlea produces excitations of the basilar membrane (BM). A second component of the input comes from the relative motion from the mass inertia of the ossicles.

Results

The vibrational direction normal to the BM surface at the base $d1$ of the cochlea produced the highest BM velocity response across all tested frequencies - higher than an excitation direction normal to the BM surface at the non-basal locations (d^2 - d^4) and their best-frequency (BF). The basal part of the human cochlea features a well-developed hook region, in which the BM undergoes a sudden curvature that produces the largest difference in fluid volume between the scala vestibuli (SV) and scala tympani (ST) not found elsewhere in the cochlea. Due to this sudden curvature, the normal direction to the BM surface in the base differs significantly from the normal directions to the BM along the mid-turns and apical regions of the cochlea. This change caused the most significant anti-symmetric pressure difference than the other direction so that the BM velocity is maximized for the $d1$ location rather than vibrations at the other locations.

Conclusion

The proximity of the hook region to the oval and round windows, combined with it having the biggest fluid volume and impedance difference between the SV and ST, results in maximization of the pressure difference between the SV and ST for BC stimulation perpendicular to the BM in this region, and consequently the resulting BM velocity to be maximized.

1060 A Finite Element "Virtual Labyrinth" Model of the Human Inner Ear Facilitates Electrode Design for a Multichannel Vestibular Prosthesis

Abderrahmane Hedjoudje^{1,2}, Russell Hayden¹, TjenSin Lie¹, Kevin Olds¹, Pei-dong Dai³, Tian-yu Zhang³, Zheng-min Wang³, Ke-qiang Wang³, Kristin Hageman¹, Charles Della Santina¹

¹Johns Hopkins School of Medicine, Baltimore, USA,

²Faculté de Médecine Paris Descartes, Paris, France,

³Fudan University, Shanghai, China

Background

Accurate modeling of prosthetic electrical current flow within the human labyrinth can facilitate optimal design of electrode arrays for a multichannel vestibular prosthesis intended to restore sensation to individuals with bilateral loss of vestibular hair cell function. Our previous research has demonstrated the ability of a finite element and neuromorphic computational model to accurately predict responses to electrical stimulation delivered by vestibular implant electrodes in chinchillas and rhesus monkeys. We extended this approach to human anatomy to create a virtual labyrinth model of the human vestibular system.

Methods

Model geometry was developed in Amira® from the Fudan University Virtual Temporal Bone Data, a 3-dimensional (3D) reconstruction of a human specimen serially sectioned at 50 μ m. Electrodes were virtually positioned within the model volume to test hypotheses regarding dependence of neural responses on electrode location, stimulus current and insulating materials displacing inner ear fluids. Finite element analysis (Comsol Multiphysics®) computed the extracellular potential field time course during current pulses from any constellation of electrodes. Extracellular potential waveforms then served as inputs to stochastic, nonlinear dynamic models for 2,415 vestibular afferent axons with spiking dynamics based on a modified Smith and Goldberg model incorporating parameters that varied with fiber location in each endorgan. Action potential propagation was implemented by a well validated model of myelinated fibers. 3D eye rotation axes were predicted from the relative proportion of model axons excited within each of the three ampullary nerves.

Results

Consistent with model predictions in rodents and nonhuman primates (in which measured 3D vestibulo-ocular reflex [VOR] responses were well-predicted by model output), the magnitude and direction of predicted 3D VOR responses depend heavily on electrode proximity to cristae (changing significantly for displacements on the order of 100 μ m), return electrode location, and the presence of insulating material (such as fat or silicone) displacing perilymph and/or endolymph. Current spread and the degree of spurious activation of nontarget afferents was similar to that observed in simulations and empiric data for rhesus monkeys.

Conclusion

Although model validation must await empiric 3D VOR and electrophysiologic measurements in humans implanted with multichannel vestibular prostheses, the success of analogous models for rodents and monkeys suggests the Virtual Human Labyrinth can facilitate optimal design of electrode arrays intended for human implantation.

1061 In Vitro Culture of Adult Mouse Cochlea

Wenyan Li^{1,2}, Yilai Shu^{1,2}, Marco Petrillo¹, Zhengmin Wang², Huawei Li², Zheng-Yi Chen¹

¹Eaton-Peabody Laboratory, Massachusetts Eye and Ear Infirmary, Harvard Medical School, ²Eye Ear Nose and Throat Hospital of Shanghai medical school, Fudan University

Background

Study of mammalian inner ear for hair cell regeneration, biophysics, genetic deafness and drug screening has been greatly hampered by the lack of a system that enables the culture of adult cochlea in vitro. In standard culture condition, adult mammalian cochleae rapidly lose all hair cells, with the degeneration of overall structure of sensory epithelium, leading to downregulation of supporting cell gene expression, further loss of supporting cells, and overgrowth of fibroblasts.

Methods

Here we developed a protocol with which the integrity of cultured adult mouse cochlea can be maintained in vitro. With the protocol, a relatively intact adult cochlear sensory epithelium structure could be preserved for 10-14 days in vitro.

Results

Supporting cells in culture were well organized with a distinct cellular pattern similar to that in vivo. Supporting cells were labeled with multiple specific makers, supporting that the identity of supporting cells was maintained. Many inner hair cells, especially those in the apex, survived while outer hair cells were lost during culture. In contrast to traditional attachment culture system, there was a minimum contamination from other cell types including fibroblasts within the sensory epithelium. When infected by adenovirus carrying a GFP reporter, the infected supporting cells and inner hair cells started to express GFP, which could be observed two days after infection, with the expression maintained for 1 to 2 weeks. While outer hair cells were rapidly lost within 12 hours in normal culture, the death of outer hair cells can be substantially delayed by blocking necrosis pathway.

Conclusion

Our in vitro culture system thus provides a new tool to investigate the adult mammalian cochlea through genetic manipulation and pharmacological interference.

1062 Hypotonic Condition Induces Hearing Impairment in TRPV4 Knock-Out Mice

Kohei Kawamoto¹, Narinobu Harada², Nobuo Kubo¹, Makoto Suzuki³, Koichi Tomoda¹

¹Kansai Medical University, ²Harada Ear Institute, ³Jichi Medical School

Background

Changes of osmolality in the inner ear fluids have been considered to cause some clinical disorders such as tinnitus, fluctuating hearing loss, and Meiniere's disease. Transient receptor potential vanilloid 4 (TRPV4) has been recently proposed as an osmo- and mechanosensitive channel and reported to be involved in cellular volume regulation and affect cellular function. In the cochlea, TRPV4 was confirmed to express in the outer hair cells, inner hair cells as well as spiral ganglion cells. To investigate the influence of osmotic pressure on cochlear function, we investigated whether the hypotonic condition in the inner ear fluids causes hearing impairment in TRPV4 knock-out mice.

Methods

Hypotonic solution was introduced into the inner ear of mouse through the left side of posterior semicircular canal by an osmotic mini-pump (Alzet®: 1003D). Wild type (C57BL/6) and TRPV4 knock-out (KO) mice were implanted with the pump and cannula for delivery of artificial perilymph (300 ± 2mOsm) or hypotonic saline (150 ± 2mOsm) continuously for 3days. Auditory brainstem responses (ABRs) were measured on day0, day3 and day7 after the surgery at the pump-implanted side. Both sides of cochleae were removed at day7, and then processed for further histological assessment.

Results

At day7, mice implanted pump with artificial perilymph showed less than 10dB threshold shifts at all frequencies. Wild type mice showed statistically significant smaller ABR threshold shifts compared to KO mice at all frequencies 7 days after the implantation of pump with hypotonic solution. The non-pump-implanted (contralateral) side showed significant higher OHC survival rate than the pump with hypotonic solution implanted (experimental) side in KO mice at day7. On the other hand, difference of the IHC survival rate was not significant.

Conclusion

Hypotonic condition induced hearing impairment in TRPV4 knock-out mice which was statistically significant compared to that of the wild type mice. It indicates that TRPV4 might be involved in hearing impairment by changing of osmolality in the inner ear fluids. Any disturbance in the homeostasis of inner ear fluids may thus affects the functional properties of OHCs via TRPV4, thereby causing some hearing impairment.

1063 Auditory System in Knock-In Mouse Models of Pendred Syndrome

Shin Koyama¹, Yasuhiro Ikehara¹, Michio Murakoshi¹, Sigenari Hashimoto², Shinya Nishio², Yutaka Takumi², Shin-ichi Usami², Hiroshi Wada¹
¹Tohoku University, ²Shinsyu University

Background

Among all persons with congenital hearing loss, 4~10% are cases of Pendred syndrome (Morton and Nance, 2006), which is an autosomal recessive disorder. This syndrome is caused by mutations in the pendrin gene. Mutations in pendrin also cause nonsyndromic hearing loss (Usami et al., 1999). Pendrin is a membrane protein and expressed in the inner ear. In the inner ear, pendrin is involved in the conditioning of the ion concentration of the endolymph. Generally, membrane proteins are transported to the plasma membrane; however, some protein mutants are retained in the cytoplasm. In the case of pendrin mutants, the amount of pendrin that localizes on the plasma membrane is low, and the ion concentration of the inner ear is abnormal. So far, no effective therapy for hearing loss caused by these mutations has been established. In this study, to clarify the mechanisms of the Pendred syndrome or nonsyndromic hearing loss caused by the H723R pendrin mutant, which is a major cause of sensorineural hearing loss among Japanese, and to find a curative method for hearing loss in humans, a knock-in mouse model with H723R pendrin mutant was developed as a first step.

Methods

Two strains of knock-in mice, namely, mice carrying the knock-in point mutation of H723R pendrin (murine-type knock-in mice) and mice in which the mouse pendrin was replaced by the human H723R pendrin mutation (human-type knock-in mice) were generated using a recombineering approach. The hearing ability of these mice was assessed using the ABR test.

Results

In this study, the hearing of thirty-three murine-type knock-in mice was assessed. Twenty-one of them had hearing thresholds of less than 40 dB SPL (Fig. 1) and twelve showed mild to moderately severe hearing loss (hearing thresholds of 40~70 dB SPL) at various ages of onset (Fig. 2). All human-type knock-in mice at the age of 4 weeks had a profound hearing loss (> 90 dB SPL).

Conclusion

It is suggested that the murine-type knock-in mouse model may be comparable to cases of human patients since various shift patterns of hearing among patients with mutations in the pendred gene have been reported (Napiontek et al., 2004). There is a possibility that hearing loss of the mice with early onset was caused by H723R mutation in the pendred gene. Human-type knock-in mice had profound hearing loss. This result is comparable to studies on knock-out mouse models (Wangemann et al., 2007).

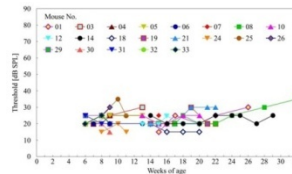


Fig. 1. Changes in hearing thresholds of knock-in mice which showed no abnormalities. ABR measurements were taken at various weeks of age.

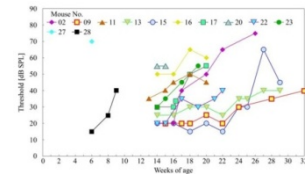


Fig. 2. Changes in hearing thresholds of knock-in mice which showed hearing impairment. ABR measurements were taken at various weeks of age.

1064 Optimizing a 2f1-f2 DPOAE Measurement for Extended High Frequencies

Gayla L. Poling¹, Sumaya Sidique¹, Tracey Moskatel¹, Claire Beers¹, Daniela Wijnperle¹, Jungwha Lee², Jonathan H. Siegel¹, Jungmee Lee¹, Sumitrajit Dhar¹
¹Hugh Knowles Center, Roxelyn & Richard Pepper Dept. of CSD, Northwestern University, ²Feinberg School of Medicine, Dept. of Prev. Med., Northwestern University

Background

Given the variation in cochlear mechanics from base to apex, it is not surprising that different stimulus conditions are necessary to generate the most robust distortion at different frequencies. Specifically, sharper tuning (due to reduced spread of excitation) would dictate that narrower frequency ratios between the stimulus tones (f_1 and f_2 , $f_2 > f_1$) used to elicit $2f_1$ - f_2 DPOAEs would be necessary to produce optimal overlap between mechanical excitation patterns. Typically, the stimulus parameters that elicit the most robust DPOAEs up to ~8 kHz in normal-hearing ears are used in clinical applications (Gorga et al. 1997). Commonly used (standard) parameters include $f_2/f_1=1.22$ and stimulus levels of 65/55 dB SPL. However, Dreisbach and Siegel (2001) have shown the optimal frequency ratio ($f_2/f_1=1.22$ at 1 kHz) decreases with increasing frequency (~1.16 at 10 kHz). Additionally, DPOAEs are most sensitive to hearing loss when recorded using low or moderate stimulus levels; however, DPOAEs are more difficult to obtain at higher frequencies using these levels. Taken together, this body of evidence suggests that stimulus parameters used routinely at frequencies <8 kHz are suboptimal for measurements at higher frequencies. This study aimed to optimize DPOAE measurements up to 20 kHz using stimulus parameters chosen to account for underlying variations in the mechanical properties over the length of the cochlea to further enhance our ability to detect cochlear damage.

Methods

Accurate and stable measurements of DPOAE amplitudes using custom hardware and calibration procedures for swept- (up to 16 kHz; $n=15$) and discrete-frequency (up to 20 kHz in ~1/8-octave steps; $n=15$) stimuli were obtained in normal-hearing individuals. An innovative test paradigm, comprising three fixed-level combinations and varying f_2/f_1 ratios in comparison to a "standard" protocol and/or a "fixed" ratio protocol was evaluated.

Results

Larger DPOAEs were measured with narrower frequency ratios than the standard ($f_2/f_1=1.22$) at frequencies ≥ 6 kHz in normal-hearing ears. Increasing stimulus level elicited larger DPOAEs (most notably at higher

frequencies). Evaluation in 15 ears with hearing loss revealed no compromise to the sensitivity of DPOAEs as a screener for mild hearing loss.

Conclusion

Preliminary results support the hypothesis that using stimulus conditions optimized for variations in presumed underlying cochlear mechanics are needed to elicit robust DPOAEs at higher frequencies. Further evaluation is needed to explore whether DPOAE test performance improves when optimal stimuli are utilized.

1065 Investigating Stimulus-Frequency Otoacoustic Emissions and Threshold Fine Structure at High Frequencies

James Dewey¹, Sumitrajit Dhar¹

¹Northwestern University, Evanston, IL

Background

When the inner ear is stimulated by a tone, energy at the stimulus frequency propagates back out to the ear canal via mechanisms that depend on active cochlear processes. These stimulus-frequency otoacoustic emissions (SFOAEs) can be extracted from the ear canal signal using techniques that exploit cochlear nonlinearity. Additional evidence for backwards-propagating energy within the cochlea can be found in the quasiperiodic fluctuations in hearing sensitivity, termed threshold fine structure. This fine structure pattern is thought to arise from standing waves produced by multiple reflections of energy between the middle-ear boundary and the site of SFOAE generation. The high frequency limits of the mechanisms underlying SFOAE generation and threshold fine structure have not been thoroughly explored; here we report both acoustic and behavioral evidence for these mechanisms extending beyond 8 kHz.

Methods

Behavioral hearing thresholds and SFOAEs were obtained from adult participants in an exploratory fashion. Pure-tone detection thresholds for frequencies between .125 and 20 kHz were measured using a modified Bekesy tracking procedure, with frequency steps ranging from 1 to 1/100th of an octave. SFOAEs were evoked by both swept and discrete tones for probe frequencies between .4 and 18 kHz, and extracted from the ear canal pressure via either the compression or suppression method. Stimuli were calibrated using a method that compensated for the depth of probe insertion in the ear canal. Spontaneous OAEs were identified via spectral averaging of the ear canal signal obtained without stimulation.

Results

Threshold fine structure was observed at frequencies that approached the start of the steeply sloping high-frequency portion of the audiogram, which typically ranged from 11-14 kHz, even in an ear with a broad mid-frequency region of elevated thresholds. The depth of the high-frequency fine structure was often comparable to that found at lower frequencies (~10 dB). Robust high-frequency SFOAEs were also measurable in some ears when elicited by

discrete tones, with amplitudes peaking around 10-13 kHz, and reliable phase gradients measurable up to ~15 kHz. Swept-tone SFOAE measurements above 10-12 kHz were complicated by excessive variability in the pressure at the probe frequency, most likely due to small changes in probe position across stimulus repetitions.

Conclusion

The mechanisms underlying SFOAE generation and threshold fine structure extend to the highest frequency regions of sensitive hearing. Further work is needed to determine precisely how SFOAE amplitudes are related to fluctuations in threshold.

1066 Latency of Tone-Burst-Evoked Auditory Brainstem Responses and Otoacoustic Emissions: Level, Frequency, and Rise-Time Effects

Daniel Rasetshwane¹, Michael Argenyi^{1,2}, Stephen Neely¹, Judy Kopun¹, Michael Gorga¹

¹Boys Town National Research Hospital, ²Boston University, School of Social Work

Background

Auditory brainstem responses (ABRs) and otoacoustic emissions (OAEs) are two physiological measures that have been used to indirectly estimate basilar membrane (BM) delays. Simultaneous measurement of ABRs and OAEs may provide insights into effects of level, frequency and stimulus rise time on BM delay.

Methods

Tone-burst-evoked ABRs and OAEs (TBOAE) were measured simultaneously in 46 normal-hearing human subjects. Total data-collection time was 620 hours. Stimuli included a wide range of frequencies (0.5 to 8 kHz, 1/2-octave steps) and levels (20 to 90 dB SPL, 10-dB steps). Multiple tone-burst rise times at each frequency allowed characterization of the dependence of latency on rise time. ABR latencies were estimated by three judges and averaged. TBOAE latencies were estimated as the group delay of the OAE waveform. In an effort to facilitate comparisons between ABR and TBOAE latencies, the level-dependent component of ABR latency (i.e., forward latency) was derived by subtracting level-independent estimates of synaptic and neural delays (5 ms) from wave-V latency.

Results

ABR latencies showed the same orderly frequency and level dependence as previously reported [Gorga et al., *J. Speech Hear. Res.* 31, 87-97 (1988)]. The level-dependence of TBOAE latencies was similar to that of ABR latencies across all frequencies, although the TBOAE latencies were more variable by a factor of five. Additionally, the frequency dependence of TBOAE latencies was similar to ABR latencies only for mid-frequencies. Rise time also had a significant effect on ABR latency, but this effect was independent of its level dependence. Comparison between simultaneously-measured ABR and TBOAE latencies showed that TBOAE

latency is about twice ABR forward latency for frequencies above 1.5 kHz, but the two latency estimates were roughly equal for lower frequencies.

Conclusion

The level dependence of ABR latency must be either mechanical or neural, whereas TBOAE latency is determined by cochlear mechanics. Thus, the similarity at all frequencies of the level dependence of ABR latency to that of OAE latency supports the view that most of this level dependence is due to cochlear mechanics. This view is further supported (1) by independence of level and rise-time effects and (2) by similarity of frequency dependence at mid-frequencies. [Work supported by the NIH R01 DC2251 and P30 DC4662].

1067 Towards a Clinical Test for the Medial-Olivocochlear Reflex (MOCR)

Lynne Marshall¹, Judi Lapsley Miller¹, Charlotte Reed²

¹Naval Submarine Medical Research Laboratory,

²Research Laboratory of Electronics, MIT

Background

A clinical test for the medial-olivocochlear reflex (MOCR) must be fast, reliable, valid, and the MOCR strength measured by the test must vary widely in the population. Such a test must also be as free as possible from confounds, such as multiple OAE components, middle-ear muscle reflexes (MEMR), negative middle-ear pressure, and spontaneous OAEs.

Methods

In a series of experiments, we have developed and evaluated (and continue to refine) three OAE-based MOCR tests based on transient-evoked OAEs (TEOAEs), stimulus-frequency OAEs (SFOAEs), and most recently swept-frequency OAEs (SWOAEs). All three measure the reflection-component OAE that is more sensitive to the MOCR.

Results

Our SFOAE and TEOAE-based tests take around 3 minutes per ear to run, with repeated testing needed to assure stability. Avoiding the MEMR is nigh-on impossible in many ears - it is both difficult to reliably measure in many ears and its magnitude is often at the same level as the raw MOCR effect. But for SFOAE and SWOAE tests we can show which measurements are affected by this confound.

Conclusion

All methods have their pros and cons, with SWOAEs showing the most potential, but needing more development.

1068 Binaural Measurements of Otoacoustic Emissions in Humans

Katharina Jäger¹, Manfred Kössl¹

¹Goethe University

Background

The efferent system has been shown to be involved in the protection of the cochlea against acoustic trauma and the facilitation of signal detection from background noise, but the precise function is still controversial. Due to the fact that the efferent fibers innervate the outer hair cells (OHCs), otoacoustic emission (OAE) measurements are a suitable tool to assess efferent function. Especially distortion-product OAEs (DPOAEs), which are evoked by two-tone stimuli are often used to study cochlear mechanics. Two types of DPOAEs are distinguishable, the cubic distortion tone ($2f_1-f_2$) and the quadratic distortion tone (f_2-f_1). The present project investigates efferent effects on cubic and quadratic DPOAEs under binaural stimulation using the same two-tone stimuli in both ears, which should produce a natural hearing impression.

Methods

Thirteen subjects participated in two measurement series. OAEs were recorded using two identical Etymotic ER-10C probe systems. Part I: Level-growth-functions in the level range of 10 to 70 dB SPL were measured at 6, 4, 2 and 1 kHz during binaural and monaural two-tone stimulation to evoke cubic DPOAEs. The f_2/f_1 ratio was adjusted to 1.2. The measurements were repeated with levels up to 80 dB SPL at 6 and 4 kHz with the individual optimal ratio to evoke quadratic DPOAEs. Part II: The recordings on the cubic and quadratic emissions were repeated with repetitive amplitude-modulated two-tone complexes.

Results

Three types of efferent effects occurred in the subjects. (i) Level-dependent suppression in one ear versus enhancement of DPOAE levels in the other ear, resulting in a strong lateralization. (ii) Level-dependent suppression or enhancement in both ears and (iii) effects at DPOAE level maxima or minima. In some cases, only one ear showed suppression and the other ear was not affected by binaural stimulation. The type of effect could change when instead of pure tone stimuli amplitude-modulated pure tones were used. The effects were independent of the stimulus frequency, but highly level-dependent, with largest changes of up to 4-6 dB in the low-level stimulus ranges. The effects on the quadratic emissions were less stable than the ones on the cubic emissions, but had the same magnitude.

Conclusion

The results indicate a different processing of pure tone and amplitude-modulated sound signals already at the level of the cochlea, which may be mediated by a shift in the OHC's operating point.

1069 Estimates of Human Cochlear Tuning Derived from DPOAE Reflection-Component Delays

Carolina Abdala^{1,2}, François Guérit³, Ping Luo¹, Christopher A. Shera^{4,5}

¹House Research Institute, ²University of Southern California, ³Technical University of Denmark, ⁴Eaton-Peabody Laboratories, ⁵Harvard Medical School

Background

Past work has shown a consistent relationship between reflection emission phase-gradient delay and cochlear tuning in a variety of mammalian species, as predicted by filter theory and models of otoacoustic emission (OAE) generation (Shera et al., 2010). Here, we exploit this relationship and explore methods of estimating delay trends, with the long-term aim of studying cochlear tuning throughout the human lifespan.

Methods

The 2f₁-f₂ DPOAE was recorded with pure tones (L₁, L₂ = 65, 55 dB SPL; f₂/f₁ = 1.22) swept at 8 s/oct in 186 subjects from prematurely born neonates to elderly adults. DPOAEs were measured from 0.5–4 kHz in all groups and extended to 8 kHz in young adults. DPOAE reflection components were separated via inverse FFT and their phase-gradient delays calculated and expressed in periods. Following parametric study to optimize variables, trend lines were fit to group data using two strategies: energy-weighted loess and a loess fit to segments at amplitude peaks only. A mean trend combining both approaches was also computed. Tuning ratios derived from measurements in non-human mammals and shown to be species invariant were applied to the human data to generate measures of filter bandwidth.

Results

The phase-gradient delay versus frequency function shows a typical bend (putative apical-basal transition) between 0.8 and 1.2 kHz, consistent with past OAE work. Q_{erb} estimates from young adults roughly match those obtained from SFOAEs and ranged between 10–15 for frequencies below 4 kHz, increasing to approximately 17–18 for higher frequencies. The infant groups tend to show sharper tuning than the adult subjects over much of the frequency range. The middle-aged and elderly groups manifest greater variability in Q_{erb} across frequency, including a slight decrease at the highest frequency tested.

Conclusion

DPOAE reflection components can provide reliable estimates of delay and tuning. The match with SFOAE-based tuning estimates is imperfect for predictable reasons: a) The strength of the probe generating reflection at 2f₁-f₂ is not controlled in the DPOAE paradigm and undoubtedly varies among individuals, increasing the variance of the tuning estimates; b) F₁ in the DPOAE paradigm produces suppression at the DP place (Kalluri and Shera, 2001), influencing reflection generation. Despite these caveats, the Q_{erb} values derived here approximate those reported by Shera and colleagues

(2010) in humans and represent a first step towards quantifying the maturation and aging of human cochlear tuning.

1070 Aging of the Medial Olivocochlear Reflex: Associations with Speech Perception in Noise

Carolina Abdala^{1,2}, Sumitrajit Dhar³, Mahnaz Ahmadi¹

¹House Research Institute, ²University of Southern California, ³Northwestern University

Background

The medial olivocochlear reflex (MOC) has modulatory effects on cochlear mechanics, typically producing inhibition by hyperpolarizing outer hair cells. Otoacoustic emissions (OAEs) can gauge this reflex. Little is known about how MOC effects change throughout the human lifespan. Here, we studied aging effects on the MOC reflex using an expanded repertoire of indices while considering the effects of MOC activation on both the 2f₁-f₂ distortion product OAE and on its dual components. Also, we preliminarily examine the links between age-related changes in medial efferent effects and speech perception in noise.

Methods

DPOAEs were recorded with pure tones (L₁, L₂ = 65, 55 dB SPL; f₂/f₁ = 1.22) swept at 8 s/oct in 116 subjects, with and without contralateral acoustic stimulation (CAS) to activate the MOC reflex. Age groups included teens and young, middle-aged and elderly adults. The MOC reflex was calculated as the vector difference between baseline and +CAS conditions at fine structure peaks only, to minimize the effects of component interference. Additionally, the DPOAE was separated into distortion and reflection components via inverse FFT and the effects of CAS on the amplitude and phase of each were calculated. The middle ear muscle reflex (MEMR) was monitored during testing. Speech perception was assessed under headphones using a variety of speech tokens, for a range of signal-to-noise ratios.

Results

CAS presented at 60 dB SPL produced a reduced contralateral MOC reflex in middle-aged subjects compared to teens and young adults. In general, MOC activation reduced emission magnitude most strongly at low frequencies and tended to produce shallower reflection-component phase slope. Unexpectedly, the elderly group showed the largest reductions in emission level, and over half of these subjects also showed a pronounced increase in DPOAE fine structure when contralateral noise was presented, most notably at 65 and 70 dB SPL. Links between these findings and speech perception in noise are currently being probed.

Conclusion

By middle age, the medial efferent reflex is weakened; however, the oldest subjects show seemingly incongruous effects of MOC activation. Both observations in the elderly—stronger MOC reflexes and increases in DPOAE fine

structure- might be explained by unintended activation of the MEMR during presentation of the contralateral noise elicitor. Middle ear muscle contractions could increase multiple internal reflections, producing the pronounced fine structure noted here; they might also increase the size of the MOC reflex by reducing DPOAE levels during reverse transmission.

1071 The Half-Octave Shift Revisited: Evidence from Middle-Ear Power Transmittance and Stimulus Frequency Otoacoustic Emissions in Humans

Shaum Bhagat¹, Chelsea Kilgore¹

¹University of Memphis

Background

Following exposure to an intense tone, the largest temporary otoacoustic emission level shift (TES) occurs approximately one-half octave above the exposure frequency. Variation in TES between individuals may be partially explained by individual differences in middle-ear sound transmission. The aim of this study was to examine the contribution of middle-ear sound transmission to measured amounts of TES.

Methods

Pre-exposure measurements of middle-ear power transmittance (MEPT) and stimulus frequency otoacoustic emissions (SFOAE) at 1.4 and 2.0 kHz were obtained from normal-hearing adults. SFOAE levels were derived from probe alone and probe plus suppressor conditions. SFOAE measurements were repeated as a check of test/retest reliability. Following a 1-minute exposure to a 105 dB SPL tone at 1.4 kHz, SFOAE measurements at 1.4 and 2.0 kHz were completed at 2 and 4 minutes after the exposure. Shifts in SFOAE levels at 2 minutes (TES₂) and 4 minutes (TES₄) were calculated.

Results

The mean SFOAE test/retest reliability was within 1 dB at both 1.4 and 2.0 kHz. The mean amount of TES was greater than one standard deviation above the mean value of test-retest reliability only at 2.0 kHz. The amount of TES₂ and TES₄ was similar at both test frequencies. Trends in the data indicated that MEPT was related to the amount of TES. Individuals with higher MEPT values at 1.4 and 2.0 kHz tended to have larger TES₄ at 2.0 kHz, while individuals with lower MEPT values tended to have smaller TES₄ at 2.0 kHz.

Conclusion

The results of this study are consistent with previous research indicating the maximum effect of tonal overexposure occurs one-half octave above the exposure frequency. For SFOAEs, the amount of TES₄ appears to be related to a) MEPT at the exposure frequency and b) MEPT at one-half octave above the exposure frequency. These findings suggest that MEPT of intense sound may play a role in explaining some of the variability seen in the amount of TES across individuals. Exploration of the role of MEPT in temporary threshold shift is warranted.

1072 Otoacoustic-Emission Detection When the Middle Ear Contains Amniotic Fluid: A Chinchilla Animal Model

Olubunmi Akinpelu¹, Robert Funnell¹, Sam Daniel¹

¹McGill University

Background

Otoacoustic emissions (OAE) have frequently been used for newborn hearing screening. However, OAE screening tests have a low specificity and have referral rates higher than recommended by the Joint Committee on Infant Hearing. The presence of residual amniotic fluid in the middle ear is one of the reasons for these problems. The aim of this study was to determine the effects of human amniotic fluid on distortion product OAEs and noise levels across various frequencies. The effects of normal saline were also studied in order to investigate the role of viscosity.

Methods

Forty-six adult female chinchillas with normal Preyer's reflex were used. The animals were initially screened using auditory brainstem responses and tympanometry. Only animals with normal hearing and middle-ear status were included. They were randomly divided into 8 groups based on the type (amniotic fluid or saline) and volume (0.5, 1, 1.5, 2 ml) of liquid introduced into the middle ear. OAE measurements were taken at the Montréal Children's Hospital using a SmartOAE system (Intelligent Hearing Systems) under inhalational anaesthesia. After an initial OAE measurement, liquid was introduced into the middle ear by trans-bullar injection and then a second OAE measurement was made.

Results

Both the type and the volume of liquid made a difference in both the OAE amplitudes and the noise level. Significant reductions of OAE amplitudes occurred across all frequencies, with more reduction for greater volumes. Changes in the noise level had important effects on the signal-to-noise ratio at some frequencies.

Conclusion

Both human amniotic fluid and saline in the middle ear of a chinchilla animal model resulted in changes in OAE detection patterns that may be relevant to newborn hearing screening with OAEs.

1073 Exploring Stimulus Conditions for Measurement of the Quadratic F2-F1 Distortion Product Otoacoustic Emission

Rachael Baiduc¹, Sumitrajit Dhar¹

¹Northwestern University

Background

Measurement of distortion product otoacoustic emissions (DPOAEs) aids in diagnosis of sensorineural hearing loss. Clinically, the cubic DPOAE 2f1-f2 is most commonly employed. However, quadratic DPOAEs (e.g., f2-f1) may also be sensitive to outer hair cell physiology. The clinical

utility of DPOAEs may increase if f2-f1 can be used to pinpoint subtle cochleopathies, including those that result from stria vascularis damage. Previous work by Bian and Chen (2008) suggests optimal stimulus parameters for f2-f1 differ from those used to elicit robust 2f1-f2 DPOAEs for an f2 of 4 kHz. Here, we explore the optimal f2/f1 ratio for eliciting f2-f1 over a wide frequency range in normal hearing and hearing impaired adults.

Methods

Fifteen young adults (18-30 years) with clinically normal hearing (0.25-8 kHz) in at least one ear participated in this study. In addition, a small cohort of subjects with hearing loss were also examined. The DPOAE at f2-f1 was tested at six f2/f1 ratios (1.14, 1.18, 1.22, 1.30, 1.32, and 1.36) for f2 frequencies ranging from ~660-19,220 Hz. Sweep tones (L1,L2=70 dB SPL) were used to elicit emissions. In addition, behavioral hearing thresholds were obtained from 125-20,000 Hz in the test ear. DPOAE data were averaged in 1/3-octave bins to assess the effect of f2/f1 ratio on f2-f1 amplitude across frequency. The influence of high frequency hearing thresholds on f2-f1 amplitude was also explored.

Results

In contrast to previous reports (Bian and Chen, 2008), these data revealed that f2/f1 ratio was not highly influential in determining f2-f1 level. Although wider ratios did occasionally produce more robust emissions in individual subjects, mean data do not support a ratio or frequency-dependent trend. In some subjects, prominent 2f1-f2 DPOAEs could be measured while little, if any, f2-f1 could be recorded. Conversely, f2-f1 was more robust than 2f1-f2 in some individuals. Hearing impaired subjects demonstrated reduced f2-f1 compared to the normal hearing group.

Conclusion

The f2/f1 ratio did not have a significant impact on mean f2-f1 emission amplitude, with the exception of some individual differences. These preliminary results suggest that the DPOAE at f2-f1 may provide information about cochlear health that is complementary to that obtained from the 2f1-f2 DPOAE.

1074 Estimating Cochlear Frequency Selectivity with Stimulus-Frequency Otoacoustic Emissions

Karolina Charaziak¹, Jonathan Siegel¹

¹Hugh Knowles Center, Roxelyn and Richard Pepper Dept. of Comm. Sci. and Disord, Northwestern Univ.

Background

Each point along the basilar membrane of the cochlea is tuned to a specific frequency. At low stimulation levels this mechanical filtering is sharpened due to action of the outer hair cells (OHC). It has been suggested that the tuning of the cochlear filters can be derived from measures of otoacoustic emissions – byproducts of OHC action. Two approaches have been proposed for estimating cochlear frequency selectivity using single frequency OAEs

(stimulus-frequency OAEs), based on (a) SFOAE group delays (GDs) and (b) SFOAE suppression tuning curves (STCs). We aim to compare these estimates of frequency selectivity with more direct measurements of cochlear tuning – compound action potential tuning curves (CAP TCs) – obtained in the same animal.

Methods

Twelve chinchillas served as experimental subjects. The CAP and SFOAE STC data were obtained at up to four probe frequencies (1, 4, 8, and 12 kHz). SFOAE STCs were measured as iso-response curves where the level of a suppressor tone is adjusted until a predefined change in ear canal pressure at the probe frequency is recorded. An analogous paradigm was used for CAP TC measurements. The SFOAE GDs were measured using the suppression method for probe frequencies ranging from 0.3 to 12 kHz. The SFOAE data were collected at probe levels of 30 – 40 dB SPL and CAP data for tone-burst levels resulting in a clear response above the noise floor (25 – 60 dB SPL). Q10 values were calculated for all tuning measures.

Results

On average there was good agreement between Q10 derived from SFOAE STCs and CAP TCs at all frequencies except 1 kHz, where emission tuning curves were considerably broader. Q10 derived from SFOAE GD were in good agreement with CAP data at 1 and 12 kHz while for mid frequencies SFOAE GD indicated sharper tuning. When compared to published Q10s for auditory nerve (AN) TCs, CAP TC and SFOAE STC seemed to underestimate sharpness of tuning, while the opposite trend was observed for SFOAE GD Q10s. When individual data were analyzed there was no clear one-to-one positive relationship between Q10s derived with any pair of the three methods.

Conclusion

Although, on average, the sharpness of tuning derived with all methods changed in a similar way across the frequency range, the individual data indicate that neither SFOAE measure allows for precise estimation of CAP tuning within a given subject.

Supported by NIH Grant DC-00419 (M. Ruggero) and Northwestern University.

1075 The Influence of Compression on Evaluating Dynamic Changes in Frequency Selectivity in Forward Masking

Skyler Jennings¹, Ali Almishaal¹

¹University of Utah

Background

Frequency selectivity has been reported to increase as a function of the duration of a forward masker [e.g. Bacon and Jesteadt, J. Acoust. Soc. Am. 82, 1926-1932 (1987)]. This finding suggests that the tuning of the auditory system may sharpen shortly after being stimulated; however, this interpretation does not consider the influence of nonlinearity in the cochlea. The current study tests the

hypothesis that an increase in frequency selectivity with masker duration is a product of cochlear nonlinearity. This was done by measuring frequency selectivity psychophysically and correcting these measurements with an estimate of cochlear nonlinearity.

Methods

Frequency selectivity was estimated from “input filter patterns” (IFPs) where the detection threshold for a 4-kHz probe was measured in the presence of a masker whose level was held constant and whose frequency varied. Cochlear non-linearity was estimated from on- and off-frequency growth of masking (GOM) and “output filter patterns” (OFPs) were obtained by transforming IFPs by this estimate.

Results

Preliminary results suggest that corrected measurements of frequency selectivity (i.e. OFPs) do not differ between long and short maskers. This suggests that compression may be responsible for the increased frequency selectivity observed in IFPs measured with a long masker.

Conclusion

These results can be interpreted as suggesting, 1) that the tuning of the auditory system does not change during stimulation, or 2) that manipulating masker duration may be an insensitive way to study how auditory tuning changes with stimulation. The influence of the medial olivocochlear reflex on frequency selectivity supports the latter interpretation as this reflex has been reported to reduce frequency selectivity when elicited [e.g. Cooper and Guinan, *J. Physiol.* 576, 49-54 (2006)].

1076 Heart Rate Responses of Big Brown Bats (*Eptesicus Fuscus*) to Conspecific Vocalizations

Marie Gadziola^{1,2}, Kelsey Gerbig¹, Jeffrey Wenstrup^{1,2}
¹Northeast Ohio Medical University, ²Kent State University

Background

Acoustic communication plays a primary role in social interactions among many species of bats. Our previous work revealed a complex acoustic communication system among big brown bats in which acoustic cues and call structure signal the emotional state of the vocalizing animal. We found that heart rate of a calling bat scaled to the intensity level of evoked vocal aggression, confirming our behavioral state classifications assessed by vocalizations and behavioral displays. However, it is not known how these social vocalizations modify the behavior and affective state of a listener.

Methods

In this study we monitored the heart rate responses of big brown bats (n=4) to the presentation of conspecific vocalizations. An external heart rate monitor was attached and signals were transmitted to a wireless receiver (TBSI). Bats were allowed to roost freely within a small cage, in which heart rate, video, and vocalizations were recorded over 5-min trials. Bats were presented with sound stimuli

that corresponded to one of five different contexts: high aggression, lower aggression, appeasement, and neutral pure tones at two different intensity levels. Stimuli were presented 30 times at a rate of 1/s, and the sound context of trials was randomized within each recording session.

Results

Bats generally showed a significant increase in heart rate in response to sound (81%, 57 trials), including pure tones. However, we found that the conspecific vocalizations evoked a greater increase in heart rate than pure tones (p<0.05). Surprisingly, lower aggression vocalizations evoked the largest change in heart rate magnitude (p<0.001) and remained elevated for longer durations (p<0.001) compared to any other sound context. Heart rate responses also showed level dependence, with the higher-intensity tones evoking a larger increase in heart rate than lower-intensity tones (p<0.005).

Conclusion

The results of the current study suggest that factors influencing heart rate changes in response to conspecific vocalizations may be different for the sender and receiver. Lower aggression vocalizations, which evoked the greatest increase in heart rate of receivers, are more likely to be associated with close physical contact and biting. In contrast, vocalizations of a highly aggressive bat are more likely to prevent physical contact and reduce the probability of biting. The increased probability of biting associated with lower aggression vocalizations may explain why receivers show a greater elevation in heart rate in response to these vocalizations. Supported by NIDCD grant R01 DC00937.

1077 Two-Step Cluster Analysis for Automated Classification of Mouse Pup Isolation Syllables

Jeffrey Wenstrup¹, Jasmine Grimsley¹, Marie Gadziola^{1,2}
¹Northeast Ohio Medical University (NEOMED), ²Kent State University

Background

Acoustic communication signals can be used as behavioral markers of stress or diseased state. For example, mouse pups vocalize at higher rates when they are cold or isolated from the nest. Beyond rate of calling, recent work also suggests that changes in the types or proportion of emitted syllables can also carry significant information about the internal state of the animal. However, current methods of manual syllable categorization are time consuming and vulnerable to experimenter bias.

Methods

In this study we use an automated two-step clustering technique to determine the number of statistically distinct syllable types produced by CBA/CaJ mouse pups, and compare the results to prior manual classification methods. A total of 15,116 CBA/CaJ mouse pup syllables were used to determine the number of distinct syllables within the repertoire at different ages (p5, 3,145 syllables; p7, 4,329; p11, 4,560; p13, 3,082). For each syllable, an automated 9-point fundamental frequency contour was first computed.

Next, the distribution of frequency transitions was analyzed to develop a criterion for indicating discontinuous frequency steps. The two-step cluster analysis was computed using four variables for each syllable: the total number of frequency steps and the start, middle, and end frequency of the fundamental.

Results

Manual classifications of these vocalizations had previously identified ten syllable types based on spectro-temporal features (Grimsley et al., PLoS One, 6 (3), 2011). The automated cluster analysis identified four distinct clusters: two syllable types with continuous frequency-time structure that were distinct based on their frequency bands, and two syllable types that featured single or multiple discontinuous frequency transitions. Although the cluster analysis computed fewer syllable types than manual classification, the clusters are more acoustically distinct and represent the probability distributions of the acoustic features within syllables.

Conclusion

Using fixed categorical boundaries informed by the cluster analysis, we generated a Microsoft Excel-based mouse syllable classification calculator that rapidly classifies syllables, with over 90% correspondence. This tool can be used by behavioral neuroscientists to investigate the relationship between mouse pup vocal signals and genetic makeup, health status, or emotional state. Supported by NIDCD grant R01 DC 00937.

1078 Measurement of the Frequency Dependence of Medial Olivocochlear Activation During an Auditory Intensity Discrimination Task

Wei Zhao^{1,2}, John Guinan^{1,2}

¹Massachusetts Eye and Ear Infirmary, ²Harvard Medical School

Background

In awake humans in passive listening (i.e. not doing a task), tones and narrow-band noise evoke medial olivocochlear (MOC) efferent activation over broad frequency regions with the largest MOC inhibition not necessarily centered on the frequency of the presented sound. Recently, it has been shown that during an intensity discrimination task, MOC activity is increased compared to passive listening to the same sounds. Since the MOC efferents have been postulated to facilitate stimulus intensity discrimination in noise, the task-related increase in MOC activity might be near the frequency of the target tone where it might best help the auditory discrimination. With this in mind, we sought to determine whether task-related MOC activity is restricted to, or correlated with, the target frequency of the task.

Methods

Human subjects with normal hearing are recruited for a two-interval forced choice intensity discrimination task. In each trial, two 20 ms tone pips at the same frequency, separated by 380 ms, are embedded in a broadband noise

and presented to one ear per subject. The task is to indicate whether the two tone pips are of the same intensity, or not. MOC activity is monitored by click-evoked otoacoustic emissions (CEOAEs), in the task ear before and immediately after the task, and, sometimes, in the contralateral ear also during the task. The decrease in CEOAE level, relative to the level at the beginning of the task, is taken as an index of the MOC inhibition. In each subject, two target frequencies (>1 octave apart) are used with sets of trials at one target frequency alternated with sets of trials at the other target frequency. For comparison, subjects are also tested using the same sounds but without doing a task.

Results

Preliminary results indicate that the pattern of MOC activation across frequency shows a dependency on the task frequency.

Conclusion

The paradigm has great potential for showing the extent to which the cochlear frequency region receiving MOC inhibition follows the task frequency. We will have more complete results at the ARO meeting.

Supported by NIH NIDCD RO1 DC005977

1079 Relationship Between Middle-Ear Transmission Characteristics and Frequency Modulation Detection

Sho Otsuka¹, Shinpei Yamagishi², Koichi Hirota¹, Shigeto Furukawa³, Makio Kashino^{2,3}

¹The University of Tokyo, ²Tokyo Institute of Technology, ³NTT Communication Science Laboratories

Background

The frequency-modulation difference limen (FMDL) with a low modulation rate has been used as a measure of the listener's sensitivity to the temporal fine structure (TFS) of a stimulus, which is represented by the pattern of neural phase-locking at the auditory periphery. However, factors that determine inter-listener variation of FMDL have not been thoroughly explored. This study examined the extent to which non-neuronal factors, specifically mechanical middle ear transmission characteristics, can account for inter-listener variation of FMDL. The middle-ear transmission characteristics and the FM detection performance in normal-hearing listeners were compared.

Methods

The middle-ear transmission was assessed by wideband energy reflectance measurement, in which the reflectance and admittance are derived from the sound reflected by the middle ear. The reflectance and admittance frequency response were measured as a function of frequency from 0.2 to 6 kHz. FMDLs were measured by using a 2I-2AFC transformed up-down method. A stimulus was a 750-ms long tone burst with a frequency of 1 kHz. The modulation rate was 2 Hz. Sixteen audiometrically normal adults participated in the experiment as listeners. In the analysis, participants were divided into two groups: the lower-FMDL

group (nine listeners) and the higher-FMDL group (seven listeners).

Results

The reflectance was typically near 1.0 (all of the sound energy was reflected) at low frequencies (<0.5 kHz). The reflectance-versus-frequency function exhibited a minimum at frequencies within a range between 1 and 4 kHz (the resonance frequency). The resonance frequency of the higher-FMDL group was distributed around 1 kHz, while that of the lower-FMDL group was distributed above 1 kHz. Consistently, the admittance value at 0.25 kHz (which is generally assumed to be negatively correlated with the stiffness of the middle ear; a decrease in the stiffness is associated with a lower resonance frequency), exhibited a significant correlation with FMDL (Pearson's $r=0.57$, $p=0.02$).

Conclusion

The results showed that an appreciable fraction of inter-listener variability in FMDL could be accounted for by the listener's middle ear characteristics: FM detection performance tended to be poor when the stimulus frequency was close to the listener's resonance frequency. When an FM detection task is used to evaluate the degree of neural phase-locking, the inter-listener variation of middle-ear transmission should be considered.

1080 Auditory Cortex Is Highly Tuned to the Emergence of Regular Patterns in Sound Sequences

Nicolas Barascud¹, Maria Chait¹

¹UCL Ear Institute

Background

We used psychophysics and magnetoencephalography (MEG) functional brain imaging to assess listeners' ability to detect the emergence and violation of complex regularities (characterized by long repeating patterns) in ongoing sound sequences and the degree to which this process is bottom-up driven or dependent on explicit attention. Stimuli were tone pip sequences that contained transitions between random and regular frequency patterns. Transitions from a regularly alternating to a random tone sequence (**REG-RAND**) are immediately detectable as the first tone to violate the established regularity pattern is sufficient to signal the transition. In contrast, listeners must wait longer (at least one regularity cycle) to detect the opposite transition –from a random to a regular pattern (**RAND-REG**).

Methods

We used sequences of 50ms tone pips arranged according to 4 frequency patterns: **REG** sequences consisted of a regularly repeating pattern of X tones (X=10, 15, 20; new pattern for each trial). **RAND** sequences consisted of a sequence of tones of random frequencies. **REG-RAND** and **RAND-REG** sequences contained a transition between a regular and a random pattern. Additionally a proportion of **CONTROL** stimuli consisting of a simple step change in frequency between two long pure tones were

used to estimate basic response times (RT). In all signals, the time of change was jittered across trials.

In the behavioural experiments (N=16), subjects were actively detecting the transitions in **REG-RAND**, **RAND-REG** and **CONTROL** stimuli (change occurred in 50% of the trials). The time required to detect the emergence/violation of regularity was estimated by subtracting the RT to **CONTROL** signals from that to **RAND-REG** and **REG-RAND**. In the MEG experiment (N=16; different subjects), naïve participants listened to **RAND-REG** and **REG-RAND** stimuli while performing an unrelated visual decoy task.

Results

Behavioural response times reveal that subjects required about a cycle and a half to detect the emergence of regularity in **RAND-REG** signals. Since the transition is not detectable before the first regularity cycle, our results show that listeners only required an additional half cycle to recognize the onset of regularity. Analysis of MEG data is ongoing. Preliminary results indicate that brain response latencies (when the subjects were not actively listening to the transitions) reliably match the RT data.

Conclusion

Our data reveal that the auditory system is remarkably efficient at detecting the appearance and disappearance of regularities in sound sequences, even for very long patterns.

1081 A Perceptual Measure of Cochlear Gain Control by the Medial Olivocochlear System

Mark Fletcher¹, Jess de Boer¹, Katrin Krumbholz¹

¹MRC Institute of Hearing Research, Nottingham UK

Background

The medial branch of the efferent olivocochlear (MOC) system controls the gain of the cochlear amplifier. This gain-control function is thought to play an important role in speech-in-noise perception. Otoacoustic emissions (OAEs) offer a qualitative measure of the MOC system's effect on cochlear gain, but a quantitative measure is still lacking. The aim of the current study was to develop such a measure.

Methods

Cochlear gain affects the ear's input-output (I/O) function, that is, the function relating the size of the ear's response to the intensity of the input stimulus. The I/O function can be measured behaviourally by measuring the temporal masking curve (TMC) of a given stimulus. The TMC measures the forward-masking effectiveness of the stimulus as a function of time after stimulus offset. Here, we measure the effect of contralateral noise, which is known to activate the MOC system, on the TMC. In order to control for any longer-lasting effects of MOC activation, the conditions with and without contralateral noise were presented either in a blocked or interleaved sequence. For comparison, we also measured the effect of contralateral noise on OAEs under the same conditions.

Results

The TMCs exhibited a significant effect of contralateral noise, suggesting a gain reduction of ~6 dB. This effect was observed equally in the blocked and interleaved sequences. The OAE also showed a significant effect of contralateral noise (of 0.5 dB, on average), but, in this case, the effect was observed only for the interleaved sequence. There was also no correlation across participants between the sizes of the contralateral noise effects on the TMCs and OAEs.

Conclusion

Our results suggest that TMCs are sensitive to cochlear gain control through the MOC system. However, the lack of correspondence with OAE estimates of MOC-mediated gain control suggests that the two methods are sensitive to different aspects of MOC function. The differences between the two methods may be related to the influence of attention; in the TMC measurements, participants were engaged in an active task, whereas the OAEs were measured under passive listening conditions. Under this assumption, TMCs would appear to offer an ecologically more valid measure of MOC function than OAEs.

1082 Specific Deficits of Basic Auditory Processing in High-Functioning Pervasive Developmental Disorders

Makio Kashino^{1,2}, Shigeto Furukawa¹, Tamami Nakano^{3,4}, Shiho Washizawa², Shinpei Yamagishi², Atsushi Ochi^{1,5}, Atsushi Nagaike⁶, Shigeru Kitazawa^{3,4}, Nobumasa Kato^{7,8}

¹NTT Communication Science Laboratories, NTT Corporation, ²Interdisciplinary Graduate School of Science and Engineering, Tokyo Institute of Technology, ³Graduate School of Medicine, Juntendo University, ⁴Graduate School of Frontier Biosciences and Graduate School of Medicine, Osaka University, ⁵Faculty of Medicine, The University of Tokyo, ⁶Graduate School of Medical Sciences, Kyushu University, ⁷School of Medicine, Showa University, ⁸Showa University Karasuyama Hospital

Background

Individuals with pervasive developmental disorders (PDD), such as high-functioning autism (HFA) and Asperger's syndrome (AS), often have difficulties perceiving speech in noisy environments. Here, we investigated whether this might be explained by deficits in basic auditory processing.

Methods

We conducted a set of psychophysical experiments assessing various aspects of basic auditory processing for a group of young adults with PDD (N=21; 5 AS, 9 HFA, and 7 PDD-NOS) and a group of age/IQ-matched controls (N = 37). None of them had hearing levels > 20 dB at all audiometric frequencies. The psychophysical measures included: (a) auditory filter shape at 500 and 2000 Hz estimated by the notched-noise method, (b) level increment detection threshold for noise, (c) gap detection threshold for noise, (d) frequency discrimination threshold for tones at 100 and 1100 Hz, (e) detection threshold for the shift of frequencies of otherwise harmonic components; the stimulus containing harmonics with intermediate

resolvability with a fixed spectral envelope, (f) discrimination threshold of interaural time difference (ITD) for noise, (g) discrimination threshold of interaural level difference (ILD) for noise, (h) binaural masking level difference, (i) discrimination threshold of Huggins pitch, and (j) speech reception threshold (SRT), defined as the speech-to-noise ratio at which approximately 50% of Japanese monosyllables are correctly identified.

Results

Statistically significant differences in the median and distribution of psychophysical measures between the PDD and control groups were found for the discrimination thresholds of ITD (f) and ILD (g), as well as SRT (j). In these three tasks, the performance for the PDD group was worse than those for the control group. For the frequency-shift detection task (e), where the temporal fine structure of sounds was the major cue, the difference in the median between the groups was not significant but that in the distribution was significant. In this task, the proportion of good and bad performers was also significantly different between the groups. No statistically significant difference was found for other tasks.

Conclusion

The results indicate that a certain proportion of individuals with PDD have reduced ability to detect temporal fine structure and binaural disparities of sounds, which may contribute to the speech-in-noise perception difficulties experienced by them. The deficits may be related to the malformation of the superior olivary complex found recently in autistic spectrum disorders.

1083 Multiple Sound Sources in an Australian Amphibian?

Peter Narins¹, Michel Ohmer², Ikkyu Aihara³, Phil Bishop⁴, Jean-Marc Hero⁵

¹UCLA, ²U. Brisbane, ³RIKEN Brain Sci. Inst., ⁴U. Otago, ⁵Griffiths U. Gold Coast

Background

Terrestrial vertebrates are capable of producing a wide variety of sounds. Among these are vocalizations which are generated by the larynx in the case of amphibians, reptiles and mammals, or by the syrinx in birds. While the syrinx has the ability to produce separate sound components on each side of its bipartite structure, the larynx is not so well endowed, being restricted to generating one sound at a time that is then subjected to post-filtering by the structures inside the head. Nevertheless, the calls of the Cascade Tree Frog (*Litoria pearsoniana*) exhibit clear examples of simultaneous production of multiple vocalization components.

Methods

All field recordings of this species were made between 2000 and 2200 h from 5 to 10 February, 2012. Males of *L. pearsoniana* were found in their natural habitat in Springbrook, Queensland, Australia, calling along streams and near waterfalls. Vocalizations of seven males of *L. pearsoniana* were recorded with a broadband, directional

microphone (G.R.A.S. 40 BE) and preamplifier (G.R.A.S. 26 CB) and a portable digital recorder (Sound Devices 722) at 48 kHz sampling rate. Before each recording, it was determined that no other calling males were in the vicinity of the focal male, thus ensuring that the recorded vocalizations were all coming from a single individual. Data were saved as .wav files and analyzed (FFT, 1024), and displayed using SELENA, a custom-designed program (S. Andrzejewski, St. Petersburg).

Results

Sound spectrograms of the advertisement calls of males of *L. pearsoniana* revealed that the advertisement calls consisted of multiple harmonic stacks in which the fundamental frequencies ranged between 0.5-0.6 kHz, and exhibited various degrees of FM. Multiple instances of simultaneous occurrences of two call components were found. These were most often seen when one harmonic stack disappeared abruptly and a second stack with a new fundamental frequency would commence before the first stack ended.

Conclusion

One interpretation of our findings is that the observed "stack overlaps" reflect the existence of a second sound source in this frog species. The vocal cords within the larynx are one source; the other is unknown. Several potential candidates for the second source are discussed.

1084 Probing the Auditory Attention Filter Along the Auditory Pathway

Sarah Verhulst^{1,2}, Christopher Shera², Barbara Shinn-Cunningham¹

¹Boston University, ²Harvard Medical School

Background

Evidence that auditory attention can be focused in a particular frequency range was discovered by Greenberg and Larkin (1968) using the probe-signal method. Listeners were presented with a cue tone and asked to detect a subsequent tone embedded in noise whose frequency was either the same as the cue (signal tone) or different (probe tones). For tones within 150 Hz of the cue-tone frequency, performance was better for the signal tone than for nearby probe tones, suggesting that listeners focused attention on the cue frequency with an "attentional filter". However, the mechanism by which such filtering arises is unknown. Moreover, for the just-detectable tones used, listeners were unaware of the signal and probe tone frequencies, thereby excluding a purely cortically mediated explanation. The current study uses the probe-signal method along with physiological measures of auditory response (otoacoustic emissions and EEG) to investigate responses at different levels along the auditory pathway.

Methods

Subjects were presented with three intervals: a cue interval, consisting of a clearly audible cue tone embedded in a 450-ms noise, followed by two 450-ms noise bursts, one of which was randomly selected to contain a near-threshold test tone. The test tone was either presented at

the same frequency as the cue tone (75% of the trials) or at a frequency within 150 Hz of the cue frequency (25% of the trials). Performance was analyzed as a function of test tone frequency and then compared across trials differing in the cue-tone frequency. Click trains were presented immediately before and after each three-interval trial to simultaneously record click-evoked otoacoustic emissions (CEOAEs). Additionally, electrical potentials (EEG) from the scalp were recorded using a 32-electrode cap, enabling measurement of both brainstem and cortical responses to the stimuli.

Results

Physiological measures were recorded during the attention task so that their amplitudes could be directly related to task performance. The signal-to-noise ratio for the brainstem and cortical correlates were optimized using principal component analysis across the 32 channels. The CEOAE spectra in the pre- and post-trial conditions were used to assess peripheral changes during the task.

Conclusion

Simultaneous recording of CEOAEs and EEG signals during a behavioral task allows probing of related physiological responses at different stages of the auditory pathway. We expect that a full analysis of the data will elucidate peripheral, sub-cortical, and cortical correlates of the auditory attention filter.

1085 Glycinergic Inhibition Controls Synaptic Integration in the Medial Superior Olive

Michael H Myoga¹, Simon Lehnert¹, Leibold Christian¹, Felix Felmy¹, Benedikt Grothe¹

¹Ludwig-Maximilians-Universität München

Background

The brainstem nucleus of the medial superior olive (MSO) encodes differences in the arrival time of sounds between the ears (interaural time difference or ITD), providing information about the location of sounds in the horizontal plane. MSO neurons receive bilateral phase-locked excitation and glycinergic inhibition. MSO neurons integrate all four synaptic inputs, but it is not understood how these inputs interact at the cellular level to generate ITD output functions. Here, we investigated whether the precise timing of inhibition is important for synaptic integration in the MSO.

Methods

We performed patch-clamp recordings of MSO neurons in acute slices from adult (postnatal day 60 – 90) Mongolian gerbils (*Meriones unguiculatus*) at near physiological temperature (35 °C). We investigated the interaction between EPSPs and IPSPs using fiber stimulation and conductance-clamp recordings. We also created a computational model of an MSO neuron, based largely on our measured membrane properties.

Results

We first measured excitatory and inhibitory synaptic conductances evoked by putative single presynaptic fibers in voltage-clamp in many neurons. From these data, we selected representative conductance waveforms as templates and then simulated excitatory and inhibitory potentials (EPSPs and IPSPs) in conductance-clamp. We found that the peak of a combined EPSP and IPSP is advanced when the EPSP occurs during the hyperpolarizing phase of an IPSP, but is delayed when the EPSP occurs during the re-depolarizing phase of the IPSP. This suggests that precisely timed inhibition can shift the peak timing of excitation arising from either the ipsilateral or contralateral side. We went on to investigate how the timing of an IPSP influences the summation of two EPSPs. Without inhibition, two EPSPs summated maximally when they occur simultaneously. However, when a pair of EPSPs occurred during the hyperpolarizing phase of the IPSP, maximal summation was observed when the first EPSP led the second. Moreover, when the EPSPs occurred during the re-depolarizing phase of the IPSP, maximal summation was observed when the first EPSP trailed the second. We also used the same conductance templates as inputs for our model simulations and found that if the model quantitatively matches the voltage responses, it provides a good prediction for the effect of inhibition on the peak timing and summation of EPSPs.

Conclusion

Our findings indicate that precisely timed inhibition can influence the coincidence detection of ipsilateral and contralateral excitation. This provides evidence for a crucial role for inhibition in ITD tuning in vivo.

1086 Cross-Correlation Based Characterization of Axonal Delays in the Nucleus Laminaris of the Barn Owl Using a Microelectrode Array

Thomas McColgan^{1,2}, Richard Kempter¹, Hermann Wagner²

¹Humboldt University Berlin, ²RWTH Aachen

Background

The barn owl localizes sound sources in the azimuthal plane by measuring the Interaural Time Difference (ITD). The proposed mechanism for the calculation of these ITDs involves axonal delay lines. The properties of these structures, such as axonal conduction velocities, have been a subject of research for many years.

Methods

In this study, we analyzed data collected in vitro using a Microelectrode Array (MEA) from barn owl chicks aged from postnatal day 2 to day 13. The aim of the analysis was to verify the existence of the axonal delay lines and to characterize the conduction velocities. Improvements with respect to previous studies were made in the preprocessing of the electrophysiological data leading to a higher signal-to-noise ratio and better temporal precision. Furthermore, an algorithm for the determination of the conduction velocity based on cross-correlation was

developed and employed. The new algorithm allowed the simultaneous and unsupervised measurement of conduction velocities across the MEA involving recordings from multiple electrodes.

Results

Using these methods, the data was found to show a structured delay distribution consistent with the existence of delay lines. The conduction velocities obtained were lower than reported from in-vivo experiments in mature barn owls as well as from similar in-vitro experiments in chicken.

Conclusion

One factor causing the lower conduction velocities may be that the delay lines are still developing at this age. The methods used in this study might be applicable to future MEA experiments and experiments using multiple simultaneous recordings in general.

1087 Glycine Receptors Expressed in "Timing" Neurons of the Avian Auditory Brainstem Modulate GABAergic Inhibition

Matthew Fischl¹, Sonia Weimann¹, Michael Kears¹, R.

Michael Burger¹

¹Lehigh University

Background

Glycine (GLY) transmission is prominent in the mammalian sound localization circuit, but has not been a focus of investigation in the avian brainstem for several reasons. First, inhibitory input is completely blocked by application of the GABA_A receptor antagonist bicuculline in the nuclei known to process temporal features, nucleus magnocellularis (NM) and nucleus laminaris (NL). Additionally, GLY immunoreactivity appears much less robust compared to GABA staining in these nuclei. However, recent studies from our group and others have shown that GLY is co-released with GABA in other auditory nuclei within this circuit such as the nucleus angularis (Kuo et al. 2009) and the superior olivary nucleus (SON) (Coleman et al. 2011). Here we show that functional glycine receptors are ubiquitously expressed in all brainstem auditory nuclei.

Methods

Glycine receptor expression was characterized using immunocytochemistry and whole cell voltage clamp recordings. We used pressure application of glycine to test the functionality of glycine receptors in the NM, NL and SON. We also used pressure application and presynaptic fiber stimulation to explore the effects of glycine receptor activation on synaptically evoked inhibitory postsynaptic currents.

Results

We show that GLY receptors are present at all four of the above-mentioned nuclei throughout development of the auditory system and demonstrate that exogenous GLY application evokes strychnine sensitive currents in these neurons. Indeed, these currents were observed in nuclei

such as the NM and NL, where GLY responses could not be synaptically evoked via electrical stimulation. To assess the functional role of GLY signaling we evaluated the effect of an exogenous GLY pre-pulse on synaptically evoked GABA or mixed GABA/GLY inhibitory currents in the NM and the SON, respectively. Surprisingly, activation of GLY receptors reduced the amplitude of inhibitory postsynaptic currents evoked during a 100Hz train stimulus in both nuclei. This occlusion effect was blocked during application of strychnine and recovered after washout. This modulation was not dependent on phosphatase 2B activity but did require the flux of ions through the receptor channel.

Conclusion

Functional GLY receptors were located in all four primary nuclei in the chicken auditory brainstem. Pre-application of glycine suppressed the amplitude of both synaptically evoked IPSCs and spontaneous IPSCs. Activation of the GLY receptor without Cl⁻ flux was insufficient to induce the suppression. These results suggest that ionic transmission through the GLY receptor occludes inhibition via GABA_A receptors, providing a possible modulatory mechanism for inhibition in the sound localization pathway.

1088 Variability of Sound Source Position and Temporal Feature Representation in Across-Frequency Integrating Neurons of the Barn Owl

Philipp Tellers¹, Kerstin Buelles¹, Hermann Wagner¹
¹RWTH Aachen

Background

The acoustic system needs to code where a sound source is located and what kind of source it is. Keller and Takahashi (J Neurophysiol 84:2638 (2000)) showed that neurons of the central nucleus of the inferior colliculus (ICC) are able to code both, the “where” and the “what”. The location of a sound source was represented by the maximum firing rate in response to interaural time (ITD) and level (ILD) differences, while temporal feature of the sound were represented by the discharge pattern of the neurons.

The acoustic pathway branches at the level of the ICC to create a forebrain and a midbrain pathway (Fig. 1). Both pathways receive input from the ICC, both integrate information of different frequency channels, and the neurons of both pathways are significantly tuned to ITD. ICC neurons exhibit a high firing rate with low variability in response to ITD stimuli (Christianson and Pena, J Neurosci 26:5948 (2006)).

Methods

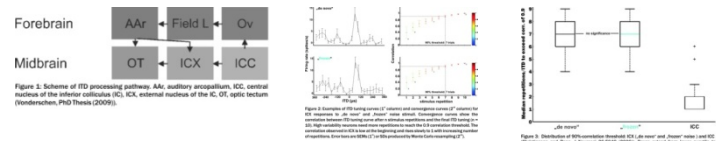
We recorded extracellularly from single neurons of the external nucleus of the inferior colliculus (ICX, midbrain) and the auditory arcopallium (AAR, forebrain). We used “de novo” generated noise and different “frozen” noise samples to examine to what degree and how precise the sound source position and the temporal features of acoustic sounds are represented in these nuclei.

Results

While firing rate decreased from ICC to ICX, variability increased (Fig. 2). Preliminary data of AAR neurons showed the same effect. We could not observe any difference between the firing rate and the variability in response to “de novo” and “frozen” stimuli neither at the population (Fig. 3) nor at the neuron level.

Conclusion

Across-frequency integration leads to increased variability and is accompanied by a decrease in firing rate. The missing difference between “de novo” and “frozen” noise indicated a stimulus independent rate code for ITD representation in these neurons.



1089 Previous Stimulation Does Not Affect the Representation of Sound Source Location by Units of the Inferior Colliculus of the Mongolian Gerbil

Sandra Tolnai¹, Laura Endres¹, Georg M. Klump¹
¹Carl von Ossietzky University Oldenburg

Background

Previous stimulation, particularly the number of stimuli preceding a target stimulus has been shown to affect the localization ability (e.g., Feinkohl & Klump 2012). Here we compare the representation of sound source location in neurons of the inferior colliculus (IC) of anesthetized Mongolian gerbils in relation to the number and location of preceding stimuli with behavioral data collected from gerbils trained in an absolute and relative localization task.

Methods

In a first set of experiments, extracellular recordings from IC units in anesthetized gerbils were obtained in response to 125-ms broadband noise bursts or tones. Stimuli were presented over headphones using virtual acoustic space techniques to mimic free-field conditions. Target signals were presented from positions to the left or the right of the midline following a variable number of stimuli from the midline. Response rates and response latencies were subjected to a receiver operating characteristic (ROC) analysis. In a second set of experiments, two Mongolian gerbils were trained in a two-alternative forced choice task to indicate the direction of a target sound after the presentation of sounds from the midline that varied in number using the same stimulus types. The animals received a food reward if they approached the side of the target stimulus. Thresholds were determined applying signal detection theory.

Results

Units in the IC were spatially tuned to sounds as indicated by their response rate and/or response latency. In the vast majority of units the number of preceding sounds did not

affect the spatial tuning to the target sound and thus the neurons' discrimination ability for spatial positions as shown by the ROC analysis. Contrary to this, the discrimination ability of the gerbils performing in a localization task depended on the number of sounds that preceded the target signal. The more preceding sounds were presented, the smaller the thresholds were. Thus, while units in the IC faithfully encode the location of sound sources irrespectively of the number of preceding sounds from a reference position, behavioral thresholds are affected by stimulation history.

Conclusion

The discrepancy between the neurophysiological and the behavioral data suggests that IC neurons do not represent the observed behavior. Additional factors not related to the stimulus source location per se may affect the behavioral response.

1090 Analysis of Localization Cues in Globular Bushy Cell with a Sound Localization Model

Marek Rudnicki¹, Christian Wirtz^{1,2}, Werner Hemmert¹
¹Technische Universität München, ²Med-El Detuschland GmbH

Background

Globular Bushy Cells (GBCs) are one of principal cells in cochlear nucleus. They receive major excitatory inputs from auditory nerve fibers (ANFs) and project their axons to the contralateral medial nucleus of the trapezoid body. GBCs are directly involved in the sound localization pathway to the lateral superior olive. We show how GBCs improve temporal cues in spike trains by combining them with a sound localization model. The localization model is sensitive both to interaural time differences and interaural level differences.

Methods

We simulated auditory nerve responses with an auditory periphery model including power-law adaptation described by Zilany et al. (2009), which we tuned to reproduce human hearing thresholds. The GBC model was a single compartment representing a soma with Hodgkin-Huxley-like channels (Rothman and Manis 2003). It received purely excitatory inputs from ANFs. Synaptic weights were fitted to reproduce firing patterns of high-sync neurons in cochlear nucleus. They achieved a synchronization index above 0.9 and entrainment of 1 for frequencies up to 600 Hz. Simulated responses from both ears were fed to a binaural cross-correlation model (Lindermann 1986). It consisted of delay lines inspired by Jeffress (1948) and additional inhibitory elements. This combination makes the model both ITD and ILD sensitive.

Results

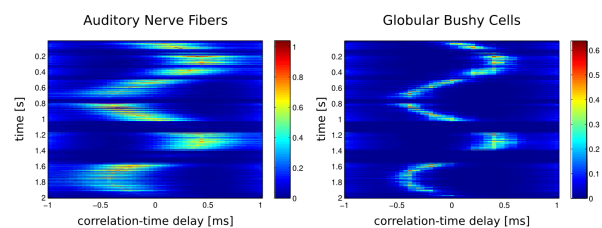
We simulated two types of sounds: pure tones and speech. In both cases, the sound source was moving around the listener (1 rotation/s). Our results show that GBCs greatly enhance localization cues over ANFs. GBCs are known to enhance the temporal precision of

their spike trains by coincidence detection. They lock on low-frequency pure tones and enhance amplitude modulations, which are present in speech sounds. Therefore, the internal representation of the sound source location in the Lindermann model is much sharper with GBCs compared with ANFs (supplemented Figure). With speech sounds this sharpening effect is particularly pronounced.

Conclusion

The analysis of spike trains derived from GBCs and ANFs using a sound localization model showed a large improvement of localization cues in GBCs. We observed improved precision of sound source localization for simple and complex sounds. The improvement was mostly due to the higher temporal precision of action potentials in GBCs. In summary, our analysis demonstrates how temporal information is processed in the localization pathway to achieve sharp localization cues.

This work was supported by the German Research Foundation (SPP 1608), the Bernstein Center for Computational Neuroscience Munich (BMBF 01GQ1004B and 01GQ1004D) and MedEl.



Internal representation of sound source location in the Lindermann (1986) model for auditory nerve fibers (left panel) and globular bushy cells (right panel). Data is shown for the 400 Hz characteristic frequency for a spoken sentence emitted by a source circling around the listener once per second.

1091 Simulations of Auditory Periphery to Study the Effects of Sound Level and Duration on Spectral Cues to Localization

Yan Gai¹, Janet Ruhland¹, Tom Yin¹, Daniel Tollin¹
¹University of Wisconsin-Madison

Background

Changes in sound level or duration have been shown to affect localization performance for human and cats, especially for targets in elevation. An interesting finding is that, for short-duration sound, localization performance in elevation decreases at high sound levels, whereas for long duration sound, this "negative level effect" is minimal. The integration model predicts that localization of long-duration sound benefits from "multiple looks" of consecutive short-term spectral analyses of the ongoing information. In contrast, the adaptation theory predicts that the later part of the long-duration response is more sensitive to spectrum changes than the onset. Previous studies have also suggested that a broad and flat spectrum of the sound source is critical for localization in the elevation.

Methods

An AN model (Zilany et al. 2009) for the cat was used to simulate populations of AN responses to targets in

elevation. The input of the model was broadband noise filtered with cat directional transfer functions (DTFs). Three sets of broadband stimuli including long-duration random noise, short-duration (5-ms) random noise, and long-duration (100-ms) repeated noise made of identical concatenated copies of the short-duration noise were tested. The correlation between the simulated AN firing rates under these stimuli and the DTFs was used as a metric to study the level and duration effects on vertical localization.

Results

The correlation was significantly higher for the 100-ms random noise than for the 5-ms noise. However, the correlation was non-monotonic with level for sound of both durations.

Replacing the 100-ms random noise with the 100-ms repeated noise had a small effect on the correlation at low and high sound levels and no effect at intermediate levels. Introducing neural adaptation during the steady-state AN response showed a large effect at high levels. The largest improvement of correlation was observed when providing the model with “multiple looks” throughout the stimulus duration.

Conclusion

The flatness of sound spectrum and peripheral adaptation benefit localization only at low and high levels, whereas neural integration that relies on “multiple looks” of the spectral analysis is critical for the peak performance at intermediate levels. The release of negative level effect observed for long-duration sound cannot be explained at the periphery and therefore, is likely a result of higher-center processing. Supported by NIH DC-00116 and DC-02840 (Yin) and DC-00376.

1092 Effects of Forward Masking on Sound Localization in Cats

Yan Gai¹, Janet Ruhland¹, Tom Yin¹

¹University of Wisconsin-Madison

Background

Forward masking is traditionally measured as an increased signal-detection threshold as a consequence of the addition of a preceding masking sound. The present study examined the influence of forward masking on localization of free-field sound in cats, which has not been previously studied in human or animal subjects.

Methods

Gaze positions of head-unrestrained cats were monitored using a search-coil technique. The masker speaker was fixed at the front center, while the signal could come from one of 17 speaker locations in the frontal hemifield. Cats were required to saccade from a central fixation LED to the perceived source of the target, with (i.e., the forward-masking condition) or without (i.e., the control condition) the masker. The masker was a broad-band noise (50 dB SPL, 600 to 700 ms). The target signal (25-ms) was either a broadband or a narrowband noise. The level of the signal

ranged from 30 to 80 dB SPL. The gap between the end of the masker and the beginning of the target was 0 or 10 ms.

Results

When the target was a short broadband noise, the presence of the forward masker reduced localization accuracy of the target at all target sound levels, along both horizontal and vertical dimensions. The detrimental effect was larger when gap = 0 ms than when gap = 10 ms. When the target was a narrowband noise, the effect of the forward masker was considerably larger for low-frequency (0.2–2 kHz) than for high-frequency (7–15 kHz) target, in both horizontal and vertical dimensions. At certain target sound levels, forward masking had no effect on localization of the high-frequency target. For all narrowband targets, localization accuracy for targets in elevation was significantly lower than for targets in azimuth, whether a forward masker was presented or not.

Conclusion

Localization of a short sound can be affected by a preceding noise masker, even when the target was well detected. Adding a gap between the masker and the target released the masking effect to a certain degree. The detrimental effect of the broadband masker acted mostly on the low-frequency component of the target, where the interaural timing cue dominates. Supported by NIH DC-02840 (Yin).

1093 In Vivo Response Properties of Neurons from Low-Frequency Nucleus Laminaris in the Chicken

Nicolas Palanca-Castan¹, Christine Koeppel¹

¹Carl von Ossietzky University Oldenburg

Background

Locating the source of a sound in the environment is a critical task for any animal. One of the most important cues animals use to accomplish this is interaural time difference (ITD), the minute difference between the moment when a sound reaches the ear closest to the source and the moment it reaches the opposite. However, how different animals compute these ITDs has been the subject of much debate. Here, we present new data from the low-frequency region of nucleus laminaris (the first brainstem nucleus that processes ITDs) in the chicken, aiming for a greater overlap in frequency range with comparable mammalian data.

Methods

Recordings were obtained from the low-frequency region of nucleus laminaris in vivo, under anesthesia, from chickens aged P28 to P48. Best frequency (BF), best interaural phase, best ITD, and frequency tuning were determined using pure tones.

Results

Approximately half of our data set is comprised of single-unit recordings, which showed no systematic differences to the multi-unit and neurophonic recordings. BFs ranged from 300 to 1600 Hz, corresponding to the caudolateral

part of the tonotopically organized NL. Most interestingly, best ITDs scattered symmetrically around zero within a range of up to $\pm 500\mu\text{s}$, i.e., nearly equal numbers of recording sites showed a preference for contra- and ipsilaterally leading sounds, respectively. This is consistent with published, preliminary data.

Conclusion

The available data for the chicken NL now suggest a symmetrical distribution of best ITDs around a value of zero at low BFs, up to approximately 1500 Hz. At higher BFs (up to the limit of 3500 Hz in the chicken) the distribution changes to a contralaterally biased representation of auditory space. Furthermore, the range of best ITDs is in good agreement with the physiologically relevant (i.e., naturally heard) range for the chicken. These features are consistent with a Jeffress-type neural code of ITD. However, the symmetrical distribution of best ITDs around the acoustic midline at low frequencies is unorthodox. It remains to be shown whether the topographic representation of ITD, previously shown for the majority of chicken NL, also persists into the caudolateral, low-frequency region.

1094 Mechanisms of Auditory Spatial Selectivity in Barn Owls

Ulrike Langemann¹, Rainer Beutelmann¹, Georg Klump¹
¹Carl-von-Ossietzky-Universität Oldenburg

Background

The physiological mechanisms of interaural time difference (ITD) encoding in birds and mammals are a matter of ongoing debate. The avian encoding strategy is assumed to be based on coincidence detection of excitatory inputs fed by neuronal delay lines, while the mammalian strategy is assumed to involve precisely timed interaction of excitatory and inhibitory inputs resulting in ITD-dependent activation balance between the left and right hemisphere (e.g., Grothe 2003, *Nature Neuroscience*). Given such differences it is interesting to test whether one model can explain spatial perception of sound sources both in birds and mammals. Wiegrebe and Binetti (2010, ARO) presented an experimental paradigm aimed at determining spatial selectivity in humans in a binaural unmasking task. We adopted this paradigm using barn owls as an avian species. The observed data from both humans and owls were compared to predictions of a computational model.

Methods

Three barn owls (*tyto alba*) were trained in a Go/NoGo paradigm using operant conditioning to detect a narrow-band noise target in broad-band masking noise. The stimuli were presented under free-field conditions, with two independent masker sources placed symmetrically to the target source in the horizontal plane. The masker was played continuously and the target duration was 110 ms including ramps. Detection threshold levels were measured as a function of target-masker separation (7.5° - 110°), target center frequency (2, 8 kHz), and target location (front, left, right). The computational model is

based on the equalization-cancellation model by Durlach (1963, JASA).

Results

In barn owls, the detection thresholds generally decreased with increasing target-masker separation, and there were significant interactions between both target frequency and target location with target-masker separation. The lowest thresholds were observed for an 8 kHz target in front of the subject. In humans (Wiegrebe and Binetti 2010), the thresholds generally also decreased with increasing target-masker separation and increasing target frequency, but in contrast to the owl data a target on the interaural axis leads to lower thresholds than a target in front. Especially at 8 kHz the barn owl's spatial resolution revealed by the unmasking was far superior to that of humans.

Conclusion

One computational model can explain the data in both humans and owls. Only the head-related transfer functions and the phase locking cut-off frequency need to be adjusted in the model in order to explain the observed detection threshold differences across species.

1095 Optimizing Parameters for Efficient Acquisition of the Binaural Interaction Component of the Auditory Brainstem Response

Alexander T Ferber^{1,2}, Kelsey Anbuhl¹, Daniel J Tollin^{3,4}
¹Neuroscience Training Program, ²Medical Scientist Training Program, ³Department of Physiology and Biophysics, ⁴Department of Otolaryngology, University of Colorado School of Medicine, Aurora, CO 80045 USA

Background

The sound-evoked binaural interaction component (BIC) is the residual auditory brainstem response (ABR) after subtracting the sum of both monaurally-evoked ABRs from the binaurally-evoked ABR. The β peak (i.e., DN1) is the first negative peak of the BIC. Latencies of β in human and animal studies indicate a brainstem origin for this electrophysiological potential related specifically to binaural processing at the inferior colliculus. The BIC may be diagnostically important: altered β latencies and amplitudes in children and adults correlate with and predict long-term behavioral deficits in binaural processing associated with chronic conductive hearing loss. In humans, cats, chinchillas and guinea pigs, β amplitude also depends systematically on binaural cues to location, exhibiting maximal amplitude for interaural time (ITD) and level (ILD) differences of zero (midline sources); β is often no longer detectable once ITDs and/or ILDs exceed physiological range. In this regard, the BIC is also informative for perception, as changes in β peak latencies and amplitudes occurring with varied stimulus ITD or ILD are correlated with psychophysical performance (lateralization, discrimination, binaural masking level differences) in normal and hearing-impaired subjects.

Methods

While the BIC β peak is theoretically clinically useful, it can be difficult and time-consuming to measure. The ABRs from which the differential BIC is calculated are themselves very small potentials ($\sim 1 \mu\text{V}$) measured using signal averaging to cumulatively amplify the small potentials (such as the β peak). The large series of stimulus trials required for ABR acquisition typically ranges from the hundreds to thousands or more, while acquisition of a subtractive potential like the BIC β peak is yet more elusive. Manipulation of stimulus ITD and ILD requires even more time.

Results

While presentation of thousands of stimulus iterations is laborious but feasible in a laboratory setting, introduction of the BIC β peak as a practical clinical assessment tool is more challenging. Laboratory experiments can allow for many hours of stimulus repetitions and recordings, but such an acquisition protocol is clinically impractical. Likewise in longitudinal animal experimentation, an expedited measurement of the BIC β peak is also desirable.

Conclusion

To this end, we assess and discuss parameters for quickly and accurately obtaining reliable BIC β peak measurements in chinchillas. The resultant protocol allows for reliable BIC β peak measurement within a more clinically-feasible time period. Support: NIDCD R01-DC011555

1096 Sensitivities to the Relative Phase of Interaural-Time-Difference Modulations Between Carrier Frequencies

Shigeto Furukawa¹, Tsuruyo Nishida^{1,2}, Tadahisa Kondo¹, Kazuhiko Takehi²
¹NTT Comm. Sci. Labs, ²Chukyo Univ.

Background

Evidence suggests that the human auditory system integrates information about interaural-time difference (ITD) across frequencies (e.g., Buell & Hafter, JASA, 1991; Hill & Darwin, JASA, 1996). The present study examined the dynamic properties of the across-frequency integration mechanism, specifically the extent to which the information about the *direction* of ITD change is integrated across frequencies.

Methods

The stimulus was a 1000-ms-long complex tone (flanked with 50-ms raised-cosine onset/offset ramps), consisting of two sinusoidal carriers at 400 and 700 Hz. A sinusoidal modulation in ITD was imposed on one carrier alone or the two carriers simultaneously. The ITD of each carrier was centered at 0 μs , and the modulation started and ended with the zero phase. Modulation rates of 1, 2, 4, and 8 Hz were tested. ITD modulations, when imposed on the two carriers simultaneously, were in-phase or anti-phase between the carriers. Listeners with normal hearing participated in the experiments. Experiment 1 measured

the threshold modulation depth for detecting the modulation with an adaptive method. The three-interval, three-alternative forced-choice (3I-3AFC) method was used; one "signal" interval contained a modulated stimulus, and the other two "non-signal" intervals contained unmodulated stimuli. Experiment 2 measured the discriminability between in-phase and anti-phase modulations. Modulation depth was fixed at a supra-threshold value (600 μs). In the 3I-3AFC task, the "signal" interval contained anti-phase modulations and the other two "non-signal" intervals contained stimuli with in-phase modulations. The method of constant stimuli was used to obtain the percentage of correct answers.

Results

Experiment 1 showed generally lower thresholds when the two carriers were modulated than when only one was modulated, indicating across-frequency integration of the information about the *presence* of modulation. The threshold, however, was not significantly different between the in-phase and anti-phase conditions, even when the modulation rate was as low as 1 Hz. In Experiment 2, the discrimination performance was generally at the chance level for the majority of listeners even for a 1-Hz rate.

Conclusion

The study failed to present compelling evidence that the auditory system is sensitive to the relative phase of ITD modulations for the conditions tested. This suggests that the *directional* information of even slow (~ 1 Hz) ITD modulation is lost at or below the level of across-frequency processing, or is not effectively combined at that level.

1097 The Influence of Low Frequency Distortion Products on ITD Sensitivity to Transposed Tones

Jessica Monaghan¹, Mathias Dietz^{2,3}, David Greenberg³, David McAlpine³

¹University of Southampton, ²University of Oldenburg, ³University College London

Background

A long-standing controversy concerns brain mechanisms underlying the perception of the pitch of complex sounds, particularly the so-called 'pitch of the missing fundamental' in which the perceived pitch corresponds to the reciprocal of the harmonic spacing. One potential contributing factor to missing fundamental pitches is intermodulation distortion; the non-linear mechanics of the cochlea generate an excitation pattern at the low-frequency location of the basilar membrane corresponding to the periodicity in the stimulus. The salience of distortion-generated missing fundamentals (and the level of distortion generated in the cochlea) is modulated by factors such as the phase, number and order of harmonic components, the relative timing of click trains eliciting pitch percepts, and the overall stimulus level. Pressnitzer and Patterson [Pressnitzer D and Patterson RD 2001, Distortion products and the perceived pitch of harmonic complex tones. In: Breebaart, DJ, Houtsma, AJM, Kohlrausch, A, Prijs, VF, and Schoonoven, R (Eds)

Physiological and Psychophysical Bases of Auditory Function, pages 97-104. Shaker Publishing BV, Maastricht, The Netherlands.] assessed the level of the distortion spectrum using the “cancellation of beats” method. They showed that adding low pass noise reduced the pitch percept for bandpass complex tones at high frequencies. Here, we assess the magnitude of intermodulation distortion using a binaural discrimination task.

Methods

We assessed the sensitivity of human listeners to ITDs conveyed in the envelopes of transposed tones as a function of sound level of the transposed tone and as a function of low-frequency noise level. ITD discrimination was determined for transposed tones with a fixed envelope ITD. Psychometric functions d' as a function of both stimulus level and noise level were measured with a constant stimulus procedure in a forced choice paradigm.

Results

Preliminary data indicate that, in the absence of low-pass masking noise, subjects' performance can be as good (low) as those for pure tones. Adding low-pass masking noise considerably elevates thresholds to the point that thresholds are unobtainable.

Conclusion

The exquisite sensitivity of the early auditory pathways to low-frequency binaural temporal information may mean that distortion products are particularly relevant in binaural experiments. Here we determine the minimum level of noise necessary to mask distortion products at each stimulus level.

1098 Electrical Stimulation of the Dorsal Inferior Colliculus Modulates the Auditory Lemniscal Pathway: Implications for Tinnitus

Sarah Offutt¹, Kellie Ryan¹, Lauren Berger¹, Babak Tabesh¹, Hubert Lim¹

¹University of Minnesota

Background

Hyperactivity and increased neural synchrony have been linked to tinnitus. These neural changes have been observed in the central nucleus of the inferior colliculus (ICC) of tinnitus animals and patients. Thus the inferior colliculus (IC) is a potential target for treating tinnitus. We are planning a clinical trial to investigate a new IC-based auditory midbrain implant (AMI) for hearing restoration. Many of the selected AMI patients will also have tinnitus, providing a unique opportunity to assess IC stimulation effects on tinnitus suppression directly in humans. Since the AMI array can only stimulate a few IC regions, prior to implantation it is critical to determine optimal regions for tinnitus suppression. The dorsal region of the IC (ICD) is known to modulate the ICC. Therefore, our goal is to identify regions within ICD that may lead to more effective tinnitus suppression to guide AMI implantation in humans.

Methods

Multi-site electrode arrays were positioned across ICC and ICD in ketamine-anesthetized guinea pigs. Spike activity in ICC was recorded in response to broadband noise stimulation both before and after repeated electrical stimulation of the ICD to identify any residual changes in neural activity. Histological steps were taken to produce 3D reconstructions of the midbrain and to identify the location of the electrode sites across the IC.

Results

Our results reveal complex suppression and enhancement patterns. Every ICD stimulation location resulted in suppression or enhancement of at least one ICC recording location, and every recording location was suppressed or enhanced by at least one stimulation location. Interestingly, we observed a spatial gradient of suppression strength for stimulation across the ICD that could affect just one site up to all the sites across the ICC array. The caudal-medial ICD region induced the strongest suppression across the ICC.

Conclusion

Based on our data, stimulation of any ICD location causes some suppression or enhancement within the ICC, and stimulation of specific ICD regions will induce dramatic suppression across the ICC. This complex activation pattern is favorable for tinnitus in which neural changes are highly variable across patients, and thus the location of stimulation can be altered per tinnitus case. Future studies will be performed in animal models of tinnitus to verify that ICD stimulation can suppress or enhance the appropriate neural patterns to eliminate tinnitus, including suppression of spontaneous hyperactivity and hypersynchrony.

This research was funded by University of Minnesota start-up funds and NIH NIDCD R03DC011589.

1099 Sound-Triggered Suppression of Neuronal Firing as an Underlying Mechanism of the Residual Inhibition of Tinnitus

Sergiy Voytenko¹, Ryan Longenecker¹, Alexander Galazyuk¹

¹Northeast Ohio Medical University

Background

Tinnitus can be suppressed briefly following the offset of an external sound. This phenomenon, termed “residual inhibition,” has been known for almost four decades, although its underlying cellular mechanism(s) remains unknown. In our previous work we demonstrated that many neurons in the inferior colliculus exhibit long lasting suppression of spontaneous activity following the offset of an external sound. Hyperactivity or elevated spontaneous activity in the central auditory system often correlate with tinnitus; thus we hypothesize that sound evoked suppression underlies residual inhibition. To test this hypothesis, we studied the sound evoked suppression phenomenon in animals with behavioral evidence of tinnitus.

Methods

Experiments were conducted on CBA/CAJ mice. For tinnitus induction mice were exposed to a narrowband noise centered at 12.5 kHz presented at 116 dB SPL unilaterally for 1 hour under general anesthesia (Ketamine/Xylazine). Tinnitus was assessed with gap-induced prepulse inhibition of the acoustic startle reflex. Extracellular recordings were performed in IC both contra- and ipsilateral to the exposed ear in awake restrained animals. Pure tones at neurons' characteristic frequency and/or wideband noise stimuli with 5 sec duration were delivered in the free-field.

Results

We found that mice with behavioral signs of tinnitus exhibited abnormally high spontaneous activity in the contralateral IC. Although most of these neurons showed abnormally high spontaneous firing, less than 25% of them exhibited sound triggered suppression of spontaneous firing. In contrast, more than 80% of ipsilateral ("unexposed") IC neurons exhibited long lasting suppression following the offset of a sound stimulus. Bursting patterns within spontaneous firing were not evident in either the contra- or ipsilateral IC. It is important to note that even in response to a relatively short sound duration in about 10% of recorded neurons the duration of this suppression approximated the duration of the residual inhibition of tinnitus observed in humans.

Conclusion

Unilateral tinnitus induction causes a dramatic increase of spontaneous activity in the contralateral ("exposed") IC, whereas the ipsilateral ("unexposed") IC remains similar to the control (not exposed) animals. The majority of neurons in the contralateral "exposed" IC did not exhibit long lasting sound evoked suppression. The time course of suppression in the ipsilateral IC corresponds to the time course of residual inhibition in tinnitus patients.

This research was supported by grant R01 DC011330 from the National Institute on Deafness and Other Communication Disorders of the U.S. Public Health Service.

1100 Blast-Induced Tinnitus and Changes in Spontaneous Firing Rates Along the Auditory Axis in Rats

Hao Luo¹, Xueguo Zhang¹, Srinivas Kallakuri¹, Jinsheng Zhang¹

¹Wayne State University

Background

High-pressure blast shock waves are known to cause tinnitus. Although the underlying mechanism may be due to damage to structures in the ear and/or direct brain impact that triggers a cascade of neuroplastic changes in both auditory and non-auditory centers, there is a lack of investigation of electrophysiological changes following blast-induced tinnitus. In this study, we used a rat model and investigated how blast influenced behavioral evidence of tinnitus and spontaneous firing rates (SFR) in the dorsal cochlear nucleus (DCN), inferior colliculus (IC) and

auditory cortex (AC) at different time points after blast exposure.

Methods

Forty-two adult Sprague-Dawley rats were divided into three groups: one day, one month and three months after a single blast exposure in the left ear. Each group had nine blasted and five age-matched control rats. Gap detection acoustic startle reflex behavior was used for evaluating tinnitus and auditory brainstem responses were measured before and after the blast exposure. SFRs were simultaneously recorded in the DCN, IC and AC after blast exposure. At the end of experiments, all animals were euthanized and their brains were processed histologically to verify the electrode positions.

Results

Our behavior data showed that blast-induced tinnitus occurred at all frequency bands immediately after, at high frequency bands one month after, and eventually at a high- and a low-frequency band three months after the blast exposure. Compared to control rats, an early onset increase in SFR was found in the DCN of rats with tinnitus, which lasted for a month before returning to a normal level three months after the blast exposure. An increased SFR in the IC of rats with tinnitus persisted through all recording sessions. In the AC of rats with tinnitus, onset decrease in SFR occurred, which lasted for one month before reversing to an increase in SFR at three months after the blast exposure.

Conclusion

These results demonstrated that blast-induced tinnitus does not involve a uniform manifestation of increased SFR along the auditory axis. Instead, changes in SFR happen in different directions at different levels of the central auditory system. The data also suggest that blast-induced early onset tinnitus may be related to increased SFR in the brainstem whereas delayed tinnitus may be attributed to increased SFR in the IC and AC. This information may be important for developing treatment strategies of blast-induced tinnitus based on hyperactivity change patterns along the auditory axis.

1101 Behavioural, Neural and Histological Correlates of Tinnitus in the Guinea Pig

Joel Berger¹, Ben Coomber¹, Trevor Shackleton¹, Mark Wallace¹, Alan Palmer¹

¹MRC Institute of Hearing Research

Background

Animal models of tinnitus are essential to furthering our understanding of neural changes accompanying the condition. Deficits in gap detection in behavioural tests and increased spontaneous neuronal firing rates (SFRs) in the inferior colliculus (IC) are used as markers for tinnitus.

Methods

We sought a histochemical marker of tinnitus in guinea pigs (GPs) by studying changes in the expression of nitric oxide synthase (NOS), a pathological marker, in the

ventral cochlear nucleus (VCN). 16 GPs were subjected to unilateral noise trauma, tested behaviourally over an 8-week period and IC recordings were performed. Hearing status was assessed using auditory brainstem responses.

Results

Using strict criteria, 45% of GPs exhibited behavioural evidence of tinnitus. These same animals also showed a 30% increase in the number of NOS containing neurones in the VCN of the deafened side at eight weeks after noise exposure. By contrast, deafened animals with no behavioural evidence of tinnitus at eight weeks showed symmetric NOS staining. Increased SFRs were evident in noise-exposed GPs, when compared with control GPs, whether or not there was behavioural evidence of tinnitus.

Conclusion

The behavioural test reliably indicated the presence of tinnitus. However, our data indicate that elevated SFRs in the IC are not an unequivocal marker for tinnitus, as increased SFRs were apparent after noise exposure regardless of whether tinnitus was present or not. However, sustained changes in NOS expression in the VCN do appear to be a robust marker for tinnitus.

1102 Unexpected Increases in Ipsilateral Inferior Colliculus Spontaneous Activity in a Rat Model of Tinnitus

Stefanie Kennon-McGill¹, Dianne Durham¹, Hinrich Staecker¹, Thomas Imig¹

¹University of Kansas Medical Center

Background

Although common, tinnitus is not yet well understood. One hypothesis is that damage to the peripheral auditory system changes the balance of excitatory and inhibitory inputs to the central auditory system, causing an increase in spontaneous activity (SA) in central auditory structures that is perceived as tinnitus. We measured changes in SA in the central auditory system by utilizing radioactively labeled 2-deoxyglucose (2DG). 2DG is used to measure metabolic activity in the nervous system, and we used it to evaluate changes in SA of the inferior colliculus (IC) following sound damage.

Methods

We exposed anesthetized male Long-Evans rats to a unilateral 118 dB SPL, 16 kHz pure tone for 4 hours. A minimum of two weeks after sound damage, following electrophysiological recordings, we injected rats with 2DG. Because many tinnitus studies evaluate SA in anesthetized animals, half of the animals were anesthetized with a ketamine-xylazine mix prior to 2DG injection, allowing for a direct comparison of activity in anesthetized and unanesthetized animals. Each rat was placed in a sound proof chamber for 45 minutes following injection, to allow for optimal 2DG uptake. We then sacrificed the animals, harvested the brains, and sectioned them in 40 µm sections to be placed on film. One week later, the film was developed and the radioactivity was

measured in ten sectors along the tonotopic axis of the central nucleus of the IC (ICc).

Results

All four groups (control, anesthetized, n=5; damaged, anesthetized, n=4; control, unanesthetized, n=9; damaged, unanesthetized, n=15) displayed an increase in uptake along the tonotopic map of the ICc, which corresponds with our previously published data. However, the overall level of 2DG uptake was lower in the anesthetized groups compared to the unanesthetized groups. In both the anesthetized and unanesthetized damaged animals, the ICc contralateral to the damaged ear, which receives the majority of its input from that ear, displayed levels of uptake similar to that in control animals. However, the ipsilateral ICc, in both anesthetized and unanesthetized damaged animals, had significantly higher uptake compared to contralateral ICc or ICc in control animals.

Conclusion

The use of anesthesia appears to have an effect on the overall level of metabolic activity in the IC. Interestingly, both the anesthetized and unanesthetized groups displayed a significant increase in activity in the IC ipsilateral to the damaged ear.

1103 Hyperactivity in Animals with a Tonal Tinnitus Percept Is Narrowband

Tessa-Jonne Ropp¹, Kerrie Tiedemann¹, Eric Young¹, Brad May¹

¹Johns Hopkins University

Background

In previous work, little attention has been paid to the differences between neural responses to a sound exposure that did or did not produce a tinnitus percept. Here, neurons in rat central nucleus of the inferior colliculus were studied in noise-exposed rats characterized for the presence of a tonal tinnitus percept using a gap inhibition acoustic startle response paradigm. Recordings were done in three groups of animals: normal, exposed with tinnitus, and exposed without tinnitus. Presumably the neural correlates of tinnitus can be isolated from the effects of sound exposure in this way.

Methods

Rats were unilaterally exposed to a 16kHz tone at 120 dB SPL for 2 hours. One month post-exposure, animals were screened for tinnitus using GIASR.

For electrophysiology, animals were anesthetized (im Ketamine-Acepromazine,30:1). A fenestration was made anterior to lambda and single neurons were recorded by advancing a tungsten microelectrode (AM Systems) through occipital cortex to ICC.

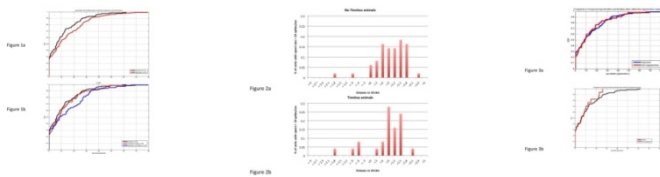
The ear contralateral to the exposure was stimulated using a free-field speaker with tones (1 to 50kHz). Once a neuron was isolated, response maps, rate-level functions and a 10-minute recording of spontaneous activity were recorded.

Results

Relative to normal baselines, sound-exposed rats showed an increase in spontaneous activity across all BFs (Figure 1a). When sound-exposed rats were divided into tinnitus versus no-tinnitus subgroups based on behavioral screening results, the no-tinnitus group showed significant hyperactivity, while the tinnitus subgroup did not (Figure 1b). We attribute this result to the narrowband elevation of spontaneous rates in the tinnitus subgroup (Figure 2a) versus the global elevation of spontaneous rates in the no-tinnitus subgroup (Figure 3b). Within this narrowband region of hyperactivity, the spontaneous rates of the tinnitus subgroup matched the global rate elevations of the no-tinnitus subgroup (Figure 3a). Outside the region of hyperactivity, the tinnitus subgroup showed lower spontaneous rates than normal controls (Figure 3b).

Conclusion

Rats that test positive for tonal tinnitus display elevated spontaneous rates that are confined to a narrow range of frequencies. The region of hyperactivity is predicted by the tinnitus pitch, and it may be enhanced by abnormally low levels of activity at surrounding frequencies. Global hyperactivity may fail to produce a positive tonal tinnitus test either because these subjects experience a broadband tinnitus percept not captured by our current behavioral paradigm, or tinnitus is derived from the frequency-organized contrast of hyperactive and hypoactive neurons.



1104 Co-Activation of the Somatosensory and Auditory Pathways to Induce Central Auditory Plasticity as a New Approach for Treating Tinnitus

Benjamin Smith¹, Craig Markovitz¹, Luke Parker¹, Cory Gloeckner¹, Hubert Lim¹

¹University of Minnesota

Background

We propose a new noninvasive stimulation approach for treating tinnitus, which we call Multi-modal Stimulation Therapy (MST). An underappreciated organization of the brain for treating neurological disorders is the dense and topographic interconnectivity among the sensory, motor, cognitive, and limbic centers. Relevant for MST, receptive fields across the entire body project onto and can modulate auditory neurons. Considering that tinnitus has been associated with abnormal spiking patterns of central auditory neurons, including those within the central nucleus of the inferior colliculus (ICC) and primary auditory cortex (A1), we conceived of the idea of electrically stimulating across the body to modulate tinnitus-affected neurons. We present our initial feasibility studies in guinea pigs.

Methods

We positioned 32-site electrode arrays in different locations throughout the ICC and A1 in ketamine-anesthetized guinea pigs and recorded spontaneous and acoustic-driven activity. Acoustic stimuli consisted of pure tones and broadband noise. We compared the ICC and A1 neural activity before and after MST, which consisted of body stimulation using subcutaneous needle electrodes. For the MST paradigm, we repeatedly stimulated (≥ 100 trials) each of eight body regions (left leg, right leg, back, genital area, left shoulder, right shoulder, neck, tongue) paired with acoustic stimulation to induce long-term neural changes within ICC and A1. The delays between electrical and acoustic stimulation as well as stimulus levels varied across body locations.

Results

MST induced long-term changes (e.g., tens of minutes) across ICC and A1. These changes included increases or decreases in spontaneous and/or acoustic-driven activity. Interestingly, different body locations affected different central auditory neurons, which suggests that different MST parameters may be able to target specific and different neurons driving the tinnitus. Only a small percentage of auditory neurons were affected by each body location, and thus additional MST parameters (e.g., multi-site stimulation, varying pulse trains, customized acoustic stimuli) need to be investigated to induce greater auditory plasticity.

Conclusion

Our preliminary animal studies demonstrate the potential for modulating central auditory neurons using MST. Further studies need to be performed in tinnitus animals to demonstrate that MST can fix abnormal tinnitus-related neural activity, including suppression of hyperactivity and hypersynchrony. Additional body locations and stimuli will be investigated to identify effective MST parameters that can be tested in tinnitus patients.

1105 Discovery of Somatotopy Within the Inferior Colliculus: Implications for a New Tinnitus Treatment

Cory Gloeckner¹, Jake Tilleson¹, Daniel Kastl¹, Benjamin Smith¹, Hubert Lim¹

¹University of Minnesota

Background

The brain has an immense capacity to integrate and coordinate information across multiple sensory and motor modalities necessary for daily function and survival. Even a simple reflex orienting the body and head towards a visual and/or auditory cue requires precise and rapid coordination among sensory and motor circuits. Previous studies have identified superimposed topographic maps of visual space, sound localization, and somatosensory representation within the superior colliculus. Considering the large number of somatosensory projections to the inferior colliculus (IC) and the involvement of the IC in the orienting reflex, we performed experiments to identify a

similar topographic map of somatosensory responses within the IC.

Methods

We positioned a 32-site electrode array into the IC of anesthetized guinea pigs at various locations to form a 3-D grid of placements across the entire IC. We characterized the acoustic-driven responses on each site to confirm their placement within different IC subregions. We then electrically stimulated each of eight different body locations and recorded the corresponding neural activity across the IC. Histological reconstruction of the IC and the locations of recording sites were obtained for analysis.

Results

Electrical stimulation of each body site elicited excitatory responses within specific regions of the IC in a spatially-ordered pattern. Stimulation of the legs and back activated more caudal-medial regions of the IC while stimulation of regions closer to the head activated more lateral regions. Although each body region projected predominantly to a unique IC area, there were also projections to overlapping regions across IC. Additionally, PSTH shape, activation threshold and latency generally varied for different IC locations and for different body stimulation locations.

Conclusion

Our discovery of a somatotopic map within an auditory-dominant nucleus reveals an even stronger coupling and organization among the different sensory modalities than previously reported. Considering the large and well-organized projection of the body to the auditory pathways and the ability to electrically stimulate the body regions noninvasively, we conceived of the idea of activating the somatosensory pathways to modulate auditory neurons for tinnitus treatment. We are currently investigating if stimulation across the body in a coordinated pattern can induce long-term changes within the central auditory system to suppress/fix the tinnitus-affected neurons. Further details are presented in our companion poster (Benjamin Smith et al., ARO 2013).

This research was supported by University of Minnesota start-up funds and NSF IGERT grant DGE-1069104.

1106 Generation of Induced Neurons from Cochlear Non-Sensory Epithelial Cells in Adult Mice

Koji Nishimura¹, Rachel Weichert², Alain Dabdoub^{1,3}

¹Sunnybrook Research Institute, ²SDSU Department of Audiology, ³Department of Otolaryngology, University of Toronto

Background

Spiral ganglion neurons (SGNs), which are auditory primary neurons, transmit electrical stimulation from cochlear hair cells to the cochlear nucleus in the brainstem. Once lost, SGNs do not regenerate; therefore, the development of methodologies that could be used to induce the regeneration of SGNs in a damaged ear has the potential to significantly increase the likelihood of

positive outcomes for hearing impaired individuals. A recent study has demonstrated that a combination of transcriptional factors, including *Ascl1*, a neurogenic bHLH transcription factor, sufficed to convert mouse embryonic and postnatal fibroblasts into functional induced neurons (iNs) *in vitro* (Vierbuchen *et al.*, 2010). We previously generated iNs by overexpression of *Ascl1* from cochlear non-sensory epithelial cells (NSECs) at high efficiency at early developmental stages (Weichert *et al.*, 35th ARO). In this study, our aim was to examine whether we could generate iNs from NSECs in juvenile or adult stages and to elucidate the mechanism of neural induction.

Methods

Cochleae from ICR mice at embryonic day 13.5, postnatal day 1, 5, 10 and 20 were dissected out. Following dissection and exposure of the sensory epithelium, individual cochlear explants were transfected with the *Ascl1.nucEGFP* expression vector or control vector. Explants were cultured for seven days *in vitro* and analyzed for immunohistochemistry. To determine the efficiency of induction of a neuronal fate, the percentage of transfected cells that also expressed the neuronal marker β III-tubulin was determined for cells transfected with *Ascl1.nucEGFP* or a control vector *pCIG.nucEGFP*. Explants at E13.5 were exposed to BrdU three days after electroporation until day 7 to determine whether iNs from NSECs proliferate during conversion.

Results

91% of cells transfected with *Ascl1.nucEGFP* were positive for β III-tubulin at E13.5, and this efficiency remained high at P20 (46%). No cells transfected with the control vector were positive for β III-tubulin indicating the specificity of the result. β III-tubulin positive NSECs transfected with *Ascl1.nucEGFP* did not uptake BrdU, suggesting that direct conversion by *Ascl1* occurred without cell proliferation.

Conclusion

Overexpression of *Ascl1* is sufficient to reprogram cochlear NSECs into neurons in adult mice. Gene therapy presents an attractive strategy for treating neurodegenerative disease and direct reprogramming of mature cells from one lineage to another constitutes an alternative approach for the generation of specific cell types. Our finding is an important step in understanding and achieving the induction of regeneration of SGNs in the mature cochlea.

1107 Gross Neural Responses Shown to Be from the Cochlear Apex by Ototoxic Injections

Jeffery Lichtenhan¹, Jared Hartsock¹, John Guinan^{2,3}, Alec Salt¹

¹Washington University in St. Louis, ²Eaton-Peabody Laboratory, ³Harvard Medical School

Background

We recently reported that the auditory nerve overlapped waveform (ANOW) recorded from the round window provides an objective measure of low-frequency (<=700

Hz) neural thresholds (Lichtenhan et al. Ear Hear. In Press). In the present study, a pharmacological method was used to assess the origin along the cochlea of simultaneously recorded ANOW, cochlear microphonics (CM), and onset action potentials (AP) evoked by low-frequency stimuli. Compound action potentials (CAP) to high-frequency (≥ 2 kHz) tone bursts aided the interpretation of the low-frequency measures.

Methods

Ototoxic pharmaceuticals were 150 mM KCl, 250 ng/ml tetrodotoxin (TTX), or 20 mM sodium salicylate in artificial perilymph. Injection into perilymph was with a pipette sealed into the cochlear apex. Injection at this site induces a volume flow from the injection toward the cochlear aqueduct at the base of scala tympani. This results in an increase in drug concentration progressing from apex to base. Injections were started at a rate of 50 nl/min, increased to 100 nl/min after 10 mins, and to 200 nl/min after 30 mins, to partially compensate for the increasing cross-sectional area of scala tympani along the cochlear partition.

Results

ANOW and AP to low-frequency (353, 500, and 707 Hz), low-level (50 dB SPL) stimuli were rapidly abolished by injections, demonstrating the predominantly apical origins of these responses. ANOW and AP responses to the higher-level stimuli (65 dB SPL) were abolished later, confirming the broader origins of high-level responses. CAP thresholds to higher frequencies were abolished even later and sequentially in low- to high-frequency order, in accordance with their well-known spatial origins. Approximately 15 minutes after the start of a TTX injection, the CM to low-frequency tones was partially reduced, suggesting a neural component to CM originating in the apical turn. About 60 minutes after a KCL injection, the CM was fully abolished, suggesting the component of the CM that remains after TTX originates predominantly from hair cells in the basal turn.

Conclusion

The results confirm that the ANOW response from low-frequency, low-level tones originates in the cochlear apex with little contamination by basal-turn responses, and that ANOW provides a good metric for cochlear sensitivity at low frequencies.

Supported by 5R01DC001368-20

1108 Modeling the Time-Varying and Level Dependent Effects of the Olivocochlear Reflex in Auditory Nerve Responses

Christopher J. Smalt¹, Michael G. Heinz^{2,3}, Elizabeth A. Strickland³

¹School of Electrical and Computer Engineering, Purdue University, West Lafayette, IN, ²Weldon School of Biomedical Engineering, Purdue University, West Lafayette, IN, ³Department of Speech, Language, and Hearing Sciences, Purdue University, West Lafayette, IN

Background

The medial olivocochlear reflex (MOCR) has been implicated as a source of benefit for listening in noisy environments. This benefit is an anti-masking effect enabled by a reduction in auditory nerve (AN) firing to continuous background noise, resulting in increased sensitivity to a stimulus of interest. MOC neurons synapse on outer hair cells (OHCs), and inhibit basilar membrane responses through the reduction of cochlear amplifier gain. The current study implements the time-varying, characteristic frequency (CF), and level dependent effects of the MOCR within the framework of a well-established computational model for normal and impaired hearing AN responses (Zilany and Bruce, 2006) based on physiological evidence in humans and cats.

Methods

A second order linear system was used to model the time-course of the efferent feedback loop, and was based on measurements in humans using stimulus-frequency otoacoustic emissions. The stimulus level dependence of the MOCR was determined using a tone-in-noise paradigm, fitting model parameters to previous data from AN fibers in decerebrate cats. The model includes the effect of efferent feedback for both the ipsilateral and contralateral pathways.

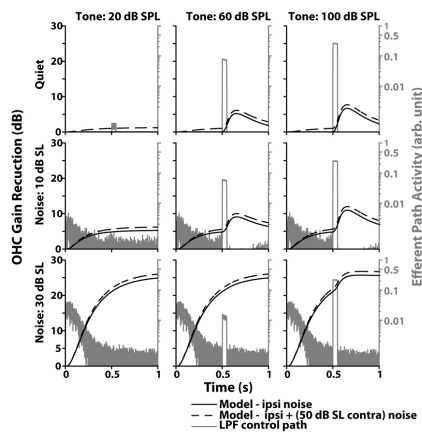
Results

The time-course of the model, after being fit to AN data, is shown in the supplemental figure for a tone at 8 kHz with ipsilateral (solid) and binaural broadband noise (dashed). OHC gain reduction is shown as a function of time, with increasing tone level (horizontally), and with increasing noise levels (vertically). The result is a time-varying, level-dependent OHC gain dependent on both ipsilateral and contralateral stimulus amplitude. Also included is the physiologically observed CF dependent nature of the MOC efferents, which has been shown to be correlated with the innervation density of efferent terminals. The MOCR improves detection of a tone in noise by decreasing the gain of the OHCs, consistent with AN data in cats.

Conclusion

The AN model presented here allows us to study the complex interactions of the MOCR within the peripheral auditory system, including the bilateral interaction of stimuli to both ears. The MOCR may be important for speech recognition in noisy situations as well as for protection from acoustic trauma. Further study of this model and its efferent feedback loop may contribute to our

understanding of sensorineural hearing loss in noisy situations for hearing-impaired listeners. [Research supported by NIH(NIDCD) R01 DC008327 and T32 DC00030.]



1109 Expression of Axon Guidance Molecules in Developing Avian Auditory Pathways

Michelle Allen-Sharpley¹, Michelle Tjia¹, Karina Cramer¹
¹University of California, Irvine

Background

The development of connections between the ear and the brain occurs with great fidelity during early embryogenesis. To explore the mechanisms underlying this process, we investigated expression patterns of five axon guidance molecules in the avian inner ear, eighth cranial nerve (nVIII) and hindbrain from E5 – E8 when the central connections are being formed. The molecules tested were chosen to survey classes of candidate molecules and include characterized molecules with opposing effects on axon growth. Further selection included molecules with suspected involvement in cranial nerve and/or inner ear development.

Methods

We performed immunolabeling of coronally sectioned chick hindbrain together with nVIII and inner ears using antibodies against Neuropilin-1 (NPN-1), Cadherin-6 (Cad-6), Semaphorin-3A (Sema-3A), Slit-2, and Netrin-1. In some cases we counterstained with Neurofilament (NF) to identify axons, TUBB-3 to identify neurons, and/or Sox10 to identify glial lineages.

Results

We found low and overlapping expression of the respectively repellent and attractant molecules, Slit-2 and Netrin-1, from E5-E6 that disappeared by E7 when central auditory connections are being formed. Patterns consistent with nVIII axon guidance were seen with NPN-1, Cad-6, and Sema-3A. NPN-1 is highly expressed in glia along the peripheral edge of the PNS-CNS junction, and in vestibular axons. Cad-6 is expressed briefly in a gradient at the PNS-CNS transitional zone as nVIII axons enter this region. Cad-6 appears differentially expressed in prospective auditory and vestibular components of nVIII.

Sema-3A is expressed in patches surrounding vestibular projections, potentially consistent with its role in channeling growing axons via repulsion cues. NPN-1, Cad-6 and Sema-3A also have unique expression profiles in the central auditory nuclei n. magnocellularis (NM) and n. laminaris (NL) when NM axons project toward NL.

Conclusion

The cell-type specificity and developmental expression patterns suggest that these molecules may guide formation of auditory circuitry during embryogenesis. These observations support a role for coordinated functions of multiple classes of molecules in the formation of these pathways.

1110 Guidance of Spiral Ganglion Neurites by Micropatterned Physical Cues Involves TRP Channels, Ca²⁺ and Cyclic Nucleotide Second Messenger Systems and RhoA/Rho-Associated Kinase (ROCK) Signaling

Shufeng Li^{1,2}, Bradley Tuft³, Joseph Clarke¹, Linjing Xu¹, Scott White³, Allan Guymon³, Marlan Hansen¹

¹Departments of Otolaryngology-Head and Neck Surgery, University of Iowa, ²Departments of Otolaryngology-Head and Neck Surgery, Eye & ENT Hospital of Fudan University, ³Departments of Chemical Engineering, University of Iowa

Background

We recently demonstrated that microchannels generated by photopolymerization of methacrylate polymers guide neurite growth from spiral ganglion neurons (SGNs). While the signaling mechanisms activated by chemotactic molecules (e.g. semaphorins) to direct neurite growth have been widely explored, the mechanisms by which neurons sense changes in the physical environment and transduce them into directed growth remain largely unknown. Here we used dissociated spiral and trigeminal ganglion cultures to explore the contribution of TRP channels, Ca²⁺ and cyclic nucleotides, and the downstream effectors, RhoA and ROCK, to neurite guidance by micropatterned substrates.

Methods

SKF96365, gentamicin, and RNA interference were used to inhibit TRP channels. We increased [Ca²⁺]_i by depolarizing the cultures with elevated (25 mM and 50mM) extracellular K⁺ (25K and 50K). Ryanodine or xestospongine C, which inhibit ryanodine-sensitive channels or inositol-1,4,5-trisphosphate receptors, respectively, were used to decrease Ca²⁺ release from internal stores. We applied cpt-cAMP, a cyclic AMP analog, or 8-bromo-GMP, a cyclic GMP analog, to investigate the function of cyclic nucleotide second messenger systems. We further employed a FRET-based biosensor and in situ Rho GTPase activity assay to quantify RhoA activity in growth cones. Phosphorylated (activated) ROCK was detected by immunolabeling. RhoA and ROCK inhibitors and siRNA-mediated ROCK knockdown were used to investigate the contribution of RhoA/ROCK signaling to SGN neurite guidance by micropatterned substrates.

Results

SKF96365 and gentamicin each decreased neurite alignment to micropatterns. Further, growth cones immunolabeled with anti-TRPV1 antibodies and siRNA knockdown of TRPV1 decreased alignment. 25K and 50K significantly reduced neurite alignment suggesting that chronically elevated $[Ca^{2+}]_i$ inhibits neurite alignment. Further, ryanodine or xestospongin C also decreased neurite alignment whereas inhibition of external Ca^{2+} entry with cadmium did not affect alignment. Cpt-cAMP reduced neurite alignment while 8-bromo-GMP increased neurite alignment suggesting reciprocal antagonism between these cyclic nucleotides. Micropatterns increased RhoA activity and ROCK phosphorylation in growth cones. Inhibition of RhoA reduced neurite alignment while activation of RhoA further enhanced alignment. The ROCK inhibitors, H1152 or Y27632, each reduced neurite alignment in a dose-dependent manner. Likewise, siRNA knock-down of ROCK significantly decreased alignment to the micropatterns.

Conclusion

These results suggest a signaling network that senses and mediates growth cone responses to environmental physical cues involving TRP channels, Ca^{2+} and cyclic nucleotides as second messenger systems, and RhoA/ROCK as downstream effectors.

1111 Excitotoxic Trauma to Cochlear Afferent Synapses Is Associated with Ca^{2+} Entry Via Ca^{2+} -Permeable AMPA Receptors

Ning Hu¹, Qiong Wang¹, Dillon Harris¹, Dylan Todd¹, Steven Green¹

¹Departments of Biology and Otolaryngology, University of Iowa

Background

Excitotoxic trauma causes rapid loss of synapses between inner hair cells (IHCs) and type I spiral ganglion neurons (SGNs). Noise damage to synapses appears to be a consequence of such excitotoxicity. Ca^{2+} entry to postsynaptic terminals via NMDA receptors has been implicated as the major cause of excitotoxicity in the brain but plays a minor role, if any, in the cochlea. Here we ask whether excitotoxicity at the IHC-SGN synapse is associated with Ca^{2+} entry and what is the Ca^{2+} entry route to the SGNs.

Methods

Excitotoxic trauma to IHC-SGN synapses was quantified by counting contacts between IHC-SGN axon contacts in kainate-exposed four days *in vitro* (DIV) organotypic cochlear cultures (Wang & Green J. Neurosci., 2011). Ca^{2+} imaging was done using 1DIV dissociated SGN cultures (Hegarty et al. J. Neurosci., 1997). Oregon Green-BAPTA1 was used as the Ca^{2+} reporter. All cultures were from postnatal day 4-6 rats.

Results

Two-hour exposures of cochlear cultures to 100-500 μ M kainate caused a dose-dependent loss of IHC-SGN contacts, with complete loss at 500 μ M. Cotreatment with IEM1460, a blocker of Ca^{2+} -permeable (GluA2-lacking) AMPA receptors (CP-AMPA) partially reduced loss of IHC-SGN contacts in 500 μ M kainate. In contrast, nifedipine and isradipine, blockers of L-type voltage-gated Ca^{2+} channels (L-VGCCs) had no protective effect, although it did potentiate the protection of IEM1460. Kainate (100-500 μ M) caused an increase in intracellular Ca^{2+} concentration, $[Ca^{2+}]_i$. IEM1460 (20-100 μ M) completely blocked this Kainate-induced increase in $[Ca^{2+}]_i$, implying that CP-AMPA is the Ca^{2+} entry route in excitotoxic trauma. In contrast, the increase in $[Ca^{2+}]_i$ following depolarization with 30 mM K^+ , previously shown (Hegarty et al., 1997) to be due primarily to Ca^{2+} entry via L-VGCCs, was unaffected by IEM1460. Immunohistochemistry using isoform-specific anti-GluA antibodies suggests that GluA3 and GluA4 are the predominant GluA subunits in these postnatal rats, consistent with the presence of CP-AMPA.

Conclusion

Blockade of CP-AMPA by IEM1460 reduces excitotoxic trauma and prevents Kainate-induced Ca^{2+} entry in SGNs *in vitro*. L-VGCC blockers are not protective. Taken with previous data showing that NMDAR agonists do not contribute to excitotoxic trauma at IHC-SGN synapses, we infer that excitotoxic trauma at these synapses in postnatal rats involves Ca^{2+} entry via CP-AMPA, not L-VGCCs or NMDARs.

(Supported by NIH R01 DC009405 & P30 DC010362)

1112 Trade-Off Between Reliability of Spiking and High-Frequency Phase-Locking in the Barn Owl's Auditory Nerve

Christine Koepl¹, G. Bjorn Christianson², Jose L. Peña³
¹Carl von Ossietzky University Oldenburg, ²UCL Ear Institute, University College London, ³Department of Neuroscience, Albert Einstein College of Medicine

Background

Transduction by hair cells and coding by primary afferents are crucial stages in auditory sensory coding. Auditory receptors do not reproduce every aspect of a stimulus equally well, which in turn constrains central processing. In order to accurately encode both the identity and the fine timing of complex sounds, the neural response should be as similar as possible over multiple presentations of the same stimulus while preserving phase information. However, the response pattern of single auditory nerve fibres can be highly variable. We hypothesised that the spiking mechanism, which emerges at the primary afferent synapse with the hair cell, plays a role in the variability. The barn owl's auditory afferents are known for their ability to phase-lock to frequencies up to 10 kHz, allowing us to explore the relationship between response variability and phase locking over a broad frequency range.

Methods

We recorded the responses of single auditory-nerve fibres in anaesthetised barn owls to repeated presentations of the same noise token and characterised their phase-locking using tones and their spectral tuning using reverse correlation to unfrozen noise.

Results

Surprisingly, the increased temporal precision of auditory-nerve fibres at high best frequencies (BF) did not correlate with repeatable spike timing for complex sounds. The reliability of spiking, quantified as signal-related power, decreased with increasing best frequency, while the temporal dispersion of phase-locked discharges also decreased. However, within fibres of similar BF, there was no correlation between reliability and temporal dispersion. A spiking model with BF-dependent parameters drawn from the data was able to reproduce the decline of response reliability with increasing BF.

Conclusion

Our data suggest that reliability of discharge and spike timing precision are not directly linked in single auditory-nerve fibres. While both measures correlated tightly with BF, we found no direct relation between them. Thus, the major source of unreliability in the auditory-nerve discharge was not temporal jitter. Rather, it appeared to be a frequent failure to spike to preferred segments of the stimulus. We propose that the inability to respond to every cycle at higher frequencies is the source of increasing frequency of spiking failures. Higher-order neurons are able to mitigate such failures through convergence of many primary inputs. Thus, the representation of phase at high frequencies may come at the expense of decreased reliability of spiking. This requires an increased total number of auditory nerve fibres to adequately represent sounds.

1113 Functional Changes in Spiral Ganglion Neurons Following Exposure to Neurotrophins

Karina Needham¹, Bryony Nayagam¹, Ricki Minter¹, Stephen O'Leary¹

¹University of Melbourne

Background

Neurotrophins such as brain-derived neurotrophic factor (BDNF) and neurotrophin-3 (NT3) provide an effective tool for the rescue and regeneration of spiral ganglion neurons (SGNs) following sensorineural hearing loss. Applied separately, BDNF and NT3 alter the firing properties of SGNs and differentially regulate ion channel expression *in vitro*. The present study examines the impact of combined BDNF and NT3 application on the activity of SGNs, and the contribution of hyperpolarization-activated currents (I_h).

Methods

Dissociated SGNs from early post-natal rats (P3-7) were cultured for 1 or 2 days *in vitro* (DIV). Untreated SGNs were grown in Neurobasal media alone, while neurotrophin-treated (NT) cultures were supplemented

with both BDNF and NT3 at 50 ng/ml or 10 ng/ml each. Whole-cell patch-clamp recordings were made in both current- and voltage-clamp modes to assess neural activity and the contribution of I_h respectively.

Results

Current-clamp recordings revealed a rapidly-adapting response during sustained depolarization for 96% of SGNs (n=117), with no difference observed between NT and untreated SGNs. Resting membrane potential was consistent between all groups, whilst input resistance was significantly reduced in SGNs exposed to 10 ng/ml neurotrophins only. Firing threshold and latency were influenced by the presence of combined neurotrophins as well as time *in vitro*. In voltage-clamp, membrane hyperpolarization induced a slowly activating, non-inactivating inward current sensitive to the hyperpolarization-activated (HCN) channel blocking compound, ZD7288. The ZD7288-sensitive I_h increased significantly in SGNs exposed to combined BDNF and NT3. At 2 DIV, current density was -15.1 ± 3.0 pA/pF (n=21) in untreated SGNs, compared to -25.9 ± 3.2 pA/pF (n=25) at 50 ng/ml NT, and -28.5 ± 5.3 pA/pF (n=16) for NT at 10 ng/ml. The increase in I_h magnitude was also accompanied by a shift in the activation curve and kinetics. SGNs treated with neurotrophins at 50 ng/ml displayed a 9 mV hyperpolarizing shift in half-activation compared to untreated SGNs, whilst NT at 10 ng/ml did not display a significant shift from either group. In addition, time constants were slower at 50 ng/ml NT compared to both untreated and 10ng/ml NT SGNs.

Conclusion

Exposure to combined BDNF and NT3 increases the activity of hyperpolarization-activated currents, but does not generate a shift in SGN firing adaptation.

1114 Dynamic Range Adaptation in the Mouse Auditory Nerve

Bo Wen^{1,2}, Ann E. Hickox^{1,3}, Luke Shaheen^{1,3}, Tobias Moser⁴, M. Charles Liberman^{1,2}, Bertrand Delgutte^{1,2}
¹Eaton-Peabody Laboratories, Massachusetts Eye and Ear Infirmary, Boston, MA 02114, ²Department of Otolaryngology and Laryngology, Harvard Medical School, Cambridge, MA 02115, ³Harvard-MIT Division of Health Sciences and Technology, Harvard University, Cambridge, MA 02115, ⁴Dept. of Otorhinolaryngology, Göttingen University Medical School, D-37075 Göttingen, Germany

Background

Dynamic range adaptation refers to the shift of a neuron's dynamic range toward the most probable levels in a continuous, dynamic stimulus, thereby improving the precision of stimulus level coding. This phenomenon has been shown at several processing centers of the auditory pathway, including the auditory nerve (AN), the inferior colliculus, and the auditory cortex, and in different species including guinea pigs, monkeys, and cats. Here for the first time, we demonstrate this phenomenon in the AN fibers of wild-type and Bassoon knockout mice. In the

knockout mice, the synaptic ribbons are not anchored to the active zone of inner hair cells.

Methods

We investigated both the amount and the time course of dynamic range adaptation by recording from AN fibers in anesthetized mice using CF-tone stimuli in which the mean sound level of the stimuli switches between two values every 3 s. During each 3-s half-cycle, the level was randomly drawn every 25 ms from a distribution containing a 12-dB wide high-probability region (HPR) imposed on a uniform background.

Results

We found that AN fibers in both wild type and Bassoon knockout mice show dynamic range shift in response to these "switching-HPR" stimuli. Adaptation of AN average firing rate occurs over a few hundreds of milliseconds, comparable to that found in the cat AN (Wen et al., *J. Neurophysiol*, 108: 69-82).

Conclusion

Overall, our work suggests that the adaptive processing in response to changes in sound level distribution occurs at the hair-cell/AN synapse and does not require the pre-synaptic ribbon.

Supported by NIH grants R03 DC011156, R01 DC002258, R01 DC000188, and P30 DC005209.

1115 The Representation of Vocalizations in the Mouse Auditory System

Jose Garcia-Lazaro¹, Nicholas Lesica¹

¹University College London

Background

One of the main functions of the auditory system is to process sounds elicited by conspecifics, therefore, it is plausible that the mechanisms underlying hearing and vocalizing have co-evolved to match each other. Mice are an increasingly important model in biomedical and auditory research that seem peculiar because there is a mismatch between the acoustic features of the communication calls that they produce and the capabilities of their auditory system to process these sounds. In other words, we cannot as yet, explain how mice hear each other given what we know of their auditory system.

Methods

To investigate the mechanisms underlying the processing of high frequency vocalizations, we recorded extracellular responses of single auditory nerve (AN) fibers and neurons in the inferior colliculus (IC) of anesthetized CBA/Ca mice using a combination of glass micropipettes and silicon array electrodes. The basic response properties of neurons at these two levels of the auditory pathway were characterized using stimuli that consisted of pure tones with frequencies between 1 and 90 kHz. In addition to tones, we recorded responses to conspecific vocalizations whose frequency components were contained within the range from 60 to 90 kHz. These sounds were carefully chosen to be representative of the vocal repertoire of the

CBA/Ca strain and other strains extensively used for biomedical research.

Results

We found that most AN fibers exhibit characteristic frequencies (CFs) that lie between 10 and 30 kHz. In contrast, CFs higher than 40 kHz are more commonly observed in the responses of neurons in the central nucleus of the IC.

Conclusion

These results suggest that the representation of high frequency sounds is transformed along the ascending auditory pathway and that this transformation enhances responses to vocalization stimuli.

1116 Elevated SP/AP Ratio in the Mouse

Model of Endolymphatic Hydrops

Yiping Li¹, Sami Melki¹, Maroun Semaan^{1,2}, Qing Yin

Zheng¹, Kumar Alagramam¹, Cliff Megerian¹

¹University Hospitals Case Medical Center, ²Louis Stokes

VA medical Center

Background

An elevated Summating Potential (SP) over Action Potential (AP), or SP/AP ratio, on electrocochleography (ECoG) suggests endolymphatic hydrops (ELH) in humans. The male mouse carrying the *Phex*^{Hyd-Duk} (*Phex*^{HD/Y}), a mutant allele of the phosphate-regulating gene *Phex*, develops spontaneous postnatal ELH by postnatal day P21. In animals, (ECoG) has been recorded from primates, guinea pigs and rats but never on a spontaneous ELH mouse model. A survival procedure was developed and applied to the *Phex*^{HD/Y} mouse to determine whether it exhibited similar electrocochleographic changes seen in humans with ELH. Concurrent histological studies would also definitely prove that an enlarged SP/AP is associated with ELH. These studies would identify direct correlation between severity of hydrops, hearing loss and the SP/AP ratio.

Methods

A percutaneous recording of (ECoG) was developed and applied to *Phex*^{HD/Y} mice and wild-type controls at P21. The mice were then euthanized and their cochleae harvested for histological analysis. Each hydropic cochlea was assigned a grade ranging from 0 (normal) to 4 (severely hydropic). SP/AP ratios were compared between both groups using a ttest, and a linear regression test was applied to determine correlation among hydrops grade, hearing loss and SP/AP ratio.

Results

42 control ears and 26 *Phex*^{HD/Y} ears were successfully tested. All *Phex*^{HD/Y} mice ears had ELH on histology. The *Phex*^{HD/Y} mice had a significantly elevated SP/AP ratio compared to the wild-type animals (mean±SD: 0.439±0.038 and 0.278±0.010, respectively, p=0.0002). The regression test between ELH and the SP/AP ratio showed no significant correlation (p=0.978). However,

hearing loss was found to correlate positively with ELH grade ($p=0.0002$).

Conclusion

(ECoG) was successfully recorded in a mouse model of ELH for the first time. As seen in human studies, the Phex^{HD}/Y mouse demonstrated an elevated SP/AP ratio. While elevation of the SP/AP shadows ELH, it does not correlate with severity; ELH however, correlated positively with elevated hearing thresholds. Elevated SP/AP has been suggested to be linked to ELH in the literature, but this is the first study to prove that with histologic evidence. The evidence presented in this report, combined with unique advantages of the Phex^{HD}/Y model, provides new drivers to understand the pathophysiology linked to the development of hearing loss associated with the ELH scenario, including Ménière's disease.

1117 Mouse Model of the Fluctuating Hearing Loss Associated with Enlargement of the Vestibular Aqueduct in Pendred Syndrome

Taku Ito¹, Byung Yoon Choi¹, Philine Wangemann², Andrew Griffith¹

¹NIDCD/NIH, ²Kansas State University

Background

Hearing loss associated with enlargement of the vestibular aqueduct (EVA) is commonly caused by *SLC26A4* mutations. The hearing loss is predominantly sensorineural, variable in severity, asymmetric or unilateral, with an onset in the first few years of life. The hearing loss often shows fluctuation and overall downward progression. We previously reported a binary transgenic mouse line, in which *Slc26a4* expression is induced by doxycycline (dox). *Slc26a4* expression during E16.5 to P2 was required for the acquisition of normal hearing at 1 month of age. The purpose of the present study was to characterize the natural history of hearing loss in this model.

Methods

Dox was included in the drinking water provided to the mother from the time of conception through embryonic day 17.5. ABR thresholds were measured at 1, 2, 3, 4, 5, 6, 9 and 12 months of age. Endocochlear potential (EP) was measured in the basal turn of the cochlea. We performed quantitative real-time PCR analysis of total RNA isolated from microdissected stria vascularis. PCR primers were designed to amplify *cd68*, *cd45* and *lyzs* as macrophage expression markers. Plastic-embedded cochlear tissue sections of 4 μ m thickness were stained with toluidine blue. Numeric data are presented at average \pm sem. Statistical analyses included Pearson correlation and one-way ANOVA.

Results

ABR thresholds showed fluctuating hearing loss from 1 through 3 months of age. The EP correlated with ABR thresholds at both time points, suggesting that fluctuations of hearing are primarily associated with stria dysfunction

and fluctuating EP. Quantitative real-time PCR and immunohistochemistry analyses showed a significant inverse correlation of macrophage parameters in the stria vascularis with hearing ability at 1 month of age. Kcnj10 and Kcnq1 immunoreactivity appeared normal even with severe hearing loss. ABR testing at 9-12 months of age revealed progressive overall loss of hearing. Light microscopic evaluation showed atrophy and degeneration of the stria vascularis, without EVA.

Conclusion

This mouse model closely approximates the fluctuating and progressive hearing loss observed in many human EVA patients. Macrophage proliferation in the stria vascularis and loss of the EP appear to be primary events caused by a decrease of pendrin function. EVA is a radiologic marker for, but not a cause of, hearing loss. This is a valuable animal model to explore the molecular and cellular pathogenesis of, as well as potential therapeutics for, hearing loss associated with EVA. Supported by NIH R01-DC012151.

1118 Restoration by Salicylate of Transport Function and Anion Exchanger Activity of Missense Pendrin Mutations

Hiroshi Wada¹, Kenji Ishihara², Shuhei Okuyama¹, Shun Kumano¹, Koji Iida¹, Hiroshi Hamana¹, Michio Murakoshi¹, Toshimitsu Kobayashi¹, Shin-ichi Usami³, Katsuhisa Ikeda⁴, Yoichi Haga¹, Kohei Tsumoto⁵, Hiroyuki Nakamura⁶, Noriyasu Hirasawa¹

¹Tohoku University, ²Ibaraki University, ³Shinshu University, ⁴Juntendo University, ⁵The University of Tokyo, ⁶Gkusuyn University

Background

In the inner ear, pendrin is detected in the stria vascularis, spiral prominence and outer sulcus. It is a member of the *solute carrier 26A* (*SLC26A*) family and known as an anion exchanger involving in the conditioning of ion concentration of the endolymphatic fluid. Its mutations are responsible for hereditary hearing loss. In Japanese, 10 missense mutations, i.e., P123S, M147V, K369E, A372V, N392Y, C565Y, S657N, S666F, T721M and H723R, have been found. We have reported that salicylate restores the localization and function of mutants of prestin, which is a member of the *SLC26A* family and has about 45% similarity with the amino acid sequences of pendrin. Thus, it is hypothesized that salicylate restores pendrin mutants as in the case of prestin. In this study, the effects of salicylate on the localization and anion transporter activity of the 10 mutants were analyzed *in vitro*.

Methods

HEK 293 cells were transfected with each expression vector with the 10 mutants. After the cells were incubated with salicylate for 12 h, for the analysis of localization, they were stained with TRITC and its fluorescence was observed using a confocal laser scanning microscope. For the analysis of anion transporter activity, they were incubated in high I^- buffer containing 200 kBq/ml ¹²⁵I, promoting uptake of ¹²⁵I, and then incubated with high Cl^-

buffer, leading to the export of ^{125}I from the cells to extracellular media by transfected pendrin. Radiolabeled iodide in the cell lysates was measured using a scintillation counter.

Results

Immunofluorescent staining revealed that K369E and C565Y, as well as wild-type pendrin, were transported to the plasma membrane while 8 other mutants were retained in the cytoplasm (Fig. 1). Incubation with salicylate induced the transport of 4 pendrin mutants (P123S, M147V, S657Y and H723R) from the cytoplasm to the plasma membrane (Fig. 2(a)). The remaining radioactivity in cells transfected with such 4 mutants was significantly decreased by salicylate treatment as in the case of WT pendrin, indicating that their anion exchanger activity was restored (Fig. 2(b)).

Conclusion

Incubation with salicylate restored the transport function and anion exchanger activity of 4 pendrin mutants (P123S, M147V, S657Y and H723R). These findings suggest that salicylate possibly contribute to development of a new method of medical treatment for sensorineural hearing loss caused by pendrin mutations.

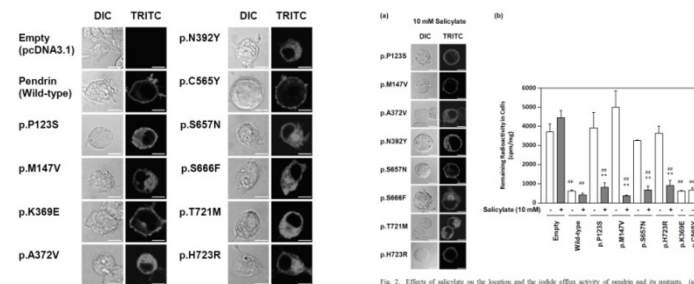


Fig. 1. Intracellular localization of pendrin and its mutants expressed in HEK293 cells. TRITC indicates pendrin. Scale bars represent 10 μm .

Fig. 2. Effects of salicylate on the location and the iodide efflux activity of pendrin and its mutants. (a) Fluorescence micrographs. TRITC indicates pendrin. Scale bars represent 10 μm . (b) Remaining radioactivity in cells. The remaining radioactivity in the cells transfected with p.P123S, p.M147V, p.S657Y and p.H723R was significantly decreased by salicylate. ** $P < 0.01$ vs. corresponding control (the cells lacking salicylate), or $P < 0.01$ vs. empty without salicylate.

1119 A Balanced Chromosome Translocation Reveals a Predicted Lipase's Involvement in Sensorineural Hearing Loss

Benjamin Currell^{1,2}, Nahid Robertson¹, Tatiana Hoyos^{2,3}, Ann Hickox^{2,4}, Kristen Wong¹, Charles Liberman^{2,4}, Eric Liao^{2,3}, Cynthia Morton^{1,2}

¹Brigham and Women's Hospital, ²Harvard Medical School, ³Massachusetts General Hospital, ⁴Massachusetts Eye and Ear Infirmary

Background

Chromosomal translocations, an abnormal exchange of genetic material between chromosomes, are estimated to be as frequent as 1 in 500 newborns and may result in abnormal phenotypes due to gene disruption or dysregulation. The Developmental Genome Anatomy Project (DGAP, www.DGAP.Harvard.edu) systematically examines subjects with chromosomal translocations and abnormal phenotypes to identify disrupted genes etiologic in the disorder. Of particular interest for DGAP are chromosomal translocations associated with congenital hearing loss. DGAP056 is an archetypal case with congenital profound sensorineural hearing loss, as well as

a constellation of other symptoms including mild craniofacial abnormalities (coloboma, exotropia, blepharophimosis, and low-set posteriorly rotated ears), mitral valve prolapse, hypospadias, and early onset prostate cancer.

Methods

Several standard methods were used including protein homology modeling, karyotyping, fluorescent *in situ* hybridization (FISH), 3' RACE, qPCR, whole-mount *in situ* hybridization (WISH), mouse KO, Western blot (WB), immunohistochemistry (IHC), ABR and DPOAE.

Results

The karyotype, confirmed by FISH and PCR analysis, reveals that DGAP056 has a *de novo* apparently balanced translocation involving chromosomes 2 and 13, t(2;13)(p24.1;q22.3)dn. The translocation results in a breakpoint in chromosome 2 that disrupts an unannotated gene, designated *C2ORF43*. Analysis of the subject's immortalized lymphoblast cells reveals a marked reduction in *C2ORF43* expression, as well as expression of two abnormal, truncated isoforms. Homology analysis indicates that *C2ORF43* produces an evolutionarily conserved protein that is part of the alpha/beta hydrolase clan of proteins, many of which act as serine-based lipases, whose central motif, the catalytic triad, is dismantled in the abnormal transcripts. Further investigation of *C2ORF43* was carried out in model organisms. WISH demonstrated that staining of *C2ORF43* orthologs was localized to the developing inner ear of both zebrafish and mice. A newly developed mouse KO model demonstrated, by WB and IHC, that protein synthesis of the *C2ORF43* ortholog was essentially absent in the KO mouse ear compared to the WT. Physiological measurements of hearing, using ABR and DPOAE, indicate that at six months, some KO mice exhibit signs of hearing loss.

Conclusion

C2ORF43 appears to play an important role in development and/or maintenance of the inner ear. While it is unclear what the role of this putative serine-based lipase might play in the inner ear, analysis of DGAP056's chromosomal translocation has revealed some of the genetic components of hearing loss and highlights the power of the DGAP model.

1120 ACEMg Diet Supplement Influences

Progression of Hereditary Deafness

Shaked Shivatzki¹, Diane M Prieskorn², Lisa A Beyer², Cynthia J Schoen³, Karen B Avraham¹, Marci M Lesperance⁴, Margit Burmeister³, Josef M Miller², Glenn E Green⁴, **Yehoash Raphael²**

¹Department of Human Molecular Genetics & Biochemistry, Sackler Faculty Medicine, Tel Aviv University, ²KHRI, Dept. of Otolaryngology, Head & Neck Surgery, The Univ. of Michigan, ³Dept. of Human Genetics, The Univ. of Michigan, ⁴Dept. of Otolaryngology, Head & Neck Surgery, The Univ. of Michigan

Background

Dietary supplements have been shown to reduce auditory insults caused by aminoglycosides and overstimulation. Vitamins A-C-E and Mg (ACEMg) have been shown to reduce cochlear acoustic and ototoxic trauma. When given to an 11-year-old boy with Connexin 26 (*GJB2*) mutations 35delG/167delT and progressive hearing loss, hearing thresholds showed an average improvement of 2 dB/year over two years. To understand the mechanism of this outcome and extend it to other forms of hereditary hearing loss, we tested the influence of ACEMg on hearing loss and pathology in two mouse models of human mutations, *DIAPH3* (AUNA1) and *GJB2* (DFNB1).

Methods

Gjb2 conditional knock-out (*Gjb2*-CKO) mice were created by breeding *Gjb2*^{loxP/loxP} mice with *Sox10*-Cre PAC mice, abolishing expression of *Gjb2* in supporting cells of the organ of Corti. *Diap3* (mouse *DIAPH3* ortholog) transgenic mice (*Diap3*-Tg) overexpressed wild-type *Diap3* on an FVB background [FVB-Tg(CAG-Diap3)924Lesp/J]. ABRs to pure tones at 12, 16 and 24 (*Gjb2*-CKO) or 32 (*Diap3*-Tg) kHz were measured at 4 and 12 (*Diap3*-Tg) or 16 (*Gjb2*-CKO) weeks of age. Mice were fed an ACEMg-enhanced or control diet starting at 4 weeks of age until euthanasia at 12 (*Diap3*-Tg) or 16 (*Gjb2*-CKO) weeks. Cochleae were prepared as whole-mounts stained for actin and myosin-VIIa.

Results

ABR thresholds for *Gjb2*-CKO mice fed ACEMg were significantly better than the control diet group. *Gjb2*-CKO mice also had a robust preservation of hair cells (HCs) compared to control chow mice. The opposite was true for the *Diap3*-Tg mice, which displayed worse thresholds and accelerated HC loss compared to mutants fed a control chow. Combined, the results indicate a negative effect of the ACEMg treatment on hearing and HCs in the *Diap3*-Tg mice and a positive effect in the *Gjb2*-CKO mice.

Conclusion

ACEMg significantly influenced deafness progression in the cochleae of both *Gjb2*-CKO and *Diap3*-Tg mice. In *Diap3*-Tg mice, there was a deleterious effect whereas in *Gjb2*-CKO mice there was robust preservation of HCs and significant preservation of auditory thresholds. These data link dietary supplements with modulation of phenotypes in hereditary deafness and suggest that effects may vary

depending on the mutation. The positive influence of ACEMg on structure and function in *Gjb2*-CKO ears is especially important considering the prevalence of *GJB2* mutations in humans.

1121 Viral-Mediated Gjb2 Gene Expression Partially Restores the Gap Junction Function in the Cochlea of Conditional Connexin26 Null Mouse

Qing Yu¹, Qing Chang², Jianjun Wang², Shusheng Gong¹, **Xi Lin²**

¹Beijing Tongren Hospital, Beijing, ²Emory University

Background

Mutations in the *Gjb2* gene, which codes for connexin 26 (Cx26), are the most common causes of human nonsyndromic hereditary deafness. Non-sensory supporting cells in the cochlea are connected extensively by gap junctions (GJs), heteromerically assembled from both Cx26 and Cx30, to facilitate intercellular ionic and biochemical coupling. The cCx26 null mouse model is deaf and intercellular coupling mediated by GJs among non-sensory cells in the cochlea was severely impaired.

Methods

Cx26 was tagged with green fluorescence protein (GFP) and inserted into an adeno-associated viral vector driven by the CMV promoter (AAV1-CMV-Cx26-eGFP). The recombinant viruses were directly injected into the scala media of one side of the cochlea of early postnatal (either P0 or P1) cCx26 null mice in order to rescue the impaired GJ functions. The contralateral side was used as a control for the same animal. In order to check the effect of surgery procedures on the hearing, the same injections were performed in wild type mice.

Results

We found that the hearing thresholds were normal in wild type mice observed one month after injections as measured by ABR tests. The earliest Cx26-GFP expression was detected about 5 days after injections and lasted for at least 3 months. The expression was found in many types of supporting cells of the organ of Corti, fibrocytes of connective tissues and marginal cells in the stria vasculares, with the strongest Cx26-GFP signal found in the outer sulcus cells, marginal cells and spindle shaped cells.

We found significantly more cells in the injected side survived in the sensory epithelium of cCx26 null mouse at one month. GJs biochemical coupling in the supporting cells was tested using the fluorescent dye transfer assay (injection of propidium iodide, PI) and the fluorescent recovery after photobleach (FRAP) assay. Both PI transfer and FRAP assays demonstrated a significant amount of restoration of GJ-mediated biochemical coupling among the outer sulcus cells in the injected cochlea of cCx26 mice. However, the tunnel of Corti remained closed and the hearing test of the injected mice did not show significant hearing recovery so far.

Conclusion

This study demonstrated partial restoration of GJ-mediated biochemical coupling in the cochlea of cCx26 null mice after gene delivery via AAV1-CMV-Cx26-eGFP. Late and incomplete expression by various types of cochlear cells may be responsible for the failure of hearing rescue in the cCx26 null mice.

1122 Absence of Tricellulin Affects the Ultrastructural Organization of the Tricellular Tight Junctions and Leads to Degeneration of Cochlear Hair Cells

Gowri Nayak¹, Sue I. Lee², Rizwan Yousaf¹, Stephanie E. Edelman³, Christina M. Van Itallie⁴, Ghanshyam P. Sinha³, Maria Rafeeq⁵, Sherri M. Jones⁶, Inna A. Belyantseva², James M. Anderson⁴, Andrew Forge⁷, Gregory I. Frolenkov³, Saima Riazuddin^{1,8}

¹Div. of Pediatric Otolaryngology, CCHRF & Dept. of Otolaryngology, UC., Cincinnati, Ohio, USA, ²Laboratory of Molecular Genetics, NIDCD, NIH, Rockville, Maryland, USA, ³Department of Physiology, University of Kentucky, Lexington, Kentucky, USA, ⁴National Heart, Lung, and Blood Institute, National Institutes of Health, Bethesda, Maryland, USA, ⁵National Center of Excellence in Molecular Biology, University of the Punjab, Lahore, Pakistan, ⁶Dept. of Special Education and Communication Disorders, University of Nebraska, Omaha, Nebraska, USA, ⁷Centre for Auditory Research, University College London, London, United Kingdom, ⁸Div. of Pediatric Ophthalmology, CCHRF & Dept. of Ophthalmology, UC., Cincinnati, Ohio, USA

Background

In the cochlea, tight junctions between the epithelial cells lining the scala media are responsible for isolating the endolymph from the perilymph, which is indispensable for normal cochlear function. Mutations in *TRIC*, which encodes a tricellular tight junction protein, are known to cause autosomal recessive nonsyndromic hearing loss (DFNB49) in humans, but the exact mechanism leading to deafness is unknown.

Methods

We generated a mouse model for DFNB49 that carries a mutation in *Tric*, p.R497*, orthologous to a previously identified mutation, p.R500*, in humans. Inner ear function was determined by ABR, DPOAE and vestibular evoked potential measurements. The cochlear and vestibular sensory epithelia were examined by immunofluorescence and scanning electron microscopy. The effects of the mutation on the ultrastructure of tight junctions in the inner ear were determined by freeze fracture microscopy. Tracer assays and endocochlear potential measurements were performed to establish the integrity and functional state of the stria vascularis. Whole cell patch clamp recordings were performed to determine the functional maturation in early postnatal outer hair cells (OHCs). Serum chemical, hemotological and histological analysis were performed by using the services of the Division of Veterinary Resources at NIH.

Results

Mice homozygous for the p.R497* knockin mutation displayed early onset rapidly progressing hearing loss and were completely deaf by P30. Progression of hearing loss coincided with OHC degeneration, followed by loss of inner hair cells. The mutation neither affected the maturation of voltage-gated ion channels in young postnatal OHCs, nor endocochlear potential nor vestibular evoked potentials. However, the mutation appeared to affect the ultrastructure of the tricellular tight junctions in the reticular lamina of the organ of Corti, marginal cell layer of the stria vascularis and the vestibular epithelia. Consistent with the hypothesis that the barrier function of the reticular lamina is lost in *Tric* knockin mice, the hair cell loss in these animals was rescued *in vivo* when the endocochlear potential was eliminated by deleting *Pou3F4* that is necessary for normal development of the stria vascularis. Finally, the *Tric* knockin mice showed phenotypic changes in mandibular salivary glands, thyroid follicles, olfactory epithelium and heart.

Conclusion

Loss of tricellulin leads to organ of Corti degeneration that is likely due to defective paracellular barrier function of the reticular lamina. Although mutations in tricellulin are known to cause non-syndromic deafness in humans, orthologous mutations in mouse result not only in deafness but also in abnormalities beyond the inner ear.

1123 Connexin26 (Cx26) Deficiency Impairs MiRNA Expression in the Cochlea

Hong-Bo Zhao¹, Yan Zhu¹, Liang Zong¹, Chun Liang¹

¹University of Kentucky Medical Center

Background

Gap junctions play an important role in hearing. Connexin 26 (Cx26, GJB2) mutations are responsible for 50-70% of nonsyndromic hearing loss. Cx26 deficient mice demonstrate cochlear developmental disorders, reduction of endocochlear potential (EP), and degeneration of cochlear cells including hair cells. We recently found that cell degeneration is not a primary cause for Cx26 deficiency induced hearing loss (Liang et al., 2012). Some mechanisms other than cell degeneration, such as cochlear development disorders, may play an essential role in this prevalent genetic hearing loss. However, the molecular genetic mechanism underlying cochlear developmental disorder associated with Cx26 deficiency is little known. During organic development, intercellular communication between cells is necessary and required for synchronizing cell proliferation and differentiation. MicroRNAs (miRNAs) are naturally-occurring regulatory RNAs and play critical roles in cell differentiation and organisms. In another report (Zhao et al., 2013 ARO meeting), we have demonstrated that miRNA can pass through gap junctions. In this study, we studied whether miRNA can pass through inner ear gap junctions *in vivo* and whether Cx26 deficiency can impair miRNA expression and intercellular communication in the cochlea.

Methods

Fluorescence-tagged miRNA intracellular injection was used to assess miRNA intercellular diffusion between the cochlear native cells. We also used quantitative real-time PCR (qRT-PCR) to measure miRNA expression in the Cx26 deficient mouse cochlea during postnatal development.

Results

By intracellular injection of fluorescence-tagged miRNA, we directly demonstrated that miRNA could pass through gap junctions between cochlear supporting cells. Gap junctional blockers could eliminate this miRNA intercellular transferring. Using Cx26 knockout mice, we further found that Cx26 deficiency disrupted miRNA intercellular transferring in the cochlear sensory epithelium and reduced miRNA expression in the cochlea during postnatal development.

Conclusion

These studies provide direct evidence for miRNA intercellular exchanges between native cochlear cells in vivo. These studies also provide important information about gap junctional function in the regulation of cochlear development.

1124 Mutation in a Novel Actin-Binding Protein, Exhibiting an Arl2 GAP Activity, Is Associated with Nonsyndromic Deafness DFNB88

Elodie M. Richard^{1,2}, Thomas J. Jaworek¹, Anna A. Ivanova³, Arnaud P.J. Giese^{1,2}, Shaheen N. Khan⁴, Richard A. Kahn³, Saima Riazuddin^{1,2}

¹Division of Pediatric Ophthalmology, Cincinnati Children's Hospital Medical Center, Cincinnati, USA, ²Division of Pediatric Otolaryngology, Cincinnati Children's Hospital Medical Center, Cincinnati, USA, ³Department of Biochemistry, Emory University School of Medicine, Atlanta, USA, ⁴CEMB, University of the Punjab, Lahore, Pakistan

Background

Hearing loss is an etiologically diverse condition that can be genetic in origin. While mutations in over 100 loci have been causally linked with hearing impairment, less than half of them have had their gene identified. The purpose of our study was to identify a new gene responsible for nonsyndromic recessively inherited prelingual hearing loss in a large human pedigree.

Methods

We have enrolled a large consanguineous Pakistani family PKDF468 segregating prelingual, recessively inherited, nonsyndromic, moderate to profound sensorineural hearing loss. Genome wide analysis was performed after excluding the linkage to known recessively inherited nonsyndromic loci (DFNB). Whole exome followed by Sanger sequencing was performed using the DNA from the affected individuals of the PKDF468 family. Fluorescently tagged constructs were used to evaluate the effect of the mutant allele. Cosedimentation and GTPase

activating protein (GAP) activity assays were performed as initial characterizations of this newly identified deafness protein.

Results

We mapped a new deafness locus, designated as DFNB88 on chromosome 2p11 in family PKDF468. Our sequencing analyses revealed a missense mutation in a candidate gene encoding a novel actin-binding protein. The DFNB88 protein is largely uncharacterized with no known biochemical activities reported to date. Our RT-PCR studies demonstrated the expression of DFNB88 protein in both cochlear and vestibular epithelia of mouse. In cochlear explant, fluorescently tagged DFNB88 protein is targeted to the actin-base structures of hair cells. Similarly, in CL-4 cells, it targets to the microvilli on the cell surface while this ability is impaired in the mutant protein with missense mutation identified in family PKDF468. DFNB88 protein is also colocalized with actin-cytoskeleton in MDCK cells. When treated with cytochalasinD, MDCK cells show a disrupted actin cytoskeleton that leads to the mislocalization of the DFNB88 protein. We found a direct interaction between F-actin and DFNB88 protein in a highspeed cosedimentation assay. Moreover, DFNB88 protein possesses GAP activity against Arl2 GTPase. Arl2 belongs to the Ras superfamily of GTPases, containing multiple members known to be involved in the regulation of the actin cytoskeleton architecture and membrane traffic.

Conclusion

Taken together, these data suggest that the DFNB88 protein is linked to the actin cytoskeleton and might regulate it through small GTPases. Our data expand the genetic basis of nonsyndromic hearing loss and highlight the indispensable function of DFNB88 protein in sound perception. To our knowledge, this is the first report of this protein associating with hearing impairment in humans.

1125 Identification of Target Proteins Involved in Cochlear Otosclerosis

Celine Richard¹, Jose Fayad², Fred Linthicum Jr², Joni Doherty²

¹CHU of St Etienne, University of Saint-Etienne, France,

²House Research Institute

Background

Otosclerosis, is a bone remodeling disorder limited to the endochondral layer of the otic capsule within the temporal bone. Clinical onset, audiometry, and progression of the disease are unpredictable and vary from subject to subject, probably due to genetic factors. Some authors have suggested an inflammatory etiology for otosclerosis due to persistent measles virus infection involving the otic capsule. Despite numerous genetic studies, implication of candidate genes in the otosclerotic process remains elusive. Recently, a reliable method for liquid chromatography-mass spectrometry (LC-MS) analysis on formalin fixed celloidin-embedded temporal bone tissues was successfully developed, and we have employed this proteomic technique for post-mortem investigation of otosclerosis.

Methods

Proteomic analysis was performed using two human temporal bones: one from a patient with severe otosclerosis and a control temporal bone from a patient without otological disease. Sections were dissected under microscopy to remove otosclerotic lesions for proteomic analysis. We utilized a modification of the Liquid Tissue Protein Extraction kit® (MS Protein Prep Kit, Expression Pathology, Rockville, MD) for celloidin-embedded temporal bones. For shotgun MS analysis, tandem 2D chromatography MS/MS using an LTQXL Orbitrap (Thermo Fischer) was employed. The MS/MS data analysis and peptide matching to FASTA human databases was done using SEQUEST and proteome discoverer software.

Results

Several proteins were revealed in both normal otic capsule bone and otosclerosis-infiltrated otic capsule, and many were identified only in otosclerosis. Of interest, TGFβ1 was identified in otosclerosis but not in the normal control temporal bone specimen. Aside from TGFβ1, many proteins and predicted cDNA-encoded proteins were observed, with implications in cell death and/or proliferation pathways, suggesting a possible role in otosclerotic bone remodeling. Immunostaining using TGFβ1 monoclonal antibody (pTyr369, Novus Biologicals, CO) directed against the extra-cellular matrix revealed marked staining of the spongiotic otosclerosis lesion and scant staining in normal bone adjacent as well as in the control temporal bone.

Conclusion

Mechanisms involved in cochlear extension of otosclerosis are still unclear, but the implication of TGFβ1 is supported by the present proteomic data. Our immunostaining results support this data. The established role of TGFβ1 in the chondrogenesis process support the theory of a reaction targeting the globulae interossei within the otic capsule.

1126 Determinants of Discharge Regularity

Jay M. Goldberg¹

¹University of Chicago

Background

To study the cellular basis of discharge regularity, intra-axonal recordings made in the turtle posterior crista were compared with simulations run in an updated version of a model (Smith and Goldberg 1986).

Methods

Recordings were from bouton afferents, were close enough to the neuroepithelium to include mEPSPs and AHPs, and were obtained from both regular and irregular units.

Results

The interspike voltage trajectory of regular units is dominated by a deep, slow AHP that crosses threshold, whereas the AHP of irregular units is fast and shallow and

remains below threshold presumably because of the presence low-voltage ionic currents (Iwasaki et al. 2008; Kalluri and Eatock 2010). mEPSPs of regular units are small and hardly affect the times when AHPs cross threshold. Because the AHPs are deterministic, discharge is regular. In contrast, mEPSPs of irregular units are large and discharge is determined by the crossing of a favorable mEPSP; because the timing of mEPSPs is random, discharge is irregular. In short, discharge regularity is determined by AHP size and time course and by mEPSP size. To determine the efficacy of the AHPs and mEPSPs in determining discharge regularity, they were independently varied in the model. AHPs were by far the more influential. Regular units have much lower rotational gains than do irregular units, which is related to differences in the afferents' sensitivity to depolarizing inputs. This can be explained as follows. Depolarizing inputs in regular units result in relatively small shifts in the threshold crossings of AHPs. Such inputs in irregular units lift the interspike voltage trajectory and result in many previously ineffective mEPSPs crossing threshold. Discharge regularity and response dynamics are highly correlated. Yet simulations confirm that the two discharge properties are not causally related. The close association of the two discharge properties presumably reflects some functional advantage. One such advantage has to do with information transmission as developed in another Abstract.

Conclusion

The results corroborate a previous analysis (Goldberg et al. 1986; Smith and Goldberg 1986). In the present study, cellular events are observed rather than inferred. The fact that simulations reproduce all of the features of our recordings, including the cellular events, supports the proposed mechanisms of discharge regularity.

Author Index (Indexed by abstract number)

- Abaya, Homer, 399
Abbas, Leila, 188
Abbas, Paul, 389
Abdala, Carolina, 1069, 1070
Abdolazimi, Yassan, 276
Abdulhadi, Khalid, 726
Abes, Generoso, 731
Abidi, Omar, 14
Abrams, Daniel, 877
Abu Rayyan, Amal, 718
Acosta, Amanda, 818
Adams, David, 717
Adams, Joseph, 733
Adams, Meredith, 134
Adelman, Cahtia, 121
Adelman, John P., 1008
Adelstein, Robert, 117, 269
Adjamian, Peyman, 232
Adler, Henry, 469
Adunka, Oliver, 130
Agrawal, Sumit, 439, 443
Agrawal, Yuri, 802, 810, 816
Agterberg, Martijn, 220
Aguar, Daniel, 999
Aguillon, Blanca N., 663
Ahlstrom, Jayne, 523, 909
Ahmad, Iram, 435
Ahmad, Shoeb, 703, 713
Ahmad, Wasim, 881
Ahmadi, Mahnaz, 1070
Ahmed, Zubair, 729, 881
Ahn, Jheeyae, 70
Ahn, Joong Ho, 237, 255
Ahn, Kang-Hun, 1053
Ahn, Kyung, 721
Ahn, Okjin, 456, 755, 756
Aihara, Ikkyu, 1083
Akamatsu, Yusuke, 430
Akbergenov, Rashid, 309
Akeroyd, Michael, 851, 852
Akhoun, Idrick, 982
Akil, Omar, 335
Akinpelu, Olubunmi, 1072
Akyurek, Elkan, 317
Alagramam, Kumar, 606, 1116
Alain, Claude, 892, 931
Alami, Aurash, 335
Alamilla, Javier, 350
Alasti, Fatemeh, 27
Alexandrov, Vladimir, 251
Alexandrova, Tamara, 251
Ali, Rouknuddin, 457
Alisch, Mareike, 636
Alkhaury, Samiya, 1050
Allan, Chris, 416
Allen, Emily, 484
Allen, Nicola, 840
Allen, Paul, 180, 505, 510
Allen, Prudence, 416
Allen-Sharp, Michelle, 1109
Allison, Jerome, 240
Allman, Brian L., 532, 657
Almishaal, Ali, 1075
Althen, Heike, 102
Altschuler, Richard, 224, 311, 706
Alvaro, Giuseppe, 936
Amitay, Sygal, 475
Ammer, Julian, 354, 360
An, Yang, 312
Ananthakrishnan, Saradha, 921, 952
Anbuhl, Kelsey, 511, 1095
Andeol, Guillaume, 506
Anderson, Carly, 367
Anderson, Charles T., 72, 874
Anderson, Elizabeth S., 398
Anderson, James M., 1122
Anderson, Lucy, 85, 857, 930
Anderson, Samira, 61, 62, 645, 891
Andrade-Elizondo, Paula B., 881
Andreou, Andreas G., 545
Angeles, Alicia, 251
Angeli, Simon, 424
Ansar, Muhammad, 881
Antunes, Flora, 366
Anwar, Abbas, 690
Anwar, Saima, 881
Aparicio, M-Auxiliadora, 98
Applebaum, Eric, 326
Applegate, Brian, 781
Appler, Jessica, 296
Argenyi, Michael, 1066
Årnlund-Richter, Lars, 457
Ari-Even Roth, Daphne, 614
Aronoff, Justin, 977, 983
Arun Gundram, Sailaja, 163
Asai, Yukako, 468
Ashford, Alex, 537
Ashihara, Takanori, 175
Ashmore, Jonathan, 472
Asimacopoulos, Eleni, 733
Asimacopoulos, Eleni P., 333
Askew, Charles, 468
Asuncion, James, 1006
Atala, Anthony, 571
Athanasakis, Emmanouil, 726
Atiani, Serin, 386
Atligan, Huriye, 908, 944
Auer, Manfred, 608, 838
Auer, Veronika, 67
Augustine, George, 263, 268, 694
Avci, Ersin, 740
Avenarius, Matthew, 608, 728
Avenidaño, Carlos, 327
Avraham, Karen B., 16, 23, 718, 720, 1120
Ayala, Yaneri A., 639, 662
Ayub, Muhammad, 881
Baş, 989
Baat, John E., 786
Baba, Yuto, 826
Babic, Kristen, 680
Back, Sang A, 50
Badii, Ramin, 726
Baguley, David, 582
Bai, Junping, 158
Bai, Jun-Ping, 149, 154
Baiduc, Rachael, 1073
Bailey, Erin, 1024, 1025
Baizer, Joan, 649
Bajo, Victoria M, 879
Bakay, Warren, 938
Baker, Robert, 540
Balaban, Carey, 247
Balachandrar, Kapilesh, 519
Ball, Gregory, 606, 844, 1035
Ball, Leila, 524
Ballesterro, Jimena, 357
Balogova, Zuzana, 626
Baltzell, Lucas, 379, 962
Banai, Karen, 477, 873
Bandyopadhyay, Saurav, 124
Banfi, Botond, 1012
Bao, Jianxin, 55, 223
Bao, Shaowen, 260
Barakat, Abdelhamid, 14
Barascud, Nicolas, 197, 1080
Barber, Carol, 925
Barbour, Dennis, 819
Barboza Jr, Luiz, 184
Barchi, Jonathan, 52
Bardins, Stanislav, 802
Barral, Jérémie, 616
Barria, Andres, 355
Barry, Johanna, 415
Bartels, Matthias, 268, 694
Barth, Jeremy L, 786
Bartlett, Edward, 634, 858
Barton, Matthew, 108
Bas, Esperanza, 58, 137, 138, 337, 341, 745
Basch, Martin, 270, 575
Basinou, Vasiliki, 51
Basiri, Reza, 43
Basit, Sulman, 881
Baskent, Deniz, 34, 211, 316, 317, 636, 684, 797, 800, 863
Basta, Dietmar, 77, 395, 806, 868
Basura, Gregory, 957
Bateschell, Michael, 267
Bathellier, Brice, 283
Batrel, Charlene, 126
Battistutta, Roberto, 557
Baumann, Simon, 380, 486, 950
Baumgartner, Robert, 509
Baumhoff, Peter, 655, 696
Baxter, Caitlin, 2
Bazan, Nicolas, 757
Beaton, Kara, 810
Beauchamp, Michael S., 399
Bee, Mark, 209, 210, 512, 902
Beers, Claire, 1064
Beim, Jordan A., 168, 613
Beisel, Kirk, 186, 555, 618
Beitel, Ralph, 89, 401
Belding, Heather M., 604
Bell, Andrew, 167
Belmont, John, 731
Belyantseva, Inna, 881, 1122
Belzner, Katharine A., 1020
Benard, Michel Ruben, 800
Benedict-Alderfer, Cindy, 24
Benito Gonzalez, Ana, 275
Benson, Chelsea, 389, 390
Benson, Thane, 680
Bento, Ricardo, 184
Berezina-Greene, Maria A., 170
Berger, Joel, 1101
Berger, Jonathan, 877
Berger, Lauren, 1098
Bergevin, Christopher, 169
Bergkvist, Magnus, 872
Bergles, Dwight E., 578
Berglund, Ken, 262
Berkowitz, Bruce, 865, 871
Berliner, Karen, 1027
Bernardo, F.-Javier, 98
Bernstein, Joshua, 687
Bajo, Victoria M, 879
Bernstein, Sara R., 495
Berrebi, Albert, 98, 642, 643
Bertoncini, Josiane, 212
Beurg, Maryline, 473, 554
Beutelmann, Rainer, 671, 1094
Beyer, Lisa, 288, 1120
Bhagat, Shaum, 1071
Bharadwaj, Hari, 887, 923, 927
Bhargava, Pranesh, 797
Bhat, Manzoora, 469
Bhatta, Puspanjali, 307, 759
Bhonker, Yoni, 718
Bianco, Isaac, 540
Bidelman, Gavin, 880, 892, 931
Biel, Martin, 969
Bielefeld, Eric, 310
Bierer, Julie, 402
Bierer, Julie Arenberg, 981
Bierer, Steven, 402
Biino, Ginevra, 725
Billig, Alex, 602
Billig, Alexander J., 981
Billings, Curtis, 379, 945, 962
Binley, Katie, 702
Bishop, Brian, 514, 515
Bishop, Phil, 1083
Bissig, David, 871
Bizley, Jennifer, 504, 908, 944
Blakley, Brian, 820
Blanco, Cynthia, 351
Blankenship, Sara, 848
Blanton, Susan, 424
Blatt, Melissa, 818
Bleeck, Stefan, 994
Bleser, Tana, 814
Bloomberg, Jacob J., 811
Bockisch, Christopher, 539
Bodmer, Daniel, 306
Boese, Benjamin J., 28
Bohlen, Peter, 488, 641, 674
Böhmen, Katharina, 636
Bohorquez, Jorge, 58
Boian, Melissa, 390
Bok, Jinwoong, 106, 1007, 1009
Bones, Oliver, 932
Bonham, Ben, 692
Boothroyd, Arthur, 560
Borck, Guntram, 14
Boreki, Alexander A., 338
Borenstein, Jeffrey, 700, 704
Bornuth, Volker, 616
Borse, Vikrant, 760
Bortfeld, Heather, 399
Bosen, Adam, 505
Böske, Tobias, 636
Böttger, Erik C., 309
Botti, Teresa, 164
Boulet, Jason, 985
Boulouiz, Redouane, 14
Bourien, Jérôme, 126, 461, 911
Boutros, Peter J., 255
Bouy, Jean Christophe, 506
Boven, Christopher, 910
Boyden, Edward, 261, 265, 695
Boyen, Kris, 229, 231, 280
Boyle, Patrick, 395
Bozorg Grayeli, Alexis, 590
Bozovic, Dolores, 763, 764, 767, 896
Bradfield, Colby, 113, 1004
Bradley, Allison, 956
Braidia, Louis, 215
Brand, Yves, 306
Brandewie, Eugene, 502
Brandon, Carlene, 843
Brant, Jason, 721
Brechmann, Andre, 603
Bremen, Peter, 382, 387, 508
Bremova, Tatiana, 802
Brenner, Michael, 307
Bress, Andreas, 162
Brette, Romain, 172
Brichta, Alan, 542
Bertoncini, John, 267
Brignull, Heather, 576
Brill, Sandra, 516
Brimjoin, W. Owen, 852
Brinker, Whitney, 421
Brinkmeier, Jennifer, 325
Briscoe, Adams, 240
Bronkema, Danielle, 390
Brons, Inge, 864
Bhonker, Michael, 603
Brough, Douglas, 456
Brown, David, 993
Brown, Kevin, 925
Brown, M. Christian, 265, 400, 680, 695
Brown, Maile, 936
Brown, Steve D. M., 606
Brownstein, Zippora, 23, 718, 720
Bruce, Ian, 214, 914, 985
Brughera, Andrew, 356
Brumberg, Jonathan, 527
Brun, Emilie, 238
Brunette, Katyarina E., 59, 825
Brungart, Douglas, 219, 521, 853
Buchholz, Jule, 344
Buchman, Craig, 130, 688
Büchner, Andreas, 474
Buckey, Jay, 673
Buden, Cameron, 403, 572, 683
Buelles, Kerstin, 1088
Bullen, Anwen, 744
Buniello, Annalisa, 17, 719
Burger, R. Michael, 68, 1087
Burgess, Ann, 538
Burghard, Alice, 686
Burke, Brian, 23
Burke, Catherine, 385
Burke, Kevin, 335
Burmeister, Margit, 1120
Burns, Joseph, 571
Buschbeck, Elke, 881
Buss, Emily, 204, 498, 503
Butt, Sehrish, 682
Cabrera, Laurianne, 212
Cacace, Anthony, 234, 870, 872
Cadieux, Jamie, 563
Caessens, Bernie, 690
Cai, Hongxue, 438
Cai, Qunfeng, 56, 57, 319
Cai, Rui, 80
Cai, Tiantian, 273
Calderon, Nicole, 83
Caldwell, Amanda, 612
Caldwell, Jillian S., 253
Caldwell, Michael, 512
Camarena, Vladimir, 248
Camenga, Elizabeth, 373
Carnegie, Colleen A., 28
Campbell, Dean, 115
Campbell, Kathleen, 46
Campbell, Sean, 787
Campbell, Tara, 700
Canlon, Barbara, 51, 595
Cant, Nell, 639
Cao, Xiao-Jie, 74
Carcagno, Samuele, 476
Carey, John, 28, 541, 808, 809, 810
Carey, Thomas, 331, 332
Carlile, Simon, 519
Carlin, Michael, 86
Carlisle, Francesca, 20
Carlyon, Robert, 176, 402, 602, 981, 984
Carney, Laurel, 169, 181, 666, 914
Carruthers, Isaac, 10
Carter, Paul, 690
Caruso, Paul, 714
Carver, Courtney, 493
Caspari, Franziska, 67
Caspary, Donald, 80, 365, 624, 625
Castracane, James, 872
Cazals, Yves, 479
Cediel Algovia, Rafael, 300
Cediel, Rafael, 327
Celaya, Adelaida, 327
Cervantes Constantino, Francisco, 373
Chabbert, Christian, 238
Chad-Friedman, Avi, 700
Chadwick, Richard, 766, 1052
Chae, Sung Won, 1046
Chai, Renjie, 569, 783
Chait, Maria, 197, 202, 888, 1080
Chalasanani, Kavita, 569
Chambers, Robert, 673
Chandrakasan, Anantha, 124
Chandrasekaran, Bharath, 876
Chang, Edward, 96
Chang, Jiwon, 1046

- Chang, Qing, 18, 328, 703, 712, 1121
 Chang, Sun O, 711
 Chang, Weise, 291, 299
 Charaziak, Karolina, 122, 123, 1074
 Chatterjee, Monita, 211, 392, 393, 482, 483, 660, 889
 Chavez, Eduard, 450, 451
 Chays, Andre, 479
 Cheatham, Mary Ann, 142, 156, 553
 Cheatham, MaryAnn, 155, 295
 Chen, Chen, 7, 8
 Chen, Daniel H.-C., 606
 Chen, Dongyang, 758
 Chen, Fangyi, 769
 Chen, Fu-Quan, 48
 Chen, Guang-Di, 534, 597
 Chen, Guoyou, 222, 650
 Chen, Jin, 827
 Chen, Jing, 20, 717
 Chen, Jun, 822
 Chen, Po-Yin, 813
 Chen, Xiaowei, 285
 Chen, Yan, 833
 Chen, Yen-Jung Angel, 707, 708
 Chen, Yixin, 223
 Chen, Zhengyi, 324
 Chen, Zheng-Yi, 833, 1061
 Chen, Zuxin, 75
 Cheng, Alan, 569, 783
 Cheng, Christopher J., 784
 Cheng, Jeffrey, 440
 Cheng, Weihua, 320
 Chertoff, Mark, 414, 915
 Cheung, Linda, 465
 Chhan, David, 454
 Chi, Fang-Lu, 789
 Chi, Le, 1034
 Chiang, Bryce, 545
 Chida, Izumi, 724
 Chidavaenzi, Robstein, 152
 Chien, Wade, 191, 193
 Chintanpalli, Ananthkrishna, 909
 Chiong, Charlotte, 731
 Chiossone, Juan, 924
 Cho, Dong-Woo, 406
 Cho, Soyoun, 459
 Choi, Byung Yoon, 711, 1117
 Choi, Chul-Hee, 738
 Choi, Dongseok, 42, 425
 Choi, Inyong, 381, 527
 Choi, Jae Young, 160, 427, 434, 727
 Choi, Jin Woong, 831
 Choi, June, 1046
 Choi, Sang Beak, 1009
 Choi, Seong Jun, 1044
 Choi, Seung-Hyo, 749
 Choi, Soo-Young, 722
 Choi, Yoon Gi, 298
 Chong, Xiaoge, 396
 Choo, Daniel, 40
 Choudhury, Niloy, 769
 Choung, Yun-Hoon, 1044, 1045
 Chow, Cynthia, 790
 Choy, Kristel, 241
 Christensen-Dalsgaard, Jakob, 512
 Christian, Leibold, 1085
 Christianson, G. Bjorn, 1112
 Chung, Jong Woo, 237, 749
 Chung, Juyong, 711
 Chung, Yoojin, 972
 Clare, Simon, 717
 Clark, Emily, 505, 510
 Clark, John, 412
 Clark, William, 593
 Clarke, Jason, 435
 Clarke, Jeanne, 211
 Clarke, Joseph, 1110
 Clarkson, Cheryl, 929
 Clause, Amanda, 859
 Clavier, Odile, 673
 Clifton, William, 49
 Clinard, Christopher, 638
 Cloninger, Christina, 510
 Coate, Thomas, 293
 Coddou, Claudio, 343
 Coenen, Maraike, 636
 Cohen, Bernard, 546, 547
 Cohen, Helen S., 552, 811
 Cohen, Julie, 853
 Cohen, Shira, 614
 Cohen, Yale, 203
 Colburn, Steven, 500, 947
 Cole, Erika, 480
 Cole, Susan, 270
 Coles, Deborah, 683
 Connelly, Catherine, 63, 338, 646, 679
 Contini, Donatella, 460
 Contreras, Julio, 327
 Cook, Rebecca, 536
 Cook, Tiffany, 881
 Cooley, Amanda, 796
 Coomber, Ben, 1101
 Cooper, Benjamin, 75
 Copley, Catherine, 271
 Cord, Mary, 853
 Corey, David P., 471, 605, 606
 Corfas, Gabriel, 841
 Cornella, Miriam, 103
 Corwin, Jeff, 291
 Corwin, Jeffrey, 290
 Cosentino, Stefano, 218
 Cosgrove, Dominic, 465
 Costa-Faidella, Jordi, 922
 Cotin, Stephane, 590
 Cox, Brandon C., 145, 568, 569, 570
 Crabtree, Mark, 570
 Cramer, Karina, 1109
 Crane, Alison, 987, 988
 Crane, Benjamin, 550
 Crenshaw III, E. Bryan, 721
 Cress, John, 513
 Crew, Joseph, 685, 983
 Criter, Robin, 812
 Crozier, Robert, 904, 916
 Cruz, Ivan, 576
 Cullen, Kathleen E., 253
 Culling, John, 218
 Cunnane, MeryBeth, 714
 Cunningham, Lisa, 191, 783, 843, 844, 1035
 Cureoglu, Sebahattin, 134, 426, 436
 Currall, Benjamin, 619, 1119
 Curthoys, Ian, 538
 Curtin, Hugh D., 433
 Cusack, Rhodri, 890
 Cute, Stephanie, 523
 Cutiongco-de la Paz, Eva Maria, 731
 Cyr, Janet, 44
 Dabdoub, Alain, 791, 1106
 Dagan-Rosenfeld, Orit, 23
 Dai, Chenkai, 255, 544, 545
 Dai, Chunfu, 158, 1030
 Dai, Lengshi, 927
 Dai, Min, 754
 Dai, Pei-dong, 1060
 Dai, Pu, 18
 Dailey, Michael E., 1025
 D'Alessandro, Lisa M., 678
 Dalhoff, Ernst, 171
 Dallman, Julia, 324
 Dallos, Peter, 155, 156, 295, 553
 Danashi, Ahmad, 28
 Dang, Kai, 997
 Daniel, Sam, 444, 445, 1072
 Darrow, Keith, 265, 680, 695
 Darville, Lancia, 143
 Dash-Wagh, Suvarna, 457
 Dau, Torsten, 216, 478
 Daudet, Nicolas, 119
 Davalos, Marcela, 810
 Davatzikos, Christos, 312
 David, Stephen, 100
 Davidson, Lisa, 563
 Davis, Matthew, 602
 Davis, Robin, 904, 913, 916
 Dawson, Sally J., 830
 de Boer, Egbert, 782
 de Boer, Jess, 1081
 de Cheveigné, Alain, 920
 de Kleine, Emile, 229, 231, 280
 De Ridder, Dirk, 233, 661
 De Vel, Eddy, 982
 Deans, Michael, 271
 Dearman, Jennifer, 145
 Decker, Brandon, 529, 534, 535
 Decorsière, Rémi, 216
 Deeks, John, 176, 602, 984
 Deeks, John M., 981
 Deerinck, Tom, 1014
 Dehoff, Marlin, 1014
 Deike, Susann, 603
 Delano, Paul H., 101, 654
 Delgutte, Bertrand, 972, 1019, 1114
 Delhorme, Lorraine, 215
 Delimont, Duane, 465
 Della Santina, Charles, 28, 255, 541, 544, 545, 807, 808, 1060
 Demany, Laurent, 201, 476
 Deng, Lili, 1022
 Deng, Nan, 311
 Dent, Micheal, 182, 194, 481, 490, 601
 Depireux, Didier, 43
 DeRemer, Susan, 1038
 Deroche, Mickael L.D., 393, 482, 483
 Deshpande (Balvalli), Shruti, 412, 993
 Deshpande, Aniruddha, 412, 421
 Desloge, Joseph, 215, 407
 Desloovere, Christian, 907
 DeSmidt, Alexandra A., 324
 Dewald, Jules, 956
 Dewan, Isha, 1004
 Dewey, James, 1065
 Dewey, Rebecca, 367, 953
 Dhandusaria, Henisha, 651
 Dhar, Sumitrajit, 1064, 1065, 1070, 1073
 Dhooge, Ingeborg, 474, 982
 Diepenbrock, Jan, 670
 Dietz, Beatrice, 343
 Dietz, Mathias, 358, 1097
 Ding, Bo, 628, 629, 630, 632
 Ding, Dalian, 178, 529, 837, 1021, 1022, 1047
 Ding, Nai, 527, 889, 961, 1002
 Dinh, Christine, 137, 337
 Dinh, John, 137
 Dipresa, Savina, 726
 Disanza, Andrea, 467
 Dlugaiczyk, Julia, 53
 Doetzlhofer, Angelika, 275
 Doetzlhofer, Angelika, 115, 116
 Doherty, Joni, 710, 1027, 1125
 Dolan, David, 224, 311, 331, 332
 Dollezal, Lena-Vanessa, 671
 Dombrowski, Katya, 373
 Donaldson, Gail, 796
 Donato, Roberta, 357
 Dong, Fengping, 567
 Dong, Junzi, 947
 Dong, Wei, 169, 772, 777
 Donnay, Gabriel, 383
 Dougan, Gordon, 717
 Dougherty, Brian, 918
 Dragicevic, Constantino, 101, 654
 Drennan, Ward R., 398
 Dresbach, Thomas, 340
 Drescher, Dennis, 150, 885
 Drescher, Marian, 150, 885
 Dreschler, Wouter A., 864
 Drga, Vit, 173
 Dror, Amiel A., 23
 Druckenbrod, Noah, 577
 Drummond, Meghan, 729
 Du, Xiaoping, 320, 784
 Duan, Chongwen, 155, 295
 Dubbaka, Srinivas R., 309
 Dubno, Judy, 523, 627, 653, 909
 Duchon, Michael, 1036
 Duelli, Dominik, 757
 Duffey, Megan, 790
 Dufour, Eric, 151
 Duncan, R. Keith, 144
 Dunlap, Myles, 239
 Dunn, Andrew, 942
 Dunne, Sara Fernandez, 566
 Dunnon, Askia, 130
 Duret, Guillaume, 620, 761
 Durham, Dianne, 1102
 Duriez, Christian, 590
 During, Matthew, 335
 Duscha, Stefan, 309
 Dweik, Dima, 718
 Dygert, Michael, 182
 Dylla, Maggie, 488, 641, 674
 Dziennis, Suzan, 423
 Earl, Brian, 915
 Easter, James, 775
 Eatock, Ruth Anne, 131, 246
 Eby, Thomas, 537
 Eckert, Mark, 523, 653
 Eddins, Ann, 313
 Eddins, David, 313
 Edeline, Jean-Marc, 644
 Edelmann, Stephanie, 470, 1122
 Edge, Albert, 585, 669, 705, 787, 1020
 Edge, Roxanne, 142
 Edmundson-Jones, Mark, 227, 232, 417
 Eduardo, Chavez, 105
 Edwards, Brent, 561
 Edwards, Jan, 420
 Edwards, Robert, 335
 Efferz, Thomas, 610
 Egami, Naoya, 159, 737
 Egger, Katharina, 489
 Eggermont, Jos, 278
 Eggleston, Jessica, 688
 Ehlers, Erica, 520
 Eisenberg, Daniel, 1000
 Eisenman, David, 732
 Eladari, Dominique, 579
 El-Amraoui, Aziz, 147, 151
 Elgoyhen, Ana Belen, 463
 Elgueda, Diego, 377
 Elhaili, Mounya, 12, 86, 372, 377, 496
 Elkan-Miller, Tal, 16
 Elkon, Rani, 732
 Elledge, Heather, 607
 Ellinger, Chris, 548
 Elliott, Karen, 274, 294
 Ellis, Dan, 501
 Ellisman, Mark, 1014
 Endres, Laura, 1089
 Engdahl, Bo, 633
 Engert, Florian, 540
 Englitz, Bernhard, 100, 377, 385
 Epp, Bastian, 489
 Ercolino, José Miguel, 924
 Ernst, Arne, 77, 395, 806, 868
 Escabi, Monty, 7, 8
 Escera, Carles, 102, 103, 663, 922
 Eshraghi, Adrien, 58, 138, 745
 Esterberg, Robert, 1040
 Estrada, Jose, 298
 Ewert, Donald, 320
 Fahlke, Christoph, 558
 Falcon, Romina, 101
 Faletra, Flavio, 726
 Falk, Tiago, 218
 Fallon, James, 38, 39, 394
 Fang, Jie, 117
 Faria, Andreia V., 659
 Farley, Brandon, 939
 Farrahi, Shirin, 161, 780, 1051
 Farris, Hamilton, 757
 Favrot, Sylvain, 407
 Fayad, Jose, 710, 1027, 1125
 Feeney, M. Patrick, 418
 Feinkohl, Arne, 507
 Fekete, Donna, 905
 Fekete, Donna M., 112
 Fellows, Abigail, 673
 Felmy, Felix, 354, 359, 360, 1085
 Feng, Albert, 573
 Fensky, Luisa, 344
 Ferber, Alexander, 511, 1095
 Ferguson, Melanie A., 526
 Ferman, Sara, 614
 Fernando, Augusta, 435, 912
 Ferrary, Evelynne, 590
 Ferrucci, Luigi, 312
 Fettiplace, Robert, 473, 554, 609, 898
 Fiering, Jason, 704
 Filippini, Kaitlyn, 825
 Finale, Michael, 341
 Firkins, Lester, 235
 Firszt, Jill, 563
 Fischl, Matthew, 1087
 Fisher, Jonathan, 615
 Fisher, Rachel, 729
 Fishman, Yonatan, 3
 Fitzgerald, Matthew, 978, 979, 1002
 Fitzgibbons, Peter, 622
 Fitzpatrick, Douglas, 130
 Flaherty, Mary M., 194
 Flanagan, Colleen, 589
 Flanagan, Sheila, 176
 Fleck, Roland, 744
 Fletcher, Mark, 1081
 Fletcher, Russell, 298
 Floyd, Robert, 320
 Folmer, Robert L., 418
 Fontaine, Bertrand, 903
 Forge, Andrew, 119, 135, 136, 744, 830, 840, 1122
 Forgues, Mathieu, 130
 Forshell Hederstierna, Christina, 436
 Forsythe, Ian D., 69
 Fortnum, Heather, 54, 227, 417
 Foster, Nichole, 677, 681
 Foster, Sarah, 60
 Foster, Simon, 357
 Foth, Hans-Jochen, 405
 Fox, Daniel, 46
 Francis, Nikolai, 385, 963
 Francis, Shimon, 843, 1037
 Frank, Thomas, 882
 Franken, Tom P., 353
 Franz, Christoph, 53, 1008
 Fredman, Elisha, 24
 Fredrickson, Karin, 28
 Free, Rolien, 34, 989
 Freeman, Dennis, 161, 780, 1051
 Freihofer, Pietro, 309
 Frerck, Micah, 254, 464
 Freyman, Richard, 213
 Fridberger, Anders, 766, 838, 895
 Friderici, Karen, 729
 Fridman, Gene, 807
 Fridman, Gene Y., 255, 545
 Friedman, David, 987, 988
 Friedman, Lilach M., 16, 718
 Friedman, Thomas, 729, 881
 Friedrich, Jr., Victor L., 546
 Friesen, Lendra, 660
 Frisina, Robert, 628, 629, 630, 632
 Fritz, Jonathan, 377, 378, 385, 963

- Fritzs, Bernd, 28, 133, 274, 294, 574, 1011, 1012
 Froemke, Robert, 90, 95
 Frolenk, Gregory I., 157, 466, 470, 881, 1122
 Frydman, Moshe, 23, 718, 720
 Fu, Qian-Jie, 685, 977
 Fugain, Claude, 200
 Fuhrman, Susan, 815
 Fuji, Hironori, 803
 Fujikawa, Taro, 26, 458
 Fujioka, Masato, 826
 Fujita, Takeshi, 141, 829
 Fujita, Tomoki, 836
 Fukazawa, Yugo, 339
 Fukui, Hideto, 548, 702
 Fukushima, Keizo, 52
 Fuller, Christina, 34, 989
 Fullgrave, Christian, 54
 Füllgrabe, Christian, 475
 Fullmer, Tanner, 987, 988
 Funnell, Robert, 444, 445, 1072
 Furlong, Cosme, 440
 Furman, Joseph, 815, 817
 Furness, David N., 467, 606, 1008
 Furukawa, Shigeto, 175, 1079, 1082, 1096
 Fuzessery, Zoltan, 675
 Gaboyard, Sophie, 238
 Gabriele, Mark, 1013
 Gadziola, Marie, 1076, 1077
 Gai, Yan, 513, 1091, 1092
 Galazyuk, Alex, 221
 Galazyuk, Alexander, 1099
 Gale, Jonathan, 843, 844, 1035, 1036
 Gallun, Frederick, 379, 604, 848
 Galvin III, John, 685
 Gan, Lin, 117
 Gan, Rong, 441, 591
 Gandour, Jackson, 952
 Gantz, Bruce J., 28
 Gao, Changxin, 18
 Gao, Fei, 643
 Gao, Simon, 49, 781
 Gao, Xinsheng, 784
 Gao, Yanhong, 758
 Garcia de Diego, Antonio M., 472
 Garcia-Lazaro, Jose, 1115
 Gardner, Stephanie, 858
 Garipey, Brian, 445
 Garnham, Carolyn, 58, 268, 694
 Gartrell, Brian, 449
 Gasparini, Paolo, 17, 725, 726
 Gati, Joseph S., 890
 Gaucher, Quentin, 644
 Gaudet, Rachelle, 605, 606
 Gaudrain, Etienne, 211
 Geffen, Maria, 10
 Geisler, Hyon-Soon, 53
 Geleoc, Gwenaëlle S.G., 468
 Gellibolian, Robert, 710
 Geng, Ruishuang, 606
 Gentner, Timothy, 9
 Genualdi, Alisa, 189
 Gerbig, Kelsey, 1076
 Gerig, Rahel, 437
 Gerka-Stuyt, John, 606
 Ghaffari, Roozbeh, 161, 780, 1051
 Ghazanfar, Asif, 6
 Ghisleni, Peter, 224
 Ghobreal, Bemin, 818
 Giebel, Armin, 396
 Giersch, Anne, 15, 455
 Giese, Arnaud, 881
 Giese, Arnaud P.J., 1124
 Giesse, Cora, 396
 Gifford, Adam, 203
 Gilels, Felicia, 730
 Gill, Ruth M., 701
 Gillespie, Deda, 350
 Gillespie, Peter, 118, 469, 608
 Gim, Jungsoo, 711
 Girotto, Giorgia, 17, 725, 726
 Glassman, E. Katelyn, 979
 Glassman, Katelyn, 1002
 Gloeckner, Cory, 1104, 1105
 Glogowski, Carolina, 73
 Glueckert, Rudolf, 127, 128
 Gnansia, Dan, 200, 479, 996, 997
 Godar, Shelly, 449
 Goeckel, Tom, 517
 Goh, Joshua, 312
 Goldberg, Jay M., 132
 Golden, Erin, 116
 Golder, Zoe J., 823
 Golding, Nace, 353, 364
 Goldstein, Alamea, 1038
 Goldstein, Bradley, 138
 Goldwyn, Joshua, 352
 Gómez-Álvarez, Marcelo, 98
 Gonçalves, Stefania, 924
 Gong, Shusheng, 109, 1121
 Goodman, Shawn, 37
 Goodrich, Lisa, 296, 577
 Goodyear, Richard, 14, 467, 840
 Gopal, Kamakshi, 83
 Gopal, Suhasini R., 606
 Gorbunov, Dmitry, 557
 Gordon, Karen, 564
 Gordon, Karen A., 652
 Gordon-Salant, Sandra, 622, 990
 Gore, Emma, 499
 Gorga, Michael, 1066
 Goto, Fumiyouki, 806
 Götze, Romy, 77
 Goupell, Matthew, 522, 974, 975, 990, 1000, 1001
 Goutman, Juan, 884
 Govil, Nandini, 978
 Goyer, David, 345
 Gracewski, Sheryl, 1056
 Graham, Heather, 646, 648
 Grande, Giovanbattista, 346
 Grandjean, Nicolas, 400
 Grant, Wally, 239
 Grati, M'hamed, 26, 424, 469
 Gratton, Michael Anne, 325, 326
 Gray, Lincoln, 480
 Green, David, 965
 Green, Glenn, 589, 1120
 Green, James, 469
 Green, Steven, 1023, 1024, 1025, 1111
 Greenberg, David, 358, 1097
 Gregg, Melissa, 208
 Greinwald, Emily, 40
 Greters, Mario Edwin, 806
 Gridley, Thomas, 270
 Griffin, Amanda, 213
 Griffith, Andrew, 1117
 Griffith, Kia, 990
 Griffiths, Timothy, 380, 486, 492, 888, 950, 951
 Grigoryan, Gevorg, 673
 Grigsby, Jason, 488, 641, 674
 Grillet, Nicolas, 607
 Grimm, Sabine, 102, 103, 922
 Grimm-Gunter, Eva-Maria, 119
 Grimsley, Jasmine, 370, 1077
 Grolman, Wilko, 94, 397, 779
 Gröschel, Moritz, 77, 395, 868
 Grose, John, 204, 658
 Grosh, Karl, 403, 773, 1057
 Gross, Guenter, 83
 Grothe, Benedikt, 359, 360, 969, 970, 1085
 Grover, Mary, 566
 Groves, Andrew, 49, 270, 273, 575
 Guan, Xiyang, 441, 591
 Gubbels, Samuel, 449, 790
 Guérit, François, 1069
 Guex, Amélie, 400
 Guinan Jr., John J., 170
 Guinan, John, 765, 1078, 1107
 Guinand, Nils, 543
 Gummer, Anthony, 153, 171
 Guo, Hong, 788
 Guo, Weiwei, 18
 Guo, Wei-Wei, 631
 Gupta, Chhavi, 58, 137, 138, 337, 341, 745
 Gurgel, Richard, 399
 Gürkov, Robert, 804
 Guthrie, O'neil, 900, 901
 Gutierrez-Hernandez, Sergio, 808
 Gutsche, Katja, 53
 Guymon, Allan, 1110
 Guyot, Jean-Philippe, 543
 H. McDermott, Josh, 197
 Hackett, Troy, 79, 674
 Hackney, Carole, 467, 473
 Haddad, Luciana, 184
 Haefele, Ben, 84
 Haefele, Benjamin, 92
 Haga, Yoichi, 1118
 Hageman, Kristin, 545, 1060
 Hahn, Tim, 847
 Hakizimana, Pierre, 766, 895
 Hall, Amanda, 110
 Hall, Deborah, 232, 235, 236, 942
 Hall, III, Joseph W., 498
 Hall, Joseph, 204
 Hallman, Timothy, 186
 Hallworth, Richard, 318, 556, 619
 Halsey, Karin, 224, 311
 Hamacher, Volkmar, 740
 Hamade, Mohamad A., 433
 Hamana, Hiroshi, 1118
 Hamlet, William, 362
 Hammerschmidt, Matthias, 14
 Hammill, Tanisha, 592
 Han, Chul, 1047
 Han, Duyeol, 1007
 Han, Fengchan, 24
 Han, Kyu-Hee, 711
 Hance, Zahra, 20
 Hancock, Kenneth, 365, 400, 972
 Hansberry, Mitchell, 704
 Hansen, Marlan, 28, 37, 435, 912, 1110
 Hanson, Coral, 201
 Hao, Xiping, 627, 786
 Hara, Akira, 1034
 Harada, Narinobu, 1062
 Harada, Tatsuhiko, 806
 Harasztsi, Csaba, 153
 Harasztsi, Emese, 153
 Harbidge, Donald, 579
 Harbison, R.Alex, 447
 Hardisty-Hughes, Rachel E., 606
 Hargrove, Tim, 46
 Harkins, Tim T., 28
 Harpole, Bethany, 912
 Harris, Dillon, 1111
 Harris, J. Aaron, 1013
 Harris, Kelly C., 653
 Harrison, Robert V., 346, 678
 Hartley, Douglas, 33, 367, 953
 Hartsoc, Jared, 701, 1107
 Hartwich, Heiner, 347
 Hasegawa, Shingo, 141, 829
 Hashimoto, Makoto, 139, 803
 Hashimoto, Sigeneri, 1063
 Hashimoto, Yuriko, 829
 Hashino, Eri, 192
 Hassan, Ahmed, 838
 Hasson, Dan, 281
 Hastings, Michelle, 757
 Hausman, Fran, 42, 425
 Hausman, Frances, 322
 Havens, Luke T., 786
 Haverkate, Maj, 864
 Haward, Simon, 741
 Hayasaka, Takahiro, 743
 Hayashi, Ken, 826
 Hayashi, Yushi, 302, 303
 Hayden, Russell, 1060
 Hayes, Sarah H., 532, 657
 Hazlett, Emily, 370
 Hazrati, Oldooz, 795
 He, David, 555, 618
 He, Shuman, 658
 He, Wenxuan, 120
 He, Zhizhou, 621
 Heavenrich, Miriam, 196
 Hebert, Sylvie, 281
 Heckler, Dietmar J., 53, 405
 Hedjoudje, Abderrahmane, 1060
 Hedrick, Mark, 494
 Heeringa, Amarins, 220
 Hegde, Rashmi, 881
 Hegemann, Stefan, 539
 Hegland, Erica L., 183
 Heil, Peter, 906
 Heinz, Michael, 497, 917, 1108
 Heiser, Marc, 89
 Heller, Stefan, 787
 Helms, Cynthia, 586
 Hemmert, Werner, 391, 396, 849, 1090
 Hempel, John-Martin, 391
 Henkemeyer, Mark, 292
 Henry, James, 258, 583
 Henry, Kenneth, 917
 Henshaw, Helen, 526
 Hernandez, Victor H., 268, 694
 Hernandez-Rojas, Jorge, 924
 Hero, Jean-Marc, 1083
 Hershnhoren, Itai, 366
 Hertzano, Ronna, 732
 Hess, Christi, 420
 Hesse, Lara Li, 930, 938
 Hickox, Ann, 1119
 Hickox, Ann E., 333, 1114
 Hidaka, Hiroshi, 410
 Hide, Winston, 585
 Hideko, Nakajima, 774
 Higgins, Nathan, 959
 Highstein, Stephen, 244, 254
 Higuchi, Hitomi, 429
 Hildebrand, Michael, 27
 Hill, Kayla, 822
 Hinduja, Sneha, 304
 Hinrich, Anthony, 757
 Hirasawa, Noriyasu, 1118
 Hirose, Keiko, 751, 752, 845
 Hirose, Kenzo, 742
 Hirose, Yoshinobu, 139, 746, 747
 Hirota, Koichi, 1079
 Hisa, Yasuo, 836
 Hladek, Lubos, 518
 Ho Sui, Shannan, 585
 Hoch, Gerhard, 268, 462, 694
 Hoffman, Howard J., 633
 Hoffman, Larry, 148, 241
 Hoffpauir, Brian, 1014
 Hofmann, Kay, 14
 Hogan, Patrick, 651
 Holcomb, Paul, 1014
 Holfoth, David, 182, 481
 Holley, Matthew C., 467, 1008
 Hollister, Scott, 589
 Holly, Jan, 551, 552
 Holman, Holly, 163, 254, 464
 Holmes, Emma, 525
 Holstein, Gay, 546, 547
 Holt, Avril Genene, 234, 871, 872
 Holt, Jeffrey, 296
 Holt, Joseph C., 252, 253
 Homma, Kazuaki, 155, 156, 553
 Honaker, Julie, 409, 812
 Hong, Amy, 513
 Hong, Bo, 665
 Hong, Jason S., 14
 Hong, Ki Hwan, 805
 Hood, Linda, 926
 Hopkins, Kathryn, 932
 Horii, Arata, 249
 Horikawa, Junsei, 368
 Horn, David, 600
 Horn, Henning F., 23
 Hornak, Aubrey, 1026
 Hornickel, Jane, 919
 Hosoi, Hiroshi, 448, 452, 453
 Hotehama, Takuya, 408
 Houben, Rolph, 864
 Housley, Gary D., 26
 Howard, Matthew, 960
 Hoyos, Tatiana, 1119
 Hrabé de Angelis, Martin, 720
 Hsieh, Chia-Lung, 739
 Hsu, Chuan-Jen, 709, 712, 715
 Hu, Bo Hua, 56, 57, 319, 631
 Hu, Jinwei, 900, 901
 Hu, Ning, 1111
 Hu, Zhengqing, 567
 Huang, Chengcheng, 104
 Huang, Genevieve, 569, 783
 Huang, Hai, 66
 Huang, Juan, 493
 Huang, Teng, 996
 Huang, Tzu-Hui, 813
 Huang, Zhen, 72
 Huber, Alex, 404
 Huber, Alexander M., 437
 Hubka, Peter, 655, 980
 Hudspeth, A. J., 599, 615, 617
 Hudspeth, Jim, 25
 Huebner, Patrick, 542
 Hullar, Timothy, 819
 Hulleit, Patrick, 96
 Huma, Andreea, 719
 Humes, Larry, 562
 Hummel, Jennifer, 762
 Huppert, Theodore, 815
 Hurd, Elizabeth, 288
 Hurley, Laura, 667, 734
 Hussain, Kiran, 830
 Hwang, Juen-Haur, 715
 Hyde, Elizabeth, 683
 Hyeon, Jae-Hwan, 242
 Hyun Kwon, Jae, 734
 Ibrahim, Ibrahim, 626
 Ibrahim, Rasha A., 914
 Ifeanyi, Chuka, 37
 Ihrle, Sebastian, 437
 Iida, Koji, 45, 1118
 Iizuka, Takashi, 190
 Ikeda, Katsuhisa, 107, 190, 329, 330, 699, 1118
 Ikeda, Ryoukichi, 105
 Ikeda, Takuo, 803
 Ikehara, Yasuhiro, 1063
 Ilbegi, Nima, 220
 Illing, Robert, 65, 647
 Im, Gi Jung, 1046
 Imai, Takao, 249
 Imaizumi, Kazuo, 97
 Imig, Thomas, 1102
 Indrakanti, Divya, 146
 Indzhukilian, Artur, 466, 470, 881
 Ingham, Neil, 19, 20, 717, 719, 823, 1008
 Inohara, Hidenori, 249
 Inokuchi, Go, 411
 Inoshita, Ayako, 190
 Irino, Toshio, 491
 Irsik, Vanessa, 208
 Irvine, Dexter, 394
 Irving, Samuel, 38, 394
 Isaiah, Amal, 33, 955
 Isakov, Ofer, 16
 Ise, Momoko, 1010
 Ishida, Tomohiro, 368
 Ishida, Yusuke, 249
 Ishihara, Kenji, 1118
 Ishii, Satoshi, 964
 Ishimitsu, Shunsuke, 1049
 Ishiyama, Akira, 148
 Ishiyama, Gail, 148
 Ismail, Ozama, 717
 Isoguchi, Tomoyo, 82
 Ison, James, 180
 Issa, John, 84, 92

- Itatani, Naoya, 949
Ito, Juichi, 111, 187, 302, 303, 736
Ito, Rindy, 688
Ito, Taku, 1117
Ivanova, Anna A., 1124
Ives, David, 479, 487
Ives, Timothy D., 398
Iwakura, Takashi, 452
Iwasaki, Shinichi, 430, 431
Iwata, Ayaka, 47
Iyer, Nandini, 219, 521
Jabre, Nicholas, 40
Jackson, Dakota, 1014
Jackson, John, 571
Jackson, Ryan, 438
Jacques, Bonnie, 791
Jacques, Steven, 769
Jäger, Katharina, 1068
Jahan, Israt, 28, 274, 574, 1012
Jajoo, Sarvesh, 760
Jamal, Lena, 682
Jamesdaniel, Samson, 304
Jameyson, Elyse M., 398
Jansen, Sebastian, 395
Janz, Philipp, 647
Jara, Natalia, 101, 654
Jason, Pecka, 618
Jaworek, Thomas J., 1124
Jeang, Kuan-Teh, 23
Jeanne, James, 9
Jedrzeczak, Wiktor, 167
Jeevarajan, Jerome, 551
Jeffers, Penelope W.C., 334
Jenkins, Herman A., 30
Jennings, Skyler, 1075
Jennings, Todd, 970
Jensen Smith, Heather, 318, 1004
Jeon, Chang-Jin, 722
Jernigan, Courtney, 240
Jesteadt, Walt, 485
Jiang, Haiyan, 1021, 1047
Jiang, Hui, 567
Jiang, Meiyang, 1032
Jiang, Zhi-Gen, 267, 834, 835, 1032
Jin, Kai, 789
Jin, Yongming, 98
Jing, Zhiyi, 268, 694, 882
Jiradejvong, Patpong, 383, 493, 991
Jiwani, Salima, 652
Jodelka, Francine, 757
Joglekar, Samidha, 660
Johnson, Angélique, 403
Johnson, Kenneth, 607
Johnson, Stuart, 53, 119, 467, 1008
Johnsrude, Ingrid, 196, 495, 894
Johnstone, Patti, 494
Joly, Olivier, 486
Jones Huyck, Julia, 196
Jones, Adam P., 955
Jones, Bianca, 95
Jones, Heath, 973
Jones, Sheri, 812, 1122
Jones, Simon, 967
Jönsson, Radoslava, 798
Jordan, Paivi M., 253
Jorgensen, Erik, 464
Jørgensen, Søren, 216
Joris, Philip, 352, 353
Joris, Pierre, 400
Joshi, Suyash, 485
Jovanovic, Sasa, 343
Juhn, Steven, 426
Jüllicher, Frank, 616
Jung, Enja, 636
Jung, Hak Hyun, 1046
Jung, Jae-Yun, 225, 242
Juul, Holger, 798
Kabara, Lisa, 331, 332, 683
Kachar, Bechara, 26, 458, 467, 469
Kachelmeier, Allan, 753, 838, 1030
Kaczmarek, Leonard, 936
Kadokia, Sama, 693
Kahn, Kayla, 378
Kahn, Richard A., 1124
Kajikawa, Yoshinao, 79
Kakaraparthy, Bala Naveen, 331, 332
Kakehi, Kazuhiko, 1096
Kakigi, Akinobu, 159, 430, 431, 699, 737
Kalayjian, Zaven, 545
Kale, Shusrut, 691, 917
Kalinec, Federico, 707, 708, 827, 828
Kalinec, Gilda, 828
Kallakuri, Srinivas, 1100
Kalluri, Sridhar, 487, 853
Kaltenbach, James, 222, 530, 650
Kalwani, Neil, 714, 741
Kam, Alice, 820
Kamakura, Takefumi, 249
Kamasawa, Naomi, 339
Kamiya, Kazusaku, 190, 329, 330
Kammerer, Robert, 162
Kamogashira, Teru, 430
Kampel, Sean, 848
Kan, Alan, 449, 520, 522, 973
Kanaan, Moien, 718
Kanagawa, Eijyu, 139, 746, 747
Kane, Catherine J., 1025
Kaneko, Hiroki, 716
Kaneshiro, Blair, 877
Kang, Woo Seok, 749
Kanicki, Ariane, 224, 311, 331, 332
Kannengießler, Marc, 405
Kanold, Patrick, 284, 1016, 1017
Kanold, Patrick O., 955
Kantner, Claudia, 804
Kanwisher, Nancy, 948
Kanzaki, Ryohei, 82, 941
Kanzaki, Sho, 826
Kao, Albert, 767
Kao, Chung-Lan, 813
Karasawa, Keiko, 329, 330
Karasawa, Takatoshi, 1029, 1032
Karavitaki, K. Domenica, 471
Karet Frankl, Fiona E., 823
Karfunkel, Daphne, 718, 720
Karg, Sonja, 396
Karim, Helmet, 815
Karino, Shotaro, 430, 431, 742
Kashanian, Nina, 532
Kashino, Makio, 175, 197, 202, 1079, 1082
Kashio, Akinori, 430, 431, 635, 737
Kastl, Daniel, 1105
Kästner, Sabine, 623
Kataoka, Kazunori, 742
Kato, Nobumasa, 1082
Katsunuma, Sayaka, 141
Kaur, Tejbeer, 752, 760
Kawahara, Hideki, 501
Kawai, Hideki, 87
Kawamoto, Kohei, 1062
Kawano, Satoyuki, 187
Kawasaki, Hiroto, 960
Kawase, Tetsuaki, 410
Kawauchi, Satoko, 140
Kawaura, Mitsuhiro, 826
Kaya, Emine Merve, 496
Kazmierczak, Piotr, 607
Kazmitcheff, Guillaume, 590
Keane, Thomas, 20
Kearse, Michael, 1087
Keefe, Douglas, 587
Keine, Christian, 640
Keith, Robert, 390, 412
Keller, Jacob, 156
Keller, Jesse, 792
Keller, Matthew, 794
Kelley, Matthew, 193, 272, 290, 291, 293, 299
Kelley, Phillip, 885
Kelly, Heather, 519
Kempfle, Judith, 265, 585, 695
Kempter, Richard, 1086
Kempston, Beth, 42, 425
Kennon-McGill, Stefanie, 1102
Kent, Deniz, 989
Keplinger, Stefan, 969
Kersigo, Jennifer, 274, 574, 1011, 1012
Kesser, Bradley, 480
Kettler, Lutz, 516
Khalifa Alkowiari, Moza, 726
Khan, Aziz, 682
Khan, Shaheen, 729, 881, 1124
Khojasteh, Elham, 539
Khouri, Leila, 366
Kidd Jr., Gerald, 407
Kidd, Gary R., 418
Kidd, Grahame, 650
Kidokoro, Yoshinobu, 190, 330
Kikuchi, Yukiko, 950
Kilgore, Chelsea, 1071
Killius, Jeanette, 676
Kim, Ah Reum, 711
Kim, Bo Gyung, 427
Kim, Bong Jik, 242, 711
Kim, Chang-Hee, 237
Kim, Dong Kee, 50
Kim, Duck, 514, 515
Kim, Ernest, 704
Kim, H. Jeffrey, 228
Kim, Hong Lim, 50
Kim, Hongkyung, 106, 1007
Kim, Hwi Ram, 727
Kim, Hyung Jin, 1009
Kim, Jichul, 1055
Kim, Jin Woo, 1009
Kim, Jin Young, 160
Kim, Jinsook, 422
Kim, Jun Hee, 351
Kim, Jung Min, 427
Kim, Kyunghee X., 609
Kim, Kyu-Sung, 805
Kim, Namkeun, 1058, 1059
Kim, Sei Eun, 351
Kim, Seung Won, 1044, 1045
Kim, Suejin, 24
Kim, Sung Huhh, 160
Kim, Sung Won, 406
Kim, Tae Su, 237, 749
Kim, Un-Kyung, 427, 722, 727
Kim, Ye-Hyun, 296
Kim, Yeon Ju, 1044, 1045
Kim, Yeunjung, 328, 713
Kim, Young Sun, 1044, 1045
Kimura, Akinori, 724
Kimura, Tohru, 107
Kinder, Kimberly, 606
King, Andrew, 33, 908
King, Andrew J., 879
King, Mary-Claire, 26
Kinoshita, Makoto, 750
Kishon-Rabin, Liat, 614
Kitahara, Tadashi, 249
Kitamura, Ken, 724
Kitazawa, Shigeru, 1082
Kitsunai, Yoko, 45
Kitterick, Padraig, 525
Klis, Sjaak, 397
Klotz, Caitlyn, 1013
Kludt, Eugen, 474
Klump, Georg, 507, 1094
Klump, Georg M., 671, 949, 1089
Knipper, Marlies, 53, 162, 277, 467, 1008
Knisely, Katherine, 403
Knudson, Inge, 230
Knyazeva, Stanislava, 603
Ko, Hyukwan, 1007
Ko, Kwang Woo, 364
Kobayashi, Kota, 52
Kobayashi, Takayuki, 187
Kobayashi, Toshimitsu, 45, 410, 1118
Koch, Fred, 969
Koch, Ursula, 67
Kochanek, Krzysztof, 167
Kodali, Vikas, 679
Koehler, Carla M., 14
Koehler, Seth, 531, 957
Koehn, Heather, 130
Koelewijn, Thomas, 862
Koepl, Christine, 1093, 1112
Koessl, Manfred, 762, 1048
Kohlrausch, Armin, 177
Kohrman, David, 331, 332, 728
Koka, Kanthaiah, 30, 447, 511, 775
Kol, Nitzan, 718
Kollmar, Richard, 573
Komatsu, Hirokazu, 411
Kommareddi, Pavan, 331, 332
Komune, Shizuo, 588, 1003
Kondo, Tadahisa, 1096
Koning, Raphael, 998
Konnerth, Arthur, 285
Koo, Jawon, 1028
Koo, Soo Kyung, 1009
Kopco, Norbert, 518
Kopelovich, Jonathan, 37
Kopke, Richard, 320, 784
Köppel, Christine, 903
Köpschall, Iris, 53
Kopun, Judy, 1066
Korchagina, Julia, 840
Korenic, Andrej, 640
Koretsky, Alan, 866
Kössl, Manfred, 166, 1068
Kotak, Vibhakar, 384
Kotak, Vibhu, 1015
Koulich, Elena, 323
Koyama, Shin, 1063
Kozlov, Serguei, 23
Kral, Andrej, 623, 655, 686, 696, 740, 980
Kramarenko, Inga, 843
Kramer, Kenneth, 114
Kramer, Richard H., 364
Kramer, Sophia, 862
Kratz, Megan, 93
Kraus, Nina, 61, 62, 645, 873, 875, 891, 919
Kraut, Michael, 312
Kreeger, Lauren, 70
Kremmyda, Olympia, 802
Krey, Jocelyn, 118, 608
Krishnamoorthy, Gayathri, 832
Krishnan, Ananthanarayan, 921, 952
Kristiansen, Arthur G., 334
Krizman, Jennifer, 645, 875
Krug, Edward L., 786
Krüger, Alexander, 696
Krumbholz, Katrin, 1081
Kruper, Gregory, 528
Ku, Yuan-Chieh, 108, 290, 586
Kuberan, Balagurunathan, 163
Kubisch, Christian, 14
Kubo, Nobuo, 1062
Kuchinsky, Stefanie, 523
Kuenzel, Thomas, 344, 345
Kügler, Sebastian, 268, 694
Kuhn, Stephanie, 53, 1008
Kujawa, Sharon, 334, 637, 700, 1020
Kulesza, Randy, 925
Kulkarni, Aditya, 392, 660
Kumano, Shun, 45, 1118
Kumar, Shaun, 690
Kumar, Sukhbinder, 380, 888, 950, 951
Kumaraguru, Anand, 935
Kumoi, Kazuo, 411
Kunz, Lars, 969
Knyazeva, Stanislava, 640
Kuriki, Shinya, 99
Kurioka, Takaomi, 140
Kurita, Akihiro, 140
Kurth, Stefanie, 344, 345
Kuwada, Shigeyuki, 514, 515
Kwak, Eunye, 413
Kwak, Sangyeop, 413
Kwon, Bomjun, 793, 799
Kwon, Tae Jun, 727
Laback, Bernhard, 509
Lackner, Christina, 396
Lacour, Stéphanie, 400
Laczkovich, Irina, 331, 332
Lad, Yatish, 702
Ladak, Hanif M., 439, 443
Ladrech, Sabine, 126
Laflen, J. Brandon, 999
Lahann, Joerg, 706
Lai, Jesyin, 634
Lakemeyer, Gerhard, 517
Lall, Kumud, 637, 1020
Lalor, Edmund, 527, 943
Lamb, Jessica, 1052
Lammers, Marc, 94
Lancelin, Denis, 200
Land, Rüdiger, 655
Landry, Tom, 39
Landsberger, David, 976, 977, 983, 986
Lang, Dustin, 58, 745
Lang, Hainan, 627, 786, 905
Lang, Kathrin, 309
Langemann, Ulrike, 1094
Langenbacher, Achim, 405
Langer, Robert, 700
Langers, Dave, 229, 231, 280
Lansky, Beate, 714
Lapsley Miller, Judi, 1067
Large, Charles, 930, 936
Larrain, Barbara, 322
Larson, Eric, 886, 940
Lasker, David, 255
Laudanski, Jonathan, 172, 996, 997
Lauer, Amanda, 338, 646, 648
Lazard, Diane, 200
Lazarini, Paulo, 134
Le Goff, Nicolas, 177
Le Prell, Colleen, 1038
Leach, Nicholas D., 879
Leake, Patricia, 401, 692
Leal, Suzanne, 731, 881
Leaver, Amber, 228
Ledoux, Joseph E., 854
Lee, Adrian K.C., 527, 940, 954
Lee, Calvin, 222
Lee, Changwon, 1053
Lee, Charles, 97, 855
Lee, Choongheon, 409
Lee, Daniel, 265, 400, 433, 695, 779
Lee, Jae Wook, 225
Lee, Jianyi, 269
Lee, Jungnak, 422
Lee, Jungmee, 1064
Lee, Jung-Seob, 406
Lee, Jungwha, 1064
Lee, Kwanghyuk, 881
Lee, Kyu-Yup, 722
Lee, Min Young, 225
Lee, Norman, 209, 512
Lee, Patrick, 668
Lee, Roger, 43
Lee, Sang-Heun, 722
Lee, Sangmin, 805
Lee, Sue, 881, 1122
Lee, Won-Sang, 160
Lee, Wookey, 805
Lee, Yoojin, 456, 755, 756
Lee, Yungling Leo, 715
Leek, Marjorie, 848
Leek, Marjorie R., 604
Legan, Kevin, 840
Léger, Agnès, 200, 217, 479
Lehmann, Alexandre, 928
Lehnert, Simon, 1085
Lei, Debin, 55, 223
Leibold, Lori, 503
Leman, Marc, 474

- Lenarz, Thomas, 29, 442, 686, 696, 740
 Lenoir, Mark, 126
 Lentz, Jennifer, 468, 757
 Lenz, Danielle R., 23, 720
 Leong, Ng Chyan, 309
 LeRoith, Derek, 297, 297
 Lesica, Nicholas, 1115
 Lesicko, Alexandria, 88
 Lesperance, Marci M., 1120
 Leung, Sumie, 103
 Levano, Soledad, 306
 Lewis, Morag, 17, 20
 Lewis, Rebecca, 792
 Lezirovitz, Karina, 184
 Li, Cheng, 28
 Li, Chuan-Ming, 633
 Li, Gang Q., 246
 Li, Geng-Lin, 129
 Li, Hongzhe, 1028, 1030, 1031
 Li, Huawei, 703, 833, 1061
 Li, Jennifer, 540
 Li, Jin, 71
 Li, Muwei, 659
 Li, Na, 968
 Li, Shufeng, 1110
 Li, Song-Zhe, 751
 Li, Tianhao, 666
 Li, Wei, 320, 784
 Li, Wenyang, 833, 1061
 Li, Xiangming, 579, 824
 Li, Yingxing, 788
 Li, Yiping, 1116
 Li, Yizeng, 773
 Li, Yun, 14
 Liang, Chun, 827, 1123
 Liang, Ruqiang, 55
 Liang, Ru-Qiang, 723
 Liao, Eric, 1119
 Liberman, Charles, 256, 637, 669, 1018, 1019, 1114, 1119
 Licastro, Danilo, 726
 Lichtenhan, Jeffery, 125, 1107
 Lie, TjenSin, 1060
 Lim, David, 456, 755, 756
 Lim, Hubert, 405, 651, 668, 1098, 1104, 1105
 Lim, Hye Jin, 1044, 1045
 Lim, Rebecca, 542
 Limb, Charles, 195, 383, 393, 474, 493, 991
 Lin, Chia-Cheng, 817
 Lin, Frank, 312
 Lin, I-Fan, 202
 Lin, Qin, 833
 Lin, Shu-Wha, 712
 Lin, Wei, 72
 Lin, Xi, 18, 328, 703, 712, 713, 1121
 Lin, Ying-Hung, 712
 Lin, Yin-Hung, 715
 Lin, Yi-Tsen, 709
 Lin, Yung-Song, 393
 Linbo, Tor, 1033
 Linden, Jennifer, 85, 930, 938
 Ling, Harrod, 253
 Ling, Lynne, 625
 Lingner, Andrea, 359
 Linke, Annika C., 890
 Linthicum, Jr., Fred, 710, 1027, 1125
 Lipovsek, Marcela, 463
 Lippard, Stephen, 72
 Litovsky, Ruth, 420, 449, 520, 522, 973
 Litovsky, Ruth Y., 495
 Little, David F., 371
 Liu, Dong, 788
 Liu, Hong, 837
 Liu, Huihui, 788
 Liu, Huizhan, 555, 618, 621
 Liu, Jian, 443
 Liu, Jianping, 1030
 Liu, Lijie, 1039
 Liu, Liqian, 144
 Liu, Qiang, 464
 Liu, Qiaoyun, 36
 Liu, Qing, 916
 Liu, Tien-Chen, 715
 Liu, Wei, 127, 128
 Liu, Xue Zhong, 26, 324, 337, 424
 Liu, Yanju, 1056
 Liu, Yi-Wen, 1054
 Liu, Zhiyong, 570
 Llano, Daniel, 88, 624
 Lobarinas, Edward, 178, 597
 Locastro, Michael, 377
 Loera, Katherine, 689
 Loizou, Philip, 794, 795
 Longenecker, Ryan, 221, 1099
 Longo, Federica, 164
 Lonsbury-Martin, Brenda, 165, 596
 Lopez Valdes, Alejandro, 388
 Lopez, Ivan, 148, 241
 López-González, Mónica, 383
 Lorente, Beatriz, 17
 Lorente-Canovas, Beatriz, 823
 Lorenzi, Christian, 31, 200, 212, 217, 398, 479, 487, 644
 Loughlin, Patrick, 817
 Lovas, Sandor, 555, 618
 Love, Emily, 142
 Lovett, Michael, 108, 290, 291, 586
 Lovett, Rosemary, 419
 Low, Sean, 25
 Lowenstein, Joanna, 612
 Lu, Chin-Chun, 791
 Lu, Fengqing, 567
 Lu, Hui-Ping, 393
 Lu, Jianzhong, 320
 Lu, Jingqiao, 713
 Lu, Xiaowei, 269
 Lu, Ying-Chang, 709, 712, 715
 Lu, Yong, 362, 363
 Lu, Zhongmin, 324, 424
 Lu, Zoe, 223
 Luan, Chi-Hao, 566
 Luecke, Anne E., 253
 Lui, Hui-Zhan, 631
 Lukashina, Victoria, 735
 Lukose, Richard, 925
 Lumbreras, Vicente, 341
 Lunner, Thomas, 861
 Luo, Hao, 1100
 Luo, Ping, 1069
 Luo, Xin, 35
 Luo, Xuemei, 567
 Lupo, J. Eric, 30, 447, 775
 Lustig, Lawrence, 335
 Luu, Grace, 450
 Lysaght, Andrew, 124, 714, 741
 Lysakowski, Anna, 152, 245
 Lyu, Ah-Ra, 831
 Ma, Eva, 576
 Ma, Jihyun, 1007
 Ma, Ji-Hyun, 106
 Ma, Leung-Hang, 540
 Ma, Rui, 789
 Ma, Xuefei, 117
 Maass, Juan, 575
 Maat, Bert, 34, 989
 MacArthur, Carol, 425
 MacDonald, Ewen, 216
 MacDonald, Glen, 243
 Macherey, Olivier, 984
 Mackinnon, Robert, 54
 MacLeod, Katrina, 70
 Maddox, Ross, 886, 954
 Maerten, Karlee, 178
 Maftoon, Nima, 444, 445
 Magezi, David, 847
 Magistretti, Jacopo, 460
 Magnusson, Lennart, 798
 Mahendrasingam, Shanthini, 473
 Mahmood, Gulrez, 528
 Mahoney Rogers, Amanda, 289
 Maier, Hannes, 29, 442, 696
 Maison, Stéphane F., 1018
 Majdak, Piotr, 316, 509
 Majumder, Paromita, 1036
 Mak, Tak, 107
 Makishima, Tomoko, 536
 Maklad, Adel, 133, 240
 Mallinckrodt, Lisa, 34
 Malmerica, Manuel, 639, 662, 663
 Malone, Brian, 89
 Manak, J. Robert, 1024
 Mangiore, Rachael, 819
 Manis, Paul, 64, 93
 Mann, Mary Anne, 244
 Mann, Zoe, 290, 291
 Manohar, Senthilvelan, 529, 534, 535, 1022
 Manor, Uri, 467
 Manoussaki, Daphne, 1052
 Mantokoudis, Georgios, 816
 Manzoor, Nauman, 222, 530, 650
 Mao, Junwen, 181
 Mao, Olivia, 223
 Marcotti, Walter, 53, 119, 467, 1008
 Marcus, Daniel C., 579, 824
 Markovitz, Craig, 651, 1104
 Marquardt, Torsten, 218, 358, 967
 Márquez, Emmanuel, 98
 Marrs, Glen, 1014
 Marshall, Lynne, 1067
 Martin, Amanda K., 194
 Martin, Cathy, 311
 Martin, Donna, 288
 Martin, Glen, 165, 596
 Martin, Karen Ann, 494
 Martin, Pascal, 616
 Martin, William, 584
 Martinelli, Giorgio P., 546, 547
 Martinez, Carlos, 236
 Martinez-Vega, Raquel, 719
 Martins, Ana Raquel, 90
 Masetto, Sergio, 460
 Mason, Christine, 407
 Masood, M. Arjumand, 552
 Massaad, Cynthia, 869
 Masterson, Megan, 35
 Masud, Salwa, 887
 Masuda, Sawako, 716
 Masutomi, Keiko, 197
 Mathias, Samuel R., 174
 Matic, Agnella, 693, 697
 Matsui, Jonathan, 1006
 Matsui, Toshie, 448, 452, 491
 Matsumoto, Nozomu, 588
 Matsumoto, Yu, 742
 Matsunaga, Tatsuo, 716
 Matsunobu, Takeshi, 140
 Matt, Tanja, 309
 Matthews, Jacob, 890
 Mattley, Jane, 85
 Mattox, Douglas, 713
 May, Andrew P., 28
 May, Brad, 257, 1103
 May, Lindsey, 783, 843, 844, 1035
 Mayerhoff, Ross, 528
 May-Simera, Helen, 291
 McLaughlin, Myles, 382, 387, 388
 McAlpine, David, 218, 357, 358, 930, 938, 967, 1097
 McBride, Ethan, 349
 McCaffrey, Kate, 757
 McColgan, Thomas, 1086
 McCormack, Abby, 227
 McCormack, Abigail, 417
 McCormick, David, 958
 McDermott, Brian, 146
 McDermott, Josh, 13, 501, 948
 McDougald, Devin, 191
 McFerran, Don, 236
 McGee, JoAnn, 59, 621, 825
 McGinley, Matthew, 958
 McGuire, Brian, 648
 McKenna, Michael J., 334
 McKinley, Gareth, 741
 McKinnon, Melissa, 454
 McLaughlin, Myles, 352
 McLaughlin, Susan, 893, 959
 McIntyre, Rebecca, 717
 McMahan, Melissa, 668
 McMillan, Garnett P., 418
 McNulty, Bridgett, 270
 Meaud, Julien, 1057
 Meech, Robert, 46
 Meehan, Dan, 465
 Meenderink, Sebastiaan, 764, 767
 Megerian, Cliff, 1116
 Mehta, Anahita, 946
 Meinen-Derr, Jareen, 993
 Melcher, Jennifer, 230
 Melki, Sami, 1116
 Mellado Lagarde, *Marcia, 735
 Mellott, Jeffrey, 676, 677, 681
 Meltser, Inna, 51, 595
 Menardo, Julien, 1043
 Mendus, Diana, 21
 Meng, Xiangying, 1017
 Meno, Chikara, 1003
 Menon, Vinod, 877
 Merchant, Gabrielle R., 433
 Merchant, Saumil N., 433
 Mercier, Patrick, 124
 Mertens, Griet, 976
 Mescher, Mark, 704
 Mesgarani, Niman, 96, 527
 Metter, E. Jeffrey, 312
 Meyer, Bernard, 200
 Meyer, Martin, 309
 Meyer, Nicole C., 28
 Mi, Xiaoxiao, 788
 Miah, Mahfuzur, 937
 Michalakos, Stylianos, 969
 Michel, Christophe, 911
 Michel, Vincent, 151
 Micheyl, Christophe, 3, 174, 201, 209
 Middlebrooks, John C., 1, 382, 387, 508
 Middleton, Jason W., 874
 Mieda, Takuya, 87
 Migliaccio, Americo, 542, 801
 Mikuriya, Takefumi, 139, 746
 Milenkovic, Ivan, 343, 640
 Miller, Christopher, 811
 Miller, Danielle, 331, 332
 Miller, Josef, 224, 706, 1120
 Miller, Richard, 311
 Miller, Roger, 44
 Mineta, Hiroyuki, 743
 Mingroni-Netto, Regina, 184
 Minoda, Ryosei, 41, 185, 1010
 Minor, Lloyd B., 28, 808
 Minowa, Osamu, 190, 329, 330
 Minter, Ricki, 1113
 Miroir, Mathieu, 590
 Mirza, Najab, 871
 Mistry, Nina, 135
 Misurelli, Sara M., 495
 Mitrophanous, Kyriacos, 702
 Mitsak, Annie, 589
 Miwa, Toru, 41, 185, 1010
 Miyamae, Ryosuke, 452
 Miyazaki, Hiromitsu, 410
 Mizrahi, Adi, 286
 Mizuta, Kunihiko, 743
 Mizutari, Kunio, 705
 Mlynarczyk, Gregory, 226, 533
 Moayed-Esfahani, Yalda, 575
 Mochizuki, Hideki, 190
 Moeckel, Doreen, 166
 Moglie, Marcelo, 463
 Mohamad, Najibah, 235
 Moleti, Arturo, 164
 Moline, Mckay, 536
 Moles, Michelle R., 604
 Molloy, Katharine, 475
 Monaghan, Jessica, 994, 1097
 Monsell, Edwin, 567
 Monstrey, Jolijn, 602, 984
 Montbrio, Ernest, 374
 Montgomery, Scott, 325
 Montoya, Jose, 336
 Monzack, Elyssa, 843
 Moon, Il Joon, 497
 Moon, In Seok, 434, 727
 Moon, Seo, 337
 Moon, Sung, 456, 755, 756
 Mooney, Chance, 620
 Moore, Brian, 217, 580
 Moore, Charles, 713
 Moore, Dave, 54, 227
 Moore, David, 415, 417, 475, 526
 Moore, Ernest, 83
 Moores, Carolyn, 744
 Morata, Thais, 598
 Morell, Robert, 729
 Moreno, Sylvain, 931
 Morgan, Clive, 608
 Morgan, Susan, 228
 Mori, Susumu, 659
 Morizono, Tetsuo, 429
 Morley, Barbara, 885
 Morris, David, 798
 Morse-Fortier, Charlotte, 213
 Morton, Cynthia, 15, 455, 1119
 Moser, Tobias, 14, 268, 462, 694, 882, 883, 1114
 Moskatel, Tracey, 1064
 Moss, Cynthia, 971
 Motallebzadeh, Hamid, 445
 Mountain, David, 771, 778
 Mowery, Todd, 1015
 Mueller, Ulrich, 607
 Mukherhea, Debashree, 305, 307, 321, 759, 760
 Mulavara, Ajitkumar P., 811
 Müller, Susanne, 868
 Muniak, Michael, 679
 Murakami, Yasuki, 1049
 Murakoshi, Michio, 45, 1063, 1118
 Murata, Junko, 107, 699
 Murillo-Cuesta, Silvia, 300, 327
 Murphy-Courter M., Dora, 389
 Musiek, Frank, 673
 Mustain, William, 240, 537
 Mustapha, Mima, 21
 Mutai, Hideki, 716
 Myoga, Michael H., 359, 1085
 Myth, Gordon, 27
 Na, Woo Sung, 225
 Nadol, Joseph, 336
 Nagaike, Atsushi, 1082
 Nagatani, Yoshiki, 453
 Nair, Thankam, 331, 332
 Najmabadi, Hossein, 28
 Nakagawa, Seiji, 99, 408
 Nakagawa, Takashi, 429
 Nakagawa, Takayuki, 111, 187, 301, 302, 303, 736
 Nakajima, Heidi, 779
 Nakajima, Hideko H., 433
 Nakamagoe, Mariko, 1034
 Nakamoto, Kyle, 676
 Nakamura, Hiroyuki, 1118
 Nakamura, Yukiko, 249
 Nakanishi, Hiroshi, 743
 Nakano, Tamami, 1082
 Nakano, Toru, 107
 Nakano, Yoko, 1012
 Nakayama, Masahiro, 1034
 Nam, Jong-Hoon, 898, 1056
 Namba, Kazunori, 716
 Namiki, Shigeyuki, 742
 Nandamuri, Sri Pratima, 881
 Nara, Takeshi, 190
 Narins, Peter, 1083
 Naruse, Taeko, 724
 Natan, Ryan, 10
 Nataraj, Pratik, 702
 Nauwelaers, Tim, 740
 Navaratnam, Dhasakumar, 149, 154
 Navarro, Marco, 734

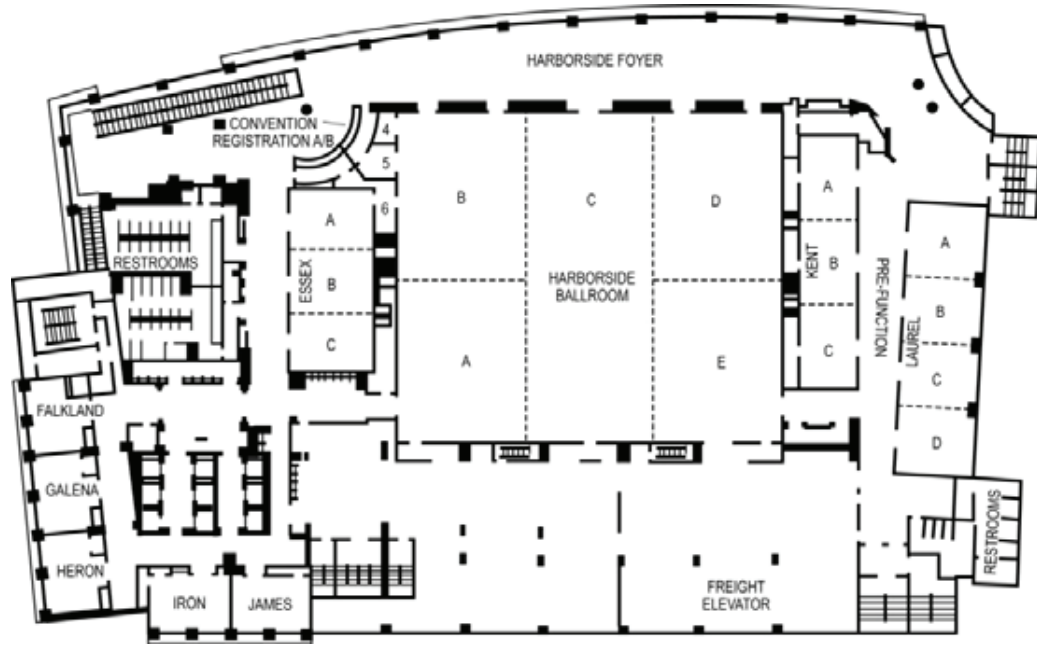
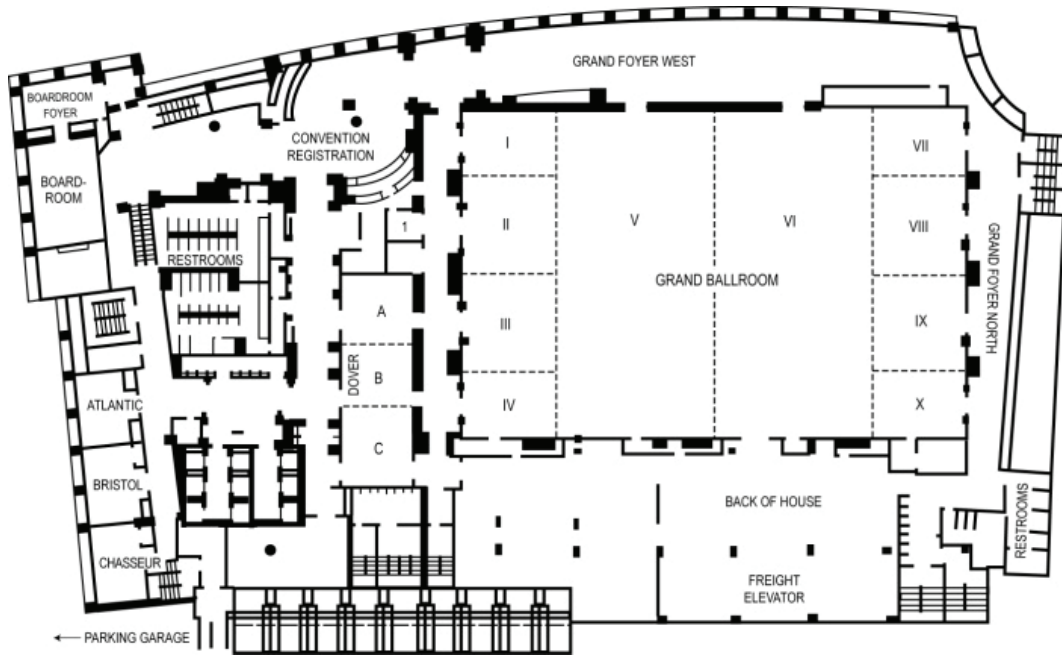
- Nayagam, Bryony, 1113
Nayak, Gowri, 1122
Nayak, Shruti, 248
Necciari, Thibaud, 509
Needham, Karina, 1113
Neely, Stephen, 1066
Negandhi, Jaina, 346
Neilans, Erikson, 182, 194, 481, 601
Nelken, Israel, 282, 366
Nelson, Brian, 2
Nelson, Mark, 1038
Neng, Lingling, 753, 754, 838, 839
Nerlich, Jana, 343, 640
Neuman, Arlene, 978, 1002
Newlands, Shawn, 549
Ngai, John, 298
Nguyen, Lynn, 163
Nguyen, Minh, 113
Nguyen, Tot Bui, 243
Nguyen, Yann, 590
Nguyen-Huynh, Anh, 689
Nibu, Ken-ichi, 141, 829
Nichols, Michael, 318, 619
Nicoletti, Michele, 396, 849
Nie, Liping, 758
Nies, Florian, 557
Niesten, Marlien, 433, 779
Nieto, Javier, 663
Nihira, Tomoko, 190
Niksch, Paul D., 471
Nin, Fumiaki, 615
Nishida, Tsuruyo, 1096
Nishimura, Bungo, 1034
Nishimura, Koji, 1106
Nishimura, Masahiko, 699
Nishimura, Tadashi, 448, 452, 453
Nishio, Ayako, 724
Nishio, Shinya, 1063
Nishitani, Allison, 296
Nittrouer, Susan, 612
Niu, Yuguang, 935
Niwa, Katsuki, 140
Noda, Takahiro, 82, 941
Noda, Teppi, 1003
Noda, Tetsuo, 190
Nodal, Fernando R., 879
Noguchi, Yoshihiro, 724
Nolan, Lisa S., 136
Nookala, Vikas, 569, 783
Norena, Arnaud, 939
Norgett, Elizabeth E., 823
Norman-Haignere, Sam, 948
Nothwang, Hans Gerd, 347
Nourski, Kirill, 960
Nouvian, Régis, 126, 461, 911
Nowotny, Manuela, 166, 762, 1048
Numata, Ryouta, 368
Nürnberg, Gudrun, 14
Nürnberg, Peter, 14
Nuttall, Alfred, 60, 267, 423, 768, 769, 782, 835
Nutter, Heather, 36
O Maoileidigh, Daibhid, 617
Ochi, Atsushi, 1082
Oda, Kazuha, 410
O'Donovan, Adam, 527
Oertel, Donata, 74, 180
Oesterle, Elizabeth, 787
Offutt, Sarah, 1098
Ogata, Erika, 430
Ogawa, Kaoru, 826
Oghalai, John, 49, 399, 781
Ogun, Oluwatobi, 465, 1005
Oh, Jeong-Hoon, 406
Oh, Sejo, 755
Oh, Se-Kyung, 722
Oh, Seung-Ha, 711
Ohashi, Mitsuru, 588
Ohl, Frank, 670
Ohlemiller, Kevin K., 594
Ohmer, Michel, 1083
Ohyama, Takahiro, 270
Oishi, Kenichi, 659
Oishi, Naoki, 822
Oiticica, Jeanne, 184
Ojima, Hisayuki, 368
Okada, Teruhiko, 699
Okamura, Jun, 743
Okano, Hideyuki, 107
Okano, Takayuki, 272, 299
Okazaki, Suzuyo, 249
Okou, David, 713
Okubo, Hideki, 1034
Okuyama, Shuhei, 1118
Olds, Cristen, 399
Olds, Kevin, 1060
O'Leary, Stephen, 1113
Oline, Stefan, 68
Oliver, Dominik, 557
Oliver, Douglas, 639
Olson, Elizabeth, 691, 772, 777
Olt, Jennifer, 467
O'Malley, Jennifer, 455
Omelchenko, Irina, 60, 267
O'Neill, William, 505, 510
Ong, Bonnie, 983
Ong, Cheng, 455, 739, 741
Oron-Karni, Varda, 718
Osborne, Lucy, 333
Osmanski, Michael, 179
Otsuka, Asuka, 99
Otsuka, Sho, 175, 1079
Ou, Henry, 1040, 1041, 1042
Ouellette, Christine, 234
Ovaska, Noora, 369
Overath, Tobias, 197, 950, 951
Owens, Kelly, 1033, 1041
Oxenham, Andrew, 174, 198, 199, 201, 484, 613, 942
Oya, Hiroyuki, 960
Ozmeral, Erol J., 498
Paasche, Gerrit, 686
Packer, Mark, 592
Padilla, Monica, 977, 986
Pagana, James, 1037
Page, Scott, 161
Paige, Gary, 505, 510
Pak, Kwang, 105, 308, 450, 451
Palan, Vikrant, 441, 591
Palanca-Castan, Nicolas, 1093
Palmer, Alan, 232, 965, 1101
Pals, Carina, 684, 863
Pan, Ning, 274, 574, 1012
Panu, Francesco, 725
Paolone, Nicholas, 649
Papal, Samantha, 147
Paparella, Michael, 134, 426, 436
Papesh, Melissa, 962
Papsin, Blake C., 652
Pararas, Erin, 704
Parbery-Clark, Alexandra, 891
Parikh, Malav, 531
Park, Eunjin, 805
Park, Gibeum, 711
Park, Hong Ju, 237, 749
Park, Hong-Joon, 427
Park, Hun Yi, 1044
Park, Hyun-Young, 1009
Park, Il Yong, 225
Park, Joo Hyun, 1028
Park, Kyoung-Ho, 50
Park, Mi-Hyun, 1009
Park, Raekil, 755, 756
Park, Shi-Nae, 50
Park, Sukyung, 1053
Park, Tae-Sung, 711
Park, Wookje, 805
Park, Woong-Yang, 711
Park, Yong-Ho, 785, 831
Park, Young-Min, 225
Parker, Andrew J., 606
Parker, Helen, 69
Parker, Luke, 1104
Parsa, Arya, 827, 828
Parthasarathy, Aravindakshan, 634
Parzefall, Thomas, 720
Pass, Johanna, 20, 719
Patel, Chirag, 573, 682
Patel, Minal, 319
Patil, Kailash, 372
Patterson, Jessie, 812
Pautler, Robia, 869
Pawlowski, Karen S., 323
Payne, Christopher, 888
Pear, Warren, 270
Pearson, Selina, 19, 20
Pecka, Jason, 186, 555
Pecka, Michael, 359
Peguero, Braulio, 314
Pelizzone, Marco, 543
Pellieux, Lionel, 506
Peña, Jose L., 850, 903, 1112
Peng, Anthony, 610
Peng, Shu-Chen, 393
Peng, Zhe, 109
Penman, Tina, 945
Penninger, Richard T., 474
Peppi, Marcello, 414
Pereira, Frederick, 49, 273, 748
Pereira, Lucio, 150
Perez Fornos, Angelica, 543
Perez, Ronen, 121
Perez-Fernandez, Déborah, 309
Perez-Gonzalez, David, 662
Perry, Trevor, 793, 799
Peters, Brian T., 811
Peters, Nils, 527
Peterson, Adam, 906
Peterson, Diana, 226, 533
Petit, Christine, 147, 151
Petkov, Christopher I., 950
Petralia, Ronald S., 458
Petrie, Tracy, 769
Petrillo, Marco, 1061
Pfungst, Bryan, 683, 992
Pham, Carol Q., 382, 387
Pham, Xuan-Phien, 569, 783
Pichora-Fuller, Kathy, 860
Pierce, Marsha L., 113, 1004
Pierstorff, Erik, 707, 708
Pierzycki, Robert, 227, 417
Pineda, Mario, 441, 591
Pinsky, Peter, 1055
Pirastu, Mario, 725
Plack, Chris, 932
Plack, Christopher, 173
Plotnik, Meir, 252
Pogoda, Hans-Martin, 14
Pogson, Jacob, 538
Poirier, Colline, 486
Poling, Gayla L., 1064
Pollak, George, 968
Polley, Daniel, 265, 669, 695, 859
Pollock, Lana, 146
Pollonini, Luca, 399
Pompe, Jeffrey, 527
Pongstaporn, Katanyu, 646
Pongstaporn, Tan, 338, 679
Pontoppidan, Niels Henrik, 478
Portfors, Christine V., 481
Prabhhu, Anjana, 611
Prasol, Melanie, 298
Premkumar, Preethi, 942
Price, Steven D., 245
Prieskorn, Diane, 224, 706, 1120
Prieve, Beth, 926
Prigioni, Ivo, 460
Profant, Oliver, 626
Psaltis, Demetri, 739
Pu, Dai, 713
Pu, Ye, 739
Puel, Jean-Luc, 126, 461, 911, 1043
Pujol, Remy, 39
Puria, Sunil, 438, 1055, 1058, 1059
Puvvada, Krishna, 373
Pylawka, Serhiy, 25
Qi, Weidong, 1021
Qin, Jia, 423
Quintanilla-Dieck, Lourdes, 322
Rabang, Cal, 858
Rabbitt, Richard, 163, 244, 254, 464
Racherla, Manoj, 732
Radford, Robert, 72
Radojevic, Vesna, 306
Radulovic, Tamara, 343
Radziwon, Kelly, 481, 490
Rafeeq, Maria, 1122
Raft, Steven, 292
Rahman, Irfan, 730
Rahman, Mehdi, 544, 545
Rahmani, Sahar, 706
Raible, David, 576, 1033, 1041
Rainville, Pierre, 928
Raisen, Claire, 717
Rajah, Gary, 871
Rajaram, Siddharth, 527, 943
Rajendran, Vishnu, 589
Rajguru, Suhru, 254, 341, 995
Ramachandran, Ramnarayan, 488, 641, 674
Ramakrishnan, Neeliyath, 150, 885
Ramakrishnan, V., 309
Ramamoorthy, Sripriya, 267, 768, 769
Ramekers, Dyan, 397
Ramenahalli, Sudarshan, 527
Ramkumar, Vickram, 305, 307, 321, 759, 760
Rankin, Summer, 383
Rankin, Summer K., 195
Raphael, Patrick, 49, 781
Raphael, Robert, 620, 761
Raphael, Yehoash, 288, 403, 548, 572, 683, 702, 785, 1120
Raphan, Theodore, 547
Rasetshwane, Daniel, 1066
Rask-Andersen, Helge, 127, 128
Rathkolb, Birgit, 720
Ratnam, Rama, 315
Ratnanather, J. Tilak, 659
Rauschecker, Josef, 228
Ravicz, Michael, 440
Ray, Kausik, 44
Raynor, Graham, 196
Razak, Khaleel, 81
Read, Heather, 7, 8
Rebscher, Stephen, 692
Redfern, Mark, 817
Reed, Caitlyn, 133
Reed, Charlotte, 215, 1067
Rees, Adrian, 611
Reh, Thomas, 842
Rehman, Atteeq, 729
Rehman, Zarin, 1025
Reichenbach, Tobias, 599, 615
Reif, Roberto, 423
Reilly, Richard B., 388
Reimann, Katrin, 832
Reinhart, Katherine, 1033
Reiss, Lina, 688, 689
Remington, Evan, 376
Ren, Dong-Dong, 789
Ren, Tianying, 120, 773
Renaud, Nicole, 586
Renaud, Philippe, 400
Reppa, Joyce J., 323
Resnick, Susan, 312
Reuter, Kirsten, 268, 694
Reyes, Maribel, 251
Reyes-Quintos, Ma. Rina, 731
Rhee, Chung-Ku, 225, 242
Riazuddin, Saima, 881, 1122, 1124
Riazuddin, Sheikh, 729, 881
Ricci, Anthony, 610, 1055
Richard, Celine, 1125
Richard, Elodie M., 1124
Richards, Virginia, 206
Richardson, Ben, 365, 625
Richardson, Guy, 14, 467, 840
Richardson, Matthew, 382
Richardson, Sophie, 415
Richter, Claus-Peter, 266, 693, 697, 918, 956, 995
Rieger, Brian, 656
Rigo, Frank, 757
Rinne, Teemu, 369
Rinzel, John, 104, 352, 374
Riquimaroux, Hiroshi, 52
Risk, Omar, 840
Ritchie, Robert, 27
Ritzl, Eva K., 808
Rivero, Francisco, 118, 119
Rivolta, Marcelo N., 188
Robbins, Carol, 47
Roberts, Brock, 1033
Roberts, Dale C., 541
Roberts, Larry E., 279
Roberts, Michael T., 353
Robertson, Nahid, 15, 455, 1119
Robins, Mike, 538
Robinson, Barbara, 37
Robinson, Linda, 314
Robles, Luis, 907
Robson, Drew, 540
Rocha-Sanchez, Sonia, 59, 825
Rodríguez-de la Rosa, Lourdes, 300, 327
Roehm, Pamela, 248
Rogers, Catherine, 796
Rohani, S. Alireza, 439
Rohbock, Karin, 53
Roland Jr., J. Thomas, 690
Romershausen, Bryce, 313
Romigh, Griffin, 521
Roongthumskul, Yuttana, 763, 896
Röösli, Christof, 404, 433, 437
Ropp, Tessa-Jonne, 1103
Rosen, Stuart, 524, 934
Rosowski, John, 433, 440, 454, 774, 779
Ross, Astin, 706
Ross, Deborah, 79
Ross, Robert, 269
Rossi-Izquierdo, Marcos, 806
Rosskothén-Kuhl, Nicole, 65
Roux, Kyle J., 23
Rowell, Jennifer, 110
Roy, Alexis, 991
Roy, Soumen, 843
Rozenbaum, Vasily, 1026
Rubel, Edwin, 349, 355, 361, 569, 576, 752, 1033, 1041
Ruben, Robert, 428
Rubin, Troy, 664
Rubinstein, Jay, 31, 398, 497, 600
Rubio, Maria, 339, 929
Rübsamen, Rudolf, 343, 640
Rudner, Mary, 861
Rudnick, Eric, 1038
Rudnicki, Anya, 16
Rudnicki, Marek, 1090
Ruettiger, Lukas, 53
Ruggles, Dorea, 198
Ruhland, Janet, 513, 1091, 1092
Rumpel, Simon, 283
Runge, Christina, 987, 988
Rupprecht, Laura, 778
Russell, Benjamin, 796
Russell, Ian, 735
Russo, Giancarlo, 460
Rutherford, Mark, 14, 462, 882, 883
Rüttiger, Lukas, 162, 467
Ryan, Allen, 26, 105, 308, 450, 451
Ryan, Kellie, 1098
Rybak, Leonard, 305, 307, 321, 759, 760
Rye, Jihee, 1009
Ryll, Jana, 77
Ryugo, David, 63, 338, 646, 679
Sabratzki, Sybille, 720

- Sadow, Peter, 733
 Saeed, Shakeel, 135, 136, 830
 Sagi, Elad, 1002
 Sahel, José-Alain, 151
 Sahly, Iman, 151
 Saija, Jeffa, 317
 Saito, Osamu, 452
 Sakaguchi, Hirofumi, 836
 Sakamoto, Takashi, 430, 431, 635, 737, 750
 Sakamoto, Tatsunori, 736
 Sakashita, Tetsushi, 964
 Sakuraba, Mayumi, 107
 Salamati, Ehsan, 439
 Salcher, Rolf, 29, 442
 Saldaña, Enrique, 98, 856
 Salditt, Tim, 268, 694
 Salt, Alec, 125, 701, 1107
 Saltzman, W. Mark, 784
 Salvi, Richard, 529, 532, 534, 535, 597, 657, 837, 1021, 1022, 1047
 Salviz, Mehti, 336
 Samani, Abbas, 439
 Sametskiy, Evgeny, 625
 Samy, Ravi, 993
 Sanes, Dan, 384, 867, 1015
 Sängner, Martin R., 405
 Sangi-Haghepykar, Haleh, 811
 Sanjust, Filippo, 164
 Sanneman, Joel, 579
 Santos, Felipe, 336
 Santos-Cortez, Regie Lyn, 731
 Santos-Sacchi, Joseph, 149, 154, 158, 897, 899, 911
 Santurette, Sébastien, 478
 Sarampalis, Anastasios, 636, 684, 863
 Sarro, Emma, 384
 Sarwar, Azeem, 43
 Sato, Shunichi, 140
 Satoh, Yasushi, 140
 Saunders, Thom, 331
 Savas, Jeffrey N., 308
 Savitsky, Douglas, 875
 Savli, Richard, 178
 Sawada, Naoki, 411
 Saxena, Udit, 416
 Schachern, Patricia, 134, 426
 Schacht, Jochen, 48, 309, 822
 Schaeette, Roland, 938
 Schänzler, Michael, 558
 Scheich, Henning, 603
 Scheifele, Peter, 412, 421
 Schemitsch, Michael, 501
 Schiavon, Emanuele, 69
 Schick, Bernhard, 53, 405
 Schier, Alexander, 540
 Schiromma, Cataldo, 151
 Schimrang, Thomas, 53
 Schlee, Winfried, 233, 661
 Schmitz Lundkvist, Gabriella, 51
 Schmitz, Samuel, 668
 Schneider, Erich, 802
 Schneider, Glenn, 252
 Schnupp, Jan, 908
 Schoen, Cynthia J., 1120
 Schoenwiesner, Marc, 878
 Schofield, Brett, 676, 677, 681
 Schönwiesner, Marc, 386, 928
 Schoof, Tim, 934
 Schopf, Christian, 623
 Schoppik, David, 540
 Schreiner, Christoph, 89, 96
 Schreiter, Cathleen, 405
 Schrode, Katrina, 512, 902
 Schroeder, Charles, 79
 Schrott-Fischer, Anneliese, 127, 128
 Schubert, Michael, 801, 810, 816
 Schuchman, Gerald, 687
 Scholarick, Nathan, 435
 Schulte, Bradley A., 627
 Schultz, Michael, 696
 Schuster, Maria, 391
 Schwab, Burkard, 29, 442
 Scita, Giorgio, 467
 Scott, Michael, 389, 412, 993
 Seal, Rebecca, 335
 Sedley, Will, 951
 Segenhout, Hans, 220
 Segil, Neil, 270, 276
 Seibel, Kai-Oliver, 345
 Seidl, Armin, 355
 Seitz, Aaron, 518
 Selezneva, Elena, 603
 Sellon, Jonathan, 1051
 Selman, Yamil, 138
 Selvakumar, Dakshnamurthy, 150
 Semaan, Maroun, 1116
 Semal, Catherine, 476
 Sen, Kamal, 947
 Sendin, Gaston, 461
 Sereda, Magdalena, 232
 Sergeyenko, Yevgeniya, 637
 Serrador, Jorge, 818
 Sesena, Emmanuel, 250
 Setou, Mitsutoshi, 743
 Setz, Cristian, 306
 Seward, Keena, 978, 1002
 Sewell, William, 705
 Seydell-Greenwald, Anna, 228
 Seymour, Michelle, 273, 748
 Sha, Su-Hua, 48, 309, 822
 Shackleton, Trevor, 1101
 Shah, Hetel, 912
 Shah, Manan, 732
 Shah, Samit, 573
 Shaheen, Luke, 1019, 1114
 Shamma, Shihab, 100, 201, 375, 377, 378, 385, 527, 963
 Shanbhag, Sharad, 370
 Shannon, Robert, 983
 Shapiro, Ben, 43
 Sharpee, Tatyana, 9
 Shaver, Mark D., 446
 Shcherbakov, Dmitri, 309
 Shearer, Eliot, 27
 Sheehan, Kelly, 305, 321, 759, 760
 Sheffield, Benjamin, 687
 Sheft, Stanley, 487
 Sheikh, Aminah, 1016
 Shen, Jun, 15
 Shen, Li, 665
 Shen, Yi, 205, 206
 Shepherd, Gordon M. G., 874
 Shepherd, Robert, 38, 39, 394
 Sheppard, Adam, 535
 SHERA, Christopher, 1050, 1069, 1084
 Shi, Lei, 423
 Shi, Xiaorui, 753, 754, 838, 839
 Shigemoto, Ryuichi, 339
 Shim, Byoung Soo, 237
 Shim, Hyeon-min, 805
 Shim, Hyun Joon, 31
 Shim, Katherine, 289
 Shimada, Aki, 724
 Shimada, Shoichi, 249
 Shimogori, Hiroaki, 139, 746, 803
 Shimokura, Ryota, 448, 452
 Shimomura, Atsushi, 192
 Shin, Joong-Wook, 427
 Shin, Jung-Bum, 469, 1037
 Shinder, Michael, 549
 Shinn-Cunningham, Barbara, 1, 381, 527, 887, 923, 927, 933, 943, 1084
 Shinomiya, Hitomi, 829
 Shiotani, Akihiro, 140
 Shivatzki, Shaked, 23, 720, 1120
 Shlomovitz, Roie, 764
 Shomron, Noam, 16, 718
 Shore, Susan, 224, 531, 937, 957
 Shu, Yilai, 1061
 Shub, Daniel E., 499
 Shulenina, Nelly, 251
 Sibrian-Vazquez, Martha, 1029
 Sidique, Sumaya, 1064
 Sidorenko, Galina, 251
 Siegel, Jonathan, 122, 123, 142, 1064, 1074
 Sienko, Kethleen, 817
 Silipino, Lorna, 732
 Silver, Robert, 150
 Sim, Jae Hoon, 404, 437
 Simmons, Andrea, 52
 Simmons, Dwayne, 148, 1026
 Simmons, James, 52
 Simon, Jonathan Z., 4, 373, 889, 961
 Simon, Julian, 1041
 Simoncelli, Eero, 13
 Simpson, Brian, 521
 Singer, Wibke, 53
 Sinha, Ghanshyam, 157, 470, 881, 1122
 Sirmaci, Asli, 881
 Sisto, Renata, 164
 Siveke, Ida, 359, 360
 Skarzynski, Henryk, 167
 Skarzynski, Piotr, 167
 Koch, Antonin, 626
 Skoe, Erika, 645, 873, 875
 Slama, Michael, 265, 400, 695
 Slaney, Malcolm, 527
 Slattey, William, 707, 708
 Slee, Sean, 966
 Sloan, David, 98, 642
 Small, Christopher J., 1108
 Smith, Adam, 667, 734
 Smith, Benjamin, 1104, 1105
 Smith, Felicia L., 913
 Smith, Geoffrey M., 14
 Smith, Jacklyn, 388
 Smith, Karen, 869
 Smith, Richard J.H., 27, 28
 Smith, Sonya, 766
 Smith, Zachary, 32
 Smyth, Brendan, 325
 Smythe, Nancy, 627, 905
 Snyder, Joel, 207, 208
 Sohmer, Haim, 121
 Sohoglu, Ediz, 475
 Soken, Hakan, 37
 Sokolic, Ljiljana, 538
 Sokolowski, Bernd, 143
 Someya, Shinichi, 1047
 Son, Eun Jin, 106
 Song, Jae-Jin, 233, 661, 1046
 Song, Judy, 873
 Song, Lei, 158, 897, 899
 Song, Mee Hyun, 434, 727
 Song, Taegeun, 1053
 Songer, Jocelyn, 131
 Soto, Enrique, 250, 251
 Sotomayor, Marcos, 605, 606
 Soto-Varela, Andres, 806
 Soukup, Garret, 113, 186, 621, 1004
 Sowick, Colleen, 676
 Spallita, Matthew, 757
 Sparto, Patrick, 815, 817
 Spencer, Abigail, 704
 Spencer, Nathaniel, 500
 Spirou, George, 1014
 Sprenger, Christiane, 655
 Srinivasan, Arthri, 660, 983
 Srinivasan, Nirmal, 795
 Sripal, Prashanth, 186
 Staecker, Hinrich, 1102
 Stafford, Jim, 794
 Stafford, Ryan, 794
 Stagner, Barden, 165, 596
 Stakhovskaya, Olga, 692, 975, 990, 1001
 Stanely, Pamela, 270
 Stange, Annette, 359
 Stankovic, Konstantina, 124, 333, 455, 714, 733, 739, 741
 Stark, Gemaine, 689
 Stark, Kelsey, 619
 Stasiak, Arkadiusz, 402, 644
 Stawicki, Marnix, 316
 Stawicki, Tamara, 1033
 Steadman, Mark, 672
 Stebbings, Kevin A., 624
 Stecker, G. Christopher, 893, 959
 Steel, Karen, 17, 19, 20, 717, 719, 823, 905, 1008
 Steele, Charles, 438, 1055, 1058, 1059
 Steenson, Sharalyn, 113, 1004
 Steinhoff, Hans-Joachim, 396
 Steinschneider, Mitchell, 3, 960
 Steiner, Dietrich A., 28
 Stephens, Jill, 993
 Sterkers, Olivier, 590
 Stevens, Madelyn, 819
 Stevens, Shawn M., 786
 Stewart, Colin L., 23
 Steyger, Peter, 322, 1028, 1029, 1030, 1031, 1032
 Stieger, Christof, 774, 779
 Stilller, Barbara, 14
 Stimmmer, Sarah, 59, 825
 Stockdale, David, 235
 Stocker, Alan, 203
 Stoddart, Paul, 698
 Stoelb, Corey, 520, 522
 Stojilkovic, Stanko S., 343
 Stolzberg, Daniel, 532, 597, 657
 Stone, Jennifer, 243, 792
 Storey-Workley, Megan, 676
 Strahl, Stefan, 397
 Strain, Shinji, 620
 Straka, Malgorzata, 668
 Strauss, Bryan, 184
 Streeter, Timothy, 407
 Strelcyk, Olaf, 487
 Strenzke, Nicola, 268, 694, 882
 Strickland, Elizabeth A., 183, 1108
 Strimbu, C. Elliott, 763, 764
 Strimbu, Clark Elliott, 896
 Strome, Scott, 732
 Strong, Melissa, 752
 Strongin, Robert, 1029
 Strupp, Michael, 802
 Sturlese, Mattia, 557
 Su, Gina, 683
 Su, Jiping, 1022
 Subhash, Hreesh, 267, 769
 Sugahara, Kazuma, 139, 746, 747, 803
 Sugamura, Mayumi, 429
 Sugiyama, Kenichi, 743
 Suh, Jin Kyung, 749
 Suh, Myung-Whan, 225, 242
 Sultemeier, David, 241
 Summerfield, Quentin, 419, 525
 Summers, Van, 219
 Sumner, Chris, 78, 672
 Sun, Hong, 837
 Sun, Li, 380
 Sun, Wei, 534, 935
 Sun, Xiao-Ming, 446
 Sunami, Kishiko, 162, 964
 Sundaresan, Vidya, 21
 Sung, Michael, 306
 Suni, Karima, 942
 Suthakar, Kirupa, 63
 Suzukawa, Keigo, 450, 451
 Suzuki, Akira, 107
 Suzuki, Makoto, 1062
 Suzuki, Mitsuya, 635, 750
 Svirsky, Mario, 690, 979, 1002
 Swaminathan, Jayaganesh, 215, 479, 927
 Swarouth, Lani, 541
 Swiderski, Donald, 548, 572
 Syka, Josef, 626
 Tabesh, Babak, 1098
 Tabor, Kathryn, 361
 Tabuchi, Keiji, 1034
 Taira, Masato, 368
 Takada, Yohei, 548
 Takahashi, Hirokazu, 82, 941
 Takahashi, Terry, 2
 Takanami, Taro, 750
 Takata, Yusuke, 410
 Takeda, Noriaki, 724
 Takeda, Setsuko, 699
 Takeda, Taizo, 159, 699
 Takeshima, Chihiro, 491
 Takimoto, Yasumitsu, 249
 Takizawa, Yoshinori, 743
 Takubo, Yuya, 737
 Takumi, Yutaka, 1063
 Talavage, Thomas, 999
 Talja, Suvi, 369
 Tambis, Kristian, 633
 Tamura, Atsushi, 140
 Tan, Chin-Tuan, 690, 979, 1002
 Tan, Xiaodong, 473, 554, 555
 Tanaka, Chiemi, 689
 Tanaka, Masaaki, 964
 Tanaka, Shuho, 1034
 Tang, Jie, 555, 618
 Tang, Wenxue, 713
 Tang, Xiaolan, 632
 Tang, Xuehui, 240
 Tang, youg, 126
 Tang, Zhengquan, 363
 Tanigawa, Makoto, 679
 Tanimoto, Hitoshi, 141
 Tanokura, Masaru, 1047
 Tarabichi, Osama, 326
 Tavazzani, Elisa, 460
 Taylor, Anna M., 323
 Taylor, Ruth, 119, 135, 136, 830
 Tea, Basileid, 713
 TeGrootenhuus, Lauren T., 28
 Teitell, Michael A., 14
 Tejada, Francisco, 545
 Teki, Sundeep, 492, 888, 951
 Tekin, Mustafa, 424, 881
 Tellers, Philipp, 1088
 Tempel, Bruce, 47, 71, 314
 Terrell, David, 881
 Terreros, Gonzalo, 654
 Teudt, Ingo U., 696
 Thakkar, Tanvi, 975, 990, 1001
 Thein, Pru, 828
 Thiede, Benjamin, 290, 291
 Thiele, Alexander, 380, 486
 Thies, Scott, 791
 Thiessen, Kevin, 114
 Thomas, Andrew, 1041, 1042
 Thomas, Paul, 144
 Thompson, Alexander, 698
 Thompson, Eric, 219, 521
 Thorne, Peter R., 26
 Thornton, Jennifer, 71, 447, 511
 Tian, Chunjie, 1044, 1045
 Tian, Cong, 24
 Tiedemann, Kerrie, 1103
 Tignor, Emily, 625
 Tillein, Jochen, 655, 980
 Tilleson, Jake, 1105
 Tillingier, Joshua, 745
 Tintera, Jaroslav, 626
 Tjia, Michelle, 1109
 Todd, Dylan, 1111
 Todd, N. Wendell, 432, 713
 Tokita, Joshua, 912
 Tollin, Daniel, 30, 447, 511, 775, 1091, 1045
 Tolnai, Sandra, 671, 1089
 Tomlin, Julia, 450, 451
 Tomoda, Koichi, 1062
 Tomoriova, Beata, 518
 Tona, Yosuke, 736
 Tong, Ling, 569, 752, 787
 Tong, Mingjie, 1020
 Torii, Hiroko, 111
 Torii, Masaaki, 859
 Town, Stephen, 944
 Trahiotis, Constantine, 846
 Tran, Mina, 432

- Tran, Vy, 163
Treaaba, Claudiu, 690
Treadway, Jamie, 710
Tremblay, Kelly, 565
Trevino, Carolina, 809, 810
Tritsch, Nicolas X., 578
Trivedi, Parul, 790
Trujillo, Michael, 81
Trune, Dennis, 42, 322, 425
Truong, Kristy, 843
Trussell, Laurence, 66, 73, 76
Tsai, Ching-Hui, 715
Tsang, Joyce, 1026
Tsuchihashi, Nana, 826
Tsuda, Junko, 139
Tsumoto, Kohei, 1118
Tsuprun, Vladimir, 426, 436
Tszaki, Minoru, 491
Tuft, Bradley, 1110
Tümsmeyer, Julia, 623
Turesky, Theodore, 228
Turnbull, Daniel, 867
Turner, Jeremy, 259, 624
Tzounopoulos, Thanos, 72, 874
Uchanski, Rosalie, 819
Udayashankar, Arun, 1048
Uemaetomari, Isao, 1034
Ulfendahl, Mats, 457
Uno, Atsuhiko, 249
Uribe, Phillip, 1006
Usami, Shin-ichi, 1063, 1118
Ushakova, Lyubov, 283
Ushio, Munetaka, 737
Uthaiha, Revethy, 615
Vachhani, Jay, 418
Vaden, Kenneth, 523
Vaillencourt, Dwayne, 548
Valdes, Jose Luis, 101
Valencia, Gloria, 412
Valero, Michelle, 315
Van de Heyning, Paul, 233, 661, 976
Van De Water, Thomas, 58, 137, 138, 337, 745
van der Heijden, Marcel, 770, 776
van der Waals, Marjolijn, 94
van Dijk, Mart, 684
van Dijk, Pim, 220, 229, 231, 280
van Doorn-Bierman, Maaïke, 864
van Gendt, Margriet, 231, 280
van Iersel, Levi, 847
Van Itallie, Christina M., 1122
van Opstal, John, 847
van Wanrooij, Marc, 847
van Zanten, Gijsbert, 94
Vander Werff, Kathy, 656
Vanneste, Sven, 233, 661
Vardar, Gülcin, 67
Varela-Nieto, Isabel, 300, 327
Varghese, Lenny, 933
Varoqueaux, Frederique, 75
Vasella, Andrea, 309
Vatti, Marianna, 478
Vazquez, Ana E., 758
Veau, Nicolas, 996, 997
Vega, Rosario, 250, 251
Veile, Rose, 586
Velet, Lily, 650
Vélez, Alejandro, 209
Vélez-Ortega, A. Catalina, 466
Venkataraman, Yamini, 858
Verhey, Jesko, 670
Verhoeven, Kristien, 136
Verhulst, Sarah, 1084
Verhulst, Steven, 46
Verma, Rohit U., 400
Vermeire, Katrien, 982
Verschooten, Eric, 352, 907
Vernel, Huib, 94, 397
Versteegh, Corstiaen, 770, 776
Viani, Laura, 388
Vianna, Melissa, 134
Vickers, Deborah, 419
Vidal, Rene, 92
Villafañe-Delgado, Marisel, 373
Vlaming, Marcel, 54
Voelkel-Johnson, Christina, 843
Vogt, Gerhard, 268, 694
Volk, Alexander E., 14
Vollmer, Maïke, 89, 401
von Ameln, Simon, 14
von Gersdorff, Henrieque, 129, 459
von Kriegstein, Katharina, 873
Vongpaisal, Tara, 33
Vongtau, Habiba, 247
Voytenko, Sergiy, 1099
Vozzi, Diego, 726
Vranceanu, Florin, 791
Vu, Ly, 137
Vuckovic, Dragana, 17, 725
Vulovic, Vedran, 538
Vuong, Quoc, 611
Wada, Hiroshi, 45, 1063, 1118
Wada, Tetsuro, 1034
Wade, Scott, 698
Wagner, Hermann, 344, 345, 516, 517, 1086, 1088
Wagner, Thomas, 607
Wali, Abdul, 881
Walker, Kerry, 908
Wallace, Mark, 965, 1101
Wallace, Matthew, 1013
Wallaert, Nicolas, 479
Wallenhorst, Christopher, 236
Walsh, Benjamin, 373
Walsh, Edward J., 59, 621, 825
Walsh, Kyle P., 168
Walshe, Peter, 388
Walters, Bradley, 22, 570
Walton, Joseph P., 628, 629, 630, 632
Wan, Wankei, 443
Wang, Bo, 57
Wang, Chuansong, 335
Wang, Geng, 14
Wang, Guopeng, 109
Wang, Han Chin, 578
Wang, Hongning, 929
Wang, Jane, 700
Wang, Jian, 1039
Wang, Jianjun, 18, 703, 1121
Wang, Jing, 126, 1043
Wang, Jun, 18
Wang, Ke-qiang, 1060
Wang, Lingyan, 267
Wang, Lu-yang, 346
Wang, Ningyuan, 199
Wang, Qiong, 1011, 1023, 1111
Wang, Rosalie, 49, 781
Wang, Ruikang, 423, 769
Wang, Tian, 569, 783, 1032
Wang, Tzu-Lun, 462, 883
Wang, Xiaoqin, 91, 179, 376, 493
Wang, Ya-Xian, 458
Wang, Yuan, 349
Wang, Yunfeng, 703
Wang, Yunyan, 850
Wang, Zheng-min, 1060, 1061
Wang, Zhiyong, 791
Wangemann, Philine, 27, 579, 824, 832, 1117
wangsawihardja, felix, 21
Warchol, Mark, 108, 189, 586, 752, 845
Ward, Bryan K., 541, 808
Ward, Jessica L., 210
Ward, Jonette, 40
Ward, Kristi, 520
Washizawa, Shiho, 1082
Wasserman, Stephen, 450, 451
Watanabe, Yasuyoshi, 964
Watson, Charles S., 418
Watts, Melissa, 683
Weatherstone, Jessica, 71
Webster, Jennifer, 28
Wei, Eric, 306
Wei, Liting, 353
Wei, Shun-Hwa, 813
Wei, Wei, 537
Weichert, Rachel, 1106
Weihofen, Wilhelm A., 605
Weimann, Sonia, 1087
Weinberg, Irving, 43
Weinberg, Monica, 581
Weiner, Benjamin, 260
Weinstock, Nadav, 649
Weintraub, David, 207
Weiss, Inbal, 16
Weiss, Michael, 931
Weisz, Nathan, 661
Wells, Jonathon, 794
Wells, Toby, 78
Wen, Bo, 1114
Wenstrup, Jeffrey, 370, 1076, 1077
Wenzel, Angela, 808, 809, 810
Wenzel, Gentiana I., 405
Werner, Lynne, 600
Wersinger, Eric, 238
Wesen, Kyle, 651
Wess, Jessica, 1016
West, Matthew, 784
Weston, Michael D., 469
Wetzal, Friederike, 340
White, Jacqueline, 20, 717
White, Keith, 814
White, Patricia, 730
White, Scott, 1110
White-Schwoch, Travis, 61, 62
Whitlon, Donna S., 566
Whitmer, William, 851
Whitney, Susan, 817
Wichman, Carolin, 462, 882
Wickesberg, Robert, 910
Wiebel, Michael, 150
Wijnperle, Daniela, 1064
Wilch, Ellen, 729
Wild, Conor, 894
Wiler, James, 957
Wilkes, Bradley, 814
Williams, Anthony, 675
Williams, Whitney, 511
Williamson, Tanika T., 630
Wilson, Teresa, 60, 267
Winter, Ian, 402, 644, 994
Wirtz, Christian, 849, 1090
Wirtzfeld, Michael, 214
Wise, Andrew, 38, 39
Witteveen, Jolanda, 840
Wohlgemuth, Melville, 971
Wojtczak, Magdalena, 168, 613
Wolf, Eckhard, 720
Wollnik, Bernd, 14
Won, Jong Ho, 31, 398, 497, 600
Wong, Aaron, 816, 882
Wong, Hiu Tung, 572
Wong, Jau-Min, 712
Wong, Kristen, 1119
Wong, Rachel, 361
Woo, Hae-Mi, 1009
Woo, Jeong-Im, 456, 755, 756
Wood, Katherine, 504, 944
Wood, Scott, 551, 818
Woods, Bill, 853
Woolley, Sarah, 11
Wouters, Jan, 5, 998
Wozny, David, 688
Wright, Beverly, 371, 477, 559
Wright, Charles G., 323
Wright, James, 527
Wright, Matthew, 994
Wright, Samantha, 74
Wu, Calvin, 83
Wu, Chen-Chi, 712, 715
Wu, Ching-Chih, 35
Wu, Doris, 106, 292
Wu, Jing, 18
Wu, Jonathan, 1014
Wu, Leqing, 55
Wu, Mailing, 691
Wu, Patricia, 1040, 1041, 1042
Wu, Tao, 267
Wu, Xuewen, 837
Wu, Yuting, 788
X. Joris, Philip, 907
Xia, Anping, 49
Xie, Jing, 309
Xie, Ruili, 64
Xie, You-zhou, 437
Xin, Feng, 18
Xing, Yazhi, 627, 786, 905
Xiong, Wei, 607
Xu, Helen, 900, 901
Xu, Li, 36
Xu, Linjing, 1110
Xu, Min, 24
Xu, Yanbo, 375
Xu, Yang, 631
Xue, Angela, 569
Xu-Friedman, Matthew, 342
Yaeger, Daniel, 76
Yakushin, Sergei B., 547
Yamada, Takahiro, 249
Yamada, Takao, 41, 185, 1010
Yamagishi, Shinpei, 175, 1079, 1082
Yamamoto, Hidefumi, 964
Yamamoto, Norio, 111, 299, 302, 303
Yamane, Hideo, 964
Yamano, Takafumi, 429
Yamashita, Akinori, 453
Yamashita, Daisuke, 141, 411, 829
Yamashita, Hiroshi, 139, 746, 747, 803
Yamashita, Shinji, 737
Yamasoba, Tatsuya, 159, 430, 431, 635, 737, 742, 750
Yan, Denise, 26, 324, 424
Yan, Xukun, 18
Yang, Hua, 342
Yang, Shiguang, 44
Yang, Sungchil, 260
Yang, Tao, 27
Yang, Ting-Hua, 712
Yang, Wanwan, 707, 708
Yang, Weiping, 631
Yang, Xin, 739
Yang, Yuqin, 835
Yang, Yu-Qin, 834, 1032
Yao, Jun, 956
Yao, Justin D., 508
Yarden, Tohar, 366
Yaron, Amit, 366
Yaron, Orly, 718
Yasin, Ifat, 173, 946
Yasui, Tetsuro, 588
Yechikov, Sergey, 758
Yee, Kathleen, 348
Yehekel, Adva, 718
Yeo, Sang Won, 50
Yin, Pingbo, 375, 378
Yin, Tom, 513, 1091, 1092
Yonemura, Shigenobu, 836
Yoo, James, 571
Yoshida, Atsuhiko, 111
Yoshida, Naohiro, 45
Young, Eric, 84, 92, 664, 966, 1103
Young, Hunter, 693
Young, Samuel, 75
Yousaf, Rizwan, 881, 1122
Youzhou, Xie, 404
Yu, Heping, 24
Yu, Huiqian, 833
Yu, I-Shing, 712
Yu, Lu-Ming, 1054
Yu, Qing, 1121
Yu, Song Hee, 722
Yu, Wei-Ming, 296
Yu, Xin, 867
Yuan, Quan, 714
Yuan, Yasheng, 669
Yuan, Yongyi, 18, 713
Yue, David, 84, 92
Yumoto, Eiji, 1010
Yumoto, Masato, 99
Zador, Anthony, 287
Zahorik, Pavel, 502, 514
Zähringer, Dana, 516
Zakharenko, Stanislav, 264
Zallocchi, Marisa, 465, 1005
Zamani, Darius, 752
Zampini, Valeria, 460
Zanatta, Daniela, 184
Zatorre, Robert J., 386
Zekveld, Adriana, 862
Zelle, Dennis, 171
Zemek, Allison, 438
Zemla, Marcin, 838
Zeng, Chunhua, 937
Zeng, Fan-Gang, 387, 388
Zeng, Fang-Gang, 382
Zhai, Feng, 158
Zhang, Fawen, 389, 390
Zhang, Fei, 753, 754, 839
Zhang, Hongzhen, 120
Zhang, Huiming, 682
Zhang, Jian, 289
Zhang, Jianguo, 18
Zhang, Jin, 24
Zhang, Jin Hui, 754
Zhang, Jinhui, 839
Zhang, Jinsheng, 528, 1100
Zhang, Kaidi D., 112
Zhang, Lei, 567
Zhang, Li, 260
Zhang, Mengchao, 36
Zhang, Qian, 621
Zhang, Su-Chun, 790
Zhang, Tian-yu, 1060
Zhang, Wenjing, 838
Zhang, Xiangming, 441, 591
Zhang, Xueguo, 1100
Zhang, Yan, 24
Zhang, Yifan, 154
Zhang, Ying Xin, 578
Zhang, Yong, 223
Zhang, Yuan, 267, 769
Zhao, Bo, 607
Zhao, Hong-Bo, 723, 821, 827, 1123
Zhao, Hongyu, 608
Zhao, Ken, 995
Zhao, Lingyun, 665
Zhao, Wei, 1078
Zheng, Hong-Wei, 48, 822
Zheng, Jing, 142, 155, 156, 295, 553
Zheng, Qing, 24
Zheng, Qing Yin, 1116
Zheng, Yi, 172
Zhi, Zhongwei, 423
Zholudeva, Lyandysha, 619
Zhou, Binfei, 18, 703
Zhou, Fei, 579, 824
Zhou, Han, 55
Zhou, Hongbo, 26
Zhou, Ning, 992
Zhou, Wu, 240, 537
Zhou, Xiang, 1002
Zhou, Yi, 91
Zhu, Guangjie, 55
Zhu, Hong, 240, 537
Zhu, Juhong, 905
Zhu, Qingyan, 18
Zhu, Xiaoxia, 628, 629, 630, 632
Zhu, Yan, 723, 821, 827, 1123
Zilany, Muhammad S.A., 914
Zimmermann, Elke, 623
Zimmermann, Wolfgang, 162
Zirn, Stefan, 391
Znamenskiy, Petr, 287
Zobay, Oliver, 227, 417
Zoghbi, Huda, 273
Zong, Liang, 723, 827, 1123
Zopf, David, 589
Zosuls, Aleks, 778
Zuccotti, Annalisa, 53
Zuniga, M. Geraldine, 809, 810
Zuo, Jian, 22, 117, 145, 568, 569, 570, 735

BALTIMORE MARRIOTT WATERFRONT

MEETING SPACE FLOOR-PLANS



Baltimore Marriott Waterfront
700 Aliceanna Street • Baltimore, MD 21202
Phone: (410) 385-3000 • Fax: (410) 895-1900
www.marriott.com

SAVE THE DATES

February 22-26, 2014

37th ARO MidWinter Meeting
Manchester Grand Hyatt Hotel
San Diego, California, USA

February 21-25, 2015

38th ARO MidWinter Meeting
Baltimore Marriott Waterfront
Baltimore, Maryland, USA

February 20-24, 2016

39th ARO MidWinter Meeting
Manchester Grand Hyatt Hotel
San Diego, California, USA

Association for Research in Otolaryngology

19 Mantua Road

Mt. Royal, NJ 08061

www.aro.org